MODERN PRESTRESSED CONCRETE

Design Principles and Construction Methods

MODERN PRESTRESSED CONCRETE

Design Principles and Construction Methods

Fourth Edition

James R. Libby

James R. Libby and Associates
San Diego, California

SPRINGER SCIENCE+BUSINESS MEDIA, LLC

Originally published by Van Nostrand Reinhold in 1990
Softcover reprint of the hardcover 1st edition 1990

Library of Congress Catalog Card Number 89-21464
ISBN 978-1-4613-6747-5

16 15 14 13 12 11 10 9 8 7 6 5 4 3 2 1

Library of Congress Cataloging-in-Publication Data

Libby, James R.
Modern prestressed concrete : design principles and construction methods / by James R. Libby. — 4th ed.
p. cm.
Includes bibliographical references.
ISBN 978-1-4613-6747-5 ISBN 978-1-4615-3918-6 (eBook)
DOI 10.1007/978-1-4615-3918-6
1. Prestressed concrete construction. I. Title.
TA683.9.L47 1990
624.1'83412—dc20 89-21464
CIP

To my wife Lucy with love and gratitude for her patience and understanding during the preparation of this edition and its predecessors.

Contents

Preface

This book was written with a dual purpose, as a reference book for practicing engineers and as a textbook for students of prestressed concrete. It represents the fifth generation of books on this subject written by its author.

Significant additions and revisions have been made in this edition. Chapters 2 and 3 contain new material intended to assist the engineer in understanding factors affecting the time-dependent properties of the reinforcement and concrete used in prestressing concrete, as well as to facilitate the evaluation of their effects on prestress loss and deflection. Flexural strength, shear strength, and bond of prestressed concrete members were treated in a single chapter in the third edition. Now, in the fourth edition, the treatment of flexural strength has been expanded, with more emphasis on strain compatibility, and placed in Chapter 5 which is devoted to this subject alone. Chapter 6 of this edition, on flexural-shear strength, torsional strength, and bond of prestressed reinforcement, was expanded to include discussions of Compression Field Theory and torsion that were not treated in the earlier editions. In similar fashion, expanded discussions of loss of prestress, deflection, and partial prestressing now are presented separately, in Chapter 7. Minor additions and revisions have been made to the material contained in the remaining chapters with the exception of

Chapter 17. This chapter, which is devoted to construction considerations, has important new material on constructibility and tolerances as related to prestressed concrete.

Appendixes A, B, and C reproduce important documents on computation of the loss of prestress, which have found wide use and acceptance among practicing engineers. Appendix D, reproduced from Canadian National Standard CAN3-A23.3-M84, contains portions of Section 11 and Appendix D of that standard—information that is familiar to engineers in Canada but considerably less familiar to U.S. engineers.

The material contained in the appendixes is copyrighted resource material that has been reproduced with the permission of the publishers. This important material was included in this book because many readers, particularly students, may have difficulty accessing it. Readers are encouraged to acquire complete copies of the documents from which the reproduced material was taken because in some instances only excerpts of the original work were included here.

Frequent references are made to publications of the American Association of State Highway and Transportation Officials, the American Concrete Institute, the Canadian Standards Association, and the Prestressed Concrete Institute. Engineers and contractors concerned with the design and construction of prestressed concrete should be familiar with the publications of these organizations. This book is intended to emphasize the requirements of the *Building Code Requirements for Reinforced Concrete* (ACI 318-89), the 1989 edition of the AASHTO *Standard Specification for Highway Bridges*, and the 1984 edition of the Canadian National Standard *Design of Concrete Structures for Buildings* (CAN3-A23.3-M84). These important documents should be included in the libraries of engineers engaged in the design and construction of prestressed concrete.

The author wishes to acknowledge, with sincere thanks, the help of Geoffrey R. Cook, Victor Garcia Delgado, Donald R. Libby, and Dan Protopopescu, for their suggestions, contributions, reviewing, and checking portions of the manuscript for this book.

JAMES R. LIBBY
San Diego, California

1 Prestressing Methods

1-1 Introduction

Prestressing can be defined as the application of a predetermined force or moment to a structural member in such a manner that the combined internal stresses in the member, resulting from this force or moment and from any anticipated condition of external loading, will be confined within specific limits. The prestressing of concrete, which is the subject of this book, is the result of applying this principle to concrete structural members with a view toward eliminating or materially reducing the tensile stresses in the concrete.

The prestressing principle is believed to have been well understood since about 1910, although patent applications related to types of construction involving the principle of prestress date back to 1888 (Abeles 1949). The early attempts at prestressing were abortive, however, owing to the poor quality of materials available in the early days as well as to a lack of understanding of the action of creep in concrete. Eugene Freyssinet, the eminent French engineer, generally is regarded as the first investigator to recognize the nature of creep in concrete and to realize the necessity of using high-quality concrete and high-tensile-strength steel to ensure that adequate prestress is retained. Freyssinet applied prestressing in structural application during the early 1930s. The history

and the evolution of prestressing are controversial subjects and not well documented; so they are not discussed further in this book. The interested reader may find additional historical details in the references (Abeles 1949; Dobell 1950).

Many experiments have been conducted to demonstrate that prestressed concrete has properties that differ from those of nonprestressed reinforced concrete. Diving boards and fishing poles have been made of prestressed concrete to demonstrate the ability of this material to withstand large deflections without cracking. Of more significance, however, is the fact that prestressed concrete has proved to be economical in buildings, bridges, and other structures (under conditions of span and loading) that would not be practical or economical in reinforced concrete.

Prestressed concrete was first used in the United States (except in tanks) in the late 1940s. At that time, most U.S. engineers were completely unfamiliar with this mode of construction. Design principles of prestressed concrete were not taught in the universities, and the occasional structure that was constructed with this new material received wide publicity.

The amount of construction utilizing prestressed concrete has become tremendous and certainly will continue to increase. The contemporary structural engineer must be well informed on all facets of prestressed concrete. It is indeed unfortunate that the subject of prestressed concrete design and construction is not included in the undergraduate curriculum of many U.S. universities at this time.

1-2 General Design Principles

Prestressing, in its simplest form, can be illustrated by considering a simple, prismatic flexural member (rectangular in cross section) prestressed by a concentric force, as shown in Fig. 1-1. The distribution of the stresses at midspan is as indicated in Fig. 1-2. It is readily seen that if the flexural tensile stresses in the bottom fiber, due to the dead and live service loads, are to be eliminated, the uniform compressive stress due to prestressing must be equal in magnitude to the sum of these tensile stresses.

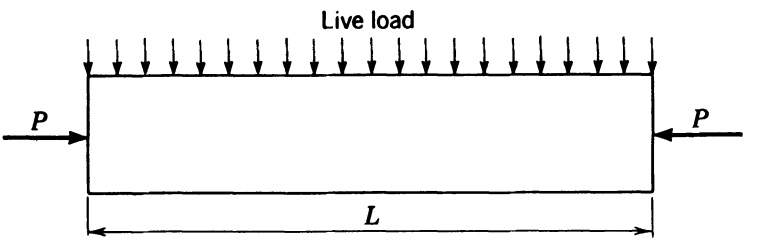

Fig. 1-1. Simple rectangular beam prestressed concentrically.

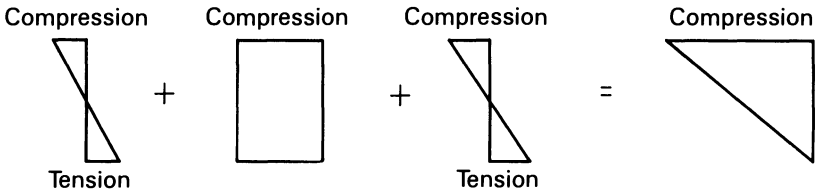

Fig. 1-2. Distribution of stresses at midspan of a simple beam concentrically prestressed.

There is a time-dependent reduction in the prestressing force, due creep and shrinkage of the concrete and relaxation of the prestressing steel (see Chapters 2, 3, and 7). If no tensile stresses are to be permitted in the concrete, it is necessary to provide an initial prestressing force that is larger than would be required to compensate for the flexural stresses resulting from the service loads alone. The prestress loss, which is discussed in detail in Secs. 7-2 and 7-3, generally results in a reduction of the initial prestressing force by 10 to 30 percent. Therefore, if the stress distributions shown in Fig. 1-2 are desired after the loss of stress has taken place (under the effects of the final prestressing force), the distribution of stresses under the initial prestressing force would have to be as shown in Fig. 1-3.

Prestressing with the concentric force just illustrated has the disadvantage that the top fiber is required to withstand the compressive stress due to prestressing in addition to the compressive stresses resulting from the service loads. Furthermore, because prestressing must be provided to compress the top fibers, as well as the bottom fibers, if sufficient prestressing is to be supplied to eliminate all of the service load flexural tensile stresses, the average stress due to the prestressing force (the prestressing force divided by the area of the concrete section) must be equal to the maximum flexural tensile stress resulting from the service loads.

If this same rectangular member were prestressed by a force applied at a point one-third of the depth of the beam from the bottom of the beam, the distribution of the stresses due to prestressing would be as shown in Fig. 1-4. In this case, as in the previous example, the final stress in the bottom fiber due to prestressing

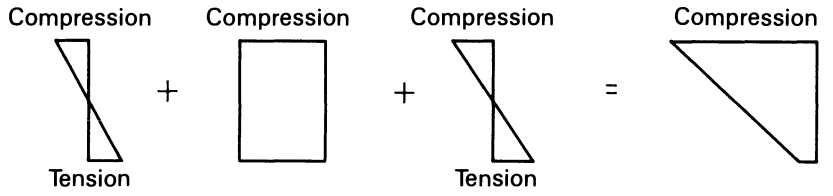

Fig. 1-3. Distribution of stresses at midspan of a simple beam under initial concentric prestressing force.

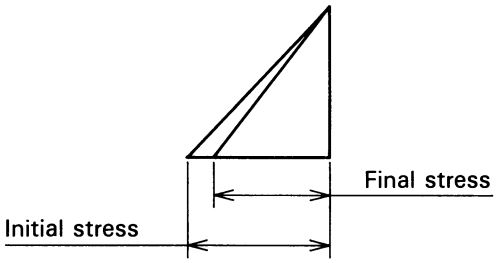

Fig. 1-4. Distribution of stresses due to prestressing force applied at lower third point of rectangular cross section.

should be equal in magnitude to the sum of the tensile stresses resulting from the service loads. By inspection of the two stress diagrams for prestressing (Figs. 1-2b and 1-4), it is evident that the average stress in the beam, prestressed with the force at the third point, is only one-half of that required to develop the amount required in the first example. In addition, the top fiber is not required to carry any compressive stress due to prestressing when the force is applied at the third point.

The economy that results from applying the prestressing force eccentrically is obvious. Further economy can be achieved when small tensile stresses are permitted in the top fibers. The tensile stresses may be due to prestressing alone or to the combined effects of prestressing and any service loads that may be acting at the time of prestressing. This is so because the required bottom-fiber prestress can be attained with a smaller prestressing force, which is applied at a greater eccentricity under such conditions. This principle is treated in greater detail in subsequent chapters.

In many contemporary applications of prestressing, the flexural tensile stresses due to the applied service loads are not completely nullified by the prestressing; nominal flexural tensile stresses are knowingly permitted under service load conditions. Economy of construction is the motivation for this practice as well. The use of flexural tensile stresses under service load conditions is considered in detail in this book.

1-3 Prestressing with Jacks

The prestressing force in the above examples could be created by placing jacks at the ends of the member, if there were abutments at each end sufficiently strong to resist the prestressing force developed by the jacks. Prestressing with jacks, which may or may not remain in the structure, depending upon the circumstances, has been used abroad on dams, dry docks, pavements, and other special structures. This method has been used to a very limited degree in North America because extremely careful control of the design (including study of the behavior under overloads), construction planning, and execution of the

construction is required if the results obtained are to be satisfactory. Furthermore, the loss of prestress resulting from this method is much larger than when other methods are used (see Sec. 3-15), unless frequent adjustments of the jacks are made, because the concrete is basically subjected to constant strain in this method of prestressing rather than to nearly constant stress as is the case in other methods. For these reasons, and because the types of structure to which this method of prestressing can be applied are very limited and beyond the scope of usual generalities, subsequent consideration of this method is not given in this book (Guyon 1953).

1-4 Prestressing with Pretensioned Tendons

Another method of creating the necessary prestressing force is referred to as pretensioning. Pretensioning is accomplished by stressing steel wires or strands, called tendons, to a predetermined stress, and then, while the stress is maintained in the tendons, placing concrete around the tendons. After the concrete has hardened, the tendons are released, and the concrete, which has become bonded to the tendons, is prestressed as the tendons attempt to regain the length they had before they were stressed. In pretensioning, the tendons usually are stressed by the use of hydraulic jacks. The stress is maintained during the placing and curing of the concrete by anchoring the ends of the tendons to rigid, nonyielding abutments that may be as much as 500 ft or more apart. The abutments and appurtenances used in this procedure are referred to as a pretensioning bed or bench. In some instances, rather than using pretensioning benches, the steel molds or forms that are used to form the concrete members are designed in such a manner that the tendons can be safely anchored to the mold after they have been stressed. As the results obtained with each of these methods are identical, the factors involved in determining which method should be used are of concern to the fabricator of prestressed concrete, but do not usually affect the designer.

The tendons used in pretensioned construction must be relatively small in diameter because the bond stress between the concrete and a tendon is relied upon to transfer the force in the tendon to the concrete. If the bond stress exceeds the bond strength of the concrete, the tendon will slip, and the prestress will be lost. The ratio of the bond area (product of the circumference and length of the wire) to the cross-sectional area of a circular wire or bar is equal to $4L/d$, where d is the diameter and L is the length over which the transfer is made; thus the bond area available per unit length of tendon decreases as the diameter increases. It follows that, for constant tendon stress, the bond stress increases as the tendon diameter increases. This explains why several tendons of small diameter normally area used in pretensioning concrete, rather than a few larger ones. Small-diameter strands composed of several small wires twisted around a straight center (core) wire are widely used in pretensioning concrete because of their excellent bond characteristics (see Sec. 6-6).

Pretensioning is widely used in the manufacture of prestressing concrete in

North America. The basic principles and some of the methods currently used here were imported from Europe, but much has been done to develop and adapt the procedures to the North American market. One of these developments was the introduction of pretensioned tendons that do not pass straight through the concrete member, but are deflected or draped into a path that approximates a curve. This procedure was first used on light roof slabs, but subsequently has been commonly used in the construction of large structural members. The use of deflected, pretensioned tendons is common in the production of large bridge girders.

Although many of the devices used in pretensioned construction are patented, the basic principle is in the public domain and has been so for many years. A detailed discussion of the construction procedures and equipment used in pretensioned construction is given in Chapter 15.

1-5 Prestressing with Post-tensioned Tendons

When a member is fabricated in such a manner that the tendons are stressed, and each end is anchored to the concrete section *after* the concrete has been cast and has attained sufficient strength to safely withstand the prestressing force, the member is said to be post-tensioned. Two types of tendons are used: bonded and unbonded.

Fully bonded post-tensioned tendons consist of bars, strands, or wires, in preformed holes, metallic ducts, or plastic tubes, that have been pressure-grouted after stressing. The tube is used to prevent the tendon from becoming bonded to the concrete at the time that the concrete is placed. After the concrete has been sufficiently cured, the tendon is stressed, and the tube is injected with grout. The cured grout effectively bonds the tendon to the tube and the concrete itself (the outside surface of the tube becomes bonded to the concrete when the concrete is placed). Rather than using metallic tubes, bonded tendons can be constructed by using holes formed in the concrete with removable rubber tubes or hoses; in this method the tendons are inserted into the preformed holes after the rubber tubes have been removed, and they are subsequently stressed and grouted. Another form of bonded tendons—which may or may not be partially bonded to the concrete section, and are commonly known as external tendons—is used in special applications, as discussed in Sec. 6-8.

Unbonded tendons normally consist of strands or wires that are wrapped or encased in plastic after having been coated with a grease or a bituminous material. The grease sometimes contains a rust inhibitor to help protect the tendons from corrosion. Also, waterproof paper wrapping has been used rather than plastic. Unbonded tendons normally are assembled in a factory, shipped to the job site, and placed in the forms before the concrete is placed. They are not grouted after they have been stressed, so they do not become bonded to the concrete.

Bonded tendons are generally used in bridge construction, but unbonded tendons have been so used quite successfully. Unbonded tendons are most frequently used in building construction, but bonded tendons are sometimes used there also. The quantity of unbonded tendons used annually greatly exceeds the amount of bonded tendons used.

Post-tensioning offers a means of prestressing on the job site, which may be necessary in some instances. Very large building or bridge girders that cannot be transported from a precasting plant to the job site (because of their weight, size, or the distance between the plant and the job site) can be made by post-tensioning on the job site. Post-tensioning is used in precast as well as in cast-in-place construction. In addition, fabricators of pretensioned concrete will frequently post-tension members for small projects on which the number of units to be produced does not warrant the expenditures required to set up pretensioning facilities. There are other advantages inherent in post-tensioned construction, which are discussed in subsequent chapters.

In post-tensioning, it is necessary to use some type of device to attach or anchor the ends of the tendons to the concrete section. Such devices usually are referred to as end anchorages or simply anchorages. The end anchorages, tendons, special jacking, and grouting equipment, if used, in post-tensioning concrete are collectively referred to as a post-tensioning system. There are several different systems in use. Chapter 16 contains a more detailed discussion of post-tensioning and post-tensioning systems.

1-6 Pretensioning vs. Post-tensioning

It is generally considered impractical to use post-tensioning on very short members because the elongation of a short tendon (during stressing) is small and requires very precise measurement. In addition, some post-tensioning systems do not function well with very short tendons. A number of short members can be made in series on a pre-tensioning bench without difficulty and with no need for precise measurement of the tendon elongation during stressing; relatively long tendon lengths result from making a number of short members in series.

It has been pointed out that very large members may be more economical when cast in place and post-tensioned, or when precast and post-tensioned near the job site, compared to transporting and handling large pretensioned structural members that are cast off-site.

Post-tensioning allows the tendons to be placed through structural elements on smooth curves of any desired path. Pretensioned tendons can be employed on other than straight paths, but not without expensive plant facilities and somewhat complicated construction procedures.

Because post-tensioning tendons can be installed in holes preformed in precast concrete elements or segments, they can be used to prestress a number of small

precast elements together to form a single large structural member. This technique, frequently referred to as segmental construction, is discussed in Sec. 8-3.

The cost of post-tensioned tendons, measured in either cost per pound of prestressing steel or cost per pound of effective prestressing force, generally is significantly greater than the cost of pretensioned tendons, because of the larger amount of labor required in placing, stressing, and grouting (where applicable) post-tensioned tendons, as well as the cost of special anchorage devices and stressing equipment. On the other hand, a post-tensioned member may require less total prestressing force than an equally strong pretensioned member. For this reason, one must be careful when comparing the relative costs of these modes of prestressing.

The basic shape of an efficient pretensioned flexural member may be different from the most economical shape that can be found for a post-tensioned design. This is particularly true of moderate- and long-span members and somewhat complicates any generalization about which method is best under such conditions.

Post-tensioning generally is regarded as a method of making prestressed concrete at the job site, yet post-tensioned beams often are made in precasting plants and transported to the job site. Pretensioning often is thought of as a method of manufacturing that is limited to permanent precasting plants, yet on very large projects where pretensioned elements are to be utilized, it is not uncommon for the general contractor to set up a temporary pretensioning plant at or near the job site. Each method of making prestressed concrete has particular theoretical and practical advantages and disadvantages, which will become more apparent after the principles are well understood. A final determination of the mode of prestressing that should be used on any particular project can be made only after careful consideration of the structural requirements and the economic factors that prevail for the particular project.

1-7 Linear vs. Circular Prestressing

The subject of prestressed concrete frequently is divided into linear prestressing, which includes the prestressing of elongated structures or elements such as beams, bridges, slabs, piles, and so, and circular prestressing, which includes pipe, tanks, silos, pressure vessels, and domes. This book has been confined to consideration of linearly prestressed structures. The reader interested in circular prestressed concrete structures will find considerable information in the technical literature of the American Concrete Institute, the American Society of Civil Engineers, the American Water Works Association, and the Prestressed Concrete Institute, as well as in civil engineering text and reference books.

1-8 Application of Prestressed Concrete

Prestressed concrete, when properly designed and fabricated, can be virtually crack-free under normal service loads as well as under moderate overload. This is believed to be an advantage in structures exposed to corrosive atmospheres in service. Prestressed concrete efficiently utilizes high-strength concretes and steels and is economical even with long spans. Reinforced concrete flexural members cannot be designed to be crack-free, cannot efficiently utilize high-strength concrete (except in compression members), and are not economical for long-span flexural members.

A number of other statements can be made in favor of prestressed concrete, but there are bona fide objections to the use of this material under specific conditions. An attempt is made to point out these criticisms in subsequent chapters. Among the more significant advantages of this material are that in many structural applications, prestressed concrete is lower in first cost than other types of construction, and, in many cases, if the reduced maintenance cost inherent in concrete construction is taken into account, prestressed concrete offers the most economical solution. Its benefits have been well confirmed by the very rapid increase in the use of linear prestressed concrete that has taken place in the United States since its introduction in the late 1940s. It is well known that the advantages of low first cost and maintenance (real economy) outweigh intangible advantages that may be claimed except for very special conditions.

The precautions that engineers must observe in designing and constructing prestressed concrete structures differ from those required for reinforced concrete structures. Some of these precautions are discussed in this book, but others, such as those related to specific construction practices and the safety of workers, are not. The prudent engineer will keep informed on such precautions and other considerations through the trade and technical literature.

Illustrations of prestressed structures and structural elements are given in Chapters 13 and 14, where the various types of building and bridge construction are described and compared.

1-9 Evolution of U.S. Design Criteria

A document entitled *Criteria for Prestressed Concrete Bridges* (Bureau of Public Roads 1955) presented the first criteria for the design of prestressed concrete published in the United States. This brief treatment of the design, materials, and construction of prestressed concrete, including a discussion of the provisions contained therein, was successfully used in the design of many of the early prestressed concrete bridges and buildings in the United States. A joint committee of members of the American Concrete Institute and the American

Society of Civil Engineers prepared a report containing tentative recommendations for prestressed concrete that was published in 1958 (ACI–ASCE 1958). This report served as the basis for the first provisions for prestressed concrete, contained in *Building Code Requirements for Reinforced Concrete* (ACI 318 1963); and all subsequent editions of this document (ACI 318) have contained provisions for prestressed concrete. Virtually all other U.S. specifications and codes for the design of bridges and buildings are based upon ACI 318 although many have individual differences in some of their provisions.

REFERENCES

Abeles, P. W. 1949. *Principles and Practice of Prestressed Concrete.* London. Crosby Lockwood & Son, Ltd.

ACI–ASCE Joint Committee 323. 1958. Tentative Recommendations for Prestressed Concrete. *Journal of the American Concrete Institute* 29(7):545–78.

ACI Committee 318. 1963. *Building Code Requirements for Reinforced Concrete.* Detroit. American Concrete Institute.

Bureau of Public Roads. 1955. *Criteria for Prestressed Concrete Bridges.* Washington, D.C. U.S. Government Printing Office.

Dobell, C. 1950. Patents and Code Relating to Prestressed Concrete. *Journal of the American Concrete Institute* 46(9):713–24.

Guyon, Y. 1953. *Prestressed Concrete.* New York. John Wiley & Sons, Inc.

2 Steel for Prestressing

2-1 Introduction

As noted in Sec. 1-2, the loss in prestress due to the effects of steel relaxation and the shrinkage and creep of concrete generally is from 10 to 30 percent of the initial prestress. Computation of prestress losses due to various causes is discussed in detail in Sec. 7-2, but it is important here for the designer of prestressed concrete to be aware that the greater portion of the loss of prestress normally is attributed to the shrinkage and creep of the concrete. Therefore, it is necessary to use a high-strength steel, with a relatively high initial stress, in the construction of prestressed concrete.

The shrinkage and creep of concrete produce inelastic volume or length changes. Because the tendons used in construction are anchored to the concrete, either by bond or by end anchorages, length changes in the concrete result in a length change in the tendons. Furthermore, because the steel used for prestressing is fundamentally an elastic material at the stress levels employed in normal designs, the reduction of stress in the tendons that results from length changes in the concrete is equal to the product of the elastic modulus of the steel and the unit length change in the concrete.

It is essential that the loss of prestress be a relatively small portion of the

total prestress, in order to attain an economical and feasible design. The elastic modulus of steel is a physical property that, for all practical purposes, cannot be altered or adjusted by manufacturing processes. In a similar manner, the inelastic volume changes of concrete of any particular quality are physical properties that cannot be eliminated by using practical construction procedures. Therefore, the product of these two factors is normally beyond the control of the designer.

It can be shown that the normal loss of prestress is generally on the order of 15,000 to 50,000 psi. It is apparent that if the loss of prestress is to be a small portion of the initial prestress, the initial stress in the steel must be very high, on the order of 100,000 to 200,000 psi. If a steel having a yield point of 40,000 psi were used to prestress concrete, and if this steel were stressed initially to 30,000 psi, the entire prestress could be lost, as was the case, indeed, in early attempts at prestressing with low-strength steel and poor-quality concrete.

Research has been conducted into the use of other materials, such as fiberglass and aluminum alloys, for prestressing concrete. Some of these materials have elastic moduli that are about one-third that of steel. If such materials could be safely and economically used, the loss of prestress would be reduced to approximately one-third of the loss obtained with steel tendons; hence, the loss of prestress possibly could be ignored in normal design practice if these materials were employed as tendons. However, many problems must be studied and overcome before these materials can be used safely and economically. The use of tendons having a low elastic modulus and plastic deformations different from those of steel would result in members having post-cracking deflection and ultimate strength characteristics different from those obtained when steel tendons are used. These problems will be apparent from this chapter's discussion of the desirable physical properties of the steel used in prestressing.

Several basic forms of high-strength steel currently are used in North American prestressed work. In general, they can be divided into three groups: uncoated stress-relieved wires, uncoated stress-relieved strand, and uncoated high-strength steel bars. Each of these types of steel is described briefly in the following sections. For a more detailed description of the method of manufacture, chemical composition, and physical properties of these materials, the reader should consult the applicable ASTM specifications and the references listed at the end of this chapter.

Other types of wire, such as straightened "as-drawn" wire and oil-tempered wire, are used for prestressing in other parts of the world. Experience in Europe has shown that oil-tempered wire may, under certain circumstances, be more susceptible to stress corrosion (see Sec. 2-11) than the types of steels commonly employed in North America. In addition, "as-drawn" wire generally exhibits greater relaxation than stress-relieved wire and strand of the types employed domestically. Hence, caution should be exercised by the engineer who specifies the use of materials that do not conform to usual ASTM standards; some adjust-

ments in the design may be necessary. These materials are not considered here because they are not normally used in North America.

2-2 Stress-Relieved Wire

Cold-drawn stress-relieved wire, which was commonly used in post-tensioned construction in North America in the past but rarely used in pretensioned members, is manufactured to conform to the "Standard Specification for Uncoated Stress-Relieved Wire for Prestressed Concrete" (ASTM A 421). These specifications provide that the wire be made in two types (BA and WA), depending upon whether it is to be used with button- or wedge-type anchorages (see Chapter 16). Other major requirements in these specifications include the minimum ultimate tensile strength, the minimum yield strength, and the minimum elongation at rupture, as well as diameter tolerances. The principal strength requirements of ASTM A 421 are summarized in Table 2-1. A supplement to these specifications covers low-relaxation wire (see Sec. 2-10).

Typical stress–strain curves for uncoated, stress-relieved wires are shown in Fig. 2-1. It should be noted that the stress–strain curves for the two wire diameters shown are similar in shape, and that the ultimate tensile strength is higher for a wire of smaller diameter. Also, ASTM A 421 requires a minimum elongation of 4.0 percent when measured in a gage length of 10 in., which means that the steel is quite ductile and has a plastic range of considerable magnitude. (The plastic range is not shown in Fig. 2-1.) The minimum yield strength for wire conforming to ASTM A 421, as a percentage of the breaking strength, is 85 percent and 90 percent for stress-relieved wire and low-relaxation wire, respectively.

The use of solid wire has diminished greatly while the use of strand (see Sec. 2-3) has increased substantially. This trend is expected to continue, for economic reasons, in spite of the fact that stress-relieved wire has performed very well in prestressed concrete.

TABLE 2-1 Properties of stress-relieved wire for prestressed concrete contained in ASTM A 421.

	Min. Tensile Strength (psi)		Min. Stress at 1% Extension (psi)*	
Nominal Diameter (in)	Type BA	Type WA	Type BA	Type WA
0.192		250,000		212,500
0.196	240,000	250,000	204,000	212,500
0.250	240,000	240,000	204,000	204,000
0.276	235,000	235,000	199,750	199,750

*Measured according to procedures specified in ASTM A 421.

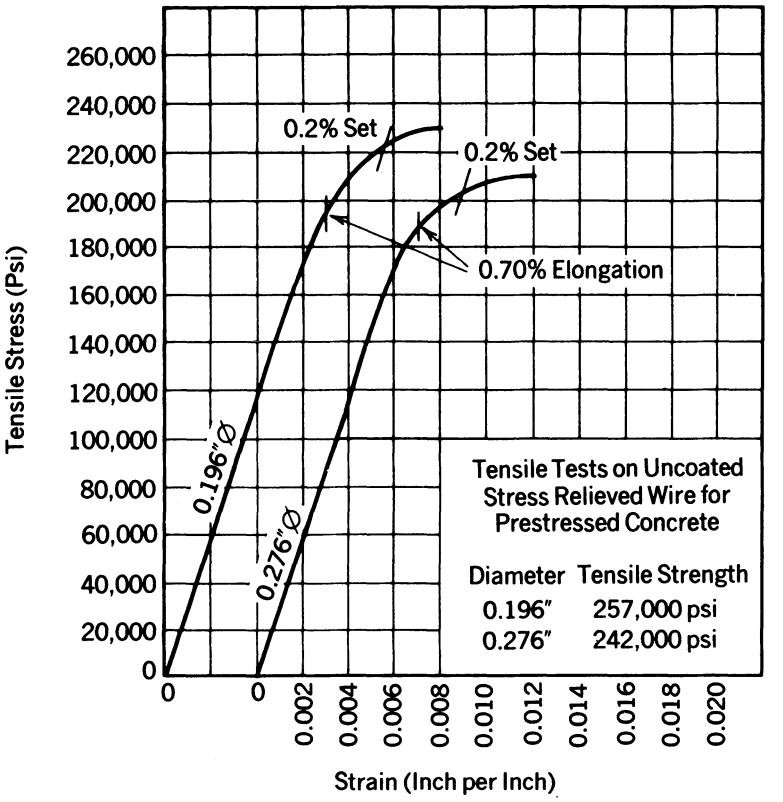

Fig. 2-1. Typical stress–strain curves for wires in elastic range. (Provided by and used with the permission of C.F. & I. Steel Corp.)

2-3 Stress-Relieved Strand

Most stress-relieved strand used in prestressed concrete construction in the United States is made to conform to the requirements of "Standard Specification for Uncoated Seven-Wire Stress-Relieved Steel Strand for Prestressed Concrete" (ASTM A 416). Basic strength, area, and weight requirements for the two grades of seven-wire strands included in ASTM A 416 are given in Table 2-2, and pieces of several types of strand are shown in Fig. 2-2. The strands are made by twisting six wires, on a pitch of between 12- and 16-strand diameters, around a slightly larger, straight central wire. The strands are stress-relieved after being stranded. Typical stress–strain curves for seven-wire strands commonly used in pretensioning and in multistrand post-tensioning tendons are shown in Figs. 2-3 and 2-4. ASTM A 416 provides for seven-wire strands in Grade 250, which has a nominal ultimate tensile strength of 250,000 psi, and in Grade 270, which has slightly larger wires than Grade 250 strand and has a nominal ultimate

TABLE 2-2 Properties of uncoated, seven-wire, stress-relieved strand for prestressed concrete contained in ASTM A 416.

Nominal Diameter of Strand (in.)	Breaking Strength of Strand (min. lb)	Nominal Steel Area of Strand (sq in.)	Nominal Weight of Strands (lb. per 1000 ft.)	Minimum Load at 1% Extension (lb)
		GRADE 250		
$\frac{1}{4}$ (0.250)	9,000	0.036	122	7,650
$\frac{5}{16}$ (0.313)	14,500	0.058	197	12,300
$\frac{3}{8}$ (0.375)	20,000	0.080	272	17,000
$\frac{7}{16}$ (0.438)	27,000	0.108	367	23,000
$\frac{1}{2}$ (0.500)	36,000	0.144	490	30,600
$\frac{3}{5}$ (0.600)	54,000	0.216	737	45,900
		GRADE 270		
$\frac{3}{8}$ (0.375)	23,000	0.085	290	19,550
$\frac{7}{16}$ (0.438)	31,000	0.115	390	26,350
$\frac{1}{2}$ (0.500)	41,300	0.153	520	35,100
$\frac{3}{5}$ (0.600)	58,600	0.217	740	49,800

tensile strength of 270,000 psi. A supplement to ASTM A 416 covers low-relaxation strand, which is discussed in more detail in Sec. 2-10. The minimum yield strength for strand conforming to ASTM A 416, as a percentage of the breaking strength, is 85 percent and 90 percent for stress-relieved strand and low-relaxation strand, respectively, and the minimum elongation at rupture is 3.5 percent for both grades of strand. The stress–strain curves of Fig. 2-3 clearly show different shapes for stress-relieved and low-relaxation strand; the higher yield stress is very apparent in the figure.

When the manuscript for this book was submitted to the publisher for publication, Subcommittee 1.05 of ASTM Committee A01 was balloting on a major revision to ASTM A 416. The revision would make low-relaxation strand the standard material to be supplied under ASTM A 416 but provide for the supply of stress-relieved strand as well, if specifically ordered by the purchaser. The reader should consult the latest version of ASTM 416 for accurate details about its contents.

Stress–strain curves are shown in Fig. 2-3 for a seven-wire strand that has a nominal ultimate tensile strength of 300 ksi, as well as for a galvanized seven-wire strand that has a nominal ultimate breaking strength of 230 ksi. Although specialty materials such as these are not covered by the ASTM specifications, there are instances where they offer benefits in either economy or serviceability, or both, that cannot be obtained with strand that strictly conforms to ASTM 416. (A strand manufacturer *may* guarantee a special strand to meet or exceed most of the *minimum* requirements of ASTM 416 and to have other physical

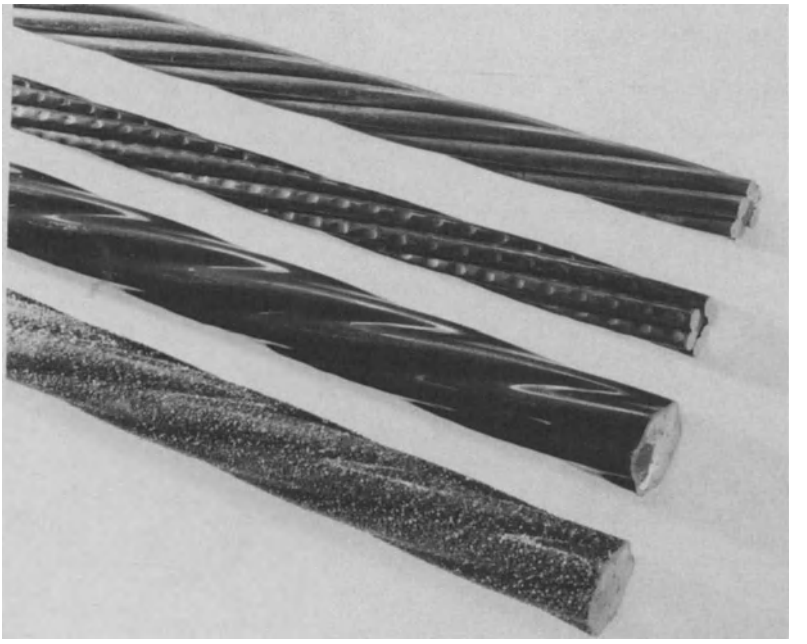

Fig. 2-2. Uncoated, uncoated indented, epoxy-coated, and epoxy-coated with grit seven-wire prestressing strand.

properties that exceed the minimum values in the ASTM specification.) Information on special strands should be obtained directly from the strand manufacturers.

Strand having properties similar to, but not strictly conforming to the requirements of ASTM A 416 is available with a factory-applied coating of epoxy (Dorsten, Hunt, and Preston 1984). The coating can be specified to be smooth or to have a hard grit material embedded in the exposed surface of the epoxy coating. The grit is used to improve bond characteristics in pretensioning applications. Special anchorage devices are available for use with the epoxy-coated strand; these anchorages have teeth that are long enough to extend through the coating and penetrate into the surface of the strand itself. The purpose of the epoxy coating is to protect the strand from corrosion—an important consideration for strands that may be exposed to corrosive environments in service. The epoxy-coated strand is not covered by an ASTM standard, so the engineer considering specifying the use of this type of material should investigate its properties and performance record thoroughly before so doing. The relaxation characteristics, fire resistance, bond stress, creep characteristics at temperatures above 120°F, cost, and safety precautions to be followed in the use of all special

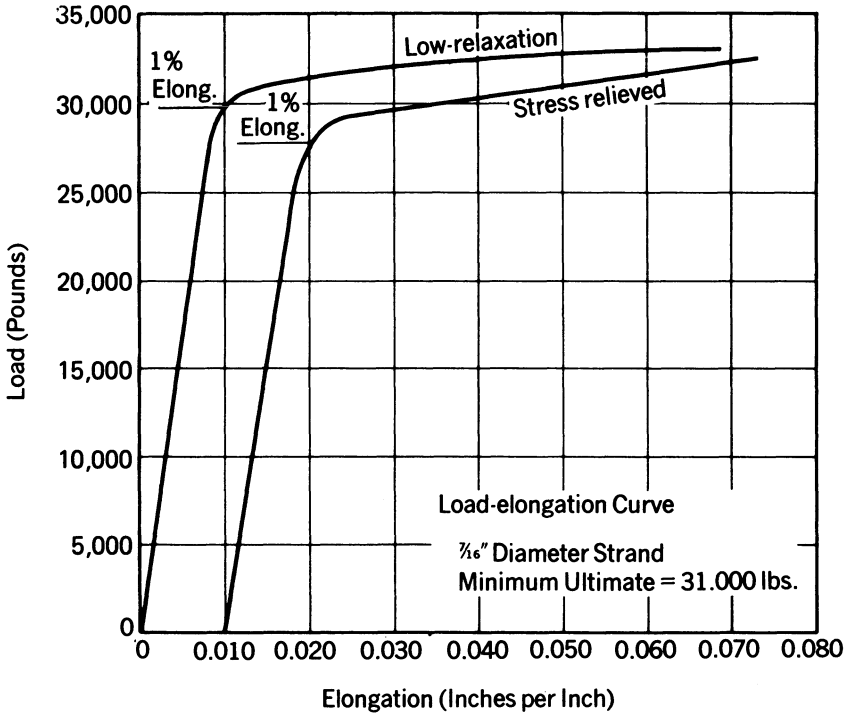

Fig. 2-3. Typical load-elongation curves for $\frac{7}{16}$-in. diameter, low-relaxation and stress-relieved seven-wire strands. (Provided by and used with the permission of C.F. & I. Steel Corp.)

materials should be carefully investigated before any strand is used on a specific project.

Strand having indentations in the outer wires, for the purpose of reducing the longitudinal movement of pretensioned tendons within the concrete, is covered by ASTM A 886. The properties of the indented strand are identical to those for strands conforming to ASTM 416 shown in Table 2-2 except that a 5/16-in. nominal size strand, with a breaking strength of 16,500 lb, is also available in Grade 270.

Another type of uncoated, stress-relieved strand for prestressing concrete is covered by ASTM A 779. This material is "compacted," having been drawn through a die after being stranded; hence, strands of this type have a cross-sectional shape as shown in Fig. 2-5. The material is stress-relieved or processed for low-relaxation properties after being stranded and compacted. The minimum total elongation of compacted strand under maximum load is 3.5 percent in a gage length of 24 in. or more. This type of strand has a greater cross-sectional area, for any nominal diameter, compared to strand that has not been compacted.

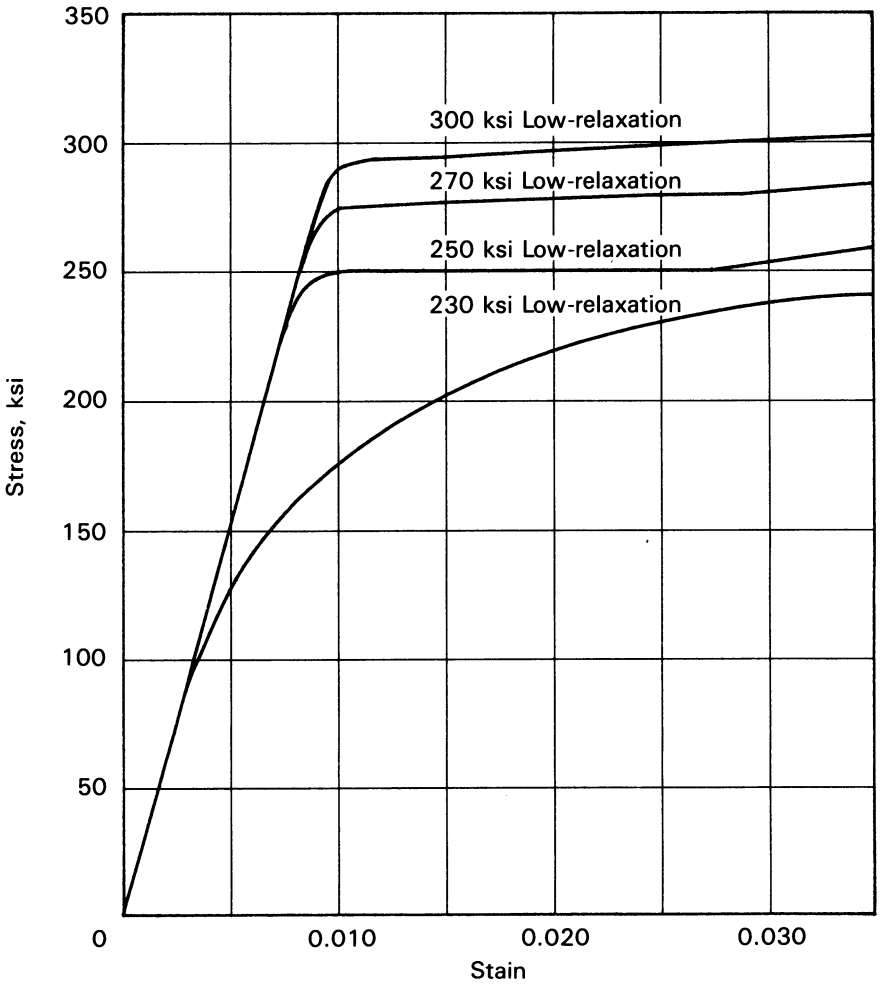

Fig. 2-4. Partial stress–strain curves for uncoated low-relaxation prestressing strand of different grades compared to galvanized strand.

The result is a larger ultimate tensile strength for the compacted strand of a particular diameter. Basic strength, area, and weight properties for compacted strand are given in Table 2-3.

2-4 High-Tensile-Strength Bars

Both plain (Type I) and deformed (Type II) high-tensile-strength, alloy steel bars are available in nominal diameters from 0.75 to 1.375 in. Bars of other

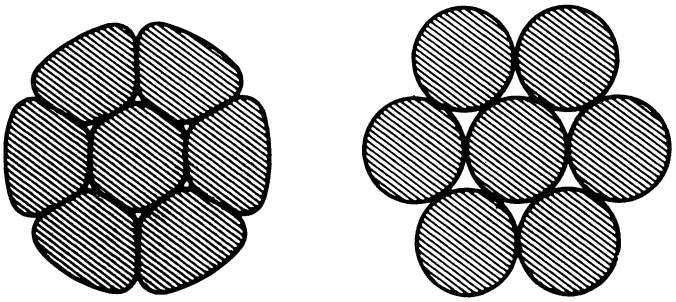

Fig. 2-5. Comparison of cross sections of compacted and noncompacted seven-wire strand.

sizes are available by special arrangement with some bar manufacturers. The bars are made from an alloy steel and conform to the "Standard Specification for Uncoated High-Strength Steel Bar for Prestressing Concrete," ASTM A 722.

The bars are generally cold-stretched in order to raise the yield point and to render them more elastic at stress levels below the yield point. After cold-stretching, they frequently are stress-relieved in order to improve the ductility and stress–strain characteristics. Principal minimum requirements in ASTM A 722 include a minimum tensile strength of 150,000 psi, minimum yield strengths for plain and deformed bars of 85 percent and 80 percent of the minimum ultimate tensile strength, respectively, and a minimum elongation after rupture of 4.0 percent in a gage length equal to 20 bar diameters, or of 7 percent in a gage length equal to 10 bar diameters. Bars sometimes are produced with properties exceeding the minimum requirements of ASTM A 722.

A typical stress–strain curve for a high-tensile-strength bar is given in Fig. 2-6. Deformed bars (Type II) are shown in Fig. 2-7.

TABLE 2-3 Properties of uncoated, seven-wire, stress-relieved, compacted, steel strand for prestressed concrete contained in ASTM A 779.

Nominal Diameter (in.)	Breaking Strength of Strand (min. lb)	Nominal Steel Area ($in.^2$)	Nominal Weight of Strand (per 1000 ft lb)
$\frac{1}{2}$	47,000	0.174	600
0.6	67,440	0.256	873
0.7	85,430	0.346	1176

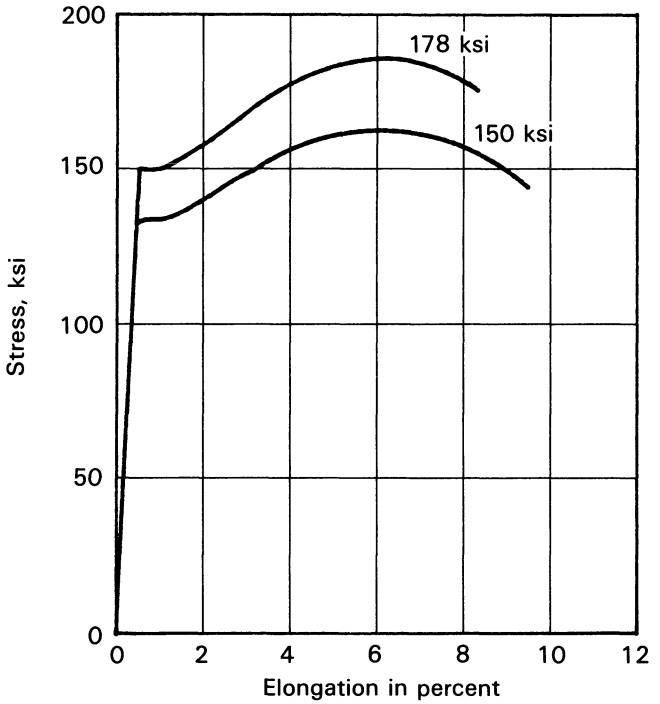

Fig. 2-6. Typical load-strain curves for Grade 150 and 178 prestressing bars. (*Based upon data obtained from and used with permission of Dywidag Systems International USA, Inc.*)

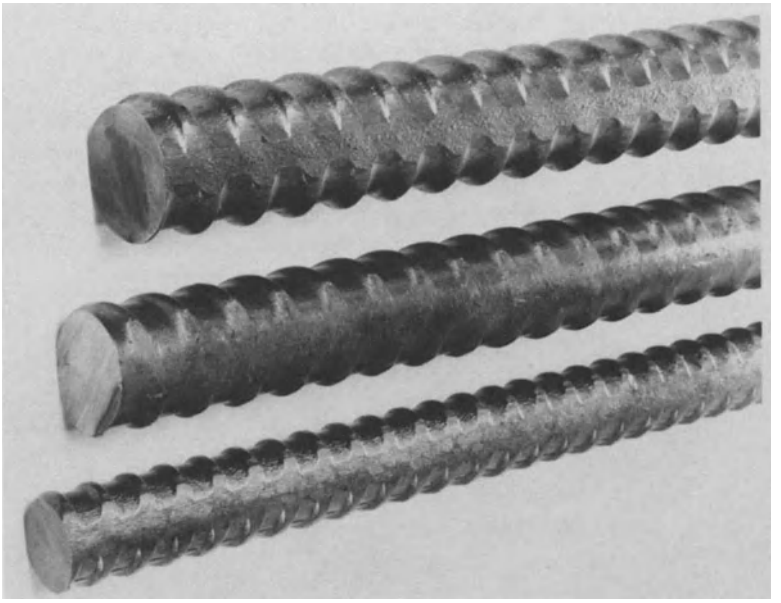

Fig. 2-7. ASTM A 722, Type II (deformed) prestressing bars.

2-5 Yield Strength

An examination of the stress–strain curves for the various types of prestressing steels shows that these steels do not have definite yield points. Therefore, an arbitrary stress must be specified in order to define the stress that is taken to be the yield strength. Because there is no definite yield strength, the term does not have the meaning that it would have for a steel with a yield point. Yield strengths taken as the stress at a 0.20 percent offset often are used for materials that lack a definite yield strength. (In this case the yield stress is the stress at the intersection of the stress–strain curve with a line parallel to the linear portion of the curve that originates on the abscissa at a strain of 0.20 percent.) Minimum yield strengths at 1 percent extension (an elongation of 1 percent of the gage length) are specified in the standard ASTM specifications for wire and strand. Minimum yield strengths at 0.7 percent extension and at 0.2 percent offset are specified for high-strength bars. Some research work has been done using the stress at a 0.10 percent offset as the yield strength. Hence, the term yield strength as related to prestressing materials is not precise, and the reader is cautioned to use the term with care, being certain of its definition in any discussion or recommendations where it is used.

Some engineers consider the minimum yield strength specified in ASTM A 416 or ASTM A 421—85 percent and 90 percent of the strength of the material for stress-relieved and low-relaxation strand and wire, respectively—as equal to the actual yield strength at 0.10 percent offset (see eq. 2-1, in Sec. 2-10) as well as equal to the 1 percent extension. This practice is generally regarded as conservative, as it will result in overestimating the loss due to relaxation. An examination of several stress–strain curves revealed that the 0.10 percent offset strength varied only +1.3 percent from the actual stress at 1 percent extension for one manufacturer; for another, the strength at 0.10 percent offset was consistently 2 to 3 percent lower than the stress at 1 percent extension.

The methods to be used in determining the yield strength of prestressing steels are given in "Test Methods and Definitions for Mechanical Testing of Steel Products" (ASTM A 370). Yield strength requirements for the various types of steels used in prestressed concrete are specified in the ASTM specifications applicable to each type of steel.

2-6 Modulus of Elasticity

The elastic modulus of reinforcing steel that is not prestressed is generally taken to be equal to 29,000,000 psi, as provided in Sec. 8.5.2 of ACI 318. The elastic modulus of reinforcing steel that is to be prestressed generally is based upon load–deformation data provided by the manufacturer of the specific material used. The reason for this is that prestressing bars and strands frequently are made to sizes that are different from their nominal diameter. By this means the

bars or strands are intended to have breaking strengths that equal or slightly exceed the minimum breaking strengths required by the applicable ASTM specifications, but the ultimate unit tensile stresses actually may be less than the nominal ultimate unit tensile strength. For this reason, the stress–strain characteristics of prestressing materials used in stressing calculations (see Chapter 16) and in flexural strength calculations (see Chapter 5) should be based on test data provided by the manufacturer of the actual material to be used and not on theoretical values computed by using nominal areas and unit stresses for minimum yield strength requirements.

2-7 Ultimate Tensile Strength

Because prestressing bars and strands normally are marketed on the basis of *nominal* areas or diameters that are frequently *smaller* than their actual cross-sectional areas or diamters, the actual ultimate tensile strength of the materials may be different from their guaranteed ultimate tensile strengths (GUTS). The designer of prestressed concrete should be aware of this possibility.

2-8 Plasticity

Plasticity at very high stress levels is as essential in prestressing steel as it is in ordinary reinforcing steel. It is needed to ensure that ultimate bending moments will be reached only after large and very apparent plastic deformations have taken place. The use of brittle steel could result in a sudden failure similar to that which is characteristic of an overreinforced concrete flexural member. To avoid this possibility, the normal practice is to specify that the prestressing steel will have a minimum elongation at rupture of 3.5 to 4.0 percent, depending upon the type of steel used and the method used to measure the elongation at rupture (see ASTM A 416, ASTM A 421, ASTM A 722, ASMT A 779, and ASTM A 886). The stress–strain curves of Figs. 2-3, 2-4, and 2-6 clearly show the significant plastic deformations that prestressing materials can withstand when loaded to high stress levels.

2-9 Stress–Strain Characteristics

The stress–strain characteristics of a prestressing steel, which can be shown as a plot of either unit stress (units of force per unit area) or load (units of force) versus strain, can be represented by a curve as shown in Fig. 2-8, where stress has been used for the ordinate, and the abscissa represents unit strain. (This type of plot often is used for prestressing wire, whereas load vs. unit strain is more commonly used for strand.) Six points on the curve have been numbered for the purpose of illustrating the principal load–deformation characteristics of

prestressing materials. The first portion of the curve is a straight line extending from the origin of the plot to point 1. The slope of this portion of the curve (i.e., an increment of stress divided by the corresponding increment of strain) normally is referred to as the elastic modulus of the material. The ordinates of point 1 can be taken to be the stress and strain at the proportional limit. The strain at point 2 defines the stress taken to be the yield stress. The material standards for the various prestressing steels specify the strain at point 2 as well as the minimum value of stress it must have in order to conform to the standard (e.g., a minimum stress of 212,500 psi at an extension of 1 percent in ASTM A 421 for a stress-relieved prestressing wire having a diameter of 0.192 in.). Points 3 and 4 have ordinates that define a portion of the curve that can be taken as a straight line, as a means of facilitating equilibrium and strain compatibility computations for strength design of prestressed members (see Sec. 5-2), without introducing significant error. Point 5 is defined by the greatest stress (load) that the material is able to withstand, and point 6 defines the stress and strain at failure of the material.

2-10 Relaxation and Creep

Relaxation is defined as the loss of stress in a material that is placed under stress and held at a constant strain; creep is defined as the change in strain for a member held at constant stress. Although tendons in prestressed concrete are not subjected to constant strain or to constant stress, it generally is agreed that

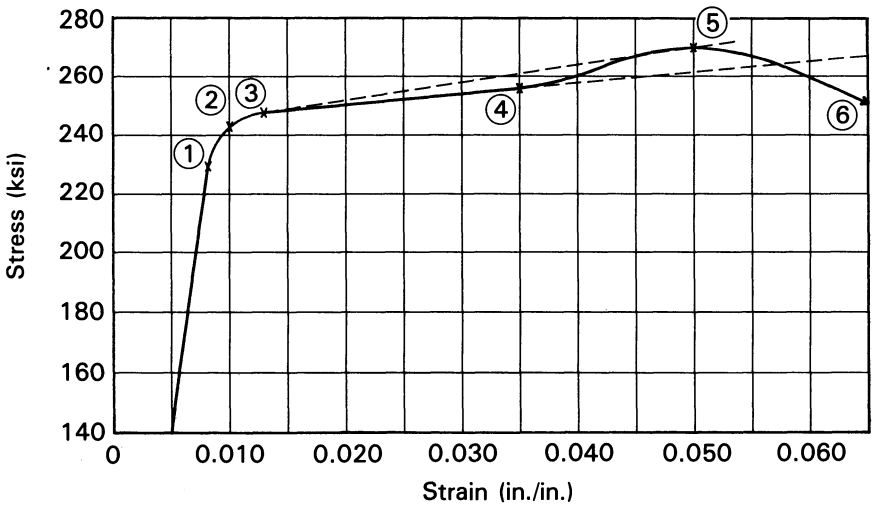

Fig. 2-8. Curve used to identify typical characteristics of stress–strain curves for reinforcement used for prestressing concrete.

the condition more closely approximates a condition of constant strain; hence, relaxation studies are used to evaluate the loss of prestress that can be attributed to the time-dependent inelastic behavior of the steel. A typical relaxation curve, showing relaxation as a function of time for a wire specimen initially loaded to 70 percent of its ultimate tensile strength and held at constant strain and a constant temperature of 85°F, is shown in Fig. 2-9. A comparison of the relaxations of cold-drawn (not post-treated), stress-relieved, and low-relaxation strand after 1000 hours at constant strain and constant temperature of 68°F at various levels of initial stress (expressed as a ratio to the guaranteed ultimate tensile strength) is given in Fig. 2-10.

For stress-relieved wire or strand, the loss of stress due to relaxation at normal temperatures can be estimated with sufficient accuracy for design purposes using the following relationship:

$$\Delta f_{sr} = f_j \frac{\log t}{10} \left(\frac{f_j}{f_y} - 0.55 \right) \tag{2-1}$$

where Δf_{st} is the relaxation loss at time t hours after prestressing, f_j is the jacking stress, and f_y' is the 0.10 percent offset stress for the steel under consideration (Magura, Sozen, and Siess 1962). The logarithm of time t is to the base 10. This relationship is applicable only when the ratio of f_j/f_y' is equal to or greater than 0.55. It should be noted that f_y' is used here rather than f_{py}, which is the

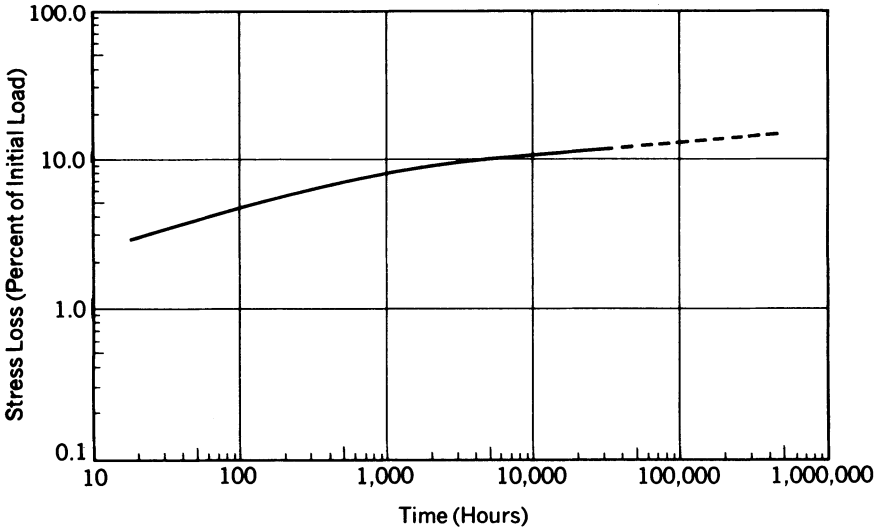

Fig. 2-9. Stress loss versus time for a stress-relieved wire initially loaded at 70 percent of the guaranteed ultimate tensile strength and held at constant length at 85°F (Provided by and used with the permission of C.F. & I. Steel Corp.)

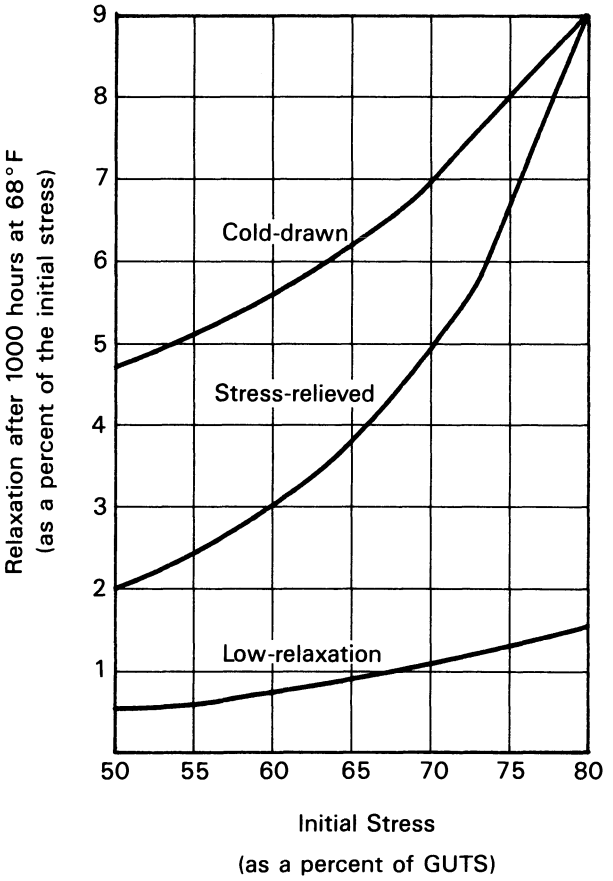

Fig. 2-10. Comparison of the relaxation of cold-drawn, stress-relieved, and low-relaxation strand initially loaded to 70 percent of the guaranteed ultimate tensile strength after being under constant strain at 68°F for 1000 hours. (*Based upon data obtained from and used with permission of Florida Wire and Cable Company.*)

notation used for the specified yield strength of prestressing steel in ACI 318-89, because of the difference in definitions of the two yield strengths.

ILLUSTRATIVE PROBLEM 2-1 Using eq. 2-1 with a 0.10 precent offset stress of 256,000 psi and a jacking stress in the steel of 189,000 psi, the approximate values for the 270 k grade strand illustrated in Fig. 2-3, compute the relaxation loss after 100,000 hours (11.4 years) and 400,000 hours (45.6 years). Note that the ratio of the jacking stress to the 0.10 precent offset stress is $0.738 > 0.55$.

SOLUTION: For t = 100,000 hours:

$$\Delta f_{cr} = 189 \times \frac{5.00}{10}(0.74 - 0.55) = 18 \text{ ksi}$$

For t = 400,000 hours:

$$\Delta f_{cr} = 189 \times \frac{5.60}{10}(0.74 - 0.55) = 20.0 \text{ ksi}$$

Using eq. 2-1, the efficiency of the steel at various levels of jacking stress after 50 years of service can be studied with the aid of Fig. 2-11. From this plot it will be seen that the increase in effective stress f_{se} is nearly equal to the increase in jacking stress f_j up to the point where f_j equals $0.60f'_y$. Above this stress, the efficiency is progressively reduced. For a jacking stress ratio of 0.90, virtually no gain in effective stress is realized for increases in jacking stress.

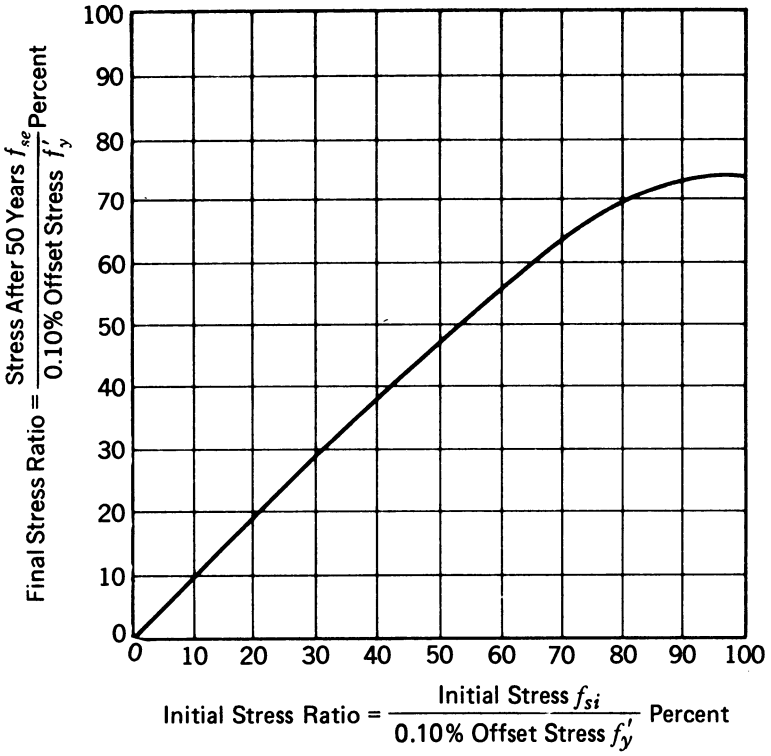

Fig. 2-11. Effect of jacking stress on the final stress of prestressing steel subjected to constant strain (relaxation).

In the fabrication of pretensioned concrete members, the tendons are stressed to a jacking stress, held at constant elongation for a period of time, and then released. At the time when the prestressing force is transferred to the concrete (tendons released), the stress in the tendons, f'_{sj}, is less than the original jacking stress, f_{sj}. This is due to the relaxation than has taken place in the interval between stressing and transfer. In addition, elastic shortening of the concrete takes place upon transfer of the prestressing force to the concrete, and this reduces the stress in the prestressed reinforcement to the initial stress, f_{si}, as illustrated in Fig. 2-12a. The effect of relaxation of the steel can be estimated

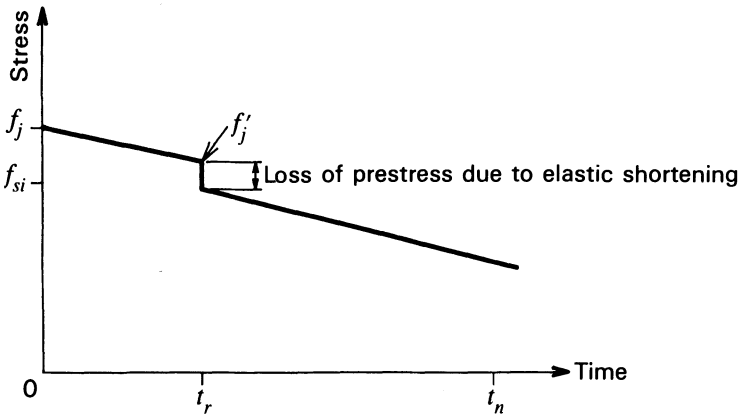

(a) Pretensioned Reinforcement

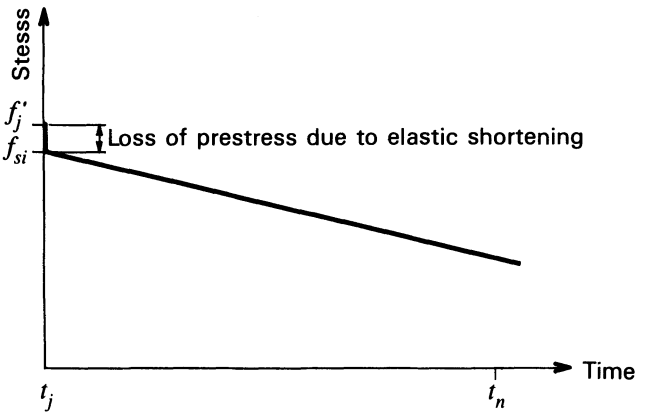

(b) Post-tensioned Reinforcement

Fig. 2-12. Relationships between stress and time in reinforcement that is (a) pretensioned and (b) post-tensioned.

at time t_n, assuming the tendon was stressed at time zero and released at time t_r, by using the following relationship:

$$\frac{f_{stn}}{f_j'} = 1 - \left(\frac{f_j'}{f_y} - 0.55\right)\frac{\log t_n - \log t_r}{10} \tag{2-2}$$

in which f_j' is the stress in the prestressed reinforcement at the time of release of the tendons, and f_{stn} is the stress in the prestressed reinforcement at time t_n (Magura, Sozen, and Siess 1962). In eq. 2-2, the stresses are in ksi and time is in hours. In using eq. 2-2, with pretensioned reinforcement, one must first compute the relaxation loss from the time of initial jacking until the time of release, using eq. 2-1. This relaxation loss should be subtracted from the original jacking stress in the reinforcement to determine the value of f_j' for use in eq. 2-2. The computation of the loss due to elastic shortening is explained in Sec. 7-2 of this book.

As explained in Sec. 7-2 and illustrated in Fig. 2-12b, post-tensioned reinforcement is not subjected to the same sequence of jacking stresses as pretensioned reinforcement, and eq. 2-2 is not used with post-tensioned reinforcement.

ILLUSTRATIVE PROBLEM 2-2 During the production of pretensioned members for a large project, the normal production cycle provided for an 18-hour period between the times when the tendons were stressed and were released. Occasionally, because of weekends, holidays, or other events beyond the control of the contractor, the time interval between stressing and releasing the tendons was as great as 90 hours. Determine the stress in the stress-relieved prestressing steel at transfer for time intervals between stressing and release of 18, 42, 66, and 90 hours for grade 270 k strand having a 0.10 percent offset stress of 240 ksi if the initial stress of the strands is always 202.5 ksi.

SOLUTION: From eq. 2-1:

$$\Delta f_{sr} = 202.5\frac{\log t}{10}\left(\frac{202.5}{240} - 0.55\right) = 5.948 \log t$$

The computations are summarized in Table 2-4.

Ghali and Trevino have used the term intrinsic relaxation, L_r, rather than relaxation to define the loss of stress in a prestressing tendon held at constant strain for a specific period of time (Ghali and Trevino 1985). The intrinsic relaxation is assumed to reach its maximum value, $L_{r\infty}$, after being under constant strain for 500,000 hours. In addition, the term reduced relaxation, L_{rr}, has been used for the loss of stress in a prestressing tendon. The reduced relax-

TABLE 2-4 Summary of calculations for I.P. 2-2.

t (hr)	ΔF_{sr} (ksi)	f_j at transfer (ksi)
18	7.5	195.0
42	9.7	192.8
66	10.8	191.7
90	11.6	190.9

ation includes the effects of concrete creep and shrinkage as well as the fact that the steel is not subjected to constant strain, as it must be for intrinsic relaxation. The relationship between the intrinsic and reduced relaxations is expressed as:

$$L_{rr} = \chi_r L_{r\infty} \tag{2-3}$$

where χ_r is a dimensionless coefficient having a value less than unity.

The ultimate value of intrinsic relaxation has been found to be function of the ratio, λ, of the stress in the reinforcement immediately after elastic shortening (initial stress) to the strength of the steel (CEB-FIP 1978). The ratio can be expressed as:

$$\lambda = \frac{f_{si}}{f_{pu}} \tag{2-4}$$

where f_{si} is the stress in the prestressed reinforcement immediately after stressing of the concrete (i.e., the stress in post-tensioned reinforcement immediately after anchoring [see Sec. 16-6] or the stress in pretensioned reinforcement immediately after elastic shortening of the concrete [see Sec. 7-2]), and f_{pu} is the tensile strength of the prestressed reinforcement, either the actual or the minimum specified.

Values of the ratio of intrinsic relaxation to initial steel stress for various values of the ratio λ are given in Table 2-5 and plotted in Fig. 2-13. These

TABLE 2-5 Values of the ratio of intrinsic relaxation to initial steel stress for different steel types and different ratios of initial steel stress to steel tensile strength (after CEB-FIP 1978).

Type of prestressing steel	Ratio of initial steel stress to steel tensile strength		
	0.60	0.70	0.80
Stress-relieved group 1	0.06	0.12	0.25
Low-relaxation group 2	0.03	0.06	0.10

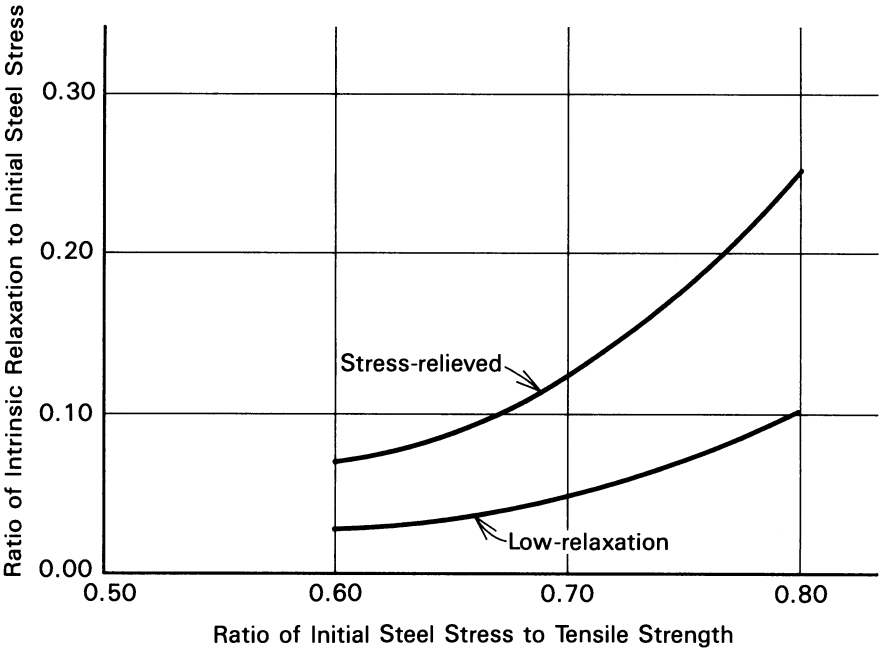

Fig. 2-13. Plot of the relationships between the ratio of intrinsic relaxation to initial steel stress and the ratio of initial steel stress to steel tensile strength, for stress-relieved and low-relaxation prestressing reinforcement (after CEB).

values are recommended by CEB for use when actual relationships between intrinsic relaxation and initial steel stress are not known for the specific steel to be used on a project. Ghali and Trevino have proposed equations for approximating the CEB recommendations for the relationship between the intrinsic relaxation/initial steel stress and λ. The relationship, which is intended for use with values of λ greater than 0.4, is:

$$\frac{L_r}{f_{si}} = -\eta_\infty (\lambda - 0.40)^2 \tag{2-5}$$

in which η_∞ is equal to 1.5 and 0.67 for stress-relieved and low-relaxation steels, respectively. The ultimate value of intrinsic relaxation, $L_{r\infty}$, which is very small and can be neglected for values of the ratio λ less than 0.40, is projected to reach its limiting value in 57 years (500,000 hours).

The value of the intrinsic relaxation at time t, for a tendon stressed at time t_i, can be computed for time increments, $(t - t_i)$, up to 1000 hours after stressing, from:

$$L_{r(t)} = L_{r\infty} \left\{0.0625 \ln \left[1 + 0.10(t - t_i)\right]\right\} \tag{2-6}$$

For time increments greater than 1000 but less than 500,000 hours, the relaxation can be computed from:

$$L_{r(t)} = L_{r\infty}\left\{2 \times 10^{-6}(t - t_i)\right\}^{0.2} \tag{2-7}$$

The value of $L_{r(t)}$ should be taken to be equal to the limiting value for intrinsic relaxation, $L_{r\infty}$, when $(t - t_i)$ exceeds 500,000 hours.

As explained above, because of the effects of concrete creep and shrinkage (see Sec. 3-10 through 3-13), prestressing tendons are not held at constant length after they have been stressed. The creep and shrinkage cause the lengths of the prestressed concrete member, and the tendons provided to prestress them, to shorten. The shortening results in a reduction in the stress in the tendons. Consequently, the relaxation in the tendon also is reduced from what it would have been without the shortening (i.e., the reduced relaxation is less than the intrinsic relaxation). Ghali and Trevino have proposed the use of a relaxation coefficient, χ_r, to account for this phenomenon. The relaxation coefficient can be computed from

$$\chi_r = e^{(-6.7 + 5.3\lambda)\Omega} \tag{2-8}$$

in which:

$$\Omega = \frac{|L_{ps(t)}| - |L_{r(t)}|}{f_{si}} \tag{2-9}$$

where $|L_{ps(t)}|$ is the absolute value of the change in stress in the prestressing steel due to the combined effects of concrete creep and shrinkage together with relaxation of the prestressing steel (total loss of stress in the steel) at time t, and $|L_{r(t)}|$ is the absolute value of the intrinsic relaxation at time t. This calculation must be done by trial and error because it involves computation of the total loss of prestress in the steel as well as the intrinsic relaxation, where the total loss of prestress includes the reduced relaxation loss of the prestressing steel. Rather than using eq. 2-8, the value of χ_r can be obtained from tabulated data or a plot, such as Table 2-6 and Fig. 2-13, both of which are from Ghali and Trevino.

Elevated temperatures have an adverse effect on the relaxation of prestressing steel. For applications where the prestressing tendons will be subjected to temperatures in excess of 100°F for extended periods of time, larger allowances should be made for the relaxation of the steel (de Strycker 1959; Papsdorf and Schwier 1958).

Relaxation curves for low-relaxation strand stressed initially to 70 percent of the guaranteed ultimate tensile strength and held at various temperatures are shown in Fig. 2-14. The curves clearly demonstrate the adverse effect of elevated temperatures on the long-term relaxation of prestressing steel. In Fig. 2-15, values of the relaxation for stress-relieved strand and for low-relaxation strand,

TABLE 2-6 Values of the relaxation reduction coeficient χ, for various values of Ω and λ (after Ghali and Trevino 1985).

	Values of λ					
Ω	0.55	0.60	0.65	0.70	0.75	0.80
0.0	1.000	1.000	1.000	1.000	1.000	1.000
0.1	0.6492	0.6978	0.7282	0.7490	0.7642	0.7757
0.2	0.4168	0.4820	0.5259	0.5573	0.5806	0.5987
0.3	0.2824	0.3393	0.3832	0.4166	0.4425	0.4630
0.4	0.2118	0.2546	0.2897	0.3188	0.3429	0.3627
0.5	0.1694	0.2037	0.2318	0.2551	0.2748	0.2917

stressed initially to 70 percent of the guaranteed ultimate tensile strength and stored at different temperatures, are compared after 1000 hours; the effects of temperature and level of initial stress are clearly evident. From these examples, it is apparent that the relaxation of prestressing strand is temperature-sensitive as well as sensitive to the level of stress to which it is initially stressed. The designer of prestressed concrete must be cautious when designing prestressed concrete structures that will be exposed to elevated temperatures during their service life.

From the above, one can conclude that the relaxation of the low-relaxation

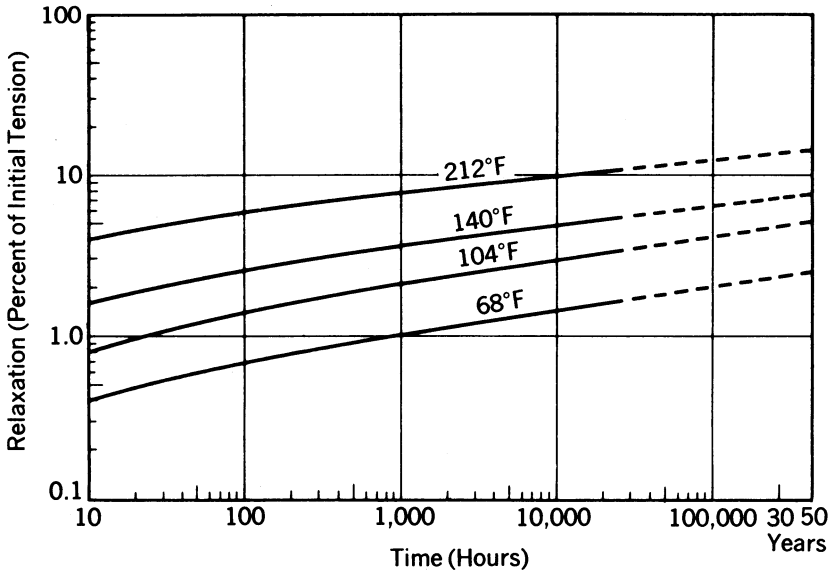

Fig. 2-14. Relaxation versus time for low-relaxation strand stressed initially to 70 percent of the guaranteed ultimate tensile strength and held at various temperatures. (*Provided by and used with the permission of C.F. & I. Steel Corp.*)

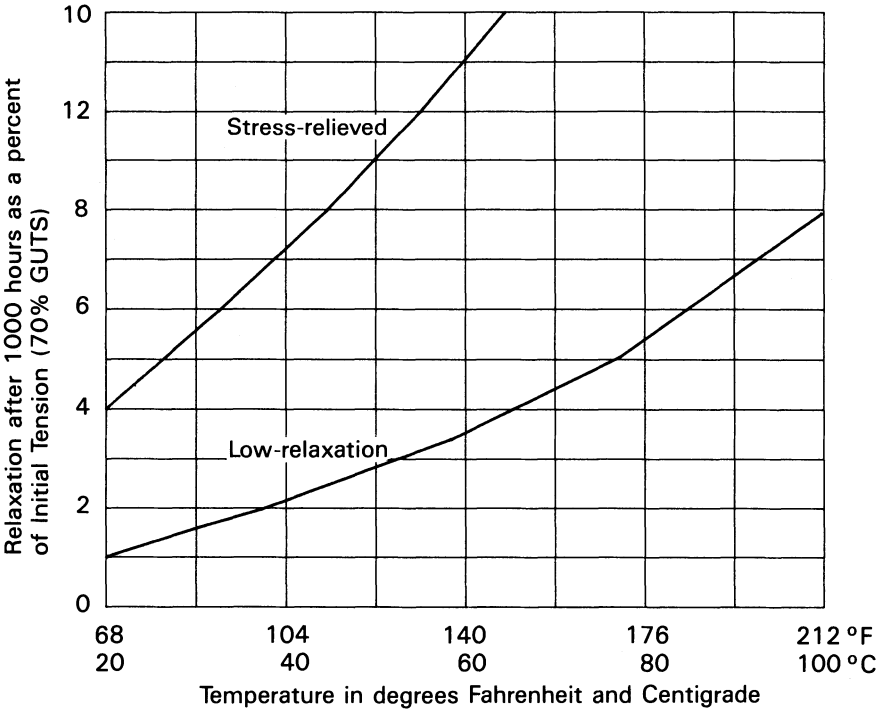

Fig. 2-15. Effect of temperature on the relaxation of stress-relieved and low-relaxation seven-wire strand, stressed initially to 70 percent of the guaranteed ultimate tensile strength, after 1000 hours at constant strain. (*Based upon data obtained from and used with permission of Florida Wire and Cable Company.*)

strand could be taken as approximately 20 percent of that for stress-relieved strand for applications at normal temperatures. For applications in which the tendons may be exposed to temperatures above 100°F, only low-relaxation-type strand should be used.

In order to determine if prestressing wire or strand is low-relaxation or stress-relieved, one can perform a short-term constant-strain test on a sample of the material. The strain should approximate the strain in the material under the initial prestressing stress. For a test period of 30 minutes at constant or nearly constant temperature, the relaxation of low-relaxation material should be less than 0.50 percent, whereas that of stress-relieved material should be less than 2 percent. There is no ASTM standard for this test known to the author.

2-11 Corrosion

The strength of a prestressed-concrete flexural member is dependent upon the condition of its tendons throughout their service life; so they must not experi-

ence serious deterioration due to corrosion. Prestressing steels are subject to normal oxidation in approximately the same degree as structural-grade steels. Because wire and strand tendons are normally of small diameter, it is essential that they be protected against significant oxidation. Bar tendons should be protected too, but, because of their relatively large diameter, normal oxidation is of somewhat less concern with them than with wire and strand tendons.

Protection against corrosion is effected in pretensioned construction by the concrete that surrounds the tendons. In bonded post-tensioned construction, the tendons are protected by grout injected into the ducts containing the tendons after the tendons have been stressed. Unbonded tendons normally are coated with grease, wax, or bituminous materials and covered with plastic tubing or waterproof paper in a factory before being shipped to the construction site; chemicals that inhibit oxidation of ferrous metals sometimes are included in the coating applied to tendons used in unbonded construction. Hydrated portland cement concrete provides an alkaline environment (pH on the order of 11–13) that is very effective in preventing corrosion of steel tendons. Cracks or porosity in the concrete however, can, cause this protection to be lost (FIP Comission on Prestressing 1986). It must be emphasized that research has shown a light, hard oxide on the tendons to be desirable in pretensioned members because its existence improves the transfer and flexural bond characteristics of the tendons (see Sec. 6-6). Light, hard oxides also should be desirable in bonded, post-tensioned tendons, because of the improved flexural bond.

To protect prestressing steel against corrosion between the time when it leaves the factory and the time when it is processed at a construction site for placement in the work, it has become standard practice in some areas to require the steel to be wrapped in waterproof paper, with a vapor-phase corrosion inhibitor included within the packaging.*

A vapor-phase corrosion inhibitor is a white, fine-grained powder consisting of an organic compound containing nitrogen. The material vaporizes (sublimes), and, if the vapors are confined, it will recrystallize on the surface of the steel and prevent oxidation. The action of vapor-phase inhibitors can be nullified by the following:

1. Temperatures greater than 160°F.
2. Free-running water over the surface of the steel.
3. An acidic environment (pH less than 6.5).
4. Free circulation of fresh air.
5. Coatings or films on the steel that prevent the vapor from contacting the steel.

*A convenient way to specify the protective packaging of prestressing materials is to use the provisions of "Standard Recommended Practices for Packaging, Marking, and Loading Methods for Steel Products for Domestic Shipment" (ASTM A 700).

6. The powder's not being in the immediate vicinity of the steel (farther than 12 in. away).
7. An environment containing a high concentration of chlorides.

The material will work in either air or water, provided that the above conditions do not exist to nullify its action.

Post-tensioned construction occasionally is protected against the effects of corrosion by the use of galvanized tendons. This procedure is not used frequently because galvanized tendons are less strong than bright tendons of the same size, as some of the diameter of galvanized tendons is composed of low-strength zinc rather than high-strength steel. Moreover, galvanized tendons are more expensive than bright tendons of equal strength. (For equal-diameter tendons, galvanized, seven-wire strands are approximately 15 percent lower in strength and 10 percent higher in cost.) Furthermore, the various types of anchorage devices that have been used in post-tensioning with the older parallel-wire systems (rarely used any longer in North America) either cannot anchor galvanized wire, because of its low coefficient of friction, or cannot be used without damaging its zinc coating. For these reasons, the use of galvanized wire generally is considered to be impractical with parallel-wire systems. The use of galvanized, large-diameter strand is feasible under some conditions, however. Galvanized, seven-wire strand can be used in some of the more modern anchorage devices, but rarely is, because of the cost.

Galvanized wire and strand are not used in pretensioned concrete because the concrete provides adequate protection of the steel against corrosion.

A type of corrosion referred to as pitting corrosion is the cause of some deterioration (and even failures) of prestressed concrete structures. Calcium chloride or sodium chloride in the concrete or grout generally is thought to be the cause of this type of corrosion. For this reason, chlorides must never be permitted, except in very small (trace) amounts, in the concrete or grout used in prestressed-concrete construction (Szilard 1969).

Prestressing steels, particularly wires and strands, are susceptible to a type of deterioration termed stress corrosion, which has occurred relatively infrequently. Stress corrosion is characterized by a breakdown of the cementitious portion of the steel resulting in fine cracks, which can render the steel nearly as brittle as glass. Because little is known about this type of corrosion, there is no way to be certain that it will not occur during construction of a prestressed member. It is true that nitrates (not to be confused with the rust-inhibiting nitrites), chlorides, sulfides, and some other agents can result in stress corrosion under certain conditions. It is also known that steel is more susceptible to this type of corrosion when highly stressed—hence the name "stress corrosion."

Another cause of delayed failure, which can occur in high-strength steels, is called hydrogen embrittlement. This phenomenon, which apparently results when steel is exposed to hydrogen ions (atomic hydrogen) but does not occur

when it is exposed to molecular hydrogen, is characterized by a decrease in ductility and tensile strength. Hydrogen embrittlement may be promoted by electroplating steel with cadmium or zinc, as well as by corrosion and electrical currents. Confining the prestressing steel in an environment with a pH greater than 8 is thought to be the best protection against the absorption of hydrogen.

It is interesting to note that aluminum powder, which causes the release of hydrogen gas (molecular hydrogen), has been used for many years as an expansion additive for the grouting of post-tensioned tendons. This practice apparently has not been harmful because failures have not been reported in structures so constructed. Additives that cause expansion by the release of nitrogen gas also are used.

2-12 Effect of Elevated Temperatures

In estimating the effect of elevated temperatures on prestressed concrete elements, such as temperatures due to uncontrolled fires in buildings, it is necessary to know the effect of such temperatures on the types of steel used in prestressing concrete. The report of ACI Committee 216 (ACI 216 1981) contains a plot showing the ultimate strengths of two types of prestressing steel, as compared to a steel commonly used in structural steel construction, as a function of different temperatures. This plot is reproduced here as Fig. 2-16. In

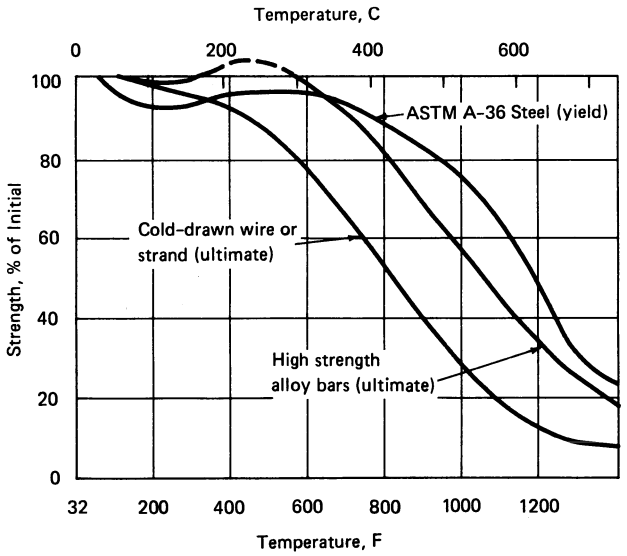

Fig. 2-16. Strength of prestressing wire and strand, high-strength alloy bars and structural steel conforming to ASTM A 36 at high temperatures. (*Reproduced with the permission of the American Concrete Institute.*)

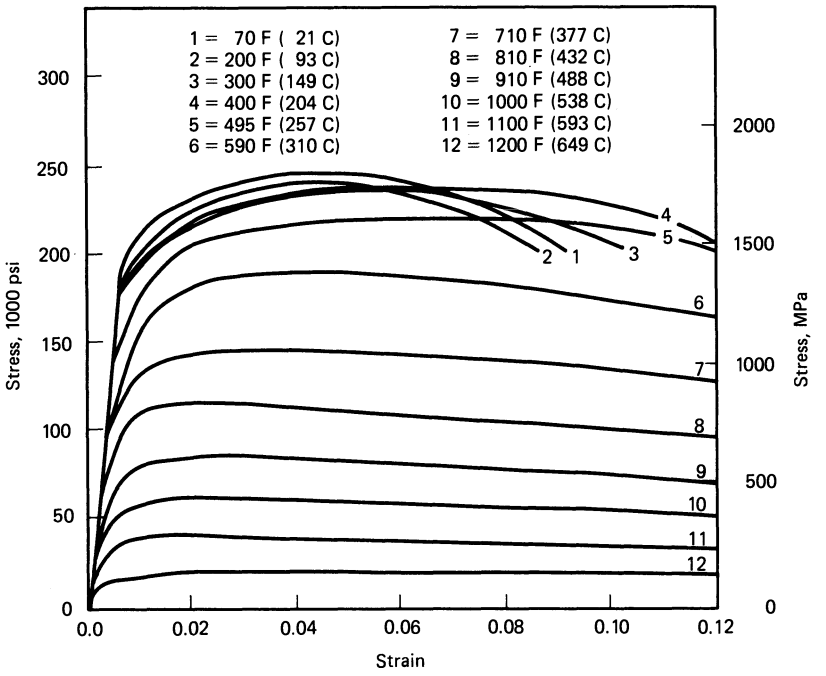

Fig. 2-17. Stress-strain curves for uncoated wire used to prestress concrete, conforming to ASTM A 421, at various high temperatures. (Reproduced with the permission of the American Concrete Institute.)

addition the report contains a plot comparing the stress–strain curves for stress-relieved wire conforming to ASTM A 421 at various elevated temperatures, which is shown here as Fig. 2-17. The tensile strength of stress-relieved and low-relaxation strand as a function of temperature is shown plotted in Fig. 2-18, and the effect of time and heat on the tensile strength of low-relaxation prestressing strand is illustrated in Fig. 2-19. These plots clearly show the sensitivity of prestressing steel to temperatures of the levels frequently encountered in fires. The reader is referred to the latest edition of the report of ACI Committee 216 and material-specific information from the manufacturers of prestressing steels for more information on this subject.

2-13 Application of Steel Types

The same basic steel can be used in pretensioning and post-tensioning, but in the former it is necessary that the individual tendons not be so large that they cannot be adequately bonded to the concrete, as the bond is relied upon to transfer the prestressing force from the steel to the concrete. In post-tensioning, as has been explained, end anchorages are used to transfer the prestressing force

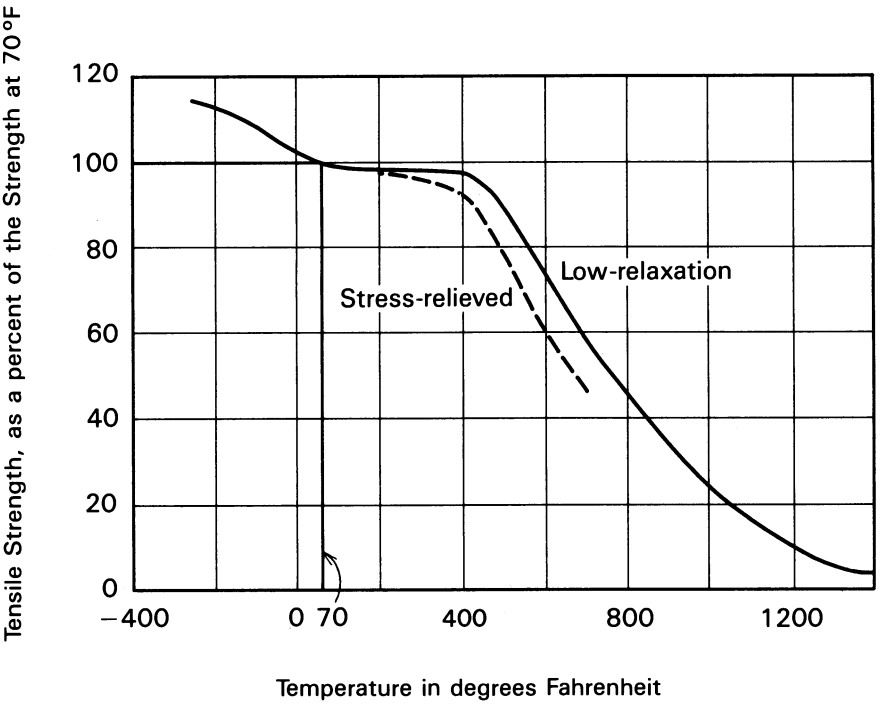

Fig. 2-18. Tensile strength of stress-relieved and low-relaxation prestressing strand, expressed as a percentage of its strength at 70°F, as a function of strength at various temperatures. (Based upon data obtained from and used with permission of Florida Wire and Cable Company.)

to the concrete, and the grout, when used, is relied upon to protect the steel against corrosion as well as to develop flexural bond stress (i.e., bond stress resulting from changes in the externally applied loads). Bond stresses are discussed in detail in Secs. 6-6 and 6-7. It should be mentioned here that, although in Europe it has been customary to use wires up to 0.276 in. in diameter as pretensioning tendons, the usual practice in the United States has been to use the uncoated, seven-wire strands described in Sec. 2-3. Little or no use of high-tensile alloy bars has been made in pretensioning in North America, although favorable results have been obtained experimentally in Europe with bars up to $\frac{5}{8}$ in. in diameter (Base 1958).

2-14 Idealized Tendon Material

One may wish to consider the properties that an ideal material for prestressing concrete would have. Some characteristics are desirable from one standpoint and not from another. For example, high tensile strength coupled with a low elastic modulus would permit a high strain under initial stress and minimize the

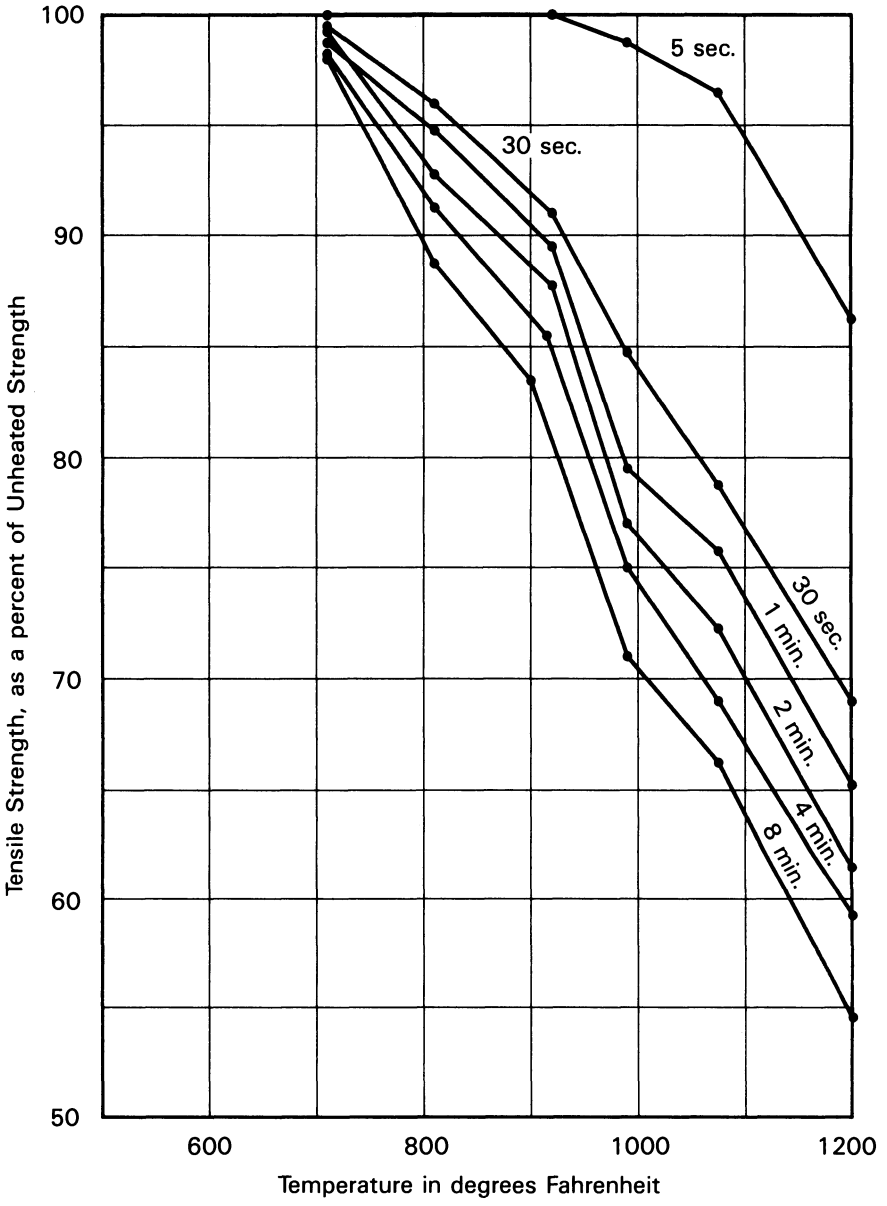

Fig. 2-19. Effect of duration of exposure to high temperatures on the tensile strength of low-relaxation prestressing reinforcement. (Based upon data obtained from and used with permission of Florida Wire and Cable Company).

loss of stress due to the inelastic properties of the concrete. On the other hand, with a high tensile strength only a small area of tendon is required, which, coupled with a low modulus of elasticity, could result in very high deflections upon the application of an overload that caused cracking. In actuality, use of the currently available steels generally results in designs that are efficiently balanced in serviceability and strength characteristics. Perhaps steels with somewhat higher strengths could be used efficiently. Steels without any relaxation loss obviously would be advantageous.

It is also possible that materials of very high strength and low elastic modulus eventually will be used in combination with nonprestressed mild reinforcing to achieve efficient and economical construction.

The major desirable physical characteristics of material used for prestressing tendons can be summarized as follows:

1. High strength that allows high prestressing stresses.
2. Elasticity up to high stress levels.
3. Plasticity at very high stress levels.
4. Low elastic modulus at time of stressing to minimize the loss of prestress.
5. High elastic modulus after bonding to contribute to the stiffness of the member.
6. Low creep and relaxation losses at the stress levels normally employed in prestressing and at elevated temperatures.
7. Resistance to corrosion.
8. Small diameter or relatively large surface area for the individual tendons to achieve good bond characteristics.
9. Absence of dirt and lubricants on the surface.
10. Straightness when uncoiled to facilitate handling and placing.

No material known has all of these desirable qualities, but the high-strength steels currently used possess most of them.

2-15 Allowable Prestressing Steel Stresses

The two most significant design criteria for prestressed concrete in the United States are the *Standard Specifications for Highway Bridges*, which is published by the American Association of State Highway and Transportation Officials (AASHTO 1989), and the *Building Code Requirements for Reinforced Concrete* (ACI 318 1989), published by the American Concrete Institute.

The following allowable stresses in prestressed reinforcement are those permitted in Sec. 9.15.1 of the *AASHTO Standard Specifications for Highway Bridges*, *14th Edition* (Copyright 1989. The American Association of State Highway and Transportation Officials, Washington, D.C. Used by permission). The quantities f'_s and f^*_y are the ultimate (tensile) strength and the yield point stress of the prestressing steel, respectively. The specific provisions are:

9.15.1 Prestressing steel

Stresses at anchorages after seating

Pretensioned members

.....$0.70 f'_s$ for stress relieved strands

.....$0.75 f'_s$ for low relaxation strands

Slight overstressing up to $0.85 f_s^*$ for short periods of time may be permitted to offset seating losses, provided the stress after seating does not exceed the above values.

Post-tensioned members.....$0.70 f'_y$

Overstressing up to $0.90 f_y^*$ for short periods of time may be permitted to offset seating and friction losses provided the stress at the anchorage does not exceed the above value. The stress at the end of the seating loss zone must not exceed $0.83 f_y^*$ immediately after seating.

Stress at service load† after losses .....$0.80 f_y^*$

The stresses permitted by ACI 318-89 are as follows:

1. Due to tendon jacking force, $0.94 f_{py}$ but not greater than $0.80 f_{pu}$, or maximum value recommended by manufacturer of prestressing tendons or anchorages.
2. Pretensioning tendons immediately after prestress transfer, $0.82 f_{py}$ but not greater than $0.74 f_{pu}$.
3. Post-tensioning tendons, at anchorages and couplers, immediately after tendon anchorage, $0.70 f_{pu}$.

It can be seen that both sets of criteria permit higher stresses in the reinforcement during the stressing operation than after seating of the anchorages. In addition, both have more restrictive limitations on the initial stress in post-tensioned reinforcement than in pretensioned reinforcement. Initial stress, in pretensioned tendons, is defined as the stress immediately after transfer (release); in post-tensioned tendons, it is the stress immediately after anchoring.

REFERENCES

ACI Committee 216. 1981 (1987). Guide for Determining the Fire Endurance of Concrete Elements. *Concrete International* 3(2):13–47 and 9(11):65.

ACI Committee 318. 1989. *Building Code Requirements for Reinforced Concrete.* Detroit. American Concrete Institute.

American Association of State Highway and Transportation Officials. 1989. *Standard Specifications for Highway Bridges. Fourteenth Edition.* Washington, D.C.

American Society for Testing and Materials. Test Methods and Definitions for Mechanical Testing of Steel Products. A 370-87c. Philadelphia.

†Service load consists of all loads contained in Article 3.2 but does not include overload provisions.

American Society for Testing and Materials. Specification for Uncoated Seven-Wire Stress-Relieved Steel Strand for Prestressed Concrete. A 416-87a. Philadelphia.

American Society for Testing and Materials. Specification for Uncoated Stress-Relieved Wire for Prestressed Concrete. A 421-80(1985). Philadelphia.

American Society for Testing and Materials. Practices for Packaging, Marking, and Loading Methods for Steel Products for Domestic Shipment. A 700-81. Philadelphia.

American Society for Testing and Materials. Specification for Uncoated High-Strength Steel Bar for Prestressing Concrete. A 722-86. Philadelphia.

American Society for Testing and Materials. Specification for Steel Strand, Seven-Wire, Uncoated, Compacted, Stress-Relieved for Prestressed Concrete. A 779-80(1985). Philadelphia.

American Society for Testing and Materials. Specification for Steel Strand, Indented, Seven-Wire Stress-Relieved for Prestressed Concrete. A 886-88. Philadelphia.

Base, G. P. 1958. An Investigation of Transmission Length in Pretensioned Concrete. Research Report No. 5. London. Cement and Concrete Association.

CEB-FIP. 1978. *CEB-FIP Model Code for Concrete Structures.* London. Federation International de la Precontraint. 201–2.

de Strycker R. 1959. The Influence of Temperature and Variations of Stress on the Creep of Prestressing Steels. Paris. *Revue de Metallurgie* 56(1):49–54.

Dorsten, V., Hunt, F. F., and Preston, H. K. 1984. Epoxy Coated Seven-Wire Strand for Prestressed Concrete. *PCI Journal* 29(5):120–29.

FIP Commission on Practical Construction. 1986. *Corrosion and Corrosion Protection of Prestressed Ground Anchorages.* London. Thomas Telford, Ltd.

FIP Commission on Prestressing Steels and Systems. 1986. *Corrosion Protection of Unbonded Tendons.* London. Thomas Telford, Ltd.

Ghali, A. and Trevino, J. 1985. Relaxation of Steel in Prestressed Concrete. *PCI Journal* 30(5):82–94.

Magura, D. D., Sozen, M. A., and Siess, C. P. 1962. A Study of Stress Relaxation in Prestressing Reinforcement. Civil Engineering Studies, Structural Research Series No. 237. Urbana. University of Illinois.

Papsdorf and Schwier. 1958. Creep and Relaxation of Steel Wire, Particularly at Slightly Elevated Temperatures. *Stahl und Eisen* 78(14):937–47.

Szilard, Rudolph. 1969. Corrosion and Corrosion Protection of Tendons in Prestressed Concrete Bridges. *Journal of the American Concrete Institute* 66(1):42-59.

PROBLEMS

1. A prestressed member requires an effective prestressing force of 980 kips. Determine the area of steel required for stress-relieved strand, low-relaxation strand, and high-tensile-strength bars, if the strain change in the concrete surrounding the prestressing steel in 700×10^{-6} in./in. owing to concrete elastic shortening, shrinkage, and creep. Assume a 25-year useful life for the structure, normal temperatures during service, and that the elastic modulus of steel is 29,000 ksi; assume that f_y' and f_{pu} are equal to 256 and 270 ksi, respectively; and assume that the tendons are stressed to $0.70\,f_{pu}$

initially. Make the computations on the basis of (1) full relaxation of the prestressing steel, and (2) reduced relaxation as expounded by Ghali and Trevino.

SOLUTION:

Using eq. 2-1 with $t' = 25 \times 365 \times 24 = 219{,}000$ hr, and taking $f_{si} = 0.70 \times 270 \times 189$ ksi for strands and $f_{si} = 0.70 \times 150 = 105$ ksi for bars, the losses due to relaxation alone are:

Stress-relieved strand:

$$\Delta f_{sr} = 189 \frac{\log 219{,}000}{10} \left(\frac{189}{256} - 0.55 \right) = 19.0 \text{ ksi}$$

Low-relaxation strand:

$$\Delta F_{sr} = 0.25 \times 19.0 = 4.8 \text{ ksi}$$

High-tensile-strength bars:

$$\Delta f_{sr} = 0.70 \times 105 \times 0.03 = 3.2 \text{ ksi}$$

A summary of the calculations for full relaxation is found in Table 2-7, and a summary for reduced relaxation in Table 2-8. For reduced relaxation, with the value of λ equal to 0.70, the values of Ω are computed as follows:

$$\text{S.R. strand, } \Omega = \frac{20.3}{189} = 0.107, \chi_r = e^{(-6.7 + 5.3 \times 0.70)0.107} = 0.726$$

$$\text{L.R. strand, } \Omega = \frac{20.3}{189} = 0.107, \chi_r = 0.726$$

$$\text{H.T. bars, } \Omega = \frac{20.3}{105} = 0.193, \chi_r = e^{(-6.7 + 5.3 \times 0.7)0.193} = 0.562$$

The reduced relaxations become: $0.762 \times 19.0 = 14.5$ ksi, $0.762 \times 4.8 = 3.7$ ksi, and $0.562 \times 3.2 = 1.8$ ksi, for stress-relieved strand, low-relaxation strand, and high-tensile strength bars, respectively. (See Table 2-8.)

2. For a pretensioned stress-relieved strand that is released 24 hours after having been stressed to 175 ksi, determine the stress remaining in the tendon after

TABLE 2-7 Summary of computations for full relaxation for Problem 1.

Steel type	Initial stress (ksi)	Relax. loss (ksi)	Concrete loss (ksi)	Total loss (ksi)	A_s req'd (ksi)
S.R. strand	189	19.0	20.3	39.3	6.55
L.R. strand	189	4.8	20.3	25.1	5.98
H.T. bars	105	3.2	20.3	23.5	12.02

TABLE 2-8 Summary of computations for reduced relaxation for Problem 1.

Steel type	Initial stress (ksi)	Relax. loss (ksi)	Concrete loss (ksi)	Total loss (ksi)	A_s req'd (ksi)
S.R. strand	189	14.5	20.3	34.8	6.36
L.R. strand	189	3.7	20.3	23.7	5.93
H.T. bars	105	1.8	20.3	22.1	11.82

50 hours, if $f_{pu} = 250$ ksi and $f' = 225$ ksi. Assume that the elastic shortening is 170×10^{-6} in./in., and the deferred deformation of the concrete (creep and shrinkage) is 825×10^{-6} in./in. Use an elastic modulus for the steel of 28,000 ksi.

SOLUTION: At 24 hours:

$$\Delta f_{sr} = 175 \frac{\log 24}{10} \left(\frac{175}{225} - 0.55 \right) = 5.5 \text{ ksi}$$

The loss due to elastic shortening is $28{,}000 \times 170 \times 10^{-6} = 4.8$ ksi, the initial loss at the time of the stressing is $5.5 + 4.8 = 10.3$ ksi, or approximately 10 ksi, and the stress remaining after release is 165 ksi. Using eq. 2-2 to determine the stress remaining in the steel after 50 years (438,000 hr), one finds:

$$\frac{f_{st}}{165} = 1 - \left(\frac{165}{225} - 0.55 \right) \left(\frac{\log 438{,}000 - \log 24}{10} \right) = 0.922$$

and $f_{st} = 0.922 \times 165 = 152$ ksi. The loss due to the deferred concrete strain is equal to $28{,}000 \times 825 \times 10^{-6} = 23.1$ ksi; hence, the effective stress after 50 years (using full or intrinsic relaxation) is 129 ksi.

3 Concrete for Prestressing

3-1 Introduction

It is presumed that the reader is familiar with the basic physical properties of portland-cement concrete, which is the principal constituent of prestressed concrete. It is important that a proper concrete be employed in prestressed concrete construction, but only the factors that are of particular interest in this type of construction are considered here. General data pertaining to the factors affecting the physical properties of concrete can be found in the many publications and standards of the American Concrete Institute.

Concretes with compressive strengths of 5000 to 6000 psi at the age of 28 days, as measured on standard cylindrical specimens, are rather easily obtained in most localities today, but little, if any, economic advantage results from the use of concretes in this strength range in nonprestressed reinforced concrete flexural members. For this reason, concretes with compressive strengths on the order of 3000 to 4000 psi are much more commonly used for nonprestressed flexural members than are the higher-strength concretes. (The use of concrete of moderate and high strength can be both functionally and economically advantageous in columns and other compression members reinforced with nonprestressed reinforcement, however.) This is not the case for prestressed flexural

members, where the use of concretes of moderate to high strength is common and efficient because of the reduction in weight and cost of the members that it makes possible. Furthermore, as has been explained, the time-dependent volume changes of concrete (creep and shrinkage) significantly affect the amount of prestressing that is lost. Because the higher-strength concretes normally undergo substantially smaller volume changes than the lower-strength ones, their use is desirable, if not necessary, in many applications.

Strength and volume changes in concrete are affected by many variables, but in practice the engineer's control of these variables normally is limited to the writing of specifications intended to govern the amount of water, the types and proportions of the aggregates, and the type and amount of cement, as well as the types and amounts of admixtures that can be used in the concrete mixture. On many projects the engineer is not at liberty to specify particular materials available from a single source (producer), but must write specifications relying upon nonproprietary standard specifications to obtain the desired results. The water content of the concrete mixture should be kept to the minimum required for proper placing; by this means its strength is increased and its shrinkage reduced. On the other hand, care must be exercised to ensure that sufficient water will be present in the plastic concrete mixture so that it can be placed and consolidated with conventional methods and equipment and with a reasonable amount of labor. The engineer also should specify the method and duration of curing the concrete after it has been placed and finished.

3-2 Cement Type

The cement used in most prestressed concrete construction is portland cement that conforms to "Standard Specification for Portland Cement" (ASTM C 150). Blended cements, conforming to "Standard Specifications for Blended Hydraulic Cements" (ASTM C 595), also are used.

The most common types of cement used in prestressed concrete vary from one locality to another. Types I (normal), II (modified), and III (high early strength) cements, conforming to ASTM C150, all are used extensively, as are the air-entraining blends, Types IA, IIA, and IIIA. All give satisfactory results under specific local conditions if properly used.

Type III cement is intended for use when high early strength is desired. Because high early strength can permit prestressing at an earlier than usual age, the time required to produce prestressed concrete members, especially under plant conditions, sometimes is reduced through its use. Type III cement has a higher heat of hydration (heat evolved as a result of chemical reactions with water during mixing and hardening) than Types I and II cements, and this is sometimes found to be objectionable; on the other hand, the heat generated by the hydration process, if properly controlled, can be used to accelerate the curing of the concrete. Concrete admixtures, which are discussed in the following

section, in combination with Types I and II cements and accelerated curing methods, also can be used to produce concrete having high early strength, but with a more moderate heat of hydration than that of Type III cement. The use of Type II cement is required by some agencies because of its greater sulfate resistance and a lower heat of hydration than is encountered with cement Types I and III. Because the various cements perform in different ways with the variety of aggregates and admixtures that are available, concrete mixture designs normally are determined by using a number of trial batches made with the different materials available in a locality.

A technical report published by the Prestressed Concrete Institute (Pfeifer and Marusin 1981) contains specific recommendations regarding cement chemistry for optimum results in the manufacture of precast concrete products.

Calcium-aluminate cement, also known as high-alumina cement and aluminous cement, has been used to some extent in prestressed concrete in Europe but not extensively in North America. Because some of these cements are reported to contain significant quantities of sulfides that can undergo chemical change and form atomic hydrogen embrittlement of prestressing steel, this cement is not recommended for use in prestressed concrete (Szilard 1969).

3-3 Admixtures

An admixture is defined as a material other than water, aggregates, hydraulic cement, and fiber reinforcement, which is used as an ingredient of concrete or mortar, and is added to the batch immediately before or during its mixing (ACI 116 1985). The use of admixtures has increased dramatically in the past 30 years with the development of many new types. Admixtures are used in prestressed concrete to make the plastic concrete more plastic, retard the initial set, accelerate the final set, reduce the amount of water required in the mixture, and entrain air in the concrete in order to enhance the durability of the hardened product. Admixtures frequently are used to facilitate the placing and handling of concrete, as well as to obtain high strength at an early age.

The admixtures used in concrete for entraining air normally must conform to the requirements of ASTM C 260, "Specification for Air-Entraining Admixtures for Concrete." Technical specifications for admixtures that reduce the amount of water required in the plastic concrete, or retard or accelerate the setting of the concrete, as well as those that cause combinations of these effects, are contained in "Specification for Chemical Admixtures for Concrete" (ASTM C 494).

The use of concrete admixtures has become very sophisticated, in many instances involving combinations of admixtures, some added to the concrete during the original batching and others added at the job site after the concrete has been mixed for a period of time. Experimentation generally is needed to determine the best combination of admixtures to use with the other specific

ingredients that will go into a concrete for a particular application. The engineer generally relies on the advice of concrete suppliers, consultants, suppliers of admixtures, and past experience in initiating a testing program to determine what admixtures will perform best on a specific project.

The adverse effect of chloride ion on reinforcing steel has been recognized for many years. It can be particularly serious in prestressing steels, where it can cause pitting and stress corrosion. It is for this reason that "Building Code Requirements for Reinforced Concrete" (ACI 318-89) limits the amount of water-soluble chloride ion in prestressed concrete, at the age of 28 days, to 0.06 percent of the weight of the cement. Materials containing significant amounts of chlorides should not be used in prestressed concrete, but trace amounts, whether in the mixing water, the aggregates, or admixtures, are unavoidable and should not be of concern.

The engineer always should be careful to check the chloride ion content of chemical admixtures proposed for use in a concrete mixture. This often requires more investigation than simply reading the sales literature provided for the product.

3-4 Slump

In the European technical literature on prestressed concrete of the 1940s and 1950s, there was a strong emphasis on using no-slump or very low-slump concrete in prestressed concrete. The purpose behind the recommendation was to obtain high concrete strength together with relatively low creep and shrinkage. Experience in the United States indicates that the use of no-slump and very low-slump concrete generally should be confined to products made on vibrating tables or vibrating pallets, and perhaps to shallow members that are of such configuration that all areas of the member are readily accessible to internal vibrators. For example in North America low-slump concrete commonly is used in precast hollow core slabs, which are sometimes made by an extrusion process and sometimes with a slip form. However, for average prestressed members that are too large to be produced on a vibrating table, or that have large bottom flanges that cannot be readily vibrated with internal vibrators, it has been found that good results are obtained when the slump of the plastic concrete is about 4 in. With modern high-range water-reducing admixtures, low water–cement ratios can be maintained with slumps in the 4 to 6 in. range; hence, the need for the use of low-slump concrete no longer exists if modern admixtures are used in the concrete.

3-5 Curing

After concrete has been placed and consolidated, the cement used as one of the constituents combines (hydrates) with some of the mixing water. This process

is essential for the concrete to gain strength and other desirable properties. To ensure that sufficient water is available for the hydration process, the concrete must be kept from drying; and it is this prevention of drying during hydration that is called curing. It is generally recognized that the best method of curing concrete is to keep its surfaces wet by the application of water or by sealing the surfaces through the application of a coating or moisture barrier. The manufacturer can accelerate the hydration process by heating the concrete while preventing it from drying. Methods of heating concrete to accelerate hydration include the use of steam at high pressure; the use of hot, moist air at atmospheric pressure (see Sec. 3-16); and the use of radiant heat from circulating hot water or hot oil, electric heating pads, and so on. Covering the concrete surfaces with carpets, burlap, or other absorbent material that is kept wet by the application of hot water also is an effective means of accelerating the hydration process during the curing period.

Accelerating the hydration process is more important in the manufacture of plant-produced prestressed concrete than it is in prestressed concrete products produced on site. This is so because of the need to achieve frequent reuse of plant facilities through reduction in production time; the cost of products produced is reduced if the time required to produce them is reduced.

The reader should consult "Standard Practice for Curing Concrete" (ACI 308-81) for a comprehensive treatment of concrete curing.

3-6 Concrete Aggregates

The aggregates used in the manufacture of normal concrete members usually are satisfactory for prestressed concrete. However, because of the higher strengths required for prestressed concrete, it has been difficult, in some localities, to find suitable natural aggregates for prestressed construction. Where a choice of aggregates is available, one should make the selection after considering the ease of obtaining the necessary strength, as well as the magnitude of the elastic and inelastic volume changes that might be expected with the different types available. Lightweight aggregates of the expanded shale or clay type have been used with good results in North America. When lightweight aggregates are used in prestressed concrete, one must be careful to make a reasonable assessment of anticipated volume changes when estimating the loss of prestress.

Normal concrete aggregates should conform to the requirements of "Standard Specifications for Concrete Aggregates" (ASTM C 33). Aggregates for lightweight prestressed concrete should conform to "Standard Specifications for Lightweight Aggregates for Structural Concrete" (ASTM C 330).

3-7 Strength

A principal reason why concrete with a minimum 28-day cylinder compressive strength of the order of 4000 to 6000 psi is used in prestressed concrete members

is that concrete of higher strength generally will exhibit lower volume changes than concretes of lower strength. In addition, concrete in this strength range is relatively easy to produce with contemporary materials and production facilities. Another reason for using higher-strength concretes is that efficient use generally can be made of them in prestressed concrete flexural members; this is not the case in nonprestressed reinforced concrete members.

In some localities it is difficult to consistently produce concrete of high quality with locally produced concrete materials. The designer of prestressed-concrete structures should carefully investigate this problem on each project undertaken. It is generally possible to prepare reasonably economical designs with concretes of moderately high strength, and thereby avoid the need for strengths that may be difficult to obtain under job-site conditions. It is better to anticipate this problem and provide for it in the design stage than to struggle with what may be an almost impossible situation during construction.

Whenever possible, and always on major jobs, the concrete mixtures used should be trial-patched and laboratory-tested before use on the job. The mixtures employed in the work should be proportioned on the basis of field experience and/or trial mixtures as provided in Sec. 4.3 of ACI 318. The strength test results obtained during the work should be evaluated by using "Recommended Practice for Evaluation of Strength Test Results of Concrete" (ACI 214-77).

A general equation for predicting the compressive strength of concrete at any age has been proposed (Branson and Christianson 1971; ACI 209 1982). This relationship is:

$$f'_{ct} = \frac{t}{a + \beta t} f'_c \tag{3-1}$$

where f'_{ct} is the compressive strength at age t in days, a and β are constants, and f'_c is the compressive strength at the age of 28 days. The average values of constants a and β have been found to be as shown in Table 3-1. Variations in compressive strength as a function of time, using eq. 3-1 and the values of the constants a and β given in Table 3-1, are shown in Fig. 3-1.

The compressive strength that eventually will be achieved by moist-cured

TABLE 3-1 Values of concrete strength coefficients a and β for use in eq. 3-1 and ratios of eventual strength to 28-day strength (after ACI Committee 209 1982).

Concrete curing	Cement type	a	β	Curve in Fig. 3-1	Eventual str. / 28-day str.
Moist	I	4.00	0.85	1	1.18
Moist	II	2.30	0.92	2	1.09
Steam	I	1.00	0.95	3	1.05
Steam	III	0.70	0.98	4	1.02

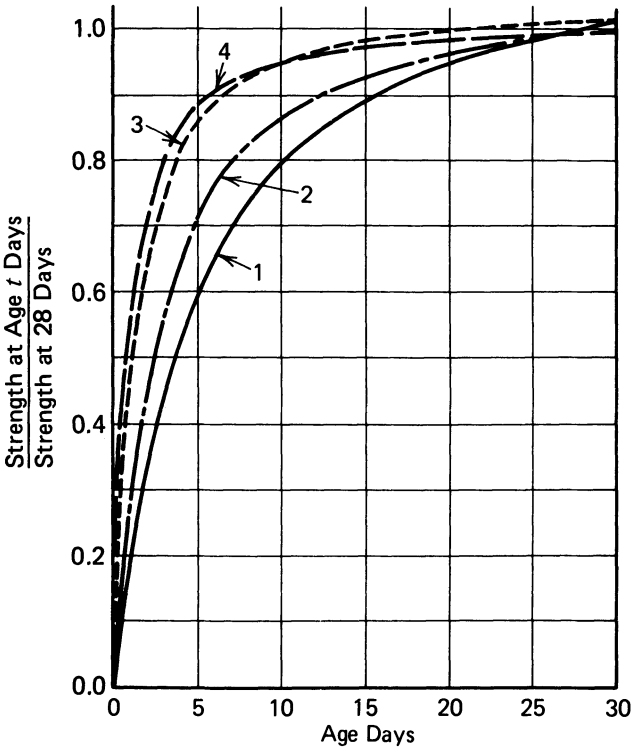

Fig. 3-1. Strength–time curves for concrete as predicted by eq. 3-1 for the concretes listed in Table 3-1.

concrete, expressed as a ratio of eventual strength to strength at the age of 28 days, can be estimated to be as shown in Table 3-1 (ACI 209 1986).

On important projects, and in precasting plants, strength–time curves should be developed for the particular concrete mixtures being used. This approach permits the work to be accurately planned in advance and monitored during construction, and it facilitates the identification of low-strength concrete at an early age.

The 28-day compressive strength of concrete as a function of the water–cement ratio for air-entrained and non-air-entrained concrete is illustrated in Fig. 3-2; and in Fig. 3-3, the 28-day compressive strength of concrete is shown as a function of the voids–cement ratio. These curves are useful in estimating the quantities of cement and water that must be used to achieve a desired concrete strength with and without entrained air.

The tensile strength of concrete, sometimes called the direct tensile strength, can be estimated from:

$$f'_t = g_t \left[w(f'_{ct}) \right]^{1/2} \tag{3-2}$$

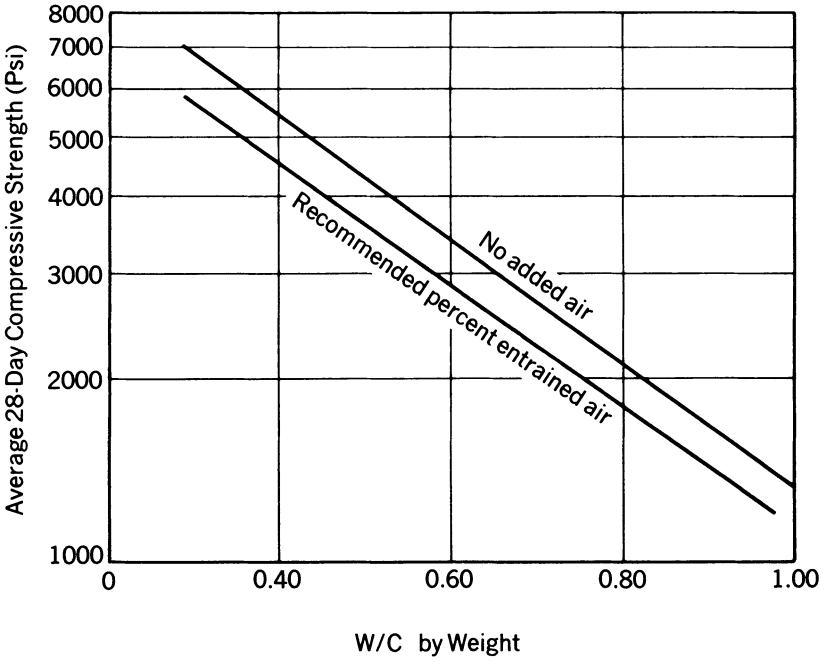

Fig. 3-2. Concrete compressive strength in relation to water–cement ratio for air-entrained and non-air-entrained concrete. The strength decreases with an increase in the water–cement ratio; or with the water–cement ratio held constant, the use of air entrainment decreases the strength by about 20 percent (Bureau of Reclamation 1966).

in which w is the unit weight of the concrete in pounds per cubic foot, f'_{ct} is the comrpessive strength at time t in days, and g_t is equal to 0.33 (ACI 209 1982). For g_t taken to be equal to 0.33 and a concrete having a unit weight, w, equal to 144 pcf, eq. 3-2 becomes:

$$f'_t = 4\sqrt{f'_{ct}} \tag{3-2a}$$

The modulus of rupture can be taken as follows:

$$f_r = g_r\left[w(f'_{ct})\right]^{1/2} \tag{3-3}$$

in which g_r is a constant that normally varies between 0.60 and 0.70. For concrete having a unit weight, w, of 144 pcf, the values of the modulus of rupture using eq. 3-3 would become:

$$f_r = 7.2\sqrt{f'_{ct}} \tag{3-3a}$$

and:

$$f_r = 8.4\sqrt{f'_{ct}} \tag{3-3b}$$

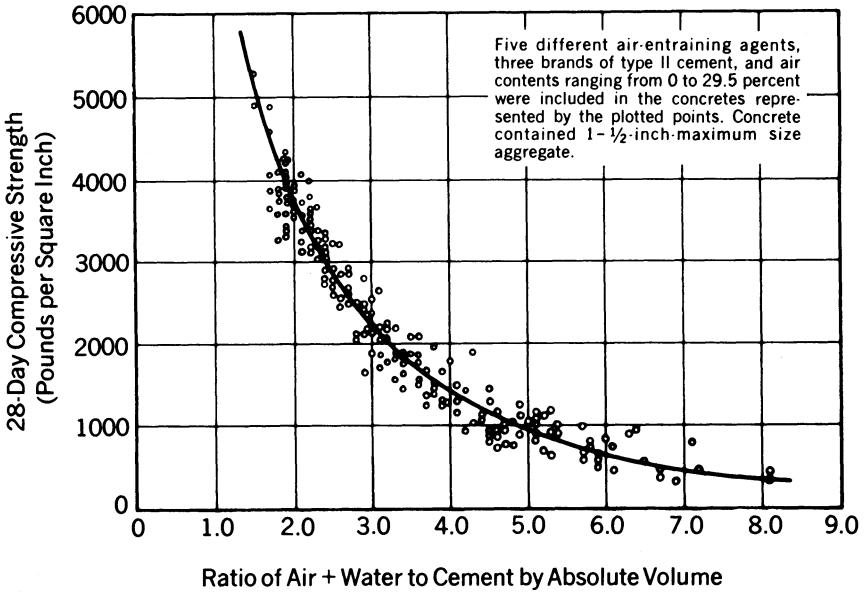

Fig. 3-3. Compressive strength of concrete in relation to voids–cement ratio (Bureau of Reclamation 1966).

for values of g_r of 0.60 and 0.70, respectively. Because of the variation that is found in the modulus of rupture, the upper or lower limit of eq. 3-3 should be used in computations in such a manner that the result will be conservative (Branson and Christianson 1971; ACI 209 1982). (It should be noted that the values specified for the modulus of rupture in *Building Code Requirements for Reinforced Concrete*, ACI 318, are as low as $6\sqrt{f'_c}$ and as high as $7.5\sqrt{f'_c}$.)

The strength of lightweight concrete should always be determined by tests. The curves of Figs. 3-1, 3-2, and 3-3 should not be expected to apply to lightweight concrete.

3-8 Elastic Modulus

The value of the elastic modulus of concrete is important to the designer of prestressed concrete because it must be used in computing deflections and losses of prestress. Unfortunately, the elastic modulus of concrete is a function of many variables, including the types and amounts of ingredients used in making the concrete (cement, aggregates, admixtures, and water), as well as the manner and duration of curing the concrete, age at the time of loading, rate of loading, and other factors (Troxell, Davis, and Kelley 1956). When possible, it is recommended that the elastic modulus be determined by tests for the concrete to be used in a specific application; especially in applications where deflections and

loss of prestress are particularly important. When the elastic modulus of the concrete is not determined by tests, it may be assumed to be:

$$E_{ct} = 33\, w^{1.5} \sqrt{f'_{ct}} \tag{3-4}$$

in psi, for values of w, the unit weight of the concrete, between 90 and 155 pcf (ACI 209 1982). For normal-weight concrete, eq. 3-4 can be taken as:

$$E_{ct} = 57{,}000 \sqrt{f'_{ct}} \tag{3-5}$$

Based upon test data, eq. 3-4 may give a good representation of the elastic modulus for a particular concrete if a value other than 33, as given in eq. 3-4, is used. This should be an acceptable procedure if the test data are available. ACI Committee 363, High Strength Concrete, has recommended the following relationship for the elastic modulus for use in lieu of eq. 3-5 (ACI 363):

$$E_{ct} = \left[40{,}000\, (f'_{ct})^{1/2} + 1 \times 10^6\right] \left[\frac{w_c}{145}\right]^{1.5} \tag{3-6}$$

Equations 3-5 and 3-6 are compared graphically in Fig. 3-4. It should be noted that eq. 3-5 was based upon test data for concrete having 28-day compressive strengths of 6000 psi and less, and eq. 3-6 is intended to better predict the elastic modulus for concretes having strengths as high as 14,000 psi. It should also be noted that f'_{ct} in eqs. 3-5 and 3-6 is the compressive strength of concrete, as determined by tests of standard 6 × 12 in. cylinders made in accordance with ASTM C 192 and tested in accordance with ASTM C 39, at the age of t days.

Klink reported experimental work that led him to conclude that the procedure for determining the elastic modulus of concrete in ASTM C 469 produces results that are approximately 55 percent lower than those found by measurements made with internal strain gages (Klink 1985). The accuracy of Klink's conclusions have been questioned by others; hence, the reader is advised to carefully review the technical literature on this subject when designing structures that could be adversely affected by differences as great as those reported by Klink (Baidar, Jaeger, and Mufti 1989).

It should be pointed out that eqs. 3-5 and 3-6 are intended to predict the values of the elastic modulus that would be obtained if the concrete were tested in accordance with ASTM C 469. Because the value of the elastic modulus thus obtained is the chord modulus at a stress of 40 percent of the ultimate compressive strength of the cylinder, a value as much as 10 percent higher could be anticipated in applications where the concrete is not stressed to such high a level. The differences between the tangent moduli at different stress levels and the secant modulus are illustrated in Fig. 3-5.

In prestressing concrete, the prestressing force often is transferred to the concrete at a relatively early age (1 to 14 days, depending upon the materials and method of curing used). Hence, at the time of stressing the concrete

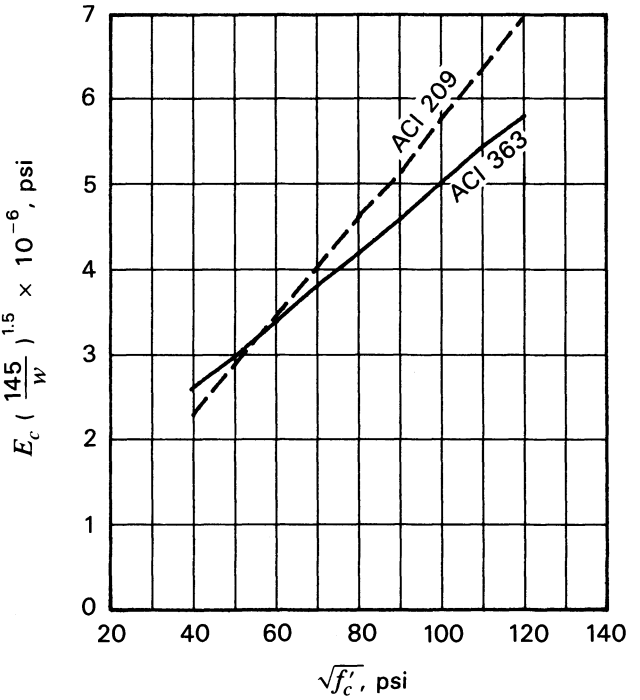

Fig. 3-4. Comparison of relationships for the modulus of elasticity of concrete as contained in Sec. 8.5.1 of ACI 318 and as recommended by ACI Committee 363 (ACI 318 1989; ACI 363 1984).

frequently has a strength that is somewhat less than the minimum specified at the age of 28 days. Equations 3-5 and 3-6 give a means of approximating the modulus of elasticity of the concrete at a given age by relating it to the cylinder strength, which varies with age.

ILLUSTRATIVE PROBLEM 3-1 A post-tensioned beam is to be stressed when the concrete strength is 4000 psi. The specifications also provide that the minimum cylinder compressive strength at the age of 28 days shall be not less than 5000 psi. Compute the elatic modulus that should be used in determining instantaneous deflections and stress losses at the time of stressing and at the age of 28 days if (1) the concrete is normal concrete, and (2) the concrete is light-weight concrete having a unit weight of 100 pcf.

SOLUTION:

(1) $$E_{ct} = 57{,}000\,(f'_{ct})^{1/2}$$

At the time of stressing:

$$E_{ct} = 57{,}000 \times \sqrt{4000} = 3{,}600{,}000 \text{ psi}$$

At 28 days:

$$E_{ct} = 57{,}000 \times \sqrt{5000} = 4{,}030{,}000 \text{ psi}$$

(2) $$E_{ct} = 100^{1.5} \times 33(f'_{ct})^{1/2}$$

At the time of stressing:

$$E_{ct} = 33{,}000 \times \sqrt{4000} = 2{,}090{,}000 \text{ psi}$$

At 28 days:

$$E_{ct} = 33{,}000 \times \sqrt{5000} = 2{,}330{,}000 \text{ psi}$$

Creep of concrete, which is discussed in detail in Sec. 3-13, is defined as the increase in strain that occurs when a concrete member or specimen is subjected to constant stress. Because the elastic modulus of concrete is the quotient of the

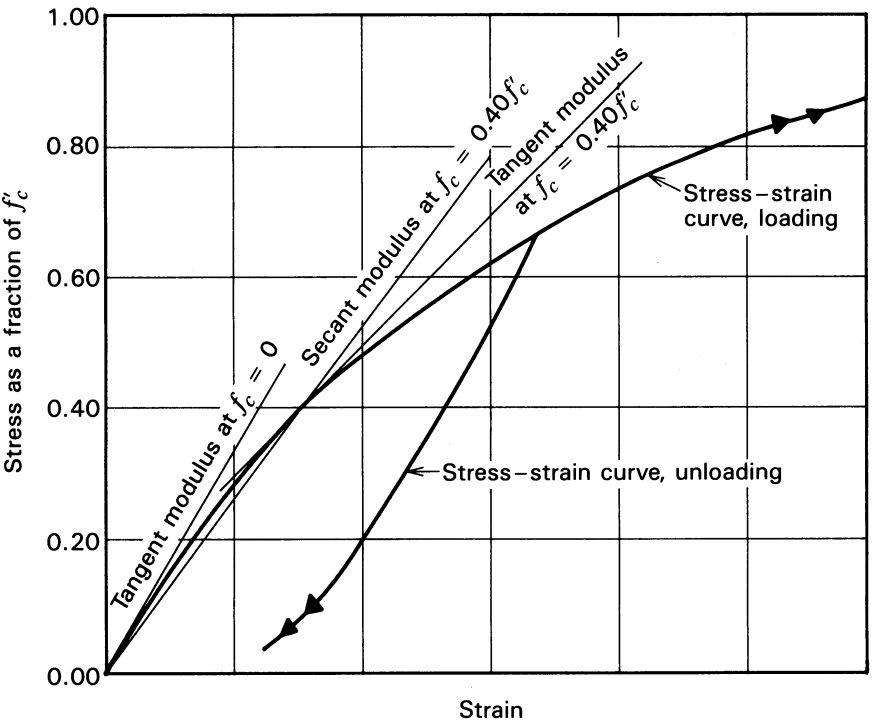

Fig. 3-5. Stress–strain curve for a concrete cylinder loaded in compression, illustrating the secant and tangent moduli at a stress of 40 percent of the compressive strength and the tangent modulus at zero stress.

stress per unit of "elastic" strain or strain that occurs "instantaneously" upon the application of stress, an increase in the amount of strain under a sustained stress level has the effect of decreasing the modulus of elasticity. Hence, one should be aware of the two moduli of elasticity commonly used in the analysis of concrete. These are the instantaneous modulus, normally referred to simply as the elastic modulus and the effective modulus, which is sometimes called the reduced or sustained modulus as well. The instantaneous elastic modulus, E_{ci}, can be expressed by:

$$E_{ci} = \frac{\text{Stress}}{\text{Strain}} \tag{3-7}$$

The effective modulus is time-dependent and includes the creep strain that has occurred during a period of time in which the concrete is subjected to a sustained load. The effective modulus, E_{ce}, can be expressed by:

$$E_{ce} = \frac{\text{Stress}}{\text{Elastic strain} + \text{Creep strain}} \tag{3-8}$$

The effective modulus, at time t, also can be written:

$$E_{ce} = \frac{E_{ci}}{1 + v_t} \tag{3-9}$$

where v_t is the creep ratio at time t. The creep ratio at time t can be defined mathematically as:

$$v_t = \frac{\text{Creep strain at time } t}{\text{Elastic strain}} \tag{3-10}$$

in which v_t is the creep ratio at the age of t days. The value of the effective modulus that eventually will be achieved for concrete held under a sustained load for a long period of time can be written as:

$$E_{cu} = \frac{E_c}{1 + v_u} \tag{3-11}$$

where v_u is the creep ratio for the ultimate creep strain, or:

$$v_u = \frac{\text{Ultimate creep strain}}{\text{Elastic strain}} \tag{3-12}$$

The values of v_u and v_t are functions of many variables, but principally of the relative humidity, concrete quality, and age of the concrete when loaded. Additional information on creep of concrete is given in Secs. 3-13 and 3-14.

The effecitve modulus frequently is used in computing deflections of reinforced and prestressed concrete, as well as the losses of prestress in

prestressed-concrete members. These subjects are discussed in greater detail in Secs. 7-3 and 7-4.

The use of an age-adjusted concrete modulus, originally proposed by Trost and subsequently supported by Banzant and ACI Committee 209, has become accepted practice in recent years (Trost 1967; Banzant 1972; ACI 209 1982). The age-adjusted concrete modulus, which compensates for time-dependent effects on the properties of concrete including concrete age at loading and duration of the load, is determined with the use of an aging coefficient. The expression for the age-adjusted modulus at time t, E_{cat}, is:

$$E_{cat} = \frac{E_c}{1 + \chi v_t} \tag{3-13}$$

in which χ is an aging coefficient normally on the order of 0.6 to 0.9, and the other terms are as defined above. Values of the aging coefficient, as computed by Bazant, are given in Table 3-2.

3-9 Poisson Ratio

When concrete is subjected to a uniaxial stress, a transverse deformation takes place simultaneously with the axial (longitudinal) deformation. The ratio of the transverse deformation to the axial deformation is known as the Poisson ratio, or as Poisson's ratio. Structural engineers must include the effects of transverse

TABLE 3-2 Concrete aging coefficients, χ (after Bazant 1972).

$t - t_{lac}$ days	v_u	t_{lac} in days			
		10^1	10^2	10^3	10^4
10^1	0.5	0.525	0.804	0.811	0.809
	1.5	0.720	0.826	0.825	0.820
	2.5	0.774	0.842	0.837	0.830
	3.5	0.806	0.856	0.848	0.389
10^2	0.5	0.506	0.888	0.916	0.915
	1.5	0.739	0.919	0.932	0.928
	2.5	0.804	0.935	0.943	0.938
	3.5	0.839	0.946	0.951	0.946
10^3	0.5	0.511	0.912	0.973	0.981
	1.5	0.732	0.943	0.981	0.985
	2.5	0.795	0.956	0.985	0.988
	3.5	0.830	0.964	0.987	0.990
10^4	0.5	0.501	0.899	0.976	0.994
	1.5	0.717	0.934	0.983	0.995
	2.5	0.781	0.949	0.986	0.996
	3.5	0.818	0.958	0.989	0.997

deformations in sophisticated structural analysis of prestressed and reinforced concrete plates, shells, and other three-dimensional structures.

Neville, in Nomograph No. 6, has reported the value of the Poisson ratio to vary between 0.11 and 0.21, with the ratio being lower for concrete of high strength (Neville 1971).

Based upon experimental work involving the measurement of transverse and longitudinal strains near the center of concrete specimens, Klink found the value of the Poisson ratio to be about 55 percent greater than when measured on the surface of the specimen, as done using the standard method in ASTM C 469. (Klink 1985; ASTM 1987). Based upon his research, Klink has proposed the following relationship for predicting the value of the Poisson ratio, ν_c, for concretes of different weights and strengths:

$$\nu_c = (67 \times 10^{-8})\,(w)^{1.75}\,(f'_{ct})^{1/2} \tag{3-14}$$

For a concrete having a unit weight of 144 pcf, eq. 3-14 becomes:

$$\nu_c = 0.0040\sqrt{f'_{ct}} \tag{3-15}$$

In eq. 3-14, ν_c is the Poisson ratio, as measured internally in a specimen, and the other terms are as previously defined. It should be pointed out that Klink's experimental work was done on concrete having unit weights that varied from 95 to 152 pcf and strengths that varied from 1350 to 7322 psi, and predicts values of the Poisson ratio about 55 percent greater than those determined following the procedures in ASTM C 469.

The results reported by Klink have been disputed, and the reader is cautioned to review contemporary technical literature on the subject of the Poisson ratio when designing structures where differences in this value on the order of 55 percent could be significant (Baider, Jaeger, and Mufti 1989).

3-10 Shrinkage

Shrinkage from three different sources is recognized in concrete: autogenous shrinkage, carbonation shrinkage, and drying shrinkage. Autogenous shrinkage, which results from the hydration of the cement, normally is small in comparison to drying shrinkage and is not considered in this book. Carbonation shrinkage results from atmospheric carbon dioxide combining with lime (calcium oxide) in the concrete to form calcium carbonate. This type of shrinkage can be significant under certain conditions of environment, but it normally is not important and is not considered in the design of concrete structural elements. Drying shrinkage results from the loss of water from concrete, and is the type of shrinkage normally referred to by structural engineers simply as shrinkage. In this book, the term shrinkage is intended to mean drying shrinkage.

3-11 Drying Shrinkage

The shrinkage of concrete is an important factor to the designer of prestressed concrete for several reasons. As has been stated, the shrinkage of the concrete contributes to the loss of prestress. The magnitude of the shrinkage, also must be known with reasonable accuracy when the deflection of prestressed members is being computed by sophisticated methods. One cannot compute the deflection of composite prestressed-concrete members without knowing the shrinkage characteristics of each of the concrete in each of the components involved. In addition, the magnitude of the concrete shrinkage must be estimated in order to evaluate secondry stresses (due to volume changes) that may result.

The effects of concrete shrinkage in prestressed-concrete structures are considerably different from those in reinforced-concrete structures. In reinforced concrete the shrinkage strains are resisted by compressive stresses in the reinforcing steel, whereas in prestressed concrete the prestressing steel is always in tension and causes compressive strains in the concrete that add to the shrinkage deformation. In addition, reinforced-concrete flexural members normally are cracked, with many closely spaced minute cracks that tend to relieve the effect of shrinkage stresses. The designer of prestressed-concrete structures must give particular attention to the effects of shrinkage, creep, and temperature variations. If these movements are restrained, forces of very high magnitude can result, with the very real possibility of serious structural and nonstructural damage. This subject is discussed in greater detail in Chapters 12 and 17.

The drying shrinkage of concrete is known to result from loss of moisture. It also has been shown that concrete will expand if, after having dried or partially dried, it is subjected to very high humidity, or if it is submerged in water. Shrinkage is known to be affected by the following variables:

A. Composition of the cement.
B. Physical properties of the aggregate.
C. Method and duration of curing.
D. Relative humidity of the service environment.
E. Volume to surface ratio/average thickness of the member.
F. Water content (related to slump).
G. Admixtures.
H. Slump of the plastic concrete.
I. Relative amount of fine aggregate.
J. Cement content.
K. Air content.

A considerable amount of data is available in the literature concerning the effect of each of these variables. The discussion that follows is of a general nature but is considered sufficiently accurate for most design purposes, as the

designer of prestressed concrete often can control shrinkage to some degree through careful consideration of the materials and methods specified for each project. The effects of the above variables can be summarized as follows, with items H, I, J, and K being included in the discussion of items A through G:

A. Cement. High early strength portland cement (type III) normally would be expected to have a shrinkage 10 percent higher than that of normal portland cement (type I) or modified portland cement (type II) (Troxell, Davis, and Kelley 1956). In addition, a cement exhibiting a large amount of shrinkage may have a total shrinkage that is 100 percent greater than that of a cement which, because of its chemical composition, exhibits a small amount of shrinkage. This is an extreme range, however, and it may be beneficial to investigate the cements available in any locality, in order to determine if any of the normally used cements have exceptionally high or low shrinkage characteristics. There is some evidence that the use of a high early strength cement of good quality may result in a concrete that exhibits somewhat lower total volume changes (creep and shrinkage combined) in prestressed concrete than would be obtained with normal cement (type I) (Troxell, Davis, and Kelley 1956; Hanson 1964).

B. Aggregates. The physical properties of the larger aggregate particles have a considerable influence on the shrinkage of concrete because the concrete aggregate reinforces the cement paste and resists its contraction. Aggregates with higher elastic moduli are stiffer and hence restrict the contraction of the paste to a greater degree than those with lower elastic moduli. Aggregates that have a low volume change in themselves, due to drying, generally lower concrete shrinkage. Concretes containing aggregates of quartz, limestone, dolomite, granite, or feldspar are generally low in shrinkage, whereas those containing standstone, slate, trap rock, or basalt may be relatively high in shrinkage. Therefore, if aggregates of the latter type, or gravels containing a large portion of such minerals, are used, an allowance should be made for a relatively high shrinkage value. Concretes made with soft, porous sandstone may shrink 50 percent more than concretes made with hard dense aggregates (Troxell, Davis, and Kelley 1956).

Aggregate size also has a marked effect on the amount of concrete shrinkage, due to the greater restraint on the shrinkage of the mortar by larger particles. In addition, increasing the maximum aggregate size results in a reduction of the amount of water needed to obtain a given slump.

Lightweight concrete aggregates manufactured by expanding clay or shale have been used to a significant extent in prestressed-concrete structures. High-quality expanded shale or clay aggregates that are not crushed after burning, and hence are coated and less absorbent than crushed materials, have been reported to have drying shrinkage characteristics that are approximately of the same magnitude and rate as those found with normal aggregates (HHFA 1949). Other research has indicated that lightweight aggregates may have shrinkages as much as 50 percent greater than those of normal aggregates (HHFA 1949).

When the use of lightweight aggregates is contemplated, the designer should investigate the shrinkage characteristics of the actual concrete mixture proposed for use.

C. Curing. There is little if any concrete shrinkage during curing, if the concrete is kept moist and the loss of moisture is prevented. Some investigators report that ultimate shrinkage is unaffected by an increase in the duration of curing time (Carlson 1938), but others report a reduction in shrinkage with longer curing periods (ACI 209 1982). There is evidence that curing concrete at an elevated temperature (atmospheric pressure steam curing) will result in a reduction in shrinkage of as much as 30 percent (Klieger 1960; ACI 517 1969). The acceleration in curing that is obtained from steam curing apparently leads to a more complete hydration of the cement; hence, less free water remains available for evaporation, and shrinkage is reduced. Atmospheric pressure steam curing has resulted in shrinkage reductions of 10 to 30 percent for type I cement and 25 to 40 percent for type III cement, when compared to specimens that were moist-cured for 6 days (Hanson 1964).

D. Humidity. The relative humidity during service has a marked effect on shrinkage, with lower humidities resulting in greater shrinkages. Relationships for estimating concrete shrinkage as a function of relative humidity were proposed by Branson and Christianson (1971), and were incorporated in the report of ACI 209 (ACI 209 1982). Variations in temperature and humidity during service result in higher shrinkage (and creep) than is obtained under constant conditions; so estimates of shrinkage made in laboratory tests may be low (Fintel and Khan 1969).

E. Volume-to-Surface Ratio or Average Thickness of Member. The size of the member affects the amount and rate of shrinkage. Because shrinkage is caused by evaporation of moisture from the surface, members that have low volume-to-surface ratios or small average thicknesses will be expected to shrink more, as well as more rapidly, than members having high volume-to-surface ratios or greater average thickness.

F. Water Content. For many years the amount of water in a concrete mixture has been considered a very important factor, if not the single most important factor, affecting the shrinkage of concrete. The shrinkage of concrete made with a particular aggregate has been reported to vary almost directly with the unit water content of concrete (Bureau of Reclamation 1966). Recent research has shown that this is not correct, and that the reduction of water in a concrete mixture through the introduction of a water-reducing admixture does not necessarily result in a reduction of the concrete shrinkage. It still is considered important to restrict the amount of water used in concrete, whether prestressed or not, to the minimum required for the consistency needed for proper placing and compaction. It is recognized that most of the properties considered desirable in concrete are improved by reducing the water content in a concrete mixture. The water required to obtain the necessary plasticity in a concrete mixture is a

function, among other things, of the amount of mortar (cement and sand) in the mixture, and for this reason it is desirable to keep the quantity of mortar as low as possible. Using the maximum size of coarse aggregate available is one way of reducing the mortar content of concrete.

G. Admixtures. Admixtures may increase, decrease, or have practically no effect on the amount of concrete shrinkage. The more commonly used admixtures in prestressed work are of the water-reducing and the water-reducing and retarding types (classified in ASTM C 494 as types A and D, respectively). Admixtures of these types can be further classified according to their general chemical composition and, as such, are categorized as lignosulfonates, organic acids, or polymers. Unpublished test data indicate that the lignosulfonates tend to increase shrinkage (from 5 to 50 percent) when compared with the control concrete (a concrete without admixture but having the same slump). In the same tests, organic acid types of admixtures showed shrinkages from 89 to 117 percent of the control concrete, and the polymer-type admixtures produced shrinkages of from 98 to 112 percent of the control concrete.

3-12 Estimating Shrinkage

The best method of estimating the amount of concrete shrinkage, which should be used in any structural design, is to use shrinkage tests. Established precasting plants and firms engaged in supplying ready mixed concrete, cement, or aggregates should have shrinkage test results available for typical concrete mixtures obtainable in the localities they serve. If such data are not available, designers must either make tests or use their own judgment in estimating the unrestrained shrinkage of concrete for particular conditions. A conservative estimate is recommended if tests are not made.

Long-term shrinkage can be estimated from short-term tests using relationships developed by Brooks and Neville (1975). The relationships for predicting the shrinkage strain at the age of one year, ϵ_{s365}, based upon the shrinkage measured at 28 days, ϵ_{s28}, for moist-cured concrete are:

For moist-cured concrete:

$$\epsilon_{s365} = 347 + 1.08\epsilon_{s28} \tag{3-16}$$

or, for values of ϵ_{s28} less than 100×10^{-6}:

$$\epsilon_{s365} = 52\epsilon_{s28}^{0.45} \tag{3-17}$$

For steam-cured concrete:

$$\epsilon_{s365} = 243 + 1.51\epsilon_{s28} \tag{3-18}$$

or, for values of ϵ_{s28} less than 100×10^{-6}:

$$\epsilon_{s365} = 27\epsilon_{s28}^{0.57} \tag{3-19}$$

The ultimate shrinkage, ϵ_{su}, can be estimated from the shrinkage at the age of one year from:

$$\epsilon_{su} = \frac{\epsilon_{s365}(1.06\epsilon_{s365} - 192)}{1.085\epsilon_{s365} - 265} \tag{3-20}$$

In eqs. 3-16 through 3-20 the shrinkages are expressed in millionth inches per in. (10^{-6} in./in.).

In the absence of experimental data, Branson and Christianson suggest using ultimate shrinkage strains of 800 and 730 millionths inches per inch for moist-cured and steam-cured concrete at relative humidity of 40 percent, respectively (Branson and Christianson 1971).

A relationship for concrete shrinkage at a time of t days after drying commences, ϵ_{st}, as a ratio of the eventual (ultimate) concrete shrinkage, ϵ_s, is contained in the report of Subcommittee II of ACI Committee 209:

$$\frac{\epsilon_{st}}{\epsilon_{su}} = \frac{t^{\alpha}}{f + t^{\alpha}} \tag{3-21}$$

in which α and f are parameters best determined experimentally for a particular concrete, and t is the time in days after drying has commenced. Values of α and f and the ultimate drying shrinkage strain, ϵ_{su}, reported by Subcommittee II are given in Table 3-3. If not determined experimentally, the value of α can be taken as unity for both moist- and steam-cured concrete. The value of f can be assumed to be 35 for concrete that has been moist-cured for seven days or more. For concrete steam-cured for 1 to 3 days before drying commences, the value of f can be taken as 55. The ultimate shrinkage of concrete is reported to vary between 415×10^{-6} and 1070×10^{-6} in./in., and an intermediate value of 780×10^{-6} is recommended for use in the absence of experimental data for a specific concrete.

The shrinkages of moist-cured and steam-cured concrete as a function of time, as predicted by eq. 3-21, are shown plotted in Figs. 3-6 and 3-7, respectively. The parameter α was taken to be equal to one, and the parameter f was taken to be 35 and 55 in Figs. 3-6 and 3-7, respectively.

TABLE 3-3 Values of concrete shrinkage coefficients for use with eq. 3-21 (after ACI Committee 209 1982).

Constant	Low value	Average value	High value	Comment
α	0.90	1.00	1.10	
f	20.00	35.00	130.00	After seven days of moist curing
f		55.00		After one to three days of steam curing
ϵ_u	415	780	1070	

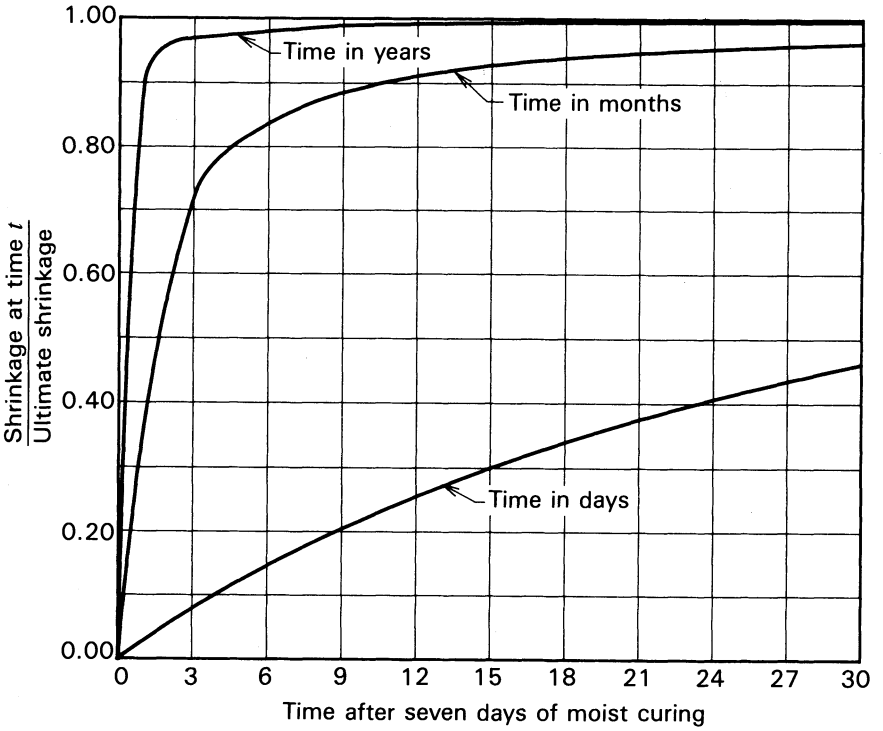

Fig. 3-6. Shrinkage of concrete after being moist-cured for seven days as predicted by eq. 3-21, using unity and 35 for the parameters α and f, respectively.

The Subcommittee II report provides guidance for adjusting the estimated ultimate shrinkage of concrete for several factors. One of these is to account for moist-curing periods other than seven days. Values of the curing period correction coefficient, γ_{cps}, are given in Table 3-4 and plotted in Fig. 3-8. It should be noted that Fig. 3-8 consists of the data from Table 3-4 connected by straight lines; Subcommittee II recommends the use of straight-line interpolation between the values given in Table 3-4. The factor for adjusting the estimated ultimate shrinkage for ambient humidities greater than 40 percent, $\gamma_{\lambda s}$, is given in Fig. 3-9. An adjustment of the estimated ultimate shrinkage for size of the concrete member can be made either on the basis of the ratio of the volume to surface area of the member, γ_{vss}, or on the basis of the average thickness of the member, γ_{hs}; values for these factors are given in Table 3-5 and Figs. 3-10 and 3-11.

Additional correction factors for concrete composition (i.e., slump of concrete γ_{ss}, ratio of fine aggregate to total aggregate content $\gamma_{\psi s}$, cement content γ_{ccs}, and air content $\gamma_{\alpha s}$) given in the Subcommittee II report are intended for use only with the average value of ultimate shrinkage (780×10^{-6} in./in.). These

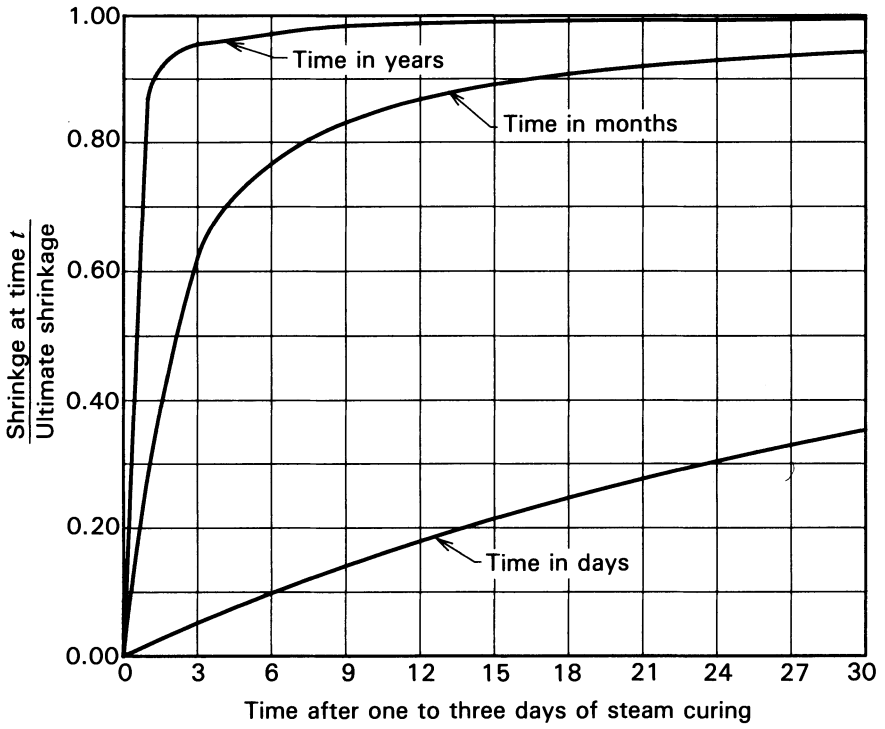

Fig. 3-7. Shrinkage of concrete after one to three days of steam curing as predicted by eq. 3-21, using unity and 55 for the parameters α and f, respectively.

coefficients, presented herein in Figs. 3-12 through 3-15, should not be used when shrinkage data have been determined experimentally for a specific concrete in accordance with ASTM C 157, "Standard Test Method for Length Change of Hardened Cement Mortar and Concrete."

TABLE 3-4 Concrete shrinkage correction coefficients for moist curing periods less than and more than seven days (after ACI Committee 209 1982).

No. of days of moist curing	Shrinkage factor γ_{cps}
1	1.20
3	1.10
7	1.00
14	0.93
28	0.86
90	0.75

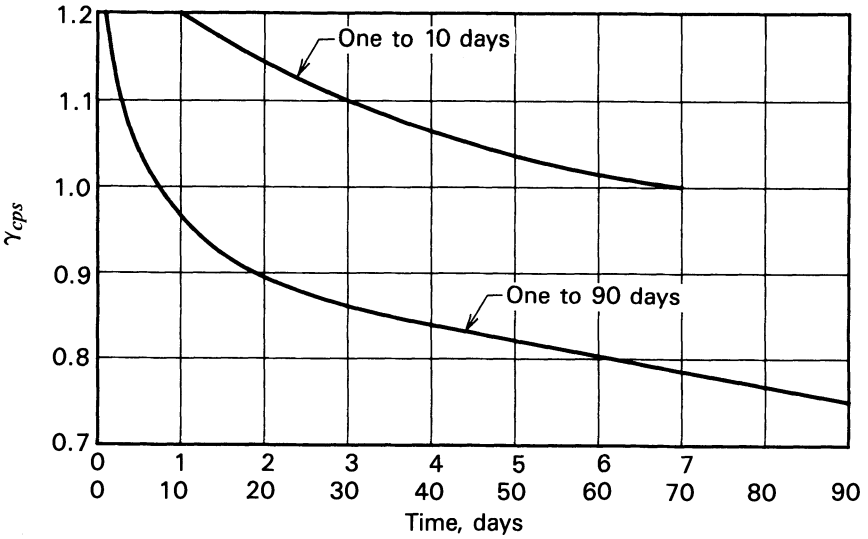

Fig. 3-8. Variation of shrinkage coefficient γ_{cps} for moist curing period as a function of the curing period in days.

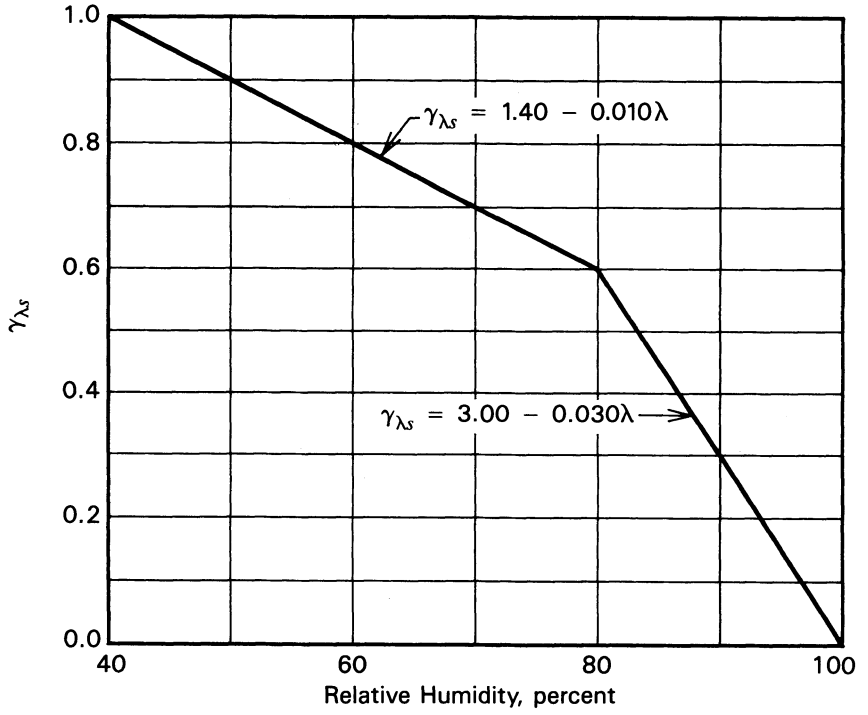

Fig. 3-9. Variation of shrinkage coefficient $\gamma_{\lambda s}$ as a function of relative humidity.

TABLE 3-5 Shrinkage correction factors γ_{hs} for average thickness of members from 2 through 5 in. (after ACI Committee 209 1982).

Average thickness (in.)	Shrinkage factor γ_{hs}
2	1.35
3	1.25
4	1.17
5	1.08

The correction factors provided in the ACI 209 Committee report are used by multiplying the product of the several factors with the average value of the ultimate shrinkage to obtain the adjusted estimated value. It must be emphasized that only one of the two correction factors for member size—that is, the one for the average thickness or the one for volume to surface area should be used. This is illustrated in the examples given on the next page.

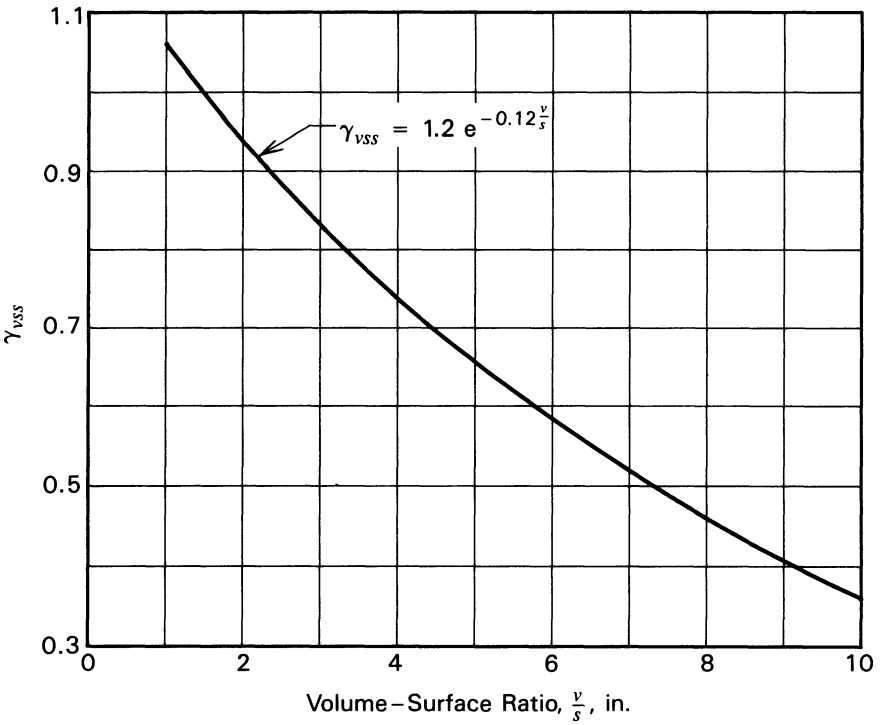

Fig. 3-10. Variation of shrinkage coefficient γ_{vss} as a function of the volume to surface ratio.

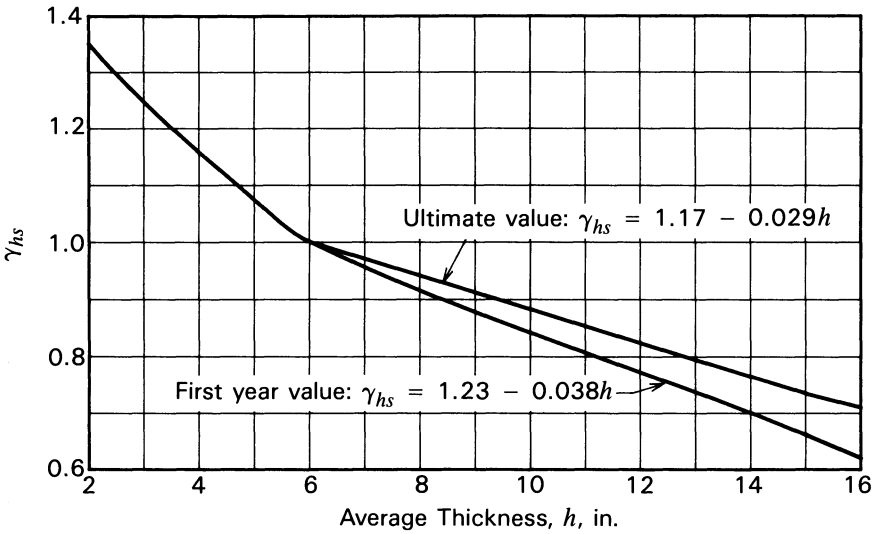

Fig. 3-11. Variation of shrinkage coefficient γ_{hs} as a function of average thickness.

ILLUSTRATIVE PROBLEM 3-2 Estimate the one-year and ultimate shrinkages of a moist-cured concrete if the shrinkage at 28 days is 300 millionths in./in. and the concrete is stored at a constant humidity.

SOLUTION: From eq. 3-16:

$$\epsilon_{s365} = 347 + 1.08 \times 300 = 671 \text{ millionths in./in.}$$

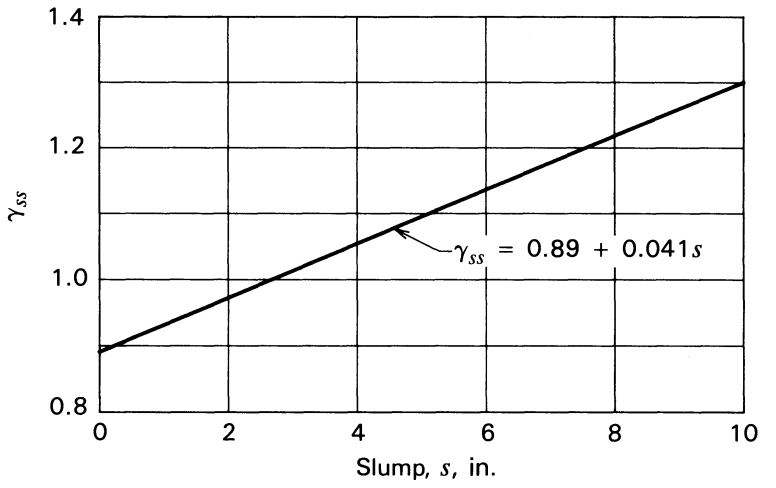

Fig. 3-12. Variation of shrinkage coefficient γ_{ss} as a function of concrete slump.

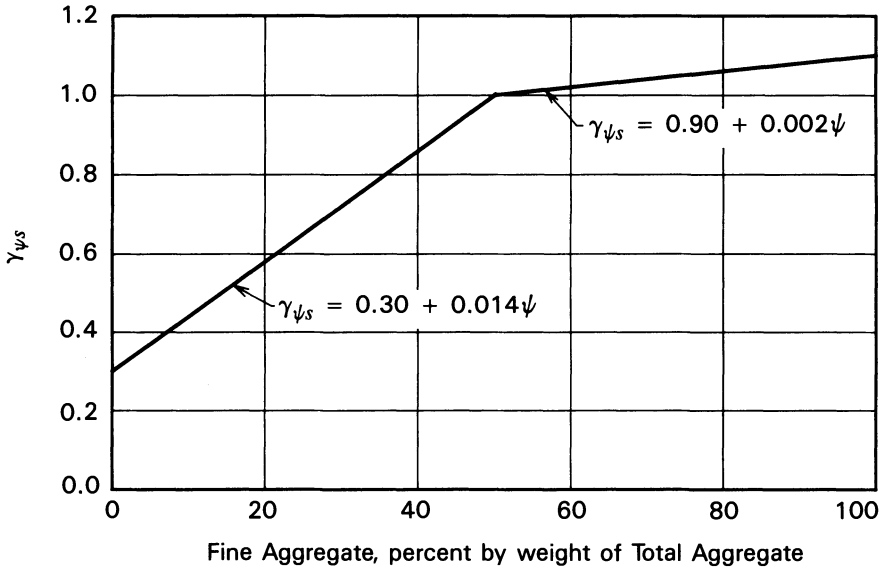

Fig. 3-13. Variation of shrinkage coefficient $\gamma_{\psi s}$ as a function of percentage of fine aggregate in total aggregate by weight.

and from eq. 3-20:

$$\epsilon_{su} = \frac{671(1.06 \times 671 - 192)}{1.085 \times 671 - 265} = 752 \text{ millionths in./in.}$$

Note that in using eq. 3-17 rather than eq. 3-16 (even though the shrinkage at 28 days is greater than 100×10^{-6}), the one-year shrinkage is:

$$\epsilon_{s365} = 25 \times 300^{0.45} = 677 \text{ millionths in./in.}$$

ILLUSTRATIVE PROBLEM 3-3 Estimate the ultimate shrinkage for an unrestrained cast-in-place concrete slab using the procedure recommended by ACI 209 and summarized in Table 3-3 and Figs. 3-8 through 3-15, assuming the following:

1. Concrete is moist-cured for seven days.
2. Ambient relative humidity in service is 50 percent.
3. Average thickness of the slab is 6 in.
4. Concrete slump is 5 in.
5. Fine aggregate content is 60 percent of the total aggregate.
6. Cement content is 650 pcy.
7. Air content is 2 percent.

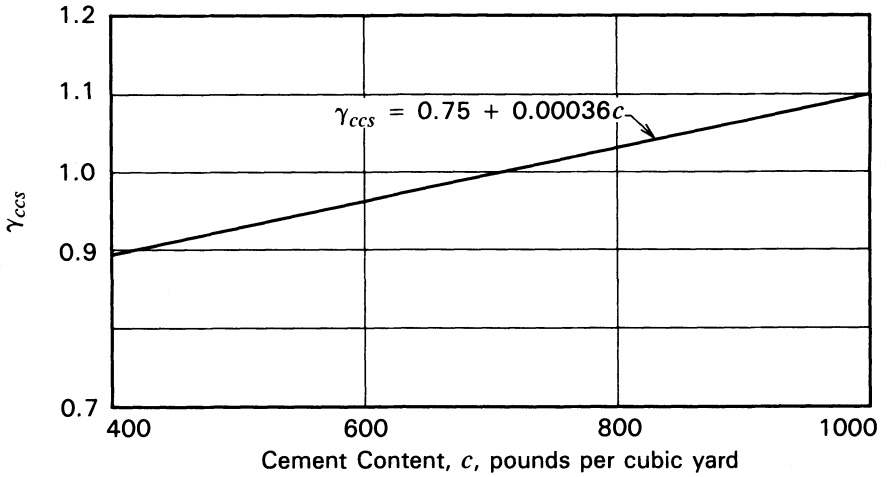

Fig. 3-14. Variation of shrinkage coefficient γ_{ccs} as a function of cement content of the concrete.

The computations are summarized in the Table 3-6. The computation for ultimate shrinkage is:

$$\epsilon_{su} = 780 \times 0.96 = 749 \text{ millionths in./in.}$$

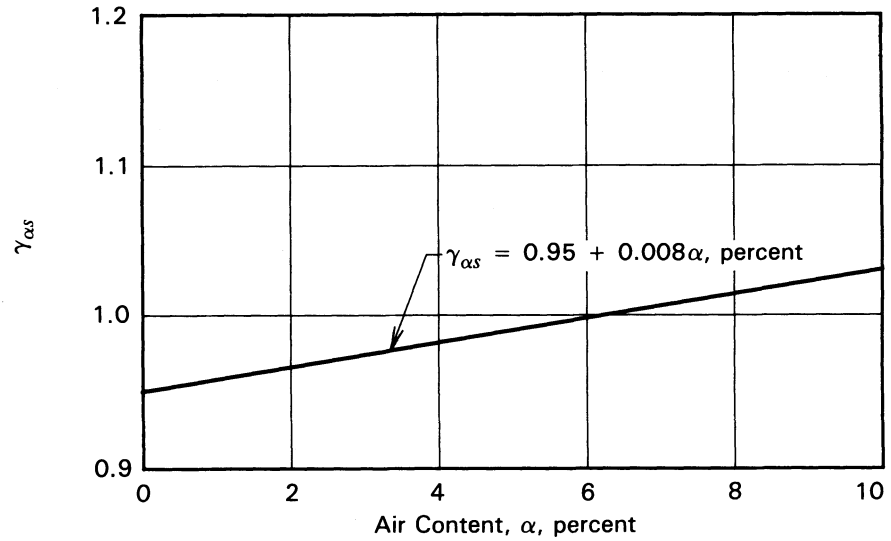

Fig. 3-15. Variation of shrinkage coefficient $\gamma_{\alpha s}$ as a function of air content of the concrete.

TABLE 3-6 Computations for I.P. 3-3.

Item	Shrinkage factor
γ_{cps}	1.00
$\gamma_{\lambda s}$	0.90
γ_{hs}	1.00
γ_{ss}	1.10
$\gamma_{\psi s}$	1.02
γ_{ccs}	0.98
$\gamma_{\alpha s}$	0.97
Product of factors	0.96

3-13 Creep

Creep of concrete is defined as the time-dependent strain that takes place in concrete subjected to constant stress. Under laboratory conditions, creep tests are made with all conditions of the environment, such as temperature and humidity in which the test specimens are stored, being kept as constant as possible. Two types of creep are recognized: basic creep and drying creep. Basic creep is not dependent upon the loss of moisture from the concrete and will occur with concrete protected from drying; however, drying creep, like drying shrinkage, is dependent upon the loss of moisture from the concrete to its environment. Unlike shrinkage, creep is affected by stress in the concrete as well as the maturity of the concrete. Maturity refers to the degree of hydration of the cement in the concrete and is a function of time and temperature history of the concrete; as an approximation, it often is taken as the age of the concrete. For a discussion of maturity as it relates to concrete technology, see "Standard Practice for Curing Concrete" (ACI 308-81). In normal structural engineering applications, one does not distinguish between basic and drying creep; and creep normally is considered to vary directly with the applied stress. The term specific creep is also found in the literature, where specific creep is defined as creep per unit of stress and has the units of inches per inch per pound per square inch.

When concrete is placed under stress, it undergoes an elastic or instantaneous deformation. If the stress is maintained, the deformation increases with the passage of time. If the load is removed after the passage of a period of time, as instantaneous recovery of strain occurs, immediately after which a time-dependent recovery of strain occurs. A permanent strain deformation will remain, however, after the removal of the load and after the creep recovery has reached its maximum value. This is illustrated in Fig. 3-16. In normal engineering practice, creep recovery, because it is relatively small, is ignored in evaluating the effects of creep strain remaining after the load has been removed.

Relaxation of concrete is defined as the loss of stress in concrete that is subjected to constant strain. It is discussed in Sec. 3-15.

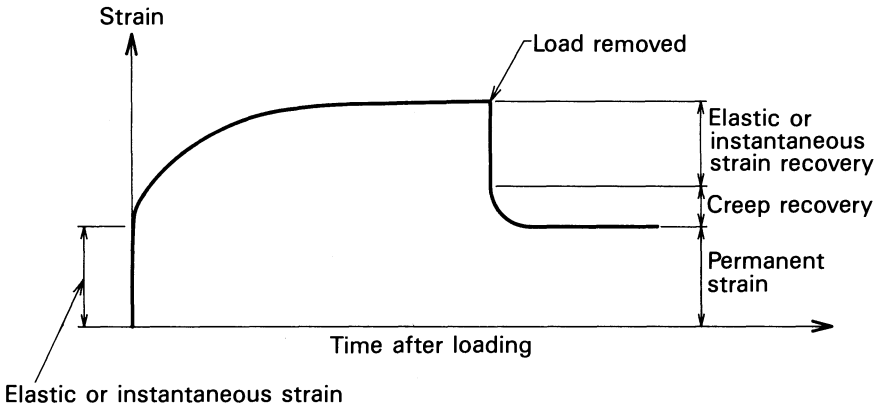

Fig. 3-16. Deformation of concrete as a function of time, illustrating instantaneous deformation, creep deformation, instantaneous recovery, creep recovery, and permanent deformation.

Prestressed concrete normally is not subjected to constant stress or to constant strain. It is subjected to time-dependent changes in stress and strain due to variations in external loads, together with changes in the prestressing forces that result from relaxation of prestressing steel and the shrinkage and creep of the concrete. However, for purposes of computing the loss of prestress and other computations, the loss due to the plasticity of concrete is more commonly based upon creep than on relaxation data for the concrete.

Determination of the creep characteristics of concrete to be used in the design of a concrete structure is best done by performing tests on the specific concrete to be used in the project under conditions that approximate the service conditions to which the actual structure will be exposed. (Neville and Liska 1973).

Progressive producers of prestressed concrete products should have test data available on the concrete normally used in their products for the information and guidance of engineers contemplating the use of those products. Unfortunately, specific test data rarely are available from suppliers of concrete and concrete products; so engineers must have methods for estimating creep at various concrete ages and under various conditions of service.

3-14 Estimating Creep

Creep at the age of one year can be estimated from the amount determined experimentally at the age of 28 days (Brooks and Neville 1975). The relationship for this calculation proposed by Brooks and Neville, in terms of specific creep in order to facilitate the computation, is:

$$\epsilon_{sc365} = 0.127 + 1.70\epsilon_{sc28} \tag{3-22}$$

in which ϵ_{sc365} and ϵ_{sc28} are the values of specific creep at the ages of one year and 28 days, respectively. Ultimate specific creep, ϵ_{scu}, can be estimated from known or estimated values of specific creep at one year by one of the following equations:

$$\epsilon_{scu} = \frac{1.15t\epsilon_{sc365}}{0.396 + t} \tag{3-23}$$

$$\epsilon_{scu} = \frac{1.45t^{0.6}\epsilon_{sc365}}{0.107 + t^{0.6}} \tag{3-24}$$

ILLUSTRATIVE PROBLEM 3-4 A concrete having an elastic modulus of 4×10^6 psi is subjected to a constant stress of 1000 psi at a constant temperature and humidity. The creep strain measured after 28 days of loading was found to be 235×10^{-6} in./in. Using eqs. 3-22 and 3-34, estimate the ultimate creep strain and that at the age of one year.

SOLUTION: The specific creep at 28 days is:

$$\epsilon_{sc28} = \frac{235 \times 10^{-6}}{1000} = 0.235 \text{ millionths in./in./psi}$$

and at 365 days, the specific creep is:

$$\epsilon_{sc365} = 0.127 + 1.70 \times 0.235 = 0.527 \text{ millionths in./in./psi}$$

Assuming ultimate specific creep is obtained at 1500 days:

$$\epsilon_{scu} = \frac{1.45(1500)^{0.6}}{0.107 + (1500)^{0.6}} = 0.763 \text{ millionths in./in./psi}$$

Therefore, the creep strains at one year and at 1500 days (ultimate) are estimated to be as follows:

$$\epsilon_{c365} = 1000\epsilon_{sc365} = 527 \times 10^{-6} \text{ in./in./psi}$$

and:

$$\epsilon_{cu} = 1000\epsilon_{sc1500} = 763 \times 10^{-6} \text{ in./in.}$$

Subcommittee II of ACI Committee 209 has proposed methods to be used in estimating creep for the cases where specific test data are not available. The time-dependent relationship proposed by Subcommittee II is:

$$\frac{\text{Creep strain at time } t}{\text{Ultimate creep strain}} = \frac{v_t}{v_u} = \frac{t^{\psi}}{d + t^{\psi}} \tag{3-25}$$

TABLE 3-7 Concrete creep coefficients for use in eq. 3-25 (after ACI Committee 209 1982).

Constant	Low value	Average value	High value
ψ	0.40	0.60	0.80
d	6	10	30
v_u	1.30	2.35	4.15

in which t is the time in days, measured from the time stress is applied (age at loading), ψ and d are parameters that can be determined experimentally for each particular concrete, and v_u and v_t are the ultimate creep ratio and the creep ratio at time t, respectively. The ranges of the parameters ψ, d, and v_u reported by Subcommittee II, as well as their average values, are given in Table 3-7.

Using the average recommended values for ψ and d, 0.60 and 10, respectively, one can solve eq. 3-25 and plot the values of the ratio of creep at time t to the ultimate creep as a function of time. The results of such a calculation are shown in Fig. 3-17. As in the case of shrinkage, Subcommittee II recom-

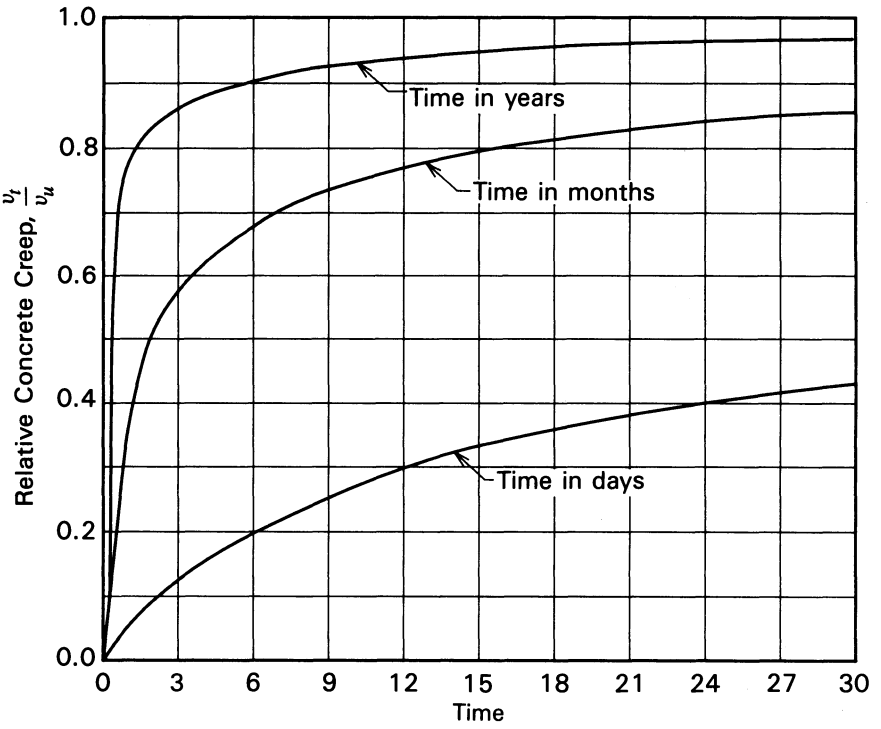

Fig. 3-17. Creep strain of concrete as a function of time using eq. 3-25, with the parameters ψ and d being taken as 0.60 and 10, respectively.

mends the use of the average values of the parameters given in Table 3-7 in the absence of data for the specific concrete to be used. In addition, correction factors are provided for several different items that influence the amount of creep, as follows:

1. Loading age of the concrete, γ_{lac}. Different recommendations are given for moist-cured and steam-cured concrete in Figs. 3-18 and 3-19, respectively. (Table 3-8 is to be used with Figs. 3-18 and 3-19.)
2. Ambient humidity, $\gamma_{\lambda c}$. See Fig. 3-20.
3. Member size, γ_{vsc} or γ_{hc}. Figs. 3-21 and 3-22 are for use with the volume to surface ratio and average thickness methods, respectively. Table 3-9 contains values for γ_{hc} for average thicknesses from 2 through 5 inches.
4. Concrete slump, γ_{sc}. See Fig. 3-23.
5. Fine aggregate to total aggregate ratio, $\gamma_{\psi c}$. See Fig. 3-24.
6. Air content, $\gamma_{\alpha c}$. See Fig. 3-25.

The correction factors are to be used in adjusting the average value of the ultimate creep ratio in the same way as for shrinkage; that is, the product of the several factors is multiplied by the average value of the ultimate creep ratio (2.35) to obtain the adjusted ultimate creep ratio. It should be noted that the engineer may select either member size correction factor (average thickness or volume—surface ratio), but only one of them should be used. As in the case of the computations for shrinkage, the correction factors for concrete slump, fine aggregate ratio, and air content should be used only when the average value of the ultimate creep ratio is being used to estimate the ultimate creep; if experimental data are being used as a basis for the computation, only the factors for loading age, humidity during service, and member size should be used.

TABLE 3-8 Table for ordinates of Figs. 3-18 and 3-19 (after ACI Committee 209 1982).

Age at loading days	$1.25\ t_{lac}^{-0.118}$	$\frac{1.13}{t_{lac}^{-0.094}}$
1	N/A	1.13
2	N/A	1.059
3	N/A	1.019
4	N/A	0.992
5	N/A	0.971
6	N/A	0.955
7	0.994	0.941
10	0.953	0.910
20	0.878	0.853
28	0.844	0.826
60	0.771	0.769
90	0.735	0.740
100	0.726	0.733

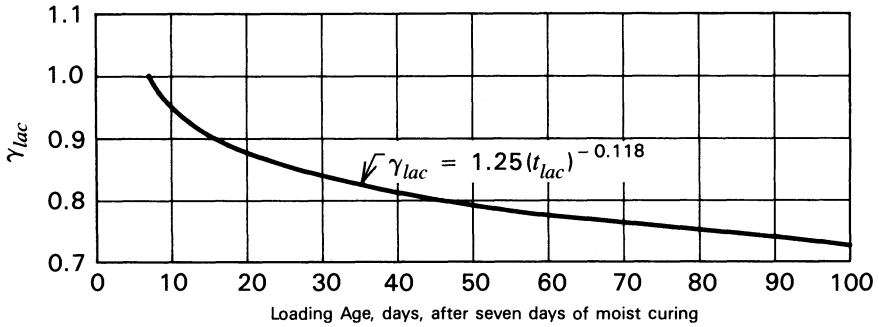

Fig. 3-18. Variation of creep coefficient γ_{lac} for concrete moist-cured for seven days, as a function of time in days.

ILLUSTRATIVE PROBLEM 3-5 Using the data of I.P. 3-3 and assuming the concrete to be 10 days old at the time of loading, compute the estimated ultimate shrinkage strain and ultimate creep ratio, using the average parameters given in Tables 3-3 and 3-7.

SOLUTION: The computations for the creep factors are summarized in Table 3-10. Using the average values for ultimate shrinkage strain and ultimate creep ratio recommended by Subcommittee II of ACI Committee 209, the computations for the ultimate creep ratio and ultimate shrinkage strain are:

$$\text{Ultimate creep ratio} = 2.35 \times 1.06 = 2.49$$
$$\text{Ultimate shrinkage strain} = 7.80 \times 0.96 = 740 \text{ millionths in./in.}$$

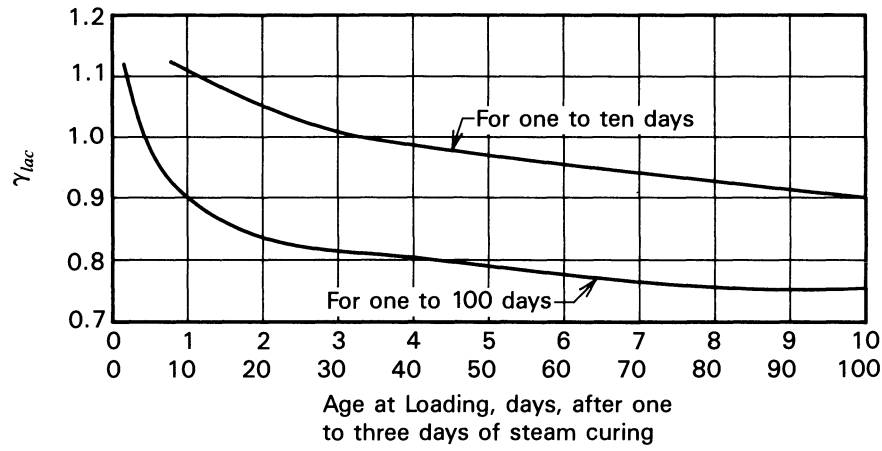

Fig. 3-19. Variation of creep coefficient γ_{lac} for concrete steam-cured for one to three days, as a function of time in days.

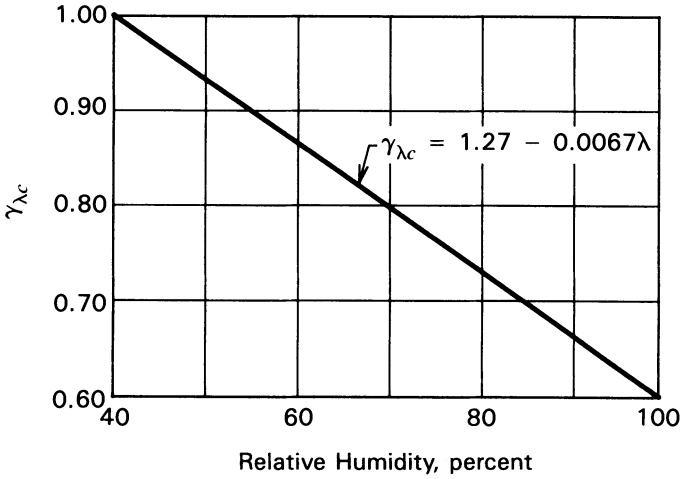

Fig. 3-20. Variation of creep coefficient $\gamma_{\lambda c}$ as a function of relative humidity.

The amount of creep is significantly affected by the age of the concrete at the time of loading. Hence, this factor requires careful consideration when one is computing the long-term deflections and stresses in some forms of prestressed concrete construction, as well as when writing specifications for their construction (see Secs. 7-2, 7-3, 7-4, and 10-9). This is illustrated in Fig. 3-26, in which concrete strains, due to both elastic deformation and creep, are plotted as a function of time (Mathivat 1979). In the figure, the strains shown are relative to the elastic deformation of the concrete when stressed at the age of 28 days. The curve that slopes downward and to the right indicates the elastic deforma-

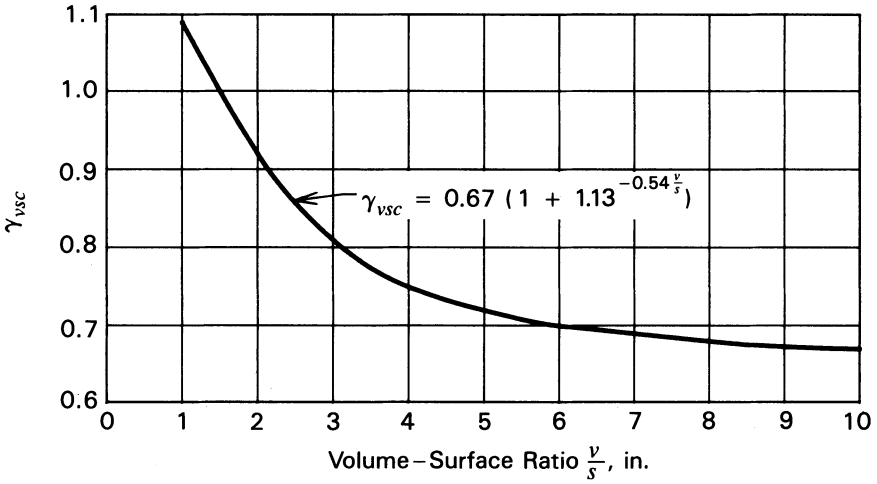

Fig. 3-21. Variation of creep coefficient γ_{vsc} as a function of volume to surface ratio.

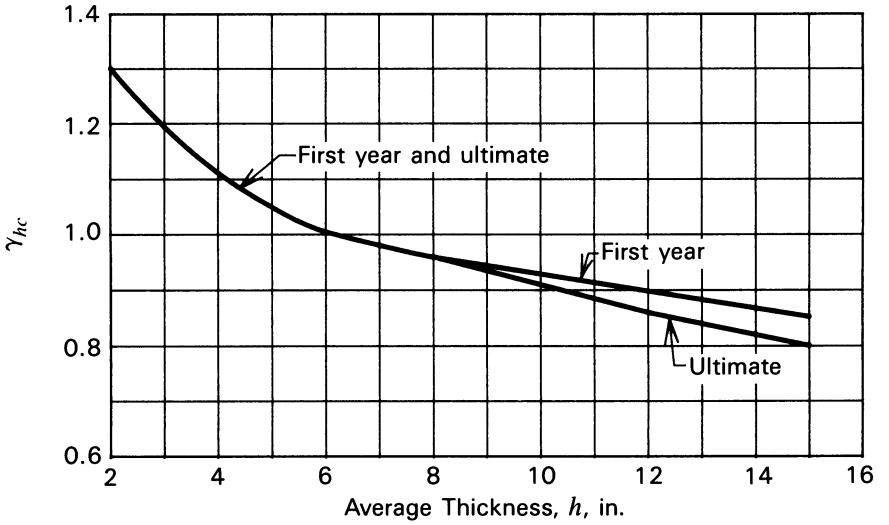

Fig. 3-22. Variation of creep coefficient γ_{hc} as a function of average thickness.

TABLE 3-9 Creep correction factors γ_{hc} for average thickness of members from 2 through 5 in. (after ACI Committee 209 1982).

Average thickness (in.)	Creep factor γ_{hc}
2	1.30
3	1.17
4	1.11
5	1.04

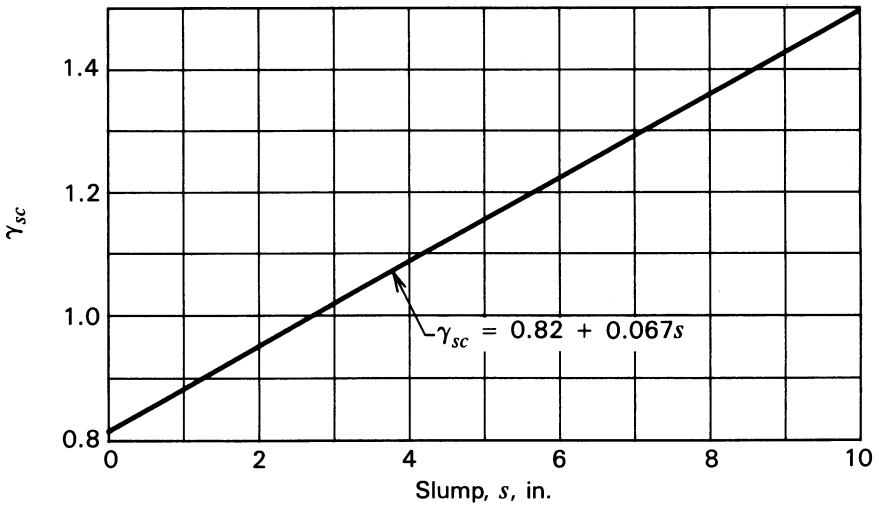

Fig. 3-23. Variation of creep coefficient γ_{sc} as a function of concrete slump.

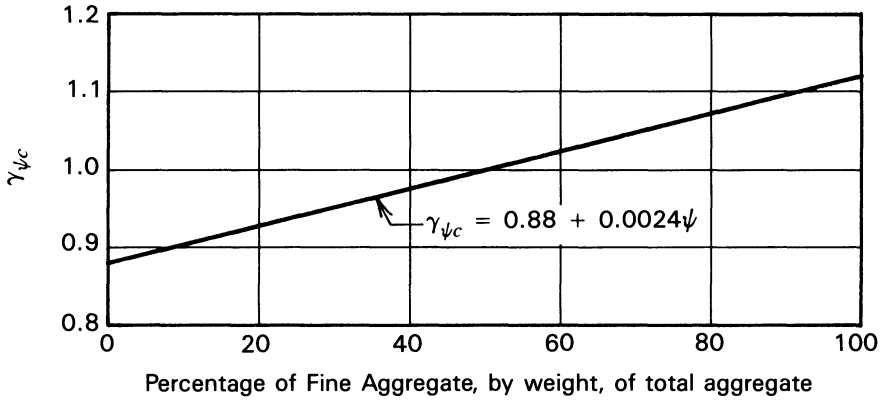

Fig. 3-24. Variation of creep coefficient $\gamma_{\psi c}$ as a function of fine aggregate percentage of total aggregate by weight.

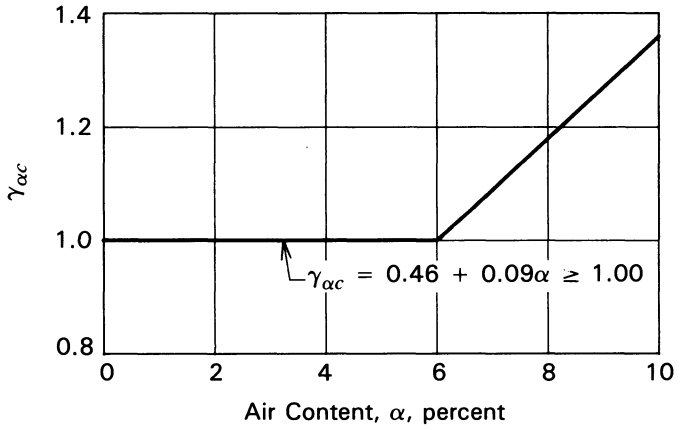

Fig. 3-25. Variation of creep coefficient $\gamma_{\alpha c}$ as a function of air content of the concrete.

TABLE 3-10 Computations for I.P. 3-5.

Item	Creep factor
γ_{lac}	0.95
$\gamma_{\lambda c}$	0.94
γ_{hc}	1.00
γ_{sc}	1.16
$\gamma_{\psi c}$	1.02
$\gamma_{\alpha c}$	1.00
Product	1.06

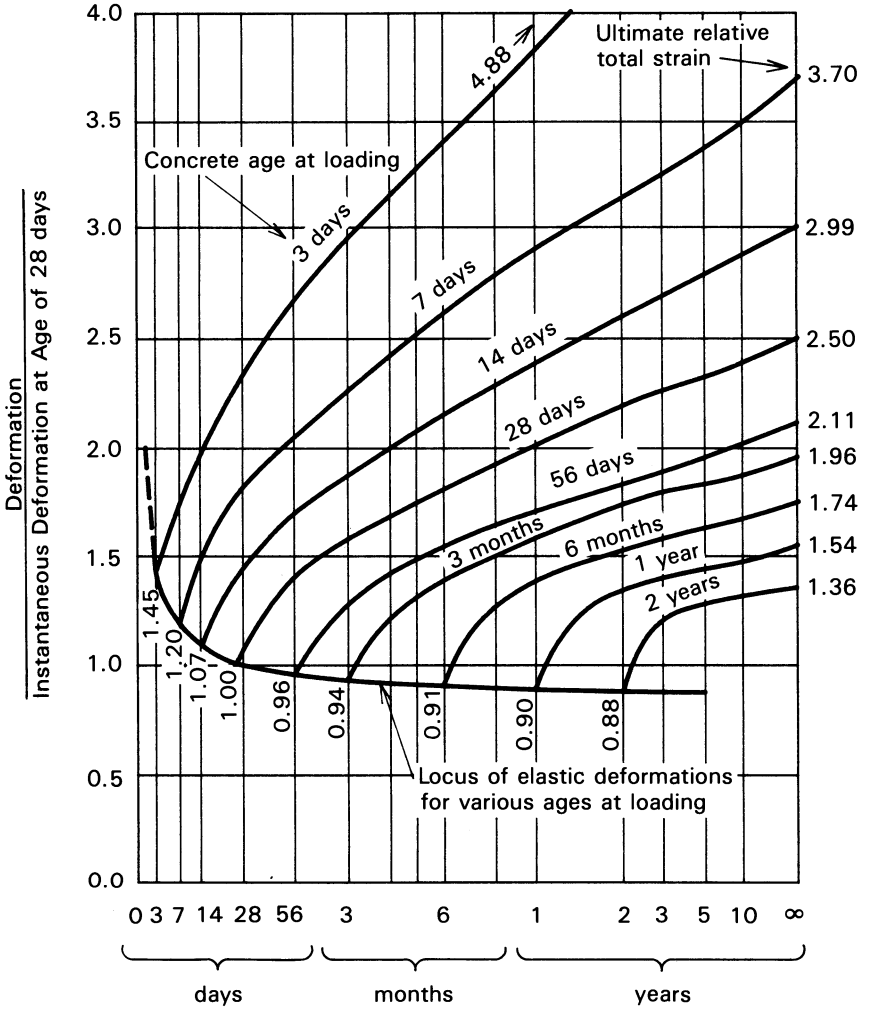

Instantaneous and Creep Strains for Concrete Loaded at Different Ages

Fig. 3-26. Instantaneous and long-term concrete strains for different concrete ages at the time of loading (after Mathivat 1979).

tion at different ages of loading. The curves that originate at the curve indicating elastic deformation and slope upward and to the right illustrate the strain due to creep. The numbers on the creep strain curves indicate the age of the concrete at the time of loading, and the numbers at the ends of the creep strain curves indicate the ultimate total strain (elastic plus creep strain) relative to the elastic strain for loading at the age of 28 days.

3-15 Relaxation of Concrete

It has been explained that when concrete is placed under stress and held at constant strain, the stress in the concrete will decrease with the passage of time. This phenomenon, known as relaxation, can have beneficial results in some cases and adverse effects in others.

If a concrete pavement slab supported on a frictionless subgrade, for example, were to be prestressed by the use of screw jacks reacting against the ends of the slab and immovable abutments, as shown in Fig. 3-27, the slab would be subjected to constant strain if the jack screws remained stationary after their installation and initial stressing (jacking) of the slab. As a result of the relaxation of the concrete, the stress in the slab would decrease with the passage of time, as illustrated in Fig. 3-28, and would eventually approach a stress of approximately one-third of the initial stress (Guyon 1953). If the prestress of the slab were being relied upon to control flexural tensile stresses in the slab, one would have to apply three times the amount of prestress needed at the time of prestressing to have sufficient stress remaining in the slab after the passage of one or two years.

In other situations, the reduction of the stress in the concrete of a reinforced or prestressed member due to relaxation can be beneficial. It is important to understand this property, and the interested reader will find additional information on this subject in Chapter 5 of the ACI Committee 209 report.

3-16 Accelerating Concrete Curing

In the manufacture of structural concrete products, it is often desirable or necessary to accelerate the early hydration of the cement in the products so that a rapid reuse can be made of the mnufacturing facilities. In the case of precast reinforced concrete, it may be necessary to obtain a concrete strength of 1000 to 2000 psi at the age of 24 hours or less so that the products can be safely (without cracking) stripped and moved to storage for further curing, and the forms or molds used to make the products can be reused. Concrete strengths from 3000 to 4500 psi are required in the manufacture of pretensioned concrete

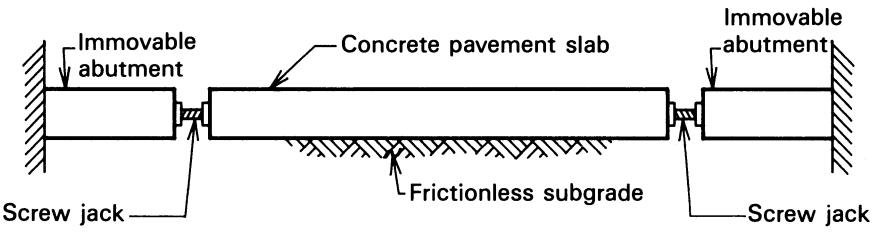

Fig. 3-27. Concrete pavement slab prestressed with screw jacks.

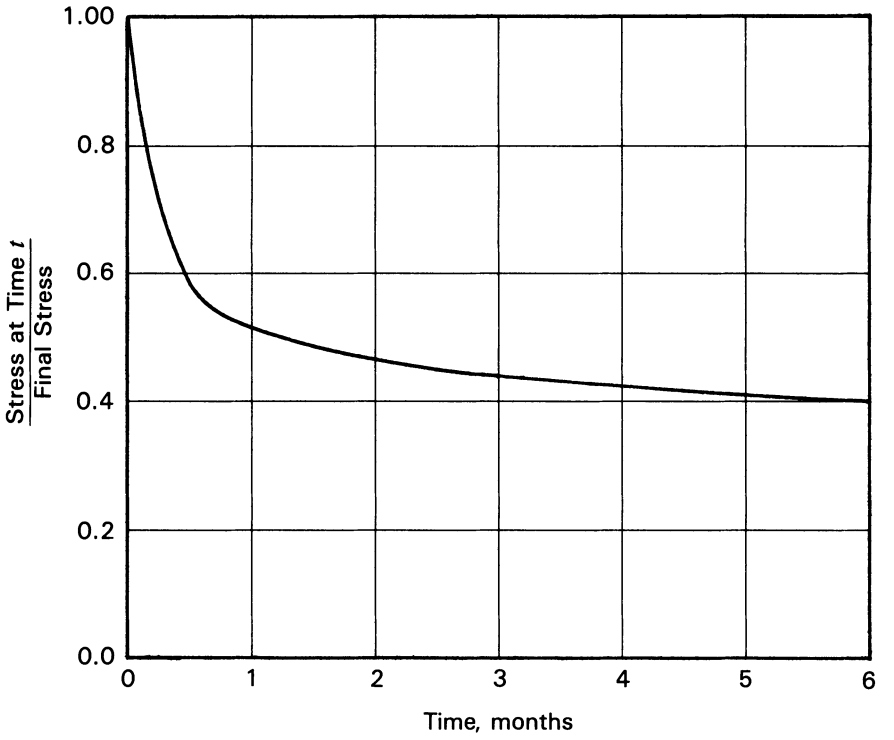

Fig. 3-28. Relaxation of concrete stress as a function of time after concrete is placed under constant strain.

before the pretensioning tendons can be released, the products removed from the prestressing bench, and the facilities reused. The forms for structural concrete and pretensioning benches represent significant capital investments that are tied up while the concrete gains the strength required to complete the production cycle and permit reuse of the facilities; so it is apparent that a nominal expenditure can be justified for accelerating the hydration of the cement if the time required for the concrete to attain the adequate strength can be sufficiently reduced.

Low-pressure or atmospheric-pressure steam curing, which is referred to simply as steam curing in this book, often has been employed to accelerate the curing of concrete. Well-executed steam curing can result in 24-hour strengths equal to or greater than 60 percent of the 28-day strength of concrete specimens cured under standard conditions. This method consists of confining the concrete products in hot, nearly saturated air at atmospheric pressure by isolating them from the normal atmosphere in an enclosure into which steam is injected at low pressure.

A process that employs steam at elevated pressure, which is referred to as

high-pressure steam curing (or autoclaving), is more effective than low-pressure steam curing and has been used in concrete-block-manufacturing plants. High-pressure steam curing requires that the concrete products be placed in a steel pressure vessel in which the pressure can be increased above atmospheric. Consequently, this method is not considered to be feasible for large, structural concrete products, particularly those that are made on pretensioning benches.

Hot water and hot oil are used in some applications, in which case the heated fluid is pumped through longitudinal cavities in the forms or through pipes in or on the casting beds, thus heating the concrete products by radiant heat. This method can give results similar to those obtained by steaming, if the products are kept from drying during heating.

Electric blankets also are used, to provide external heat and to confine the concrete in an insulated enclosure that prevents it from drying.

Chemical admixtures designed to accelerate the hydration of the cement in concrete are available, but some of them contain chloride ions. Chloride ions, except in small amounts, cannot be safely used in prestressed concrete because of the danger of chloride-induced corrosion of the prestressing steel. Furthermore, admixtures that do not contain chloride ions generally do not accelerate the hydration of normal portland cement sufficiently to achieve the strengths required for stressing at an early age. Therefore, in the manufacture of prestressed concrete, the concrete frequently is made with high-early-strength cement, an admixture that accelerates the set, and it is cured with low-pressure steam or some other source of heat.

It is generally agreed that the optimum curing cycle used when heat is employed to increase the early strength of concrete is influenced by the following considerations (Troxell, Davis, and Kelley, 1956; ACI 517 1980; Pfeifer and Marusin, 1981):

1. Delay period: After it is placed and vibrated, the concrete must be allowed to attain its initial set before steam is applied.
2. Rate of increasing the concrete temperature: The temperature of the concrete, and hence the temperature of the atmosphere surrounding it, must be raised at a specific rate to a maximum temperature.
3. Duration of maintaining the maximum temperature: The maximum temperature generally is maintained for a specific period of time.
4. Rate of cooling: The temperature of the concrete must be reduced slowly.

The normal North American procedure is to employ a delay period of two to six hours, depending upon the type of cement being used. The longer delay periods are used when slower-setting cements, retarding admixtures, and higher maximum temperatures are used. Specifications for steam curing usually provide for the temperature in the enclosure in which the concrete is located to be increased at a rate less than 1°F per minute to a maximum temperature that

does not exceed 165°F. In sophisticated plants the temperature of the concrete itself is monitored during the heating process. The concrete temperature frequently exceeds that of the surrounding atmosphere after a period of time, because of the heat released from the hydration of the cement in the concrete being cured. At a rate of 1°F per minute, the maximum concrete temperature will be reached after one or two hours once steaming is commenced, depending upon the starting temperature. The facilities used for steam curing in most prestressing plants do not permit the temperature to be increased at a precise rate; so, the temperature usually is raised in a few small increments over a period of time. The maximum temperature is maintained between 140°F and 165°F for a period that varies from 10 to 20 hours. The products are then allowed to cool more or less slowly, depending upon the practice at the particular plant. Exposing hot concrete products to cold air, particularly under windy conditions, without a controlled cooling period can result in surface cracking and, in extreme cases, complete fracturing of the concrete.

Tests should be performed to determine the optimum curing cycle for use under specific conditions. Through trial and error, one can determine the delay period, maximum temperature, and time required at maximum temperature that will yield optimum results. The optimum cycle will give the strength required at an acceptable time period and cost.

3-17 Cold Weather Concrete

Frequently, in fabricating precast, prestressed concrete members for governmental agencies during winter months, manufacturers are required to conform to standard specifications originally written for job-site winter concrete. The specifications often stipulate that concrete cannot be placed when the temperature of the ambient air reaches a particular minimum value, and that the aggregates and mixing water must be heated to temperature that will keep the temperature of the plastic concrete from falling below a specific minimum value.

These specifications may be necessary for job-site cast concrete that will be placed and allowed to cure without having the surrounding air artificially heated, but imposing them on concrete used in plant-produced products that are steam-cured frequently has detrimental effects on the eventual concrete strength. There is no question that the aggregates used in precasting plants should be kept sufficiently warm to prevent ice or frost formation in the plastic concrete, and that the plastic concrete should not be allowed to freeze. However, higher concrete strengths are obtained for concrete mixed and placed at lower temperatures than for concrete mixed and placed at higher temperatures—a phenomenon attributed to the fact that cool plastic concrete mixtures require less water for workability than do warmer concretes.

The use of very hot mixing water, if done improperly, can have a very serious

detrimental effect on the strength of concrete, and, in particular, on the early strength. If very hot water must be used as the mixing water, it should be added to the aggregates before the cement is introduced to the concrete mixer.

3-18 Fire Endurance of Concrete Elements

One very important property of concrete and concrete structural elements is their ability to resist the effects of heat generated by fire without serious loss of strength or complete collapse. Concrete construction generally is considered to be among the more fire-resistant types of construction. In the past, the fire resistance of many types of prestressed concrete structural elements was determined by testing the elements, following standards and procedures contained in ASTM E 119. Alternative methods for the determination of the fire resistance of concrete structural elements, including prestressed concrete elements, are given in the "Guide for Determining the Fire Endurance of Concrete Elements" (ACI 216R-81). The interested reader is referred to ACI 216R for further information on the alternate methods.

3-19 Allowable Concrete Flexural Stresses

The two most significant design criteria for prestressed concrete in the United States are the *Standard Specifications for Highway Bridges, 14th Edition*, published by the American Association of State Highway and Transportation Officials (AASHTO 1989), and the *Building Code Requirements for Reinforced Concrete* (ACI 318 1989), published by the American Concrete Institute.

The concrete stresses permitted in the AASHTO specifications (Copyright 1989. The American Association of State Highway and Transportation Officials, Washington, D.C. Used by permission) are:

9.15.2.1 Temporary Stresses before losses due to creep and shrinkage

Compression

Pretensioned members ..... $0.60 f'_{ci}$

Post-tensioned members ..... $0.55 f'_{ci}$

Tension

Precompressed tensile zone.....No temporary allowable stresses are specified. See Article 9.15.2.2 for allowable stresses after losses.

Other areas

In tension areas with

no bonded reinforcement ..... 200 psi or $3\sqrt{f'_{ci}}$

Where the calculated tensile stress exceeds this value, bonded reinforcement shall be provided to resist the total tension force in the concrete computed on the assumption of an uncracked section.

The maximum tensile stress shall not exceed
..... $7.5\sqrt{f'_{ci}}$

9.15.2.2 Stresses at service load after losses have occurred

Compression..... $0.40 f'_c$

Tension in the precompressed tensile zone

(a) For members with bonded reinforcement* ..... $6\sqrt{f'_c}$

For severe corrosive exposure conditions, such as coastal areas $3\sqrt{f'_c}$

(b) For members without bonded reinforcement..... 0

Tension in other areas is limited by the allowable temporary stresses specified in Article 9.15.2.1.

*Includes bonded prestressed strands.

9.15.2.3 Cracking Stresses*

Modulus of rupture from tests or if not available,

For normal weight concrete..... $7.5\sqrt{f'_c}$

For sand-lightweight concrete ..... $6.3\sqrt{f'_c}$

For all other lightweight concrete..... $5.5\sqrt{f'_c}$

9.15.2.4 Anchorage and bearing stress:

Post-tensioned anchorage at service load (but not to exceed $0.9 f'_c$). 3000 psi

*The total amount of prestressed and non-prestressed reinforcement shall be adequate to develop an ultimate load in flexure at the critical section at least 1.2 times the cracking load calculated on the basis of the modulus of rupture.

The concrete stresses permitted in ACI 318 are:

18.4 Permissible stresses in concrete—Flexural members

18.4.1 Stresses in concrete immediately after prestress transfer (before time-dependent prestress losses) shall not exceed the following:

(a) Extreme fiber stress in compression $0.60 f'_{ci}$

(b) Extreme fiber stress in tension except as permitted in (c) $3\sqrt{f'_{ci}}$

(c) Extreme fiber stress in tension at ends of simply supported members $6\sqrt{f'_{ci}}$

Where computed tensile stresses exceed these values, bonded auxiliary reinforcement (non-prestressed or prestressed) shall be provided in the tensile

zone to resist the total tensile force in concrete computed with the assumption of an uncracked section.

18.4.2 Stresses in concrete at service loads (after allowance for all prestress losses) shall not exceed the following:

(a) Extreme fiber stress in compression $0.45 f'_c$

(b) Extreme fiber stress in tension in precompressed tensile zone $6\sqrt{f'_c}$

(c) Extreme fiber stress in tension in precompressed tensile zone of members (except two-way slab systems) where analysis based on transformed cracked sections and on bilinear moment-deflection relationships show that immediate and long-time deflection comply with requirements of Section 9.5.4, and where cover requirements comply with Section 7.7.3.2. $12\sqrt{f'_c}$

18.4.3 Permissible stresses in concrete of Section 18.4.1 and 18.4.2 may be exceeded if shown by test or analysis that performance will not be impaired.

In the above, f'_c is defined as the specified compressive strength of the concrete in psi and f'_{ci} is the compressive strength of the concrete at the time of initial prestress.

The reader's attention is called to the Commentary on Building Code Requirements for Reinforced Concrete (ACI 318-89), Secs. 18.4.2(b) and 18.4.2(c), in which it is pointed out that the concrete covers specified in Secs. 7.7.3.1 and 7.7.3.2 are closely related to the allowable tensile stresses permitted by ACI 318.

Comparison of these allowable stresses will show that the requirements of AASHTO are more conservative than those of ACI 318. This is understandable and reasonable because bridge structures are exposed to more severe conditions of service (i.e., fatigue, temporary overloads, etc.) than are buildings.

REFERENCES

ACI Committee 116. 1985. Cement and Concrete Terminology, ACI 116R-85. SP-19(85). Detroit. American Concrete Institute.

ACI Committee 209. 1982 (Rev. 1986). Prediction of Creep, Shrinkage, and Temperature Effects in Concrete Structures, ACI 209R-82 (Rev. 1986). Detroit. American Concrete Institute.

ACI Committee 214. 1977 (Rev. 1983). Recommended Practice for Evaluation of Strength Test Results of Concrete, ACI 214-77 (Rev. 83). Detroit. American Concrete Institute.

ACI Committee 216. 1981 (Rev. 1987). Guide for Determining the Fire Endurance of Concrete Elements. *Concrete International Design and Construction* 3(2): 13–47 and 9(11): 65.

ACI Committee 308. 1981 (Rev. 1986). Standard Practice for Curing Concrete, ACI 308-81 (Rev. 86). Detroit. American Concrete Institute.

ACI Committee 318. 1989. *Building Code Requirements for Reinforced Concrete*, ACI 318-89. Detroit. American Concrete Institute.

ACI Committee 363. State-of-the-Art Report on High-Strength Concrete, ACI 363R-84. Detroit. American Concrete Institute.

ACI Committee 517. 1980. Accelerated Curing of Concrete at Atmospheric Pressure—State of the Art, ACI 517.2R-80. Detroit. American Concrete Institute.

ACI Committee 517. 1969. Recommended Practice for Atmospheric Pressure Steam Curing of Concrete. *Journal of the American Concrete Institute* 66(8):629–46.

American Association of State Highway and Transportation Officials. 1989. *Standard Specifications for Highway Bridges. Fourteenth Edition.* Washington, D.C.

ASTM C 33. 1986. Specification for Concrete Aggregates. Philadelphia. American Society for Testing and Materials.

ASTM C 39. 1986. Test Method for Compressive Strength of Cylindrical Concrete Specimens. Philadelphia. American Society for Testing and Materials.

ASTM C 150. 1986. Specification for Portland Cement. Philadelphia. American Society for Testing and Materials.

ASTM C 157. 1986. Standard Test Method for Length Change of Hardened Hydraulic-Cement Mortar and Concrete. Philadelphia. American Society for Testing and Materials.

ASTM C 192. 1988. Test Method of Making and Curing Concrete Test Specimens in the Laboratory. Philadelphia. American Society for Testing and Materials.

ASTM C 260. 1986. Specifications for Air-Entraining Admixtures for Concrete. Philadelphia. American Society for Testing and Materials.

ASTM C 330. 1987. Specification for Lightweight Aggregates for Structural Concrete. Philadelphia. American Society for Testing and Materials.

ASTM C 469. 1987. Test Method for Static Modulus of Elasticity and Poisson's Ratio in Concrete in Compression. Philadelphia. American Society for Testing and Materials.

ASTM C 494. 1986. Specification for Chemical Admixtures for Concrete. Philadelphia. American Society for Testing and Materials.

ASTM C 595. 1986. Specifications for Blended Hydraulic Cements. Philadelphia. American Society for Testing and Materials.

ASTM E 119. 1988. Methods of Fire Tests of Building Construction and Materials. Philadelphia. American Society for Testing and Materials.

Baidar, B., Jaeger, L. G., and Mufti, A. A. 1989. Elastic Modulus of Concrete from Compression Tests. *ACI Materials Journal* 86(3):220–24.

Bazant, Z. P. 1972. Prediction of Concrete Creep Effects Using Age-Adjusted Effective Modulus Method. *Journal of the American Concrete Institute* 69(4):212–17.

Branson, D. E. and Christianson, M. L. 1971. Time Dependent Concrete Properties Related to Design-Strength and Elastic Properties, Creep and Shrinkage. *Designing for Effects of Creep, Shrinkage, Temperature in Concrete Structures.* Raymond C. Reese, Symposium Chairman, Special Publication 27. Detroit. American Concrete Institute. 257–77.

Brooks, J. J. and Neville, A. M. 1975. Estimating Long-Term Creep and Shrinkage from Short-Term Tests. *Magazine of Concrete Research* 27(90):3–12.

Bureau of Reclamation. 1966. *Concrete Manual.* Denver. U.S. Department of Commerce.

Carlson, R. W. 1938. Drying Shrinkage of Concrete as Affected by Many Factors. *Proceedings* 38(II):419–37. Philadelphia. American Society for Testing and Materials.

Fintel, M. and Khan, F. R. 1969. Effects of Column Creep and Shortening. *Journal of the American Concrete Institute* 66(12):957–67.

Guyon, Y. 1953. *Prestressed Concrete.* New York. John Wiley and Sons, Inc.

Hanson, J. A. 1964. Prestress Loss as Affected by Type of Curing. *Journal of the American Concrete Institute* 9(2):69–93.

HHFA. 1949. *Lightweight Aggregate Concrete.* Washington, D.C. Housing and Home Finance Agency.

Klieger, P. 1960. Some Aspects of Durability and Volume Change of Concrete for Prestressing. Research Department Bulletin 118. Skokie. Portland Cement Association.

Klink, S. A. 1985. Actual Poisson Ratio of Concrete. *Journal of the American Concrete Institute* 82(6):813–17.

Mathivat, J. 1979. *The Cantilever Construction of Prestressed Concrete Bridges.* New York. John Wiley and Sons, Inc.

Neville, A. M. 1971. *Hardened Concrete: Physical and Mechanical Aspects.* Detroit. American Concrete Institute.

Neville, A. M. and Liska, W. Z. 1973. Accelerated Determination of Creep of Lightweight Aggregate Concrete. *Civil Engineering and Public Works Review* 68(803):515–19.

Pfeifer, D. W. and Marusin, S. 1981. Energy-Efficient Accelerated Curing of Concrete. Chicago. Prestressed Concrete Institute.

Szilard, Rudolph. 1969. Corrosion and Corrosion Protection of Tendons in Prestressed Concrete Bridges. *Journal of the American Concrete Institute* 66(1):42–59.

Trost, H. 1967. Implications of the Superposition Principle in Creep and Relaxation Problems for Concrete and Prestressed Concrete. *Beton und Stahlbetonbau* 10:230–38 and 261–69.

Troxell, G. D., Davis, H. E., and Kelley, J. W. 1956. *Composition and Properties of Concrete.* New York. McGraw-Hill Book Company. Chapter 3—Problems.

PROBLEMS

1. Prepare a plot showing the variations in concrete tensile strength and modulus of rupture as predicted by eqs. 3-2 and 3-3. Use the product of concrete compressive strength and unit weight as the ordinate with values of the compressive strength from 2000 psi to 10,000 psi and unit weights from 100 to 160 pcf. Use values of the tensile strength and modulus of rupture as the abscissa.

SOLUTION: The computations required for the plot are shown in Table 3-11, and the results are plotted in Fig. 3-29.

TABLE 3-11 Summary of computations for Problem 1.

wf'_c	$\sqrt{wf'_c}$	$0.33\sqrt{wf'_c}$	$0.60\sqrt{wf'_c}$	$0.70\sqrt{wf'_c}$
200,000	447	149	268	313
600,000	775	258	465	542
1,000,000	1000	333	600	700
1,400,000	1183	394	710	828
1,800,000	1342	447	805	939

2. Prepare a plot of f_{ct} versus E_{ct} for values of the variable w (unit weight of concrete) of 100, 120, 140, and 160 pcf. Use f_{ct} as the ordinate with values from 2000 to 10,000 psi.

SOLUTION: The computations are summarized in Table 3-12 and plotted in Fig. 3-30.

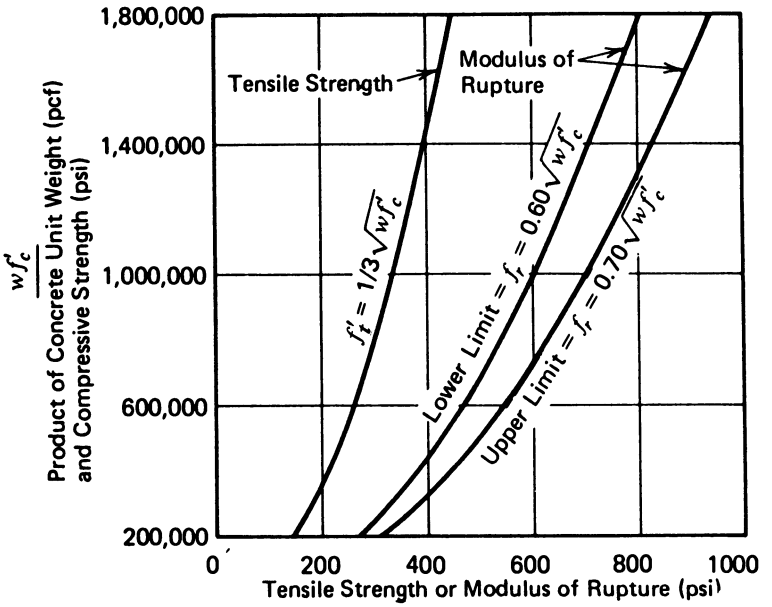

Fig. 3-29. Plot of the results of Problem 1.

TABLE 3-12 Computations for Problem 2: Values of the elastic modulus in millions of psi for unit weights of concrete from 100 to 160 pcf.

	Unit Weight of Concrete (pcf)			
f'_c	100	120	140	160
2,000	1.48	1.94	2.44	2.99
4,000	2.09	2.74	3.46	4.22
6,000	2.56	3.36	4.23	5.17
8,000	2.95	3.88	4.89	5.97
10,000	3.30	4.38	5.47	6.68

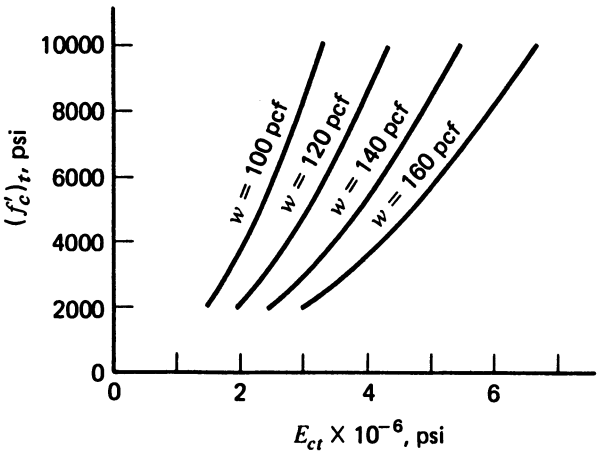

Fig. 3-30. Plot of the results of Problem 2.

3. A piece of concrete 10 ft long is stressed in compression to 500 psi. The initial (elastic) shortening is 0.020 in. After two years the total shortening is 0.065 in. Determine the creep ratio at the age of two years.

SOLUTION:

$$\text{Creep ratio} = \frac{0.065 - 0.020}{0.020} = 2.25$$

4. A particular concrete is believed to have a creep ratio of 3.10. At the time it is stressed, it undergoes a strain of 230 millionths inches per in. Determine the estimated eventual total strain if the concrete is kept under constant stress in a uniform environment.

SOLUTION:

$$\text{Creep strain} = 3.10 \times 230 = 713 \times 10^{-6} \text{ in./in.}$$

$$\text{Total strain} = 943 \times 10^{-6} \text{ in./in.}$$

5. For the concrete in Problem 4, if the modulus of elasticity is 4000 ksi at the time of stressing, determine the effective modulus that eventually will be attained.

SOLUTION: Using eq. 3-9:

$$E_{ce} = \frac{4000}{1 + 3.10} = 976 \text{ ksi}$$

6. Determine the ratio of creep strain, at the age of five years, that one might expect for a particular normal-weight concrete made with Type I cement, if

TABLE 3-13 Summary of computations for Problem 6.

Age of concrete at loading (days)	Relative strength	Relative elastic modulus	Relative elastic deform.	Relative creep deform.
7	0.70	0.84	1.19	2.38
28	1.00	1.00	1.00	2.00
90	1.12	1.06	0.94	1.76

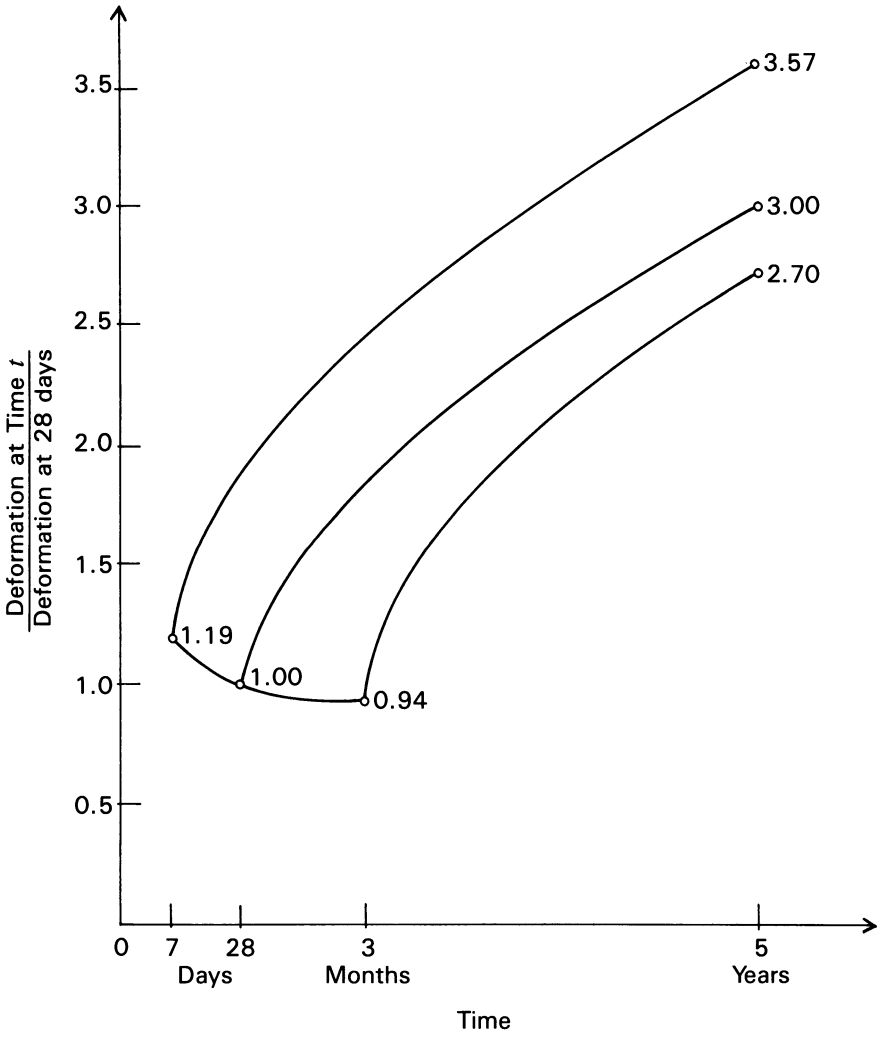

Fig. 3-31. Plot of the results of Problem 6.

TABLE 3-14 Summary of results for Problem 7.

Time (months)	Stress remaining (psi)
1	160
3	132
6	119
∞	100

the concrete were placed under constant stress at the ages of 7, 28, and 90 days. Prepare a plot of the results that is similar to Fig. 3-26, assuming that the creep ratio for loading at the age of 28 days is 2.00.

SOLUTION: The computations are made using eqs. 3-1 for strength and 3-5 for elastic modulus and Fig. 3-18 for the effect of age at loading on creep strain. The results of the computations are summarized in Table 3-13 and plotted in Fig. 3-31. It should be noted that the relative total deformations are 3.57, 3.00, and 2.70 for loading at the ages of 7, 28, and 90 days, respectively.

7. A concrete pavement for an airfield is to be prestressed by placing jacks at the ends of the pavement. The jacks are to be supported by stiff, nonyielding abutments at each end of the pavement. If the pavement is to be stressed initially to a uniform prestress of 300 psi, and assuming there is no friction between the slab and the subgrade (friction does exist in actual applications of this type), determine the stress one would expect to remain in the pavement after one, three, and six months, as well as at an infinite number of months.

SOLUTION: The jacks would cause the pavement to be placed in a condition of constant strain. Hence, the stress in the pavement would decrease with the passage of time because of relaxation of the concrete. From Fig. 3-28, one would expect the results shown in Table 3-14.

4 Basic Principles for Flexural Design

4-1 Introduction

The basic principles and mathematical relationships used in the design and analysis of prestressed-concrete flexural members are not unique to this type of construction. Virtually all of the fundamental relationships are based upon the normal, basic assumptions of elastic design, which form the basis of the study of the strength of materials. Although the form in which the relationships appear in a discussion of prestressed concrete may be somewhat modified to facilitate their application, the student of engineering should have little difficulty in understanding these modified relationships.

Two major forms of design problems are encountered by the engineer engaged in the design of prestressed concrete flexural members. Such problems frequently are referred to as the review of a member or as the design of a member.

The review of a member consists of determination of the concrete flexural stresses and deflections under various conditions of service load and prestressing in order to confirm their compliance with the applicable design criteria. In addition, the strength of the member in bending, shear, and bond must be determined to equal or exceed the minimum strength requirements of the design criteria. To review a member as described here, the dimensions of the concrete

section, the properties of the materials, the amount and eccentricity of the prestressing steel, the amount of the nonprestressed reinforcement, and the amount of the web reinforcement must be known.

The design of a member consists of selecting and proportioning a concrete section in which the stresses in the concrete do not exceed the permissible values under any combination of service loads and prestressing. Design also includes determination of the amount and eccentricity of the prestressing force required for the specific section. An important aspect of the design of a member under service load conditions is calculation of deflection and confirmation that the predicted deflections will not exceed the maximum values permitted by applicable design criteria and are within limits deemed acceptable to the designer. The design of a member must include a study of the flexural strength that the section can develop under design load, and a determination of the amount of nonprestressed flexural reinforcing that may be required. Additionally, a study of the shear stresses must be made, and the amount of web reinforcing required for adequate shear strength under design loads must be determined. Consideration of tendon development lengths, both for flexural strength and, in the case of pretensioned tendons, for transfer length, is included in the design of a member. It must be emphasized that the design of a flexural member normally is done by trial. The designer must assume a concrete section and compute the prestressing force and eccentricity required to confine the concrete stresses within the allowable limits under all conditions of service loads. In addition to confirming compliance with service loading criteria, the designer must make a complete strength analysis in order to confirm compliance with the strength requirements of the applicable design criteria. In the design process, several adjustments of the trial section normally are required before a satisfactory solution is found.

This chapter is devoted to a consideration of fundamental principles pertaining to determination of the concrete stresses due to prestressing, determination of the prestressing force and eccentricity required for a specific distribution of stresses due to prestressing, consideration of the pressure line in simple flexural members loaded in the elastic range, and other topics related to flexural analysis and design. The problems given in this chapter are confined to the review type. The procedures used in preparing preliminary designs by trial are treated in Sec. 9-8.

The elastic analysis and design of prestressed flexural members can be done rapidly and accurately only after the fundamental theorems and axioms have been thoroughly mastered. Many of the operations discussed in this chapter can be done more rapidly by the use of the simple expedients treated in Chapter 7. These classical methods should be well understood, however, before one attempts to use the expedients. The design and analysis of continuous prestressed members, which are treated in Chapter 10, also require complete familiarity with the principles presented in this chapter.

4-2 Mathematical Relationships for Prestressing Stresses

Although prestressing forces sometimes are applied to a prismatic member concentrically, it is far more common for them to be applied eccentrically, as was explained in Sec. 1-2 and is illustrated in Fig. 4-1. The stresses in a prismatic concrete section prestressed with an eccentric force are analyzed as combined stresses, that is, the stresses due to an axial force combined with the stresses due to a moment. The familiar expression for the combined stresses at a section subject to an axial force and a moment is:

$$f = \frac{F}{A} \pm \frac{My}{I} \tag{4-1}$$

in which f is the fiber stress at a distance y from the centroidal axis, F is the axial prestressing force, M is the moment acting on the section, and A and I are the area and moment of inertia of the cross section, respectively.

Because the moment due to the prestressing is equal to the prestressing force multiplied by the eccentricity of this force (i.e., $M = Pe$), and because the quotient of the moment of inertia and the area of the cross section is equal to the square of the radius of gyration of the cross section (i.e., $r^2 = (I/A)$), the general eq. 4-1 be written:

$$f = \frac{F}{A}\left(1 \pm \frac{ey}{r^2}\right) \tag{4-2}$$

The sign convention used in the following discussion, as well as in the remainder of this book, is based upon tensile stresses, forces, strains, and elongations being positive; moments causing tensile stresses at the bottom fibers being positive; curvatures and slopes of stress diagrams for positive bending moments being positive; and incremental changes in values that are increases (i.e., increases in stress, strain, etc.) being positive. The positive and negative signs are included in the symbols for a parameter; concrete shrinkage at time t (days), which is represented by ϵ_{st}, is always negative, but a change in stress,

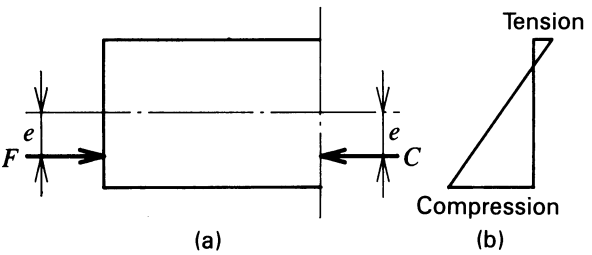

Fig. 4-1. (a) Freebody diagram of the end of a prism of concrete prestressed with an eccentrically applied force. (b) Diagram of concrete stresses.

such as Δf_t, could be positive or negative, depending upon whether it is an increase or a decrease in the stress. Furthermore, the values of the ordinates, y, such as eccentricity e and the distances to the extreme fibers of a cross section, are taken as positive when measured downward from the centroidal axis of the cross section in the computation of fiber stresses. In special cases in this book, the values of the ordinates, y, are measured from an arbitrarily selected reference point; the reader's attention will be called to this difference when it is applied to a particular computation. Using this sign convention, eq. 4-2 can be rewritten for the top and bottom fibers of a beam as:

$$f_t = \frac{C}{A}\left(1 + \frac{ey_t}{r^2}\right) \tag{4-3}$$

$$f_b = \frac{C}{A}\left(1 + \frac{ey_b}{r^2}\right) \tag{4-4}$$

where f_t and f_b are the stresses in the top and bottom fibers due to the prestressing alone, respectively. As noted above, the positive and negative signs are included in the notation used in eqs. 4-3 and 4-4 (i.e., C, the resultant compressive force acting on the section under consideration, and y_t are negative, and y_b is positive, as is e when it is below the centroidal axis).

These relationships are the same for the stresses resulting from the initial and the final prestressing forces (see Sec. 1-2). In computing these stresses, one would, of course, use the value of C for the initial prestressing force when computing the initial stresses due to prestressing and the value of C for the final prestressing force when computing the final stresses. Frequently, particularly in preliminary design, the designer assumes a ratio between the final and the initial prestressing forces for design purposes because the reduction of the prestressing force (loss of initial prestress) cannot be estimated accurately until the design is nearly complete (see Secs. 7-2 and 7-3). Therefore, if the designer bases his or her computations on the final prestressing force and has assumed that the total loss will be 15 percent of the initial force, for example, the stresses resulting from the initial prestressing force can be determined by dividing the final stresses by 0.85.

The experienced designer generally prefers to design with the final prestressing force assumed to be from 75 to 90 percent of the initial force. A comprehensive study of the losses of prestress cannot be made until the basic design is finalized. If, when the loss of prestress study is made, it is found that the loss will be greater than assumed, the initial prestressing force can be increased so that the final force will be satisfactory. In addition, strength requirements of design criteria frequently control the amount of prestressed flexural reinforcement required; serviceability requirements may or may not control the amount of prestressing required. The advantage of this procedure will be apparent after consideration of the data presented in Chapter 9.

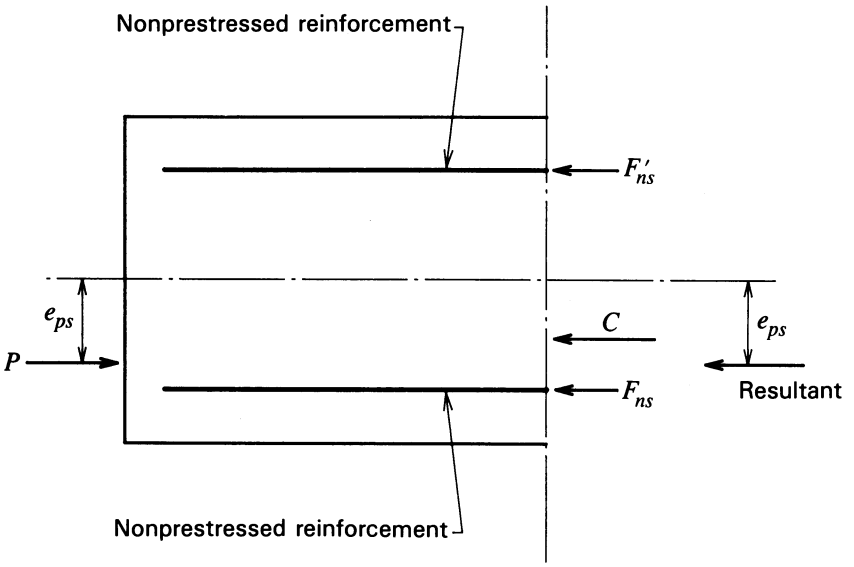

Fig. 4-2. Freebody diagram of the end of a prism of reinforced concrete prestressed with an eccentrically applied force.

It should be recognized that most prestressed concrete members contain nonprestressed bonded reinforcement in addition to the prestressed reinforcement. The nonprestressed reinforcement may be provided in the member simply to facilitate construction, or it may be included for strength or serviceability considerations. In any case, if reinforcement of this type is provided in a member, it too will become prestressed by the prestressing force. This is illustrated in Fig. 4-2. For the purposes of this discussion on the basic principles of designing prestressed concrete members, it is assumed the concrete does not contain embedded nonprestressed reinforcement, and the prestressing force P is equal and opposite to the resultant compressive force in the concrete, C. The effect of nonprestressed reinforcement, which can be significant in certain situations, is discussed in Secs. 7-2, 7-3, and 9-2.

ILLUSTRATIVE PROBLEM 4-1 Compute the stresses due to prestressing alone in a beam with a rectangular cross section 10 in. wide and 12 in. high that is prestressed by a final force of 120 k at an eccentricity of -2.5 in. (above the centroidal axis). State whether the stresses are compressive or tensile. Compute the stresses due to the initial prestressing force if the ratio between the final force and the initial force is 0.85.

SOLUTION:

$$F = 120 \text{ k}, \; C = -120 \text{ k}, \; A = 120 \text{ sq. in.}$$

$$I = \frac{10 \times 12^3}{12} = 1440 \text{ in.}^4, \; r^2 = \frac{1440}{120} = 12 \text{ in.}^2,$$

$$\frac{r^2}{y_t} = \frac{12}{-16} = -2.00 \text{ in.}, \; \frac{r^2}{y_b} = \frac{12}{6} = 2.00 \text{ in.}$$

Final stresses:

$$f_t = \frac{-120}{120}\left(1 + \frac{-2.5 \times -6}{12}\right) = -2250 \text{ psi (compression)}$$

$$f_b = \frac{-120}{120}\left(1 + \frac{-2.5 \times 6}{12}\right) = +250 \text{ psi (tension)}$$

Initial stresses:

$$f_t = \frac{-2250}{0.85} = -2650 \text{ psi (compression)}$$

$$f_b = \frac{-250}{0.85} = +294 \text{ psi (tension)}$$

ILLUSTRATIVE PROBLEM 4-2 Compute the prestressing force and eccentricity that would be necessary in the beam of I.P. 4-1, in order to obtain a bottom-fiber compression of 2400 psi and a top-fiber tension of 350 psi, by equating the relationships for stresses due to prestressing in the top and bottom fibers.

SOUTION:

$$f_t = \frac{C}{A}\left(1 + \frac{ey_t}{r^2}\right) = +350 \text{ psi}$$

$$f_b = \frac{C}{A}\left(1 + \frac{ey_b}{r^2}\right) = -2400 \text{ psi}$$

$$\frac{350}{1 + \dfrac{-6e}{12}} = \frac{-2400}{1 + \dfrac{6e}{12}}$$

$$1025e = 2750$$

$$e = 2.68 \text{ in.}$$

Using eq. 4-4:

$$C = \frac{120 \times -2400}{1 + \dfrac{2.68 \times 6}{12}} = -123{,}000 \text{ lb}$$

The familiar principle of superposition is used to determine the combined effect of the prestressing and the other loads that may be acting simultaneously on a prestressed beam. Although it is possible to write a single equation that will accurately define the stress at any particular point in a beam, for normal manual calculations it frequently is less confusing if the effect of each load (or prestressing) is computed separately, and the net effect is determined by algebraically adding the effects of the several loads.

ILLUSTRATIVE PROBLEM 4-3 Compute the net initial and final concrete stresses in the extreme top and bottom fibers at the midspan of a beam that is 10 in. wide 12 in. deep and on a span of 25 ft. The beam is to support an intermittent, uniformly distributed live load of 0.45 k/ft and is to be prestressed with a final force of 120 k positioned with an eccentricity of 2.5 in. The ratio between the final and initial prestressing forces is assumed to be 0.85. The unit weight of the concrete is 150 pcf.

SOLUTION: The initial and final stresses due to prestressing in the top and bottom fibers are opposite to those in I.P. 4-1 because the eccentricity of the prestressing force is positive; these stresses are as shown in Table 4-1, a tabulation of the combined stresses.

The section modulus of the section is equal to I/y or -240 in.^{3} for the top fiber and $+240$ in.^{3} for the bottom fiber. The stresses due to the dead load of the beam alone are:

$$w_{dl} = \frac{120}{144} \times 0.150 = 0.125 \text{ klf}$$

$$M_{dl} = 0.125 \times \frac{25^2}{8} = 9.77 \text{ k-ft}$$

$$f_t = \frac{9.77 \times 12{,}000}{-240} = -488 \text{ psi (compression)}$$

$$f_b = \frac{9.77 \times 12{,}000}{240} = +488 \text{ psi}$$

TABLE 4-1 Summary of Stresses for I.P. 4-3.

	Top fiber (psi)	Bottom fiber (psi)
Initial prestress	+294	−2650
Beam dead load	−488	+488
Initial prestress plus dead load	−194	−2162
Live load	−1760	+1760
Initial prestress plus total load	−1954	−402
Final prestress	+250	−2250
Dead load of beam	−488	+488
Final prestress plus dead load	−238	−1762
Live load	−1760	+1760
Final prestress plus total load	−1998	+2

The stresses due to the live load alone are:

$$M_{ll} = 0.45 \times \frac{25^2}{8} = 35.2 \text{ k-ft}$$

$$f_t = \frac{35.2 \times 12{,}000}{-240} = -1760 \text{ psi (compression)}$$

$$f_b = \frac{35.2 \times 12{,}000}{240} = +1760 \text{ psi (tension)}$$

The stresses are summarized in Table 4-1.

4-3 Pressure Line with Straight Tendon

At any section of an uncracked beam, the combined effect of the prestressing force and the externally applied load will result in a distribution of internal concrete stresses that can be resolved into a single resultant force that is equal to, but opposite in sign to, the prestressing force. The locus of the points of application of this force in any beam, beam-column, or frame is called the *pressure line*.

The pressure line can be illustrated by considering a rectangular beam prestressed by an eccentric, straight tendon, as shown in Fig. 4-3. Under the condition of prestressing alone, the beam would have a distribution of internal compressive stresses at every cross section as shown in Fig. 4-4a. The resultant compressive force in the beam, C, is equal in magnitude to the prestressing force, P. The prestressing force and the resultant force in the beam are applied at the same location, $d/6$ below the centroidal axis of the beam, at every section of the beam as long as other loads are not applied to the beam.

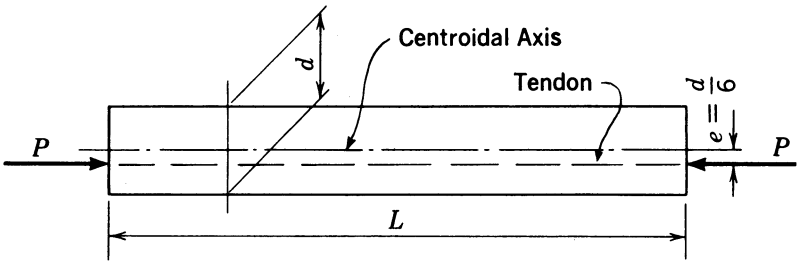

Fig. 4-3. Simple rectangular beam prestressed by an eccentric straight tendon.

If a uniformly distributed load that is of such magnitude that it results in the bottom-fiber prestress being nullified at midspan is applied to the beam, the resulting stress distribution at midspan would be as indicated in Fig. 4-4b, and the pressure line at this point would be applied at a point $-d/6$ above the centroidal axis of the beam. At the quarter points of the beam, under the effects of the uniformly distributed load alone, the stresses due to the external load alone are only 75 percent as great as those at midspan. The distribution of compressive stresses in the beam from the combination of the prestressing and the external load would be a shown in Fig. 4-4c, and the pressure line at this point would be located at a distance of $-d/12$ above the centroidal axis of the beam. At the support, because there are no flexural stresses resulting from the external load, the pressure line remains at the level of the steel. Plotting the location of the pressure line for this loading reveals that it is a parabola with its vertex at the center of the beam, as shown in Fig. 4-5.

In a similar manner, it can be shown that a larger uniformly distributed load would result in the pressure line's being moved up even higher, and for a uniform load applied upward rather than downward, the result would be a downward movement of the pressure line. Therefore, it is apparent that the location of the pressure line in simple prestressed beams is dependent upon the magnitude and

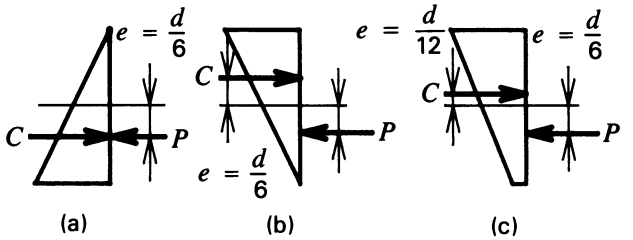

Fig. 4-4. Stress distributions and pressure-line locations for a simple rectangular beam prestressed with a straight eccentric tendon: (a) due to prestressing alone, (b) at midspan under full service load, and (c) at quarter point under full service load.

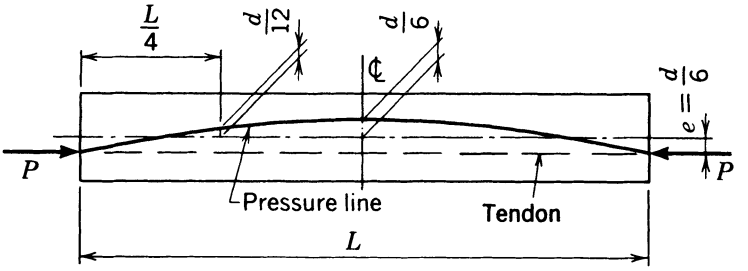

Fig. 4-5. Location of pressure line in a simple beam of rectangular cross section, prestressed by a force at $e = d/6$, together with a uniformly distributed load resulting in zero bottom-fiber stress at midspan.

direction of the moments applied at any cross section and the magnitude and distribution of stress due to prestressing: *A change in the external moments in the elastic range of a prestressed beam results in a movement of the pressure line in the beam.*

Because of the change in the strain in the concrete at the level of the steel (assuming the flexural bond strength between the steel and concrete is adequate, as it is in pretensioned and bonded post-tensioned beams), there is an increase in the stress in the prestressing steel when an external load is applied. This occasionally is of importance, but the effect normally is disregarded (see Sec. 4-11).

ILLUSTRATIVE PROBLEM 4-4 Compute and draw to scale the location of the pressure line for a rectangular beam 10 in. wide and 12 in. deep that is prestressed with a force of 120 k at a constant eccentricity of 2.5 in. and is supporting a 15 k concentrated force at midspan of a span of 10 ft. Use an exaggerated vertical scale in the sketch, and dimension the location of the pressure line at the midspan, quarter point, and end of the beam. Neglect the dead weight of the beam.

SOLUTION: From I.P. 4-3 the stresses due to final prestressing of 120 k are known to be +250 psi and −2250 psi, and the section moduli are known to be ∓ 240 in.^{3} for both the top and the bottom fibers. At the end of the beam, there is no moment due to the concentrated load; hence, the pressure line is located $e = +2.50$ in. below the centroidal axis.

At the midspan:

$$M = \frac{PL}{4} = \frac{15 \times 10}{4} = 37.5 \text{ k-ft}$$

$$f = \frac{37.5 \times 12{,}000}{\mp 240} = \mp 1875 \text{ psi (compression in top fiber)}$$

The stress distribution at midspan is:

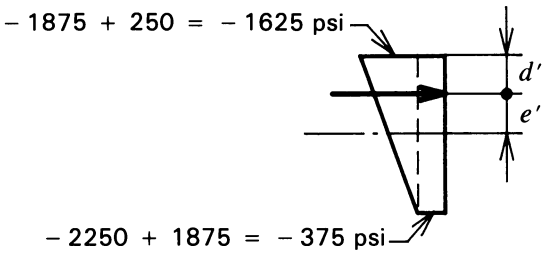

The distance from the top fiber to the resultant force in the section is computed by taking moments about the top fiber as:

$$d' = \frac{6 \times -375 \times 120 + (-1250/2) \times 120 \times 4}{-375 \times 120 + (-1250/2) \times 120} = 4.75 \text{ in.}$$

The resultant force is located at $e' = 6.00 - 4.75 = 1.25$ in. above the centroid axis ($e = -1.25$ in.).

At the quarter point, the moment due to the external load is only one-half that at the midspan. Therefore, the flexural stresses due to the applied load are only one-half of those at midspan, or ∓ 938 psi.

The stress distribution at the quarter point is:

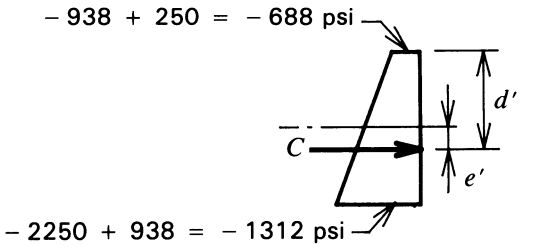

$$d' = \frac{6 \times -688 \times 120 + (-624/2) \times 120 \times 8}{-688 \times 120 + (-624/2) \times 120} = 6.625 \text{ in.}$$

The resultant is located at $e' = 6.625 - 6.00 = +0.625$ in. below the centroidal axis.

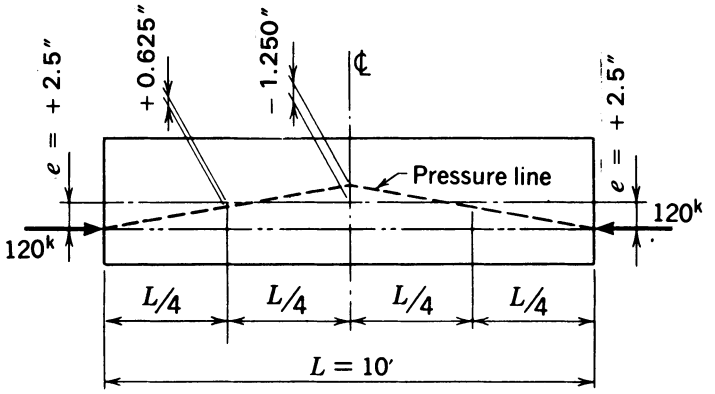

Fig. 4-6. Location of pressure line, I.P. 4-4.

The results are shown plotted in Fig. 4-6.

4-4 Variation in Pressure Line Location

If the stress in the bottom fiber of a beam is to be equal to zero, or to be under a compressive stress under the effects of the final prestressing force and service dead and live loads, as is the case for a fully prestressed member, the distribution of stresses will be as shown in Fig. 4-7a (see Sec. 7-5). A beam cross section is shown in Fig. 4-7b together with certain dimensions of importance in the design of prestressed concrete flexural members. The force C shown in Fig. 4-7a is the resultant of the unit compressive stresses in the concrete section and hence defines the location of the pressure line under the particular conditions of prestressing and service loads that cause the stress distribution illustrated. For the forces P, the prestressing force, and C, the resultant compressive force, to be in equilibrium, they must be equal in magnitude and opposite in

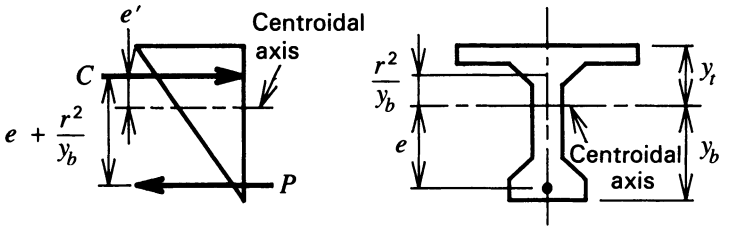

Fig. 4-7. Relationship between prestressing force, pressure line, and section properties of a beam having zero stress in bottom fiber under design load. (a) Stress distribution. (b) Beam cross section.

direction. In addition, from eq. 4-4 developed in Sec. 4-2, we can write the relationship for the stress in the bottom fiber as follows:

$$f_b = \frac{C}{A}\left(1 + \frac{e'y_b}{r^2}\right) = 0$$

from which, for C not equal to zero, one can obtain:

$$e' = \frac{r^2}{y_b}$$

The eccentricity e' of the resultant C in this example, which is negative because it is above the centroidal axis, should not be confused with the eccentricity of the prestressing force P.

Another requirement of equilibrium is that the internal and external moments be equal in magnitude and opposite in direction at every section. Hence, it follows that the total external moment that the beam is resisting at this section, and with this distribution of stresses in the concrete, is equal to:

$$M_t = M_{dl} + M_{ll} = C\left(e + \frac{r^2}{y_b}\right) = -P\left(e + \frac{r^2}{y_b}\right) \qquad (4\text{-}5)$$

in which e is the eccentricity of the prestressing force.

The above example further illustrates that prestressed beams, functioning in the elastic range, resist the moment due to externally applied loads by the movement of the resultant of the stresses in the concrete, rather than by an increase in the prestressing stress, as was brought out in Sec. 4-3. From eq. 4-5, it is apparent that if M_t is equal to zero, the product of C multiplied by the quantity $(e + r^2/y_b)$ also must be equal to zero, and the concrete stresses would be distributed as shown in Fig. 4-8. If the external moment (M_t) were some value less than that which nullifies the precompression of the bottom fibers, the force C would be applied above the location of the prestressing steel at a distance d equal to:

$$d = \frac{M_t}{C} \qquad (4\text{-}6)$$

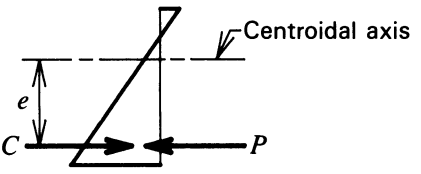

Fig. 4-8. Distribution of stress and location of C when external moment equals zero (prestress alone).

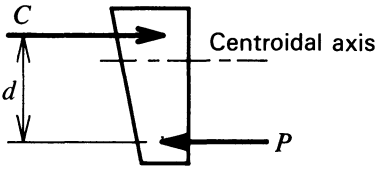

Fig. 4-9. Distribution of stress and location of resultant C when external moment is of nominal magnitude.

This condition is illustrated in Fig. 4-9. It should be noted that in using the sign convention that has been adopted for this book, positive moments due to externally applied loads cause tensile stresses in the bottom fibers of beams and thus cause upward (negative) movements of the location of the pressure line C. Conversely, a negative moment resulting from externally applied loads will cause a downward (positive) movement of the pressure line.

The relationship given by eq. 4-5 is extremely useful in the preliminary design of beams as well as in checking final designs. Because the value of $(e + r^2/y_b)$ normally is on the order of 65 percent of the depth of the beam section (it varies between the approximate limits of 33 to 80 percent for different cross sections) for a given superimposed moment, the designer can assume a dead weight for the beam and estimate the prestressing force required for different depths of construction. The use of this relationship is demonstrated in Illustrative Problem 4-5 and treated further in Sec. 9-8, in the discussion of preliminary design.

It should also be pointed out that if the point of application of the resultant compressive force in a prestressed concrete member is restricted to an area that does not exceed r^2/y_b above the centroidal axis and r^2/y_t below the centroidal axis, tensile stresses will not exist in the concrete section. This zone in which the prestressing force can be applied without tensile stresses is called the kern zone.

ILLUSTRATIVE PROBLEM 4-5 Compute the maximum concentrated load that can be applied at the midspan of a beam that is 10 in. wide, 12 in. deep, prestressed with 120 k at an eccentricity of +2.5 in., and is to be used on a span of 10.0 ft center to center of bearings, without tensile stresses resulting in the bottom fibers.

SOLUTION: Using the basic relationships for flexural design and the section properties and stresses due to prestressing known from I.P. 4-3, the moment that can be applied to the beam without tensile stresses being created in the bottom fibers is:

$$M_t = f_b \times S_b = \frac{2250 \times 240}{12{,}000} = 45.0 \text{ k-ft}$$

The moment due to the dead load of the beam itself is:

$$M_{dl} = \frac{W_{dl}l^2}{8} = \frac{120}{144} \times 0.15 \times \frac{10^2}{8} = 1.56 \text{ k-ft}$$

The moment that can be permitted from the application of the concentrated load is equal to 45.0 − 1.56 = 43.4 k-ft, and the concentrated load can be computed by:

$$P = \frac{43.4 \times 4}{10} = 17.4 \text{ k}$$

Using eq. 4-5 for computing the moment at which the stress in the bottom fiber is equal to zero yields:

$$M = 120\left(\frac{2.5 + 2.0}{12}\right) = 45.0 \text{ k-ft}$$

4-5 Pressure Line Location with Curved Tendon

It was shown in Sec. 4-3 that the pressure line for prestressing alone in a prismatic beam is coincident with the prestressing force when the beam is prestressed with a straight tendon. This can also be demonstrated for a beam prestressed with a tendon that changes slope, as shown in Fig. 4-10. By inspection, the forces acting on the concrete at the point where the tendon changes slope are determined to be as indicated in Fig. 4-11. The forces acting on the concrete are shown at their respective points of application in the freebody diagram of Fig. 4-12. In order to determine where the pressure line is acting at the center of the beam, the conditions of statics at point A are investigated. The sum of the vertical forces is equal to zero because $P \sin \alpha$ is acting downward

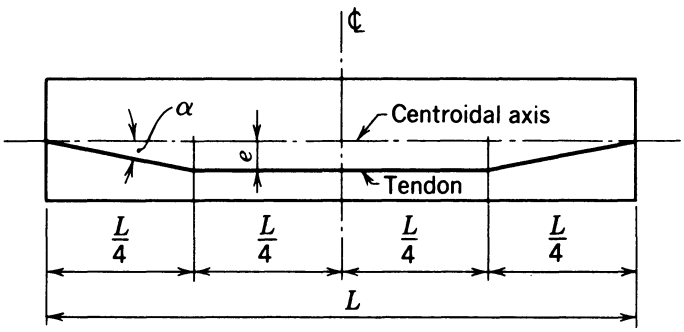

Fig. 4-10. Beam prestressed with tendon that slopes between quarter points and ends.

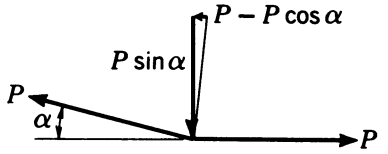

Fig. 4-11. Freebody diagram of tendon in Fig. 4-10 at quarter point.

at the end of the beam and upward at the quarter point. The sum of the horizontal forces indicates that the force R must be equal to P because:

$$\Sigma H = P \cos \alpha + (P - P \cos \alpha) - R = 0 \quad \therefore R = P$$

to determine the distance from the centroidal axis to the point of application of the force R (and hence the location of the pressure line at the center of the beam), moments are taken about point A as follows:

$$\Sigma M_A = (P \sin \alpha)\frac{L}{2} + (P - P \cos \alpha)e - (P \sin \alpha)\frac{L}{4} - Px = 0$$

and:

$$\frac{PL \sin \alpha}{4} + Pe - Pe \cos \alpha - Px = 0$$

but:

$$\tan \alpha = \frac{4e}{L} = \frac{\sin \alpha}{\cos \alpha}$$

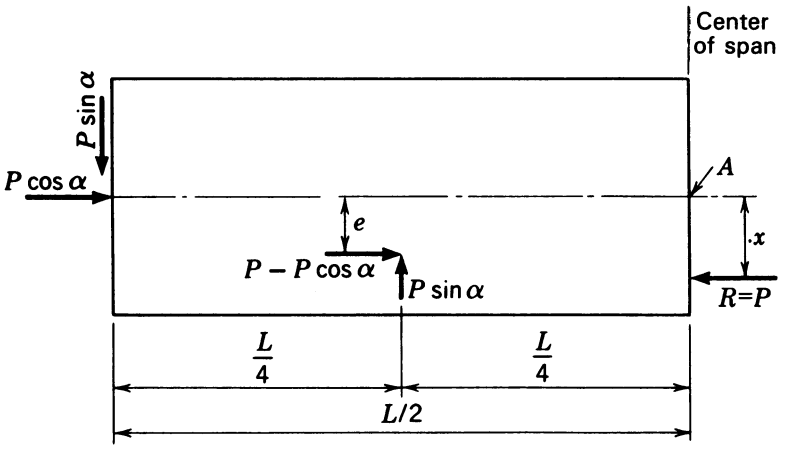

Fig. 4-12. Freebody diagram for half of the beam shown in Fig. 4-10.

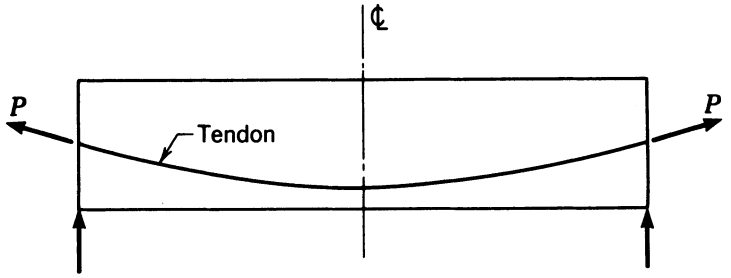

Fig. 4-13. Simple beam with curved tendon.

and:

$$\sin \alpha = \frac{4e \cos \alpha}{L}$$

Therefore:

$$Pe \cos \alpha + Pe - Pe \cos \alpha - Px = 0$$

Hence, $x = e$, and the pressure line is coincident with the location of the tendon.

If a beam with a curved tendon, as shown in Fig. 4-13, is considered, it is readily seen that in the stressing of the tendon, the natural tendency for the tendon to straighten is resisted by the concrete. If a short segment of the tendon is studied as a free body, as shown in Fig. 4-14, forces must be present normal to the tendon (neglecting friction) in order to prevent straightening. If friction is neglected, the force acting throughout the tendon is uniform in magnitude, and because the tendon is flexible, it cannot support any bending moments. Therefore, at every point such as point A, the force in the tendon is equal to P and is located at the tendon. If the force were not coincident with the tendon at A, but were located at some distance from A (as shown by the dashed vector), the tendon would have to withstand the moment Pe caused by this eccentricity.

From this analysis, then, it can be concluded that the pressure line for prestressing alone in a simple beam, prestressed with a curved tendon, is coincident with the path of the tendon because the forces in the concrete must be

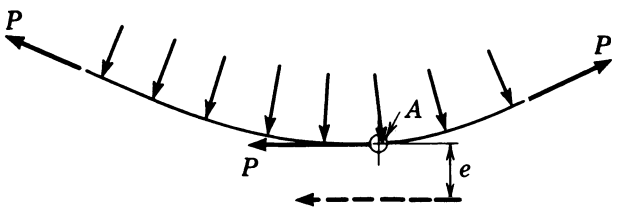

Fig. 4-14. Freebody diagram of portion of curved prestressing tendon.

equal and opposite to those in the steel to maintain equilibrium. Furthermore, it can be shown that the pressure line moves when an external load is applied to a beam with a curved tendon, just as it does in a beam with a straight tendon.

ILLUSTRATIVE PROBLEM 4-6 Compute and plot to scale the location of the pressure line for a rectangular beam that is 10 in. wide and 12 in. deep, if the beam is prestressed with a force of 120 k and placed on a second-degree parabolic path having eccentricities of +2.5 in. below the centroidal axis at midspan and zero at the supports. The beam has a span of 10 ft and supports a uniformly distributed dead and live load of 3.5 klf, including the dead load of the beam itself.

SOLUTION: At midspan:

$$M = 3.5 \times \frac{10^2}{8} = 43.8 \text{ k-ft}$$

$$\text{Pressure line movement} = \frac{43.8 \times 12}{120} = 4.38 \text{ in.}$$

Hence, the pressure line moved up 4.38 in. from its original position 2.5 in. below, to 1.88 in. above the centroidal axis.

At the quarter point:

$$M = 0.75 \times 43.8 = 32.8 \text{ k-ft*}$$

$$\text{Pressure line movement} = 0.75 \times 4.38 = 3.28 \text{ in.}$$

and the pressure line is located at 1.40 in. above the centroidal axis.

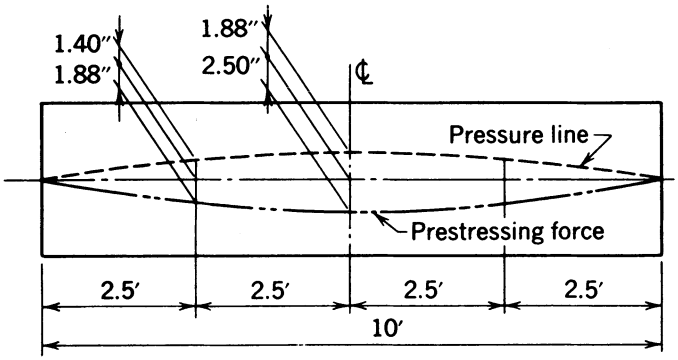

Fig. 4-15. Location of pressure line for I.P. 4-6.

*Note that the ordinate of a second degree parabola at the quarter point of the span is 0.75 times the ordinate at midspan.

At the end: $M = 0$; pressure line movement = 0.

The locations of the pressure lines for the prestressing force alone as well as for the beam under the full uniformly distributed load of 3.5 klf are shown in Fig. 4-15.

ILLUSTRATIVE PROBLEM 4-7 Calculate the maximum, uniformly distributed load that can be applied to the beam of I.P. 4-6 if the bottom fiber stress is to be zero at midspan.

SOLUTION: Under the loaded condition, the pressure line will be at $r^2 = 2.00$ in. above the centroidal axis. Hence:

$$M_T = 120 \times \frac{2.50 + 2.00}{12} = 45.0 \text{ k-ft}$$

and:

$$W_{max} = \frac{45 \times 8}{10^2} = 3.60 \text{ klf}$$

4-6 Advantages of Curved or Draped Tendons

When a simple beam, such as is shown in Fig. 4-16, is prestressed by a straight tendon, it deflects upward. From this observation, it is apparent that the dead weight of the beam itself is acting at the time of prestressing because, as the beam deflects upward, the soffit of the beam no longer is in contact with the soffit form, except at the ends of the beam. From this consideration, it can be concluded that the actual stress existing in the beam at any point along its length, at the time of prestressing, is equal to the algebraic sum of the stresses caused by the prestressing and the dead weight of the beam itself.

The variation in the stresses along the length of the beam in the extreme top and bottom fibers, for a beam prestressed with straight tendons, also is illustrated in Fig. 4-16. Ignoring loss of prestress, for the purpose of this discussion, and assuming, for the concrete in the beam under consideration, that the maximum permissible bottom-fiber compressive stress is 2000 psi and the maximum permissible top-fiber tensile stress is 200 psi, the beam as illustrated is prestressed as highly as possible. Assuming that tensile stresses are not to be permitted in the bottom fiber under the total load, it will be seen that 1500 psi, or 75 percent of the permissible compressive stress in the concrete at the midspan of the beam, is available for the superimposed loads, and 25 percent is counteracted by the dead load of the beam itself. Furthermore it is observed that the maximum concrete stresses occur at the ends of the beam, where dead-load

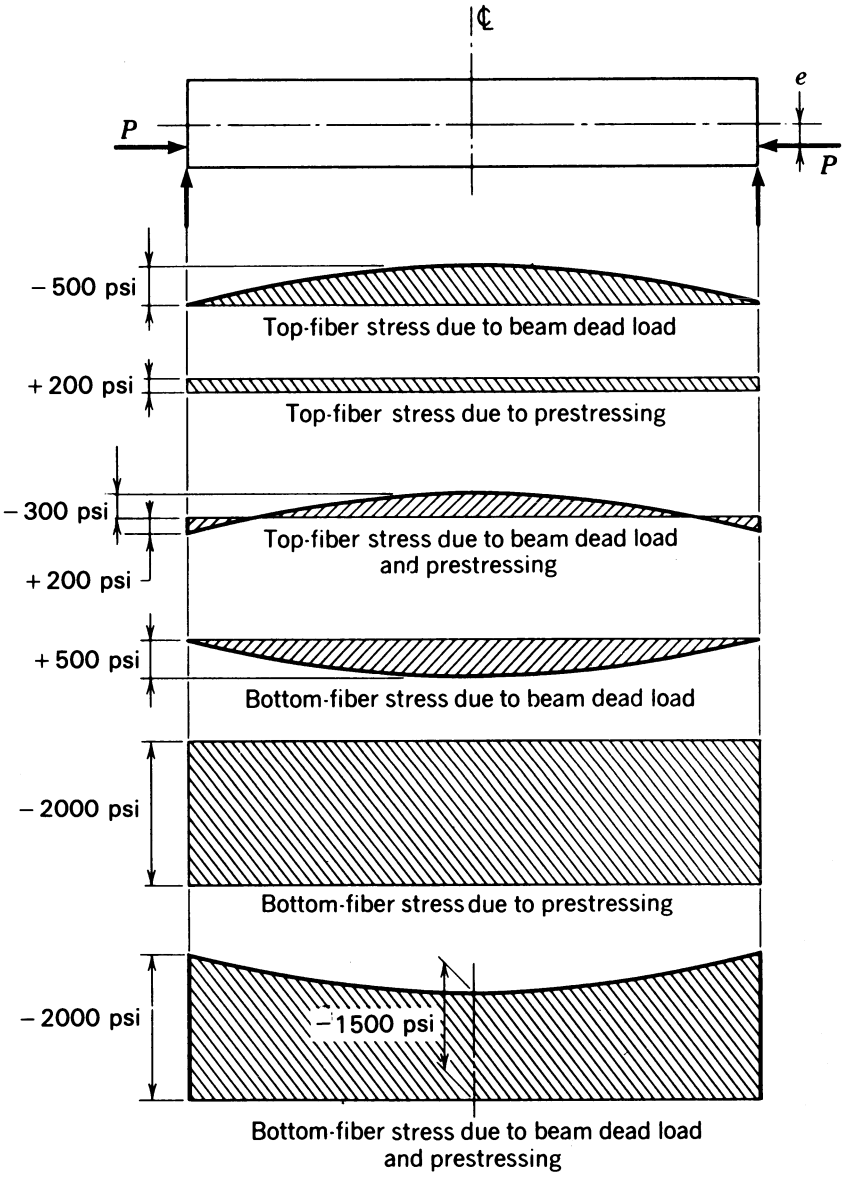

Fig. 4-16. Stress distribution of top and bottom fibers of simple prismatic beam prestressed with a straight tendon.

flexural stresses do not exist, rather than near the midspan, where the flexural stresses under the maximum service loads are the greatest.

If the tendon were placed in the member on a second-degree parabolic curve such that the eccentricity were maximum at midspan of the beam and minimum

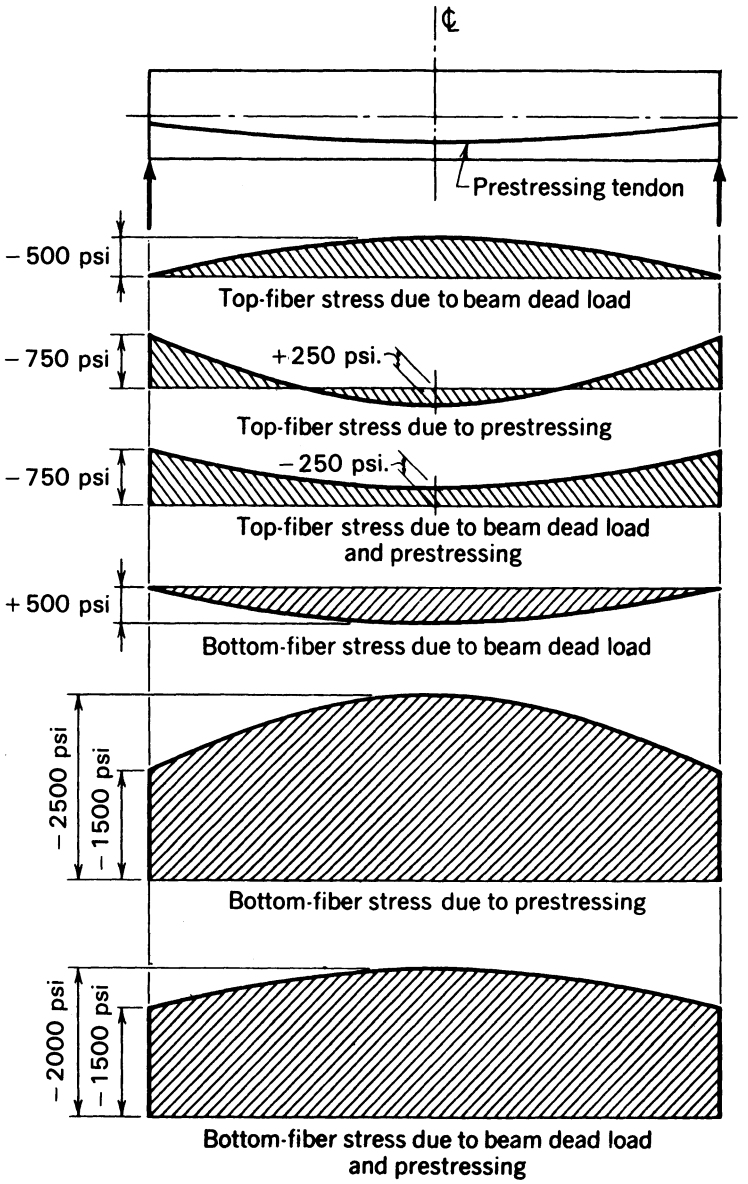

Fig. 4-17. Stress distribution in the top and bottom fibers of a simple prismatic beam prestressed with a curved tendon.

at the ends of the beam, the stresses in the top and bottom fibers would vary along the length of the beam, as illustrated in Fig. 4-17. It will be seen, from an examination of these stress distributions, that the maximum stresses resulting from prestress in both the top and bottom fibers occur at midspan of the beam.

Furthermore, it is apparent that, by careful selection of the amount and eccentricity of the prestressing, it is possible to eliminate the reduction in the capacity of the beam to withstand a superimposed load due to the dead weight of the beam itself, as was the case in the previous example. This can be explained in terms of the pressure line as follows: the prestressing force can be applied lower at midspan of the beam than at the ends, without exceeding the permissible stresses, because the dead-load moment of the beam is acting in a direction opposite to the moment due to prestressing. The increase in eccentricity that can be used is equal to M_{dl}/P.

The advantage to be gained from curving the tendons obviously is more important in members in which the external moment existing at the time of prestressing is a large percentage of the total moment. Conversely, if the dead-load moment acting at the time of prestressing is very small, there is little or no advantage (from the standpoint of flexural stresses) in having the prestressing force at a greater eccentricity at midspan than it is near the ends.

It is axiomatic in structural engineering that the dead loads of structures become progressively more important and greater, in respect to the total load, as the span lengths are increased. This is one of the important considerations influencing the normal practice of using straight tendons for short members and using tendons having variable eccentricity, either pretensioned or post-tensioned, for longer members. As is discussed in Sec. 4-9, this fact is also important in determining the proper cross-sectional shape of a flexural member.

It should be recognized that deflected or draped pretensioned tendons cannot be placed on smooth curves (see Sec. 15-6). They are often placed on a path consisting of a series of straight lines that approximate a second-degree parabola or other curve form. When the term curved tendon is used in this book, it is not meant to infer that the tendon must be post-tensioned, or that the path of the tendon is a smooth curve.

Another beneficial effect of curving prestressing tendons is reduction of the shear force that must be carried by the concrete section (see Sec. 6-3). This can be explained by considering a simple beam prestressed by a tendon placed on a second-degree parabolic path, as illustrated in Fig. 4-18 (freebody diagrams showing the forces on the tendon and the concrete are shown in Fig. 4-19). If the friction between the tendon and the concrete is assumed to not exist, the forces exerted by the concrete on the tendon, between midspan and the ends of the beam, will be normal to the tendon. If the tendon is inclined at angle α at its end, the vertical and horizontal components of the prestressing force at the end will be $P \sin \alpha$ and $P \cos \alpha$, respectively. Because the inclination of the forces the concrete applies to the tendon normally is small, it can be ignored for the purpose of this discussion, and the force the tendon applies to the concrete can be assumed to be equal to $P \sin \alpha$ applied vertically upward and uniformly distributed between midspan and the end of the beam, as shown in Fig. 4-19. If the total shear force at the end of the beam due to the design loads is taken

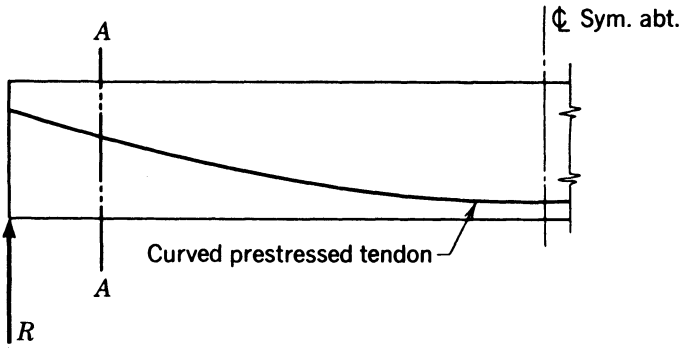

Fig. 4-18. Half-elevation of a simple beam with curved tendon.

to be V, acting vertically upward at the end of the beam, the force the concrete must resist in shear is equal to $V - P \sin \alpha$. From this example it is apparent that the curvature of the tendon has the effect of reducing the vertical shear force the concrete section must be able to resist, and, if the tendon were not curved, the concrete section would be subjected to the total shear force V.

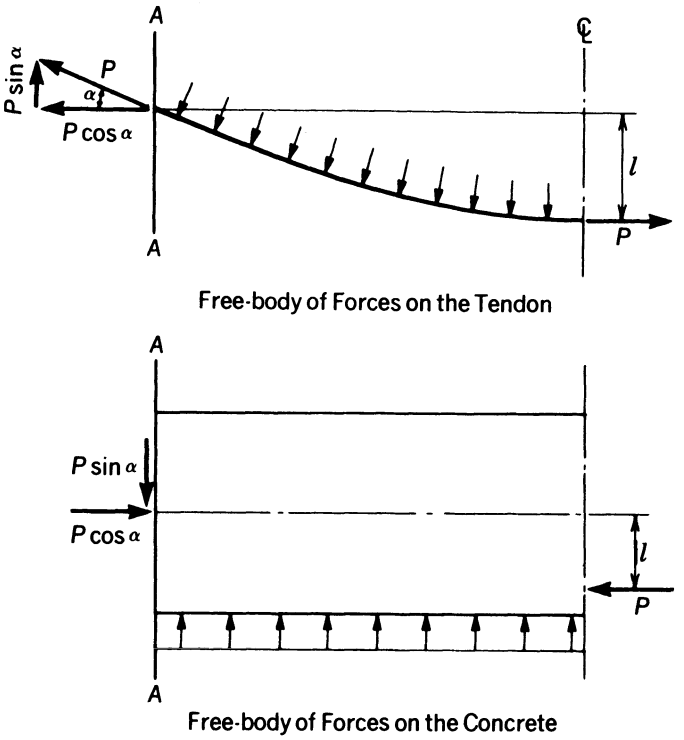

Fig. 4-19. Freebody diagrams for curved tendon and concrete section. (a) Freebody of forces on the tendon. (b) Freebody of forces on the concrete.

ILLUSTRATIVE PROBLEM 4-8 Determine the prestressing force and eccentricity required to prestress a slab, 4 ft wide, 8 in. deep, that is to be simply supported on a span of 30 ft. Maximum final compression in the bottom fibers is 2000 psi, and maximum allowable, final, top-fiber tensile stress is 300 psi. The slab is to made of normal-weight concrete and is to support a superimposed load of 45 psf. The minimum concrete cover for the prestressing tendons is $1\frac{1}{2}$ in. Assume the tendons have a diameter of $\frac{3}{8}$ in. and have a final prestress of 11 k each. If the tendons are straight and in one layer, determine how many tendons are required and how thick the concrete cover would be. Determine how many tendons would be required if they could be placed on a parabolic path with a concrete cover of $1\frac{1}{2}$ in. at midspan.

SOLUTION:

$$\begin{aligned} \text{Slab dead load} &= 100 \text{ psf} \times 4 \text{ ft} = 400 \text{ plf} \\ \text{Superimposed load} &= 45 \text{ psf} \times 4 \text{ ft} = \underline{180 \text{ plf}} \\ & \qquad\qquad\qquad\quad 580 \text{ plf} \end{aligned}$$

$$M_t = 0.58 \times \frac{30^2}{8} = 65.3 \text{ k-ft}$$

$$S = \frac{bd^2}{6} = \frac{48 \times 8^2}{6} = \mp 512 \text{ in.}^3 \text{ (top fiber negative)}$$

$$f = \frac{65.3 \times 12{,}000}{\mp 512} = \mp 1530 \text{ psi}$$

$$\frac{r^2}{y_t} = \frac{d}{-6} = -1.33 \text{ in.}, \quad \frac{r^2}{y_b} = \frac{d}{6} = 1.33 \text{ in.}$$

The distribution of stress desired for the minimum amount of prestressing with straight tendons will have a tensile stress of 300 psi in the top fiber and 1530 psi compression in the bottom fiber. Therefore:

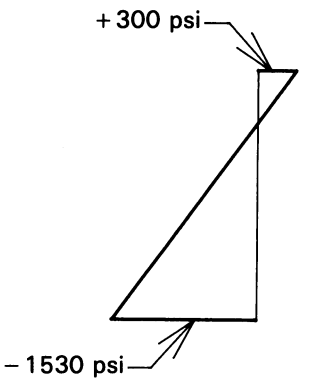

$$f_t = \frac{C}{A}\left(\frac{1 + e}{-1.33}\right) = +300 \text{ psi}$$

$$f_b = \frac{C}{A}\left(1 + \frac{e}{1.33}\right) = -1530 \text{ psi}$$

$$\frac{300}{1 + \dfrac{e}{-1.33}} = \frac{-1530}{1 + \dfrac{e}{1.33}}$$

$$300 + 225e = -1530 + 1150e$$

$$925e = 1830$$

$$e = +1.98 \text{ in.}$$

From eq. 4-4 with $e = 1.98$ in.:

$$C = \frac{-1530 \times 48 \times 8}{2.49} = -236{,}000 \text{ lb}$$

This would require 22 tendons ($P = 242$ k), and the concrete cover would be $4.00 - 1.98 - 0.375/2 = 1.83$ in.

If the tendons are placed on a curved path, the top fiber stress would not limit the eccentricity of the prestressing. The eccentricity could be $4.00 - 1.50 - 0.375/2 = 2.31$ in., and the prestressing force can be computed from eq. 4-4 as follows:

$$\frac{C}{384}\left(1 + \frac{2.31}{1.33}\right) = -1530 \text{ psi}$$

From which the resultant compressive force of -214.7 k is obtained. This solution requires 20 tendons, which will provide a force of 220 k.

ILLUSTRATIVE PROBLEM 4-9 If the maximum final, allowable top-and bottom-fiber stresses are 170 psi tension and 2000 psi compression, respectively, determine the maximum superimposed load that can be carried by a 12 in. wide beam that is 18 in. deep if flexural tensile stresses are not permitted in the bottom fiber under service load, and the beam is to be used on a span of 30 ft. Determine the minimum prestressing force and the corresponding eccentricity of the force if the beam is prestressed with straight tendons. Determine the minimum curved-tendon prestressing force that could be used to carry the same superimposed load if the maximum eccentricity is 6 in. (i.e., the center of gravity of the tendon is 3 in. above the soffit of the beam). Compute the ratio of the two forces.

SOLUTION: The area of the beam is 216 in.^{2}, the section moduli for the top and bottom fibers are ∓ 648 in.^{3}, and the upper and lower limits of the kern zone are -3.00 in. above and $+3.00$ in. below the centroidal axis of the section. The desired distribution of stress using straight tendons is controlled by the stresses at the ends of the beam; these are final top- and bottom-fiber stresses of $+170$ psi and -2000 psi, respectively. Solving eqs. 4-3 and 4-4 simultaneously, the eccentricity and prestressing force that will result in the desired stress distribution can be determined by:

$$f_t = \frac{C}{A}\left(1 + \frac{e}{-3.00}\right) = 170 \text{ psi}$$

$$f_b = \frac{C}{A}\left(1 + \frac{e}{3.00}\right) = -2000 \text{ psi}$$

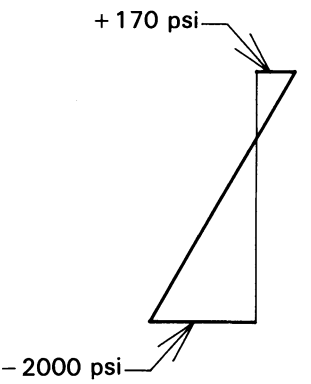

$$\frac{170}{1 - \frac{e}{3}} = \frac{-2000}{1 + \frac{e}{3}}$$

$$170 + 56.7e = -2000 + 667e$$

$$610e = 2170$$

$$e = 3.56 \text{ in.}$$

$$C = \frac{-2000 \times 216}{1 + \frac{3.56}{3.00}}$$

$$= -198{,}000 \text{ lb}$$

$\therefore$ The straight tendon requires an eccentricity of 3.56 in. and a prestressing force of 198,000 lb.

For the curved tendon, the top-fiber stress due to prestressing at midspan can be made equal to the arithmetical sum of 170 psi, the allowable tensile stress in the top fiber, plus the top-fiber stress due to dead load alone. The bottom-fiber stress due to prestressing should be 2000 psi compression in order for the beam to be able to support the same superimposed load. The moment the beam can withstand to nullify the −2000 psi in the bottom fiber is:

$$M_t = 198 \times \frac{3.00 + 3.56}{12} = 108 \text{ k-ft}$$

The total dead plus superimposed load that results in a moment of 108 k-ft is:

$$w_t = \frac{108 \times 8}{30^2} = 0.960 \text{ klf}$$

The dead load of the beam is:

$$w_d = \frac{216}{144} \times 0.150 = 0.225 \text{ klf}$$

and the superimposed dead load is 0.960 − 0.225 = 0.735 klf. The flexural stresses due to the dead and superimposed loads will be found to be $\mp$469 psi and $\mp$1531 psi, respectively. Therefore, the top-fiber tensile stress due to prestressing can equal the arithmetic sum of 170 and 469, which is 639 psi, and the bottom-fiber compressive stress due to prestressing, as explained above, should equal −2000 psi. Using these values and solving eqs. 4-3 and 4-4, one obtains:

$$f_t = \frac{C}{A}\left(1 + \frac{e}{-3.00}\right) = 639 \text{ psi}$$

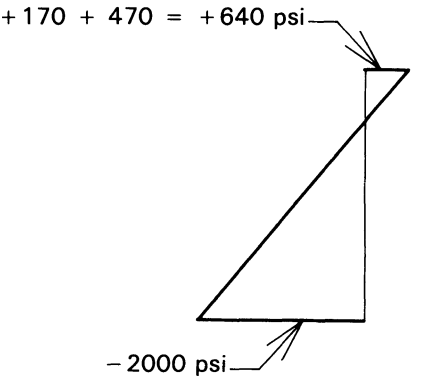

$$f_b = \frac{C}{A}\left(1 + \frac{e}{3.00}\right) = -2000 \text{ psi}$$

Equating the above, one obtains:

$$\frac{639}{1 + \dfrac{e}{-3.00}} = \frac{-2000}{1 + \dfrac{e}{3.00}}$$

from which:

$$\frac{1361e}{3} = 2639$$

and:

$$e = \frac{3 \times 2639}{1361} = 5.82 \text{ in.}$$

and the prestressing force is:

$$P = \frac{2000 \times 216}{1 + \dfrac{5.82}{3.00}} = 147 \text{ k}$$

and, finally, the ratio of the prestressing force required for straight and curved tendons is 1.35.

ILLUSTRATIVE PROBLEM 4-10 Compute the shear force carried by the prestressing tendon of 120 k and by the concrete section at the ends of the beam for the loading and dimensions shown in Fig. 4-20.

SOLUTION: The sine of the angle at the end of a second-degree parabolic curve is equal to the quotient of two times its height (ordinate) and its base (abscissa).

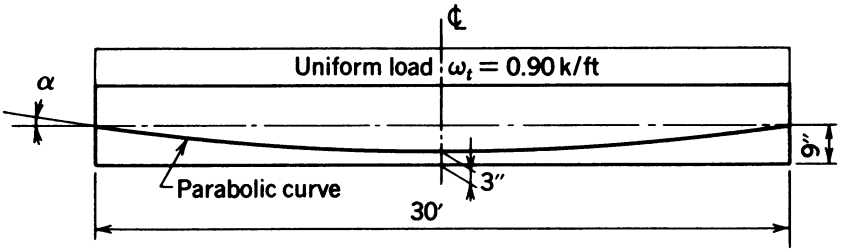

Fig. 4-20. Beam of I.P. 4-10.

For the beam in Fig. 4-20:

$$\tan a \cong \sin a = \frac{2e}{L/2} = \frac{4 \times 6}{12 \times 30} = 0.0667$$

$$P \sin a = 120 \times 0.0667 = 8.00 \text{ k}$$

$$\text{Total shear force } V_t = 0.90 \times 15 = 13.5 \text{ k}$$

$$\text{Shear on concrete } V_c = 13.5 - 8.00 = 5.5 \text{ k}$$

4-7 Limiting Eccentricities

It was explained in Sec. 4-6 that the designer frequently can allow a greater eccentricity of the prestressing force at the midspan of a beam without exceeding the allowable stresses at other locations along the span, because of the dead weight of the beam itself, which is acting at the time of prestressing. The design and analysis of prestressed concrete is further complicated, however, because normally two different criteria for permissible stresses must be satisfied: those that apply at the time of prestressing and those that apply in the completed structure after the losses of prestress have taken place. At the time of stressing, the strength of the concrete normally is less than it will be in the completed structure, and, because it is recognized the initial stresses in the concrete at the time of prestressing will decrease with the passage of time, relatively high stresses are permitted. The conditions of loading that cause maximum conditions of stress in the completed structure are different and less predictable than those at the time of prestressing; so the stresses permitted in the completed structure normally are more conservative (in terms of the ratio of allowable stress to ultimate stress) than those permitted at the time of prestressing. Both criteria normally permit a maximum tensile stress and a maximum compressive stress in the concrete, with the former being much smaller than the latter. In the case of precast, prestressed members, the allowable tensile stress is most apt to be a limiting criterion in the top fibers at the time of prestressing and in

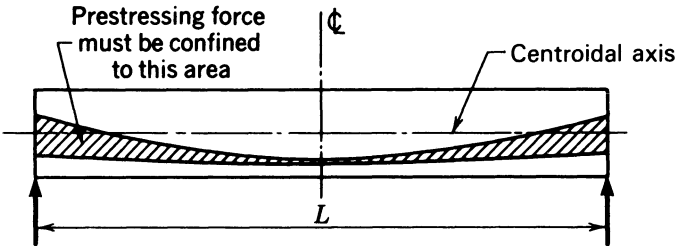

Fig. 4-21. Schematic diagram showing area in which prestress force must be confined to satisfy initial and final stress requirements.

the bottom fibers in the complete structure when subjected to full service load. The opposite is the case with the allowable compressive stresses: at the time of prestressing the compressive stress in the bottom fibers are more likely to control a design than are compressive stresses in the top fibers, and top-fiber compressive stresses are more likely to control under full service load. In most beams, a number of combinations of prestressing force and eccentricity can be found that will satisfy the conditions of allowable stress. In the interest of economy, however, the minimum prestressing force that satisfies the permissible combinations of stress at all locations along the length of the member normally is selected. Experienced designers sometimes use prestressing forces somewhat greater than the minimum size that could be used, and still comply with the minimum requirements of the applicable code, in the interest in facilitating construction.

For a force selected for a particular design, one can compute maximum and minimum eccentricities that can be used at various locations along the length of the beam without exceeding the permissible stresses enumerated above. Plotting the eccentricities in a schematic elevation of the beam, generally with an exaggerated vertical scale, reveals the limiting dimensions in which the center of gravity of the prestressing force must remain in order to satisfy the conditions of allowable stress. An example of this type of is shown in Fig. 4-21, where the area in which the center of gravity of the prestressing tendons must be confined is crosshatched. It generally is not necessary to make a diagram of this type for simple span beams designed for uniformly distributed loads, because by placing the center of gravity of the prestressing tendons on a curve approximating a second-degree parabola, the stress conditions normally can be satisfied without difficulty. The design of nonprismatic beams, continuous beams, and beams that have acute or unusual conditions of stress often is facilitated by the use of a diagram of this type.

ILLUSTRATIVE EXAMPLE 4-11 Compute the limits of the eccentricity of the prestressing force of 550 k at the midspan, quarter point, and end for a simple

TABLE 4-2 Top- and Bottom-Fiber Stresses, I.P. 4-11.

Location	Max. top (psi)	Min. top (psi)	Max. bottom (psi)	Min. bottom (psi)
End	0	0	0	0
Quarter point	−1350	−453	+1530	+328
Midspan	−1800	−605	+2038	+438

beam if the maximum allowable stresses are: (1) when the minimum condition of loading exists (beam dead load alone), 200 psi tension in the top fibers and 2000 psi compression in the bottom fibers; and (2) when the maximum loading condition exists (service dead and live loads), zero tension in the bottom fibers and 2200 psi compression in the bottom fibers. The stresses in the top and bottom fibers under maximum and minimum conditions of loading are as summarized in Table 4-2. The area of the cross section of the beam is 445 in.^{2} and the limits of the kern zone, r^2/y_b and r^2/y_t, are equal to 8.99 and 6.50 in., respectively.

SOLUTION: The average compressive stress in the concrete due to the prestressing force of 550 k is 550,000/445 = −1236 psi. At midspan, under minimum loading, compressive stress in the bottom fiber can equal −2000 − 438 = −2438 psi. Rearranging eq. 4-4 solve for the eccentricity, one obtains:

$$e = \left[\frac{f_b}{C/A} - 1\right]\frac{r^2}{y_b} = \left[\frac{-2438}{-1236} - 1\right](8.99) = 8.74 \text{ in.}$$

With this value of e, the top-fiber stress due to prestressing alone is:

$$f_t = -1236\left[1 + \frac{8.74}{-6.50}\right] = 426 \text{ psi}$$

and the net top-fiber stress is:

$$426 - 605 = -179 \text{ psi} < 200 \text{ psi ok.}$$

Under the maximum loading, tensile stress is not permitted in the bottom fibers, and the prestress must be equal to −2038 psi or more. Hence:

$$e = \left[\frac{f_b}{C/A} - 1\right]\frac{r^2}{y_b} = \left[\frac{-2038}{-1236} - 1\right](8.99) = 5.83 \text{ in.}$$

and the top-fiber stress with this eccentricity is:

$$f_t = -1236\left[1 + \frac{5.83}{-6.50}\right] = -127 \text{ psi}$$

and the net top-fiber stress is:

$$-127 - 1800 = -1927 \text{ psi} < -2200 \text{ psi ok.}$$

Summary for midspan:

$$e_{max} = 8.74 \text{ in.}, \; e_{min} = 5.83 \text{ in.}$$

At the quarter point, under minimum loading, the prestressing in the bottom fiber can equal $-2000 - -328 = -2328$ psi. The eccentricity for this bottom fiber stress is:

$$e = \left[\frac{f_b}{C/A} - 1\right]\frac{r^2}{y_b} = \left[\frac{-2328}{-1236} - 1\right](8.99) = 7.94 \text{ in.}$$

With this value of e, the top fiber stress due to prestressing alone is:

$$f_t = -1236\left[1 + \frac{7.94}{-6.50}\right] = 274 \text{ psi}$$

and the net top fiber stress is $274 - 453 = -179$ psi > 200 psi ok.

Under the maximum loading, tensile stress is not permitted in the bottom fibers, and the prestress must be equal to -1530 psi or more. Hence:

$$e = \left[\frac{f_b}{C/A} - 1\right]\frac{r^2}{y_b} = \left[\frac{-1530}{-1236} - 1\right](8.99) = 2.14 \text{ in.}$$

and the top-fiber stress with this eccentricity is:

$$f_t = -1236\left[1 + \frac{2.14}{-6.50}\right] = -829 \text{ psi}$$

and the net top-fiber stress is:

$$-829 - 1350 = -2179 \text{ psi} < -2200 \text{ psi ok.}$$

Summary for midspan:

$$e_{max} = 2.14 \text{ in.}, \; e_{min} = 7.94 \text{ in.}$$

At the end, the compressive stress in the bottom fiber can equal -2000 psi, and:

$$e = \left[\frac{f_b}{C/A} - 1\right]\frac{r^2}{y_b} = \left[\frac{-2000}{-1236} - 1\right](8.99) = 5.56 \text{ in.}$$

For an eccentricity of 5.56 in., the stress in the top fiber is:

$$f_t = -1236\left[1 + \frac{5.56}{-6.50}\right] = -179 \text{ psi} < 200 \text{ psi ok.}$$

Tensile stress is not permitted in the bottom fiber. For this condition of stress, the pressure line will be at the upper limit of the kern zone, and the eccentricity

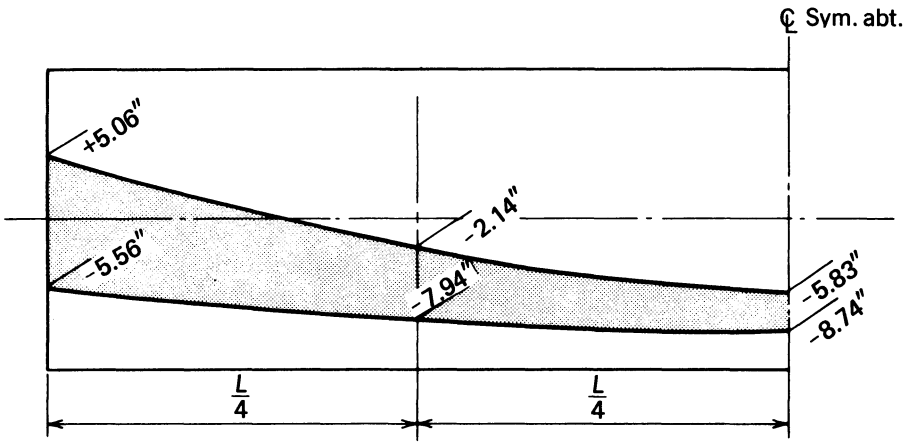

Fig. 4-22. Plot of the limits of the prestressing force for I.P. 4-11.

will be −8.99 in. This eccentricity will produce a stress in the top fiber equal to

$$f_t = -1236\left[1 + \frac{-8.99}{-6.50}\right] = -2945 \text{ psi}$$

This stress exceeds the allowable value of −2200 psi. The eccentricity for a top fiber compressive stress of −2200 psi is:

$$e = \left(\frac{2200}{1236} - 1\right)(6.50) = -5.07 \text{ in.}$$

For an eccentricity of −5.07 in., the bottom fiber stress is:

$$f_b = 1236\left(1 + \frac{-5.07}{8.99}\right) = -539 \text{ psi} > 2000 \text{ psi, ok.}$$

Summary for the end of the beam:

$$e_{\min} = -5.07 \text{ in.}, \; e_{\max} = 5.56 \text{ in.}$$

The limits in which the center of gravity of the prestressing tendons must be located are shown in Fig. 4-22.

4-8 Cross-Section Efficiency

In a rectangular beam the distribution of the unit flexural stresses in the concrete under prestress alone and under total load at the midspan may be as is illustrated in Fig. 4-23. The distribution of the forces in this beam will be identical in

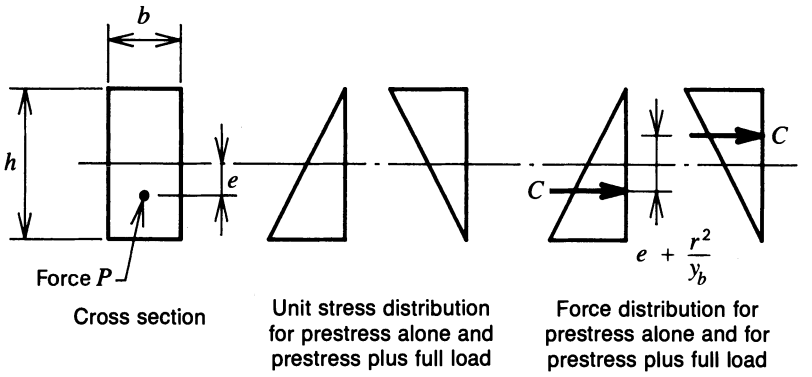

Fig. 4-23. Distribution of unit stresses and forces in a rectangular beam under prestress alone and under prestress plus full load.

shape to the distribution of the unit stresses, and the conversion of the unit stresses to forces can be made by multiplying the unit stresses by the width of the cross section. As has been explained, the total moment to which this member is subjected can be computed by determining the distance between the points of application of the resultant forces in the concrete, under the conditions of prestressing alone and when under full load, and multiplying this distance by the prestressing force.

Analysis of a beam with an I-shaped cross section, such as that illustrated in Fig. 4-24, will reveal that the distribution of unit stresses varies linearly, as in the case of the rectangular cross section; however, because of the variable width of the cross section, the distribution of forces is variable, as illustrated. It is apparent that the resultants of the force diagrams for the I-shaped member will be nearer the extreme fibers of the cross section. For this reason, the resultant force in the I-shaped concrete section moves through a greater vertical distance

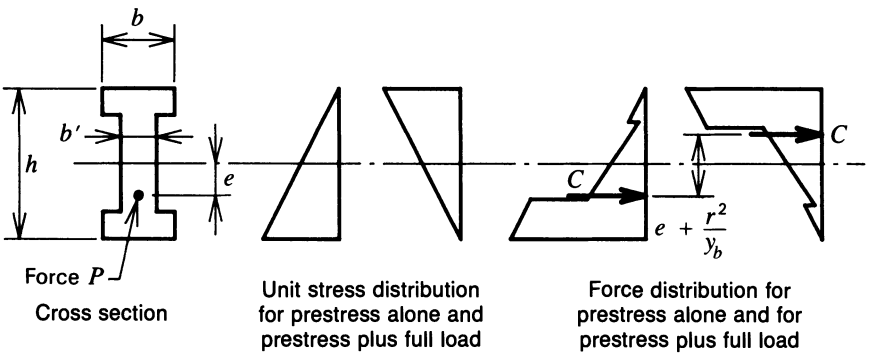

Fig. 4-24. Distribution of unit stresses and forces in a beam with I-shaped cross section, under prestress alone and under prestress plus full load.

when the external load that nullifies the bottom-fiber prestress is applied, than is the case with the rectangular cross section of equal depth. From this analysis, it is obvious that an I-shaped section will be more efficient and is capable of withstanding a greater load than a rectangular section of equal depth, provided that the sections are prestressed with forces of equal magnitude and that tensile stresses are not allowed in the sections.

This consideration is the primary reason for using I, T, and hollow shapes in prestressed flexural members where major tensile stresses must be avoided, and where construction depth is important and must be minimized. Solid slabs and rectangular beams are economical under some conditions of span, loading, and design criteria; but use of the more complicated shapes generally results in minimum quantities of prestressing steel and concrete being required to support a particular load condition, so that they frequently are the more economical choice.

The effect of allowing tensile stresses in the top and bottom fibers is discussed in Secs. 8-6 and 8-7. Selection of an efficient beam cross section for various loading conditions is discussed in Sec. 4-9.

ILLUSTRATIVE PROBLEM 4-12 Determine the maximum total moments that can be imposed upon the I-shaped and rectangular cross sections in Fig. 4-25 if each is prestressed with a straight tendon having an effective force of 200 k, and if tensile stresses are not allowed under any condition of loading.

SOLUTION: Because tensile stresses are not allowed under any conditions of loading, the prestressing force cannot be applied outside of the kern zone. The lower limit of the kern zone is located r^2/y_t below the centroidal axis, and the upper limit is located r^2/y_b above the centroidal axis (see Sec. 4-4). Therefore:

For the I shape:

$$M_t = 200 \text{ k} \left(\frac{4.22 + 4.22}{12} \right) = 140 \text{ k-ft}$$

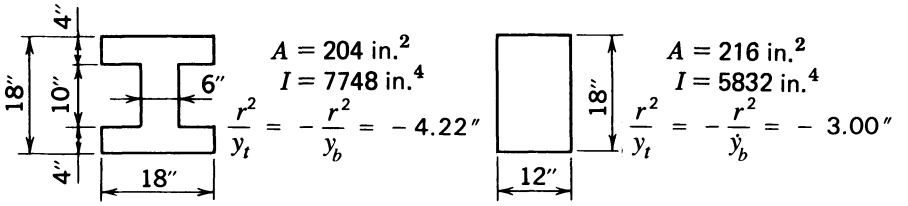

Fig. 4-25. Cross sections compared in I.P. 4-12.

For the rectangular shape:

$$M_t = 200 \text{ k} \left(\frac{3.00 + 3.00}{12} \right) = 100 \text{ k-ft}$$

4-9 Selection of Beam Cross Section

It has been shown that the location of the pressure line in a prestressed-concrete flexural member changes upon the application of external load. At the end of a member where no moment exists, the pressure line in a simple prestressed-concrete beam is always coincident with the location of the center of gravity of the prestressing force. At the center of the beam, the distance from the center of gravity of the prestressing to the pressure line is equal to the total moment acting at that point divided by the prestressing force (from eq. 4-6).

To illustrate the effect of this action on the shape of the optimum concrete section, one can consider a simple pretensioned beam that is prismatic, has straight tendons, and is subjected to a load of such magnitude that the bottom-fiber stress is zero at the midspan. At the end of the beam, the pressure line is coincident with the center of gravity of the prestressing, a condition that remains unchanged despite variations in the external load. Therefore, the optimium section at the end will be a shape that is concentric about the prestressing force because this shape will result in minimum concrete stresses. At midspan, the pressure line acts above the center of gravity of the section; so a top flange is necessary to resist this force. Because the stress in the bottom fibers is zero, no bottom flange is required to resist stress under this condition of loading.

The above discussion shows that, as would be expected, the optimum concrete section is materially influenced by the prestressing force and the loading. If, in the above example, the prestressing tendons were draped in such a manner that there was little or no eccentricity at the ends of the beam, there would be no need for any shape other than a rectangular section, which is easy to construct and is efficient in resisting large, concentric, compressive forces. If the load causing zero stress in the bottom fibers at the midspan of the beam were always present, there would be no need for a large bottom flange near midspan because the pressure line would always be acting near the top of the section, and the concrete in the bottom flange would serve only to protect the prestressing steel from the effects of fire and corrosion; therefore, a T-shaped section would be efficient. On the other hand, if the load that causes zero stress in the bottom fibers at midspan is an intermittent load, and if this intermittent load is very large in comparison to the dead load of the beam itself, a large bottom flange would be required at midspan of the beam to resist or "store" the prestressing force until the beam was again required to carry the intermittent load. An I shape is better for this purpose than a rectangular shape, for with an I shape the

distance the pressure line can move without tensile stresses resulting in the section is greater than with a rectangular shape of equal depth.

There are basic principles the designer of prestressed-concrete simple beams must keep in mind: bottom flanges are primarily for resisting and retaining the prestressing force until it is needed to resist the external load, at which time the pressure line moves upward; top flanges are needed for fully loaded, flexural members because the pressure line is in the vicinity of the top flange when the beam is fully loaded (in addition, amply proportional top flanges ensure that flexural failures of the brittle type cannot occur, as is discussed in Chapter 5); flanged shapes permit greater distance between the pressure line and the center of gravity of the prestressing force than is allowed by rectangular shapes, so that smaller prestressing forces are required; and, finally, the webs are effective primarily in resisting shear stresses. A complete understanding and appreciation of these functions will assist the designer in the rapid preliminary design of beams, as well as in obtaining economical and efficient designs.

Because the dead load of a prestressed member constitutes a small portion of the total load to which it is subjected for short spans and a large portion of the total load for long spans, the use of I-shaped, hollow-rectangular, and solid-rectangular beams is more common for short-span members, whereas T-shaped beams are more often used on long spans. (An exception to this is cast-in-place box girder bridge sections, which are often used in long-span bridges, both simply supported and continuous; see Chapter 14.

When straight pretensioned tendons are used in applications in which the dead load of the member is large in comparison with the total moment, it often is necessary to supply a large bottom flange to resist the prestressing stresses at the end. In addition, the large bottom flange may be required to ensure that the concrete cover for the tendons will be adequate to protect the tendons against corrosion throughout the length of the beam. In such applications, the stress level in the bottom flange at the center of the beam, due to the combined effects of prestressing and dead load, may be relatively low. Because of the smaller area required for post-tensioned tendons, as well as the ease of placing post-tensioned tendons on curved paths, the size of the bottom flange of post-tensioned beams is not frequently dictated by the stresses due to prestressing at the end or by the amount of concrete required to provide adequate concrete cover.

The designer experienced in field supervision as well as the theoretical aspects of prestressed concrete will bear in mind that thin webs of 4 or 5 in. width may be theoretically satisfactory with minimum web reinforcement, but their use often is problematic, resulting in a member in which it is difficult to place and consolidate the concrete. Honeycomb then becomes a real danger. Under normal conditions, 6 in. should be regarded as the minimum web width for a precast I-shaped beam, and 7 in. is the preferred minimum web width if post-tensioning is used. The minimum web width some agencies permit in cast-in-place post-

tensioned box girder bridge superstructure is 12 in.; experience has shown this width is needed in order to provide sufficient space for shear reinforcement, post-tensioning tendons, and consolidating the concrete with internal vibrators.

Extremely narrow top flanges are dangerous in prestressed concrete, just as they are in structural steel. The top flange of a beam can buckle like a column if it is of narrow dimensions, unsupported laterally, and too highly stressed. Field experience has shown the desirability of using reasonably wide flanges to reduce the transverse flexibility of girders during handling. This subject is treated further in Sec. 17-8.

The usual ratio for depth of beam to span for simple prestressed-concrete beam varies from 1 in 16 to 1 in 22, depending upon the conditions of loading, allowable vertical clearance, and type of construction. In lightly loaded, simple T-shaped roof members, the depth-to-span ratio may be as great as 1 in 30. Simply supported cored slabs of prestressed concrete have been successfully used with depth-to-span ratios as great as 1 in 40. Solid, continuous, post-tensioned roof slabs with depth-to-span ratios as great as 1 in 45 have given satisfactory performance. Excessive deflection and vibration under transient live loads are more likely to be problems in slender members than in deeper, stiffer ones.

4-10 Effective Beam Cross Section

The most commonly used procedure in prestressed-concrete design is to base the flexural computations in the elastic range upon the section properties of the *gross concrete section*, defined as the concrete section from which the area of the reinforcement, the ducts in the case of post-tensioning, has not been deducted, and to which the transformed area of the reinforcement has not been added. This procedure is considered to render sufficiently accurate results in the usual application of prestressed concrete. The accuracy in the computation of stressses that would result by basing the computation on the net and transformed section properties is not normally justified or significant. One must keep in mind that the dimensions of sections are never constructed exactly as specified, and the elastic properties of the concrete and reinforcement are not known precisely; so assumed values must be used in computing transformed section properties. It is important, however, that the designer of prestressed concrete be aware of the nature of the actual section involved in the various types of construction, and that the use of net section and transformed section properties can be important under special conditions. Furthermore, Sec. 18.2.6 of ACI 318 requires the consideration of the net section in computing the section properties in post-tensioned members.

When the prestressing force is applied (at transfer) to pretension a concrete member that does not contain nonprestressed flexural reinforcement, the deformation of the concrete is a function of its *net section* properties because the

concrete alone is compressed by the tensile force in prestressing steel. In this case, at the time of applying the prestressing force, the prestressing reinforcement shortens and does not assist the concrete in resisting the prestressing force. The net section is defined as the section that results when the area occupied by the pretensioned reinforcement (or ducts in the case of post-tensioning) is deducted from the gross section. Because the pretensioned reinforcement is bonded to the concrete, when there is a change of strain in the concrete at the level of the prestressed reinforcement after the transfer of the prestressing force to the concrete, there must be a corresponding and equal change of strain in the presetressing reinforcement. Therefore, when external loads, other than the dead load of the beam, which is acting at the time of prestressing, are applied, the deformation of a member is a function of the *transformed net section*, which can be defined as the section that results when the area of bonded reinforcement (prestressed and nonprestressed) is transformed into an elastically equivalent area of concrete, with the area of concrete displaced by the reinforcement taken into account. This accomplished by multiplying the areas of the reinforcement by the appropriate modular ratios and adding these transformed areas to the net concrete section at the proper locations. If the transformed areas are added to the gross concete section, the result is the *gross-transformed section;* if added to the net section, the result is the *net-transformed section*. In normal pretensioning practice, the effect of the transformed section is small, and little normally is gained by taking these effects into account. The effect of the transformed section normally will be greater in large members with bundled pretensioned tendons (see Sec. 8-8). However, little can be gained under normal conditions by including these refinements in the computations. (See Sec. 9-2 for methods of computing section properties.)

In the case of post-tensioned construction, the deformation of a member that does not contain bonded nonprestressed reinforcement is a function of the net section under all conditions of prestressing and external load, until such time as grout is injected into the ducts and allowed to harden and thereby bond the tendons to the concrete section. After bond is established, the deformation of the member is a function of the net-transformed section. As in the case of pretensioning, under normal conditions little is gained by including these effects in the computations.

The use of the net section properties for the computation of stresses that occur before the bonding of post-tensioned reinforcement is required by ACI 318, but the use of the transformed section is optional for stresses that occur after bonding.

The net section and net-transformed section properties should be used in computing stresses in long-span, post-tensioned girders that have large concentrations of ducts in relatively small bottom flanges. In such cases, the areas of the ducts can have a significant influence on the compressive stresses in the bottom flange resulting from the prestressing, because the area occupied by the

ducts may be a large portion of the total bottom flange area. In addition, the area of the prestressing reinforcement generally is large and can have a significant effect upon the stresses due to superimposed loads.

In transforming an area of nonprestressed reinforcement (tension or compression), or an area of pretensioned reinforcement, the area of the reinforcement should be multiplied by the quantity $(n - 1)$, or in the case of pretensioned reinforcement by the quantity $(n_p - 1)$, to account for the concrete area occupied by the reinforcement (A_s, A'_s, or A_{ps}). In the case of post-tensioned reinforcement that is bonded by grouting after stressing, it is appropriate to use $n_p A_{ps}$ as the area of the transformed reinforcement that is added to the net section or net-transformed section. The values of n and n_p, the modular ratios for nonprestressed and prestressed reinforcement, respectively, used in the computations of transformed section properties should be computed by using the value of the elastic modulus of the concrete appropriate for the age of the concrete at the time when the change in loading is being considered. The details of the different types of sections are illustrated in Fig. 4-26, and computations of section properties for the various types of sections are discussed in Sect. 9-2.

ILLUSTRATIVE PROBLEM 4-13 For the pretensioned girder illustrated in Fig. 4-27, compute the stresses in the concrete due to prestressing, based upon the gross and net section properties. In addition, compute the combined concrete stresses, based upon the gross, net, and transformed-net sections at the center of a span of 40 ft, when the externally applied load is 3.13 klf, the dead load of the beam is 0.44 klf, the area of the prestressing steel is 3.20 in.^{2}, the eccentricity of the prestressing is 9.40 in., the effective prestressing force is 440 k and the modular ratio is 6.

The section properties of the gross section are:

$$A = 418.5 \text{ in.}^2 \qquad I = 44{,}700 \text{ in.}^4$$

$$y_t = -15.39 \text{ in.} \qquad y_b = 14.61 \text{ in.}$$

$$\frac{r^2}{y_t} = -6.94 \text{ in.} \qquad \frac{r^2}{y_b} = 7.31 \text{ in.}$$

$$S_t = -2904 \text{ in.}^3 \qquad S_b = 3060 \text{ in.}^3$$

The area of the net section is 415.3 in.^{2}, the eccentricity of the prestressing is 9.48 in. (note the slight increase in the eccentricity due to the larger value of y_b for the net section), and other section properties for the net section are:

$$y_t = -15.32 \text{ in.} \qquad y_b = 14.68 \text{ in.}$$

$$\frac{r^2}{y_t} = -6.98 \text{ in.} \qquad \frac{r^2}{y_b} = 7.29 \text{ in.}$$

$$S_t = -2899 \text{ in.}^3 \qquad S_b = 3025 \text{ in.}^3$$

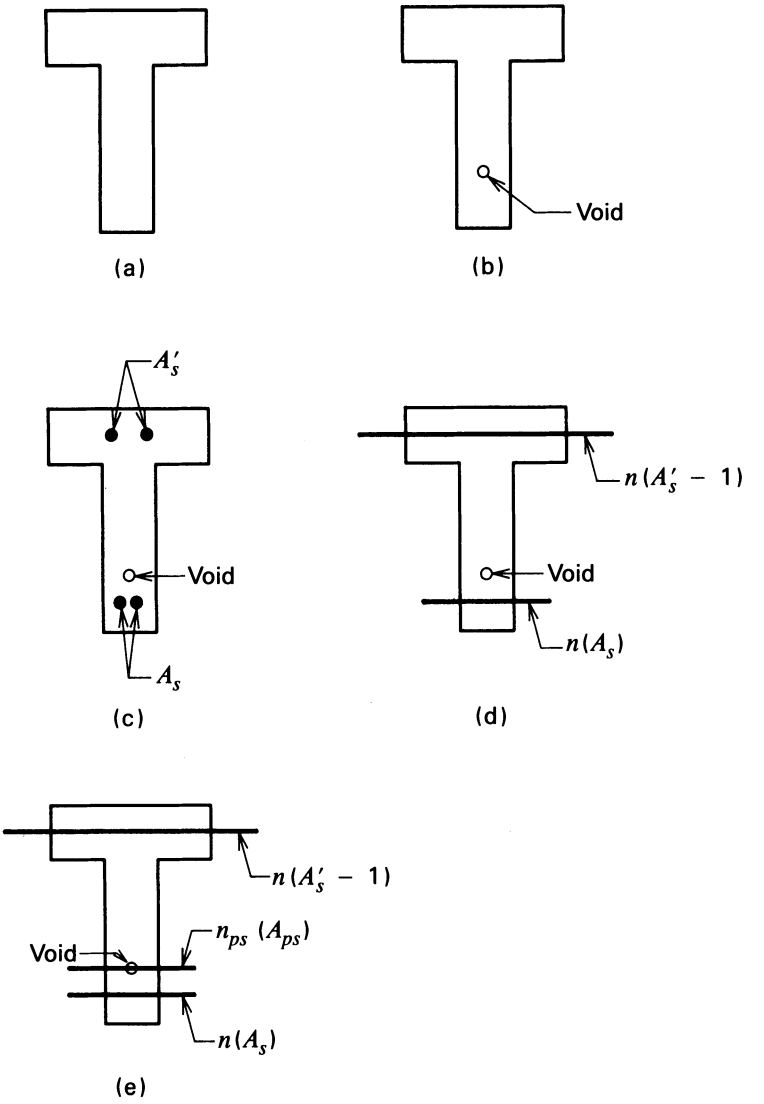

Fig. 4-26. Cross sections of a beam illustrating: (a) gross concrete section; (b) net concrete section having void for either pretensioned reinforcement or duct, or preformed hole for post-tensioned reinforcement; (c) gross section (containing nonprestressed tension and compression reinforcement as well as a void for prestressed reinforcement); (d) transformed net section (containing transformed nonprestressed reinforcement and void for post-tensioning reinforcement, duct, or pretensioned reinforcement); (e) gross transformed section (containing prestressed and nonprestressed reinforcement).

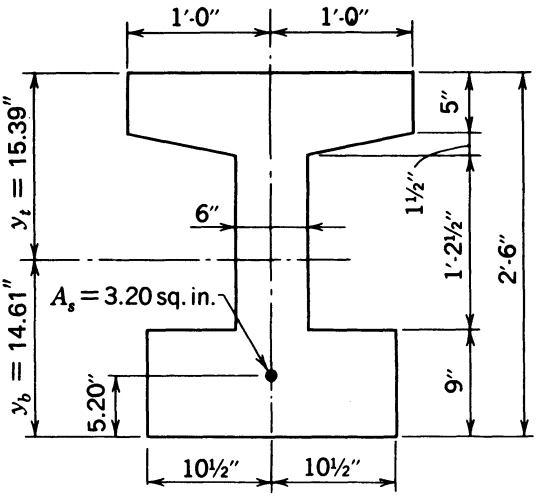

Fig. 4-27. Cross section used to demonstrate the effect of the transformed and net beam cross sections as compared to gross cross section in I.P. 4-13.

The section moduli for the transformed-net section are $S_t = -2926$ in.^{3} and $S_b = 3230$ in.^{3}

SOLUTION:

The stresses due prestressing based upon the gross section are:

$$f_t = \frac{-440{,}000}{418.5}\left(1 + \frac{9.40}{-6.94}\right) = 373 \text{ psi}$$

$$f_b = \frac{-440{,}000}{418.5}\left(1 + \frac{9.40}{7.31}\right) = -2403 \text{ psi}$$

The stresses due to prestressing based upon the net section are:

$$f_t = \frac{-440{,}000}{415.3}\left(1 + \frac{9.48}{-6.98}\right) = 379 \text{ psi}$$

$$f_b = \frac{-440{,}000}{414.3}\left(1 + \frac{9.48}{7.29}\right) = -2437 \text{ psi}$$

The moments due to dead and superimposed load are:

$$M_d = 0.44\,\frac{40^2}{8} = 88 \text{ k-ft}$$

$$M_{sl} = 3.13\,\frac{44^2}{8} = 626 \text{ k-ft}$$

The stresses due to the dead and superimposed load based upon the gross section are:

$$f_t = (88 + 626)\frac{12{,}000}{-2904} = -364 - 2587 = -2951 \text{ psi}$$

$$f_b = (88 + 626)\frac{12{,}000}{3060} = 345 + 2455 = 2800 \text{ psi}$$

The combined stresses, based upon the selection properties for the gross section, are:

$$f_t = 373 - 364 - 2587 = -2578 \text{ psi}$$

$$f_b = -2403 + 345 + 2455 = 397 \text{ psi}$$

The combined stresses in the top and bottom fibers due to prestressing and dead load on the net section combined with those due to the superimposed load on the transformed-net section are:

$$f_t = 379 - 364 - 2567 = -2552 \text{ psi}$$

$$f_b = -2437 + 349 + 2326 = +238 \text{ psi}$$

ILLUSTRATIVE PROBLEM 4-14 Using the section properties for the gross, net and transformed sections listed below, compute the stresses due to prestressing in the top and bottom fibers for the post-tensioned girder of Fig. 4-28 based upon an effective prestressing force of 2380 k located 5.3 in. above the soffit based upon:

1. The gross section properties.
2. The net section properties if the area of the post-tensioning ducts is 39.0 in.^{2}.

In addition, determine the allowable uniformly distributed superimposed live load on the girder, if the design span is 200 ft based upon:

1. The gross section properties.
2. The transformed section properties if $nA_{ps} = 8.35$ in.^{2}. Finally, compute the ratio between the computed allowable superimposed live loads.

Gross Section Properties

$A = 2051$ in.^{2} $\quad I = 3{,}735{,}950$ in.^{4}

$y_t = -53.7$ in. $\quad y_b = 69.3$ in.

$S_t = -69{,}700$ in.^{3} $\quad S_b = 54{,}000$ in.^{3}

$\dfrac{r^2}{y_t} = -34.0$ in. $\quad \dfrac{r^2}{y_b} = 26.3$ in.

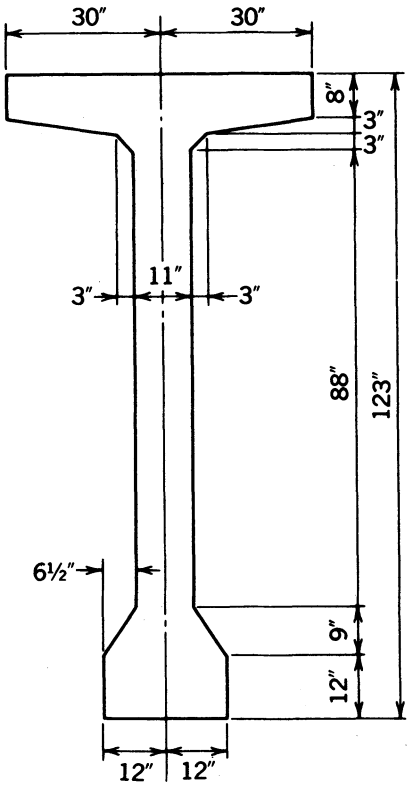

Fig. 4-28. Girder cross section for Problem 4-14.

Net section properties

$A = 2012$ in.^{2} $I = 3{,}572{,}900$ in.^{4}

$y_t = -52.5$ in. $y_b = 70.5$ in.

$S_t = -68{,}000$ in.^{3} $S_b = 50{,}750$ in.^{3}

$\frac{r^2}{y_t} = -33.8$ in. $\frac{r^2}{y_b} = 25.2$ in.

Transformed section properties

$A = 2096$ in.^{2} $I = 3{,}915{,}500$ in.^{4}

$y_t = -55.0$ in. $y_b = 68.0$ in.

$S_t = -71{,}300$ in.^{3} $S_b = 57{,}600$ in.^{3}

SOLUTION:

(1) Stresses due to prestressing using the gross section:

$$f_t = \frac{-2380}{2051}\left(1 + \frac{64.0}{-34.0}\right) = 1024 \text{ psi}$$

$$f_b = \frac{-2380}{2051}\left(1 + \frac{64.0}{26.3}\right) = -3984 \text{ psi}$$

(2) Stresses due to prestressing using the net section:

$$f_t = \frac{-2380}{2012}\left(1 + \frac{65.2}{-33.8}\right) = 1099 \text{ psi}$$

$$f_b = \frac{-2380}{2012}\left(1 + \frac{65.2}{25.2}\right) = -4243 \text{ psi}$$

The dead load of the beam is 2.14 klf, and M_d = 10,700 k-ft. Therefore, the allowable superimposed live loads for the gross and net sections are computed as:

(1) For the gross section:

$$f_{dt} = \frac{10{,}700 \times 12{,}000}{-69{,}700} = 1842 \text{ psi}$$

$$f_{db} = \frac{10{,}700 \times 12{,}000}{54{,}000} = 2378 \text{ psi}$$

$$\text{Final top-fiber stress} = -1842 + 1024 = -818 \text{ psi}$$

$$\text{Final bottom-fiber stress} = 2378 - 3984 = -1606 \text{ psi}$$

$$w_{sll} = \frac{1606 \times 54{,}000}{12{,}000 \times 5{,}000} = 1.44 \text{ klf}$$

(2) For the net and transformed sections:

$$f_{db} = \frac{10{,}700 \times 12{,}000}{-68{,}000} = -1888 \text{ psi}$$

$$f_{bt} = \frac{10{,}700 \times 12{,}000}{50{,}750} = 2530 \text{ psi}$$

$$\text{Final top-fiber stress} = -1888 + 1099 = -789 \text{ psi}$$

$$\text{Final bottom-fiber stress} = 2530 - 4243 = -1713 \text{ psi}$$

$$w_{sll} = \frac{1713 \times 57{,}600}{12{,}000 \times 5{,}000} = 1.64 \text{ klf}$$

Ratio = 1.14 (less for gross section)

4-11 Variation in Steel Stress

Because the prestressing steel never is located at the extreme fiber of a prestressed beam but is at some distance from the surface of the concrete, the maximum change in concrete stress that normally can be expected to occur at the level of the center of gravity of the steel is approximately 70 to 80 percent of the bottom-fiber stress that results from superimposed loads. With concrete that has a cylinder strength of 5000 psi, the stress change in the concrete at the level of the steel could be expected to be on the order of 1500 psi. The modular ratio between the prestressing steel and the concrete can be assumed to be 6 for loads of short duration. As a result, the application of the short-duration, superimposed load would cause an increase in steel of approximately 9000 psi, provided that the steel and the concrete were adequately bonded. If the steel is not bonded to the concrete but is anchored at the ends of the member only, the increase in steel stress resulting from the application of the superimposed load will be less than 9000 psi because the steel can slip in the ducts. The increase in steel stress in unbonded tendons tends to be proportional to the average change in the concrete stress at the level of the steel, and thus is affected by the tendon shape and the depth of the concrete section.

It should be noted that the increase in stress of 9000 psi due to the application of the superimposed load is only about 7 percent of the final stress normally employed in wire or strand tendons, and about 11 percent of the final stress normally employed in bar tendons. The reduction in stress in the prestressing steel due to relaxation of the steel, shrinkage of the concrete, and creep of the concrete is on the order of 10 to 30 percent under average conditions (see Sec. 7-2). Hence, the stress that exists in the tendon under the superimposed load after all of the losses of prestress have taken place is not so high as the initial stress in the steel.

The small variation in steel stress that occurs in a normal prestressed member subjected to frequent application of the design load is responsible for the high resistance to fatigue failure that is associated with this material (see Sec. 11-6).

ILLUSTRATIVE PROBLEM 4-15 Compute the increase in the stress in the steel at the midspan of the beam in I.P. 4-13 by using the transformed section properties. The distances from the centroidal axis of the section to the top and bottom

fibers are −15.74 in. and +14.26 in., respectively, and the section moduli for the top and bottom fibers are −2926 in.^{3} and +3230 in.^{3}, respectively.

SOLUTION: The concrete stress at the level of the steel due to the external load of 3.13 klf is:

$$y_{cgs} = 14.26 - 5.20 = 9.06.$$

$$f_{cgs} = \frac{626 \times 12{,}000 \times 9.06}{3230 \times 14.26} = 1478 \text{ psi}$$

The increase in steel stress due to the superimposed load is:

$$\Delta f_s = nf_c = 6 \times 1478 = 8868 \text{ psi (tension)}$$

PROBLEMS

1. The double-tee slab shown in Fig. 4-29 has an area of 180 sq. in., and a moment of inertia of 2860 in.^{4}, with the distance from the top fiber to the centroid of the cross section 4.00 in. Assume that the concrete weighs 150 pcf and the member is to be used on a simple span of 24.0 ft. If it is pretensioned with one tendon in each stem with an initial force of 16,100 lb each, located 2 in. above the bottom fiber, determine the initial stresses due to prestressing and dead load at the support and at midspan. If the loss of prestress is 20 percent of the initial force, determine the maximum superimposed service load that can be imposed on the member if the allowable bottom fiber tensile stress under service load is zero, 200, 400, and 800 psi.

SOLUTION:

$$r^2 = \frac{2860}{180} = 15.89 \text{ in.}^2, \quad \frac{r^2}{y_t} = \frac{15.89}{-4.00} = -3.97 \text{ in.}, \quad \frac{r^2}{y_b} = \frac{15.89}{10.00} = 1.59 \text{ in.}$$

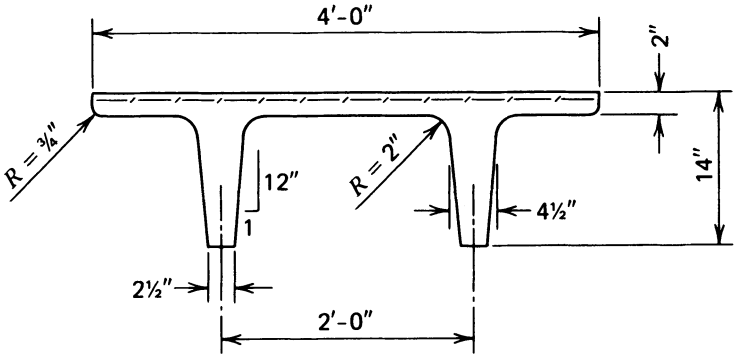

Fig. 4-29. Double-tee slab used in Problem 1.

Stresses due to initial prestressing:

$$f_t = \frac{-2 \times 16{,}100}{180} = \left(1 + \frac{8.00}{-3.97}\right) = 182 \text{ psi}$$

$$f_b = \frac{-2 \times 16{,}100}{180} = \left(1 + \frac{8.00}{1.59}\right) = -1079 \text{ psi}$$

Load and moment due to dead load:

$$w_d = \frac{180}{144} \times 150 = 187.5 \text{ plf}$$

$$M_d = \frac{187.5 \times 24^2}{8} = 13{,}500 \text{ lb-ft}$$

Stresses due to dead load:

$$f_t = \frac{13{,}500 \times 12 \times -4}{2860} = -227 \text{ psi}$$

$$f_b = \frac{13{,}500 \times 12 \times 10}{2860} = 566 \text{ psi}$$

Initial stresses at support:

$$f_t = 182 \text{ psi}$$

$$f_b = -1079 \text{ psi}$$

Initial stresses at midspan:

$$f_t = 182 - 227 = -45 \text{ psi}$$

$$f_b = -1079 + 566 = -513 \text{ psi}$$

Final stresses at support:

$$f_t = 0.80 \times 182 = 146 \text{ psi}$$

$$f_b = 0.80 \times -1079 = -863 \text{ psi}$$

Final stresses at midspan:

$$f_t = 146 - 227 = -81 \text{ psi}$$

$$f_b = -863 + 566 = -297 \text{ psi}$$

The allowable superimposed service load will be limited by the bottom-fiber is 2.5 times that of the section modulus for the bottom fiber. The results of the allowable superimposed service load computations are summarized in Table 4-3.

TABLE 4-3 Summary of Computations for Problem 1.

Allowable bottom fiber stress at service load (psi)	Bottom fiber stress due to superimposed service load (psi)	Superimposed service load (plf)	(psf)	Top fiber stress due to total service load (psi)
0	297	98	24	−200
200	497	165	41	−280
400	697	231	58	−360
800	1097	363	91	−520

Note: Flexural strength requirements, rather than service loads, can be shown to govern the allowable loading on this member when the greater tensile stresses are permitted (see Chapter 5).

2. For the condition of prestressing alone, as well as for the four allowable bottom-fiber stresses investigated in Problem 1, construct the locations of the pressure lines. Use a horizontal scale of 1.0 in. = 4.0 ft and a vertical scale of 1.0 in. = 6.0 ft.

SOLUTION:

Taking f_b to be the bottom-fiber stress due to the total service load, one can write:

$$d = \frac{M}{C} = \frac{f_b I}{y_b C} = \frac{2860 f_b}{10 \times 12 \times 0.80 \times -32{,}200} = -0.000925 f_b \text{ ft}$$

The computations are summarized in Table 4-4 and Fig. 4-30.

3. For the beam of Problem 1 loaded as shown in Fig. 4-31, compute and plot the location of the pressure line if the effective prestressing force is 24,000 lb. Include the dead load of the beam.

TABLE 4-4 Summary of Computations for Problem 2.

Allowable bottom fiber stress due to total service load (psi)	f_b (psi)	Midspan d (ft)
0	863	0.798
200	1063	0.983
400	1263	1.169
800	1663	1.539

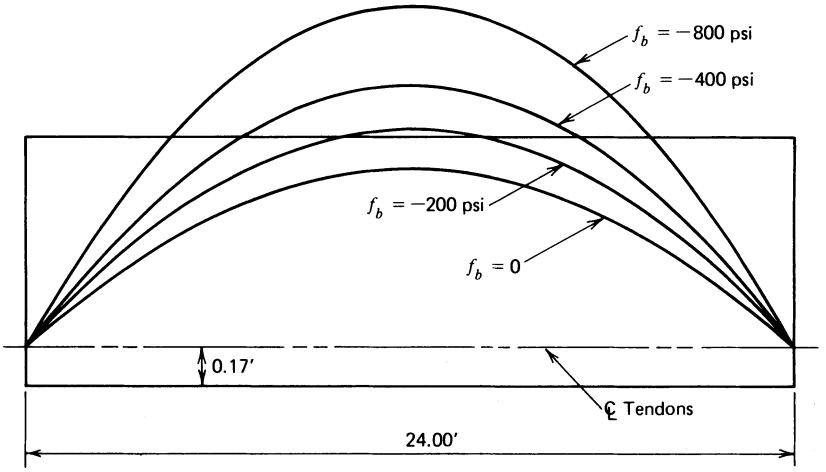

Fig. 4-30. Pressure line locations for Problem 2.

SOLUTION:

For the concentrated load:

$$M_{\max} = \frac{4500 \times 24}{4.5} = 24{,}000 \text{ ft-lb}$$

For the beam dead load:

$$M_{\max} = \frac{187.5 \times 24^2}{8} = 13{,}500 \text{ ft-lb}$$

The locations of the pressure line are summarized in Table 4-5. The results are plotted in Fig. 4-32.

4. Solve Problem 3 as if the effective prestress were equal to 48,000 lb.

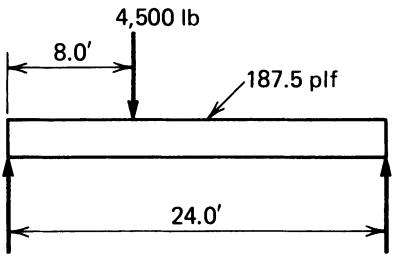

Fig. 4-31. Beam used in Problem 3.

TABLE 4-5 Summary of Pressure Line Locations for Problem 3. Values of $d = M/C$ (ft).

Dist. from left end:	0	6	8	12	18	24
For conc. load:	0	−0.750	−1.000	−0.750	−0.375	0
For unif. load	0	−0.422	−0.500	−0.563	−0.422	0
Total	0	−1.172	−1.500	−1.313	−0.797	0

SOLUTION:

The total movement of the pressure line will be half as much with an effective prestressing force of 48,000 lb. The pressure line locations are summarized in Table 4-6.

5. For the beam shown in Fig. 4-33a, and the total service loads shown in Fig. 4-33b, plot the location of the pressure line at midspan and the quarter points.

SOLUTION:

The solution is shown plotted in Fig. 4-34.

6. For the beam in Fig. 4-35, plot the location of the pressure line for a prestressing force of 100,000 lb if the beam is subjected to a uniform service load of 3000 plf. Use scales of 1 in. = 5.00 ft and 1 in. = 1.00 ft horizontally and vertically, respectively.

SOLUTION:

The negative moment at the right support due to the load on the overhanging end of the beam is:

$$M_{oh} = \frac{-3000 \times 10^2}{2} = -150{,}000 \text{ ft-lb}$$

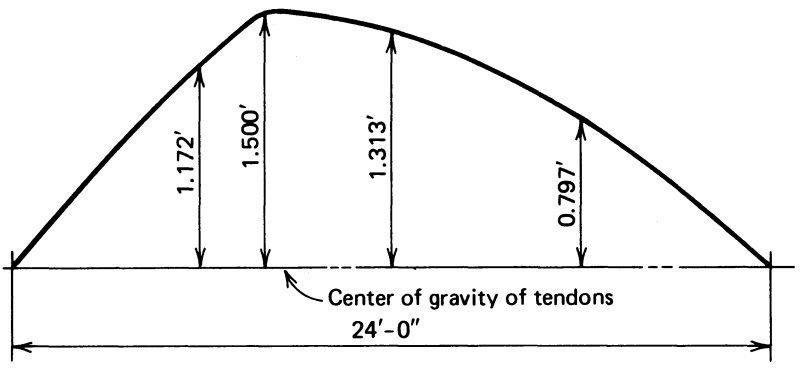

Fig. 4-32. Pressure line for Problem 3.

TABLE 4-6 Summary of Pressure Line Locations for Problem 4. Values of $d = M/C$ (ft).

Dist. from left end:	0	6	8	12	18	24
Total	0	−0.586	−0.750	−0.657	−0.399	0

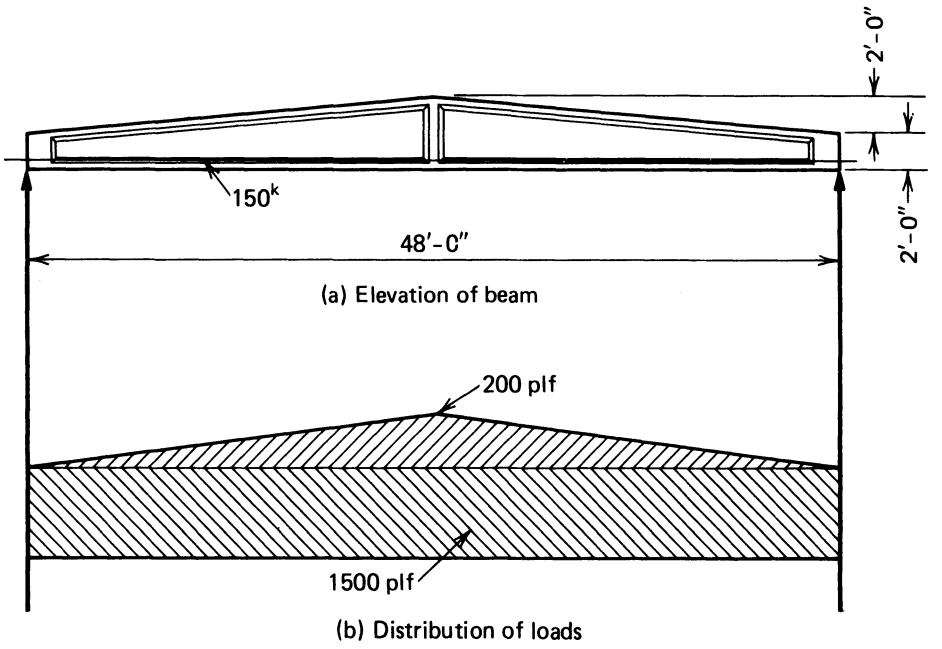

Fig. 4-33. Beam for Problem 5.

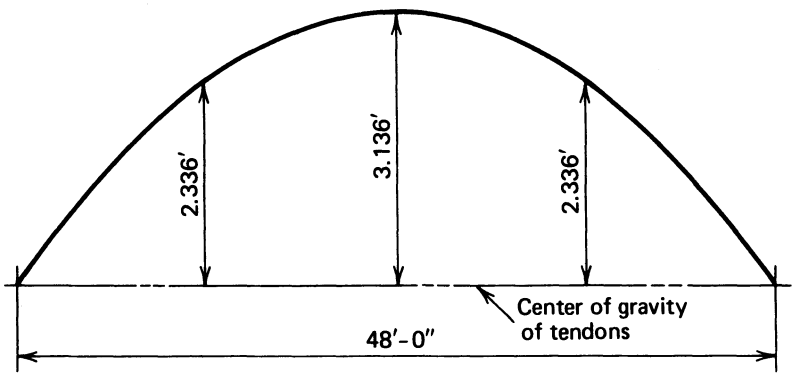

Fig. 4-34. Pressure line for beam of Problem 5.

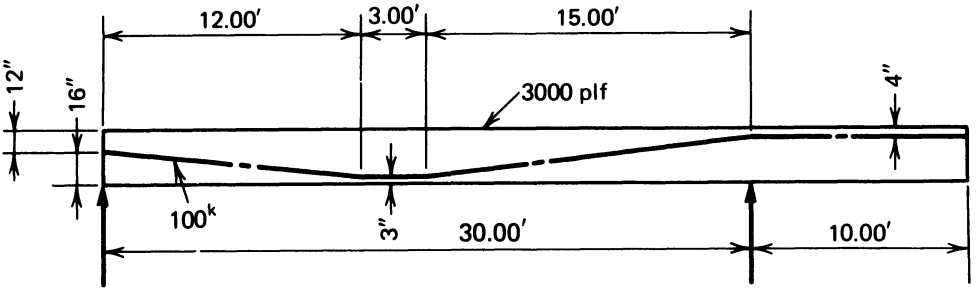

Fig. 4-35. Beam for Problem 6.

The simple-span moment for the load on the 30 ft span only is:

$$M_{sp} = \frac{3000 \times 30^2}{8} = 337{,}000 \text{ ft-lb}$$

The moments for various distances from the left support are summarized in Table 4-7. The solution is completed by dividing the total of the moments by the prestressing force, 100 k, and plotting the results as shown in Fig. 4-36.

7. For the beam shown in Fig. 4-37a, plot the location of the pressure line when the uniformly distributed load is acting alone as well as the location when the uniformly distributed load and the concentrated loads both are acting.

SOLUTION:

The moment diagrams for the uniformly distributed load alone, the concentrated loads alone, and the combination of the uniform and concentrated loads are

TABLE 4-7 Summary of Computation of Moments for Problem 6.

Dist. (ft)	M_{sp} (ft-k)	M_{oh} (ft-k)	M_t (ft-k)
0	0.0	0.0	0.0
3	121.5	−15.0	106.5
6	216.0	−30.0	186.0
9	283.5	−45.0	238.5
12	324.0	−60.0	264.0
15	337.5	−75.0	262.5
18	324.0	−90.0	234.0
21	283.5	−105.0	178.5
24	216.0	−120.0	96.0
27	121.5	−135.0	−13.5
30	0.0	−150.0	−150.0
35	0.0	−37.5	−37.5
40	0.0	0.0	0.0

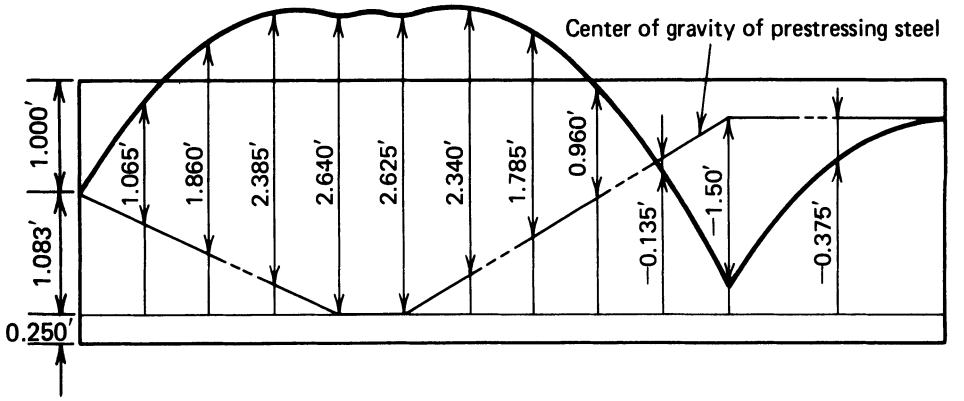

Fig. 4-36. Pressure line for Problem 6.

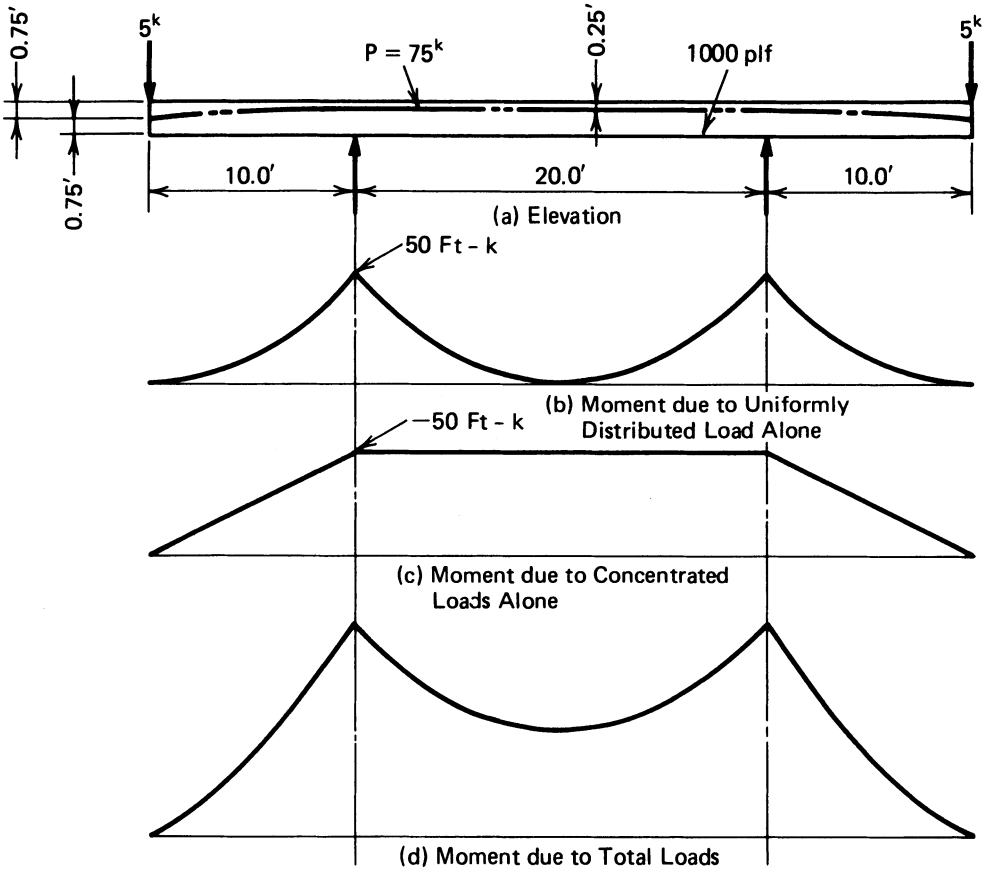

Fig. 4-37. Beam and moment diagrams for Problem 7.

TABLE 4-8 Summary of Pressure Line Locations for Problem 7.

Point	Prestress only	Prestress and uniform load	Prestress and total load
Left end	0.00	0.00	0.00
Midcant. span	−4.50	−2.50	+1.50
Left support	−6.00	+2.00	+10.00
0.10L	−6.00	−0.88	+7.12
0.20L	−6.00	−3.12	+4.88
0.30L	−6.00	−4.72	+3.28
0.40L	−6.00	−5.68	+2.32
0.50L	−6.00	−6.00	+2.00

shown plotted in Fig. 4-37a–c. The locations of the pressure line at various points along the span for the conditions of prestressing alone, prestressing plus the uniformly distributed load, and prestressing plus the combined effects of the loads are summarized in Table 4-8 and plotted in Fig. 4-38.

8. The two-span continuous beam in Fig. 4-39 has variable depth and prestressing force. The location of the pressure line and the magnitude of the prestressing force are given in Table 4-9. Also given in the table are the

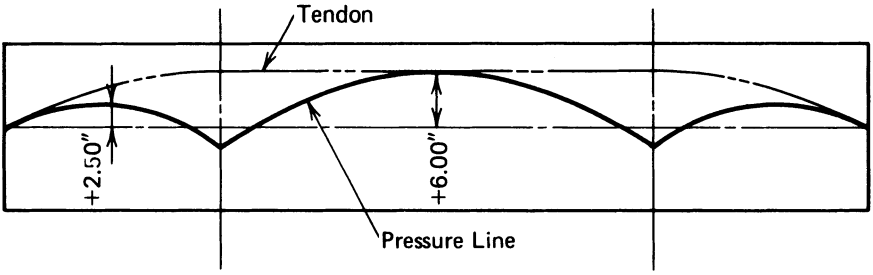

(a) Prestress Plus Uniformly Distributed Load

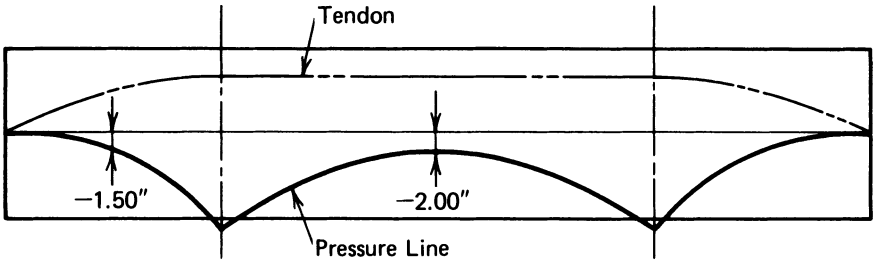

(b) Prestress Plus Total Load

Fig. 4-38. Plots of computations for Problem 7.

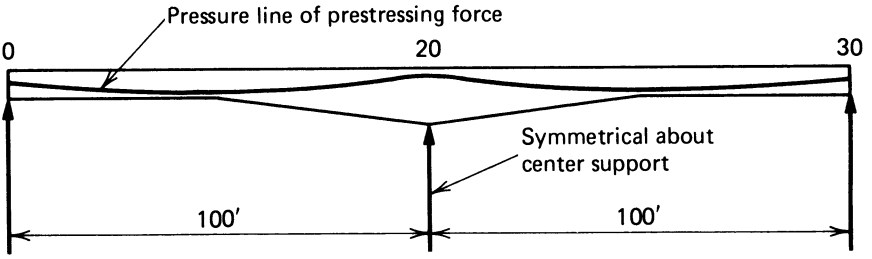

Fig. 4-39. Beam for Problem 8.

dead load moment and the maximum and minimum live load moments. Tabulate the location of the pressure line for the beam when under dead load alone as well as when under dead load plus maximum and dead load plus minimum live loads.

SOLUTION:

The eccentricities of the pressure line in inches, resulting from the computations are summarized in Table 4-10.

9. If f'_{ci} = 4000 psi and f'_c = 5000 psi, compute the maximum uniformly distributed load that the beam in Fig. 4-40 can withstand on a span of 70 ft. Make the determination for the tendons being straight as well as curved. Use the stresses permitted by ACI 318 (see Sec. 3-19). Assume that the loss of prestress is 20 percent, and the curved tendons can be placed with their center of gravity as low as 3.25 in. from the soffit of the beam. The beam has a weight of 488 plf, an area of 468 sq. in., and moment of inertia of 94,184 in.^{4}. The distance from the top fiber to the centroidal axis is 22.54 in.

TABLE 4-9 Given Information for Problem 8.

Pt.	e (in.)	P (k)	M_d (k-ft)	M_{max} (k-ft)	M_{min} (k-ft)
0	0.00	1012	0	0	0
1	2.52	1047	203	416	146
2	4.68	1088	330	697	216
3	6.48	1122	379	839	209
4	7.56	1157	352	846	126
5	8.16	1198	247	715	−35
6	4.56	1164	65	446	−274
7	−0.24	1115	−200	34	−596
8	−6.96	1074	−555	−527	−1007
9	−14.76	1026	−1005	−1244	−1753
10	−21.24	916	−1558	−2123	−2689

TABLE 4-10 Summary of Results for Problem 8.

Pt.	P only	P plus M_{dl}	P plus $M_{dl} + M_{max}$	P plus $M_{dl} + M_{min}$
0	0.00	0.00	0.00	0.00
1	2.52	0.19	−4.57	−1.48
2	4.68	1.03	−6.67	−1.35
3	6.48	2.43	−6.55	0.19
4	7.56	3.91	−4.87	2.60
5	8.16	5.69	−1.48	6.04
6	4.56	3.89	−0.71	6.71
7	−0.24	1.91	1.55	8.33
8	−6.96	−0.76	5.13	10.49
9	−14.76	−3.01	11.54	17.50
10	−21.24	−0.83	26.98	34.40

SOLUTION:

The limits of the kern zone and the section moduli are computed as follows:

$$y_b = 42 - 22.45 = 19.46 \text{ in.}, \quad r^2 = \frac{94{,}184}{468} = 201 \text{ in.}^2$$

$$\frac{r^2}{y_t} = \frac{201}{-22.54} = -8.92 \text{ in.}, \quad \frac{r^2}{y_b} = \frac{201}{19.46} = 10.3 \text{ in.}$$

$$S_t = \frac{94{,}184}{-22.54} = -4178 \text{ in.}^3, \quad S_b = \frac{94{,}184}{19.46} = 4840 \text{ in.}^3$$

The allowable initial stresses are 2400 psi in compression and 190 psi in tension. The allowable final stresses are 2250 psi in compression and 848 psi in tension.

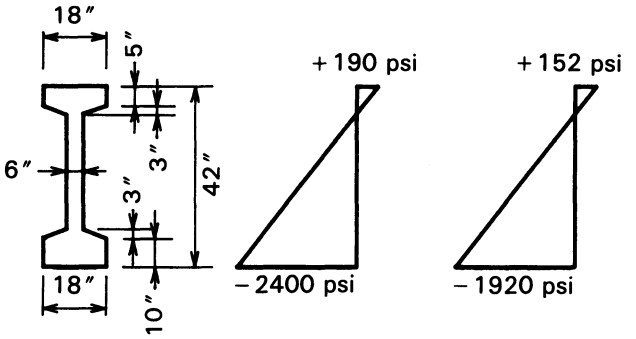

(a) Cross section. (b) Initial stress straight tendon. (c) Final stress straight tendon.

Fig. 4-40. Beam and stress distribution for Problem 9.

(a) Straight tendons: The average prestress for the initial prestressing force is computed as follows (see Fig. 4-40b):

$$\frac{C}{A} = -[190 - (-2400)]\left(\frac{22.54}{42}\right) + 190 = -1200 \text{ psi}$$

Solving for e using eq. 4-4:

$$e = \left(\frac{-2400}{-1200} - 1\right)(10.34) = 10.34 \text{ in.} < y_b - 3.25 \text{ in.}$$

$$= 19.46 - 3.25 = 16.21 \text{ in. ok}$$

$$C = -1200 \times 468 = -561.6 \text{ k}$$

The moment capacity, as limited by the service load stresses in the top and bottom fibers (see Fig. 4-40c), is computed as follows:

By top fiber:

$$M = \frac{(2250 + 152)}{12{,}000}(4178) = 836 \text{ k-ft}$$

By bottom fiber:

$$M = \frac{(1920 + 848)}{(12{,}000)}(4840) = 1116 \text{ k-ft}$$

$$w = \frac{8 \times 836}{70^2} = 1365 \text{ plf}$$

(b) Curved tendons: The dead load moment due to the weight of the beam is:

$$M_{dl} = \frac{488}{1000} \times \frac{70^2}{8} = 298.9 \text{ k-ft}$$

The stresses due to dead load at midspan are:

$$f_t = -858 \text{ psi}, \quad f_b = 741 \text{ psi}$$

The shift in the location of the pressure line due to the dead load moment would be:

$$d = \frac{M_{dl}}{C} = -\frac{298.0}{561.6} \times 12 = -6.39 \text{ in.}$$

The eccentricity of the prestressing force can be greater with the curved tendon than with the straight tendon by the amount of 6.39 in., for a total of 6.39 + 10.34 = 16.73 in. The maximum eccentricity, as limited by the minimum distance from the soffit to the centroid of the prestressing steel (3.35 in.), is:

$$e_{max} = 19.34 - 3.25 = 16.21 \text{ in.} < 16.73 \text{ in.}$$

Using 16.21 in. and solving for the prestress needed to produce an initial bottom-fiber stress that is equal to the arithmetical sum of the bottom-fiber stress due to beam dead load, 741 psi, and the allowable initial stress, −2400 psi, which is 3141 psi, one obtains:

$$-3141 = \frac{C}{468}\left(1 + \frac{16.21}{10.34}\right)$$

$$C = -572 \text{ k}$$

The top and bottom fiber stresses due to the initial prestressing force of −572 k are:

$$f_t = \frac{-572{,}000}{468} = \left(1 + \frac{16.21}{-8.93}\right) = 996 \text{ psi}$$

$$f_b = \frac{-572{,}000}{468} = \left(1 + \frac{16.21}{10.34}\right) = -3138 \text{ psi}$$

$$\text{Net initial top-fiber stress} = 996 - 858 = 138 \text{ psi}$$

$$\text{Net initial bottom-fiber stress} = -3138 + 741 = -2397 \text{ psi}$$

The 20 percent loss of prestress results in final top and bottom fiber stresses due to prestressing alone of 797 psi and −2510 psi, respectively.

Moment capacity limitations of service loads are:

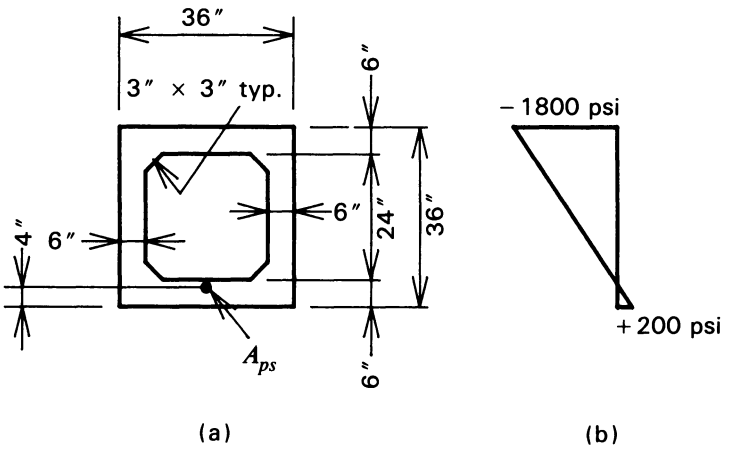

Fig. 4-41. Cross section of beam and stresses for Problem 10. (a) Cross section. (b) Distribution of stresses.

TABLE 4-11 Summary of Computations for Problem 10.

y	f	b	b'	P	P'
36	−1800	36	—	−64.8	—
30	−1467	36	18	−52.8	−26.4
27	−1300	12	—	−15.6	—
9	−30	12	—	−3.6	—
6	−133	36	18	−4.79	2.39
0	+200	36	—	+7.20	—

By top fiber:

$$M = \frac{(2250 + 797)\,4178}{12{,}000} = 1061 \text{ k-ft}$$

By bottom fiber:

$$M = \frac{(2510 + 848)\,4840}{12{,}000} = 1354 \text{ k-ft}$$

$$w = \frac{8 \times 1061}{70^2} = 1732 \text{ plf}$$

$$\text{Ratio} = \frac{1732}{1365} = 1.27$$

10. For the hollow-box girder shown in Fig. 4-41a, plot the distribution of force in the section for the stress distribution indicated in Fig. 4-41b.

SOLUTION:

The computations required for preparing the plot are summarized in Table 4-11. The plot of the distribution of the forces is shown in Fig. 4-42.

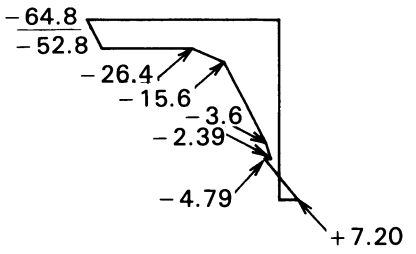

Fig. 4-42. Distribution of forces in kips per inch for Problem 10.

5 Flexural Strength

5-1 Beams under Overloads

It has been shown that a variation in the external load acting on a prestressed concrete beam results in a change in the location of the pressure line, for beams in the elastic range. This is a fundamental principle of prestressed construction. In a normal prestressed concrete beam, this shift in the location of the pressure line continues at a relatively uniform rate as the external load is increased, to the point where cracks develop in the tension fiber. After the cracking load has been exceeded, the rate of movement in the pressure line decreases as additional load is applied, and a significant increase in the stress in the prestressing tendon and the resultant concrete force begins to take place. This change in the action of the internal moment continues until all movement of the pressure line virtually ceases. The moment caused by loads that are applied thereafter is offset entirely by a corresponding and proportional change in the internal forces, just as in nonprestressed reinforced concrete construction. The range of loading that is characterized by these different actions is illustrated in the load deflection curve of Fig. 5-1. The fact that the load is carried by actions that are fundamentally different in the elastic range and in the plastic range is very significant, making strength computation essential for all designs of prestressed concrete flexural

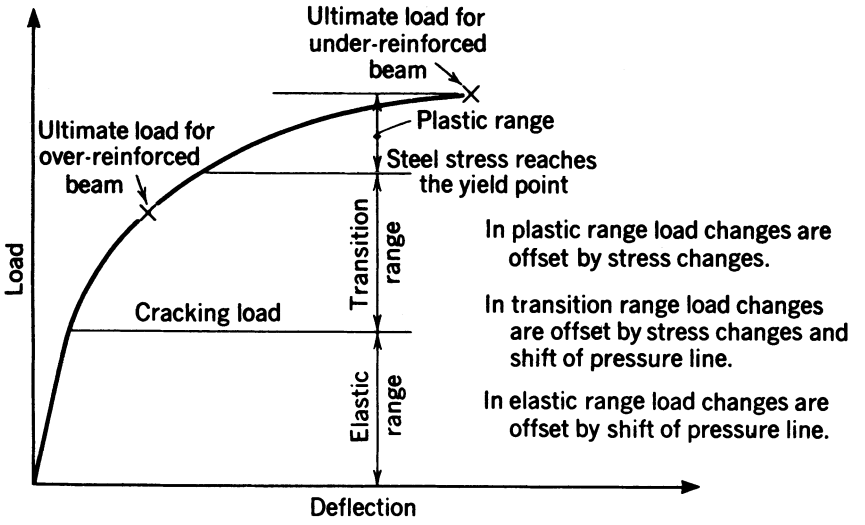

Fig. 5-1. Load–deflection curve for a prestressed-concrete beam.

members, to ensure that adequate safety exists. This is true even though the stresses in the elastic range may conform to a recognized elastic design criterion.

It should be noted that the load deflection curve in Fig. 5-1 is very close to a straight line up to the cracking load, and that the curve becomes progressively more curved as the load is increased above the cracking load. The presence of nonprestressed reinforcing steel in the tensile flange will tend to make the cracking load more difficult to detect from a load–deflection curve, as well as from observations of a beam during loading. The curvature of the load–deflection curve for loads exceeding the cracking load is due to the change in the basic internal resisting moment action that counteracts the applied loads, as described above, as well as to inelastic strains that begin to take place in the steel and the concrete when stressed to high levels.

It may be essential for some flexural members to remain crack-free even under significant overloads, perhaps because of their being exposed to exceptionally corrosive environments during their useful life. In designing prestressed concrete members for use in special applications such as this, it may be necessary to compute the load that causes cracking of the tensile flange to ensure that adequate safety against cracking is provided. Computation of the moment that will cause cracking also is necessary, to ensure compliance with some design criteria (see last paragraph of Sec. 5-4).

Many tests have demonstrated that the load–deflection curves of prestressed beams are approximately linear up to and slightly in excess of the load that causes the first cracks in the tensile flange. (This linearity is a function of the

rate at which the load is applied.) For this reason, normal elastic-design relationships can be used in computing the cracking load by simply determining the load that results in a net tensile stress in the tensile flange (prestress and the effects of the applied loads) that is equal to the tensile strength of the concrete. It is customary to assume that the flexural tensile strength of the concrete is equal to its modulus of rupture in computing the cracking load. The modulus of rupture can be estimated from eq. 3-3.

It should be recognized that the performance of bonded prestressed members is actually a function of the transformed section rather than the gross concrete section (see Sec. 4-10), as well as of concrete creep and shrinkage (see Sec. 7-2). If it is desirable to make a precise estimate of the cracking load, as is required in some research work, these effects must be considered.

ILLUSTRATIVE PROBLEM 5-1 Compute the total uniformly distributed load required to cause cracking in a beam that is 10 in. wide, 12 in. deep, and supported on a simple span of 25 ft, if the final prestressing force is 120,000 lb applied at an eccentricity of 2.50 in. Assume $f'_c = 5000$ psi and $f_r = 7.2\sqrt{5000} = 509$ psi.

SOLUTION:

$$A = 120 \text{ in.}^2, \; I = 1440 \text{ in.}^4$$

$$r^2/y = \mp 2.00 \text{ in. (top/bottom fibers, respectively)}$$

$$S = \frac{1440}{6} = \mp 240 \text{ in.}^3 \text{ (top/bottom fibers, respectively)}$$

$$f_b = \frac{-120{,}000}{120} = \left(1 + \frac{2.50}{2.00}\right) = -2250 \text{ psi}$$

Therefore, the moment that causes cracking must result in a bottom-fiber tensile stress equal to 509 psi + 2250 psi = 2759 psi.

$$M_{cr} = \frac{w_t l^2}{8} = \frac{f_b S_b}{12{,}000} = \frac{2759 \times 240}{12{,}000} = 55.18 \text{ k-ft}$$

$$w_t = \frac{55.18 \times 8}{25.0^2} = 0.706 \text{ klf}$$

5-2 Principles of Flexural Capacity for Members with Bonded Tendons

When prestressed flexural members that are stronger in shear and bond than in bending are loaded to failure, they fail in one of the following modes:

1. *Failure at Cracking Load.* In very lightly prestressed members, the cracking moment may be greater than the moment the member can withstand in the cracked condition so that the cracking moment is the ultimate moment. This condition is rare and is most likely to occur in members that are prestressed concentrically, or with small eccentricities and with relatively small amounts of prestressing steel. It also can occur in hollow or solid prestressed concrete members that have relatively low levels of reinforcement. Determination of the possibility that this type of failure will occur is accomplished by comparing the estimated moment that would cause cracking to the estimated flexural strength of the member. If the estimated cracking load is larger than the computed ultimate load, this type of failure would be expected to take place if the member were subjected to the required load. Because this type of failure is brittle, it occurs without warning. Members that would fail in this fashion should be avoided.

2. *Failure Due to Rupture of Steel.* In lightly reinforced members subject to externally applied load that results in flexural failure, the strength of the steel may be attained before the concrete is subjected to high stresses and has reached a significantly inelastic state. This type of behavior is likely to be encountered in structures that have very large compression flanges and relatively low percentages of flexural reinforcement, such as composite bridge stringers. Computation of the flexural strength of members subject to this type of failure can be done with a high degree of precision. The method of computation, as well as the determination of which members are subject to this mode of failure, is described below.

3. *Failure Due to Concrete Strain.* The usual underreinforced, prestressed flexural members encountered in practice are of such proportions that if they are loaded to their flexural strength, the steel would be stressed well above its yield strength, and the members would attain large deflections before failure. Failure of an underreinforced member occurs when the concrete attains the maximum strain that it is capable of withstanding. Research has shown that the flexural strength of underreinforced flexural members, made with concrete of the normal quality used in prestressed concrete work, is attained when the concrete reaches a strain on the order of 0.003. The flexural strengths of members of this type are limited by concrete strain, load–deformation characteristics, and the amount of the flexural reinforcement. The flexural strength of underreinforced concrete can be predicted with relatively high precision.

4. *Failure Due to Crushing of the Concrete.* Flexural members that have relatively large amounts of prestressing steel or relatively small compressive flanges are said to be overreinforced. Overreinforced members, when loaded to their flexural capacities, do not attain the large deflections associated with underreinforced members, and at failure the stress in the steel does not exceed the yield strength by a significant amount if at all. The failure of the member is limited by the compressive strength (crushing of the concrete compression

flange) and not by the strain in the concrete, as is the case with underreinforced members. The flexural strength of overreinforced concrete flexural members is computed by a trial-and-error procedure, involving assumed strain patterns, as well as by empirical relationships. Both methods are discussed below (Muller 1956).

It must be emphasized that there are no precise definitions of the boundaries between the different classifications of failures listed above. Provisions are included in the *Building Code Requirements for Reinforced Concrete*, ACI 318, to alert the structural designer to the special problems associated with lightly reinforced, underreinforced, and overreinforced members (see Sec. 5-4). Important parameters used in the analysis of the flexural strength of prestressed concrete members include the percentage of reinforcement, ρ_p, which is defined as follows:

$$\rho_p = \frac{A_{ps}}{bd_p} \tag{5-1}$$

where A_{ps} is the area of the prestressed reinforcement in the tension zone, b is the width of the compression flange of the member, and d_p is the distance from the extreme compression fiber to the centroid of the prestressing reinforcing. Another factor is the reinforcement index, ω_p. This dimensionless parameter, which is used in contemporary building codes, is defined as follows:

$$\omega_p = \frac{A_{ps}}{bd_p f_c} = \rho_p \frac{f_{ps}}{f'_c} \tag{5-2}$$

where f_{ps} represents the stress in the prestressing steel under the load resulting in the ultimate moment, and f'_c is the specified concrete compressive strength.

It should be noted that f'_c used in eq. 5-2, is defined as the *specified compressive strength of concrete, psi*, in Chapter 4 of ACI 318 (ACI 318 1989). The value of f'_c normally is specified by an engineer who has designed reinforced concrete members that are included in contract plans and specifications for a unique project. It is, of course, normal and appropriate that the provisions of building codes refer to specified concrete strengths rather than actual concrete strengths. It also should be recognized that actual concrete strengths, which normally but not always will exceed the specified concrete strengths, are appropriately used in the analysis of experimental data and for explaining the basic behavior of reinforced concrete members. For this reason, the term f_{cu} is used henceforth in this discussion to refer to the concrete cylinder compressive strength, in psi.

In order to simplify the explanation of strain compatibility theory as it relates to the computation of ultimate flexural strength, a rectangular beam cross section will be assumed throughout the following discussion. This is done to eliminate the variable of flange width, which is frequently encountered with I or T cross sections. In addition, the following assumptions are made:

1. Plane sections are assumed to remain plane.
2. The stress–strain properties of the steel can be represented by a smooth curve without a definite yield point.
3. The limiting strain of the concrete is equal to 0.003 regardless of the strength of the concrete.
4. The steel and concrete are completely bonded.
5. The stress diagram of the concrete at failure is such that the average concrete stress is $0.85f_{cu}$, the depth of the stress block is $0.85k_u d_p$, and the resultant of the stress in the concrete acts at a distance of $0.42k_u$ from the top of the compression block, as is illustrated in Fig. 5-2.
6. The strain in the top fiber of the concrete section under prestressing alone is equal to zero.
7. The section is subject to pure bending.
8. The analysis is made for the condition of static loads of short duration.

The strains illustrated in Fig. 5-2 and used in the derivation are defined as follows:

ϵ_c: concrete strain at extreme fiber due to prestressing (assumed = 0).
ϵ_u: maximum concrete strain at ultimate moment (assumed = 0.003).
ϵ_{ce}: concrete strain at the level of the steel due to prestressing.
ϵ_{cu}: concrete strain at the level of the steel at ultimate moment.
ϵ_{se}: steel strain due to the effective prestress.
ϵ_{ps}: steel strain at ultimate moment.

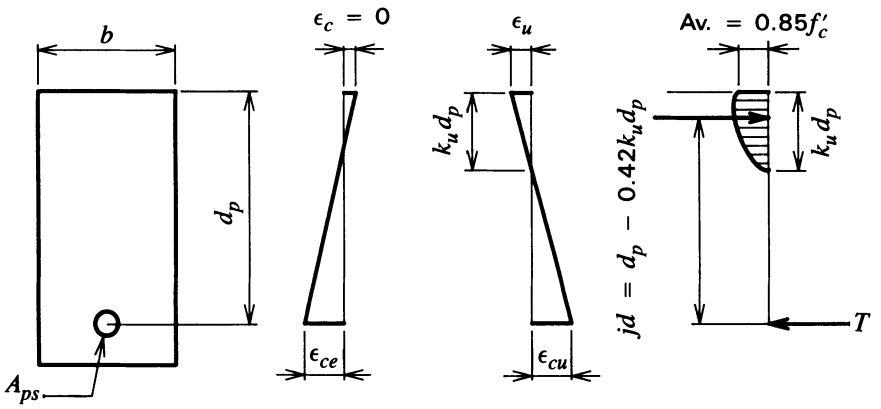

Fig. 5-2. Cross section, strain distributions, and stress distribution used in flexural strength computations. (a) Cross section of beam. (b) Strains due to prestress. (c) Strains at ultimate flexural capacity. (d) Stresses at ultimate flexural capacity.

Because equilibrium of the section requires that the tensile force in the prestressing steel and the compressive force in the concrete be equal, one can write:

$$T = C$$

or:

$$A_{ps} f_{ps} = 0.85 f_{cu} b k_u d_p$$

and:

$$f_{ps} = \frac{0.85 f_{cu} d k_u d_p}{A_{ps}}$$

or:

$$f_{ps} = \frac{0.85 f_{cu} k_u}{\rho_p} \tag{5-3}$$

Expressed in terms of force, eq. 5-3 is written:

$$F_{ps} = 0.85 f_{cu} b k_u d_p \tag{5-3a}$$

By comparing the similar triangles of the concrete strains at ultimate shown in Fig. 5-2, the following relationship is seen:

$$\frac{\epsilon_{cu}}{d_p - k_u d_p} = \frac{\epsilon_u}{k_u d_p}$$

or:

$$\epsilon_{cu} = \epsilon_u \left(\frac{1 - k_u}{k_u} \right) \tag{5-4}$$

The strain in the prestressing steel at ultimate moment, ϵ_{ps}, which consists of the sum of the strains due to the effective prestress, ϵ_{se}, the strain in the concrete at the level of the steel resulting from prestressing, ϵ_{ce}, and the strain in the concrete at the level of the steel at ultimate moment, ϵ_{cu}, can be expressed by:

$$\epsilon_{ps} = \epsilon_{se} + \epsilon_{ce} + \epsilon_{cu} \tag{5-5}$$

Substituting eq. 5-4 into eq. 5-5, one obtains:

$$\epsilon_{ps} = \epsilon_{se} + \epsilon_{ce} + \epsilon_u \left(\frac{1 - k_u}{k_u} \right) \tag{5-6}$$

which can be rearranged to:

$$k_u = \frac{\epsilon_u}{\epsilon_u + \epsilon_{ps} - \epsilon_{se} - \epsilon_{ce}} \tag{5-7}$$

Substituting the value of k_u given in eq. 5-7 into the relationship of eq. 5-3, the general equation for the stress in the prestressing steel and the strains in the concrete and steel under ultimate flexural loading is obtained:

$$f_{ps} = \frac{0.85 f_{cu}}{\rho_p} \times \frac{\epsilon_u}{\epsilon_u + \epsilon_{ps} - \epsilon_{se} - \epsilon_{ce}} \tag{5-8}$$

All of the terms in this relationship are known or assumed except the strain, ϵ_{su}, and the stress, f_{ps}, in the prestressing steel at failure. The stress–strain curve for the prestressing steel actually used in the construction of the flexural member represents the second relationship needed to solve eq. 5-8.

A solution using the strain compatibility procedure described above is illustrated in Fig. 5-3, in which the basic assumptions used in the analysis are given in the figure itself, and the values of the steel index q'' are shown plotted on the stress–strain curve for the particular steel that was studied. The steel index is defined as:

$$q'' = \frac{A_{ps} f_{pu}}{b d_p f_{cu}} = \rho_p \frac{f_{pu}}{f_{cu}} \tag{5-9}$$

The steel index was used by some of the early proponents of strain compatibility analysis, rather than the reinforcement index (eq. 5-2) that is commonly used today. In addition, some of the early analyses were based upon a maximum concrete stress of $0.80 f'_c$ rather than 0.85, and the maximum concrete strain at failure was assumed to be 0.0034 rather than 0.003 in./in. (Muller 1956). The results obtained by using these slightly different values are almost identical to those obtained using the contemporary assumptions, which were listed above

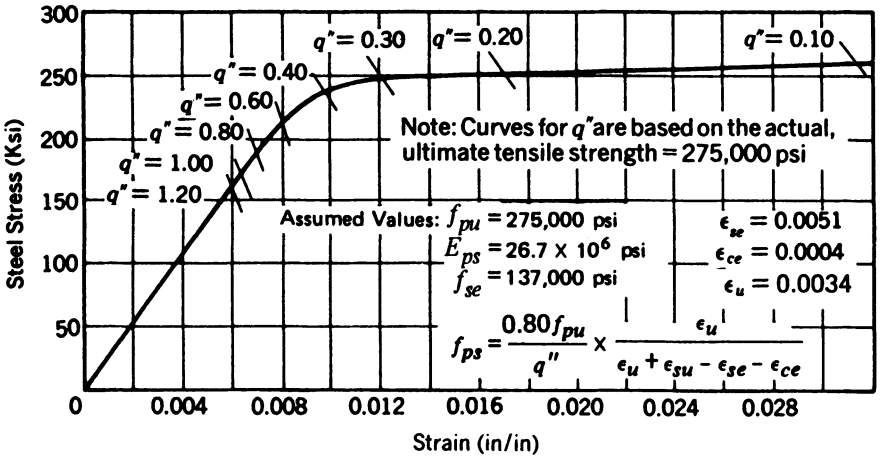

Fig. 5-3. Stress–strain diagram with curves for various values of q'' superimposed.

and are discussed further in Sec. 5-4. The following discussion, which is based upon the paper presented in 1956 by Muller, is used as a means of further illustrating the basic principles of using strain compatibility in the flexural strength analysis of reinforced concrete beams; *it is not intended to imply that the limiting stresses and strains used therein are recommended for use today.*

The intersections of the curves for q'' with the stress–strain curve in Fig. 5-3 define the values of steel stress and steel strain that are compatible for different values of q''. Stress–strain curves are a function of the physical properties of the prestressing steel and can be obtained experimentally for each heat of steel manufactured; they are not derived mathematically. A trial-and-error procedure must be followed if these curves for q'' are used in solving strain compatibility relationships with a stress–strain curve that cannot be expressed mathematically. However, it sometimes is feasible to mathematically approximate an actual stress–strain curve, or at least the portions of the curves for stresses that are greater than the yield strength of the steel, and thereby avoid the use of the trial-and-error procedure.

Values of f_{ps}, as a function of the steel index, resulting from the analysis summarized in Fig. 5-3 are compared graphically in Fig. 5-4 with values obtained from the approximate relationship:

$$f_{ps} = f_{pu}(1 - 0.5\rho_p) \tag{5-10}$$

This approximate relationship, which was included in the ACI–ASCE Joint Committee 323 report "Tentative Recommendations for Prestressed Concrete"

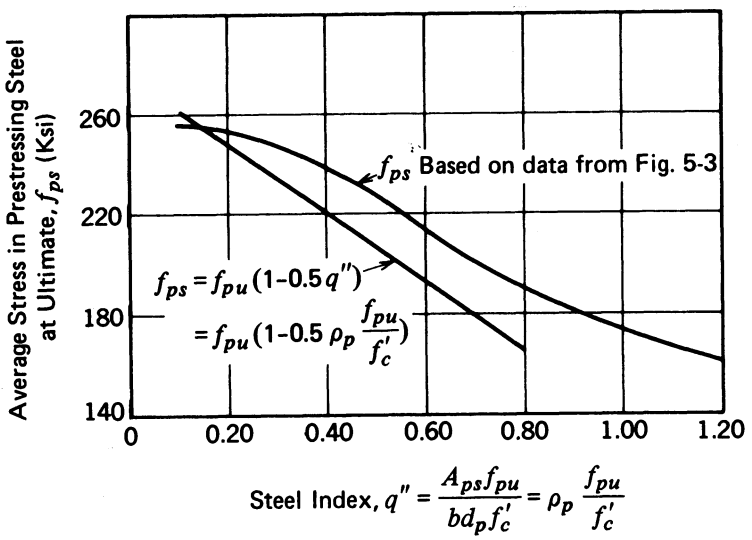

Fig. 5-4. Variation of f_{ps} with the steel index. The actual values of f_{ps} shown are based on the stress–strain curve of Fig. 5-3, and the approximate values are from eq. 5-10.

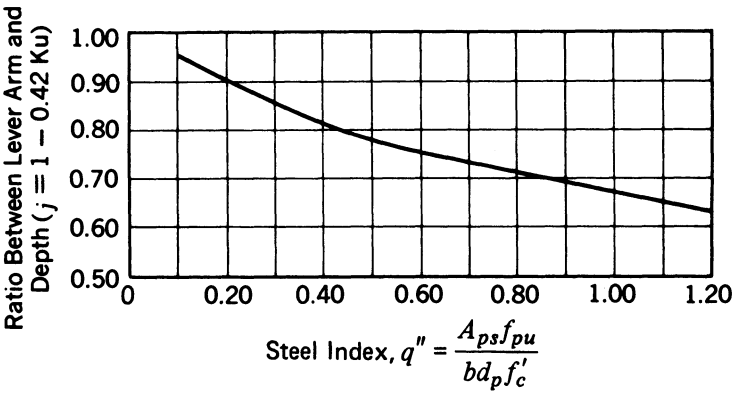

Fig. 5-5. Variation of lever-arm–depth ratio, j, with steel index.

(ACI-ASCE Committee 323 1958), has been included in the major U.S. building codes since 1963. In recent years it has been modified to better reflect the effects of concrete strength and type of prestressing steel (see Sec. 5-4). As can be seen from Fig. 5-4, the values predicted by the approximate relationship are conservative *for this particular steel*, as would be expected. The variation of j, the ratio of the resisting moment lever arm to the effective depth of the section, is shown as a function of the steel index in Fig. 5-5, and the ratio of the ultimate moment capacity to $f_{pu}A_{ps}d_p$ is shown as a function of the steel index in Fig. 5-6.

Tests have shown that for lightly reinforced members, arbitrarily defined as

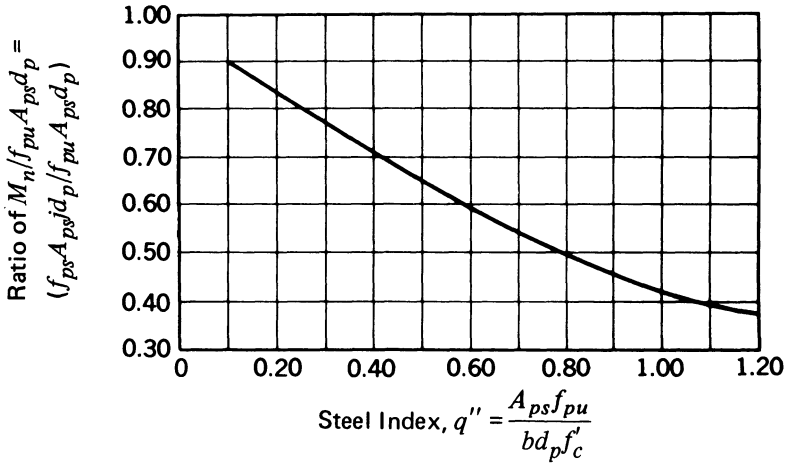

Fig. 5-6. Variation in the factor $M_n/f_{pu}A_{ps}d_p$ with the steel index.

those with steel indices less than 0.08, the flexural capacity can be calculated with sufficient accuracy by the relationship:

$$M_n = 0.95 f_{pu} A_{ps} d_p \tag{5-11}$$

The lightly reinforced members fail as a result of the failure of the prestressing steel, and before the concrete has become highly stressed.

The results summarized in Figs. 5-3 and 5-4 indicate that for the particular steel studied, the moment capacity is very nearly linear for the lower values of the steel index. Members made with this steel, and having relatively low amounts of reinforcement (as measured by the steel index), would be expected to experience large deformations of the flexural reinforcement before collapse. This behavior has previously been described as characteristic of underreinforced members. Figures 5-3 and 5-4 also indicate that if this steel were to be used in relatively large quantities, the steel stress would be relatively low, and the members would perform as described above for overreinforced concrete members.

As was stated above, the relationships that have been developed in this section are applicable to flexural members having rectangular cross sections. These relationships are equally applicable for flanged sections, provided that the neutral axis of the section when loaded to its flexural capacity is within the limits of the compression flange. If, when subjected to the ultimate loading, the neutral axis is located outside of the flange area, the same strain distribution applies as in the case of rectangular sections, but because of the variable width of the section that is subjected to compressive stresses, the distance from the extreme compressive fiber to the neutral axis is no longer equal to $0.42 k_u d_p$, and its location must be calculated. To facilitate calculation of the location of the resultant of the compressive stresses, the compression block can be assumed to be rectangular rather than curved, as shown in Fig. 5-2, without the introduction of significant error.

When complete strain compatibility analyses are not made, and small quantities of nonprestressed flexural reinforcement are used in combination with small quantities of prestressed reinforcement in underreinforced members, the additional flexural strength due to provision of the nonprestressed reinforcement can be approximated by:

$$M_n = 0.90 A_s f_y d \tag{5-12}$$

where d is the distance from the extreme compression fiber to the centroid of the nonprestressed reinforcement, and A_s and f_y are the area and yield strength (60,000 psi maximum) of the nonprestressed reinforcement, respectively. When significant amounts of nonprestressed reinforcement are used in combination with prestressed reinforcement, strain compatibility analyses should be performed.

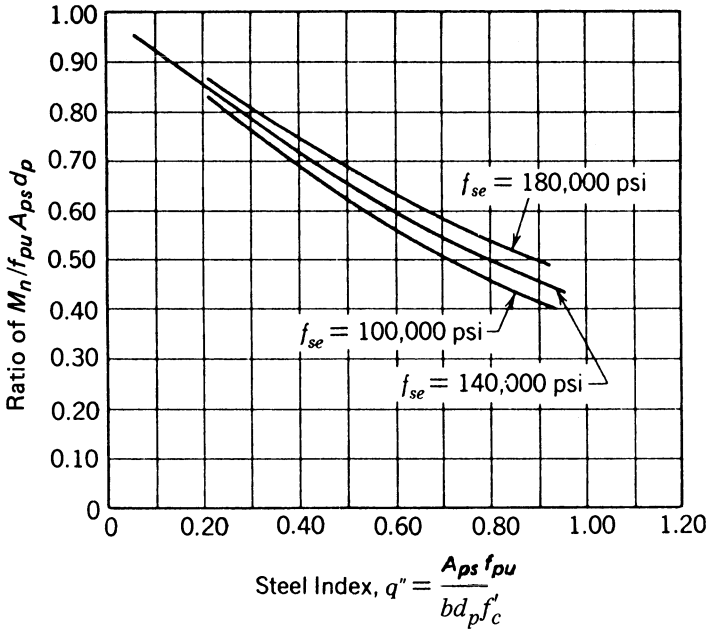

Fig. 5-7. Effect of effective prestressing stress, f_{se}, on the ratio $M_n/A_{ps}f_{pu}d$ for various values of steel index, q'' (after J. Muller).

The effect that unintended variations in the effective stress in prestressed reinforcement have on the flexural capacity of prestressed concrete members is shown in Fig. 5-7. This figure illustrates the fact that small variations in the effective prestress have no significant effect on the flexural strength of prestressed members having bonded tendons. It is important to note that even if errors are made in estimating the losses of prestress, or in estimating the friction during prestressing, or even if the stressing is not carried out with reasonably high precision in the field, the effect on the flexural strength is generally small for flexural members *having bonded tendons*.

An obvious difficulty with applying strain compatibility in the design of prestressed concrete flexural members is related to determining the stress–strain curve for the prestressed reinforcement that will be used. At the time when prestressed members are designed, the designer rarely knows the source of the prestressing steel to be used in construction, and thus cannot have access to the stress–strain characteristics of the prestressing steel that will be used in the actual construction. More often than not, the steel that will be used has not yet been produced when the structure is being designed. Consequently, it has been customary for designers to use mathematical relationships that conservatively approximate the stress in the prestressing steel in strength calculations; the provisions of virtually all U.S. codes and standards for the design of prestressed

concrete permit the use of relationships of this type. It should be recognized, however, that designs based upon strain compatibility analysis, which utilize less conservative stress–strain relationships, frequently will be more economical that those based upon these approximate relationships. For this reason, there is considerable interest in avoiding the commonly used approximate relationships and instead performing strain compatibility analyses based upon stress–strain curves intended to reasonably approximate the stress–strain characteristics of prestressing steel obtained from any of several sources. Curves of this type, which have been included in the publications of the Precast Prestressed Concrete Institute since 1978, are reproduced herein as Fig. 5-8 (PCI 1978, 1985). It is well known that the shapes of the stress–strain curves are not the same for prestressing strand produced by different manufacturers, and this probably is the case for prestressing wire and high-tensile-strength bars as well. The designer of prestressed concrete should exercise care in selecting a stress–strain curve for use in a strain-compatibility analysis, and should provide a means of confirming that the curve used is reasonably representative of *all* of the prestressing steel used in the actual construction.

The manufacturers of prestressing steel normally do not provide stress–strain curves for their products. Upon request, however, they will provide load–strain curves that are either typical of their products or are prepared for a particular heat or production lot of the products. Load–strain curves are preferred by manufacturers, and should be by designers, because they illustrate the actual measurements made on test specimens and have not been converted from force to unit stress—a process that can result in erroneous results if theoretical areas of the test specimens are used. It should be recognized that the diameters, and hence the areas, of individual prestressing wires and bars vary from their theoretical dimensions. Because strands are made from seven individual wires, their dimensions must be expected to vary from the theoretical dimensions as well. The variations should be within certain tolerances, set either by the applicable ASTM standard or, in the absence of an ASTM standard, by the manufacturer's specifications. The load–strain curves are easily employed in performing strain-compatibility analyses using the principles and relationships explained herein, by simply rearranging the relationships from expressions of stress to those of force.

To facilitate strain-compatibility computations, the stress–strain curve for nonprestressed reinforcement normally is taken to be bilinear, as shown in Fig. 5-9. The curve is based upon the premise that the slope of the first portion of the curve is equal to the elastic modulus of the nonprestressed reinforcement for stresses up to and including its yield strength, and for stresses above the yield strength, the strain increases without an increase in stress. For prestressed reinforcement, the stress–strain curve can simplistically be assumed to consist of three straight lines, as shown for Grades 250 and 270 strand in Figs. 5-10a

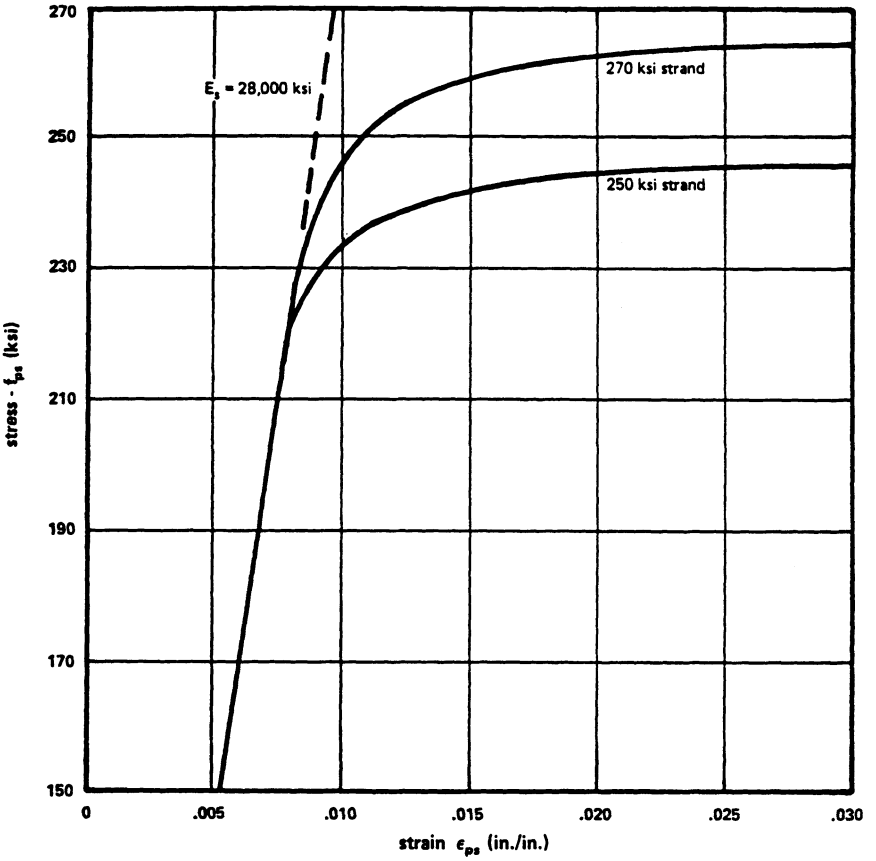

These curves can be approximated by the following equations:

$\epsilon_{ps} \leq 0.008$: $f_{ps} = 28{,}000\ \epsilon_{ps}$ (ksi)

$\epsilon_{ps} > 0.008$:

250 ksi strand: $$f_{ps} = 248 - \frac{0.058}{\epsilon_{ps} - 0.006} < 0.98\ f_{pu}\ \text{(ksi)}$$

270 ksi strand: $$f_{ps} = 268 - \frac{0.075}{\epsilon_{ps} - 0.0065} < 0.98\ f_{pu}\ \text{(ksi)}$$

Fig. 5-8. Typical stress–strain curves for seven-wire stress-relieved and low-relaxation prestressing strand. (Reproduced with the permission of the Precast/ Prestressed Concrete Institute.)

and 5-10b, respectively. The first of these lines, which extends from zero stress up to an arbitrary stress (point 1) that is somewhat less than the yield strength, as in the case of nonprestressed reinforcement, can be assumed to have a slope equal to the elastic modulus of the steel. The second line connects the first and third lines (points 1 and 2). The coordinates of point 2, the intersection of the

Reinf. grade	Elastic modulus (ksi)	Yield strength (psi)	Yield strain (in./in.)
40	29,000	40,000	0.00138
60	29,000	60,000	0.00207
40	30,000	40,000	0.00133
60	30,000	60,000	0.00200

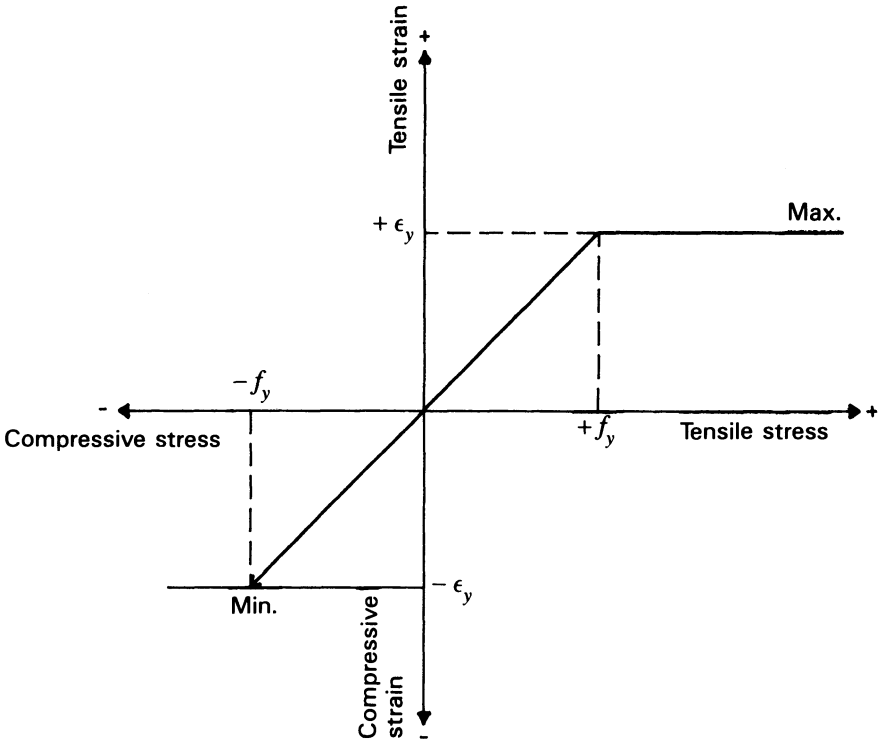

Fig. 5-9. Idealized stress–strain diagram for nonprestressed reinforcement of Grades 40 and 60.

second and third lines, can be taken to have coordinates of one percent extension (strain) and the stress equal to the minimum strength at the one percent extension required by the applicable ASTM specification. Alternatively, the coordinates of point 2 can be taken from points approximating the stress–strain curve of a particular prestressing steel as shown in Fig. 5-10c.

The slopes of the third lines in Fig. 5-10a–c, which are the parameters of the "curves" that are of the greatest importance in most designs, present the greatest

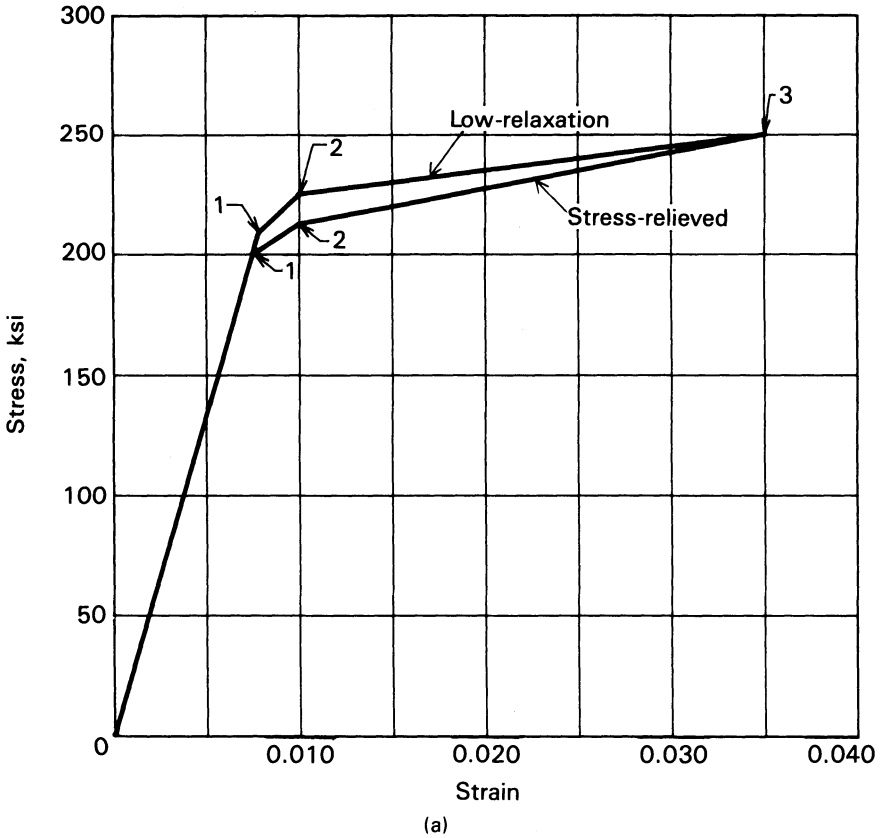

(a)

Fig. 5-10. Simplistic stress–strain curves for Grades 250 and 270 stress-relieved and low-relaxation seven-wire strand for prestressing concrete. (a) Grade 250 seven-wire strand.

challenge in determining reasonable values. The ASTM specifications provide minimum elongations at rupture (normally 3.5 percent for seven-wire strand and 4.0 percent for prestressing wire) and a minimum ultimate tensile strength, but these elongations may not and most frequently will not occur simultaneously: the elongation at rupture is normally significantly greater than the minimum elongation required by the ASTM specifications, and the ultimate tensile strength may or may not exceed the minimum guaranteed strength by a significant margin. For this reason a conservative end point for the slope of the third line might be taken as the point identified by the specified minimum ultimate tensile strength and an elongation equal to 5 to 7 percent, as is the case for the curve in Fig. 5-10c. An idealized stress–strain curve for 270 grade strand, proportioned as shown in Fig. 5-10c and consisting of two straight lines connected by a curved transition section, could be more representative of the

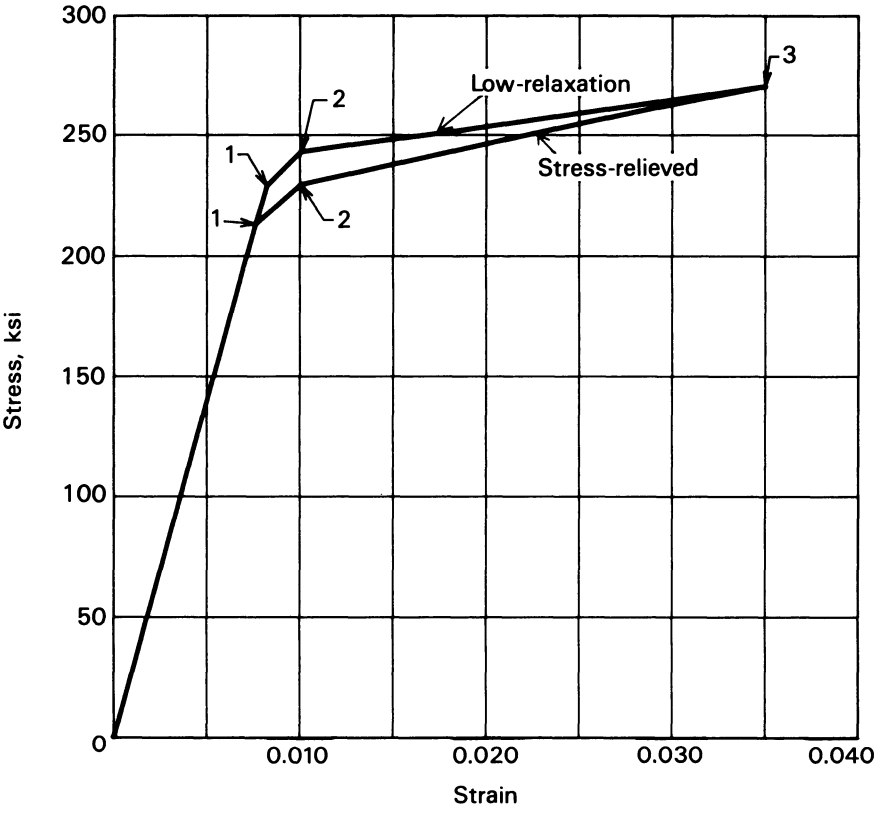

(b)

Fig. 5-10. (*Continued*) (b) Grade 270 seven-wire strand.

actual prestressing steel than the curves in Figs. 5-10a and 5-10b. One should not use an idealized curve for design without prior confirmation that it reasonably represents the stress–strain characteristics of the actual steel to be used in construction.

It is hoped that the ASTM standards eventually will be modified to include stress–strain or load–deformation curves that:

1. Are acceptable to the prestressing steel manufacturers.
2. Structural designers can use in approximating the load–elongation curves of the various prestressing materials without having to assume that the material is capable of attaining ultimate strains greater than the minimum values required by the applicable ASTM standard.
3. Reasonably approximate the load–elongation curves of the various prestressing materials.

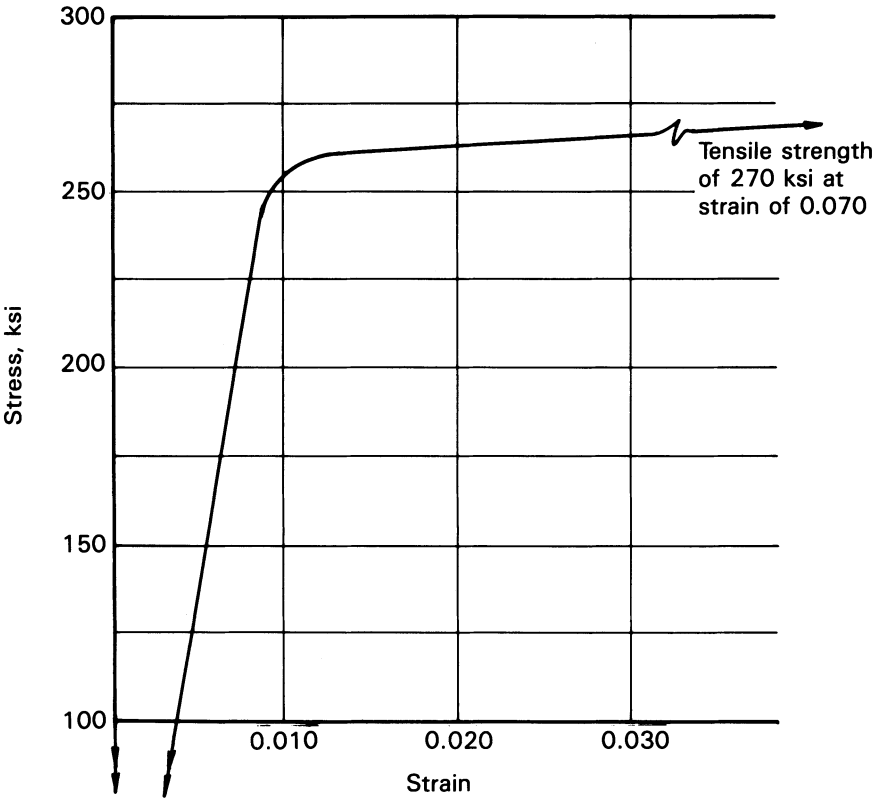

(c)

Fig. 5-10. (*Continued*) (c) Curve approximating a portion of an actual stress–strain curve for Grade 270 low-relaxation prestressing strand.

The stress–strain characteristics of prestressing steels are discussed in detail in Sec. 2-9.

An iterative procedure for determining the relationship between the stress and strain in prestressed reinforcement for use in computing the flexural strength of prestressed concrete members utilizing a computer program written in BASIC, and an approximate, noniterative procedure suitable for hand calculations, have been described by Skogman, Tadros, and Grasmick (1988). This work, which is based upon previous work by Mattock (1979), Naaman (1977), and by Menegotto and Pinto (1973), depends upon the assumption that plane sections remain plane and the equation:

$$f_i = \epsilon_i E_{ps}\left[Q + \frac{1 - Q}{(1 + \epsilon_i^{*R})^{1/R}}\right] \leq f_{pu} \qquad (5\text{-}13)$$

in which:

$$\epsilon_i^* = \frac{\epsilon_i E_{ps}}{K f_{py}} \tag{5-14}$$

and:

f_i = Stress in prestressed reinforcement corresponding to strain ϵ_i
f_{py} = Specified yield strength of prestressed reinforcement
ϵ_i = Strain in the prestressed reinforcement in layer i;
E_{ps} = Elastic modulus of the prestressed reinforcement

and the dimensionless constants K, Q, and R are specific values for the stress–strain curve for a particular steel. (*Note:* If eq. 5-13 is used for nonprestressed reinforcement, then E_s, the elastic modulus of nonprestressed reinforcement, should be substituted for E_{ps}. Abort values for E, K, Q, and R, proposed by the authors for use when values are not determined for a specific prestressed reinforcement, are given in Table 5-1. Two curves, adapted from the work of Skogman, Tadros, and Grasmick, included herein as Figs. 5-11 and 5-12, compare the stress ratio for the prestressed reinforcement (ratio of the stress in

TABLE 5-1 Reinforcement stress–strain constants and dimensionless constants for eqs. 5-13 and 5-12. (From Skogman, Tadros, and Grasmick 1988.)

f_{pu}(ksi)	f_{py}/f_{pu}	E (psi)	K	Q*	R
270 strand	0.90	28,000,000	1.04	0.0151	8.449
	0.85	28,000,000	1.04	0.0270	6.598
250 strand	0.90	28,000,000	1.04	0.0137	6.430
	0.85	28,000,000	1.04	0.0246	5.305
250 wire	0.90	29,000,000	1.03	0.0150	6.351
	0.85	29,000,000	1.03	0.0253	5.256
235 wire	0.90	29,000,000	1.03	0.0139	5.463
	0.85	29,000,000	1.03	0.0235	4.612
150 bar	0.85	29,000,000	1.01	0.0161	4.991
	0.80	29,000,000	1.01	0.0217	4.224

*Q is based upon the strain in the prestressed reinforcement, ϵ_{pu}, being equal to 0.05.

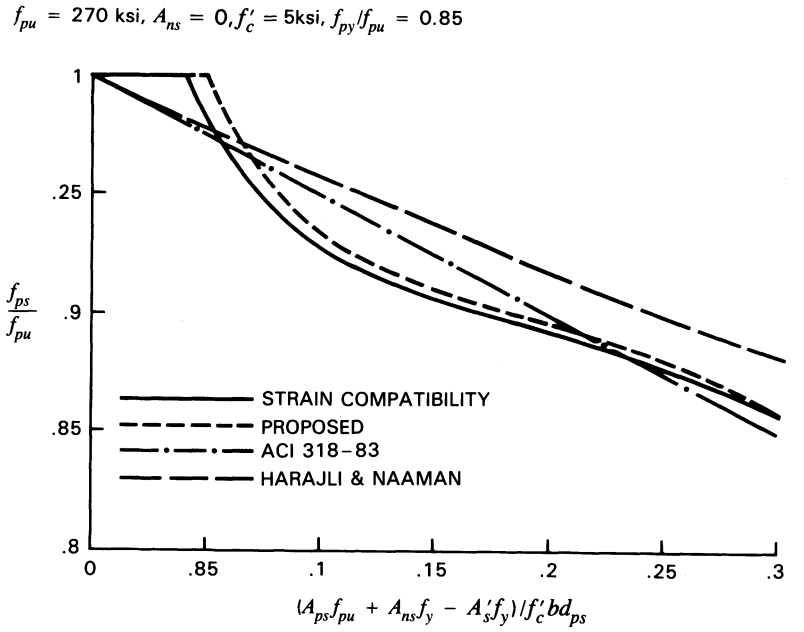

Fig. 5-11. Stress in prestressed tendon at ultimate flexure as a function of the total steel index (after Skogman, Tadros, and Grasmick 1988). (Reproduced with the permission of the Precast/Prestressed Concrete Institute.)

the prestressed reinforcement at ultimate flexural strength to its specified strength) to the reinforcement index. The figures show the results obtained by:

1. A strain compatibility analysis.
2. The hand-calculation method proposed by the authors.
3. The equation contained in ACI 318 (eq. 5-34 in this book; eq. 18-3 in ACI 318).
4. The method proposed by Harajli and Naaman (1985).

The curves clearly show the proposed noniterative method to give excellent agreement with the results obtained with the computer program based upon strain compatibility, when the constants E, K, Q, and R have been determined for the stress–strain curve for a particular steel.

The hand-calculation method includes six steps:

1. The stresses in the tension reinforcements, both prestressed and nonprestressed, are assumed to be equal to their respective yield strengths, and the stress in the compression reinforcement is assumed to be equal to zero. Based upon these assumptions, the total compressive stress in the concrete is computed

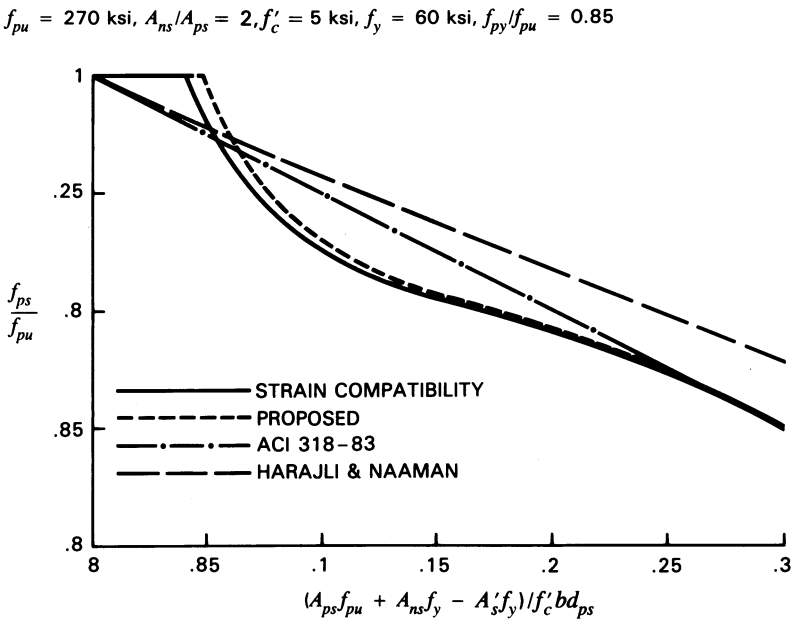

Fig. 5-12. Stress in prestressed tendon at ultimate flexure as a function of the total steel index (after Skogman, Tadros, and Grasmick 1988). (Reproduced with the permission of the Precast/Prestressed Concrete Institute.)

under ultimate bending moment based upon equilibrium of the forces in the concrete and reinforcement. This is expressed mathematically as:

$$F_c = A_{ps}f_{py} + A_sf_{sy} \tag{5-15}$$

2. Using the value of F_c computed in step 1, the depth of the compression block is then computed by:

$$a = \frac{F_c}{\sum 0.85\,(f'_cb\beta_1)} \tag{5-16}$$

3. Compute the depth to the neutral axis from:

$$c = \frac{a}{\beta_1} \tag{5-17}$$

For composite sections, the average values of β_1, based upon the strengths of the different concretes in the compression block, is to be used. This is computed as:

$$\beta_{1\,ave} = \frac{\sum\limits_k 0.85(f'_cA_c\beta_1)_k}{F_c} \tag{5-18}$$

4. The concrete strains at the levels of the reinforcement are computed as follows:

$$\epsilon_i = \epsilon_{cu}\left(\frac{d_i}{c} - 1\right) + \epsilon_{idec} \tag{5-19}$$

in which ϵ_{cu} is normally taken to be 0.003, d_i is the depth from the extreme compression fiber to the reinforcement layer under consideration, c is the depth of the neutral axis, and ϵ_{idec} is the decompression strain at the level of the layer under consideration (the decompression strain being the strain that takes place as a result of loading the member in such a way that the compressive strain in the concrete due to the effective prestressing force is nullified). The decompression strain can be computed by:

$$\epsilon_{idec} = f_{se}/E_i \tag{5-20}$$

or:

$$e_{idec} = (f_{pi} - 25{,}000)/E_i \tag{5-21}$$

at the designer's option. The terms f_{se} and f_{pi} are the effective and initial stresses in the prestressed reinforcement, respectively (see Sec. 7-2), and E_i is the elastic modulus for the layer of reinforcement at the level under consideration. The 25,000 psi used in eq. 5-21 for the computation of ϵ_{idec} is a commonly used, but not necessarily accurate, value for loss of prestress. Equation 5-20, which requires computation of the loss of prestress, is the preferred relationship because the computed loss of prestress is frequently a value other than 25,000 psi.

5. Computations now are made for the values of f_i for the various layers of reinforcement, using eq. 5-13. Normally it will be found that the strains at the levels of the nonprestressed reinforcements exceed their strains at yield; hence, the stresses in the nonprestressed reinforcements are taken to be equal to their yield strengths.

6. The computations are completed by first computing new values of F_c and a, based upon the stresses in the tension and compressive reinforcements determined in steps 4 and 5. The depth to the resultant of the compressive force in the compression reinforcement and the concrete section, d_c, is found next, after which the flexural strength of the member can be determined by using:

$$M_n = A_{ps}f_{ps}(d_p + d_c) + A_sf_y(d - d_c) \tag{5-22}$$

ILLUSTRATIVE PROBLEM 5-2 Compute the flexural capacity of the composite section of Fig. 5-13, which consists of the AASHTO-PCI type III bridge stringer with a 6.50 in. cast-in-place slab. The area of the prestressing steel, which is Grade 270, is 4.00 sq. in., and it is located with its centroid 5.85 in. above the bottom of the beam. The prestressing steel has the stress–strain characteristics

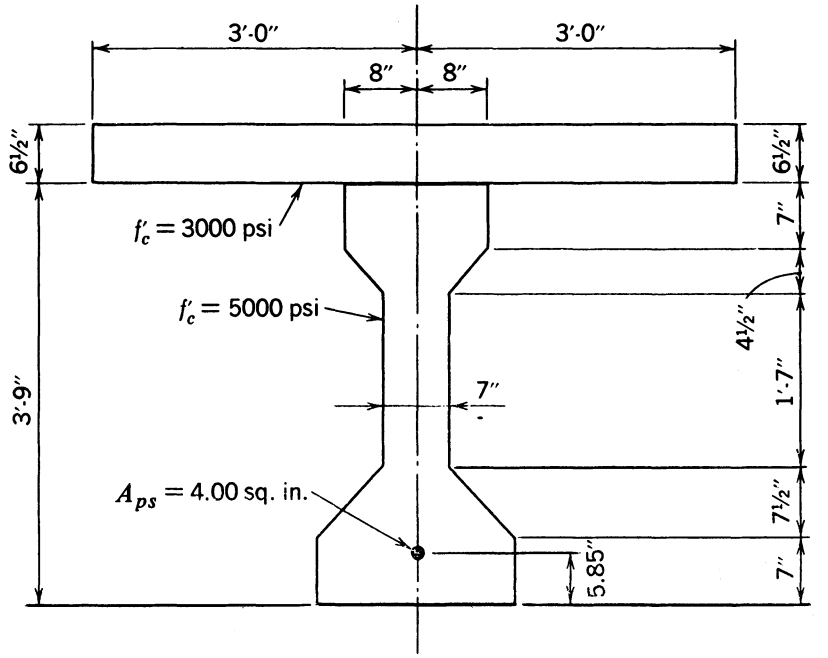

Fig. 5-13. AASHTO-PCI type III bridge stringer with a composite deck.

given in Fig. 5-10c. The concrete cylinder compressive strengths are 5000 psi and 3000 psi for the stringer and the cast-in-place deck, respectively. Use the principle of strain compatibility, assuming the following strains: $\epsilon_u = 0.003$; $\epsilon_{ce} = 0.0004$; $\epsilon_{se} = 0.0058$. Assume the stress–strain curve for the prestressed reinforcement to be a straight line for values of f_{ps} greater than 248 ksi. Assume that the equation of the line is:

$$f_{ps} = 242 + 400\epsilon_{ps} \text{ ksi}$$

SOLUTION: The steel index is:

$$q'' = \frac{4 \times 275}{72 \times 45.65 \times 3} = 0.112$$

The relationship for strain compatibility, eq. 5-8, is written as follows:

$$f_{ps} = \frac{0.85 f_{cu}}{\rho_p} \times \frac{\epsilon_u}{\epsilon_u + \epsilon_{ps} - \epsilon_{se} - \epsilon_{ce}}$$

By substituting the appropriate values for the terms that are known, this becomes:

$$f_{ps} = \frac{0.85 \times 3 \times 72 \times 45.65}{4.00} \times \frac{0.003}{\epsilon_{ps} - 0.0032} = \frac{6.286}{\epsilon_{ps} - 0.0032}$$

Solving the equation for the slope of the stress–strain curve simultaneously with eq. 5-8 gives a value of f_{ps} equal to 253.21 ksi and a value for ϵ_{ps} of 0.0280 in./in. The force in the prestressing steel is 1013 kips, and k_u, the ratio of the depth of the neutral axis to the effective depth, is computed as follows:

$$k_u = \frac{0.003}{0.0280 - 0.0032} = 0.121$$

The depth of the compression block is:

$$a = 0.85 \times 0.121 \times 45.65 = 4.70 \text{ in.}$$

For a compression block having a depth of 4.70 in., the concrete stress is:

$$f_c = \frac{1013}{72 \times 4.70} = 3.00 \text{ ksi} > 0.85 f_{cu} = 2.55 \text{ ksi}$$

To prevent the concrete stress from exceeding the maximum permissible value of $0.85 f_{cu}$, the strength of the concrete would have to be increased to a value not less than 3530 psi.

The moment capacity of the section is computed as follows:

$$M_n = \frac{1013}{12} \times \left(45.65 - \frac{4.70}{2}\right) = 3655 \text{ k-ft}$$

ILLUSTRATIVE PROBLEM 5-3 Compute the flexural strength of the stringer of I.P. 5-2 using the noniterative hand-calculation procedure proposed by Skogman, Tadros, and Grasmick, assuming the prestressing steel to be low-relaxation, Grade 270.

SOLUTION: The value of the compressive stress in the concrete is computed as:

$$F_c = 4.00 \times 0.90 \times 270 = 972 \text{ kips}$$

The depth of the compression block is computed as:

$$a = \frac{972}{72 \times 0.85 \times 3} = 5.29 \text{ in.}$$

The depth to the neutral axis is computed as:

$$c = \frac{5.29}{0.85} = 6.22 \text{ in.}$$

The strain for decompression is computed as:

$$\epsilon_{idec} = \frac{162}{28{,}000} = 0.00578$$

and the ultimate strain is computed to be:

$$\epsilon_i = 0.003\left[\frac{45.65}{6.22} - 1\right] + 0.00578 = 0.0248$$

The stress in the prestressed reinforcement, based upon the strain $\sigma_i^* = 2.748$, is computed to be:

$$f_{ps} = 0.0248 \times 28{,}000\left[0.0151 + \frac{1 - 0.0151}{(1 + 2.748^{8.449})^{1/8.449}}\right]$$

$$= 247 \text{ ksi}$$

and the new value of F_c is 988 kips, $a = 5.38$ in., and the nominal flexural strength is computed to be:

$$M_n = 988\left(\frac{45.65 - 2.69}{12}\right) = 3537 \text{ k-ft}$$

ILLUSTRATIVE PROBLEM 5-4 Compute the flexural capacity of the stringer of I.P. 5-2, neglecting the composite action of the deck and assuming that the prestressing steel has stress–strain characteristics as shown in Fig. 5-3.

SOLUTION: Assume the compressive stress block to be rectangular in shape with the average concrete stress equal to $0.85f_{cu}$. Assume the concrete strain at the level of the prestressing steel due to prestressing, e_{ce}, to be 0.0004, the steel strain due to the effective prestress, e_{se}, to be 0.0050, and the maximum concrete compressive strain at the time of flexural failure, e_u, to be 0.003. The effective depth of the prestressing steel is $45.00 - 5.85 = 39.15$ in. and the steel index is:

$$q'' = \frac{4.00 \times 275}{16 \times 39.15 \times 5} = 0.351$$

A review of the stress–strain curve in Fig. 5-3 will show that this value of the reinforcement index (the reinforcement index and the steel index are of a similar order) may cause the beam to be overreinforced in flexure; hence it will be analyzed as such. The strain in the steel at flexural capacity will be computed using eq. 5-6 and a trial-and-error procedure to determine the depth of the compression block. The compression block will be assumed to extend from the top of the compression fiber to $0.85k_u d_p$.

Try:

$$k_u d_p = 15 \text{ in.}$$

$$C = 0.85 \times 5[7 \times 15 \times 0.85 + 9 \times 7 + 9 \times 4.5/2] = 733 \text{ k}$$

$$\epsilon_{ps} = 0.0054 + 0.003\left(\frac{39.15 - 15.00}{15.00}\right) = 0.102$$

From Fig. 5-3:

$$f_{ps} = 240 \text{ ksi}, \quad T = 960 \text{ k}$$

$$C < T; \text{ try a larger value of } k_u d$$

Try:

$$k_u d_p = 21.5 \text{ in.}$$

$$C = 0.85 \times 5[7 \times 21.5 \times 0.85 + 9 \times 7 + 9 \times 4.5/2] = 897 \text{ k}$$

$$\epsilon_{ps} = 0.0054 + 0.003\left(\frac{39.15 - 18.50}{18.50}\right) = 0.0087$$

$$f_{ps} = 225 \text{ ksi}, \quad T = 900 \text{ k} \cong C = 897 \text{ k}$$

Compute the distance from the top fiber to the centroid of the compression block:

$0.85 \times 7 \times 21.5 =$	$127.9 \times 9.14 =$		1169.3
$9 \times 7 =$	$63.0 \times 3.50 =$		220.5
$0.5 \times 9 \times 4.5 =$	$20.3 \times 8.5 =$		172.1
Totals =	211.2		1561.9

$$d_t = 7.40 \text{ in.}$$

$$M_n \cong 900\left[\frac{39.15 - 7.40}{12}\right] = 2381 \text{ k-ft}$$

As will be shown subsequently, the principle of strain compatibility is easily applied to cross sections other than rectangular, in the cases of underreinforced and overreinforced sections alike, as well as in members that are provided with nonprestressed reinforcement in both the compression and tensile zones.

5-3 Principles of Flexural Capacity for Members with Unbonded Tendons

The flexural strength relationships developed in Sec. 5-2 for members having bonded tendons do not apply to members not having bonded tendons because, without bonding, the prestressing tendons can slip (with respect to the concrete) during the application of a load. The reader will recall that one of the basic assumptions made prior to the derivation of the relationships of Sec. 5-2 was that the concrete and steel are completely bonded. Because the tendons can slip with respect to the concrete, other variables affect the ultimate moment capacity of unbonded prestressed concrete members. After the "Tentative Recommen-

dations for prestressed Concrete'' appeared, the normal U.S. practice was to consider the stress in unbonded prestressing steel loaded to flexural failure to be as follows:

$$f_{ps} = f_{se} + 15{,}000 \tag{5-23}$$

(in psi) with the requirements that the effective stress in the prestressing steel be between $0.50f_{pu}$ and $0.60f_{pu}$ and that the reinforcement index not exceed 0.30 (ACI-ASCE Joint Committee 323 1958).

Variables that affect the ultimate moment capacity of an unbonded beam, but affect bonded beams in a different manner or not at all, include the following:

1. Magnitude of the effective stress in the tendons.
2. Span-to-depth ratio.
3. Characteristics of the materials used in the members.
4. Form of loading (shape of the bending moment diagram).
5. Profile of the prestressing tendon.
6. Friction coefficient between the prestressing steel and the sheath.
7. Amount of bonded nonprestressed reinforcing.

Another relationship has been suggested for the value of f_{ps} in members with unbonded tendons (to be used in lieu of eq. 5-23), as follows:

$$f_{ps} = f_{se} + \left(30{,}000 - \frac{\rho_p}{f_c} \times 10^{10}\right) \tag{5-24}$$

in which f_{se} is limited to $0.60f_{pu}$, ρ_p is the percentage of prestressing steel, and f_{ps}, f_{se}, and f'_c are in psi. Still another relationship has been more recently proposed:

$$f_{ps} = f_{se} + \frac{1.4f'_c}{100\rho_p} + 10{,}000 \text{ psi} \tag{5-25}$$

Equations 5-24 and 5-25 contain the notation for the specified concrete compressive strength, f'_c, because they were suggested for use in building codes.

The results of tests of members with unbonded tendons as well as eqs. 5-23, 5-24, and 5-25 are shown in Fig. 5-14 (Yamazaki, Kattula, and Mattock 1969). Equations 5-24 and 5-25 have not been widely used because they have not been included in any of the U.S. codes or standards.

A method of computing the ultimate strength of prestressed members (with unbonded tendons) that takes into account the variables listed above has been proposed (Pannell 1969). This method, which is based upon experimental data and is considered slightly conservative, provides the following relationship for the ultimate moment:

$$M_n = q_u(1 - 0.80q_u)f'_c bd_p^2 \tag{5-26}$$

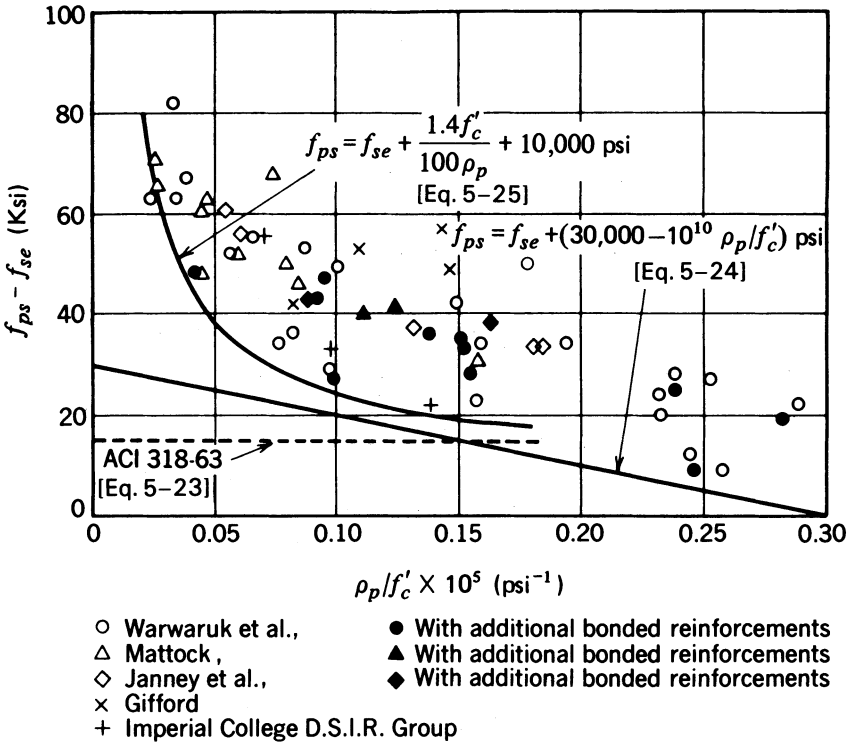

Fig. 5-14. Comparison of values of $f_{ps} - f_{se}$ for unbonded beams. Test data and suggested mathematical relationships are shown (after Yamazaki, Kattula, and Mattock 1969). (Reproduced with the permission of the Precast/ Prestressed Concrete Institute.)

in which:

$$q_u = \frac{q_e + \lambda}{1 + 1.6\lambda} \tag{5-27}$$

with:

$$q_e = \frac{\rho_p f_{se}}{f_{cu}} \tag{5-28}$$

$$\lambda = \frac{10^6 \rho_p d_p}{f_{cu} L} \tag{5-29}$$

In eqs. 5-26 through 5-29 the notation is standard, and it should be recognized that the depth of the member, d_p, and the span length, L, must be in the same units.

A plot showing the accuracy of eq. 5-26 is given in Fig. 5-15, where the

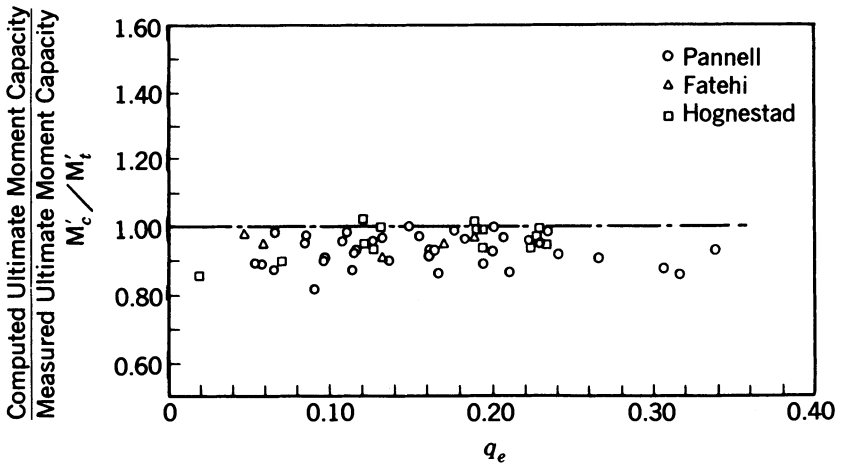

Fig. 5-15. Plot showing the ratio of the computed ultimate moment to that found by tests for various effective steel indices (after Pannell 1969).

ordinate is the ratio of the calculated flexural capacity to the flexural capacity measured in tests conducted by various investigators.

Readers interested in the development in the U.S. practice with unbonded tendons will find the 1983 and 1989 reports of ACI-ASCE Committee 423 to be sources of valuable information.

It should be recognized that the flexural capacity of a member prestressed with unbonded tendons, *unlike members with bonded tendons* (see Fig. 5-7), may be adversely affected by unintentional variations in the effective prestress. Hence, it is considered prudent to exert more care in estimating the losses of prestress and in supervising the stressing of unbonded members than would be considered necessary for bonded members, to ensure that the desired results are obtained.

5-4 Flexural Strength Code Requirements for Members with Bonded Tendons

The building code requirements for reinforced concrete contained in virtually all model building codes, building codes, building codes written for specific political jurisdictions and government agencies, and standards used in the United States are based upon the ACI standard *Building Code Requirements for Reinforced Concrete* (ACI Committee 318 1989). References in this book to ACI 318 or "the code" are intended to mean this particular standard of the American Concrete institute.

The basic design assumptions for the computation of flexural strengths, or flexural capacities, of members are contained in Sec. 10.2 of ACI 318. The

reader should consult the original document for the actual wording of the basic design assumptions, but the following summary is presented to facilitate this discussion:

1. The principles of strain compatibility and equilibrium are to be satisfied.
2. Plane sections remain plane (except for deep flexural members).
3. The maximum strain at extreme compression fibers in the concrete section is equal to 0.003.
4. Stress in nonprestressed reinforcement is equal to the product of the strain in the concrete at the level of the steel (assuming bond between the steel and the concrete is perfect) and the elastic modulus of the steel, with the maximum (tensile) and minimum (compressive) values being numerically equal to the minimum guaranteed yield strength, f_y, of the steel; see Fig. 5-9 for the assumed stress–strain curve for nonprestressed reinforcement. *Compression reinforcement in members having prestressed tensile reinforcement, as is the case for reinforced concrete members having nonprestressed tensile reinforcement, must be tied to guard against buckling, as provided in Sec. 7.10.5 of ACI 318.*
5. The tensile strength of concrete is to be neglected in flexural strength computations (except for investigating the possibility of failure at the cracking load, as described in Sec. 5-2 and subsequently in this section).
6. The concrete compressive stress distribution may be assumed to be of parabolic shape (as shown in Fig. 5-2), trapezoidal, or rectangular (as shown in Fig. 5-16), or of other shapes that can be substantiated with the results of comprehensive tests.
7. For simplicity, a rectangular distribution of concrete compressive stress, as shown in Fig. 5-16, may be assumed, with the following limitations:

   a. The concrete stress shall be taken as being equal to $0.85f'_c$.
   b. The depth of the compression block shall be taken as being equal to a distance of $a = \beta_1 c$, in which c is the distance from the extreme compression fiber to the neutral axis ($c = k_u d_p$ in Sec. 5-2).
   c. The factor β_1 shall be taken to be equal to 0.85 for concrete compressive strengths up to and including 4000 psi; for strengths greater than 4000 but less than 8000 psi:

$$\beta_1 = 0.85 - \frac{0.05(f'_c - 4000)}{1000} \tag{5-30}$$

   For concrete strengths equal to or greater than 8000 psi, β_1 shall be taken to be equal to 0.65.

It should be emphasized that the assumptions from ACI 318 listed above differ from those assumed by some of the early proponents of the use of strain compatibility methods of analysis as described in Section 5–2, in that the limiting concrete strain is taken to be 0.003, rather than 0.0034, and the compression

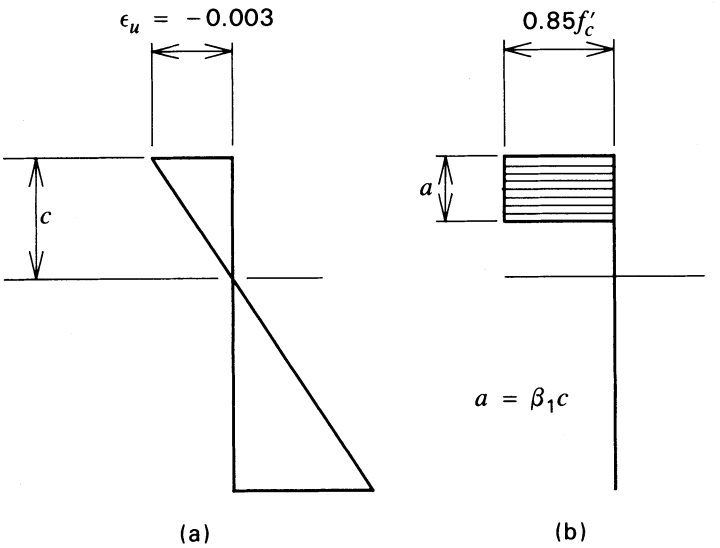

Fig. 5-16. Concrete strain and stress distribution assumed by ACI 318 at limit of flexural strength. (a) Strain. (b) Concrete stress.

stress block may be assumed to be rectangular with a uniform distribution of stress equal to $0.85f'_c$ to a depth of $\beta_1 c$, rather than a parabolic distribution having an average stress of $0.80f_{cu}$ acting to a depth of $k_u d_p$. It should be noted that the term β_1 is included in ACI 318 to account for the effect of concrete strength on the depth of the compressive stress block; experimental studies confirmed the need for its inclusion. Note that the term β_1 is equal to 0.85 for concrete strengths of 4000 psi and less, is equal to 0.65 for concrete strengths of 8000 psi or more, and varies linearly between 4000 psi and 8000 psi (at the rate of 0.05 per 1000 psi). This is illustrated in Fig. 5-17.

Using the ACI 318 assumptions listed above, one can rewrite eq. 5-8 for strain compatibility as follows:

$$f_{ps} = \frac{0.85\beta_1 f_{ps}}{\omega_p} \times \frac{\epsilon_u}{\epsilon_u + \epsilon_{ps} - \epsilon_{se} - \epsilon_{ce}} \tag{5-31}$$

It should be noted that the difference between this equation and eq. 5-8 is only the β_1 in the numerator.

The principles of strain compatibility explained above can be applied to flexural members reinforced with a combination of bonded prestressed and nonprestressed reinforcement. In this case, the equations of equilibrium for a rectangular section, as shown in Fig. 5-18, become:

$$T = C$$

$$A_{ps} f_{ps} + A_s f_s = 0.85 f'_c ba + A'_s f'_s \tag{5-32}$$

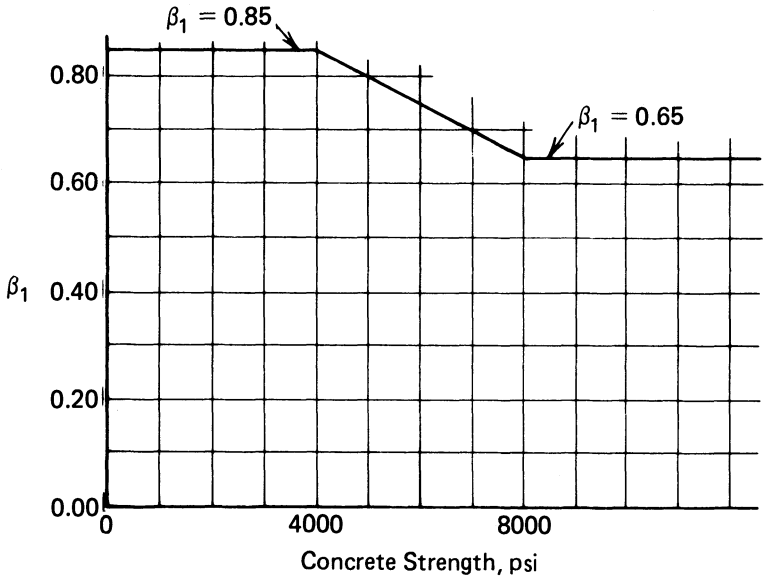

Fig. 5-17. Variation of β_1 and f'_c.

in which the terms not previously defined are as follows:

A_s = Area of nonprestressed tension reinforcement
A'_s = Area of nonprestressed compression reinforcement

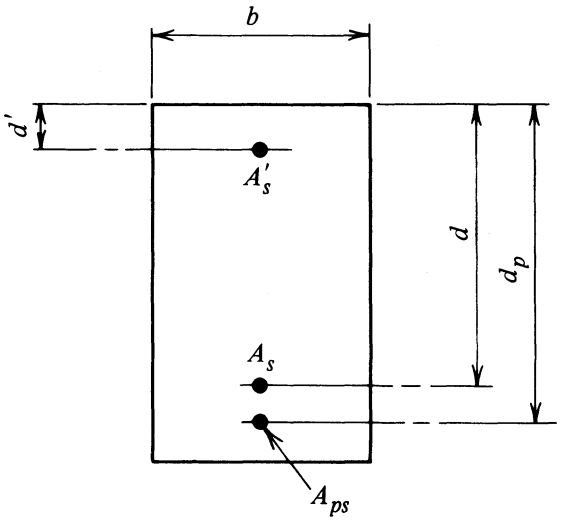

Fig. 5-18. Cross section of a rectangular flexural member having bonded nonprestressed tension and compression reinforcement in addition to bonded prestressed tension reinforcement.

d = Distance from extreme compression fiber to centroid of nonprestressed tension reinforcement

d'_e = Distance from extreme compression fiber to centroid of compression reinforcement

d_p = Distance from extreme compression fiber to centroid of prestressed tension reinforcement

f_s = Stress in the nonprestressed tensile reinforcement ($\leq f_y$)

f'_s = Stress in the nonprestressed compressive reinforcement ($\leq f_y$)

f_y = Specified minimum yield strength of nonprestressed reinforcement

Equilibrium relationships based upon the conditions of strain in the concrete and the prestressed and nonprestressed steels, similar to those in eqs. 5-3 through 5-8, can be written for the stresses in the prestressed and nonprestressed reinforcements as well as the nonprestressed compression reinforcement. Once the stresses in all the different steels are known, the nominal moment capacity of the section can be calculated as in I.P. 5-5 and I.P. 5-6.

In a similar manner, equations for conditions of equilibrium and compatibility of strains can be written for members having other than rectangular cross sections. For a T-shaped member, as shown in Fig. 5-19, the basic equation for equilibrium is:

$$A_{ps} f_{ps} + A_s f_s = 0.85 f'_c [(b - b_w) h_f + b_w a] + A'_s f'_s \qquad (5\text{-}33)$$

in which b_w = web width.

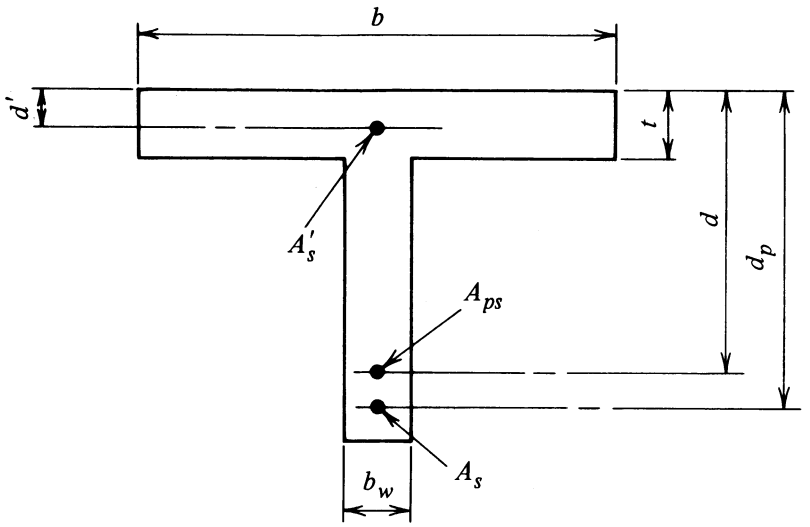

Fig. 5-19. Cross section of a T-shaped flexural member having bonded nonprestressed tension and compression reinforcement in addition to bonded prestressed reinforcement.

In using eqs. 5-32 and 5-33, the stress in the nonprestressed tension reinforcement normally will be found to be equal to its yield strength. As shown in Fig. 5-9, the strain required in the nonprestressed reinforcement to stress it to the yield strength, based upon an elastic modulus of 29,000 ksi, is 0.00138 and 0.00207 for Grades 40 and 60, respectively. Because prestressed steels, when stressed from the effective stress level to the yield stress, normally will increase in stress from 45 to 80 ksi, the stress in the nonprestressed tensile steel normally will go through a similar stress increase. As will be seen below, the stress in the nonprestressed compression reinforcement may, depending upon its location with respect to the extreme compression fiber, be significantly below its yield strength at ultimate flexural strength.

In lieu of requiring the designer to perform a strain compatibility analysis in computing the flexural strength of prestressed concrete members, ACI 318 permits f_{ps} to be taken as follows for bonded tendons, provided that f_{se} is not less than $0.50f_{pu}$:

$$f_{ps} = f_{pu}\left(1 - \frac{\gamma_p}{\beta_1}\left[\rho_p \frac{f_{pu}}{f'_c} + \frac{d}{d_p}(\omega - \omega')\right]\right) \tag{5-34}$$

in which:

d = Distance in inches from extreme compression fiber to centroid of nonprestressed tension reinforcement
d_p = Distance from extreme compression fiber to centroid of prestressed reinforcement
β_1 = Factor defined above in this section
γ_p = Factor for type of prestressing tendon
= 0.53 for f_{py}/f_{pu} not less than 0.80 (high-tensile-strength prestressing bars)
= 0.40 for f_{py}/f_{pu} not less than 0.85 (stress-relieved wire and strand)
= 0.28 for f_{py}/f_{pu} not less than 0.90 (low-relaxation wire and strand)
ρ_p = Ratio of prestressed reinforcement, A_{ps}/bd_p
ω = Nonprestressed tension reinforcement index $= \dfrac{A_s f_y}{bdf'_c}$
ω' = Nonprestressed compression reinforcement index $= \dfrac{A'_s f_y}{bdf'_c}$

The use of eq. 5-34 is further restricted by ACI 318 in that if compression reinforcement is included (i.e., $\omega' > 0$), the term:

$$\rho_p \frac{f_{pu}}{f'_c} + \frac{d}{d_p}(\omega - \omega')$$

shall be taken not less than 0.17, and d' shall be no greater than $0.15d_p$. Equation 5-34 also includes factors intended to compensate for the effects of nonprestressed tension reinforcement, concrete strengths greater than 4000 psi ($\beta_1 = 0.85$ for f'_c of 4000 psi or less), and minimum yield strength (at 1% extension) of the prestressing steel, as well as the presence of nonprestressed compression reinforcement (if any).

The value of f_{ps} computed with eq. 5-34 can be used for the computation of the nominal design flexural strength of rectangular sections with tension reinforcement alone by:

$$M_n = A_{ps}f_{ps}\left(d_p - \frac{a}{2}\right) + A_sf_y\left(d - \frac{a}{2}\right) \tag{5-35}$$

where:

$$a = \frac{A_{ps}f_{ps} + A_sf_y}{0.85f'_cb} \tag{5-36}$$

Equation 5-35 also can be used in flanged sections if the thickness of the flange h_f is not less than the depth of the compression block a as given in eq. 5-36. When the depth of the compression block exceeds the flange thickness, the nominal design flexural strength of a section can be computed by:

$$M_n = A_{pw}f_{ps}\left(d_p - \frac{a}{2}\right) + A_sf_y(d - d_p) + 0.85f'_c(b - b_w)\,h_f\left(d_p - \frac{h_f}{2}\right) \tag{5-37}$$

in which:

$$A_{pw}f_{ps} = A_{ps}f_{ps} + A_sf_y - 0.85f'_c(b - b_w)h_f \tag{5-38}$$

and:

$$a = \frac{A_{pw}f_{ps}}{0.85f'_cb_w} \tag{5-39}$$

The tensile force represented by $A_{pw}f_{ps}$ (eq. 5-38) is the force the web must develop; that is, it is the tensile force not developed by the flange.

The effect of compressive reinforcement is taken into account by basic principles. For compression reinforcement to be most effective in rectangular beams, it must be positioned in such a way that it will be stressed to its yield strength under design load. For this to be the case, using the notation defined in Fig. 5-20, the following relationships must be satisfied:

$$\frac{c}{d'} = \frac{\epsilon_u}{\epsilon_u - \epsilon'_s}$$

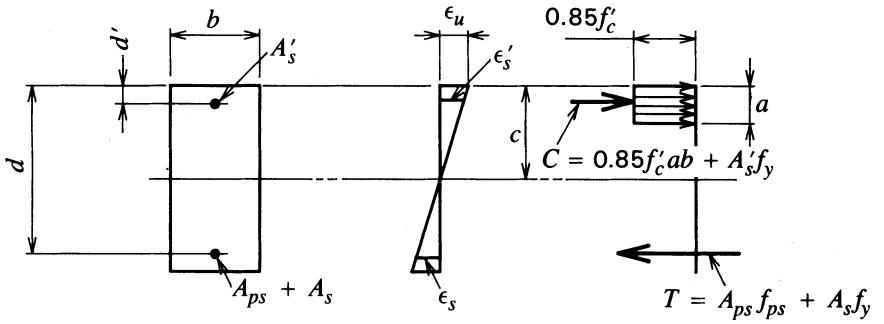

(a) Cross section. (b) Strain distribution. (c) Force distribution.

Fig. 5-20. Rectangular beam with compression reinforcement.

For yielding of the compression reinforcement, the strain in the concrete at the level of the compressive reinforcement ϵ_s' must equal to exceed its yield strain ϵ_u and:

$$c = d' \frac{\epsilon_u}{\epsilon_u - \epsilon_y'}$$

Because $\Sigma F_y = 0$, one can write:

$$A_{ps}f_{ps} + A_sf_y = 0.85f_c'ab + A_s'f_y$$

By taking $a = \beta_1 c$ and rearranging, the expression can be written:

$$\omega_p + \omega - \omega' = \frac{0.85\beta_1 c}{d} = 0.85\beta_1 \times \frac{d'}{d} \times \frac{\epsilon_u}{\epsilon_u - \epsilon_y'}$$

Using $\epsilon_y' = f_y/E_s$ and taking ϵ_u to be equal to 0.003, one obtains:

$$\omega_p + \omega - \omega' = 0.85\beta_1 \times \frac{d'}{d} \times \frac{87{,}000}{87{,}000 - f_y} \qquad (5\text{-}40)$$

One can conclude that the term on the left side of eq. 5-40 must be equal to or greater than the term on the right side of the equation if the compression reinforcement is to be stressed to its yield strength. If not stressed to its yield strength, the compression reinforcement should either be ignored or its effect determined from a study of the strain in the compression reinforcement. If the compression reinforcement is stressed to its yield strength as predicted from eq. 5-40, the nominal flexural strength of a rectangular section with compression reinforcement can be computed from:

$$M_n = A_{ps}f_{ps}\left(d_p - \frac{a}{2}\right) + A_sf_y\left(d - \frac{a}{2}\right) + A_s'f_y\left(\frac{a}{2} - d'\right) \qquad (5\text{-}41)$$

where:

$$a = \frac{A_{ps}f_{ps} + A_s f_y - A'_s f_y}{0.85 f'_c b}$$

Equations 5-35, 5-37, and 5-41 are intended for use in computing the nominal flexural strength of members that are underreinforced. Underreinforced members are proportioned in such a way that the stress in the tension reinforcement will reach the yield strength of the reinforcement before the compressive strain in the concrete reaches its limiting value of 0.003. The ACE 318 provisions covering this point are contained in Sect. 18.8.1, in which the reinforcement index is limited to $0.36\beta_1$. This can be expressed mathematically by:

$$\omega_p \leq 0.36\beta_1 \tag{5-42}$$

or:

$$\omega_p + \frac{d}{d_p}(\omega - \omega') \leq 0.36\beta_1 \tag{5-43}$$

for rectangular sections, and by:

$$\omega_{pw} + \frac{d}{d_p}(\omega_p - \omega'_w) \leq 0.36\beta_1 \tag{5-44}$$

for flanged sections. The ratio d/d_p is used to account for the difference in the effective depths of the prestressed and nonprestressed reinforcement, and the term β_1 accounts for the effect of concrete strength as previously described.

Combining the reinforcement index limit of $0.36\beta_1$ with eq. 5-30 and solving for d' gives the following:

$$d' = 0.424d\frac{87{,}000 - f_y}{87{,}000} \tag{5-45}$$

which can be reduced to $d' = 0.229d$ and $0.132d$ for Grades 40 and 60 reinforcement, respectively. The compression reinforcement will not be stressed to its yield strength if it is placed farther from the extreme compression fiber than the value of d' given by eq. 5-45. Using these values, the structural designer can rapidly check to determine the feasibility of using compression reinforcement to enhance the strength of a particular member. In so doing, the structural engineer should not overlook the normal tolerances in concrete construction and should determine if, in view of the normal tolerances, compression reinforcement should be used, and if special inspection should be required to ensure that the work is performed in an acceptable way.

Rectangular sections, or flanged sections having their neutral axes located within the depth of their flanges, having reinforcement indices exceeding $0.36\beta_1$

are considered to be overreinforced, and their nominal capacity may be computed from basic principles (see I.P. 5-4) or from:

$$M_n = f'_c b d_p^2 (0.36\beta_1 - 0.08\beta_1^2) \tag{5-46}$$

For flange sections having reinforcement indices equal to or greater than $0.35\beta_1$ and their neutral axes not located within the flange depth, the following approximate relationship is permitted for computing the nominal moment capacity:

$$M_n = f'_c b d_p^2 (0.36\beta_1 - 0.08\beta_1^2) + 0.85 f'_c (b - b_w) h_f (d_p - 0.5h_f) \tag{5-47}$$

Another important requirement in ACI 318 (Sec. 18.8.3), which is equally applicable to bonded and unbonded tendons, provides that the minimum factored load a section is capable of developing must be at least 1.2 times the cracking load, based upon a modulus of rupture equal to $7.5\sqrt{f'_c}$ for normal-weight concrete (additional provisions are provided in Sec. 9.5.2.3 of ACI 318 for concretes other than normal-weight concrete). An exception contained in Sec. 18.8.3 provides that members having shear and flexural strengths not less than twice the minimum required in Sec. 9.2 of ACI 318 are exempt from this requirement. This provision is to guard against failure at the cracking load, which was described in Sec. 5-2.

ILLUSTRATIVE PROBLEM 5-5 For the beam cross section shown in Fig. 5-21, compute the nominal flexural capacity as well as the stress in the prestressing steel at flexural capacity if the span of the beam is 40 ft, the weight of the beam is 0.44 kpf, and the dead load moment at midspan is 88.0 k-ft. Use the stress–strain properties as given in Fig. 5-8 in a strain-compatibility analysis. Compare the stress in the prestressing steel computed with the strain-compatibility analysis with that computed with the approximate relationship in ACI 318. Assume the following materials properties:

Concrete:

$$f'_c = 7500 \text{ psi}$$

$$E_c = 5000 \text{ ksi}$$

$$\beta_1 = 0.85 - \frac{(f'_c - 4000)0.05}{1000} = 0.675$$

Prestressing steel:

$$f_{ps} = 270 \text{ ksi}$$

$$f_{py} = 243 \text{ ksi}$$

$$E_{ps} = 28{,}000 \text{ ksi}$$

$$\gamma_p = 0.28$$

$$A_{ps} = 2.75 \text{ sq. in.}$$

$$P_{se} = 440 \text{ kips}$$

The section properties and other dimensional data are:

$$A_c = 415.8 \text{ in.}^2,\ I = 44{,}386 \text{ in.}^4$$

$$y_t = -15.3 \text{ in.},\ S_t = -2900 \text{ in.}^3,\ r^2/y_t = -6.97 \text{ in.}$$

$$y_b = 14.7 \text{ in.},\ S_b = 3020 \text{ in.}^3,\ r^2/y_b = 6.25 \text{ in.}$$

$$d_p = 30.00 - 5.20 = 24.8 \text{ in.}$$

$$e = 14.7 - 5.20 = 9.50 \text{ in.}$$

$$r^2/e = 11.24 \text{ in.}$$

SOLUTION: The percentage of prestressing reinforcement is computed as:

$$\rho_p = \frac{2.75}{24 \times 24.8} = 0.00462$$

This moderate value of the steel index indicates that the strain in the prestressing steel will be greater than 0.008 in./in. Hence, the equation for the Grade 270

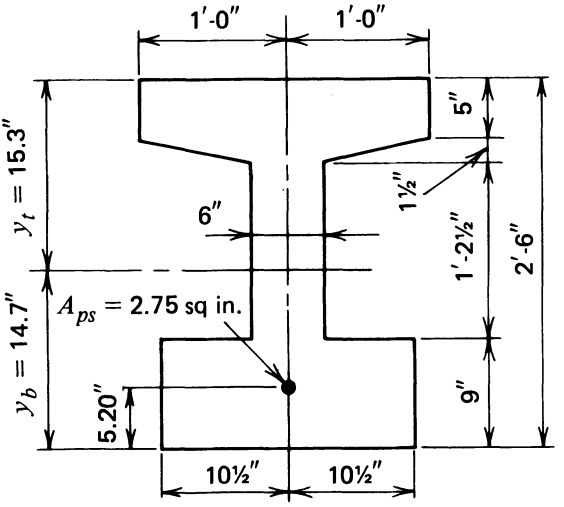

Fig. 5-21. Beam cross section for I.P. 5-5.

prestressing steel in Fig. 5-9 would be expected to be applicable. This relationship, which is one of the two required for the strain compatibility solution, is:

$$f_{ps} = 268 - \frac{0.075}{\epsilon_{ps} - 0.0065} < 0.98 f_{ps} = 264.6 \text{ ksi}$$

The stress in the concrete at the level of the prestressing steel due to effects of dead load and the prestress in the steel is:

$$f_e = \frac{-440{,}000}{415.8}\left(1 + \frac{9.50}{11.24}\right) + \frac{88.0 \times 12000 \times 9.50}{44{,}386} = -1727 \text{ psi}$$

The strains required for the analysis are:

$$\epsilon_c = 0$$

$$\epsilon_u = 0.003 \text{ in./in.}$$

$$\epsilon_{ce} = \frac{-1727}{5{,}000{,}000} = 0.00034 \text{ in./in.}$$

$$\epsilon_{se} = \frac{440{,}000}{28 \times 10^6 \times 2.75} = 0.0057 \text{ in./in.}$$

Substituting these values into the basic relationship for strain compatibility (eq. 5-8) gives:

$$f_{ps} = \frac{0.85 \times 0.65 \times 7.5}{0.00462} \times \frac{0.003}{0.003 + \epsilon_{ps} - 0.0057 - 0.00034}$$

$$f_{ps} = \frac{2.6907}{\epsilon_{ps} - 0.00304}$$

Solving the two equations gives $\epsilon_{ps} = 0.013498$ and $f_{ps} = 257.28$ ksi, from which one calculates the tensile force, k_u, and a as follows:

$$T = 257.28 \times 2.75 = 707.52 \text{ k}$$

$$k_u = \frac{0.003}{0.003 + 0.013498 - 0.0057 - 0.00034} = 0.287$$

$$a = 0.675 \times 0.287 \times 24.8 = 4.80 \text{ in.} < h_r = 5.00 \text{ in.}$$

Hence, the section should be analyzed as a rectangular beam. The maximum compressive force that the concrete section is capable of resisting is:

$$C = -0.85 \times 7.5 \times 24 \times 4.80 = 734.4 \text{ k} > T = 707.52 \text{ k}$$

and the nominal moment capacity is:

$$M_n = \frac{707.52}{12}\left(24.8 - \frac{4.80}{2}\right) = 1321 \text{ k-ft}$$

By using eq. 5-24 rather than strain compatibility, the calculations become:

$$f_{ps} = 270\left(1 - \frac{0.28}{0.675}\frac{2.75 \times 270}{24 \times 24.8 \times 7.5}\right) = 251.4 \text{ ksi}$$

$$\omega_p = \frac{2.75 \times 251.4}{24 \times 24.8 \times 7.5} = 0.155 < 0.36\beta_1 = 0.243, \text{ not overreinforced}$$

$$a = \frac{2.75 \times 251.4}{0.85 \times 7.5 \times 24} = 4.52 \text{ in.} < 5.00 \text{ in.}$$

$$M_n = \frac{2.75 \times 251.4}{12}\left(24.8 - \frac{4.52}{2}\right) = 1298.6 \text{ k-ft.}$$

The basic principle of strain compatibility can be developed for a rectangular beam having both prestressed and nonprestressed tensile reinforcement with the same methods used in developing the relationship for beams having only prestressed tensile reinforcement. Equilibrium requires that the tensile and compressive forces at a section to be equal in magnitude and opposite in direction, or $T = C$, which can be expanded to:

$$\frac{d}{d_p}(A_s f_y) + A_{ps} f_{ps} = 0.85 f'_c \beta_1 b k_u d_p$$

in which A_s and f_y are the area and stress at yield for the nonprestressed reinforcement located below the neutral axis at a depth d from the compression flange. It should be noted that the above relationship is valid only if the strain in the nonprestressed reinforcement equals or exceeds 0.0014 and 0.0021 for Grades 40 and 60 reinforcement, respectively. Note that multiplying the term $A_s f_y$ by the ratio of the effective depths of the nonprestressed and prestressed reinforcements, d/d_p, converts the effect of the nonprestressed reinforcement into an equivalent amount of nonprestressed reinforcement acting at a distance d_p from the extreme compression fiber. The above relationship can be rearranged to:

$$f_{ps} = \frac{0.85 f'_c \beta_1 b k_u d_p - \frac{d}{d_p}(A_s f_y)}{A_{ps}}$$

or the equivalent relationship:

$$f_{ps} = \frac{0.85f'_c\beta_1 k_u}{\rho_p} - \frac{d(A_s f_y)}{d_p A_{ps}}$$

By substituting eq. 5-7 for k_u, one obtains the general equation for a rectangular beam having both prestressed and nonprestressed reinforcement in the tensile flange:

$$f_{ps} = \frac{0.85f'_c\beta_1}{\rho_p} \times \frac{\epsilon_u}{\epsilon_u + \epsilon_{ps} - \epsilon_{se} - \epsilon_{ce}} - \frac{d(A_s f_y)}{d_p A_{ps}} \qquad (5\text{-}48)$$

The strain-compatibility principle can be extended to include sections with compression reinforcement by adding the compressive force carried by the compression reinforcement to the equilibrium equation. The result is:

$$\frac{d}{d_p}(A_s f_y) + A_{ps} f_{ps} = 0.85f'_c\beta_1 b k_u d_p + A'_s f'_s$$

By rearranging this relationship in a manner similar to what was done above in developing the relationship for nonprestressed tensile reinforcement, one obtains:

$$f_{ps} = \frac{0.85f'_c\beta_1}{\rho_p} \times \frac{\epsilon_u}{\epsilon_u + \epsilon_{ps} - \epsilon_{se} - \epsilon_{ce}} + \frac{A'_s f'_s}{A_{ps}} - \frac{d(A_s f_y)}{d_p A_{ps}} \qquad (5\text{-}49)$$

ILLUSTRATIVE PROBLEM 5-6 For the beam of I.P. 5-5, compute the nominal moment capacity of the beam if the area of the Grade 270 prestressed reinforcement is 2.00 sq. in., and, in addition to the prestressed reinforcement, the beam is provided with nonprestressed reinforcement having a yield strength of 60.0 ksi and an area of 3.00 sq. in., located with its center of gravity 4.50 in. from the soffit.

SOLUTION: The values needed for eq. 5-48 are:

$$\rho_p = \frac{2.00}{24 \times 24.8} = 0.00336$$

$$f_e = \frac{-320{,}000}{415.8}\left(1 + \frac{9.5}{11.24}\right) + \frac{88.0 \times 12{,}000 \times 9.50}{44{,}386} = -1194 \text{ psi}$$

$$\epsilon_u = 0.003$$

$$\epsilon_{se} = \frac{320{,}000}{28{,}000{,}000 \times 2.00} = 0.0057$$

$$\epsilon_{ce} = \frac{-1194}{5{,}000{,}000} = -0.00024$$

Using eq. 5-48:

$$f_{ps} = \frac{0.85(0.65)(7.5)}{0.00336} \times \frac{0.003}{0.003 + \epsilon_{ps} - 0.0057 - 0.00024} - \frac{25.5(3.0)(60)}{24.8 \times 2.00}$$

$$f_{ps} = \frac{3.700}{e_{ps} - 0.00294} - 92.54$$

Solving the above relationship with that for the Grade 270 prestressing strand from Fig. 5-8 gives $\epsilon_{ps} = 0.013904$ and $f_{ps} = 257.87$, from which the tensile force, T, k_u, and a are determined to be:

$$T = 3.0 \times 60 + 257.87 \times 2.00 = 695.74 \text{ k}$$

$$k_u = \frac{0.003}{0.013904 - 0.00294} = 0.274$$

$$a = 0.675 \times 0.274 \times 24.8 = 4.59 \text{ in.}$$

The concrete compressive stress is:

$$f_c = \frac{695.74}{4.59 \times 24} = 6.32 \text{ ksi} < 0.85f'_c$$

The nominal moment capacity of the section is:

$$M_n = \frac{180}{12}\left(25.5 - \frac{4.59}{2}\right) + \frac{516}{12}\left(24.8 - \frac{4.59}{2}\right) = 1316 \text{ k-ft}$$

Using eq. 5-34:

$$\omega = \frac{3.00 \times 60}{24 \times 25.5 \times 7.5} = 0.0392$$

$$\omega' = 0$$

$$\rho_p = 0.00336$$

$$f_{ps} = 270\left(1 - \frac{0.28}{0.675}\left[\frac{0.0336 \times 270}{7.5} + \frac{25.5 \times 0.0392}{24.8}\right]\right)$$

$$= 251.9 \text{ ksi}$$

The tensile forces carried by the nonprestressed and prestressed steel areas are 180 and 504 kips, respectively, the depth of the compression block is computed as:

$$a = \frac{180 + 504}{0.85 \times 7.5 \times 24} = 4.47 \text{ in.}$$

and the nominal moment capacity is:

$$M_n = \frac{180}{12}\left(25.5 - \frac{4.47}{2}\right) + \frac{504}{12}\left(24.8 - \frac{4.47}{2}\right) = 1296 \text{ k-ft}$$

ILLUSTRATIVE PROBLEM 5-7 Compute the nominal moment capacity of the T-shaped beam having nonprestressed tension and compression reinforcement in addition to prestressed reinforcement, as shown in Fig. 5-22. Use the approximation given in ACI 318 for the stress in the prestressing steel when loaded to its moment capacity. The dimensions of the section are given in the figure. The properties of the materials are given in the following summary:

$$f'_c = 4000 \text{ psi}$$

$$f_{pu} = 270 \text{ ksi}$$

$$f_{py} = 229.5 \text{ ksi}$$

$$f_y = 60 \text{ ksi}$$

$$f'_y = 60 \text{ ksi}$$

The parameters needed are computed as follows:

$$\rho_p = \frac{3.5}{60 \times 27.75} = 0.00210$$

$$\omega = \frac{4.0 \times 60}{60 \times 30 \times 4.0} = 0.03333$$

$$\omega' = \frac{1.0 \times 60}{60 \times 30 \times 4.0} = 0.00833$$

$$\frac{f_{py}}{f_{pu}} = \frac{229.5}{270.0} = 0.85$$

$$\beta_1 = 0.85$$

Note that from eq. 5-45 for $f_y = 60$ ksi, $0.132 \times 27.75 = 3.66$ in. $> d' = 1.50$ in.; hence, compression reinforcement will be effective.

b = 60.0 in. (flange width)	f'_c = 4.0 ksi
b_w = 16.0 in. (web width)	f_{pu} = 270 ksi
h = 32.5 in. (overall height)	f_{py} = 229.5 ksi
d_p = 27.75 in. (depth to A_{ps})	f_y = 60 ksi
d = 30.0 in. (depth to A_s)	A_s = 4.00 in.^{2}
d' = 1.5 in. (depth to A'_s)	A'_s = 1.00 in.^{2}
h_f = 4.5 in. (flange thickness)	

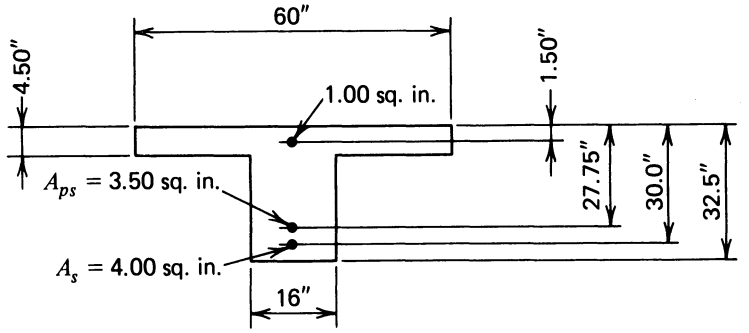

Fig. 5-22. Cross section of T-beam having compression reinforcement.

Using eq. 5-34:

$$f_{ps} = 270\left(1 - \frac{0.40}{0.85}\left[(0.00210)\frac{270}{4.0} + \frac{30}{27.75}(0.025)\right]\right) = 248.6 \text{ ksi}$$

$$\omega_p + \frac{d}{d_p}(\omega - \omega') = 0.158 < 0.36\beta_1 = 0.306$$

$$T = 3.5 \times 248.6 + 4.0 \times 60 = 870.1 + 240 = 1110.1 \text{ k}$$

Considering the section to be rectangular—that is, the compression block cannot extend below the thickness of the flange (4.50 in.)—the maximum compressive force is:

$$C = 0.85 \times 4.0 \times 60.0 \times 4.50 + 1.0 \times 60 = 918.0 + 60.0 = 978.0 \text{ k}$$

Because $T > C_{max}$, the member must be analyzed as a flanged section. The compressive force that must be resisted by the web of the beam is determined by subtracting the maximum allowable compressive force that can be imposed on the overhanging flanges of the member from the tensile force, T, that can be developed by the tensile reinforcement. This computation is done as follows:

$$A_{pw}f_{ps} = 1110.1 - 0.85 \times 4.0(60.0 - 16.0)4.5 - 1.0 \times 60$$

$$= 1110.1 - 673.2 - 60 = 376.9 \text{ k}$$

and:

$$\omega_{pw} = \frac{376.9}{16 \times 27.75 \times 4.0} = 0.2122$$

$$\omega_{pw} + \frac{d}{d_p}(\omega - \omega') = 0.239 < 0.36\beta_1 = 0.306$$

Using eq. 5-37, modified to include compression reinforcement (see eq. 5-41):

$$a = \frac{376.9}{0.85 \times 4.0 \times 16.0} = 6.93 \text{ in.}$$

$$M_n = \frac{376.9}{12}(27.75 - 6.93/2) + \frac{240}{12}(30.0 - 27.75)$$

$$+ \frac{673.2}{12}(27.75 - 2.25) + \frac{60}{12}(27.75 - 1.50)$$

$$= 762.3 + 45.0 + 1430.6 + 131.3 = 2369.2 \text{ k-ft}$$

5-5 Design Moment Strength Code Provisions for Members with Unbonded Tendons

The design moment strength provisions in ACI 318 that may be used for members prestressed with unbonded tendons if an analysis based upon strain compatibility is not performed, as is the case for members with bonded tendons, are restricted to use in members where f_{ps} is not less than $0.5f_{pu}$.

For members prestressed with unbonded prestressing tendons that have span-to-depth ratios of 35 or less, the value of f_{ps} permitted is:

$$f_{ps} = f_{se} + 10{,}000 + \frac{f'_c}{100\rho_p} \tag{5-50}$$

but f_{ps} in eq. 5-50 may not be taken greater than f_{py} or $(f_{se} + 60{,}000)$. For span-to-depth ratios greater than 35, the value of f_{ps} permitted is:

$$f_{ps} = f_{se} + 10{,}000 + \frac{f'_c}{300\rho_p} \tag{5-51}$$

with the value not to exceed f_{py} or $(f_{se} + 30{,}000)$. In eqs. 5-50 and 5-51, f_{ps}, f_{se}, and f'_c are in psi. When information is available for determining a more accurate value of f_{ps}, it may be used. Similarly to eq. 5-34, eqs. 5-50 and 5-51 are limited for use in applications where f_{se} is not less than $0.5f_{pu}$.

The relationships given in eqs. 5-42 through 5-44 for determining if members are to be analyzed as under- or overreinforced are also applicable to members with unbonded tendons. Members with unbonded tendons, in general, must be

able to develop factored loads equal to or greater than 1.2 times the cracking load with the modulus of rupture equal to $7.5\sqrt{f'_c}$, as with bonded members. Flexural members having flexural and shear strengths at least twice the minimum values required by Sec. 9.2 of ACI 318 are exempt from the minimum cracking load requirements.

Unbonded members lacking bonded, nonprestressed reinforcement could be subject to sudden brittle failure. For this reason, except as provided in Sec. 18.9.3.2 of the UBC, which applies to the positive moment areas of two-way flat plates having tensile stresses less than $2\sqrt{f'_c}$, the code requires a minimum amount of nonprestressed reinforcement in the tensile zone of members stressed with unbonded tendons. The minimum amount of bonded reinforcing, A_s, except for two-way flat plates (solid slabs of uniform thickness), is specified to be:

$$A_s = 0.004A \tag{5-52}$$

in which A is the area of the concrete section between the flexural tension face and the center of gravity of the gross section. The reinforcing must be placed as close as possible to the extreme tension fiber and uniformly distributed. It is required regardless of the stresses existing in the member under service loads.

It is interesting to note that Sec. 2618(j)B of the Uniform Building Code requires that one-way post-tensioned beams and slabs having unbonded reinforcement be designed to carry the dead load plus 25 percent of the unreduced superimposed live load tributary to the member by some method other than the unbonded post-tensioned reinforcement. (See the UBC for the complete requirements.) This provision applies to the design moment strength based upon load and strength reduction factors of unity (see Sec. 5-6). Compliance with this requirement normally is achieved through the provision of nonprestressed reinforcement detailed to comply with all requirements of the UBC (i.e., development lengths, minimum embedments, etc.). This provision is not included in the ACI 318 requirements.

In the case of flat plates, no bonded reinforcement is required in areas of positive moment when the concrete tensile stresses do not exceed $2\sqrt{f'_c}$ after all losses. If the tensile stress does exceed $2\sqrt{f'_c}$, the minimum area of bonded steel is:

$$A_s = \frac{N_c}{0.5f_y} \tag{5-53}$$

in which f_y cannot exceed 60,000 psi, and N_c is the tensile force in the concrete under the sum of the service dead and live loads. Again, the steel must be uniformly distributed over the section and as close as practicable to the tension fiber. In areas of negative moment, the minimum amount of bonded reinforcement required in each direction is:

$$A_s = 0.00075hl \tag{5-54}$$

in which l is the length of the span in the direction parallel to the reinforcement being considered, and h is thickness of the member. The bonded reinforcing is to be placed in a width not exceeding the width of the supporting column plus $3h$, the maximum spacing of the bars is 12 in., and there must be at least four bars or wires in each direction. The code contains other provisions for determining the minimum lengths of the reinforcement (UBC 1988).

ILLUSTRATIVE PROBLEM 5-8 Compute the nominal moment capacity for the member shown in Fig. 5-23. The member is stressed with an unbonded tendon, $f_{se} = 144$ ksi, $f_{py} = 240$ ksi, $f_{py} = 192$ ksi, $f'_c = 6.0$ ksi, and the span is 40.0 ft. Use the provisions of ACI 318 for f_{ps} and the method proposed by Pannell.

SOLUTION:

$$\text{Span–depth ratio} = \frac{L}{d} = \frac{40.0}{2.5} = 16$$

and the ratio of the effective stress to the ultimate tensile strength is:

$$\frac{f_{se}}{f_{pu}} = \frac{144}{240} = 0.60 > 0.50$$

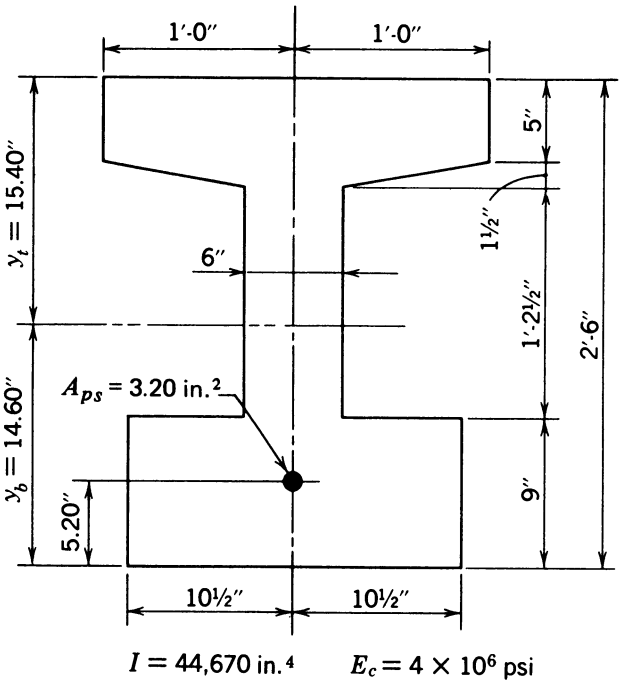

Fig. 5-23. Cross section of beam used in I.P. 5-8.

Hence, the use of eq. 5-50 is appropriate for the analysis in conformance with ACI 318. The steel ratio is:

$$\rho_p = \frac{3.20}{24 \times 24.8} = 0.00538$$

and:

$$f_{ps} = 144 + 10 + \frac{6.0}{100 \times 0.00538} = 165 \text{ ksi}$$

This value of $f_{ps} < f_{pu} = 192$ ksi $< f_{se} + 60 = 204$ ksi.

$$A_{ps}f_{ps} = 3.20 \times 165 = 528 \text{ kips}$$

$$a = \frac{528}{0.85 \times 6 \times 24} = 4.31 \text{ in.}$$

$$M_n = \frac{528(24.8 - 2.16)}{12} = 996 \text{ k-ft}$$

Using Pannell's method:

$$\rho_p = 0.00538$$

$$q_e = \frac{0.00538 \times 144}{6} = 0.129$$

$$\lambda = \frac{10^6 \times 0.00538 \times 2.5}{6000 \times 40.0} = 0.056$$

$$q_u = \frac{0.129 + 0.056}{1 + 0.0895} = 0.170$$

$$M_n = \frac{0.170(1 - 0.80 \times 0.170)6 \times 24 \times 24.8^2}{12} = 1084 \text{ k-ft}$$

5-6 Strength Reduction and Load Factors

The relationships given in Secs. 5-2 through 5-5 were provided for use in computing the nominal design moment in prestressed concrete flexural members. The nominal design moment is the flexural strength one would expect if the equations used in the calculations were accurate, the materials used in the construction had the stress and strain properties assumed in the calculations, and the members were constructed with dimensions equal to those assumed in the calculations. These conditions do not exist consistently in practice; so a

strength reduction factor, ϕ, is used to reduce the nominal strengths calculated with the equations given previously in this chapter. The product of the strength reduction factor and the nominal strength is referred to as the *reduced nominal strength*. The reduced nominal strength must equal or exceed the required strengths (sometimes referred to as the factored strengths or minimum strengths) mandated by the applicable code or standard being used as the design criterion. The six different relationships for required strengths are specified in Chapter 9 of ACI 318. The basic relationship is:

$$U = 1.4D + 1.7L \tag{5-55}$$

in which U is the required strength needed to resist the factored loads or related internal moments and forces, D is the dead loads or related internal moments and forces, and L is the live loads or related external moments and forces. The numerical factors, 1.4 and 1.7, are commonly referred to as load factors. The other relations for the required strength contained in Chapter 9 of ACI 318 are applicable to members subject to loads from wind, earthquake, earth pressure, fluids, impact, differential settlement of supports, concrete creep, concrete shrinkage, and temperature change.

The strength reduction factors given in ACI 318 for flexure and shear are 0.90 and 0.85, respectively. The factor for shear is lower than that for flexure in view of the more brittle (less ductile) nature of shear failures as compared to flexural failures of underreinforced members.

Hence, when one is applying the flexural strength relationships given in this chapter in actual design, the nominal moment capacity, M_n, is to be multiplied by the strength reduction factor, ϕ, and the product (i.e. the reduced nominal flexural strength) is to be compared to the required flexural strength, M_u (i.e., the minimum factored flexural strength permitted by the criteria being used). This relation can be expressed as:

$$\phi M_n \geq M_u = 1.4M_d + 1.7M_l \tag{5-56}$$

where M_d is the service load moment due to dead load and M_l is the service load moment due to live load. If ϕM_n is less than the required strength, M_u, adjustments must be made in the design in order to increase the reduced nominal flexural strength to equal or exceed the minimum required.

The codes and standards of some countries use an approach somewhat different from the one used in ACI 318 to ensure that adequate strength is provided. For example, the Canadian Standards Association building standard provides for the use of various strength reduction factors for the different materials commonly used in reinforced concrete construction (CSA 1984). The strength reductions factors for concrete, prestressed reinforcement, nonprestressed reinforcement, and structural steel are 0.60, 0.90, 0.85, and 0.90, respectively. These strength reduction factors (referred to as "resistance

factors'' in the CSA document), are used with load factors that are different and somewhat lower than those required by ACI 318. For example, the basic load-combination equation for strength contained in the CSA document is:

$$\alpha_D D + \gamma\psi(\alpha_L L + \alpha_Q Q + \alpha_T T) \tag{5-57}$$

in which α_D, α_L, α_Q, and α_T are load factors for dead load, live load, wind or earthquake, and the cumulative effects of temperature, creep, shrinkage, and differential settlement, respectively; γ is an importance factor; and ψ is a load-combination factor. The values of the load factors for dead, live, wind/earthquake, and ''T-loads'' are 1.25 (except that when dead load is resisting overturning, uplift, or stress reversal, the dead load factor is 0.85), 1.50, 1.50, and 1.25, respectively. The importance factor normally is not to be taken to be less than 1.0, and has a minimum value of 0.8 for unimportant structures not likely to cause injury or other serious consequences in the event of collapse. The load combination factor, ψ, is to be taken as 1.0 when only one of the loads L, Q, or T is included in eq. 5-57. If two of the loads L, Q, or T are included in eq. 5-57, the load combination factor is 0.70, and if all three loads are included, the factor becomes 0.60. The load combination for service load checks (i.e., cracking and deflection) is:

$$D + \psi(L + Q + T) \tag{5-58}$$

in which the terms are as defined above.

The above discussion of the provisions of the Canadian standard is not complete and is given here only to illustrate the difference between the ACI 318 approach to safety and those used in other countries. The reader should consult and use the complete CSA document if any of its provisions are to be used; it normally is considered risky to use only portions of a code or a standard.

REFERENCES

ACI Committee 318. 1989. *Building Code Requirements for Reinforced Concrete*. Detroit. American Concrete Institute.

ACI Committee 318. 1989. *Commentary on Building Code Requirements for Reinforced Concrete*. Detroit. American Concrete Institute.

ACI-ASCE Joint Committee 323. 1958. Tentative Recommendations for Prestressed Concrete. *Journal of the American Concrete Institute* 29(7):545–78.

ACI-ASCE Committee 423.3R. 1983. Recommendations for Concrete Members Prestressed with Unbonded Tendons. *Journal of the American Concrete Institute* 5(7):61–76.

ACI-ASCE Committee 423.3R. 1989. Recommendations for Concrete Members Prestressed with Unbonded Tendons. *Journal of the American Concrete Institute* 86(3):301–18.

Canadian Standards Association. 1984. *Design of Concrete Structures for Buildings*. Rexdale (Toronto). Canadian Standards Association.

Harajli, M. H. and Naaman, A. E. 1985. Evaluation of the Ultimate Steel Stress in Partially Prestressed Flexural Members. *PCI Journal* 30(5):54–81.

Mattock, A. H. 1979. Flexural Strength of Prestressed Concrete Sections by Programmable Calculator. *PCI Journal* 24(1):32–54.

Menegotto, M. and Pinto, P. E. 1973. Method of Analysis for Cyclically Loaded R.C. Plane Frames, Including Changes in Geometry and Non-Elastic Behavior of Elements Under Combined Normal Force and Bending. In *Preliminary Report for Symposium on Resistance and Ultimate Deformability of Structures Acted on by Well-Defined Repeated Loads*. Lisbon. International Association for Bridge and Structural Engineering. 15–32.

Muller, J. 1956. Flexural Strength of Prestressed Concrete Continuous Structures. Paper read at the Knoxville Convention of the American Society of Civil Engineers. 9–19.

Naaman, A. E. 1977. Ultimate Analysis of Prestressed and Partially Prestressed Sections by Strain Compatibility. *PCI Journal* 22(1):32–51.

Pannell, F. N. 1969. The Ultimate Moment Resistance of Unbonded Prestressed Concrete Beam. *Magazine of Concrete Research* 21(66):43–54.

PCI Design Handbook. 1978. Chicago. Prestressed Concrete Institute.

PCI Design Handbook. 1985. Chicago. Prestressed Concrete Institute.

Skogman, B. C., Tadros, M. K., and Grasmick, R. 1988. Flexural Strength of Prestressed Concrete Members. *PCI Journal* (33)5:96–123.

Uniform Building Code. 1988. Whittier, California. International Conference of Building Officials.

Yamazaki, J., Kattula, B. T., and Mattock, A. H. 1969. A Comparison of the Behavior of Post-Tensioned Prestressed Concrete Beams with and without Bond. Structures Mechanics Report SM69-3. Seattle. Department of Civil Engineering, University of Washington.

PROBLEMS

1. Determine ultimate moment capacity for the double-tee slab of Problem 1 of Chapter 4 using eq. 5-34 for f_{ps}. Assume that $A_{ps} = 0.171$ in.^{2}, $f_{pu} = 270$ ksi, the strand is low-relaxation, and $f'_c = 5000$ psi.

SOLUTION:

$$\rho_p = \frac{0.171}{48 \times 12} = 0.000297,\ \gamma_p = 0.28,\ \beta_1 = 0.80$$

$$f_{ps} = 270\left(1 - \frac{0.35 \times 0.000279 \times 270}{5}\right) = 268.5 \text{ ksi}$$

$$\omega_p = \rho_p \frac{f_{ps}}{f'_c} = 0.0159 < 0.80 \times 0.36 = 0.288$$

$$a = \frac{0.171 \times 268.5}{0.85 \times 48 \times 5} = 0.225 \text{ in.} < 2.00 \text{ in.}$$

and the member can be analyzed as a rectangular section.

$$\phi M_n = \frac{0.90 \times 0.171 \times 268.5}{12}\left[12.00 - \frac{0.225}{2}\right] = 40.93 \text{ k-ft}$$

The design load (factored) for the simple span of 24 ft that will result in the moment of 40.93 k-ft is 568.5 plf. Assuming all the superimposed service load to be live load, its maximum permitted value would be:

$$w_{ll} = \frac{568.5 - 1.4 \times 187.5}{1.7} = 180 \text{ plf}$$

This should be compared to the allowable loads as controlled by stresses at service load, computed in Problem 1, Chapter 4. If the modulus of rupture of the concrete is $7.5\sqrt{5000} = +530$ psi and the bottom fiber compressive stress due to the final prestressing force is -863 psi as calculated in Problem 1 of Chapter 4, the cracking moment for the slab is:

$$M_{CR} = \frac{(530 + 863)2860}{12000 \times 10} = 33.20 \text{ k-ft}$$

and the full reduced moment capacity of the section can be utilized because:

$$\phi M_n = 40.83 > 1.20 \times 33.20 = 39.84 \text{ k-ft}$$

2. If the double-tee slab analyzed in Problem 1 had a concrete strength of 6500 psi, determine what steps would be necessary to fully utilize the flexural capacity of the member.

SOLUTION:

$$\beta_1 = 0.725$$

$$f_{ps} = 270\left[1 - \frac{0.386 \times 0.000297 \times 270}{6.5}\right] = 268.7 \text{ ksi}$$

$$a = \frac{268.7 \times 0.171}{0.85 \times 48 \times 6.5} = 0.173 \text{ in.}$$

$$\phi M_n = \frac{0.90 \times 0.171 \times 268.7}{12}\left[12 - \frac{0.173}{2}\right] = 41.06 \text{ k-ft}$$

By using a modulus of rupture of 605 psi, the minimum reduced flexural strength computation becomes:

$$1.2M_{CR} = \frac{1.2(605 + 863)2860}{12000 \times 10} = 41.98 \text{ k-ft} > 41.06 \text{ k-ft}$$

The flexural strength is 2.2% less than the minimum required to conform to the cracking moment limitation of the code. One option is to increase the flexural strength by adding nonprestressed flexural reinforcement. Another would be to

increase the quantity of prestressed reinforcement. With Grade 40 nonprestressed reinforcement, the amount required would be approximately:

$$A_s = \frac{0.022 \times 268.7 \times 0.171}{40} = 0.25 \text{ in.}^2$$

The provision of a number 3 bar in each leg in addition to the prestressing would result in the following (using $d = 12.5$ in. for the nonprestressed reinforcement):

$$f_{ps} = 270\left(1 - 0.386\left[\frac{0.000297 \times 270}{6.5} + \frac{12.5}{12}\left(\frac{0.22}{48 \times 12.5 \times 6.5}\right)\right]\right)$$

$$= 268.7 \text{ ksi}$$

and:

$$a = \frac{0.171 \times 268.7 \times 0.22 \times 40}{0.85 \times 6.5 \times 48} = 0.206 \text{ in.}$$

and:

$$\phi M_{CR} = 0.90\left(\frac{0.171 \times 268.7}{12}\left(12 - \frac{0.206}{2}\right) + \frac{0.22 \times 40}{12}\left(12.5 - \frac{0.206}{2}\right)\right.$$

$$= 49.18 \text{ k-ft} > 1.2M_{CR} = 41.98 \text{ k-ft}$$

3. Analyze the double-tee beam of Problem 1 for ultimate moment capacity under conditions of $f'_c = 5000$ psi and the tendon being unbonded. Assume that the effective prestress is equal to 80 percent of the initial prestress of 16,100 lb per tendon.

$$f_{se} = \frac{0.80 \times 2 \times 16{,}100}{0.171} = 150.6 \text{ ksi}$$

$$\rho_p = \frac{0.171}{48 \times 12} = 0.000297$$

The span-to-depth ratio is:

$$\frac{L}{d} = \frac{24 \times 12}{14} = 20.6$$

Hence, eq. 5-50 should be used to determine f_{ps}.

$$f_{ps} = 150{,}600 + 10{,}000 + \frac{5000}{100 \times 0.000297}$$

$$= 329{,}000 \text{ psi} > f_{py}$$

Use $f_{ps} = 150{,}600 + 60{,}000 = 210{,}600$ psi $\leq f_{py}$, $a = 0.176$ in., and:

$$\phi M_n = \frac{0.90 \times 0.171 \times 210.6}{12}\left[12 - \frac{0.176}{2}\right] = 32.17 \text{ k-ft}$$

The cracking moment (from Problem 1) was shown to be 33.20 k-ft. Hence, nonprestressed reinforcement must be provided, or some other means must be used, to increase the moment capacity of the section to not less than $1.20 \times 33.20 = 39.84$ k-ft. The flexural strength of the member must be increased approximately 24 percent, or the permissible service loads must be restricted to a level that provides twice the load factors permitted in Sec. 9.2 of ACI 318.

4. The double-tee beam shown in Fig. 5-24 is to be used on a span of 40 ft with an overhang of 8 ft at one end. If the member is prestressed with bonded stress-relieved strand tendons having an area of 0.58 sq in., an effective prestress of 90,000 lb, and $f_{pu} = 270.0$ ksi, determine the adequacy of the member from the standpoint of negative moment flexural strength. The tendons are located 2.50 in. from the top of the member and $f'_c = 5000$ psi. For the double-tee section, $A = 187.5$ in.^{2}, $I = 4256$ in.^{4}, $y_t = 5.17$ in., and $y_b = 10.83$ in.

SOLUTION:

For negative moment the ratio of the prestressed reinforcement is:

$$\rho_p = \frac{0.58}{5.25 \times 13.5} = 0.00818$$

The stress in the prestressed reinforcement at design strength is:

$$f_{ps} = 270\left(1 - \frac{0.5 \times 0.00818 \times 270}{5}\right) = 210.34 \text{ ksi}$$

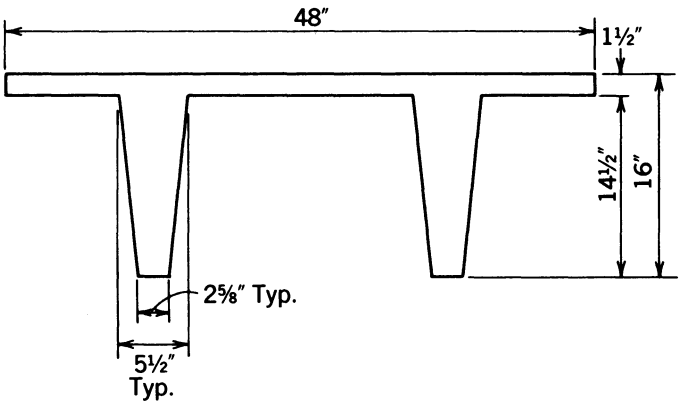

Fig. 5-24. Double-tee slab.

The index of the prestressed reinforcement is:

$$\omega_p = \frac{210.34 \times 0.00818}{5} = 0.344 > 0.36\beta_1 = 0.288$$

and the section is overreinforced. The flexural strength is computed, using eq. 5-46, as:

$$\phi M_n = \frac{0.90 \times 5 \times 5.25 \times 13.5^2}{12}(0.288 - 0.08 \times 0.80^2) = 85.0 \text{ k-ft}$$

The compressive stress in the top fiber due to the effective prestress of 90,000 lb is computed as follows:

$$f_t = \frac{-90{,}000}{187.5}\left(1 + \frac{-2.67}{-4.39}\right) - 772 \text{ psi}$$

and the cracking moment is:

$$M_{CR} = \frac{(772 + 530)823}{12{,}000} = 89.3 \text{ k-ft}$$

and $1.2M_{CR} = 107.2$ k-ft. In this case the cracking moment is greater than reduced nominal flexural capacity, and if flexural failure were to occur, it would be expected to be sudden and complete. The flexural strength is limited by the compressive strength of the section, as is the case in overreinforced concrete sections; and because of the narrow width of the bottoms of the stems of the double-tee beam, providing tied compression reinforcement in the stems to increase the compressive strength is not a feasible alternative.

The reduced flexural strength of 85.0 k-ft amounts to a uniformly distributed loading, over the 8 ft length of the overhanging ends, of 2.66 klf or 0.66 ksf. Assuming that the superimposed load is primarily live load, for which the load factor is 1.7, by using two times the normal load factor the total load that could be applied *if the cracking moment were controlling rather than the flexural strength* would be approximately $0.66/2 \times 1.7 = 194$ psf. The only feasible way of increasing the flexural capacity of the section if used as a prestressed member with the dimensions given in this analysis is to increase the compressive strength of the concrete so that the cracking moment will control. Alternatively, either the eccentricity or the amount of the prestressing reinforcement could be reduced and thereby cause the cracking moment to control, or the prestressing in the overhanging section could be eliminated and the negative moment areas could be designed as nonprestressed reinforced concrete.

5. Investigate the double-tee beam of Problem 4, under the identical conditions given there, if the tendons are unbonded rather than bonded.

SOLUTION:

The span–depth ratio for the cantilever is equal to 12 if the actual length of the overhanging end is used as the span length, and 24 if two times the span length is used (because it is not a simple span). In either case, eq. 5-50 should be used in determining the stress in the prestressed reinforcement for the strength analysis. The value found from eq. 5-50 is 171 ksi, which is less than the effective prestressing stress plus 60 ksi (215 ksi) and less than the minimum specified yield stress (243 ksi). The value of the prestressed reinforcement index is 0.28; hence, the member is underreinforced. The reduced nominal moment capacity is:

$$\phi M_n = \frac{0.90 \times 171 \times 0.58}{12}\left[13.5 - \frac{4.44}{2}\right] = 83.89 \text{ k-ft}$$

The moment capacity is less than 120% of the cracking moment (107.2 k-ft), and the member does not conform to the code requirements. Addition of flexural tensile reinforcement will not correct the situation because additional reinforcement will result in the member becoming overreinforced.

6. Two identical one-story buildings, having the dimensions shown in Fig. 5-25, are composed of a continuous post-tensioned roof slab that is 6 in. thick supported on concrete bearing walls. One building has bonded tendons; the other does not. The roof slab is prestressed with stress-relieved strand tendons placed on parabolic paths, as shown in Fig. 5-26. The effective stress in the tendons is 15.0 kips per foot of width. The tendons have an area of 0.11 sq. in./ft, and $f_{pu} = 270$ ksi. If a catastrophic accident caused a downward load of 950 psf to act along the full length and width of one of the 4-ft-wide overhangs of the structure, determine its effect on each of the buildings. If the catastrophic accident caused a downward load of 1200 psf on the overhang, determine its effect on the structures with each type of tendons. Assume $f'_c = 4500$ psi.

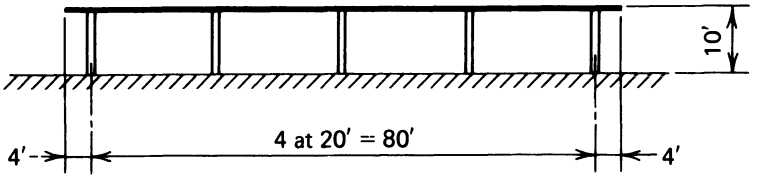

Fig. 5-25. Elevation of single-story building having a 6 in. one-way slab roof supported by bearing walls, used in Problem 6.

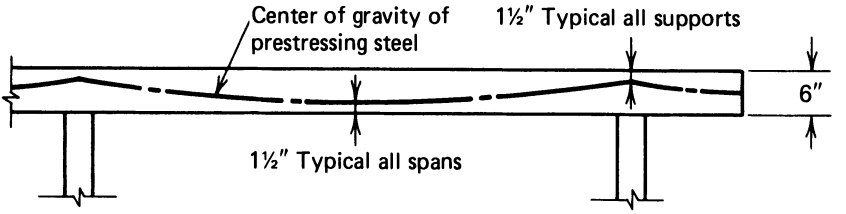

Fig. 5-26. Tendon layout for 6 in. slab roof for building in Problem 6.

SOLUTION:

Bonded tendons:

$$\rho_p = \frac{0.11}{12 \times 4.5} = 0.00204 \qquad f_{ps} = 253.3 \text{ ksi}$$

$$\omega = 0.115 \qquad \phi M_n = 8.78 \text{ k-ft/ft}$$

$$f_t = \frac{-15{,}000}{72}\left(1 + \frac{-1.5}{-1.0}\right) = -521 \text{ psi}$$

$$M_{CR} = \frac{(503 + 521)72}{12{,}000} = 6.14 \text{ k-ft/ft}$$

$$1.2M_{CR} = 7.37 \text{ k-ft/ft} < 8.78 \text{ k-ft/ft} \quad \text{ok.}$$

Unbonded tendons:

$$\frac{\text{Span}}{\text{Depth}} = \frac{20 \times 12}{6} = 40 \qquad \therefore \text{ Use eq. 5-51.}$$

$$f_{ps} = 136 + 10 + \frac{4.5}{300 \times 0.00204} = 153.4 \text{ ksi}$$

$$\text{Use } f_{ps} = 153.4 < 136 + 60 = 166 < f_{py}$$

$$\phi M_n = 5.46 \text{ k-ft/ft}$$

$$1.2M_{CR} = 7.37 \text{ k-ft/ft} > 5.46 \text{ k-ft/ft} \quad \text{NG.}$$

Nonprestressed reinforcing must be added to the slab with unbonded tendons to increase the moment to 7.37 k-ft/ft.

$$A_s \cong \frac{12(7.37 - 5.46)}{60 \times 4.5} = 0.085 \text{ in.}^2\text{/ft}$$

Use No. 4 bars at 28 in. on centers, $A_s = 0.086$ in.^{2}/ft. For 950 plf, $M = 7.60$ k-ft/ft, and for 1200 plf, $M = 9.60$ k-ft/ft.

CONCLUSIONS: For the load of 950 plf the moment in the overhang due to the applied load, exceeds the moment capacity of the slab having unbonded tendons (7.37 k-ft/ft). The slab overhang would be expected to break off and release the prestress in the tendons. Without the prestress in the tendons, the slab in the interior spans would be expected to collapse because of its own dead load. The moment due to the load of 950 plf would not cause the overhang to fail in the slab with bonded tendons.

For the load of 1200 psf, the overhang on the building with bonded tendons would fail. The roof would not collapse, however, because the stress in the bonded tendons would not be released by the failure of the overhang.

6 Flexural-Shear Strength, Torsional Strength, and Bond of Prestressed Reinforcement

6-1 Introduction

The topics of flexural-shear strength and bond of prestressed reinforcement are closely associated with flexural strength design. For a flexural member to perform as intended, it must not fail in bending, flexural shear, or torsional shear, or because of inadequate bond of the reinforcement. Torsion is not necessarily related to flexure, but it is included in this chapter because it frequently occurs in flexural members, and reinforcement for torsional strength frequently is closely associated with reinforcement for flexural shear strength.

6-2 Shear Consideration for Flexural Members

Reinforced concrete members, when subjected to loads that cause significant flexural stresses, often develop cracks that originate in the extreme tensile fibers of the members in the vicinity of the larger bending moments. Cracks of this type normally are nearly vertical, are caused by flexural tensile stresses, and are considered to be relatively unimportant at relatively low loads or bending moments. As flexural cracking progresses with the application of load, the area over which the cracking occurs extends, and cracks farther away from the areas

of highest bending moments tend to become flatter (i.e., less vertical). At higher loads (moments), the cracks extend in length, their ends nearest the compression flange assume a more horizontal path, and they become what are known as flexural-shear cracks (as opposed to simple flexural cracks). Flexural-shear cracks are potentially dangerous from the standpoint of complete collapse. In addition, members having prestressed reinforcement will, on occasion, develop web cracks that do not extend to the extreme fibers (tensile or compressive) in areas of low bending moment. The latter type of cracking, which is more likely to occur in flexural members having T-or I-shaped cross sections, (i.e., cross sections with thin webs), is caused by principal tensile stresses that exceed the tensile strength of the concrete; they normally originate near the centroidal axis of the cross section of the member.

The existence of shear cracks of these two types may or may not be precursors of catastrophic collapse of a flexural member; but, because "shear failures" that originate from these types of cracking can occur suddenly and with little warning, prudent engineers generally provide reinforcement (shear reinforcement) when the conditions of a design indicate reinforcement may be needed to ensure that the flexural shear strength of a member equals or exceeds its flexural bending strength.

The two types of flexural shear cracking currently are recognized in one way or another in all contemporary design standards for concrete flexural members having prestressed and nonprestressed reinforcement. Illustrated in Fig. 6-1, they are further described as follows:

Type I Cracking. This is the type of cracking associated with flexural cracking. Some authorities believe that for this type of crack to adversely affect the capacity of a member, it must extend in such a manner that the horizontal projection of the crack has a length approximately equal to the depth of the

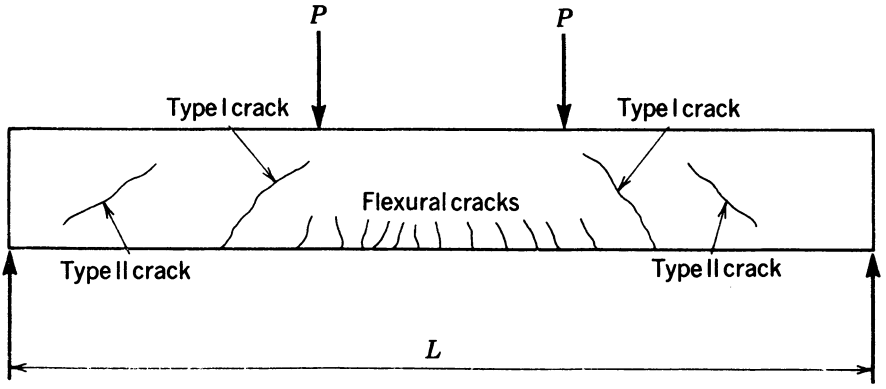

Fig. 6-1. Illustration of flexural cracks and Types I and II shear cracks.

member. For this reason, some researchers believe that a Type I crack located at a distance equal to the depth of the member away (in the direction of lesser moment) from a section being investigated for flexural shear strength can be the source of a critical flexural shear crack (PCA 1963). In addition, principal tensile stresses along a potential Type I crack may be aggravated by flexural cracks that occur in the vicinity of the potential Type I crack; and, because principal tensile stresses normally are maximum at the centroidal axis of a beam (can be taken to be approximately at the middepth of the beam), a flexural crack at one-half the beam depth from a section under consideration can be considered a potential cause for a Type I crack. Shear cracking in members having nonprestressed and prestressed reinforcement most commonly results in Type I cracks. The cracks begin as flexural cracks extending approximately vertically into the beam. When a critical combination of flexural and shear stresses develops near the top of a flexural crack, the crack becomes more inclined, and the potential for failure is enhanced.

Type II Cracking. This type of cracking, which is associated with principal tensile stresses in areas where there are no flexural cracks, originates in the web of the member near the centroidal axis, where shear and thus principal tensile stresses are the greatest. With an increase in loading, they extend towards the flanges (PCA 1963). Type II cracking is fairly unusual. It may appear near the supports of highly prestressed simple beams that have thin webs, and it also may occur near the inflection points and bar cutoff points of continuous, reinforced-concrete members subjected to axial tension (MacGregor and Hanson 1969).

In view of the above distinctions, it should be apparent that in designing flexural members for the effects of shear stresses, one must consider each type of cracking and determine the amount of reinforcing that is required to negate the adverse effects of each type. Some members must be designed for movable live loads, variable spacings between the live loads, and variable conditions of loading (as functions of span lengths, continuity, etc.); so designing for the different types of "shear cracking" can be confusing. A good understanding of the fundamental differences between the types of cracking can help one to gain confidence and proficiency in flexural shear design. The reader will find interesting discussions of the classical theories related to the shear strength of reinforced and prestressed concrete members in the references listed at the end of this chapter.

In some parts of the world, it has been customary to assume that once a crack has formed in a reinforced concrete flexural member, whether reinforced for flexure with prestressed or with nonprestressed reinforcement, the total shear force must be carried by shear-reinforcing steel without any of the shear force being resisted by the uncracked portion of the concrete section. On the other

hand, it has been traditional in U.S. practice to assume that a portion of the shear force is carried by the concrete section, with shear reinforcing needed only for the shear forces that are in excess of those the concrete can safely resist itself. Hence, shear design criteria commonly used in the United States have been formed with two purposes: to establish the amount of shear force the concrete can carry alone and to determine the amount of shear reinforcing required to carry the shear force, if any, in excess of that which the concrete can sustain itself.

In recent years a new approach to the design for shear in reinforced concrete members has emerged from research work done in Canada (Mitchell and Collins 1974). This theory was originally presented as the Compression Field Theory. More recently it has been modified to include the effects of tension stiffening, and the updated version is known as the Modified Compression Field Theory (Vecchio and Collins 1986). This theory is an extension of the truss analogy approach to the design of reinforced concrete flexural members originally proposed by Ritter and subsequently enhanced by Moersch (Ritter 1899; Moersch 1902). It recognizes the importance of reinforcement placed in each of the two orthogonal directions on the shear strength of reinforced concrete flexural members, as well as its effect on the inclination of shear cracks. The method has been used to explain the strength behavior of reinforced concrete flexural members, with and without prestressing, without relying upon the assumption that web cracks must occur at an angle of 45° from the centroidal axis of the member regardless of the amounts of longitudinal and transverse reinforcement. In its complete form, the method is relatively difficult to apply, especially to members that must be designed for many, variable combinations of loading; so it is probably most useful in research and the investigation of failures. It is interesting to note that simplified code provisions based upon the Compression Field Theory are included in the Canadian Standards Association publication *Design of Concrete Structures for Buildings* (CSA 1984).

Another area in which U.S. practice in shear design differs from the practice in other parts of the world concerns the design in the support regions of beams, areas of beams subjected to concentrated loads, and portions of members having abrupt changes in cross section (corbels, haunches, daps, etc.) and discontinuities. A comprehensive treatment of this subject will be found in the paper "Toward a Consistent Design of Structural Concrete" (Schlaich, Schaefer, and Jennewein 1987), and a brief but enlightening treatment will be found in the *Design of Concrete Structures for Buildings* (CSA 1984). The areas in question are referred to as disturbed areas, and these areas are modeled as trusses for the purpose of determining the concrete compressive stresses in the diagonal struts, the tensile forces in the ties, and the stresses in the connections—the latter being termed nodal zones. Figure 6-2, which is based upon Fig. D13 in CSA 1984 (see Appendix D), illustrates the components of the truss model and is used here to facilitate this discussion of the basic concept. Threaded ends of ties with

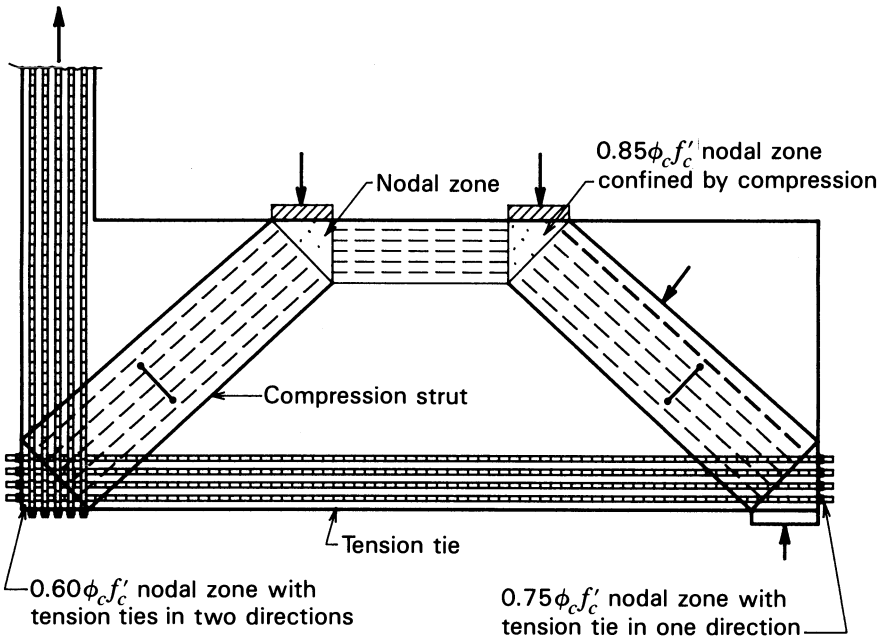

Note: Threaded ends of rods and nuts used to emphasize the need for anchoring the ends of tension elements in the nodal areas.

Fig. 6-2. Model employed to illustrate the trusslike action of a reinforced concrete beam using the truss analogy (after CSA 1984).

nuts are used to emphasize the need for anchoring the ends of tension elements in the nodal areas. The provisions contained Sec. 11.4.7, "Design of Regions Adjacent to Supports, Concentrated Loads, or Abrupt Changes in Cross Section," in CSA 1984 are discussed in detail in Sec. 6-5 of this chapter.

6-3 Flexural Shear Design Provisions of ACI 318

The flexural shear provisions for prestressed concrete members contained in ACI 318 include an approximate method that may used to determine the shear force that a concrete section can resist without transverse (shear) reinforcement. This relationship is:

$$V_c = \left(0.6\sqrt{f'_c} + 700\frac{V_u d}{M_u}\right) b_w d \qquad (6\text{-}1)$$

The use of the approximate method is limited to members with an effective prestress equal to at least 40 percent of the strength of the tensile flexural reinforcement. In eq. 6-1, V_u and M_u are the total required (factored) design

shear force and moment applied at a section, respectively. When the approximate relationship is used, the limitations on V_c are:

$$2\sqrt{f'_c}b_w d \leq V_c \leq 5\sqrt{f'_c}b_w d$$

In addition, $V_u d/M_u \leq 1$. The term d in eq. 6-1 is the distance from the extreme compression fiber to the centroid of the longitudinal tension reinforcement, and b_w is the width of the web.

When applied to simply supported spans subjected to uniformly applied loads alone, eq. 6-1 becomes:

$$V_c = \left(0.6\sqrt{f'_c} + 700\frac{d(l-2x)}{x(l-x)}\right)b_w d \qquad (6\text{-}2)$$

where l is the span length, and x is the distance from the support to the point under consideration. Equation 6-2 can be represented graphically in terms of unit stress, as shown in Fig. 6-3 (from ACI 318R 1983).

The designer may elect to make a more detailed analysis for the shear design of prestressed concrete flexural members by determining the amount of shear reinforcing required to guard against failure as a result of Types I and II cracking. If this is done, two separate analyses are required because Type I cracking is a function of both moment and shear, whereas Type II cracking is not a function of moment. In the case of moving loads, maximum moment and

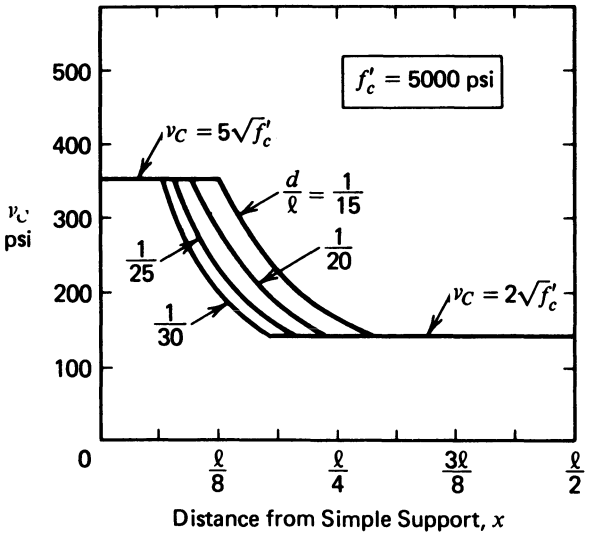

Fig. 6-3. Diagram showing the relationship of unit shear stress v_c as a function of the span length for a simple prestressed concrete beam supporting a uniformly distributed load. Reproduced with the permission of the American Concrete Institute.

maximum shear do not usually occur at any one section under the same condition of loading; so more effort is required to make a complete analysis for members designed for moving loads than is needed in the case of a member subjected to nonmoving live loads.

The shear force that can safely be carried by the concrete in areas subject to flexural cracking (Type I shear cracks) is computed by:

$$V_c = 0.6\sqrt{f'_c}b_w d + V_d + \frac{V_i M_{cr}}{M_{\max}} \tag{6-3}$$

in which:

V_d = The shear force due to service dead load (unfactored). The service dead load includes the self-weight of the member, cast-in-place slabs, cast-in-place toppings, and superimposed dead loads, whether acting compositely or noncompositely with the member

V_i = V_u minus V_d

$M_{\max}$ = M_u less the moment due to service dead load (unfactored) from the self-weight of the member and all superimposed dead load moments ($M_{\max}$ and V_i are concomitant)

b_w = the width of the web

d = the effective depth

M_{cr} = the cracking moment

In applying eq. 6-3, one must use the loading combination resulting in the greatest value of $M_{\max}$, not V_i. It is worth repeating that V_i is the shear force concomitant with $M_{\max}$ and not necessarily the greatest design shear force at the section under consideration. (This fact has caused considerable difficulty among structural designers who have become accustomed to using the loading that causes the greatest shear force, rather than the loading that causes the greatest moment, when designing for shear.)

The cracking moment is defined as:

$$M_{cr} = \frac{I}{y_t}(6\sqrt{f'_c} + f_{pe} - f_d) \tag{6-4}$$

The equation for M_{cr} is given as it appears in ACI 318; f_{pe} and f_d are both taken to be positive. In eq. 6-4, the terms are defined as follows:

f_d = Stress due to total service dead load, at the extreme fiber of a section at which tensile stresses are caused by applied load, psi

f_{pe} = Compressive stress in concrete due to prestress only after all losses, at the extreme fiber of a section at which tensile stresses are caused by applied loads, psi

I = Moment of inertia of section resisting externally applied design loads, in.^{4}

y_t = Distance from the centroidal axis of the gross section, neglecting the reinforcement, to the extreme fiber in tension, in.

The limits for V_{ci} are:

$$1.7\sqrt{f'_c}b_w d \leq V_{ci} \leq V_{cw}$$

Equation 6-5, which is discussed below, is used to compute V_{cw}.

The shear force that can be carried by the concrete in areas where Type II (principal tensile stress) cracking controls, rather than flexural-shear cracking, is given in ACI 318 to be as follows:

$$V_{cw} = (3.5\sqrt{f'_c} + 0.3f_{pc})b_w d + V_p \qquad (6\text{-}5)$$

In lieu of using eq. 6-5, V_{cw} can be taken as the shear corresponding to a multiple of dead load plus live load, which results in a computed principal tensile stress of $4\sqrt{f'_c}$ at the centroidal axis of the member, or at the intersection of the flange and the web when the centroidal axis is located in the flange.

The definitions of the terms in eq. 6-5 not previously defined are:

b_w = Web width, or diameter of circular section, in.

d = Distance from extreme compression fiber to centroid of tension reinforcement, in.

f_{pc} = Compressive stress in the concrete, after all prestress losses have occurred, at the centroid of the cross section resisting the applied loads, or at the junction of the web and flange when the centroid lies in the flange, psi (In a composite member, f_{pc} will be the resultant compressive stress at the centroid of the composite section, or at the junction of the web and flange when the centroid lies within the flange, due to both prestress and to the bending moments resisted by the precast member acting alone. The reduction in the effective prestressing force at a section, due to the length required to transfer the prestress to the concrete, must be taken into account when computing V_{cw} in pretensioned members.) (See Sec. 6-6.)

V_p = Vertical component of the effective prestress force at the section considered, lb

At the option of the designer, in members that are prestressed in one direction only, eq. 6-6, which follows, may be used to determine the shear force or unit shear stress that will cause a principal tensile stress of $4\sqrt{f'_c}$:

$$V_{cw} = [\sqrt{4f'_c(4\sqrt{f'_c} + f_{pc})}]b_w d + V_p \qquad (6\text{-}6)$$

If the member is provided with prestressing in two orthogonal directions, such as in a beam prestressed with vertical stirrups in addition to longitudinal prestressed reinforcement, the relationship for V_{cw} becomes:

$$V_{cw} = \left[\sqrt{(\sqrt{4f'_c} + f_{pcv})(4\sqrt{f'_c} + f_{pc})}\right] b_w d + V_p \qquad (6\text{-}7)$$

in which f_{pcv} is the prestressing stress acting at 90° from f_{pc}.

It should be noted that in the relationships given above in eqs. 6-1, 6-2, 6-3, 6-4, and 6-5, it is assumed that the concrete is made of normal sand and gravel and does not contain lightweight concrete aggregates. ACI 318 provides that in lieu of $\sqrt{f'_c}$, $0.75\sqrt{f'_c}$ be used if the concrete is made with lightweight sand and coarse aggregate (''all-lightweight concrete''), and $0.85\sqrt{f'_c}$ be used if the concrete made with normal sand and lightweight coarse aggregates (''sand-lightweight concrete''). In eqs. 6-6 and 6-7, the actual tensile strength of the concrete should be used in lieu of $4\sqrt{f'_c}$ if it is known.

In applying the above equations for V_c, V_{ci}, and V_{cw}, d is to be taken as the depth from the extreme compression fiber to the centroid of the longitudinal tension reinforcement, or 0.8 times the overall thickness of the member, whichever is greater.

The shear design at each section is to be based upon:

$$V_u \leq \phi V_n \qquad (6\text{-}8)$$

and:

$$V_n = V_c + V_s \qquad (6\text{-}9)$$

Terms in eqs. 6-8 and 6-9 are:

V_c = Nominal shear strength provided by the concrete; either that obtained from eq. 6-1 or the lesser of that obtained from eq. 6-3 or eq. 6-5.
V_n = Nominal shear strength
V_s = Nominal shear strength provided by shear (transverse) reinforcement
V_u = Total design (factored) shear force at a section (Note that for use in computing V_c and V_{cw} from eqs. 6-1 and 6-5, the value of V_u to be used in eq. 6-8 is the greatest value that occurs at the section. For use with V_{ci} from eq. 6-3, the value of V_u to be used in eq. 6-8 is a function of the shear force occurring from the load distribution causing maximum moment; *this may not be the greatest shear force that can occur at the section.*)
ϕ = Capacity reduction factor, which for shear design is 0.85
b_w = Web width
d = Depth from extreme compression fiber to the centroid of the longitudinal tension reinforcement, but not less than 0.8 times the thickness of the member

When the value of V_u is greater than ϕV_c, shear reinforcement must be provided for the shear force in excess of the amount that the concrete can carry. For the

usual case of shear reinforcement placed perpendicular to the longitudinal reinforcement, the amount of shear force the reinforcement can sustain is:

$$V_s = \frac{A_v f_y d}{s} \tag{6-10}$$

in which A_v is the area of the shear reinforcement perpendicular to the flexural tension reinforcement within a distance s, and the other terms have been defined previously. Note that eq. 6-10 can be rewritten as:

$$\frac{V_s}{b_w d} = v_s = \frac{A_v f_y}{b_w s} \tag{6-11}$$

or:

$$A_v = \frac{V_s b_w s}{f_y} \tag{6-12}$$

in which v_s is the unit shear stress.

Other provisions are contained in ACI 318 for the case of shear reinforcing that is not placed perpendicular to the longitudinal reinforcing. Reinforcing of this type rarely is used in prestressed concrete construction, and it is not discussed in this book.

It should be noted that vertical stirrups normally are placed at a maximum spacing of 0.75 times the thickness of prestressed members, but when V_s exceeds $4\sqrt{f'_c}\, b_w d$, the maximum spacing permitted by ACI 318 is 0.375 times the thickness. To guard against principal compression failures, the value of V_s is limited to $8\sqrt{f'_c}\, b_w d$.

It is interesting to note that the reduction of the shear force acting upon the section due to the vertical component of the prestressing is included in eq. 6-5 but not in eq. 6-3. Tests of prestressed concrete members with and without inclined tendons have shown this to be appropriate. In designing for shear in prestressed member it also is appropriate to include the effects of variation of depth of the section (see below) and shear forces resulting from prestress-induced deformations in continuous members (see Chapter 10).

Beams of variable depth and normal configuration have less shear force on their webs in areas where the compression flange is inclined to the gravity axis than would be revealed from a usual analysis of the flexural shear forces. The principle, known as the Résal effect, is illustrated in Fig. 6-4, in which a freebody diagram of a portion of a variable-depth continuous beam is shown. The portion of the beam shown is near the support, where both the shear force and the negative moment are large. If the angle of inclination of the bottom flange with respect to the gravity axis of the member is taken as α, and the force in the compression flange is designated as C_f, there is a vertical component of the force C_f equal to $C_f \sin \alpha$. This vertical component of the force acts in a

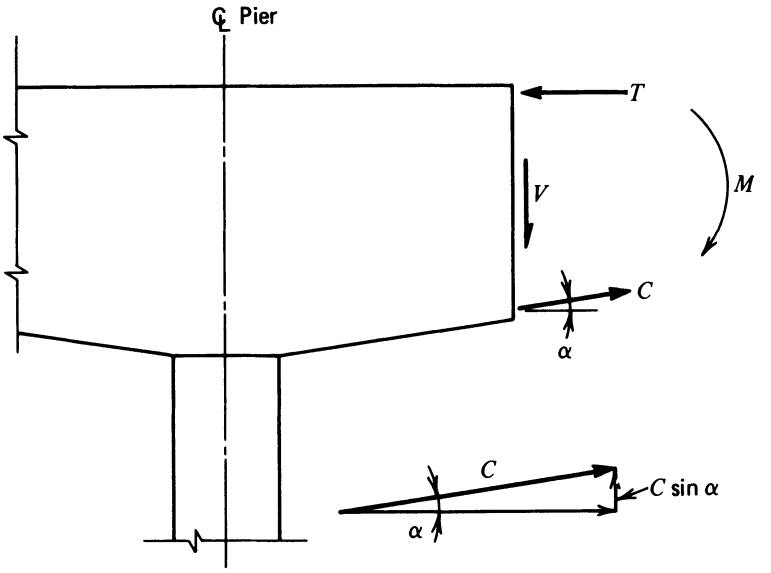

Fig. 6-4. Freebody diagram of a portion of a bridge superstructure having variable depth.

direction that reduces the shear force applied to the webs of the member. When this effect is applied in an analysis under design loads, the force should be determined on the basis of the design moment that is concomitant with the design shear force being considered.

Minimum shear reinforcing provisions are contained in ACI 318 for prestressed concrete, as they are for reinforced concrete. Slabs, footings, and concrete joist construction are exempt from these requirements. The minimum amount of shear reinforcing is:

$$A_v = \frac{50 b_w s}{f_y} \tag{6-13}$$

for reinforced or prestressed members not subject to significant torsional moments (see ACI 318). For prestressed members, the relationship:

$$A_v = \frac{A_{ps} f_{pu} s}{80 f_y d} \sqrt{\frac{d}{b_w}} \tag{6-14}$$

may be used if the effective prestress is at least 40 percent of the tensile strength of the flexural reinforcement. (As is discussed in Sec. 6-4, ACI 318 does not include specific requirements for prestressed concrete members subject to significant torsional moment.)

For prestressed concrete flexural members having reactions that induce

compression into their end regions, ACI 318 permits the maximum shear force to be taken to be the shear force at a distance equal to one-half the thickness of the member, $h/2$, from the support. This recognizes the arch or truss action of the concrete in the vicinity of the support. For flexural members reinforced with nonprestressed reinforcement that have reactions that induce compression into their end regions, ACI 318 permits the maximum shear force to be taken as equal to the shear force at a distance of d (the effective depth of the reinforcement) from the support.

The end regions of flexural members having prestressed or nonprestressed reinforcement and reactions that do not induce compression in the end regions must be designed for the maximum calculated shear force.

Punching shear stresses, as might be caused by a concentrated wheel load on a prestressed slab or by the supporting column on a flat plate structure, are a source of concern to the prestressed-concrete designer. Provisions are made for punching shear in concrete slabs and footings, reinforced with prestressed or nonprestressed reinforcement, in Sec. 11.11 of ACI 318. The design for shear stresses in the vicinity of the columns in flat plates and flat slabs involves a determination of shear stresses resulting from the vertical concentric load as well as from the moment that must be transferred between the column and the slab. The method used in that type of analysis is described in Sec. 13-13 of this book.

The basic prestressed concrete shear provisions of the AASHTO specification (AASHTO 1989) are similar to those contained in ACI 318. It is interesting to note, however, that the AASHTO specifications permit the use of the shear design provisions of the 1979 Interim AASHTO *Standard Specifications for Highway Bridges* as an alternative to those contained in AASHTO 1989.

It should be noted that the shear provisions for prestressed concrete described herein, and found in the commonly used U.S. design criteria and codes, are written in terms of force rather than unit stress. Before the publication of the 1977 edition of ACI 318, U.S. design criteria and codes contained shear design provisions for reinforced and prestressed concrete members expressed in unit stress. The change to expressions of force made in the 1977 edition of ACI 318 was done in the interest of having consistency of units throughout the code—that is, having all of the code provisions (except those for the development of reinforcing) in terms of force. Unit stress relationships are more desirable than force terms for the designer because it is possible to memorize certain limiting unit stresses. It is not possible to memorize limiting forces because they are the product of unit stresses and dimensions of the cross section, and thus vary from member to member. For this reason, it is recommended the structural designer consider the use of unit shear stresses rather than shear forces in routine design work. The forces can be computed and shown at the completion of the calculations if necessary to demonstrate specific compliance with the applicable

building code. This approach is particularly useful in the evaluation of Type II shear cracking in prestressed concrete flexural members, as the maximum unit stress is the limiting factor for Type II cracking. (This is occasionally overlooked by designers who are not familiar with the basis for the force relationships contained in the codes for V_{cw}.)

The limiting stresses that the designer should keep in mind are as follows:

1. Minimum value for shear stress in eq. 6-3 for V_{ci} is $v_c = 1.7\sqrt{f'_c}$.
2. The minimum value for shear stress V_c in eq. 6-1 is $v_c = 2.0\sqrt{f'_c}$.
3. The maximum value of shear stress for shear reinforcement used at normal spacing is $v_c = 4.0\sqrt{f'_c}$.
4. The maximum value of shear stress V_c in eq. 6-1 is $v_c = 5.0\sqrt{f'_c}$.
5. The maximum value for shear stress to be carried by shear reinforcement, to guard against a failure due to diagonal compression stresses, is $v_s = 8.0\sqrt{f'_c}$.

ILLUSTRATIVE PROBLEM 6-1 Using the provisions of ACI 318, investigate the double-tee slab shown in Fig. 6-5 for web reinforcing using the simplified analysis. The dead load of the double-tee slab is 200 plf, the superimposed live load is 240 plf, the design span is 40 ft, f'_c is 5000 psi, and the prestressing consists of straight tendons with A_{ps} = 0.58 sq. in., P_{se} = 90.0 kips, and f_{pu} = 270 ksi. The tendons are located 2 in. above the soffit. Plot the results. Use b_w = 8.00 in.

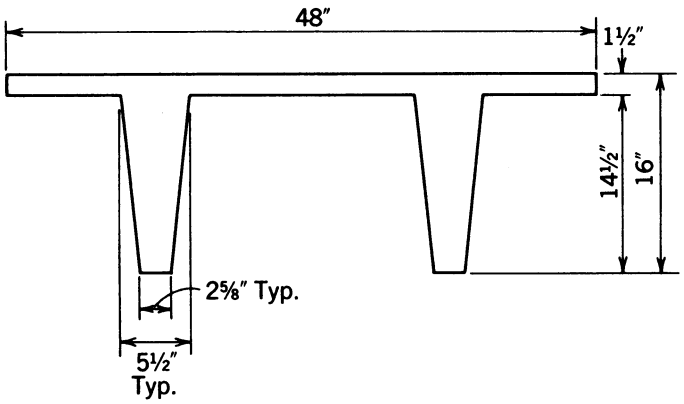

Fig. 6-5. Double-tee slab.

SOLUTION:

		Service load	*Design load*
Dead load	= 0.200 klf × 20 ft	= 4.00 k × 1.4	= 5.60 k
Live load	= 0.240 klf × 20 ft	= 4.80 k × 1.7	= 8.16 k
	Total reactions	= 8.80 k	= 13.76 k

$$V_{u\max} = 13.76 \text{ k}$$

$$v_{u\max} = \frac{13{,}760}{8 \times 14} = 123 \text{ psi}$$

$$\frac{V_{u\max}}{\phi} = \frac{13.76}{0.85} = 16.19 \text{ k}$$

$$\frac{v_{u\max}}{0.85} = \frac{16{,}190}{8 \times 14} = 145 \text{ psi}$$

$$v_{c\min} = 2\sqrt{5000} = 141 \text{ psi}$$

$$v_{c\max} = 5\sqrt{5000} = 353 \text{ psi}$$

Using eq. 6-2, the relationship for the approximate method with simple spans having uniformly distributed loads, expressed in unit stress rather than force, gives:

$$v_c = \left(0.6\sqrt{5000} + \frac{700 \times 14(40 - 2x)}{12x(40 - x)}\right)$$

Solving for v_c gives values of v_c of 429, 223, and 154 psi for values of x of 2, 4, and 6 ft, respectively.

The computations of the minimum shear reinforcement according to eqs. 6-13 and 6-14, respectively, are as follows:

$$A_v = \frac{50 \times 8 \times 12}{40{,}000} = 0.12 \text{ sq. in.}$$

$$A_v = \frac{0.58}{80}\frac{270}{40}\frac{12}{14}\sqrt{\frac{14}{8}} = 0.055 \text{ sq. in.}$$

The ratio of f_{se} to f_{pu} is $0.57 \geq 0.40$; hence, the use of eq. 6-14 is appropriate, and the minimum area of shear reinforcement of 0.055 sq. in. per foot may be used.

The results are plotted in Fig. 6-6. It should be noted that v_c is greater than v_u/ϕ throughout the length of the member; so shear reinforcement is not

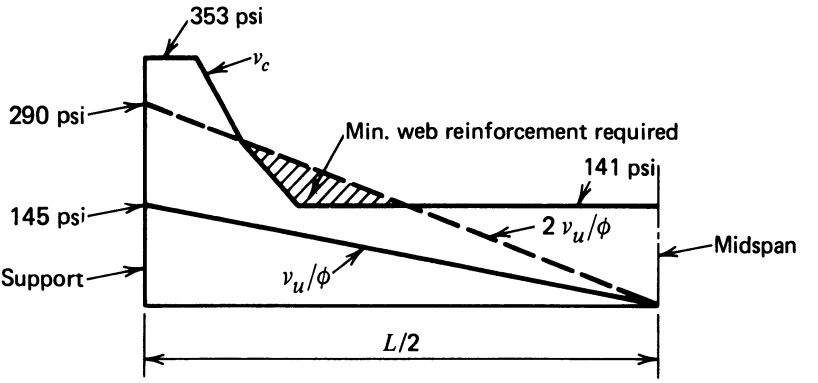

Fig. 6-6. Plot of the results of a shear stress analysis for a double-tee slab.

required for strength considerations. For a small distance, v_c is less than $2v_u/\phi$; so minimum reinforcement is required in this area.

ILLUSTRATIVE PROBLEM 6-2 For the double-tee slab of Problem 6-1, determine the web reinforcing required using both simplified and detailed analyses if the design span is 30 ft, the supports are simple, and the superimposed live load is 650 plf. The section properties of the slab are:

$$A = 189.5 \text{ sq. in.}, I = 4256 \text{ in.}^4, y_t = -5.17 \text{ in.}$$

SOLUTION: Simplified analysis:

$$V_u = (1.4 \times 0.2 + 1.7 \times 0.65)15 = 20.78 \text{ kips}$$

$$\frac{v_u}{\phi} = \frac{20{,}780}{0.85 \times 8 \times 14} = 218 \text{ psi}$$

$$v_{c\max} = 5\sqrt{5000} = 353 \text{ psi}$$

$$v_{c\min} = 2\sqrt{5000} = 141 \text{ psi}$$

At 6 feet from the support, $x = 6.00$ in eq. 6-2,

$$v_c = 42 + \frac{(700)(14)(18)}{(12)(6)(24)} = 144 \text{ psi}$$

The computations are plotted in Fig. 6-7a.

Detailed analysis: The computations are summarized in Table 6-1 and plotted in Fig. 6-7b.

$$v_{c\min} = 1.7\sqrt{5000} = 120.2 \text{ psi}$$

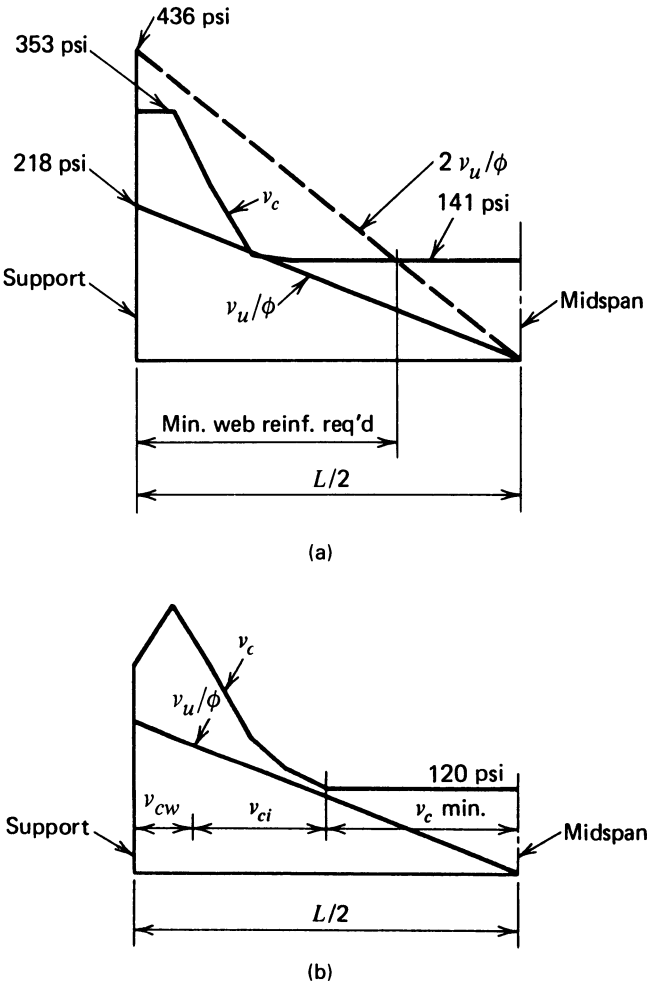

Fig. 6-7. Plots of the results of simplified and detailed shear analyses for a double-tee slab. (a) Simplified analysis. (b) Detailed analysis.

The transmission length for the tendons (see Sec. 6-6) has been taken as 18.75 in.

The area of the shear reinforcement provided is based upon the use of Grade 40 reinforcement and eq. 6-14. Note that with an area of reinforcement of 0.0554 sq. in. per foot:

$$V_s = \frac{0.0554 \times 40{,}000 \times 14}{12} = 2585 \text{ lb}$$

TABLE 6-1 Summary of Computations for I.P. 6-2.

Pt.	Length (ft)	v_{ci} (psi)	v_{cw} (psi)	v_c (psi)	v_u (psi)	A_v (in.^{2}/ft)
.00	.000	infin	247.4	247.4	218.2	.0554
.05	1.500	563.4	384.2	384.2	196.4	.0554
.10	3.000	295.5	389.9	295.5	174.5	.0554
.15	4.500	198.7	389.9	198.7	152.7	.0554
.20	6.000	149.2	389.9	149.2	130.9	.0554
.25	7.500	118.3	389.9	120.2	109.1	.0554
.30	9.000	96.6	389.9	120.2	87.2	.0554
.35	10.500	79.9	389.9	120.2	65.4	.0554
.40	12.000	66.1	389.9	120.2	43.6	.0554
.45	13.500	53.9	389.9	120.2	21.8	.0554
.50	15.000	42.4	389.9	120.2	000.0	.0554

and

$$v_s = 23.1 \text{ psi}$$

COMMENTS: In this example the simplified analysis is only slightly conservative when compared to the detailed analysis. In the detailed analysis, the value of v_c increases rapidly between the end of the member and 1.50 ft from the end because of the transmission length (transfer distance) required for the pretensioned tendons (see Sec. 6-6).

ILLUSTRATIVE PROBLEM 6-3 Investigate the post-tensioned beam shown in Fig. 6-8 for shear reinforcing if the beam has the following section properties:

$$A = 876 \text{ in.}^2,\ I = 433{,}350 \text{ in.}^4,\ y_t = -25.0 \text{ in.}$$

The design dead loads are as follows:

Girder dead load = 0.911 klf
Superimposed dead load = 0.500 klf
Total dead load = 1.411 klf

The design span is 80.0 ft, and the design live load is 2.00 klf. The beam is stressed with an effective force of 670 kips and:

$$f'_c = 5000 \text{ psi}$$

$$f_y = 40{,}000 \text{ psi}$$

$$f_{pu} = 270{,}000 \text{ psi}$$

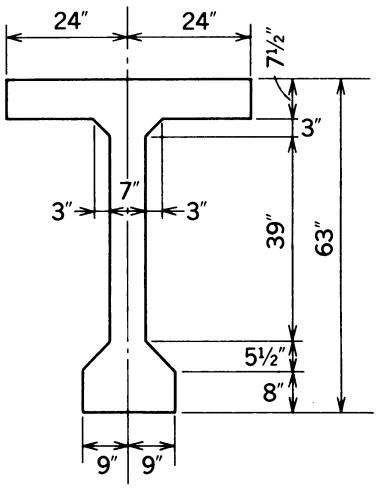

Fig. 6-8. Cross section of a beam analyzed for shear stresses.

The tendon is on a parabolic curve with $e = 0$ at the support and $e = 32.1$ in. at midspan. Use load factors of $1.4D + 1.7L$, and analyze the beam by the detailed analysis. The area of the prestressed reinforcement is 4.00 in.^{2}. Neglect the nonprestressed longitudinal reinforcement.

SOLUTION: See Table 6-2 for a summary of the computed values of v_{ci}, v_{cw}, v_c, v_u, and A_v. The data in Table 6-2 are shown plotted in Fig. 6-9.

ILLUSTRATIVE PROBLEM 6-4 Investigate the beam of I.P. 6-3 for shear reinforcement if the live load consists of one concentrated load of 100 kips applied 20 ft from the left support.

TABLE 6-2 Summary of Computations for I.P. 6-3.

Pt.	Length (ft)	v_{ci} (psi)	v_{cw} (psi)	v_c (psi)	V_u/ϕ (psi)	A_v (in.^{2}/ft)
.00	.000	infin	730.9	730.9	717.0	0.1050
.05	4.000	1029.6	705.5	705.5	645.3	0.1050
.10	8.000	601.5	680.1	601.5	573.6	0.1050
.15	12.000	440.0	654.7	440.0	501.9	0.1299
.20	16.000	344.9	629.3	344.9	430.2	0.1790
.25	20.000	276.1	603.9	276.1	358.5	0.1727
.30	24.000	214.9	575.8	214.9	278.1	0.1360
.35	28.000	162.3	547.7	162.3	199.9	0.1050
.40	32.000	118.4	522.8	120.2	129.4	0.1050
.45	36.000	79.3	499.4	120.2	63.6	0.1050
.50	40.000	42.4	476.9	120.2	000.0	0.1050

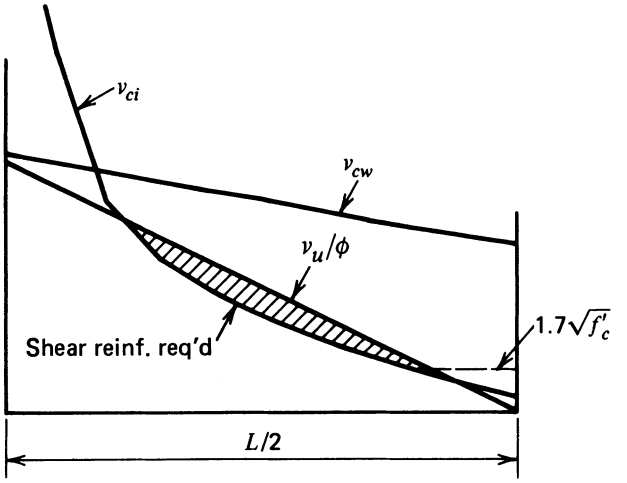

Fig. 6-9. Plot of the results of a shear analysis of the beam shown in Fig. 6-8.

SOLUTION: The computations are summarized in Table 6-3, and the results are shown plotted in Fig. 6-10.

6-4 Torsion Considerations for Flexural Members

Flexural members frequently are subjected to the effects of torsion. The torsional moments often are small and frequently can be neglected without serious consequences. On the other hand, in some instances torsional stresses can be significant and lead to failure if not addressed in the designing and detailing of reinforced concrete members. Spandrel or facia beams probably are the most commonly encountered members in building construction for which torsion design can be important.

The torsional moment acting upon a beam cross section is measured from the shear center of the section. The locations of the shear centers for commonly encountered cross sections are illustrated in Fig. 6-11 (Oden 1967). The principles involved in determining the torsional moments on L-shaped spandrel beams and a box-girder bridge are illustrated in Figs. 6-12 and 6-13, respectively.

It is important to recognize the fact that the torsional stiffness and torsional strength of "open" sections, such as I-shaped or T-shaped beams, are low in comparison to those for a "closed" section such as the cross section of a box-girder bridge. (See Chapter 14 for illustrations of open and closed bridge members.) The torsional strength and stiffness are an important consideration in the design of bridges because these structures are frequently subjected to significant torsional moments due to eccentrically applied live loads or due to

TABLE 6-3 Summary of Computations for I.P. 6-4.

Pt.	Length (ft)	e (in.)	V_d (k)	M_d (k-ft)	V_i (k)	M_{max} (k-ft)	V_u (k)	V_p (k)	v_{ci} (psi)	v_{cw} (psi)	v_u (psi)	v_c (psi)	A_v (in.^{2}/ft)
.00	.000	.00	−56.440	.000	−150.076	.000	−206.516	−89.6	infin	730.9	688.6	730.9	.1050
.05	4.000	6.10	−50.796	214.472	−147.818	595.788	−198.614	−80.7	1069.7	705.6	662.3	705.6	.1050
.10	8.000	11.55	−45.152	406.368	−145.560	1182.547	−190.712	−71.7	647.8	680.1	635.9	647.8	.1050
.15	12.000	16.37	−39.508	575.688	−143.303	1760.275	−182.811	−62.7	493.2	654.6	609.6	493.2	.2443
.20	16.000	20.54	−33.864	722.432	−141.045	2328.972	−174.909	−53.8	405.2	629.4	583.2	405.2	.3738
.25	20.000	24.08	−28.220	846.600	31.212	2888.640	2.992	−44.8	172.2	603.9	9.9	172.2	.1050
.30	24.000	26.69	−22.576	948.192	33.469	2759.276	10.893	−35.8	160.8	575.8	35.4	160.8	.1050
.35	28.000	29.21	−16.932	1027.208	35.727	2620.883	18.795	−26.9	149.3	547.8	58.2	149.3	.1050
.40	32.000	30.82	−11.288	1083.648	37.984	2473.459	26.696	−17.9	140.7	522.7	80.3	140.7	.1050
.45	36.000	31.78	−5.644	1117.512	40.242	2317.004	34.598	−9.0	134.7	499.5	102.4	134.7	.1050
.50	40.000	32.10	.000	1128.800	42.500	2151.520	42.500	.0	131.0	476.9	125.0	131.0	.1050
.55	44.000	31.78	5.644	1117.512	44.757	1977.004	50.401	9.0	158.4	499.5	149.1	158.4	.1050
.60	48.000	30.82	11.288	1083.648	47.015	1793.459	58.303	17.9	189.8	522.7	175.5	189.8	.1050
.65	52.000	29.21	16.932	1027.208	49.272	1600.883	66.204	26.9	227.6	547.8	205.2	227.6	.1050
.70	56.000	26.69	22.576	948.192	51.530	1399.276	74.106	35.8	274.9	575.8	240.9	274.9	.1050
.75	60.000	24.08	28.220	846.600	53.788	1188.640	82.008	44.8	331.2	603.9	273.4	331.2	.1050
.80	64.000	20.54	33.864	722.432	56.045	968.972	89.909	53.8	393.2	629.4	299.8	393.2	.1050
.85	68.000	16.37	39.508	575.688	58.303	740.275	97.811	62.7	482.2	654.6	326.1	482.2	.1050
.90	72.000	11.55	45.152	406.368	60.560	502.547	105.712	71.7	637.8	680.1	352.5	637.8	.1050
.95	76.000	6.10	50.796	214.472	62.818	255.788	113.614	80.7	1060.8	705.6	378.8	705.6	.1050
1.00	80.000	.00	56.440	.000	65.076	.000	121.516	89.6	infin	730.9	405.2	730.9	.1050

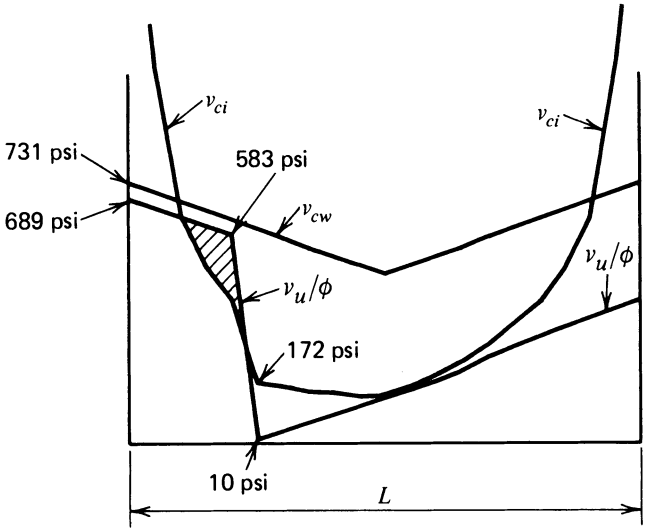

Fig. 6-10. Plot of the results of the analysis of a prestressed concrete beam supporting a concentrated live load of 100 k.

the configuration of the bridge itself. The superstructures as well as the substructures of curved bridges can be subjected to significant torsional moments from dead as well as from live loads simply because of their shape.

Uncracked concrete box girder sections can be analyzed for the effects of torsion using the membrane analogy (Timoshenko 1956) or by solving the equations of equilibrium (Oden 1967). For the section shown in Fig. 6-14a), shear flows, ϕ, exist as shown in Fig. 6-15 due to the torsional moment M_t. The equations for the web shear flows at sections B–B' through E–E' are:

$$\phi_6 = \phi_2 - \phi_1 \tag{6-15}$$

$$\phi_7 = \phi_3 - \phi_2 \tag{6-16}$$

$$\phi_8 = \phi_3 - \phi_4 \tag{6-17}$$

$$\phi_9 = \phi_4 - \phi_5 \tag{6-18}$$

Shear flow is equal to the product of the torsional shear stress and the wall thickness of the element at the location under consideration.

The relationship for the torsional couple is:

$$2\phi_1 A_1 + 2\phi_2 A_2 + 2\phi_3 A_3 + 2\phi_4 A_4 + 2\phi_5 A_5 = M_t \tag{6-19}$$

in which the notation is as defined in Fig. 6-14a, the areas are as defined in Fig. 6-14b, and M_t is the torsional moment applied to the member.

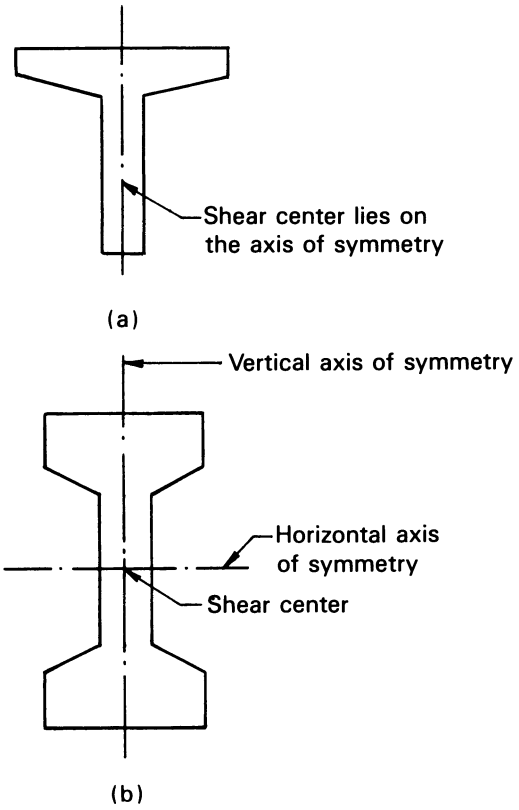

Fig. 6-11. Beam cross section illustrating the locations of shear centers. (a) Member with a single axis of symmetry. (b) Member having biaxial symmetry.

The relationships between the shear flows and the rate of twist θ, using the same notation from Fig. 6-14a, are:

$$\phi_1\left[\frac{B_1}{t_{b1}}+\frac{H_{01}}{t_{01}}+\frac{T_1}{t_{t1}}\right]-\phi_6\frac{H_{12}}{t_{12}}=2GA_1\theta \tag{6-20}$$

$$\phi_6\frac{H_{12}}{t_{12}}+\phi_2\left[\frac{B_2}{t_{b2}}+\frac{T_2}{t_{t2}}\right]-\phi_7\frac{H_{23}}{t_{23}}=2GA_2\theta \tag{6-21}$$

$$\phi_7\frac{H_{23}}{t_{23}}+\phi_3\left[\frac{B_3}{t_{b3}}+\frac{T_3}{t_{t3}}\right]-\phi_8\frac{H_{34}}{t_{34}}=2GA_3\theta \tag{6-22}$$

$$\phi_8\frac{H_{34}}{t_{34}}+\phi_4\left[\frac{B_4}{t_{b4}}+\frac{T_4}{t_{t4}}\right]-\phi_9\frac{H_{45}}{t_{45}}=2GA_4\theta \tag{6-23}$$

$$\phi_9\frac{H_{45}}{t_{45}}+\phi_5\left[\frac{B_5}{t_{65}}+\frac{T_5}{t_{65}}+\frac{H_{56}}{t_{56}}\right]=2GA_5\theta \tag{6-24}$$

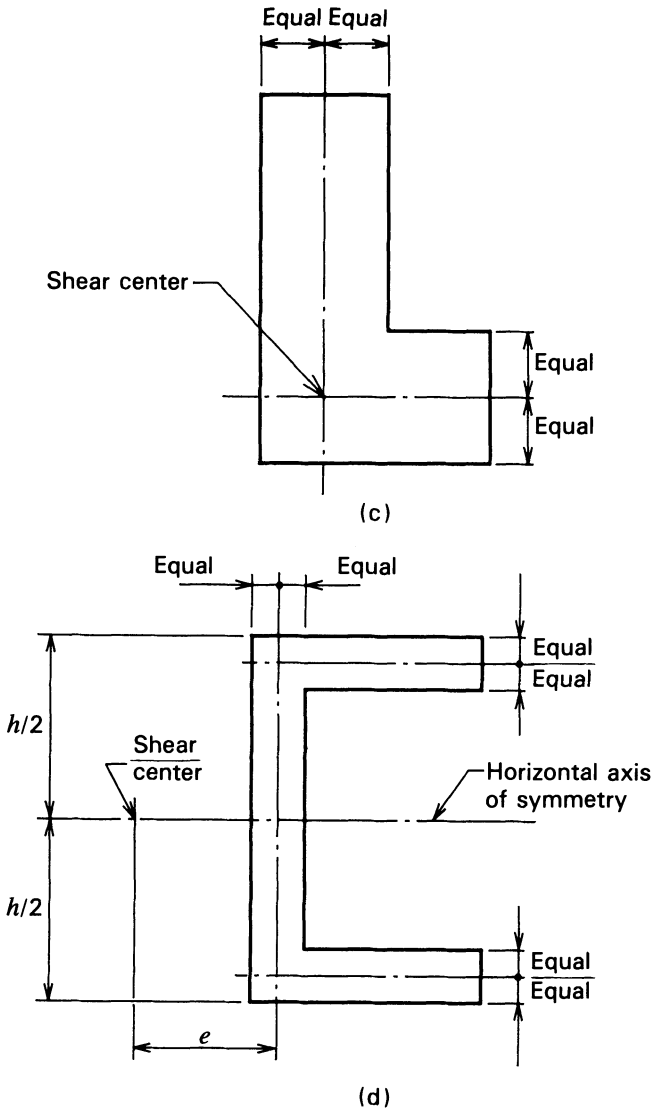

Fig. 6.11. (*Continued*) (c) Member not having symmetry. (d) Channel-shaped member having a single axis of symmetry.

It should be recognized that the terms representing the areas of the components of the section, such as B_1/t_{b1} in eqs. 6-20 through 6-24, must include the effect of variations in thickness for slabs and webs not having uniform thicknesses. The relationship between the rate of twist and the applied moment is:

$$\theta = \frac{M_t}{JG} \tag{6-25}$$

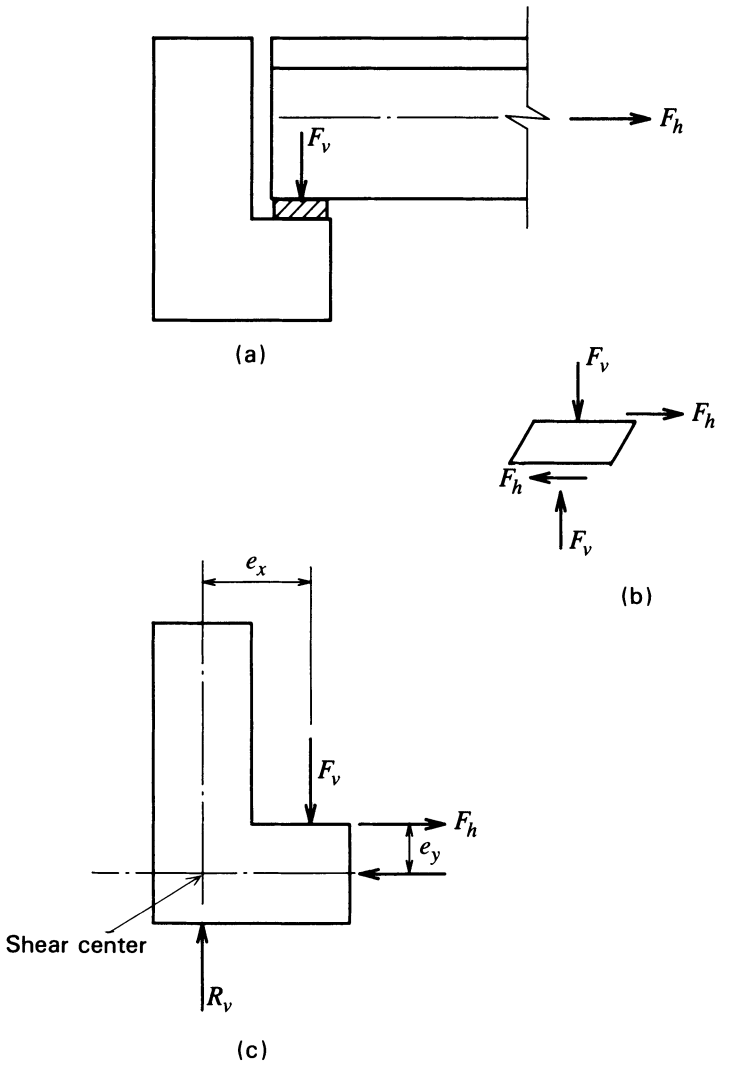

Fig. 6-12. L-shaped spandrel beam illustrating torsional moment due to vertical and horizontal forces. (a) L-shaped beam supporting a double-tee beam. (b) Freebody diagram of elastomeric bearing pad. (c) Freebody diagram of L-shaped spandrel beam.

In eqs. 6-20 through 6-25, G is the shear modulus of the concrete, J is the torsional constant for the box-girder cross section, and the other notation has been defined above. Solving these equations, one can determine the values of the shear flows and the torsional stresses in the components ($v_t = \phi/t$), as well as the value of the torsional constant. (The solution is facilitated by using a unit

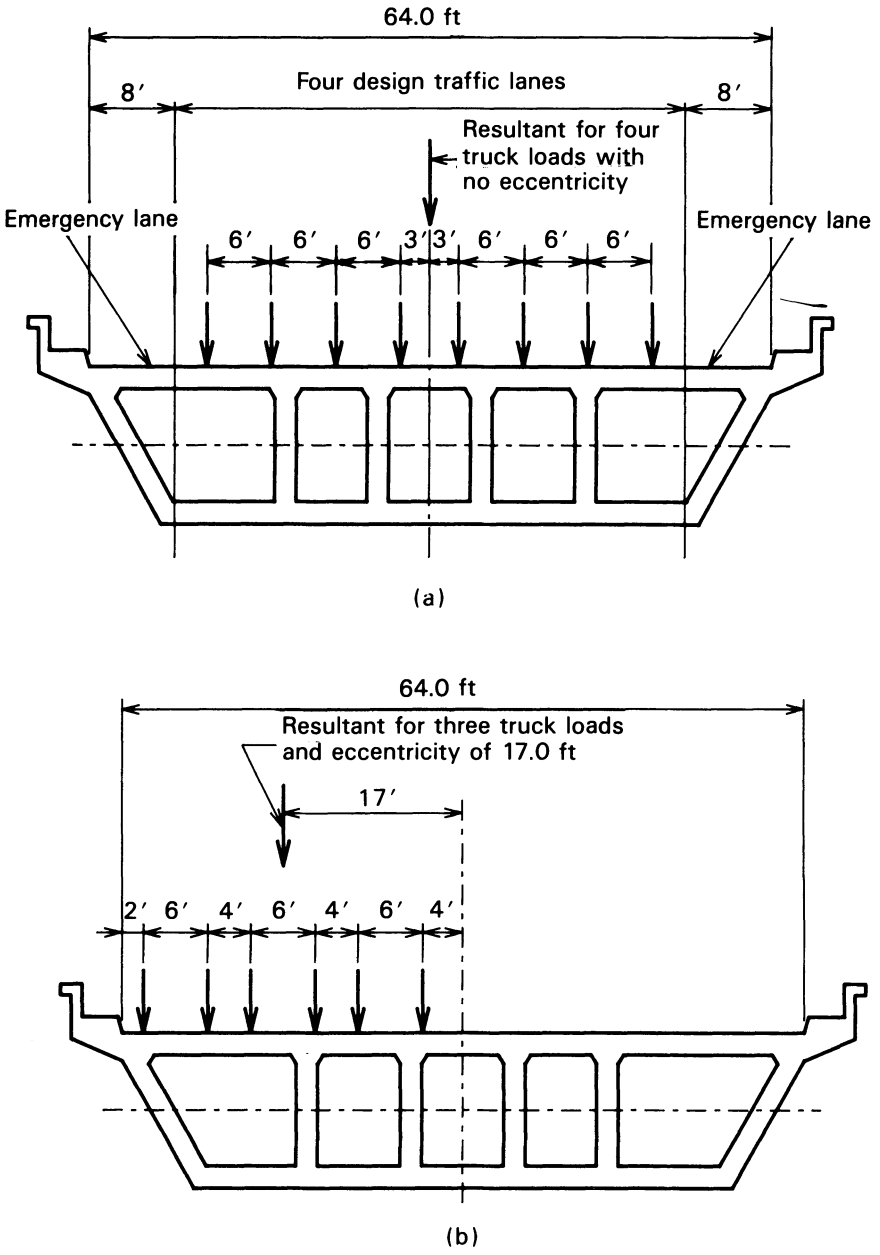

Fig. 6-13. Cross section of box-girder bridge illustrating loading conditions for maximum bending moment and maximum torsion. (a) Box-girder bridge with four lanes of concentric truck live load (no torsional moment). (b) Box-girder bridge with three lanes of eccentric truck live load (with torsional moment).

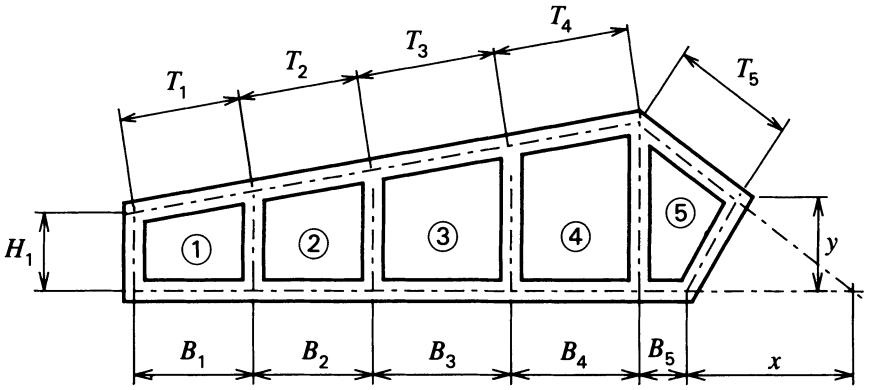

(a) Cross section of the closed section.

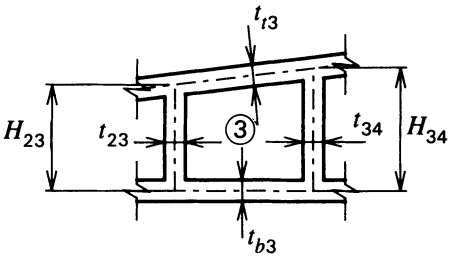

$$A_3 = \left[\frac{H_{23} + H_{34}}{2} \right] B_3$$

(b) Dimensions of cell 3.

Fig. 6-14. Cross section of a closed section and a detail of a panel of the member illustrating the terminology used in the analysis of shear flow. (a) Cross section of the member. (b) Definition of panel element dimensions.

torsional moment, i.e., substituting unity for M_t in eq. 6-25 and substituting $1/J$ for $G\theta$ in eqs. 6-20 through 6-24.) With these parameters known, one can determine the torsional moment that would be expected to cause cracking in a box-girder cross section.

In reinforced concrete members, relatively small torsional moments can be resisted by the uncracked concrete section. Larger torsional moments may cause the concrete section to crack. After cracking has occurred, the torsion must be resisted by a combination of transverse and longitudinal reinforcement, both of which are stressed in tension, and portions of the uncracked concrete section that act as compression struts. The cracked concrete member can be thought of as a three-dimensional, trusslike system, as illustrated in Fig. 6-16, that resists the torsion by axial tension and compression forces.

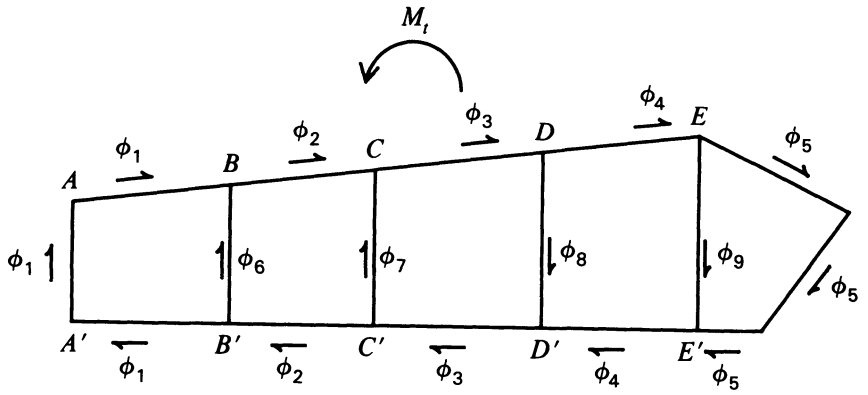

Fig. 6-15. Shear flows due to a torsional moment for the cross section shown in Fig. 6-14.

Under a torsional moment approaching the capacity of the member, the concrete cover over the reinforcement nearest the outer surface tends to spall off and can no longer be counted upon to anchor the transverse reinforcement or to serve as a part of the compression struts. Ducts for post-tensioned tendons located near the external surfaces of members subjected to high torsional moments can further decrease the thickness in the areas of the concrete section and adversely affect the compressive strength of the concrete struts. The hooks of the transverse reinforcement must extend around the longitudinal reinforcement and be anchored in the interior core of the member to be effective after the spalling (Collins and Mitchell 1980). Because of the loss of concrete cover and the reduction in area caused by post-tensioning ducts, the Canadian Standard requires the use of a reduced thickness of the concrete section in computing the torsional strength of concrete members subject to torsional moments that are greater than 25 percent of the torsional moment that would be expected to cause torsional cracking (CSA 1984).

Although ACI 318 (Secs. 11.3.1.4 and 11.6) contains provisions for the torsion design of concrete members with nonprestressed reinforcement, it does not contain similar provisions for members having prestressed reinforcement. Code provisions for the design of members with prestressed reinforcement are, however, contained in the standards of other countries, such as the Canadian building standard (CSA 1984). In addition, publications of trade associations, such as the Prestressed Concrete Institute (PCI 1985), contain guidance for the design of prestressed concrete members for torsion.

The reader's attention is called to the fact that in statically indeterminate structures redistribution of torsional moment can take place after concrete cracking has occurred. In statically determinate structures, however, and particularly those composed of precast members with connections that do not develop

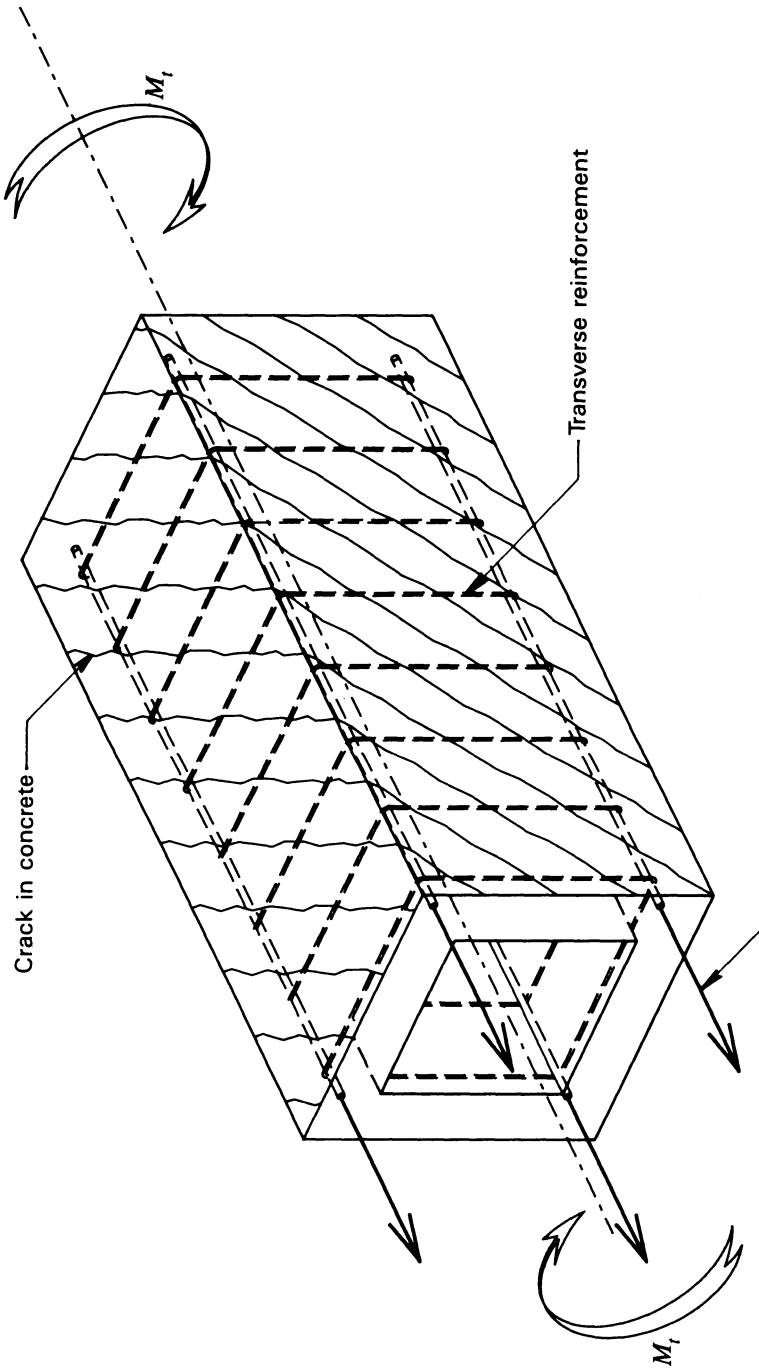

Fig. 6-16. Reinforced concrete box beam subjected to a torsional moment showing the locations of the concrete cracks, compression struts, transverse torsional shear stress reinforcement, and forces in the longitudinal reinforcement.

continuity, redistribution cannot take place (ACI 318 1983; ACI 318R 1983; CSA 1984).

6-5 Flexural Shear and Torsion Provisions of CAN-A23.3-M84

The Canadian standard *Design of Concrete Structures for Buildings*, unlike ACI 318, contains minimum design requirements for flexural shear and torsional moment for members with prestressed reinforcement as well as with nonprestressed reinforcement. The shear and torsion provisions in CSA 1984 are contained in the 11 sections of Clause 11. Five of these sections (11.0 Notation; 11.1 Scope; 11.2 General Requirements; 11.3 Shear and Torsion Design—Simplified Method; 11.4 Shear and Torsion Design—General Method) are reproduced herein, with the permission of the publisher, in Appendix D. The subclauses not reproduced herein include: 11.5 Special Provisions for Deep Shear Spans; 11.6 Special Provisions for Walls; 11.7 Shear Friction; 11.8 Special Provisions for Brackets and Corbels; 11.9 Transfer of Moments to Columns in Frames; and 11.10 Special Provisions for Slab and Footings. Also reproduced herein in Appendix D, with the permission of the publisher, are excerpts from *Explanatory Comments to Clause 11, Shear and Torsion*, (excluding those pertaining to Secs. 11-5 through 11.10) of CSA 1984.

The simplified method of shear design contained in Section 11.3 of CSA 1984 is based upon the provisions of ACI 318. It differs from ACI 318 in several respects, however, as it is intended for use with the *Systeme International* (SI) units of measure, it contains provisions for torsion, and so on. The general method of Section 11.4 is based upon the Compression Field Theory. The design professional using CSA 1984 may use either of the two methods.

(The reader is cautioned that the materials in Appendix D are written for use with SI units and are only a portion of the original document. Persons who wish to use the provisions of CAN3-A23.3-M84 in actual design should become familiar with all of its provisions and not rely solely upon the contents of Appendix D contained herein.)

The main provisions of the general method, converted to customary units, are presented in the following paragraphs of this section for the purpose of acquainting the reader with the code procedures that are being used in applying the Compression Field Theory in Canada. To simplify the following discussion, reference to the Canadian Standard will be indicated by CSA 1984 for the document as a whole, CSA eq. 11-2 for an equation from it, and CSA Sec. 11.2 for a subclause from the Canadian Standard.

The expression given in CSA 11.2.4.1 for the torsional moment resistance at cracking (CSA eq. 11-2), T_{cr}, for a prestressed concrete member is

$$T_{cr} = \frac{A_c^2}{p_c}(4.8\phi_c\lambda\sqrt{f'_c})\sqrt{1 + \frac{f_{pc}}{4.8\phi_c\lambda\sqrt{f'_c}}} \qquad (6\text{-}26)$$

in which A_c is the area within the outside perimeter of the concrete section without deducting the areas of holes or voids (sq. in.), p_c is the outside perimeter of the concrete section (in.), ϕ_c is the dimensionless strength reduction factor for concrete (see Sec. 5-6), λ is the factor to account for density of the concrete, and the remaining terms have been defined previously. The torsional cracking moment is expressed in inch-pounds. Torsional effects must be considered in the design if:

$$T_u > 0.25T_{cr} \tag{6-27}$$

where T_u is the design (factored) torsional moment.

It should be noted that the last term in eq. 6-26 contains the term f_{pc}, the compressive stress in the concrete at the centroid of the section due to the effective prestress, a term that is equal to zero for members that only have nonprestressed reinforcement. Hence, the last term in the eq. 6-26 is equal to one for members without prestressed reinforcement.

CSA Sec. 11.4.2 covers the requirements for the diagonal compressive stress in the concrete "struts." The diagonal compressive stress, f_2, must not exceed the maximum permissible value, $f_{2\max}$. This is expressed mathematically (CSA eq. 11-17) as:

$$f_2 \leq f_{2\max} \tag{6-28}$$

where (CSA eq. 11-19):

$$f_{2\max} = \frac{\lambda\phi_c f'_c}{0.8 + 170\epsilon_1} \leq \phi_c f'_c \tag{6-29}$$

in which ϵ_1 is the principal tensile strain in the cracked concrete due to design (factored) loads. If the concrete is triaxially confined, $f_{2\max}$ is permitted to exceed $\phi_c f'_c$.

In eq. 6-29 (CSA eq. 11-19), the terms ϵ_1 may be taken to be:

$$\epsilon_1 = \epsilon_x + \frac{\epsilon_x + 0.002}{\tan^2 \theta} \tag{6-30}$$

The relationships given above in eqs. 6-29, and 6-30 can better be understood by considering the free body of a portion of a beam that is subject to nearly uniform shear stress over the effective shear depth (d_v) as illustrated in Fig. 6-17. The angle θ is the angle of inclination of the compression struts measured from the longitudinal axis of the member. The strains in the concrete web of the beam in Fig. 6-17 are illustrated in Fig. 6-18 and, from the Mohr's circle for strain given in Fig. 6-19, it will be seen that the following relationships for $\tan \theta$ can be written:

$$\tan \theta = \frac{\epsilon_x - \epsilon_2}{y}$$

$$\tan \theta = \frac{y}{\epsilon_1 - \epsilon_x}$$

Equating these relationships and eliminating the term y, the following is obtained:

$$\epsilon_1 = \epsilon_x + \frac{\epsilon_x - \epsilon_2}{\tan^2 \theta}$$

Setting the limiting compressive strain, ϵ_2, to -0.002, the relationship given above as eq. 6-30 is obtained. The relationship given above as eq. 6-29, which was determined experimentally, relates the principal compressive stress in a strut, $f_{2,\max}$, to the principal tensile strain, ϵ_1.

The relationship for f_2, the compressive stress in the concrete strut is:

$$f_2 = \left(\tan \theta + \frac{1}{\tan \theta}\right)\left(\frac{V_u}{b_v d_v}\right) \qquad (6\text{-}31)$$

in which θ is the angle of inclination of the concrete compressive stress (struts) measured in degrees from the longitudinal axis of the member (see discussion of θ below), and V_u is the design (factored) shear force with d_v *the minimum effective shear depth* and b_v *the minimum effective web width* within the depth d_v. The effective shear depth, d_v, can be taken as the distance, measured perpendicular to the neutral axis, between the resultants to the tensile and compressive

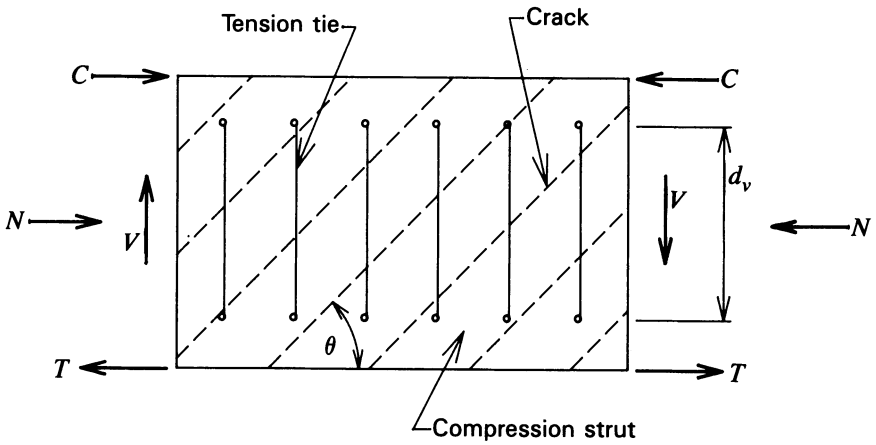

Fig. 6-17. Freebody diagram of beam web subjected to uniform shear stress.

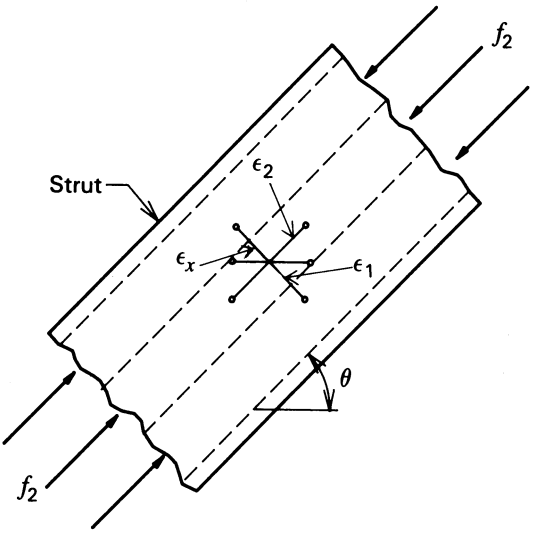

Fig. 6-18. Freebody diagram illustrating the stress in the compression strut, f_2, the angle of inclination of the compression strut, θ, and the strains ϵ_1, ϵ_2, and ϵ_x.

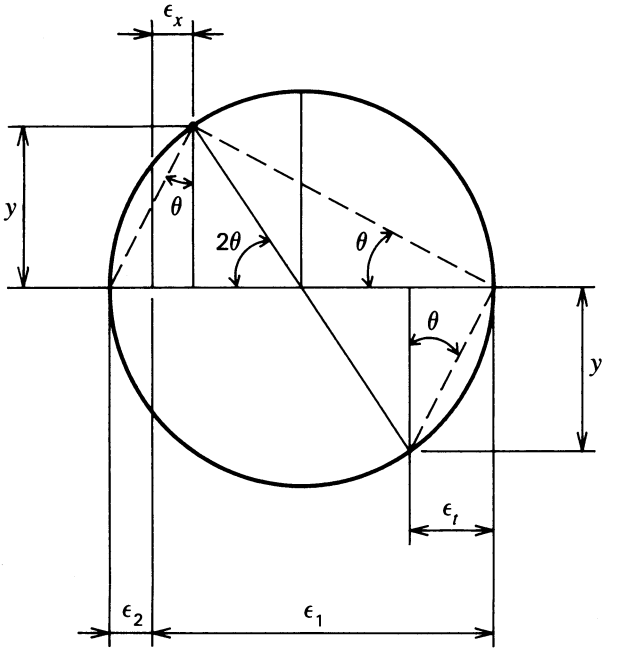

Fig. 6-19. Mohr's circle for strain at the middepth of a beam web.

forces due to flexure (inches), but does not need to be taken less than $0.9d$. The symbol d represents the distance from the extreme compression fiber to the centroid of the longitudinal tension reinforcement, but not less than 0.8 times the overall height of the member (inches). (Therefore, the minimum value of d_v is $0.72d$.) The last term in eq. 6-31, $V_u/b_v d_v$, should be replaced with:

$$\frac{V_u - \phi_p V_p}{b_v d_v}$$

for members that have variable depth or inclined prestressed reinforcement; or with:

$$\frac{V_u - \phi_s A_{vi} d \cos \alpha / s}{b_v d_v}$$

for members with inclined stirrups used as shear reinforcement, but the term may not be taken to be less than $0.66V_u$ or:

$$\frac{V_u}{b_v d_v} + \frac{T_u p_h}{A_{oh}^2}$$

if torsional reinforcement is required. In these expressions A_{oh} is the concrete area section enclosed by the centerline of exterior closed transverse torsion reinforcement including areas of holes, if any, A_{vi} is the cross sectional area of inclined shear reinforcement within the distance s, α is the angle, in degrees, between the inclined stirrups or bent-up bars and the longitudinal axis of the member, and p_h is the perimeter of the centerline of the closed transverse torsion reinforcement.

In using the Compression Field Theory, the designer selects a value of θ, the angle of the inclination of the concrete compressive stresses. The value selected affects the amount of transverse (shear) reinforcement needed as well as the amount of the longitudinal reinforcement required. Small values of θ (less than 45°) will result in less transverse reinforcement but more longitudinal reinforcement than would be required if θ were taken to be 45°. Values of θ greater than 45° will result in greater amounts of transverse reinforcement being required.

The minimum value of θ that can be used is controlled by eq. 6-28. Values of θ less than the minimum value will result in diagonal compression stresses greater than the maximum value permitted by eq. 6-28. Figure 6-20, which is based upon Fig. D7 (see Appendix D herein) of CSA 1984, is useful in assisting the designer in selecting the minimum value of θ that can be used in a particular design. Figure 6-20 illustrates the relationship between the shear stress ratio and the angle θ, for limiting values of longitudinal strain at mid-depth, ϵ_x, of zero and 0.002 (tension). In addition, the limiting values of tensile strain in the

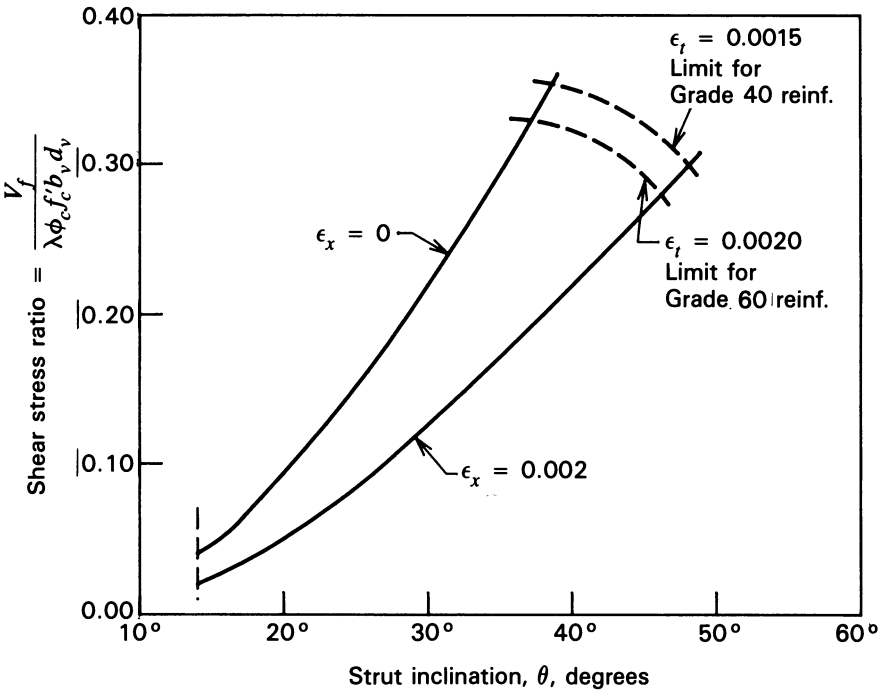

Fig. 6-20. Diagram showing the relationship between the angle θ, at which $f_2 = f_{2max}$, and the shear stress ratio. (Based upon Fig. D7 of CSA 1984.)

transverse reinforcement, ϵ_t, for Grades 40 and 60 reinforcement, are shown as upper limits. The ordinate of Fig. D7 in Appendix D, the shear ratio, should include the effects of stresses from the vertical component of prestressing, variable depth (see Sec. 6-3), and torsion, if applicable, rather than the design (factored) shear force alone.

Whatever value of θ is selected, it must be used throughout the analysis. CSA Sec. 11.4.2.6 provides that the value of θ must not be less than 15° or more than 75°. The designer may elect to select a low value of θ because it causes a reduction in the amount of transverse reinforcement, coupled with an increase in the longitudinal reinforcement, and thereby obtain an economical design.

Spalling of the concrete from the centerline of the outermost layer of reinforcement to the exterior surface of the concrete must be assumed in the design computations of b_v, by CSA Sec. 11.4.2.7, if:

$$V_u \geq \lambda\phi_c\sqrt{f'_c}\, b_w d \tag{6-32}$$

in which b_w is the width of the web, or if torsional reinforcement is required. In addition, in computing b_v, one-half the diameter of grouted ducts for post-tensioned tendons and the full diameter of the ducts for unbonded post tensioned

tendons must be deducted from the web thickness to determine the value of b_v. The purpose of this provision is, of course, to obtain the minimum width of the concrete section of the compressive struts for use in computing f_2. In hollow sections subjected to torsion, according to CSA Sec. 11.4.2.12, the wall thickness is considered adequate if the distance from the centerline of the outermost layer of transverse torsional reinforcement to the inside face of the wall exceeds $1.5a_o$. The thickness of the torsional depth, a_o, in inches, is determined from:

$$a_o = \frac{A_{oh}}{p_h}\left[1 + \sqrt{1 - \frac{T_u p_h}{0.7\phi_c f_c A_{oh}^2}\left(\tan\theta + \frac{1}{\tan\theta}\right)}\right] \qquad (6\text{-}33)$$

CSA Sec. 11.4.3 addresses concerns regarding the yielding of the transverse (shear and torsional) reinforcement. The transverse reinforcement must yield before the concrete crushes in order to assure a more ductile behavior. Yielding can be considered to occur before crushing of the concrete if the strain in the transverse reinforcement, ϵ_t, is greater than the strain at the yield strength of the reinforcement. This is expressed as:

$$\epsilon_1 > \frac{f_y}{E_s} \qquad (6\text{-}34)$$

(The yield strains, ϵ_t, are 0.0014 and 0.0021 for Grades 40 and 60 reinforcements are based upon the guaranteed minimum yield strengths and an elastic modulus of 29,000 ksi, respectively.) For transverse reinforcement perpendicular to the axis of the member, ϵ_t can be computed from (CSA eq. 11-22):

$$\epsilon_t = \epsilon_1 - \epsilon_x - 0.002 \qquad (6\text{-}35)$$

Equation 6-35 can be derived using the notation in Fig. 6-21 and the Mohr's circle for strain in Fig. 6-22. Using a value of $\epsilon_x = 0.002$, as provided in CSA Sec. 11.4.2.5, results in $\epsilon_t = \epsilon_1 - 0.004$. For inclined transverse reinforcement:

$$\epsilon_t = 0.5(\epsilon_1 - 0.002) - 0.5(\epsilon_1 + 0.002)\cos 2(\theta + \alpha) \qquad (6\text{-}36)$$

The CSA provisions for the design of transverse (shear and torsion) reinforcement are given in CSA 11.4.4. The basic requirement is that the amount of transverse reinforcement provided will equal or be greater than the sum of the amounts required for coexisting shear and torsion. This can be expressed as:

$$A_{vst} \geq A_v + A_t \qquad (6\text{-}37)$$

where A_{vst} is the sum of the areas of the transverse reinforcement required for flexural shear, A_v, and torsion, A_t, both of which are defined in the following discussions. The factored shear resistance (strength) of the member, V_r, must equal or exceed the minimum required strength, V_u, or:

$$V_r \geq V_u \qquad (6\text{-}38)$$

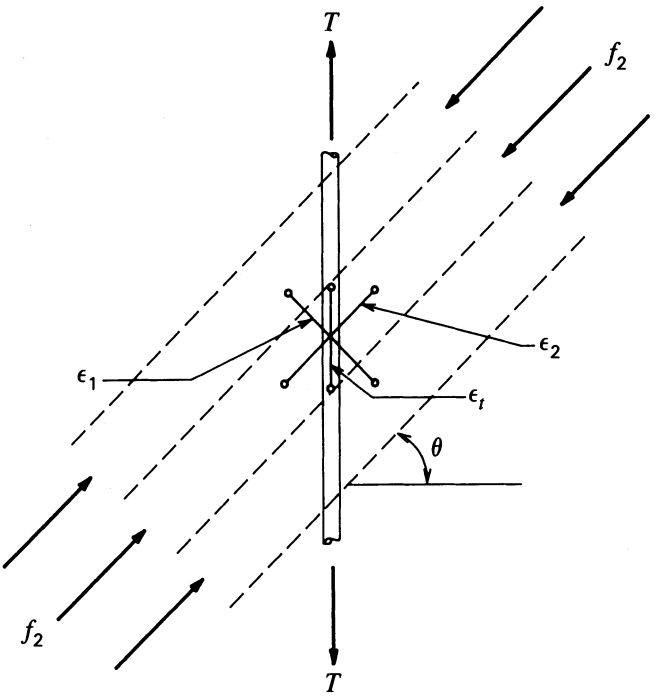

Fig. 6-21. Freebody diagram illustrating the stress in the compression strut, f_2, and the strains ϵ_1, ϵ_2, and ϵ_t.

The factored shear resistance for members not having transverse reinforcement inclined to the axis of the member is:

$$V_r = \frac{\phi_s A_v f_y}{s} \frac{d_v}{\tan \theta} + \phi_p V_p \qquad (6\text{-}39)$$

in which A_v is the area of the transverse reinforcement perpendicular to the axis of the member within a length s, in inches, along the axis of the member.

For members with nonprestressed reinforcement and having inclined transverse reinforcement (see CSA Secs. 11.4.4.4 and 11.4.4.5), eq. 6-39 becomes:

$$V_r = \frac{\phi_s A_v f_y}{s} \frac{d_v}{\tan \theta} + \frac{\phi_s A_{vi} f_y}{s} d_v \left(\frac{\sin \alpha}{\tan \theta} + \cos \alpha \right) + \phi_p V_p \qquad (6\text{-}40)$$

The factored torsional resistance of members with prestressed and nonprestressed reinforcement must be designed in such a way that the torsional resistance equals or exceeds the minimum required torsional moment. This relationship is expressed as:

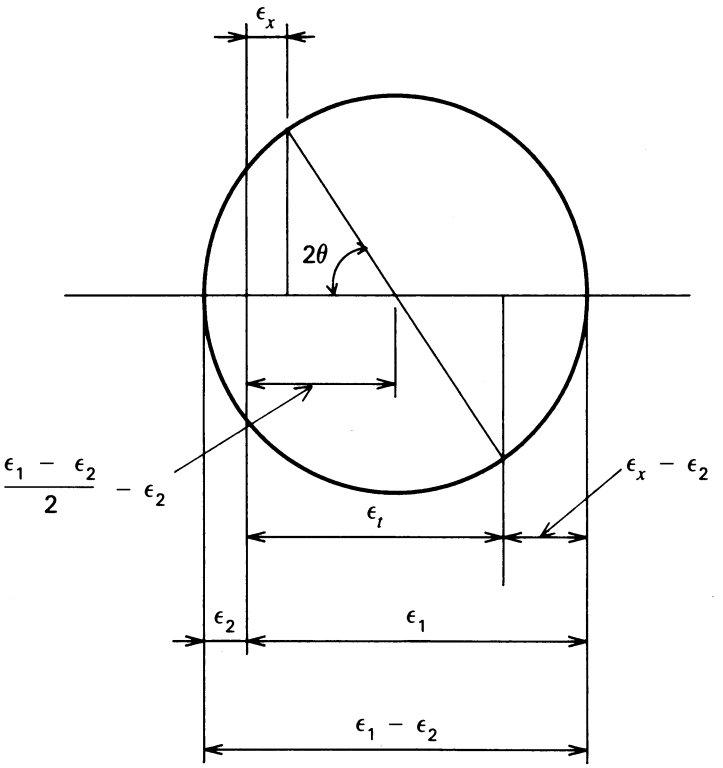

Fig. 6-22. Mohr's circle for strain.

$$T_r \geq T_u \tag{6-41}$$

in which the factored torsional resistance, T_r, is equal to:

$$T_r = \frac{\phi_s A_t f_y}{s} \frac{2A_o}{\tan \theta} \tag{6-42}$$

where

$$A_o = A_{oh} - \frac{a_o p_h}{2} \tag{6-43}$$

a_o is as defined in eq. 6-33 and A_t is the area of one leg of a closed transverse reinforcement (stirrup or tie) within a distance s.

The spacing limitations for shear and torsional reinforcement, which are found in CSA Sec. 11.4.5, provide that the spacing, s, for shear reinforcement placed perpendicular to the axis of the member shall not exceed the least of d_v, 24 in., or $d_v/3 \tan \theta$, and, the spacing, s, for torsional reinforcement placed perpen-

dicular to the axis of the member shall not exceed $p_h/8 \tan \theta$. See CSA Sec. 11.5.2 for the spacing provisions when inclined transverse reinforcement is used.

The longitudinal reinforcement is to be designed to provide flexural and axial load resistances that equal or exceed the minimum required flexural strength and axial load using classical methods (the strength reduction factors are included in the resistance computations using the CSA procedures). Reduced nominal strengths, ϕM_n and ϕP_n, as are commonly used with ACI procedures, are not used with the CSA procedures. In addition, the design must include a tensile load, N_v, acting at mid-depth of the member, to account for the additional axial force that results from the use of values for the angle, θ, of diagonal cracking other than 45°. For members not subjected to significant torsional moment, the value of the axial force is computed from:

$$N_v = \frac{V_u}{\tan \theta} \tag{6-44}$$

and for members for which torsion must be considered, the axial force is computed from:

$$N_v = \frac{1}{\tan \theta} \sqrt{V_u^2 + \left(\frac{T_u p_o}{2A_o}\right)^2} \tag{6-45}$$

The value of V_u can be reduced by the amount ϕV_p in eqs. 6-44 and 6-45 for members having variable depth or inclined prestressing tendons. The term p_o in eq. 6-45 is equal to $p_n - 4a_o$. For members having inclined shear reinforcement for use as shear reinforcement, the term V_u in eqs. 6-44 and 6-45 can be reduced by the amount:

$$\frac{\phi_s A_{vi} f_y d_v \cos \alpha}{s}$$

but the reduced term must not be taken to be less than $0.66V_u$.

Because the values of the design shear force and the design torsion normally vary along the length of a flexural member, the values of N_v computed with eqs. 6-44 and 6-45 also will vary along the length of the member. (See Fig. D11 in Appendix D.)

For members having axial compressive forces, P_u that exceed the design load causing balanced strain conditions (ACI 318, Sec. 10.3.2 and CSA Sec. 10.3.2), the flexural strength of the section must equal or exceed M_u with a concomitant axial load equal to the sum of P_u and N_v from eqs. 6-44 and 6-45.

The provisions in Section 11.4.7 of CSA 1984 apply to the evaluation of disturbed areas when the Compression Field theory is being used. Disturbed areas are defined as regions having abrupt changes in cross-sectional dimensions or forces such as concentrated loads and reactions. Examples of disturbed areas

are given in Figs. 6-2, 6-28, 6-29, as well as in Figs. D12, D13, D15, and D17 in Appendix D. Disturbed areas also are defined as regions where it is inappropriate to assume that shear stresses are uniformly distributed over the effective shear depth.

The analysis of disturbed areas can involve the investigation of the stresses in the concrete struts, the reinforced concrete ties, and the nodal zones of an imaginary two- or three-dimensional truss or truss-like system. The compressive stress in the concrete struts must not exceed $f_{2\max}$ (eq. 6-29) with the value of ϵ_1 (eq. 6-30) reflecting the conditions of strain of the concrete and reinforcement in the vicinity of the strut. As is the case in investigating the value of $f_{2\max}$ in struts in undisturbed areas, a value of -0.002 can conservatively be used for the maximum compressive strain, ϵ_2, in computing the value of ϵ_1. The maximum stress in the tension ties must not exceed the yield strength of the reinforcement used in the ties, and, of course, as is the case with all trusses, the struts and ties must be connected to the nodal zones (connections of the truss) by bond, hooks, bearing plates, or other types of connection devices.

Four conditions of confinement of the concrete in the nodal zones are possible. One of these is the case where a nodal zone is bounded by two compressive struts and bearing areas (i.e., the nodal zone concrete is subjected to biaxial compressive stresses). Another is the case where a single tension tie is anchored in a nodal zone. A third is the case where more than one tension tie is anchored in the nodal zone. The allowable concrete stresses in the nodal zones for these three conditions of stress in the nodal zones are $0.85\phi_c f'_c$, $0.75\phi_c f'_c$, and $0.60\phi_c f'_c$, respectively (see Fig. 6-2). The fourth possible condition of confinement at a nodal zone can exist in a three-dimensional structure where a node is triaxially confined by struts or reinforcement. A specific value is not given in CSA 1984 for the maximum permissible stress for the fourth condition and, owing to the complexity of establishing such a value, it is believed the only reliable way to do so would be by experimentation. Compliance with the stress limits in the nodal zones is considered to exist if: the compressive stresses in the struts bearing against a nodal zone do not exceed the maximum values for nodal zone compressive stresses listed above; the bearing stresses due to supports or concentrated loads at a nodal zone do not exceed the maximum values for nodal zone compressive stresses listed above; and the effective stress due to tension tie loads at a nodal zone does not exceed the allowable nodal zone compressive stresses listed above. The effective stress due to a tension tie is computed by using the concrete area within an imaginary line surrounding the tension tie reinforcement, with the further requirement that the centroidal axes of the tension tie reinforcement and the effective concrete area must be coincident.

CSA 11.4.8 contains provisions intended to control diagonal cracking in flexural members. The provisions are applicable in members in which the shear

force due to service loads exceed the force, V_{cr}, that will cause diagonal cracking. For members not required to be designed for torsion, that is $T_u \leq 0.25T_{cr}$, one may assume that diagonal cracking is adequately controlled if the spacing of the transverse reinforcement does not exceed 12 in. and the required (factored) shear force does not exceed $7.2\phi_c \sqrt{f'_c} b_w d$. Alternatively, diagonal cracking may be assumed to be adequately controlled if: the spacing of the transverse reinforcement does not exceed 12 in.; the spacing of the longitudinal reinforcement along the sides of the member does not exceed 12 in.; and either the calculated strain in the transverse reinforcement under service loads does not exceed 0.0010 for interior exposure or 0.0008 for exterior exposure, or the value of f_y used in calculating the required amount of transverse reinforcement is taken to be equal to or less than 43.5 ksi. The strain in the transverse reinforcement under service loads can be computed from:

$$\epsilon_{sl} = \left[\frac{V_{sl}s}{A_v E_s d_v} + \frac{T_{sl}s}{1.6A_t E_s A_{oh}}\right]\left[\left(1 - \frac{f_y}{200}\frac{f_{pc}}{f'_c}\right)\tan\theta\right]^2 \times \left[1 - \left(\frac{V_{cr}}{V_{sl}}\right)^3\right] \tag{6-46}$$

in which V_{sl} and T_{sl} are the shear force and torsion due to service loads, respectively, and A_v and A_t are the areas of the transverse reinforcement provided for shear and torsion, respectively. The shear force at cracking for members not subject to torsion or axial tension, V_{cr}, can be determined from:

$$V_{cr} = 2.4\lambda\sqrt{f'_c}\left(\sqrt{1 + \frac{f_{pc}}{4.8\lambda\sqrt{f'_c}}}\right)b_w d + \theta_p V_p \tag{6-47}$$

If the member is subjected to torsion, eq. 6-47 should be divided by:

$$\sqrt{1 + \left(\frac{p_c b_w d}{2A_o^2}\frac{T_{sl}}{V_{sl}}\right)^2} \tag{6-48}$$

and if the member is subject to a service load axial tension, N_{sl}, the term f_{pc} in eq. 6-47 should be replaced with the term $(f_{pc} - (N_{sl}/A_g))$, in which A_g is the gross area of the concrete section. The second term in eq. 6-46 is provided to estimate the direction of the principal compressive stress at service load, and the third term in the equation is intended to make an allowance for the influence of the tensile stresses in the cracked concrete (tension stiffening).

This summary of the provisions of the CSA provisions for the design for shear and torsion is incomplete. The excerpts from the CSA standard in Appendix D should be consulted for exact wording and more details. Before one uses the provisions of the CSA standard, the complete document should be consulted.

ILLUSTRATIVE PROBLEM 6-5 Investigate the single-tee beam shown in Fig. 6-23 for transverse and longitudinal reinforcement requirements using the general method in Chapter 11 of CSA 1984. The service dead and live loads are 594 and 600 plf, respectively, and the member is not subject to torsion. Use the load and strength reduction factors contained in Chapter 9 of CSA 1984 as described in Sec. 5-6 herein. Assume that the concrete cover to the transverse reinforcement is 1.5 in., the specified concrete strength is 3000 psi, and the concrete is normal weight (i.e., $\lambda = 1$). The gross area of the concrete section is 570 sq. in., the moment of inertia of the section is 68,917 in.^{4}, and, the centroid of the concrete section is 9.99 in. measured from the top of the section. Assume that the member is prestressed with an effective prestressing force (after losses) of 173.5 kips, the beam has a simple span of 60 ft, and the effective depth, d_p, which varies linearly between midspan and the ends of the member, is 32.86 in. and 30.93 in., at midspan and at the supports, respectively.

SOLUTION: The loads are:

	Service	*Design*
Dead Load	594 plf × 1.25 =	743 plf
Live Load	600 plf × 1.5 =	900 plf
Total	1194 plf	1643 plf

The design shear force at the ends of the member equal

$$V_u = 1643 \times 30 = 49{,}290 \text{ plf}$$

and because, with $d = 30.93$ in. ($> 0.80h$) at the supports,

$$\lambda\phi_c\sqrt{f'_c}b_w d = 1 \times 0.60\sqrt{3000} \times 8 \times 33 = 8676 \text{ lb} < V_u$$

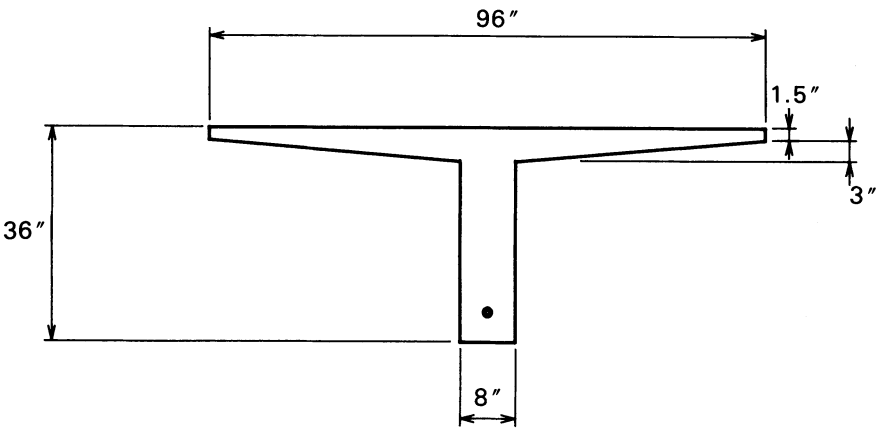

Fig. 6-23. T-shaped beam used in I.P. 6-5.

spalling must be considered. The vertical component of the prestressing force is:

$$V_p = \frac{(32.86 - 30.93) \times 173.5}{30 \times 12} = 0.93 \text{ kips}$$

and

$$\phi_p V_p = 0.90 \times 0.93 = 0.84 \text{ kips}$$

Assuming the transverse reinforcement to have a diameter of 0.5 in. and a concrete cover of 1.5 in., the effective shear width, $b_v = 8.00 - (2 \times 1.50 + 0.50) = 4.50$ in. The minimum value of the effective shear depth, d_v, permitted to be used in the calculations can be calculated as $0.72h$ which is equal to 25.92 in. At midspan, assuming $A_{ps}f_{ps}$ is equal to 173.5 kips/0.58 or approximately 300 kips, the distance between the resultants of the tensile and compressive forces can be taken as $32.86 - 300/0.85 \times 3 \times 96 = 32.25$ in. and, at the support, the effective shear depth can be taken as $0.90 \times 30.93 = 27.84$ in. Hence, d_p could be assumed to vary linearly from 27.84 in at the support to 32.25 in at midspan. To facilitate the computations, d is conservatively taken to be 27.84 in. throughout the length of the member. Therefore, the shear stress, including the effect of the prestressing, is computed to be:

$$\frac{V_u - \phi_p V_p}{b_v d_v} = \frac{49{,}290 - 840}{4.5 \times 27.84} = 387 \text{ psi}$$

and the shear stress ratio, for use in Fig. D7 in the CSA Appendix D, is found to be:

$$\frac{387}{0.60 \times 3000} = 0.215$$

The shear stress ratio should be used to determine the value of the angle of the principal compressive stress, θ, that results in $f_2 = f_{2\max}$ using Fig. D7 of Appendix D of CSA 1984. As explained by Collins and Mitchell, diagonal crushing is avoided because the diagonal compressive stress is less than the diagonal compressive strength if the angle selected is greater than those defined by the appropriate curve in Fig. D7 (Collins and Mitchell 1987). Using 0.215 for the shear stress ratio, the minimum value of θ that should be used is estimated to be 38°. Adopting a value of 40° for θ, the computations for the compressive stress in the concrete struts becomes:

$$f_2 = 387 \left(\tan 40° + \frac{1}{\tan 40°} \right) = 783 \text{ psi}$$

$$e_1 = 0.002 + \frac{0.004}{\tan 40°} = 0.00768$$

$$f_{2\max} = \frac{1 \times 0.60 \times 3000}{0.80 + 170 \times 0.00768} = 855 \text{ psi}$$

Forty degrees will be used for θ in the subsequent calculations because $f_2 < f_{2\max}$. The factored shear resistance provided by the transverse reinforcement and the vertical component of the prestressing force, using Grade 60 transverse reinforcement spaced at 12 in. on centers, is computed as:

$$V_n = \frac{0.85 \times 60 A_v}{12} \times \frac{22.84}{\tan 40°} + 0.90 \times 0.93 = 141 A_v + 0.84 \text{ kips}$$

and the maximum amount of transverse reinforcement is needed at a distance of $d_v/\tan\theta$ ($27.84/\tan 40° = 33.2$ in.) from the support. The shear force at this location is equal to

$$\frac{(49.29)(360 - 33.2)}{360} = 44.74 \text{ kips}$$

and the maximum area of shear reinforcement needed is $44.74/141 = 0.32$ sq. in. per foot of length or No. 3 stirrups spaced 8.5 in. on centers. The amounts of reinforcement needed at various distances from the supports are summarized in Table 6-4.

The minimum area of shear reinforcement computed with CSA eq. 11-3 is 0.045 sq. in. per foot and the maximum spacing is $0.75 \times 36 = 27$ in. The area of No. 3 U-shaped stirrups at the maximum spacing is 0.098 sq. in. per foot. The spacing adopted for No. 3 stirrups is shown in Fig. 6-24.

The design is completed by determining the axial force for which longitudinal

TABLE 6-4 Amounts of Shear Reinforcement Required at Various Locations in the Beam Analyzed in I.P. 6-5.

Distance from Support (in.)	Area required (sq. in.)
0.00	0.32
33.2	0.32
168.0	0.19
276.0	0.08
360.0	0.00

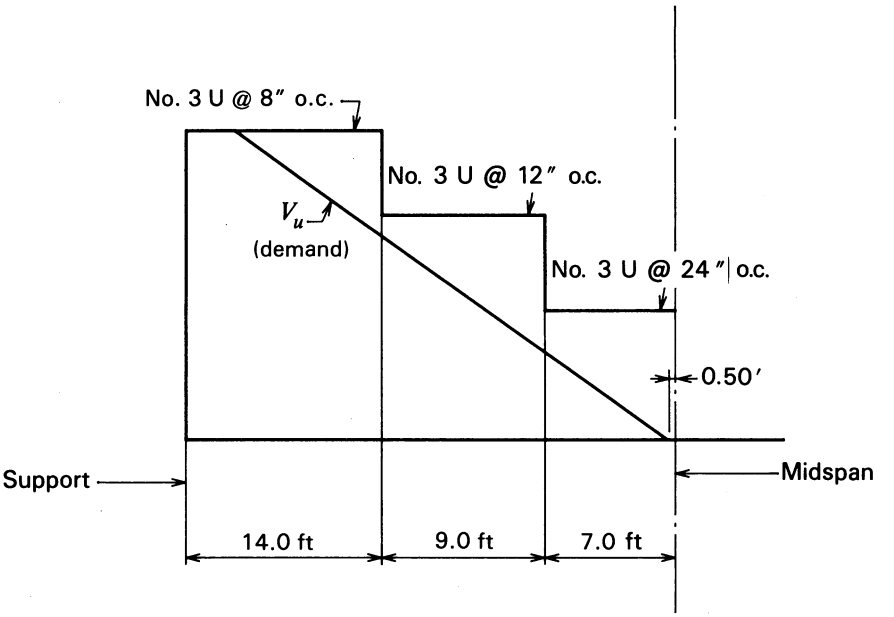

Fig. 6-24. Spacing of no. 3 U-shaped stirrups for I.P. 6-5.

reinforcement, in addition to that required for flexure, must be provided. This force is computed as follows:

$$N_v = \frac{V_u - \phi_p V_p}{\tan \theta} = \frac{49.29 - 0.84}{0.839} = 57.7 \text{ kips}$$

This axial tensile force can be resisted by the prestressed reinforcement, if the amount provided is sufficient for both the flexural requirements and the axial force, by supplementing the amount of prestressed reinforcement, or by providing Grade 60, nonprestressed reinforcement in the amount of 57.7/60 = 0.96 sq. in.

ILLUSTRATIVE PROBLEM 6-6 Determine the shear, torsional, and axial longitudinal reinforcements required for a spandrel beam having the cross section shown in Fig. 6-25 if the span of the beam is 36 ft, the applied service dead and live loads, P_{DL} and P_{LL}, are 6.0 and 5.0 kips, respectively, and the loads are applied with an eccentricity of 10 in. and with a spacing of 4 ft on centers commencing 2 ft from the supports. The specified concrete compressive strength is 4000 psi and the yield strength of the nonprestressed reinforcement is 60 ksi. The flexural reinforcement consists of four straight ($V_p = 0$) seven-wire prestressed strands having an effective prestress of 24.78 kips per strand with their centroid located 2.75 in. above the soffit of the beam. The gross area of

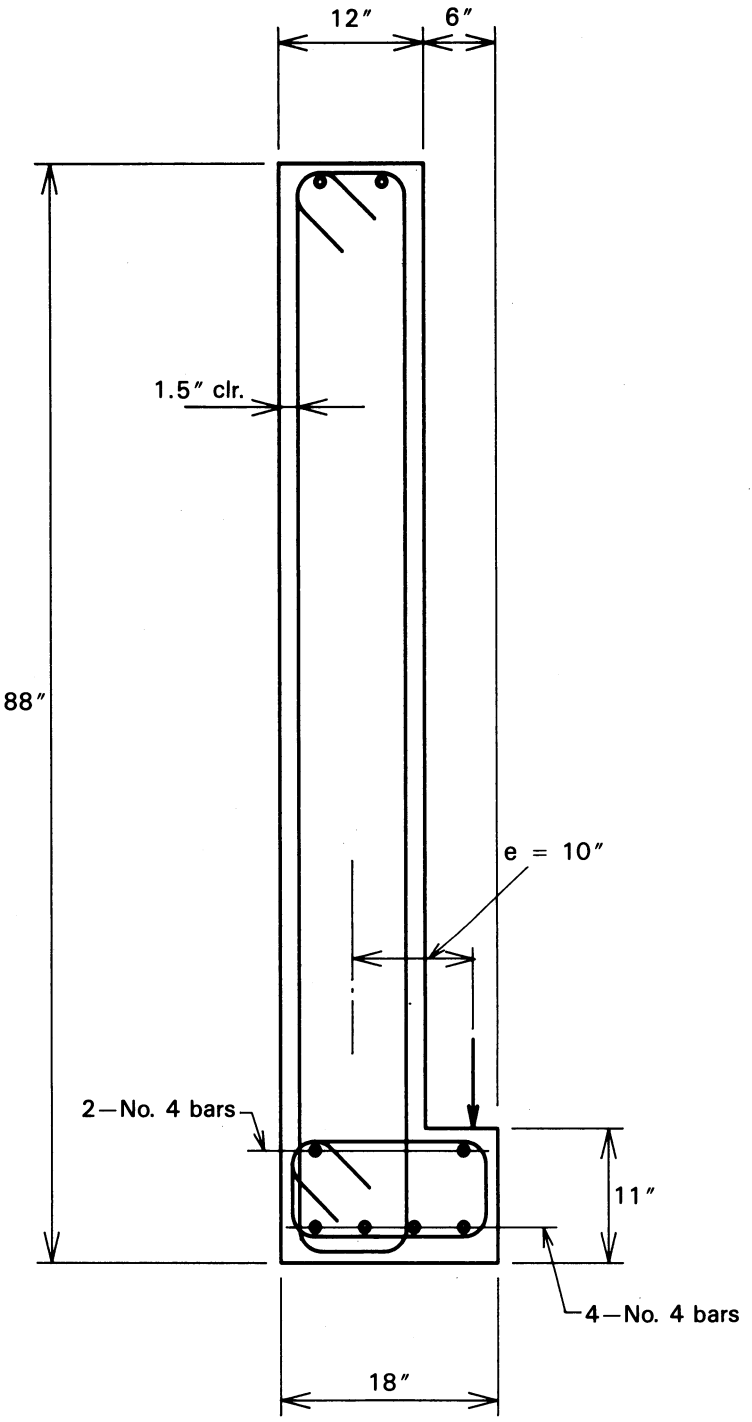

Fig. 6-25. Cross section of the spandrel beam for I.P. 6-6.

the concrete section (A_c in CSA) is equal to 1122 in.^{2}, the moment of inertia is 797,000 in.^{4}, and the centroid of the concrete section is located 46.26 in. from the top fiber. The concrete is normal weight, and the beam service dead load is 1.17 klf. Use the strength reduction and load factors contained in CSA 1984 as described in Sec. 5-6 herein. Use a concrete cover of 1.5 in. and use No. 4 bars for the transverse reinforcement.

SOLUTION: The design dead load of the beam is $1.17 \times 1.25 = 1.46$ klf. The design concentrated dead and live loads, of which there is a total of 9, are equal to $1.25 \times 6 = 7.5$ and $1.50 \times 5 = 7.5$ kips, respectively. Other dimensions and parameters needed in the analysis include the following:

$$d_p = 88.00 - 2.75 = 85.25 \text{ in.}$$

$$d_v = 0.90 \times 85.25 = 76.7 \text{ in.}$$

$$b_w = 12 \text{ in.}$$

$$b_v = 12.00 - 2(1.5 + 0.25) = 8.5 \text{ inches.}$$

$$p_c = 2 \times 88 + 12 + 6 + 18 = 212 \text{ in.}$$

$$p_h = 2[(88.00 - 2 \times 1.75) + (12.00 - 2 \times 1.75)] = 198 \text{ in.}$$

$$A_{oh} = 8.5(88.00 - 3.5) + 6(7.5) = 763.25 \text{ sq. in.}$$

$$f_{pc} = \frac{4 \times 24{,}780}{1122} = 88 \text{ psi}$$

The end reactions due to the design loads are:

$$R_u = 1.46 \times 18 + 4.5 \times 15.00 = 93.78 \text{ kips}$$

and the shear diagram is as shown in Fig. 6-26. The torsional moments at the supports are equal to:

$$T_u = 4.5 \times 15.00 \times 10 = 675 \text{ kip-in.}$$

and the torsion diagram is as shown in Fig. 6-27. The design moment at midspan is:

$$M_u = 1.46\left(\frac{36^2}{8}\right) + 4 \times 15\left[\frac{4.5}{2} + 3.5 + 2.5 + 1.5 + 0.5\right]$$

$$= 851.5 \text{ k-ft}$$

and the service load moment is equal to 640.5 k-ft.

The need for torsional reinforcement is determined by comparing the

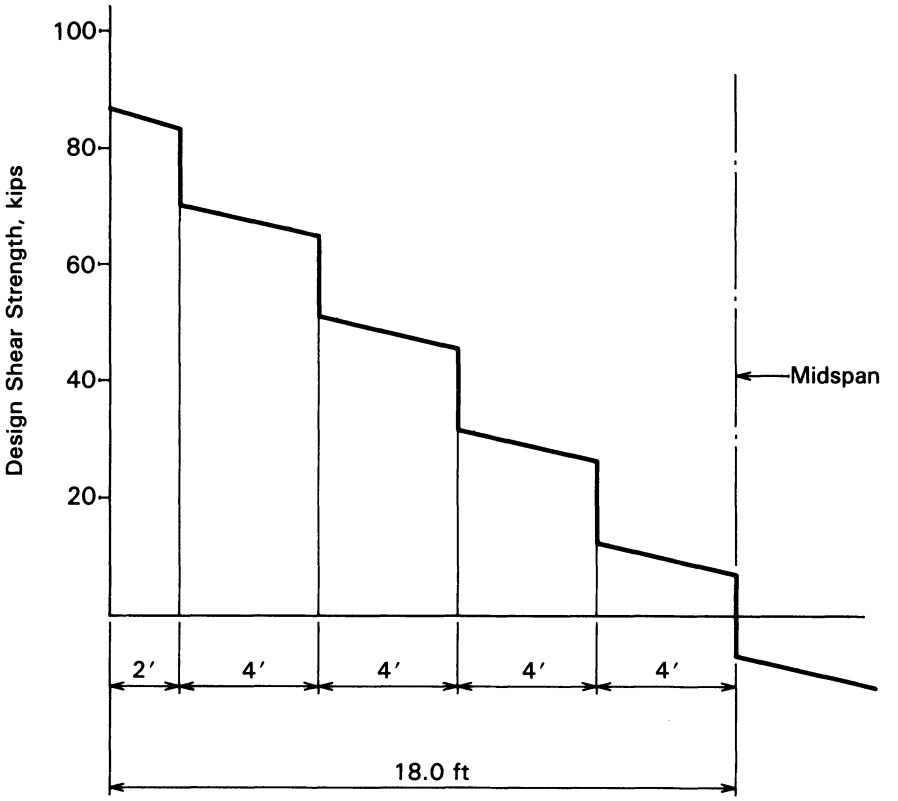

Fig. 6-26. Shear diagram for one-half span of beam analyzed in I.P. 6-6.

computed torsional cracking moment to the maximum torsional moment. The torsional moment at which cracking would be expected is computed as:

$$T_{cr} = \left(\frac{1122^2}{212}\right) 4.8 \times 1 \times 0.85\sqrt{4000}\sqrt{1 + \frac{88}{4.8 \times 1 \times 0.60\sqrt{4000}}}$$

$$= 1860 \text{ k-in.}$$

and the maximum value of T_u, 675 k-in. is equal to $0.36T_{cr}$ and torsional reinforcement is required.

Using the maximum values of design shear force and torsional moment, computation of the shear and torsional unit stresses give:

$$\frac{V_u}{b_v d_v} + \frac{T_u p_h}{A_{oh}^2} = \frac{93.78}{8.5 \times 76.7} + \frac{675 \times 198}{763.24^2}$$

$$= 144 + 229 = 373 \text{ psi}$$

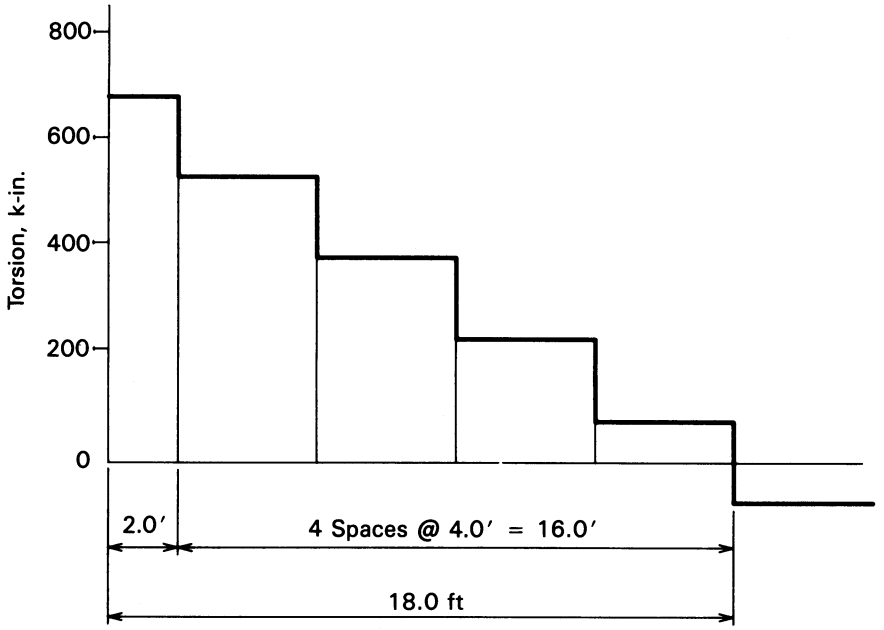

Fig. 6-27. Torsion diagram for one-half span of beam analyzed in I.P. 6-6.

and the ratio of the sum of the shear and torsional stress to $\lambda\phi_c f'_c$ is:

$$\frac{373}{1 \times .60 \times 4000} = 0.155$$

From Fig. D7 from CSA 1984, the angle θ at which f is equal to $f_{2\max}$ is approximately 32°. By adopting a value of θ equal to 35°, the diagonal compressive stress computations are:

$$f_2 = \left(\tan 35° + \frac{1}{\tan 35°}\right)(373) = 794 \text{ psi}$$

$$\epsilon_1 = 0.002 + \frac{0.004}{\tan^2 35°} = 0.01016$$

$$f_{2\max} = \frac{1 \times 0.60 \times 4000}{0.80 + 170 \times 0.01016} = 950 \text{ psi} > f_2$$

The strain in the transverse reinforcement is computed as:

$$\epsilon_1 = 0.01016 - 0.002 - 0.002 = 0.00616 > 0.002$$

Hence, the use of Grade 60 reinforcement is acceptable. The relationship for the amount of transverse reinforcement required for the factored shear resistance within the length s placed perpendicular to the axis of the member is:

$$V_r = \frac{0.85A_t 60}{12} \frac{76.7}{\tan 35°} = 465A_t$$

To determine the relationship for the computation of the amount of torsional reinforcement, one must compute the values of d_v and $A_{ps}f_{ps}$

$$a_o = \left[1 - \sqrt{1 - \frac{675{,}000 \times 198}{0.7 \times 1 \times 0.60 \times 4000(763.25)^2}\left(\tan 35° + \frac{1}{\tan 35°}\right)}\right]$$

$$\times \frac{763.25}{198} = 1.77 \text{ in.}$$

$$A_o = 763.35 - \frac{1.77 \times 198}{2} = 588 \text{ in.}^2$$

The relationship for the torsional resistance developed by reinforcement having an area of A_t in one leg of a closed stirrup spaced at intervals of s is:

$$T_r = \frac{0.85A_t 60}{12} \frac{2 \times 588}{\tan 35°} = 7140A_t$$

The amounts of reinforcement, in the form of U-shaped stirrups (two legs), required for shear and torsion are summarized in Table 6-5. In Table 6-5, the areas listed in the third column are for one leg of the reinforcement required for torsion.

The spacing of stirrups required for shear stresses cannot exceed:

$$\frac{d_v}{3 \tan 35°} = 36.5 \text{ in.}$$

$$d_v = 76.7 \text{ in.}$$

or 24 in. whichever is the least. For torsion the spacing is limited to:

$$\frac{p_n}{8 \tan 35°} = 35.3 \text{ in.}$$

TABLE 6-5 Summary of Shear Reinforcement Requirements for I.P. 6-6.

Distance, (ft)	Shear Reinf. (in.^{2})	Torsion Reinf. (in.^{2})	Total Reinf. (in.^{2})	Spacing No. 4 (in.)
2	0.195	0.095	0.385	12
6	0.150	0.074	0.298	16
10	0.106	0.053	0.212	22
14	0.061	0.032	0.125	38
18	0.016	0.010	0.036	133

The maximum spacing of No. 4 stirrups (two legs, Grade 60) is:

$$s = \frac{A_v f_y}{50 b_w} = \frac{2 \times 0.20 \times 60{,}000}{50 \times 12} = 40.0 \text{ in.}$$

if the flexural tensile reinforcement is not prestressed with an effective force equal to or greater than 40 percent of its tensile strength. If the tensile flexural reinforcement is prestressed with a force equal to or greater than 40 percent of the tensile strength of the flexural reinforcement, the maximum spacing of the transverse reinforcement can be determined by using eq. 6-14.

The additional axial load, resulting from the effects of shear and torsion and the angle of 35° selected for the slope of the compression struts, is computed as follows:

$$N_v = \frac{1}{\tan 35} \sqrt{(93.79)^2 + \left(\frac{675 \times 190.0)}{2(588)}\right)^2}$$

$$= 205 \text{ kips}$$

where $p_o = 198 - 4 \times 1.77 = 190.0$ in. Nonprestressed reinforcement in the amount of 3.43 sq. in. or additional prestressing in the amount of 205 kips could be provided to resist the axial load.

To investigate the need for diagonal cracking control, the value of the shear cracking load must be determined. Based upon the assumption that the axial load computed immediately above will be resisted by nonprestressed reinforcement, an average prestress of 88 psi is used in determining the shear cracking load as follows:

$$V_{cr} = \left[2.4 \times 1 \times \sqrt{4000} \sqrt{1 + \frac{88}{4.8 \times 1 \times \sqrt{4000}}}\right] 12 \times 85.25$$

$$= 176 \text{ ksi} > V_{se} = 1.17 \times 18 + 4.5 \times 11 = 70.56 \text{ kips}$$

Hence, if torsion were not present, diagonal cracking would not require further study. In view of the fact that torsion does exist, the effect can be taken into account by adjusting the value of V_{cr} computed above by dividing it by the following term and comparing the result with the value of V_{se}:

$$\sqrt{1 + \left(\frac{p_c b_w d}{2A_c^2} \frac{T_{se}}{V_{se}}\right)}$$

$$= \sqrt{1 + \left(\frac{212 \times 12 \times 85.25}{2 \times 1122^2} \times \frac{495}{70.56}\right)} = 1.27$$

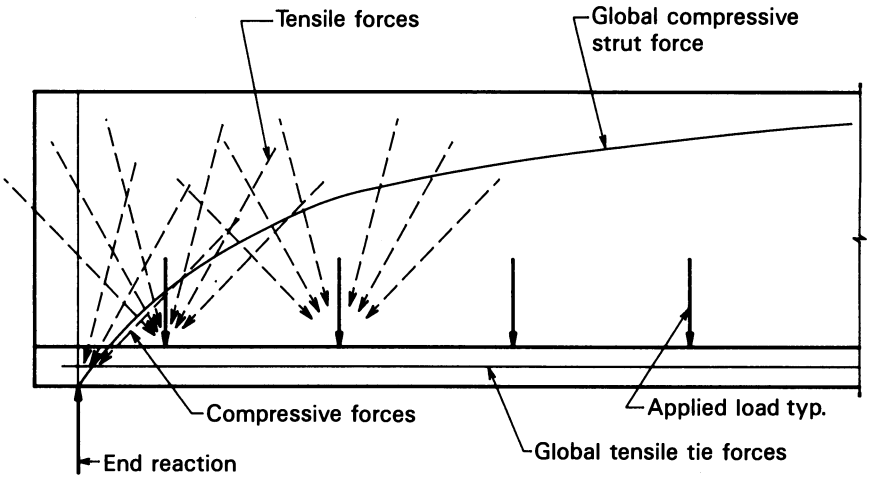

Fig. 6-28. Illustration of orientation of tensile and compressive forces in the web of an L-shaped spandrel beam having the superimposed loads applied to a ledger near the bottom of the beam.

Dividing the value of the shear cracking load computed above by this factor results in an adjusted value of 138 kips $> V_{se}$; hence control of diagonal cracking does not need further consideration.

An elevation of a portion of the beam at the support is shown in Fig. 6-28. The approximate locations and shapes of the local compression forces at the support of the beam are shown by light-weight solid lines and the approximate locations and shapes of local tensile forces due to the effect of the applied loads are shown by light-weight broken lines. Because of the number of applied loads (nine loads applied at a spacing of 4 ft on centers), their effect is not much different from the effects one would anticipate for the same amount of load uniformly distributed along the length of the beam. Because the loads are applied near the bottom of the beam, they will create tensile forces for which added reinforcement should be provided. In this example the design loads are relatively small (15 kips) and the amount of added reinforcement to transfer the effect of the loads upward into the beam is small (0.25 sq. in. of Grade 60 reinforcement would be sufficient for each load). The end reaction of the beam is 93.78 kips, and the nodal zone at the support has only one tension tie. Hence, the concrete compressive stress must be limited to $0.75\phi_c f'_c$, which, for a concrete having a specified strength of 4000 psi is equal to 1800 psi, is easily accommodated with commonly used bearing details. Anchorage of the tensile tie reinforcement must be provided in order to preserve the integrity of the nodal zone. The anchorage could be accomplished by providing sufficient development length in combination with hooks, or with special anchorage devices. If the loads were

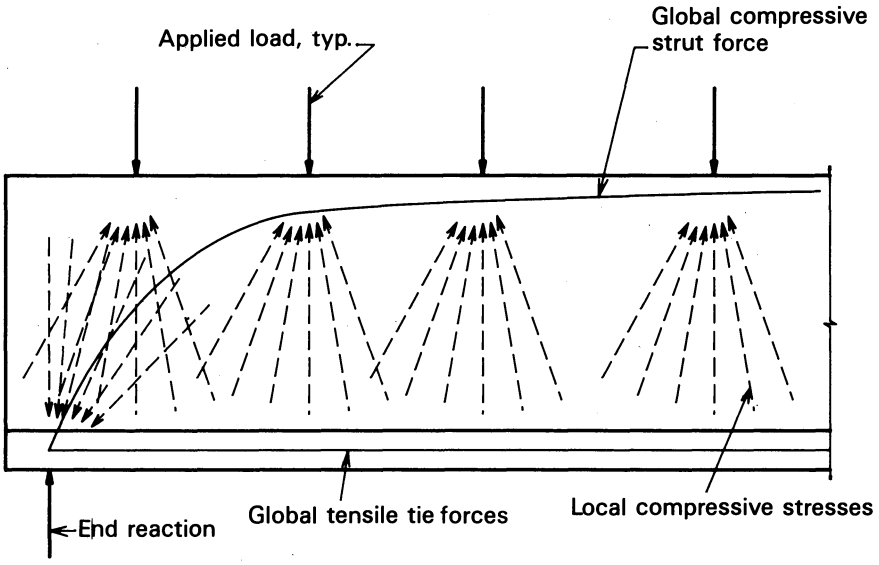

Fig. 6-29. Illustration of the orientation of compressive forces in the web of an L-shaped beam having the superimposed loads applied to the top surface of the beam.

applied to the top of the beam, rather than near the bottom, the locations and shapes of the local compressive forces would be approximately as shown in Fig. 6-29, and the added tensile reinforcement would not be needed to transfer the effect of the applied loads up into the beam.

6-6 Bond of Prestressed Reinforcement

Two types of bond stress must be considered in the case of prestressed concrete. The first of these, referred to as transfer bond stress, has the function of transferring the force in a pretensioned tendon to the concrete. Two different basic forms of transfer bond stresses are recognized: elastic and plastic transfer bond stresses. Transfer bond stresses come into existence when the forces in pretensioned tendons are transferred from the prestressing beds to the concrete section after the concrete has cured. The second type of bond stress, referred to as flexural bond stress and as development bond stress, comes into existence in pretensioned and in bonded, post-tensioned members when the members are subjected to external loads. Flexural bond stresses do not exist in unbonded, post-tensioned construction, which accounts for the term "unbonded post-tensioned tendon."

When a prestressing tendon is stressed, the elongation of the tendon is accompanied by a reduction in the diameter due to the Poisson effect. When the tendon is released, the diameter increases to its original diameter at the ends of the

prestressed member where the tendon is not encased in concrete and, hence, not restrained. This phenomenon has generally been regarded as an important factor in effecting the transfer of stress from pretensioned tendons, generally wires or strands, to the concrete. The stress in the tendon is zero at its extreme end, where it is not encased in concrete, and is at a maximum value at some distance from the end of the member. Within the length of the tendon from its extreme end to the point where it attains maximum stress, called the transmission length, there is a gradual decrease in the diameter of the tendon, which results in the tendon having a slight wedge shape over the length. This phenomenon is often referred to as the Hoyer effect after the German engineer E. Hoyer, who was one of the early engineers to develop this theory. Hoyer, and others more recently, derived elastic theory to compute the transmission length as a function of Poisson's ratio for steel and concrete, the moduli of elasticity of steel and concrete, the diameter of the tendon, the coefficient of friction between the tendon and the concrete, and the initial and effective stresses in the steel (Janney 1954). Laboratory studies of transmission lengths have indicated a relative close agreement between theoretical and actual values. There can be wide variation in bond lengths and stress, however, due to differing dimensions and physical properties between concretes and steels, as well as the several different surface conditions of prestressing tendons that can exist. All of these factors can affect the bond stresses and transfer lengths.

There is reason to believe that the configuration of a seven-wire strand (i.e., six small wires twisted about a slightly larger center wire) results in very good bond characteristics. The transfer lengths of strands have been assumed to be half as long as those for solid wires of the same nominal diameter for many years. It is believed the relatively large surface area and twisted configuration of strands effect a significant mechanical stress transfer.

Although these theoretical relationships are of academic interest, the profession has relied heavily upon experimental data for the transmission and development lengths required for different types and sizes of pretensioning tendons. Over the years there has been considerable research concerning development and transfer lengths, under both laboratory and actual production conditions (Base 1958; Hanson 1969; Cousins, Johnston, and Zia 1990). This research has led to the following significant conclusions:

1. The bond characteristics of clean three- and seven-wire prestressing strands and concrete are adequate for the majority of pretensioned concrete elements.
2. Members that are of such a nature that high moments may occur near their ends, such as short simple spans and short cantilevers, require special consideration with respect to transfer and development lengths.
3. Clean smooth wires of small diameter are adequate for use in pretensioning, but the transmission and development lengths for tendons of this

type are known to be greater than those for seven-wire strands (expressed as a multiple of the diameter).

4. For many years, based upon a provision in ACI 318, the transmission length for clean seven-wire strands has been assumed to be equal to 50 times the nominal diameter of the strand, and a very large number of structures that have been constructed under this assumption have given excellent service. Recent research, however, has shown that actual transfer lengths may be significantly longer than 50 diameters (Cousins, Johnston, and Zia 1990).
5. The transmission length of tendons can be expected to increase from 5 to 20 percent between the time of release and one year after release.
6. The transmission length of tendons released by flame cutting or with an abrasive wheel can be expected to be as much as 20 percent greater than the transmission length of tendons that are released gradually.
7. Hard, nonflaky surface rust and surface indentations effectively reduce the transmission lengths required for strand and some forms of wire tendons.
8. Concrete compressive strengths between 1500 and 5000 psi at the time of release result in transmission lengths of the same order, except for strand tendons larger than 1/2 in.
9. Because of relaxation and concrete shrinkage, a small length of tendon (3 in. $\pm$) at the end of a member can be expected to become completely unstressed.
10. The degree of compaction of the concrete at the ends of pretensioned members is very important if good bond and short transmission lengths are to be obtained. Honeycombing must be avoided at the ends of pretensioned beams.
11. There is little if any reason to believe that the use of end blocks improves the transfer bond of pretensioned tendons, other than that gained by facilitating the placing and compacting of the concrete. Hence, the use of end blocks is considered unnecessary in pretensioned beams if sufficient care is given to consolidation of the concrete.
12. Tensile stresses and strains develop in the ends of pretensioned members along the transmission length as a result of the wedge effect of the tendons. Little if any benefit can be gained in attempting to reduce these stresses and strains by providing mild reinforcing steel around the ends of the tendons, because the concrete must undergo large deformations and probably would crack before such reinforcing steel could be stressed enough to become effective. The seriousness of the effect increases with tendon size.
13. Lubricants and dirt on the surface of tendons have a detrimental effect on their bond characteristics.

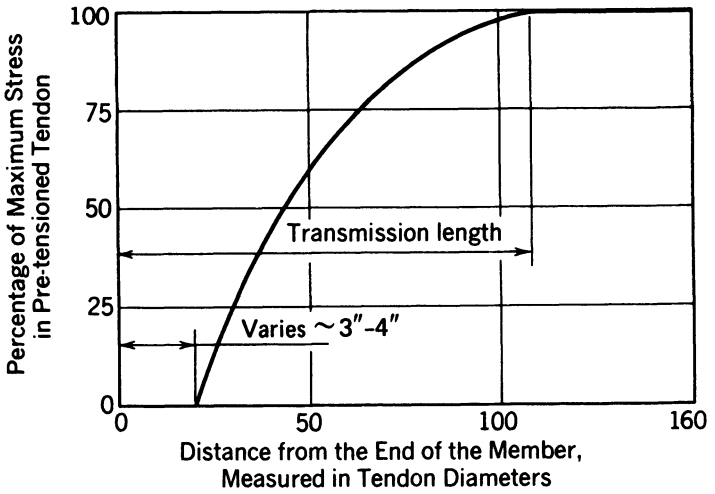

Fig. 6-30. Variation in stress in pretensioned wire tendon near end of beam after relaxation.

A curve showing typical variation of stress along the length of a pretensioned tendon near the end of a beam is given in Fig. 6-30. It will be seen that this curve is approximately hyperbolic. The stress is zero at the extreme end and for a distance of approximately 3 to 4 in., as is assumed to be the case in most applications. This should be considered in the design of pretensioned members and their connections.

Flexural bond stresses occur between the tendons and the concrete in both pretensioned and bonded, post-tensioned members, as a result of changes in the external load. There are, of course, no transfer bond stresses in post-tensioned members because the end anchorage devices transfer the stress from the tendons to the concrete. Although it is known that flexural-bond stresses are relatively low in prestressed members for loads less than the cracking load, there is an abrupt and significant increase in these bond stresses after the cracking load is exceeded. Because of the indeterminacy that results from the plasticity of the concrete for loads exceeding the cracking load, accurate computation of the flexural-bond stresses cannot be made under such conditions. Tests are relied upon as a guide for design (Hanson and Kaar 1959; Cousins, Johnston, and Zia 1990).

The effect of flexural bond is most evident when two identical post-tensioned members, one with bonded and one with unbonded tendons, are tested to destruction and the results are compared. The load–deflection curves for such tests, when plotted together, would appear as in Fig. 6-31. From these curves, it will be seen that the beam with bonded tendons does not deflect as much

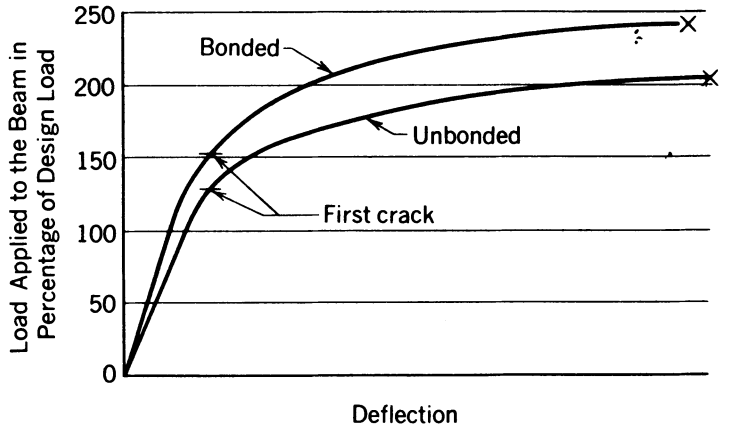

Fig. 6-31. Comparison of load–deflection curves for bonded and unbonded post-tensioned construction.

under a specific load as the one with unbonded tendons. The explanation for this behavior is that the tendon in the bonded beam must undergo changes in strain equal to the strain changes in the concrete to which it is bonded, whereas the unbonded tendon can slip in the duct and the strain changes are averaged. Hence, the beam with bonded tendons deforms and deflects as a function of a transformed section. This difference can result in the cracking load of the beam with bonded tendons being from 10 to 15 percent greater than that of the unbonded beam, and the ultimate load may be as much as 50 percent higher. The presence of flexural bond results in many very fine cracks in a bonded member in which the cracking load is exceeded, whereas in an identical unbonded member subjected to the same load, only a few wide cracks occur. This is a significant difference because removal of the load from the bonded member will result in the fine cracks closing completely, but in the unbonded member the wider cracks are less likely to completely close.*

It is generally believed that once a member with bonded tendons is cracked, a significant increase in flexural-bond stress occurs at the point of cracking. As load on the beam is increased, the flexural bond stresses at the crack increase until slip occurs at the cracked section. Further increase in the external loads will be accompanied by additional slip in the tendon. This action will continue until the member fails, either by rupture of the steel, by excessive compressive strain in the concrete, or, in the case of a pretensioned member, by lack of anchorage, when the flexural bond stress is destroyed over a length of a tendon that reaches the zone in which the pretension is developed by transfer bond

*The provision of nonprestressed reinforcement, if in sufficient quantity, will result in a nonbonded beam having deflection and cracking characteristics similar to those of a bonded beam.

(Nordby 1958; Hanson and Kaar 1959). Research has shown that the embedment length, the length from the free end of the beam to the point at which a specific steel stress can be developed, for stands having nominal diameters of $\frac{1}{4}$, $\frac{3}{8}$, and $\frac{1}{2}$ in., is of the order given in Table 6-6 (Hanson and Kaar 1959). The data in the table are applicable to concrete with a cylinder compressive strength of 5500 psi and steel stresses of the order of 150,000 psi. *If the distance from the section at which the critical stress in the steel occurs is less than the embedment length required to develop the required stress in the steel, the flexural strength of the member may be controlled by bond rather than by flexure.* In such instances, the design should be revised because it is more desirable for the controlling mode of failure to be flexural rather than bond.

Bond considerations for prestressed concrete members are treated in several different parts of ACI 318. The first of these is in Sec. 11.4.3, where the effect of transfer bond on shear strength near the ends of pretensioned beams is considered. It is in this section that it is said to be permissible to consider the transmission length of strand and wire tendons to be 50 and 100 diameters, respectively. *As stated above, these provisions are not considered conservative.* Section 11.4.4 contains provisions related to shear strength computations near the ends of pretensioned members that have some tendons not bonded to the concrete for all of the distance to the end of the member. (See Sec. 6-3 and I.P. 6-2.) The development length for prestressed three- and seven-wire strand is treated in Sec. 12.9 of ACI 318, where it is provided that strands of these types be extended a distance beyond the critical section (for moment) equal to:

$$\left(f_{ps} - \frac{2}{3} f_{se}\right) d_b \tag{6-49}$$

TABLE 6-6 Maximum Stresses (psi) That Can be Developed at the Section of Maximum Moment for Various Sizes of Seven-Wire Strands and Embedment Lengths (Hanson and Kaar 1959).

Embedment Length (in.)	$\frac{1}{4}$-in. Strand	$\frac{3}{8}$-in. Strand	$\frac{1}{2}$-in. Strand
20	194,000	160,000	—
30	218,000	187,000	166,000
40	234,000	201,000	180,000
50	250,000	211,000	192,000
60	264,000	220,000	200,000
70	—	229,000	206,000
80	—	238,000	213,000
90	—	247,000	219,000
100	—	257,000	226,000
120	—	—	244,000
140	—	—	272,000

Here d_b is the nominal diameter of the strand, and f_{ps} and f_{se} are as defined elsewhere in this chapter and have the units of ksi, although the quantity within the parenthesis is considered to be dimensionless. If the bonding of the tendons does not extend to the end of the member, the length given in eq. 6-49 must be doubled if the design allows tensile stresses in the precompressed tensile zone. (See Sec. 12.9.3 of ACI 318.) It should be noted that some designers think that the development length specified by eq. 6-49 is nonconservative, and that the embedment lengths given in Table 6-6 more accurately reflect what is needed.

Bond is also discussed in Secs. 18.7 and 18.9 of ACI 318, in which flexural strength and minimum amounts of bonded reinforcement are treated; these topics already have been discussed in detail in this book.

ILLUSTRATIVE PROBLEM 6-7 The 4-ft-wide double-tee beam in Fig. 6-32a is supported by an inverted-tee beam, as shown in Fig. 6-32b. The span of the double-tee beam is 40 ft, the dead load is 46 psf, the area of the concrete is 180 in.^{2}, the superimposed dead load is 10 psf, and the live load is 30 psf. The member is prestressed with two harped pretensioned strands in each leg. A_{ps} = 0.4668 in.^{2} (total for both legs), f_{pu} = 270 ksi, and P_{se} = 72.0 kips. The center of gravity of the prestressed reinforcement is 5.50 in. above the soffit at the supports, is 2.07 in. above the soffit of the member for a length of 4 ft at midspan, and varies linearly in between. Assume that the coefficient of friction between the double-tee beam and the elastomeric pad is 0.20. The effects of shrinkage and creep will cause slippage in the joint. Investigate the member for shear with the assumption that the transfer length is 22 in. and the stress in the tendon varies linearly in the transfer zone. Design reinforcement for shear and support stresses, taking into account the fact that the stress in the tendon is null for the first 3 to 4 in. Use load factors of 1.4 and 1.7 for dead and live loads, respectively, and f'_c = 4000 psi and f_y = 400 ksi.

SOLUTION: From eq. 6-13:

$$A_v = \frac{50 \times 8 \times 12}{40{,}000} = 0.120 \text{ in.}^2 \text{ per foot}$$

and from eq. 6-14:

$$A_v = \frac{0.4668}{80}\frac{270}{40}\frac{12}{d}\sqrt{\frac{d}{8}} = \frac{0.167}{\sqrt{d}} \text{ per foot}$$

The latter controls.

The computation for v_{ci}, v_{cw}, v_c, v_u/ϕ, and A_v are shown in Table 6-7. Note that $2v_u/\phi < v_c$ in the centermost 14 ft±; hence stirrups could be omitted over this length.

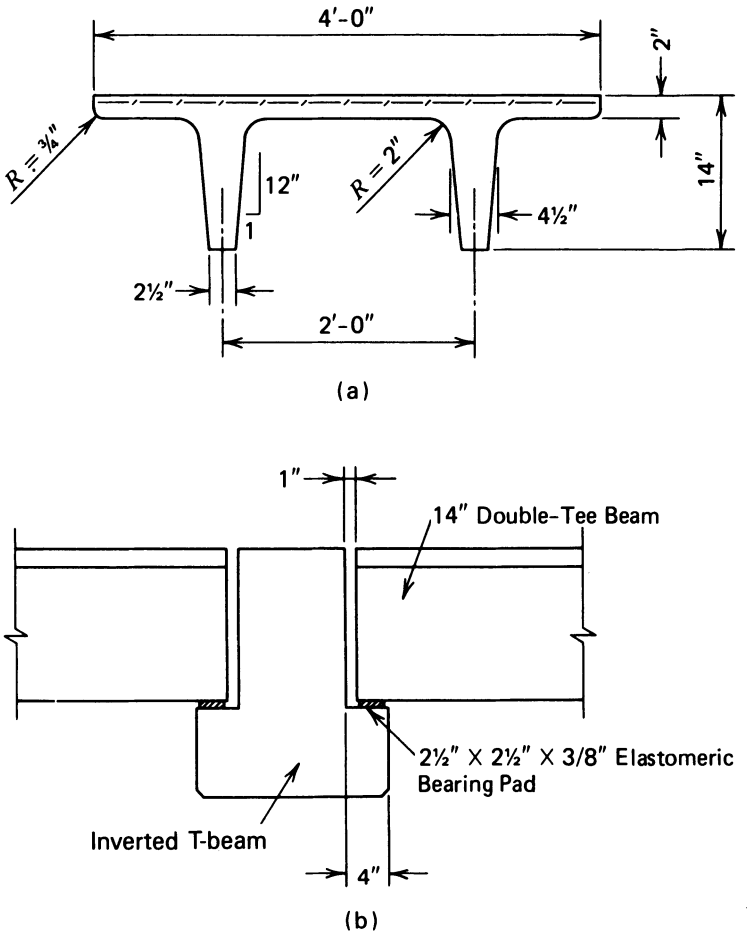

Fig. 6-32. Double-tee beam and inverted-tee beam used in I.P. 6-7. (a) Cross section dimensions of double-tee beam. (b) Cross section of inverted-tee beam.

The effect of the transfer length shows in the computation of v_{cw} at the support. Because $0.3f_{pc} = 0$ at the support, eq. 6-5 yields a value of v_{cw} equal to 234 psi at this location (including the last term of eq. 6-5). Note that the value v_{cw} is constant from 2.0 ft to 14.0 ft (points 0.05 to 0.35) from the left support. This is explained by the fact that $V_p/b_w d$ is a constant 12.8 psi between these limits, d being taken equal to $0.80h$ from the support to 14.0 ft from the support and its actual value at points 16 ft and farther from the supports.

At the supports, the design (factored) reaction can be computed as follows:

$$R_u = [1.4(46 + 10) + 1.7(30)]4 \times 20 = 10{,}352 \text{ lb}$$

TABLE 6-7 Summary of the Shear Stress Computations for I.P. 6-7.

Pt.	Length (ft)	v_{ci} (psi)	v_{cw} (psi)	v_c (psi)	v_u/ϕ (psi)	A_v (in.^{2}/ft)
.00	.000	infin	234.1	234.1	135.9	.0573
.05	2.000	290.9	354.1	290.9	122.3	.0560
.10	4.000	162.3	354.1	162.3	108.7	.0549
.15	6.000	118.2	354.1	118.2	95.1	.0538
.20	8.000	95.2	354.1	107.5	81.5	.0527
.25	10.000	80.3	354.1	107.5	67.9	.0518
.30	12.000	69.4	354.1	107.5	54.3	.0508
.35	14.000	60.6	354.1	107.5	40.7	.0500
.40	16.000	52.3	353.7	107.5	26.3	.0491
.45	18.000	44.9	353.3	107.5	12.7	.0483
.50	20.000	37.9	341.3	107.5	000.0	.0483

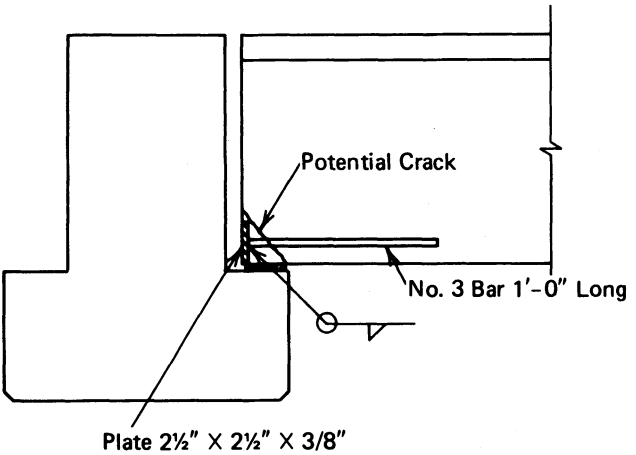

Fig. 6-33. Detail of inverted-tee beam supporting a double-tee beam.

and the maximum horizontal force at each of the four stem supports is equal to $10{,}352 \times 0.2/2 = 1035$ lb. Hence, to control cracking, steel reinforcement must be provided across and anchored on each side of the potential crack. In order to control crack width, the stress in the steel should be confined to 10,000 to 20,000 psi. Using one No. 3 bar in each leg, the stress would be 9400 psi, which is adequate. A good means of anchoring the bar is shown in Fig. 6-33.

ILLUSTRATIVE PROBLEM 6-8 For the double-tee beam in I.P. 6-7, assuming the flexural bond characteristics of the strand to be the same as given for the $\frac{1}{2}$-in.-diameter strand in Table 6-6, determine the ultimate moment capacity of

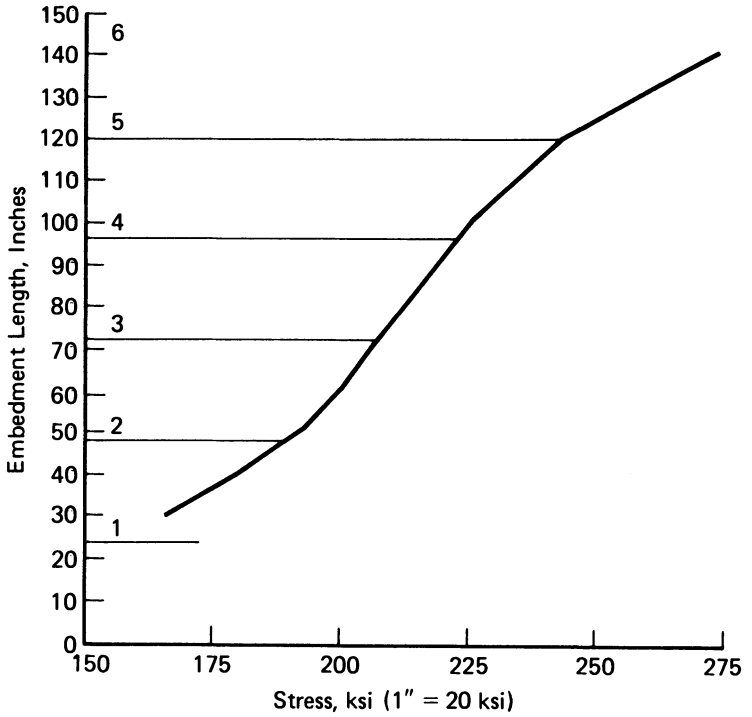

Fig. 6-34. Curve showing the stress that can be developed by the strand as a function of embedment length.

TABLE 6-8 Table for I.P. 6-8.

		By Flexure			By Bond		
Pt.	d	f_{ps}	$a/2$	M_u	f_{ps}	$a/2$	M_u
0	8.50 in.	260	0.372	74	0		0
1	8.88	260	0.372	77	0		0
2	9.26	260	0.372	81	189	0.270	59
3	9.64	261	0.373	85	207	0.296	68
4	10.02	261	0.373	88	223	0.319	76
5	10.40	261	0.374	92	244	0.349	86
6	10.78	262	0.374	95	270		
7	11.17	262	0.374	99	270		
8	11.55	262	0.375	103	270		
9	11.93 in.	263	0.376	106	270		
10	11.93 in.	263	0.376	106	270		

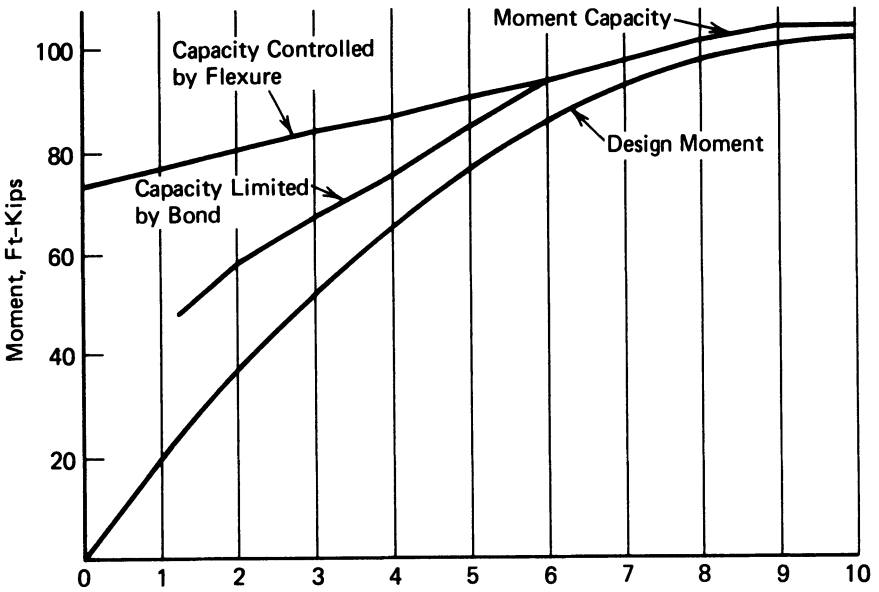

Fig. 6-35. Diagram showing the design moment, the moment capacity limited by flexure, and the moment capacity limited by embedment length (bond).

the member at the 20th points as controlled by bond and flexural strength considerations. Determine which controls.

SOLUTION: The stress versus embedment length curve based upon the data in Table 6-6 is given in Fig. 6-34. The computations for the moment capacity are summarized in Table 6-8, and the design moment and moment capacities, as limited by flexure and bond, are plotted in Fig. 6-35. The curve would indicate that the flexural capacity is adequate with a possible exception very near the ends of the beam where flexural strength, as a function of embedment length, is uncertain because of lack of data in Table 6-6. This uncertainty is the reason why many engineers provide nominal amounts of nonprestressed reinforcement near the end of simply supported members.

6-7 Bonded vs. Unbonded Post-tensioned Construction

The structural advantages gained by bonding post-tensioned tendons should be apparent from the preceding section. Yet, in spite of these advantages, unbonded tendons are widely used; literally millions of square feet of post-tensioned construction with unbonded tendons are reported to be constructed each year in the United States alone.

Suppliers of post-tensioning materials, as well as post-tensioning contractors and prestressed-concrete fabricators, have reported that the cost of using tendons coated with a rust inhibitor and wrapped with plastic or paper is lower than the cost of using tendons placed in performed or steel ducts that are grouted in place after stressing. The proponents of unbonded tendons point out that lower cracking and ultimate moments that are characteristic of unbonded construction, as well as the few widely spaced cracks that would appear in the tensile flange at loads that exceed the cracking load, can be controlled by providing nonprestressed reinforcing steel in the tensile flanges to supplement the prestressing tendons. It is claimed the supplementary reinforcing steel can be provided at less cost than would be required to bond the tendons.

The difference in spacing of the cracks that appear at overloads in unbonded and bonded construction is clearly illustrated in Figs. 6-36 and 6-37. In Fig. 6-36 an overloaded, unbonded beam is shown; wide cracks, spaced 2 to 3 ft apart, are clearly visible. The portion of bonded beam shown in Fig. 6-37 is immediately adjacent to a section of the beam that was demolished when the

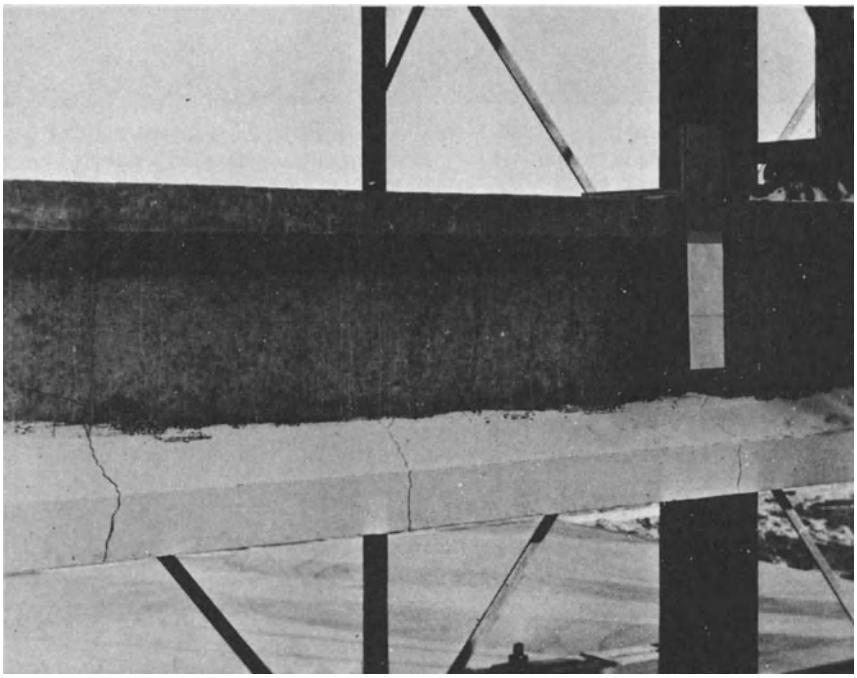

Fig. 6-36. Beam with unbonded post-tensioned tendons under a load exceeding the cracking load. Note wide spacing and relatively great width of the flexural cracks in the bottom flange. (Courtesy U.S. Naval Civil Engineering Research and Evaluation Laboratory, Port Hueneme, California.)

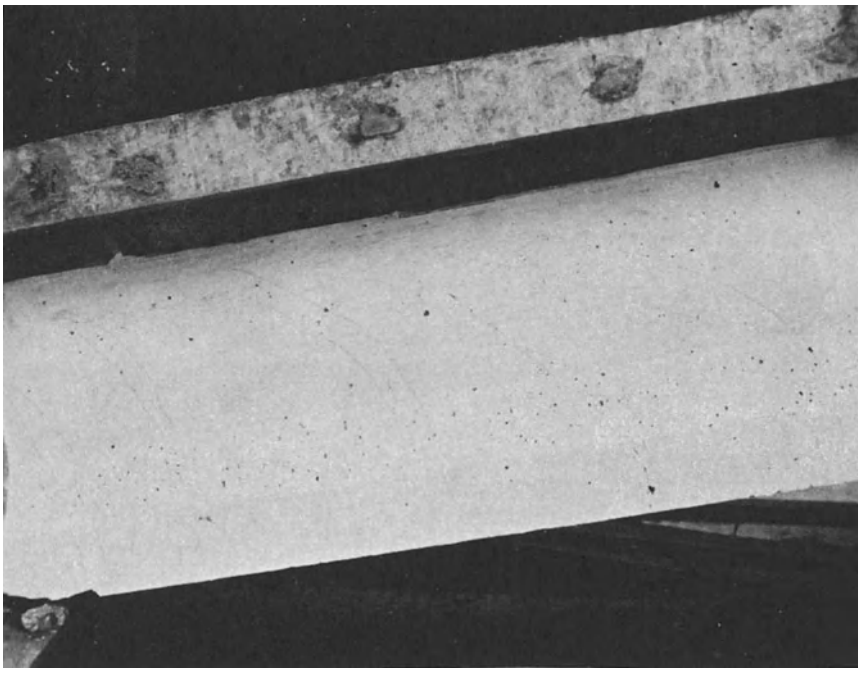

Fig. 6-37. A portion of a beam with bonded post-tensioned tendons after having been tested to destruction. Note the close spacing of cracks located between the pencil lines. The effectiveness of the grouting is confirmed by the fact the cracks are closed and virtually invisible to the unaided eye. (Courtesy U.S. Naval Civil Engineering Research and Evaluation Laboratory, Port Hueneme, California.)

beam collapsed during testing. The cracks that were open in the bottom flange and web of the beam immediately before collapse lie between the easily seen pencil lines. The cracks in the bonded beam were only faintly visible to the unaided eye after the failure of the beam. The effectiveness of the grouting in the beam of Fig. 6-38 is demonstrated by the fact that the cracks closed so completely after flexural failure of the beam.

During the testing of the beam shown in Fig. 6-37, the effectiveness of the grouting also was clearly evidenced by the location of the neutral axis of the beam. The location of the neutral axis, determined by measuring flexural strains, was found where it would be expected for the transformed concrete section, and lower than would be expected for the net or gross concrete section.

The sections of the grouted post-tensioning tendons shown in Fig. 6-38 were taken from the beam shown in Fig. 6-37. Notice that the metal sheath is very well filled with grout and virtually without voids. In addition, friction tape, which was used to seize the wires when they were being inserted in the metal

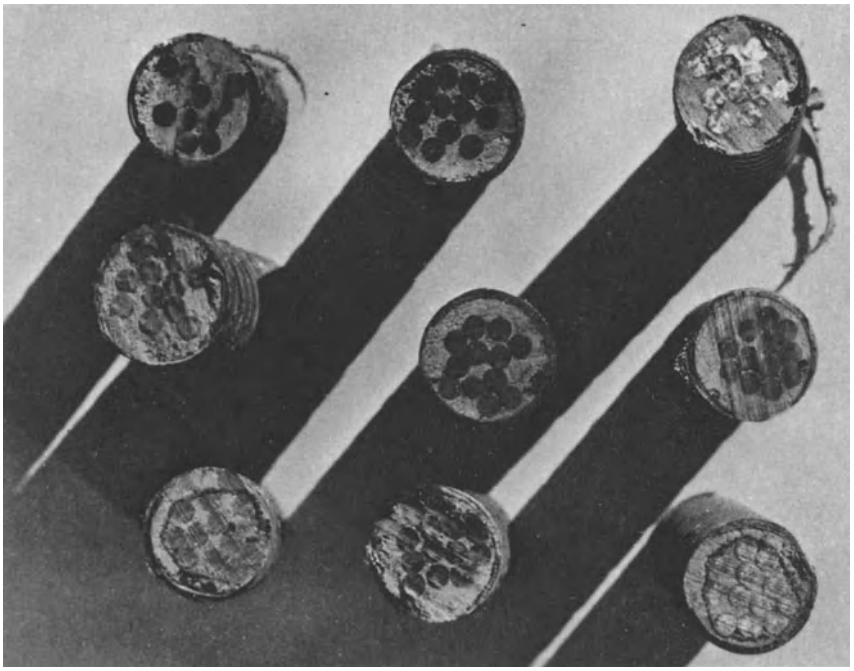

Fig. 6-38. Section of grouted post-tensioned tendons removed from the portion of the test beam shown in Fig. 6-37. (Courtesy U.S. Naval Civil Engineering Research and Evaluation Laboratory, Port Hueneme, California.)

sheath, is clearly seen in two sections of the tendon. The friction tape did not seriously restrict the flow of grout.

These comments are not intended to imply that grouting is always done perfectly. It often is not. (See Chapter 15.)

The use of unbonded tendons will certainly result in satisfactory construction if they are properly designed and fabricated. This has been demonstrated by the large amount of building construction done successfully with this method in the United States and elsewhere. Structural elements designed to be constructed with unbonded tendons should be made to conform to, or exceed, the minimum provisions of ACI 318 *Building Code Requirements for Reinforced Concrete*, as well as the "Recommendations for Concrete Members Prestressed with Unbonded Tendons" (ACI 423.3R 1989).

6-8 Internal vs. External Post-tensioned Reinforcement

In recent years there has been an increase in use of post-tensioned tendons that are not embedded within the primary concrete structural section throughout their

length. Tendons of this type are referred to as external tendons to differentiate them from internal tendons that are encased in the structural concrete section throughout their length. External tendons normally are positioned within the concrete section near their ends, at which points they are anchored to the concrete, and at intermediate points where the slopes of their paths change. Members with internal and external tendons are illustrated in Figs. 6-39 and 6-40.

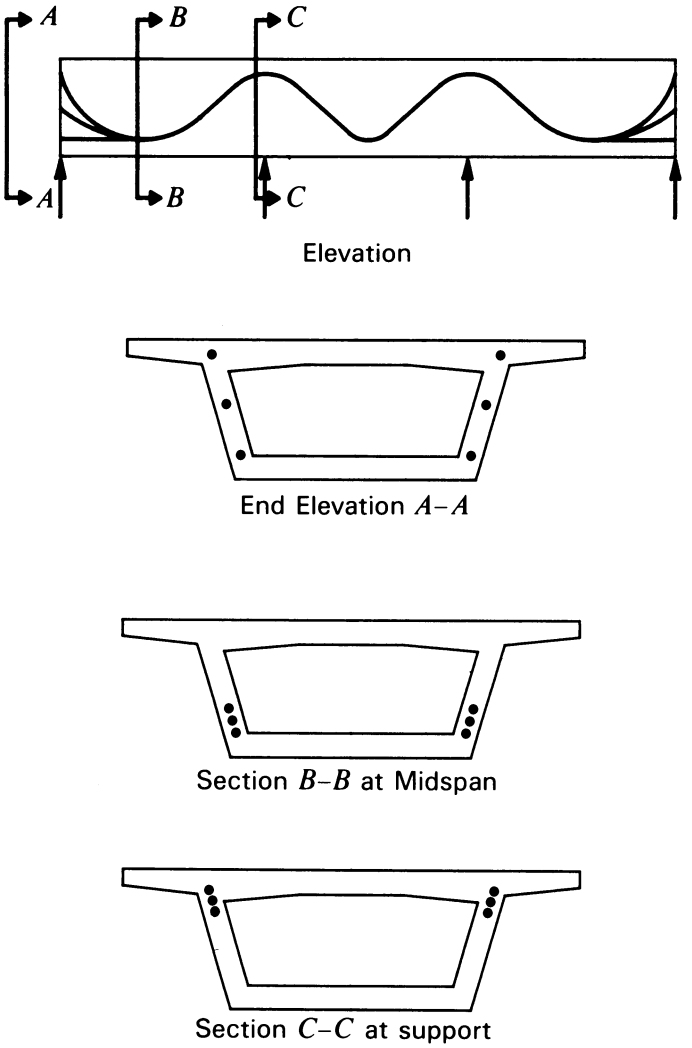

Fig. 6-39. Elevation of a three-span continuous beam illustrating typical paths of internal post-tensioned tendons.

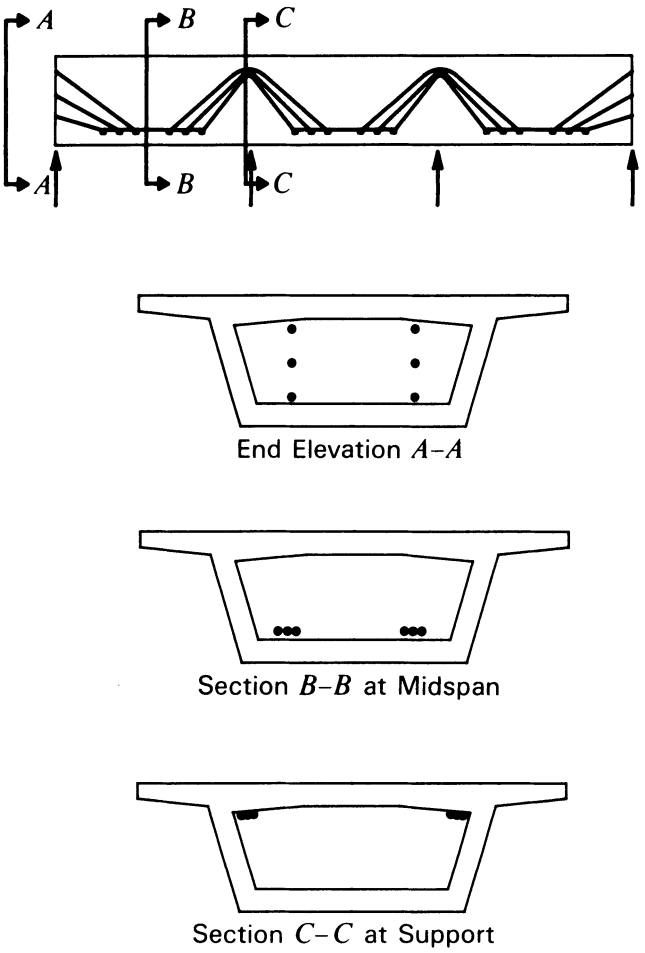

Fig. 6-40. Elevation of a three-span continuous beam illustrating the paths commonly used with external tendons.

In the early days of prestressing (late 1940s and early 1950s), the use of external tendons was most often done with zinc-coated prestressed reinforcement placed within the voids of hollow-box-girder bridge superstructures. Saddles or rockers fabricated from steel commonly were provided at the points where the slopes of the tendons were changed in order to optimize the effect of the tendons. In contemporary practice, external tendons most often are placed within the interior of a hollow box girder where they are not exposed to view or weather. In order to take advantages gained through the use of tendon paths that are not straight, the tendons frequently are anchored fairly high in the section at the ends and follow a path approximating a curve between the ends. When

this is done, the tendons are held down at the intermediate points where they pass through reinforced concrete blocks or beams especially provided for this purpose.

External tendons generally are enclosed within a metallic or plastic duct (or a combination of the two), and are protected against corrosion by portland cement grout. On occasion, materials especially compounded for corrosion protection are used rather than grout.

When the tendons are physically connected to the primary concrete structural section at the hold-down locations, where the slopes of the tendons change, they are not able to slip with respect to the primary concrete member. This restraint results in the tendons' performing structurally very nearly the same as they would if they were placed within the concrete section (i.e., internal tendons) and bonded to the concrete section after stressing (Figg and Muller 1987).

External tendons that are not structurally connected to the primary structural concrete member between the ends of the tendons must be expected to be able to slip with respect to the concrete member and thus perform as one would expect for unbonded tendons.

REFERENCES

AASHTO. 1989. *Standard Specifications for Highway Bridges*. Washington, D.C. American Association of State Highway and Transportation Officials.

ACI Committee 318. 1983. *Building Code Requirements for Reinforced Concrete*. Detroit. American Concrete Institute.

ACI Committee 318. 1983. *Commentary on Building Code Requirements for Reinforced Concrete*. Detroit. American Concrete Institute.

ACI Committee 318. 1989. *Building Code Requirements for Reinforced Concrete*. Detroit. American Concrete Institute.

ACI Committee 318. 1989. *Commentary on Building Code Requirements for Reinforced Concrete*. Detroit. American Concrete Institute.

ACI Committee 423. 1983. Recommendations for Concrete Members Prestressed with Unbonded Tendons. *Journal of the American Concrete Institute* 5(7):61–76.

ACI Committee 423. 1989. Recommendations for Concrete Members Prestressed with Unbonded Tendons. *ACI Structural Journal* 86(3):301–18.

ACI–ASCE Committee 426. 1974. *The Shear Strength of Reinforced Concrete Members*. Detroit. American Concrete Institute.

Base, G. D. 1958. *An Investigation of Transmission Length in Pretensioned Concrete*. Research Report No. 5. London. Cement and Concrete Association.

Canadian Standards Association. 1984. *Design of Concrete Structures for Buildings*. Rexdale (Toronto). Canadian Standards Association.

Collins, M. P. and Mitchell, D. 1980. Shear and Torsion Design of Prestressed and Non-prestressed Concrete Beams. *PCI Journal* 25(5):32–100.

Collins, M. P. and Mitchell, D. 1987. *Prestressed Concrete Basics*. Ottawa. Canadian Prestressed Concrete Institute.

Cousins, T. E., Johnston, D. W., and Zia, P. 1990. Transfer Length of Epoxy Coated Prestressing Strand. *ACI Structural Journal* (to be published in 1990). Detroit. American Concrete Institute.

Figg and Muller Engineers, Inc. 1987. *Ultimate Behavior of Precast Segmental Box Girders with External Tendons*. Tallahassee, Florida. Figg and Muller Engineers, Inc.

Hanson, N. W., 1969. Influence of Surface Roughness of Prestressing Strand on Bond Performance. *PCI Journal* 14(1):32–45.

Hanson, N. W. and Kaar, P. H., 1959. Flexural Bond Tests of Pretensioned Prestressed Beams. *Journal of the American Concrete Institute* 30(7):783–802.

Janney, J. R. 1954. Nature of Bond in Pretensioned Concrete. *Journal of the American Concrete Institute* 50(44):717–36.

MacGregor, J. G. and Hanson, J. M. 1969. Proposed Changes in Shear Provisions for Reinforced and Prestressed Concrete Beams. *ACI Journal* 66(4):276–88.

Mattock, A. H. 1979. Flexural Strength of Prestressed Concrete Sections by Programmable Calculator. *PCI Journal* 24(1):32–54.

Menegotto, M. and Pinto, P. E. 1973. Method of Analysis for Cyclically Loaded R.C. Plane Frames, Including Changes in Geometry and Non-elastic Behavior of Elements under Combined Normal Force and Bending. In *Preliminary Report for Symposium on Resistance and Ultimate Deformability of Structures Acted On by Well-Defined Repeated Loads*. Lisbon. International Association for Bridge and Structural Engineering. 15–32.

Mitchell, D. and Collins, M. P. 1974. Diagonal Compression Field Theory—A Rational Model for Structural Concrete in Pure Torsion. *Journal of the American Concrete Institute* 71(28):396.

Moersch, E. 1902. *Concrete-Steel Construction*. New York. McGraw-Hill.

Nordby, G. M. 1958. Fatigue of Concrete—A Review of Research. *Journal of the American Concrete Institute*. 31(2):210–15.

Oden, J. T. 1967. *Mechanics of Elastic Structures*. New York. McGraw-Hill Book Company.

PCI 1978. *PCI Design Handbook*. Chicago. Prestressed Concrete Institute.

PCI 1985. *PCI Design Handbook*. Chicago. Prestressed Concrete Institute.

Portland Cement Association. 1963. *Notes from the Building Code Seminar*. Chicago. 8–31.

Ritter, W. 1899. Die Bauweise Hennebique (Construction Techniques of Hennebique). *Schweizerische Bauzeitung* Feb. 1899.

Schlaich, J., Schaefer, K., and Jennewein, M. 1987. Toward a Consistent Design of Structural Concrete. *PCI Journal* 32(3):74–150.

Timoshenko, S. 1956. *Strength of Materials Part II*. New York. D. Van Nostrand Company Inc.

Vecchio, F. J. and Collins, M. P. 1986. The Modified Compression Field Theory for Reinforced Concrete. *Journal of the American Concrete Institute* 83(2):219–31.

PROBLEMS

1. The girder shown in Fig. 4-27 is designed to support precast rectangular beams and a cast-in-place slab. The girder, which had a dead load of 440

plf, is to be used on a span of 40 ft and support a superimposed dead load of 2.00 kips/ft and a superimposed live load of 1.13 kips/ft. Assuming that the compressive strength of the all-lightweight aggregate concrete is 5000 psi, the lightweight concrete shear strength coefficient is 0.75, the effective prestressing force is 440 kips, the area of the prestressed reinforcement is 3.20 in.^{2}, and the ultimate tensile strength of the prestressed reinforcement is 250 ksi, design the member for shear reinforcing using Grade 40 nonprestressed reinforcement for the stirrups and the criteria contained in ACI 318. Assume that the bonded reinforcing is post-tensioned on a parabolic path having distances between the center of gravity of the steel and the soffit of 5.20 in. at midspan and 12.76 in. at the supports. The girder is simply supported. Use load factors of 1.5 and 1.8 for deal load and live load, respectively (these load factors were commonly used in U.S. design practice some years ago). Plot the results. Confirm that the design conforms to all of the shear requirements of Chapter 11 of ACI 318.

SOLUTION:

The properties of the beam cross section needed for the analysis are:

$$y_b = 14.61 \text{ in.}, I = 44{,}700 \text{ in.}^4, h = 30.0 \text{ in.}$$

$$A_c = 418.5 \text{ in.}^2, t = 6.50 \text{ in.}, b_w = 6.00 \text{ in.}$$

The computations are summarized in Table 6-9. The asterisk in the A_v column at the support (point .00) indicates:

$$\frac{v_u}{\phi} > 0.75 \times 8\sqrt{f'_c}$$

TABLE 6-9 Table for Problem 1.

Pt.	Length (ft)	v_{ci} (psi)	v_{cw} (psi)	v_c (psi)	v_u/ϕ (psi)	A_v (in.^{2}/ft)
.00	.000	infin	378.1	378.1	930.3	*
.05	2.000	1574.6	673.9	673.9	837.3	.2942
.10	4.000	828.3	654.6	654.6	744.3	.1613
.15	6.000	563.4	635.4	563.4	651.2	.1581
.20	8.000	418.3	616.1	418.3	558.2	.2517
.25	10.000	320.8	596.9	320.8	465.1	.2598
.30	12.000	246.4	577.6	246.4	372.1	.2261
.35	14.000	184.1	558.1	184.1	277.7	.1684
.40	16.000	128.5	538.3	128.5	182.2	.0967
.45	18.000	78.8	519.3	90.1	90.3	.0900
.50	20.000	31.8	500.6	90.1	000.0	.0900

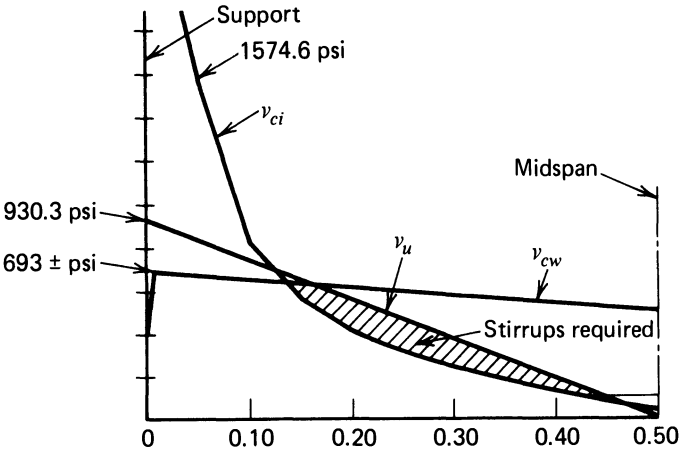

Fig. 6-41. Shear stress diagram for Problem 1.

in which 0.75 is the concrete shear strength coefficient for all-lightweight concrete, and $8\sqrt{f'_c}$ is the greatest shear stress permitted by ACI 318 to be carried by the shear reinforcement. This illustrates one of the constraints of ACI 318, but it should be pointed out that it does not apply in this example because the maximum shear stress for which it is necessary to design is located at a distance equal to one-half of the effective depth of the girder ($d/2$) or 8.63 in. from the support. Furthermore, in the case of this post-tensioned beam, the transfer distance, which is an important consideration in the design of members with pretensioned tendons, is not a consideration. The value of 378.1 psi for v_{cw} shown in the summary was computed on the basis of zero compressive stress due to prestressing at the centroidal axis—normally a conservative assumption for post-tensioned concrete but not for pretensioned concrete. The results are shown plotted in Fig. 6-41.

2. For the girder cross section and conditions specified in Problem 1, design the central span of the girder for shear, using the detailed analysis of ACI 318, if the girder has a central span of 40 ft and overhangs of 8 ft at each end. The tendon path is composed of compounded second-degree parabolas passing through the points indicated in Fig. 6-42. The service loads are shown in Fig. 6-43. The concrete is all-lightweight, and the load factors are 1.5 and 1.8 for dead and live loads, respectively. Plot the results.

SOLUTION:

The loads shown in Fig. 6-43 cause the service load and design load end moments summarized as follows:

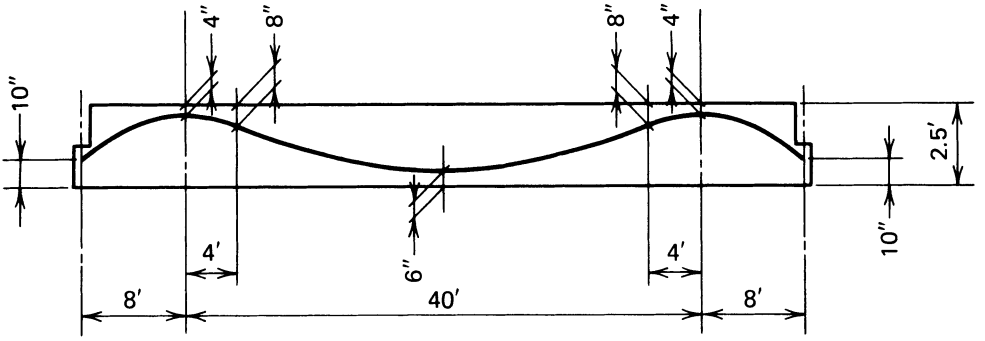

Fig. 6-42. Elevation of the beam used in Problem 2.

	Service loads (*k-ft*)	*Design loads* (*k-ft*)
Girder dead load	−56.32	−84.48
Superimposed dead load	−256.00	−384.00
Live load	−435.20	−783.36

The computations are summarized in Table 6-10, where the data are given at the 20th points. The girder and loading are symmetrical. It should be noted, as indicated by the asterisks in the tabulated data at points .00, .05, .95, and 1.00, that:

$$\frac{v_u}{\phi} - v_c > 0.75 \times 8\sqrt{f'_c}$$

To conform to the shear provisions of ACI 318, the web thickness needs to be increased in the vicinity of the supports as a means of reducing the shear stresses below the maximum acceptable level. The results are shown plotted in Fig. 6-44.

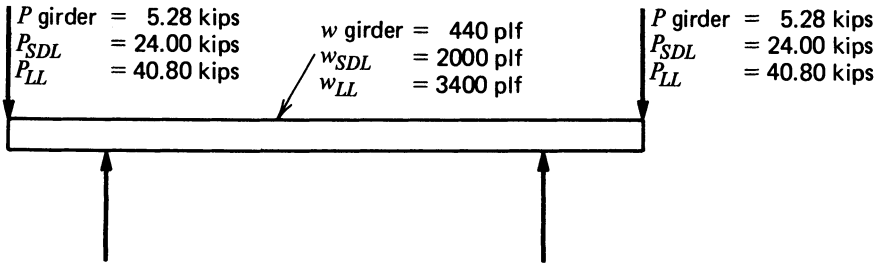

Fig. 6-43. Service loads for beam in Problem 2.

TABLE 6-10 Summary of Computations for Problem 2.

Pt.	Length (ft)	e (in.)	V_d (k)	M_d (k-ft)	Vi (k)	M_{max} (k-ft)	V_u (k)	V_p (k)	v_{ci} (psi)	v_{cw} (psi)	v_u/ϕ (psi)	v_c (psi)	A_v (in. 2/ft)
.00	.000	−11.390	48.800	−312.320	146.800	−939.520	195.600	.000	781.7	591.0	1475.1	500.6	*
.05	2.000	−10.390	43.920	−219.600	132.120	−660.600	176.040	36.700	981.2	745.6	1380.7	745.3	*
.10	4.000	−7.390	390.040	−136.640	117.440	−411.040	156.480	73.300	1226.4	1010.0	1278.4	1009.6	.4837
.15	6.000	−3.640	34.160	−63.440	102.760	−190.840	136.920	64.200	1769.0	946.8	1118.6	946.4	.3098
.20	8.000	−.390	29.280	.000	88.080	.000	117.360	55.000	infin	882.9	958.8	882.5	.1372
.25	10.000	+2.360	24.400	53.680	73.400	161.480	97.800	45.800	1405.0	810.0	799.0	818.7	.0900
.30	12.000	+4.610	19.520	97.600	58.720	293.600	78.240	36.700	750.6	755.8	639.2	750.6	.0900
.35	14.000	+6.360	14.640	131.760	44.040	396.360	58.680	27.500	480.6	691.6	479.4	480.6	.0900
.40	16.000	+7.610	9.760	156.160	29.360	469.760	39.120	18.300	304.1	628.1	319.6	304.1	.0900
.45	18.000	+8.360	4.880	170.800	14.680	513.800	19.560	9.200	161.7	564.5	159.8	161.7	.0900
.50	20.000	+8.610	.000	175.680	.000	528.480	.000	.000	31.8	501.0	000.0	90.1	.0900
.55	22.000	+8.360	−4.880	170.800	−14.680	513.800	−19.560	−9.200	161.7	564.5	159.8	161.7	.0900
.60	24.000	+7.610	−9.760	156.160	−29.360	469.760	−39.120	−18.300	304.1	628.1	319.6	304.1	.0900
.65	26.000	+6.360	−14.640	131.760	−44.040	396.360	−58.680	−27.500	480.6	691.6	479.4	480.6	.0900
.70	28.000	+4.610	−19.520	97.600	−58.720	293.600	−78.240	−36.700	750.6	755.8	639.2	750.6	.0900
.75	30.000	+2.360	−24.400	53.680	−73.400	161.480	−97.800	−45.800	1405.0	810.0	799.0	818.7	.0900
.80	32.000	−.390	−29.280	.000	−88.080	.000	−117.360	−55.000	infin	882.9	958.8	882.5	.1372
.85	34.000	−3.640	−34.160	−63.440	−102.760	−190.840	−136.920	−64.200	1769.0	946.8	1118.6	946.4	.3098
.90	36.000	−7.390	−39.040	−136.640	−117.440	−411.040	−156.480	−73.300	1226.4	1010.0	1278.4	1009.6	.4837
.95	38.000	−10.390	−43.920	−219.600	−132.120	−660.600	−176.040	−36.700	981.2	745.6	1380.7	745.3	*
1.00	40.000	−11.390	−48.800	−312.320	−146.800	−939.520	−195.600	.000	781.7	591.0	1475.1	500.6	*

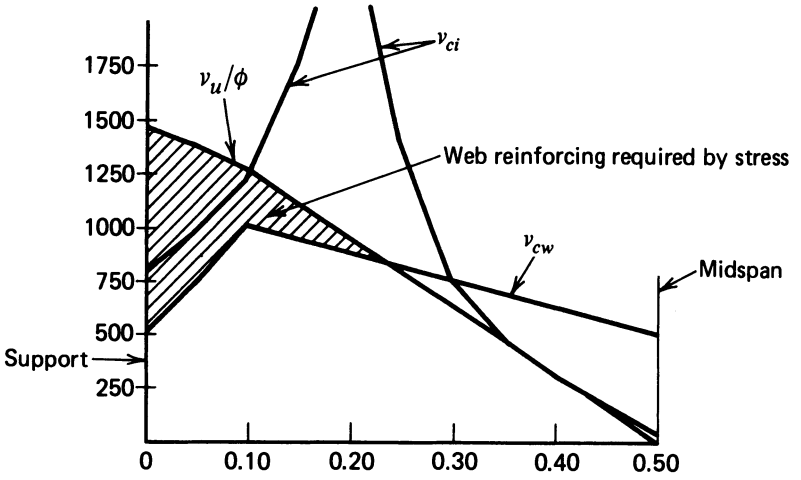

Fig. 6-44. Shear stress diagram for Problem 2.

3. The double-tee beam shown in Fig. 6-45 is pretensioned with nine $\frac{1}{2}$-in. strands in each leg. Each strand has an area of 0.153 in.^{2} and a minimum guaranteed ultimate tensile strength of 270,000 psi. The strands are positioned in three rows of three strands in each leg. The rows are at 2 in. on center with the center of the lowest strands being 2 in. above the soffit. The lower three strands in each leg are not bonded to the concrete for 12 ft at each end. The member is designed for the following loads:

Double-tee beam	671 plf
Concrete topping	375 plf
Roofing and insulation	156 plf
Live load	192 plf

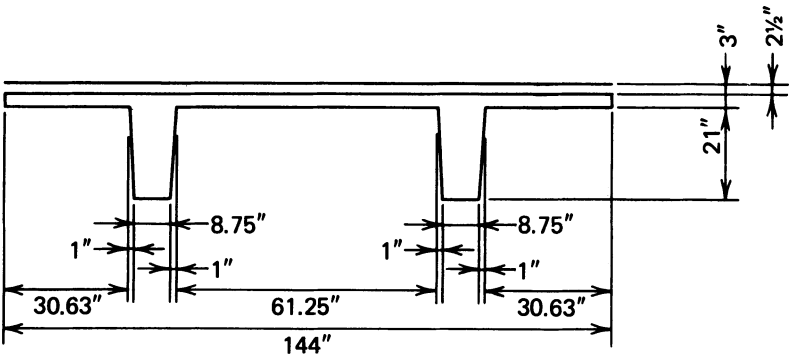

Fig. 6-45. Double-tee beam used in Problem 3.

The load factors to be used in the design are 1.5 and 1.8 for dead and live loads alone. Plot the design load moment diagram and the flexural capacity for the member, taking into account the development length requirements of ACI 318 (eq. 6-49). Assume concrete compressive strengths of 5000 and 3500 psi for the double-tee beam and the cast-in-place topping, respectively. The effective prestress in the strands is taken to be 154 ksi. The beam is to be used on a simple span of 64.3 ft.

SOLUTION:

For 18 strands, the center of gravity of the prestressed reinforcement is located 4 in. above the soffit. The effective depth of the composite section is 22.50 in. (26.50 − 4.00) and:

$$\rho_p = \frac{18 \times 0.153}{144 \times 22.50} = 0.00085$$

$$f_{ps} = 261.1 \text{ ksi}, \ \omega_p = 0.0634, \ a = 1.67 \text{ in.}$$

$$\phi M_n = \frac{0.90 \times 18 \times 0.153 \times 261.1}{12}\left[22.50 - \frac{1.67}{2}\right] = 1168 \text{ k-ft}$$

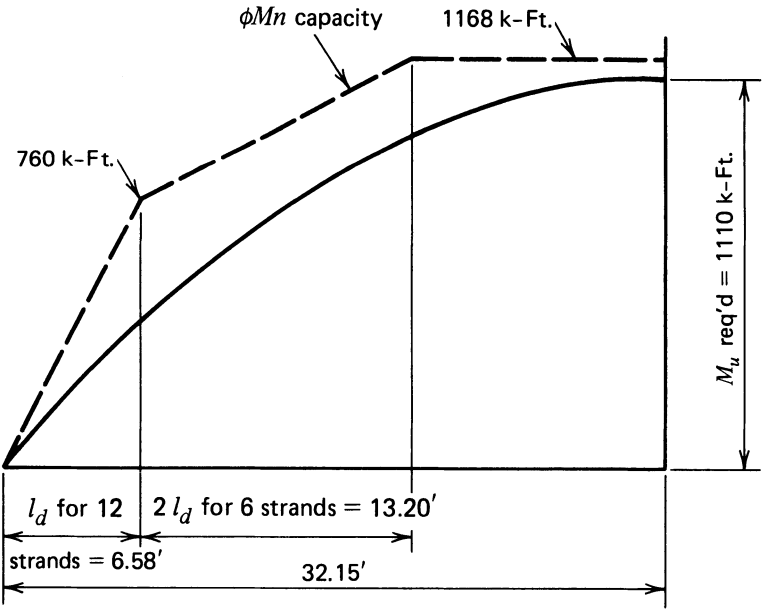

Fig. 6-46. Diagram showing the reduced moment capacity from the support to midspan for the beam in Problem 3.

For 12 strands, the effective depth of the composite section is 26.50 − 5.00 = 21.50 in. and:

$$\rho_p = \frac{12 \times 0.152}{144 \times 21.50} = 0.000593$$

$$f_{ps} = 263.8,\ a = 1.12 \text{ in.}$$

$$\phi M_n = \frac{0.90 \times 12 \times 0.153 \times 263.8}{12}\left[21.50 - \frac{1.12}{2}\right] = 760 \text{ k-ft}$$

For the 12 strands, the development length for an effective prestressing stress of 154 ksi is:

$$\left(261.1 - \frac{2}{3} \times 154\right) 0.50 = 79 \text{ in.}$$

For the six strands that are not bonded for 12 ft at each end of the member, the development length is:

$$2\left(261.1 - \frac{2}{3} \times 154\right) 0.50 = 158 \text{ in.}$$

The results are shown plotted in Fig. 6-46.

7 Loss of Prestress, Deflection, and Partial Prestress

7-1 Introduction

This chapter includes discussions of several important, frequently encountered subjects that pertain to the elastic design of simple prestressed concrete flexural members. An engineer who frequently is engaged in the design of prestressed structures will become familiar with these relationships through design experience. An engineer who is only occasionally involved in the design or review of prestressed members will find that this chapter contains valuable, concise reference material, presented in a manner that facilitates its use.

7-2 Factors Affecting Loss of Prestress

The final stress required in the prestressing steel at each of the critical sections in a prestressed member should be specified by the designer. If specific details of the method of prestressing are specified, complete stressing schedules and sequences, including jacking, initial, and final stresses required in the prestressing tendons should be determined and indicated on the construction drawings or in the specifications. To do this, it is necessary either to compute or assume a value for the loss of stress in the prestressing tendons that results

from the several contributing phenomena. The losses of prestress, including those due to friction, must be included in the computation of gage pressures and elongations for post-tensioned tendons, as is explained in Chapter 16.

The various phenomena that contribute to the loss of prestress as well as the method of calculation are discussed below.

Elastic Shortening of Concrete

When the prestressing force is applied to a concrete section, a deformation of the concrete takes place simultaneously with the application of the prestress. Because the prestressing reinforcement normally is located in the portion of the concrete member that is compressed by the prestressing, the deformation normally is a shortening; and because the deformation normally is relatively small and takes place over a very short period of time, it commonly is referred to as an elastic shortening.

If the entire prestressing force is applied to the concrete in a single operation, as is normally the case in pretensioned construction, a single change in strain takes place in the prestressed and nonprestressed reinforcement embedded within the concrete member as a result of prestressing. The application of the pretensioning force to the concrete frequently is referred to as the transfer of the prestressing force, because immediately before the prestressing force is applied to the concrete, the force is being resisted by the prestressing bed to which the tendons are anchored during the placing and curing of the concrete. In a sense, the force is transferred from the prestressing bed to the concrete member. The loss in stress in bonded reinforcement resulting from the elastic shortening is equal to the product of the stress in the concrete at the level of the reinforcement and the modular ratio of the reinforcement to the concrete. In a simple beam, the critical section for flexural stress, and hence the section at which the losses of prestress should be considered, normally will be at or near the midspan of the beam. The critical section for flexural stresses is defined as the section subject to the greatest flexural tensile stress, or the minimum compressive stress, under service load. When pretensioning is used, the concrete stress that should be used in computing the reduction in prestress due to elastic shortening is equal to the net, initial concrete stress that results from the algebraic sum of the stresses due to initial prestressing and the dead load of the beam at the level of the steel at the critical section.

In the case of post-tensioning, the prestressing normally is done by stressing a number of tendons one at a time. Hence, the first tendon stressed is shortened by the subsequent stressing of all other tendons, and the last tendon is not shortened by subsequent stressing. Therefore, in post-tensioning, an average value of stress change can be computed and assumed to affect all tendons equally.

For the case of all prestressing being applied simultaneously (as in pretensioning), the stress in the concrete at the level of the center of gravity of the

prestressed reinforcement (after elastic shortening), f_{ccgps}, resulting from an initial prestressing force (before elastic shortening) P'_j, can be computed from:

$$f_{ccgps} = -\frac{P'_j + n_{ps} f_{ccgps} A_{ps}}{A}\left(1 + \frac{e_{ps} e_{pl}}{r^2}\right) + \frac{M_d e_{ps}}{I} \tag{7-1}$$

which can be written:

$$f_{ccgps} = -\frac{P'_j k_s + A M_d e_{ps}/I}{A + n_{ps} A_{ps} k_s} \tag{7-2}$$

in which:

$$k_s = 1 + \frac{e_{ps} e_{pl}}{r^2} \tag{7-3}$$

In the above, e_{ps} is the eccentricity of the prestressing reinforcement, e_{pl} is the eccentricity of the pressure line due to prestressing only (both e_{ps} and e_{pl} are positive below the centroidal axis), n_{ps} is the modular ratio of the prestressed reinforcement to the concrete, and dead load moments causing tension in the bottom fibers are positive. In the case of statically determinate members, the term k_s becomes:

$$k_s = 1 + \frac{e_{ps}^2}{r^2} \tag{7-4}$$

because the eccentricities of the prestressed reinforcement and the pressure line due to prestressing alone are one and the same. As will be seen in Chapter 10, this may not always be true for statically indeterminate members.

In the case of simple, precast, pretensioned members, the value of f_{ccgps} can be computed at the critical section and the design adjusted accordingly. The critical section may be near the supports with members stressed with straight tendons, or it may be between the supports near the point of maximum moment due to total service load for members with draped tendons. If the critical section is near midspan, a higher jacking force may be permissible without exceeding $0.70\, f_{pu}$ in the prestressed reinforcement immediately after transfer; in other words, it may be possible to increase the jacking stress by the amount of $n_{ps} f_{ccgps}$ (see Sec. 2-15).

For pretensioned members, the value of the stress in the prestressed reinforcement, f_{si}, immediately after elastic shortening is computed from:

$$f_{si} = f'_j + n_{ps} f_{ccgps} \tag{7-5a}$$

in which f'_j is the stress in the prestressed reinforcement due to the force P'_j. In post-tensioned members, as is explained below, the stress in the prestressed reinforcement after elastic shortening is:

$$f_{si} = f'_j + \frac{n_{ps} f_{ccgps}}{2} \tag{7-5b}$$

The initial stress in the concrete at any fiber y from the centroidal axis of a pretensioned or post-tensioned section can be computed from:

$$f_{cy} = -\frac{f_{si} A_{ps}}{A}\left(1 + \frac{e_{pl}\, y}{r^2}\right) \tag{7-6}$$

Equation 7-1 is applicable to members having nonprestressed reinforcement in addition to prestressed reinforcement except that the terms A, e_{ps}, e_{pl}, and I are for the transformed section rather than the gross concrete section.

As stated above, in the case of post-tensioned members having a number of tendons that are stressed sequentially, the stress in the first tendon stressed is reduced slightly by the elastic shortening of each of the tendons stressed subsequently. The stress in the last tendon stressed is not affected by the elastic shortening caused by the other tendons. Hence, the effect of elastic shortening is less than that which occurs when all tendons are stressed simultaneously. In post-tensioned members with several tendons, the effect of elastic shortening generally is taken to be 50 percent of the value of f_{ccgps} computed with eq. 7-1.

It should be recognized that the effect of elastic shortening varies along the length of the member. In simple spans where there may be one section in the span that is most critical from the standpoint of flexural stresses under service load, it is a simple matter to adjust the design for elastic shortening at the critical section. In continuous spans there may be several critical sections along the span, as frequently result from different conditions of loading. Hence, in continuous members one may or may not be able to adjust the stress in the tendons to eliminate reduction in the prestressing force due to elastic shortening to the same degree that is possible in simple span members.

Creep of Concrete

The loss in stress in the prestressed reinforcement resulting from the creep of the concrete also should be computed on the basis of stresses that occur at the critical section for service load flexural stresses rather than for average values of service load flexural stresses, because the greatest margin of safety against cracking generally is needed at the section of maximum moment. In bonded construction, because creep is time-dependent and does not take place to a significant degree until after bond has been established between the prestressed reinforcement and the concrete, the effect of creep on the loss of prestress is not averaged along the tendon length. In the case of post-tensioned construction in which the tendons are not bonded to the concrete after stressing, the effect of creep becomes averaged along the tendon length because the tendon can slip

in the member; and, for this reason, the concrete stress at the average centroid prestressed reinforcement can be used in the computation of this stress loss. Concrete creep is discussed in Secs. 3-13 and 3-14.

Shrinkage of the Concrete

The rate at which concrete shrinks as well as the magnitude of the ultimate shrinkage can be estimated using the data of Secs. 3-11 and 3-12. The entire shrinkage strain is effective in reducing the steel stress in pretensioned construction, but only the amount of shrinkage that occurs after stressing is of significance in post-tensioned members.

Relaxation of Prestressing Reinforcement

The relaxation of prestressing reinforcement is discussed in Sec. 2-10. Three basic methods for estimating the effect of relaxation are available to the structural designer. The first of these is to estimate the effect through the use of information published by the manufacturers of prestressing steel (see Figs. 2-9 and 2-10). The second is to use eqs. 2-1 and 2-2 for estimating the relationship between relaxation, stress levels, and time. The third procedure is to use the methods suggested by Ghali and Trevino, which are discussed in Sec. 2-10.

Friction Loss

Although some authors include the loss of stress due to friction between post-tensioned tendons and their ducts or sheaths with the losses due to the deformation of the materials incorporated in a post-tensioned beam, this is not done in this book. Post-tensioning friction losses are treated in Chapter 16, rather than in this chapter. The accurate evaluation of friction loss requires knowledge of the details given in the post-tensioning placement documents, including the placing plans, the details to be used in the placing, the calculations made for the stressing procedure, and the anchorage set characteristics of the end anchorages that are to be used. In the case of continuous post-tensioned members, however, prudent engineers evaluate friction losses during the design phase. In addition, they specify, in the contract documents, the friction coefficients used in their evaluation, together with the minimum jacking forces at the ends of the tendons that will be accepted during prestressing. This preliminary work, however, does not eliminate the need for the calculations to be redone by the post-tensioning contractor at the time of construction when the actual details of the post-tensioning materials, tendon paths, and equipment are known.

7-3 Computation of Prestress Loss

The computations of the losses of prestress due to the shrinkage and elastic deformation of the concrete, are straightforward, provided that the parameters governing these phenomena are known. The losses due to concrete creep and

relaxation of the prestressing reinforcement are more difficult to determine accurately because they are functions of both time and level of stress. The amount of concrete creep in prestressed concrete varies with the age of the concrete at the time of loading, the stress levels in the concrete, and other factors, as explained in Chapter 3. The amount of relaxation of the prestressing steel is affected by the time-dependent changes in length of the concrete to which the tendons are anchored. In other words, these actions are interdependent.

Numerous methods of providing for the loss of prestress have been used over the years. These have included the use of lump sums (e.g., 35,000 and 25,000 psi, for pretensioned and post-tensioned reinforcement, respectively); methods based upon average values of the several parameters; and, step-function methods based upon basic relationships for concrete creep, shrinkage, and elastic modulus, prestressed reinforcement relaxation, and the effects of time. The prestressed concrete designer must select and use a method that, based upon his or her own knowledge and experience, is applicable for the type of design work at hand (ACI–ASCE Joint Committee 323 1958; AASHTO 1989; PCI Committee on Prestress Losses 1975; Zia, Preston, Scott, and Workman 1979; Branson 1974; Ghali 1986; and Subcommittee 5, ACI Committee 435 1963).

Prestress loss recommendations of the PCI Committee on Prestress Losses, the American Association of State Highway and Transportation Officials, and the method recommended by Zia et al. are included herein in Appendixes A, B, and C. Readers should become familiar with these methods and use them in their design work as they deem appropriate.

In the more sophisticated methods of analysis, the creep and recovery deformations of the concrete have been modeled by using the rate-of-creep principle or the superposition principle, as described in ACI 435.1R, or the principles described by Neville, Dilger, and Brooks (1983). These methods are illustrated in Figs. 7-1, 7-2, and 7-3, respectively. The rate-of-creep method assumes that

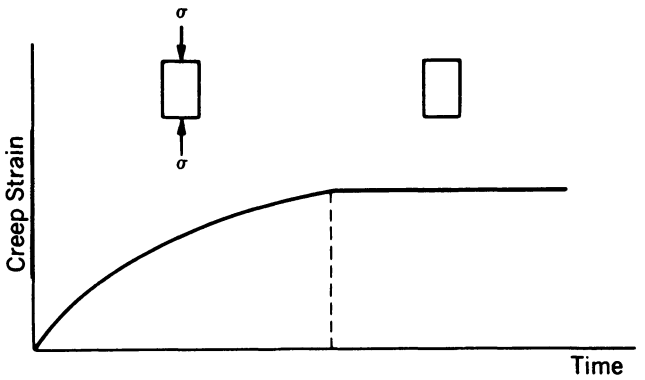

Fig. 7-1. Creep strain by the rate-of-creep method.

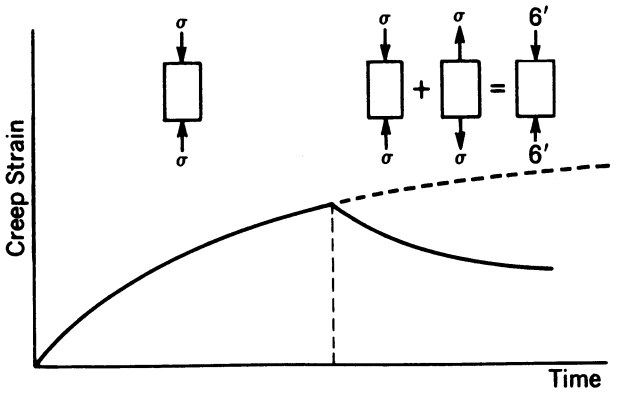

Fig. 7-2. Creep strain by the superposition method.

the creep deformation at time t is equal to the product of the stress and the ordinate of the specific creep curve corresponding to time t. Once the stress is removed, there is no further change in the creep deformation. The superposition method predicts the same initial deformations as the rate-of-creep method, but assumes that the member is subjected to a tensile stress that is equal in magnitude, but of opposite sign, upon removal of the original stress. Furthermore, the superposition method assumes that the concrete sustains further creep deformation under the original load and additional time-dependent creep recovery under the fictitious tensile stress applied to counteract the original compressive stress. The creep-recovery model described by Neville et al. includes an instantaneous deformation and time-dependent recoveries after removal of a load. The creep–time deformation characteristics of concrete normally are assumed to be identical, but of opposite sign, in tension and in compression.

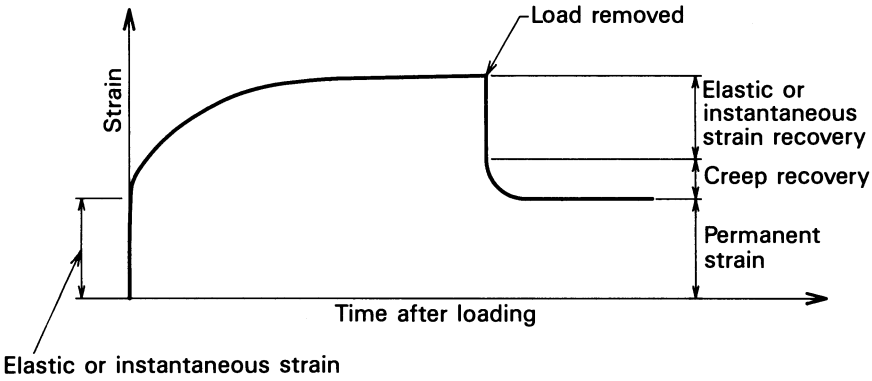

Fig. 7-3. Deformation of concrete as a function of time, illustrating instantaneous deformation, creep deformation, instantaneous recovery, creep recovery, and permanent deformation.

The Neville model is believed to be the most accurate method, but its use, which is more laborious than the rate-of-creep and superposition methods, is considered to be worthwhile only when the creep and other properties of the materials are carefully selected, high precision is desired, and the computations can be performed by computer or programmable calculator.

A method of computing the stress loss that is considered to be among the more accurate procedures uses a numerical integration procedure that treats the several variables as interdependent time functions. This method utilizes mathematical relationships that define the creep–time function of the concrete creep phenomenon, the concrete shrinkage–time function, and the prestressing reinforcement relaxation–time function for the materials that are to be used. With this procedure, the incremental changes in stress in the concrete and reinforcement (both prestressed and nonprestressed) are computed for short time intervals and the effects integrated over a specific period of time. The individual phenomena are treated as time-dependent step functions to facilitate the computations (ACI Committee 435 1963). The effect of cracking can be included in this type of analysis, following the procedures described below in Sec. 7-5.

The following basic assumptions are made in employing the numerical integration method for predicting prestress losses, as well as in computing deflections (see Sec. 7-4).

1. The initial stresses in the member under consideration are known.
2. The specific creep versus time relationship for the concrete under constant stress is known and can be approximated with sufficient accuracy with a step function.
3. Creep deformations of the concrete are proportional to the concrete stress at up to 50 percent of the concrete strength.
4. The shrinkage versus time relationship is known for the concrete under consideration and can be treated as a step function.
5. The shrinkage characteristics of the concrete are uniform over the section.
6. The stress–strain relationship for the concrete is linear at up to 50 percent of the flexural strength for loads of short duration.
7. Strains vary linearly over the depth of the section; that is, plane sections remain plane.
8. The relaxation versus time relationship for the prestressed reinforcement is known and can be treated as a step function.
9. The stress–strain relationships for prestressed and nonprestressed reinforcement are linear under short-duration loads.

This method lends itself to solution by programmable calculator or computer. The accuracy of the computations should be enhanced through the use of many short time increments (one day, for example) rather than fewer and longer time increments.

The numerical integration procedure described above is not widely used in computing the loss of prestress, for several reasons. If done without the assistance of an electronic device, the computations are tedious and time-consuming, and mathematical errors are easily made. In addition, the designer frequently does not have specific data for the creep, shrinkage, and elastic properties for the concrete or relaxation information for the reinforcement that actually will be used in a project. Consequently, the use of the more sophisticated method frequently cannot be justified. On important projects, however, the designer can use this method to study losses of prestress (and deflections) for several combinations of concrete and reinforcement properties, and to determine upper and lower bounds for the loss of prestress (and deflection). This method is recommended for the analysis of concrete structures constructed segmentally (See Secs. 8-3, 10-9 and 14-5).

ILLUSTRATIVE PROBLEM 7-1 Compute the loss of prestress for the composite bridge girder shown in Fig. 7-4. Use the numerical integration method of analysis.

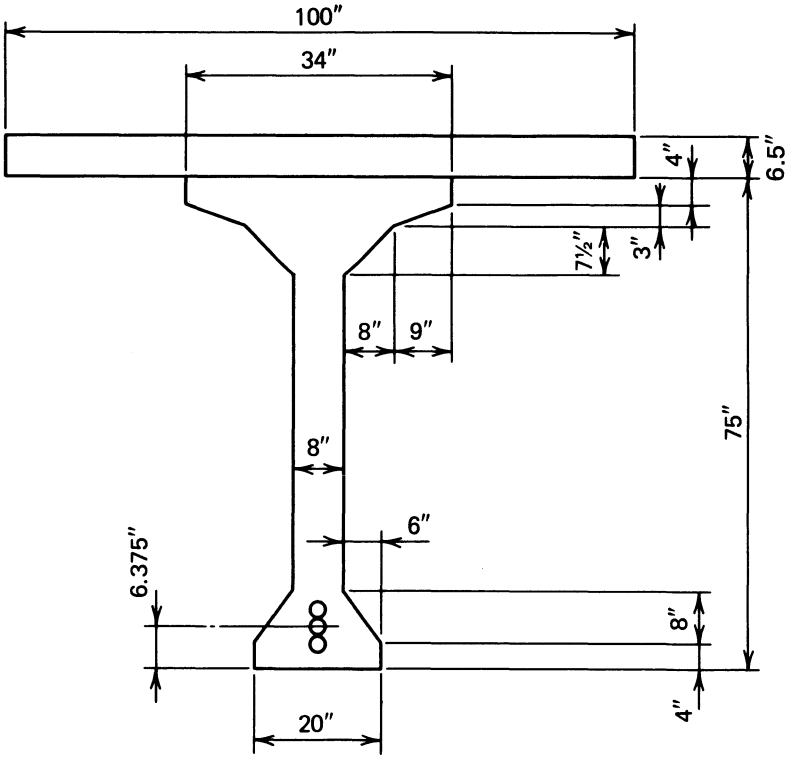

Fig. 7-4. Cross section of beam used in I.P. 7-1.

The concrete parameters are:

Concrete type	Precast	CIP
Compressive strength at 28 days (ksi)	5,500	5,000
Unit weight (pcf)	115	114
Concrete elastic modulus coefficient (eq. 3-4)	26	26
Ultimate concrete shrinkage, millionths of in./in.	350	300
Creep ratio	1.5	—

Time-dependency parameters for the concrete are:

Strength (eq. 3-1)	a	2.24	2.24
	β	0.92	0.92
Shrinkage (eq. 3-21)	α	1.00	1.00
	f	35.00	35.00
Creep (eq. 3-25)	ψ	0.60	—
	d	10.00	—

The properties of the prestressed reinforcement are as follows:

$$f_{pu} = 270 \text{ ksi}$$

$$f_{py} = 247 \text{ ksi}$$

$$f_{si} = 189.5 \text{ ksi (after elastic shortening of concrete)}$$

$$E_{ps} = 27{,}800 \text{ ksi}$$

$$A_{ps} = 5.52 \text{ sq. in.}$$

$$A_{\text{DUCTS}} = 16.23 \text{ sq. in.}$$

Assume that the relaxation of the prestressing steel can be predicted by eq. 2-1.

The construction time sequence is as follows:

End precast cure: 7 days after girder cast—shrinkage begins
Prestress: 12 days after girder cast—creep begins
Cast slab: 197 days after girder cast
End slab cure: 204 days after girder cast
Apply SDL: 206 days after girder cast
End analysis: 600 days after girder cast

Midspan section properties are as follows:

	Area *(in.^{2})*	*I* *(in.^{4})*	y_t *(in.)*	y_b *(in.)*
Net precast	949	625158	−30.87	44.12
Transformed, net precast	1013	710047	−33.23	41.76
Transformed, composite	1637	1226561	−19.32	55.67

TABLE 7-1 Summary of the Loss of Prestress Computations for I.P. 7-1.

Time (days)	Steel stress (ksi)	Concrete Fiber Stresses (ksi) Beam			Slab		Rotation $\times 10^6$
		Bottom	CGS	Top	Bottom	Top	
12	+189.5	−2.588	−2.373	−0.062			14.67
197	+144.5	−1.825	−1.689	−0.228			21.26
197′	+152.9	−0.923	−0.925	−0.946			12.62
206	+152.7	−0.919	−0.922	−0.949	+0.020	−0.010	11.41
206′	+154.3	−0.756	−0.777	−1.006	−0.035	−0.086	11.41
600	+149.4	−0.670	−0.701	−1.038	+0.159	−0.184	10.24

The midspan moments are as follows:

Due to precast D.L.: 1535 k-ft
Due to slab D.L.: 1278 k-ft
Due to superimposed D.L.: 300 k-ft

SOLUTION: The numerical integration method, as described in Sec. 7-2, was used to solve this problem, with a programmable calculator used to facilitate the computations. The computed values are shown in Table 7-1, from which it will be seen that the computed loss of stress is 40.1 ksi at 600 days. Note that values are given for the stress remaining in the steel, the concrete stresses in the top and bottom fibers of the precast section, and of the slab, as well as for rotation of the section. (The rotation is used in deflection calculations, as described in Sec. 7-4.) Two sets of data are given for day 197 and 206—for before and after the application of the cast-in-place slab and the superimposed dead load, respectively. In this example, the limiting value for loss of prestress was taken to be reached at 600 days; a more realistic time would be 1200 or 1600 days.

Another approach to the computation of the loss of prestress has been proposed by Ghali and others (Ghali and Trevino 1985; Ghali and Tadros 1985; Ghali 1986). The method is relatively simple to apply, but the use of a small special-purpose computer with programs dedicated to this calculation facilitates the computations (Ghali and Elbadry 1985). The method can be applied to fully prestressed members and partially prestressed members (see Sec. 7-5), as well as nonprestressed members. It relies upon ordinary computation procedures that are somewhat complicated by the need to use the net, net-transformed, transformed, and age-adjusted transformed section properties at different steps of the process. Prestress loss can be determined for prestressed members that contain prestressed and nonprestressed reinforcement, whether fully prestressed or not. The method relies upon basic strain compatibility and equilibrium principles, without the use of empirical relationships.

The procedure is based upon computing the strains and stresses at the section under consideration, beginning at the time of first loading and ending after a specific time interval. Also, the computations sometimes are made at specific points in time that mark notable events in the loading history of the member under study. The most simple of the loading histories consists of a single time interval that begins with the application of the member's dead load simultaneously with its prestressing and ends, after a long period of time, when the effects of creep and shrinkage are considered to have reached their ultimate values. A more complicated history, which must be divided into two separate analyses, includes the application of a second increment of dead load at some point in time after prestressing and the application of the dead load of the member itself.

The fundamental process involves an evaluation of the effects of concrete creep, concrete shrinkage, and relaxation of the prestressing steel over the time increment by the following steps:

1. Determine the stress and strain, with respect to a reference axis, due to the effects of dead load and the initial prestressing force using the net-transformed section properties (i.e., prestressed reinforcement not bonded to the section). The reference axis may be located at the centroidal axis of the net-transformed section or at some other convenient location. Because different section properties are used at various points in the analysis, the location of the centroidal axis, with respect to the top and bottom extreme fibers, varies as the analysis progresses. For this reason the computations may be facilitated by using the sections properties computed with respect to the reference axis located at the top of the member (top of the composite member if a slab or other element is to be added to the original section at another point in the analysis).
2. Determine the amount of concrete creep and shrinkage deformation that would occur if not restrained between the time of prestressing (beginning of the analysis time period) and the end of the time interval under consideration. In addition, determine the amount of the relaxation of the prestressed reinforcement during the time interval under consideration. The end of the time period considered may or may not coincide with the application of another increment of load.
3. The time-dependent deformations due to concrete creep and shrinkage are assumed to take place at a slow rate during the time interval under study. It is further assumed that these deformations are artificially restrained by stresses in the *net concrete section alone* and are a function of the age-adjusted elastic modulus for the concrete (for the period of time under consideration). The restraining stresses have resultant forces and moments (taken with respect to the reference axis) due to concrete creep and shrinkage that can be computed as follows:

$$\Delta N_{creep} = -E_{ca}\delta v\,[A_n\epsilon_{rat} + A_n y\psi_t] \tag{7-7}$$

$$\Delta M_{creep} = -E_{ca}\delta v\,[A_n y\epsilon_{rat} + I_n\psi_t] \tag{7-8}$$

$$\Delta N_{shrinkage} = -E_{ca}\delta\epsilon_{sht}A_n \tag{7-9}$$

$$\Delta M_{shrinkage} = -E_{ca}\delta\epsilon_{sht}A_n y \tag{7-10}$$

in which A_n, $A_n y$, and I_n are the net area, first moment of the net area, and moment of inertia of the net area of the concrete section (exclusive of prestressed and nonprestressed reinforcements), respectively, with respect to the reference axis. E_{ca} is the age-adjusted elastic modulus of the concrete, δv is the increment of the creep ratio for this time period under consideration, ϵ_{rat} is the strain at the reference axis at the beginning of the time period under consideration, $\delta\epsilon_{sht}$ is the unrestrained or free shrinkage deformation of the concrete for the time period under consideration, and ψ_t is the curvature (slope of the strain diagram) at the beginning of the time period under consideration. The concrete shrinkage deformation is assumed to be uniform over the depth of the section. The concrete strain due to the relaxation of the prestressed reinforcement, during the time period under consideration, can be taken into account with the following force and moment:

$$\Delta N_{relaxation} = \sum (A_{ps}\Delta f_{psr}) \tag{7-11}$$

$$\Delta M_{relaxation} = \sum (A_{ps}y_{ps}\Delta f_{psr}) \tag{7-12}$$

in which A_{ps}, Δf_{psr}, and y_{ps} are the area, relaxation loss of stress, and distance from the reference axis to the individual layers of the prestressed reinforcement, respectively.

The total force, ΣN, and moment, ΣM, required to prevent the deformations due to creep and shrinkage, including the effect of relaxation of the force in the prestressed reinforcement, are equal to the sums of the above equations for change in force and change in moment (eqs. 7-7 through 7-12).

4. The effect the artificial restraining force and moment, as described in step 3, on the actual reinforced concrete member is taken into account by applying them *in the reverse direction* (i.e., $-\Sigma N$ and $-\Sigma M$) to the age-adjusted transformed section of the member. The use of the age-adjusted transformed section accounts for the presence of the prestressed and nonprestressed reinforcements as well as the fact that the concrete creep and shrinkage and the relaxation of the prestressed reinforcement take place slowly over a period of time.

5. The strain at the reference point and the curvature at the section under consideration, at the end of the time period under consideration, are determined by summing the strains and curvatures determined in the first and fourth steps of the above analysis. The stress at the reference point and the slope of the stress diagram, γ, are determined by summing the stresses obtained in the first, third, and fourth steps of the analysis.

The use of this procedure is illustrated in illustrative problems at the end of this section.

Ghali has shown that the computations of stresses and strains in reinforced concrete members containing prestressed and nonprestressed reinforcements are facilitated, when the effects of time on concrete properties (i.e., creep, shrinkage, instantaneous elastic modulus, and age-adjusted modulus of concrete) are taken into account, by computing the section properties of the cross sections under consideration with respect to an axis that does not pass through the centroid of one of the cross sections used in the analysis (see Sec. 9-2) (Ghali 1986). When this is done, the concrete strain at the location of the reference axis, ϵ_{cra}, is computed as:

$$\epsilon_{cra} = \frac{I_{ra}N - (Ay)_{ra}M}{E_c[AI_{ra} - (Ay)_{ra}]} \tag{7-13}$$

and the curvature at the section, ψ, can be determined from:

$$\psi = \frac{-(Ay)_{ra} + AM}{E_c[AI_{ra} - (Ay)_{ra}]} \tag{7-14}$$

in which I_{ra} is the moment of inertia of the section with respect to the reference axis, $(Ay)_{ra}$ is the first moment of the area with respect to the reference axis, A is the area of the section, N is the axial force applied at the reference axis, and M is the moment of the resultant force acting on the section with respect to the reference axis.

It should be noted that the term for the first moment of the area with respect to the reference axis in eqs. 7-13 and 7-14, $(Ay)_{ra}$, is equal to zero if the reference axis passes through the centroid of the area, and, noting that $\gamma = E_c\psi$, eqs. 7-13 and 7-14 can be written:

$$N = A\epsilon_{cra}E_c = f_{cra}A \tag{7-15}$$

$$M = \psi E_c I = \gamma I \tag{7-16}$$

in which I is the moment of inertia of the section about its centroid.

ILLUSTRATIVE PROBLEM 7-2 Using the general method proposed by Ghali et al., compute the loss in prestress for the pretensioned, T-shaped beam having the dimensions and reinforcements at midspan shown in Fig. 7-5. Assume, at the time of prestressing, that the concrete strength is 3000 psi, and the elastic modulus is 3122 ksi. Assume that the ultimate concrete shrinkage is 800×10^6 in./in., and the ultimate creep ratio is 2.00. The areas of the nonprestressed reinforcements are 1.00 in.^{2} for the upper layer and 4.00 in.^{2} for the lower

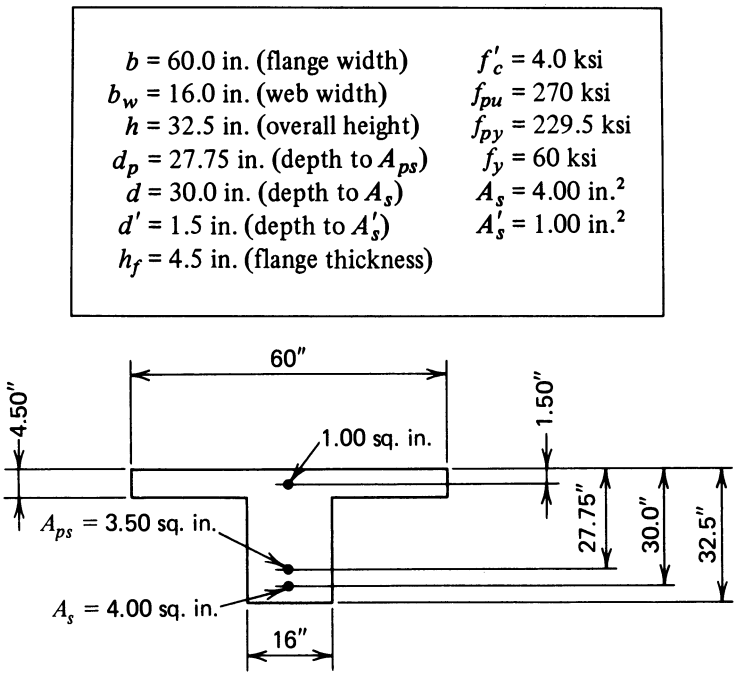

Fig. 7-5. Cross section of T-beam having compression reinforcement.

layer. The area of the prestressed reinforcement is 2.00 in.^{2}. The initial stress in the prestressed reinforcement, after elastic shortening, is 189 ksi, and the ultimate reduced relaxation of the prestressed reinforcement is taken to be 9.1 ksi. The beam, which has a self weight of 748 plf, is to be used on a span of 40 ft, and will not support superimposed dead loads but will be subjected to occasional uniformly distributed live loads of 750 plf applied for short durations. The section properties of the net, net-transformed, transformed, and age-adjusted transformed sections, with respect to the top fibers of the sections (the reference axis), using elastic moduli of 28 and 29 $\times$ 10^6 psi for the prestressed and nonprestressed reinforcement, respectively, and an age-adjusted elastic modulus for the concrete of 1200 ksi, are given in Table 7-2.

SOLUTION: The first step in the procedure requires the determination of the stresses in the concrete under the effects of initial prestressing and beam dead load. The initial force in the prestressed reinforcement (after elastic shortening of the concrete) is 189 ksi $\times$ 2.00 in.^{2} = 378 kips, and the midspan moment due to initial prestressing and the dead load of the beam, with respect to the reference axis, is:

TABLE 7-2 Section Properties for I.P. 7-2.

Section	Area ($in.^2$)	First Moment of the Area ($in.^3$)	Second Moment of the Area ($in.^4$)
Net	711.0	8718.5	179,277.5
Net-transformed	757.5	9847.1	212,738.5
Transformed	775.4	10,344.9	226,551.3
Age-adjusted transformed	878.6	12,949.8	302,268.2

$$378 \times 27.75 = -10{,}489.5 \text{ kip-in.}$$

$$\frac{0.748 \times 40^2 \times 12}{8} = +1{,}795.2 \text{ kip-in.}$$

$$\text{Total} = -8{,}694.3 \text{ kip-in.}$$

The initial stresses in the top and bottom fibers of the concrete due to prestressing and the dead load of the beam, using the net-transformed section, are +81 and −1369 psi, respectively, and the slope of the stress diagram, γ, is −44.6 psi/in. Note that the net-transformed section was used in determining the initial stresses (i.e., prestressed reinforcement not bonded and the nonprestressed reinforcement bonded to the concrete) because the stress of 189 ksi in the prestressed reinforcement is specified to be the stress after elastic shortening of the concrete. The initial strain in the top fiber is $+25.9 \times 10^{-6}$ in./in., and the initial curvature, ψ, is -14.3×10^{-6} $in.^{-1}$. The initial stress and strain diagrams determined in step 1 are shown in Fig.7-6.

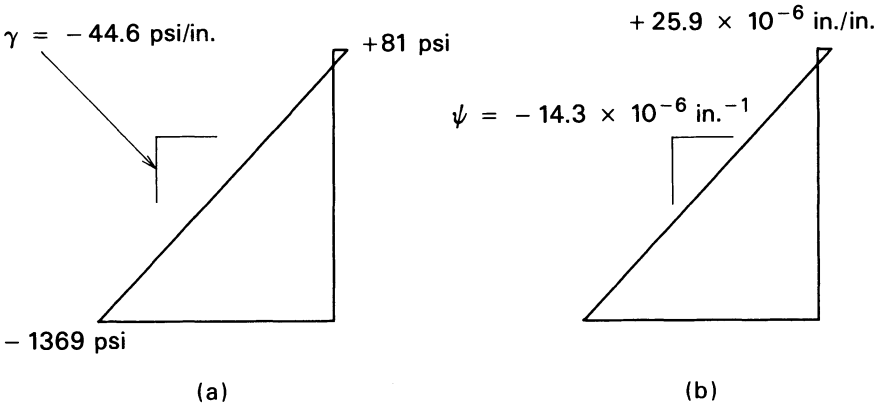

Fig. 7-6. Initial stress and strain diagrams for I.P. 7-2. (a) Stress distribution. (b) Strain distribution.

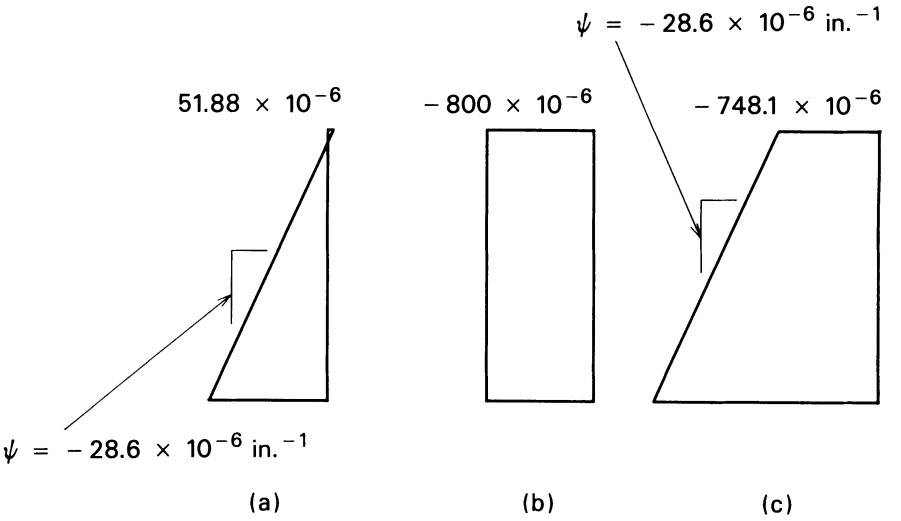

Fig. 7-7. Unrestrained creep, shrinkage, and total deformation for I.P. 7-2. (a) Creep deformation. (b) Shrinkage deformation. (c) Total deformation.

The concrete shrinkage that could occur over the time interval, if free to do so without restraint, is 800 millionths in./in., and it would be the same (uniform distribution) over the full depth of the cross section. The unrestrained creep deformation, which varies over the depth of the member, is equal to the product of the initial strain in the concrete and the increment of the ultimate creep ratio that occurs during the time period under consideration. These deformations are illustrated in Fig. 7-7. By using these values for concrete shrinkage and creep, the resultant forces and moments required to restrain the free concrete shrinkage and creep can be determined from eqs. 7-7 through 7-10. In a similar manner, the resultant force and moment required to compensate for the effect of the relaxation of the prestressing steel that takes place over the time interval are computed by using eqs. 7-11 and 7-12. The forces and moments required for the restraints are found to be as follows:

$$\Delta N_{creep} = 254.9 \text{ kips} \qquad \Delta M_{creep} = 5610 \text{ in.-kips}$$

$$\Delta N_{shr} = 683.0 \text{ kips} \qquad \Delta M_{shr} = 8375 \text{ in.-kips}$$

$$\Delta N_{relax} = -18.2 \text{ kips} \qquad \Delta M_{relax} = -505.0 \text{ in.-kips}$$

$$\Sigma N = 919.7 \text{ kips} \qquad \Sigma M = 13480 \text{ in.-kips}$$

By using these values for ΣN and ΣM, the time-dependent changes in strain and stress are found to be as shown in Fig. 7-8, and the strain and stress diagrams after the time-dependent change are as illustrated in Fig. 7-9. (*Note*: The strain

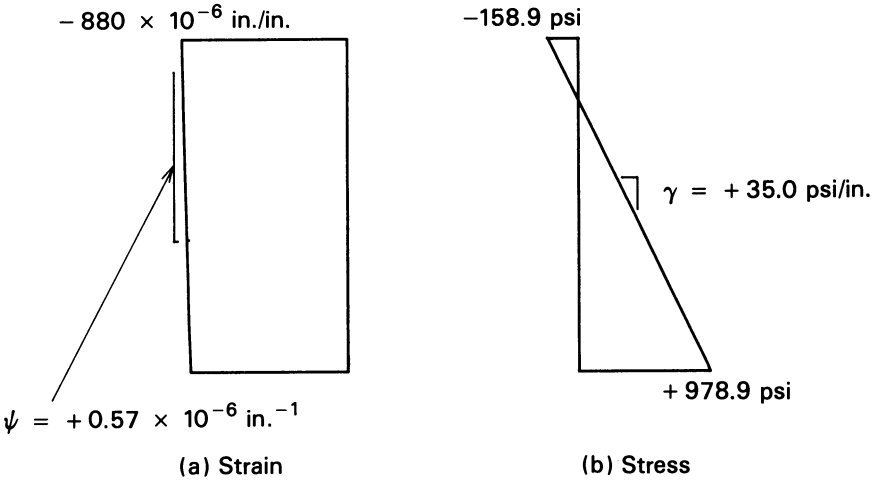

Fig. 7-8. Time-dependent changes in stress and strain in I.P. 7-2. (a) Strain. (b) Stress.

at the reference axis and the curvature in Fig. 7-9 are the sums of those values shown in Figs. 7-6 and 7-8. Also, the stresses and the slope of the stress diagram shown in Fig. 7-9 are the sums of the values shown in Figs. 7-6 and 7-8.)

The live load of 750 plf that is applied to the beam causes a midspan moment of 1800 in.-kips. When it is applied to the beam after the concrete creep and shrinkage, as well as the relaxation of the prestressed reinforcement, have reached their maximum values, the strains and stress diagrams at midspan are as shown in Fig. 7-10.

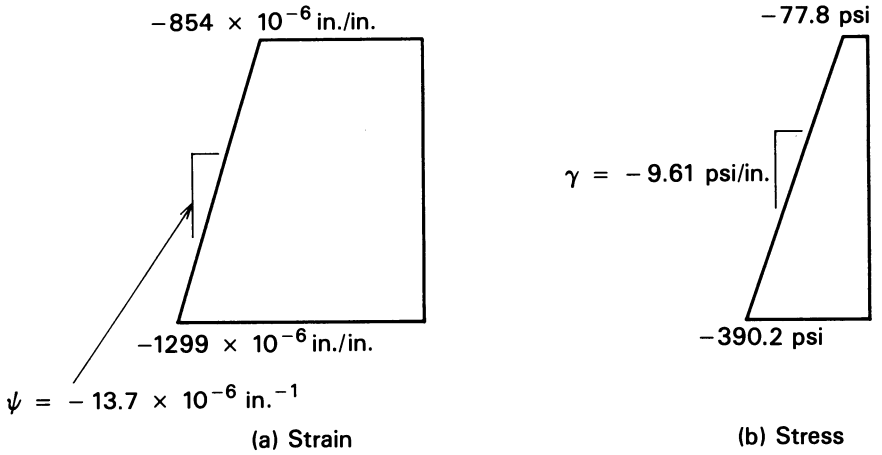

Fig. 7-9. Strain and stress distributions after time-dependent change for I.P. 7-2. (a) Strain. (b) Stress.

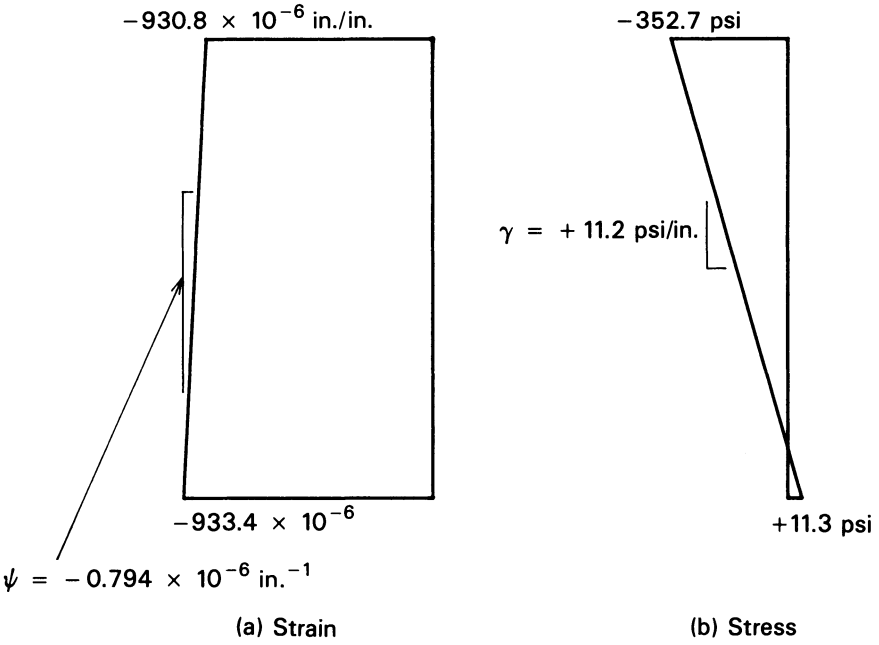

Fig. 7-10. Strain and stress distributions at midspan after all losses of prestress for I.P. 7-2. (a) Strain. (b) Stress.

The loss-of-prestress computations are completed by determining the stresses and forces in the reinforcements and the concrete under different states—in this case, (1) the first or initial state (i.e., at the time of prestressing when the beam dead load alone is acting with the prestressing force); (2) the second or ultimate state (i.e., at the time when the creep and shrinkage deformations in the concrete and the relaxation in the prestressed reinforcement have reached their maximum values, and live load is not present); and (3) the third state, a transient state consisting of the second state but including the short-term effects of the live load. The computations for the stresses and forces in the reinforcements are summarized in Table 7-3. The force in the concrete is equal to and opposite the sums of the forces in the reinforcements. The forces in the concrete for the three states can be summarized as follows:

State 1	−331.41 kips
State 2	−139.16 kips
State 3	−153.16 kips

A review of the forces in the prestressed reinforcement will show that the force in the prestressed reinforcement is on the order of 82 to 84 percent of its

TABLE 7-3 Summary of Stresses and Forces in the Nonprestressed and Prestressed Reinforcements in the Beam Analyzed in I.P. 7-2.

	Reinf. Stress and Force (KSI and KIPS)					
	Nonprestressed				Prestressed	
	Upper Layer		Lower Layer			
State	Stress	Force	Stress	Force	Stress	Force
Initial (1)	+0.13	+0.13	−11.68	−46.72	+189.00	+378.00
Ultimate (2)	−25.38	−25.38	−36.71	−146.84	+155.69	+311.38
Transient (3)	−27.34	−27.34	−33.90	−135.60	+158.02	+316.10

initial value in this particular case. A review of the forces in the concrete summarized above will show that under States 2 and 3 the force in the concrete is on the order of 42 to 46 percent of the initial force in the concrete in this case.

The general method proposed by Ghali and his colleagues can be used to calculate the loss of prestress in members that are constructed sequentially, such as precast elements having composite toppings, as well as members constructed in a single monolith. The major difference in the analysis of a simple beam that has a composite topping, when compared to a member that does not, involves the treatment of the differences in the creep and shrinkage timetables of the two different concretes. This is illustrated in I.P. 7-3, in which the computer program Crack was used to facilitate the computations (Ghali and Elbadry 1985).

ILLUSTRATIVE PROBLEM 7-3 For the beam used in I.P. 7-2, assume that a composite concrete topping 4 in. thick is placed upon the top of the beam 28 days after the prestressing of the beam. Assume that the ultimate shrinkage of the concrete topping is 800×10^{-6} in./in., and its ultimate creep ratio is 2.5. Assume that 40 percent of the shrinkage and 40 percent of the creep have occurred in the beam at the age of 28 days, and the remainder of each occurs before the application of a short-term transient live load that results in a midspan moment of 4000 in.-kips. Determine the stresses and forces in the reinforcements at the time of stressing, at the age of 28 days, and after concrete creep and shrinkage have reached their ultimate values.

SOLUTION: The problem is solved by following the basic procedures used in I.P. 7-2. The single major difference is that an additional step must be added to the analysis at the age of 28 days after the time of prestressing, in order to take the effect of the weight of the cast-in-place slab into account, as well as to

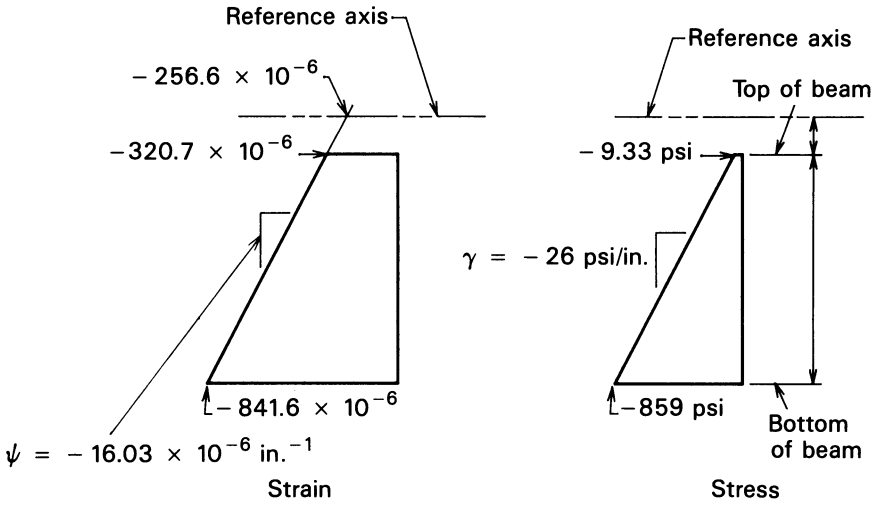

Fig. 7-11. Strain and stress distributions at midspan of the beam of I.P. 7-3 at State 1 (time = 28 days, prestress plus beam dead load).

initiate the effect of composite action and shrinkage of the concrete in the concrete topping. To facilitate the computations, the concrete is assumed to be cured, and shrinkage is presumed to commence, at the same instant that the topping is placed (at the age of 28 days after prestressing of the beam). It should be noted that the creep of the concrete topping will not have an influence on the computations unless an additional step is introduced between the time of

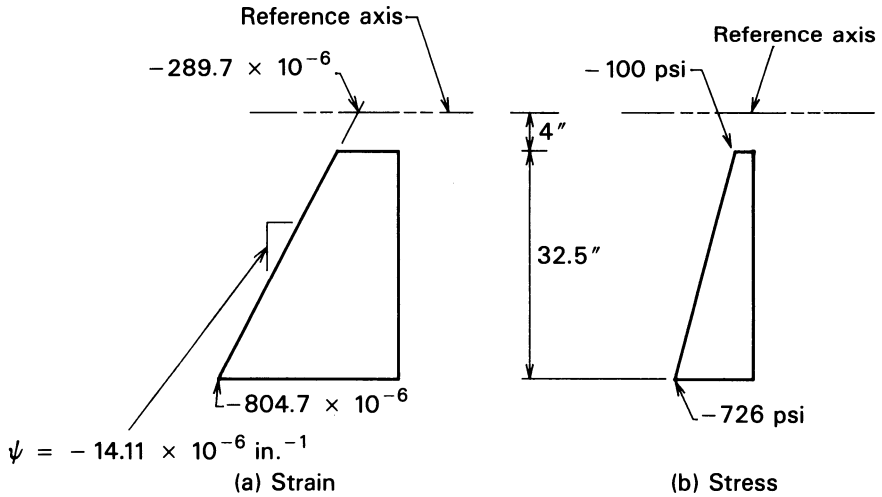

Fig. 7-12. Strain and stress distributions at midspan of the beam of I.P. 7-3 at State 2 (time = 28 days, prestress plus beam dead load plus slab dead load).

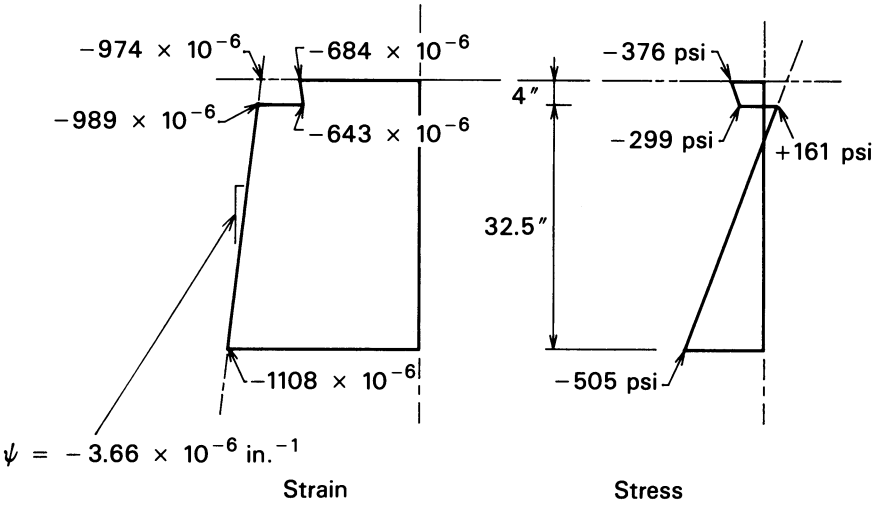

Fig. 7-13. Strain and stress distributions at midspan of the beam of I.P. 7-3 at State 2 (time = ∞, prestress plus beam and slab dead loads).

placing the topping and the time when the effects of creep and shrinkage of the two concretes reach their ultimate values. The strain and stress diagrams for the section at midspan for the various steps in the analysis are illustrated in Figs. 7-11 through 7-14. The stresses and forces in the reinforcement layers are summarized in Table 7-4. The forces resisted by the concrete are summarized for the various steps as follows:

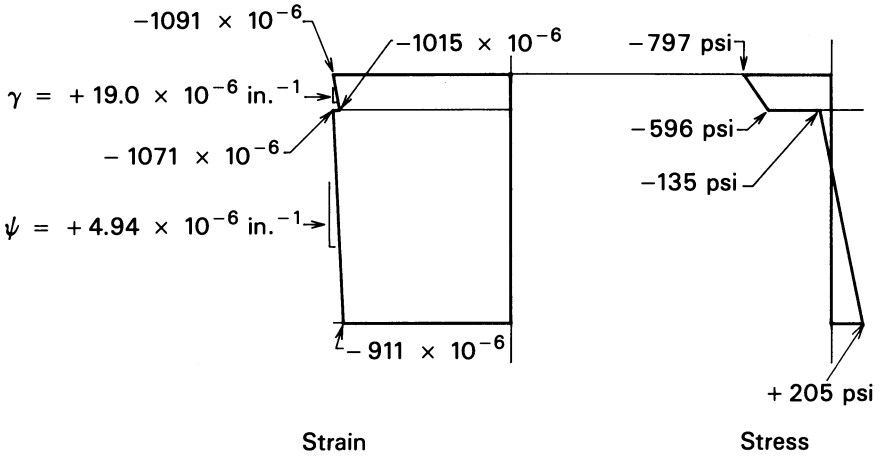

Fig. 7-14. Strain and stress distributions at midspan of the beam of I.P. 7-3 at State 3 (time = ∞, prestress plus beam, slab, and live loads).

TABLE 7-4 Summary of Stresses and Forces in the Nonprestressed and Prestressed Reinforcements in the Beam Analyzed in I.P. 7-3.

	Reinf. Stress and Force (KSI and KIPS)					
	Nonprestressed				Prestressed	
	Upper Layer		Lower Layer			
State	Stress	Force	Stress	Force	Stress	Force
Initial (1) 28-Day	+0.13	+0.13	−11.68	−46.72	+189.00	+378.00
W/O Slab (1)	−10.00	−10.00	−23.25	−93.00	+168.84	+337.68
W/Slab (2)	−10.65	−10.65	−22.31	−89.24	+169.63	+339.26
Ultimate						
W/O L. Load (2)	−28.84	−28.84	−31.86	−127.44	+150.65	+301.30
W/L. Load (3)	−30.85	−30.85	−26.77	−107.08	+155.02	+310.04

Initial	−331.31 kips
28 days	
W/O Slab	−234.68 kips
W/Slab	−239.37 kips
Ultimate	
W/O L. load	−145.02 kips
W/L. load	−172.11 kips

The force in the prestressed reinforcement in the ultimate state is on the order of 80 percent of the initial force. The force resisted by the concrete in the ultimate state is from 44 to 52 percent of the initial force, depending upon whether the live load is acting or not.

Ghali, Tadros and Trevino derived a method of determining the loss of prestress for members that have all of the reinforcement, both prestressed and nonprestressed, either in one layer or concentric with the concrete section (Ghali and Tadros 1985; Ghali and Trevino 1985). The method is more easily applied that the general method described above and gives the same results as the general method when the conditions described above exist. This method is based upon the recognition that the loss of prestress can be expressed as:

$$\Delta C + \Delta P_{ps} + \Delta P_{ns} = 0 \qquad (7\text{-}17)$$

in which the three terms represent changes in the forces in the concrete, the prestressed reinforcement, and the nonprestressed reinforcement during an increment of time. It should be recognized that the loss of prestress normally results in a reduction in the compressive force in the concrete, a reduction in

the tensile force in the prestressed steel, and an increase in the compression (or reduction in the tension) in the nonprestressed reinforcement. With the sign convention used in this book, as explained in Sec. 4-2, an incremental change in a tensile force that increases the tensile force is positive, and one that decreases the tensile force is negative. In a similar manner, an incremental change that decreases a compressive force is positive, and one that increases a compressive force is negative. Therefore, in the normal case, ΔC in eq. 7-17 is positive, and the other two terms are negative. In this method the change in the compressive force resisted by the concrete can be expressed as:

$$\Delta C = -\beta\left[\delta v f_{cst} n A_{st} + \delta\epsilon_s (E_{st} A_{st}) + L_{rr} A_{ps}\right] \tag{7-18}$$

in which:

$$\beta = \frac{1}{\left[1 + \dfrac{k_s n A_{st}}{A_c}(1 + \chi\delta v)\right]} \tag{7-19}$$

and:

δv = Incremental creep coefficient for the time period commencing at prestressing, t_p, and ending at the time, t_e, selected for terminating the analysis.

f_{cst} = Initial stress in the concrete, at the location of the center of gravity of the combined areas of the prestressed and nonprestressed steels, due to prestressing and the dead load acting at the time of prestressing, based upon the properties of the transformed, net concrete section.

n = The ratio of the modulus of elasticity of the steel, using a single value for the prestressed and nonprestressed steel, and the elastic modulus of the concrete at the time of prestressing.

A_{st} = The sum of the areas of the prestressed and nonprestressed (tension and compression) reinforcements; that is, $A_{st} = A_{ps} + A_s + A'_s$.

$\delta\epsilon_s$ = Increment of concrete shrinkage occurring from the time of prestressing, t_p, until the time selected for terminating the analysis, t_e.

E_{st} = The elastic modulus selected to represent the elastic properties of the prestressed and nonprestressed reinforcement; namely, a single value between 28×10^6 and 30×10^6 psi.

L_{rr} = The reduced relaxation of the prestressing steel (see eq. 2-3, in Sec. 2-10).

$k_s = 1 + \dfrac{e^2}{r^2}$; for use in computing β.

r = Radius of gyration of the net or transformed, net concrete section with respect to its centroid as appropriate.

χ = Concrete aging coefficient (see Sec. 3-8) for the concrete for the time increment between t_p and t_e.
A_c = The net or transformed, net area of the concrete section as appropriate (see Sec. 4-10).
t_p = Time of prestressing.
t_e = Time at the end of the analysis.

The three terms within the brackets of eq. 7-18 are factors that determine the effect of concrete creep, concrete shrinkage, and relaxation of the prestressing steel, respectively, on the loss of prestress. The dimensionless coefficient β is intended to reduce the full effects of the three terms within the brackets in order to correct for the effects of concrete creep and the areas and locations of the prestressed and nonprestressed reinforcement in the section.

In applying the method proposed by Ghali and Trevino, a value of χ, the concrete aging coefficient, must be assumed at the outset of the computations and checked when they are completed. If the assumed value differs significantly from the value computed upon completion of the computations, a new value of χ should be assumed and the computation repeated. Normally, only one iteration is needed to obtain acceptable accuracy.

After the value of ΔC has been determined, the combined effect of creep, shrinkage, and the change in ΔC on the distribution of strain on the section as well as on the curvature can be determined. The effect of the compressive force, ΔC, on the strain at the centroid of the section can be computed from:

$$\Delta\epsilon_{ci} = \delta v\epsilon_{ci} + \delta\epsilon_{si} + \frac{\Delta C}{E_{cae}A_{nt}} \tag{7-20}$$

in which the first term on the right is used for the effect of concrete creep, and ϵ_{ci} is the initial strain in the concrete; the second term represents the effect of concrete shrinkage; and the third term gives the effect of the change in the force on the section, during the time increment. The term E_{cae} represents the age-adjusted elastic modulus of the concrete. The effect on the initial curvature, ψ_i, can be determined from:

$$\Delta\psi_i = \delta v\psi_i + \frac{\Delta Ce_c}{E_{cae}I_{nt}} \tag{7-21}$$

where e_c is the eccentricity of ΔC with respect to the centroid of the section.

It will be noted that in eq. 7-21 concrete shrinkage is not included. This is so because concrete shrinkage does not affect the curvature of the section. The incremental change in concrete stress at any point in the section, located at a distance y from the centroid axis of the net, transformed concrete section, can be determined from:

$$\Delta f_c = \frac{\Delta C}{A_{nt}} + \frac{\Delta Ce_c y}{I_{nt}} \tag{7-22}$$

in which I_{nt} is the moment of inertia of the net, transformed concrete section. Finally, the change in stress in the prestressing steel can be determined by:

$$\Delta f_{ps} = E_{ps}(\Delta\epsilon_i + y_{ps}\Delta\psi_i) + L_{rr} \tag{7-23}$$

In eq. 7-23, y_{ps} is measured from the centroid of the net, transformed concrete section to the centroid of the prestressed reinforcement; the first term in parentheses accounts for concrete shrinkage; the second term in parentheses accounts for the effects of creep and change in force on the concrete section; and the last term in the equation represents the relaxation of the prestressed reinforcement.

ILLUSTRATIVE PROBLEM 7-4 Using the method of Ghali and Trevino, compute the loss of prestress for a 12-in.-high segment of a 12-in.-thick concentrically post-tensioned wall of a concrete water tank (a) if the wall does not have any nonprestressed reinforcement, and (b) if the wall has concentric nonprestressed reinforcement with a ratio, ρ, of 0.0050 in addition to the prestressed reinforcement in (a). The area of the post-tensioning duct is 4.90 in.^{2}; A_{ps} = 1.53 in.^{2}; the initial stress in the prestressed reinforcement (after anchorage set and elastic shortening), f_{si}, is 189 ksi; the elastic modulus of the concrete at the time of prestressing is a 4000 ksi; assume the elastic modulus is 29,000 ksi for both the prestressed and nonprestressed reinforcement; the ultimate creep ratio, γ_u, is 2.60; the ultimate concrete shrinkage, ϵ_{cu}, is -300 millionths in./in.; the concrete aging coefficient, χ, is 0.80; the reduced relaxation of the prestressing steel is 7.0 ksi; and the maximum service load on the section of the wall is 209 kips. Determine the residual stress in the section if the service load is not applied to the concrete section until after all losses of prestress have occurred.

SOLUTION: (a) With no nonprestressed reinforcement in the section.

$$P_i = 1.53 \times 189 = 289 \text{ ksi}$$

$$A_n = 144 - 4.9 = 139.1 \text{ in.}^2$$

$$A_{nt} = 139.1 + \frac{29}{4.0} \times 1.53 = 150.2 \text{ in.}^2$$

$$f_{ci} = \frac{-289}{139.1} = -2.08 \text{ ksi}$$

$$\beta = \frac{1}{1 + \left[\dfrac{1.53 + 0}{139.1}\right][7.25(1 + 0.80 \times 2.6)]} = 0.803$$

$$\Delta P_c = -0.803\left\{[2.6(-2.08)(1.53)(7.25)] + [-300 \times 10^6(29000)(1.53)] + [-7.0 \times 1.53]\right\}$$

$$= +67.4 \text{ kips}$$

$$P_c = -289 + 67.4 = -221.6 \text{ kips}$$

$$P_{se} = +221.6 \text{ kips}$$

The axial force due to applied load = +209 kips. The stress in the concrete due to axial load = (209/150.2) = +1.39 ksi. The effective concrete stress before the application of the axial load = (−221.6/139.1) = −1.59 ksi and the concrete stress under service load = −0.20 ksi.

(b) With 0.005×144 in.^{2} = 0.72 in.^{2} of Grade 60 nonprestressed reinforcement:

$$A_n = 144 - (0.72 + 4.90) = 138.4 \text{ in.}^2$$
$$A_{nt} = 138.4 + 7.25(0.72) = 143.6 \text{ in.}^2$$
$$A_{gt} = 138.4 + 7.25(0.72 + 1.53) = 154.7 \text{ in.}^2$$
$$f_{ci} = \frac{-289}{143.6} = -2.01 \text{ ksi}$$
$$P_s = -2.01 \times 7.25 \times 0.72 = -10.5 \text{ kips}$$
$$P_c = -2.01 \times 138.4 = -278.2 \text{ kips}$$
$$\beta = \frac{1}{\left\{1 + \left[\frac{1.53 + 0.72}{138.8}\right][7.25(1 + 0.80 \times 2.6)]\right\}} = 0.734$$
$$\Delta P_c = -0.734\{[(2.60)(-2.01)(2.25)(7.25)] + [-300 \times 10^{-6} \times 29000 \times 2.25] + [-7.0 \times 1.53]\}$$
$$= -0.734[-85.25 - 19.58 - 10.71] = +84.9 \text{ kips}$$
$$P_c = -278.2 + 84.9 = -193.3 \text{ kips}$$
$$\Delta P_s = \frac{0.734 \times 0.72}{2.25}(-85.25 - 19.58) = -24.66 \text{ kips}$$
$$\Delta P_p = \frac{0.734 \times 1.53}{2.25}(-85.25 - 19.58) + (0.734 \times -10.71) = -60.18 \text{ kips}$$

The total force change in the reinforcement is equal in magnitude, but of opposite sign, to the force change in the concrete. This relationship is expressed mathematically as:

$$\Delta P_{nt} \cong -\Delta P_c$$

and numerically as:

$$\Delta P_{nt} \; -60.18 - 24.66 = -84.8 \text{ kips}$$

$$\Delta P_c \; +84.9 \text{ kips.}$$

The total stress in the nonprestressed reinforcement due to elastic shortening, creep, and shrinkage is:

$$\Delta f_s = -2.01 \times 7.25 - \frac{24.66}{0.72} = -48.82 \text{ ksi}$$

The stress on the composite section due to the application of the service load equals $(+209/154.7) = +1.351$ ksi and the residual stress in the concrete after the application of service load equals $-(193.3/138.4) + 1.351 = -0.046$ ksi.

The computation of the loss of prestress, using the Step Function Method (Branson 1974), incorporates the creep and shrinkage recommendations of ACI Committee 209 as described in Chapter 3. The method includes the effect of nonprestressed reinforcement and the effect of loads applied at times after prestressing. The relationships presented here can be used for the computation of the ultimate loss of prestress (at a long time after prestressing) or the loss at a lesser time. As presented, the relationships are for the ultimate values but by using values of the creep ratio and shrinkage deformation for a time less than infinity, the relationships can be used for computing prestress loss at any time. The original Branson paper is detailed and not limited to the information presented herein; hence, the reader is encouraged to consult the original work for additional information about the underlying assumptions on which the loss of prestress computations are based, as well as their extension for use in the computation of deflections.

Equations for the loss of prestress and for stress in the prestressed reinforcement, based upon Branson's work, are presented here for two types of members. The first is a prestressed concrete flexural member that is constructed at one time and has no structural, composite concrete topping or slab placed on it at some period of time after the prestressing of the member. The second is for a prestressed concrete flexural member that is provided with a structural, composite concrete slab or topping, put into place some time after the original member has been prestressed. The procedure presented herein consists of consideration of the effects of several different factors that contribute to the loss of prestress, which can be represented by several different terms, some using notation unique to this discussion. To facilitate understanding Branson's methods, the notation used is listed as follows:

A_g = Gross area of the section.

$$b_{12} = (n\rho)\frac{1 + (e_{ps})(e_s)}{r^2}(1 + \eta v_u)$$

$$b_{22} = n\rho\left(1 + \frac{e_s^2}{r^2}\right)(1 + \eta v_u)$$

f_{ccgps} = Initial stress in the concrete at the level of the center if gravity of the prestressed reinforcement under consideration, immediately after prestressing.

f_{cdcgps} = Concrete stress at the level of the center of gravity of the prestressed reinforcement due to differential shrinkage and creep of the concretes in composite construction.

e_{ps} = Eccentricity of the prestressed reinforcement in the noncomposite section.

e_s = Eccentricity of the nonprestressed reinforcement in the noncomposite section.

$e_{ps\,comp}$ = Eccentricity of the prestressed reinforcement in the composite section.

$f_{c\,cgs}$ = Stress in the concrete at the level of the center of gravity of the reinforcement under consideration.

$f_{cd\,cgs}$ = Stress in the concrete at the level of the center of gravity of the reinforcement under consideration due to the effects of differential concrete creep and shrinkage.

f_{si} = Stress in the prestressed reinforcement immediately after transfer (after elastic shortening).

E_{ps} = Elastic modulus of the prestressed reinforcement.

E_s = Elastic modulus of the nonprestressed reinforcement.

I = Moment of inertia for the noncomposite section.

I' = Moment of inertia for the composite section.

$k_r = \dfrac{1}{1 + b_{12}}$ = Factor accounting for the effects of nonprestressed reinforcement in resisting creep and shrinkage deformations. For ratios of area of nonprestressed reinforcement to prestressed reinforcement equal to or less than 2, the value of k_r can be taken as:

$$k_r = \frac{1}{1 + A_s/A_{ps}}$$

and for very low values of A_s, k_s can be taken equal to unity.

$k_s = 1 + \dfrac{e_{ps} + e_{pl}}{r^2}$, or $1 + \dfrac{e_{ps}^2}{r^2}$ (see Sec. 7-2).

m = Ratio of the modulii of elasticity for the nonprestressed reinforcement and the concrete at the time of application of sustained superimposed load.

m_{ps} = Ratio of the modulii of elasticity for the prestressed reinforcement and the concrete at the time of application of sustained superimposed load.

n = Ratio of the modulii of elasticity of the nonprestressed reinforcement and the concrete.

n_{ps} = Ratio of the modulii of elasticity of the prestressed reinforcement and the concrete.

P_i = Initial prestressing force (after elastic shortening).

Q = Force generated by the differential deformation due to creep and shrinkage in composite construction.

TABLE 7-5 Values of α_s and γ_{lac} for Different Ages of Loading (see Chapter 3) (after Branson).

Time interval between prestressing and load application, in days	α_s	γ_{lac}
21	0.38	0.85
30	0.44	0.83
60	0.54	0.78
90	0.60	0.75

y_{cs} = Distance from the centroidal axis of the composite section to the centroidal axis of the slab.

$\alpha_s = t^{\psi}/(d + t^{\psi})$ = Factor used to proportion creep deformation between noncomposite and composite sections (see Table 7-5).

Δf_{cdcgps} = Change in concrete stress at the level of the center of gravity of the prestressed reinforcement due to the effects of differential shrinkage and creep.

Δf_i = Change in the initial stress in the prestressed reinforcement.

Δf_{sr} = Change in stress in the prestressed reinforcement due to relaxation.

ϵ_{su} = Concrete shrinkage deformation.

γ_{lac} = Factor to correct for the effect of concrete age at time of loading (see Figs. 3-18 and 3-19 and Table 7-5).

ΔP_s = Loss of prestressing force at time of applying superimposed dead load or composite slab.

ΔP_u = Total loss of prestressing force.

η = Concrete relaxation coefficient, ranging from 0.75 to 0.90 with an average value of 0.88, intended to account for the effect of reducing prestressing force on concrete creep.

$\lambda = 1 - \dfrac{\Delta P_u}{2P_i}$ = Factor that is a function of the ultimate loss of prestress and the initial prestressing force (see Table 7-6).

$\lambda' = 1 - \dfrac{\Delta P_s}{2P_i}$ = Factor that is a function of the loss of prestress at the time a superimposed load or a composite slab is placed (see Table 7-6).

v_u = Ultimate concrete creep ratio.

ρ = Nonprestressed reinforcement ratio (A_s/bd).

$$\zeta = 1 + (nk_s)\frac{A_{ps}}{A_g}(1 + \eta v_u)$$

The terms to be considered in an analysis are described as follows:

TABLE 7-6 Typical Values for the Ratio of Loss of Initial Prestressing Force to the Total Initial Prestressing Force $\Delta P_i / P_i$ for Different Time Intervals and Different Concrete Types. Note that $P_u \cong P_i$ after the Passage of a Long Time (after Branson 1974).

Time interval (days)	Type of Concrete		
	Normal weight	Sand-lightweight	Lightweight
20 to 30	0.10	0.12	0.14
60 to 90	0.14	0.16	0.18
1000	0.18	0.21	0.23

1. *Elastic shortening of the concrete at the level of the prestressed reinforcement:* This is an important factor that contributes to the loss of prestress in the case of pretensioned members because the tendons are normally all released at the same time (for all practical purposes). It does not contribute to the loss of prestress in post-tensioned members if the procedure used in stressing of post-tensioned reinforcement provides for the loss. This term is $n_{ps}f_{ccgps}$ and consists of the product of n_{ps}, the modular ratio of the moduli of the prestressed reinforcement and the concrete, and f_{ccgps}, the stress in the concrete at the level of the center of gravity of the prestressed reinforcement immediately after prestressing.

2. *Concrete creep:* Creep is especially important in members having concrete stressed to relatively high levels of compression at the location of the prestressed reinforcement. The creep terms are: (a) for noncomposite members:

$$k_r \lambda n_{ps} f_{ccgs} v_u$$

in which k_r is a factor that accounts for the effect of the nonprestressed reinforcement in resisting creep and shrinkage deformations, λ is a factor that is a function of the ratio of the ultimate loss of prestress and the initial prestressing force, and v_u is the ultimate creep ratio. The factor k_r is defined as follows:

$$k_r = \frac{1}{1 + b_{12}}$$

where:

$$b_{12} = (n\rho)\frac{1 + (e_{ps})(e_s)}{r^2}\eta v_u)$$

in which η is defined as the concrete relaxation coefficient (similar to χ_r in Ghali's work described in Sec. 2-10), which ranges from 0.75 to 0.90 and, according to Branson, has an average value of 0.88. For ratios of the area of

nonprestressed reinforcement to the area of prestressed reinforcement equal to or less than 2, the value of k_r can be taken to be:

$$k_r = \frac{1}{1 + A_s/A_{ps}}$$

The factor λ is defined as:

$$\lambda = 1 - \frac{\Delta P_u}{2P_i}$$

in which ΔP_u is the total loss of prestress (excluding the loss due to elastic shortening), and P_i is the initial prestressing force. (See Table 7-6 for typical values of $\Delta P_u/P_i$.)

(b) for composite members: The computation of the effect of concrete creep involves two computational steps. The first for the portion that occurs before composite action is established, and the second for that which occurs after. Composite action is established: (a) For before the composite action is established:

$$\alpha_s k_r \lambda' n f_{ccgs} v_u$$

and (b) for the Section after composite action is established:

$$k_r n f_{ccgs} v_u [\lambda - \alpha_s \lambda'] \frac{I}{I'}$$

In these expressions α_s is the ratio of the concrete creep ratio at time t to the ultimate creep ratio (from eq. 3-25, $\alpha_s = t^{\psi}/d + t^{\psi}$), and λ' is a function of the loss of prestress at the time when the slab is cast, ΔP_s, excluding the initial elastic shortening loss, and of the initial prestressing force (after elastic shortening loss), P_i, and is equal to

$$\lambda' = 1 - \frac{\Delta P_s}{2P_i}$$

(See Table 7-6 for typical values of $\Delta P_s/P_i$.)

3. *Concrete shrinkage.* All of the concrete shrinkage has an influence on the loss of prestress in a pretensioned member, but only the concrete shrinkage that occurs after prestressing has an influence in the case of post-tensioned members. The term:

$$k_r \epsilon_{su} E_{ps}/\zeta$$

where:

$$\zeta = 1 + (nk_s)\frac{A_{ps}}{A_g}(1 + \eta v_u)$$

is used to account for the effect of concrete shrinkage on the loss of prestress, and ϵ_{su} is the ultimate concrete shrinkage.

4. *Relaxation of the prestressed reinforcement.* This factor, Δf_{sr}, is equally important for members made with both methods of prestressing. The computation of the relaxation of prestressed reinforcement is discussed in Sec. 2-10.

5. *The elastic effect of superimposed loads.* Superimposed dead and live loads have an elastic effect on the loss of prestress. The term used for this effect is $m_{ps}f_{ccgs}$, in which m_{ps} is the modular ratio of the prestressed reinforcement and concrete at the time when the loads are applied, and f_{ccgs} is the stress in the concrete at the center of gravity of the prestressed tensile reinforcement due to the application of the load(s).

6. *The creep effect of permanent superimposed dead loads.* This effect is a multiple of the elastic effect of superimposed loads discussed in item 5. The term used is:

$$mf_{ccgps}\gamma_{lac}k_r v_u/\zeta$$

in which γ_{lac} is the correction factor for beam concrete age when loaded (See Figs. 3-18 and 3-19) and the other terms have been defined.

7. *Deferential deformation of beam and slab.* The change in stress in the reinforcement as a result of the differential deformations of the concretes in a composite beam is an important consideration in composite construction. The term for this effect is Δf_{cdcgps} in which f_{cdcgps} is the concrete stress at the level of the center of gravity of the prestressed reinforcement due to the effects of differential shrinkage and creep and is computed by:

$$\Delta f_{cdcgps} = m_{ps}\frac{Qy_{cs}e_{pscomp}}{I'}$$

where Q is the force generated by the differential shrinkage and creep, y_{cs} is the distance from the centroidal axis of the composite section to the centroidal axis of the slab, e_{pscomp} is the eccentricity of the prestressed reinforcement in the composite section, and I' is the moment of inertia of the composite section.

The loss of prestress is determined as the algebraic sum of the several items discussed above. The factor k_r accounts for the effect of nonprestressed reinforcement; if there is none, or if the amount present is not significant, k_r can be taken to be equal to unity and eliminated from the computation.

Summing the terms described above for prestressed reinforcement, the equation for noncomposite members is:

$$\Delta f_{si} = n_{ps}f_{ccgs} + k_r\lambda n_{ps}f_{ccgs}v_u + \frac{k_r\epsilon_{su}E_{ps}}{\zeta} + \Delta f_{sr} + m_{ps}f_{ccgs} + \frac{m_{ps}f_{ccgs}\gamma_{lac}k_r v_u}{\zeta} \qquad (7\text{-}24)$$

For composite members that are not shored at the time when the composite topping or slab is placed, the equation becomes:

$$\Delta f_{si} = n_{ps} f_{ccgs} + \alpha_s k_r \lambda' n_{ps} f_{ccgs} v_u + n_{ps} f_{ccgs} k_r v_u [\lambda - \alpha_s \lambda'] \frac{I}{I'}$$
$$+ \frac{k_r \epsilon_{su} E_{ps}}{\zeta} + \Delta f_{sr} + m_{ps} f_{ccgs}$$
$$+ \left[\frac{m_{ps} f_{ccgs} \gamma_{lac} k_r v_u}{\zeta} \right] \frac{I}{I'} + \Delta f_{cdcgps} \qquad (7\text{-}25)$$

Relationships for the stress in the nonprestressed reinforcement, similar to eqs. 7-24 and 7-25, also have been included to Branson's work. These relationships can be used to determine the stress in nonprestressed reinforcement at any location within a member because they are based upon the stresses and strains in the concrete at the level of the nonprestressed reinforcement under consideration. The relationship for noncomposite members is

$$\Delta f_s = n_{ps} f_{ccgs} + \frac{n_{ps} f_{ccgs} v_u}{1 + b_{22}} + \frac{\epsilon_{su} E_s}{1 + b_{22}}$$
$$+ m_{ps} f_{ccgs} + \frac{m_{ps} f_{ccgs} \gamma_{lac} v_u}{1 + b_{22}} \qquad (7\text{-}26)$$

and, for composite members that are not shored at the time when the composite topping or slab is placed, the relationship is:

$$\Delta f_s = n_{ps} f_{ccgs} + \frac{\alpha_s n_{ps} f_{ccgs} v_u}{1 + b_{22}} + n_{ps} f_{ccgs} v_u \left[\frac{\lambda - \alpha_s \lambda'}{1 + b_{22}} \right] \frac{I}{I'}$$
$$+ \frac{\epsilon_{su} E_s}{1 + b_{22}} + m_{ps} f_{ccgs} + \left[\frac{m_{ps} f_{ccgs} \gamma_{lac} v_u}{1 + b_{22}} \right] \frac{I}{I'} + \Delta f_{cdcpgs} \qquad (7\text{-}27)$$

ILLUSTRATIVE PROBLEM 7-5 For the composite post-tensioned girder shown in Fig. 7-4 and the data given in I.P. 7-1, estimate the loss of prestress at midspan at the age of 600 days using the Branson method. Assume the concrete cylinder compressive strength is 4000 psi at the time of prestressing.

$$E_c = (115)^{1.5} 26 \sqrt{4000} = 2.03 \times 10^6 \text{ psi}$$

$$n_{ps} = \frac{27800}{2030} = 13.7$$

SOLUTION: The initial stress in the prestressed reinforcement, after the elastic shortening of the concrete, f_{si}, is given as 189.5 psi in I.P. 7-1. With e_{ps} =

44.12 − 6.37 = 37.75 in., r^2 = (625158/949) = 659 in.^{2}, and k_s = 1 + (37.75^2/659) = 3.16 in. (eq. 7-4), the average initial stress in the prestressed reinforcement of 189.5 ksi would result in a stress in the concrete at midspan, at the level of the center of gravity of the prestressed reinforcement, that is equal to:

$$f_{ci} = -\frac{(189.5)(5.52)(3.16)}{949} + \frac{(1535)(12)(37.75)}{625158} = -2.371 \text{ ksi}$$

If the beam were pretensioned rather than post-tensioned, the average stress in the prestressed reinforcement immediately before transfer, f'_j, using eq. 7-5, would be:

$$f'_j = f_{si} + n_{ps} f_{ci}$$

$$f'_j = 189.5 + 13.7 \times 2.374 = 222.0 \text{ ksi}$$

If post-tensioned, the average initial stress in the tendons at the time of stressing would be:

$$f'_j = f_{si} + \frac{n_{ps} f_{ci}}{2}$$

$$f'_{sj} = 189.5 + \frac{13.7 \times 2.374}{2} = 205.8 \text{ ksi}$$

After elastic shortening of the concrete, the initial prestressing force, P_i, is 189.5 × 5.52 = 1046 kips. The concrete slab is placed at 197 days (girder age) at which times the concrete strength (eq. 3-1), elastic modulus, and modular ratio for beam concrete and the prestressed reinforcement are

$$f_{ct} = \frac{197}{2.24 + 0.92 \times 197}(5500)$$

$$= 5900 \text{ psi}$$

$$E_c = 2.46 \times 10^6 \text{ psi}$$

$$m_{ps} = \frac{27800}{2460} = 11.3$$

The concrete stress at the level of the center of gravity of the prestressed reinforcement due to the application of the slab and superimposed dead load is

$$f_{ccgps} = \frac{1278 \times 12 \times 35.39}{710{,}047} + \frac{300 \times 12 \times 49.30}{1{,}226{,}561}$$

$$= 0.764 + 0.145 = 0.909 \text{ ksi}$$

The relaxation loss of the prestressing reinforcement at 600 days is:

$$\Delta f_{sr} = -189.5 \frac{(\log 24 \times 600)}{10} \left(\frac{189.5}{247} - 0.55 \right) = -17.11 \text{ ksi}$$

The value of α_s at 197 days, from eq. 3-25, is

$$\alpha_s = \frac{197^{0.6}}{10 + 197^{0.6}} = 0.70$$

and the creep ratio at the age of 600 days, from eq. 3-25, v_{600} is (v_{lac})

$$v_{600} = \left(\frac{600^{0.60}}{10 + 600^{0.60}} \right) 1.50 = 1.23$$

and γ_{lac}, from Fig. 3-18 is

$$\gamma_{lac} = 1.25(197)^{-0.118} = 0.67$$

The effect of differential shrinkage and creep strain can be estimated as follows:

For slab concrete shrinkage from 204 days (end of curing) to 600 days using eq. 3-21:

$$\epsilon_s = -300 \left(\frac{396}{35 + 396} \right) = -276 \text{ millionths in./in.}$$

For beam concrete shrinkage between 197 and 600 days:

$$\epsilon_s = -350 \left(\frac{600}{35 + 600} - \frac{197}{35 + 197} \right) = -33 \text{ millionths in./in.}$$

The initial top fiber stress in the beam is computed to be:

$$f_t = -\frac{1046}{949} \left(1 + \frac{(37.37)(-30.87)}{659} \right) + \frac{(1535)(12)(-30.87)}{625158}$$

$$= +0.827 - 0.910 = -0.083 \text{ ksi}$$

At the time when the concrete slab and superimposed dead loads are applied, 197–206 days, the estimated value of λ' is:

$$\lambda' \cong 1 - \frac{\Delta P_s}{2P_i} = 1 - \frac{0.20P_i}{2P_i} = 0.90$$

and the stress in the top fiber of the precast beam is:

$$f_t = (0.90)(-0.083) + \frac{(1278)(12)(-33.23)}{710047} + \frac{(300)(12)(-19.32)}{1226561}$$

$$= -0.075 - 0.718 - 0.057 = -0.850 \text{ ksi}$$

and the creep deformation of the top fiber between 197 and 600 days for a stress of −0.850 ksi is:

$$\frac{-850}{2.46}\left(\frac{600^{0.6}}{10 + 600^{0.60}} - \frac{197^{0.6}}{10 + 197^{0.6}}\right) 1.50 = -61 \text{ millionths in./in.}$$

in which 2.46×10^6 psi is the elastic modulus of the concrete at the age of 600 days. Therefore, the differential strain between the top fiber of the beam and the slab is:

$$\delta e_t = -276 - (-33 - 61) \cong -182 \text{ millionths in./in.}$$

Elastic deformation and relaxation of the slab concrete would slightly reduce the effect of the differential strain. For the purposes of this analysis, it will be assumed that the effective differential strain is -180 millionths in./in., and the elastic modulus of the slab concrete is 2.2×10^6 psi. Hence, the computation of the force resulting from the differential strain is:

$$Q = \frac{2.2 \times -180 \times 8.33 \times 12 \times 6.5}{1000} = -257 \text{ kips}$$

and the change in the stress in the prestressing reinforcement as a result of the differential strain is:

$$f_{cdcgps} = \frac{(11.3)(-257)(49.30)(22.57)}{1226561} = +2.63 \text{ ksi}$$

Assuming that $k_r = 1.0$, because nonprestressed reinforcement is not present in a significant amount and:

$$\zeta = 1 + \frac{11.8 \times 5.52 \times 3.16}{949}(1 + 0.88 \times 1.5) = 1.50$$

in which $k_s = 3.16$, $\eta = 0.88$, $v_u = 1.5$, $\lambda = 0.88$, $\lambda' = 0.90$, $I/I' = 0.579$, $n = 29/2.46 = 11.8$, $A_{ps} = 5.52$ in.^{2}, and $A_g = 949$ in.^{2}. The computation for the loss of prestress using eq. 7-25 is:

$$\begin{aligned}
\Delta f_{si} &= 0 + (0.70)(1.0)(0.90)(13.7)(-2.371)(1.5) \\
&\quad + (13.7)(-2.371)(1.0)(1.5)[0.88 - (0.70)(0.90)]0.579 \\
&\quad + \frac{(1.0)(-350)(27.8)}{(1.50)(1000)} + (-17.11) + (11.3)(+0.909) \\
&\quad + \left[\frac{(11.3)(+0.909)(0.67)(1.5)}{1.50}\right](0.579) + 2.63 \\
&= 0 - 30.7 - 7.1 - 6.5 - 17.1 + 10.3 + 4.0 + 2.6 \\
&= -44.5 \text{ ksi} \\
f_{se} &= 189.5 - 44.5 = 145.0 \text{ ksi}
\end{aligned}$$

$$\Delta P_u = -44.5 \times 5.52 = 245.6 \text{ kips}$$

$$\Delta P_u / P_i = 0.235 \text{ (not including elastic shortening)}.$$

ILLUSTRATIVE PROBLEM 7-6 For the double-tee beam shown in Fig. 7-15, estimate the ultimate loss of prestress using the Branson method. The dead load of the double-tee beam is 200 plf, the superimposed dead load is 40 plf, and the design span is 40 ft. Assume that the transfer of prestress occurs 24 hours after the jacking (stressing) of the pretensioned tendons, and that the stress in the prestressed reinforcement immediately before transfer is 200 ksi. Assume that $A_{ps} = 0.58$ in.^{2}, $f_{pu} = 270$ ksi, and $f_{py} = 250$ ksi. The gross area of the section is 189.5 in.^{2} and the moment of inertia is 4256 in.^{4} Assume $n_{ps} = 7.3$, $m_{ps} = 6.0$, $\gamma_{lac} = 0.83$, $v_u = 2.00$, $\epsilon_s = -400$ millionths in./in., and the elastic modulus for the prestressed reinforcement is equal to 28,000 ksi.

SOLUTION:

$$P_j' = 200 \times 0.58 = 116 \text{ kips}, \quad C_j = -116 \text{ kips}$$

$$e_{ps} = 8.33 \text{ in.}, \quad r^2 = \frac{4256}{189.5} = 22.46 \text{ in.}^2$$

$$k_s = 1 + \frac{8.83^2}{22.46} = 4.47$$

$$M_d = \frac{200 \times 40^2}{8 \times 1000} = 40.0 \text{ k-ft}$$

$$f_{c\,cgps} = -\frac{(-116)(4.47) + \dfrac{(189.5)(40)(12)(8.83)}{4256}}{189.5 + (7.3)(0.58)(4.47)} = -1.582 \text{ ksi}$$

and:

$$n_{ps} f_{ccgps} = 7.3 \times -1.582 = 11.55 \text{ ksi}$$

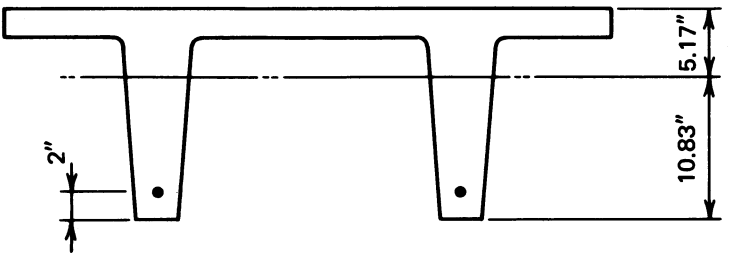

Fig. 7-15. Cross section of double-tee beam used in I.P. 7-6.

$$f_{si} = 200 - 11.55 = 188.45 \text{ ksi}$$

$$P_i = (200)(0.58) + (7.3)(-1.582)(0.58) = +109.3 \text{ kips}$$

Use $P_i = 109$ kips, $f_{si} = 188.5$ ksi, and $n_{ps}f_{ccgps} = -11.5$ ksi.

$$\text{Because } \frac{A_s}{A_{ps}} = 0, \; k_r = 0.$$

The moment due to the superimposed dead load is:

$$M_{sdi} = \frac{0.04 \times 40^2}{8} = 8.0 \text{ k-ft}$$

The concrete stress at the level of the center of gravity of the prestressed reinforcement due to the superimposed dead load is

$$f_{csdi} = \frac{8 \times 12 \times -8.83}{4246} = -0.200 \text{ ksi}$$

Using eq. 2-2 for computing the relaxation of the prestressed reinforcement at time $t_n = 100{,}000$ hours:

$$\frac{f_{stn}}{f_{si}} = 1 - \left(\frac{188.5}{250} - 0.55\right)\frac{\log 10^5 - \log 24}{10} = 0.926$$

and:

$$f_{stn} = 0.926 \times 188.5 = 174.6 \text{ ksi}$$

and the relaxation loss, after 100,000 hours have passed after elastic shortening of the concrete is:

$$188.5 - 174.6 = 13.9 \text{ ksi}$$

Assuming $\lambda = 0.91$ and $\zeta = 1.25$:

$$\Delta f_i' = -11.5 + (0.91)(-11.5)(2.00) + \frac{-400 \times 28}{1.25 \times 1000}$$

$$+ (-13.9) + (6.0 \times -0.20) + \frac{(6.0)(-0.20)(0.83)(2.00)}{1.25}$$

$$= -11.5 - 20.9 - 9.0 - 13.9 + 1.2 + 1.6 = -52.5 \text{ ksi}$$

$$f_{se} = 200 - 52.5 = 147.5 \text{ ksi}$$

The ratio of the loss of prestressing force, ΔP_u ($-52.5 \times 0.58 = -30.45\ k$), to the initial prestressing force, P_i, ($109\ k$), is -0.28. This is greater than the 0.18 assumed ($\lambda = 0.91$) hence, a second iteration is performed. The use of

$\lambda = 0.86$ rather than 0.91 in the second term in the above computation, changes the loss due to concrete creep from -20.9 ksi to -19.8 ksi, the total loss of prestress becomes -51.4 ksi, and the ratio of the total loss of prestressing force to the initial force becomes -0.27. This is acceptably close to the assumed value of -0.28, and further iterations are not needed.

In many applications of prestressed concrete, especially in pretensioned members and post-tensioned flat slab and flat plate structures, little if any nonprestressed reinforcement is included in the prestressed concrete, and the average prestressing stresses are relatively low. In cases such as these, the less sophisticated methods of determining the loss of prestress have proved to give satisfactory results. The method of Zia et al. (Zia 1979) is easy to apply and intended for use in making a reasonable estimate of loss of prestress for usual design conditions (i.e., ordinary structures, simple beams, short-to-moderate spans, moderate loads, etc.). The method is not intended for use in special structures, such as water tanks. Zia and his colleagues suggest that the methods recommended by the PCI Committee on Prestress Losses (Appendix A) be used for unusual design conditions. With the PCI Committee method, the total loss of prestress is computed as the sum of the effect of elastic shortening, concrete creep, concrete shrinkage, and relaxation of the prestressed reinforcement. A negative criticism of this method, which can be important in some special instances, is that it does not account for the effects of cracking or the provision of nonprestressed reinforcement.

7-4 Deflection

Computations of short-term deflections in prestressed concrete flexural members are made with the assumption that the concrete section acts as an elastic and homogeneous material. This assumption is only approximately correct, as the elastic modulus for concrete is not a constant value for all stress levels; in addition, the elastic modulus varies with the age of the concrete and is influenced by other factors. Furthermore, differences between assumed and actual dimensions of the concrete cross section and prestressed and nonprestressed reinforcements often exist, as do differences between assumed and actual initial stresses in the prestressed reinforcement. As a result, deflection computations for prestressed concrete are approximations and should not be considered to have high precision.

The deflections for dead and live loads are calculated by using the fundamental principles of the mechanics of materials. Normally, the moment of inertia of the gross section is used in the computations, but in members that have significant amounts of reinforcing steel, the moment of inertia of the transformed section should be used. The deflection resulting from the prestressing

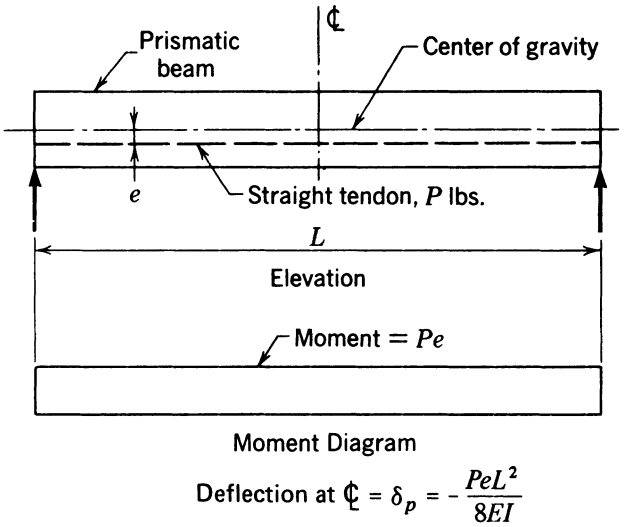

Fig. 7-16. Layout and prestressing-moment diagram for a beam having a straight tendon.

can be readily calculated for prismatic members with known prestressing force and eccentricity by use of the area-moment principle. The results of a calculation of this type for a simple, prismatic member with straight tendons (see Fig. 7-16) is:

$$\delta_p = -\frac{PeL^2}{8EI} \tag{7-28}$$

where P is the prestressing force in pounds, e is the eccentricity in inches, L is the span in inches, E is the modulus of elasticity of the concrete in psi, and I is the moment of inertia of the gross section in inches to the fourth power. Positive eccentricities in the above relationship result in upward deflections.*

In Fig. 7-17, the moment diagram and corresponding deflection due to prestressing are shown for a simple, prismatic beam prestressed with a tendon having a second-degree parabolic path with no eccentricity at the ends and maximum eccentricity at midspan; and in Fig. 7-18, the moment diagram and corresponding deflection are indicated for a simple, prismatic member prestressed with a tendon that has a path composed of three straight lines, symmetry about the midspan, and no eccentricity at the ends.

It is assumed that the deflections due to the various loads that will be applied to a beam can be algebraically superimposed in order to determine the resultant

*In this book, upward deflections are negative, and downward deflections are positive. The word "camber" is reserved for out-of-planeness or flatness built into a member, other than by prestressing, for the purpose of achieving a desired shape.

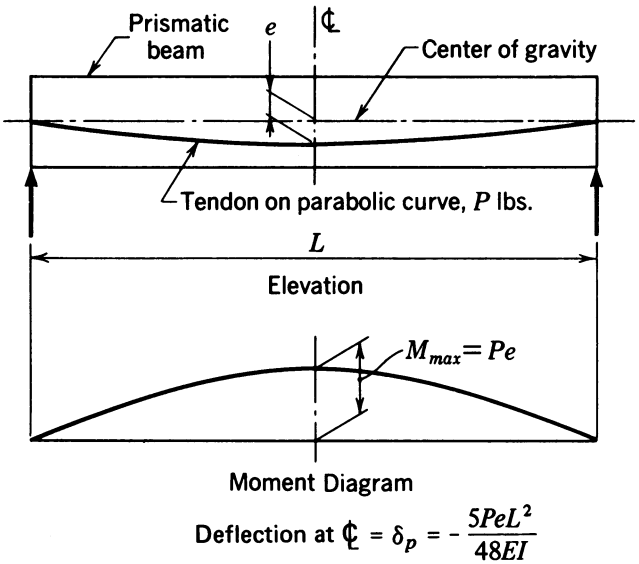

Fig. 7-17. Layout and prestressing-moment diagram for a beam having a tendon on a parabolic path and no eccentricity at the ends.

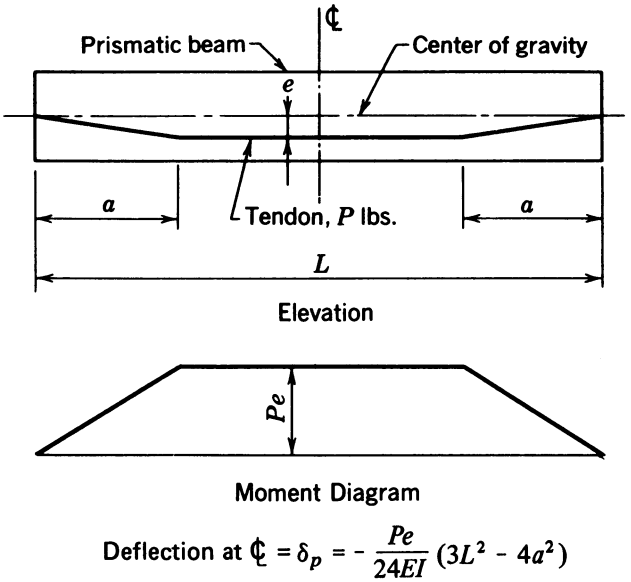

Fig. 7-18. Layout and prestressing-moment diagram for a beam having a tendon path with constant eccentricity in the midspan area and no eccentricity at the ends.

deflection of the member. In this manner, the deflection of a beam under the effects of its dead load and prestressing is computed as the algebraic sum of the deflections due to dead load of the beam and due to prestressing. In a similar manner, if a beam is prestressed with a tendon that follows a parabolic path that has equal eccentricity at the ends, the deflection of the beam due to prestressing could be determined by computing the algebraic sum of the deflections due to dead load plus the effects of prestressing with a straight tendon and with a parabolic tendon, as illustrated in Fig. 7-16 and 7-17, respectively. In applying the principle of superposition as described above, it is necessary to divide the moment due to prestressing into two portions that can be substituted into the appropriate relationships for the terms P_e. For unusual conditions of prestressing-moment diagrams, or if the designer questions the results obtained through the use of the superposition principle, the deflection can be easily calculated from the basic, area-moment principle. When members with variable moments of inertia are used, it is necessary to compute the deflections by use of basic principles. Basic principles should be used when the prestressing force varies along the length of the tendon, or when the tendon does not follow a mathematical curve, as is frequently the case in cast-in-place post-tensioned bridges.

The deflections at the ends of beams that overhang the ends of adjacent spans differ from those at the ends of cantilever beams. The difference is due to the rotation that occurs at the support where the overhanging portion of the beam adjoins the supported span. Cantilever beams have no slope at the supported end, and hence have deflections due to the deformations that occur within the length of the cantilever span alone. This is illustrated in Fig. 7-19. It frequently is found that the deflection at the end of an overhanging beam resulting from the deformation of the overhand itself is considerably smaller than that due to the deformation of the span to which it is attached. For this reason, deflection calculations should always be made for beams having overhanging ends.

It is well known that in beams having only nonprestressed reinforced concrete, the tendency is for the deflection to increase with time as a result of creep. In addition, the amount of flexural cracking in a nonprestressed reinforced concrete member has a significant influence on the deflection of the member. In a fully prestressed concrete beam, the change in deflection is a function of time as well as of the distribution of stress in the member under the normal condition of loading. For example, if the effects of the prestressing and the dead and live loads at the average section of a member were such that the distribution of stress was a uniform compression over the thickness of the member, the effect of creep would be to shorten the member (deform it axially) without changing its shape vertically. If, under the same conditions, the stress in the bottom flange were greater than the average compression, the tendency would be for the member to increase in upward deflection with the passage of time. If the top-fiber

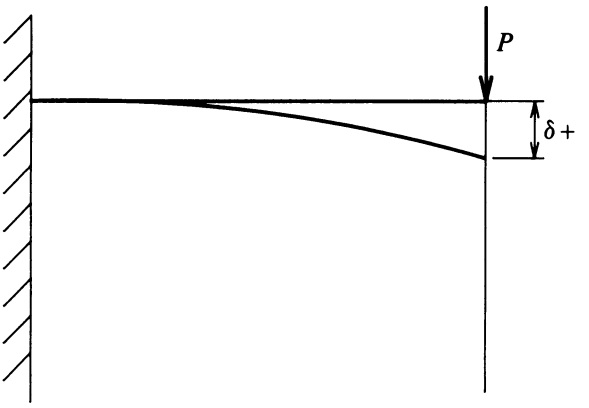

(a) cantilevered beam

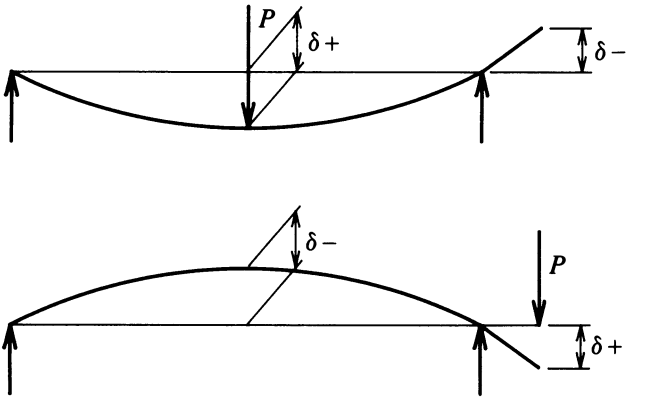

(b) Overhanging beams

Fig. 7-19. Deflections of (a) the end of a cantilevered beam and (b) two overhanging beams.

compressive stresses under the normal loading were greater than the average compression, the tendency would be for the deflection to increase downward as a result of the creep.

It is interesting to note that for the deflection due to prestressing alone, the effects of concrete shrinkage and steel relaxation are to reduce the deflection due to prestressing, because these two effects tend to reduce the prestressing force. The effect of creep is to alter the deflection for cases where the resultant force in the concrete is significantly eccentric, because the rotational changes

due to creep normally are greater than the shortening effect is on reducing the prestress.

It should be recognized that the curvature at any section of a beam is equal to:

$$\psi = \frac{M}{EI} \tag{7-29}$$

This relationship is useful in computing the theoretical deflections, including time-dependent deformations, in concrete members having prestressed reinforcement, nonprestressed reinforcement, or a combination of both. Computations of this type must be made with the more sophisticated methods, such as the Ghali or numerical integration methods, because these methods include the computation of the curvatures at the sections of the members analyzed. The mathematical relationships for the deflection of beams due to prestressing of different types, such as those illustrated in Figs. 7-16, 7-17, and 7-18, can be rewritten in the form:

$$\delta = \frac{\psi L^2}{K} \tag{7-30}$$

which K is a constant depending upon the path of the tendon. From Fig.7-20 it will be seen that the curvature at any section can be computed if the strain distribution is known. The curvature is equal to:

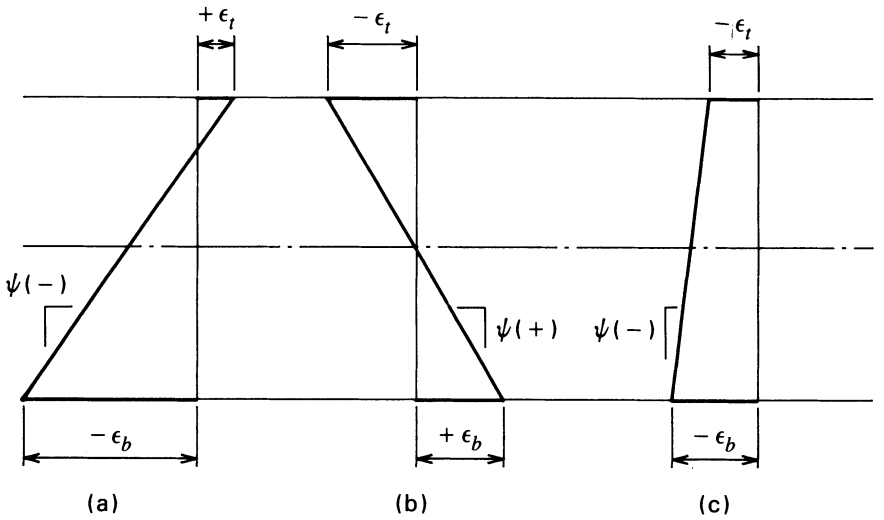

Fig. 7-20. Strain distributions due to (a) prestressing, (b) transverse loads, and (c) the combination of both.

$$\psi = \frac{\epsilon_b - \epsilon_t}{h} \tag{7-31}$$

in which compressive strains are negative, tensile strains are positive, curvatures that cause downward deflections are positive, and curvatures that cause upward deflection are negative. The relationship applies equally to short- and long-term rotations.

In computing long-term deflections, using the numerical integration method, the loss-of-prestress computations are made as a part of the deflection computations. The effects of variations in strains and stresses in the nonprestressed and prestressed reinforcements must be taken into account, and the curvature must be computed at each time increment. The accuracy of the deflection computations is improved if the strain, stress, and curvature computations are made at several sections along the length of the beam rather than at the location of the maximum moment alone. After the curvatures have been determined at the desired locations along the beam length, the deflection can be determined by classical methods.

The step-by-step procedure for computing the deflection of a precast beam with a composite cast-in-place slab (such as that shown in Fig. 7-4), using the numerical integration method, is as follows:

1. Determine shrinkage and creep characteristics of the concrete, as a function of time, for use in the analysis. In addition, determine the relaxation characteristics of the prestressing steel as a function of time.
2. Divide the beam into a number of incremental lengths for use in the analysis. The computations described in the following steps must be performed for each section between the various increments. (Beam symmetry, use of incremental lengths, and loading conditions reduce the calculations required.) Determine the time increments to be used. Small time increments are desirable from the standpoint of improving accuracy in the numerical integration procedure, but the amount of computation required is affected by the number of time increments considered (this is not an important consideration when a programmable calculator or computer is used.)
3. Compute the stresses in the concrete at the top and bottom fibers as well as at the center of gravity of the prestressed steel. The stresses should include the effects of the initial prestressing force and all transverse loads. (The effect of transverse loads or restraints that are applied at later ages must be taken into account at the appropriate time, as is explained below in step 10.)
4. Compute the initial strains in the top and bottom fibers and the curvature at the section due to the initial loading condition.
5. For the duration of the first time increment, compute the changes in strains at the top and bottom fibers and at the centroid of the prestressed

reinforcement due to creep and to shrinkage. In addition, compute the relaxation of the steel during the first time increment.

6. Compute the total incremental change in stress in the prestressing steel due to creep, shrinkage, and relaxation, and, applying this force as a tensile force on the concrete section at the location of the centroid of the prestressed reinforcement, compute the stresses in the top and bottom fibers as well as at the level of the prestressed reinforcement.
7. Add the stresses from step 6 to those of step 3 in order to find the stresses at the end of the time increment.
8. Compute the strains in the top and bottom fibers as well as the curvature at the end of the time interval.
9. Using the stresses from step 7, repeat the procedure (steps 5 through 8). The procedure is repeated until the total time has been considered.
10. At the appropriate times, the effects of superimposed loads are taken into account by computing the changes in stress at the top and bottom fibers and at the centroid of the prestressed reinforcement due to the loads. The stress at the centroid of the prestressed reinforcement should be multiplied by the modular ratio that is appropriate for the time increments under study, and the force resulting from the change in stress then applied as an incremental change in the prestressing force. The effect of the incremental change in the prestressing force on the stresses in the top and bottom fibers and at the centroid of the prestressed reinforcement should be computed. From these computations, the resulting strains and curvature in the concrete can be determined.
11. The procedure continues (steps 5 through 8) until the total time has been considered.
12. The effect of the differential strains in the cast-in-place concrete and the precast concrete is taken into account by first computing the difference in the unrestrained changes in strain in the cast-in-place concrete and the precast concrete at the interface between the two concretes. Strain compatibility is then forced by applying equal and opposite forces to the cast-in-place concrete and the beam at their interface.
13. The stresses from the forces computed in step 12 are to be computed in each subsequent time-interval computation and taken into account in the routine of steps 5 through 8.
14. The deflections at various points along the span of the beam, at the end of any time interval, can be computed by using the Area-Moment, the Conjugate Beam, or another method of analyzing statically indeterminate beams. The calculation involves the integration of the curvature diagram for the beam.

It should be apparent that a large amount of tedious computation is needed to apply this method. Consequently, the method can best be applied with the aid of a programmable calculator or computer.

Special structures, such as prestressed concrete bridges that are constructed segmentally in cantilever fashion (see Fig. 10-20), may require many time-dependent steps in their construction. Each time that increments of load or prestressing are added to the structure, new stresses, strains, rotations, and changes in the forces in the concrete and steel must be determined for each segment joint. The numerical integration method of estimating losses of prestress and deflection is a logical method to be used in such a case. This method permits the effect of time to be computed independently for each of the components.

The general method of analysis derived by Ghali et al. which is described in Sec. 7-3, can be used for the computation of deflections in lieu of the numerical integration method. The procedure involves performing all of the steps required for the determination of loss of prestress at several locations along the length of a member, after which the deflections are computed by using the computed curvatures and one of the classical methods of analyzing statically indeterminate beams, such as the Conjugate Beam Method.

When use of the numerical integration or Ghali methods of computing the deflection of prestressed reinforced concrete members is not considered warranted because of the computational effort involved, one can use the modified step function method recommended by Branson. In this method, the deflection is computed as the algebraic sum of the effects of dead and live loads combined with the effects of creep and loss of prestress. The effects of concrete elastic shortening, creep, and shrinkage, as well as relaxation of the prestressed reinforcement, on the prestressing force are, of course, included in the loss of prestress used in the analysis. Two basic relationships are used: one is for the analysis of prestressed concrete beams that do not have composite slabs and may or may not have superimposed dead loads, and the second is for prestressed concrete beams having composite slabs constructed without or with shoring supporting the beam at the time when the composite slab is placed. The following notation and definitions, which differ in some respects from those used in Branson's paper and supplement the notation given in Sec. 7-3, are used in these relationships:

δ_d = Deflection due to beam dead load
δ_{ds} = Deflection due to differential shrinkage between beam and slab concretes (see eq. 7-34)
δ_l = Deflection due to beam live load
δ_p = Deflection due to prestressing
δ_s = Deflection due to slab dead load
δ_{sdl} = Deflection due to superimposed dead load
δ_u = Ultimate deflection

For a noncomposite fully prestressed concrete beam (i.e., free of cracking under maximum loading), the ultimate total load deflection is computed by:

$$\delta_u = \delta_p \left[1 + \frac{\Delta P_u}{P_i} + \lambda(k_r v_u) \right] + \delta_d [1 + k_r v_u] + \delta_{sdl} [1 + \gamma_{lac} k_r v_u] + \delta_l \tag{7-32}$$

For a composite beam that is not shored at the time when the composite topping or slab is placed, the ultimate total load deflection is:

$$\delta_u = \delta_p \left[1 + \frac{\Delta P_s}{P_i} + \alpha_s k_r v_u \lambda' + \frac{I}{I'} \left(\frac{\Delta P_u - \Delta P_s}{P_i} + k_r v_u (\lambda - \alpha_s \lambda') \right) \right] + \delta_d \left[1 + \alpha_s k_r v_u + (1 - \alpha_s)(k_r v_u) \frac{I}{I'} \right] + \delta_s \left[1 + \alpha_s k_r v_u \frac{I}{I'} \right] + \delta_{ds} + \delta_l \tag{7-33}$$

For a precast beam that is shored at the time the composite topping or slab is placed, the deflections due to the composite topping or slab load is computed using eq. 7-33 with the ratio moments of inertia of the beam to the composite section deleted from the term for slab deflection.

For a simple beam, the deflection due to differential shrinkage and creep between the slab and beam concretes is computed from

$$\delta_{ds} = \frac{Q y_{cs} L^2}{8 E_c I} \tag{7-34}$$

in which Q is the force resulting from the differential shrinkage and creep, y_{cs} is the distance from the centroid of the composite time based upon the initial and final values computed as described above, or employ the more detailed procedures suggested by Branson (1974).

In using eqs. 7-32 and 7-33, the losses of prestress should be estimated by using the methods described in Sec.7-3.

Allowable tensile stresses as high as $12\sqrt{f'_c}$ are permitted in flexural members by Sec. 18.4.2 of ACI-318 (ACI Committee 318 1989), provided that computations are made to confirm that the immediate and long-term deflections comply with the requirements of Sec. 9.5 of ACI 318. The latter computation requires that the effects of creep, shrinkage, relaxation, and cracking be accounted for in the deflection computations. The load–deflection curve of a prestressed concrete beam loaded past the cracking load can be represented simplistically as shown in Fig. 7-21. It must be pointed out that this curve does not accurately depict the deflection characteristics of prestressed concrete beams because, in reality, the components of the figure should be curved lines rather than straight ones.

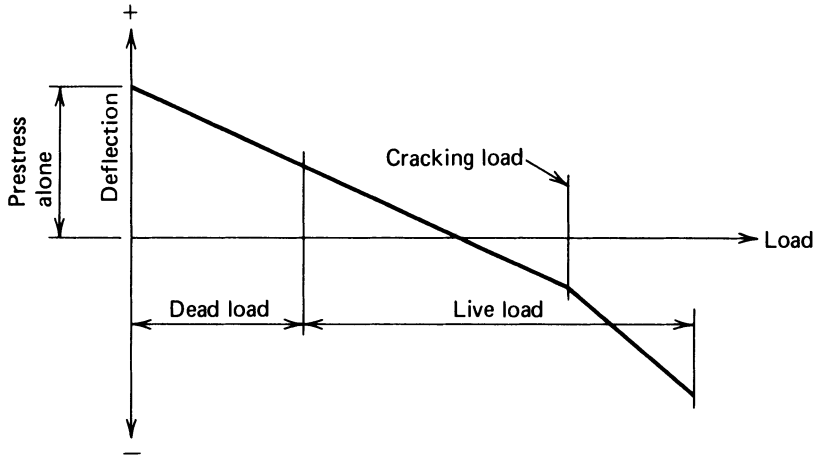

Fig. 7-21. Simplistic representation of a load–deflection curve for a prestressed concrete flexural member.

For loads below the cracking loads, the deflections can be computed by using any of the methods described above. For loadings that cause flexural cracking, ACI 318 further provides that the "effective moment of inertia" be used in the computations. This term is defined in Sec. 9.5.2.3 as follows:

$$I_e = \left(\frac{M_{cr}}{M_a}\right) I_g + \left[1 - \left(\frac{M_{cr}}{M_a}\right)^3\right] I_{cr} \qquad (7\text{-}35)$$

The terms in the above are defined as follows:

I_{cr} = Moment of inertia of the cracked transformed section with respect to the centroidal axis.

I_g = Moment of inertia of the gross concrete section about the centroidal axis, neglecting the reinforcement.

M_a = Maximum moment in member at stage for which deflection is being computed.

M_{cr} = Cracking moment based upon the modulus of rupture of $7.5\sqrt{f'_c}$ for normal weight concrete. See ACI 318, Sec. 9.5.2.3 for lightweight concrete.

The deflections of members subject to cracking can also be made using Ghali's method, as is described in the Section 7-5, Partially Prestressed Concrete. Because Ghali's method includes the effects of inelastic deformations of the concrete, the presence of nonprestressed reinforcement, as well as cracking, the author recommends its use.

The methods currently available to the structural designer for making deflection computations for fully-prestressed concrete members are considerably better than those that were available past. If done manually, as opposed to using

programmable calculators or computers, the effort required to use the contemporary methods is considerably greater than that required for nonprestressed reinforced concrete or for the methods used in the past for fully prestressed members. The trend towards the use of partially prestressed concrete, which is discussed in the next section, further complicates the computations for deflections. As stated previously, the more sophisticated methods are needed only for the more sophisticated structures, such as those with long spans or uncommon loadings, or those utilizing unusual construction methods or procedures.

ILLUSTRATIVE PROBLEM 7-7 Using the numerical integration method, determine the midspan deflections of the composite beam having the cross section shown in Fig. 7-4 if the span is 126.3 ft. The beam is the end span of a three-

TABLE 7-7 Section Properties for I.P. 7-7.

Net Precast Section			
Point	Area ($in.^2$)	Moment of inertia ($in.^4$)	y_b (in.)
0 & 10	949	650,070	43.41
1 & 9	949	647,179	43.67
2 & 8	949	640,206	43.87
3 & 9	949	632,685	44.01
4 & 6	949	627,168	44.10
5	949	625,158	44.12
Precast Transformed Section			
Point	Area ($in.^2$)	Moment of inertia ($in.^4$)	y_b (in.)
0 & 10	1013	650,140	43.48
1 & 9	1013	675,091	42.86
2 & 8	1013	673,860	42.37
3 & 7	1013	691,947	42.03
4 & 6	1013	705,214	41.82
5	1013	710,047	41.76
Composite Transformed Section			
Point	Area ($in.^2$)	Moment of inertia ($in.^4$)	y_b (in.)
0 & 10	1637	1,119,276	56.74
1 & 9	1637	1,143,025	56.35
2 & 8	1637	1,173,053	56.06
3 & 9	1637	1,200,732	55.84
4 & 6	1637	1,219,788	55.72
5	1637	1,226,561	55.67

TABLE 7-8 Dead Load Moments, Initial Stress in the Prestressed Reinforcement, and Distance from the Beam Soffit to the Center of Gravity of the Prestressed Reinforcement at the Tenth Points of the Beam in I.P. 7-7.

Pt.	Precast DLM (ft-k)	CIP Slab DLM (ft-k)	SDL Moment (ft-k)	f_{si} (ksi)	Soffit Dist. (in.)
0	0	0	0	189.5	44.50
1	553	460	125	189.5	30.77
2	982	818	200	189.5	20.10
3	1289	1074	250	189.5	12.47
4	1473	1227	300	189.5	7.90
5	1535	1278	300	189.5	6.38
6	1473	1227	250	189.5	7.90
7	1289	1074	150	189.5	12.47
8	982	818	0	189.5	20.10
9	553	460	−175	189.5	30.77
10	0	0	−445	189.5	44.50

span beam that is continuous for superimposed dead load and live load but simply supported for other dead loads. The 10th point section properties are as shown in Table 7-7. Plot a curve illustrating the variation of deflection at midspan as a function of time. The dead load moments, initial stress in the prestressed reinforcement, and distance from the centroid of the prestressed reinforcement to the beam soffit (soffit distance) are shown in Table 7-8. The properties of the materials of construction and the time sequence are as given in I.P. 7-1.

SOLUTION: The curvatures at the 10th points, based upon the use of the numerical integration method of analysis, made with the aid of a programmable calculator, are found to be as shown in Table 7-9. The deflections at the 10th

TABLE 7-9 Curvatures at the Tenth Points for the Beam in I.P. 7-7.

	Curvature: × 10^6					
Pt.	12 Days	197 Days	197′ Days	206 Days	206′ Days	600 Days
0	+0.76	+1.33	+1.33	+1.37	+1.37	+2.06
1	−4.61	−6.93	−3.58	−3.54	−3.01	−2.23
2	−8.90	−13.29	−7.46	−7.42	−6.61	−5.72
3	−12.06	−17.75	−10.30	−10.26	−9.26	−8.13
4	−14.02	−20.40	−12.05	−12.01	−10.83	−9.66
5	−14.67	−21.26	−12.62	−12.58	−11.41	−10.24
6	−14.02	−20.40	−12.05	−12.01	−11.03	−9.90
7	−12.06	−17.75	−10.30	−10.26	−9.66	−8.63
8	−8.90	−13.29	−7.46	−7.42	−7.42	−6.57
9	−4.61	−6.93	−3.58	−3.54	−4.27	−3.69
10	+0.76	+1.33	+1.33	−1.37	−0.53	−0.42

TABLE 7-10 Deflections at the Tenth Points of the Beam in I.P. 7-7.

	Deflections (in.)					
Pt.	12 Days	197 Days	197′ Days	206 Days	206′ Days	600 Days
0	0	0	0	0	0	0
1	−1.05	−1.54	−0.88	−0.88	−0.80	−0.70
2	−1.99	−2.93	−1.69	−1.68	−1.54	−1.35
3	−2.74	−4.02	−2.33	−2.32	−2.13	−1.88
4	−3.22	−4.72	−2.74	−2.73	−2.51	−2.22
5	−3.39	−4.96	−2.89	−2.88	−2.65	−2.35
6	−3.22	−4.72	−2.74	−2.73	−2.53	−2.25
7	−2.74	−4.02	−2.33	−2.32	−2.17	−1.93
8	−1.99	−2.93	−1.69	−1.68	−1.59	−1.41
9	−1.05	−1.54	−0.88	−0.88	−0.84	−0.75
10	0	0	0	0	0	0

points for the significant points in the history of the beam are summarized in Table 7-10, and the plot of midspan deflection versus time is given in Fig. 7-22.

ILLUSTRATIVE PROBLEM 7-8 For the composite post-tensioned beam shown in Fig. 7-4 and the loss of prestress computations of I.P. 7-5, compute the dead load midspan deflection at 600 days using the Branson method. Assume the

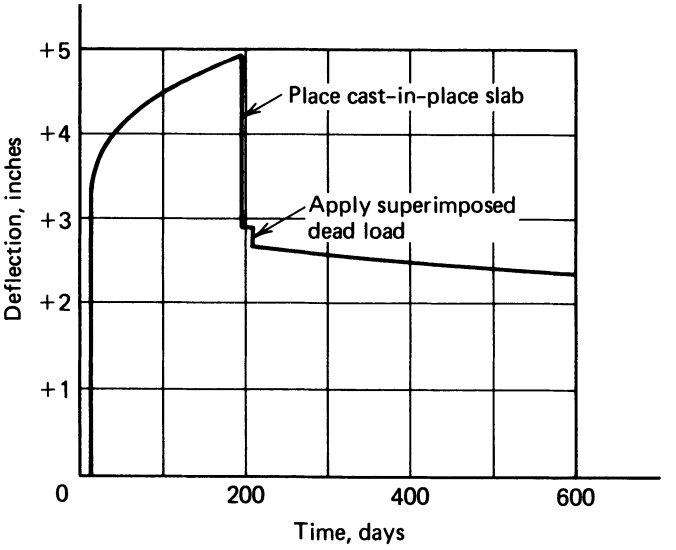

Fig. 7-22. Midspan deflections as a function of time for the beam in I.P. 7-7.

tendon to be on a second-degree parabolic path with no eccentricity at the supports and an eccentricity at midspan of 37.75 in. The span length is 126.3 ft. The superimposed dead load of 263 plf results in a moment of −445 k-ft at one end of the beam only. Use $P_i = 1046$ kips and $\Delta P_u/P_i = -0.235$.

SOLUTION: The elastic deflections are computed to be:

$$\delta_p = -\frac{(5)(1046)(37.75)(126.3)^2 \times 144}{48 \times 2030 \times 625158} = -7.44 \text{ in.}$$

$$\delta_d = \frac{(5)(1535)(126.3)^2 \times 1728}{48 \times 2030 \times 625158} = +3.47 \text{ in.}$$

$$\delta_s = \frac{(5)(126.3)^2(1728) \times 1278}{48 \times 2460 \times 710{,}047} = +2.10 \text{ in.}$$

With $Q = -257$ kips, $y_{cs} = -19.32 - 3.25 = -22.57$ in.,

$$\delta_{ds} = \frac{-257(-22.57)(126.3^2)(144)}{(8)(2460)(1226561)} = +0.55 \text{ in.}$$

The midspan deflection due to the superimposed dead load, computed with basic principles is:

$$\delta_{sdl} = +0.25 \text{ in.}$$

From I.P. 7-5:

$$\Delta P_u = -44.5 \times 5.52 = -245.6 \text{ kips (at 600 days)}$$

$$\frac{\Delta P_u}{P_i} = -0.236 \text{ (at 600 days)}$$

Assume:

$\frac{\Delta P_s}{P_i} = -0.18$ at 200 days, $\lambda = 0.88$, $\lambda' = 0.91$, $\alpha_s = 0.70$, $\gamma_{lac} = 0.67$, $k_r = 1.0$, $v_t = 1.23$ (at 200 days), and $\frac{I}{I'} = 0.51$.

Using eq. 7-33:

$$\delta_p = -7.44\big[1 + (-0.18) + (0.70)(1.00)(1.50)(0.91) + 0.51\big(0.055 + (1.00)(1.50)(0.88 - 0.70(0.91))\big)\big]$$

$$= -7.44(2.255) = -16.77 \text{ in.}$$

$$\delta_d = +3.47\big[1 + (0.70)(1.00)(1.50) + (1 - 0.70)(1.00)(1.50)(0.51)\big]$$

$$= +7.77 \text{ in.}$$

$$\delta_s = +2.31[1 + (0.70)(1.00)(1.50)(0.51)]$$

$$= +3.55 \text{ in.}$$

$$\delta_{ds} = +0.55[1 + (0.67)(1.00)(1.50)]$$

$$= +1.10 \text{ in.}$$

$$\delta_{sdl} = +0.25 \text{ in.}$$

$$\delta_u = -16.77 + 7.77 + 3.55 + 1.10 + 0.25 = -4.10 \text{ in.}$$

ILLUSTRATIVE PROBLEM 7-9 For the double-tee beam of I.P. 7-6, compute the ultimate dead load deflection using the modified step function method.

SOLUTION:

$$E_c = \frac{28}{7.3} = 3.83 \times 10^6 \text{ psi}$$

For the total loss of prestress of 63.60 ksi, and an elastic shortening loss of 11.5 ksi,

$$\Delta P_u = -52.1 \times 0.58 = -30.2 \text{ kips}, \quad P_u/P_i = -0.28$$

$$\delta_p = -\frac{(109)(-8.83)(40)^2(144)}{(8)(3830)(4256)} = -1.70 \text{ in.}$$

$$\delta_d = \frac{(5)(0.20)(40)^4(1728)}{(384)(3830)(4256)} = 0.71 \text{ in.}$$

$$\delta_{sdl} = \frac{(5)(0.04)(40)^4(1728)}{(384)(3830)(4256)} = 0.14 \text{ in.}$$

$$\delta_u = -1.70[1 - 0.27 + (0.865)(2.00)]$$

$$+ 0.71[1 + 2.00] + 0.14[1 + (0.83)(2.00)]$$

$$= -4.18 + 2.13 + 0.37 = -1.68 \text{ in.}$$

7-5 Partially Prestressed Concrete

Partial prestressing was first suggested as a means of permitting the use of higher stresses in nonprestressed reinforcement, together with supplementary pretensioned tendons, as a means of reducing the cracking of the concrete. Later, Abeles suggested the use of high-tensile steel for the entire tensile reinforcement but with only a portion of the steel being prestressed (Abeles 1949). In this manner, economy would result from the reduction in labor required to stress

and grout the tendons. In addition, the use of high-tensile steel for all of the tensile reinforcement was determined to be the most economical alternative because the unit cost per unit of ultimate tensile strength is less for high-tensile-strength steel than for steel having lower tensile strengths.

Currently there are three motivations for the use of partial prestressing. The first is economy of labor and steel costs (i.e., not prestressing and grouting all of the flexural reinforcement). Partially prestressed beams of this type will normally have somewhat lower flexural strengths than fully prestressed members because the average stress in the reinforcement will be lower than it would be if all of the flexural reinforcement in the member were prestressed. Therefore, the nominal flexural strength of members of this type is best determined by using strain compatibility computations. The fundamental principles of flexural strength analysis developed in Sec. 5-2 are appropriate for the analysis of partially prestressed members of this type.

If partial prestressing is used in a member because the concrete cross section to be used is inefficient, but all of the flexural reinforcement is stressed to normal levels, the ultimate moment will not be affected as a result of the use of partial prestressing. This can be better understood if the basic reason for using I- and T-shaped members (Secs. 4-8 and 4-9) is analyzed and compared to using a rectangular section. The preference for the use of I and T shapes normally is based upon service load and not strength considerations. If a rectangular section, which is easier to manufacture and more resistant to large shear stresses, can be found that will work satisfactorily at service loads with moderate tensile stresses in the tensile flange, the flexural strength may very well be as high as would be found for an I or T beam that had been designed for the same loads, but without tensile stresses in the bottom flange under full load. This is particularly true for short-span members, in which the dead weight itself is not important in comparison to the total moment. The motivations for using partial prestressing of this second type are the reductions of form and labor costs that can be derived through the use of simple rectangular or tapered sections.

Deflections due to prestressing and differential deflections between members, under member dead load and prestress, have been significant problems in the manufacture of prestressed-concrete members. The total deflection due to prestressing as well as the variation of deflection between individual members, which is assumed to be a function of the total deflection, can be reduced by not fully prestressing the members in some cases. Assuming that the flexural strength is still adequate, this procedure will result in satisfactory construction for many types of applications. Hence, the third motivation, which is the principal one, is the desire to achieve better performance at service loads without sacrificing the minimum safety requirements of the codes.

Some engineers look forward to the time when the building code provisions for reinforced concrete will be applicable for reinforced concrete flexural

members regardless of their degree of prestressing. Defining partial prestressed concrete is a problem in itself. The degree of prestressing can be thought of in terms of the level of prestressing in the flexural tensile reinforcement, or in terms of the amount of tension in the concrete under service loads. There is no universally accepted definition of partially prestressed concrete at this time. For example, a member in which all of the flexural tensile reinforcement is high-strength steel prestressed to the maximum permissible level permitted by the building code might be considered to be fully prestressed by some persons. Others may consider fully prestressed concrete to be the condition of no tensile stresses in the concrete under service loads. Others may think of partial prestressing as a condition that is between these two states of stress. Even though not all engineers can agree upon a definition, the use of partially prestressed concrete is common.

Partially prestressed members, designed in conformance with the requirements of ACI 318 (i.e., limited flexural tensile stresses in the concrete under service loads, designed on the basis of a noncracked section), normally can be used without significant risk in building floor and roof members because the applied loads normally are predictable with reasonable accuracy, and fatigue is not a design consideration.

Up to now, the principles of prestressing concrete discussed in this book basically have been limited to members that are fully prestressed, or that for all practical purposes are fully prestressed. The exceptions to this are members that take advantage of the provision in ACI 318 permitting the use of flexural tensile stresses as great as $12\sqrt{f'_c}$ when the design is made to conform with special requirements for deflection and corrosion protection. (It should be recognized, however, that this level of allowable tensile stress anticipates flexural cracking.) The code requires that members using the higher allowable tensile stress must be shown to meet the deflection criteria of Sec. 9.5.4 for short- and long-term deflections, using bilinear moment–deflection relationships, as well as to meet the special concrete cover requirements of Sec. 7.7.3.2. Considerations for designing members to conform with the deflection criteria were discussed briefly in the preceding section (Sec. 7-4).

The principle of prestressing concrete, as defined by the originators of the method, was stated in the first paragraph of Chapter 1. This definition has, in recent years, become the definition of fully prestressed concrete. Thus, fully prestressed concrete members are defined, for the purposes of this book, as concrete members that do not contain a significant amount of nonprestressed reinforcement, and are prestressed to a level of compression that either prevents flexural tensile stresses under service loads or restricts them to levels equal to or less than the lower-bound flexural tensile strength of the concrete, when analyzed with due regard to: strain compatibility, the principles of equilibrium, the effects of prestressed and nonprestressed reinforcement, concrete shrinkage,

concrete creep, and elastic deformations. In general, the lower-bound concrete tensile strength should be taken to be on the order of:

$$f_r = 0.50\sqrt{wf'_c} \tag{7-36}$$

which, for concrete having a unit weight of 144 pcf, is:

$$f_r = 6\sqrt{f'_c} \tag{7-37}$$

This is the lowest value for the modulus of rupture for normal-weight concrete contained in ACI 318 and is intended to be a conservative value (see Sec. 3-7).

Partially prestressed concrete members are defined, for the purposes of this book, as concrete members that: are prestressed to a level of compression that will permit cracking under the maximum service loads; may contain significant amounts of nonprestressed reinforcement in addition to prestressed reinforcement; contain prestressed reinforcement that may or may not be stressed to the maximum levels permitted by the applicable building code; but will have sufficient flexural strength to resist the minimum design loads required by the applicable code. This definition presumes that the analysis of members of this type includes consideration of: strain compatibility; the principles of equilibrium; the effects of prestressed and nonprestressed reinforcements; concrete shrinkage, creep, and elastic deformations; the concrete's being incapable of supporting tensile stresses after decompression of the section; and the assumption that a change in mechanical behavior in flexure occurs as a result of decompression (i.e., a change from behavior based upon the properties of the transformed gross section to behavior based upon a cracked, transformed section).

The concept of partially prestressed concrete, as defined herein, requires a determination of the combination of axial force and moment that defines the transition point between behavior that can be considered to be that of an uncracked member and the behavior of a cracked member. The loading that defines this transition is called the decompression loading.

In the determination of the combination of force and moment that causes decompression in a member, the amount of axial force and moment remaining after decompression has taken place also is determined.

Decompression for a partially prestressed member is said to exist when the stress across the thickness of a section (from top to bottom) equals zero at the section under consideration. This is best understood by considering the states of stress illustrated in Fig. 7-23. The condition of stress in Fig. 7-23a is that existing under final prestress and dead load. The application of a significant amount of additional load, as shown in Fig. 7-23b, results in combined stresses (prestress plus applied loads), based upon an uncracked section analysis, as shown in Fig. 7-23c. Because the concrete section is presumed to be unable to withstand tensile stresses, and indeed cannot withstand tensile stresses greater than its modulus of rupture, the section cracks and the stress distribution take the shape shown in Fig. 7-23d. To evaluate the stresses in the cracked section,

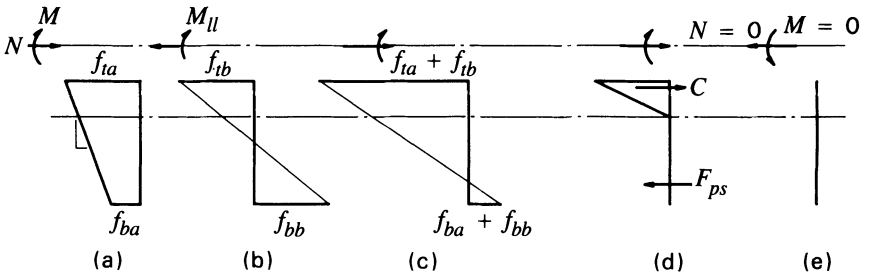

Fig. 7-23. Distribution of stresses considered in the determination of the state of decompression. (a) Distribution of stress in an uncracked flexural member under final prestress plus service dead load. (b) Distribution of stresses on the uncracked section due to the service live load. (c) Distribution of stresses resulting from the combination of final prestress, service dead, and service live loads. (d) Distribution of stresses on a cracked section. (e) Distribution of stress, equal to zero over the full thickness of the member, when the section is decompressed.

one must first determine the decompression force and moment. The decompression force and moment are those required to nullify the condition of stress shown in Fig. 7-23a and create a state of zero stress across the full thickness of the section, as shown in Fig. 7-23e. By deducting the decompression force and moment from the total force and moment producing the combined service live load stresses shown in Fig. 7-23c, the axial force and moment to be used in the determination of the stresses on the cracked section, as illustrated in Fig. 7-23d, are obtained.

By employing Ghali's methods, as explained in Sec. 7-3, the normal force and concomitant moment (or eccentricity of the normal force), required for decompression loading can be computed from a known concrete stress at a reference axis, f_{cra}, and the known slope of the stress diagram, γ, using the following two equations:

$$\Delta N_{decom} = A(-f_{cra}) + Ay(-\gamma) \tag{7-38}$$

$$\Delta M_{decom} = Ay(-f_{cra}) + I_{ra}(-\gamma) \tag{7-39}$$

in which f_{cra}, y, and I_{ra} are with respect to a reference axis that may or may not pass through the centroidal axis of the cross section of the member. The negative signs for the values of f_{cra} and γ in eqs. 7-38 and 7-39 are provided because the purpose of the computations is to determine the force and moment that will nullify the condition of stress shown in Fig. 7-23a.

If the reference axis passes through the centroidal axis of the cross section of the member, eqs. 7-38 and 7-39 become:

$$\Delta N_{decom} = A(-f_{cra}) \tag{7-40}$$

$$\Delta M_{decom} = I_{ra}(-\gamma) \tag{7-41}$$

The changes in the strain at the reference axis and the curvature due to the decompression force and moment are computed from:

$$\Delta\epsilon_{cra\,decom} = \frac{-f_{cra}}{E_c} \tag{7-42}$$

$$\psi_{decom} = -\frac{\gamma}{E_c} \tag{7-43}$$

The axial force and moment to be applied to the cracked section (Fig. 7-23d) are computed from:

$$N - N_{decom} = N_{cracked\text{-}sec} \tag{7-44}$$

$$M - M_{decom} = M_{cracked\text{-}sec} \tag{7-45}$$

in which N and M are the axial force and bending moment applied to the section as a result of prestressing and all applied dead and live loads (Ghali 1986).

Ghali and his colleagues have written computer programs that facilitate the implementation of the methods and procedures they have derived (Elbadry and Ghali 1989; Ghali and Elbadry 1985). Although these methods are not needed for the more common applications of prestressed concrete, the informed engineer must know of their existence, their intended use, and where detailed information on them can be obtained. It is hoped that this discussion will help one to accomplish these objectives.

ILLUSTRATIVE PROBLEM 7-10 Using the general method proposed by Ghali et al., compute the stresses, strains, and deflections of the T-beam analyzed in I.P. 7-2 if the intermittently applied live load is 1667 plf rather 750 plf. Compute the decompression force and bending moment as well as the force and moment applied to the cracked section.

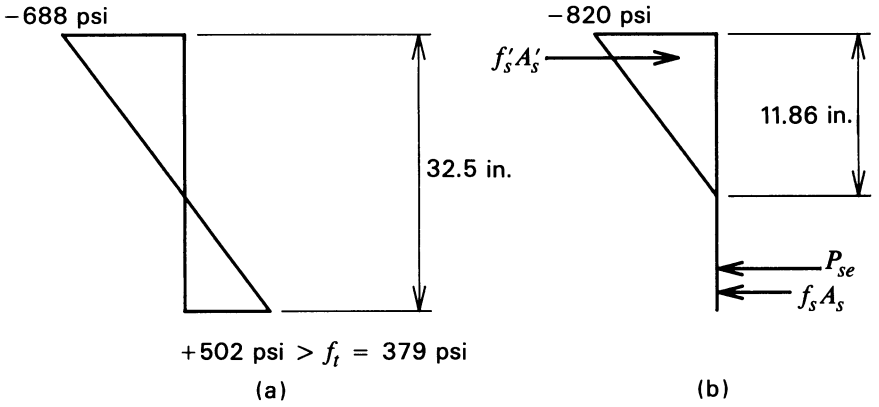

Fig. 7-24. Distribution of stresses under final prestress, dead load, and live load based on the uncracked and cracked sections. (a) Stresses on the uncracked section. (b) Stresses and forces on the cracked section.

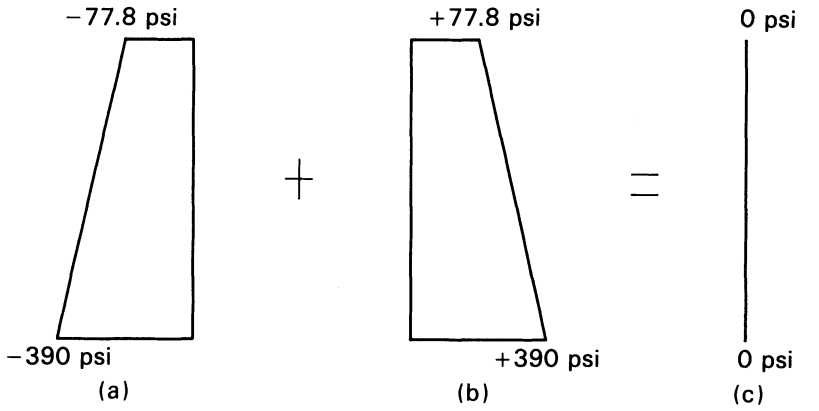

Fig. 7-25. Illustration of the effect of the decompression load and moment on the beam analyzed in I.P. 7-10. (a) Stress distribution under full pressure plus dead load at $t = \infty$. (b) Stress distribution required to decompress the section. (c) Stress distribution with the section decompressed.

SOLUTION: The stresses, strains, curvatures, rotations, and deflections of the beam are identical to those computed in I.P. 7-2 under the effects of prestressing and dead load. The higher intermittent live load that is applied to the beam in this problem, however, causes a moment at midspan of 4000 k-in. and flexural tensile stresses, based upon an uncracked section, that exceed the tensile strength. For this reason, the condition of stress under the full live load must be evaluated by using a cracked section. The distributions of stress under dead and live loads for the uncracked and cracked sections are shown in Fig. 7-24. The effect of the decompression load is shown in Fig. 7-25. By using the

TABLE 7-11 Summary of Stresses and Forces for Reinforcement and Concrete Section for I.P. 7-10.

		State of Loading and Deformations							
		State 1		State 2		State 3		State 4	
Item	Area (in.^{2})	Stress (ksi)	Force (k)	Stress (ksi)	Force (k)	Stress (ksi)	Force (k)	Stress (ksi)	Force (k)
A_s'	1.00	+13.1	+13.1	−25.4	−25.4	−24.5	−24.5	−30.4	−30.4
A_s	4.00	−11.7	−46.9	−36.7	−146.8	−33.8	−135.2	−23.7	−94.8
A_{ps}	2.00	+189.0	+378.0	+155.7	+311.4	+158.4	+316.8	+166.9	+333.8
$A_{c\,net}$			−344.2		−139.2		−157.0		−208.6

State 1. After initial prestressing, elastic deformation, and under beam dead load.
State 2. After time-dependent deformation under prestressing and beam dead load.
State 3. After application of the decompression load and bending moment.
State 4. After cracking under final prestressing and full dead and live load.

computer program called Crack, the stresses and forces in the reinforcements and the concrete section were found to be as shown in Table 7-11 for the different states in the history of the member (Ghali and Elbadry 1985).

REFERENCES

AASHTO. 1989. *Standard Specifications for Highway Bridges, Fourteenth Edition*. Washington, D.C. American Association for State Highway and Transportation Officials.

Abeles, P. W. 1949. *Principles and Practice of Prestressed Concrete*. London. Crosby Lockwood & Son, Ltd.

ACI-ASCE Joint Committee 323. 1958. Tentative Recommendations for Prestressed Concrete. *Journal of the American Concrete Institute* 29(7):545–78.

ACI Committee 318. 1989. *Building Code Requirements for Reinforced Concrete*. Detroit. American Concrete Institute.

ACI Committee 435.1R. 1963. Deflections of Prestressed Concrete Members. *Journal of the American Concrete Institute* 60(12):1697–728.

Branson, D. E. 1974. The Deformation of Noncomposite and Composite Prestressed Concrete Members. In *Deflections of Concrete Structures*. Detroit. American Concrete Institute.

Committee on Prestress Losses. 1975. Recommendations for Estimating Prestress Losses. *PCI Journal* 20(4):43–75.

Elbadry, M. M. and Ghali, A. 1985. Manual of Computer Program CPF: Cracked Plane Frame in Prestressed Concrete. Research Report No. CE85-2, Department of Civil Engineering, The University of Calgary. Calgary, Alberta, Canada.

Elbadry, M. M. and Ghali, A. 1989. Serviceability Design of Continuous Prestressed Concrete Structures. *PCI Journal* 34(1):54–91.

Ghali, A. 1986. A Unified Approach for Serviceability Design of Prestressed and Nonprestressed Reinforced Concrete Structures. *PCI Journal* 31(2):119–37.

Ghali, A. and Elbadry, M. M. 1985. Manual for Computer Program CRACK, Research Report No. CE85-1, Department of Civil Engineering, The University of Calgary. Calgary, Alberta, Canada.

Ghali, A. and Tadros, M. K. 1985. Partially Prestressed Concrete Structures. *Journal of Structural Engineering American Society of Civil Engineers* 111(8):1846–65.

Ghali, A. and Trevino, J. 1985. Relaxation of Steel in Prestressed Concrete. *Journal of the American Concrete Institute* 30(5):82–94.

Neville, A. M., Dilger, W. H., and Brooks, J. J. 1983. *Creep of Plain and Structural Concrete*. London. Construction Press.

Zia, P., Preston, H. K., Scott, N. L., and Workman, E. B. 1979. Estimating Prestress Losses. *Journal of the American Concrete Institute* 1(6):32–38.

PROBLEMS

1. For the double-tee beam shown in Fig. 7-26, compute the ultimate loss of prestress based upon the concrete's being heat-cured normal-weight concrete

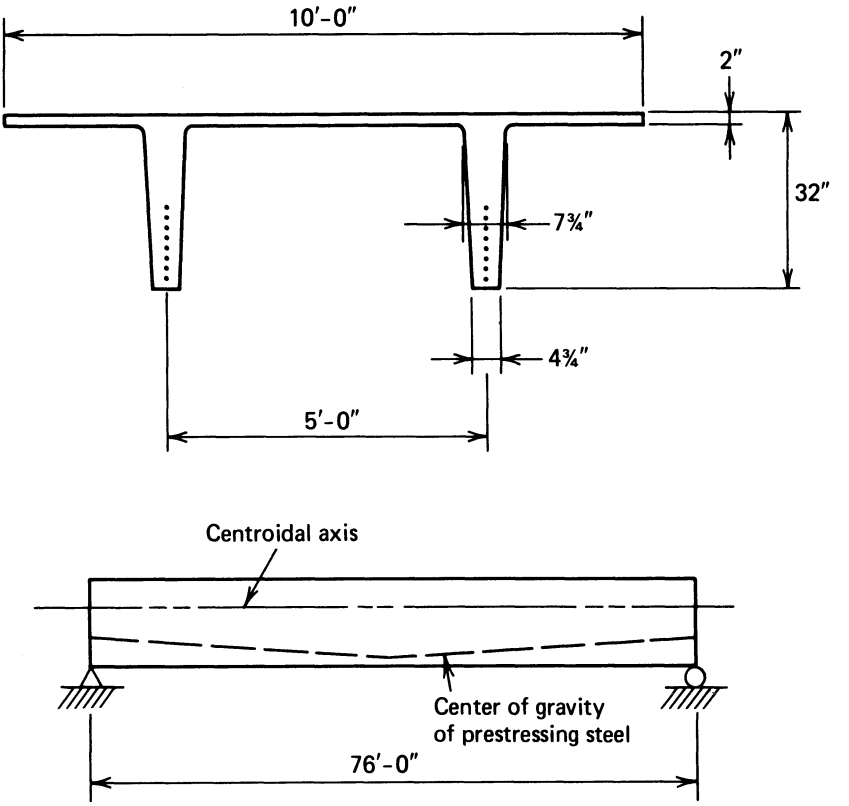

Fig. 7-26. Double-tee beam used in Problem 1. (a) Cross section. (b) Elevation.

having a compressive strength of 4000 psi at transfer and a specified minimum strength of 5000 psi at the age of 28 days, using Branson's modified step function method. Consider slab dead load alone. The prestressed reinforcement is Grade 270 stress-relieved seven-wire strand. The section properties, areas, and loadings are:

$$A_g = 615 \text{ in.}^2 \quad y_b = +21.98 \text{ in.} \quad I_g = 59{,}720 \text{ in.}^4$$

The dead load of the slab is 641 plf, the area of the prestressed reinforcement is 2.14 in.^{2}, the initial stress in the prestressed reinforcement immediately before transfer is 189 ksi, the beam is to be used on a simple span of 76 ft, and the eccentricities of the prestressed reinforcement are +18.48 in. and +11.12 in. at the midspan and ends, respectively. Assume the ambient relative humidity to be 70 percent, the modular ratio to be 7.3, the creep ratio for ultimate creep to be 1.88, the ultimate concrete shrinkage to be -546×10^6 in./in., the elastic modulus of the reinforcement to be 28,000 ksi, $\Delta P_u/P_i = -0.18$, $1 + b_{11} = 1$, and the ultimate relaxation loss of

the prestressed reinforcement to be $0.075f_{si}$. Compare the results with the general and simplified methods recommended by the Prestressed Concrete Institute (Appendix A) and the AASHTO requirements (Appendix B).

SOLUTION:

From eq.7-4:

$$k_s = 1 + \frac{(18.48)^2(615)}{59720} = 4.52$$

From eq. 7-2:

$$f_{ccgs} = -\frac{(189)(2.14)(4.52) + (615)(462.8)(12)(-18.48)/59720}{615 + (7.3)(2.14)(4.52)}$$

$$= -1.125 \text{ ksi}$$

$$P_i = (189)(2.14) + (-1.125)(7.3)(2.14) = 386.9 \text{ kips}$$

$$f_{si} = 180{,}8 \text{ ksi}, f_{sr} = -0.075 \times 180.8 = -13.6 \text{ ksi}$$

Assuming $\zeta = 1 + (7.3)(4.52)2.14/615(1 + 0.88 \times 1.88) = 1.30$, $E_c = 3.83 \times 10^{-6}$ psi, $\eta = 0.88$, $k_r = 1$, $\lambda = 0.91$, and using the modified step function method with only the first four terms of eq. 7-32, because there is no superimposed sustained dead load, the loss of stress in the prestressed reinforcement becomes:

$$\Delta f_{si} = (7.3)(-1.125) + (0.91)(7.3)(-1.125)(1.88) + \frac{(-546)(28)}{(1.30)(1000)} - 0.075(180.8)$$

$$= -8.20 - 14.04 - 11.76 - 13.56 = -47.57 \text{ ksi}$$

Using the PCI General Method:

Elastic shortening:

$$f_{cr} = f_{ccgs} = -1.125 \text{ ksi}$$

$$\text{ES} = nf_{cr} = 7.3 \times -1.125 = -8.21 \text{ ksi}$$

Creep loss:

$$\text{UCR} = 63 - (20)(3.83) = -13.6 \therefore \text{Use } 11$$

Volume to surface ratio $\cong 1.70$ in.

$$\text{SCF} = 1.05 - 0.70(1.05 - 0.09) = 0.99$$

$$\text{MCF} = 1.0$$

$$\text{CR} = (11)(0.99)(1.0)(-1.124) = -12.25 \text{ ksi}$$

Shrinkage loss:

$$\text{USH} = -\frac{27{,}000 - (3000)(3.83)}{1000} = -15.51 \text{ ksi}$$

$$\text{SSF} = 1.04 - 0.70(1.04 - 0.96) = 0.98$$

$$\text{SH} = (-15.51)(0.98) = -15.20 \text{ ksi}$$

Relaxation loss (at $t = 10^5$ hours and with $f'_y = 0.90 \times 270 = 243$ ksi):

$$\text{RET} = (189)\frac{\log 10^5}{10}\left(\frac{189}{243} - 0.55\right) = -21.52 \text{ ksi}$$

Summation:

$$\Delta f_{si} = -8.21 - 12.24 - 15.20 - 21.52 = -57.17 \, k_{si}$$

Using PCI simplified method:

$$\Delta f_{si} = -33.0 + (-13.8)(1.125) = -48.5 \text{ ksi}$$

Using the AASHTO methods:

$$\text{SH} = -\frac{17{,}000 - (150)(70)}{1000} = -6.50 \text{ ksi}$$

$$\text{ES} = (7.3)(-1.125) = -8.21 \text{ ksi}$$

$$\text{CR} = (12)(-1.125) = -13.5 \text{ ksi}$$

$$\text{Relaxation} = -20 + 0.4(8.21) + 0.2(6.5 + 13.5) = -12.72 \text{ ksi}$$

Summation:

$$\Delta f_{si} = -6.50 - 8.21 - 13.50 - 12.72 = -40.93 \text{ ksi}$$

Comparison of results:

Method	Total Loss (ksi)
Branson's	−47.57
PCI General	−57.18
PCI Simplified	−48.50
AASHTO	−40.93

2. A concrete has an elastic modulus of 3000 ksi and is under an initial axial compressive stress of 600 psi. The stress is induced by a tendon prestressed to 200 ksi. The tendon has an elastic modulus of 30,000 ksi and is perfectly elastic (not subject to relaxation). The concrete is free of shrinkage. If the creep characteristics of the concrete are defined by eq. 3-25 with $\psi = 0.60$

and $d = 10.0$, and if the creep ratio is 3.00, determine the stress remaining in the concrete and in the tendon after a period of ten days using the numerical integration procedure with time intervals of one and ten days.

SOLUTION:

The initial strain in the concrete is equal to -600 psi$/3 \times 10^6$ psi or -200×10^{-6} in./in. The computations with a time interval of one day involve the following:

$$\frac{\text{Creep deformation at time } t}{\text{Ultimate creep deformation}} = \left(\frac{t^{0.60}}{10 + t^{0.60}}\right)$$

Increment of creep deformation between times t and $t - 1$ if subject to constant stress:

$$\left(\frac{t^{0.60}}{10 + t^{0.60}} - \frac{(t-1)^{0.60}}{10 + (t-1)^{0.060}}\right)\gamma_u$$

Because the stress on the concrete varies over the time period, the increment of creep must be reduced by the ratio of the stress in the prestressed reinforcement at the beginning of the time period, $t - 1$, to the stress in the prestressed reinforcement at the end of the time period, t. This can be expressed as:

$$\Delta\epsilon_{creep} = \left(\frac{t^{0.60}}{10 + t^{0.60}} - \frac{(t-1)^{0.60}}{10 + (t-1)^{0.060}}\right)\gamma_u \frac{f_{s\,t-1}}{f_{st}}$$

The stress in the prestressed reinforcement at time t is:

$$f_{st} = f_{s\,t-1} - \Delta\epsilon_{creep} \times E_{ps}$$

The strain in the concrete at time t is:

$$\epsilon_{ct} = \epsilon_{ct-1} - \Delta\epsilon_{creep}$$

and the stress in the concrete at time t is:

$$f_{ct} = f_{c\,t-1} \times \frac{f_{st}}{f_{s\,t-1}}$$

The computations for the ten-day period using time increments of one day are summarized in Table 7-12.

For a time interval of ten days, the computation becomes:

$$\text{Creep deformation} = \left(\frac{10^{0.60}}{10 + 10^{0.60}}\right) - 600 \times 10^{-6}$$

$$= -170.8 \times 10^{-6} \text{ in./in.}$$

$$f_s = +200 + \frac{-171 \times 30}{1000} = +194.9 \text{ ksi}$$

$$f_c = \frac{+194.9}{+200.0} \times -600 = -584.7 \text{ psi}$$

3. For the conditions of Problems 2, compute the steel stress and concrete stress remaining at the age of ten days if, in addition to the creep strain, the concrete shrinks as described by eq. 3-17 with $e = 1$ and $f = 35$. Use time intervals of one day and ten days. Ultimate shrinkage, which is to commence at day 0, can be assumed to be -400 millionths in./in.

SOLUTION:

The computations for a time interval of one day are summarized in Table 7-13.

For 10-day interval, $\Delta\epsilon = -170.8 - 88.9 = -259.7 \times 10^6$ in./in.
$\Delta f_s = -7.79$ ksi, $f_s = 192.21$ ksi, $f_c = -576.62$ psi

4. For the double-tee beam shown in Fig. 7-26, determine the deflection assuming $E_{ci} = 3.89 \times 10^6$ psi, $E_c = 4.03 \times 10^6$ psi, $\Delta P_u/P_i = -0.22$ and the remaining data is as given in Problem 1.

TABLE 7-12 Summary of Computations for Effects of Concrete Creep after Ten Days Using an Integration Interval of One Day.

Day	γ_t/γ_u	$\Delta\gamma_t/\gamma_u$	$\Delta\epsilon_{creep}$ (10^{-6} in./in.)	f_s (ksi)	ϵ_c (10^{-6} in./in.)	f_c (psi)
0	0			200	−200	−600
		0.0909	−54.54			
1	0.0909			198.36	−254.54	−595.08
		0.0407	−24.22			
2	0.1316			197.64	−278.76	−592.92
		0.0304	−18.03			
3	0.1620			197.09	−296.79	−591.27
		0.0248	−14.66			
4	0.1868			196.66	−311.45	−589.97
		0.0212	−12.507			
5	0.2080			196.28	−323.96	−588.84
		0.0186	−10.952			
6	0.2266			195.95	−334.91	−587.86
		0.0166	−9.758			
7	0.2432			195.66	−344.67	−586.98
		0.0151	−8.863			
8	0.2583			195.39	−353.53	−586.18
		0.0137	−8.03			
9	0.2720			195.15	−361.56	−585.46
		0.0127	−7.435			
10	0.2847			194.93	−368.99	−584.79

TABLE 7-13 Summary of Effects of Concrete Creep and Shrinkage after a Period of Ten Days Using an Integration Interval of One Day.

Day	$\epsilon_{shrinkage}$ (10^{-6} in./in.)	$\Delta\epsilon_{shrinkage}$ (10^{-6} in./in.)	$\Delta\epsilon_{creep}$ (10^{-6} in./in.)	f_s (ksi)	$\epsilon_{concrete}$ (10^{-6} in./in.)	f_c (psi)
0	0			200.00	−200.00	−600
		−11.11	−54.54			
1	−11.11			198.03	−265.65	−594.09
		−10.51	−24.18			
2	−21.62			196.99	−300.34	−590.97
		−9.96	−17.97			
3	−31.58			196.15	−328.27	−588.46
		−9.45	−14.59			
4	−41.03			195.43	−352.31	−586.29
		−8.97	−12.43			
5	−50.00			194.79	−373.71	−584.36
		−8.54	−10.87			
6	−58.54			194.20	−393.12	−582.61
		−8.12	−9.67			
7	−66.66			193.67	−410.91	−581.01
		−7.76	−8.77			
8	−74.42			193.17	−427.44	−579.52
		−7.40	−7.93			
9	−81.82			192.71	−442.78	−578.14
		−7.07	−7.34			
10	−88.89			192.28	−457.19	−576.85

SOLUTION:

$$f_{ci} = -1.125 \text{ ksi}, f_{si} = 180.8 \text{ ksi, and } P_i = 387 \text{ kips}$$

$$\delta_p = -\frac{(387)(11.2)(76^2)(144)}{(8)(3890)(59{,}720)} - \frac{(387)(7.36)[3(76^2) - 4(38^2)](144)}{(24)(3890)(59{,}720)}$$

$$= -1.93 - 0.85 = -2.78 \text{ in.}$$

$$\delta_d = +\frac{(5)(0.641)(76^4)(1728)}{(384)(3890)(59{,}720)} = +2.07 \text{ in.}$$

$$\delta_u = -2.78[1 + (-0.22) + (1.00)(0.91)(1.88)]$$

$$+2.07\,[1 + (1.00)1.88] = -6.92 + 5.96 = -0.96 \text{ in.}$$

Note: E_{ps} of 4.03×10^6 psi should be used in the computations of deflections for loads applied after the concrete has attained its specified minimum strength.

5. A rectangular beam 12 in. wide and 42 in. deep is to be prestressed with a single bonded tendon having a steel area of 0.918 sq. in. The beam is to be used on a span of 60.0 ft. The stress in the prestressed reinforcement after elastic shortening will be 189 ksi. Immediately after prestressing, a super-

imposed load of 825 plf is to be applied to the beam. The parabolic tendon path is located 3 in. above the soffit at midspan and 21 in. above the soffit at each end. Compute the deflection of the beams using a bilinear deflection analysis. Use $E_c = 4000$ ksi, $E_{ps} = 28{,}000$ ksi, and $f'_c = 5000$ psi.

SOLUTION:

The parameters for the gross section needed in the analysis are: $A_c = 504$ in.^{2}, $I_g = 74{,}088$ in.^{4}, and $r^2 = 147$ in.^{2}, and the section weights 525 plf. The stresses in the concrete section due to prestressing and the applied loads are summarized in Table 7-14.

The bottom-fiber stress under full load exceeds $6\sqrt{f'_c}$ but is less than $12\sqrt{f'_c}$. Hence, a bilinear analysis is required. The cracking moment and total uniformly distributed load that will result in cracking are:

$$M_{CR} = \frac{74088}{21}\frac{1230 + 7.5\sqrt{5000}}{12000} = 517 \text{ k-ft}$$

$$W_{CR} = \frac{8 \times 517}{60^2} = 1.149 \text{ klf}$$

The superimposed load required to crack the section is $1149 - 525 = 624$ plf. The transformed area of the reinforcement, nA_{ps}, equals 6.426 in.^{2}, and the depth to the neutral axis is computed as follows:

$$\frac{12y^2}{2} = 6.426(39 - y)$$

$$y = 5.95 \text{ in.}$$

The moment of inertia of the cracked section and the effective moment of inertia, as provided in ACI 318 (see eq. 7-35) are computed as follows:

$$I_{CR} = \frac{12 \times 5.95^3}{3} + 6.426(39.0 - 5.95)^2 = 7862 \text{ in.}^4$$

$$I_e = \left(\frac{1149}{1350}\right)^3 + (74088) + \left[1 - \left(\frac{1149}{1350}\right)^3\right] 7862 = 48693 \text{ in.}^4$$

TABLE 7-14 Summary of Concrete Stresses for Problem 5.

	Top fiber (psi)	Bottom fiber (psi)
Initial prestressing	+540	−1230
Beam dead load	−804	+804
Superimposed load	−1263	+1263
Total	−1527	+837

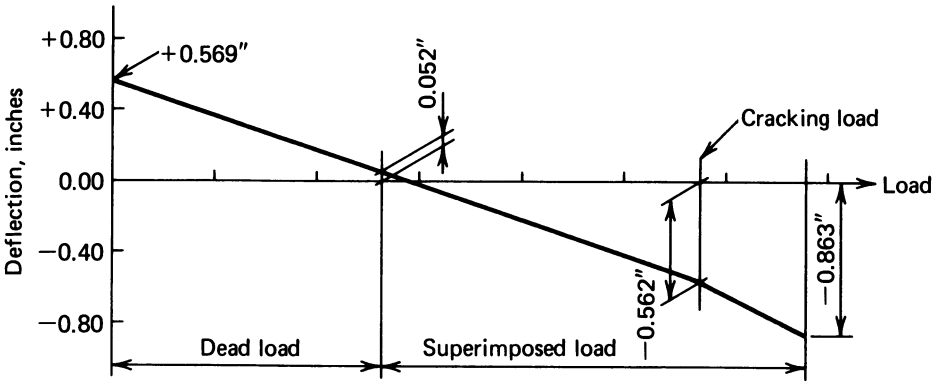

Fig. 7-27. Results of the computations for Problem 5.

The instantaneous deflections are computed as follows:

$$\delta_p = -\frac{(5)(0.918)(189)(18)(60^2)(144)}{(48)(4000)(74{,}088)} = -0.569 \text{ in.}$$

$$\delta_{sL1} = \frac{(5)(1.149)(60^4)(1728)}{(384)(4000)(74{,}088)} = 1.131 \text{ in.}$$

$$\delta_{sL2} = \frac{(5)(1.201)(60^4)(1728)}{(384)(4000)(48{,}693)} = 0.301 \text{ in.}$$

The results are plotted in Fig. 7-27.

6. Compute the initial deflection of the simply supported box girder bridge of Example IV in Appendix B using the initial stress distribution given in the example. Assume the loss of prestress due to elastic shortening is accounted for in the stressing procedure (i.e., slight overstressing to offset the loss due to elastic shortening). Use $A_{ps} = 44.37$ in.^{2} and $w_d = 8.36$ klf.

SOLUTION:

The computations are summarized in Table 7-15.

7. For the double-tee beam in Fig. 7-26, determine the prestressing force, P_i, at the 20th points immediately after transfer, using eq. 7-2. Note that the eccentricity varies from 11.12 in. at each end to 18.48 in. at midspan. Use $n = 7.3$, $A_{ps} = 2.14$ in.^{2}, $I = 59{,}720$ in.^{4}, $A_c = 615$ in.^{2}, $P_j' = 404.46$ kips, and $M_{dmax} = 462.8$ k-ft.

SOLUTION:

$$f_{ci} = \frac{(404.46)k_s + \dfrac{(615)(12)M_d e}{59{,}720}}{615 + (7.3)(2.14)k_s} = \frac{404.46k_s + 0.12357M_d e}{615 + 15.622k_s}$$

TABLE 7-15 Summary of Computations for Problem 6.

20th Pt.	Dist. (ft)	Prestress Force (k)	e (in.)	Moment (k-ft)	Defl. (in.)
0	.000	8129.000	.000	.000	.000
1	8.100	8154.000	5.950	1167.721	−.167
2	16.200	8180.000	11.280	2183.792	−.330
3	24.300	8206.000	15.970	3065.921	−.483
4	32.400	8232.000	20.040	3804.547	−.623
5	40.500	8257.000	23.490	4405.657	−.746
6	48.600	8283.000	26.310	4876.505	−.849
7	56.700	8309.000	28.500	5222.856	−.931
8	64.800	8334.000	30.070	5444.365	−.991
9	72.900	8360.000	31.000	5554.063	−1.026
10	81.000	8386.000	31.320	5537.520	−1.037
11	89.100	8412.000	31.000	5419.730	−1.024
12	97.200	8392.000	30.070	5299.027	−.986
13	105.300	8366.000	28.500	5087.481	−.926
14	113.400	8341.000	26.310	4749.340	−.843
15	121.500	8315.000	23.490	4292.122	−.740
16	129.600	8289.000	20.040	3709.357	−.617
17	137.700	8263.000	15.970	2990.063	−.479
18	145.800	8238.000	11.280	2129.272	−.327
19	153.900	8212.000	5.950	1138.962	−.166
20	162.000	8186.000	.000	.000	.000

$$P_i = 404.46 - nf_{ci}A_{ps} = 404.46 - 15.622f_{ci}$$

The computations are summarized in Table 7-16.

8. For the double-tee of Problem 7, determine the instantaneous deflection due to prestressing alone, using the values of P_i computed in Problem 7 as well as with P_i being a constant value of 386.91 kips. $E_c = E_{ps}/n = 3836$ ksi.

TABLE 7-16 Summary of Computations for Problem 7.

Pt.	e (in.)	k_s	M_d (k-ft)	f_{ci} (ksi)	P_o (kips)
0	11.12	2.273	0	−1.489	381.21
1	11.86	2.449	87.9	−1.319	383.85
2	12.59	2.632	166.6	−1.227	385.29
3	13.33	2.830	236.0	−1.147	386.55
4	14.06	3.036	296.2	−1.077	387.64
5	14.80	3.256	347.1	−1.024	388.46
6	15.54	3.487	388.8	−0.991	388.97
7	16.27	3.726	421.1	−0.981	389.14
8	17.01	3.980	444.3	−0.998	388.87
9	17.74	4.241	458.2	−1.043	388.16
10	18.48	4.517	462.8	−1.123	386.91

TABLE 7-17 Summary of Computations for Problem 8 with Variable P_i.

20th Pt.	Dist. (ft)	Prestress Force (k)	e (in.)	Moment (k-ft)	Defl. (in.)
0	.000	381.210	11.120	−353.254	.000
1	3.800	383.850	11.860	−379.371	−.501
2	7.600	385.290	12.590	−404.233	−.960
3	11.400	386.550	13.330	−429.392	−1.376
4	15.200	387.640	14.060	−454.184	−1.745
5	19.000	388.460	14.800	−479.100	−2.064
6	22.800	388.970	15.540	−503.716	−2.332
7	26.600	389.140	16.270	−527.608	−2.544
8	30.400	388.870	17.010	−551.223	−2.699
9	34.200	388.160	17.740	−573.829	−2.794
10	38.000	386.160	18.480	−594.686	−2.826

SOLUTION:

The deflections at the 20th points are summarized in Tables 7-17 and 7-18—the first for a variable P_i and the second for a constant P_i. As will be seen from a review of the tables, the variation in the initial prestressing force does not have a significant effect on the deflections in this instance.

TABLE 7-18 Summary of Computations for Problem 8 with Constant P_i.

20th Pt.	Dist. (ft)	Prestress Force (k)	e (in.)	Moment (k-ft)	Defl. (in.)
0	.000	386.910	11.120	−358.536	.000
1	3.800	386.910	11.860	−382.396	−.500
2	7.600	386.910	12.590	−405.933	−.958
3	11.400	386.910	13.330	−429.792	−1.373
4	15.200	386.910	14.060	−453.329	−1.740
5	19.000	386.910	14.800	−477.189	−2.058
6	22.800	386.910	15.540	−501.048	−2.325
7	26.600	386.910	16.270	−524.585	−2.536
8	30.400	386.910	17.010	−548.444	−2.691
9	34.200	386.910	17.740	−571.981	−2.785
10	38.000	386.910	18.480	−595.841	−2.818

8 Additional Design Considerations

8-1 Composite Beams

Flexural members formed of two concrete components made at different times, such as precast and cast-in-place elements, frequently are employed in construction. Beams so constructed are referred to as composite beams. An illustration of a typical composite bridge beam is given in Fig. 8-1.

Composite construction permits the precasting of portions of concrete members that: (a) may be difficult to form because of their shape, (b) are difficult from the standpoint of placing and consolidating the concrete, and (c) contain relatively large amounts of reinforcement. Precasting allows the members to be made under working conditions more favorable than those normally found on construction sites. The need for falsework frequently is avoided with composite construction because the precast elements often can be designed to support the dead load of the precast concrete elements as well as the cast-in-place elements without supplementary temporary support. Dead and live loads, applied after the cast-in-place deck has hardened, are supported by the composite beam. Composite cast-in-place concrete toppings frequently are used as a means of providing flat or level surfaces and to connect precast elements together to form horizontal diaphragms for resisting lateral loads.

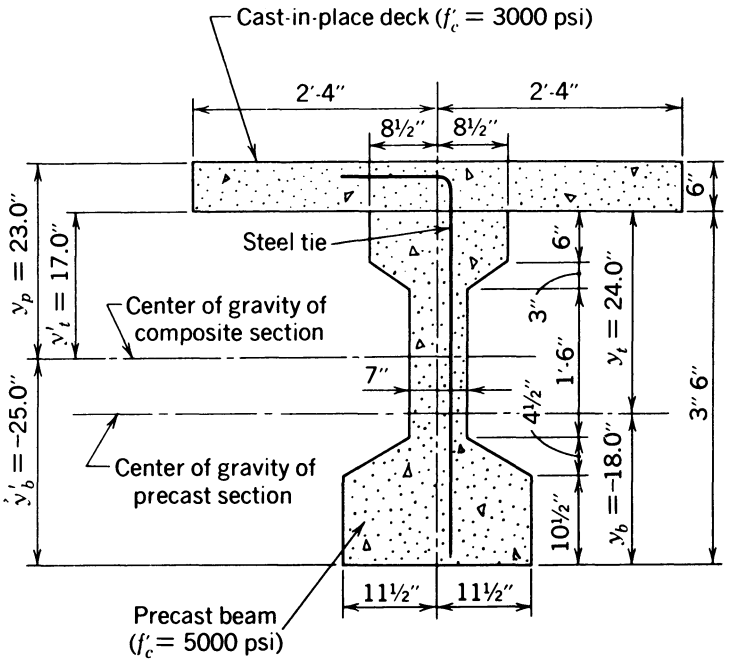

Fig. 8-1. Cross section of a composite beam.

The use of large, composite top flanges contributes to flexural strength at both service and design loads, but does not significantly improve the shear strength of prestressed beams. For this reason, there is little structural advantage, if any, to be gained in using composite construction for short-span members, in which shear strength generally is more critical than is flexural strength.

In designing composite beams, it is necessary to know the section properties of the various sections involved in the analysis, which may include the gross, net, net-transformed, transformed, and age-adjusted section properties of the precast and composite sections (see Sec. 4-10). The flexural stresses and strains resulting from the various loading effects can be computed only after the section properties have been determined.

In addition, to achieve composite action, the designer must provide a means of transferring shear stresses from the concrete that is cast first (hardened concrete) to that which is cast subsequently. Nominal shear stresses can be transferred by bond alone if the surface of the hardened concrete is clean, saturated, and rough, the stress transfer being made by frictional forces at the joint between the two concretes. Larger shear stresses can be transferred between the two components if, in addition to the above, reinforcement is extended from one component into the other and anchored on each side of the joint. The

reinforcement develops tensile stresses as a result of small in-plane displacements of the joint between the two components adding to the shear strength of the joint. Shear keys normally are not used for transferring shear stresses between the elements of a composite member.

Using the provisions of Sec. 17.5 of ACI 318-89, composite sections must be designed for shear based upon

$$V_u \leq \phi V_{nh} \tag{8-1}$$

in which V_u is the design (factored) shear force at the section under consideration, ϕ is equal to 0.85 and V_{nh} is the nominal horizontal shear strength of the joint (contact surface or surfaces) between the two concrete members intended to act as a single composite member. The nominal horizontal shear stress, v_{nh}, is computed as

$$v_{nh} = \frac{V_{nh}}{b_v d} \tag{8-2}$$

in which b_v is the width of the cross section at the contact surface, in inches and d is the distance from the extreme compression fiber to the centroid of the tension reinforcement for the entire composite section, in inches. The permissible values for v_{nh} are:

1. 80 psi when ties, in the form of nonprestressed reinforcement, are not provided, but the contact surfaces are clean, free of laitance, and intentionally roughened to a full amplitude of approximately 0.25 in.
2. 80 psi when vertical nonprestressed reinforcement is provided, and the contact surfaces are clean but not intentionally roughened. The reinforcement can be in the form of ties or extended stirrups, proportioned to equal to or exceed the requirements of eq. 6-13 (minimum shear reinforcement required in Sec. 11.5.5.3 of ACI 381), provided at spacings that do not exceed four times the least dimension of the supported element or 24 in. It is essential the strength of the reinforcement be developed on each side of the contact surface.
3. 350 psi when the conditions of both (1) and (2) are met.
4. $0.20f'_c \leq 800$ psi when the code provisions for shear friction are met (ACI 318 Sec. 11.7).

The reader should review the complete requirements of ACI 318 regarding composite concrete flexural members. Only the more important points have been presented here.

Differential-shrinkage stresses in composite construction can result in the development of tensile stresses being developed in the cast-in-place concrete and a reduction in the precompression of the tensile flange of the precast element. The differential shrinkage has no effect on the flexural strength of the composite

beam, but it does slightly reduce the load required to crack the tensile flange of the precast element. This effect should be considered in structures in which the cracking load is believed to be critical, but it normally is ignored.

When one is computing the properties of transformed sections, the difference in the elastic properties of the cast-in-place concrete and the concrete and the concrete in the precast element must be taken into account by adjusting the width of the composite flange in proportion to the modular ratio of the two concretes. An example of this type of calculation is given in I.P. 8-1.

ILLUSTRATIVE PROBLEM 8-1 Using the gross section properties, compute the flexural stresses in the precast and cast-in-place concrete for the composite bridge beam section shown in Fig. 8-1 when the sum of the moments due to the dead load of the beam, slab, and diaphragms is 673 k-ft, and the sum of the moments due to the future wearing surface, live load, and impact is 830 k-ft. The section properties for the gross precast and composite sections are as follows:

Precast section:

$$y_t = -24.0 \text{ in.} \quad S_t = -4450 \text{ in.}^3 \quad y_b = 18.0 \text{ in.} \quad S_b = 5950 \text{ in.}^3$$

Composite section: It is assumed that the ratio of the elastic moduli of the concretes in the slab and girder is 0.60, and the width of the top flange of the transformed section is $0.60 \times 56 = 33.6$ in. The section properties are:

$$y_p = -23.0 \text{ in.}, \quad S_p = -9400 \text{ in.}^3, \quad I = 216{,}000 \text{ in.}^4$$

$$y_t = -17.0 \text{ in.}, \quad S_t = -12{,}700 \text{ in.}^3$$

$$y_b = 25.0 \text{ in.}, \quad S_b = 8650 \text{ in.}^3$$

SOLUTION:

	Stress in Extreme Fibers (psi)		
	CIP slab	*Precast top*	*Precast bottom*
Dead load		−1810	+1360
Live load plus impact	−1060	−785	+1150
Totals	−1060	−2595	+2510

ILLUSTRATIVE PROBLEM 8-2 Compute the gross section properties of the precast and composite sections for the cross section shown in Fig. 8-1 when the precast beam is made of sand-lightweight concrete having a unit weight of 112 pcf, and the cast-in-place deck slab is normal-weight concrete (145 pcf). Assume the 28-day compressive strengths to be 4500 and 3500 psi for the beam and deck concretes, respectively. Assume that eq. 3-4 is accurate for both concretes.

TABLE 8-1 Computations for the Centroid of the Precast I-Section Shown in Fig. 8-1.

Part	Area computation $b \times h = A$	Distance y	First moment Ay
1	$7 \times 42 = 294$	21	6174
2	$10 \times 6 = 60$	3	180
3	$0.5 \times 10 \times 3 = 15$	7	105
4	$0.5 \times 16 \times 4.5 = 36$	30	1080
5	$16 \times 10.5 = 168$	36.75	6174
	573		13,713

SOLUTION: The elastic moduli for the concretes in the precast beam and the cast-in-place slab, using eq. 3-4, are 2620 ksi and 3400 ksi, respectively. The ratio of the moduli for the concretes is 1.30.

The section properties are calculated by first determining the centroid of the section under consideration by taking moments about the top of the section, and subsequently computing the moment of inertia of the section with respect to a horizontal axis passing through the centroid. The computation of the moment of inertia is done by summing the moments of inertia, with respect to the reference axis, of the individual components or parts of the section. For a section having n components, this can be expressed mathematically as:

$$I = \sum_{1}^{n} [I_{cg} + Ay^2]$$

TABLE 8-2 Computations for the Moment of Inertia for the Precast I-Section Shown in Fig. 8-1 with Respect to its Centroidal Axis.

1	$\left[(-23.9 + 21.0)^2 + \frac{42.0^2}{12}\right] 294$	$= 45{,}690$
2	$\left[(-23.9 + 3.0)^2 + \frac{6.0^2}{12}\right] 60$	$= 26{,}389$
3	$\left[(-23.9 + 7.0)^2 + \frac{3.0^2}{18}\right] 15$	$= 4292$
4	$\left[(-23.9 + 30.0)^2 + \frac{4.5^2}{18}\right] 36$	$= 1380$
5	$\left[(-23.9 + 36.75)^2 + \frac{10.5^2}{12}\right] 168$	$= 29{,}284$
		$I = 107{,}035 \text{ in.}^4$

TABLE 8-3 Computations of the Transformed Composite Section Properties.

$1.30 \times 56 \times 6 =$	$437 \times 3 = 1{,}310$		$234 + 3$	103,569
	$573 \times 29.9 = 17{,}132$		$135 + 0$	77,355
	1,010	18,442		107,031
				287,955

$$y_p = \frac{18{,}442}{1{,}010} = 18.3''$$

Computations for the centroid of the section, computed by taking moments about the top fiber, are shown in Table 8-1. The distance from the top fiber to the centroid is equal to:

$$y_t = \frac{-13{,}713}{573} = -23.9 \text{ in.}$$

Computations for the moment of inertia about the reference axis that passes through the centroid of the precast section are given in Table 8-2. The distance from the top of the cast-in-place slab to the centroid of the composite section, y_p, and the moment of inertia of the transformed composite section can be computed in an abbreviated form, as shown in Table 8-3; and the distance from the top fiber to the centroidal axis, b, is equal to $18{,}442/1010 = 18.3$ in., and the moment of inertia of the transformed composite section is 287,955 in.^{4}.

8-2 Beams with Variable Moments of Inertia

The moment due to prestressing with straight tendons can be made to vary along the length of a simple beam by varying the depth of the member. Members having a variable depth can, of course, be prestressed with curved tendons to optimize the effectiveness of the prestressing if that is desired.

A sloped beam, shown in Fig. 8-2, has variable depth and moment of inertia. This type of beam is adaptable to roof construction where the slope of the top flange can be used to provide roof drainage. Although beams of this shape have been produced, they are not used extensively, as they have several disadvantages that limit their use:

1. The design of variable-depth beams must be done with care, because the maximum moment and maximum flexural stresses may not (probably do not)

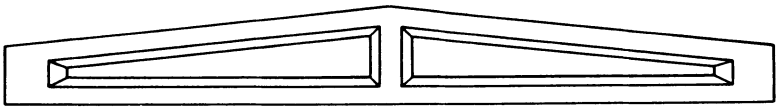

Fig. 8-2. Elevation of a beam with a sloping top flange.

Fig. 8-3. Vector diagram of forces at ridge of beam with sloping top flange.

occur at the same section. Therefore, in order to be certain that the critical sections are considered, the service load stresses and flexural strength must be investigated at several points along the span. This refinement normally is not required in the design of simple beams; so the need for it is not always recognized.

2. The sloping top flanges intersect at the center of the beam, and the large inclined compressive forces resisted by the top flanges intersect at an angle, as shown in the vector diagram of Fig. 8-3. Provision must be made for the vertical components of the forces if upward buckling of the top flanges is to be avoided. This danger is enhanced when penetrations are provided in the webs of the beams at midspan for utilities.

3. Forms for members with sloping flanges are relatively expensive and not easily converted for manufacturing the many different span lengths encountered in modern commercial and industrial building construction.

Another type of beam with a variable moment of inertia and depth, which can be used to advantage in roof as well as bridge construction, is illustrated in Fig. 8-4. This beam can be stressed with straight tendons, and, because the depth of the section is greater at the ends, the eccentricity of the prestressing force at the ends will be relatively less than at midspan. As a result, the stresses in the concrete due to prestressing will not be as great at the ends as they are at midspan. In this manner, an effect similar to curving the tendons in a prismatic beam can be obtained.

Another economical method of forming a beam with a variable moment of inertia is to use a box section, as illustrated in Fig. 8-5. In a beam of this type, the hollow core frequently is made with inexpensive plywood or paper forms that can be placed lower near midspan than at the ends. In this manner, the thicker concrete flanges are placed where needed to resist the larger compressive stresses due to pretensioning at the ends and those due to applied loads at midspan.

Beams with variable moments of inertia and depth frequently are used in

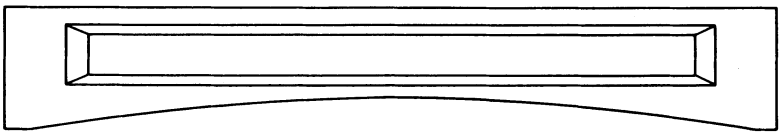

Fig. 8-4. Elevation of beam with variable bottom-flange thickness.

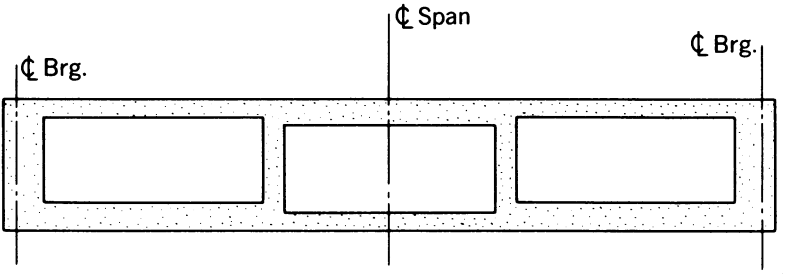

Fig. 8-5. Longitudinal cross section of a hollow box beam showing a method of varying the moment of inertia.

continuous prestressed-concrete structures, for the same reasons that variable depths are employed in continuous members made of other materials. Continuity in prestressed-concrete construction is discussed in Chapter 10.

8-3 Segmental Beams

Post-tensioned beams consisting of two or more elements or components held together by prestressing sometimes are used to facilitate fabrication, transportation, or erection, or for other considerations. An example of a multielement beam formed of three precast units is shown in Fig. 8-6.

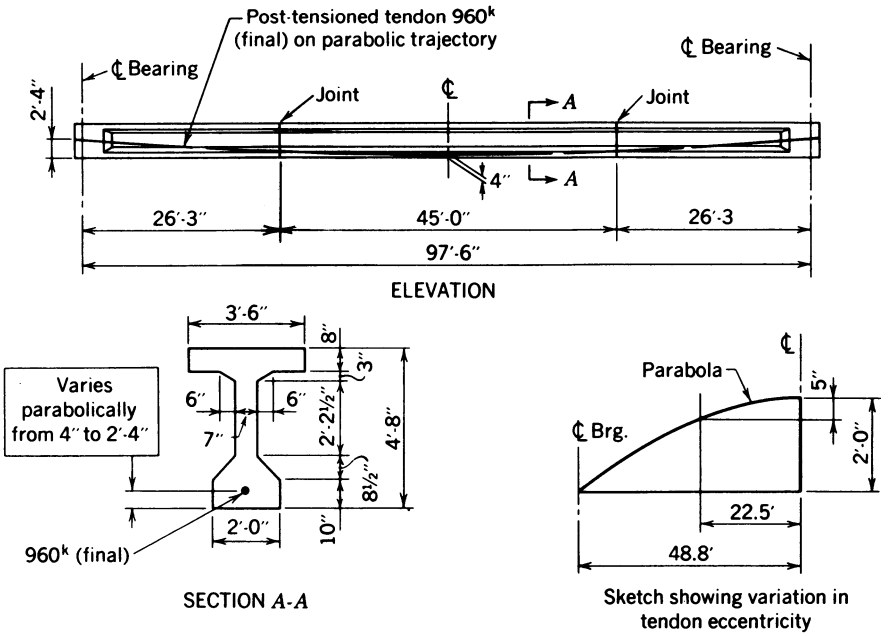

Fig. 8-6. Segmental post-tensioned beam. Adapted from bridge over Naugatuck River, Route 68, Connecticut.

Fig. 8-7. A precast segment of the Downstream Bridge at Auteuil Boulogne Saint-Cloud, Paris. (Provided by and reproduced with the permission of the Freyssinet Company, Inc., Charlotte, N.C.)

In beams on which this method is employed, the prestressing force generally is very large in comparison to the shear force that must be developed between the elements. This is true in part because this method is used most often on large, long beams, in which shear forces are not as important as in short beams. As a result, the friction that can be developed between the elements due to the prestressing force normally is sufficiently large to provide high factors of safety against slipping. Keys frequently are provided to facilitate assembly of the units, but they normally are not needed for the transfer of shear forces.

A precast segment of the Downstream Bridge at Autevil in Paris during its erection is shown in Fig. 8-7. The long-span girders of this bridge are composed of many precast segments held together by longitudinal prestressing.

ILLUSTRATIVE PROBLEM 8-3 For the beam shown in Fig. 8-6, compute the factor of safety against slipping at the joint if the maximum shear load at the joint is 70 k. Include the effect of the inclination of the tendons resulting from their parabolic path. Assume that the coefficient of friction between the concrete units is 1.0

SOLUTION: The vertical displacement through which the tendon moves between midspan and the joint is:

$$\left(\frac{22.5}{48.8}\right)^2 \times 24 = 5 \text{ in.}$$

Taking α as the angle of inclination of the tendons at the joint:

$$\tan \alpha = \frac{2 \times 5}{12 \times 22.5} = 0.037$$

$$P \sin \alpha = 0.037 \times 960 = 35.5 \text{ kips}$$

$$V_{concrete} = V - P \sin \alpha = 34.5 \text{ kips}$$

$$\mu P = 1.0 \times 960 = 960 \text{ kips}$$

Hence, the factor of safety against slipping is calculated as:

$$\text{Safety factor} = \frac{960}{34.5} \cong 27.8$$

8-4 Tendon Anchorage Zones

In post-tensioned beams it is customary, and often necessary, to curve the tendons vertically and horizontally at the ends of the beams as a means of reducing the eccentricity of the prestressing force and providing space in which to embed the tendon anchorages in an acceptable configuration. To accomplish this objective, as well as to provide sufficient space for nonprestressed secondary reinforcement in the anchorage zones, a short section at the end of the beam often is enlarged and made rectangular in cross section. This rectangular section, commonly called an end block, is illustrated in Fig. 8-8. End blocks occasionally are used with pretensioned members as well, but experience has shown that they usually are not needed. The provision of end blocks greatly facilitates the placing and compacting of the concrete at the ends of the beams—an important consideration in pretensioned as well as post-tensioned members.

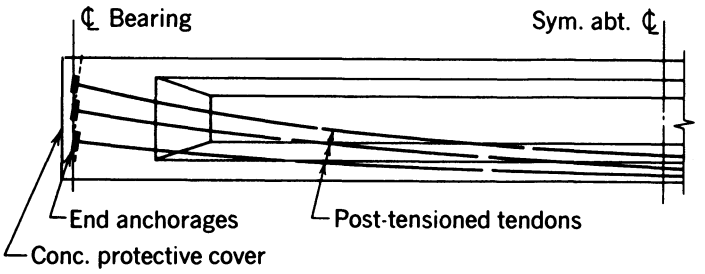

Fig. 8-8. Half elevation of a post-tensioned beam.

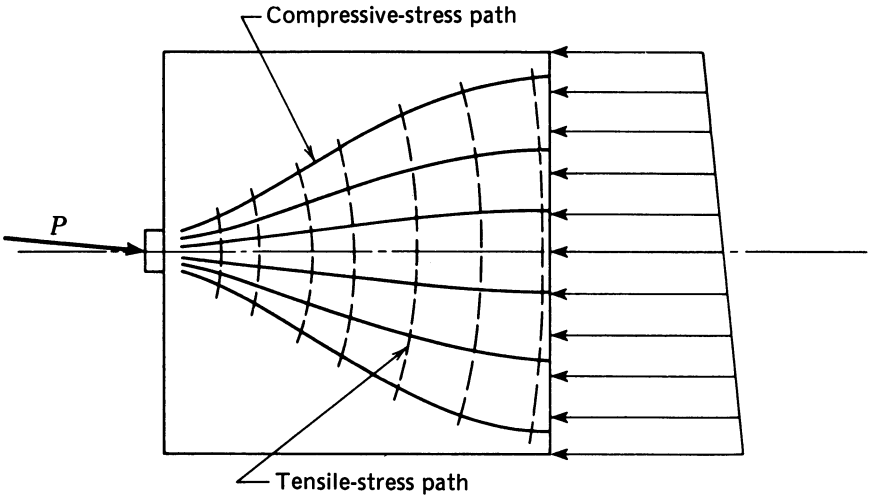

Fig. 8-9. Idealized stress paths in end block with a single load.

The distribution of the principal tensile and compressive stress paths at the ends of prismatic members can be visualized by considering the schematic diagram, as shown in Fig. 8-9. From this diagram, it will be seen that the stress paths are closely spaced near the loaded surface of the member, and that they spread to a more uniform distribution some distance from the end of the member. The distance from the point of bearing to the section at which the distribution of stress can be considered to be without the effects of the concentration of the load is approximately equal to one times the thickness of the beam.

If a prestressing force is applied to the beam, either by a number of smaller tendons distributed over the end of the beam or by a single tendon having a large bearing plate that has a flexural stiffness similar to that of the concrete on which it bears, the condition of stress can be approximated by the diagram of Fig. 8-10. In this figure, the load is represented as several small forces acting on a common bearing plate. Under this condition of loading, the stress paths are seen to be farther apart near the point where the loads are applied, but the stresses at one times the depth of the beam from the end of the beam are similar to those in Fig. 8-9.

The above illustrations are oversimplifications of the problem because:

1. The bearing plates or end anchorages for post-tensioned tendons normally do not extend across the full width of a beam; hence, the stress field is three-dimensional rather than two-dimensional.
2. Bearing plates are not provided for pretensioned tendons, but pretensioned members do, on occasion, experience each of the types of cracking.
3. Highly stressed concrete is a nonlinear material at high stress levels and does not deform in the manner of an elastic material. Hence, elastic

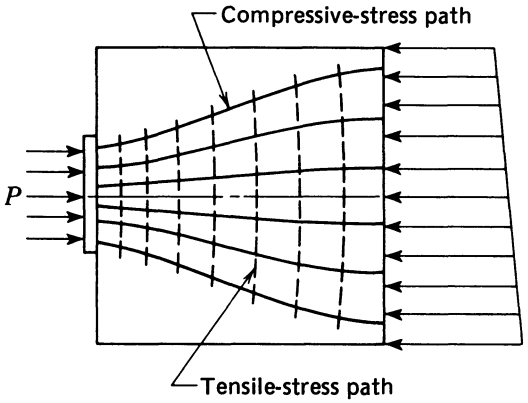

Fig. 8-10. Idealized stress paths in end block with several small loads.

mathematical models cannot accurately predict the behavior of concrete that is subject to high stresses.

These factors result in the actual stresses in the ends of many post-tensioned beams being indeterminate by elastic methods of analysis, and, for this reason, the results of elastic analyses of anchorage zone stresses should be considered to be approximations and not exact solutions of the problem. The design of end blocks and end-block reinforcing is best done by using empirical data if available. This is especially true for anchorages that cannot logically be modeled as elastic plates on elastic supports (i.e., embedded post-tensioning anchorages having shapes that do not approximate the shape of a bearing plate).

Cracking along the paths of tendons near the ends of prestressed beams, as illustrated in Fig. 8-11, is not uncommon. One type of cracks is commonly called splitting-tensile or bursting cracks, and the other frequently is referred to as spalling cracks. Both types of cracks are caused by tensile stresses resulting from the distribution of the highly concentrated compressive bearing stresses at the ends of the members.

The term "bursting" has been used to describe a type of failure that sometimes occurs in post-tensioned members during the prestressing operation or, in some instances, shortly thereafter. More often than not, when this type of failure occurs, the highly stressed concrete in the immediate vicinity of the post-tensioned anchorage, or anchorages, explodes or bursts. The failures normally occur suddenly, without warning, and are somewhat similar to the mode of failure associated with the compression testing of high-strength concrete cylinders. Because the failures do happen suddenly and result in almost complete fragmentation of the concrete, the tensile cracks identified as splitting-tensile cracks in Fig. 8-11 normally cannot be observed before, during, or after the failure. Investigation of such failures frequently reveals that they are due to the

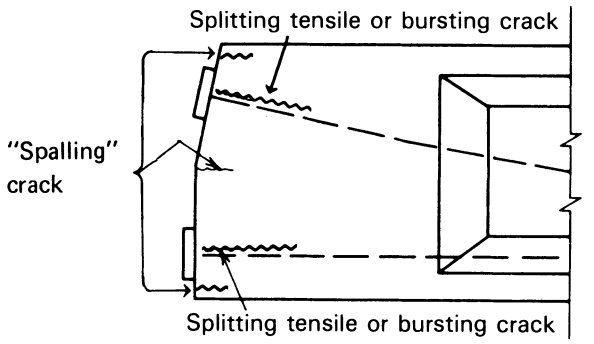

Fig. 8-11. Elevation of an end block showing cracks due to tensile stresses.

concrete in the highly stressed area being of poor quality (low strength, poorly compacted, etc.), rather than due to a lack of anchorage zone reinforcement. If the concrete fails frequently under a specific set of conditions, either explosively or by the appearance of wide splitting-tensile cracks, it is most likely that the problem could be corrected by the provision of additional nonprestressed reinforcement in the anchorage zone regions. On the other hand, if the concrete fails explosively on only a few occasions under a given set of conditions, the failure is most likely due to concrete of low quality having been provided at the location(s) of the failure(s). It should be pointed out, however, that the provision of anchorage zone reinforcement in amounts greater than "nominal amounts"—even though the designer's experience, the history of the tendons and anchorage devices being used, and structural calculations indicate that it is not needed if the concrete is of the specified quality—normally would be expected to cause an anchorage zone to fail less explosively if the concrete is of inadequate quality.

Although the major building codes in use in North America recognize the existence of splitting-tensile and spalling stresses in anchorage zones (see Sec. 18.13.1 of ACI 318), they do not provide specific criteria for determining when reinforcement is required to control them (i.e., maximum tensile stresses). Hence, the designer must make this determination based upon his or her own knowledge and experience, guidance found in the technical literature, and data provided by the suppliers of prestressing materials.

The studies of anchorage zone stresses performed by Guyon, both photoelastic and mathematic, confirmed the locations and nature of spalling and splitting-tensile stresses in prisms loaded with concentrated loads (Guyon 1953). In his book, Guyon included relationships, in the form of plots, for the following: distribution of the splitting-tensile stresses; the location of the maximum tensile stress, X_{max}; position of zero stress,, X_0; and values of the maximum splitting-tensile stress, $f_{sts\,max}$, and of the resultant splitting-tensile force, F_{RSTF}—all as

functions of the ratio a/d, the height of the loaded area a (assumed to extend across the width of the prism) to the depth of the concrete prism d. (See Figs. 8-12, 8-13, and 8-14.) Guyon's nonlinear relationship for the resultant splitting-tensile force predicts a maximum force of $0.3P_j$, for the condition of the load being applied on a very narrow loaded area ($a/d \cong 0$) and a resultant splitting-tensile force of null for $a/d \cong 1$ (see Fig. 8-15).

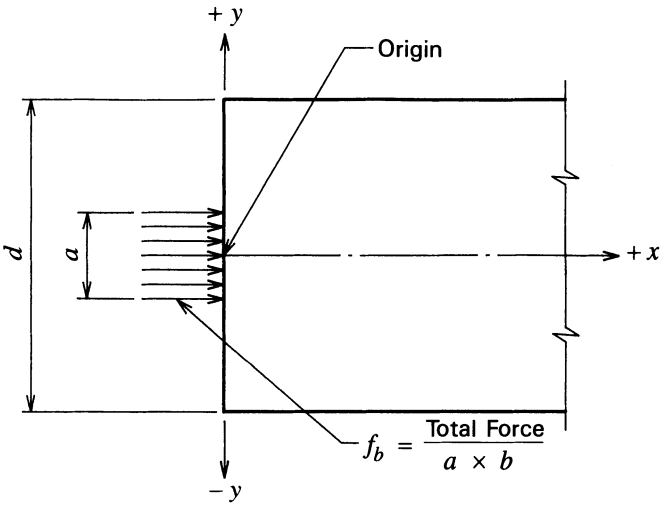

(a) Side Elevation

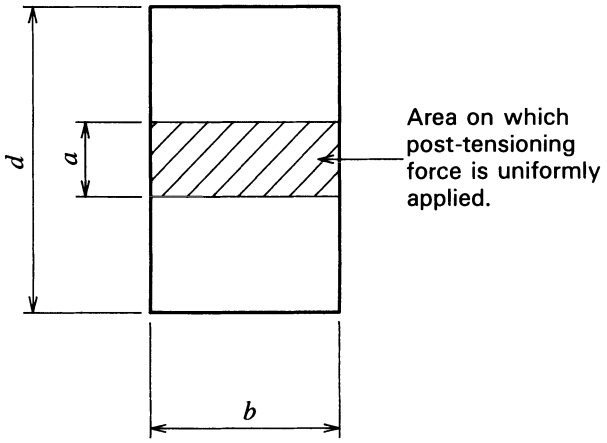

(b) End Elevation

Fig. 8-12. End and side elevations of end-block models used by Guyon in the analysis of end-block stresses.

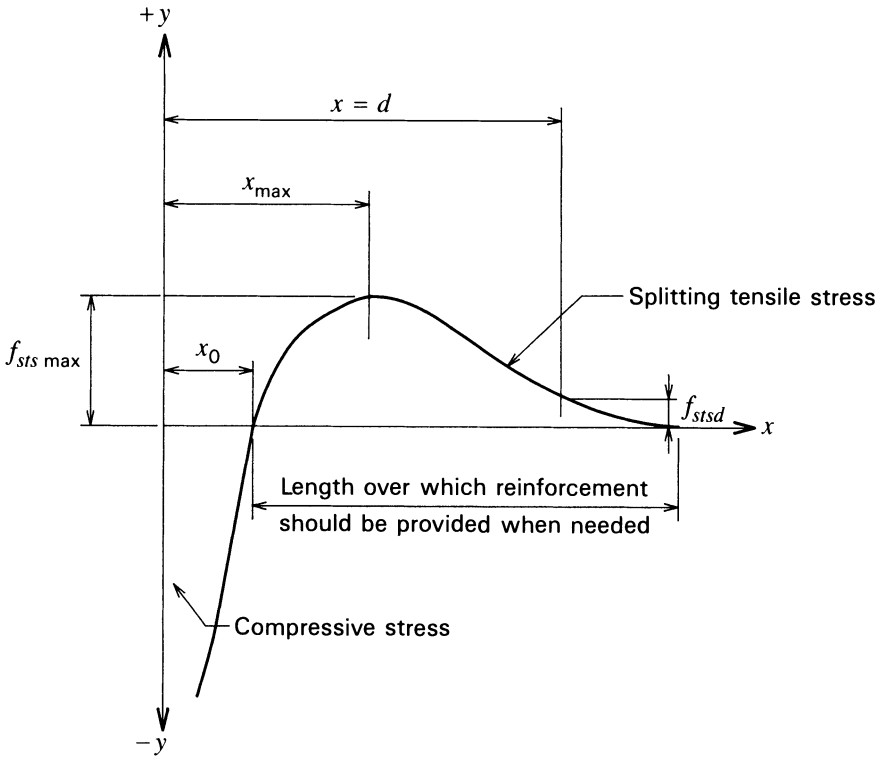

Fig. 8-13. Definition of terms Guyon used in end-block analysis.

The linear relationship of eq. 8-3 for the resultant splitting-tensile force, F_{RSTF}, appears to be a conservative approximation of Guyon's curve:

$$F_{RSTF} = 0.3F_j\left(1 - \frac{a}{d}\right) \tag{8-3}$$

This curve has been recommended by Leonhardt and is included in the CEB-FIP Model Code (MC78) for use in determining the resultant splitting tensile force (Leonhardt 1964; CEB-FIP 1978). The CEB-FIP model code provides that the reinforcement used to resist the splitting-tensile stresses should be uniformly spaced over a length extending from $0.1d$ to $1.0d$ measured from the loaded area, as shown in Fig. 8-16.

A unique relationship for the resultant splitting-tensile force, which predicts forces greater than those described above, is found in the *Ontario Highway Bridge Design Code* (1983). This relationship is:

$$F_{RSTF} = 0.70F_j\psi \tag{8-4}$$

in which the parameter ψ is computed from:

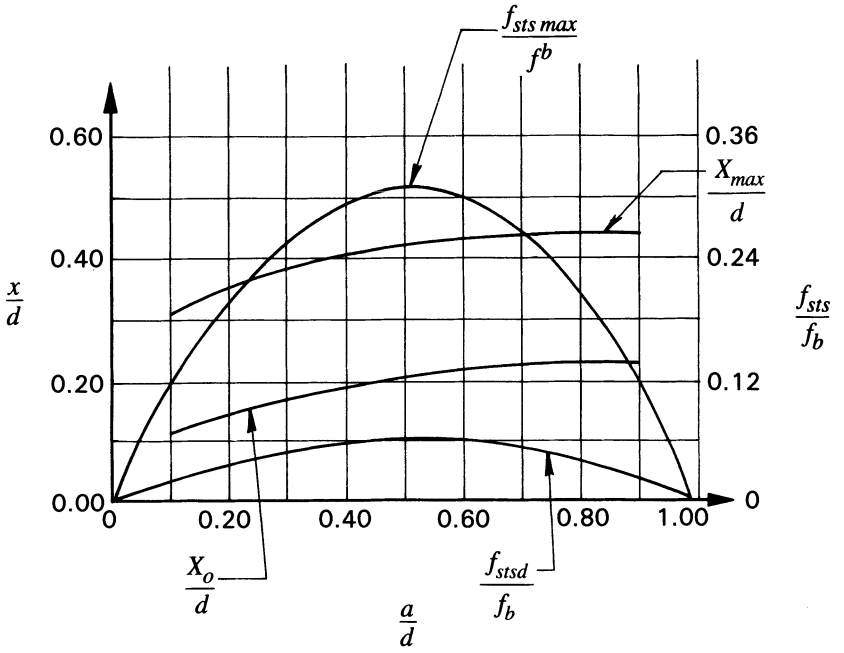

The ratios in Fig. 8–14 are defined as follows:

$\frac{f_{sts\,max}}{f^b}$ = ratio of maximum splitting tensile stress to uniformly distributed bearing stress at end of prism.

$\frac{X_{max}}{d}$ = ratio of distance location of maximum splitting tensile stress to depth of section.

$\frac{X_o}{d}$ = distance to point of zero splitting tensile stress.

$\frac{f_{stsd}}{f_b}$ = ratio of splitting tensile stress at distance of d from origin to uniformly distributed bearing stress at end of prism.

Fig. 8-14. Plot of maximum splitting-tensile stress, splitting-tensile stress at a distance of d from the loaded face, and the location of X_0 and X_{max} as functions of x/d and a/d based upon Guyon's work.

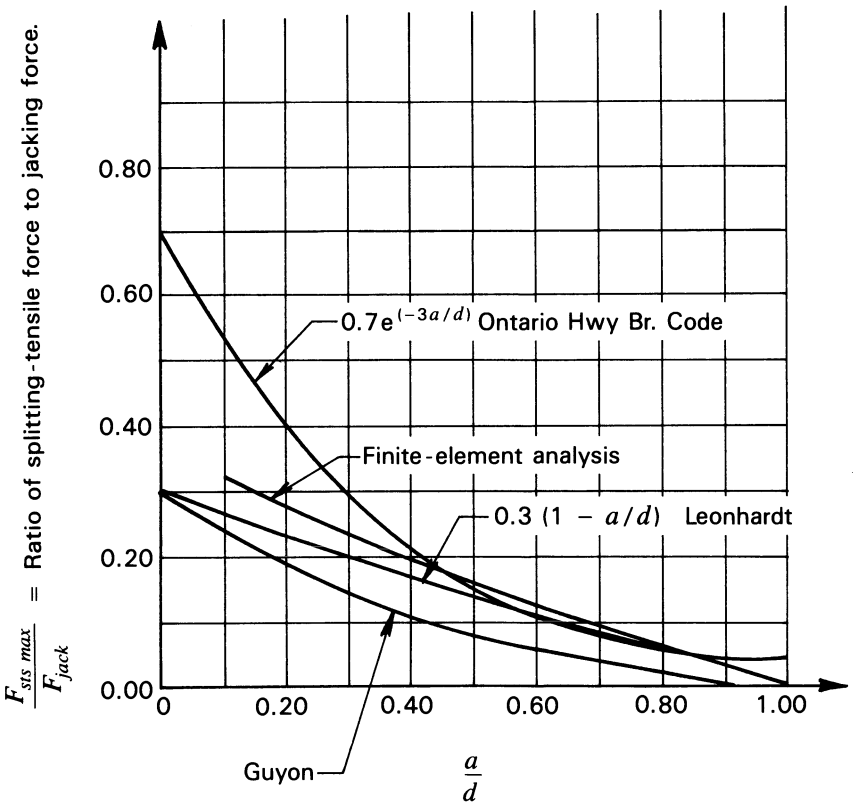

Fig. 8-15. Comparison of splitting-tensile forces predicted by methods proposed by Guyon, Leonhardt, the Ontario Highway Bridge Design Code, and a finite-element analysis.

$$\psi = e^{-3(a/d)} \tag{8-5}$$

In eq. 8-5, e is the base of the Napierian logarithms, and the other terms are as previously defined. According to the provisions in the Ontario Code, the distance from the loaded face to the maximum splitting tensile stress, X_{max}, can be computed from:

$$X_{max} = 0.54(1 - \psi)d \tag{8-6}$$

and the reinforcement provided to resist the splitting tensile force should be distributed uniformly from $0.52X_{max}$ to d measured from the loaded face. Because the provisions from the Ontario Code described herein are brief excerpts, and thus possibly subject to misinterpretation by the reader as well as the author, the reader is advised to consult the complete document for a comprehensive understanding of all of the provisions and official updates before using the information presented herein for actual design.

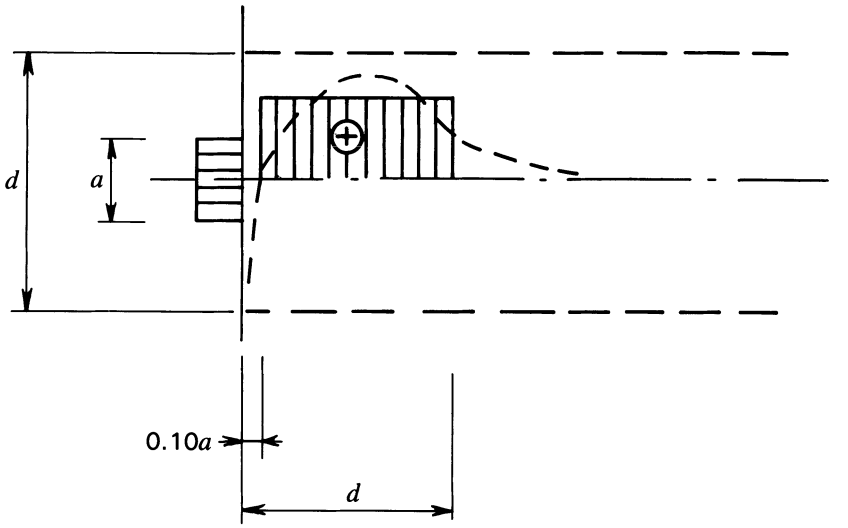

Note: Notation changed from original to that used in Fig. 8-12.

Fig. 8-16. Area over which placing of splitting tensile reinforcement is recommended by the CEB-FIP Model Code.

When a number of prestressed tendons, pretensioned or post-tensioned, are concentrated at one or more locations at the end of a beam, vertical and horizontal reinforcing sometimes may be provided to resist spalling-tensile cracks and to restrict the widths of the cracks produced. The amount of reinforcing required can be estimated by computing the area of reinforcing steel required to control the tensile stresses, based upon the following assumptions:

1. As in Fig. 8-17, the end of the beam can be represented by a free body subjected to the components of a force, as shown. To simplify the analysis, the vertical forces can be ignored.
2. With the vertical components of the forces neglected, and with the variable width of the cross section taken into account, one obtains the free body shown in Fig. 8-18.
3. Moments acting on horizontal planes between the top and bottom flanges can be computed at various locations and the results plotted, as shown in Fig. 8-19a.
4. Assuming a resisting couple, as shown in Fig. 8-19b, one can compute a tensile force for which nonprestressed reinforcement can be supplied from:

$$T = \frac{M}{h - z} \tag{8-7}$$

5. To restrict the crack width resulting from the tensile force to approximately 0.005 in., the stress in the reinforcing steel should be restricted to a stress on the order of:

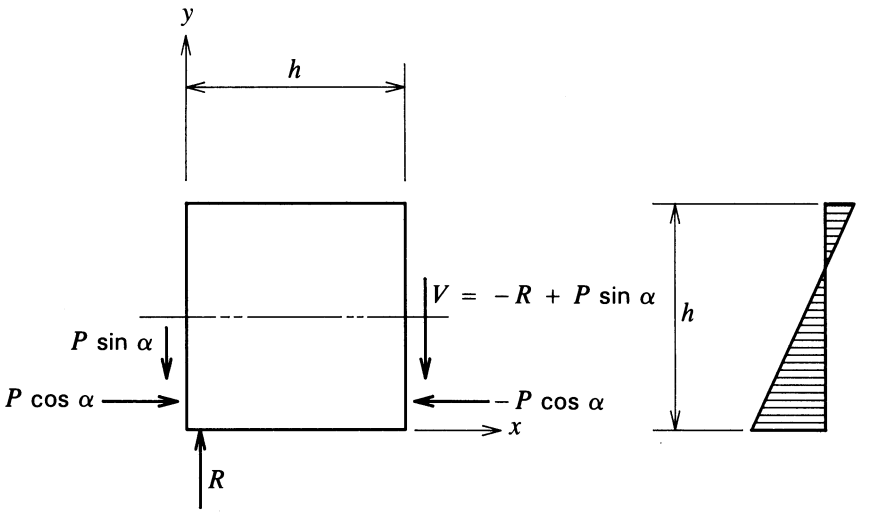

Fig. 8-17. Free body of model used in the analysis of spalling stresses at the ends of beams.

$$f_s = 775\left(\frac{\sqrt{f'_c}}{A_b}\right)^{1/2} \tag{8-8}$$

in which f_s and f'_c are in psi and A_b is the area of the size of the bars used in the reinforcing.

6. It should be recognized that the tensile stresses usually occur on horizontal

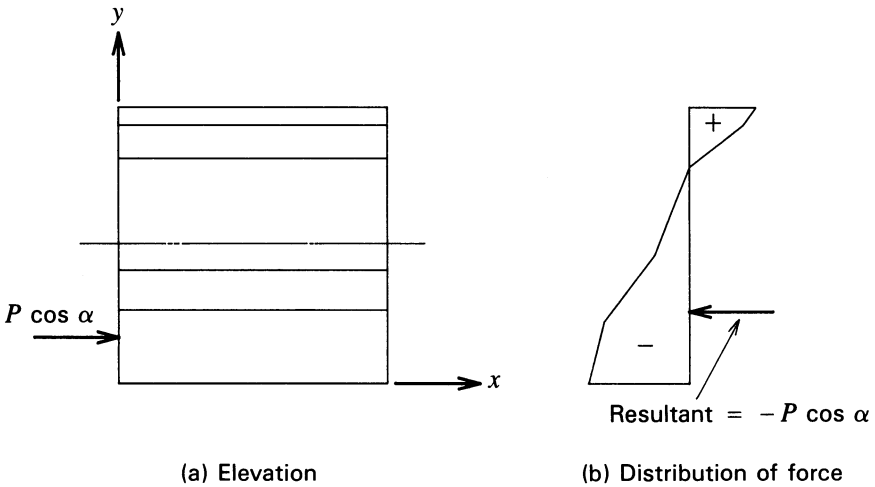

Fig. 8-18. Forces on the end of the model used in the analysis of spalling stresses.

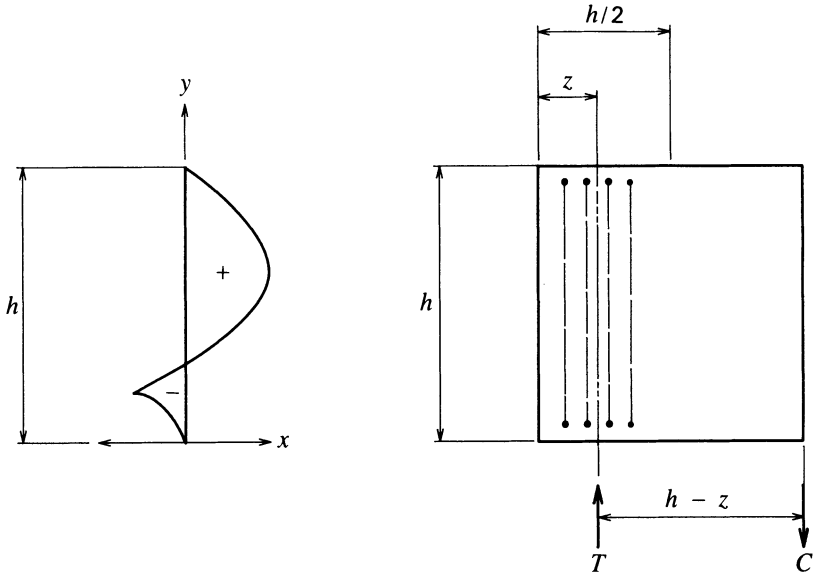

(a) Distribution of moments

(b) Dimensions used in analysis of end blocks

Fig. 8-19. Distribution of moments and dimensions used in end-block analysis.

as well as vertical planes; so horizontal as well as vertical reinforcing should be provided.

ILLUSTRATIVE PROBLEM 8-4 For the pretensioned beam shown in Fig. 8-20 compute the vertical reinforcing steel required to confine the tensile-crack width to 0.005 in. Assume $f'_c = 4000$ psi and that No. 3 bars are to be used.

SOLUTION: The distribution of force is plotted in Fig. 8-21a. The unit stress and force for various locations between the top and bottom flanges of the section are shown in Table 8-4. The distribution of moments shown in Fig. 8-21b is computed from the forces given in Fig. 8-21a.

The allowable steel stress is:

$$f_s = 755 \left(\frac{\sqrt{4000}}{0.11} \right)^{1/2} = 18{,}100 \text{ psi}$$

Assuming $z = 6$ in. and $A_s = 4 \times 0.11 = 0.44$ sq. in.:

$$f_s = \frac{165}{(30 - 6)(0.44)} = 15.6 \text{ ksi} \leq 18.1 \text{ ksi}$$

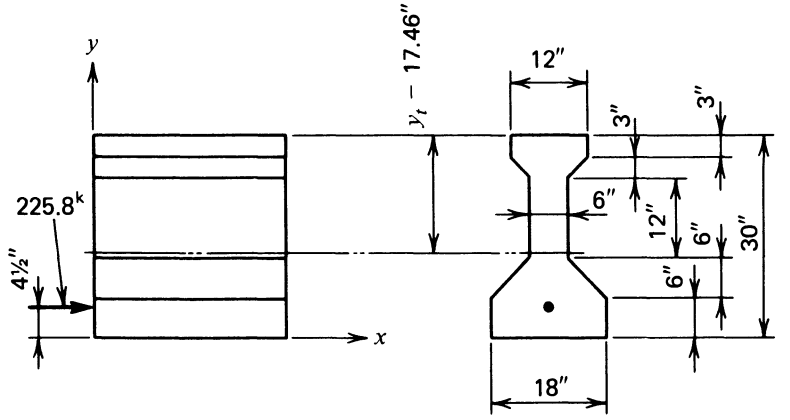

(a) Elevation (b) Cross Section

Fig. 8-20. Beam analyzed in I.P. 8-4.

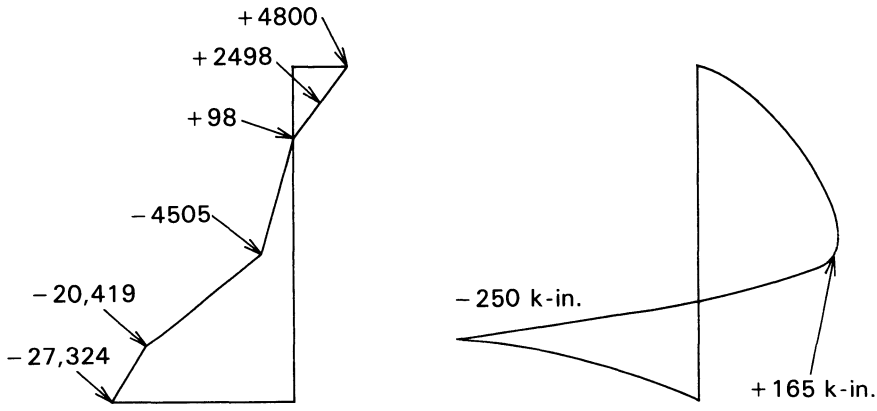

(a) Distribution of force, lb/in. (b) Distribution of moment

Fig. 8-21. Results of analysis of I.P. 8-4.

TABLE 8-4 Unit Stresses, Widths, and Forces for Various Locations Used in the Analysis of I.P. 8-4.

y (in.)	*f* (psi)	Width (in.)	Force (lb/in.)
0	1518.0	18	27,324
6	1134.4	18	20,419
12	750.8	6	4505
24	−16.4	6	−98
27	−208.2	12	−2498
30	−400.0	12	−4800

Use two No. 3 U-shaped stirrups 4 in. on center, with the first stirrup located 2 in. from the end of the beam.

8-5 Spacing of Pretensioned Tendons

The bond between the tendons and the concrete section at the ends of pretensioned members is relied upon to transfer the prestressing force from the tendons to the concrete section. Flexural bond stresses are necessary to provide resistance to cracking, minimize crack width, and ensure the development of flexural strength under design loads. To achieve the needed bond strength, it is essential that the concrete be placed and well compacted around the tendons. To facilitate concrete compaction, the dimensioning of embedded materials (i.e., tendons, bearings, nonprestressed reinforcement, etc). must be done with care.

In the manufacture of pretensioned concrete, internal vibration is relied upon to a high degree to ensure that the concrete is well consolidated. For this reason, particularly in deep beams, it is important that the pretensioning tendons be spaced in positions that facilitate extending the head of an internal concrete vibrator to the extreme bottom of forms. In addition, the tendons should not be placed in a configuration that unduly restricts the flow and consolidation of the plastic concrete in spaces not directly accessible to the vibrator head.

In the interest of lower production costs, through saving labor in handling and stressing the prestressed reinforcement in the manufacture of pretensioned concrete, the trend has been toward the use of fewer, large seven-wire strands in lieu of many small strands or solid wires. As progress has been made in prestressed-concrete manufacturing techniques, and as more has been learned about the action of transfer bond and fatigue on flexural bond stresses, the size of tendons commonly used has been increased from $\frac{1}{4}$ to $\frac{1}{2}$ in. Strands as large as 0.60 in. in diameter also have been used in pretensioned construction in recent years. It should be recognized that the head of the internal vibrator used in compacting the concrete in beams with 0.50 in. tendons spaced at 2 in. on centers, which is a common spacing with tendons of this size, is restricted to a space less than $1\frac{1}{2}$ in. in diameter. Because internal vibrators with large heads are much more effective than those with smaller heads, the placing of the concrete often is materially facilitated if at least one, relatively wide, vertical opening (through which a large internal vibrator head can be inserted) is provided at the center of deep members. This is illustrated in Fig. 8-22, in which it will be seen that omission of strands in the center row allows the use of a vibrator head having a diameter of 3 in. or more.

Concentrating groups of tendons at the ends of pretensioned members, as is often done when deflected pretensioned tendons are used, can result in a tendency for spalling-tensile cracks at the ends of the members, just as large concentrations of prestressing forces may cause cracking in the ends of post-

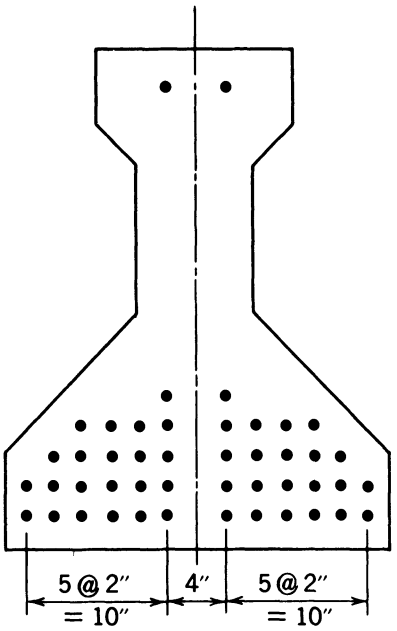

Fig. 8-22. Cross section of a pretensioned beam showing tendon spacing to facilitate placing and vibrating concrete.

tensioned members. Designers should be aware of this possibility and adjust their design accordingly.

The clear concrete cover (i.e., the distance from the edge of tendons to the surface of the concrete and the clear space between tendons within a member, in the area in which transfer bond must be developed, also must be chosen with care. Placing the tendons too close to the surface of a member can cause splitting along the tendons. Smaller tendons have been placed as close as 1 in. to the surface without adverse effects, but experience has shown that larger tendons should not be closer than 2 in. to the surface. The model building codes (see Sec. 7.6.7 of ACI 318-89) generally restrict the center-to-center spacing of seven-wire strands to four times the nominal diameter of the strand. Strands larger than $\frac{1}{2}$ in. in nominal diameter, especially those having strengths greater than 41.3 kips (the minimum required for 270 grade strand by ASTM 416; see Chapter 2), may require greater spacings to achieve acceptable results.

8-6 Stresses at Ends of Pretensioned Beams

In simple prismatic beams of normal configuration, pretensioned with straight tendons, the eccentric pretensioning force results in compressive stresses in the bottom flange and a tendency for tensile stresses in the top flange. Furthermore,

in well-proportioned beams, the service-load compressive stresses in the top flange at midspan do not approach the maximum values permitted and, thus normally do not present a problem. The amount of prestressing required, as a rule, is controlled by the flexural tensile stress in the bottom flange caused by the service loads, which the prestressing force must fully or partially nullify. The usual design criteria permit some tensile stress in the top flange from the combination of initial prestressing and service dead load without provision of nonprestressed reinforcement, and higher tensile stresses if nonprestressed reinforcement is provided in an amount proportioned to resist the entire tensile force in the concrete.

To see the effect of top-flange tensile stresses on the quantities of materials required for a given design, consider the beam shown in Fig. 8-23. Assume that this beam will be used on a span of 70 ft, no tensile stress is to be allowed in the bottom fibers under full service load, and the flexural stresses due to the dead load of the girder and the superimposed load are as summarized in Table 8-5. Under these conditions, the minimum prestressing force needed to produce the required 2000 psi compression in the bottom fibers with various amount of tensile stress in the top fibers is as summarized in Table 8-6. From Table 8-6, it can be seen that a reduction of 12% can be made in the amount of prestressing steel required if a tensile stress of 160 psi is permitted in the top fibers, and 23.7% if a tensile stress of 320 psi is permitted.

Another consideration is that, as was explained in Sec. 6-6, the stress in a pretensioned tendon is null at its end but increases to a maximum value at a

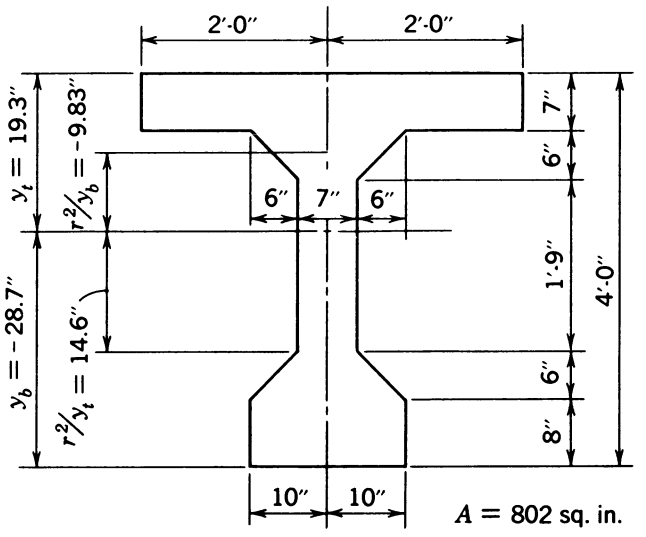

Fig. 8-23. Beam cross section used in illustrating the effect of top-fiber tensile stresses on the prestressing force.

TABLE 8-5 Summary of Stresses for Discussion in Sec. 8-6.

	Top fiber (psi)	Bottom fiber (psi)
Stress due to dead load of girder only	−524	+780
Stress due to superimposed load only	−826	+1220
Total stress	−1350	+2000

short distance, the transmission length, from the end of the beam. The size of the transmission length is primarily a function of the type and size of the tendon. Values of 50 and 100 diameters normally are used in estimating the transmission length for strand or wire tendons, respectively. The initial stress in a strand tendon having a diameter of $\frac{1}{2}$ in. varies along the transmission length approximately as shown in Fig. 8-24.

An additional consideration is that a force applied to an elastic body causes stresses in the body that flow out along smooth curves or stress paths. A large force applied to the end of a prism, such as shown in Fig. 8-25, results in principal compressive stresses that follow a pattern similar to the soiled lines, and principal tensile stresses that follow along lines similar to the dashed lines. At a distance of about one times the depth of the block from the end, the stresses are approximately equal to the values that would be computed from the usual combined stress relationship used in structural design. In other words, the effect of the concentration of the load is virtually eliminated at a distance of one times the depth of the prism from the end of the member.

As a result of the combined effects of the transmission length required to develop full bond and the distance required for the concentrated prestressing force to fully distribute, the maximum tensile stress in the top fibers does not occur at the immediate end of the beam. This is a significant phenomenon that can affect the economy of a design.

Returning to the example used above, if the effects of transmission length and distribution of the concentrated force are taken into account on the beam, acting on a span of 70 ft, the tensile stress of 320 psi resulting from the 45 tendons in this example would not be acting at the immediate end of the beam, but would be acting at a distance of from 4 to 8 ft from the end of the beam. The actual tensile stress in the top fibers of the beam would be less than 320

TABLE 8-6 Summary of Stresses, Forces, and Tendons for Discussion of Sec. 8-6.

Allowable top-fiber tensile stress (psi)	zero	160	320
Minimum prestressing force required (k)	644	570	491
No. of tendons (11 k) required	59	52	45

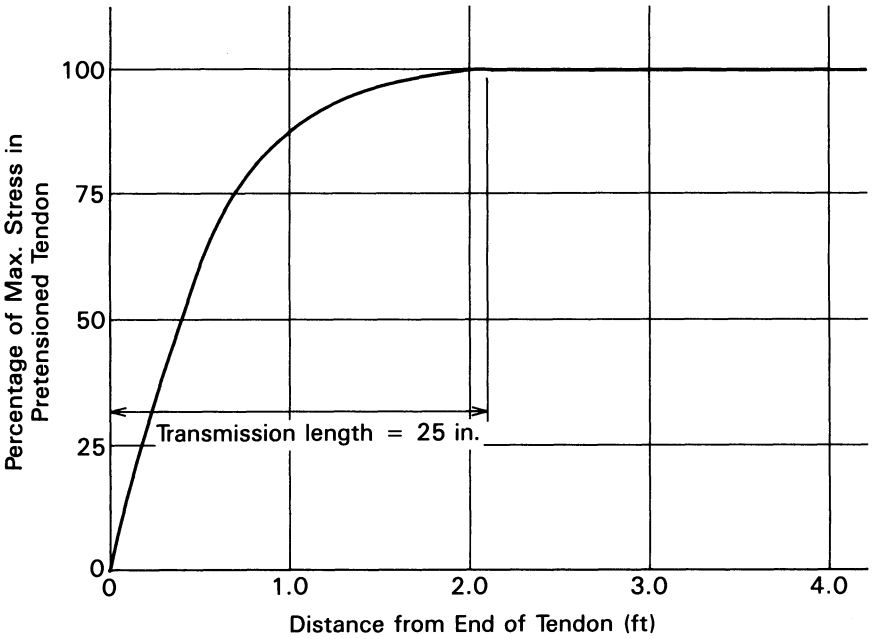

Fig. 8-24. Variation in initial stress in a pretensioned tendon near the end of a beam.

psi, owing to the effect of the dead load of the beam. Table 8-7 summarizes the effect of the stress in the top fiber of the beam resulting from the dead weight of the beam on the net, final tensile stress in the top fibers, as well as the amount of unstressed reinforcing that would be required to control tensile stresses exceeding 160 psi.

From this study it is apparent that, in taking all of these factors into consideration, the designer may be able to reduce the amount of prestressed reinforcement required in a specific elastic service load design as much as 25 percent without adding nonprestressed reinforcement in the top flange to resist tensile stresses in the concrete.

8-7 Bond Prevention in Pretensioned Construction

In Sec. 4-6, it was shown that the concrete stresses at the ends of a member prestressed with straight tendons may limit the service load capacity of the member. Furthermore, it is shown that by varying the eccentricity of the prestress, the stresses at the ends can be reduced, and the service load capacity of the member can be increased. The moment caused by prestressing and the stresses at the ends of members prestressed with straight pretensioned tendons also can be reduced by varying the prestressing force. This can be accomplished by varying the prestressing force. This can be accomplished by preventing a portion of the tendons from bonding to the concrete at the immediate ends of

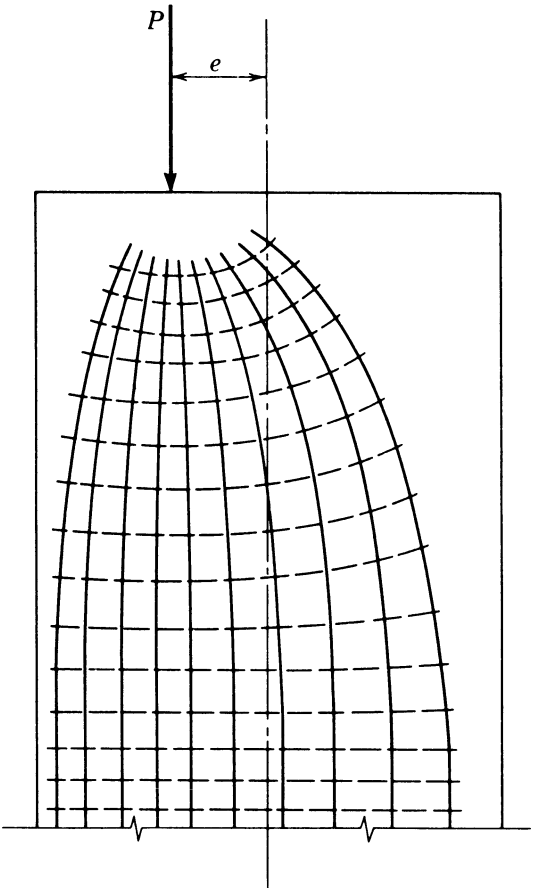

Fig. 8-25. Approximate paths of principal tensile and compressive stresses in an eccentrically loaded prism.

TABLE 8-7 Summary of Stresses and Areas of Nonprestressed Reinforcement for Discussion of Sec. 8-6.

Distance from the end to the point under consideration (ft)	0	4	6	8
Theoretical top-fiber stress (psi)	+320	+320	+320	+320
Top-fiber stress due to girder dead load (psi)	0	−113	−164	−213
Net tension under dead load of girder plus prestress (psi)	+320	+207	+156	+107
Area of nonprestressed reinforcement required (in.^{2})	3.00	1.42	0	0

the member, and, in so doing, preventing the unbonded tendons from prestressing the concrete at the ends.

This principle can best be explained by considering an example such as the beam shown in Fig. 8-26. The pretensioning tendons, as located in the figure, result in an initial, top-fiber tensile stress due to prestressing of 384 psi. It can be shown that by preventing bond on five tendons in the bottom row and four tendons in the second row, as indicated in the figure, the initial tensile stress in the top fibers at the ends can be reduced to 270 psi.

The length over which the bond must be prevented is a function of the beam dead load stresses. In most cases, they reduce the initial stresses to permissible values only a few feet from the end of the beam. The transmission length required for the tendons to develop full tension, as well as the distance required for the pretensioning force to distribute, which are discussed in Sec. 8-6, also should be taken into account when calculating the maximum tensile stresses at the ends of members.

It is believed that bond prevention can be used to advantage with complete safety if the tendons that will remain unbonded are sheathed with a split, plastic tube, or a heavy paper or cloth tape having a waterproof adhesive. Grease and

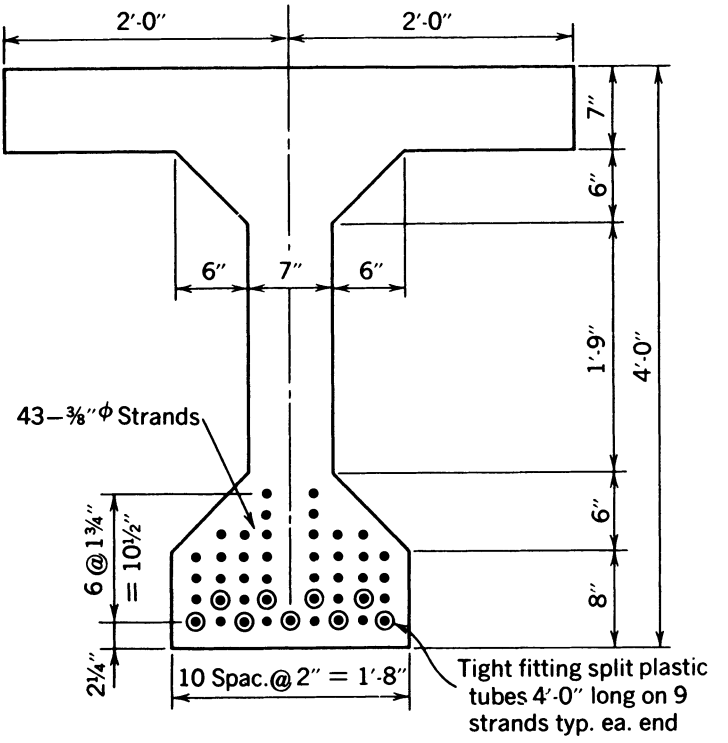

Fig. 8-26. Beam section indicating method of preventing bond on pretensioned tendons.

chemicals that retard the concrete set have been used in lieu of plastic tubes or tape as a means of preventing bond. Because of the danger of a worker's inadvertently or carelessly applying the grease or retarder to incorrect tendons or an incorrect number of tendons, this procedure should be permitted only when strict, continuous supervision and inspection can be provided to prevent errors.

As pointed out in Sec. 6-6, if bond is prevented at the end of a strand tendon, and the design allows tension in the precompressed tensile zone, the length required for flexural bond stresses to develop the strength of the tendon is taken to be *twice as great* as that for a tendon that is bonded to the end of the member (see Sec. 12.9.3, ACI 318).

ILLUSTRATIVE PROBLEM 8-5 Compute the stresses due to a prestressing force of 11 k per tendon for the AASHTO-PCI bridge stringer, type III, pretensioned as shown in Fig. 8-27, sections *A-A* and *B-B*. The plastic tubes indicated are used to reduce the stresses due to prestressing. The section properties of the concrete section are:

$$A = 560 \text{ in.}^2,\ y_t = -24.63 \text{ in.},\ r_2/y_t = -9.06 \text{ in.}$$

$$I = 125{,}400 \text{ in.}^4,\ y_b = 20.27 \text{ in.},\ r_2/y_b = 11.03 \text{ in.}$$

The computations for the center of gravity of the prestressed reinforcement at section *A-A*, by taking moments about the bottom (soffit) of the section, are summarized in Tables 8-8 and 8-9. The top and bottom fiber stresses are computed as follows:

At Section *A-A*:

$$e = 20.27 - \frac{292.5}{50} = 14.43 \text{ in.}$$

$$f_t = -\frac{50 \times 11{,}000}{560}\left(1 + \frac{14.43}{-9.06}\right) = 580 \text{ psi}$$

$$f_b = -\frac{50 \times 11{,}000}{560}\left(1 + \frac{14.43}{11.03}\right) = -2270 \text{ psi}$$

At Section *B-B*:

$$e = 20.27 - \frac{247}{38} = 13.75 \text{ in.}$$

$$f_t = -\frac{38 \times 11{,}000}{560}\left(1 + \frac{13.75}{-9.06}\right) = 386 \text{ psi}$$

$$f_b = -\frac{38 \times 11{,}000}{560}\left(1 + \frac{13.75}{11.03}\right) = -1680 \text{ psi}$$

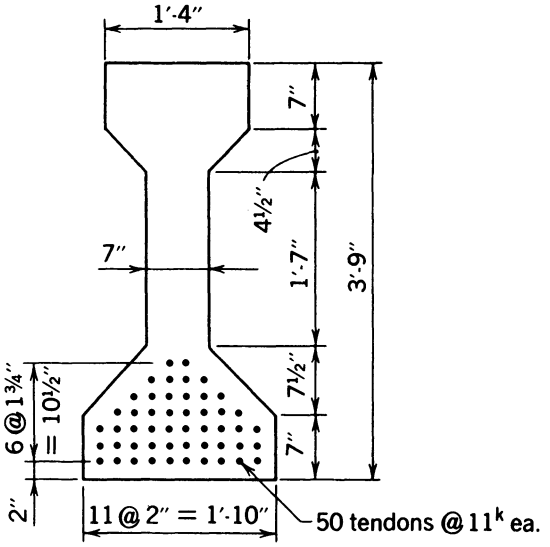

Section *A-A*

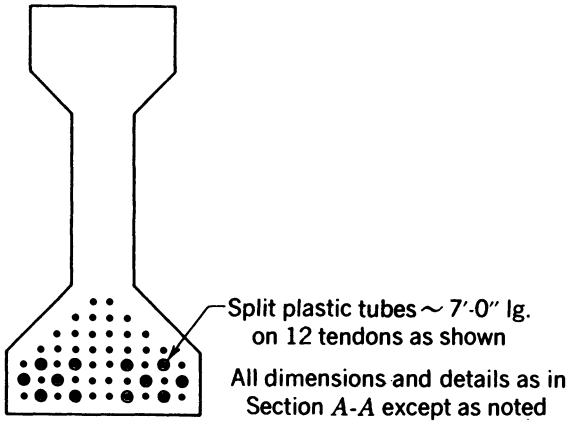

Section *B-B*

Fig. 8-27. AASHTO-PCI type III bridge stringer pretensioned with 50 tendons. Section *A-A* shows details in typical section. Section *B-B* shows details near end where plastic tubes are used to prevent 12 tendons from bonding.

8-8 Deflected Pretensioned Tendons

For the reasons explained in Sec. 4-6, it frequently is desirable to have pretensioned tendons follow a path more eccentric near midspan than at the ends of a beam. This method also is used as a means of reducing the deflection due to prestressing. It generally is preferable to use this method of controlling the

TABLE 8-8 Calculations for the Location of the Center of Gravity of the Prestressed Reinforcement with Respect to the Bottom of the Concrete Section for Section *A-A* of Fig. 8-27.

Number of tendons	Distance (in.)	Product (in.)
10	2.00	20.00
10	3.75	37.50
10	5.50	55.00
8	7.25	58.00
6	9.00	54.00
4	10.75	43.00
2	12.50	25.00
50	5.85	292.50

stresses in pretensioned members rather than to use bond prevention (see Sec. 8-7).

When applied to double-tee roof and floor slabs, the tendons commonly are deflected at one or two points within the span and supported in a higher position at the ends, in a configuration similar to that shown in Fig. 8-28. It should be noted that the tendons are stacked, one on top of the other, in the low portion of their paths near midspan and are spaced out at the ends. In this manner, the tendons are spaced apart where they must develop the all-important transfer bond and are stacked or bundled at midspan where flexural bond stresses must be developed. This construction practice has been used a great deal with very satisfactory results. The flexural bond strength at the center of such members is considered as good as or better than that achieved in grouted, post-tensioned construction.

Deflected tendons have been used extensively in the construction of bridge beams. The theoretical principles involved in their use in bridge construction are the same as in roof slabs. It can be shown that the same flexural strength that is obtained with spaced, deflected tendons normally can be achieved by

TABLE 8-9 Computation of Center of Gravity of Bonded Tendons for Section *B-B* of Fig. 8-27.

Number of tendons	Distance (in.)	Product (in.)
50		292.50
−4	2.00	−8.00
−4	3.75	−15.00
−4	5.50	−22.00
38	6.51	247.5

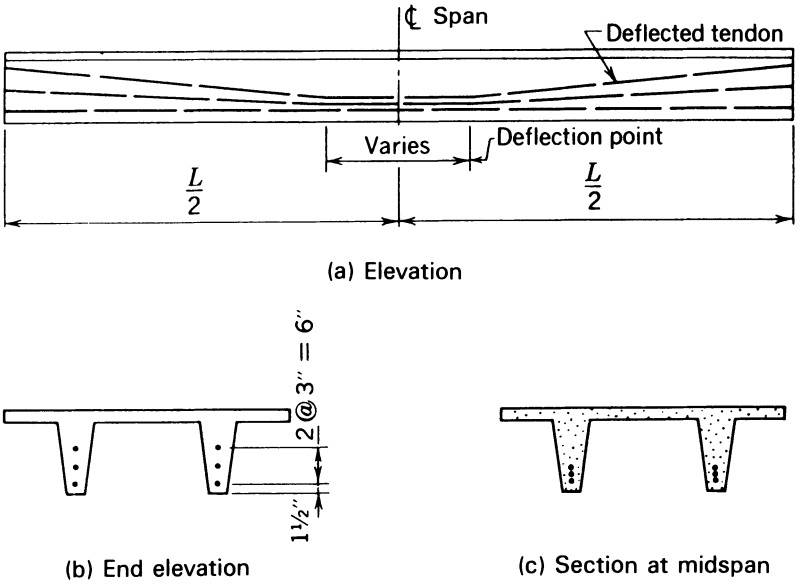

Fig. 8-28. Pretensioned double-tee roof slab with deflected tendons.

using bond prevention on selected tendons near the ends of the beams, but some nonprestressed reinforcing may be required with the unbonded tendons. Although the use of unbonded tendons avoids the need for the large capital investment required for deflecting equipment, as well as the labor required in the deflecting operation, the labor involved in bond prevention is significant in itself. Details of both methods of pretensioning are illustrated in Fig. 8-29, with AASHTO-PCI type III bridge stringers.

If the deflected, pretensioned tendons in the AASHTO-PCI type III stringer were bundled at the center instead of being spaced out, the stress in the bottom flange at the midspan due to prestressing alone, and therefore the capacity of the stringer, could be increased 4 percent without additional materials or labor being required. If the number of bundled, deflected tendons were increased to 20, and each tendon had an initial prestressing force of 13,000 lb, the initial net bottom-fiber compressive stress (prestress + dead load) at the center of the girder would be on the order of 2425 psi if the girder had a span of 70 ft. This latter tendon layout would develop the maximum practical capacity of this concrete section for the span of 70 ft, which would not be possible with spaced tendons of the same size.

8-9 Combined Pretensioned and Post-tensioned Tendons

The structural advantages of draped tendons can be obtained without materially reducing the economy of pretensioned construction with straight tendons by using a combination of pretensioned and post-tensioned tendons. This is illus-

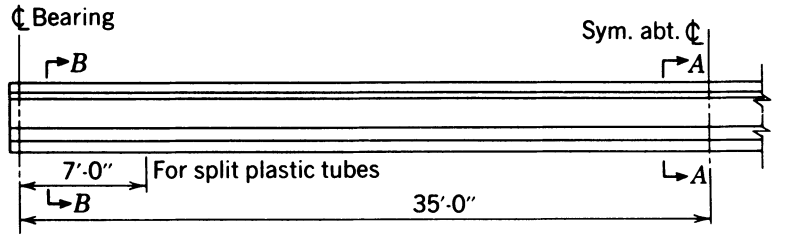

(a) Elevation AASHO-PCI, Type III, Bridge Stringer with Bond Prevention

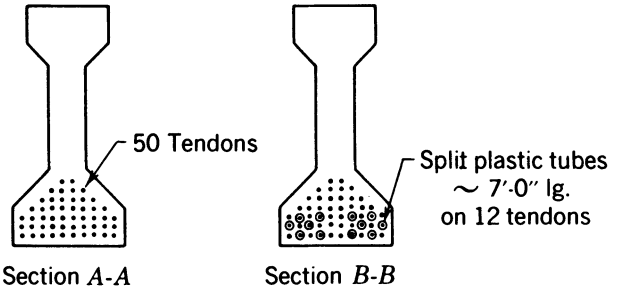

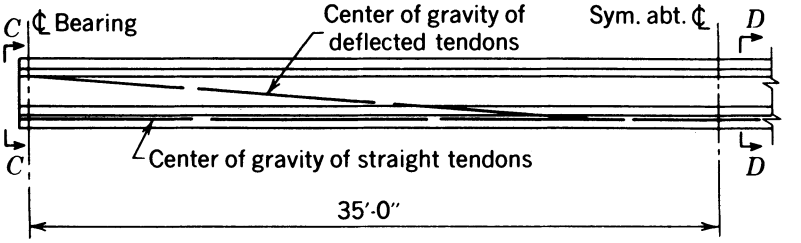

(b) Elevation AASHO-PCI, Type III, Bridge Stringer with a Portion of the Tendons Deflected.

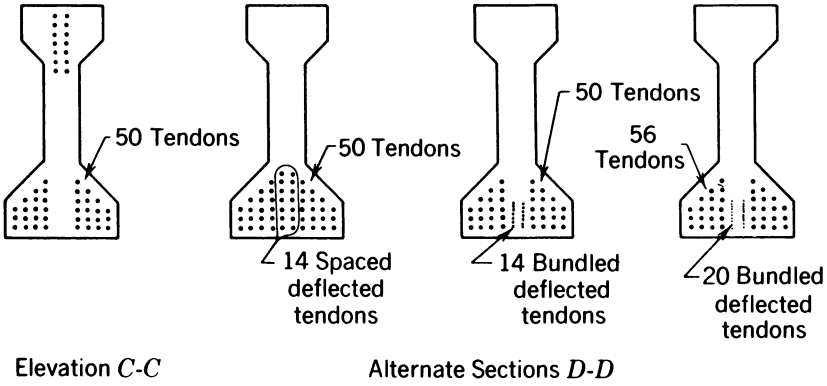

Fig. 8-29. Elevations and sections of AASHTO-PCI type III bridge stringer shown (a) prestressed with pretensioned tendons utilizing bond prevention, and (b) pretensioned with a portion of the tendons deflected.

trated in Fig. 8-30, in which the details of the AASHTO-PCI type III bridge stringer are shown with two combinations of pretensioned and post-tensioned tendons.

The use of 48 pretensioned tendons and one small post-tensioned tendon (59 k initial force) results in a distribution of prestressing stresses equivalent to that obtained with 36 straight and 14 deflected tendons (50 tendons total) and with bond prevention in combination with 50 tendons, as shown in Fig. 8-29. The number of pretensioned tendons in this solution could be reduced to 42 tendons if the post-tensioned tendons were stressed before the pretensioning force was completely released on the concrete section. With this procedure, if steam curing were to be used, it would be necessary to partially release the pretensioned tendons and allow the girders to cool somewhat before post-tensioning and completing the release of the pretensioning force; this is done to eliminate the

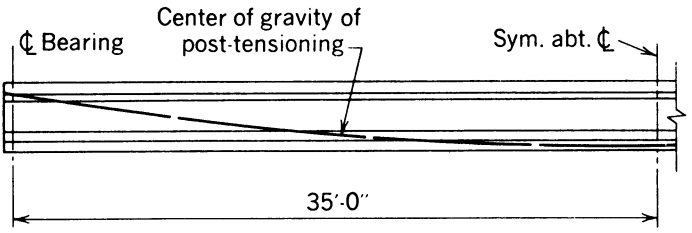

(a) Half Elevation AASHO-PCI, Type III, Bridge Stringer with Combined Pre- and Post-tensioned tendons

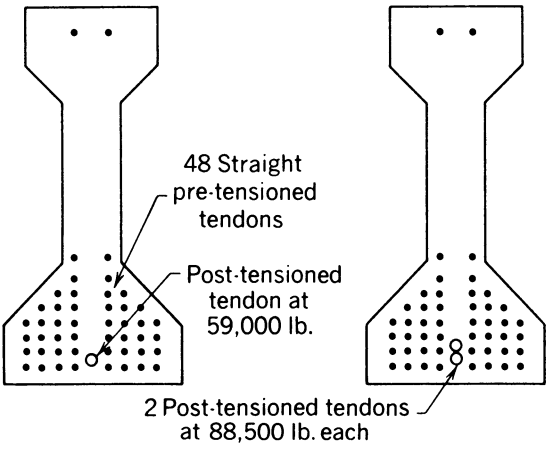

(b) Alternate Sections at Center Line

Fig. 8-30. Half-elevation and section of beam prestressed with pretensioned and post-tensioned tendons.

possibility of vertical cracks forming in the girder as a result of the strain changes that take place in the concrete and in the pretensioning tendons during curing and cooling (see Sec. 17-3). However, with 48 tendons, as shown, the pretensioning force could be released when the concrete attained a strength of 4000 psi, and the girders could be removed from the casting bed immediately and post-tensioned subsequently.

If two larger post-tensioned tendons were used rather than one small tendon (Fig. 8-30), the stresses due to prestressing would be nearly equivalent to those, in the same beam section, that would result from 56 tendons with 20 of them deflected, as shown in Fig. 8-29—which, as was explained previously, would be the maximum stresses that normally could be imposed on this section if it were to be used on a 70-ft span.

For combined pretensioning and post-tensioning, it is not necessary to use end blocks if the post-tensioned tendons can be terminated at the top of the member rather than at the end. Small post-tensioning tendons are readily adaptable to this detail.

8-10 Buckling Due to Prestressing

All structural engineers are aware of the danger of buckling of columns or other long, slim compression members. The question of possible buckling of a prestressed member as a result of the prestressing force, as differentiated from an externally applied load, is raised frequently. Obviously, when prestressing is done by the application of external load such as jacking against abutments, the possibility exists that the member will buckle. In such a case, it is essential that buckling be investigated in the conventional manner. Also, if tendons are used to prestress the member, and the tendons are placed externally in such a fashion that they are in contact with the member at its ends alone, there is some possibility of buckling.

When the tendons are placed internally and are in contact with the member at points between its ends, the tendency to buckle is reduced significantly. When the tendons are in intimate contact with the member throughout its length, as is the normal case, in post-tensioning and in pretensioning, there is no possibility of buckling due to the prestressing force. This fact has been demonstrated experimentally and mathematically and can be understood by considering the difference between the action of prestressing and column action.

Column action is characterized by an increase in eccentricity of the load as the load is increased above a critical value. This is illustrated in Fig. 8-31, in which it is seen that the column load has an eccentricity of e at load P, and if the load is increased to ΔP, the member deflects an additional amount, Δe. This action continues until the critical value of $P + \Delta P$ is reached, and the column buckles.

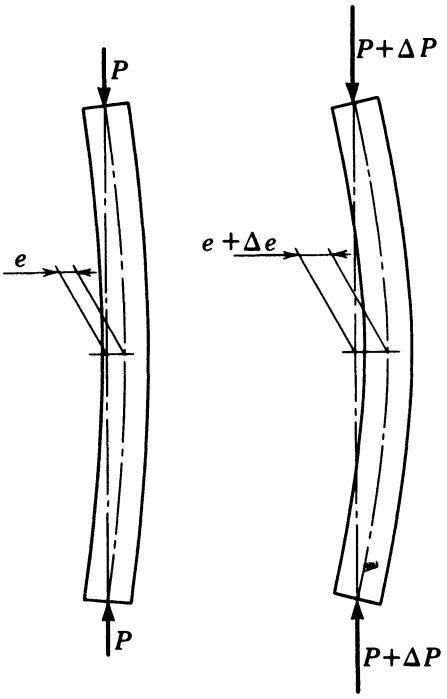

Fig. 8-31. Illustration of column action.

Prestressing action results in a specific distribution of stresses in a member. The eccentricity of the prestressing force remains constant, even if the member is deflected laterally, provided that, as was mentioned above, the tendons and concrete are in intimate contact with each other. If the concrete section were cast slightly curved or crooked, as is often the case, the effect of the prestressing alone would be to straighten the concrete member (opposite to column action) because the tendon would attempt to assume a straight path.

Prestressed columns and piles, which are pretensioned or post-tensioned with the tendons in ducts through the members in the normal manner, of course can buckle under externally applied loads, and these members must be designed with care. Prestressed columns and prestressed piles are treated in Sec. 11-3.

Consider a square, prismatic concrete member cast as a segment of a circular arc and having a single post-tensioned tendon located at the center of gravity of the member throughout its length. When the tendon is stressed, the concrete is subjected to a compressive stress uniformly distributed over the square cross section. In addition, a transverse force exists between the tendon and the concrete; this force, which can be calculated by using the methods in the following section, must exist because if it did not, the tendon would not retain its curved shape. If one draws a free body of the concrete section alone, it will

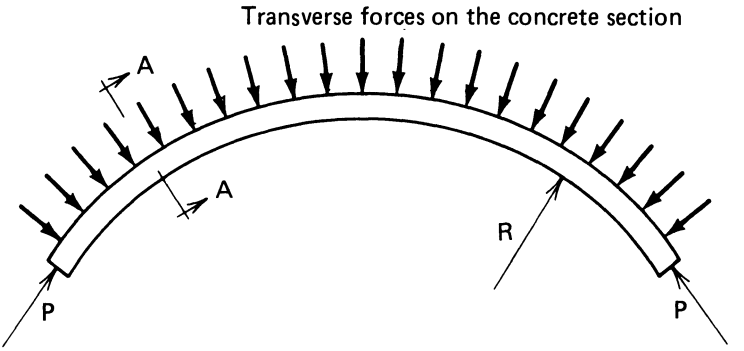

(a) Elevation of a curved post-tensioned concrete member

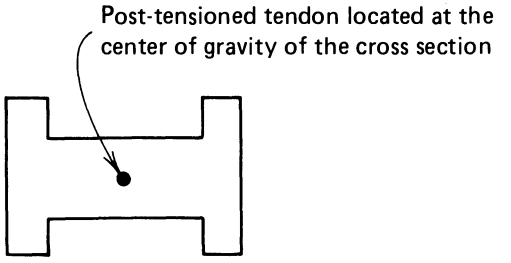

(b) Section A-A

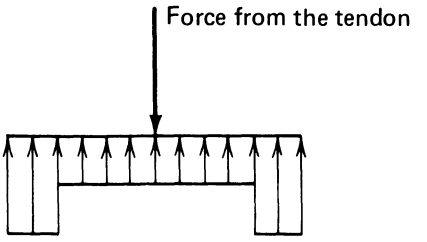

(c) Distribution of forces in the concrete section

Fig. 8-32. Global and local force distributions on a curved, prismatic post-tensioned member.

be apparent it is stressed in an archlike manner, as shown in Fig. 8-32a. If the member were to have an I-shaped cross section, as shown in Fig. 8-32b, instead of being solid and square, the global archlike action would remain for the member as a whole, but secondary or local stresses would exist within the cross section. The local stresses would include transverse shear and flexural stresses because the radial force distribution in the concrete section and the tendon would be as shown in Fig. 8-32c. This can be an important consideration in curved, flanged sections such as box-girder bridges.

The top flanges of flexural members that do not have adequate lateral support also can fail as a result of buckling. For this reason, the designer should give attention to the conditions of support and loading when selecting the dimensions of the concrete section. This is subject is discussed in Secs. 4-9 and 17-8.

8-11 Secondary Stresses Due to Tendon Curvature

In considering a short segment of a curved post-tensioned tendon, such as that shown in Fig. 8-33, neglecting friction between the tendon and the concrete, it will be seen that the forces acting upon the tendon include the axial tension P, which acts throughout the length of the tendon, and the radial forces c, applied to the tendon by the concrete in keeping the tendon in the curved path. If the segment under consideration is infinitesimal, the length of the segment can be taken as ds, the angular change in length ds can be designated as $d\alpha$, and the radius of curvature of the tendon is ρ. Because a very small angle is equal to the tangent of the angle, one can write:

$$\tan \alpha = d\alpha = \frac{ds}{\rho}$$

and:

$$\rho = \frac{ds}{d\alpha}$$

It is evident from the vector diagram, Fig. 8-34, that the unit stress exerted by the steel on the concrete is:

$$cds = P\, d\alpha$$

which can be rewritten:

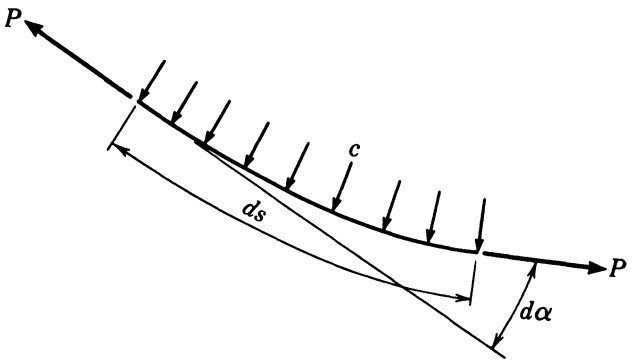

Fig. 8-33. Freebody diagram of an infinitesimal length of a curved tendon.

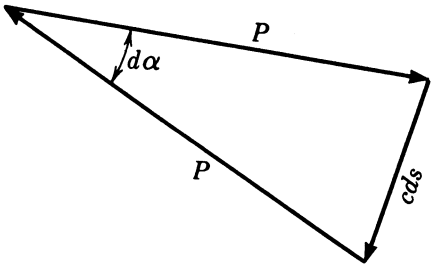

Fig. 8-34. Vector diagram of forces acting on curved tendon.

$$c = \frac{P d\alpha}{ds}$$

and because:

$$\rho = \frac{ds}{d\alpha}$$

the expression becomes:

$$c = \frac{P}{\rho} \tag{8-9}$$

This expression is useful in determining the secondary stresses that result when a tendon is placed on a curve in thin webs or on a curved path in an end block. Only on rare occasions are the unit stresses between the concrete and the tendon intense enough to cause difficulty. The curvatures must be high, and the concrete cover must be small to produce critically high stresses.

ILLUSTRATIVE PROBLEM 8-6 Compute the secondary stress between a curved tendon and the duct if the radius of curvature is 25 ft, and the force in the tendon is 500 k.

SOLUTION: Using eq. 8-9;

$$c = \frac{P}{\rho} = \frac{500}{25} = 20 \text{ klf}$$

8-12 Differential Tendon Stress

The question of the effect of differences in the stresses in the individual elements in parallel-wire and parallel-strand post-tensioning, or in the individual tendons in a pretensioned member, is sometimes raised. It can be stated that the normal

variations in stress encountered in practice do not exceed the normal tolerances expected in structural design.

Consider the case of a parallel-wire, post-tensioned tendon composed of n wires stressed to a total force of P. The force P is measured during construction by determining the elongation of the tendon during stressing as well as by measuring the force required to stress the tendon. The value as P normally can be controlled within the required tolerance without difficulty.

The average stress in the individual wires is P/n. There will be a variation in the unit stresses between the individual wires for the following reasons:

1. The wires are not connected to the jack in such a manner that the length of each wire is precisely equal, but all wires are elongated the same amount. The effect is small in almost all instances because the wires are very stiff and are confined in a relatively small duct or sheath that renders it physically impossible for one wire to have significantly more curvature, hence length, than the average wire.
2. The difference in the length between individual wires is important only with respect to the amount of the elongation of the tendon that is obtained during stressing. If, for example, the elongation of a tendon that is 100 ft long is 7 in., a difference in length of $\frac{1}{4}$ in. between an individual wire and the average wire length will result in a stress variation of only ± 3.5 percent from the average stress in the tendon. The total force in the tendon will not be affected because the average elongation is not affected.
3. Variation in the modulus of elasticity of prestressing wire, along the length of one wire and from coil to coil, of as much as ± 4 percent is not uncommon.
4. Although the relaxation loss of a wire that is more highly stressed than average will be greater than the average relaxation loss, this will be offset by wires stressed less than the average.
5. The estimate of losses of stress in the tendons is generally not as precisely known as the initial prestressing stresses in the tendon.

For relatively short, large, multi-wire or multi-strand tendons placed on small radii and through considerable curvature (such as in nuclear reactor vessels), the difference in length between individual wires or strands on the inside and outside of the curvature can be significant and thus cannot be permitted. It instances such as this, the tendons frequently are assembled twisted rather than parallel to equalize the lengths of their individual wires or strands.

In general, the same factors that affect parallel-wire post-tensioned tendons affect pretensioned tendons. The exception is that the pretensioned tendons are not confined in a sheath or a duct; so the variation is length could be significant if the tendons were not laid out approximately parallel, prior to stressing. Although the wires usually are sufficiently parallel before stressing, a small force normally is applied to each tendon before the tendons are stressed to their

final value. This force straightens the tendons and equalizes the lengths. This procedure is not necessary when the tendons are stressed individually, as is discussed in Chapter 15.

8-13 Standard vs. Custom Prestressed Members

Prestressed-concrete manufactures tend to favor the production of selected types of members that they are equipped to produce rather than members customized for an individual project. The primary reason for this is that the manufacturers of prestressed concrete prefer to use the same concrete forms many times to reduce the amount of form cost that must be charged to each unit, and the labor needed to produce the prestressed concrete can be reduced to a minimum if workers perform the same duties each day and are not confronted with variable duties and operations. Furthermore, when a standard products are made, load tables and advertising literature can be prepared for distribution to purchasers and specifiers of prestressed concrete products, and the manufacturers often can operate with a smaller sales–engineering force than would be required if custom products were used exclusively.

Standard prestressed-concrete members often have been used on small structures where the use of custom-made members would not have been cost-effective, because of the high cost of the special forms required. Because all structural methods and framing schemes have their limitations, and because many large structures have peculiar framing or loading requirements, the designer should carefully consider the economy that could result from the use of custom-made members on large projects.

8-14 Precision of Elastic Design Computations

Prestressed-concrete flexural members normally are designed with the assumption that the concrete is an elastic material under the service loads, and the stresses under such conditions of loading are made to conform to a standard or to design criteria. In addition, as has been pointed out, the flexural strength must be computed to ensure that the elastic design has resulted in adequate safety factors.

It is well known that concrete is not as elastic material, however, and that the stresses computed on the basis of elastic assumptions can be considered only as approximations. Furthermore, in order to facilitate the design of prestressed members, most engineers base their computations upon the gross concrete section instead of using the net and transformed sections. Errors in the elastic computations are introduced as a result of this simplification, as is apparent from the discussions in Secs. 4-10 and 4-11. These considerations lead to the conclusion that normal elastic-design computations can only be considered

approximate, and that nothing is gained by using more than three significant figures in such computations.

It is significant that strength computations of bonded prestressed concrete construction can be made with good precision if the characteristics of the steel are known. Flexural strength capacity computations are virtually independent of the elastic properties of the concrete and are not materially influenced by variations in the effective prestress. For these reasons, the flexural strength computations usually are more important and precise than the elastic design computations.

8-15 Load Balancing

Consider a tendon that is placed on a parabolic path in a simple beam in such a fashion that the sag of the tendon at midspan, as measured vertically from a straight line connecting the ends of the tendon, is equal to e, as shown in Fig. 8-35. If the total uniformly distributed dead load supported by the beam is equal to w, the load will be exactly balanced by the upward force of the tendon:

$$Pe = \frac{wl^2}{8} \tag{8-10}$$

because, for the tendon to retain its parabolic path, a uniformly distributed upward force (neglecting friction) must be acting on it. In this particular case, if there is no eccentricity of the tendon at the ends of the beam, the pressure line acts along the centroidal axis of the member, and the compressive stress in the concrete section will be equal to the force in the tendon divided by the area

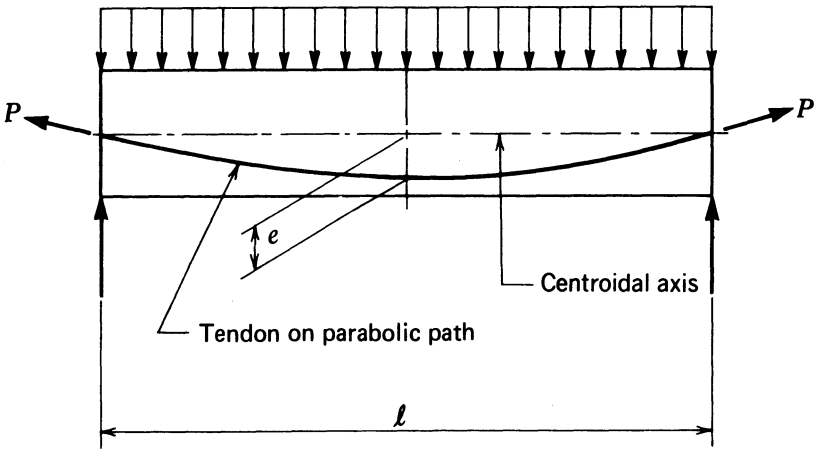

Fig. 8-35. The principle of load balancing with prestressed tendons.

of the concrete member at each section of the beam. This principle of load balancing is a useful design aid in certain circumstances.

Some structural engineers use the load balancing principle in the design of prestressed concrete flexural members, both simple beams and continuous beams. In the 1950s and early 1960s, before tensile stresses were commonly used in prestressed concrete flexural members, some designers used the load balancing principle to determine the prestressing force for balancing the dead load on a member and simply reviewed the design under total service load and design load, using the selected prestressing force. If the stress in the tensile flange was close to nil under the total service load, the prestressing force selected by the load balancing principle was adopted and used.

In contemporary practice, significant flexural tensile stresses are permitted by the major building codes, and some designers, who continue to employ the load balancing concept in their preliminary designs, do so by selecting prestressing forces and tendon paths that will balance a portion of the service dead load rather than the full dead load. In this procedure, after the load balancing concept is used to select a prestressing force for the preliminary design, a review is made of the flexural and shear stresses, as well as deflection, under full service load, and the flexural strength is checked under design loads. Modifications are made on a trial basis until an acceptable solution is found (see I.P. 13-1 in Sec. 13-11).

The load balancing principle also can be used for determining the loads that prestressed tendons impose upon concrete members. This is useful in the analysis of members having continuous as well as simple spans (see Chapter 10).

REFERENCES

ACI Committee 318. 1989. *Building Code Requirements for Reinforced Concrete.* Detroit. American Concrete Institute.

CEB-FIB Model Code for Concrete Structures. 1978. London. Federation International de la Precontraint. 201-02.

Guyon, Y. 1953. *Prestressed Concrete.* New York. John Wiley and Sons, Inc. 127-74.

Leonhardt, F. 1964. *Prestressed Concrete Design and Construction.* Berlin. Wilhelm Ernst und Sohn. 270-73.

Ontario Highway Bridge Design Code. 1983. Toronto. Ontario Highway Engineering Division. 212.

9 Design Expedients and Computation Methods

9-1 Introduction

A deterrent to the use of prestressed concrete in the past has been the greater amount of effort required to design prestressed structures in comparison to that required to design reinforced-concrete or structural-steel structures. The contemporary structural designer typically did not study prestressed concrete as a part of his or her formal education and is not familiar with the basic design principles. The fact that prestressed concrete design now is being taught at the graduate level in most universities will help alleviate this situation.

This chapter is intended to bridge the gap between theoretical considerations and practical design methods. The methods explained here can be applied in many different ways, and can be modified by individual designers for special conditions or to suit their preferences.

The discussions included in this chapter are intended to apply to concrete members that can be classified as fully prestressed. Fully prestressed members (see Sec. 7-5), for the purposes of the discussions contained herein, are defined as members in which: (1) the amount of nonprestressed principal flexural reinforcement is not significant and is limited to support bars for the web reinforcement and other secondary reinforcements; (2) the service load tensile

stresses are limited to values that do not exceed the assumed tensile strength of the concrete (i.e., the members are not expected to suffer flexural cracking under service loads); and (3) the stresses in the concrete are considered to be unaffected by the effects of concrete creep and shrinkage except for their affect on the loss of prestress. Section 7-3 discusses the important effects of significant amounts of nonprestressed reinforcement, as well as the effects of concrete creep and shrinkage and relaxation of prestressed reinforcement, on the stresses in the concrete.

The design expedients discussed herein originally were developed to facilitate design calculations made with a slide rule. Experience has shown slide rule accuracy to be sufficient. The use of modern electronic calculators and computers will render some of these methods unnecessary under usual conditions, but they still can be very useful under some circumstances.

9-2 Computation of Section Properties

The computation of axial and flexural stresses in a concrete section due to prestressing, and of external loads and moments, requires a determination of the area, the first moment of the area, and the moment of inertia (second moment of the area) of the section under study. The other properties frequently used to facilitate the computation of stresses are determined from these basic properties.

The computation of the basic properties of a section can be done by several methods, all producing the same results. These methods differ only in the organization of the computations and in the reference axis used in computing the first and second moments of the area. One convenient approach is to use an axis parallel and tangent to the top of the section as the reference axis for computing the area of the section, the first moment of the area, and the location of the centroidal axis with respect to the reference axis. The moment of inertia of the section then can be computed about the reference axis, the centroidal axis, or another reference axis. Whichever procedure is used in a design office or by an individual engineer, it should be used consistently in order to facilitate the checking and reviewing of the computations.

Moment-of-inertia computations can be made by using one or more variations of the basic relationship:

$$I_{ra} = I_0 + Ay^2 \tag{9-1}$$

which can be expressed in words as follows: The moment of inertia of a section about a reference axis (I_{ra}) is equal to the sum of the moment of inertia of the section with respect to the axis parallel to the reference axis that passes through the centroid of the section (I_0) and the product of the area of the section (A) and the square of the distance between the two axes (y^2). This relationship is illustrated in Fig. 9-1.

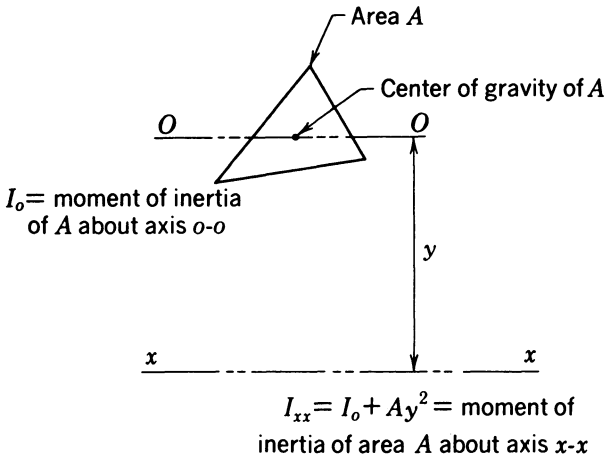

Fig. 9-1. Notation for moment-of-inertia computations.

Figure 9-2 gives the location of the centroids, and the moments of inertia about their centroids, of various shapes frequently encountered in prestressed-concrete design. The locations of the centers of gravity and the moments of inertia of other, less common sections that may be encountered can be found in standard engineering references or calculated by using basic mathematical relationships. It should be noted that the moments of inertia given in Fig. 9-2

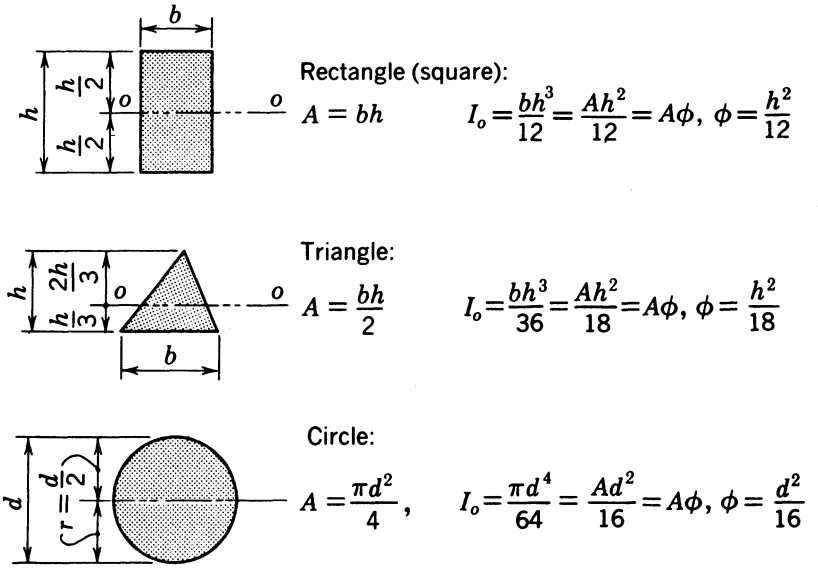

Fig. 9-2. Areas and moments of inertia for common geometric shapes.

are expressed in terms of the dimensions of the section, and as a function of the area of the section and the section height or diameter. The expressions giving the moments of inertia in terms of the areas of the sections are used to facilitate the computation of moments of inertia for complex shapes when done in tabular form. This is illustrated in the following discussion.

The method of computation is best explained with an example. The area, the first moment of the area with respect to a horizontal axis passing through the top of the section, the location of the centroid of the area, and the moment of inertia about a horizontal axis passing through the centroid of the area of the AASHTO-PCI standard bridge beam, type IV, are computed, as an illustration of a recommended procedure. Referring to Fig. 9-3 and Table 9-1, the procedure is as follows:

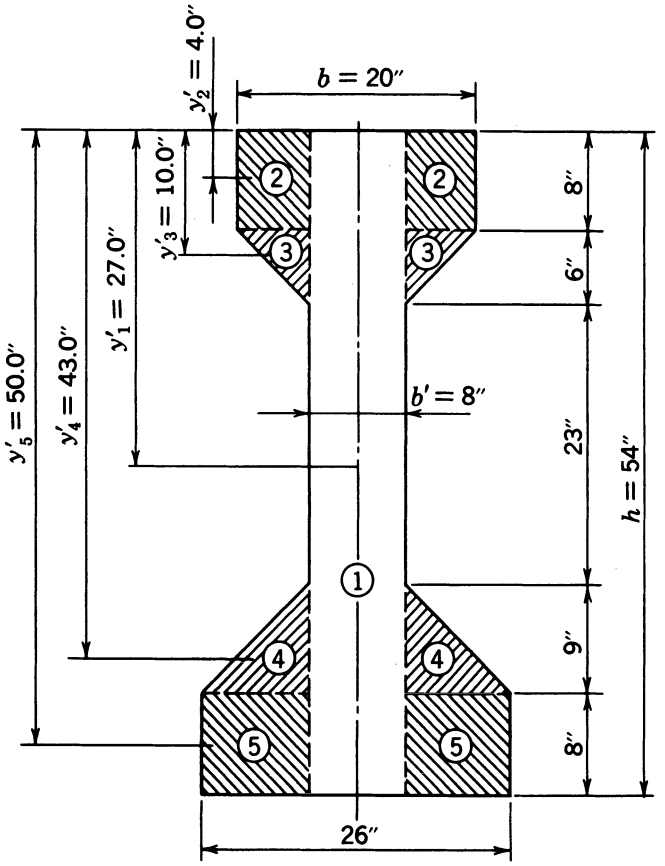

Fig. 9-3. AASHTO-PCI bridge beam, type IV, divided into rectangles and triangles to facilitate the computation of section properties.

TABLE 9-1 Computation of Section Properties of the AASHTO Type IV Bridge Beam, in Tabular Form.

Part	Area (A) Computation (in. × in. = in.^{2})	y' (in.)	Ay' (in.^{3})	y (in.)	y^2 (in.^{2})	ϕ (in.^{2})	$y^2 + \phi$ (in.^{2})	$A(y^2 + \phi)$ (in.^{4})
1	8 × 54 = 432	27.0	11,700	2.30	5.3	243	248	107,000
2	12 × 8 = 96	4.0	384	25.3	640	5.33	645	62,000
3	12 × 6/2 = 36	10.0	360	19.3	373	2.0	375	13,500
4	18 × 9/2 = 81	43.0	3,480	13.7	188	4.5	193	15,600
5	18 × 8 = 144	50.0	7,200	20.7	428	5.33	433	62,300

$\Sigma A = 789 \quad \Sigma Ay' = 23{,}124 \quad I = 260{,}400$

$y_t = 23{,}124/789 = -29.3$ in. $\quad S_t = 260{,}400/-29.3 = -8880$ in.^{3}

$$r^2/y_t = \frac{260{,}400}{789 \times -29.3} = -11.3 \text{ in.}$$

$y_b = +54.0 - 29.3 = +24.7$ in. $\quad S_b = 260{,}400/+24.7 = +10{,}500$ in.^{3}

$$r^2/y_b = \frac{260{,}400}{789 \times +24.7} = +13.4 \text{ in.}$$

1. Divide the cross section into shapes of known area, centroid locations, and moments of inertia with respect to their centroids, such as the rectangles and triangles numbered 1 through 5 in Fig. 9-3. To facilitate the computations, the number of component areas that must be included in the table was reduced: the rectangular areas listed as parts 2 and 5 in Table 9-1, as well as the triangular areas listed as parts 3 and 4, each consist of two parts in the figure.
2. Prepare a table, such as Table 9-1, as follows: compute the areas of component parts; determine and list the distances, y', from the top of the section to the centroids of the component areas; compute and list the moments of the component areas with respect to the top of the section (reference axis), A'_y; and compute the area of the section (ΣA), as well as the first moment of the section with respect to the top of the section ($\Sigma Ay'$).
3. Divide the first moment of the section ($\Sigma Ay'$) by the area of the section (ΣA), to obtain the distance from the top of the section to the centroid of the section (y_t). It should be noted that y_t is negative because it is measured upward from the centroidal axis.
4. Compute and tabulate the distances from the centroids of the component areas tot he centroid of the section of the component areas, y, by using $y_t - y'$.
5. Tabulate the squares of y.
6. Compute and tabulate the factors ϕ by which the component areas are to be multiplied to obtain their moments of inertia with respect to their centroids (see Fig. 9-2).

7. Tabulate the sums of $(y^2 + \phi)$.
8. Multiply, tabulate, and sum the terms $A(y^2 + \phi)$ for each of the component areas. The summation of these terms is the moment of inertia of the section.
9. The distance from the centroidal axis to the bottom fiber is computed as $y_b = h + y_t$, and the section moduli for the top and bottom fibers and the distances to the upper and lower limits of the kern zone are computed as follows:

$$S_t = \frac{I}{y_t} \quad \frac{r^2}{y_t} = \frac{I}{Ay_t}$$

$$S_b = \frac{I}{y_b} \quad \frac{r^2}{y_b} = \frac{I}{Ay_b}$$

Bridge stringers, such as the AASHTO-PCI standard prestressed-concrete beams for highway bridges, frequently are used with a cast-in-place deck slab that acts compositely with the stringers, as a result of shear stresses that develop between the slab and the top of the stringers (see Sec. 8-1). Computation of the composite section properties for an AASHTO-PCI bridge beam, type IV, with a 6 × 36 in. cast-in-place top flange, as illustrated in Fig. 9-4, can be done by using the same fundamental procedure as described above. This is illustrated in Table 9-2.

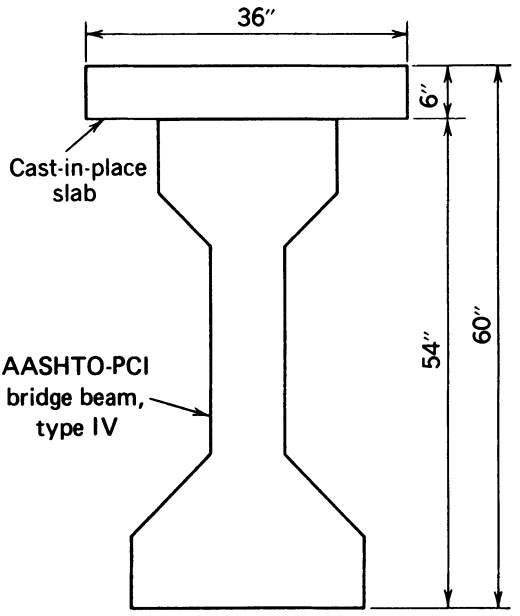

Fig. 9-4. Composite section composed of AASHTO-PCI bridge beam, type IV, and 6 × 36 in. cast-in-place concrete slab.

TABLE 9-2 Computation of the Section Properties of the Composite Beam Illustrated in Fig. 9-4.

Part	Area Computation (in. × in. = in.^{2})	y' (in.)	Ay' (in.^{3})	y (in.)	y^2 (in.^{2})	ϕ (in.^{2})	$y^2 + \phi$ (in.^{2})	$A(y + \phi^2)$ (in.^{4})
Slab	36 × 6 in. = 216	3.0	648	25.3	640	3.0	643	139,000
Beam	= 789	35.3	27,800	7.0	49	*	49	38,600
								260,400*
	ΣA = 1005 in.^{2}		$\Sigma Ay'$ = 28,448 in.^{3}					I = 438,000 in.^{4}

$y_p = -28.3$ in. $\quad S_p = -15{,}500$ in.^{3}

$y_t = -22.3$ in. $\quad S_t = -19{,}600$ in.^{3}

$y_b = +31.7$ in. $\quad S_b = +13{,}800$ in.^{3}

*The value of I_0 is known to equal 260,400 in.^{4} for the precast section. Hence, the value of ϕ is not computed for this portion of the composite section and the value of I_0 for the precast section is simply added in the $A(y^2 + \phi)$ column.

The concrete in the deck slab does not have the same elastic modulus as the concrete in the precast, prestressed concrete stringers under usual conditions because the quality of the concrete used in cast-in-place bridge decks normally is not as high as that used in the stringers. In computing the properties of the composite section, this effect is taken into consideration by using a transformed cross section that consists of the gross section of the prestressed beam and a slab section having a depth equal to that of the actual slab (less any allowance for wearing surface) plus the elastically equivalent slab width. The width normally assumed to be effective (as provided in the applicable design criteria) is multiplied by the ratio of the elastic modulus of the slab concrete to the elastic modulus of the concrete in the beam to give the elastically equivalent slab width. If the slab and beam concretes are assumed to have moduli of 3.5×10^6 psi and 5.0×10^6 psi, respectively, the elastically equivalent width of the slab that should be used in the composite section would be $3.5/5.0 = 0.70$ times the effective width.

Note that y_p and y_t are used to denote the distances from the centroidal axis of the composite section to the top fibers of the cast-in-place deck and the top fibers of the precast stringer, respectively. This procedure is recommended to avoid confusion, with the subscript t being used to denote the top fibers of the precast section in the computations of the section properties of the precast section.

In Table 9-2, it will be noted that there is no entry for the beam in the ϕ column. The moment of inertia of the precast section about its center of gravity is known, and so is simply added to the last column.

After the designer becomes accustomed to the use of this tabular form, the computation of section properties becomes rapid and routine. The effects of

minor adjustments in the concrete sections often are determined by subtracting or adding areas to the section that is being modified, rather than by recomputing the section properties of the modified section. In addition, the column headed $(y^2 + \phi)$ often is eliminated in actual calculations, and the terms y^2 and ϕ are added mentally as their sum is multiplied by the area. When electronic calculators are used, the columns headed y, y^2, ϕ, and $(y^2 + \phi)$ frequently can be eliminated from the table, thereby reducing the amount of written work needed for the computations.

As was explained in Sec. 7.3, in some methods of analysis used with prestressed concrete, it is more convenient to use the section properties computed about a reference axis other than the centroidal axis or axes of the member. This is a result of the different locations of the centroidal axis of a member at the different stages in an analysis. The computation of the first moments of the area and the moments of inertia of the different sections that must be considered actually is facilitated by using a single axis for all of the computations. In the case of a member that is first put into service in one configuration but later changed to another, such as a precast beam that eventually is modified to include a composite slab, the computation of the section properties is facilitated by performing all section-property calculations about a reference line coincident with the top surface of the composite slab.

ILLUSTRATIVE PROBLEM 9-1 Compute the areas, first moments of the area, and moments of inertia of the gross, net, net-transformed, and age-adjusted transformed sections for the member analyzed in I.P. 7-2. The dimensions of the concrete section and the prestressed and nonprestressed reinforcements are shown in Fig. 7-5. The elastic modulus of the concrete at the time of prestressing is 3122 ksi, the aging coefficient for the concrete is 0.80, and the ultimate creep ratio is 2.00. The elastic moduli for the prestressed and nonprestressed reinforcements are 28×10^3 and 29×10^3 ksi, respectively. The computations are summarized in Table 9-3.

9-3 Allowable Concrete Stresses for Use in Design Computations

Most prestressed-concrete design criteria specify maximum allowable initial, or temporary, compressive and tensile stresses, as well as maximum allowable final, or permanent, compressive and tensile stresses. This approach generally is considered necessary or justified for several reasons:

1. In order to obtain an economical and realistic production schedule under many conditions, it is essential that the prestress be applied to the member before the concrete attains the specified minimum 28-day cylinder strength. Hence, it is normal practice to apply the prestress to the concrete when the

TABLE 9-3 Computation of the Areas, First Moments, and Moments of Inertia, as Described in I.P. 9-1, for the Section in Fig. 7-5.

Gross Section: $(n-1)$	b	h	A	y'	Ay'	$y'^2+h^2/12$	I
na	16 ×	32.5 =	520 ×	16.25 =	8450	352	183,083
na	44 ×	4.5 =	198 ×	2.25 =	445	6.75	1,336
			718		8895		184,419

Net Section: $(n-1)$	b	h	A	y'	Ay'	$y'^2+h^2/12$	I
na			718		8895		184,419
na			1 ×	1.50 =	−1.5	2.25	−2
na			−2 ×	27.75 =	−55.5	770	−1,540
na			−4 ×	30.00 =	−120.0	900	−3,600
			711		8718		179,277

Net-Transformed Section: $(n-1)$	b	h	A	y'	Ay'	$y'^2+h^2/12$	I
na			718		8895		184,419
8.29			8.3 ×	1.50 =	12	2.25	19
na			−2.0 ×	27.75 =	55.5	770	−1,540
8.29			33.2 ×	30.00 =	994.7	900	29,844
			757.5		9847.1		212,742

Age-Adjusted Transformed Section: $(n-1)$	b	h	A	y'	Ay'	$y'^2+h^2/12$	I
na			718		8895		184,419
(23.17)1			23.17 ×	1.50 =	34.8	2.25	57
(22.33)2			−44.67 ×	27.75 =	1239.5	770	34,396
(23.17)4			92.67 ×	30.00 =	2780.1	900	83,403
			878.5		12,950		302,277

strength of the concrete is on the order of 4000 psi (or less) although the specified minimum cylinder strength of the concrete at the age of 28 days generally is on the order of 5000 psi (or more). Therefore, the temporary, or initial, allowable stresses are based upon a cylinder strength lower than that used in determining the final, or permanent, allowable concrete stresses.

2. The initial prestressing force is the maximum prestressing force ever to be imposed on the member. This force is subject to a reduction in the amount of 10 to 30 percent. The reduction or relaxation of the prestressing force starts to take place immediately after stressing and requires years to reach its practical maximum value.

3. The stresses imposed on the member due to prestressing are of opposite direction to those imposed by the service loads; that is, the prestressing normally

causes small tensile stresses in the top fibers and large compressive stresses in the bottom fibers of simple beams, whereas the superimposed loads that will be carried by the beams cause tensile stresses in the bottom fibers and compressive stresses in the top fibers.

4. The stresses resulting from prestressing can be controlled by the fabricator with relatively high precision, but for normal applications neither the designer nor the fabricator can control or predict very precisely the loads that will be imposed on the structure while it is in service. For this reason, and in view of the reasons listed in items (2) and (3), the safety factor required to guard against failure of the concrete during stressing does not need to be as high as that required for the design loads.

In a beam pretensioned with straight tendons, the highest initial stresses occur near the ends where there is no dead load moment to counteract the effects of the prestressing (see Sec. 4-6). Therefore, the restrictions on the temporary allowable stresses at the ends of the beam, provided that the beam does not contain significant amounts of nonprestressed reinforcement, can be expressed mathematically as follows:

$$\frac{C_i}{A}\left(1 + \frac{ey_t}{r^2}\right) \leq 6\sqrt{f'_{ci}} \tag{9-2}$$

and:

$$\frac{C_i}{A}\left(1 + \frac{ey_b}{r^2}\right) \leq 0.6f'_{ci} \tag{9-3}$$

where C_i is the resultant compressive force in the concrete section, and is equal, but of opposite sign, to the product of f_{si}, the initial stress in the prestressing steel, and A_{ps}, the area of the prestressed reinforcement; A is the area of the concrete; e is the eccentricity of the tendon; r is the radius of gyration; f'_{ci} is the concrete cylinder strength at the time of stressing; and y_t and y_b are the distances from the centroidal axis to the top and bottom fibers, respectively.*

If C is the force in the concrete resultant to the product of f_{se}, the effective stress in the tendons, and A_{ps}, the area of the prestressed reinforcement, and f'_c is the cylinder strength at 28 days, and f_{tt} and f_{tb} designate the total stresses due to dead and live loads in the top and bottom fibers at the section of maximum moment, respectively, the restrictions on the final allowable stresses can be expressed mathematically as follows:

$$\frac{C}{A}\left(1 + \frac{ey_t}{r^2}\right) + f_{tt} \leq 0.40f'_c \tag{9-4}$$

*Values of e and y are positive when below the centroidal axis, and negative above. The terms on the right side of eqs. 9-2 through 9-5 are based upon the stresses allowed by the AASHTO *Standard Specifications for Highway Bridges* (see Sec. 3-19).

and:

$$\frac{C}{A}\left(1 + \frac{ey_b}{r^2}\right) + f_{tb} \leq 3\sqrt{f'_c} \tag{9-5}$$

In eqs. 9-2 through 9-5, the symbols for the forces and stresses include the required signs.

For an assumed concrete section and an assumed ratio, m, of the effective steel stress to the initial steel stress, one can write:

$$m = \frac{C}{C_i} = \frac{f_{se}}{f_{si}}$$

and the values of f_{tt} and f_{tb} can be computed and substituted in eqs. 9-2 through 9-5, in which case all of the terms that appear in the equations will be known or assumed except for the values of C and e. Because a number of combinations of these terms normally will satisfy each of the four equations, the combinations that will satisfy all of the equations can be determined by plotting each of the four relationships as shown in Fig. 9-5. The shaded area of Fig. 9-5 indicates the combinations of C^{-1} and e that satisfy the conditions of the allowable stresses for the assumed section.

Although the procedure for plotting a figure similar to that shown in Fig. 9-5, first suggested by Magnel (1948), will yield accurate results and is useful as an instructional aid, it is too cumbersome and time-consuming to be used as a general design procedure. It illustrates the fact that there frequently are several combinations of prestressing force and eccentricity that will result in compliance with specific combinations of maximum and minimum allowable stresses.

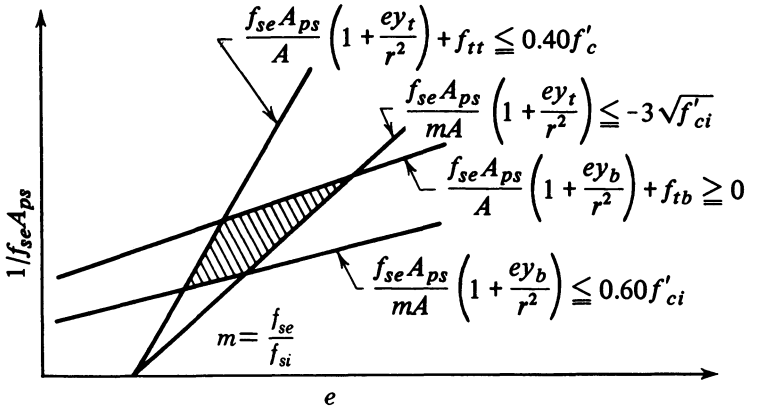

Fig. 9-5. Graphical solution of four equations for the prestressing force and eccentricity (after Magnel).

9-4 Limitations of Sections Prestressed with Straight Tendons

It should be apparent that fully bonded, straight pretensioning tendons can be used only in prismatic beams in which the maximum flexural stress in the bottom fibers, due to the total load, does not exceed the arithmetic sum of either (a) the allowable tensile stress and the final bottom-fiber stress due to prestressing or (b) the allowable tensile stress and the allowable compressive stress. If, for example, the maximum stress in the bottom fiber due to the total external load were 2300 psi, and the allowable tensile stress and the final compressive stress due to prestressing (assuming the final stress due to prestressing to be less than the allowable final compressive stress) were +400 psi and −2000 psi, respectively, the design would not be restricted by the bottom-fiber stress. The maximum load that could be applied without exceeding the allowable stresses would be one that resulted in a maximum bottom-fiber stress of +2400 psi.

In a similar manner, the top-fiber stress may limit the capacity of a prismatic beam section if the maximum flexural stress in the top fiber, due to the total load, is greater than the arithmetic sum of the allowable compressive stress in the member, after loss of prestress, and the allowable permanent tensile stress.

As a result of these limitations, the designer normally can determine if a specific concrete section can be used with straight tendons without calculating the magnitude and eccentricity of the prestressing force. It is necessary only to determine the stresses in the section due to the total load and compare these values with the sum of the appropriate, allowable stresses.

ILLUSTRATIVE PROBLEM 9-2 Determine the maximum moment that the section in Fig. 9-6 can withstand if pretensioned with straight tendons having initial and final stresses of 180 and 154 ksi, respectively, if f'_{ci} and f'_c are 4000 and 5000 psi, respectively, and the initial tensile stress cannot exceed the following:

Top fiber:

$$\text{Initial tensile stress} = 3\sqrt{4000} = +190 \text{ psi}$$

$$\text{Final compressive stress} = 0.40 \times -5000 = -2000 \text{ psi}$$

Bottom fiber:

$$\text{Initial compressive stress} = 0.60 \times -4000 = -2400 \text{ psi}$$

$$\text{Final tensile stress} = 3\sqrt{5000} = +212 \text{ psi}$$

$$\text{Final compressive stress} = 0.40 \times -5000 = -2000 \text{ psi}$$

SOLUTION: The stresses at the time of stressing will reduce to $\frac{154}{180} = 0.856$ of their initial value as a result of the prestressing losses. Therefore, the maximum stress due to all loads will be limited as follows:

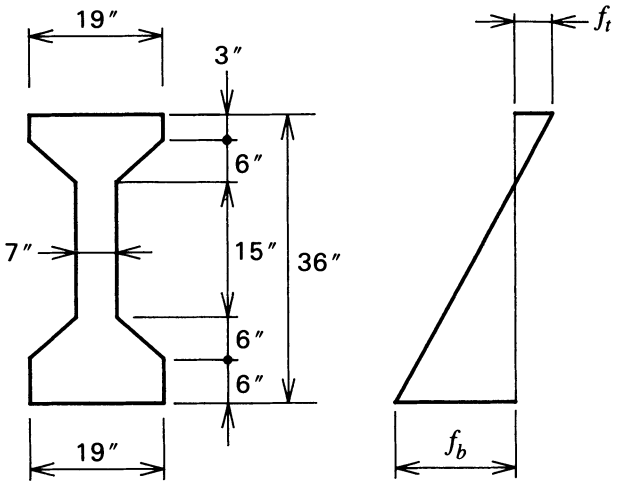

Fig. 9-6. Beam section and stress distribution for I.P. 9-2.

$$\text{Top fiber} = 2000 + 0.856 \times 190 = 2163 \text{ psi}$$

$$\text{Bottom fiber} = 212 + 0.856 \times 2400 = 2266 \text{ psi}$$

$$\text{Bottom fiber} = 212 + 2000 = 2212 \text{ psi}$$

The allowable moments as controlled by the top and bottom fibers are:

$$M_t = \frac{-2163 \times 63{,}300}{-18.9 \times 12000} = 604 \text{ k-ft}$$

$$M_t = \frac{2212 \times 63{,}300}{17.1 \times 12000} = 682 \text{ k-ft}$$

The stresses in the top fiber control the capacity of this section with these design criteria.

9-5 Limitations of Sections Prestressed with Curved Tendons

In considering the stress in the bottom fiber at any specific section of a simple beam prestressed with a curved tendon, it should be apparent that the maximum stress due to external loads must not exceed the arithmetic sum of the stress due to the effective prestressing force and the allowable tensile stress in the completed structure. In addition, the algebraic sum of the stress due to the initial prestressing force and the stress due to the minimum loading condition must not exceed the allowable, initial compressive stress.

ILLUSTRATIVE PROBLEM 9-3 Determine the maximum allowable total moment on the beam section of Fig. 9-6 if a curved tendon is used, and the initial and final stresses in the prestressed reinforcement are 187 and 162 ksi, respectively. The design span is 50.0 ft. The allowable stresses are those used in I.P. 9-2. The compressive strength at the time of prestressing is -4000 psi, and the specified compressive strength at 28 days is -5000 psi.

SOLUTION: The beam dead load is equal to 0.450 klf, and the dead load moment at midspan is equal to 141 k-ft. Dead load flexural stresses:

$$f_t = \frac{141 \times 12}{-3350} = -0.505 \text{ ksi}$$

$$f_b = \frac{141 \times 12}{3700} = +0.457 \text{ ksi}$$

Maximum allowable stress and moment as limited by top fiber:

$$f_t = -0.40 \times 5000 - 505 - \frac{162}{187}(3\sqrt{4000}) = -2669 \text{ psi}$$

$$M_t = \frac{-2669 \times 3350}{12000} = 745 \text{ k-ft}$$

Maximum allowable stresses and moment as limited by bottom fiber:

$$f_b = (0.60 \times 4000)\frac{162}{187} + 457 + 3\sqrt{4000} = 2726 \text{ psi}$$

$$f_b = (0.40 \times 5000) + 457 + 3\sqrt{5000} = 2669 \text{ psi}$$

$$M_b = \frac{2669 \times -3700}{12000} = 823 \text{ k-ft}$$

It should be recognized that the maximum allowable top and bottom fiber stresses due to prestressing may not always be attainable (see Sec. 9-7).

The initial tensile stresses in the top fibers of beams prestressed with curved tendons normally are not critical at the section of maximum moment in beams of good proportions. If the top-fiber stresses do limit the design of beams with curved tendons, the problem usually is due to excessive, compressive stress under maximum loading conditions. Top-fiber stresses are much more apt to be a concern in a beam with a thin, narrow top flange than in a beam with a thick, wide top flange.

9-6 Minimum Prestressing Force for Straight Tendons

In the design-by-trial procedure commonly used in designing prestressed flexural members, a beam with known cross-sectional properties is tentatively adopted and reviewed to determine the stresses due to the external loads. If the external loads result in stresses within practical limits (see Sec. 9-4), then the prestressing force and concomitant eccentricity required to develop the desired net concrete stresses must be determined. When straight tendons are used in prismatic simple beams subjected to usual loading conditions, the maximum stresses under minimum loading conditions (dead load of the beam alone, usually) occur at the ends of the beam where there is no moment due to external loads. The maximum stresses under the maximum loading conditions occur near midspan. The procedures recommended for determining the minimum prestressing force and its required eccentricity for different specific conditions are illustrated with explanations in I.P. 9-4 through I.P. 9-6.

ILLUSTRATIVE PROBLEM 9-4 Determine the prestressing force and eccentricity required to prestress a slab, 4 ft wide and 8 in. deep, with straight tendons. The slab is to be used, simply supported, on a span of 30 ft and is to be composed of normal concrete (150 pcf) with $f'_{ci} = 4000$ psi and $f'_c = 5000$ psi. The superimposed load is 45 psf, and the member will be exposed to a corrosive atmosphere in service.

SOLUTION:

Loads and moments:

$$\text{Slab dead load} = 4 \times 100 = 400 \text{ plf}$$

$$\text{Superimposed load} = 4 \times 45 = \underline{180 \text{ plf}}$$

$$\text{Total load} = 580 \text{ plf}$$

The bending moment due to the total load is:

$$M_{TL} = 0.580 \frac{30^2}{8} = 65.25 \text{ k-ft}$$

The section modulus of the slab is:

$$S = \frac{48 \times 8^2}{6} = 512 \text{ in.}^3$$

and the top and bottom fiber stresses due to the total load are:

$$f_t = \frac{65.25 \times 12{,}000}{-512} = -1530 \text{ psi}$$

$$f_b = \frac{65.25 \times 12{,}000}{512} = +1530 \text{ psi}$$

Assume that nonprestressed reinforcement is not to be used in the top flange to resist tensile stresses in the concrete. The final stress in the bottom fiber due to prestressing must be equal to +1530 psi. (Because the slabs are to be exposed to a corrosive atmosphere, to guard against cracking and to protect the prestressed reinforcement against corrosion, the net bottom-fiber stress should not be tensile under full load.) If nonprestressed reinforcement is not to be provided at the ends, the top-fiber tensile stress at the ends, due to initial prestress, should be equal to or less than $3\sqrt{4000} = 190$ psi. Assuming that the ratio of the effective stress to the initial stress in the prestressed reinforcement is 0.85, the tensile stress in the top fiber resulting from the effective prestress must not exceed $0.85 \times 190 = 160$ psi. Therefore, the stress distribution due to the final prestressing force should be as shown in Fig. 9-7.

The prestressing stress at the centroid of a section is equal to the average compressive stress in the concrete due to the prestressing force ($-P/A$) because the distance from the centroidal axis of the concrete section, y, is equal to zero for the fiber at the centroidal axis, and the familiar equation for stress due to prestressing:

$$f = \frac{P}{A}\left(1 + \frac{ey}{r^2}\right)$$

becomes:

$$f = \frac{P}{A}$$

This fundamental principle is applicable for sections that are symmetrical or asymmetrical about the centroidal axis. The average stress can be rapidly

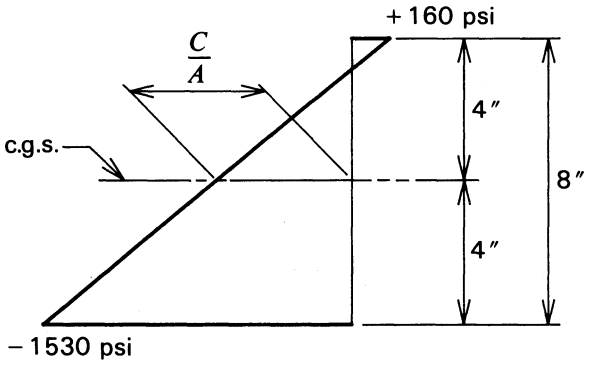

Fig. 9-7. Distribution of stresses due to final prestressing force for I.P. 9-4.

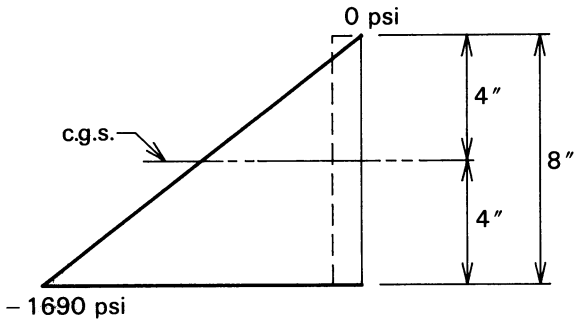

Fig. 9-8. Distribution of stresses for I.P. 9-4.

computed by use of the relationships indicated in Fig. 9-8, from which it will be seen that:

$$\frac{p}{A} = (f_b - f_b)\frac{y_t}{d} + f_t = -1690\left(\frac{4.0}{8.0}\right) + 160 = -685 \text{ psi}$$

Therefore, the final prestressing force can be computed by:

$$P = -\frac{(-685 \times 48 \times 8)}{1000} = 263 \text{ kips}$$

This force must develop -1530 psi in the bottom fiber, and the familiar relationship for the bottom-fiber stress due to prestressing:

$$f_b = \frac{C}{A}\left(1 + \frac{ey_b}{r^2}\right)$$

can be rewritten:

$$e = \left(\frac{f_b}{C/A} - 1\right)\frac{r^2}{y_b} = \left(\frac{-1530}{-685} - 1\right)\left(\frac{8}{6}\right) = 1.65 \text{ in.}$$

Note that $r^2/y = d/6$ for a rectangular section.

If it is decided to use nonprestressed reinforcement in the top fibers to resist the tensile stresses in the concrete due to prestressing, the initial, top-fiber tensile stress might be as great as $6\sqrt{f'_{ci}} = 380$ psi, and the top-fiber tensile stress due to the effective prestressing force could be as great as $0.85 \times 380 = 320$ psi. Assuming that it is desired to limit the top-fiber tensile stress to 300 psi, the required distribution of prestress will be as shown in Fig. 9-9, and the computation of C and e will be:

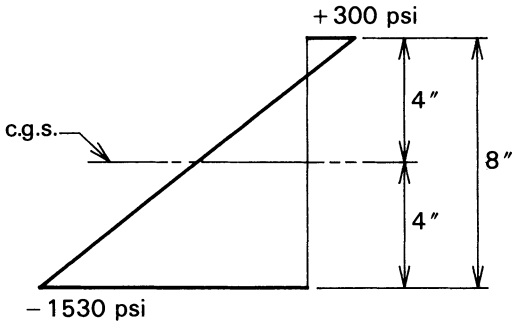

Fig. 9-9. Required prestress distribution for I.P. 9-4.

$$\frac{C}{A} = -1830 \times \frac{4.0}{8.0} + 300 = -615 \text{ psi}$$

$$P = 236 \text{ kips}$$

$$e = \left(\frac{-1530}{-615} - 1\right)\left(\frac{8.0}{6}\right) = 1.98 \text{ in.}$$

Compare the simplicity of this computation to the effort required using the classical relationship demonstrated in I.P. 4-8.

ILLUSTRATIVE PROBLEM 9-5 For the slab of I.P. 9-4, assume that the superimposed load will be 100 psf. Compute the required prestressing force and eccentricity, assuming: (1) the final top-fiber tensile stress due to prestressing must not exceed 300 psi, and no tension is to be allowed in the bottom fibers; and (2) the final top-fiber stress due to prestressing must not exceed 300 psi, and the net stress in the bottom fiber under full load must not exceed 400 psi.

SOLUTION: Loads and moments:

$$\text{Slab dead load} = 4 \times 100 = 400 \text{ plf}$$

$$\text{Superimposed load} = 4 \times 100 = \underline{400 \text{ plf}}$$

$$\text{Total load} = 800 \text{ plf}$$

$$\text{Total moment} = 0.80 \times \frac{30^2}{8} = 90.0 \text{ k-ft}$$

$$\text{Top-fiber stress} = \frac{90.0 \times 12{,}000}{-512} = -2110 \text{ psi}$$

$$\text{Bottom-fiber stress} = \frac{90.0 \times 12{,}000}{512} = 2110 \text{ psi}$$

Part (1): The bottom-fiber stress of −2110 psi is too high for $f'_{ci} = -4000$ psi because $0.85 \times 0.60 \times -4000 = -2040$ psi. If this solution is to be used, and if the design is to conform to the allowable stresses specified above, the value of f'_{ci} must be equal to $-2110/(0.85 \times 0.60)$, which is equal to −4150 psi. It should be pointed out that the net compression in the top fiber will be $-2110 + 300$ psi $= -1810$ psi. If the final net compressive stress is to be 0.40 f'_c or less, the minimum value of f'_c is 4500 psi. Assuming that these values of initial and final concrete strength are to be used, the required values of C and e are (see Fig. 9-10):

$$\frac{C}{A} = -2410 \times \frac{4.0}{8.0} + 300$$

$$= -905 \text{ psi}$$

$$P = 348 \text{ kips}$$

$$e = \left(\frac{-2110}{-905} - 1\right)\left(\frac{8.0}{6}\right) = 1.77 \text{ in.}$$

Part (2): The desired distribution of concrete compressive stresses due to prestressing is as shown in Fig. 9-11, and the values of P and e become:

$$\frac{C}{A} = -2010 \times \frac{4.0}{8.0} + 300$$

$$= -705 \text{ psi}$$

$$P = 271 \text{ kips}$$

$$e = \left(\frac{-1710}{-705} - 1\right)\left(\frac{8.0}{6}\right) = 1.90 \text{ in.}$$

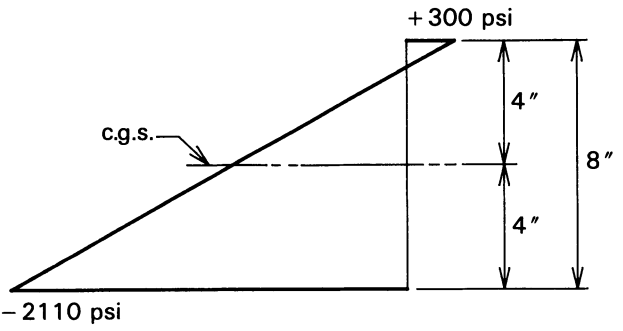

Fig. 9-10. Distribution of stresses, part (1) of I.P. 9-5.

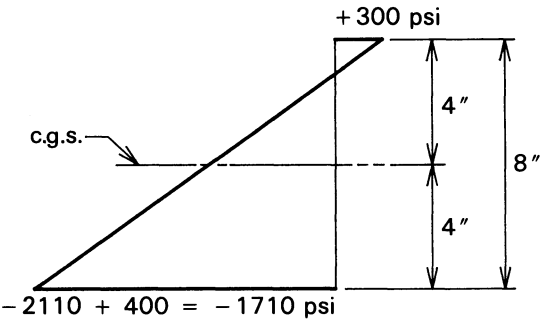

Fig. 9-11. Distribution of stresses, part (2) of I.P. 9-5.

This example illustrates a procedure that can be adopted if the initial concrete stresses (or final stresses) are nominally higher than would be allowable for the quality of concrete that was at first assumed; the designer can increase the value of the concrete strength at the time of prestressing and at the age of 28 days (within reasonable limits) in order to confine the stresses within the allowable limits. Also illustrated is the procedure used in the calculation of the prestressing required for members in which tensile stresses are permitted in the bottom fibers of the members under full load.

ILLUSTRATIVE PROBLEM 9-6 Compute the prestressing force and eccentricity required to produce a final stress of +300 psi in the top fibers and −2000 psi in the bottom fibers of an AASHTO-PCI type III bridge beam, as shown in Fig. 9-12. The section properties required for the analysis are as follows: $A = 560$ in.^{2}, $y_t = 24.7$ in., and $r^2/y_b = 11.03$ in.

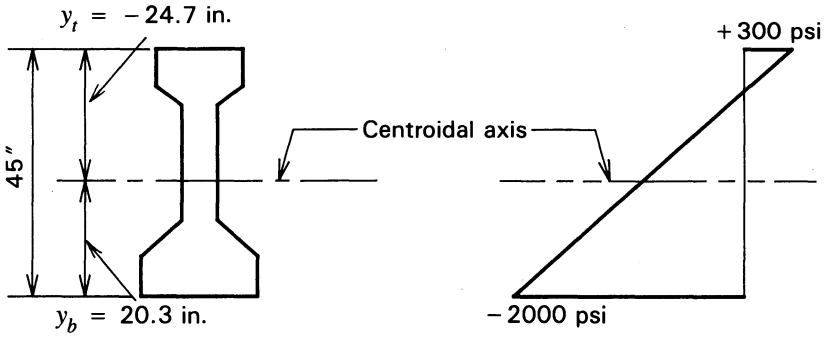

(a) AASHTO-PCI Type III bridge beam.

(b) Distribution of effective prestress

Fig. 9-12. Cross section of AASHTO-PCI type III bridge beam and distribution of effective prestress required.

SOLUTION: The desired distribution of stresses is illustrated in Fig. 9-12, and P and e are computed as follows:

$$\frac{P}{A} = -\left(-2300 \times \frac{24.7}{45.0} + 300\right) = -962 \text{ psi}$$

$$P = 539 \text{ kips}$$

$$e = \left(\frac{-2000}{-962} - 1\right)(11.03) = 11.90 \text{ in.}$$

9-7 Minimum Prestressing Force for Curved Tendons

Because the dead load of a beam is acting at the time of prestressing, the eccentricity of prestressed reinforcement can be greater near midspan of a simple beam than at the ends, without the net concrete stresses exceeding the allowable values, as was explained in Sec. 4-6. This is the reason for draping or curving the tendons. This procedure results in a variable prestressing moment along the length of the beam; hence, the stresses in the concrete due to curved prestressing tendons should be investigated at several locations along the length of the beam. For prismatic members having straight tendons, the amount of prestressing needed is controlled by the conditions of stress at the position of maximum moment; this remains true for members having curved tendons if the maximum eccentricity of the prestressed reinforcement occurs at the location of the maximum moment. *For members having variable depth, the amount of prestressing needed may be controlled by the conditions of stress at a section other than the section at which maximum moment occurs.*

In detailing a member, the prestressing force must be developed by a specific number of whole tendons. Fractions of tendons cannot be used, and, to avoid errors, all tendons in a pretensioned concrete member are normally of the same size and grade. For reasons of economy, the number of tendons should be as low as possible, and they should be stressed to their maximum allowable stress.

ILLUSTRATIVE PROBLEM 9-7 For the AASHTO-PCI bridge beam, type III, which is to be used on a span of 70 ft, compute the minimum prestressing force and eccentricity that can be used if the member must withstand a superimposed moment of 800 k-ft at midspan. The superimposed moment varies parabolically from a maximum value at midspan to zero at the support. Assume that the minimum specified concrete strength and the minimum concrete strength at the time of prestressing are 5000 psi and 4000 psi, respectively. The centroidal axis measured from the top fiber, the area, and the moment of inertia of the AASHTO-PCI bridge beam, type III, are 24.7 in., 560 in.^{2}, and 125,400 in.^{4}, respectively. The dead load of the beam itself is 0.585 klf.

TABLE 9-4 First Table for I.P. 9-7.

	Top Fiber	Bottom Fiber
Stresses due to total moment	−2740 psi	+2250 psi
Stresses due to dead load only	−845 psi	+695 psi

SOLUTION:

$$\text{Moment due to dead load of beam} = 0.585 \times \frac{70^2}{8} = 358 \text{ k-ft}$$

$$\text{Moment due to the superimposed load} = 800 \text{ k-ft}$$

$$\text{Total moment at midspan} = 1158 \text{ k-ft}$$

The stresses due to dead load and total load are summarized in Table 9-4.

The distribution of concrete stresses due to the effective prestress at midspan must be as shown in Fig. 9-13a, if the net top-fiber stress due to total load plus effective prestress is to be held to $0.40f'_c = 0.40 \times 5000 = 2000$ psi, and if the tensile stresses in the bottom fiber due to the total load are to be exactly nullified by the effective prestress, nonprestressed reinforcement is not to be used, and the top-fiber concrete stress due to initial prestressing plus dead load of the beam is to be limited to 190 psi. Assuming $f_{se}/f_{si} = 0.85$, the prestressing distribution shown in Fig. 9-13b limits the top-fiber stress to the allowable value and exactly nullifies the total load stress in the bottom fiber. The bottom-fiber stress, due to the effective prestress, could be as high as $0.40f'_c + 695 = 2695$ psi. The most economical design will result from a prestressing force that can develop the required minimum effective prestress in the bottom fibers (+2250 psi) without exceeding the allowable, initial tensile stress in the top fibers, such

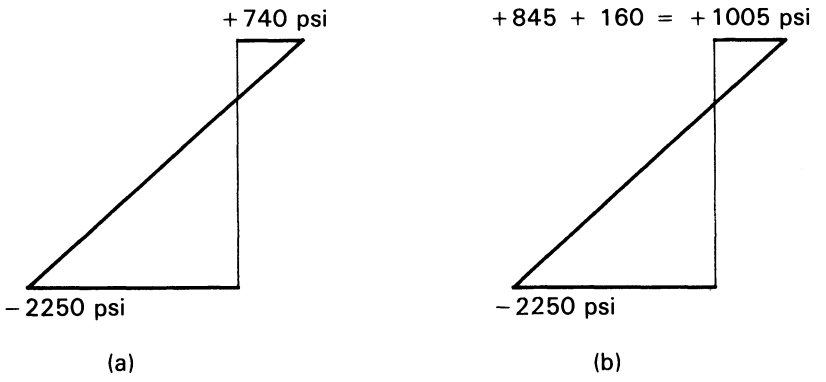

Fig. 9-13. Stress distributions for I.P. 9-7.

as is shown in Fig. 9-13b, if such a stress distribution can be obtained with a practical eccentricity.

For the distribution of stress shown in Fig. 9-13b, the values of C and e are:

$$\frac{C}{A} = -3255 \times \frac{24.7}{45.0} + 1005 = -782 \text{ psi}$$

$$P = 438 \text{ kips}$$

$$e = \left(\frac{-2250}{-782} - 1\right)(11.03) = 20.70 \text{ in.}$$

It is apparent that this is not a solution for this case because the required eccentricity is greater than the distance from the centroidal axis of the section to the bottom fibers (y_b); hence, if this solution were used, the centroid of the prestressed reinforcement would be below the bottom of the beam. Therefore, the distribution of stress due to the effective prestress must be revised in such a manner that the eccentricity is reduced.

Using the distribution of stress indicated in Fig. 9-13a, the values of C and e are:

$$\frac{C}{A} = -2990 \times \frac{24.7}{45.0} + 740 = -900 \text{ psi}$$

$$P = 504 \text{ kips}$$

$$e = \left(\frac{-2250}{-900} - 1\right)(11.03) = 16.5 \text{ in.}$$

This solution is reasonable for the conditions at midspan, and should be adopted, because the stresses are allowable and the eccentricity of 16.5 in. results in the centroid of the prestressed reinforcement being 3.8 in. from the bottom of the beam, allowing adequate concrete cover.

Because the dead-load moment and the moment due to the superimposed loads vary parabolically (from maximum at the center of the span to zero at the supports), it can be specified that the eccentricity of the prestressing is zero at the support. Nominal eccentricities above or below the center of gravity of the section could be allowed at the supports without exceeding the allowable stresses.

At the quarter point, the stresses due to the dead and superimposed loads are only 75 percent of the stresses due to these loads at midspan, or -2060 and $+1690$ psi in the top and bottom fibers, respectively. Assume that the effective force in the prestressed reinforcement is 504 k, and the eccentricity is 16.5 in. at midspan; if the eccentricity varies parabolically to zero at the supports, it would be 75 percent of 16.5 in. at the quarter point, and the stresses due to the effective prestress would be:

TABLE 9-5 Second Table for I.P. 9-7.

	Top Fiber	Bottom Fiber
Stress due to dead load of beam	−634	+521
Effective prestress	+332	−1912
Net, minimum loading	−302	−1391
Stress due to superimposed load	−1420	+1165
Net, maximum loading	−1722	−226

$$f_t = -\frac{504{,}000}{560}\left(1 + \frac{12.4}{-9.06}\right) = 332 \text{ psi}$$

$$f_b = -\frac{504{,}000}{560}\left(1 + \frac{12.4}{11.03}\right) = -1912 \text{ psi}$$

It can be shown that these stresses due to prestressing will result in net concrete stresses, under minimum and maximum loading conditions at the quarter point of the span, that are within the allowable values. The stresses are summarized in the Table 9-5.

ILLUSTRATIVE PROBLEM 9-8 For the beam and the conditions specified in I.P. 9-7, determine the number of high-tensile-strength steel rods, in sheaths having a diameter of 1.5 in., that could be used, if the rods were to be used with an effective prestress of 82 k each, and $f_{se}/f_{si} = 0.85$.

SOLUTION: Assume six rods, so that:

$$P = 6 \times 82 = 492 \text{ kips}$$

$$M_T = P(e + r^2/y_b) = 1158 = 492(e + 11.03)$$

$$e = 17.3 \text{ in.}$$

Check the computations:

$$f_t = -\frac{492{,}000}{560}\left(1 + \frac{17.3}{-9.06}\right) = 800 \text{ psi}$$

$$f_b = -\frac{492{,}000}{560}\left(1 + \frac{17.3}{11.03}\right) = -2250 \text{ psi}$$

This solution is satisfactory. It should be noted the stress distribution is between those of parts (a) and (b) of Fig. 9-13, and the distance from the soffit of the

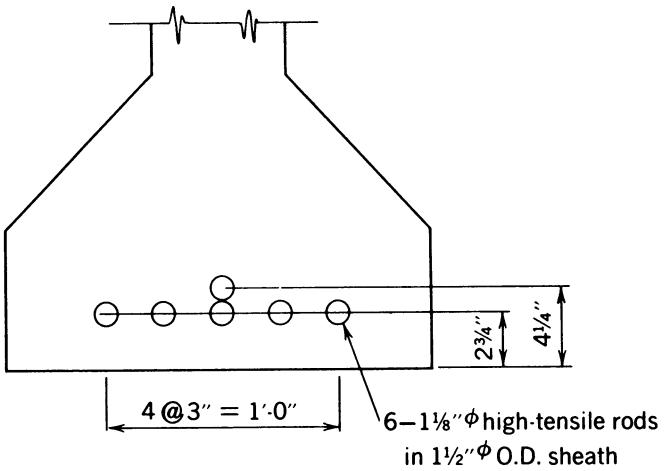

Fig. 9-14. Position of post-tensioning tendons, I.P. 9-8.

beam to the centroid of the tendons is 3.0 in.—a distance that will allow a clear concrete cover of 2 in. for sheaths if placed as shown in Fig. 9-14.

ILLUSTRATIVE PROBLEM 9-9 Assume that the beam for I.P. 9-7 is to be stressed with a combination of pretensioned and post-tensioned reinforcement. Determine the amount and eccentricity of the prestressing required for each of these methods, if it is assumed that the maximum, initial, tensile and compressive concrete stresses are 350 psi and −2400 psi, respectively, and $f_{se}/f_{si} = 0.85$. The amount of the post-tensioned reinforcement is to be kept as small as possible. Assume that the post-tensioned reinforcement is not to be prestressed until the beam has been pretensioned and removed from the casting bed.

SOLUTION: The maximum distribution of stress that can be allowed by the effective prestress in the straight pretensioned tensions is as shown in Fig. 9-15, for which the values of P and e are:

$$\frac{C}{A} = -2340 \times \frac{24.7}{45.0} + 300 = 985 \text{ psi}$$

$$P = 551 \text{ kips}$$

$$e = \left(\frac{-2040}{-985}\right)(+\ 11.03) = +11.81 \text{ in.}$$

Assuming that the supplementary prestressing is accomplished with one post-tensioned tendon at an eccentricity of 17.5 in. (2.8 in. from the bottom of the beam to the centroid the tendon), the prestressing force required to increase the

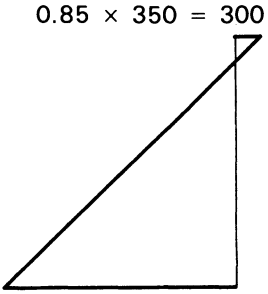

Fig. 9-15. Distribution of stresses, first solution, I.P. 9-9.

bottom-fiber stress, −210 psi, to a total value of −2250 psi, is calculated as follows:

$$\frac{C}{A} = \frac{-210}{1 + \left(\frac{17.5}{11.03}\right)} = -81.2 \text{ psi}$$

$$P = +45.5 \text{ kips}$$

$$f_t = -\frac{45{,}500}{560}\left(1 + \frac{17.5}{-9.06}\right) = +76 \text{ psi}$$

$$f_b = -\frac{45{,}500}{560}\left(1 + \frac{17.5}{11.03}\right) = -210 \text{ psi}$$

Summarizing, the net concrete stresses for this solution are as shown in Table 9-6.

If this combination of prestressing is adopted, the value of f'_c required for conformance to the design criteria is $-2364/0.40 = -5900$ psi. If this value is too high, the member must be redesigned with a larger top flange, in order to resist the compressive stresses, or the tensile stresses in the top flange due to prestressing must be increased.

Because the top-fiber tensile stress resulting from the effective pretensioning is confined to +300 psi, to revise the prestressing so that the value of f'_c does

TABLE 9-6 First Table for I.P. 9-9.

	Top Fiber	Bottom Fiber
Stress due to total moment	−2740 psi	+2250 psi
Effective prestress: pretension	+300 psi	−2040 psi
Effective prestress: post-tension	+76 psi	−210 psi
Net concrete stresses	−2364 psi	0 psi

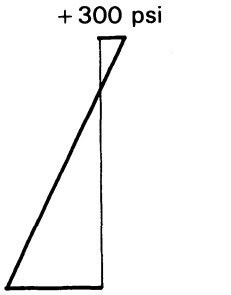

Fig. 9-16. Distribution of stresses, second solution, I.P. 9-9.

not have to exceed −5000 psi, the post-tensioning must develop +440 psi in the top fiber. Thus, the top-fiber compressive stress will not exceed −2000 psi under maximum loading conditions. Assuming that the centroid of the post-tensioned reinforcement is 4.40 in. above the bottom of the beam (e = 15.9 in.), the force required to develop the required tensile stress of +440 psi in the top fiber and the concomitant compressive stress in the bottom fiber are:

$$f_t = 440 = -\frac{P}{560}\left(1 + \frac{15.9}{-9.06}\right)$$

$$P = 326 \text{ kips}$$

$$f_b = -\frac{326{,}000}{560}\left(1 + \frac{15.9}{11.03}\right) = -1420 \text{ psi}$$

Hence, the required stress distribution due to the supplementary effective pretensioning is as shown in Fig. 9-16, and the P and e required are as follows:

$$\frac{C}{A} = -1130 \times \frac{24.7}{45.0} + 300 = -320 \text{ psi}$$

$$P = 179 \text{ kips}$$

$$e = \left(\frac{-830}{-320} - 1\right)(+ 11.03) = 17.6 \text{ in.}$$

TABLE 9-7 Second Table for I.P. 9-9.

	Top Fiber	Bottom Fiber
Stresses due to M_t	−2740 psi	+2250 psi
Stresses due to post-tensioning	+440 psi	−1420 psi
Stresses due to pretensioning	+300 psi	−830 psi
Net concrete stresses	−2000 psi	0 psi

The net concrete stresses resulting from this combination of prestress are summarized in Table 9-7.

The above problem illustrates that the capacity and method of prestressing used may be limited by compressive stresses in the top fiber of the beam. This condition is particularly acute in beams having long spans and narrow top flanges.

9-8 Preliminary Design of Flexural Members

The preliminary design of a prestressed concrete flexural member, from an analytical point of view, involves proportioning of a concrete section, selection of the strength of concrete to be used, selection of the types and grades of reinforcements to be used, and determination of the quantities of prestressed and nonprestressed reinforcements needed to conform to the applicable design standards. In actual engineering practice, however, economic considerations are very important, and preliminary design normally involves the study of several preliminary design alternatives for the purpose of determining the relative cost of the different designs considered acceptable from analytical considerations alone.

In Sec. 4-4, it was shown that for a simple beam that has zero bottom-fiber stress in the loaded state, the total moment that the beam can withstand is expressed by:

$$M_T = M_D + M_{SL} = P(e + r^2/y_b) \tag{9-6}$$

In a similar manner, if the stress in the top fiber due to the effects of prestressing alone is to be zero, it can be shown that the eccentricity of the prestressing force must not be greater than r^2/y_t below the centroidal axis of the section (i.e., $e = -r^2/y_t$). Therefore, if tensile stresses are not to be permitted in a section under the conditions of no load and maximum loads, the relationship of eq. 9-6 can be written:

$$M_T = M_D + M_{SL} = P(r_2/y_t + r^2/y_b) \tag{9-7}$$

The relationships are useful in making preliminary designs of fully prestressed members because, by assuming values for M_D and P, the required value of the quantity $(e + r^2/y_b)$ can be computed. In employing these relationships in preliminary design, the engineer should keep the following fundamental factors in mind:

1. Most economical designs of simple beams have values of C/A (the average compressive stress in the concrete) between -500 and -900 psi. This gives a means of making a rough check on the estimated dead weight of the beam

without assuming a specific cross section. (Considerably lower values of average prestress, C/A, generally are used in precast members with large top flanges, such as T-shaped beams, as well as in solid slabs.)

2. The dead weight of the beam itself is a small portion of the total load for short-span beams, whereas for long-span beams, the dead load of the beam itself may be of great importance.

3. When straight tendons are used in short, simple-span members, the value of the quantity $(e + r^2/y_b)$ approaches the lower limit as given in eq. 9-7 $(r^2/y_t + r^2/y_b)$.

4. When curved or draped tendons are used in beams of moderate to long spans, the value of e frequently is limited by the dimensions of the concrete section, rather than by top- or bottom-fiber stresses, and eq. 9-6 approaches:

$$M_T = P(y_b + r^2/y_b) \tag{9-8}$$

5. When tensile stresses are allowed in the bottom fibers in the fully loaded state, the pressure line goes higher than r^2/y_b above the center of gravity of the section, and the relationship given by eq. 9-6 can be rewritten:

$$M_T = \psi P(e + r^2/y_b) \tag{9-9}$$

The value of ψ to be assumed in the above relationship must be estimated by considering the absolute value of the allowable bottom-fiber tensile stress with respect to the absolute value of the bottom-fiber stress resulting from prestressing alone. For example, if the bottom-fiber stress due to the effective prestress must be confined to -2000 psi, and the allowable tensile stress in the bottom fiber is $+400$ psi, the value of $(e + r^2/y_b)$ must be increased by the ratio $\psi = 2400/2000 = 1.20$ to give an accurate estimate of the movement of the pressure line that will take place when the beam is loaded from the condition of zero bottom-fiber stress (due to external loads) to the point where the stress in the bottom fiber is $+400$ psi. If the bottom-fiber stress due to the effective prestress alone is as high as -3000 psi, as it frequently is in long-span, post-tensioned members, an allowable tensile stress of $+400$ psi in the bottom fiber would result in a ratio for ψ of $3400/3000$, which is equal to 1.13.

6. The value of the term $(e + r^2/y_b)$ varies from 33 to 80 percent of the depth of the beam, depending upon the efficiency of the cross section, the allowable stresses, and the dead-load moment. Average values of this factor for use in estimating the preliminary design of roof and bridge girders are between 60 and 75 percent of the depth of the member, with the larger values being applicable to the longer spans and to members with relatively large flanges.

7. The average value for the depth-to-span ratio for most simple beams can be assumed to be $1/20$. This ratio does vary between relatively wide limits, but for simple beams it is rarely greater than $1/6$ or less than $1/24$, except for solid and cored slabs.

ILLUSTRATIVE PROBLEM 9-10 Estimate the depth of a beam required to carry a superimposed moment of 800 k-ft on a span of 70 ft using curved tendons.

SOLUTION: Assume the weight of the girder will be 400 plf.

$$\text{Total moment} = 0.40 \times \frac{70^2}{8} + 800 = 1045 \text{ k-ft}$$

If $(e + r^2/y_b) = 0.70d$, and $P = 400$ kips:

$$d = \frac{1045}{0.70 \times 400} = 3.73 \text{ ft}$$

This amounts to a depth-to-span ratio of 1 to 18.8. If the average compressive stress due to prestressing is -1000 psi, $P = 400$ k, and $A = 400$ in.^{2}, then the weight of the girder will be 415 plf. The estimated dead weight of the beam is reasonably close to the assumed value, but the depth is somewhat greater than normal for this span. Therefore, try $P = 450$ k, $A = 450$ in.^{2}, and $w_d = 470$ plf.

$$\text{Total moment} = 0.45 \times \frac{70^2}{8} + 800 = 1088 \text{ k-ft}$$

$$d = \frac{1088}{0.70 \times 450} = 3.46 \text{ ft}$$

The depth-to-span ratio for this prestressing force is 1 to 20.2, which is reasonable and slightly more slender than average. It is apparent that a preliminary estimate can be made with the data developed here, as the magnitude of the prestressing force and the concrete quantity are known approximately.

ILLUSTRATIVE PROBLEM 9-11 For the conditions states for I.P. 9-10, assume that the depth of the beam cannot exceed 3.5 ft, owing to headroom restrictions. Estimate the prestressing force required, and determine a preliminary cross-sectional shape. Assume that the member is to be post-tensioned, $f'_c = -5000$ psi, and no tensile stresses are to be allowed in the bottom fibers. Check the estimate.

SOLUTION: Assume $w_d = 0.50$ klf and $(e + r^2/y_b) = 0.70d$; then:

$$M_T = 0.50 \times \frac{70^2}{8} + 800 = 1106 \text{ k-ft}$$

$$P = \frac{1106}{0.70 \times 3.5} = 451 \text{ kips}$$

For a beam 42 in. deep, the web thickness normally is about 7 in. The average stresses in the flanges can be estimated to be −2000 psi for the purpose of selecting dimensions of the trial section. For the top flange, the total force that must be resisted is 451 k because the pressure line will be quite high when the beam is fully loaded. Furthermore, the top flange of a member that is 70 ft long should be about 70/35 or 2 ft wide. Therefore, the thickness of the top flange can be computed by:

$$t = \frac{451{,}000}{2000 \times 24} \cong 9.40 \text{ in.}$$

The bottom flange must resist a smaller force than the top flange because the dead load of the beam is acting at the time of stressing. The force that the bottom flange must resist can be approximated by multiplying the estimated prestressing force by the ratio of the moment due to the superimposed load and the moment due to the total load, or:

$$451 \text{ kips} \times \frac{800}{1106} \cong 330 \text{ kips}$$

Assuming that the width of the bottom flange is to be 18 in., the thickness of the bottom flange can be computed by:

$$t = \frac{330{,}000}{2000 \times 18} \cong 9.20 \text{ in.}$$

The assumed trial section is shown in Fig. 9-17, where the estimated values of the thicknesses for the top and bottom flanges calculated are shown superimposed.

To check the estimated prestressing force and concrete area, the section properties of the trial section are computed as follows:

$$A = 576.5 \text{ in.}^2 \qquad I = 115{,}680 \text{ in.}^4$$

$$y_t = -19.7 \text{ in.} \qquad S_t = -5860 \text{ in.}^3 \qquad r^2/y_t = -10.2 \text{ in.}$$

$$y_b = +22.3 \text{ in.} \qquad S_b = +5180 \text{ in.}^3 \qquad r^2/y_b = +9.00 \text{ in.}$$

The moment due to dead load is computed as follows:

$$M_D = 0.60 \times \frac{70^2}{8} = 368 \text{ k-ft}$$

and when combined with the moment due to superimposed load, 800 k-ft, the moment due to total load is found to be 1168 k-ft. Assuming $e = +22.3 - 4.5 = +17.8$ in., the prestressing force is computed to be:

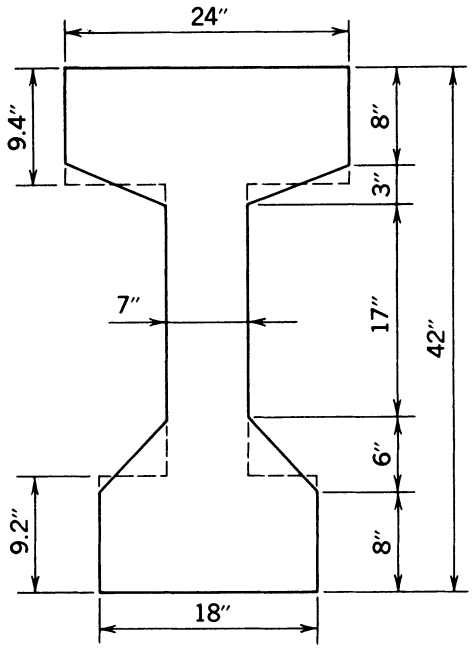

Fig. 9-17. Cross section of a beam, I.P. 9-11.

$$P = \frac{1168 \times 12}{17.8 \times 9.0} = 523 \text{ kips}$$

and the stresses are summarized in Table 9-8.

Examination of the stresses will reveal that the net compressive stress in the top fiber is −1713 psi when the beam is under full load. This value is substantially below the value of −2000 psi, allowable for the assumed concrete compressive strength of 5000 psi. In addition, if f'_{ci} is to be −4000 psi because the dead load of the beam is acting at the time of stressing, the −1850 psi compression in the bottom fibers is below the allowable initial stress. Therefore, the area of the flanges can be reduced.

TABLE 9-8 First Table for I.P. 9-11.

	Top Fiber	Bottom Fiber
Stress due to dead load	−753 psi	+853 psi
Stress due to superimposed load	−1640 psi	+1850 psi
Total	−2393 psi	+2703 psi
Stress due to prestressing	+680 psi	−2700 psi
Net stress	−1713 psi	+3 psi

In addition to considerations of stress, the following factors must be evaluated in selecting the final shape of the section:

1. Flanges must not be so thin that they might be broken during the handling and transportation of the members.
2. The top flange should have sufficient width to protect against undue lateral flexibility during transportation and erection, as well as to ensure that the flange will not buckle under load if it is to be used in the completed structure without supplementary lateral support (see Secs. 4-9 and 17-8).
3. The bottom flange must be of such shape that the prestressing tendons can be positioned with adequate cover and spacing to protect them against corrosion and to facilitate placing of the concrete, and, when post-tensioning is used, the shape of the bottom flange must allow curving of the tendons (without small radii of curvature) up into the web while the minimum cover is maintained.
4. For reasons of economy, the shape should be simple as possible to facilitate the fabrication.
5. The slopes provided as transitions between the flanges and the webs should be of such size and shape that danger of honeycomb and the entrapment of air bubbles in the bottom flange is minimized. In addition, stripping of the form is facilitated by large slopes on the flanges.

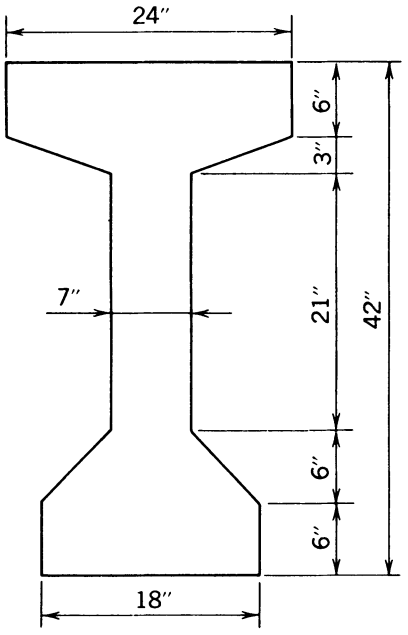

Fig. 9-18. Beam cross section, revised, I.P. 9-11.

TABLE 9-9 Second Table for I.P. 9-11.

	Top Fiber	Bottom Fiber
Stress due to dead load	−735 psi	+814 psi
Stresses due to superimposed load	−1770 psi	+1960 psi
Total	−2505 psi	+2774 psi
Stress due to prestressing	+665 psi	−2770 psi
Net stresses	−1840 psi	+4 psi

In this example, it is assumed that the flanges can be reduced to 6 in. in thickness at their extremities, as shown in Fig. 9-18, and the revised section properties and stresses are computed as follows:

$$A = 520.5 \text{ in.}^2 \qquad I = 108{,}090 \text{ in.}^4$$

$$y_t = -19.9 \text{ in.} \qquad S_t = -5430 \text{ in.}^3 \qquad r^2/y_t = -10.4 \text{ in.}$$

$$y_b = +22.1 \text{ in.} \qquad S_b = +4900 \text{ in.}^3 \qquad r^2/y_b = +9.39 \text{ in.}$$

The dead load of the member is found to be 0.542 klf, and the midspan moment due to dead load is 332 k-ft. The superimposed dead load moment is 800 k-ft, and the moment due to dead plus superimposed loads is equal to 1132 k-ft. Assuming the eccentricity of the prestressed reinforcement to be equal to $+22.1 - 4.5 = +17.6$ in., the prestressing force is computed as:

$$P = \frac{1132 \times 12}{9.39 \times 17.6} = 503 \text{ kips}$$

and the stresses are summarized in Table 9-9.

It should be noted that the prestressing force required in the final design is about 11 percent higher than the preliminary estimate, and the concrete quantity is about 4 percent higher in the final design. The errors result from assuming $(e + r^2/y_b)$ to be equal to $0.70d$ and its being only $0.644d$ in the final design.

The initial stress in the bottom fiber should be checked. Assuming $f_{se}/f_{si} = 0.85$, the initial bottom-fiber stress would be −2445 psi, and the value of f'_{ci} should be −4450 psi if the initial compression is restricted to $0.55f'_{ci}$, and −4100 psi if the initial compression is limited to $0.60f'_{ci}$.

ILLUSTRATIVE PROBLEM 9-12 Design a pretensioned T-beam to be used in a roof on a simple span of 60 ft. The superimposed dead load is 16 psf, and the live load is 30 psf. Use a noncomposite section, $f'_c = 4000$ psi, $f_{pu} = 270$ ksi, loss of prestress = 40,000 psi, and $f_y = 60{,}000$ psi. Allowable stresses and load factors are to conform to ACI 318. Use normal-weight concrete and a width of 8 ft.

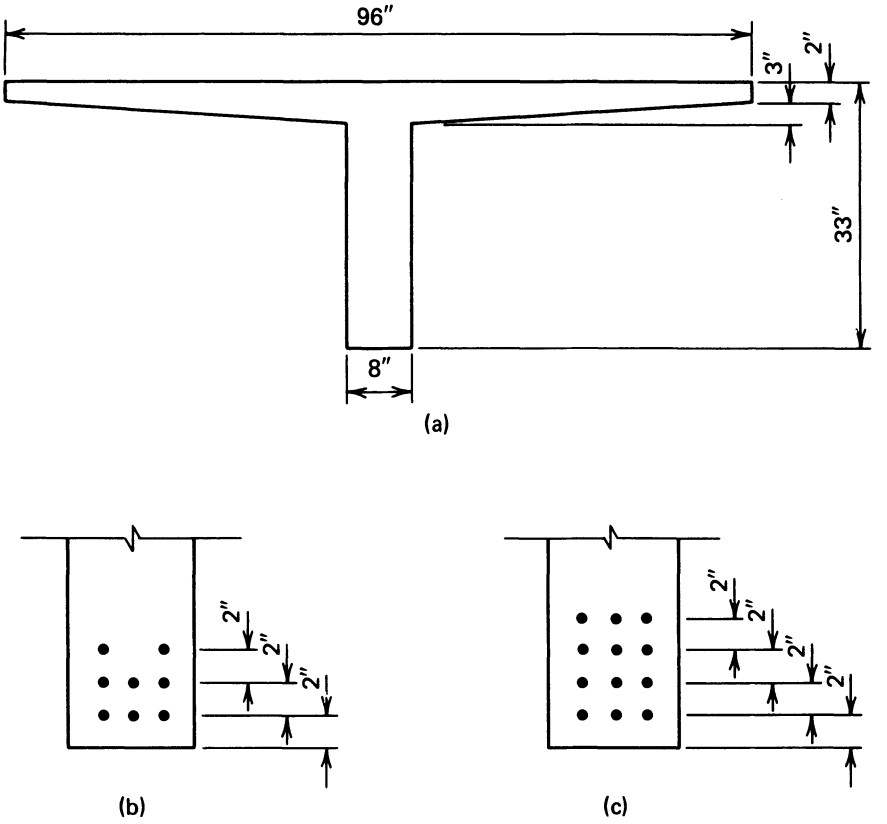

Fig. 9-19. Cross section and details of T-beam used in I.P. 9-12.

SOLUTION: The depth-to-span ratio for simple prestressed beams is usually between 1 in 16 and 1 in 22 but may be as shallow as 1 in 40. For a span of 60 ft, the depth would be expected to be between 3.75 ft and 2.75 ft. Because the span is relatively long, a depth-to-span ratio of 1 in 40 probably is not feasible. For a first try, assume a depth of 2.75 ft. The top flange can have a variable depth to save dead load and to give greater depth at the face of the web where the cantilever moment is greatest. Shear would not be expected to be a problem on a span of 60 ft with roof loads. An 8-in.-wide web probably will provide sufficient space for the tendons. In view of these considerations, adopt the trial section shown in Fig. 9-19a. The properties of the section are summarized as follows:

$$A = 572 \text{ in.}^2 \qquad I = 54{,}863 \text{ in.}^4$$

$$y_t = -8.62 \text{ in.} \qquad S_t = -6365 \text{ in.}^3 \qquad r^2/y_t = -11.13 \text{ in.}$$

$$y_b = +24.38 \text{ in.} \qquad S_b = +2250 \text{ in.}^3 \qquad r^2/y_b = +3.93 \text{ in.}$$

TABLE 9-10 First Table for I.P. 9-12.

	Load	Moment
Total dead load	596 plf	268.2 k-ft
Superimposed dead load	128 plf	57.6 k-ft
Superimposed live load	240 plf	108.0 k-ft

The loads and maximum moments are summarized in Table 9-10, and the stresses at midspan are summarized in Table 9-11.

The stresses are relatively low and it is apparent that a solution can be found with this depth. Allowing a bottom-fiber tensile stress of $8\sqrt{f'_c} = +506$ psi, the prestress must equal -1807 psi in the bottom fibers.

Assume that the centroid of the prestressed reinforcement is located 4.0 in. from the soffit of the beam, and, hence, its eccentricity is -20.38 in. By using this eccentricity, the prestressing force required for a bottom fiber stress of -1807 psi is computed as follows:

$$\frac{C}{A} = \frac{-1807}{1 + \dfrac{-20.38}{+3.93}} = -292 \text{ psi}$$

$$P = -(-292)(572) = 167 \text{ kips}$$

Assuming that the strands have an initial stress of $0.70f_{pu} = 189$ ksi (after transfer) and the loss of prestress is 40 ksi, each strand will have an effective force of $(0.153)(149) = 22.8$ k, and 7.32 strands would be required to provide a force of 167 kips. Using the eight-tendon layout shown in Fig. 9-19b, the distance from the soffit to the centroid of the prestressed reinforcement is:

$$d' = \frac{3 \times 2 + 3 \times 4 + 2 \times 6}{8} = 3.75 \text{ in.}$$

and the eccentricity is $+20.63$ in. Using these values for the initial prestressing force and the eccentricity, the top- and bottom-fiber stresses due to prestressing

TABLE 9-11 Second Table (midspan stresses) for I.P. 9-12.

	Top Fiber (psi)	Bottom Fiber (psi)
T.D.L.	−506	+1430
S.D.L.	−109	+307
S.L.L.	−204	+576
Total	−819	+2313

are:

$$f_t = \frac{8 \times 22{,}800}{572} = \left(1 + \frac{20.63}{-11.13}\right) = +272 \text{ psi}$$

$$f_b = \frac{8 \times 22{,}800}{572} = \left(1 + \frac{20.63}{+3.93}\right) = -1993 \text{ psi}$$

This results in a satisfactory design from an elastic design viewpoint with an average prestress of −319 psi. The stresses at the end of the member would have to be controlled by preventing bond on two or three tendons or deflecting the tendons upward at the ends to reduce the eccentricity.

For this solution, the midspan flexural strength is computed as follows:

$$A_{ps} = 8 \times 0.153 = 1.224 \text{ in.}^2,\ b = 96 \text{ in.},\ d = 29.25 \text{ in.}$$

$$\rho_p = \frac{1.224}{96 \times 29.25} = 0.000436$$

$$f_{ps} = 270\left(1 - \frac{0.5 \times 0.000436 \times 270}{4.0}\right) = 266.0 \text{ ksi}$$

$$\omega_p = \frac{0.000436 \times 266.0}{4.0}$$

$$= 0.0290 < 0.30 \therefore \text{ underreinforced}$$

$$1.4\, d\omega_p = 1.19 \text{ in.} < 2.00 \text{ in.}$$

Therefore, analyze as a rectangular beam:

$$a = \frac{A_{ps} f_{ps}}{0.85 b f'_c} = 1.00 \text{ in.}$$

$$\phi M_n = \frac{0.90\, A_{ps} f_{ps}}{12}\left(d - \frac{a}{2}\right) = 702 \text{ k-ft}$$

$$M_u = 1.4[268.2 + 57.6] + 1.7[108.0] = 639.7 \text{ k-ft}$$

The flexural capacity is about 10 percent greater than the minimum required. The design shear at each reaction is:

$$V_u = \left[1.4(724) + 1.7(240)\right]\frac{60}{2} = 42{,}650 \text{ lb}$$

$$v_u = \frac{42{,}650}{8 \times 29.25} = 182 \text{ psi} = 2.88\sqrt{f'_c}$$

$$A_{v\min} = \frac{1.224 \times 270 \times 12}{80 \times 60 \times 29.25}\sqrt{\frac{29.25}{8}}$$

$$= 0.054 \text{ in.}^2/\text{ft}$$

$$v_s = \frac{A_v f_y}{b_w s} = \frac{0.054 \times 60{,}000}{8 \times 12} = 34 \text{ psi}$$

Therefore, with minimum reinforcement:

$$\phi v_n = 0.85(126 + 34) = 136 \text{ psi}$$

Using eq. 6-2 converted to unit stress:

$$v_c = 0.6\sqrt{4000} + 700\frac{29.25(60 - 2x)}{12x(60 - x)}$$

$$= 37.9 + \frac{1706(60 - 2x)}{x(60 - x)}$$

The computations for v_c are summarized in Table 9-12. Note that $5\sqrt{f'_c} = 316$ psi and $2\sqrt{f'_c} = 126$ psi, and stirrups are not required by stress considerations.

The design should be completed by making short-and long-term deflection studies and comparing the results to the design criteria being used, or to other performance standards that the designer may wish to adopt.

If the designer were to elect to use a depth-to-span ratio of 1 in 30, the depth would be 24 in. rather than 33 in., and the section properties would become:

$A = 500 \text{ in.}^2$ $\quad I = 12{,}810 \text{ in.}^4$

$y_t = -5.75 \text{ in.}$ $\quad S_t = -3793 \text{ in.}^3$ $\quad r^2/y_t = -7.59 \text{ in.}$

$y_b = +18.25 \text{ in.}$ $\quad S_b = +1195 \text{ in.}^3$ $\quad r^2/y_b = +2.39 \text{ in.}$

Loads and midspan moments are as summarized in Table 9-13, and the flexural stresses at midspan are shown in Table 9-14. Using $8\sqrt{f'_c}$ tension in the bottom

TABLE 9-12 Third Table for I.P. 9-12.

x (ft)	v_c (psi)	$v_{s\min.}$ (psi)	$\phi(v_c + v_s)$ (psi)	v_u (psi)
0	316	34	298	182
6	316	34	298	146
9	194	34	194	127
12	145	34	152	109
15	126	34	136	91

TABLE 9-13 Fourth Table for I.P. 9-12.

	Load	Moment
Beam dead load	521 plf	234.4 k-ft
Superimposed dead load	128 plf	57.6 k-ft
Superimposed live load	240 plf	108.0 k-ft

fiber, the required bottom-fiber prestress is −3511 psi. Assuming $e = 18.25 - 4.0 = 14.25$ in.:

$$P = -\frac{500 \times -3511}{1 + \dfrac{14.25}{2.39}} = 252 \text{ kips}$$

This requires 11 strands, and the average prestress in the concrete is −504 psi. Using 12 strands spaced 2 in. on center, as shown in Fig. 9-19c, $e = 18.25 - 5.00 = +13.25$ in., and:

$$f_t = -\frac{22{,}800 \times 12}{500}\left(1 + \frac{13.25}{-7.59}\right) = +408 \text{ psi}$$

$$f_b = -\frac{22{,}800 \times 12}{500}\left(1 + \frac{13.25}{2.39}\right) = -3581 \text{ psi}$$

This, too, is a satisfactory solution for elastic flexural stresses. The average prestress of −547 psi is greater than the −319 psi required with a depth of 33 in.; hence, more creep deformation must be accommodated in the structure if the 24 in. depth is used. Bond prevention or tendon deflection must be used to control the stresses. The latter would be preferred for the 24 in. depth because of the high bottom-fiber prestress.

TABLE 9-14 Fifth Table for I.P. 9-12.

	Top (psi)	Bottom (psi)
B.D.L.	−742	+2354
S.D.L.	−182	+578
S.L.L.	−342	+1085
Total	−1266	+4017

TABLE 9-15 Sixth Table for I.P. 9-12.

x (ft)	v_c (psi)	v_s (psi)	$\phi(v_c + v_s)$ (psi)	v_u (psi)
0	316	63	322	260
3	316	63	322	234
6	202	63	225	208
9	139	63	172	182
12	126	63	160	156
15	126	63	160	130
18	126	63	160	104

The flexural strength computations become:

$$\rho_p = \frac{12 \times 0.153}{96 \times 19} = 0.00101$$

$$f_{ps} = 260.8 \text{ ksi}$$

$$\omega_p = 0.0656 < 0.30$$

$$1.4\, d\omega_p = 1.75 \text{ in.} < 2.00 \text{ in.}$$

$$a = 1.47 \text{ in.}$$

$$\phi M_n = 656 \text{ k-ft}$$

$$M_u = 592.4 \text{ k-ft}$$

The flexural strength is about 11 percent greater than the minimum required. The design shear at each reaction is 39,500 lb, and:

$$v_u = \frac{39{,}500}{8 \times 19.0} = 260 \text{ psi}$$

$$A_{u\min} = \frac{1.836 \times 270 \times 12}{80 \times 60 \times 19}\sqrt{\frac{19}{8}} = 0.100 \text{ in.}^2/\text{ft}$$

Using eq. 6-2 converted to unit stress:

$$v_c = 37.9 + \frac{1108(60 - 2x)}{x(60 - x)}$$

and the computations for shear stresses are as summarized in Table 9-15. As will be seen, shear reinforcing greater than the minimum permitted is required by stress considerations between 6 and 12 ft from the ends of the beam.

To complete the design, a deflection study should be made.

The above example demonstrates that there is a family of acceptable designs. One designer may prefer the deeper T-beam over the more shallow one because of the lower average prestress, and hence lower deferred strain, as well as because of the smaller deflections associated with deeper members. *Concrete stresses are only one design parameter that must be considered;* frequently, the designer selects a design with concrete stresses lower than the maximum permitted under service loads.

ILLUSTRATIVE PROBLEM 9-13 Prepare the preliminary design for a simple post-tensioned beam that is to be used on a span of 32 ft. The beam is to have a composite concrete slab that is 5 in. thick. Superimposed dead and live loads are 20 psf and 125 psf, respectively. The width tributary to the beam is 30 ft. Assume the beam and slab concrete has a specified compressive strength of 4000 psi at age 28 days, and that the beam and slab are cast in place monolithically. Use the allowable stresses of ACI 318.

SOLUTION: The relatively short span and high superimposed loads will render shear stresses an important design consideration. The loads without the beam stem are as follows:

Slab (tributary width of 30 ft): 1875 plf
Superimposed dead load: 600 plf
Superimposed live load: 3750 plf

The live load is greater than the dead loads; hence, a bottom flange may be required to resist the prestressing force when the live load is not applied.

The span–depth ratio for a heavily loaded beam is generally lower than for a lightly loaded beam. In view of these considerations, for a first trial section, adopt a beam that has an overall depth of 2 ft (span–depth ratio of 16) and a width of 12 in. with no bottom flange. The trial section is shown in Fig. 9-20. The top flange width is taken to be 16 times the flange thickness plus the width of the web. For the assumed section, the area is 688 in.^{2}, and the moment of inertia is 29,768 in.^{4}. The other section properties are as follows:

$$y_t = -6.48 \text{ in.} \quad S_t = -4594 \text{ in.}^3 \quad r^2/y_t = -6.68 \text{ in.}$$

$$y_b = +16.52 \text{ in.} \quad S_b = +1600 \text{ in.}^3 \quad r^2/y_b = +2.47 \text{ in.}$$

The weight of the beam stem is 238 plf, and the midspan moments are:

Beam/slab dead load	$(238 + 1875)(128)$	= 270.5 k-ft
Superimposed dead load	$(600)(128)$	= 76.8 k-ft
Superimposed live load	$(3750)(128)$	= 480.0 k-ft
	Total moment	= 827.3 k-ft

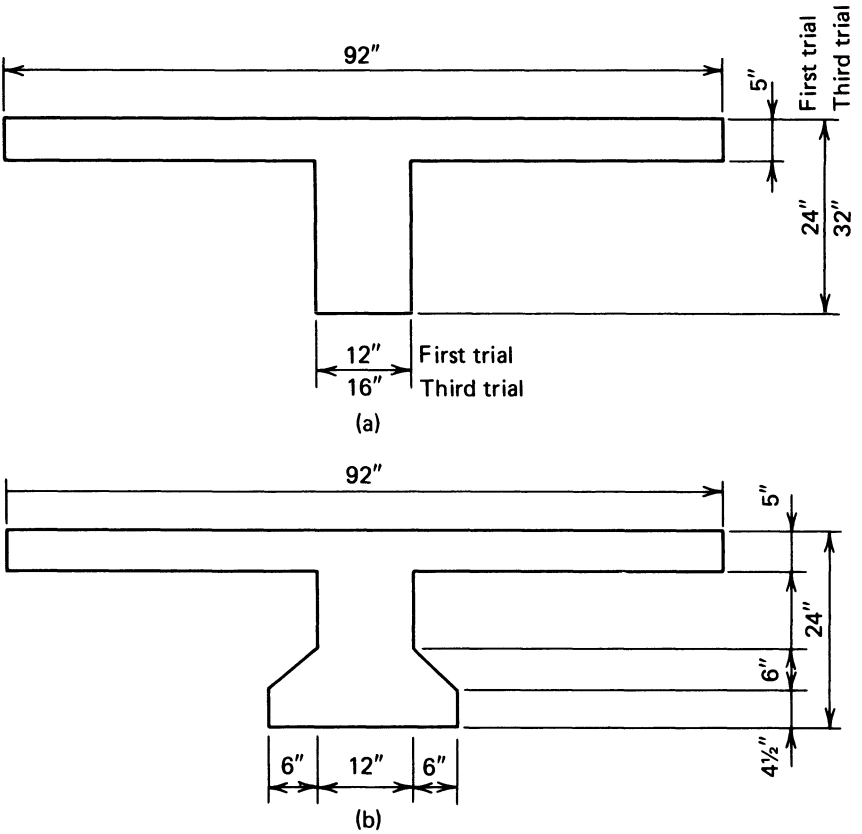

Fig. 9-20. Beam cross sections used in I.P. 9-13.

Midspan flexural stresses are summarized in Table 9-16. A review of the flexural stresses reveals that the section will not be satisfactory because the bottom-fiber stresses are too high for concrete having a specified strength of 4000 psi. If the bottom flange were increased in width to 24 in., the bottom-fiber stress due to total load should be reduced to an acceptable value and result in an acceptable solution.

TABLE 9-16 First Table for I.P. 9-13.

	Top (psi)	Bottom (psi)
Beam/slab dead load	−707	+1911
Superimposed dead load	−201	+542
Superimposed live load	−1254	+3390
Total load	−2162	+5843

Adding a bottom flange to the section, as shown in Fig. 9-20b, is another alternative. With the bottom flange, the area of the section is 778 in.^{2}, the moment of inertia is 44,985 in.^{4}, and other section properties become:

$$y_t = -8.05 \text{ in.} \qquad S_t = -5588 \text{ in.}^3 \qquad r^2/y_t = -7.18 \text{ in.}$$

$$y_b = +15.95 \text{ in.} \qquad S_t = +2820 \text{ in.}^3 \qquad r^2/y_b = +3.63 \text{ in.}$$

The additional dead load due to the bottom flange is 94 plf, and the loads and midspan moments are:

Beam/slab dead load: 2207 plf, 282.5 k-ft
Superimposed dead load: 600 plf, 76.8 k-ft
Superimposed live load: 3750 plf, 480.0 k-ft

and the midspan flexural stresses are as summarized in Table 9-17. If tensile stresses were used, a solution would be possible with this section, provided that the tendon could be sufficiently eccentric to nullify the effects of dead load. The maximum tension necessary is $+3571 + (-1202 - 327 - 1800) = +242$ psi. (It should be noted that 1800 psi is equal to $0.45f'_c$ for a specified concrete compressive strength of 4000 psi.) With a tension of +242 psi and an assumed eccentricity of +12.00 in., the prestressing force required its:

$$P = \frac{3329 \times 778}{1 + \dfrac{12.00}{3.63}} = 601.5 \text{ kips}$$

and the average compressive stress in the concrete due to prestress is −773 psi. This value of average prestress is not unrealistic but would cause significant creep deformation.

A shear analysis for the member, based upon $f_y = 60{,}000$ psi and a parabolic path for the tendon ($e = +12.00$ in. at midspan), is summarized in Table 9-18. A review of this table will show that the 12-in.-thick web results in only minimum shear reinforcement being required. Hence, the web thickness could be reduced if the designer so desired.

TABLE 9-17 Second Table for I.P. 9-13.

	Top (psi)	Bottom (psi)
Beam/slab dead load	−607	+1202
Superimposed dead load	−165	+327
Superimposed live load	−1031	+2042
Total load	+1803	−3571

TABLE 9-18 Summary of Shear Stresses, I.P. 9-13.

Pt.	Length (ft)	v_{ci} (psi)	v_{cw} (psi)	v_c (psi)	v_u (psi)	A_v (in.^{2}/ft)
.00	.000	infin	779.0	779.0	841.8	0.2419
.05	1.600	1303.7	747.0	747.0	757.7	.1200
.10	3.200	870.8	714.3	714.3	673.5	.1200
.15	4.800	682.6	681.7	681.7	589.3	.1200
.20	6.400	555.4	649.1	555.4	505.1	.1200
.25	8.000	452.3	616.4	452.3	420.9	.1200
.30	9.600	361.0	583.8	361.0	336.7	.1200
.35	11.200	276.2	551.2	276.2	252.5	.1200
.40	12.800	192.1	517.3	192.1	165.1	.1200
.45	14,400	113.2	484.7	113.2	81.1	.1200
.50	16.000	37.9	453.3	107.5	000.0	.1200

The cost of forming the bottom flange, and the added costs of placing reinforcing steel stirrups in a beam of this shape, are barriers to the adoption of this section as a final one.

Rather than adding the bottom flange, another solution would be to increase the depth of the beam.

Still another solution would be to increase the depth as well as the stem width. Increasing the depth to 32 in. and increasing the stem width to 16 in. will be the basis for another trial. Using a top flange width of 8 ft ($L/4$), the area and moment of inertia of the section are 912 in.^{2} and 85,450 in.^{4}, respectively, and the other properties needed for flexural stress computations are:

$$y_t = -10.08 \text{ in.} \quad S_t = -8477 \text{ in.}^3 \quad r^2/y_t = -9.30 \text{ in.}$$

$$y_b = +21.92 \text{ in.} \quad S_b = +3898 \text{ in.}^3 \quad r^2/y_b = +4.27 \text{ in.}$$

The midspan stresses become as shown in Table 9-19.

An examination of these stresses will show that the superimposed dead and live loads cause a bottom-fiber stress of +1713 psi. Hence, tensile stresses can be avoided with the solution, if so desired. It also should be apparent that the height or thickness of the stem could be reduced if that is desired.

TABLE 9-19 Fourth Table for I.P. 9-13.

	Top (psi)	Bottom (psi)
Beam/slab dead load	−421	+916
Superimposed dead load	−109	+236
Superimposed live load	−679	+1477
Total load	−1209	+2629

The prestressing force required can be determined for the case of zero tension by:

$$P_{se} = \frac{M_T}{e + r^2/y_b} = \frac{854.4 \times 12}{17.92 + 4.27} = 462.0 \text{ kips}$$

in which $e = +21.92 - 4.00 = +17.92$ in.

This solution can be checked as follows

$$f_t = -\frac{462{,}000}{912}\left(1 + \frac{17.92}{-9.30}\right) = +470 \text{ psi}$$

$$f_b = -\frac{462{,}000}{912}\left(1 + \frac{17.92}{4.27}\right) = -2633 \text{ psi}$$

If one wished to permit tensile stresses under full load, the prestressing force could be reduced.

For a tensile stress of $6\sqrt{f'_c} = 379$ psi, the prestressing force can be determined from eq. 4-4 as follows:

$$P = -\frac{912 \times (-2629 + 379)}{1 + \dfrac{17.92}{-4.27}} = 394.9 \text{ kips}$$

To complete the design, one must investigate short-and long-term deflections, design the shear reinforcement, and confirm the adequacy of the flexural strength.

9-9 Shear Reduction Due to Parabolic Tendon Curvature

In Sec. 4-6, it was shown that the curvature of prestressing tendons results in a reduction in the shear force that the concrete must withstand. Furthermore, it was shown that this reduction is equal to the vertical component of the prestressing force at the point under consideration. The vertical component of the prestressing force is equal to $P \sin \alpha$, in which α is the angle of inclination of the tangent to the prestressing tendon, with respect to the centroidal axis of the member, at the point under consideration.

Because the angle is small in almost all instances, the sine and tangent are practically equal. Hence, the tangent can be used in computing the vertical component of the prestressing force without introducing significant error.

The computation of the tangent of the angle of inclination for tendons placed on a series of chords is basic and requires no explanation. For tendons on second-degree parabolic curves, the computation of the tangent of the angle of inclination is equally simple if the properties of a parabola are understood.

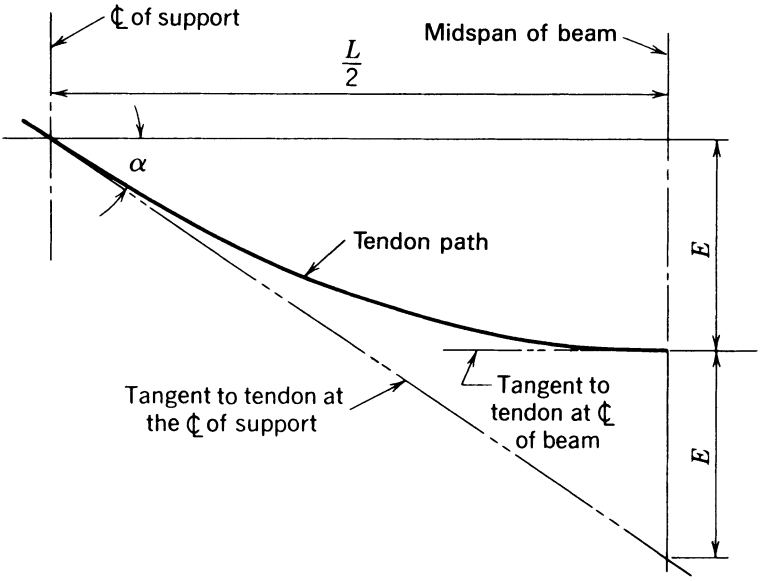

Fig. 9-21. Diagram of fundamental properties of a parabola.

A parabola is shown in Fig. 9-21 with the dimensions and tangents that are most important in the analysis of prestressing shear forces. It will be seen from the figure that the tangent to the parabola at the centerline of the support is inclined at an angle of α to the reference line parallel to the centroidal axis of the member, and that the tangent of the angle α is equal to:

$$\tan \alpha = \frac{2E}{L/2} = \frac{4E}{L} \tag{9-10}$$

The dimension E is the total displacement of the prestressing force and is equal to the normal eccentricity of the force only when the eccentricity of the prestressing force is zero at the ends. The units of E and L must be the same.

It is apparent from the freebody diagram of Fig. 9-22, in which the forces that act on the concrete as a result of prestressing with a parabolic tendon are shown, that the vertical component of the prestressing force results in a uniformly distributed upward load on the beam. It also should be apparent that the internal shear forces resulting from the vertical component of the prestressing force vary uniformly from a maximum value at the support to zero at midspan. Hence, the vertical component of the shear stress carried by the tendon at points between the end and the midspan of the beam can be determined by the following relationship:

$$P \sin \alpha = P \sin \alpha \times \frac{L/2 - x}{L/2} \tag{9-11}$$

in which x is the distance from the support to the point under consideration.

Although the relationships presented here are derived for tendons placed on second-degree parabolic paths, they normally can be applied to tendons placed on other curves without introducing significant error. If the displacement of a tendon is very large in comparison to the span, as is sometimes the case in post-tensioned folded plates or shells, it is advisable to compute the reduction in shear using the sine of the angle at the point under consideration as determined from the tendon layout.

An example of the computation of the shear component for a tendon on a second-degree parabolic curve is given in I.P. 4-10.

9-10 Locating of Pretensioning Tendons

The selection of the location or pattern of the pretensioning tendons must be made after the cross-section shape, the prestressing force, and the eccentricity have been determined. This is done by trial, and generally can be accomplished quickly if the computations are made according to a specific procedure. The procedure consists of first determining the number of tendons required, by dividing the required effective prestressing force by the maximum allowable effective prestressing force for one tendon. Second, the positions of the required number of tendons are determined by computing moments of the tendons at assumed locations, which are adjusted and readjusted as required until the centroid of the tendons is at the desired location. The procedure can be illustrated by the sketch of Fig. 9-23, which represents the cross section of a beam that requires N tendons placed with their centroid at a distance d' from the bottom of the beam. If n_1, n_2, n_3, . . . n_n represent the number of tendons in the first, second, third, and nth rows from the bottom of the beam, and y_1, y_2, y_3, . . . y_n represent the distances from these rows to the bottom of the beam,

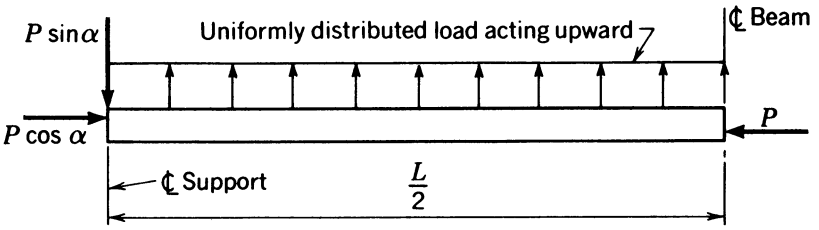

Fig. 9-22. Freebody diagram of the forces exerted on a beam prestressed by a tendon having a second-degree parabolic path.

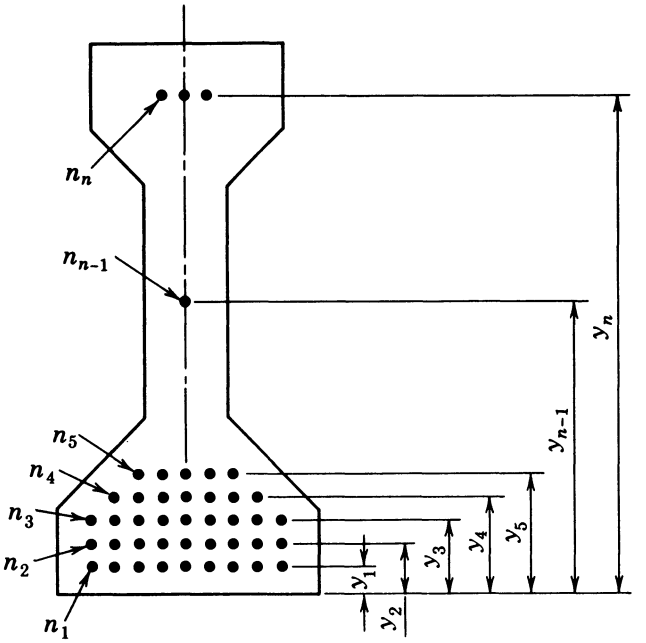

Fig. 9-23. End elevation of a pretensioned concrete beam.

it is apparent that in order to obtain the desired location, the following relationship must be satisfied:

$$Nd' = \Sigma (y_1 n_1 + y_2 n_2 + y_3 n_3 + \ldots y_n n_n) \qquad (9\text{-}12)$$

Because the values of N and d' are known, the majority of the tendons can be located, and the value of the term to the right of the equals sign adjusted to the desired value with the remaining tendons.

It is apparent that the majority of the tendons will be near the bottom of the member in order to achieve the required eccentricity. It is desirable that some tendons be supplied near the top of most members for the purpose of supporting the reinforcing, inserts, and other embedded items. This frequently can be done with the required number of tendons, without supplying additional tendons specifically for this purpose.

In tendon patterns that have some tendons high in the section, the upper tendons should be disregarded in computing the flexural strength of the section. The distance to the centroid of the lower group of tendons, which would be highly stressed at ultimate load, should be determined for use in calculating the ultimate moment capacity.

ILLUSTRATIVE PROBLEM 9-14 Compute the location of the tendons required to produce a prestressing force of 538 k at an eccentricity of +11.9. in. in the

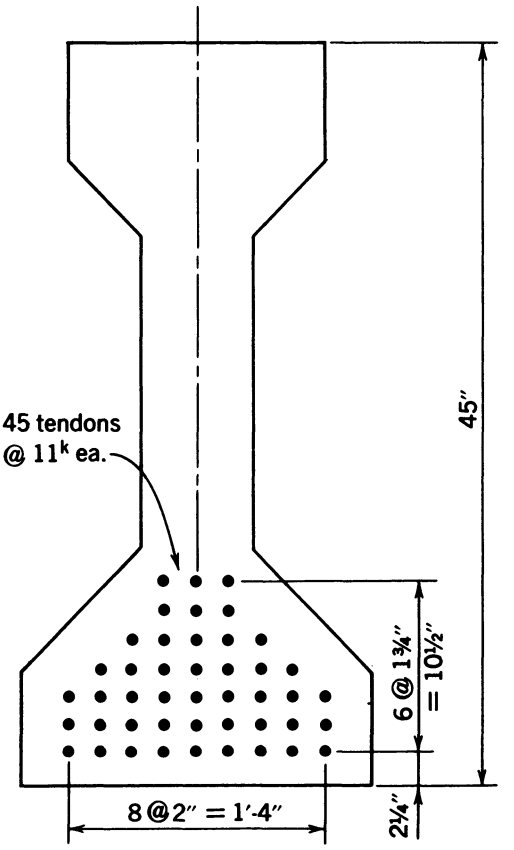

Fig. 9-24. End elevation of pretensioned concrete beam, showing tentative tendon layout, I.P. 9-14.

AASHTO-PCI bridge beam, type III, if the tendons to be used have an effective force of 11 k each, and $y_b = +20.3$ in.

SOLUTION: The number of tendons required is computed as $538/11 = 49$ each. The distance from the soffit of the beam to the center of gravity of the steel is computed as $d' = 20.3 - 11.9 = 8.4$ in., and $Nd' = 49 \times 8.4 = 412$. The summation of the moments of the tendons in their final location should equal 412. Forty-five of the tendons are tentatively positioned as shown in Fig. 9-24, and the moment of the tendons computed about the bottom of the section is equal to 278. Therefore, the remaining four tendons must have an average distance from the bottom of the beam equal to:

$$y_{\text{average}} = \frac{412 - 278}{4} = 33.5 \text{ in.}$$

This average distance is of the order of 75 percent of the depth of the beam, and it appears that the tendon layout should be adjusted in order to include one more tendon in the bottom group. Therefore, the pattern is revised by increasing the number of tendons in the sixth row, from the bottom of the second, to 5 and reducing the number of tendons in the seventh row, to 2. The moment of the 45 tendons in the revised tendon pattern is 287.25. The average distance required for the three remaining tendons is computed as follows:

$$y_{\text{average}} = \frac{412 - 287.25}{3} = 41.5 \text{ in.}$$

The final tendon layout is illustrated in Fig. 9-25. The values of d' and d'_u

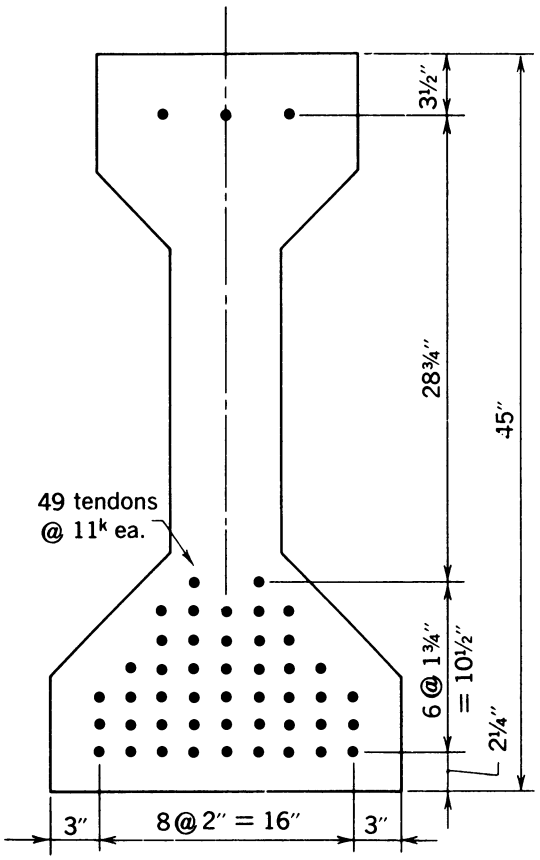

Fig. 9-25. End elevation of pretensioned concrete beam, showing final tendon layout, I.P. 9-14.

are computed as follows:

$$d' = \frac{411.75}{49} = 8.40 \text{ in.}$$

$$d'_u = \frac{287.5}{46} = 6.25 \text{ in.}$$

The flexural strength should be computed on the basis of the lowest 46 tendons having their center of gravity located 6.25 in. from the soffit of the beam.

9-11 Stresses at Ends of Prismatic Beams

In employing bond prevention or in using nonprestressed reinforcing as a means of controlling the stresses resulting from initial prestress at the end of a beam, it is necessary to analyze the flexural stresses resulting from the dead weight of the beam near its end. This is needed to determine the limits over which the bond must be prevented or over which the special end reinforcement should be provided. This can be done by using the fundamental principles of strength of materials through the use of factors selected from unit parabolic curves, or by computing the location of the required dead load stresses through the use of the known properties of parabolas. These methods should yield identical results. The use of the latter method is shown in the following problem.

ILLUSTRATIVE PROBLEM 9-15 Compute the length over which nonprestressed reinforcing is required at the ends of a simple prismatic beam in which the top-fiber stresses due to initial prestressing are equal to +360 psi, and the maximum,

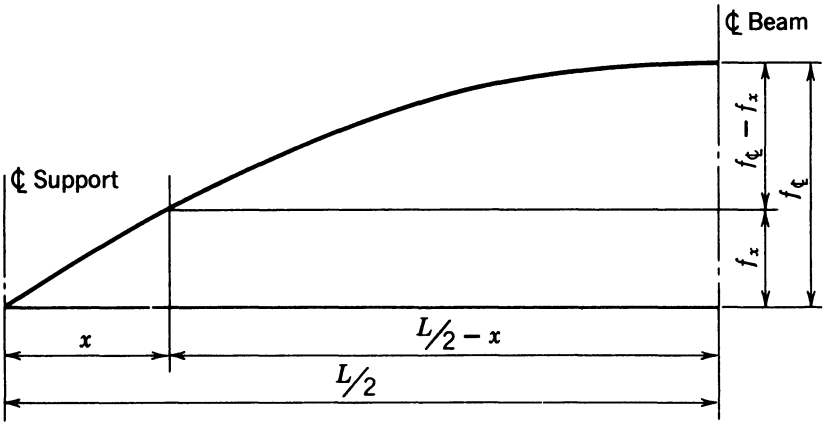

Fig. 9-26. Diagram used to compute stresses at different locations along the length of a beam having a parabolic moment diagram, I.P. 9-15.

allowable tensile stress without nonprestressed reinforcing is +190 psi. The stress in the top fibers at midspan of the beam due to dead load alone is −730 psi. The beam has a span of 70 ft.

SOLUTION: The stress due to dead load in the top fiber varies parabolically, as shown in Fig. 9-26. It is necessary to determine the distance from the end of the beam, where the top-fiber stress is 360 − 190 = 170 psi, because at this location the net concrete stress will be +190 psi, which can be allowed without nonprestressed reinforcement. The ordinates of the parabola vary according to the relationship:

$$f_{\text{midspan}} - f_x = \left(\frac{L/2 - x}{L/2}\right)^2 f_{\text{midspan}}$$

which can be written:

$$x = \frac{L}{2}\left[1 - \left(\frac{f_{\text{midspan}} - f_x}{f_{\text{midspan}}}\right)^{1/2}\right]$$

Using the values given in the example:

$$x = 35\left[1 - \left(\frac{730 - 170}{730}\right)^{1/2}\right]$$

$$= 35 \times 0.125 = 4.37 \text{ ft}$$

9-12 Length of Bond Prevention

When the initial prestressing stresses at the ends of a simple pretensioned beam exceed the allowable stresses, the effect of the prestressing can be reduced by preventing bond on a specific number of tendons over a specific length, as is explained in detail in Sec. 8-7. The length over which the bond must be prevented can be computed according to the methods suggested in Sec. 9-11. The number and location of tendons that should be prevented from bonding to the concrete can be determined by computing the effect of one tendon in each of the lower rows of the tendon pattern and then, by trial, determining the number of tendons in each row that should be prevented from bonding to the concrete.

ILLUSTRATIVE PROBLEM 9-16 The double-tee beam shown in Fig. 9-27 has a simple span of 64.3 feet and is pretensioned with nine strands, each of which has an area of 0.153 in.^{2}, in each leg. The strands, which are placed in three rows of three strands in each leg, have 2-in. center-to-center spacings, vertically

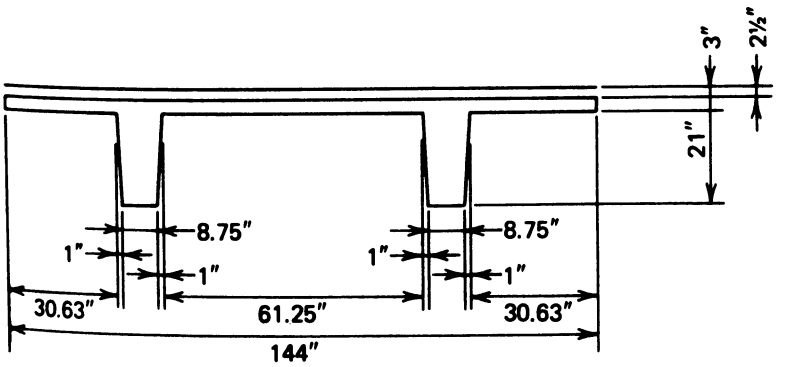

Fig. 9-27. Cross section of double-tee beam used in I.P. 9-16.

and horizontally, with the centroid of the nine-strand groups being located 4 in. above the soffits of the legs. The prestressed reinforcement has a minimum guaranteed ultimate tensile strength of 270 ksi, a jacking stress of 189 ksi, and an effective prestress of 154 ksi. The normal-weight concrete in the double-tee beam and the sand-lightweight concrete in the topping (115 pcf) have specified compressive strengths of 5000 and 3500 psi, respectively. Compute the distance over which bond must be prevented if the double-tee beam has a dead load of 671 plf,, and the allowable initial compressive and tensile stresses in the concrete are -2100 and $+177$ psi, respectively. Assume that the ratio of the elastic moduli of the prestressed reinforcement and the concrete, n, at the time of prestressing, is 14.0. The area of the double-tee beam is 840 in.^{2}, and the moment of inertia is 43,759 in.^{4}. The section properties needed for the computation of flexural stresses are:

$$y_t = -7.175 \text{ in.} \qquad S_t = -6098 \text{ in.}^3 \qquad r^2/y_t = -7.26 \text{ in.}$$

$$y_b = +16.825 \text{ in.} \qquad S_b = +2600 \text{ in.}^3 \qquad r^2/y_b = +3.10 \text{ in.}$$

SOLUTION: For 18 strands, $A_{ps} = 2.754$ in.^{2}, $e = +12.825$ in., and from eq. 7-3:

$$k_s = 1 + \frac{(12.825)^2(840)}{43759} = 4.16$$

Using eq. 7-2 with M_d expressed in kip-ft:

$$f_{cgs} = \frac{2165 - 2.954M_d}{1000.4}$$

and for 12 strands, $A_{ps} = 1.836$ in.^{2}, $e = +11.825$ in., $k_s = 3.68$, and:

$$f_{cgs} = \frac{1277 - 2.724M_d}{934.6}$$

The stress in the prestressing steel after elastic shortening, f_{si}, is:

$$f_{si} = f_{sj} - nf_{cgs}$$

The initial concrete stresses in the top and bottom fibers, respectively, are:

$$f_t = -\frac{f_{si}A_{ps}}{A}\left(1 + \frac{e_{pl}y_t}{r^2}\right) + \frac{12M_d}{S_t}$$

and:

$$f_b = -\frac{f_{si}A_{ps}}{A}\left(1 + \frac{e_{pl}y_b}{r^2}\right) + \frac{12M_d}{S_b}$$

The computations are summarized in Table 9-20. The results at the 20th points (from the support to midspan) as well as at 6 and 7 ft from the support are given for 18 strands; for 12 strands, the results are given at the support and at 2 ft from the support. Because the transmission length for $\frac{1}{2}$-in. strands is on the order of 25 in., the 12 strands can be bonded full length without exceeding the permissible stresses. All 18 strands can be fully bonded at 7 ft from the end without the stresses being excessive; in consideration of the transmission length,

TABLE 9-20 Table for I.P. 9-15.

	Distance from End (ft)	M_d (k-ft)	e_{ps} (in.)	e_{pl} (in.)	$f_{c.g.s.}$ (ksi)	f_t (ksi)	f_b (ksi)	f_{si} (ksi)	P_i (k)
18 Strands A_{ps} = 2.754 sq in.	0.000	.000	+12.825	+12.825	−2.163	+.398	−2.675	158.713	437.097
	3.215	65.888	+12.825	+12.825	−1.968	+.276	−2.417	161.438	444.600
	6,430	124.840	+12.825	+12.825	−1.794	+.166	−2.186	163.875	451.313
	9.645	176.857	+12.825	+12.825	−1.640	+.069	−1.983	166.026	457.236
	12.860	221.939	+12.825	+12.825	−1.507	−.014	−1.806	167.890	462.370
	16.075	260.085	+12.825	+12.825	−1.395	−.085	−1.657	169.467	466.713
	19.290	291.295	+12.825	+12.825	−1.302	−.144	−1.534	170.758	470.267
	22.505	315.570	+12.825	+12.825	−1.231	−.189	−1.439	171.761	473.031
	25.720	332.909	+12.825	+12.825	−1.180	−.221	−1.371	172.478	475.006
	28.935	343.312	+12.825	+12.825	−1.149	−.241	−1.331	172.908	476.191
	32.150	346.780	+12.825	+12.825	−1.139	−.247	−1.317	173.052	476.585
	0.000	.000	+12.825	+12.825	−2.163	+.398	−2.675	158.713	437.097
	6.000	117.400	+12.825	+12.825	−1.816	+.180	−2.215	163.567	450.465
	7.000	134.600	+12.825	+12.825	−1.765	+.147	−2.148	164.279	452.424
12 Strands A_{ps} = 1.836 sq in.	0.000	.000	+11.825	+11.825	−1.367	+.233	−1.789	169.851	311.847
	2.000	41.800	+11.825	+11.825	−1.245	+.153	−1.614	171.556	314.978

TABLE 9-21 Table for I.P. 9-16.

20th Pt.	Bottom Slab Thickness (in.)	Area (sq. in.)	Moment of Inertia ($in.^4$)	y_t (in.)	y_b (in.)	Weight (plf)
0.00	12.000	9744.5	8847614	−40.7	37.3	10,150
0.05	10.438	9313.4	8543251	−39.5	38.5	9,700
0.10	8.875	8882.0	8169629	−38.1	39.9	9,250
0.15	7.313	8450.1	7714397	−36.5	41.5	8,800
0.20	5.750	8019.5	7161480	−34.6	43.4	8,350

the bottom 6 strands can be prevented from bonding to the concrete for 5 ft at each end.

ILLUSTRATIVE PROBLEM 9-17 A continuous cast-in-place post-tensioned bridge is to have the cross section shown in Example IV of Appendix B. Assuming that the bottom slab thickness varies linearly from 5.75 in. to 12 in. over a length equal to 0.20 times the span length, compute the gross section properties for the cross section at the 20th points between 0 and $0.20L$.

SOLUTION: The results of the computations are summarized in Table 9-21.

REFERENCE

Magnel, G. 1948. *Prestressed Concrete*. London. Concrete Publications, Ltd.

10 Flexural Continuity

10-1 Introduction

Continuity is provided in the construction of prestressed concrete buildings, bridges, and other structures for the same basic reasons that it is used with other materials, including savings in construction materials and reductions in construction costs. Of perhaps greater importance are the advantages of improved performance under service and design loads as a result of smaller deflections, increased redundancy, and, in some cases, improved performance under dynamic loads. Because these benefits are approximately the same for structural elements made with prestressed concrete and those made with other materials used in comparable applications, they will not be discussed in detail in this book.

Continuous prestressed members, whether made of concrete or of another structural material, have a unique characteristic that the structural engineer must not overlook, involving the moments, shear forces, and reactions that result from the prestressing itself. A continuous prestressed flexural member, if free to deform (i.e., unrestrained by its supports), deforms axially and most frequently deflects transversely from its original shape. If the transverse deflec-

tions due to prestressing are restrained by the supports, moments and shear forces are created as a result of the restraint. The moments induced in the continuous members by the restraint of the transverse deformations are often referred to as the secondary moments (and secondary shear forces) due to prestressing or, more simply, the secondary moments, and the reactions at the supports that are created by restraining the deformations are often referred to as secondary reactions due to prestressing or, more simply, the reactions due to prestressing. Methods of determining the secondary effects, using the classical methods of analysis for indeterminate structures, are illustrated in this chapter.

The inelastic deformations of structural elements made from materials that are subject to time-dependent deformations, such as concrete, can be an important consideration in some prestressed-concrete continuous members. For statically indeterminate concrete flexural members constructed monolithically in a topology (configuration) that remains unchanged throughout their useful lives, the inelastic behavior of the concrete does not affect the internal moments and shear forces, except for the effect of the loss of prestress. On the other hand, a member initially constructed in a topology that is subsequently changed to another can experience significant time-dependent changes in its internal moments and shear forces. This change can be greater than those due to the loss of prestress alone. The time-dependent changes result from inelastic deformations of the concrete that tend to make the member behave as it would have done if it had been originally constructed in the final topology. This consideration is discussed in detail in Sec. 10-9.

There are many different ways of configuring continuous prestressed concrete beams and frames. Cast-in-place and precast concrete construction both are used effectively in the construction of continuous beams and frames. It is not possible to discuss all of the possible configurations in a book such as this. The reader should be aware that the structural configurations found to be economical in the construction of continuous bridges vary greatly from one region of the country to another, and the same is true for building construction. Some of the types of continuous beams used in bridge and building construction are described in Chapters 13 and 14. The reader can find much more information on these subjects through publications of numerous local and national trade associations related to the concrete construction industry.

Many engineers have the impression that continuous prestressed structures are difficult to design and analyze because of the moments that result from the deformation of the structure during prestressing. As will be seen in the following discussion, except for structures constructed by using methods that involve changes in the topology of the structure, the analysis of continuous prestressed structures is not particularly complex and involves only familiar principles used in the analysis of elastic statically indeterminate structures.

10-2 Elastic Analysis with Straight Tendons

The moment due to dead and live loads in an indeterminate prestressed-concrete structure are calculated by using the same classical methods employed in analyzing statically indeterminate structures composed of other materials. The one significant difference in a prestressed structure is that secondary moments may or may not result from the prestressing. These moments, which are due to deformation of the structure, also are calculated by the usual methods of indeterminate analysis. In most areas of structural design, the term secondary moments denotes undesirable moments that must be avoided if possible. In prestressed concrete design, the secondary moments are not always undesirable, and more often than not they cannot be avoided. It is essential that the designer be aware that such moments do exist and that they must be included in the design of statically indeterminate prestressed structures.

In the design and analysis of continuous prestressed concrete beams, the following assumptions generally are made:

1. The concrete acts as an elastic material within the range of stresses permitted in the design.
2. Plane sections remain plane.
3. The effects of each cause of moments can be calculated independently and superimposed to attain the result of the combined effect of the several causes (the principle of superposition).
4. The effect of friction on the prestressing force is small and can be neglected.
5. The eccentricity of the prestressing force is small in comparison to the span, and, hence, the horizontal component of the prestressing force can be considered uniform throughout the length of the member.
6. Axial deformation of the member is assumed to take place without restraint.

Research into the performance of continuous prestressed-concrete beams has revealed that these assumptions do not introduce significant errors in normal applications. If the cracking load of a beam is exceeded, and in cases where the effect of friction during post-tensioning of the tendon is significant, special attention should be given to these effects. The axial deformation that results from prestressing can have a significant effect on the moments and shear forces when they are restrained, as in rigid frames; hence, special investigation into the effects of this phenomenon may be required. Some of these effects will be considered subsequently, but for the general discussion that follows, the above assumptions will be assumed to be valid.

The nature of secondary moments can be illustrated by considering a two-span, continuous, prismatic beam that is not rotationally restrained by its

supports, but which must remain in contact with them, as illustrated in Fig. 10-1a. This beam is prestressed with a straight tendon that has a prestressing force of P and eccentricity, with respect to the centroidal axis of the beam, of e_{ps}. This would tend to make the beam deflect away from the center support by the amount:

$$\delta = -\frac{Pe_{ps}(2l)^2}{8EI} = -\frac{Pe_{ps}l^2}{2EI} \tag{10-1}$$

Because the beam must remain in contact with the center support, a downward reaction must exist at the location of the center support to cause an equal but opposite deflection. The deflection at the center of a beam that has a span of $2l$, due to a concentrated load (R_b) applied at the center, is equal to:

$$\delta = \frac{R_b l^3}{6EI} \tag{10-2}$$

Because the deflections must be equal in magnitude but opposite in direction, by equating eqs. 10-1 and 10-2 the value of R_b is found to be:

$$\begin{aligned} \frac{R_b l^3}{6EI} &= -\frac{Pel^2}{2eI} \\ R_b &= -\frac{3Pe_{ps}}{l} \end{aligned} \tag{10-3}$$

By applying the rules of statics, it can be shown that the forces acting upon the beam must be as shown in Fig. 10-1d in order to maintain equilibrium, and the moment diagram due to prestressing alone is as shown in Fig. 10-1e.

By dividing the moment due to prestressing at each section by the prestressing force P, the eccentricity of the pressure line, e_{pl}, can be found and plotted (Fig. 10-1f). At the ends, as would be expected, the pressure line is seen to be coincident with the location of the prestressing force, whereas at the center support the pressure line is at $-e_{ps}$ from (above) the centroidal axis of gravity of the beam. The effect of the secondary reaction, R_b, has been to move the pressure line from an eccentricity of e_{ps} below the centroidal axis of the beam to an eccentricity of $-e_{ps}/2$ above the center of gravity at the center support. Because there are no additional external loads between the end support and the center support (the weight of the beam itself being neglected), and because the path of the tendon is straight between the supports (i.e., no curvature or angle points between the supports), the pressure line is a straight line, as shown in Fig. 10-1f. It will be seen from this example that the secondary moment is secondary in nature (i.e., it results from the deformation of the beam), but not in magnitude.

As the above example illustrates, if the prestress results in a deformation of the structure (there are cases where this does not occur), secondary reactions as

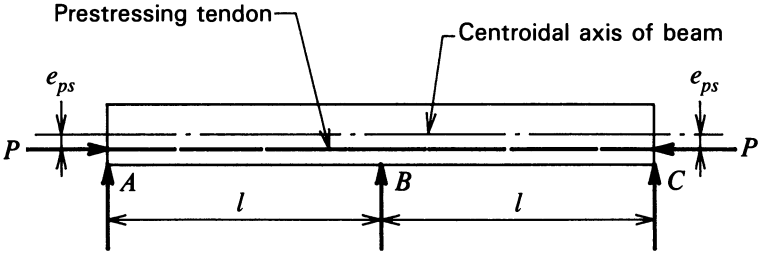

(a) Elevation

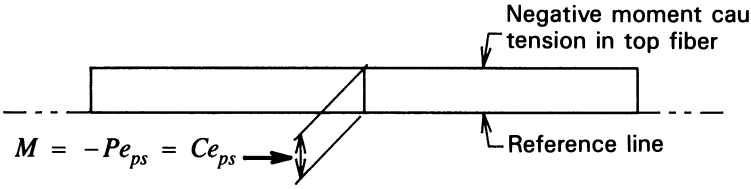

(b) Primary moment due to prestressing

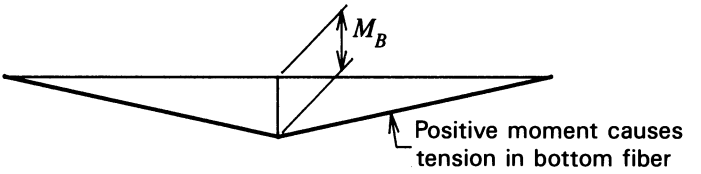

(c) Secondary moment due to prestressing

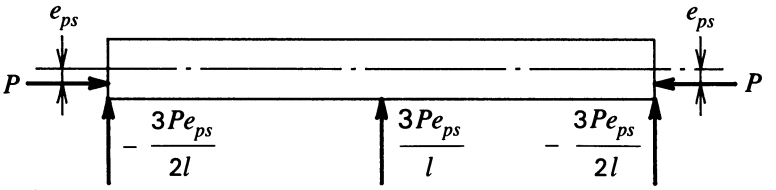

(d) Forces on beam due to prestressed reinforcement and reactions needed for beam to remain in contact with its support.

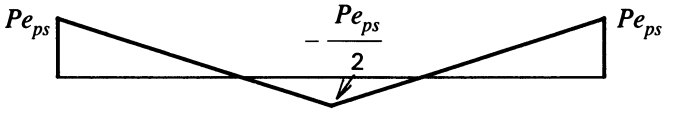

(e) Moment due to prestressing

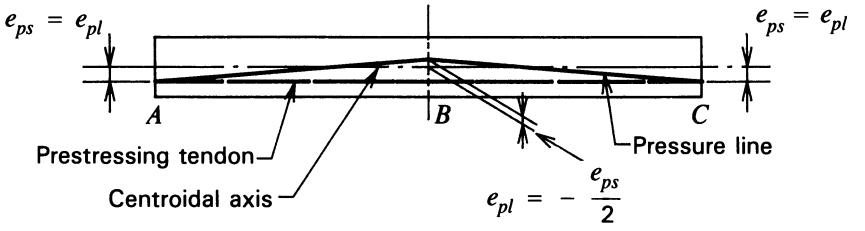

(f) Location of pressure line

Fig. 10-1. Two-span continuous beam prestressed with a straight tendon having constant eccentricity of e.

well as secondary moments are the result. (This explains why some persons refer to secondary reactions and moments as the reactions and moments due to prestressing.) Because the secondary reactions and secondary moments are functions of each other, the secondary moments vary linearly, and the secondary shear forces are constant between the supports. The addition of the secondary moment, as shown in Fig. 10-1c, to the prestressing moment diagram, Fig. 10-1b, results in the diagram of the total moment due to prestressing Fig. 10-1e. Because the secondary reactions can only cause a moment that varies linearly, its effect is to displace the pressure line linearly from the centroid of the prestressed reinforcement, in direct proportion to the distance from the supports. It is also apparent from this example that, if the reactions resulting from the prestress force are known, the locations of the pressure line and the stresses due to prestressing at any point along the length of the beam can be determined.

The stresses in the concrete at y from the centroidal axis due to prestressing in continuous beams are calculated from the basic relationship:

$$f_{cy} = \frac{C}{A}\left(1 + \frac{e_{pl}y}{r^2}\right) \tag{10-4}$$

in which e_{pl} is the eccentricity of the pressure line and not the eccentricity of the tendon, e_{ps} (although these eccentricities may be one and the same, as will be seen). An important axiom is illustrated by the above example: *the pressure line due to prestressing is not necessarily coincident with the center of gravity of the prestressed reinforcement in statically indeterminate prestressed concrete structures*. This axiom is also applicable to members made of materials other than concrete that are subjected to prestress.

If the position of the tendon in the above example is revised so that it is coincident with the location of the pressure line computed above, the resulting tendon location and moment diagram due to prestressing alone would be as shown in Fig. 10-2a and 10-2b, respectively. Removing the reaction at B, in order to render the structure statically determinate, and using the principle of elastic weights, the reactions and forces acting on the beam are as shown in Fig. 10-2c. The deflection of the beam at B due to the prestressing is equal to the moment at B resulting from the elastic weights, or:

$$\delta = \frac{Pe_{pse}l^2}{4EI} - \frac{7Pe_{pse}l^2}{27EI} + \frac{Pe_{pse}l^2}{108EI} = 0$$

Because the deflection due to prestressing at B is nil, no secondary reaction is required at B to keep the center support in contact with the beam, and there are no secondary moments. In this example, the pressure line and the center of gravity of the prestressed reinforcement are coincident, and the tendon is said to be *concordant*. In the first example, the pressure line and the center of gravity

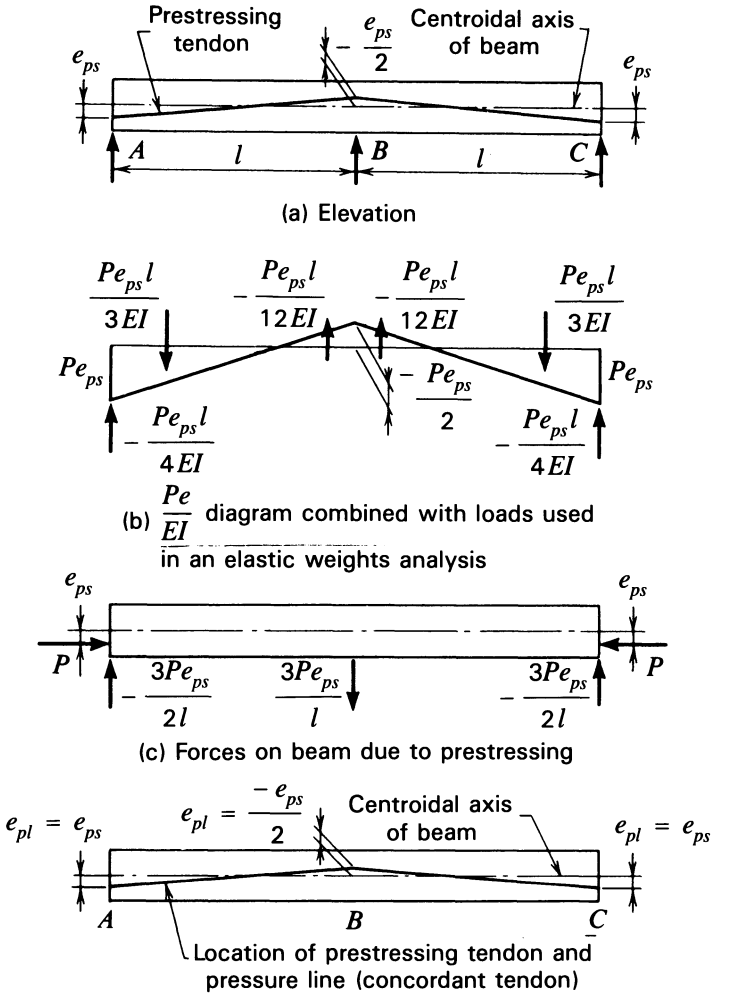

Fig. 10-2. Two-span continuous beam prestressed with a tendon on straight paths having an eccentricity of e at the ends and $-e/2$ at the center support.

of the prestressing were not coincident, and the tendon is said to be *noncon-cordant*.

If the tendon is placed in the path shown in Fig. 10-3a, the elastic weights are as shown in Fig. 10-3b, and the reactions and moments due to prestressing are found to be as shown in Fig. 10-3c and 10-3d. In this case the moment diagram due to prestressing, and hence the location of the pressure line, are the same as in the first two examples. The tendon in the third example is noncon-cordant.

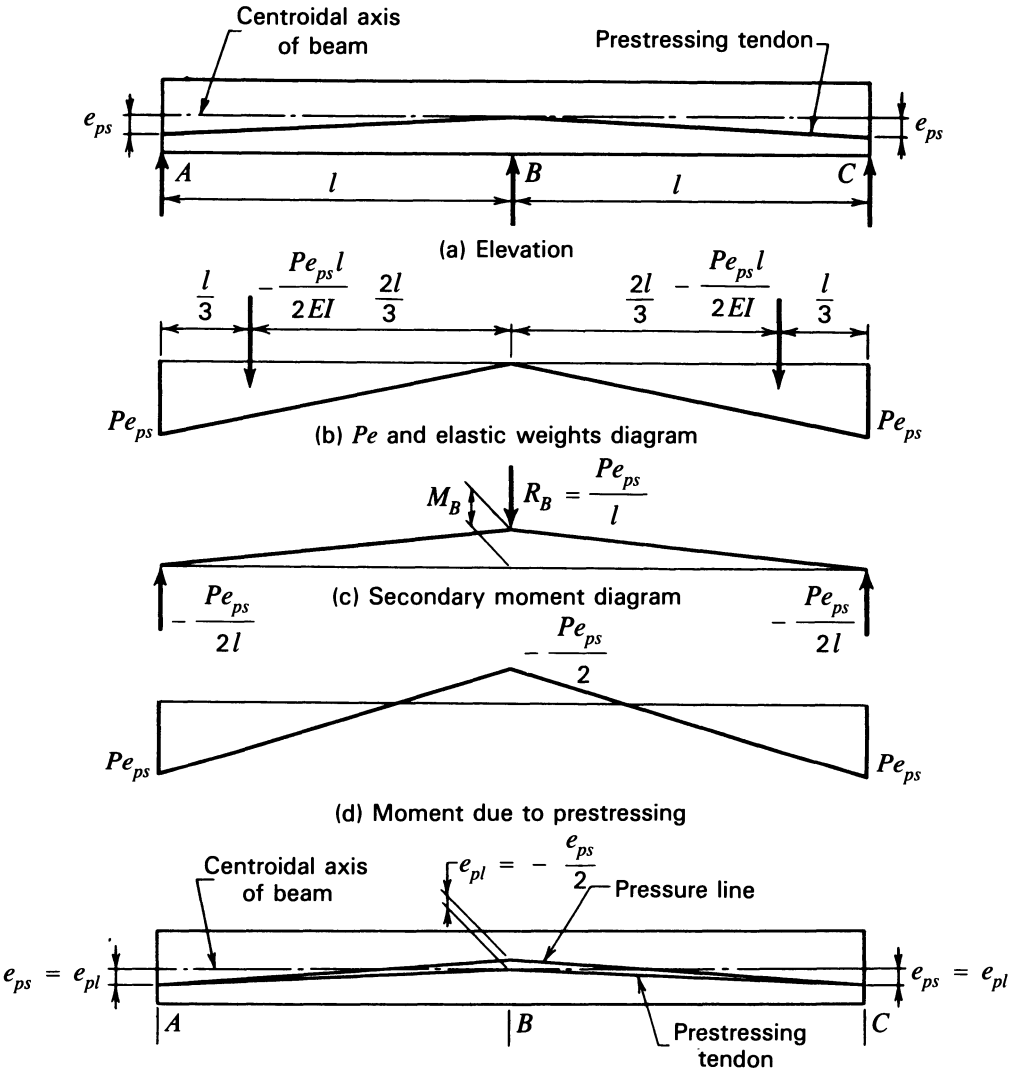

Fig. 10-3. Two-span continuous beam prestressed with a tendon on straight paths between supports with no eccentricity at the center support.

The above examples illustrate several principles that are useful in the elastic design and analysis of statically indeterminate prestressed structures. In the three examples, the only variable is the eccentricity of the prestressing tendon at the center support. The force in the tendon, P, as well as the eccentricity of the tendon at the end supports, e_{pse}, was the same in each case. Inspection of the

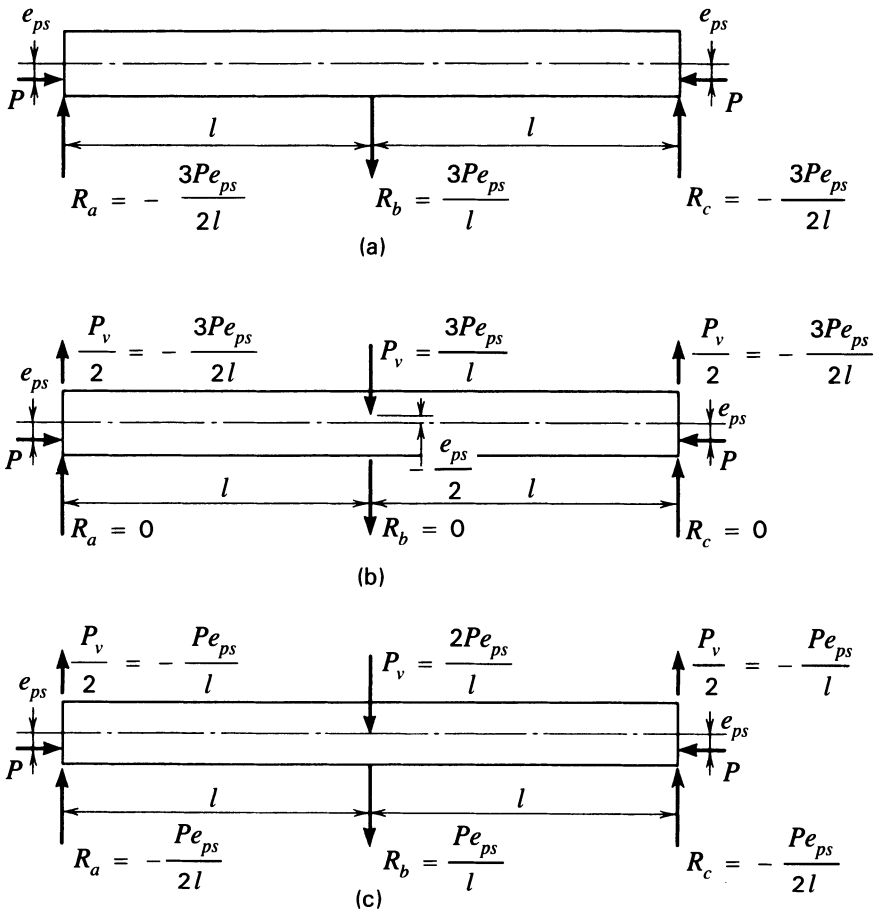

Fig. 10-4. Freebody diagrams with (a) straight tendon of eccentricity e, (b) tendon sloping from eccentricity of e at each end to $-e/2$ above the center support, and (c) tendon sloping from eccentricity of e at the ends to 0 at the center support.

three solutions shows the moments on the concrete section that resulted from each tendon layout to be identical, although the secondary reactions and secondary moments are different. It is apparent, from inspection of the moment diagrams used in these examples, that if the eccentricity at the end of the member were changed to another value, $e_{pse} + \Delta e_{pse}$, the moment due to prestressing, and thus the location of the pressure line, would be changed. Freebody diagrams for each of the three examples (Fig. 10-4) reveal that the net forces that act on the members (combination of components of the prestressing force and the secondary reactions) are identical for the three conditions of prestressing, as is to be expected if the total moments due to prestressing are equal.

The above examples also illustrate the very important principle of linear transformation, which can be stated as follows: *The path of the prestressing force in any continuous prestressed beam is said to be linearly transformed when the location of the path at the interior supports is altered without altering the position of the path at the end supports and without changing the intrinsic shape (straight, curved, or series of chords) of the path between any supports.* Linear transformation of any tendon can be made without altering the location of the pressure line.

The only difference between the three tendon paths in the above examples is that they are displaced from each other, at every section, by an amount that is in direct (linear) proportion to the distance of the section from the end of the member. The eccentricity of the tendon at the end supports and the shape of the tendon between the supports were not changed. It will be shown subsequently that the principle of linear transformation is equally applicable to tendons that are curved, and, from the above examples, it is apparent that the principle applies to concordant tendons as well as nonconcordant tendons.

The principle of linear transformation is particularly useful in designing continuous beams when it may be desirable to adjust the location of the tendon in order to provide more protective concrete cover over the prestressing tendons without altering the locations of the pressure line.

Another significant principle, apparent from these examples, is that *the location of the pressure line in beams stressed by tendons alone is not a function of the elastic properties of the concrete.* (The elastic modulus of the concrete did not appear in the value of the secondary reaction in eq. 10-3, for example.) Therefore, the only effect of changes in the elastic properties of the concrete in a statically indeterminate member (i.e., creep and shrinkage) is a reduction in the prestressing force, just as it is in statically determinate structures. This has been confirmed by tests (Saeed-Un-Din 1958). (Note that this does not apply to a structure built in a topology that is subsequently revised to a topology different from the original one; see Secs. 10-1 and 10-9.)

On the other hand, if the location of the pressure line is altered by adjustment of the reactions of a continuous beam, such as by displacing the beam upward or downward at one or more of the supports (with large hydraulic jacks), the reactions and moments induced thereby are a function of the elastic properties of the concrete. Therefore, when such methods are used, the effect of creep must be included in the analysis of the structures by employing a procedure based upon an age-adjusted elastic modulus for the concrete, similar to that used in analyzing the effects of differential settlement.

Additional understanding of the action of secondary moments can be gained by considering a prismatic beam fixed at each end in such a manner that rotation of the ends of the beam cannot take place. A beam of this type, prestressed with a straight tendon that is stressed to a force P and at eccentricity e_{ps}, is

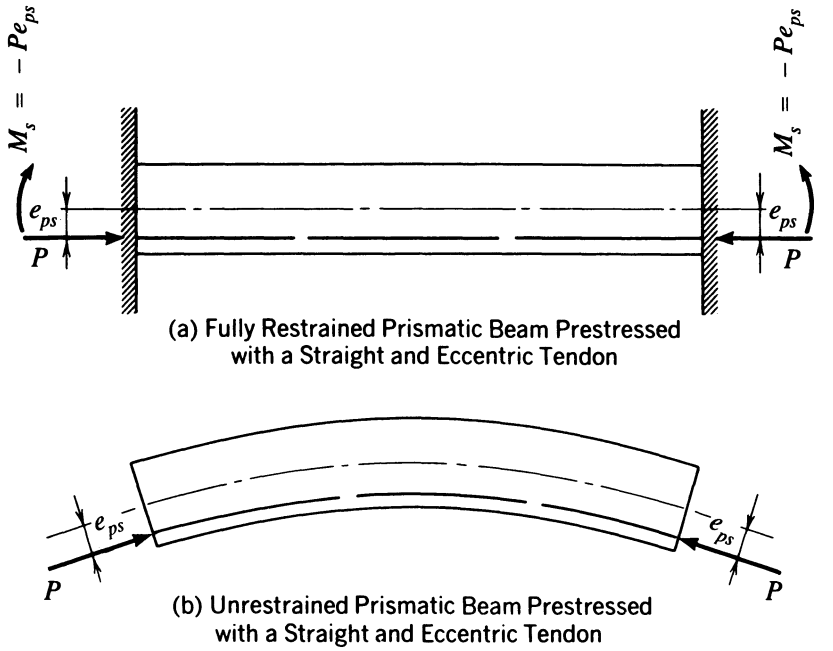

Fig. 10-5. Effect of end restraint on prismatic prestressed beams. (a) Fully restrained prismatic beam with a straight eccentric tendon. (b) Unrestrained prismatic beam with a straight eccentric tendon.

illustrated in Fig. 10-5a. Neglecting the dead weight of the beam itself, if the ends were released and allowed to rotate, the beam would deflect upward as a normal, simply supported prestressed-concrete beam would do. This is illustrated in Fig. 10-5b. Because the ends of the beam are fixed and cannot rotate, it is apparent that another (secondary) moment must be present at the ends to nullify the end rotation caused by the prestressing moment Pe_{ps}. The secondary moment must cause a rotation at each end that is equal in size, but opposite in direction, to that which results from the prestressing moment. It thus can be concluded that the secondary moment is equal to $-Pe_{ps}$. It is significant in this particular case (prismatic fixed beam prestressed by a straight tendon) that the secondary moment has the effect of nullifying the effect of the eccentricity of the prestressing force and results in a uniform compressive stress ($-P/A$) due to prestressing at every cross section. Again in this example, as has been noted previously, the secondary moment is secondary in nature but not in size.

If a haunched beam of rectangular cross section, as shown in Fig. 10-6, is prestressed with a straight tendon located at the elastic center of the member, the prestressing will result in stresses of the proper direction for resisting negative moments at the ends of the beam and positive moments at the midsec-

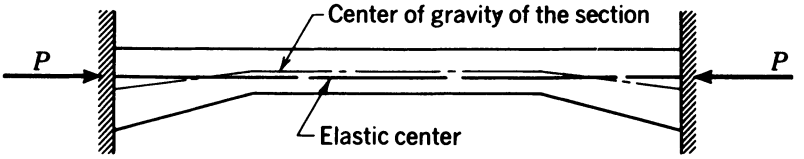

Fig. 10-6. Haunched beam of rectangular cross section prestressed with a straight tendon.

tion of the beam, and there will be no secondary moments. (The *elastic center* is defined as the location through which a force may be applied without causing rotations at the ends of the beam.) Applying the same principles used in the above discussion of the prismatic beam, it can be shown that if the straight, prestressing tendon is not located at the elastic center, secondary moments will result in combined stresses that are equal to the stresses that would occur if the tendon were located at the elastic center.

The location of the elastic center of the haunched beams of Fig. 10-7 can be determined by solving the relationship:

$$\int_0^{L/2} \frac{e_{ps}\,dx}{I} = 0 \tag{10-5}$$

The value of y that satisfies eq. 10-5 is the location of the elastic center.

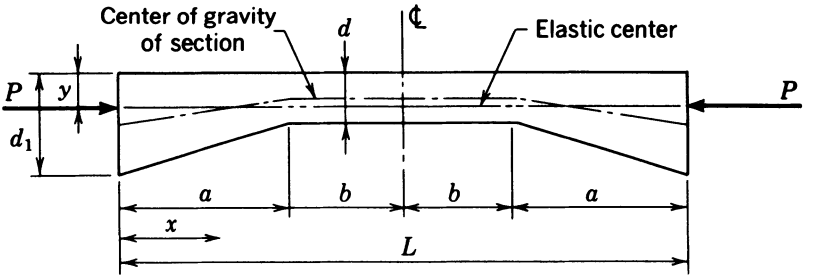

(a) Straight Haunches

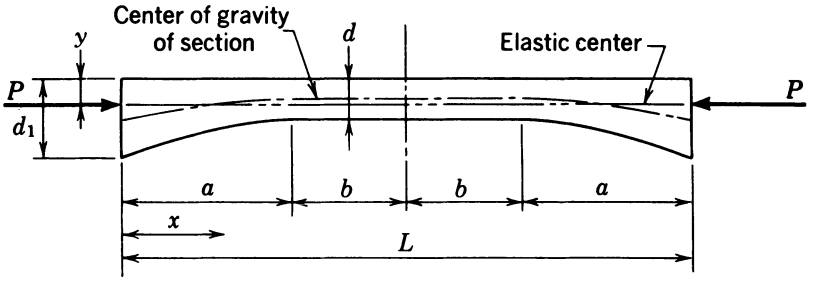

(b) Parabolic Haunches

Fig. 10-7. Beams with straight and parabolic haunches.

The examples given above for straight tendons are useful in all design problems, but are of particular use in short-span continuous slabs, such as in bridge decks.

10-3 Elastic Analysis of Beams with Curved Tendons

The introduction of curvature to the tendon path does not affect the basic methods or principles of analysis in any way. Calculation of the secondary reactions or moments can be made without the use of computers or programmable calculators, by using the principle of elastic weights, the theorem of three moments, or other classical methods, if desired. The familiar moment distribution method is considered among the easier methods for analyzing prismatic beams that have simple tendon paths. For beams with variable moments of inertia, the theorem of three moments, which may be simplified by using a semigraphical method of computing the static moments of the M/I diagram, is rapid and easily understood. Each of these methods is used subsequently in example problems, and a brief explanation is given of the procedures followed in applying them.

The methods used in the analysis of continuous prestressed-concrete members do not affect the results obtained, and those used in actual design should be selected by the designer according to the ease of application of the various methods for the particular conditions at hand.

When the moment distribution method is used, the end eccentricities, curvature, and abrupt changes in slope of the prestressing tendons are converted into specific, equivalent end moments, uniformly applied loads, and concentrated loads, respectively. Fixed end moments for the equivalent loadings are subsequently distributed in the usual manner. The conversion of end eccentricity and curvature of the tendon into equivalent loading is illustrated by considering the beam shown in Fig. 10-8a. This two-span continuous beam is prestressed by a tendon having an eccentricity of e_1 at each support. The tendon path extends downward, following a second-degree parabola between supports, with a total, vertical ordinate at midspan of e_t.

As was shown in Sec. 9-9, the tangent to a second-degree parabolic tendon path at the support is equal to:

$$\tan \theta = \frac{4e_t}{l}$$

Because the curvatures are small (see design assumptions in Sec. 10-2), $\tan \theta = \sin \theta = \theta$, and the vertical component of the force in the tendon at each end of each span is:

$$V_p = P \sin \theta = \frac{4Pe_t}{l}$$

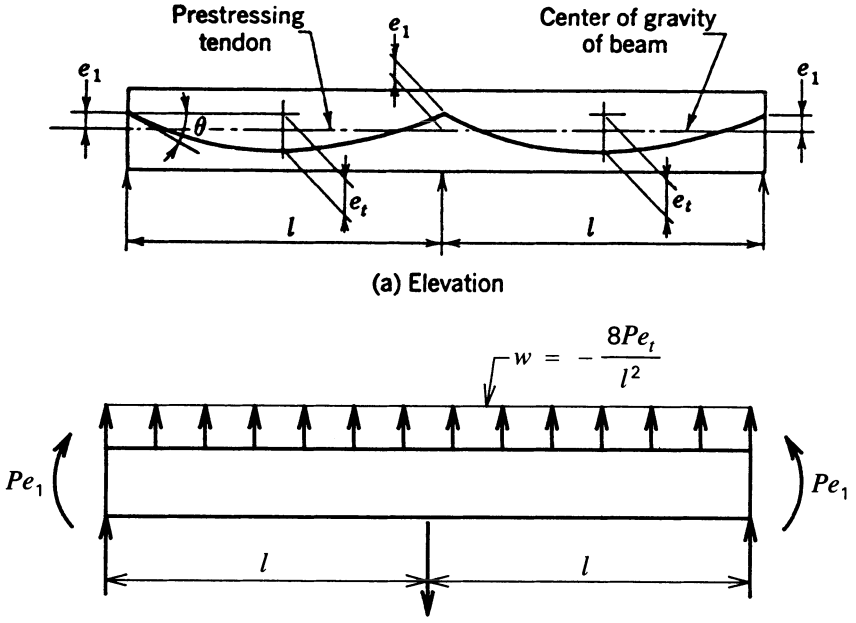

Note: To prevent upward deflection of beam at center support, center reaction for prestressing alone acts downward rather than upward as shown.

Fig. 10-8. Beam continuous over two spans prestressed with a tendon on second-degree parabolic path in each span.

Therefore, the total vertical component of the prestressing force that acts on each span of the beam is equal to twice the force that acts at each end, and the equivalent uniformly applied load is found to be:

$$wl = \frac{2 \times 4Pe_t}{l}$$

$$w = \frac{8Pe_t}{l^2} \tag{10-6}$$

The vertical components of the prestressing force that occur at the supports do not cause moments in the beam, but pass directly through the supports. For this reason, they are disregarded in the equivalent loading. The horizontal component of the prestressing tendon is eccentric by an amount equal to e_1 at each end of the beam, and the equivalent loading must, therefore, include end moments in the amounts of Pe_1. The effect of the end moment is included in the analysis in the same way that a moment due to a cantilevered end would be. The equivalent loading is shown in Fig. 10-8b.

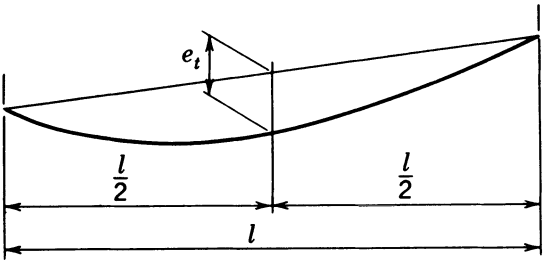

Fig. 10-9. Value of e_t to be used for tendon on second-degree parabolic path terminating at different elevations.

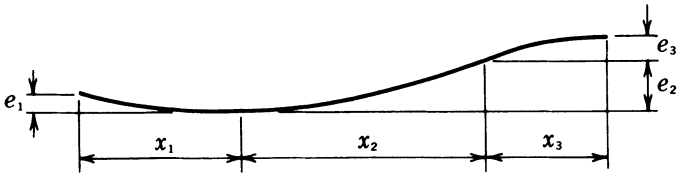

Fig. 10-10. Tendon path composed of compounded second-degree parabolas.

When the tendon curves parabolically over the length of the span but with the ends of the curve at different elevations, the values of e_t and l to be used in eq. 10-6 are as shown in Fig. 10-9. If the tendon path is formed of compounded second-degree parabolas, as shown in Fig. 10-10, the equivalent load due to tendon curvature is computed by:

$$w_n = \frac{2Pe_n}{x_n^2} \tag{10-7}$$

It usually is sufficiently accurate to assume that all curves are parabolic even though they may be circular or of other shape. Because the eccentricity normally is small in comparison to the span, the error introduced by this assumption is small.

The vertical load resulting from an abrupt change in slope of the tendons is computed as follows:

$$V_p = P \sin \theta_t \cong P \tan \theta_t$$

The value of tan θ is determined by the dimensions of the tendon, as is illustrated in Fig. 10-11.

ILLUSTRATIVE PROBLEM 10-1 Compute the moments due to prestressing and draw the pressure line for the prismatic beam shown in Fig. 10-12. Use moment distribution and the theorem of three moments.

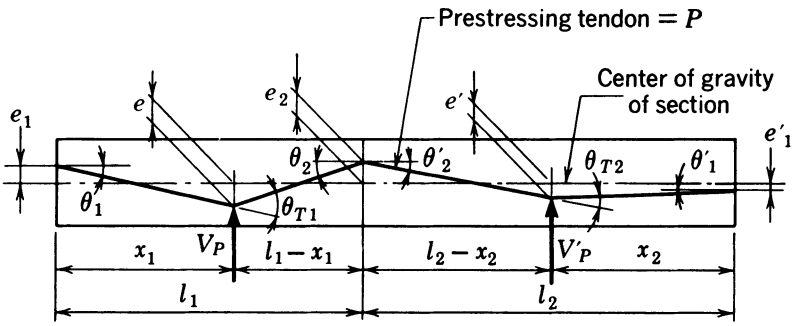

$$\theta_{T1} = \theta_1 + \theta_2 \qquad \theta_{T2} = \theta'_1 + \theta'_2$$

$$\tan\theta_{T1} \cong \theta_{T1} = \frac{e_1 + e}{x_1} + \frac{e_2 + e}{l - x_1} \qquad \tan\theta_{T2} \cong \theta_{T2} = \frac{e' - e'_1}{x_2} + \frac{e_2 + e'}{l_2 - x_2}$$

$$V_P = P\left(\frac{e_1 + e}{x_1} + \frac{e_2 + e}{l_1 - x_1}\right) \qquad V'_P = P\left(\frac{e' - e'_1}{x_2} + \frac{e_2 + e'}{l_2 - x_2}\right)$$

Fig. 10-11. Equivalent loads for tendons placed on a series of straight slopes.

SOLUTION: The equivalent uniformly distributed load due to the parabolic path of the tendon is computed from eq. 10-6, in which the prestressing force is 500 kips, the span length is 100 ft, and e_t is computed as:

$$e_t = -\left[0.80 + \frac{0.50 + 1.20}{2}\right] = -1.65 \text{ ft}$$

and the equivalent load is:

$$w = \frac{8 \times 500 \times -1.65}{100^2} = -0.66 \text{ klf}$$

The values of e_t and w are negative because they cause negative moments. The fixed end moments for use in the moment distribution method of analysis are:

$$M^F_{AB} = M^F_{BC} = -\frac{-0.66(100)^2}{12} = 550 \text{ k-ft}$$

$$M^F_{BA} = M^F_{CB} = +\frac{-0.66(100)^2}{12} = -550 \text{ k-ft}$$

The moments at the ends of the beam due to the eccentricity of the prestressing force are:

$$M_A = -[-0.50 \times 500] = 250 \text{ k-ft}$$

$$M_C = +[-0.50 \times 500] = -250 \text{ k-ft}$$

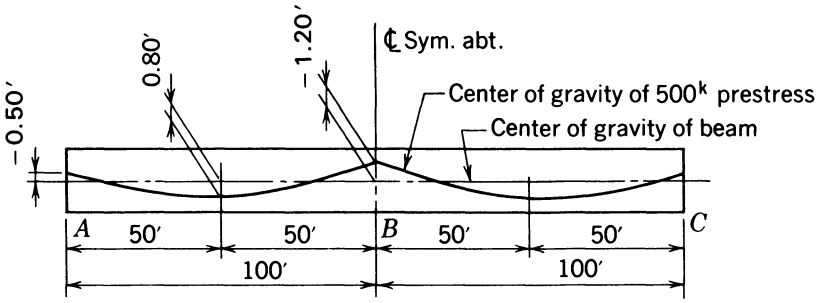

(a) Elevation of Prismatic Beam

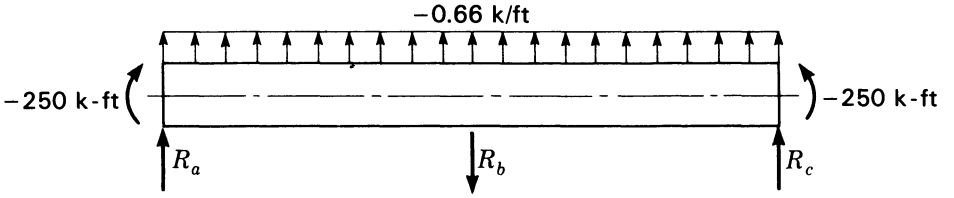

(b) Equivalent Loading Due to Prestress

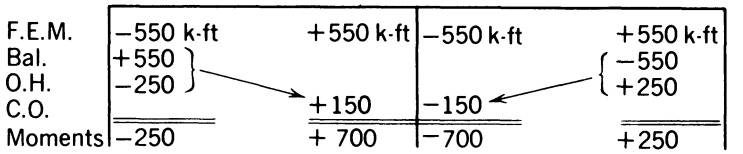

(c) Distribution of Moments

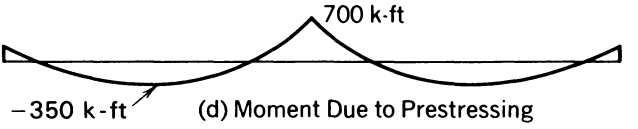

(d) Moment Due to Prestressing

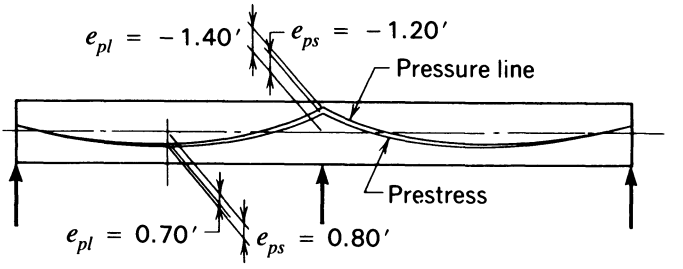

(e) Location of Pressure Line

Fig. 10-12. Analysis of two-span continuous beam with moment distribution.

The distribution of moments is performed in Fig. 10-12c, and the moment diagram due to prestressing is plotted in Fig. 10-12d. The computed moment at the interior support is 700 k-ft, and the eccentricity of the pressure line is:

$$e_{pl} = -\frac{700}{500} = -1.40 \text{ ft}$$

The pressure line is located 0.20 ft above the tendon at the interior support. At midspan of spans *AB* and *BC*, using the principle of linear transformation, the pressure line is found to be located 0.10 ft above the tendon path. This is shown in Fig. 10-12e. Because of the symmetry of the beam and the loading, the three-moment equation for this example is reduced to:

$$M_A + 4M_B + M_C = -\frac{wl^2}{2}$$

$$250 + 4M_B + 250 = -\frac{-0.66(100)^2}{2}$$

$$M_B = +700 \text{ k-ft}$$

ILLUSTRATIVE PROBLEM 10-2 Compute the moments due to prestressing for the prismatic beam and condition of loading illustrated in Fig. 10-13. Use moment distribution and the theorem of three moments.

SOLUTION: The concentrated loads in the two spans are computed as follows:

$$\text{Span } AB = 500\left(\frac{-1.50}{60} + \frac{-2.30}{40}\right) = -41.2 \text{ kips}$$

$$\text{Span } BC = 500\left(\frac{-0.80 + -1.60}{50}\right) = -24.0 \text{ kips}$$

The fixed end moments are:

$$M^F_{AB} = -\frac{-41.2 \times 60 \times 40^2}{100^2} = +395 \text{ k-ft}$$

$$M^F_{BA} = +\frac{-41.2 \times 60^2 \times 40}{100^2} = -593 \text{ k-ft}$$

$$M^F_{BC} = -\frac{-24.0 \times 50 \times 50^2}{100^2} = +300 \text{ k-ft}$$

$$M^F_{CB} = +\frac{-24.0 \times 50 \times 50^2}{100^2} = -300 \text{ k-ft}$$

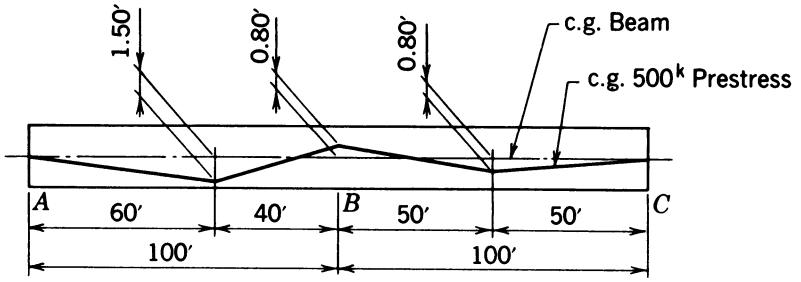

(a) Elevation

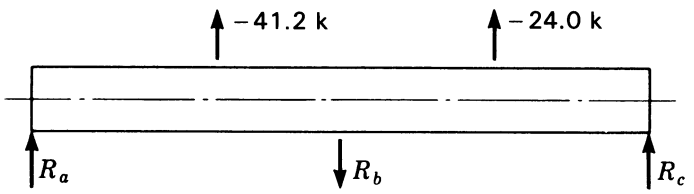

(b) Equivalent Loading

F.E.M.	−395 k-ft	+593 k-ft	−300 k-ft	+300 k-ft
Bal.	+395			−300
C.O.		+198	−150	
Bal.		−170	−170	
Moments	0	+621 k-ft	−620 k-ft	0

(c) Distribution of Moments

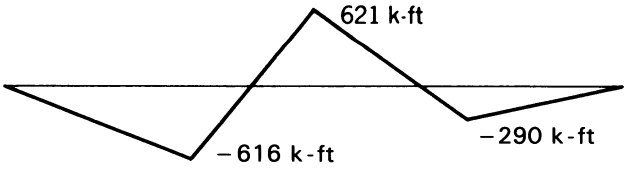

(d) Moment Due to Prestressing

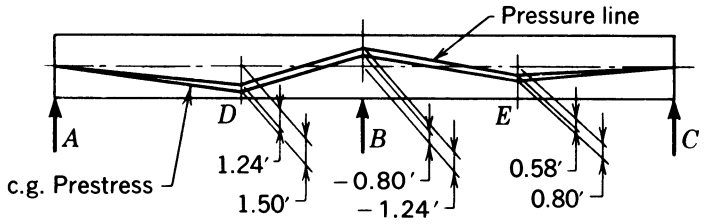

(e) Location of Pressure Line

Fig.10-13. Analysis of two-span continuous beam with moment distribution.

The moments are distributed in Fig. 10-13, and the moment at the interior support is found to be 621 k-ft, and the eccentricity of the pressure line at the interior support is:

$$e_{pl} = -\frac{621}{500} = -1.24 \text{ ft}$$

Therefore, the pressure line is 0.44 ft above the location of the tendon at the interior support. The distances from the pressure line to the tendon at points D and E are found by using linear transformation:

$$\text{At point } D\text{: } \frac{0.44 \times 60}{100} = 0.264 \text{ ft}$$

$$\text{At point } E\text{: } \frac{0.44 \times 50}{100} = 0.220 \text{ ft}$$

Using the theorem of three moments, the computation of the moment at B for the above example is as follows:

$$M_A L_1 + 2M_B(L_1 + L_2) + M_C L_2 = -\frac{-41.1 \times 60}{100}[(100)^2 - (60)^2]$$

$$-\frac{-24.0 \times 50}{100}[(100)^2 - (50)^2]$$

$$400M_B = 158{,}000 + 90{,}000$$

$$M_B = +620 \text{ k-ft}$$

ILLUSTRATIVE PROBLEM 10-3 Compute the moment due to prestressing for the beam illustrated in Fig. 10-14. Note that the relative moment of inertia is 1.00 for the outermost 60 ft of each span and 1.15 for the center 40 ft of the beam. The centroidal axis of the beam is a horizontal line (the variable moment of inertia is the result of an abrupt change in web thickness or an abrupt, symmetrical change in top and bottom flange thicknesses, or both).

SOLUTION: In Fig. 10-14, parts (b) through (e), the Pe diagram, the Pe/I diagram, the assumed M_b diagram, and the M_b/I diagram, respectively, are plotted. The value of M_b can be determined rapidly by employing the principle of elastic weights. The principle is used here by computing and equating the moments (deflections) at the center of the span AC of the beam loaded with the M/I diagrams for Pe and M_b.

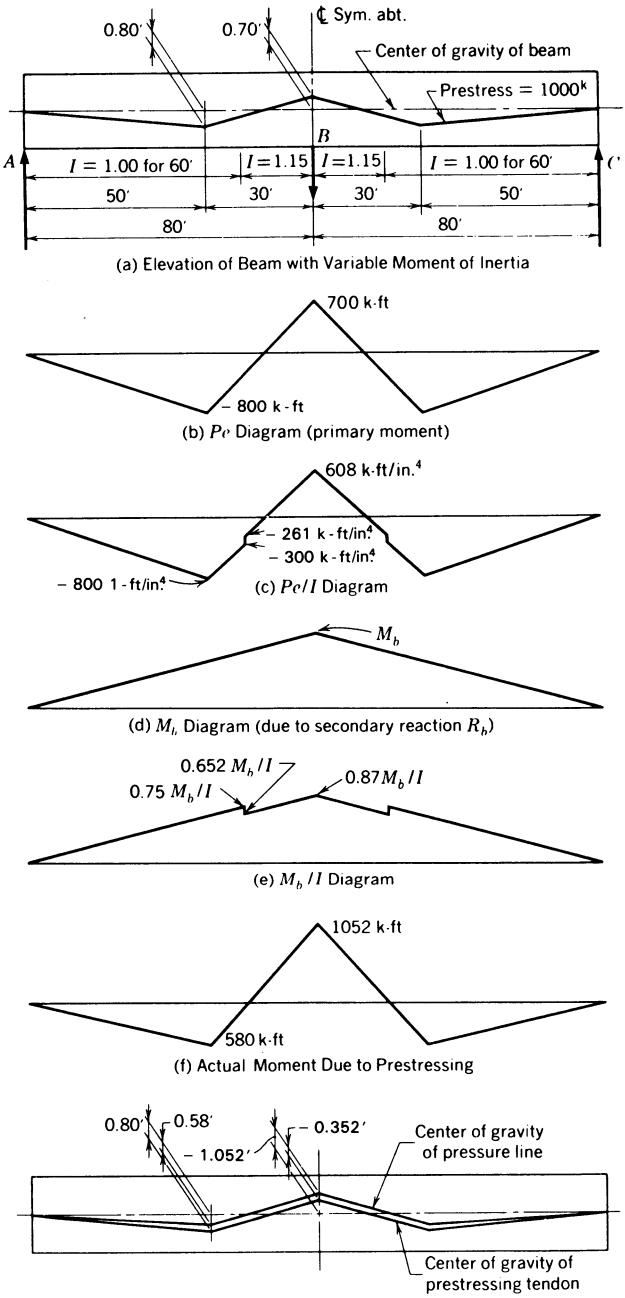

Fig. 10-14. Analysis of two-span continuous beam with a variable moment of inertia, using the principle of elastic weights.

The upward deflection due to the Pe/I diagram, δ_{pe}, is:

$$\begin{aligned}
-800 \times 50/2 &= -20{,}000 \times 46.70 = -933{,}000 \\
-300 \times 10 &= -3{,}000 \times 25.00 = -75{,}000 \\
-500 \times 10/2 &= -2{,}500 \times 26.70 = -66{,}700 \\
-261 \times 6/2 &= -783 \times 18.00 = -14{,}100 \\
+608 \times 14/2 &= +4{,}256 \times 4.67 = +19{,}800 \\
&\quad -22{,}000 \qquad\quad -1{,}069{,}000
\end{aligned}$$

$$\delta_{pe} = -22{,}027 \times 80 + 1{,}069{,}000 = -691{,}100 \text{ k-ft}^3/\text{in.}^4$$

The downward deflection due to the M_b/I diagram, δM_b, is:

$$\begin{aligned}
0.750M_b \times 60/2 &= 22.5M_b \times 40.00 = 900.0M_b \\
0.652M_b \times 20 &= 13.0M_b \times 10.00 = 130.0M_b \\
0.218M_b \times 20/2 &= 2.2M_b \times 4.67 = 14.6M_b \\
&\quad 37.7M_b \qquad\quad 1044.6M_b
\end{aligned}$$

$$\delta M_b = -37.7M_b \times 80 + 1044.6M_b = -1965M_b$$

Equating the two deflections and solving for M_b:

$$M_b = \frac{-691{,}000}{-1965} = +352 \text{ k-ft}$$

The combined (actual) moment diagram due to prestressing and the location of the pressure line are as shown in Fig. 10-14f and 10-14g, respectively.

It should be noted that the total moment due to prestressing and not the secondary moment was computed in I.P. 10-1 and I.P. 10-2. When equivalent loads are used for the analysis of moment due to prestressing, the total moment due to prestressing is computed. In I.P. 10-3, the secondary moment and not the total moment due to prestressing was computed. The secondary moment due to prestressing is computed when the effects of prestressing are analyzed, by using the basic principles of indeterminate structural analysis with the primary moment due to prestressing being considered as the initial loading condition.

With the general availability of electronic computers and programmable calculators, the analysis of continuous prestressed-concrete structures is greatly facilitated. These devices particularly aid in the analysis of members with variable prestressing forces, variable moments of inertia, and variable eccen-

tricity; so there is no longer a need for engineers to avoid the inclusion of these variations.

10-4 Additional Elastic Design Considerations

From the previous discussions, one should recognize that in applying the moment distribution method in the analysis of the moments due to prestressing, the effect of the prestressing is analyzed by determining an equivalent loading that is a function of the eccentricity of the tendon at the end supports and of the intrinsic shape of the tendon between supports, but is independent of the eccentricity of the tendon at the interior supports. There is a family of tendon paths that will result in this equivalent loading, but there will be only one pressure line for this loading. Also, the pressure line that results from an equivalent loading is the location of the concordant tendon for the particular equivalent loading (i.e., end eccentricities and intrinsic shapes of the tendon paths within the individual spans). Furthermore, the location of the pressure line is determined by dividing the moment diagram resulting from the equivalent loading by the effective prestressing force. From these considerations, the following corollary should be apparent: *A moment diagram for a particular beam, due to any condition of loading on the beam, defines a location for a concordant tendon; therefore, if a tendon is placed on a path proportional to any moment diagram for a particular loading on a beam, the tendon will be concordant.* This principle is useful in selecting a trial path for a tendon for which it is not necessary to determine the effects of secondary moments.

From the discussions of linear transformation in Sec. 10-2, the principles of elastic design that form the basis of the analysis of statically indeterminate structures, and the illustrative problems in the preceding section, the following axioms and corollaries applicable to most continuous beams can be stated (see Sec. 10-2 for an exception):

1. For any particular beam, a specific shape or path of the prestressing tendon between the supports will result in a specific pressure-line location for each specific value of eccentricity at the end supports.
2. Alteration of the eccentricity at one or both end supports, without revision to the intrinsic shape of the tendon path, will result in a linear shift in the location of the pressure line for any particular continuous beam.
3. Alteration of the eccentricity of the tendon path at the interior supports will not affect the location of the pressure line if the eccentricities at the ends of the beam and the intrinsic shapes of the tendon paths within the spans remain unchanged.
4. The conditions of continuity require that the deflection of a beam at the supports be equal to zero and that the end rotations of each span that adjoin at a common interior support be equal. These conditions apply

equally to the effect of the prestressing force (pressure line) and to the effect of external loads.

5. The distribution of moments, and hence the path of the pressure line, due to the prestressing can be determined by resolving the forces that the prestressed reinforcement exerts on a member into equivalent loads and end moments, and then, using the equivalent loads, calculating the moments resulting therefrom in the continuous structure.
6. The location of a pressure line is directly proportional to the moment in the continuous beam that results from a specific condition of (equivalent) loading.

Concordant tendon locations are not more desirable than nonconcordant tendon locations. It is true that concordant tendon paths generally do not result in a more efficient design; but sometimes it is convenient to start a design with an assumed tendon path that is concordant, in order to avoid the necessity of determining secondary moments. The tendon location then can be linearly transformed, or otherwise altered, into a nonconcordant tendon that may result in better design details.

From the discussion in Sec. 4-7, one can see that the location of the pressure line of a simple beam must be confined within certain limits in order to comply with the flexural stresses permitted by the design criteria. The same is true of continuous prestressed-concrete beams and frames. The major difference between continuous and simple beams in this respect is that in continuous beams there are more critical locations restricting the path of the pressure line than in simple beams. However, except in situations where the service load compressive stresses exceed the permissible values, the limits within which the pressure line must be contained in order to conform to the service load design criteria can be made less restrictive by increasing the effective prestressing force.

10-5 Elastic Design Procedure

It is difficult to generalize on the best procedure for the complete design of a structure because many factors must be addressed, including theoretical elastic design considerations as well as economic and construction constraints (i.e., methods of construction feasible for the specific site, minimum clearance requirements, first cost, etc.). Therefore, the procedure outlined in the following discussion is for the structural analysis portion of the "design." The process consists of reviewing a concrete section selected after due consideration has been given to all the other governing factors.

The computation of the maximum and minimum live-load moments that can occur at various sections along a continuous prestressed beam is no different from that done for other types of construction. The unique procedures in the design of continuous prestressed beams involve determination of the minimum prestressing force, together with an acceptable tendon path, that will perform

satisfactorily with the assumed concrete section. The normal design procedure is as follows:

1. Compute the moments due to dead load, superimposed dead load, and live loads. For structures subject to moving live loads, the maximum and minimum moments must be determined.
2. Adopt a trial layout and effective prestressing force for the prestressed reinforcement. The shape and location of the trial layout should consider practical controls, such as the space required to place the tendons with adequate cover, that do not interfere with the position of nonprestressed reinforcement or with other embedded items. Some engineers make preliminary flexural strength calculations at this step in the process as well, to confirm that the assumptions made up to this point appear to be acceptable from a strength standpoint.
3. Determine the secondary moments due to prestressing.
4. Compute the flexural stresses at the critical points along the span under the combinations of dead loads and prestressing alone, as well as with maximum and minimum live load.
5. If the elastic analysis reveals stresses that exceed those permitted by the applicable design criteria, or if it reveals the design of some portions of the structure to be overly conservative, the dimensions of the concrete section, the prestressing force, or the layout of the prestressed reinforcement, or all three, may be revised and the procedure repeated until an acceptable solution is obtained.
6. After the designer is satisfied with the flexural design under service loads, the adequacy of the flexural strength must be confirmed, and the member must be designed for the shear forces.

ILLUSTRATIVE PROBLEM 10-4 Determine a satisfactory means of prestressing the beam shown in Fig. 10-15. The beam is a hollow box and varies in depth from 24 to 49 in. The superimposed live load is 600 plf. Each span may be loaded independently of the other span.

SOLUTION: The section properties at the 20th points (intervals of 5 ft) of span *AB* are summarized in Table 10-1, together with the following moments:

1. Dead load on both spans.
2. Dead load on both spans plus live load on span *AB* only.
3. Dead load on both spans plus live load on span *BC* only.
4. Maximum moment.
5. Minimum moment.

Based on experience, a tendon path—whose ordinates are given in Table 10-2—is adopted for a trial, as is the effective prestressing force of 800 kips. The path does not follow a mathematical curve but was selected by plotting.

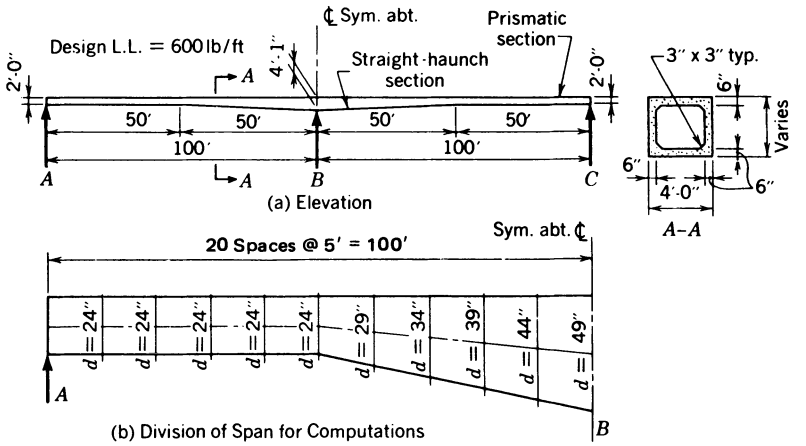

Fig. 10-15. Continuous beam analyzed in I.P. 10-4.

Using the trial path given in Table 10-2 and the force of 800 kips, the secondary moment due to prestressing is found to be 272 k-ft at *B*; there is no secondary moment at the end supports. With this secondary moment, the location of the pressure line and the stresses due to prestressing alone are computed to be as shown in Table 10-2. Combining the stresses due to prestressing with those due to the four loading conditions shown results in the stresses given in Table 10-3.

A review of Table 10-3 will reveal that the stresses under dead load and prestressing are all compressive. The maximum value is −1541 psi. Hence, the beam cannot be critical with respect to initial stresses. Under the other three loading conditions, it will be seen that the more critical stresses occur in span *AB* when the live load is on that span alone. The maximum compressive stress is −2476 psi, and the greatest tensile stress is 308 psi. If the concrete strength at 28 days were specified to be 5500 psi, the maximum compressive stress would be $0.45f'_c$, and the tensile stress would amount to $4.2\sqrt{f'_c}$; both of these values are well within those permitted by ACI 318.

With the electronic computational devices commonly used today, the most efficient method of designing continuous prestressed concrete members for service loads is by trial and review. The number of iterations needed to achieve a satisfactory design can be significantly reduced, however, by making preliminary computations before enlisting the assistance of the computer or programmable calculator.

10-6 Limitations of Elastic Action.

As stated previously, prestressed-concrete continuous structures perform substantially as elastic structures under loads that do not result in stresses that

TABLE 10-1 Section Properties and Moments for I.P. 10-4.

20th Pt.	Location (ft)	Section 1 ($in.^4$)	Area ($in.^2$)	Location (in.) CG Top	Bottom	(1) Moment (k-ft)	(2) Moment (k-ft)	(3) Moment (k-ft)	(4) Moment (k-ft)	(5) Moment (k-ft)	(6) Moment (k-ft)
0	.000	50571	738	12.000	12.000	.000	.000	.000	.000	.000	.000
1	5.000	50571	738	12.000	12.000	111.256	197.193	225.475	82.975	225.475	82.975
2	10.000	50571	738	12.000	12.000	203.288	360.161	416.725	146.725	416.725	146.725
3	15.000	50571	738	12.000	12.000	276.095	488.904	573.750	191.250	573.750	191.250
4	20.000	50571	738	12.000	12.000	329.677	583.423	696.550	216.550	696.550	216.550
5	25.000	50571	738	12.000	12.000	364.034	643.716	785.125	222.625	785.125	222.625
6	30.000	50571	738	12.000	12.000	379.166	669.784	839.475	209.475	839.475	209.475
7	35.000	50571	738	12.000	12.000	375.073	661.628	859.601	177.101	859.601	177.101
8	40.000	50571	738	12.000	12.000	351.755	619.246	845.501	125.501	845.501	125.501
9	45.000	50571	738	12.000	12.000	309.212	542.639	797.176	54.676	797.176	54.676
10	50.000	50571	738	12.000	12.000	247.444	431.808	714.626	−35.373	714.626	−35.373
11	55.000	66004	768	13.250	13.250	166.321	286.621	597.721	−144.778	597.721	−144.778
12	60.000	83838	798	14.500	14.500	65.193	106.429	445.811	−274.188	445.811	−274.188
13	65.000	104166	828	15.750	15.750	−56.719	−109.547	258.116	−424.383	258.116	−424.383
14	70.000	127081	858	17.000	17.000	−200.197	−362.088	33.857	−596.142	33.857	−596.142
15	75.000	152677	888	18.250	18.250	−366.020	−651.975	−227.747	−790.247	−227.747	−790.247
16	80.000	181048	918	19.500	19.500	−554.968	−979.987	−527.477	−1007.477	−527.477	−1007.477
17	85.000	212288	948	20.750	20.750	−767.821	−1346.903	−866.112	−1248.612	−767.821	−1346.903
18	90.000	246490	978	22.000	22.000	−1005.359	−1753.505	−1244.432	−1514.432	−1005.359	−1753.505
19	95.000	283749	1008	23.250	23.250	−1268.362	−2200.572	−1663.217	−1805.717	−1268.362	−2200.572
20	100.000	324158	1038	24.500	24.500	−1557.611	−2688.884	−2123.247	−2123.247	−1557.611	−2688.884

TABLE 10-2 Section Properties, Eccentricities of the Tendon and Pressure Line, and Stresses Due to Prestressing Alone, Span *AB*.

		Section				Tendon		Prestress Only		
20th Pt.	Location (ft)	I ($in.^4$)	Area ($in.^2$)	Location (in.) CG Top	Bottom	Eccentricity (in.)	Prestress Force (K)	Eccentricity (in.) Pressure Line	Stress (ksi) Top	Bottom
0	.000	50571	738	12.000	12.000	.000	800.00	.000	1.084	−1.084
1	5.000	50571	738	12.000	12.000	1.320	800.00	1.116	.872	−1.295
2	10.000	50571	738	12.000	12.000	2.520	800.00	2.112	.683	−1.484
3	15.000	50571	738	12.000	12.000	3.780	800.00	3.168	.482	−1.685
4	20.000	50571	738	12.000	12.000	4.680	800.00	3.864	.350	−1.817
5	25.000	50571	738	12.000	12.000	5.700	800.00	4.680	.195	−1.972
6	30.000	50571	738	12.000	12.000	6.480	800.00	5.256	.086	−2.081
7	35.000	50571	738	12.000	12.000	7.140	800.00	5.712	.000	−2.168
8	40.000	50571	738	12.000	12.000	7.560	800.00	5.929	.041	−2.209
9	45.000	50571	738	12.000	12.000	7.920	800.00	6.085	.071	−2.239
10	50.000	50571	738	12.000	12.000	8.160	800.00	6.121	.078	−2.246
11	55.000	66004	768	13.250	13.250	6.600	800.00	4.357	−.341	−1.741
12	60.000	83838	798	14.500	14.500	4.560	800.00	2.113	−.710	−1.294
13	65.000	104166	828	15.750	15.750	2.400	800.00	−.250	−.996	−.935
14	70.000	127081	858	17.000	17.000	−.240	800.00	−3.094	−1.263	−.601
15	75.000	152677	888	18.250	18.250	−3.480	800.00	−6.537	−1.526	−.275
16	80.000	181048	918	19.500	19.500	−6.960	800.00	−10.221	−1.752	.009
17	85.000	212288	948	20.750	20.750	−10.680	800.00	−14.145	−1.950	.262
18	90.000	246490	978	22.000	22.000	−14.760	800.00	−18.429	−2.133	.497
19	95.000	283749	1008	23.250	23.250	−18.720	800.00	−22.593	−2.274	.687
20	100.000	324158	1038	24.500	24.500	−21.240	800.00	−25.317	−2.301	.760

TABLE 10-3 Pressure Line Locations Together with the Combined Top and Bottom Fiber Stresses for Four Conditions of Loading, Span *AB*.

(1) Prestress and Load			(2) Prestress and Load			(3) Prestress and Load			(4) Prestress and Load		
Eccentricity (in.) Pressure Line	Stress (ksi) Top	Bottom	Eccentricity (in.) Pressure Line	Stress (ksi) Top	Bottom	Eccentricity (in.) Pressure Line	Stress (ksi) Top	Bottom	Eccentricity (in.) Pressure Line	Stress (ksi) Top	Bottom
−.000	−1.084	−1.084	−.000	−1.084	−1.084	−.000	−1.084	1.084	−.000	−1.084	−1.084
−.552	−1.188	−.979	−1.841	−1.433	−.734	−2.265	−1.514	.653	−.128	−1.108	−1.059
−.937	−1.261	−.906	−3.290	−1.708	−.459	−4.138	−1.869	.298	−.088	−1.100	−1.067
−.973	−1.268	−.899	−4.165	−1.874	−.293	−5.437	−2.116	.051	.299	−1.027	−1.140
−1.080	−1.289	−.878	−4.886	−2.011	−.156	−6.583	−2.333	.165	.616	−.967	−1.201
−.779	−1.232	−.935	−4.975	−2.028	−.139	−7.096	−2.431	.263	1.341	−.829	−1.338
−.430	−1.165	−1.002	−4.789	−1.993	−.174	−7.335	−2.476	.308	2.114	−.682	−1.485
.086	−1.067	−1.100	−4.211	−1.883	−.284	−7.181	−2.447	.279	3.056	−.503	−1.664
.652	−.960	−1.207	−3.359	−1.721	−.446	−6.753	−2.366	.198	4.046	−.315	−1.852
1.447	−.809	−1.358	−2.054	−1.473	−.694	−5.872	−2.198	.030	5.265	−.084	−2.083
2.409	−.626	−1.541	−.355	−1.151	−1.016	−4.597	−1.956	−.211	6.652	−.178	−2.346
1.862	−.742	−1.340	.058	−1.032	−1.051	−4.608	−1.781	−.301	6.529	−.006	−2.090
1.135	−.845	−1.159	.517	−.930	−1.074	−4.573	−1.635	−.369	6.226	−.140	−1.864
.600	−.893	−1.038	1.393	−.797	−1.134	−4.121	−1.464	−.467	6.115	−.226	−1.705
−.091	−.942	−.922	2.337	−.682	−1.182	−3.601	−1.317	−.546	5.848	−.306	−1.558
−1.047	−1.001	−.800	3.241	−.590	−1.210	−3.121	−1.199	−.602	5.315	−.392	−1.409
−1.897	−1.034	−.707	4.478	−.485	−1.257	−2.309	−1.070	−.672	4.890	−.450	−1.292
−2.628	−1.049	−.638	6.057	−.370	−1.317	−1.153	−.934	−.753	4.583	−.485	−1.202
−3.349	−1.057	−.578	7.873	−.255	−1.380	.237	−.801	−.834	4.287	−.511	−1.124
−3.567	−1.027	−.559	10.415	−.110	−1.476	2.354	−.639	−.948	4.492	−.499	−1.088
−1.953	−.888	−.652	15.016	.137	−1.678	6.531	−.375	−1.165	6.531	−.375	−1.165

(1) Dead load plus prestressing.
(2) Dead load plus prestressing plus live load on *AB* and *BC*.
(3) Dead load plus prestressing plus live load on Span *AB*.
(4) Dead load plus prestressing plus live load on Span *BC*.

exceed the normal working stresses permitted by recognized prestressed-concrete design criteria. Adequate experimental data are available to substantiate this.

Under normal conditions, when the service loads for which a structure has been designed are exceeded, the concrete stresses remain reasonably elastic up to the load that causes visible cracking in the structure. The first cracks are not visible to the unaided eye and do not materially affect the performance of the structure. In the testing of prestressed-concrete flexural members, when the load at which the first crack observed with the unaided eye during a beam test is plotted on a load–deflection curve, it often is found to be below the point at which pronounced deviation of the tangent to the elastic deflection curve takes place (see Fig. 5-1).

In most continuous structures, the cracking load will not be reached simultaneously in all highly stressed sections because the value of the moment varies along the length of the member, and, when members are designed for moving live loads, the largest moments that may occur at different sections under the assumed design loads do not occur under the same condition of loading. Furthermore, once the cracking load has been significantly exceeded at a section, there is a reduction in the effective moment of inertia at the cracked section and, hence, the stiffness of the member in the cracked area. At loads that result in one or more areas of a beam being stressed substantially above cracking, the effective modulus of elasticity of the concrete in the cracked areas may be lower than it is in areas that remain stressed in the elastic range, further contributing to the reduction in stiffness of the member in the cracked areas.

Because of the localized changes in stiffness of a continuous member subjected to significant overload, the distribution of moments ceases to be proportional to the distribution of moments in the elastic range. This is explained by the fact that, after cracking has occurred to a significant degree at one or more areas in a beam, the moment that results from the application of additional loads is carried in greater proportion by the parts of the member that remain uncracked. The areas first to attain a highly cracked and highly stressed condition yield more upon the application of additional load than areas that remain uncracked; hence, the cracked areas resist less of the additional loads than would be indicated by purely elastic analysis. This phenomenon is called *redistribution of the moments.*

The redistribution of moments often, but not always, causes continuous beams designed on a purely elastic basis to have very high factors of safety. This phenomenon can be illustrated by considering the fixed beam of Fig. 10-16. This beam, when subjected to loads slightly above cracking, has a distribution of moments that is virtually identical to the distribution that would result from an elastic analysis. When an additional increment of load, Δ_w, is applied, the stiffnesses of the cracked sections with respect to the uncracked sections are not as great as the relative stiffnesses were before cracking; so the distribution of

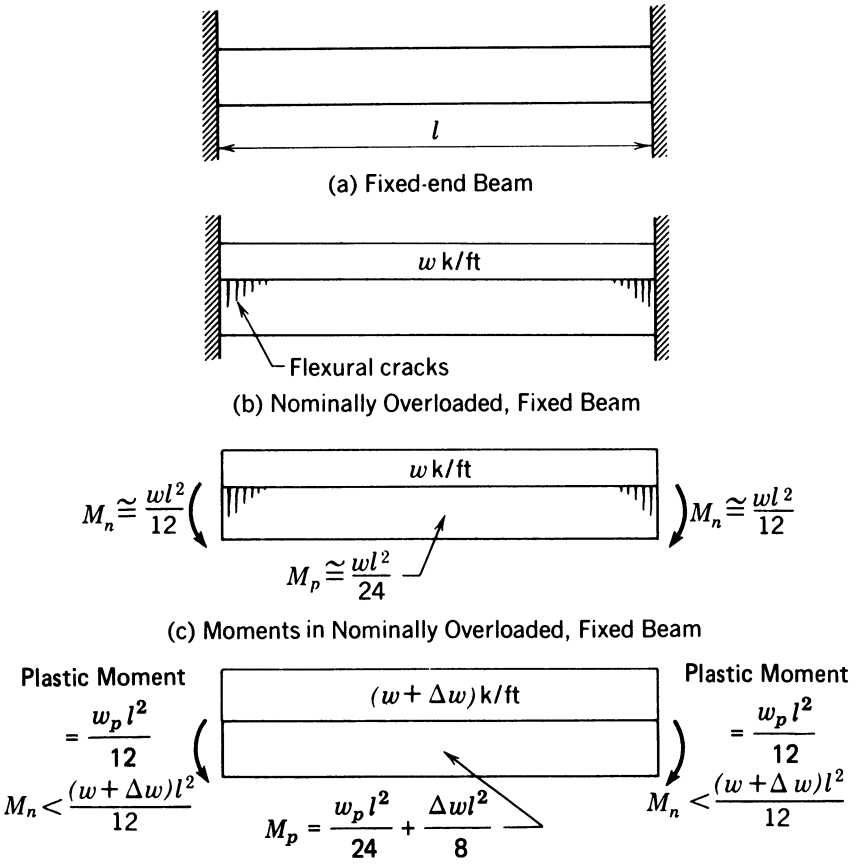

Fig. 10-16. Variations in moments in a fixed-end beam subjected to various conditions of overload.

moments deviates from the elastic distribution. For redistribution to be complete, the sections that crack first must form hinges that are completely plastic. If plastic hinges form at the ends of the beam of Fig. 10-16, the moments at the ends would not increase upon the application of additional load. The ends would simply rotate, and the positive moment would increase as a result of the application of further increases in load on the beam.

The redistribution of moments takes place in varying degrees. Redistribution is said to be complete when the various critical sections of a beam all attain a high degree of plasticity and attain the ultimate moments indicated by the flexural strength analysis developed in Sec. 5-2. Many continuous beams, if loaded to destruction, would fail before redistribution was complete. Engineers do not fully understand why this is so.

Additional research is needed on the phenomena that control the redistribution of moments, but it is now believed that the following conditions improve the redistribution of moments that occurs in a beam when loaded to destruction:

1. Low values of the steel index.
2. Good bond between the prestressing reinforcement and the concrete.
3. The use of nonprestressed reinforcement to improve cracking patterns in areas of high moment in: (a) beams with bonded prestressed reinforcement but with very low values for the steel index, and (b) beams that have unbonded tendons.
4. The prevention of large inclined shear cracks in areas of high moment because cracks of this type reduce the flexural strength and rotation capacities of sections. The use of nonprestressed shear reinforcement is considered necessary in the areas of high shear as well as in areas of high moment.
5. Use of members having large differences in flexural capacity at the various sections, in which moment distribution seems to be more complete than in members in which the flexural capacity is nearly equal at all critical sections (Guyon 1956).

The *Building Code Requirements for Reinforced Concrete* (ACI 318) permit very limited redistribution of moments in continuous prestressed concrete beams. These provisions, which are reproduced here with the permission of the American Concrete Institute, are as follows:

18.10—Statically indeterminate structures

18.10.1—Frames and continuous construction of prestressed concrete shall be designed for satisfactory performance at service load conditions and for adequate strength.

18.10.2—Performance at service load conditions shall be determined by elastic analysis, considering reactions, moments, shears and axial forces produced by prestressing, creep, shrinkage, temperature change, axial deformation, restraint of attached structural element, and foundation settlement.

18.10.3—Moments to be used to compute required strength shall be the sum of the moments due to reactions induced by prestressing (with a load factor of 1.0) and the moments due to factored loads, including redistribution as permitted in Section 18.10.4.

18.10.4—Redistribution of negative moments due to gravity loads in continuous prestressed concrete flexural members.

18.10.4.1—Where bonded reinforcement is provided at supports in accordance with Section 19.9.2, negative moments calculated by elastic theory for

any assumed loading arrangement may be increased or decreased by not more than

$$20\left[1 - \frac{\omega_p + \frac{d}{d_p}(\omega - \omega')}{0.36\beta_1}\right] \text{ percent} \qquad (10\text{-}8)$$

18.10.4.2—The modified negative moments shall be used for calculating moments at section within spans for the same loading arrangement.

18.10.4.3—Redistribution of negative moments shall be made only when the section at which moment is reduced is so designed that ω_p, $[\omega_p + d/d_p(\omega - \omega')]$, or $[\omega_{pw} + d/d_p - (\omega_w)]$, whichever is applicable, is not greater than $0.24\beta_1$.

The definitions of the steel indices (ω, ω_p, ω_w, ω_{pw}, ω', and ω'_w) are as given in Secs. 5-2, 5-4, and 5-5.

From these provisions it will be seen the redistribution of moments would be a maximum value of 20 percent for a reinforcement index of 0, and a minimum value of 6.67 percent when the applicable steel index is 0.20.

10-7 Analysis at Design Loads

Flexural strength analysis for indeterminate prestressed concrete structures should be based upon an elastic analysis or upon an elastic analysis including the limited redistribution of moments according to eq. 10-8 and the other requirements specified in Sec. 10-6 above.

In investigating the safety of a multispan continuous beam under design loading, all conditions of loading must be considered. The loading arrangement that would result in the collapse of the member due to negative moment may be quite different from the loading that would result in collapse due to positive moment or from positive and negative movement, simultaneously, in the same span. In addition, because reversal of moments occurs in continuous structures, it is possible to have critical positive moments develop under overload in areas of the beams that normally are stressed by negative moments. The opposite condition is also possible. Therefore, to facilitate the determination of the flexural strength of a member, an envelope of the maximum and minimum moment capacities that can be developed at various sections in the member is computed and plotted as shown in Fig. 10-17. Moment diagrams due to the various conditions of loading (with the appropriate load factors) are computed and plotted in the envelope. The moments can be distorted from those obtained by the elastic analysis as much as the excerpt from ACI 318 given in Sec. 10-6 permits, on projects governed by this code. If the moment diagrams so

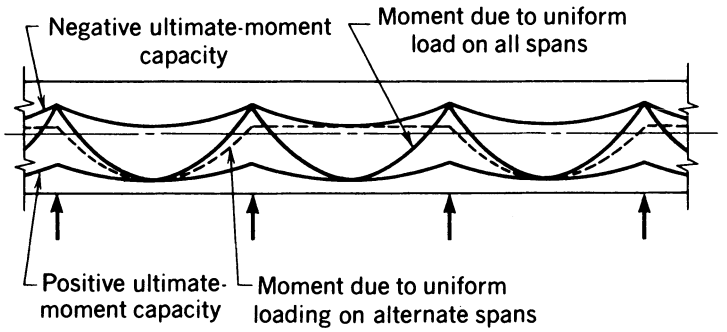

Fig. 10-17. Moment diagrams for uniform loads on all spans and on alternate spans of a multispan beam superimposed on an envelope of flexural capacities.

computed fall within the limits of the flexural strength envelopes, the design is satisfactory. If not, the design must be altered.

Before 1975, it was customary in the United States to ignore secondary moments due to prestressing in making a strength analysis. This is no longer the case. The secondary moments that exist when the member is loaded in the elastic range do not disappear as the load is increased and the member approaches its capacity. Ignoring the existence of the secondary moments in the strength analysis is the same as assuming a redistribution of moment in the amount of the secondary moment; it may very well be that this amount exceeds that permitted by the applicable design criteria.

ILLUSTRATIVE PROBLEM 10-5 Compute the ultimate moment for the beam of I.P. 10-4, using the nonconcordant tendon path in Table 10-4. Assume f'_c = 5500 psi, f_{pu} = 270 ksi, A_{ps} = 5.00 in.^{2} The design load is to be taken as $1.4D + 1.7L$, where D and L are the service dead and live loads, respectively.

SOLUTION: The design moments for various conditions of loading are shown in Table 10-4. The secondary moment, which is not factored, is included in the design (factored) dead load because both are of a "permanent" nature. These moments are used, together with the positive and negative moment capacities computed at various locations along the span, to construct the diagram shown in Fig. 10-18. An examination of this figure will reveal that for the condition of maximum design load on both spans (curve 1), the design moment diagram is well within the envelope of the positive and negative moment capacities. For the conditions of design dead load and secondary moment on both spans but with design live load on span *AB* only (Curve 2), the design moment curve slightly exceeds the positive moment capacity in span *AB* (about 2%), whereas in span *BC* the design moment curve is very close to being tangent to the negative moment capacity curve near midspan. One should not count on any redistri-

TABLE 10-4 Design Moments for I.P. 10-5.

Point	Moments (k-ft)					
	Sec. Moment and Design D. L. Moment	Design LL on Spans *AB* and *BC*	Design LL on Span *AB*	Design LL on Span *BC*	Design Maximum Moment	Design Minimum Moment
0	0	0	0	0	0	0
1	169	146	194	−48	363	121
2	312	267	363	−96	675	216
3	427	362	506	−144	933	283
4	516	431	624	−192	1140	324
5	578	476	716	−241	1294	338
6	613	494	782	−289	1395	324
7	621	487	824	−337	1445	284
8	602	455	839	−385	1441	217
9	556	397	829	−433	1385	123
10	483	314	794	−481	1277	2
11	383	205	733	−529	1116	−146
12	255	70	647	−577	902	−322
13	98	−90	535	−625	633	−527
14	−89	−275	398	−673	309	−762
15	−307	−486	235	−722	−73	−1028
16	−558	−722	46	−770	−512	−1328
17	−843	−984	−167	−818	−1010	−1827
18	−1162	−1272	−407	−865	−1569	−2434
19	−1517	−1585	−672	−914	−2189	−3102
20	−1908	−1923	−962	−962	−2870	−3831

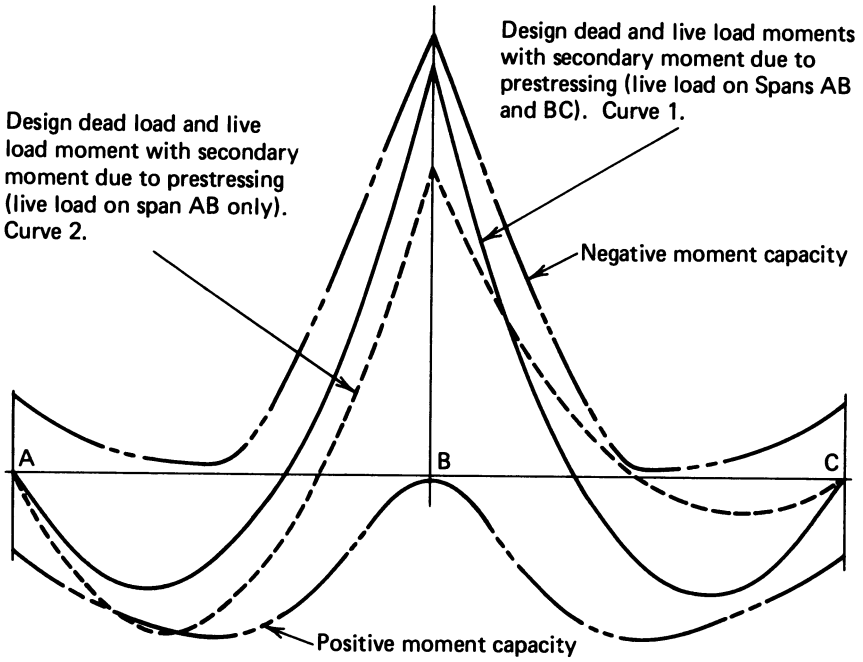

Fig. 10-18. Analysis of moment capacity of beam of I.P. 10-5 for loading on both spans simultaneously.

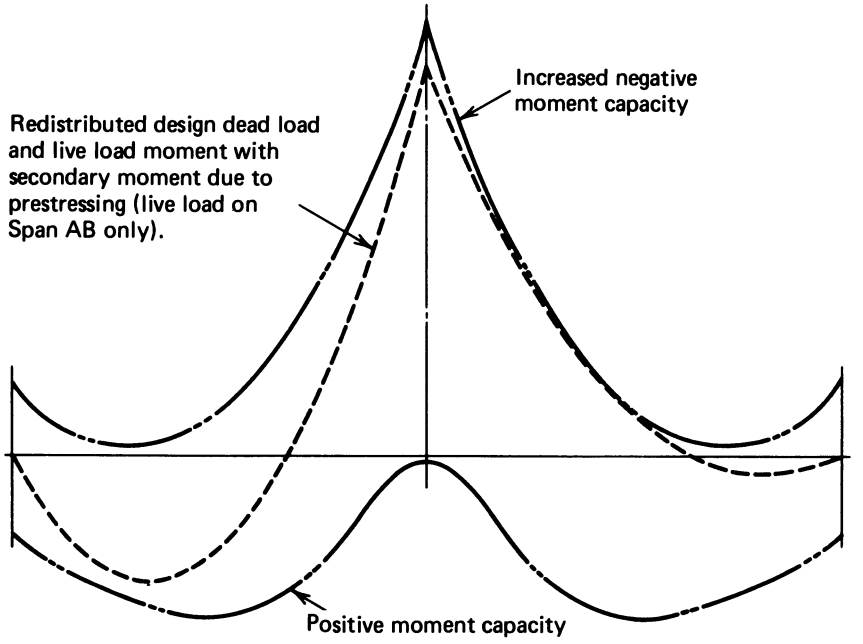

Fig. 10-19. Analysis of moment capacity of beam of I.P. 10-5 for loading on one span alone.

bution of moment in a case such as this because the formation of a plastic hinge in either span will prevent use of the "excess" negative moment capacity at the interior support. If the negative moment capacity in the spans were increased by the provisions of additional nonprestressed reinforcement in the upper portions of the beams near midspan, a diagram such as that shown in Fig. 10-19 could be obtained, and some redistribution of moment could be counted upon.

In continuous beams, the reinforcement indices can be substantially greater than is normally experienced in simple beams; in the latter, reinforcement indices of 0.10 to 0.40 are commonly found. In continuous beams, the reinforcement indices may be as high as 2.00 because the tendon may be very near the flange when the section is subject to moment reversal. Such highly reinforced areas would certainly fail suddenly; thus critical areas of this type should be investigated with great care and modified so that adequate safety of the structure is assured.

10-8 Additional Considerations

The effect of tendon friction during stressing was not discussed in the preceding sections on the design of continuous beams. The fundamental principles that govern friction loss of post-tensioned tendons are the same for simple and continuous beams; and because it is a practical rather than theoretical consideration, the discussion of tendon friction is included in the discussion of post-tensioning methods (Chapter 16).

Tendon friction can result in substantial losses of stress, and for this reason, particularly in the design of continuous structures, the designer must select a tendon layout that will minimize friction losses. The designer should estimate the friction loss as various layouts are studied; and if high losses are both significant and unavoidable, the design should be made on the basis of a variable prestressing force.

The use of sharp bends or abrupt changes of slope in the tendon generally is avoided, as these features can result in significant secondary bending stresses in the tendon.

The angular change through which the tangent to a post-tensioned tendon passes has an important influence on the friction loss that occurs during stressing. Larger losses result from the larger curvatures. From this standpoint, a tendon layout composed of two chords is theoretically preferable to a second-degree parabolic layout because the angular change with a parabola is twice that of the angular change obtained with chords.

In short-span, continuous prestressed structures, the dead load of the structure is small in comparison to the live load; and if the structure is subjected to a

moving live load, the critical sum of the maximum and minimum moments is nearly the same as the simple beam moment for the same span. Therefore, the prestressing force required for short-span continuous structures is not significantly less than that required for a simple span. This greatly reduces the economy of materials that one would normally expect from the use of continuity. The advantages of less deflection and greater resistance to lateral and longitudinal loads, among others, are still attained through the introduction of continuity in short-span structures.

When the dead-load moment is a large portion of the total moment, the variation in moment in a continuous beam is less than is found in simple beams, and, for this reason, the prestressing force is less for the continuous structure. This accounts for the fact that continuity is used on long-span bridge structures to a much greater degree than on short-span bridges.

The same general procedures of design and analysis that have been presented in this chapter are used in designing prestressed-concrete rigid frames. In such construction, special attention must be given to the moments that result from axial shortening of the members due to prestressing, creep, shrinkage, and temperature effects.

10-9 Effect Topology Change

In Sec. 10-1 it was pointed out that changes in topology (configuration) of statically indeterminate structures constructed with prestressed concrete can result in significant time-dependent changes in their internal moments and shear forces. This is best explained by considering the example of a bridge constructed in cantilever, as is shown during construction and after completion in Fig. 10-20. The method consists of constructing the bridge superstructure in a series of pieces commonly called segments, as shown in Fig. 10-20b. The segments can be constructed in place (cast-in-place segmental construction), or segments can be used that are precast at a location other than their final location, after which they are transported to the structure and set in place (precast segmental construction). With this type of construction, the structure is built in one topology, a simply supported cantilevered structure, that ultimately is changed to another topology, a statically indeterminate continuous beams (or frame) structure. To understand how this affects the moments and shear forces in the structure, consider the fixed-end cantilevered beams shown in Fig. 10-21a. After the cantilevered beams are constructed, but before the cast-in-place closure joint is constructed, the cantilevered spans have the deflected shape shown in Fig. 10-21b. If the cantilevers were not connected to each other by the cast-in-place closure joint for a long period of time, the deflection of the cantilevers would increase because of the effect of concrete creep, as shown in Fig. 10-21c; and during this period the ends of the cantilevers would experience time-dependent

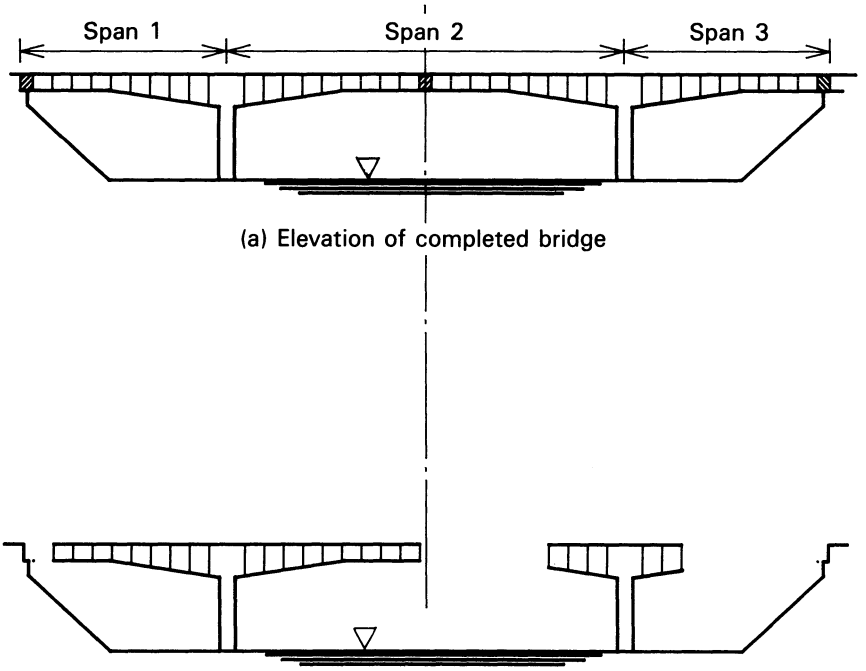

Fig. 10-20. Principle of erecting bridges segmentally in cantilever. (a) Elevation of completed structure. (b) Elevation during construction.

rotations, as shown in Fig. 10-21d. Casting the closure joint between the ends of the cantilevers completes the construction and provides restraint against further rotation of the ends of the cantilevers. The restraint results in a concrete-creep-induced positive moment in the completed fixed-end beam, and the creation of the positive moment in the span is accompanied by a reduction of the negative moments at the supports. The amount of the positive moment introduced into the completed beam is dependent upon the amount of concrete creep that has occurred before the restraint is introduced. If the restraint is not applied until the cantilevers are very old and virtually all of the creep has taken place, the amount of the positive moment introduced will be very small. If, on the other hand, the cantilevers are completely erected very rapidly and the closure joint concrete is placed and cured before very much concrete creep has taken place in the cantilevers, the amount of positive moment introduced will be significant, approaching the amount that would have existed had the structure been built in its final topology (Ketchum 1986).

The introduction of creep-induced moment into structures due to changes in topology is not limited to bridges constructed in cantilever. It occurs to varying

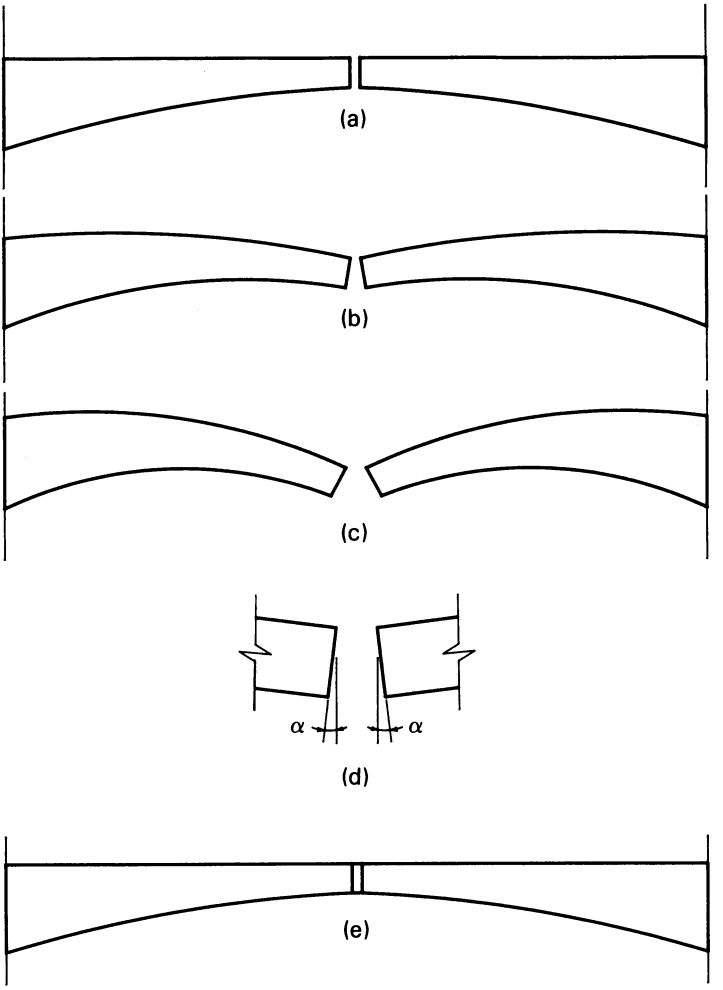

Fig. 10-21. Illustration of the redistribution of moments in a structure erected in a topology different from the final one. (a) Two cantilever spans without deflection. (b) Elastic deflection of cantilevers before closure joint is placed. (c) Deflection of cantilevers that would occur with the passage of time if the closure joint were not placed. (d) Rotation at the ends of the cantilevers due to time-dependent effects of concrete creep and shrinkage and relaxation of the prestressed reinforcement. (e) Completed fixed-end beam constructed in cantilever.

degrees in bridges and buildings constructed with precast, prestressed concrete beams and girders that are made continuous for superimposed dead loads and live loads by the provision of nonprestressed reinforcement in cast-in-place slabs cast over the tops of the beams. It occurs in bridges constructed with the span-

by-span method of erection if the spans are made continuous after erection, in bridges constructed with precast sections erected by the push-on method of erection, and in other sophisticated methods of constructing and erecting concrete structures.

The moments induced into structures by changes in topology, such as the positive moments described for the bridge built in cantilever, can be analyzed by using the time-dependent methods of analysis described in Chapter 7 for computing loss of prestress and deflection of prestressed-concrete flexural members. The same basic principles of determining time-dependent changes of strain and rotation used in determining losses of prestress and deflections are used in determining moments induced by changes in topology. The computations however, are, tedious, time-consuming, and best done with the aid of a computer (Ketchum 1986).

REFERENCES

ACI Committee 318. 1989. *Building Code Requirements for Reinforced Concrete.* Detroit. American Concrete Institute.

Guyon, Y. 1956. The Strength of Statically Indeterminate Prestressed Concrete Structures. *Proc.* of a Symposium on the Strength of Concrete Structures. 305.

Ketchum, M. A. 1986. Redistribution of Stresses in Segmentally Erected Prestressed Concrete Bridges. Report No. UCB/SESM-86107. Berkeley. Department of Civil Engineering, University of California.

Saeed-Un-Din, K. 1958. The Effect of Creep upon Redundant Reactions in Continuous Prestressed Concrete Beams, *Magazine of Concrete Research* 10(109).

PROBLEMS

1. A slab 8.333 ft long has straight haunches at each end as shown in Fig. 10-6. The slab is rectangular in cross section and is solid. The slab depth is 14 in. at each end and 7 in. for the central 3.33 ft. The length of each haunch is 2.50 ft. The top surface of the slab is level. If the slab is to be prestressed with a straight tendon that is parallel to the top surface of the slab, determine where the tendon must be placed if secondary moments due to prestressing are to be avoided.

SOLUTION:

Assume a trial location, such as at 3.50 in. from the top surface, that results in no eccentricity in the center portion of the slab, and compute the rotations at the ends of the slab. Compute the moment required at each end of the slab required to cause an equal but opposite rotation at each end of the slab. This moment is the secondary moment for the tendon positioned at the trial location. The trial location should be adjusted by an amount equal to M_{sec}/P. Adding

this adjustment to the trial location will give the location of the concordant tendon. The results can be checked by computing the rotation at the ends of the member with the adjusted tendon location; there should not be any rotations at the ends. In this case, the correct location is 4.55 in. from the top of the slab.

2. A prismatic beam has five equal continuous spans of 50 ft each. It is prestressed by a straight tendon located at an eccentricity of e_{ps} below the centroidal axis of the beams. Determine the location of the pressure line for prestressing alone.

SOLUTION:

The pressure line locations in terms of e_{ps} are as follows:

End supports: $+1.00$ in. (below the centroidal axis of the members).
First interior supports: -0.263 in. (above the centroidal axis).
Second interior supports: $+0.053$ in. (below the centroidal axis).

11 Direct Stress Members, Temperature, and Fatigue

11-1 Introduction

The first part of this chapter is devoted to a discussion of prestressed members subject to direct stress. Except for rock and soil anchors and piles, prestressed concrete is not used extensively for members that are designed primarily to resist direct stress.

The second part is devoted to a consideration of fire resistance, the effect of nominal temperature variations, and fatigue of prestressed concrete.

11-2 Tension Members

The use of rigid frames, trusses, certain types of continuous beam framing, soil-retaining anchored bulkheads (both temporary and permanent), and other types of structures frequently requires structural components that are basically subject to direct tensile stress alone. These members are frequently referred to as tension ties or more simply as ties. The cross sections of two prestressed concrete ties are shown in Fig. 11-1. For reasons of economy or function, or simply to facilitate construction, it may be preferable to use concrete ties with prestressed reinforcement rather than ties made of nonprestressed reinforced concrete or structural steel.

Prestressed concrete ties can be proportioned to have controlled deformations

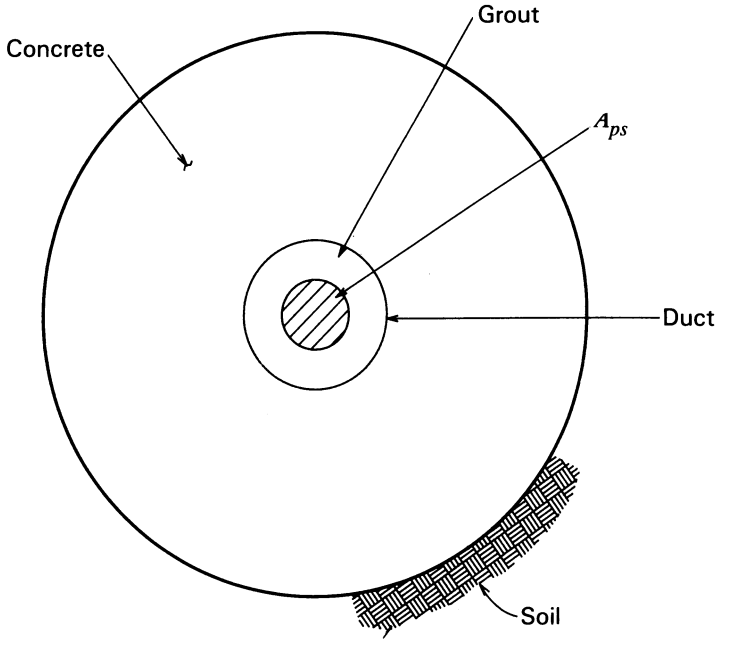

Fig. 11-1. Cross sections of prestressed concrete tension ties. (a) Prestressed concrete soil anchor. (b) Square concrete tension tie with nonprestressed confinement reinforcement, and longitudinal prestressed and nonprestressed reinforcement.

in a way not possible with steel or nonprestressed reinforced concrete. For example, steel or reinforced-concrete ties normally are designed with a stress in the steel of the order of 20,000 psi under service load. If the modulus of

elasticity of the steel is to be 29×10^6 psi, the deformation of a tie having a length of 1000 in. and stress of 20,000 psi would be:

$$\Delta L = \frac{20{,}000 \times 1000}{29 \times 10^6} = 0.69 \text{ in.}$$

If for some reason this amount of deformation is not acceptable, it could be reduced through the use of a lower allowable stress. The use of a lower stress would, of course increase the quantity of steel and the cost of the tie.

Alternatively, the concrete section of a prestressed concrete tie can be proportioned to control the stress in the concrete. Hence, the service load deformation of the tie can be restricted to any desired limits without requiring an increase in the quantity of the prestressed reinforcement over the amount needed to resist the service load. If the modulus of elasticity of the concrete in a tie is 4×10^6 psi, and the concrete stress due to the effective prestress alone is 2000 psi, the deformation of a tie 1000 in. long under full load (concrete stress being nil under full load) would be:

$$\Delta L = \frac{2000 \times 1000}{4 \times 10^6} = 0.50 \text{ in.}$$

By restricting the stress in the concrete due to prestressing to a lower limit, the deformation can be reduced to any desired quantity. If, for example, it is determined that the maximum deformation that can be permitted is 0.25 in. in a prestressed concrete tie 1000 in. long with an effective concrete stress of 2000 psi, the area of the concrete in the prestressed tie could be doubled. By this means, the stress in the concrete would be reduced to 1000 psi, and the deformation would become 0.25 in.

The use of prestressed ties in exposed roof trusses may be preferred over the use of steel ties because of the greater fire resistance and more acceptable appearance inherent in reinforced concrete members, as compared to unprotected steel members.

With correct proportioning, prestressed concrete ties can remain crack-free under service loads and thus less subject to deterioration by corrosion than ties having nonprestressed reinforcement. Therefore, in some applications prestressed concrete ties may be preferred over concrete ties having nonprestressed reinforcement or structural steel ties encased in concrete or other protective materials.

In using prestressed concrete ties, the designer must include the effects of concrete creep and shrinkage, in addition to elastic deformation, in evaluating the total deformation of the tie. If the tie were prestressed and immediately thereafter put into service, assuming the superimposed load and the prestressing force to be very nearly equal, the concrete stress in the tie would be near zero, and there would be little deferred deformation due to creep; shrinkage would

exist, however, and should be carefully evaluated in applications where corrosion of the reinforcement is of concern.

If a prestressed concrete tie were to be precast, prestressed, and stored for a period of time before being placed in service, a substantial amount of the concrete creep and shrinkage deformation would take place before its installation. For service loads of short duration applied after its installation, the tie would elongate in proportion to the modulus of elasticity of the concrete at the age when the load was applied. If the service load were to be held at a constant value that nullified the effective prestressing force, the concrete stress would be reduced to near zero, and no creep deformation would take place with the passage of time (additional concrete shrinkage would occur, however). Upon the removal of the load, an elastic shortening, in proportion to the elastic modulus of the concrete at the time when the load was removed, would take place. Furthermore, a partial recovery of the creep deformation would take place with the passing of time.

Accurate prediction of the amount of deferred strain that would be recovered upon removal of the load can be made only if the properties of the concrete are known. The strain is generally lower, however, for unloading than it is for loading, and a residual strain normally remains in the concrete after unloading. This is illustrated in the strain–time diagram of Fig. 11-2 (Guyon 1953).

The total strains occurring in a concrete of a particular quality, subjected to constant sustained stresses applied at different loading ages, are as illustrated in Fig. 11-3 (Ross 1958). Using the principles of superposition, one can employ curves like these to estimate creep effects with different concrete ages at the time of loading. For example, assume that a unit stress of 1000 psi is applied at the age of 28 days and held constant until the age of 91 days, at which time

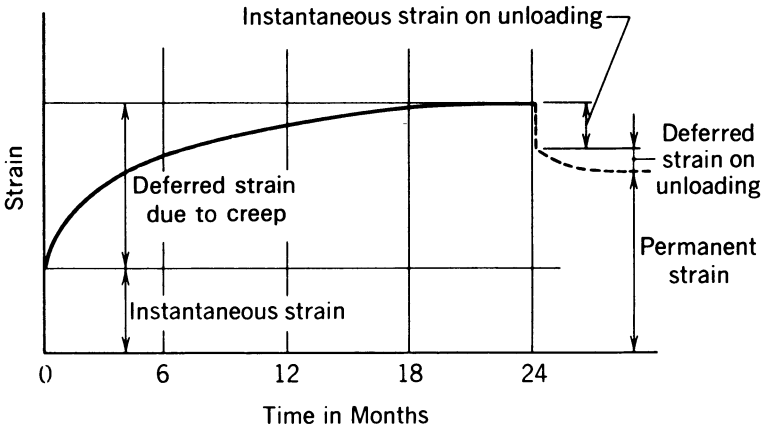

Fig. 11-2. Concrete strains under long-term loading and unloading.

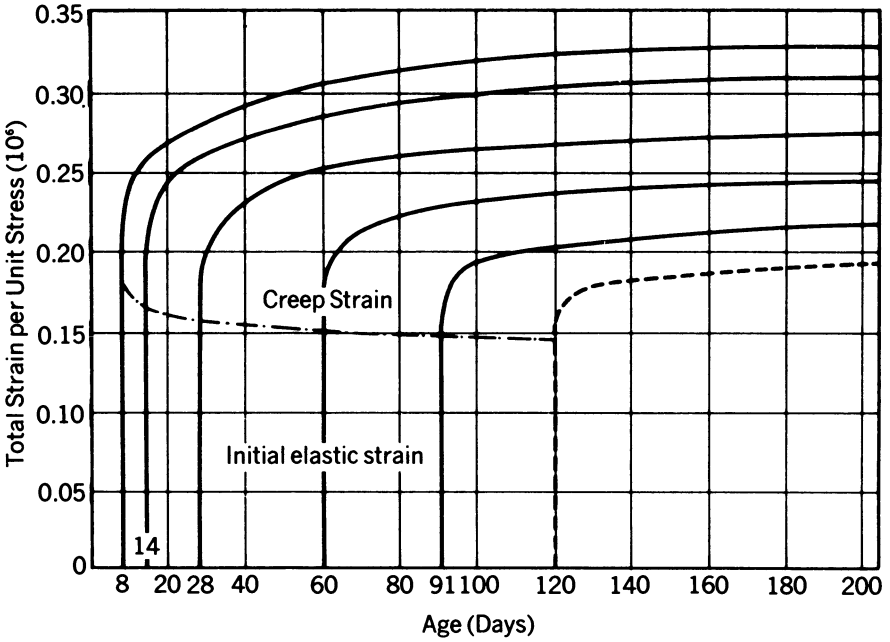

Fig. 11-3. Total strain due to constant sustained stress applied at various ages to a high-strength concrete stored at high humidity (after Ross).

it is completely removed. The strain–time diagram would be as in Fig. 11-4. The curve of Fig. 11-4 is constructed by using the curves from Fig. 11-3 with the assumption that the strain deformations upon loading and unloading at any particular age of the concrete take place at the same rate, are of the same magnitude, and are of opposite sign.

It should be apparent that as the service load applied to a prestressed concrete tie is increased, the concrete stress is reduced and the steel stress is increased in direct proportion to the strain change in the concrete. Because the elastic modulus of concrete in tension normally is taken to be the same as in compression, the action will continue until the tensile strength of the concrete is reached, at which time the concrete will crack, and the entire load must thereafter be carried by the reinforcement alone. If the load subsequently is reduced below the value of the effective prestress in the reinforcement at the time when the load is removed, the cracks in the concrete will close, and a compressive force, equal to the difference in the effective prestressing force in the reinforcement and the service load, will exist in the concrete.

If the load resisted by the concrete in a prestressed concrete tie immediately prior to cracking is greater than the tensile strength of the reinforcement, the cracking load will be the ultimate load (provided that the deformation required

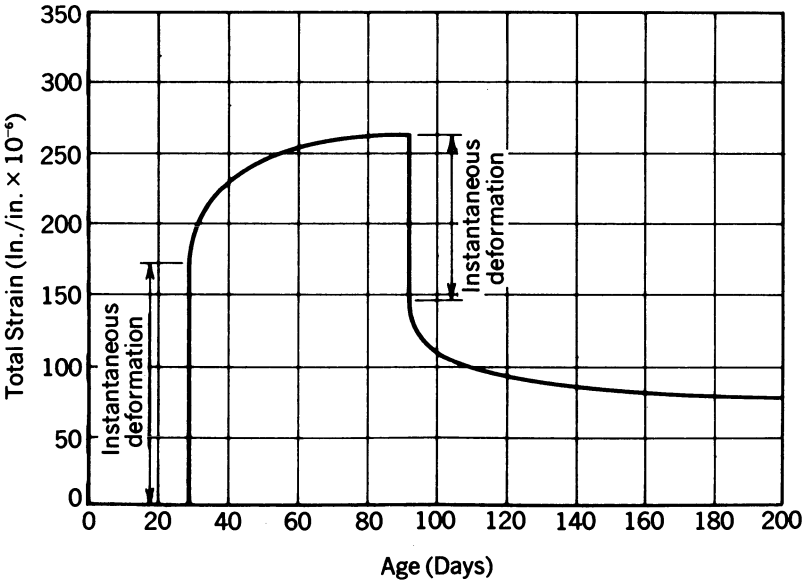

Fig. 11-4. Strain versus time diagram for concrete having creep characteristics as in Fig. 11-3, loaded to 1000 psi at the age of 28 days and unloaded at the age of 91 days.

to rupture the reinforcement can be achieved and not prevented by redundancy in the structure). This condition is more apt to exist in members prestressed with small percentages of reinforcement, as discussed for flexural members in Sec. 5-1.

Consideration of the action of prestressed ties and of the elastic and inelastic properties of concrete leads one to conclude that the designer must consider the stress level in the concrete and the duration of the applied loads in estimating the eventual deformations that will be achieved in prestressed concrete ties. The tie deformations can be large and can result in a serious deflection of the structure that they are provided to support. Such deformation could result in important, undesirable stresses or deformations in the supported structure.

11-3 Columns and Piles

Prestressed concrete members axially loaded in compression are designed by using the same principles of strain compatibility and equilibrium used in the design and analysis of concrete members having nonprestressed reinforcement. Section 18.11 of ACI 318 provides that members with an effective prestress less than 225 psi must have the minimum amount of nonprestressed reinforcement specified for concrete columns having nonprestressed reinforcement. There is

no minimum amount of nonprestressed reinforcement required for columns having an effective prestress of 225 psi or more.

Prestressed reinforcement in axially loaded compression members is required to be enclosed either by ties, spaced at the least dimension of the column but not more than 48 tie diameters, or by spirals that conform to the minimum requirements for nonprestressed reinforced concrete columns (see Sec. 18-11, ACI 318). Larger amounts of transverse reinforcement should be provided near the ends of compression members because it is at these location that splitting and shear stresses normally are the greatest, and cracking is most likely to occur.

Strength (sometimes referred to as ultimate strength) interaction diagrams can be constructed for prestressed concrete members by using the principles of strain compatibility and equilibrium. These diagrams, which graphically represent the relationship between the axial load and moment capacities of the members, typically are of the shape shown in Fig. 11-5. The figure shows that they are similar to interaction diagrams for concrete columns having nonprestressed reinforcement.

An interaction diagram can be drawn for each different column configuration. A diagram's construction is a function of the dimensions of the concrete section, the amount of the prestressed and nonprestressed reinforcements, and the physical properties of the materials. To make an interaction diagram, one preferably should have stress–strain diagrams for the prestressed and nonprestressed reinforcements to be used in the column.

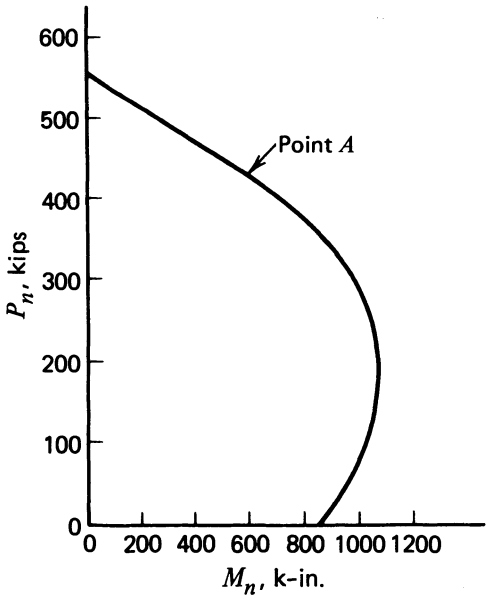

Fig. 11-5. Interaction diagram for the 14 in. square pile of I.P. 11-1.

The intersection of the interaction curve with the ordinate is the compressive strength capacity of the column under concentric load. It usually is taken to be the strength of the column when it is subjected to a uniform strain in the concrete of 0.002. The point of maximum moment capacity of the column is sometimes referred to as the balanced point. The balanced point defines the combination of axial load and moment at which crushing of the concrete in the compression flange and yielding of the longitudinal reinforcement in the tension flange will occur simultaneously. The point on the curve where the axial load is equal to zero is the flexural capacity of the section.

The capacity reduction factors specified in Sec. 9-3 of ACI 318 apply to axially loaded prestressed concrete members as well as to members that do not have prestressed longitudinal reinforcement. When the axial loads are greater than that at the balanced point, for members with normal ties for confinement reinforcement, ACI 318 provides that the capacity reduction factor (ϕ) be taken as 0.70. If spiral confinement reinforcement is used, ϕ can be taken as 0.75. The value of ϕ is permitted to vary linearly from 0.70 at the balanced point to 0.90 for zero axial load. The latter provision acknowledges that under a condition of bending alone the value of ϕ is specified to be 0.90 (ACI 318).

From Fig. 11-5, it can be observed that the interaction diagram is nearly linear for the higher values of axial load (the portion of the curve between its intercept with the ordinate and point A). For structural design computations, it is sufficiently accurate to assume that this portion of the curve is linear even though it actually has slight curvature.

The interaction curve can be constructed by computing the axial load and moment capacity of a section under different distributions of strain across the section. The assumed strains to be used are shown in Fig. 11-6, where the distribution of strain is given for three unique conditions. The first of these, which is for the condition of no moment on the section (i.e., $M_n = 0$, and P_n is equal to its maximum value), has uniform strain equal to ϵ_0 across the section (Fig. 11-6a). The second strain distribution is triangular in shape, as shown in Fig. 11-6b, and varies from nil on one face of the section to a value of ϵ_u on the other face. The third distribution of strain is for the condition of tensile strain on one face and ϵ_u on the other (Fig. 11-6c).

For the condition shown in Fig. 11-6a, the section is under uniform stress and strain because the section is under axial load alone. The reinforcement and the concrete are assumed to be perfectly bonded and stressed in the elastic range. The application of the axial force results in a reduction in the force in the prestressed reinforcement equal to:

$$\Delta f_{ps} = \epsilon_0 E_{ps}$$

where ϵ_0 is negative because it is a strain due to a compressive stress (i.e., a shortening). The forces in the prestressed reinforcement on the tensile and

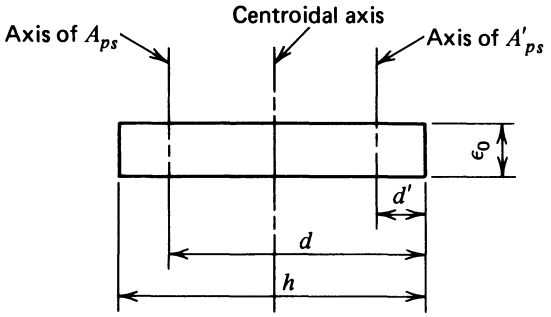

(a) Strain Distribution Assumed for Interaction Curve Point at $M_u = 0$

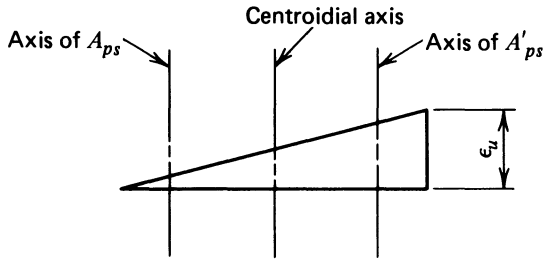

(b) Strain Distribution Assumed for Interaction Curve at Point A

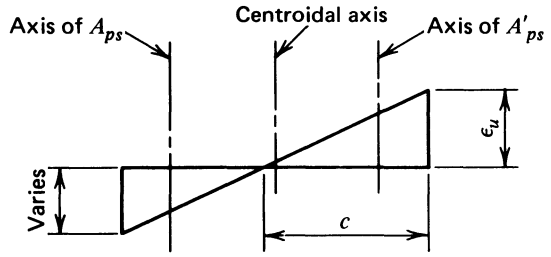

(c) Strain Distribution for Points Between Point A and Where $P_u = 0$

Fig. 11-6. Strain distributions for use in preparing interaction curves.

compressive sides of the centroidal axis are equal (for symmetrical reinforcement), and are:

$$T_T = A_{ps}(f_{ps} - \Delta f_{ps})$$

and:

$$T_C = A'_{ps}(f_{ps} - \Delta f'_{ps})$$

The strength of the concrete is taken to be $0.85f'_c$, and:

$$C_u = 0.85f'_c bh$$

where b and h are the width and depth of the concrete section, respectively. The nominal axial force strength of the section for this condition of strain becomes:

$$P_n = C_u - T_T - T_C$$

For the condition of strain shown in Fig. 11-6b, the changes in the steel stresses on the tension and compression sides of the section, respectively, become:

$$\Delta f_{ps} = \frac{\epsilon_u}{h}(h - d)E_{ps}$$

$$\Delta f'_{ps} = \frac{\epsilon_u}{h}(h - d')E_{ps}$$

and the forces in the prestressed reinforcement are:

$$T_T = A_{ps}(f_{ps} - \Delta f_{ps})$$

and:

$$T_C = A'_{ps}(f_{ps} - \Delta f'_{ps})$$

The strength of the concrete is:

$$C = 0.85\beta_1 f'_c bh$$

where β_i, as explained in Sec. 5-4, is equal to 0.85 for specified concrete strengths of 4000 psi or less, and is reduced at the rate of 0.05 for each 1000 psi in strength in excess of 4000 psi, with a minimum value of 0.65. From the above, using the principle of equilibrium, one can write:

$$P_n = C - T_T - T_C$$

and:

$$M_n = C\left(\frac{h}{2} - 0.42h\right) + T_T(d - h/2) + T_C(h/2 - d')$$

The distance $0.42h$ in the above equation is used for the location of the resultant of the concrete compressive force measured from the fiber having the ultimate strain, rather than $0.33h$, to account for the inelastic behavior of concrete at high stress levels.

For the case where tensile strains exist, as shown in Fig. 11-6c, the stress for a particular strain in the reinforcement must be determined from the stress–strain curve for the reinforcement. The strains in the reinforcements on the tensile and compressive sides of the section are determined from:

$$\epsilon_{ps} = \epsilon_{pse} + \epsilon_u \frac{d - c}{c}$$

and:

$$\epsilon'_{ps} = \epsilon_{pse} + \epsilon_u \frac{c - d'}{c}$$

where ϵ_{pse} is the strain in the prestressed reinforcement due to the effective stress at the time under study. The force in the tendons on the tensile side becomes:

$$T_T = f_{ps} A_{ps}$$

in which f_{ps} is the steel stress corresponding to a strain of ϵ_{ps} from the stress–strain curve for the prestressing steel. On the compression side, the steel continues to perform elastically and:

$$T_C = A'_{ps}\left[f_{se} - E_{ps}\epsilon_u\left(\frac{c - d'}{c}\right)\right]$$

The force in the concrete section becomes:

$$C = 0.85\beta_1 f'_c bc$$

and P_n is:

$$P_n = C - T_T - T_C$$

The moment is:

$$M_n = C(h/2 - 0.42c) + T_T(d - h/2) - (h/2 - d')$$

For the case of pure bending ($P_n = 0$), one needs to perform the nominal flexural strength analysis of the member. This is more easily done by direct solution, using the principles described in Secs. 5-2 and 5-4, rather than by trial and assuming different configurations for the distribution of strain.

The procedure described above is for the case of a rectangular column with the reinforcement confined to two rows—one in the compression side and one in the tension side of the column. The basic principles can be used for columns with more than two rows of steel.

Interaction diagrams for circular prestressed-concrete columns can be made by following the same general methods described above for rectangular columns. The relationship for the force in the concrete, based upon work done by the

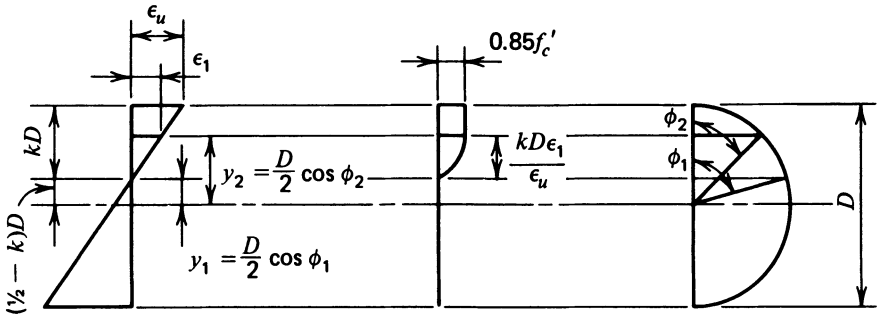

Fig. 11-7. Data for analysis of circular columns.

Portland Cement Association (1960) and the terms shown in Fig. 11-7, is:

$$C_c = \frac{0.85f_c'D^2}{2}\left(\frac{\phi_1}{2} - \frac{1}{4}\sin 2\phi_1 - \frac{1}{(1.134k)^2 j}\left\{\cos^2\phi_2\left[\frac{\phi_1 - \phi_2}{2} - \frac{1}{4}(\sin 2\phi_1 - \sin\phi_2\right] - \frac{2}{3}\cos\phi_2\,(\sin^3\phi_1 - \sin^3\phi_2) - \frac{1}{32}(\sin 4\phi_1 - \sin 4\phi_2 - 4\phi_1 + 4\phi_2)\right\}\right)$$

and the relationship for the moment in the concrete is:

$$M_c = \frac{0.85f_c'D^3}{4}\left\{\frac{1}{3}\sin^3\phi_1 - \frac{1}{(1.134k)^2}\left[\frac{\cos^2\phi_2}{3}(\sin^3\phi_1 - \sin^3\phi_2) + \frac{\cos\phi_2}{16}(\sin 4\phi_1 - \sin^2 4\phi_2 - 4\phi_1 + 4\phi_2) + \frac{\cos^2\phi_1\sin^3\phi_1 - \cos^2\phi_2\sin^3\phi_2}{5} + \frac{\sin^3\phi_1 - \sin^3\phi_2}{7.5}\right]\right\}$$

As will be seen from Fig. 11-7 the angles ϕ_1 and ϕ_2 are functions of the strain distribution and the cross section of the column. The angle ϕ_1 varies with the distance between the neutral axis and the centroid of the column. Note that cos $\phi_1 = (1 - 2k)$ when k is less than 1. The angle ϕ_2 is equal to π when k is greater than 1. The angle ϕ_1 is defined by the point on the strain diagram where the strain is equal to 0.0017 in./in. From Fig. 11-7 it will be seen that:

$$y_2 = \left(\frac{1}{2} - k\right)D + kD\frac{\epsilon_1}{\epsilon_u} = D\left[\frac{1}{2} - k + k\frac{\epsilon_1}{\epsilon_u}\right]$$

and:

$$\cos \phi_2 = \frac{1}{2} - k + k \frac{\epsilon_1}{\epsilon_u}$$

The value of P_n for $M_n = 0$ should be computed by using a concrete strain of 0.002, as was done for the rectangular column. Other points on the diagram can be found by using the maximum flexural strain of 0.003. The effects of the prestressed reinforcement, for both forces and moments, should be treated in the same manner as they are with rectangular sections.

It should be recognized that prestressed-concrete columns have lower axial load capacities than do reinforced-concrete columns. The prestressing force causes compressive stresses in the concrete and thus reduces its capacity to carry externally applied axial load. In nonprestressed reinforced-concrete columns, the reinforcement is stressed in compression, and thus assists the concrete in resisting axial load.

The effects of slenderness must be considered in the design of prestressed-concrete columns. This can be done by using the approximate methods contained in Sec. 10.11 of ACI 318 or by using a time-dependent analysis that employs the fundamental principles used by Ghali in his methods of computing the loss of prestress and deflection of prestressed concrete members (see Chapter 7). A nonlinear procedure for the analysis of slenderness effects for long concrete columns, using the Ghali approach to the analysis of prestressed concrete members for stress, strain, and deflection, has been developed by Gilbert and Mickleborough. This approach involves an iterative procedure that employs the age-adjusted effective modulus of the concrete and can be applied to cracked as well as noncracked sections. The procedure gives a means of investigating the effects of sustained loading (i.e., the charge in deflection that occurs as a result of deferred strains) on the $P(\delta + \Delta d)$ effect. A computer program has been developed to facilitate the analysis (Gilbert and Mickleborough 1989).

ILLUSTRATIVE PROBLEM 11-1 Construct the interaction curve for a square column having sides 14 in. long, an effective depth, d, of 11.5 in. to the tensile reinforcement, and a depth, d', of 2.5 in. to the compression reinforcement. The column is prestressed with four 0.5 in. strands, two on the tension side and two on the compression side of the member. The ultimate tensile strength of the prestressed reinforcement is 270 ksi, the effective stress in the prestressed reinforcement before the application of external load is 160 ksi, and the elastic modulus is 28,000 ksi. The capacity reduction factor is to be taken as 0.70 for loads greater than the balanced load, and is to vary linearly from 0.70 to 0.90 between the balanced load and zero load capacity. Assume $\epsilon_0 = 0.002$, $\epsilon_u = 0.003$, $f'_c = 5000$ psi, and $\beta_1 = 0.80$.

SOLUTION: For the case of a concentric load:

$$\Delta f_{pse} = \Delta f'_{pse} = (0.002)(28{,}000) = 56 \text{ ksi}$$

$$T_T = T_C = (2)(0.153)(160 - 56) = 31.8 \text{ k}$$

$$C = (0.85)(5)(14)(14) = 833 \text{ k}$$

$$P_n = 833 - (2)(31.8) = 769 \text{ k}$$

For the case of zero strain in the concrete on the tensile side and ϵ_u strain in the concrete on the compression side:

$$\Delta f_{pse} = 0.003\left[\frac{14.0 - 11.5}{14}\right]28{,}000 = 15.0 \text{ ksi}$$

$$\Delta f'_{pse} = 0.003\left[\frac{14.0 - 2.5}{14}\right]28{,}000 = 69.0 \text{ ksi}$$

$$T_T = (2)(0.153)(160 - 15.0) = 44.37 \text{ k}$$

$$T_C = (2)(0.153)(160 - 60.0) = 27.85 \text{ k}$$

$$C = (0.80)(0.85)(5)(14)(14) = 666.4 \text{ k}$$

$$P_n = 594.2 \text{ k}$$

$$M_n = 666.4[7.0 - (0.42)(14)] + 44.4(11.5 - 7.0) - (27.8)(7.0 - 2.5) = 821.0 \text{ k-in.} = 68.4 \text{ k-ft}$$

For the case of tensile strain on the tensile side of the section, and $\epsilon_u = 0.003$ on the compressive side, with the strain in the prestressed reinforcement due to the prestress alone being equal to $160 \div 28{,}000 = 0.00571$, the strains in the reinforcement on the tension and compression sides become:

$$\epsilon_{ps} = 0.00571 + 0.003\left[\frac{11.5 - c}{c}\right]$$

$$\epsilon'_{ps} = 0.00571 - 0.003\left[\frac{c - 2.5}{c}\right]$$

The stress in the reinforcement on the tension side must be determined from the stress–strain curve for the reinforcement being used. Assuming that the relationship between the stress and strain in the reinforcement can be taken to be as shown in Fig. 11-8, the stress in the reinforcement on the tensile side is easily determined for a particular strain. The results of the computations are summarized in Table 11-1 and shows plotted in Fig. 11-5. (The stress–strain

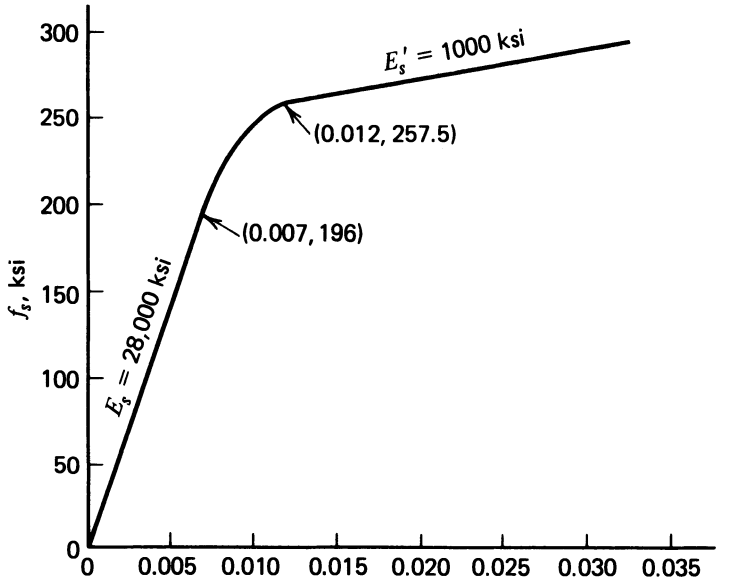

Fig. 11-8. Stress–strain curve for prestressed reinforcement used in I.P. 11-1.

TABLE 11-1 Summary of Computations for I.P. 11-1.

	$P_0 = 769.352\ k$		$.70 \times P_o = 538.546\ k$		
c (in.)	p_n (k)	M_n (k-ft)	ϕP_n	ϕM_n	ϕ
14.000	594.184	68.393	415.928	47.875	.700
13.300	559.511	81.120	391.657	56.784	.700
12.600	524.688	92.250	367.281	64.575	.700
11.900	489.688	101.791	342.781	71.253	.700
11.200	454.478	109.749	318.134	76.824	.700
10.500	419.016	116.135	293.311	81.294	.700
9.800	383.248	120.962	268.273	84.673	.700
9.100	347.103	124.248	242.972	86.973	.700
8.400	310.488	126.014	217.341	88.210	.700
7.700	272.284	126.663	192.238	89.426	.706
7.000	235.960	124.870	172.851	91.473	.732
6.300	199.878	121.215	151.721	92.010	.759
5.600	163.608	115.806	128.529	90.976	.785
4.900	126.899	108.656	103.057	88.241	.812
4.200	89.453	9.739	75.019	83.646	.838
3.500	51.369	88.774	44.442	76.804	.865
2.800	12.705	75.246	11.329	67.096	.891
2.580	.000	59.126	.000	53.213	.900

$M_{u\max} = 126.752$ k-ft at $c = 7.858$ in. $0.70M_{u\max} = 88.726$ k-ft.

curve for the prestressed reinforcement in this example is an arbitrary curve selected for the purpose of this problem and should not be used in actual design.)

Prestressed-concrete piles have been used extensively in the United States. The types of piles can be divided into three classifications: (1) cylinder piles, (2) pretensioned, precast piles, and (3) pretensioned spun piles, which are described as follows (PCI 1985):

1. Post-tensioned, multielement cylinder piles are made by precasting hollow cylinders of concrete in sections about 16 ft long with wall thickness of 5 in. or more. Holes are formed longitudinally in the walls when the sections are cast. After the precast sections have cured, they are aligned, and post-tensioning tendons are threaded through the holes in the walls, after which they are stressed and grouted. In this manner, piles up to 150 ft long have been made. Cylinder piles also are made with pretensioned reinforcement. In this process, the piles are cast either in conventional molds (wet-cast) or in traveling molds that slipform the hollow sections. Cylinder piles normally are made in diameters from 36 to 54 in. and have been used with service loads up to 550 tons. The hollow shape is efficient for resisting axial loads, as well as for resisting bending moments that may be applied from any direction. Typical details and dimensions for cylinder piles are given in Fig. 11-9.
2. Pretensioned, precast piles have been made with square, rectangular, triangular, hexagonal, octagonal, and round—both hollow and solid—cross sections. Pretensioned piles have been used extensively in the construction of waterfront structures. They are made with the normal procedures used in pretensioned construction. This type of pile has been used more than cylinder or spun piles have. Typical details and dimensions of square and octagonal prestressed piles are shown in Figs. 11-10a and 11-10b. It should be noted that the capacities in Figs. 11-10a and 11-10b are based upon stress and not on strain. The capacities listed in the figures should not be used in actual applications until an analysis has been made of the effects of slenderness, secondary moments due to deflection, and the potential for buckling for the actual conditions anticipated for the proposed use.
3. Pretensioned spun piles are made in individual molds designed to resist the pretensioning force during the casting and curing of the pile. The manufacturing procedure consists of placing the tendons and reinforcing cage in steel molds, stressing the tendons, and placing the mold on revolving wheels that turn the mold as the concrete is placed. The centrifugal force compacts the concrete and forces the excess water from the plastic concrete. The pile is then cured and stripped from the mold.

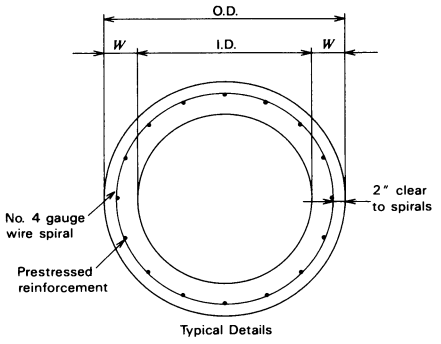

Typical Details

PILE PROPERTIES

Pile Size			Area A_c	Approx. Weight	Minimum Prestress Force (2)	Strands Per Pile Diameter (3)		Moment of/inertia	Section Modulus	Perimeter	Design Bearing Capacity (tons) Concrete Strength (4)	
OD in.	ID in.	W in.	sq in.	p/f (1)	kips	7/16"	1/2"	in.^{4}	in.^{3}	in.	5000 psi	6000 psi
36	26	5	487	508	414	24	18	60,000	3334	113	242	292
	24	6	565	590	481	28	21	66,100	3676	113	282	339
48	38	5	675	703	574	33	25	158,200	6593	151	337	405
	36	6	792	826	674	39	29	178,100	7422	151	396	475
54	44	5	770	802	655	38	28	233,400	8645	170	385	462
	42	6	904	940	769	44	33	264,600	9802	170	452	542

Fig. 11-9. Pretensioned cylinder pile cross section.

NOTES

(1). Weights are based on 150 lbs per cubic foot.

(2). Minimum prestressed force based on unit prestress of 850 psi after losses.

(3). Based on 7/16" and 1/2" strand with an ultimate strength of 31,000 lbs and 41,300 lbs respectively.

(4). Design bearing capacity based on 5000 psi and 6000 psi concrete and an allowable unit stress on the tip of the pile of $.2f'_cA_c$.

SQUARE PRESTRESSED PILES

Typical Details

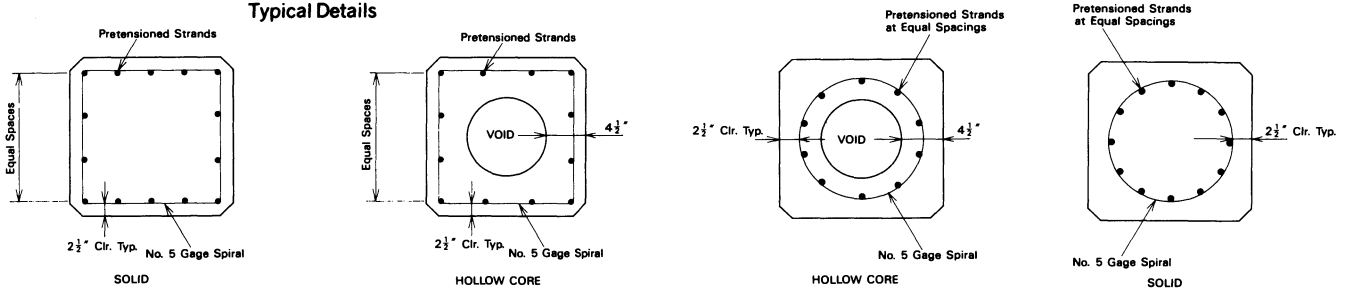

PILE PROPERTIES

Pile Size Diameter (1) in.	Area A_c sq in.	Approx. Weight p/f (2)	Minimum Prestress Force (3) kips	Strands Per Pile Diameter (4) 7/16"	Strands Per Pile Diameter (4) 1/2"	Section Modulus in.^{3}	Perimeter in.	Design Bearing Capacity (tons) Concrete Strength (5) 5000 psi	Design Bearing Capacity (tons) Concrete Strength (5) 6000 psi
10	100	105	70	4	4	167	40	50	60
12	144	150	101	6	5	288	48	72	86
14	196	205	133	8	6	457	56	98	117
16	256	265	180	11	8	683	64	128	153
18	324	335	227	13	10	972	72	162	194
20	400	415	280	16	12	1333	80	200	240
22	484	505	339	20	15	1775	88	242	290
24	576	600	404	23	18	2304	96	288	345
20 HC	305	320	214	13	10	1261	80	152	183
22 HC	351	365	246	14	11	1647	88	175	210
24 HC	399	415	280	16	12	2097	96	200	240

Fig. 11-10a. Typical pretensioned concrete pile cross sections. (See notes for the figure.)

OCTAGONAL PRESTRESSED PILES

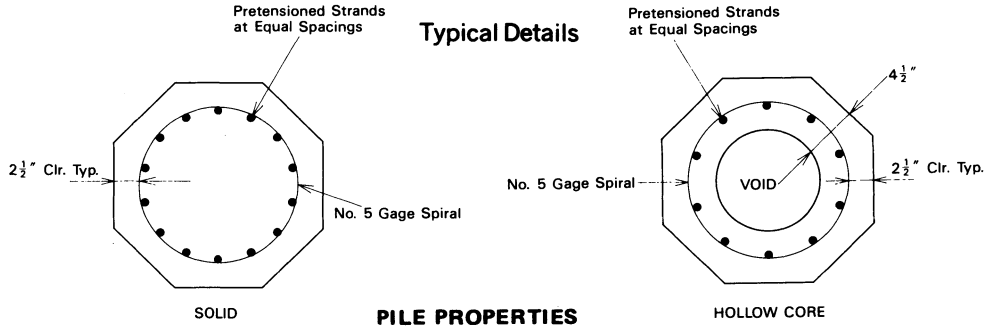

PILE PROPERTIES

Pile Size Diameter (1) in.	Area A_c sq in.	Approx. Weight p/f (2)	Minimum Prestress Force (3) kips	Strands Per Pile Diameter (4) 7/16"	Strands Per Pile Diameter (4) 1/2"	Section Modulus in.^{3}	Perimeter in.	Design Bearing Capacity (tons) Concrete Strength (5) 5000 psi	Design Bearing Capacity (tons) Concrete Strength (5) 6000 psi
10	83	85	59	4	4	111	34	41	50
12	119	125	84	5	4	189	40	59	71
14	162	170	114	7	5	301	46	81	97
16	212	220	149	9	7	449	54	106	127
18	268	280	188	11	8	639	60	134	160
20	331	345	232	14	10	877	66	165	198
22	401	420	281	16	12	1167	72	200	240
24	477	495	334	19	15	1515	80	238	286
20 HC	236	245	166	10	8	805	66	118	141
22 HC	268	280	188	11	8	1040	72	134	160
24 HC	300	315	210	12	9	1308	80	150	180

Fig. 11-10b. Typical octagonal pretensioned concrete pile cross sections. (See notes for the figure.)

Notes for Fig. 11-10 (for both square and octagonal piles)

1. Voids in 20 in., 22 in., and 24 in. diameter hollow-core (HC) piles are 11 in., 13 in., and 15 in. in diameter, respectively, providing a minimum $4\frac{1}{2}$ in. wall thickness. If a greater wall thickness is desired, properties should be increased accordingly.
2. Weights based on 150 pounds per cubic foot of regular concrete.
3. Minimum prestress force based on unit prestress of 700 psi after losses.
4. Based on $\frac{7}{16}$ in. and $\frac{1}{2}$ in. 270 grade strand with ultimate strengths of 31,000 pounds and 41,300 pounds, respectively. If 250 grade strand is used, the number of strands per pile should be increased in proportion to the ratio of strengths.
5. Design bearing capacity based on 5000 psi and 6000 psi concrete and an allowable unit stress on the tip of the pile of $0.20f'_c$. The bearing capacity values may be increased if higher strength concrete is used.

Fig. 11-10b. (*Continued*)

Prestressed-concrete piles have better driving characteristics than reinforced-concrete piles. The prestressed piles penetrate the soil better and with less effort. In addition, prestressed piles can be made longer than is practical with reinforced-concrete piles, because of their lower dead weight and higher resistance to bending moments.

Prestressed concrete sheet piles have been widely used on waterfront structures throughout the world. They generally are solid, are rectangular in cross section, and have tongue-and-groove joints formed in their edges to interlock them with adjacent piles in the completed structure. Prestressed concrete sheet piles normally are made with pretensioned reinforcement, but bonded post-tensioned reinforcement also has been used successfully.

The procedure used in the design of prestressed piles is no different from that employed in the design of columns that have axial load or combined axial load and bending. The amount of prestressing provided in the piles normally is controlled by handling stresses, but a minimum average prestress in the concrete of 700 psi is used to prevent the piles from cracking during driving. Such cracking has occurred on many projects, and is normally due to tensile stresses in the piles that result from the piles rebounding elastically from the driving hammer. This type of cracking is more likely to occur when driving is commenced (particularly in soft materials) and before significant tip resistance has developed. The cracking can be controlled by using techniques compatible with job-site conditions (Smith 1960).

11-4 Fire Resistance

Fire resistance, as determined by standard tests, has been used as a measure of the ability of a structural element to prevent the spread of fire and to retain structural strength at elevated temperatures. The fire resistance of a member generally is expressed in hours and is intended to be indicative of the length of time that the member can be subjected to a standard fire test without failing. Failure may result from the inability of the member to adequately perform in any one of these circumstances:

1. Walls, floors, and roof elements must not experience a temperature rise, on the side opposite to the fire, that would allow inflammable material to ignite by conduction.
2. Walls, floors, and roof elements must not permit flames, hot air, or gases to pass through the member and ignite or cause inflammable materials to ignite.
3. All structural members must retain sufficient strength at elevated temperatures to ensure the safety of the occupants as well as firefighters.
4. The elements must retain their structural integrity under the action of a

stream of water applied during or immediately after exposure to the standard fire test.

In detailing structural elements to resist the effects of fire, building designers traditionally have relied upon the fire resistance provision contained in the model building codes or fire ratings established by carefully controlled tests of actual structural elements. The concrete cover requirements for prestressed reinforcement, taken from Table No. 43-A of the 1988 edition of the Uniform Building Code and reproduced here as Table 11-2, are an example of commonly used data (ICBO 1988). The reader is advised to consult complete fire protection provisions in an appropriate edition of the model building codes for applicable requirements for each individual application of prestressed concrete.

Many types of prestressed concrete standard products, such as double-T slabs, cored slabs, and so on, have been tested for fire resistance and carry the approval of the various testing agencies. Manufacturers of prestressed concrete, the Prestressed Concrete Institute, and the Post-Tensioning Institute can provide specific data for different types of prestressed concrete applications.

11-5 Normal Temperature Variation

The effect of nominal atmospheric temperature variations on the performance of prestressed structures and on the effective prestress is occasionally questioned by persons who are not familiar with the use of prestressed concrete. Because the thermal coefficients of linear expansion for steel and concrete are of the same order (6.5×10^{-6} in./in./°F), if the steel and concrete have the same temperatures at all times, there is no significant effect on the effective prestress for normal changes in temperature.

If the tendons are not bonded to the member, but are exposed to the atmosphere, it would be possible for the temperature of the tendons to be different from that of the concrete section. Under such conditions, the effect of temperature variations should be studied on the basis of estimated maximum temperature differentials and their effect on the effective prestress.

Atmospheric temperature variations can result in significant stresses in structures prestressed by jacks rather than by tendons (see Secs. 1-3 and 16-9). The effect of temperature variations must be given careful consideration when this type of prestressing is used.

A prestressed member with either bonded or unbonded tendons will expand or contract with temperature variations. Provision should be made for thermal expansion and contraction in prestressed construction in the same way as is done for structures made with other materials unless conditions indicate that the effect can be reasonably neglected. It should be kept in mind that changes in the length of a member can cause stresses only if the length change is restrained.

If a temperature gradient exists within a member, such as those frequently

TABLE 11-2 Excerpts from Table No. 43-A of the 1988 Edition of the Uniform Building Code. (Reproduced With the Permission of the International Conference of Building Officials, Whittier, California.)

Structural Parts to be Protected	Item Number	Insulating Material Used	Minimum Thickness of Insulating Material for Following Fire-Resistive Periods (in inches)			
			4 Hr.	3 Hr.	2 Hr.	1 Hr.
3. Bonded Pretensioned Reinforcement in Prestressed Concrete[5]	3-1.1	Carbonate, lightweight and sand-lightweight aggregate[6] concrete				
		Beams or girders	4[7]	3[7]	$2\frac{1}{2}$[17]	$1\frac{1}{2}$
		Solid slabs[8]		2	$1\frac{1}{2}$	1
4. Bonded or Unbonded Posttensioned Tendons in Prestressed Concrete[5,10]	4-1.1	Carbonate, lightweight, sand-lightweight and siliceous aggregate concrete				
		Unrestrained Members:				
		Solid Slabs[8]		2	$1\frac{1}{2}$	
		Beams and Girders[11]				
		8 in. wide		$4\frac{1}{2}$	$2\frac{1}{2}$	$1\frac{3}{4}$
		> 12 in. wide	3	$2\frac{1}{2}$	2	$1\frac{1}{2}$
4. Bonded or Unbonded Posttensioned Tendons in Prestressed Concrete[5,10]	4-1.2	Carbonate, lightweight, sand-lightweight and siliceous aggregate				
		Restrained Members:[12]				
		Solid Slabs[8]	$1\frac{1}{4}$	1	$\frac{3}{4}$	
		Beams and Girders[11]				
		8 in. Wide	$2\frac{1}{2}$	2	$1\frac{3}{4}$	
		> 12 in. wide	2	$1\frac{3}{4}$	$1\frac{1}{2}$	
5. Reinforcing Steel in Reinforced Concrete Columns, Beams, Girders and Trusses	5-1.1	Carbonate, lightweight and sand-lightweight aggregate concrete, members 12″ or larger, square or round. (Size limit does not apply to beams and girders monolithic with floors.)	$1\frac{1}{2}$	$1\frac{1}{2}$	$1\frac{1}{2}$	$1\frac{1}{2}$
	5-1.2	Siliceous aggregate concrete, members 12″ or larger, square or round. (Size limit does not apply to beams and girders monolithic with floors.)	2	$1\frac{1}{2}$	$1\frac{1}{2}$	$1\frac{1}{2}$

Table 11-2 (*Continued*)

Structural Parts to be Protected	Item Number	Insulating Material Used	Minimum Thickness of Insulating Material for Following Fire-Resistive Periods (in inches)			
			4 Hr.	3 Hr.	2 Hr.	1 Hr.
6. Reinforcing Steel in Reinforced Concrete Joists[9]	6-1.1	Carbonate, lightweight and sand-lightweight aggregate concrete.	$1\frac{1}{4}$	$1\frac{1}{4}$	1	$\frac{3}{4}$
	6-1.2	Siliceous aggregate concrete.	$1\frac{3}{4}$	$1\frac{1}{2}$	1	$\frac{3}{4}$
7. Reinforcing and Tie Rods in Floor and Roof Slabs[9]	7-1.1	Carbonate, lightweight and sand-lightweight aggregate concrete	1	1	$\frac{3}{4}$	$\frac{3}{4}$
	7-1.2	Siliceous aggregate concrete.	$1\frac{1}{4}$	1	1	$\frac{3}{4}$

[a]Generic fire-resistance ratings (those not designated by a company code letter) as listed in the Fire Resistance Design Manual, Eleventh Edition, dated October, 1984, as published by the Gypsum Association, may be accepted as if herein listed.

[5]Where lightweight or sand-lightweight concrete having an oven-dry weight of 110 pounds per cubic foot or less is used, the tabulated minimum cover may be reduced 25 percent, except that in no case shall the cover be less than $\frac{3}{4}$ inch in slabs nor $1\frac{1}{2}$ inches in beams or girders.

[6]For siliceous aggregate concrete increase tendon cover 20 percent.

[7]Adequate provisions against spalling shall be provided by U-shaped or hooped stirrups spaced not to exceed the depth of the member with a clear cover of 1 inch.

[8]Prestressed slabs shall have a thickness not less than that required in Table No. 34-C for the respective fire-resistive time period.

[9]For use with concrete slabs having a comparable fire endurance where members are framed into the structure in such a manner as to provide equivalent performance to that of monolithic concrete construction.

[10]Fire coverage and end anchorages shall be as follows: Cover to the prestressing steel at the anchor shall be $\frac{1}{2}$ inch greater than that required away from the anchor. Minimum cover to steel bearing plate shall be 1 inch in beams and $\frac{3}{4}$ inch in slabs.

[11]For beam widths between 8 and 12 inches, cover thickness can be determined by interpolation.

[12]Interior spans of continuous slabs, beams and girders may be considered restrained.

experienced from solar heating, and the temperature distribution through the thickness of the members is known, the stresses and strains within the section are easily computed (Priestley 1978). Priestley has shown that the nonlinear distribution of temperature would yield a nonlinear distribution of strain if it were unrestrained. This imaginary strain, which is referred to as the free strain, would be equal to the product of the thermal coefficient of expansion and the temperature at each level through the thickness of the member. Because plane sections must remain plane under all loading effects in the elastic range, the strain through the thickness of the member, referred to for the purpose of this discussion as the final strain, even when under the effects of the temperature gradient, must vary linearly from the top fiber to the bottom fiber. The difference between the free strain and the final strain is the strain that is created to maintain the linear strain distribution, referred to as the restraint strain. These strains are illustrated in Fig. 11-11.

The final strain, ϵ_y, at any level y from the top of the section is:

$$\epsilon_y = \epsilon_t - \frac{(\epsilon_t - \epsilon_b)y}{d} \tag{11-1}$$

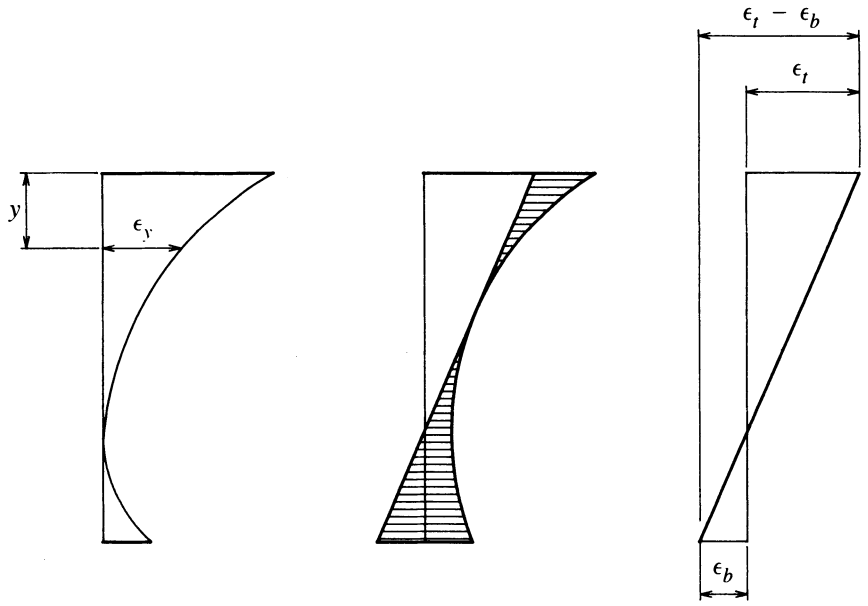

(a) Free strain (b) Restraint strain (c) Final strain

Fig. 11-11. Strain diagrams for temperature gradient analysis of concrete structures.

and, taking the free strain at any level, ϵ_{fy}, which is equal to the product of the temperature t_y, at level y, and the thermal coefficient of expansion, α, the stress at level y is:

$$f_y = E_c\,(\epsilon_y - \epsilon_{fy}) \tag{11-2}$$

The axial force on the section is equal to the summation of the forces at each level, and is expressed by:

$$P = E_c \int_0^d (\epsilon_y - \epsilon_{fy}) b_y dy \tag{11-3}$$

and the moment on the section, with respect to its centroidal axis, is:

$$M = E_c \int_0^d (\epsilon_y - \epsilon_{fy}) b_y (y - n) dy \tag{11-4}$$

in which n is the distance from the centroid to the top of the concrete section.

The force and moment on the section are each equal to zero if the section under consideration is in a simply supported beam (i.e., without axial or rotational restraints at the supports). In taking this consideration into account, Priestley has shown that the curvature, ψ, of the section and the strain at the neutral axis, ϵ_0, can be expressed by:

$$\psi = \frac{\alpha}{I} \int_0^d t_y b_y (y - n) dy \tag{11-5}$$

and:

$$\epsilon_0 = \frac{\alpha}{A} \int_0^d t_y b_y dy - n\psi \tag{11-6}$$

In eq. 11-5 I is the moment of inertia of the section about its centroidal axis, and in eq. 11-6 A is the area of the section.

The curvature from eq. 11-5 causes an upward deflection of a simple beam for the condition of a higher temperature on the top of the section (a negative deflection for the notation used in this book) with accompanying rotations at the supports. If the beam had restrained ends, like one of the interior spans of the four-span continuous beam shown in Fig. 11-12a, the rotation would be restrained by a moment that is:

$$M = -\psi E_c I \tag{11-7}$$

and a distribution of moments along the length of the member, having the shape shown in Fig. 11-12b, would result from the effects of the temperature gradient. If the moment in the continuous beam due to the effects of the temperature gradient is designated by M_{TG}, and if eq. 11-2 is rewritten in a general form

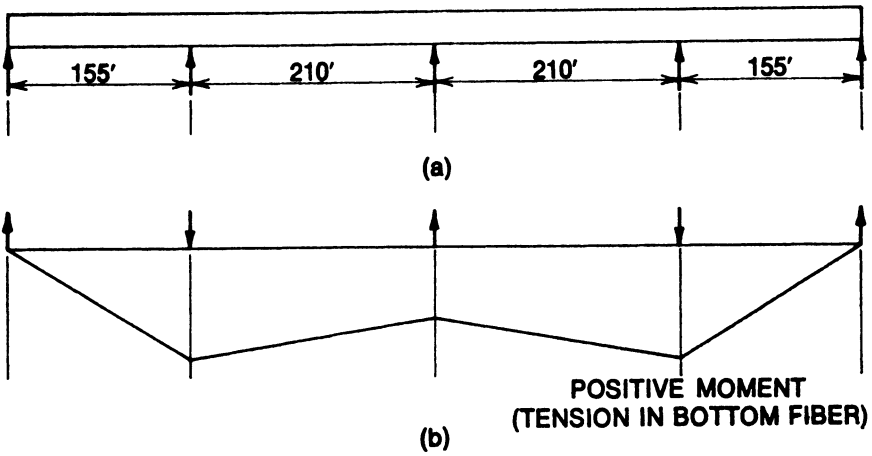

Fig. 11-12. Elevation and secondary moments due to a temperature gradient of 30°F for a four-span continuous prestressed concrete beam. (a) Elevation of beam. (b) Moment diagram.

based upon the curvature of the section, the strain at the centroidal axis, and the stress due to the temperature gradient (if one exists), the equation then takes the form:

$$f = E_c(\epsilon_0 + \psi y - \alpha\epsilon_{fy}) + \frac{M_{TG}(y - n)}{I} \qquad (11\text{-}8)$$

Priestley's research has shown the temperature gradients resulting from solar heating in bridges to vary according to a fifth-power curve. This has led to the thermal design gradient shown in Fig. 11-13, in New Zealand.

Other researchers have reported on experimental studies, field investigations, and bridge design practices with respect to the effects of temperature gradients on bridge structures. The interested reader should consult the following references: Leonhardt, Kolbe, and Peter 1965; Leonhardt and Lippoth 1970; Hoffman, McClure, and West 1983; and Imbsen et al. 1985.

ILLUSTRATIVE PROBLEM 11-2 For the double-tee beam shown in Fig. 11-14a, if used on a simple span of 50 ft, determine the deflection due a linear temperature gradient through the thickness of the member with the top fiber temperature being 58°F higher than the bottom fiber temperature. The area of the concrete section is 456 in.^{2}, and the moment of inertia is 21,670 in.^{4}. Assume that the thermal coefficient of expansion for the concrete is 6×10^{-6} in./in./°F.

SOLUTION The temperature gradient is plotted in Fig. 11-14b. Using eqs. 11-5 and 11-6, the values of the curvature and the strain at the centroidal axis

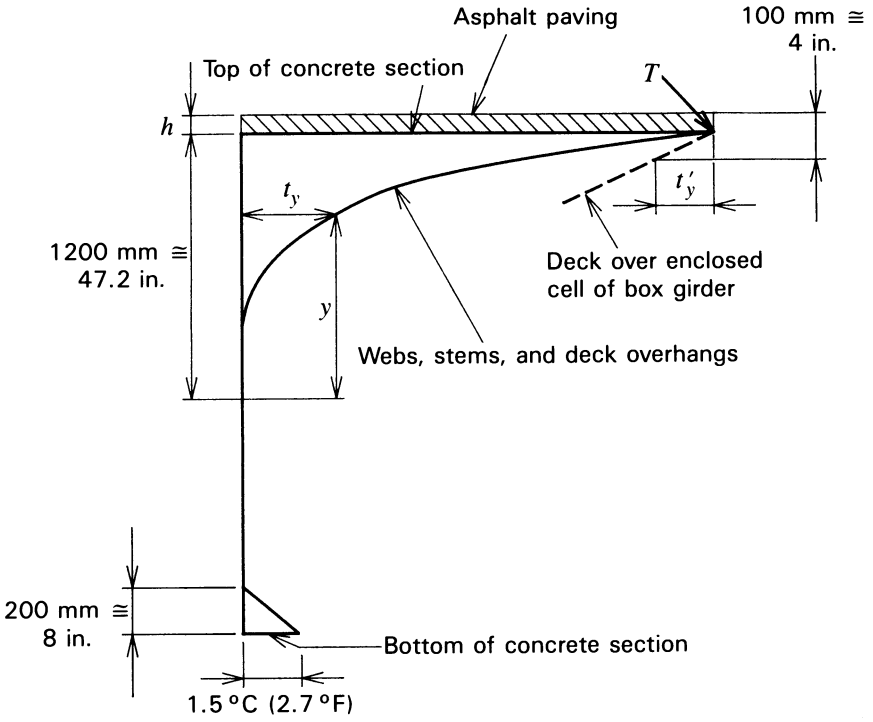

For temperature in Centigrade and y and h in mm:	For temperature in Fahrenheit and y and h in inches:
$T = 32 - 0.2h$	$T = 57.6 - 9.14h$
$t_y = T\left(\frac{y}{1200}\right)^5$	$t_y = T\left(\frac{y}{47.2}\right)^5$
$t'_y = (5.00 - 0.05h)\,°C$	$t'_y = (9.00 - 2.28h)\,°F$

Fig. 11-13. Thermal gradients used in design of concrete bridges in New Zealand (after Priestley).

are determined as follows:

$$\psi = \frac{6 \times 10^{-6}}{21{,}670}[(54)(96)(1.5 - 5.92)(3) + (25.5)(8)(10 - 5.92)(21)]$$

$$= \frac{6 \times 10^{-6}}{21{,}670}[-68{,}740 + 17{,}479] = -14.19 \times 10^{-6}$$

$$\epsilon_0 = \frac{6 \times 10^{-6}}{456}[(54)(96)(3) + (25.5)(8)(21)]$$

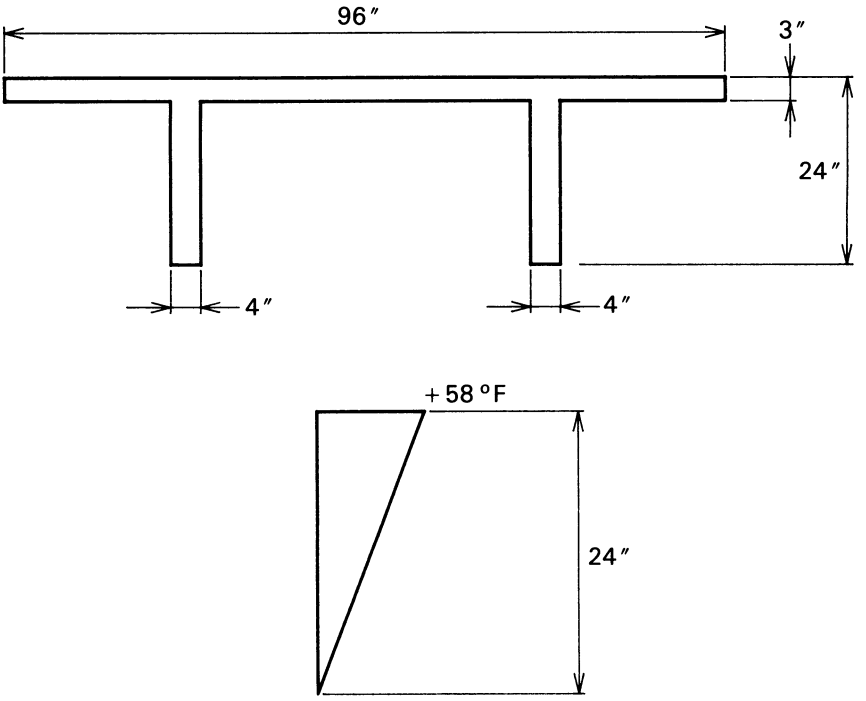

Fig. 11-14. Double-tee beam used in I.P. 11-2. (a) Cross section. (b) Temperature gradient.

$$= \frac{6 \times 10^{-6}}{456} [15{,}552 + 4{,}284]$$

$$= 0.000261 \text{ in./in.}$$

The curvature is constant over the length of the simply supported beam, and, using the conjugate beam principle, the deflection computation becomes:

$$\delta_{\text{midspan}} = \frac{\psi l^2}{8} = \frac{-14.19 \times 10^{-6}(50^2)(144)}{8} = -0.64 \text{ in.}$$

The designer frequently does not have precise information with respect to the extreme temperature gradient that a particular structure will experience in service. Knowing the location of the structure (longitude and latitude), its alignment, the superelevation, and possible shading from mountains or other objects, it is possible to estimate the maximum effect that solar heating may have on a particular structure (Priestley 1976). Therefore, some engineers believe that an

approximate method of analysis will yield results that are adequate for most design work. The approximate method consists of assuming that the top flange is raised to a uniform temperature higher than that of the other parts of the cross section. If unrestrained, the top flange would experience an increase in length as a result of the temperature increase. The expansion of the top flange is resisted by the webs and the bottom flange. By combining these effects, using the principles of equilibrium and strain compatibility, an estimate of the effect is obtained.

The first step in computations with the approximate method consists of computing the forces that would exist in the top flange due to the increase in temperature if the flange were completely restrained. The force results in a compressive stress in the top flange. The effect of the force on the section as a whole is computed by applying a tensile force equal in magnitude to the compressive force computed in the first step. The tensile force is applied at the centroid of the top flange. The sum of the stresses from the two forces gives the approximate stresses due to thermal effects in the section.

As an example, consider the bridge cross section shown in Fig. 11-15. Assume that the top flange temperature is 30°F higher than that of the webs and bottom flange. The compressive stress in the top flange, if fully restrained, would be:

$$f_c = (\Delta t)(\alpha)(E_c)$$

where α is the coefficient of thermal expansion, and E_c is the elastic modulus of the concrete. If $\alpha = 6.5 \times 10^{-6}$ and $E_c = 3 \times 10^6$ psi, $f_c = 585$ psi. The force in the top flange would be:

$$P = \frac{585 \times 5000}{1000} = 2925 \text{ k}$$

as shown in Fig. 11-16a. The tensile force applied 5.29 in. from the top of the section produces the stresses shown in Fig. 11-16b, and the combined stresses

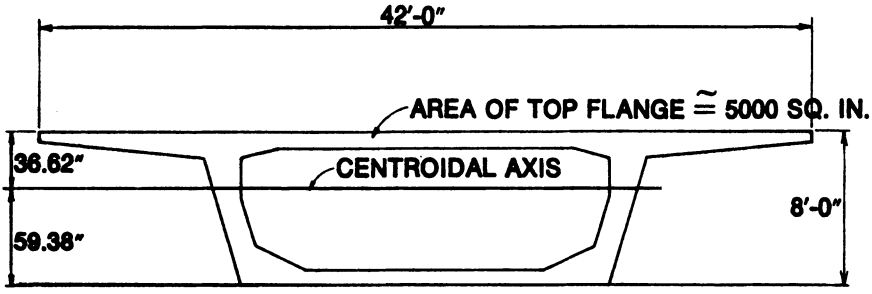

Fig. 11-15. Cross section of a single-cell concrete hollow-box girder bridge superstructure.

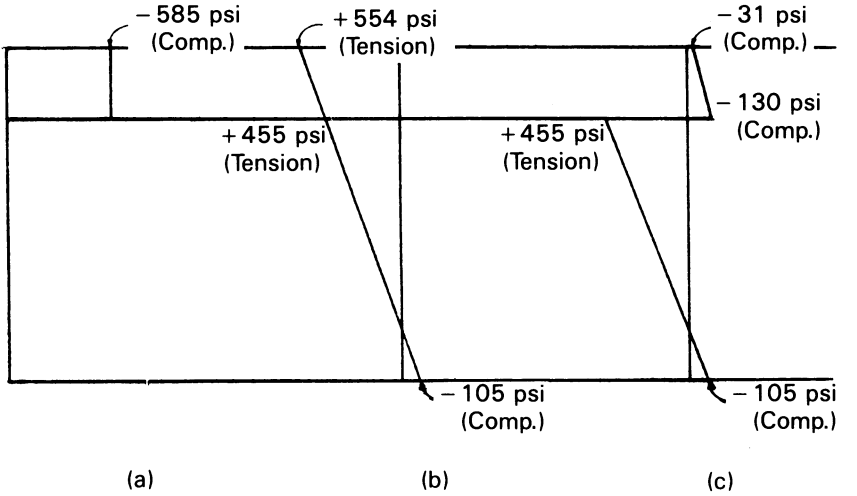

Fig. 11-16. Stresses in the bridge section of Fig. 11-15, by approximate calculation, for a linear temperature gradient of 30°F. (a) Stress in restrained top flange. (b) Stress due to axial force applied by the top flange. (c) Combined stresses.

are as shown in Fig. 11-16c. These are the approximate stresses that would exist if the beam were a single simply supported span.

If the beam were made continuous over four spans, as shown in Fig. 11-12a, it can be shown that secondary moments and reactions, as shown in Fig. 11-12b, would exist. The secondary reactions are those required to prevent the beam from deflecting upward from its supports as a result of the thermal gradient. The secondary moment at the first interior support results in a stress of 314 psi (compression) in the top fiber and 510 psi (tension) in the bottom fiber. The net stress in the member due to the effect of the differential temperature would be obtained by combining the stresses shown in Fig. 11-16c with those resulting from the secondary moment of Fig. 11-12b.

11-6 Fatigue

Fatigue strength of structural elements is important if the elements are to be subjected to frequent reversals or variations in stress. Resistance to fatigue is an essential property for bridge members, but is not normally an important consideration in building construction.

Although the effect of fatigue on prestressed-concrete beams is not completely understood, there has been considerable research into the causes and types of fatigue failures that may result under the action of stress variations of various ranges.

Fatigue failures could be expected to occur in any of the following modes:

1. Failure of the concrete due to flexural compression.
2. Failure of the concrete due to diagonal tension or shear.
3. Failure of the prestressing steel due to flexural, tensile-stress variations.
4. Failure of pretensioned beams due to loss of bond.
5. Failure of the end anchorages of post-tensioned beams.

Although the fatigue limit for concrete in compression alone generally is thought to be from 50 to 55 percent of the static compressive strength, no reports of failures of prestressed concrete flexural members due to compressive flexural stresses are known to the author. Apparently restriction of the concrete compressive stress in complete bridge structure to $0.40f'_c$ results in adequate safety (Nordby 1958). It should be pointed our that the fatigue limit mentioned above is for the load alternating from zero to the maximum value, which is a larger variation than is normally experienced in prestressed concrete flexural members in actual service.

In composite bridge stringers (f'_c = 5000 psi) of moderately long span, the compressive stress in the top fibers of the precast section may vary from 1500 psi under the loading condition of dead load alone to 2000 psi under the loading condition of dead load plus live load and impact. In a similar manner, the compressive stress in the composite flange (cast-in-place deck, f'_c = 3000 psi) may vary from zero to 900 psi. It is apparent that these ranges of stress variation and maximum values are considerably below the fatigue limit of the concrete in compression (0 to $0.50f'_c$), and for this reason fatigue of the concrete should not be a problem under these conditions. A variation of stress in the compressive flange from zero to $0.40f'_c$, due to the application of live load plus impact alone, would only be expected to occur in short-span bridge structures.

Fatigue failures due to diagonal tension or shear apparently have not been observed in prestressed concrete practice or research. Prestressed railroad ties, which are subjected to high-shear stresses, have shown distress when tested under repeated loads, as well as in service, but failure usually is caused by lack of adequate bond rather than insufficient shear or diagonal tensile strength. (Railroad ties are very special elements because of their high-shear loads and short-shear spans.)

The majority of fatigue failures found in the testing of prestressed beams have resulted from fatigue of the tendons. It appears that after the cracking load is reached, concentrations of stress or other phenomena related to the cracks develop in the tendons in the vicinity of the cracks, and failure results. It must be emphasized, however, that most tests reveal that the fatigue resistance of prestressed-concrete beams is high and generally superior to that of conventionally reinforced concrete.

In several fatigue tests conducted abroad, it was found that individual wires

contained in the prestressing tendons failed by fatigue at points where they passed over spacers used to hold the wires in position (Sawko and Saha 1968). This would lead one to suspect that the secondary stress that develops in the wire due to its passing over a spacer (usually a small-diameter wire or bar) can be sufficiently severe to cause a point of fatigue weakness and possible fatigue failure. No failures in actual structures due to this effect are known to the author, but he believes that designers should avoid the use of spacers and the use of sharp bends in prestressed reinforcement when possible, if fatigue is a consideration in the structure.

Bond failures have been found in testing very short-span members, as was mentioned above. It appears that cracking of the beam sets up conditions that result in deterioration of the flexural bond between the tendon and the concrete as additional variations in the load are applied. When the flexural bond is destroyed from the point of cracking to the vicinity of the support, in the region where transfer bond is developed, failure ensues (see Sec. 6-6).

The available experimental data lead one to conclude that the types of tendons normally used domestically in pretensioned work provide adequate safety against bond failure for members of usual proportions.

There are indications that a light, hard coating of normal oxidation on the surface of the tendons improves the dynamic bond properties, just as it improves the static bond properties (see Sec. 6-6 for other factors that affect bond stresses).

No reports of fatigue failures in the steel at the anchorages of post-tensioned members are found in the literature. This type of failure is extremely unlikely in bonded construction because the grout is very effective in developing flexural bond stresses. This was demonstrated in one test in which the end anchorages were removed from the tendons of a grouted beam, and the member was then subjected to a fatigue test. The results were satisfactory, and failure resulted from fatigue of the tendons, not from lack of bond.

In unbonded post-tensioned construction, the end anchorages could be subjected to some variation in stress under the action of variation in external load. This type of construction is not generally used in members that will be subjected to frequent variations in stress; however, there are very few experimental results available on the performance of this type of construction under repeated loads.

Existing acceptance standards for unbonded tendons include fatigue test requirements (PTI 1981).

11-7 Slabs-on-Grade

Concrete slabs-on-grade (or slabs-on-ground) are commonly used in the construction of commercial, industrial, and residential buildings. These slabs frequently are constructed of plain, unreinforced concrete or concrete that does

not contain sufficient reinforcement for it to qualify as reinforced concrete according to the provisions of ACI 318. For residential construction, slabs having a nominal thickness of 4 in. (3.5 in. actual thickness) frequently are used with welded wire fabric having W1.4 wires spaced at 6 in. on centers each way (6×6 W1.4/W1.4). If properly constructed on well-compacted soil that is nonexpansive, or on soil that is expansive but held at a constant moisture content, such slabs have performed very well.

To be properly constructed, unreinforced slabs (using the ACI 318 definition) must be provided with contraction joints if the normal cracking due to concrete shrinkage is to be confined to the locations desired by the responsible party (architect, contractor, developer, or engineer, depending upon the circumstances). It should be recognized that the reinforcement in concrete is under compressive stress and does not resist concrete shrinkage deformation until after the concrete has cracked. If slabs-on-ground are to be constructed free of cracks, special methods must be used in their construction. The use of shrinkage-compensating portland cement (type k cement), or admixtures that give normal portland cement shrinkage-compensating characteristics, together with sufficient nonprestressed reinforcement, is one means of constructing crack-free slabs-on-grade. Another method of avoiding cracks in concrete slabs-on-grade, which has been widely used, involves prestressing the concrete by using post-tensioned tendons. The use of shrinkage compensating concrete is outside the scope of this book, and the interested reader is referred to the *Standard Practice for the Use of Shrinkage-Compensating Concrete* (ACI 223).

The use of post-tensioned slabs-on-grade was developed in the 1970s with the primary purpose being to control cracking in slabs constructed on expansive or compressible soils. The original reason for the development of prestressed concrete, the elimination of cracks in concrete structures, was the motivation for this application. The principle involves the creation of compressive stresses in the concrete in such a way that the effects of creep and shrinkage will not result in axial forces that exceed the tensile strength of the concrete, the effects of friction from the soil supporting the slab will be overcome by the prestressing, and flexural stresses in the slab due to movements of the supporting soil (expansion or contraction) or the superimposed loads (posts, bearing walls, heavy objects, etc.) will not result in flexural stresses exceeding the flexural tensile strength of the concrete.

The design of post-tensioned slabs-on-ground is based upon a combination of empirical relationships and theoretical considerations. The designer must have considerable site-specific information from a soils engineer with respect to the soil parameters that should be used in the design. The design methods for slabs-on-ground recommended by the Post-tensioning Institute are included as an optional method of design in the 1988 *Uniform Building Code Standards* (ICBO 1988; PTI 1980).

REFERENCES

ACI Committee 223. 1983. *Standard Practice for the Use of Shrinkage-Compensating Concrete.* Detroit. American Concrete Institute.

ACI Committee 318. 1989. *Building Code Requirements for Reinforced Concrete.* Detroit. American Concrete Institute.

Gilbert, R. I. and Mickleborough, N. C. 1989. Creep Effects in Slender Reinforced and Prestressed Concrete Columns. Read at the Annual Convention of the American Concrete Institute, Feb. 1989, Atlanta, Georgia.

Guyon, Y. 1953. *Prestressed Concrete.* New York. John Wiley and Sons, Inc.

Hoffman, P. C., McClure, R. M., and West, H. H. 1983. Temperature Study of an Experimental Segmented Concrete Bridge. *PCI Journal* 28(2):78–97.

ICBO 1988. *Uniform Building Code Standards.* Whittier, California. International Conference of Building Officials.

Imbsen, R. A., Vandershaf, D. E., Shamber, R. A. and Nutt, R. V. 1985. Thermal Effects in Concrete Bridge Superstructures. National Cooperative Highway Research Program Report 276. Washington, D.C. Transportation Research Board.

Leonhardt, F., Kolbe, G. and Peter, J. 1965. Temperature Differences Endanger Prestressed Concrete Bridges. Berlin. *Benton- und Stahlbetonbau* 7:157–63 (in German).

Leonhardt, F. and Lippoth, W. 1970. Lessons from Damage to Prestressed Concrete Bridges. Berlin. *Benton- und Stahlbetonbau* 10:231–44 (in German).

Nordby, G. M. 1958. Fatigue of Concrete—A Review of Research. Detroit. *Journal of the American Concrete Institute* 30(2):191–219.

Portland Cement Association. 1960. *Ultimate Load Tables for Circular Columns.* Skokie, Illinois.

PCI. 1985. *PCI Design Handbook.* Chicago. Prestressed Concrete Institute.

PTI. 1980. *Design and Construction of Post-tensioned Slabs-on-Ground.* Phoenix. Post-tensioning Institute.

PTI. 1981. *Post-Tensioning Manual.* Phoenix. Post-tensioning Institute.

Priestley, M. J. N. 1976. Ambient Thermal Stresses in Circular Prestressed Concrete Tanks. *Journal of the American Concrete Institute* 73(10):553–60.

Priestley, M. J. N. 1978. Design of Concrete Bridges for Temperature Gradients. *Journal of the American Concrete Institute* 75(5):209–17.

Ross, A. D. 1958. Creep of Concrete under Variable Stress. *Journal of the American Concrete Institute* 29(9):739–58.

Smith, E. A. L. 1960. Tension in Concrete Piles during Driving. *Journal of the American Concrete Institute* 5(1):35–40.

Sawko, F. and Saha, G. P. 1968. Fatigue of Concrete and Its Effect upon Prestressed Concrete Beams. *Magazine of Concrete Research* 20(62):21–30.

ULI. 1982. *Building Materials Directory.* Chicago. Underwriters' Laboratories, Inc.

12 Connections for Precast Members

12-1 General

The connections between precast members or between precast and cast-in-place members should be designed to be capable of withstanding the design (factored) vertical and horizontal loads in which they will be subjected, without failure, excessive deformation, or rotation. It is generally preferred that the strengths of connections exceed the strengths of the members connected. In seismically active areas, ductility of the connections is as important as strength, if not more important. Details of connections should be such that they accommodate, or are readily adjusted to accommodate, construction tolerances. The tolerances considered are not just variations in length, width, and elevation, but also include unintended deviations from the specified or theoretical planes of bearing (PCI Committee on Connections 1988). Connections should be detailed to provide erection clearances, bends of the reinforcement, and clearances that may be required for special requirements such as the post-tensioning of tendons after erection.

In the interest of economy, connections should be as simple as possible and designed in such a way that during the erection of the precast members the members will be stable when set into place and can be disconnected from the

erection equipment quickly, with no need for temporary bracing. Some connections require the erection equipment to provide stability while welding or other time-consuming operations are performed in order to achieve stability; but they frequently are not economical. Connections should be of such a configuration that they are easily inspected during assembly as well as after their completion.

The designer should pay particular attention to the details of connections to be sure the structure will act as it has been assumed to act in the design of the individual elements. If the beams that are connected to opposite sides of a column are designed as simple beams, the connection details should not result in the members being continuous or partially continuous because of a cast-in-place reinforced concrete slab or topping or other mechanical fasteners. On the other hand, if the members have been designed to be continuous under certain conditions of loading, the connections should be carefully detailed to achieve the intended continuity.

Flexural members undergo rotations and deflections due to the application of transverse loads. Rotations and deflections due to other effects, such as temperature, creep, shrinkage, and so on, may also occur. Connection details, particularly for simple spans, should provide for the rotations that will occur at supports without restraint, and with no risk of spalling from a member being supported at an unreinforced edge (see Fig. 12-1).

Connections that incorporate welded reinforcing steel should be used with caution. Reinforcing steel frequently contains relatively high amounts of carbon and other elements, which can have an influence on its weldability and the

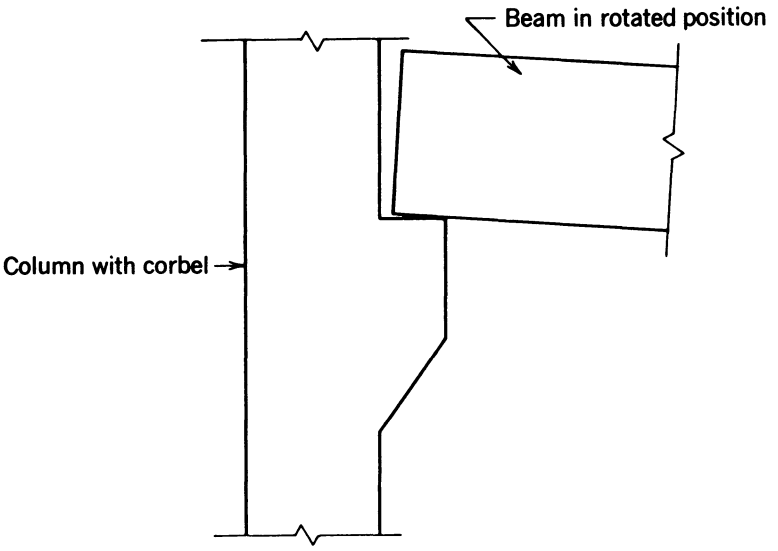

Fig. 12-1. Corbel edge loading resulting from rotation of a supported beam.

procedures that must be followed to obtain acceptable welds. This combination of carbon and other elements is known as the carbon equivalent. The codes of the American Welding Society and most building codes require that the carbon equivalents of steels being welded be known and used as the basis for the selection of welding procedures and electrodes. It is essential to use prequalified welds, workers who are certified welders for the types of welding to be done, and special inspection when needed, to assure the required quality of welds. It is considered good practice not to permit welding of reinforcing bars at their intersections (crossing bars), or welding bars close to bends (within two bar diameters) or in locations where the bars have been bent and straightened. Tack welds should be permitted only at locations where they will become part of a permanent, prequalified weld (AWS D1.4-79).

Publications containing typical connection details and methods for facilitating their design and proportioning are available from the national and regional prestressed concrete trade associations, as well as from producers of prestressed concrete products. Designers should be familiar with these details, how they evolved, and the structural theory or experimental work on which they are based. A designer should not assume that typical details are satisfactory for his or her purposes without understanding and agreeing with the basis for their ability to perform the function for which they are intended. It is sometimes useful to research the evolution of a detail contained in a contemporary publication, by reviewing previous editions of the same publication (if they exist), as a means of understanding the basis for contemporary recommendations. Several publications of the Prestressed Concrete Institute that are very useful in the design of connections are listed in the references to this chapter.

12-2 Horizontal Forces

In several of its sections, ACI 318 contains design requirements that include the consideration of horizontal forces. Section 11.9 of ACI 318, which pertains to the design of corbels and brackets, requires a minimum horizontal force of 20 percent of the vertical force supported by the corbel unless special provisions are made to avoid horizontal forces. For the designer to evaluate special provisions that might be used to avoid horizontal forces, the sources of the forces, such as concrete creep and shrinkage, temperature effects, and so on, must be evaluated, and the theoretical displacements that could result from the effects must be determined (see Secs. 3-12, 3-14, and 11-5). It is considered better practice to evaluate the forces and displacements where possible rather than to use the minimum force specified in ACI 318 because the latter can be significantly incorrect in some instances. In addition to the horizontal forces that may exist, the designer should determine the rotations that will occur at the ends of the supported members; these too are important considerations in the design of

a connection. Using well-designed connection details that avoid horizontal forces or control their magnitude is a common, proven approach.

The computation of horizontal forces to be used in the design of connections for restrained members can be done by first determining the unrestrained change in length of the member that would be expected to occur after the member is erected and the connection effected. The force from the restraint that can be developed in the connection and in the structure as whole then must be determined.

If a simple prestressed concrete beam were fully restrained, such as being attached to two infinitely stiff shear walls, as shown in Fig. 12-2, the restraining force, R_0 would be the force that would cause an increase of strain equal to δL in the bottom fibers, computed as follows:

$$R_0 = \frac{E_c A \delta L}{L\left(1 + \frac{y_b^2}{r^2}\right)} \tag{12-1}$$

In the case of a single span supported vertically and restrained against translation, but not rotation, by two columns of equal stiffness (as shown in Fig. 12-3), the value for R_0 can be computed as:

$$R_0 = \frac{3E_c I_c \delta L}{2H^3} \tag{12-2}$$

in which E_c and I_c are the elastic modulus and the moment of inertia of the column, respectively. For a multispan frame containing a number of equal spans restrained by columns of equal stiffness, such as shown in Fig. 12-4, the force in the interior spans can be approximated by:

$$R_i = R_o i(n + 1 - i) \tag{12-3}$$

in which n is the number of spans, i is the number of the span under consideration reckoned from the end, and R_0 is computed from eq. 12-2. In eqs.

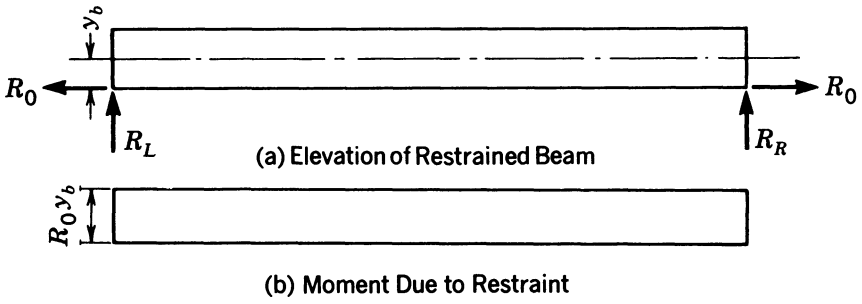

Fig. 12-2. Simple beam with horizontal eccentric forces resulting from restraint.

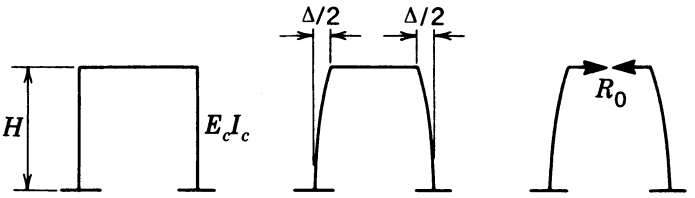

Fig. 12-3. Effect of beam shortening in a frame composed of two cantilevered columns and a beam with hinged beam-to-column joints.

12-1 and 12-2, the age-adjusted modulus of elasticity of the concrete should be used in computing R_0 (see Sec. 3-8).

In multispan structures where difficulty is experienced in applying eq. 12-3, the restraining force interior spans can be roughly approximated as being equal to 50 percent of the applied prestressing force (PCI Committee on Connections 1988; Burton, Corley, and Hognestad 1967).

12-3 Corbels

Corbels on columns, pilasters, and walls of the type commonly used for supporting precast concrete beams have been extensively studied, experimentally and analytically, by the Portland Cement Association (Kriz and Raths 1965). The testing has resulted, in part, in the recommendations shown in Fig. 12-5, which can be summarized as follows:

1. The minimum distance from the bearing plate to the edge of the corbel should be 2 in.
2. The tensile reinforcement should be welded to an anchorage bar of the same size as the tensile reinforcement.
3. The depth of the corbel at the outside face of the bearing plate should be not less than one-half the depth (d) at the face of the support.
4. If a horizontal (tensile) force is to be resisted in addition to the vertical force, a steel plate should be provided, welded to the tensile reinforcement and embedded in the top of the corbel.

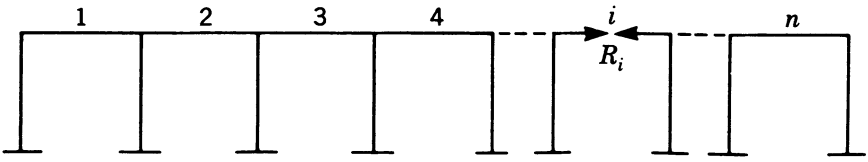

Fig. 12-4. Effect of beam shortening in a frame composed of n beams and $n + 1$ columns with hinged beam-to-column joints.

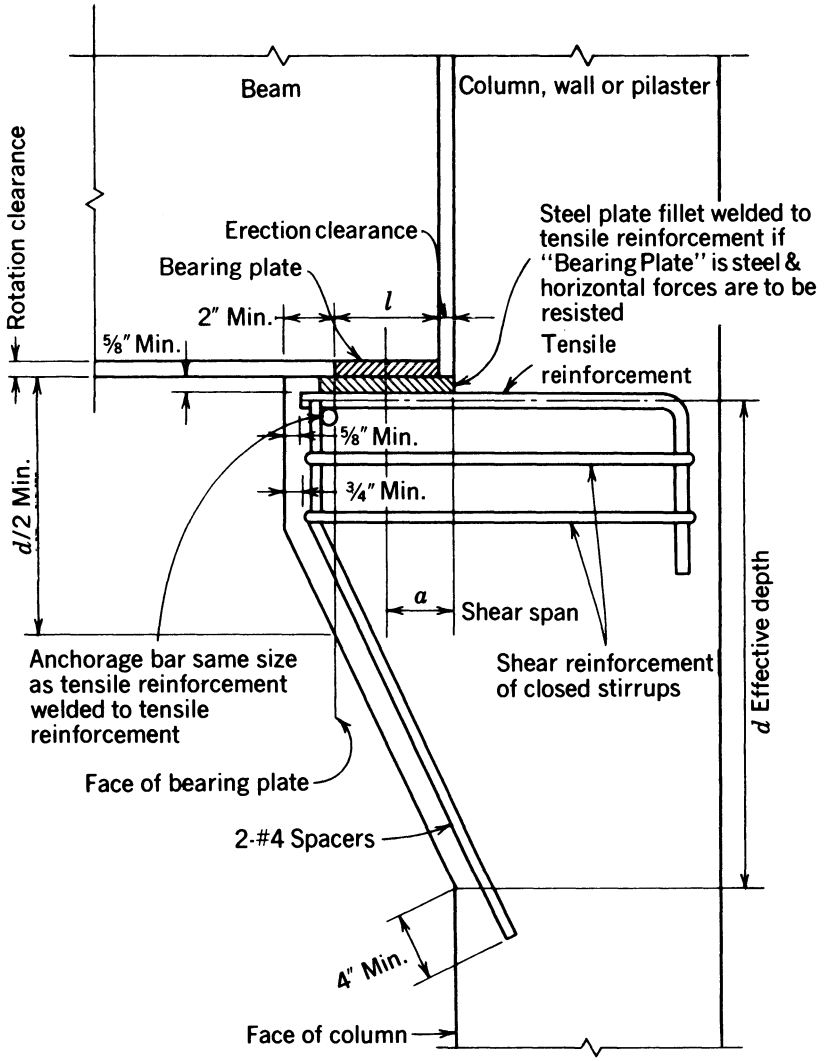

Fig. 12-5. Typical details for reinforced concrete corbels.

5. The minimum cover on the tensile reinforcement and on the shear reinforcement should be $\frac{5}{8}$ in. and $\frac{3}{4}$ in., respectively.

It should be recognized that the welding of crossing reinforcing bars, as specified in item 2 above, is not normally considered good engineering practice. On the other hand, experience has shown that in this particular detail it does provide the necessary anchorage to the tensile reinforcement without adverse effects (CRSI 1984). A preferred procedure for anchoring the end of the tensile

reinforcement to the concrete would be to fillet-weld the ends of the tensile reinforcement to flat steel plates or angles, similar to those described in Sec. 12-4, rather than to an anchorage bar.

The shear span, a, and the distance from the extreme fiber to the tensile reinforcement, d, used in the design of corbels are illustrated in Fig. 12-5.

The types of failures experienced in corbels that have not been designed, detailed, or constructed correctly are illustrated in Fig. 12-6. A toe crack in the corbel and a heel crack in the beam, both of which can result from the rotation of the supported beam, are illustrated in Fig. 12-6. In addition, a flexural-tension crack in the corbel near the surface of the column extension above is shown in Fig. 12-6. Wide flexural-tension cracks can be the result of an insufficient amount of tensile reinforcement near the top surface of the corbel or inadequate anchorage (development) of the bar on either of the two sides of the crack. Also illustrated in Fig. 12-6 are the compression strut and tensile tie forces one uses in a truss analogy analysis of a corbel.

12-4 Column Heads

The term column head is used for the structural connection consisting of a prismatic column that supports one or two beams at its top. A column head is

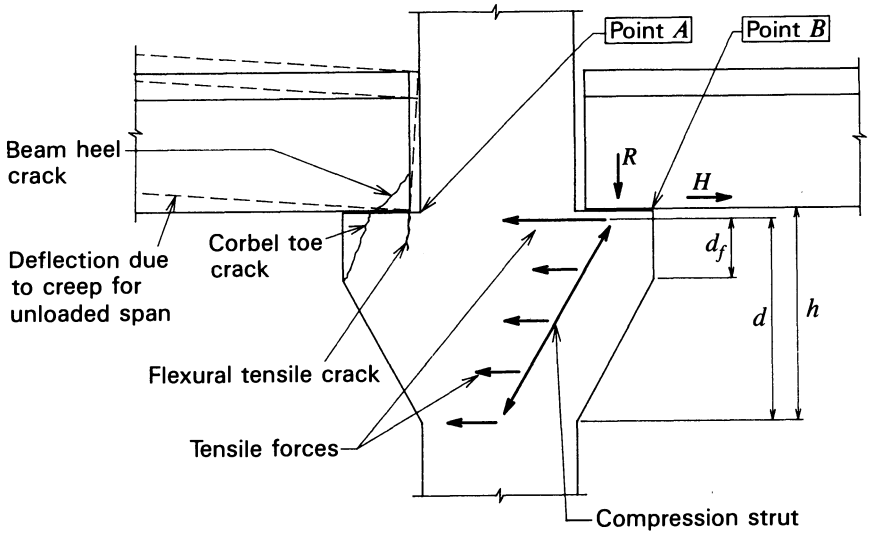

Bearing stress $= \frac{R}{A}$ where A is the contact area between the corbel and the supported member

Fig. 12-6. Typical toe crack in a reinforced concrete corbel and typical heel crack in the end of a precast concrete beam supported by a corbel.

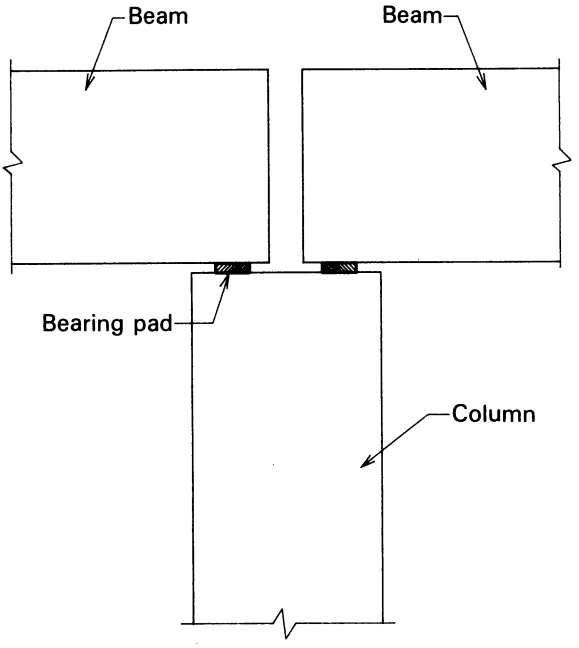

Fig. 12-7. A precast concrete column head supporting two precast concrete beams.

illustrated in Fig. 12-7. A study of the ultimate strength of column heads with various reinforcing details, loaded in various ways, was conducted by the Portland Cement Association (Kriz and Raths 1963) to determine relationships for use in the strength evaluation of this type of connection.

The study revealed that if the bearing stresses were not restricted to conventional levels, column heads reinforced with sufficient amounts of nonprestressed lateral reinforcement, when loaded to failure, would be expected to fail by concrete crushing. Without well-detailed lateral reinforcing in sufficient quantities, they would be expected to fail in shear if the load were applied at a distance of 1.5 in. or less from the edge of the column and by splitting if loaded at a distance greater than 1.5 in. from the face of the column (see Fig. 12-8). Lateral reinforcement should be anchored by welding cross bars close to the ends of the lateral reinforcement or by welding bearing plates or angles to the lateral reinforcing, as shown in Fig. 12-9. As in the case of corbels, horizontal loads have a significant effect on the strength of column heads and should be prevented or controlled at acceptable levels when possible. The uniformity of the bearing stress between the beam and the column head was found to have a significant effect on the strength of a column head.

The prudent designer will provide for the tolerances associated with the manufacture and erection of precast concrete members, as well as the effects of

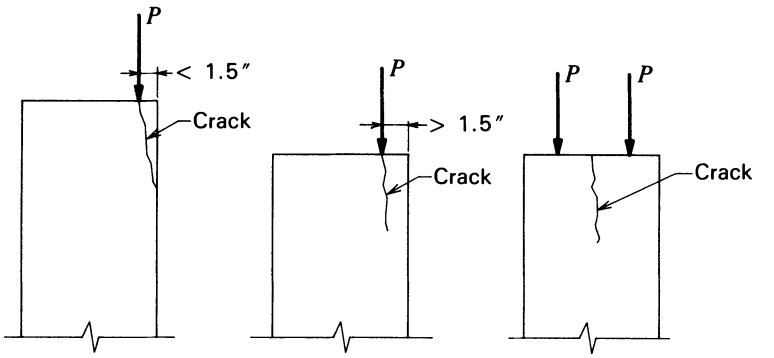

(a) $s < 1.5$ in. (b) $s > 1.5$ in. (c) Two loads, $s > 1.5$ in.

Fig. 12-8. Modes of failure for reinforced concrete column heads.

horizontal forces and beam end rotations due to loadings, when designing column heads. This is most commonly done by providing elastomeric or other types of structural bearings.

The nominal bearing strength of a laterally reinforced column head that is uniformly loaded in bearing across the width of the column head, b, in which the horizontal forces are either prevented or controlled, can be computed by:

$$f'_b = (A)(B)(C) \tag{12-4}$$

in which:

$$A = 60\sqrt{f'_c}\sqrt[3]{\frac{s}{l}} \tag{12-5}$$

$$B = 0 \text{ for } s < 2.00 \tag{12-6a}$$

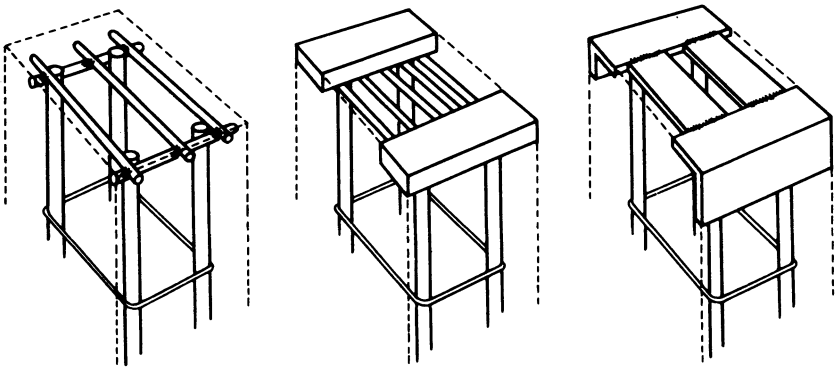

(a) (b) (c)

Fig. 12-9. Configurations of welded lateral reinforcement in concrete column heads.

and, for $s \geq 2.00$:

$$B = 1 + C_1 \sqrt{\frac{A_{sl}}{b}} \leq 2.00 \qquad (12\text{-}6b)$$

and, when the lateral reinforcement in the column head is welded to transverse bars of equal size:

$$C = \left(\frac{1}{9}\right)^{N_u/V_u} \qquad (12\text{-}7a)$$

but when the lateral reinforcement in the column head is welded to a steel bearing plate of a steel angle

$$C = \left(\frac{1}{16}\right)^{N_u/V_u} \qquad (12\text{-}7b)$$

Notation used in the above equations, and not previously defined, is as follows:

A_{sl} = Area of the lateral reinforcement (minimum yield strength of 40,000 psi) per inch of bearing plate width, b, with $A_{sl} \leq 0.16$ in.^{2}/in. of bearing plate width.
b = Width of the bearing plate measured perpendicular to the direction of s.
C_1 = Constant equal to zero when s is less than 2 in. and equal to 2.5 when s is equal to 2 in. or more.
f'_b = The nominal bearing strength in psi.
N_u/V_u = Ratio of horizontal and vertical design loads (factored).
s = Distance from the edge of the column to the center line of the bearing plate.
l = Length of the bearing plate measured in the direction of s.

Because very little increase in strength was found to be achieved by using lateral reinforcing having a yield point greater than 40,000 psi, the yield strength does not appear in the above relationships.

In eq. 12-6, the term A represents the strength of a column head that has no lateral reinforcing and is subjected to vertical loads only. The term B is a strength increase factor that reflects the effects of properly anchored lateral reinforcing when the distance s exceeds 2 in. The term B should not exceed 2, because an increase in the amount of lateral reinforcing above that which results in B being equal to 2 causes little increase in the bearing strength. The term C is a strength reduction factor that accounts for the effects of horizontal loads acting in combination with the vertical loads.

The lateral reinforcing should be placed near the top of the column with a concrete cover of $\frac{5}{8}$ in. or the minimum permitted by the applicable code. The

lateral reinforcing can be placed in two layers when necessary to facilitate concrete placing and compaction.

The nominal bearing strength computed with eq. 12-4 should be used in comparing the design (factored) load to the strength as:

$$V_u \leq \phi V_n \tag{12-8}$$

in which ϕ is taken to be 0.85 or less.

ILLUSTRATIVE PROBLEM 12-1 Design the column head for a 12 in. × 12 in. column that is to support two beams symmetrically placed about the centerline of the column. Horizontal loads are prevented. The design (factored) load for each beam is 200,000 lb, $f'_c = 4000$ psi, and the bearing pad width is 3 in.

SOLUTION: Provide a 1 in. gap between girders, and use a distance s equal to of 2.75 in. as a means of providing equal edge distances for the beam and column.

$$A = 69\sqrt{4000} \times \sqrt[3]{\frac{2.75}{3.00}} = 4239 \text{ psi}$$

Assuming that transverse reinforcement is not required, $B = 1$, and, because $N_u = 0$, $C = 1$, and:

$$\phi V_n = 0.85 \times 4239 \times 3 \times 12 \times 12 = 129{,}700 \text{ lb} < 200{,}000 \text{ lb}$$

Hence, lateral reinforcing is required and the term B from eq. 12 must equal or exceed:

$$B = \frac{200{,}000}{129{,}700} = 1.54 = 1 + 2.5\sqrt{\frac{A_{sl}}{12}}$$

because $s > 2.00$ in. and:

$$A_{sl} = 12\left(\frac{1.54 - 1.0}{2.5}\right)^2 = 12\left(\frac{0.54}{2.5}\right)^2 = 0.56 \text{ in.}^2$$

Three No. 4 bars, which are provided with a No. 4 anchorage bar welded at each end, give a lateral reinforcing area of 0.60 sq. in. and provide a good solution. Note that the actual ultimate bearing stress on the concrete with this solution would be 5560 psi, and:

$$\frac{A_{sl}}{12} = \frac{0.60}{12} = 0.050 \text{ in.}^2/\text{in.} < 0.16 \text{ in.}^2/\text{in.}$$

12-5 Ledgers and Ledges

Cast-in-place concrete walls, inverted-tee beams and L-shaped beams frequently are used to support other precast, prestressed concrete members such as double-tee beams. The portion of the wall on which the supported member bears frequently is called a ledger, and the portion of a beam on which the supported member bears is called a ledge. Typical ledges and a ledger are illustrated in Fig. 12-10. The vertical and horizontal loads that supported members impose

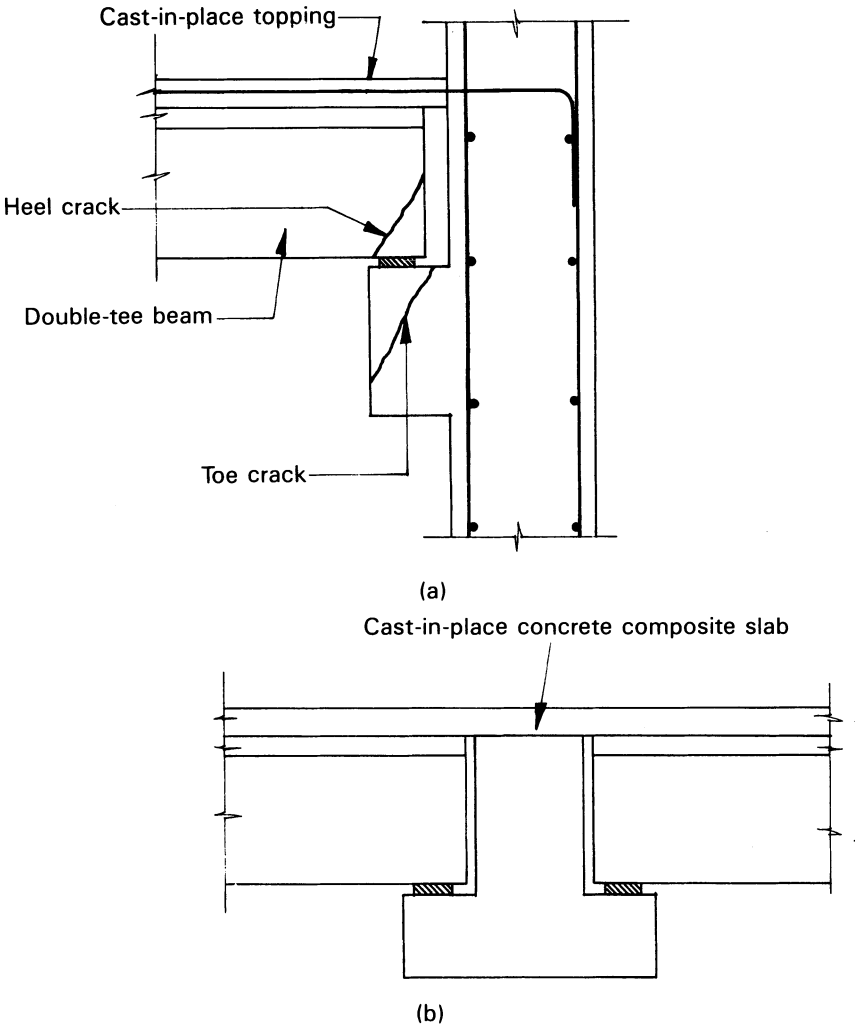

Fig. 12-10. A typical concrete ledger and a typical concrete ledge. (a) Cast-in-place concrete ledger supporting a double-tee beam. (b) Ledges of inverted-tee beam supporting double-tee beams.

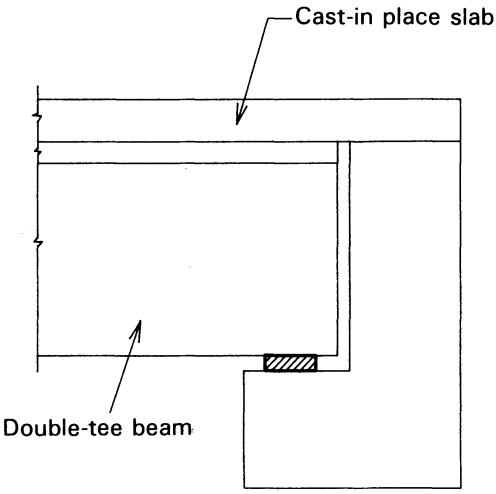

(c)

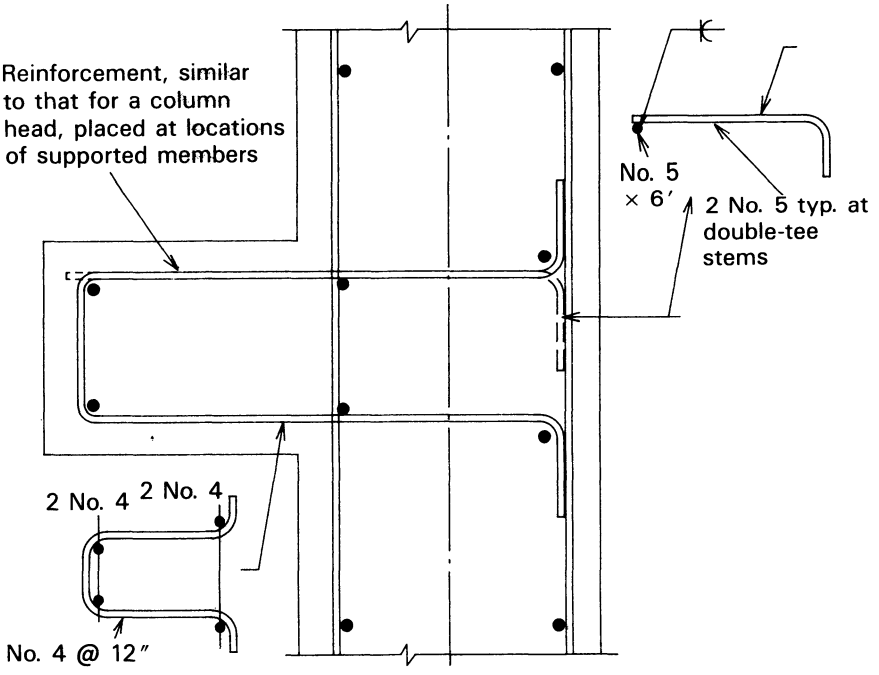

No. 4 U-shaped bars uniformly spaced along the length of the ledger

(d)

Fig. 12-10. (*Continued*) (c) Ledge at L-shaped beam supporting a double-tee beam. (d) Reinforcement in a cast-in-place ledger.

upon ledgers can cause heel cracks in the supported members and toe cracks in ledges or ledgers unless these members are correctly designed and effectively reinforced. Elastomeric bearing pads, which are discussed in Sec. 12-9, are effective in reducing the horizontal forces at the connections, as well as in reducing the incidence of heel and toe cracks, but they normally do not eliminate the need for reinforcement. The stem reinforcement in the ends of the double-tee stems frequently consists of a steel angle or plate anchored to the concrete, similar to the detail shown in Fig. 12-11.

The reinforcement in ledges and ledgers, which can be designed following the procedure contained in *Design and Typical Details of Connections for Precast and Prestressed Concrete* (PCI 1988), consists of reinforcement for flexure and axial tension (A_s), longitudinal reinforcement (A_l), and hanger (vertical axial tensile force) reinforcement (A_{sh}), as shown in Fig. 12-12. The hanger reinforcement is not needed in the walls supporting ledgers. The selection of the concrete dimensions and the detailing of the reinforcement in ledges and ledgers, as shown in Fig. 12-12, should be done by taking the actual dimensions of the reinforcing steel bars, bar bend dimensions, bar bending tolerances, bar placing tolerances, and concrete dimensional tolerances into account. It should be noted that the reinforcement is effective only if it is anchored sufficiently to develop the required stresses in the reinforcement. The minimum tension embedment lengths, l_{dh}, for 90° and 180° standard hooks can be found in reinforcing steel design and detailing aids (CRSI 1984).

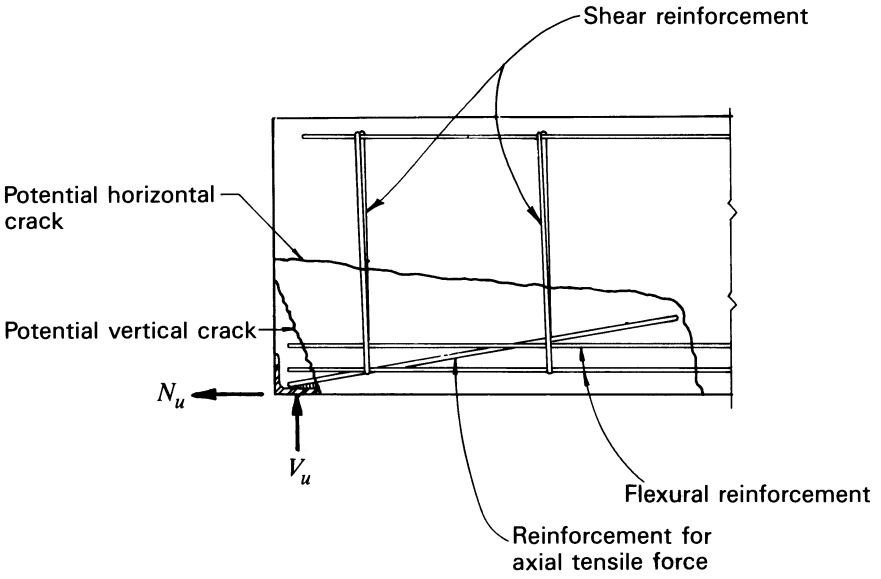

Fig. 12-11. Typical reinforcement for the bottom of a double-tee beam stem at its support.

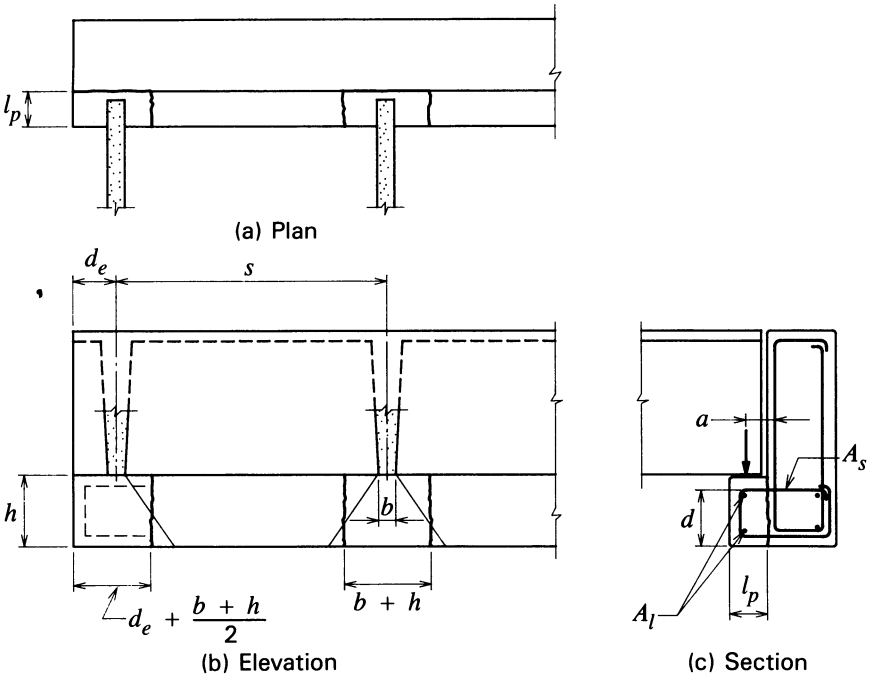

Fig. 12-12. Typical ledger and ledge reinforcement based upon the recommendations of the Precast/Prestressed Concrete Institute.

12-6 Dapped End Connections

The ends of beams sometimes are dapped, as illustrated in Fig. 12-13, to reduce the overall depths of floor and roof construction as well as to obtain the desired appearance for a building. The provision of a dap introduces a condition of

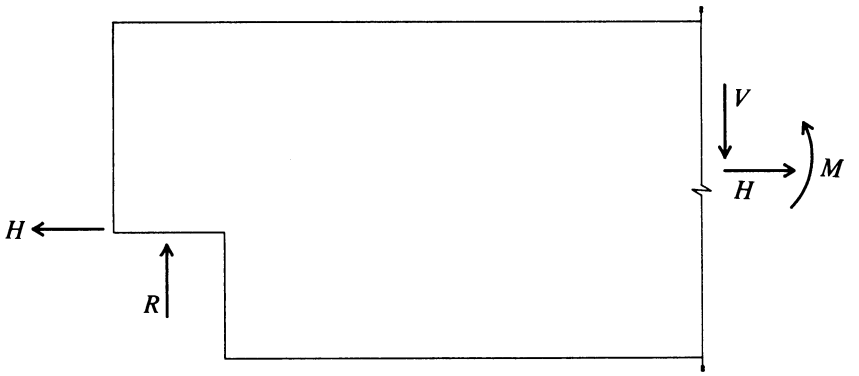

Fig. 12-13. Forces and moment on the dapped end of a prestressed concrete beam.

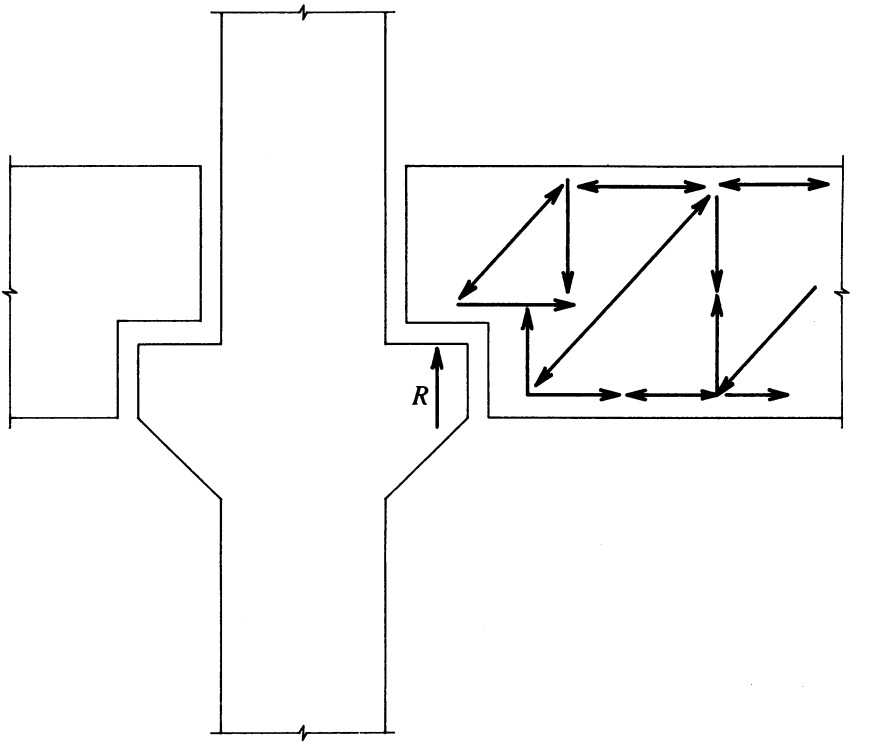

Note that compression struts are denoted by arrows toward the nodal zones and tension ties are denoted by arrows away from the nodal zones.

Fig. 12-14. Truss analogy model of the forces at the dapped end of a beam.

stress that requires reinforcing details different from those used in beams that are not dapped. The forces that must be considered in the design of beams with dapped ends are illustrated, using the truss analogy, in Fig. 12-14, and the locations of potential cracking that must be considered in proportioning the reinforcement are shown in Fig. 12-15. The cracks indicated in Fig. 12-15 are described as follows:

1. Diagonal tension (shear) crack in the extended end of the beam.
2. Potential direct shear crack used in the shear-friction analysis of the horizontal reinforcement that extends across the crack.
3. Diagonal crack (shear) emanating from the reentrant corner of the dapped end.
4. Diagonal tension (shear) crack in the full-depth section of the beam.

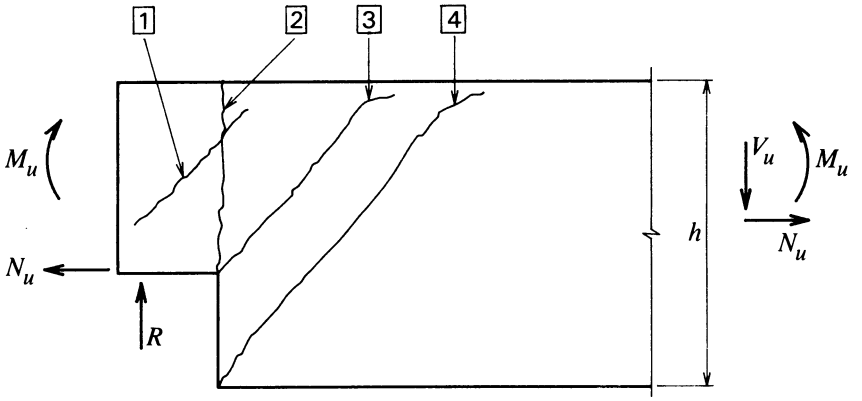

Fig. 12-15. Locations of potential cracking influencing reinforcement details in a dapped end beam.

The recommendations contained in the *PCI Design Handbook* for the design of beams with dapped ends have been different in each edition of the handbook (PCI 1971, 1978, 1985). For this reason, it is recommended that designers of beams with dapped ends consult the most recent publications of the Prestressed Concrete Institute before commencing the design of beams of this type. Furthermore, it is recommended that designers check their work by using an analysis based upon the truss analogy.

Beams with dapped ends frequently are used for spandrel beams in buildings. Spandrel beams often are subjected to torsional moments as a result of the connection details for the members supported by the spandrel beam, the support details for the spandrel beam itself, and the location of the shear center of the spandrel beam cross section. This is illustrated in Fig. 12-16. It is important that the torsional moments applied to spandrel beams be investigated during design, and that torsional reinforcement be provided when needed.

12-7 Post-tensioned Connection

Continuity of beam–column connections can be obtained by utilizing the principle of segmental construction shown in Fig. 12-17. This connection has the advantage that continuity can be developed without the use of embedded steel plates and field-welding. The principal disadvantage of this detail is that temporary shoring must be used to support the precast beams until the concrete closure pour is placed and cured, and the tendons are prestressed. This type of joint would be expected to result in a slightly longer construction time than would be experienced with other types of connections because of the time required to place and cure the cast-in-place concrete. Furthermore, shortening of the beam concrete from the effects of concrete shrinkage and creep may cause

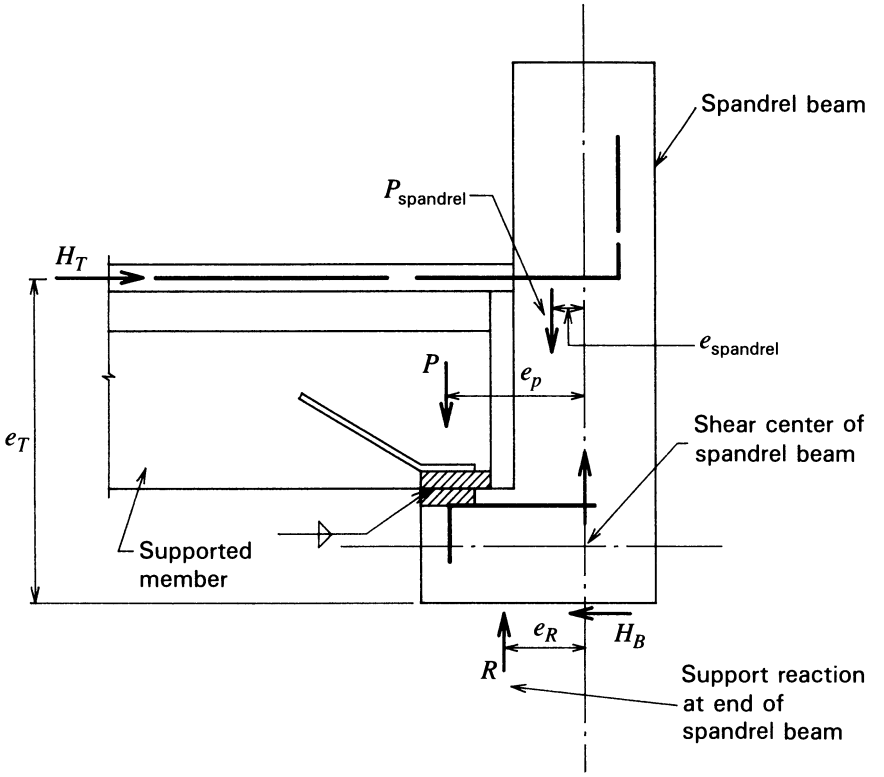

Fig. 12-16. Typical forces on a spandrel beam that cause torsional moments.

larger moments in the column than would be expected with other connection details.

12-8 Column Base Connections

Precast column base connections commonly used in precast concrete buildings are shown in Fig. 12-18. Each detail has certain advantages relative to the fabrication of the precast columns and the field work required after the erection of the columns, but there is little difference in the details from the standpoint of structural performance.

It should be observed that these details do not permit the extension of nonprestressed reinforcing steel dowels from the foundations into the columns as is commonly done in cast-in-place construction. Hence special attention must be given to the connection details if it is necessary or desired to transfer significant loads and moments between the column bases and the foundations. Welding of the longitudinal column reinforcement to the column bearing plates

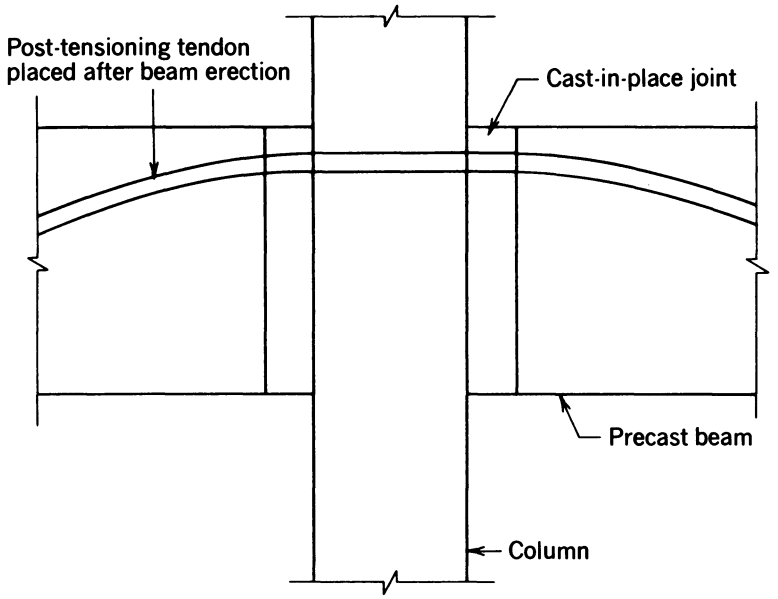

Fig. 12-17. Post-tensioned beam–column connection.

and filling of the space between the bottom of the column base plate and the top of the concrete foundation must be done well after the precast column has been erected and positioned, in order to achieve satisfactory results. The material used in filling the space should be dry-packed portland cement mortar or one of the premixed non-shrink products commercially available for this purpose. The designer must understand that the capacity of this type of connection generally is considered to be limited by the allowable bearing stress in the weaker of the two concretes. The provision of jam nuts on the anchor bolts immediately beneath the base plates facilitates plumbing and adjusting the elevation of the columns at the time of erection.

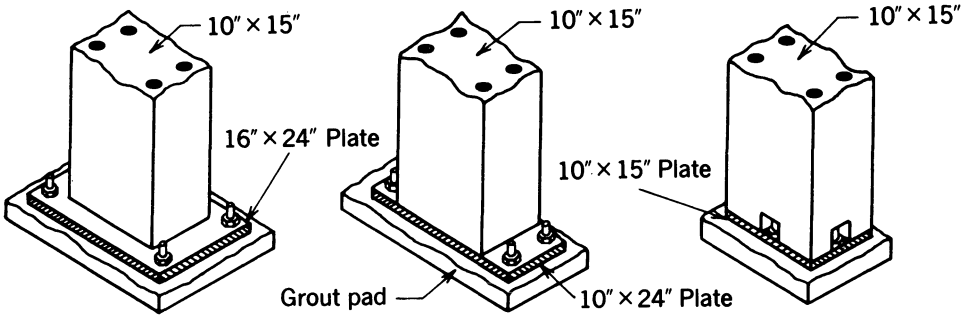

Fig. 12-18. Typical column base connections for precast concrete columns.

Column connections of the types shown should be designed by using a capacity reduction factor of 0.70, as required for tied columns by most building codes. The critical section in the design of the base plate that extends beyond the edge of the column is commonly taken as the plane tangent to the column reinforcing steel nearest the anchor bolts that are loaded in tension.

The stiffness of the connection used in design should include the effects of bolt elongation and plate deflection, as well as foundation rotations. The bolt design should be based upon the area at the root of the threads and not the nominal bolt diameter. If shear forces are to be transmitted by a connection, special consideration should be given to the stresses resulting from the combined shear and tensile stresses.

12-9 Elastomeric Bearing Pads

Elastomeric bearing pads, formulated with natural or artificial elastomers (rubber or rubber-like materials) combined with mineral fillers, have been used in both concrete and steel structures since the 1950s (Du Pont 1957). They offer some very attractive benefits if they are made of good-quality materials and correctly proportioned. Some of their advantages are:

1. Elastomeric bearing pads are capable of supporting compressive stresses in the range of 500 to 1000 psi in their most simple configuration (i.e., unreinforced and unconfined), depending upon the shape and composition of an individual pad (Fig. 12-19).
2. If used in a configuration that prevents excessive bulging at the unloaded surfaces of the pads, through lamination with steel or other materials (as shown in Fig. 12-20) or by the confinement of external restraining devices, the elastomeric materials are capable of supporting compressive stresses as high as 3000 psi.

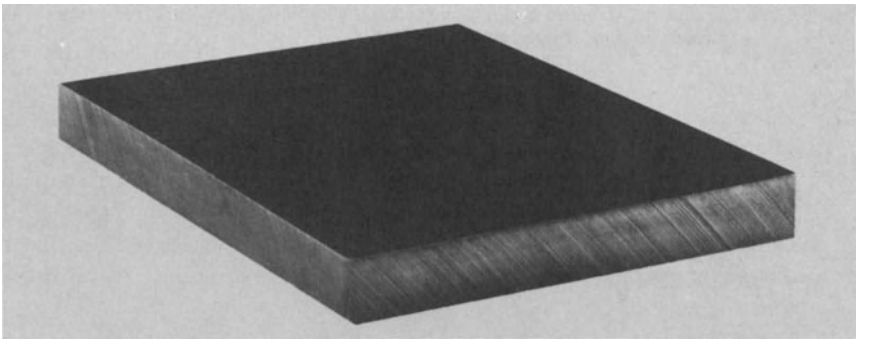

Fig. 12-19. Solid, unreinforced elastomeric bearing pad. (Based upon data obtained from and used with permission of JVI Inc., Skokie, Illinois.)

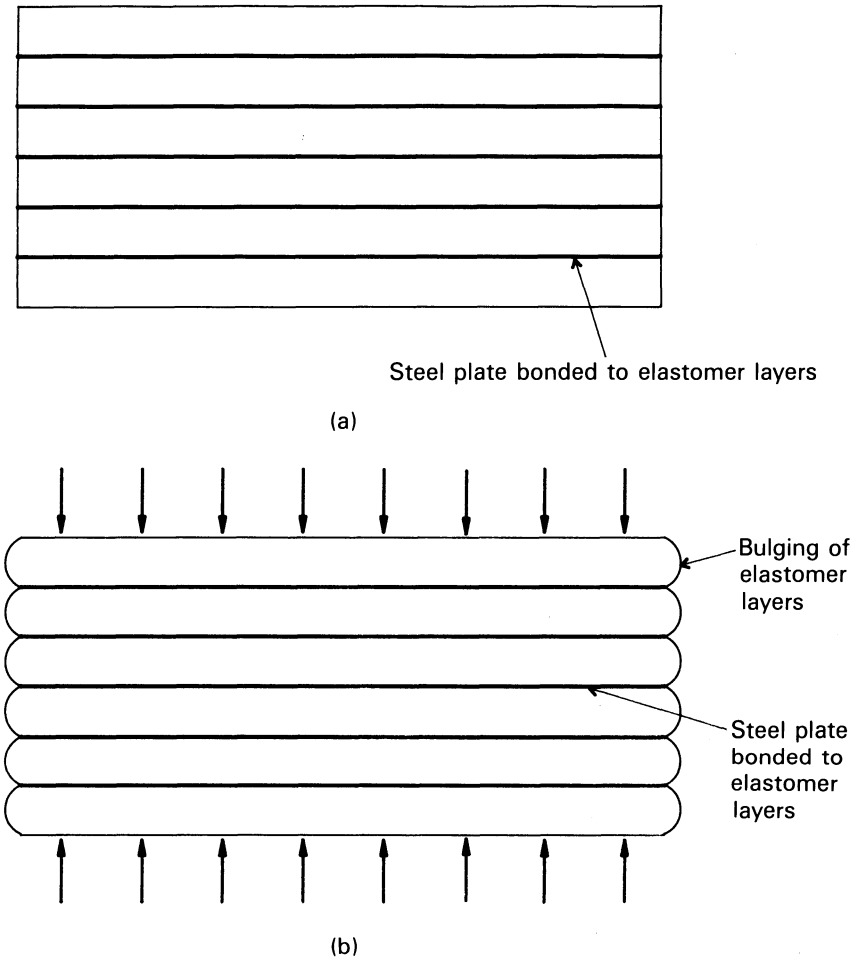

Fig. 12-20. Elastomeric bearing pad reinforced by lamination with steel plates. (a) unloaded pad. (b) Loaded pad.

3. When used between two surfaces of concrete, such as those commonly found at the ends of precast concrete flexural members where they are supported by corbels, column heads, ledgers, and so on, elastomeric bearing pads of correct proportions and composition are capable of compensating for small differences in the out-of-planeness (i.e., surfaces that are not parallel) that commonly exists at these locations. This is illustrated in Fig. 12-21.
4. When correctly designed, fabricated, and installed, elastomeric bearing pads are capable of accommodating displacements due to the effects of concrete creep and shrinkage, as well as temperature variations, without

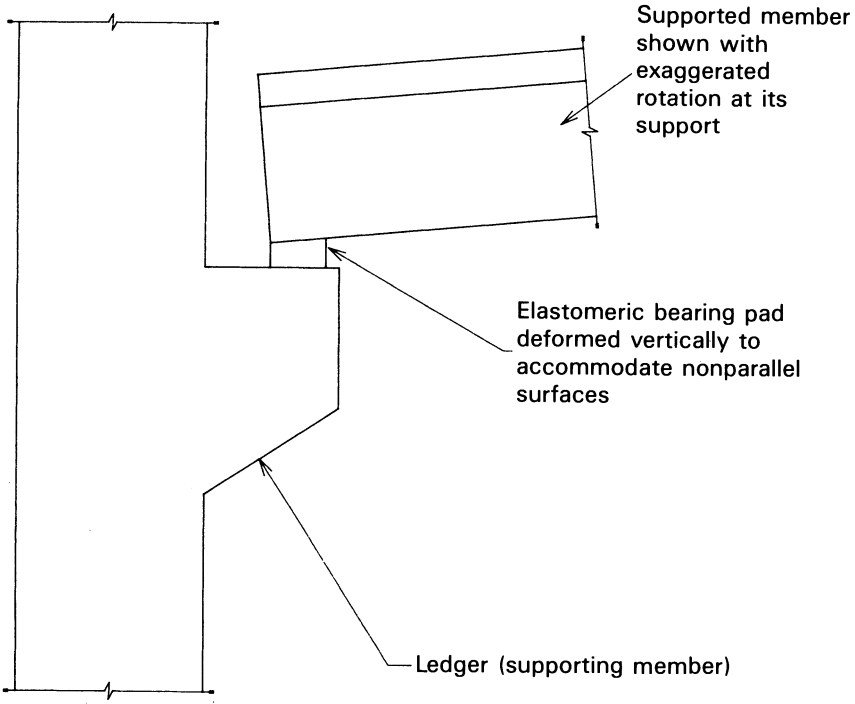

Fig. 12-21. Elastomeric bearing pad in a joint having rotational deformation.

large horizontal forces being created. This is illustrated in Fig. 12-22a. In the design of some elastomeric bearing pads, particularly in building construction, the designer sometimes relies upon the supported member's slipping over the top surface of the elastomeric bearing pad as a means of relieving the forces that would be developed because of concrete creep and shrinkage if restrained as shown in Fig. 12-22b.

5. When correctly designed, fabricated, and installed, elastomeric bearing pads are capable of accommodating rotations such as those that occur at the ends of flexural members due to the application of external loads and environmental effects (temperature changes, temperature gradients, etc.).
6. Elastomeric bearing pads function as a result of compressive and shear deformations of the material and, if well compounded with materials of good quality, are basically unaffected by corrosion, oxidation, foreign materials, inelastic deformation, and time-dependent variations in friction characteristics. (See Table 12-1 for typical values of the shear modulus for elastomers of different hardnesses.)

Some elastomeric bearing pads are composed of the elastomer alone, whereas others are formed of elastomeric materials laminated with steel plates or fabrics

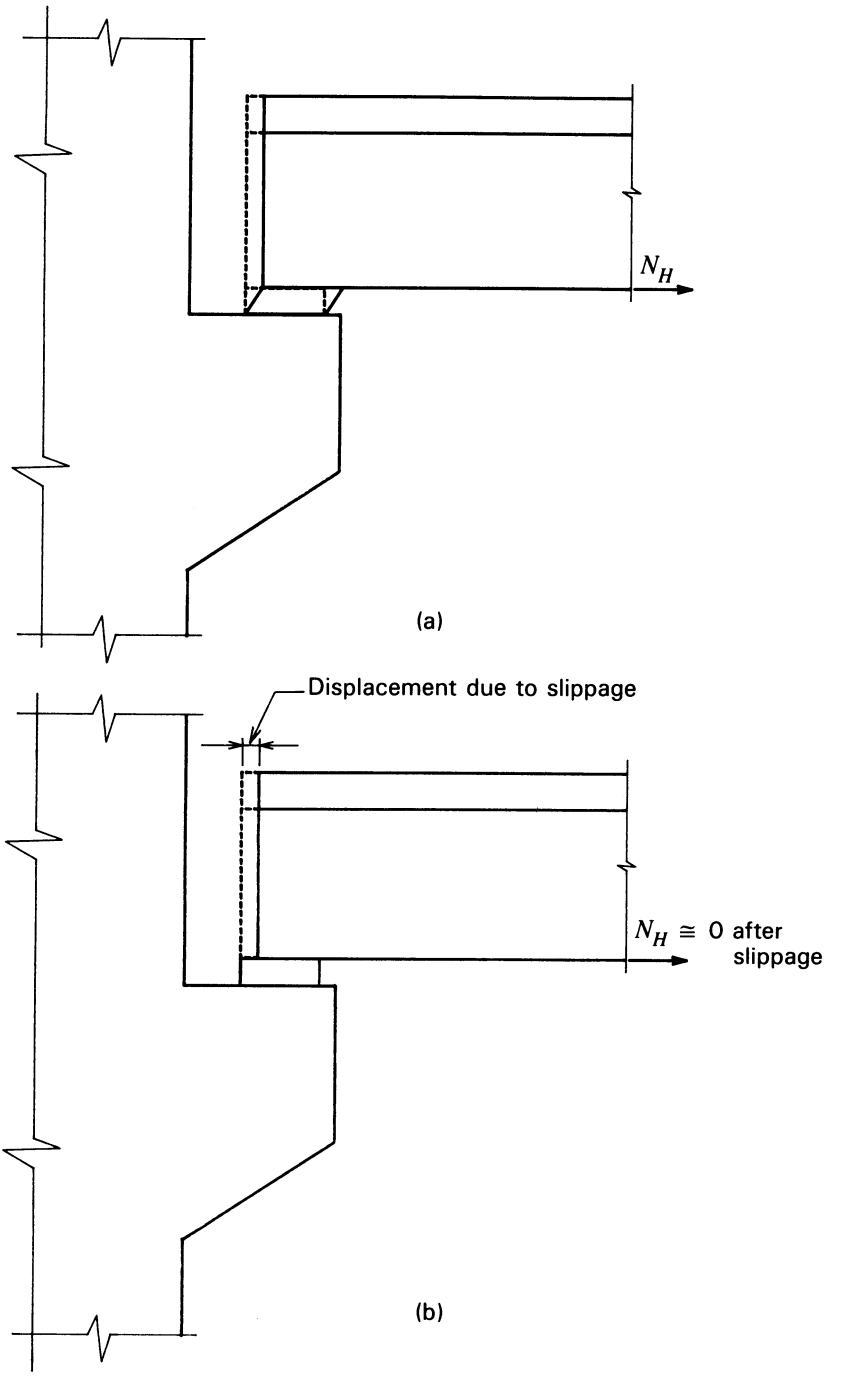

Fig. 12-22. Mechanisms relieving the forces due to concrete creep and shrinkage with elastomeric bearing pads. (a) Elastomeric bearing pad deformed because of shear stresses. (b) Slippage of a supported member.

TABLE 12-1 Modulus of Elasticity in Shear.

50 Durometer Hardness	60 Durometer Hardness	70 Durometer Hardness
110 psi at 70°F	160 psi at 70°F	215 psi at 70°F
1.10 × 110 psi at 20°F	1.1 × 160 psi at 20°F	1.10 × 215 psi at 20°F
1.25 × 110 psi at 0°F	1.25 × 160 psi at 0°F	1.25 × 215 psi at 0°F
1.9 × 110 psi at −20°F	1.9 × 160 psi at −20°F	1.9 × 215 psi at −20°F

of various types. Others are composed of elastomeric materials and randomly oriented fibers embedded within the pads, as illustrated in Fig. 12-23. The provision of laminated materials and embedded fibers within the elastomer reduces the bulging of the unloaded edges of elastomeric pads, and, because shear stresses result from the bulges, higher loads can be safely used on these reinforced pads. Cotton-fiber duck laminated with an elastomer, as shown in Fig. 12-24, has been used successfully in bearing pads for many years. Plain elastomer pads are suitable for use only in applications where relatively small compressive stresses will result from the vertical loads, and larger horizontal displacements will not be experienced.

Specifications for the design and fabrication of elastomeric bearing pads for use in highway bridges have been included in the AASHTO *Standard Specifications for Highway Bridges* for many years. (The provisions in the current edition are significantly different from those contained in the earlier editions; AASHTO 1989.) Unfortunately comparable design and fabrication standards do not exist for elastomeric bearing pads used in building construction. Recommendations for the design of elastomeric bearing pads, some based upon the AASHTO standards and some based upon information from the producers of elastomeric materials, have been included in the publications of the Prestressed

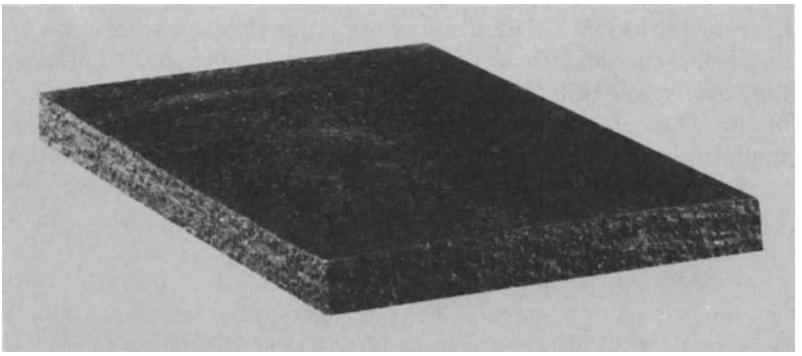

Fig. 12-23. Elastomeric bearing pad reinforced with randomly oriented fibers. (Based upon data obtained from and used with permission of JVI Inc., Skokie, Illinois.)

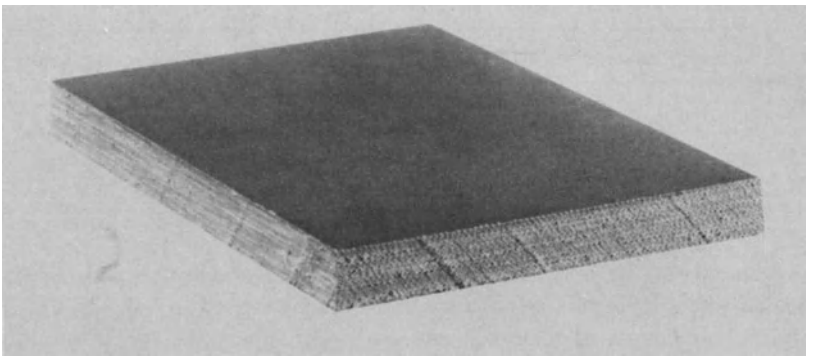

Fig. 12-24. Bearing pad composed of cotton-fiber duck laminated with an elastomer. (Based upon data obtained from and used with permission of JVI Inc., Skokie, Illinois.)

Concrete Institute for many years (see PCI 1971, 1978, 1985). In some industry publications elastomeric bearing pads that conform to the requirements in the AASHTO specifications have been referred to as structural grade pads, and pads that do not conform to the AASHTO standard have been termed commercial grade pads (PCI 1978). Unfortunately, commercial grade pads do not have to be manufactured to meet minimum standards and may or may not have physical properties that suit them for use in the construction of precast concrete structures. Numerous failures have occurred in structures constructed with commercial grade elastomeric bearing pads; some of these have been limited to the pads themselves, whereas others have resulted in damage to the supporting or supported members. In spite of the fact that there is no industry-consensus standard for elastomeric bearing pads used in building construction, knowledgeable and responsible producers of elastomeric bearing pads do exist. The designer and the user of elastomeric bearing pads should carefully investigate the source, composition, and experience record for the specific elastomeric bearing pads proposed for use on each project.

Bridge design practice in many European countries requires that elastomeric bearing pads be designed and detailed to be replaceable. This requirement is the result of a number of failures in elastomeric bridge bearings. The removal and the replacement of these pads are greatly facilitated if provided for when the bridge is designed.

Fabricated metal bearings, similar in construction to a hydraulic jack but having an elastomeric material as the compressible material rather than a fluid, are commonly used in bridge construction. Bearings of this type, which are frequently referred to as pot bearings, are covered by patents and copyrights, and for this reason it is best to obtain details about them from the manufacturers.

12-10 Other Expansion Bearings

Other materials, such as steel plates coated with low-friction coatings, graphite-impregnated materials, steel rollers, steel rockers, and bronze plates containing grooves filled with lubricants, have been used with varying degrees of success in prestressed concrete structures. The newer low-friction plastic-coated steels, as shown in Fig. 12-25, appear promising. The designer should investigate any proposed bearing material as thoroughly as possible before use, understanding that the horizontal forces that can develop when bearings do not perform as expected can be very large and can result in serious structural problems.

12-11 Fixed Steel Bearings

Bearing details similar to those shown in Fig. 12-26 have been used in many instances without difficulty. If the steel bearing plates supporting the beams are welded together, or if they become fixed to each other by the products of corrosion, they can transmit large forces that may cause cracking and eventual failure of the concrete in the connected parts. If the plates are not welded together and the center shim plate width is small, as compared to the upper and lower plates, the action of the bearing can approximate that of a rocker.

If top reinforcing is provided at a connection similar to the one shown in Fig. 12-26, and the steel bearings at the bottom of the member are welded together, rotations at the end of the beam will be restrained, and the construction will be structurally continuous for loads after continuity has been established. In a case such as this, the reinforcing, as well as the bearings, should be designed for the forces resulting from the continuity as well as from restrained concrete creep, shrinkage volume, and temperature deformations.

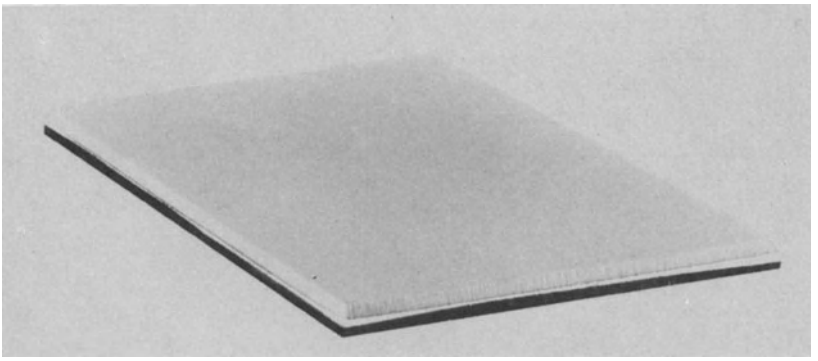

Fig. 12-25. Teflon-coated steel plate for use in a structural bearing. (Based upon data obtained from and used with permission of JVI Inc., Skokie, Illinois.)

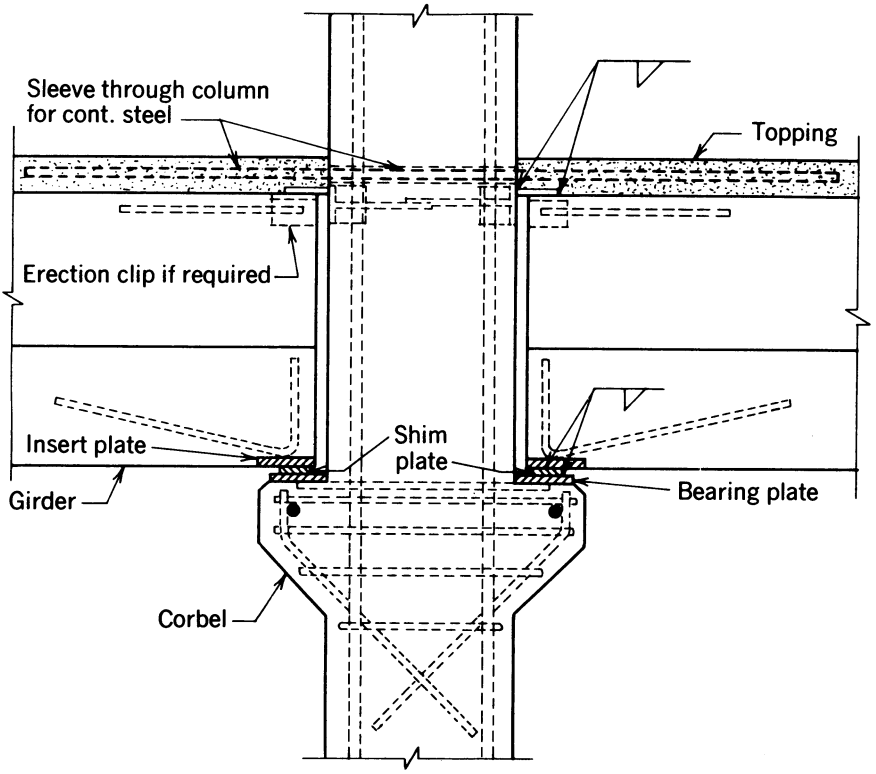

Fig. 12-26. Beam connection detail with welded steel plates at bottom and nonprestressed continuity reinforcement at top.

Fixed connections commonly are provided at the tops of beams, as shown in Fig. 12-26, through the provision of reinforcement in the cast-in-place concrete topping. Horizontal displacement of the top of the girder is prevented by the cast-in-place reinforced concrete, but the bottom supports usually are designed to move horizontally as well as to rotate. In this way, the effects of concrete creep and shrinkage, rotations due to applied loads, and deformations due to temperature effects can take place with reduced restraint and little if any cracking or other adverse effects.

12-12 Wind / Seismic Connections

It is often necessary to provide a means of transferring shear forces between individual precast concrete structural elements to provide resistance to lateral loads that will be applied to a building or other structure. A cast-in-place bonded concrete topping placed over precast members frequently is used to effect the shear transfer and form a diaphragm.

When a concrete topping is not used, connections are frequently provided between the individual precast units to transfer the shear forces. The connections can consist of concrete shear keys, adhesives, or metal inserts that are connected by welding or bolting. The use of concrete shear keys for this purpose is not common, because if they are to be effective, the precast units must be restrained against movements that would separate them. (Shear keys themselves normally are not capable of transferring tensile forces.) Although such restraint sometimes is possible by the inclusion of continuous prestressed or nonprestressed reinforcement in the end joints (over the supporting beams or girders), the details in doing so can be involved and not straightforward. Adhesives are not commonly used to provide shear strength because they are not resistant to heat and thus cannot be used structurally in fire-rated construction. In addition, the weakest part in a connection made with adhesives in a concrete structures is most often the strength of the concrete at the glue line and not that of the adhesive itself. A commonly used shear connector detail for double-tee, single-tee, and channel slabs is shown in Fig. 12-27. It should be noted that this detail includes the welding of reinforcing steel, and when it is used, the recommen-

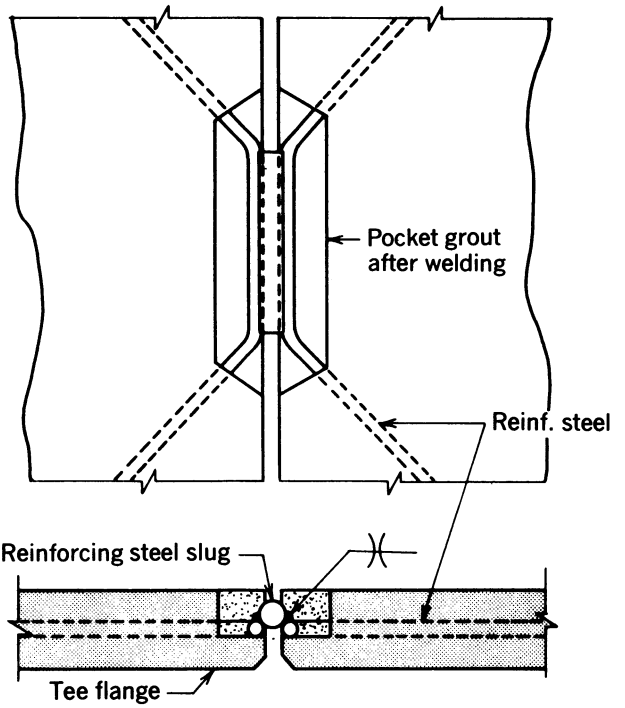

Fig. 12-27. Typical wind/seismic connection used in flanges of double-tee slabs.

dations for welding reinforcing steel of the American Welding Society should be followed (AWS 1979).

One should remember that the imposition of a force on the connection results in compression in some of the bars. Because they are positioned in thin sections, the bars cannot be tied and braced against buckling, as is customary when concrete reinforcement is used in compression. Connections of this type cannot be expected to exhibit great ductility—an important consideration in designing for seismic forces.

Hollow core slabs (for building construction) made with some processes can be provided with metallic inserts that can be used to develop the required shear forces. Other manufacturing processes do not permit the inclusion of metal inserts, and products made by these methods frequently are used with a structural topping in areas where lateral loads due to wind and earthquake must be resisted.

Concrete shear keys can be used efficiently in bridges to transfer lateral and longitudinal shear forces between bridge superstructures and substructures. The shear keys frequently are provided between the end diaphragms and bent (or pier) caps or at the abutments. The keys can be lined with thin (0.25 in.) expansion-joint material to prevent bond where they are designed to be fixed against displacements but must be free to rotate. Thicker expansion-joint material or expanded polystyrene frequently is used to line keys designed to provide for displacements (expansion bearings) as well as rotations.

12-13 Shear-Friction Connections

When it is inappropriate to consider shear as a measure of diagonal tension, contemporary engineering practice recognizes the shear-friction concept as a means of transferring shear forces. The method can be used in the design of corbels, according to the provision of ACI 318, when the ratio of the shear span to the effective depth is 0.50 or less. There are many conditions where the concept finds application in precast structural concrete elements.

In the shear-friction concept, a crack is assumed to exist in the member in the location where one might expect the element to fail in shear. Reinforcement placed across the crack is assumed to provide a force normal to the crack and develop a frictional resistance that prevents displacement of the crack. If the amount of reinforcement is sufficient, the frictional resistance will be greater than the applied shear force, and slippage will be avoided. The reinforcing should be placed approximately perpendicular to the crack.

The unit shear stress v_u is not permitted (in ACI 318) to exceed 800 psi or $0.2f'_c$, whichever is less, and the area of steel required is computed from:

$$A_{vf} = \frac{V_u}{\phi f_y \mu} \tag{12-9}$$

in which the yield strength on the nonprestressed reinforcement, f_y, cannot exceed 60,000 psi, the strength reduction factor cannot be taken to be greater than $\phi = 0.85$, and μ, the friction coefficient, is equal to 1.4 for concrete cast monolithically, 1.0 for concrete placed against clean, artificially roughened, hardened concrete (construction joints) surfaces, and 0.70 for concrete placed against clean, unpainted as-rolled steel.

If tensile stress as well as shear stress exists across the potential crack, additional reinforcement must be provided to resist the tensile stress. In any case, the reinforcement must be placed in such a manner that it is adequately anchored on each side of the assumed crack, and it must be well distributed over the area.

It should be noted that values of the friction coefficient μ recommended by the Prestressed Concrete Institute are larger than those contained in ACI 318 (PCI 1985). The PCI recommendations are based upon experimental data.

REFERENCES

AASHTO. 1983(88). *Standard Specifications for Highway Bridges, Thirteenth Edition*. Washington, D.C. American Association for State Highway and Transportation Officials.

AASHTO. 1989. *Standard Specifications for Highway Bridges*. Washington, D.C. American Association of State Highway and Transportation Officials.

ACI Committee 318. 1989. *Building Code Requirements for Reinforced Concrete*. Detroit. American Concrete Institute.

American Welding Society. 1979. *Structural Welding Code—Reinforcing Steel*. D1.4-79. Miami. American Welding Society.

Burton, K. T., Corley, W. G., and Hognestad, E. 1967. Connections in Precast Concrete Structures—Effect of Restrained Creep and Shrinkage. *PCI Journal* 12(2):18–37.

CRSI Task Group on Reinforcement Anchorages and Splices. 1984. *Reinforcement Anchorages and Splices*. Schaumburg, Illinois. Concrete Reinforcing Steel Institute.

CRSI Placing Reinforcing Bars. 1986. Schaumburg, Illinois. Concrete Reinforcing Steel Institute.

E. I. du Pont de Nemours and Company, Inc. 1957. *Design of Neoprene Bearing Pads*. Wilmington, Delaware.

Iverson, J. K. and Pfeifer, D. W. 1985. *Criteria for Design of Bearing Pads*. Chicago. Prestressed Concrete Institute.

Kriz, L. B. and Raths, C. H. 1963. Connections in Precast Concrete Structures-Strength of Column Heads. *PCI Journal*.

Kriz, L. B. and Raths, C. H. 1965. Connections in Precast Concrete Structures—Strength of Corbels. *PCI Journal* 10(1):16–61.

Long, J. E. 1974. *Bearings in Structural Engineering*. New York. John Wiley & Sons.

PCI Committee on Connection Details. 1963. *Connection Details for Precast-Prestressed Concrete Buildings*. Chicago. Prestressed Concrete Institute.

PCI Committee on Connections. 1988. *Design and Typical Details of Connections for Precast and Prestressed Concrete*. Chicago. Prestressed Concrete Institute.

PCI Design Handbook. 1971. First Edition. Chicago. Prestressed Concrete Institute.

PCI Design Handbook. 1978. Second Edition. Chicago. Prestressed Concrete Institute.

PCI Design Handbook. 1985. Third Edition. Chicago. Prestressed Concrete Institute.

The Consulting Engineers Group Inc. 1986. *Survey of Precast Concrete Parking Structures*. Chicago. Prestressed Concrete Institute.

13 Roof and Floor Framing Systems

13-1 Introduction

The subjects of prestressed and nonprestressed reinforced-concrete roof- and floor-framing systems are inseparable because identical concrete sections sometimes are used with each mode of reinforcing, and because some framing schemes incorporate elements composed of each type of construction. For this reason, each will be considered in this discussion although the emphasis will be placed upon members with prestressed reinforcement. Nonprestressed reinforced-concrete elements will be discussed only when they are used in lieu of or in combination with prestressed elements.

The desirable features of floor and roof systems frequently, but not always, will include the following:

1. Good performance at service loads with adequate strength for design loads and with minimal, if any, cracking.
2. Economy in first cost.
3. Low maintenance cost.
4. Adaptability to long and short spans with minimum revision to the manufacturing facilities.

5. Minimum total depth of construction.
6. Ease in providing vertical openings of various sizes for elevators, stairwells, plumbing, skylights, and so on.
7. High stiffness of individual precast units (low deflection).
8. Ease in developing diaphragm action of roof or floor structures for resisting horizontal loads (seismic, wind, etc.).
9. A clean, attractive soffit that is smooth or nearly so, and thus can often be left exposed in the completed building.
10. Stability of precast elements during manufacture, transportation, and erection at the job site.
11. Low, uniform, stable deflection.
12. Good fire resistance.
13. Good thermal and sound insulating qualities.
14. Large and small daily production possible with minimum capital investment.
15. Minimum erection time.
16. Large equipment and skilled labor not required for erection.
17. A minimum of additional labor, forms, or welding required for joining the elements at the time of or after erection.
18. Ability to withstand forces imposed in handling, transport, and erection without cracking or permanent deformation.

Clearly no one framing scheme can offer all these advantages. The relative importance of the factors listed above will vary from job to job, in different applications, and in different localities.

It is not possible to discuss each system and method of framing that has been used or produced as a standard product in the United States. There have been many different methods and variations of those methods. A directory of precast, prestressed-concrete producers and their products, published in 1969 by the Prestressed Concrete Institute (PCI 1969), included thirteen types of beams, girders, and joists; nine types of "stemmed" units (i.e., double-tee beams, single-tee beams, etc.); five types of members with continuous internally formed voids; eleven types of piles; and a variety of architectural and miscellaneous units. The *PCI Design Handbook* among other PCI publications, also contains valuable data regarding the commonly used prestressed concrete products (PCI 1985). The following discussion is limited to general schemes that have received reasonably widespread acceptance, and is confined to general terms.

13-2 Double-Tee Slabs

Double-tee slabs, which are used extensively in North America for both roof and floor construction, have been made in a variety of widths and depths, as illustrated in Fig. 13-1. When they are used as floor slabs, a concrete topping

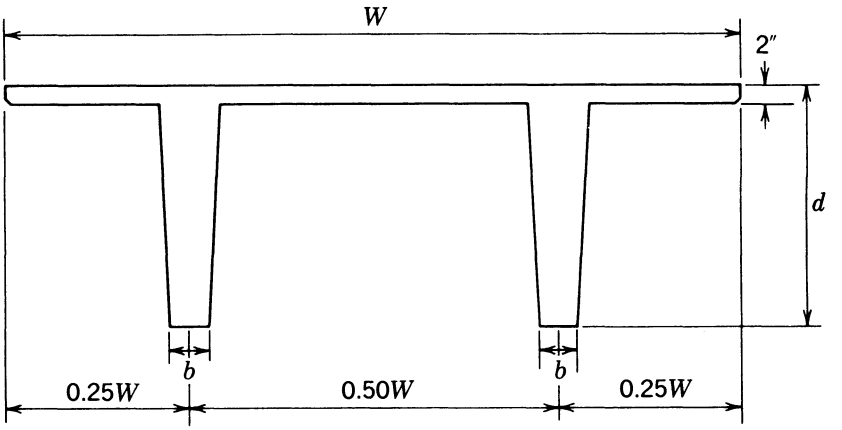

Normal Width of Slab	*Actual Width W*	*Maximum Depth d*	*Minimum Stem Width b*
8′-0″	7′-11 3/4″	30″	4 3/4″
6′-0″	5′-11 3/4″	24″	4″
4′-0″	3′-11 3/4″	16″	2 1/2″

Fig. 13-1. Typical double-tee beam dimensions.

from 2 to 4 in. thick usually is placed over the top of the slabs. The topping concrete generally is designed to be bonded to the precast double-tee slab and to perform as a composite component of the member for loads applied after curing of the topping. The topping also provides a means of obtaining a flat wearing surface, developing shear transfer through the composite construction, and installing seismic collector and chord reinforcement. Because of casting irregularities, variations in deflection, and other construction inaccuracies, the upper surface of erected double-tee slabs cannot be expected to be flat and true to line. A concrete topping frequently is not used in roof construction, the insulation and roofing often being applied directly to the precast slabs.

Owing to the poor performance of cast-in-place concrete toppings in some parts of the United States, primarily where deicing salts are used and the concrete is exposed to cycles of freezing and thawing, some manufacturers of double-tee slabs produce slabs with top flanges that are 4.5 in. thick or more, to avoid the need for a cast-in-place concrete topping on parking structures. (Minor amounts of cast-in-place concrete frequently are needed for corrosion protection of field connections, even with the thicker top flanges.) The double-tee slabs with the thicker top flanges are commonly referred to as pretopped double-tee slabs.

When a concrete topping is not used, it is normal practice to provide field-

welded connections in the edges of the top flanges to allow for the transfer of shear stresses between the individual slabs and to develop diaphragm action (see Sec. 12-12). The connections also help to eliminate differential live load deflection between the flanges of adjacent double-tee slabs. Differential deflections between adjacent slabs may result in damage to roofing applied to the slabs. Nonstructural fill material frequently is applied to the top surfaces of adjacent double-tee slabs as a means of eliminating abrupt changes in elevation at the joints and thereby helping to avoid damage to the roofing at the joints.

If field-welded connections are to be used to resist earthquake-induced forces, they should be designed for three or four times the forces to which they would be subject under the code-specified lateral force, unless tests have been made that demonstrate that the connections have sufficient ductility (energy-absorption capability) to render this requirement unnecessary. If tests are used, they should demonstrate that the diaphragms formed through the use of the connections will not displace to such an extent that the overall stability of the structure under seismic forces is questionable.

Double-tee slabs are structurally efficient. The slab portion is quite thin and has well-balanced negative and positive moments. The legs of the joists or tees are thin and normally are highly stressed. The legs do not have significant torsional stiffness, but this consideration is not normally important in roof or floor construction. The slabs are relatively light when compared to other types of framing for the longer spans, and they contain little excess material. A significant contribution to a slab's structural efficiency results from the fact that a very large portion of the total dead load is acting on the slab at the time of prestressing. Double-tee slabs can be obtained at relatively low cost in virtually all sections of the United States.

In applications that do not require beams to support the slabs, such as single-span commercial buildings with bearing walls, the depth required for double-tee slab construction is quite small. When it is necessary to support the double-tee slabs on beams and columns, the total depth of construction may become relatively great. This is particularly true if long spans are required in each direction, for, during erection, the slabs must be lowered vertically upon the supporting members, and they cannot be rotated (in a horizontal plane) into position because of their width. The inverted-tee beam, which is illustrated in Fig. 13-2, has been widely used with double-tee slabs. The inverted-tee beam may or may not be prestressed, may or may not be made continuous in the completed structure, but does not have an efficient cross-sectional shape for long simple spans. For the longer spans, a large wide top flange is necessary to achieve the required flexural strength. In applications where a cast-in-place topping will be provided to act compositely with an inverted-tee beam, the topping may provide an adequate top flange. An efficient solution for long spans in each direction is the use of double-tee slabs in combination with beams that

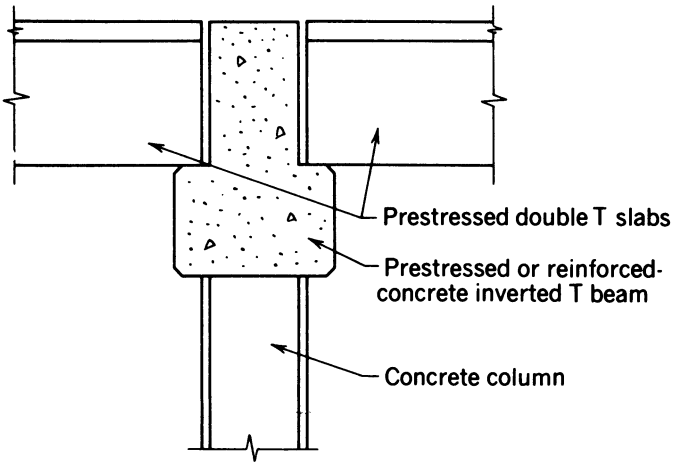

Fig. 13-2. Inverted-tee beam supporting double-tee beam.

have wide flanges, as illustrated in Fig. 13-3; the large total depth of the structure should be noted.

The size of vertical openings that can conveniently be provided in double-tee slabs is restricted to the clear width of the flange between stems unless special strengthening or intermediate support can be developed. The top flange of the slab is essential in developing flexural strength; so the openings may have to

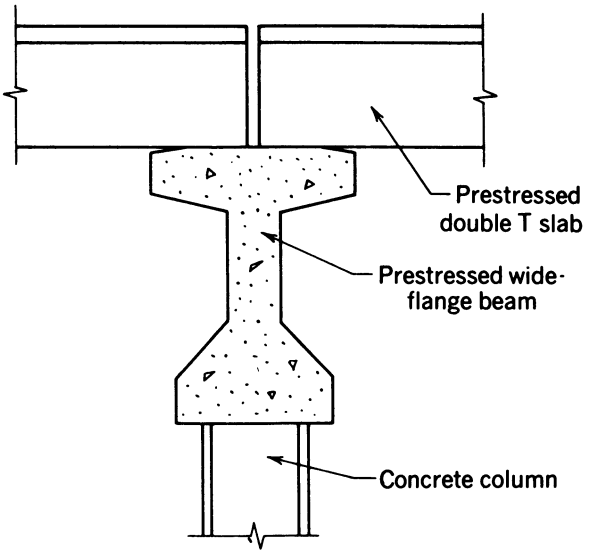

Fig. 13-3. Double-tee beam supported by prestressed concrete wide-flange beam.

be confined to the areas near the ends of the span where the moments are low. The soffits of double-tee beams are left exposed in many industrial and commercial applications.

Double-tee slabs are stable during manufacture and erection, but they must be handled with reasonable care, or the relatively fragile, outstanding flanges can be cracked. Double-tee slabs occasionally have large upward deflections due to prestressing. The deflection sometimes is not uniform from slab to slab, and, in an attempt to minimize this undesirable feature, deflected tendons and partial prestressing frequently are used. When they are fabricated with a top flange on the order of 2 in. thick, as is frequently the case, the fire resistance of double-tee slabs can be made to have a two-hour fire rating if the stems are large enough to protect the prestressed reinforcement, and if the slabs are provided supplementary insulation and built-up roofing. When they are provided with a cast-in-place concrete topping, a fire rating of two hours is easily obtained.

Double-tee slabs normally are made on pretensioning benches from 200 to 400 ft long although some manufacturers use longer beds, and some have used individual molds that resist the pretensioning force during concrete placing and curing (i.e., stress-resisting forms).

Because of the relatively large size of each double-tee slab, the erection time normally required with these members is not excessive (on a unit-area basis), and equipment of moderate size usually will work efficiently. The amount of labor required to complete the structural roof or floor during and after erection varies from job to job, depending upon the amount of welding and other tasks required to complete the structure.

Some manufacturers have supplied this type of slab made of ordinary reinforced concrete rather than prestressed concrete. Virtually all double-tee slabs currently are made pretensioned. Adequate results can be obtained with reinforced concrete on short and moderate spans if sufficient camber is provided in the members so that creep and shrinkage will not cause sagging.

Double-tee slabs fabricated by reputable and skilled manufacturers are efficient in many applications. They not only perform well, but have a pleasing appearance.

13-3 Single-Tee Beams or Joists

Single-tee beams of two general types are used in roof and floor construction. The first of these is made with the same mold that is used in double-tee beams and has the general dimensions shown in Fig. 13-4. The advantages and disadvantages of single-tee members of this type are virtually identical to those of the double-tee slab, with the exception of stability of the members during erection.

The other type of single-tee beam is made in a mold that allows the dimen-

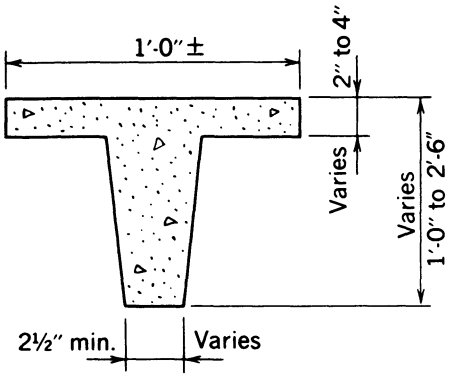

Fig. 13-4. Tee-beam made in double-tee mold.

sions to be varied approximately as is indicated in Fig. 13-5. This member can be used on roof spans up to 120 ft in length and in bridge spans up to about 60 ft. The web and flange thicknesses, which are greater than those normally used in double-tee slabs, can easily be varied. The large single-tee has been used extensively in many parts of the United States. The section is one of high structural efficiency.

Single-tee beams of each type normally are made with a constant depth (prismatic cross section) rather than variable dimensions. It is essential that some type of temporary support be provided during transportation and erection to prevent these members from falling or being accidentally tipped on their side, until such time as they are incorporated in the structure and become permanently braced.

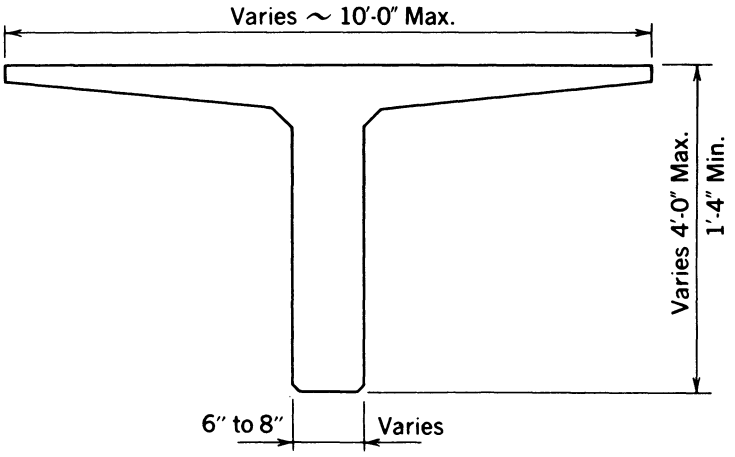

Fig. 13-5. Large tee-beam made in special mold.

13-4 Long-Span Channels

Long-span channels are members that, like double-tee slabs, incorporate a thin slab with ribs in such a way that the member can be used for relatively long spans without supplementary joists. Therefore, long-span channels have been used to span from bearing wall to bearing wall or from beam to beam, in the same way that double-tee slabs have been used. This single factor differentiates long-span channels from short-span channels, which normally do not have prestressed reinforcement. (Short-span channels require joists if used on spans that exceed 8 to 10 ft.) Long-span channels can be used on somewhat greater spans than are possible with standard double-tee slabs, as a rule, because they are narrower than a double-tee slab but have ribs comparable to or larger than those of the double-tee slab.

As with single-tees, some forms of channels are made from the same forms used to make double-tee slabs; so they have the same general attributes as double-tee slabs. There is no need to consider this form of channel any further here. The general dimensions that are used in some channels of this type are given in Fig. 13-6.

Channels of many other dimensions have been used. When the top flanges and ribs are made thicker, the strength is increased, as are the fire resistance, stiffness, weight, and cost. The deflection, and the variation of deflection between members, are less with channels of more ample proportions, such as the one illustrated in Fig. 13-7. With the thicker ribs, it is possible to develop good shear distribution between adjacent members in a structure. In addition, the heavier sections are less fragile than the lighter double-tee slabs.

End and intermediate diaphragms or flange stiffeners have been used in some types of prestressed and reinforced-concrete channels, but the provision of the secondary members greatly complicates the manufacturing facilities and techniques that must be employed. Temperature changes, shrinkage, and elastic shortening of the concrete (due to prestressing) all have a tendency to make the

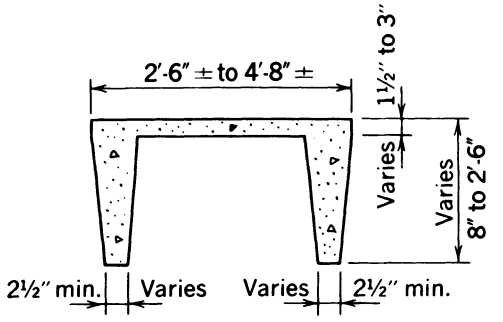

Fig. 13-6. Channel slab made in double-tee mold.

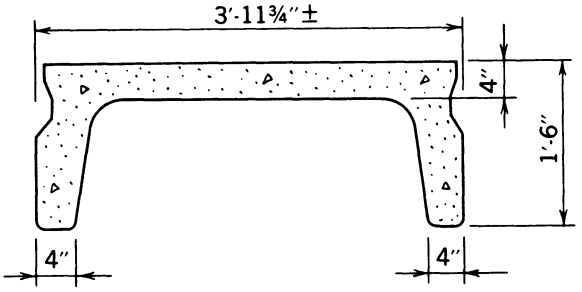

Fig. 13-7. Channel slab of moderate proportions.

precast member cling to the form or mold. These effects can be minimized by placing contraction joints in the forms.

Channels have several theoretical or practical advantages over double-tee slabs, as can be seen from the above discussion, but the advantages have not proved to be sufficiently important to justify the additional cost that results from their use. Long-span concrete channel slabs made with nonprestressed reinforcement concrete are efficient and cost-effective for moderate spans when manufactured in quantity.

13-5 Joists

Prestressed joists, or small beams, of various types and sizes are used with many types of deck materials, such as short-span channels, concrete plank, cast-in-place concrete, poured gypsum, and lightweight insulating roof materials composed of cement-coated wood fibers. Typical sizes and shapes of such joists are shown in Fig. 13-8. This type of framing is without question the most versatile because the cross-sectional shape of the joist does not restrict the maximum span on which it can be used to the same degree as with channel slab, double-tee slab, and single-tee beam construction. This versatility is due to the joist spacing's not being a fixed dimension.

The depth of construction required with joist framing is a somewhat greater than is needed in comparable spans of channel slabs and double-tee slabs when each type is used in bearing-wall construction, but it may be somewhat less when interior girders are required. The relatively lower construction depth that is possible with interior girders results from using girders that have a flat upper surface on the bottom flange on which the joists are supported. This type of girder, which is illustrated in Fig. 13-9, can be used without difficulty in joist construction; the joists can be rotated into position because of their relatively small width. As was explained previously, this cannot be done with double-tee and channel slabs because of their wide widths.

Another significant advantage with joist construction is the ease of allowing

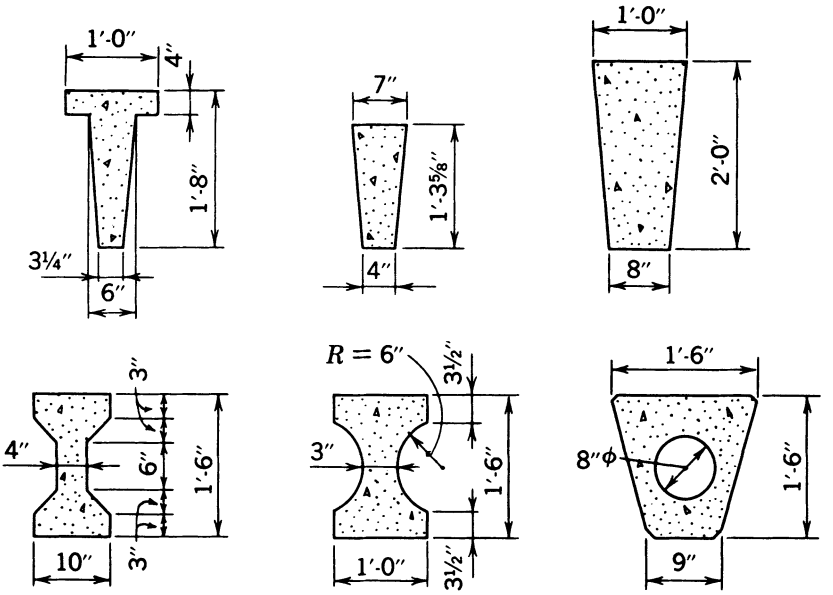

Fig. 13-8. Prestressed concrete joints.

for vertical openings. Because joist spacings normally range from 2.5 to 8.0 ft, the size of the vertical openings obtainable without special framing or strengthening is greater than that which is possible with most other types of precast framing.

Many of the other desirable characteristics of roof and floor framing systems with joists are functions of the design of the joists themselves and thus escape generalization. Included in this category are the maximum span, fire resistance, stability during handling, stiffness, appearance of the joists, and amount and stability of the deflection. Well-designed joists, however, will be satisfactory in all of these respects.

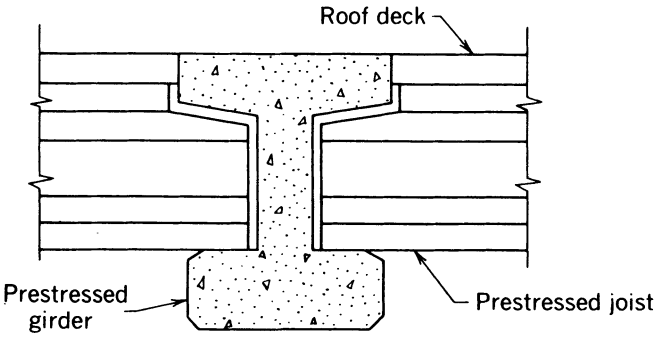

Fig. 13-9. Cross section through girder supporting prestressed concrete joints.

The degree of diaphragm action that can be developed, the appearance of the soffit, the fire resistance, and the thermal insulation characteristics, as well as the erection time and labor required, are contingent upon the type of deck selected for use with the joists.

13-6 Precast Solid Slabs

Prestressed-concrete solid slabs of two types are possible: small, prestressed planks that are 2 to 4 in. thick, and larger pretensioned slabs that are 6 to 12 in. thick. The smaller plank has been used in the United States, primarily as permanent forms for bridge decks, but some difficulty has been experienced in controlling the deflection and straightness of the individual units. Researchers believe that the variations in deflection between individual planks are combined effects of the normal variation in the quality of the concrete, the shrinkage of the concrete, and the fact that the eccentricity of the tendons is not maintained as precisely as is needed to obtain a uniform product.

Large, solid prestressed slabs capable of carrying roof loads or nominal floor loads on spans to about 30 ft are economical if made partially prestressed. Although solid pretensioned slabs have not been used to a great extent in the United States, they have been used in special applications such as precast soffit slabs for composite construction of pier decks. Hollow, precast, pretensioned slabs and solid, cast-in-place, post-tensioned slabs, which are discussed subsequently, have been widely used in building construction. The same general types of structures could be made with each type of construction. The principal advantages of pretensioned solid slabs are their ease of manufacture, small depth of construction, and smooth soffit. The presence of a smooth soffit eliminates the need for applied or suspended ceilings in some structures. The principal disadvantages of solid slabs include the dead weight of the slabs, which can be partially offset by using lightweight concrete, and the difficulty of providing large penetrations.

Solid slabs can be used with precast, prestressed beams soffits, as is illustrated in Fig. 13-10. Cast-in-place concrete, which is placed between the ends of the slabs, connects the slabs and the beam soffit so that the beam has a T-shape for all subsequently applied loads. In addition, in order to minimize deflections or to increase the flexural strength, nonprestressed reinforcement can be extended from the slabs into the cast-in-place concrete to develop continuity for superimposed loads.

13-7 Precast Hollow Slabs

Hollow or "cored" slabs have been used extensively. The primary advantages and disadvantages of these types of elements are substantially the same as for

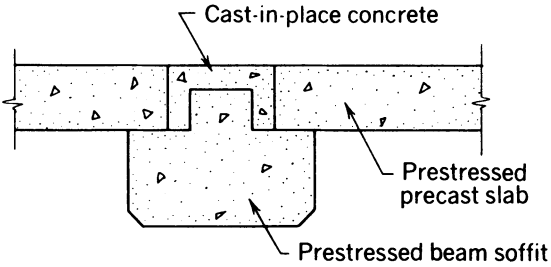

Fig. 13-10. Solid slabs with prestressed beam soffit.

the solid slabs discussed in Sec. 13-6, the primary difference being that the hollow slabs are lighter and structurally more efficient in the elastic range. Typical cross sections of the hollow slabs currently produced in the United States are illustrated in Fig. 13-11.

The slabs normally are made in long continuous castings and are cut to the desired length, with a concrete saw, after they have been cured. Sometimes, layers of slabs are cast one on top of the other (over a period of several days) until the stack is several slabs deep. The slabs cannot be cut or removed from the bench until the last slab cast has gained sufficient strength to allow it to be prestressed.

Other types of hollow slabs have been made by casting the slabs in the normal manner (wet cast) and with voids formed in the slab by using paper tubes, which are left in the member, or with metal or inflatable rubber tubes, which are removed from the slab after it has hardened.

13-8 Cast-in-Place Slabs

Four general types of cast-in-place concrete slabs, or slablike members, are commonly made using prestressed concrete.

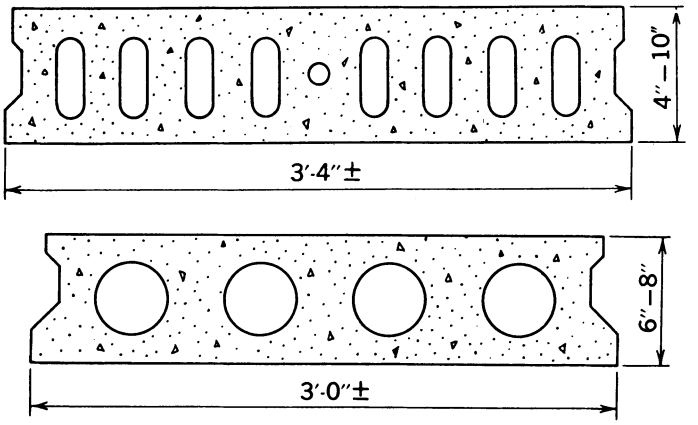

Fig. 13-11. Typical sections of hollow slabs produced in the United States.

Most frequently referred to as one-way slabs, two-way slabs, flat slabs, and flat plates, they are described briefly as follows:

1. *One-Way Slabs.* The term one-way slab is used for a type of concrete construction formed of a slab or slablike member supported in such a way as to have dead-load bending moments, for all practical purposes, in only one of the two orthogonal directions. One-way slabs are supported by wall or stiff-beam supports that extend across the entire width of the slabs and only permit deflections having single curvature. The supports usually are oriented perpendicular to the longitudinal axis of the slab but can be at an angle (skew) from the perpendicular to the longitudinal axis. One-way slabs may be simple spans or may be continuous over three or more supports.
2. *Two-Way Slabs.* Two-way slabs, which are generally square or rectangular in plan, are supported on all four sides by continuous supports of walls or stiff beams. The slabs may have several continuous spans in each of the two orthogonal directions. The deflected surfaces of two-way slabs have double curvature.
3. *Flat Slabs.* Flat slab normally are supported by a series of columns. The columns are most frequently, but not always, positioned in a square or rectangular pattern. Flat slabs do not have stiff beams or walls spanning from column to column, in either direction. Flat slabs have drop panels or capitals at the junction of the slab soffits and the tops of the columns. They normally are continuous over several supports.
4. *Flat Plates.* Flat plates basically are identical to flat slabs except that they have a flat soffit without drop panels or capitals. This type of construction commonly is used in lift-slab construction in which one or more slabs are cast on top of each other below their final position. After post-tensioning of the slab reinforcement, the slabs are lifted to their final position and connected to the supporting columns. If cast-in-place, the formwork needed for flat plates is the most simple required for cast-in-place concrete construction. Flat plates frequently have shear stresses in the concrete at locations of the columns that are relatively high and sometimes require reinforcement. Shear stresses often limit the span lengths that can be used with flat plates.

Additional specific comments on these four types of prestressed concrete construction will be found in Sections 13-9, 13-10, and 13-11. Additional information on their elastic analysis and behavior can be found in the references. (Brotchic and Wynn 1975; Kawai 1957; Kist and Bouma 1954; and Westergaard 1930.)

In the past, cast-in-place post-tensioned concrete slabs used in building construction normally had a minimum thickness of 4.5 in. in order to comply with the minimum requirements for a two-hour rating in the fire codes. Contemporary codes require thickness from 3.6 to 5.0 in., depending upon the type of aggregates used in the concrete, for a two-hour fire rating (see Table No.

43-C, UBC 1988). The slab thicknesses used in one-way slabs, which often are used on short spans, frequently are controlled by the fire code provisions of the applicable building code rather than by strength or serviceability considerations. The minimum thicknesses of two-way systems (i.e., two-way slabs, flat slabs, and flat plates) are more often than not controlled by serviceability and strength considerations rather than fire resistance.

In the interest of economy for longer spans, cast-in-place post-tensioned floors and roofs frequently are constructed with ribbed slabs in lieu of solid slabs. Construction of this type often is referred to as waffle slab construction because the ribs, which are similar in dimension to those commonly used in typical one-way pan-joist construction, are provided in each of the orthogonal directions and have soffits with a "waffle" appearance. The ribbed slabs normally are designed by following the same general procedures used in the design and analysis of solid flat slabs (Aalami 1989).

The maximum sag between the lines of supports that a tendon can have under normal conditions—that is, a tendon having an outside diameter of 0.75 in. and the slab not exposed to weather, in an interior span of a continuous slab having a thickness of 5.0 in.—is 2.75 in. If the slab is exposed to weather and the tensile stress in the concrete exceeds $6\sqrt{f'_c}$, the concrete cover requirements in ACI 318 are more stringent (Sec. 7.7.3.2), and the maximum sag that can be achieved is only 2.00 in. (ACI 318 1989). Considerable care must be exercised in constructing thin cast-in-place slabs if the intended tendon positions and sags are to be obtained; normal construction tolerances for concrete thickness, formwork, and placing of reinforcement can have a significant effect on the sags actually achieved in the field.

In the design of cast-in-place post-tensioned slabs, it is desirable to keep the average prestress reasonably low in order to minimize creep deformation (Aalami and Barth 1989). Considerable cracking has occurred in structures made with slabs of these types as a result of elastic shortening of the concrete at the time of prestressing, as well as the deformation caused by concrete creep and shrinkage (see Sec. 17-3). Therefore, the trends in design have been toward using low amounts of average prestress in the concrete (minimum value of 125 psi) and permitting flexural tensile stresses in the slabs when under total service load. One technique commonly used to reduce the average compressive stress in post-tensioned slabs and plates, when load balancing is used as the method of analysis, is to balance a portion of the total dead load rather than the full dead load. The amount of dead load balanced by the prestressing may be only 60 to 80 percent of the total dead load. When the dead load is only partially balanced, nonprestressed reinforcement frequently is needed to provide the minimum required flexural strength (see Secs. 5-3 and 5-5).

In preliminary design, and frequently in the final design as well, designers often assume that the post-tensioned tendons will be placed on paths as shown in Fig. 13-12, and they ignore the need for counter-curvature in the tendons at

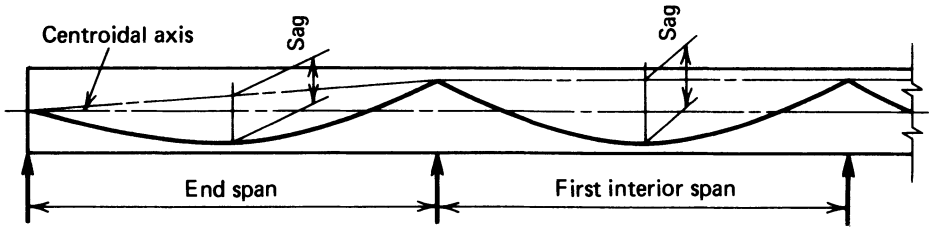

Fig. 13-12. Tendon paths used in preliminary design.

the high points in their paths (supports). With this assumption, the computations for load balancing are significantly facilitated (see Secs. 8-15 and 10-4).

It normally is necessary to terminate the tendons near middepth of the slab at the outermost ends of the end spans. The size of the end anchorages and the thickness of the slab normally dictate this. Hence, as will be seen from Fig. 13-12, it is common to have a greater sag in the interior spans than in the end spans. This has significant bearing on the amount of prestressing required because e, in eq. 8-9, is equal to the midspan sag in a span and not the eccentricity of the tendon. In the interest of economy, the designer frequently provides some tendons that extend the entire length of the structure, these being proportioned for the prestress required in the most critical of the interior spans, plus some additional shorter tendons that do not extend the full length, as shown in Fig. 13-13, in the end spans. This has proved to be an efficient method of achieving the higher prestress required in the end spans.

As pointed out above, the sag in the end spans normally is smaller than that in the interior spans. On occasion, the end spans overhang the end supports, and the tendons in the end spans can be placed on paths identical to those in the interior spans, thus eliminating the need for supplementary tendons (see Fig. 13-14).

13-9 One-Way CIP Slabs

The design of one-way slabs, with either simple or continuous spans, is done by employing the principles presented for simple and continuous flexural

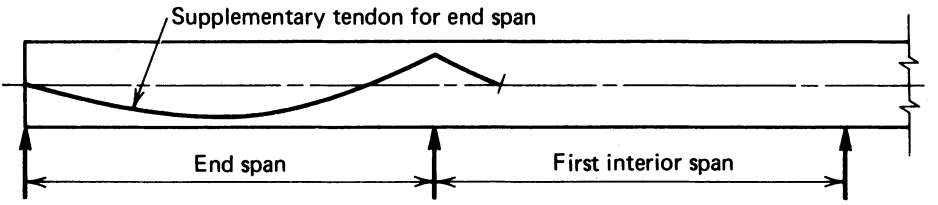

Fig. 13-13. Supplementary tendon for end spans.

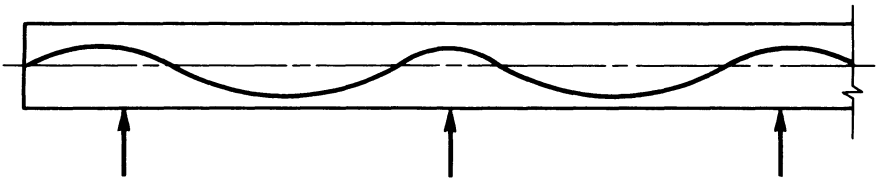

Fig. 13-14. Slab with overhanging end.

members in Chapters 4 through 10. In order to simplify the calculations, the slabs normally are modeled with a width of one foot rather than the actual width. After the amount of prestressing steel and reinforcing steel required for a width of one foot has been determined, it is a simple matter to extend these data to the actual slab width.

Transverse bending moments exist in one-way slabs subjected to concentrated loads. The transverse reinforcing required for a specific condition may be dictated by the applicable design criteria or, in special cases, may be determined by the use of an elastic analysis. The elastic analysis of transverse bending moments in one-way slabs is beyond the scope of this book; the interested reader is referred to the references listed at the end of this chapter. Bridge deck research related to the amount of reinforcement needed for wheel loads has led researchers to conclude that elastic analysis methods do not accurately predict the performance of one-way slabs reinforced with nonprestressed reinforcement. Future research may show this to be true for one-way slabs having prestressed reinforcement as well (Pucher 1964; Csagoly and Lybas 1989).

Since 1976, the Uniform Building Code (UBC 1976) has contained a provision for the minimum permissible amount of nonprestressed reinforcement in one-way slabs and beams prestressed with unbonded tendons. This provision, which will be found in Sec. 2618(j)B of the 1988 edition of the UBC and is not contained in ACI 318, is as follows:

> B. Bonded reinforcement shall be required regardless of service load stress conditions.
>
> One-way, unbonded, post-tensioned slabs and beams shall be designed to carry the dead load of the slab or beam plus 25 percent of the unreduced superimposed live load by some method other than the primary unbonded post-tensioned reinforcement. Design shall be based on the strength method of design with a load factor and capacity reduction factor of one. All reinforcement other than the primary unbonded reinforcement provided to meet other requirements of this section may be used in the design.

Additional recommendations specifically meant for one-way post-tensioned slabs having unbonded tendons are contained in Sec. 3.2 of ACI–ASCE 423.3R

(1989). Building code requirements specifically intended for one-way slabs post-tensioned with unbonded tendons are contained in Sec. 18.9.2 of ACI 318. Strength analyses are required for one-way slabs as they are for all prestressed concrete flexural members.

Cast-in-place concrete one-way slabs supported by cast-in-place concrete beams, both of which are post-tensioned with unbonded tendons, have been used extensively in automobile parking garages in the United States. These concrete structures frequently are multistory although many are only one-story high but support wood frame structures. Frequently the framing of the structures consist of slabs, 4.5 in. thick, that span between beams spaced 18 ft on centers, with larger spacings used in some cases. The beams, which frequently span from 55 to 70 ft, normally are continuous over their interior supports where possible.

13-10 Two-Way CIP Slabs

The design of buildings that incorporate two-way prestressed concrete slabs should be done following the procedures given in Sec. 13-7 of the *Building Code Requirements for Reinforced Concrete*, ACI 318 (1989). The effects of the dead and live loads and the effects of the prestressing normally are analyzed independently and subsequently superimposed. The effects of prestressing can be analyzed by using load balancing principles, equivalent loadings, or basic principles, as described in Secs. 8-15 and 10-3 of this book. Specific requirements for two-way slabs post-tensioned with unbonded tendons are contained in Sec. 3.3 of ACI–ASCE 423.3R and in Sec. 18.9.3 of ACI 318. (ACI 318 1989; ACI–ASCE 423.3R 1989). As with all prestressed-concrete flexural members, strength analyses are essential, in addition to serviceability analyses.

Two-way slabs supported by cast-in-place concrete beams are not used as extensively as flat slabs and flat plates because of the higher construction costs associated with structures that include cast-in-place beams and girders.

See Sec. 13-12 for additional information on the flexural analysis of cast-in-place slab construction with beams.

13-11 Cast-in-Place Flat Slabs and Plates

The following discussion of flat slabs is equally applicable to flat slabs and flat plates unless otherwise noted.

Flat slabs and plates should be designed following the provisions of Sec. 13-7 of ACI 318, but excluding the provisions in Secs. 13.7.7.4 and 13.7.7.5, which are not intended for slabs having prestressed reinforcement. Hence, the design of prestressed flat slabs commonly is done by analyzing the slab in each of the two principal directions, as if it were a one-way slab-beam in each direc-

tion, using the stiffness requirements for the slab-beams and columns contained in ACI 318. See Sec. 13-12 for further discussion on the flexural analysis of flat plates and slabs. The commentary to ACI 318-89 is very useful in understanding the intent of the code requirements for flat slabs and flat plates (ACI 318 1989).

In recognition of stiffness differences in the portion of the slab along the column lines (column strips) and the portion of the slab located between column lines (middle strips), it was customary in the 1970s and early 1980s to place a greater percentage of the prestressing tendons in the column strips than in the middle strips as is done with flat slabs constructed with nonprestressed reinforcement. The proportioning of the tendons between the column strips and the middle strips was left to the judgment of the designer, but guidelines for tendon distribution were available in the ACI–ASCE Committee 423 tentative report published in 1969. These recommendations were as follows:

> 3.2.4.2.—For panels with length/width ratios not exceeding 1.33, the following approximate distribution may be used:
>
> Simple spans: 55 to 60% of the tendons are placed in the column strip, with the remainder in the middle strip;
>
> Continuous spans: 60 to 70% of the tendons are placed in the column strip.
>
> When length/width ratio exceeds 1.33%, a moment analysis should be made to guide the distribution of tendons. For high values of this length/width ratio, only 50% of the tendons along the long direction shall be placed in the column strip, while 100% of the tendons along the short direction may be placed in the column strip. Tests indicate that the ultimate strength is controlled primarily by the total amount of tendons in each direction, rather than by the tendon distribution. Some tendons should be passed through the columns or at least around their edges.
>
> 3.2.4.3.—The maximum spacing of tendons in column strips should not exceed four times the slab thickness, nor 36 in. (91 cm), whichever is less. Maximum spacing of tendons in the middle strips should not exceed six times the thickness of the slab, nor 42 in. (107 cm), whichever is less.

The above recommendations were superseded in 1983 when the 1969 tentative report was withdrawn and replaced with "Recommendations for Concrete Members Prestressed with Unbonded Tendons." The spacing and distribution of tendons recommended for two-way systems in the 1983 document are illustrated in Fig. 13-15. The newer recommendations, which are based upon experimental research work, are for placing the tendons with a uniform (or nearly uniform) spacing in one direction and banding them together over the column lines in the orthogonal direction. The use of the banded tendon configuration

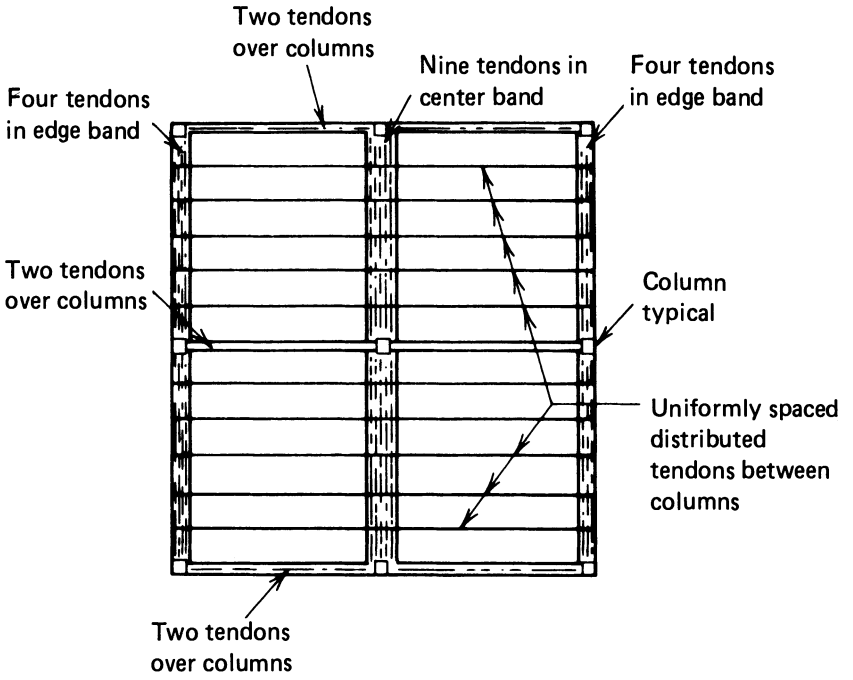

Fig. 13-15. Plan of flat plate slab showing spacing of tendons using banded tendon distribution.

greatly facilitates placing the tendons and reduces construction cost. Specific recommendations for the detailing of banded tendons are as follows:

1. The tendons required in the design strips of a slab may be banded in one direction and distributed in the other. The design strips are defined as the portions of the slabs center-to-center of adjacent panels in each direction.
2. In the distributed direction at least two tendons should be placed inside the design shear section at the columns.

The document includes numerous other detailed recommendations for minimum quantities and placing requirements for nonprestressed bonded reinforcement and maximum tendon spacings, and recommendations a minimum average prestress of 125 psi. Persons interested in the design and construction of cast-in-place flat slabs and flat plates are advised to carefully read the complete committee report as well as future revisions or new versions of the report.

For many years ACI–ASCE Committee 423 has recommended that post-tensioned tendons be placed through the columns, or close to their edges, in flat slabs and flat plates for the purpose of providing redundancy at the supports in the event of a catastrophic failure. This is an important detail that should not be overlooked. Tests have shown that flat slabs and plates tested to destruction

do not completely collapse if tendons pass through or close to the supporting columns; the failed slab remains suspended on the columns.

Office buildings, commercial buildings, and residential buildings, with and without parking levels, frequently are constructed by using cast-in-place flat slabs (and flat plates). Advantages of the method include the use of flat, or relatively flat, soffits, which facilitate the construction of the structural slab and interior partitions, in addition to providing a relatively low story height.

Experience with post-tensioned flat slab and flat plate construction utilizing unbonded banded tendons has shown them to be susceptible to the formation of relatively wide cracks parallel to the column lines perpendicular to the direction of the banded tendons—the location of the greatest negative moment when the structure is analyzed as a plate with one-way bending. It is believed that the width of cracks of this type would be significantly reduced by the provision of bonded, nonprestressed reinforcement placed near the top surface of the slabs in these areas. Present code provisions do not require, and committee recommendations do not recommend, the provision of nonprestressed reinforcement in these areas. ACI 318, in Sec. 18.9.3, and the ACI–ASCE 423.3R Recommendations, in Sec. 3.3, both require supplemental reinforcement over the columns (areas of large negative moment peaks) in each direction. Additional discussion of cracking in cast-in-place post-tensioned slabs is included in Sec. 17-3 of this book.

The deflection of prestressed flat slabs may be a significant factor in the design of this type of construction, just as it is in other types of framing. (The deflection of flat slabs can be determined by using the principles outlined in Sec. 7-4.) It should be pointed out that the deflections due to prestressing in each direction (span) are additive, as are the deflections due to the applied loads.

The original ACI–ASCE Joint Committee report for members prestressed with unbonded tendons, "Tentative Recommendations for Concrete Members Prestressed with Unbonded Tendons" (ACI–ASCE 423.1R 1969), which has been superseded by ACI–ASCE 423.3R-89, contained the following remarks relative to span–thickness ratios:

3.2.5 Deflection and Camber

3.2.5.1. Span–thickness ratios. For prestressed slabs continuous over two or more spans in each direction, the span–thickness ratio should generally not exceed 42 for floors and 48 for roofs. These limits may be increased to 48 and 52, respectively, if calculations verify that both short- and long-term deflection, camber and vibration frequency and amplitude are not objectionable.

3.2.5.2. Short- and long-term deflection and camber should be computed and checked for serviceability for all members.

Subsequent reports of ACI–ASCE Committee 423 do not contain guidelines for span–thickness ratios, and the designer must select thicknesses based upon deflection calculations, past experience, and his or her own judgment. The designer frequently is tempted to reduce the slab thickness for the purpose of reducing dead load, reducing the quantity of concrete, and thereby enhancing the economy of a design. One must remember that a reduction in slab thickness has the following results:

1. An increase in the quantity of the prestressed reinforcement, which has an adverse effect on first cost.
2. An increase in the average compressive stress in the concrete causing an adverse effect on initial and deferred concrete deformations.
3. An adverse effect on deflection and vibration characteristics.

The designer is responsible for evaluating these several points when selecting a final thickness.

ILLUSTRATIVE PROBLEM 13-1 Prepare a preliminary design for a post-tensioned flat plate that has five spans of 24 ft in each direction. The floor slab is to be designed for a superimposed dead load of 25 psf and a reducible live load of 50 psf. Assume that the live load is to be reduced at the rate of 0.08 percent per sq ft of tributary area but not more than 40 percent. Use $f'_c = 4000$ psi, $f_{pu} = 270$ ksi, and assume $f_{se} = 165$ ksi.

SOLUTION: The span-to-depth (thickness) ratio for various slab thicknesses is as follows:

Thickness (in.)	*Span/Thickness*
10	28.8
9	32.0
8	36.0
7	41.1
6	48.0

For serviceability reasons (i.e., better deflection, vibration, and deformation characteristics) adopt the 8 in. thickness. Thicknesses of 7 or 7.5 in. also could be used with reasonable performance under many types of service conditions.

Assume that the slab will be post-tensioned with tendons having an outside diameter of 0.75 in., and that a clear cover of 1.5 in. is required at the top of the slab and 0.75 in. at the bottom. The theoretical sag of an interior span would be:

$$8.00 - (1.50 + 0.38) - (0.75 + 0.38) = 5.00 \text{ in.}$$

For an end span, assuming that the centroidal axis of the tendon is at middepth of the slab at the end of the span, 1.13 in. above the slab soffit at midspan, and

1.88 in. below the top of the slab at the first interior support, the sag at midspan would be:

$$(4.00 - 1.13) + \frac{(4.00 - 1.88)}{2} = 3.93 \text{ in.}$$

In order to balance the full dead load in an interior span, the required prestressing force for a slab width of one foot, using eq. 8-10, would be:

$$P_{se} = \frac{0.125 \times 24^2 \times 12}{8 \times 5.00} = 21.6 \text{ klf}$$

and the average prestress is 225 psi. The end span requires a prestressing force of:

$$P_{se} = \frac{0.125 \times 24^2 \times 12}{8 \times 3.93} = 27.5 \text{ klf}$$

for which the average prestress is 286 psi. These levels of prestress are somewhat greater than those commonly used but not excessive, and they will be adopted for a first trial. The tendons will be designed and detailed for the paths shown in Fig. 13-16a, but actually they will be placed more like the path shown in

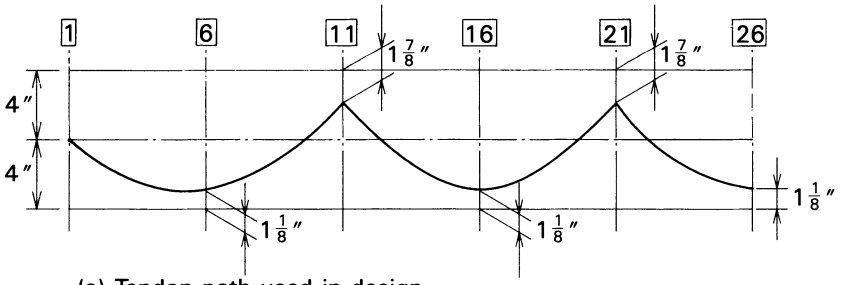

(a) Tendon path used in design.

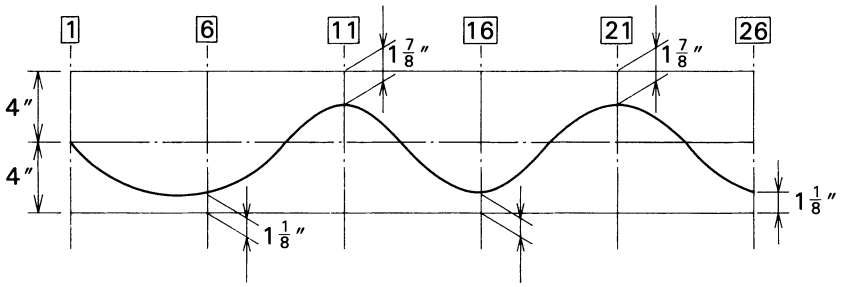

(b) Actual tendon path.

Fig. 13-16. Tendon layout for I.P. 13-1. (a) Tendon path used in design. (b) Actual tendon path as placed.

Fig. 13-16b because they cannot be placed without reversed curvature at the supports, as shown in Fig. 13-16b. The supplementary end-span tendons will terminate at the quarterpoint of the first interior span closest to the end of the slab. If the tendon path is straight from the centerline of the first interior support to its anchorage at the quarterpoint of the first interior span, an upward force, equal to the product of the force in the tendon and the sine of the angle of inclination, is applied to the concrete at the anchorage point; the existence of this relatively small force frequently is ignored in the analysis of post-tensioned flat plates. For the preliminary design, the prestressing force will be assumed to be constant and equal to 27.5 kpf for the end span and the adjacent 6.00 ft of the first interior span. For the remaining length, the prestressing force will be assumed to equal 21.6 kpf. The amount of prestressing terminating at the quarterpoint of the first interior span is 5.9 klf, and the upward component of this force, based upon a straight tendon path, is 0.174 klf. The force is ignored in the following analysis.

As explained in Chapter 10, the location of a pressure line (path of a concordant tendon) for a continuous structure is defined by a moment diagram for the structure. In this case, to balance the dead load of the beam, the desired shape of the pressure line is proportional but of opposite sign to the moment diagram for dead load. The computations are facilitated by finding the moment diagram for a uniformly distributed load of one kip per linear foot, as illustrated in Fig. 13-17, in which the unit-load moments at midspans and the interior supports are shown. The unit-load moment diagram can be used to determine the moments for the total dead load (+0.125 klf), the effective prestressing force that balances the dead load (−0.125 klf), and the live load (+0.030 klf). These moments are shown in Fig. 13-18.

Because the effective prestressing force exactly balances the dead load of the beam at every section along the length of the slab under the effects of dead load

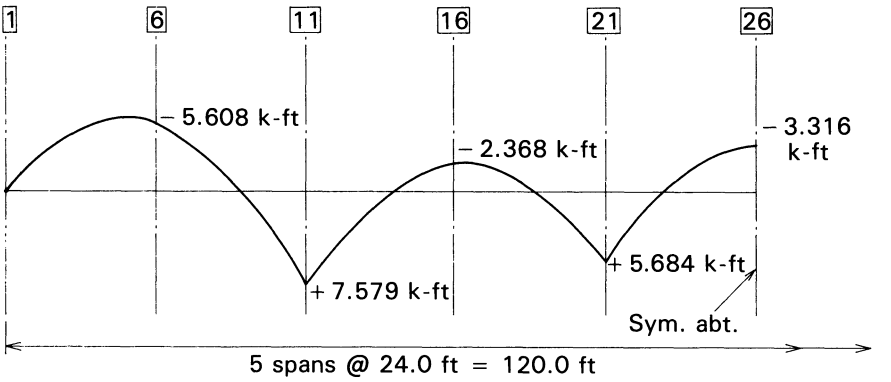

Fig. 13-17. Moment diagram for unit load of 1 klf acting upward on slab of I.P. 13-1.

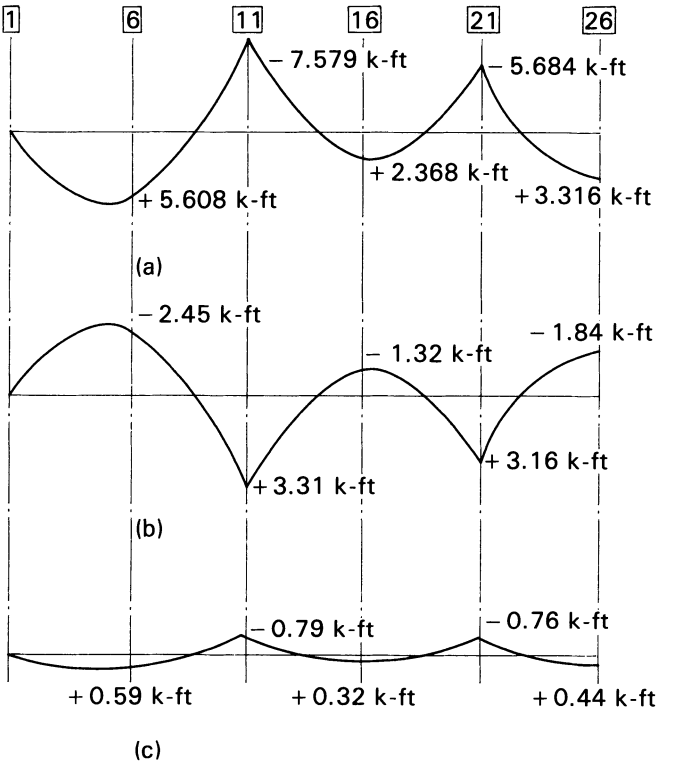

Fig. 13-18. Moment diagrams for dead load, prestressing, and live load on slab of I.P. 13-1. (a) Moment due to uniformly distributed dead load of +0.125 klf. (b) Moment diagram due to effective prestress. (c) Moment diagram due to uniformly distributed live load of 0.030 klf.

and the effective prestress alone, the concrete stress at every section is equal to the average compressive stress due to prestressing over the full thickness of the slab (i.e., the pressure line is coincident with the centroidal axis of the member). The moment due to the live load, which is equal to 24 percent of the moment due to dead load ($0.030/0.125 = 0.24$), causes an upward displacement of the location of the pressure line near the midspans. The locations of the centroidal axis of the prestressed reinforcement (e_{ps}), the pressure line due to prestressing alone (e_{pl}), as well as the pressure line plus dead load (e_{pl+dl}) and the pressure line plus total load (e_{pl+tl}), are shown as paths 1, 2, 3, and 4, in Fig. 13-19, respectively. Using the effective prestressing forces of 27.5 and 21.6 klf for the end and interior portions of the beam, respectively, the computations for the pressure line locations at various positions along the member are based on the following simple relationship:

$$\Delta e = \frac{12M}{P_{se}} = -\frac{12M}{-C}$$

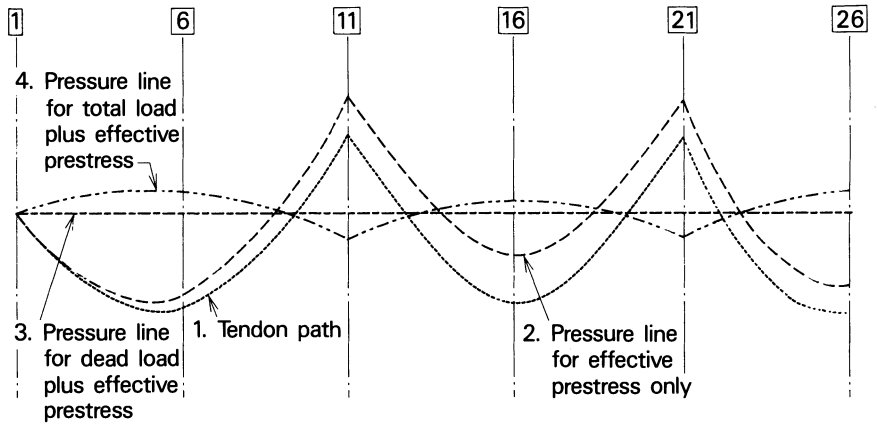

Fig. 13-19. Plot of the pressure line location for the first-trial effective prestressing forces in I.P. 13-1.

in which Δe is the change in location of the pressure line due to the moment M at a position where the effective prestressing force is P_{se}, as summarized in Table 13-1.

The stresses in the top and bottom fibers of the slab due to the resultant compressive force in the concrete (-27.5 and -21.6 kips, depending upon the location) are computed by using eqs. 4-3 and 4-4, in which e is the eccentricity of the pressure line. The stresses under the effects of effective prestress and total load, in psi, are summarized in Table 13-2.

The stresses shown in the summary are all compressive and below allowable values. It is apparent the amount of prestressing can be reduced if full load balancing is not considered necessary for deflection control or other reasons. Reducing the amount of prestressing will result in a reduction in the cost of the structure.

For a second trial, the prestressing will be reduced to balance only 60 percent of the dead load. In this case, the effective prestressing forces required are reduced to 16.5 and 13.0 klf at the end and interior portions of the member,

TABLE 13-1 Pressure Line Locations (in.) for P_{se} as Shown in Fig. 13-19.

	Nodal Point				
Load effect	6	11	16	21	26
Eff. Prestress	+2.45	−3.31	+1.32	−3.16	+1.84
δe_{dl}	−2.45	+3.31	−1.32	+3.16	−1.84
e_{pl+dl}	0.00	0.00	0.00	0.00	0.00
Δe_{ll}	−0.59	+0.79	−0.32	+0.76	−0.44
e_{pl+ll}	−0.59	+0.79	−0.32	+0.76	−0.44

TABLE 13-2 Summary of Stresses (psi) under the Effects of Total Load in First Trial of I.P. 13-1.

	Nodal Point				
	6	11	16	21	26
Top fiber	−413	−116	−279	−96	−299
Bottom fiber	−159	−456	−171	−354	−151

respectively. Following the procedure described above, the locations of the pressure line with the lower prestressing forces are summarized in Table 13-3 and plotted in Fig. 13-20, and the concrete stresses are summarized in Table 13-4.

A review of the stresses summarized above will show that the compressive stresses are well within the allowable value, the tensile stresses in the top fiber do not exceed $6\sqrt{f'_c}$, and the bottom fiber tensile stresses, except for point 6, do not exceed $2\sqrt{f'_c}$, which is equal to 126 psi. Tensile stresses in areas of positive moment are limited to $2\sqrt{f'_c}$ (by Sec. 18.9.3.1 of ACI 318) unless nonprestressed reinforcement is provided in the amount of:

$$A_s = \frac{N_c}{0.5f_y}$$

The tensile stress at point 6 exceeds 126 psi, and the amount of Grade 60 nonprestressed reinforcement that would be required for the stress of +165 is computed to be (see Fig. 13-21):

$$8\left(\frac{509}{165 + 509}\right) = 6.04 \text{ in.}$$

$$N_c = \frac{165 \times 12 \times 1.96}{2 \times 1000} = 1.94 \text{ klf}$$

$$A_s = \frac{1.94}{60} = 0.032 \text{ in.}^2/\text{ft}$$

TABLE 13-3 Pressure Line Locations (in.) for P_{se} = 16.5 and 13.0 klf as Shown in Fig. 13-20.

	Nodal Point				
Load effect	6	11	16	21	26
Eff. prestress	+2.45	−3.31	+1.32	−3.16	+1.84
δe_{dl}	−4.08	+5.51	−2.19	+5.25	−3.06
e_{pl+dl}	−1.63	+2.20	−0.88	+2.10	−1.22
Δe_{ll}	−0.98	+1.32	−0.53	+1.26	−0.73
e_{pl+tl}	−2.61	+3.52	−1.41	+3.36	−1.95

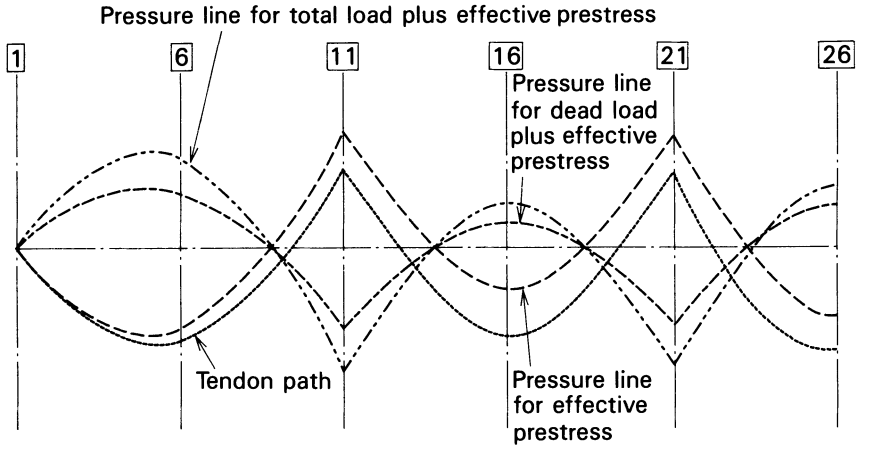

Fig. 13-20. Plot of the pressure line location for the second-trial effective prestressing forces in I.P. 13-1.

In the event that the use of nonprestressed reinforcement in positive moment areas of the end spans is to be avoided, the prestressing force in the end spans can be increased and the tensile stress in the concrete reduced.

The design is finished by completing several steps that are interdependent:

1. The flexual design in the orthogonal direction must be completed. If the tendon layout designed above is to be used in one direction, the tendon layout to be used in the other direction should be detailed to avoid conflicts between the prestressed and nonprestressed reinforcement to be provided in the two directions. (Tendons in only one direction, together with the minimum required nonprestressed reinforcement, can be placed with their centroids 1.88 in. from the top of the slab in the vicinity of the columns supporting the slab. The designer should investigate this possibility carefully before selecting the tendon paths for the orthogonal direction.)
2. The minimum reinforcement in the negative moment areas, as provided in Sec. 18.9.3.3 of ACI 318, must be computed and details selected.
3. The details for the minimum reinforcement for the positive moment areas, if needed, should be determined.
4. A flexural strength analysis, using the methods explained in Chapter 5,

TABLE 13-4 Summary of Stresses (psi) for Second Trial of I.P. 13-1.

	Nodal Point				
	6	11	16	21	26
Top fiber	−509	+283	−279	+206	−334
Bottom fiber	+165	−625	+8	−477	−63

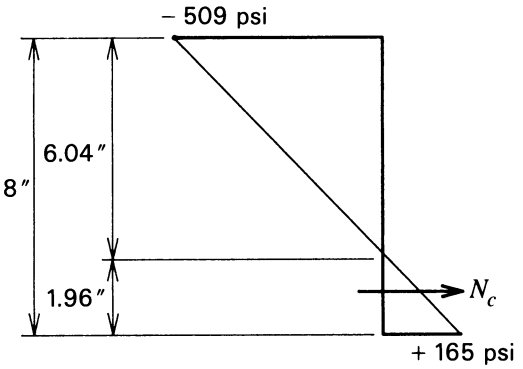

Fig. 13-21. Computation of the location of the neutral axis, the value of the axial force, N_c, and the area of nonprestressed reinforcement needed in I.P. 13-1.

should be made for each of the orthogonal directions with due consideration for differences in details.

5. Shear stresses must be investigated at the columns. The designer may find it necessary to increase column sizes or to provide drop panels in order to meet the minimum requirements of the applicable building code.
6. A deflection analysis is required by most building codes for the purpose of confirming compliance with maximum permissible values. The deflection computations should include the effects of nonprestressed flexural reinforcement, concrete creep and shrinkage, and relaxation of the prestressed reinforcement (see Sec. 7-4). The deflections of two-way slabs normally are computed as the sum of the deflections of a column strip and a middle strip, each oriented in one of the orthogonal directions.

13-12 Flexural Analysis—CIP Construction

The flexural analysis of cast-in-place construction involves making reasonable assumptions relative to the stiffnesses (or flexibilities) of the components of the structure and performing an analysis based upon these assumptions. The commentary to ACI 318-83, in Sec. 13.7, contains specific guidance on assumptions that can be made to simplify the calculations without serious compromise of accuracy. These recommendations include the dimensions of the equivalent frames, as shown in Fig. 13-22, as well as dimensions and flexural stiffnesses of the beam and column elements, as shown in Figs. 13-23 through 13-27, for use in the frame analysis. It should be noted that ACI 318 permits the moments of inertia of the slab-beams and the columns between the joint areas to be based on the gross cross section. When hand calculations are used,

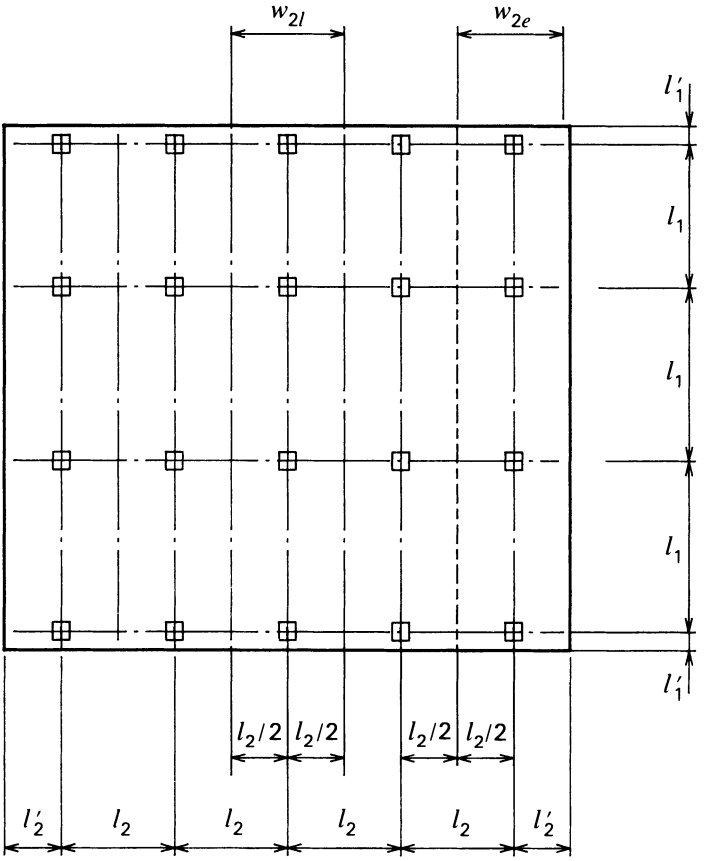

$w_{2e} = l_2/2 + l_2'$ = width of slab in an exterior equivalent frame

$w_{2l} = l_2$ = width of slab in an interior equivalent frame

Fig. 13-22. Definition of plan dimensions for equivalent frame.

the commentary to ACI 318 suggests the use of equivalent columns in the analysis of gravity loads, which combine the stiffnesses of the slab-beam and a torsional member. An equivalent column is intended to model the behavior of the columns above and below the slab-beam, normally with the far ends of the columns fixed against rotations, together with the torsional members framing into the sides of the joint of the columns and slab-beam, as shown in Fig. 13-28. The restraint of the slab-beam, which is monolithic with the torsional member and the column but not shown in Fig. 13-28, is dependent upon the rotation of the torsional member and the columns above and below. The flexi-

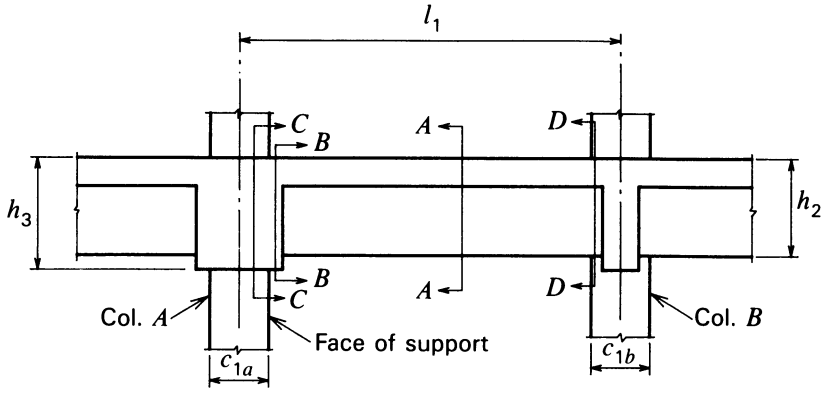

Typical section through an interior span

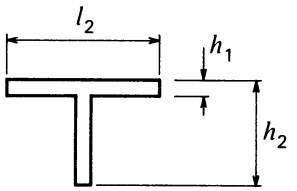

Section $A-A$ having a moment of inertia equal to I_1

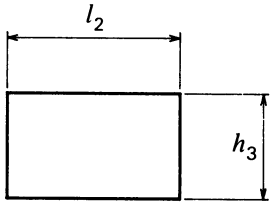

Section $B-B$ having a moment of inertia equal to I_2

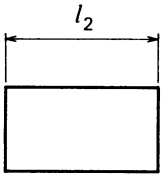

Section $C-C$ having an equivalent moment of inertia equal to $\dfrac{I_2}{\left(1-\dfrac{c_{2a}}{l_2}\right)^2}$

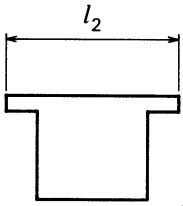

Section $D-D$ having an equivalent moment of inertia equal to $\dfrac{I_1}{\left(1-\dfrac{c_{2b}}{l_2}\right)^2}$

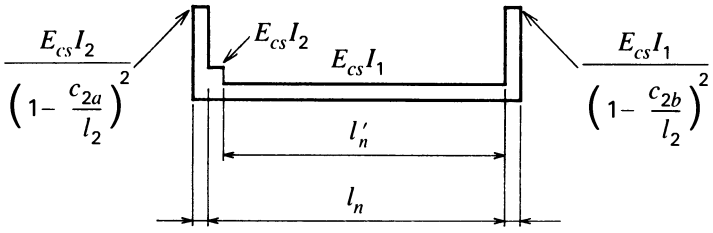

Equivalent slab-beam stiffness diagram

Fig. 13-23. Dimensions of a slab system with beams in each of the orthogonal directions (based upon Fig. 13.7.3 of ACI 318R 1983).

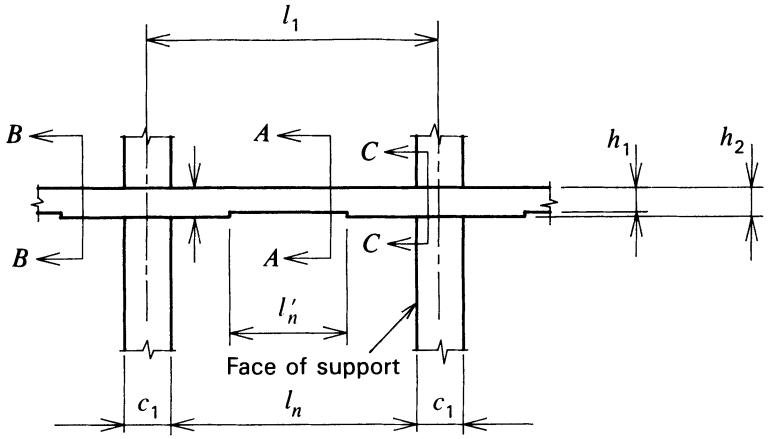

Typical section through an interior span

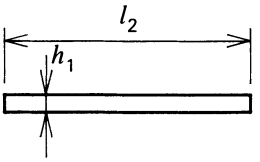

Section $A-A$ having a moment of inertia of I_1

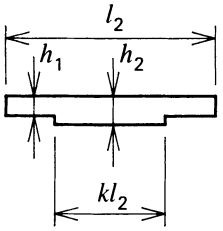

Section $B-B$ having a moment of inertia of I_2.

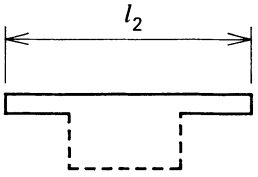

Section $C-C$ having an effective moment of inertia of $\dfrac{I_2}{\left(1 - \dfrac{c_2}{l_2}\right)^2}$

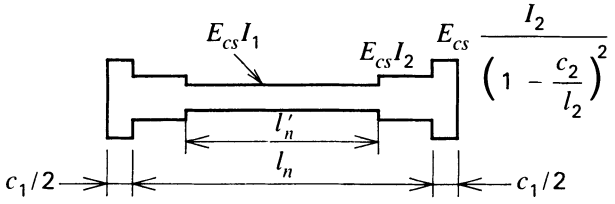

Equivalent slab-beam stiffness diagram

Fig. 13-24. Flat slab system with drop panels but without capitals (based upon Fig. 13.7.3 of ACI 318R 1983).

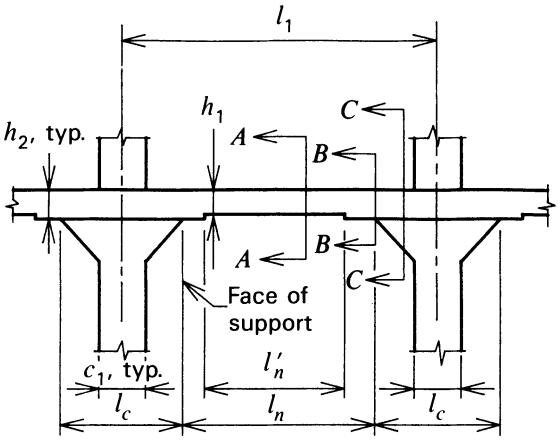

Typical section through an interior span

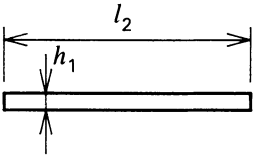

Section $A-A$ having a moment of inertia of I_1

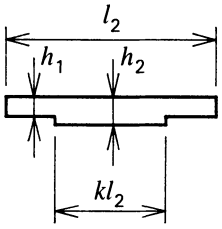

Section $B-B$ having a moment of inertia of I_2

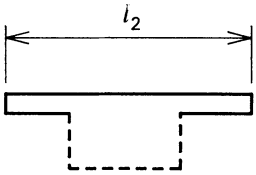

Equivalent section $C-C$ having a moment of inertia of $\dfrac{I_2}{\left(1-\dfrac{c_2}{l_2}\right)^2}$

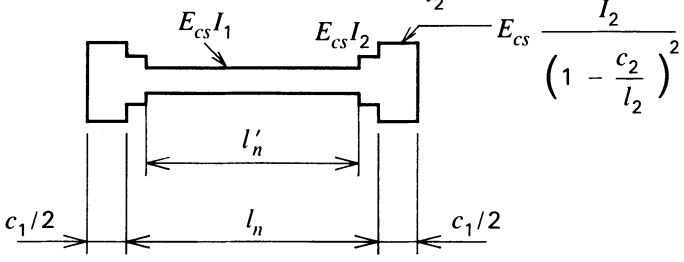

Fig. 13-25. Flat slab system with drop panels and capitals (based upon Fig. 13.7.3 of ACI 318R 1983).

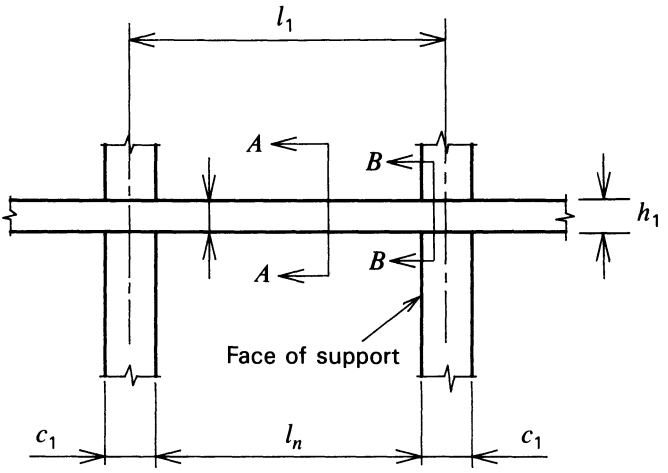

Typical section through an interior span

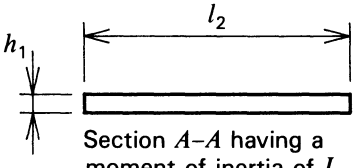

Section A–A having a moment of inertia of I_1

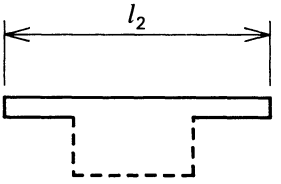

Equivalent section B–B having a moment of inertia of $\dfrac{I_1}{\left(1 - \dfrac{c_2}{l_2}\right)^2}$

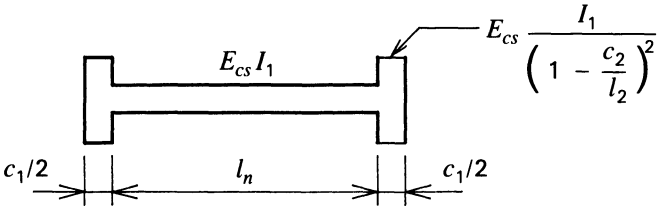

Equivalent slab-beam stiffness diagram

Fig. 13-26. Flat plate system without capitals (based upon Fig. 13.7.3 of ACI 318R 1983).

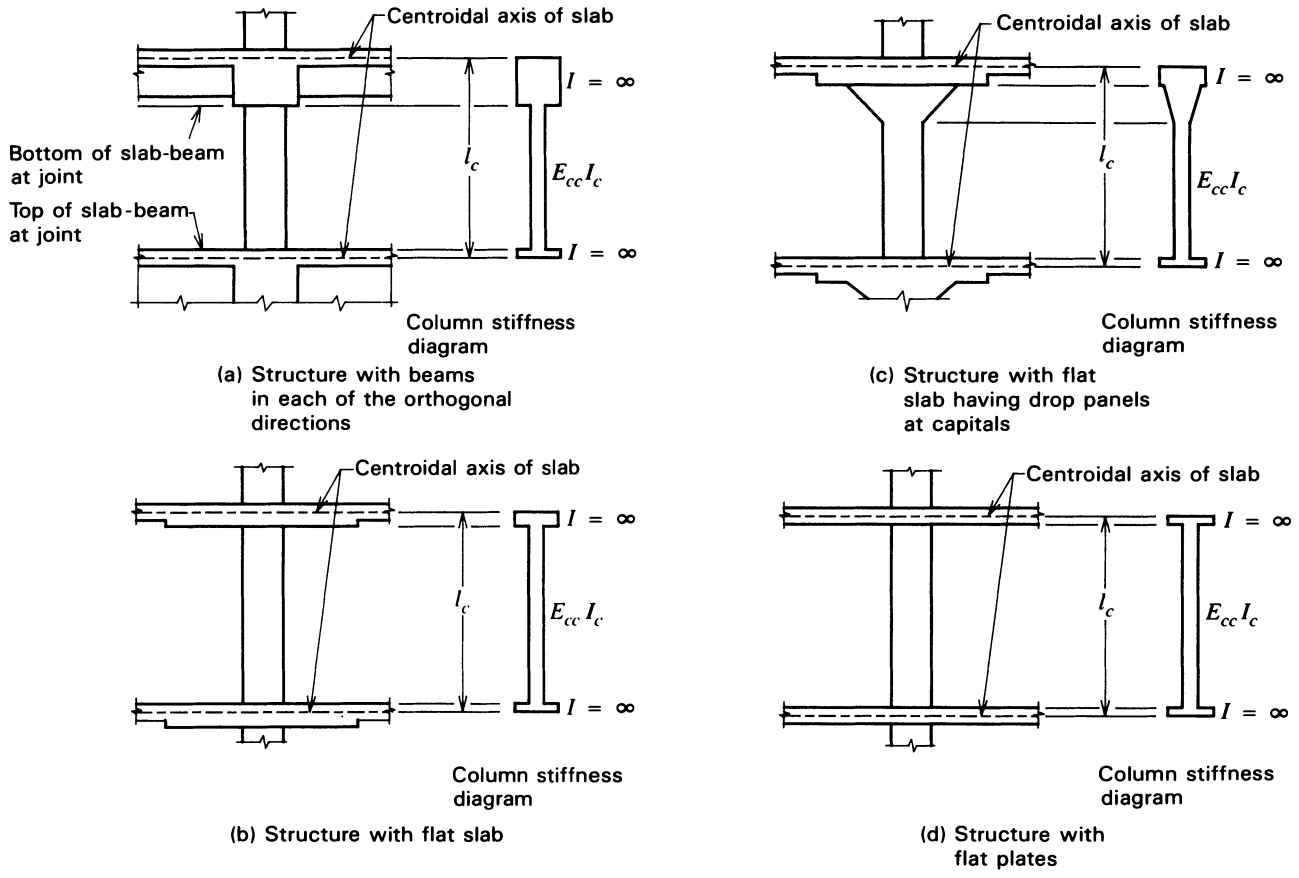

Fig. 13-27. Definition of the sections for calculating column stiffness, K_c (based upon Fig. 13.7.4 of ACI 318R 1983). (a) Structure with beams in each of the orthogonal directions. (b) Structure with flat slabs without capitals. (c) Structure with flat slabs having drop panels and capitals. (d) Structure with flat plates.

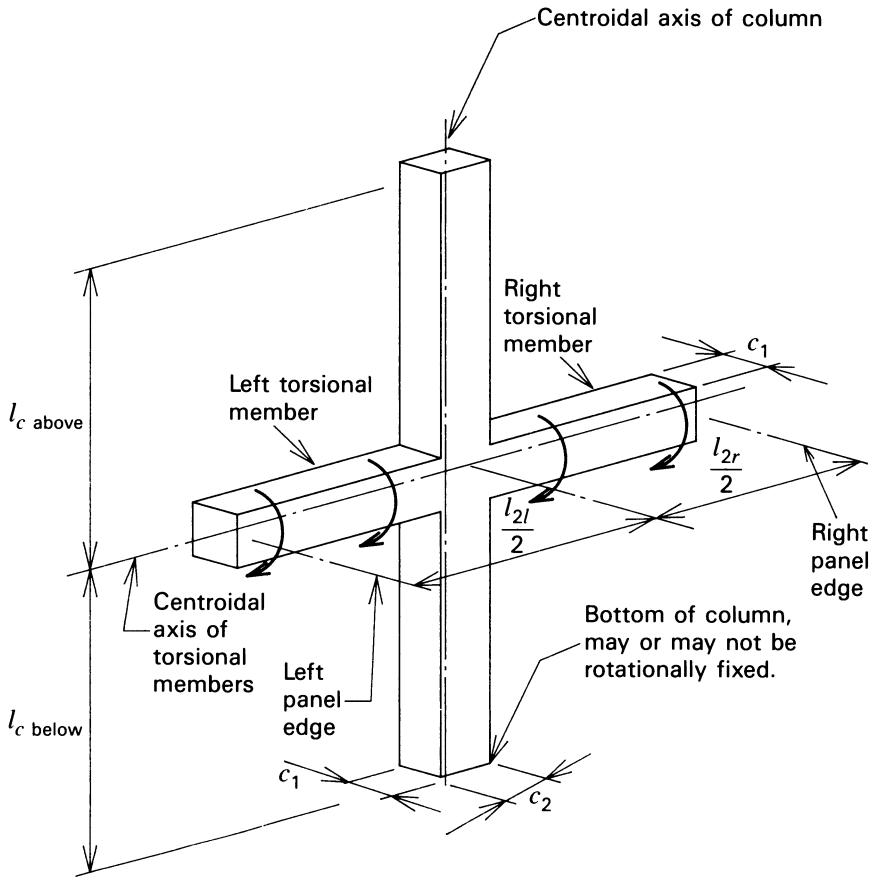

Fig. 13-28. Simplified physical model of equivalent column. Note that the slab-beam that frames into the torsional member is not shown (based upon Fig. B, ACI 318R 1983).

bility of the equivalent column can be taken as:

$$\frac{1}{K_{ec}} = \frac{1}{\sum K_c} + \frac{1}{K_t} \tag{13-1}$$

Equation 13-1 can be rewritten in terms of stiffness as:

$$K_{ec} = \frac{\sum K_c}{1 + \frac{\sum K_c}{K_t}} \tag{13-2}$$

The exploded illustration of the equivalent column shown in Fig. 13-29 defines the several separate stiffnesses to be included in the determination of its stiff-

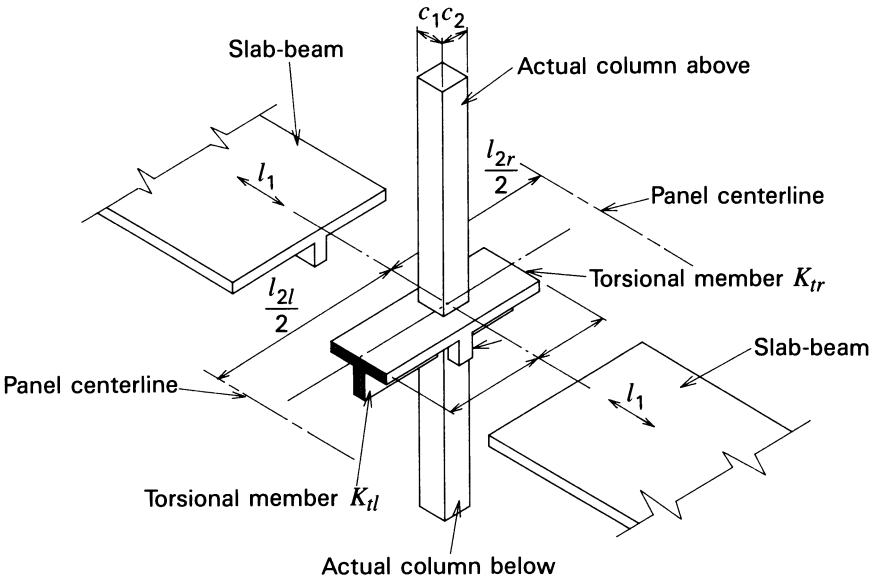

Fig. 13-29. Equivalent column consisting of column plus torsional members (based upon Fig. C, ACI 318R 1983).

ness. The term ΣK_c in eqs. 13-1 and 13-2, using the model in Fig. 13-29, becomes:

$$\Sigma K_c = K_{c\text{above}} + K_{c\text{below}} \tag{13-3}$$

for the equivalent column.

The term K_t in eqs. 13-1 and 13-2 accounts for the effect of the stiffnesses of the torsional members. For torsional members having constant cross section and elastic properties over their lengths, and extending in the transverse direction from the equivalent column a distance of $l_2/2$ from the centerline of the slab-beam under consideration (i.e., the transverse spans on each side of the centerline of the slab-beam are designated l_2), ACI 318 mandates that this term be computed from:

$$K_t = \sum \frac{9E_{cs}C}{l_2\left(1 - \frac{c_2}{l_2}\right)^3} \tag{13-4a}$$

where E_{cs} is the elastic modulus of the slab-beam concrete, C is a torsional constant (defined in eq. 13-5 below), l_2 designates the transverse spans (which do not have to have equal lengths), and c_2 is the width of the column in the transverse direction (see Fig. 13-28). It should be noted that eq. 13-4a is based upon torsional member lengths of $l_2/2$, as shown in Figs. 13-28 and 13-29. To

facilitate the computation of K_t, the 9 in the numerator of the equation accounts for the shorter lengths of the torsion members. Eq. 13-4a can be written with $l_2/2$ in the denominator, rather than l_2, and 4.5 in the numerator, rather than 9.

If the transverse spans, l_2, are of equal length on both sides of the centerline of the slab-beam, eq. 13-4a can be written:

$$K_t = \frac{18E_{cs}C}{l_2\left(1 - \frac{c_2}{l_2}\right)^3} \tag{13-4b}$$

and for the case of l_2 not having equal lengths on each side of the centerline of the slab-beam (i.e., $l_{l2} \neq l_{r2}$), eq. 13-4a can be approximated by:

$$K_t = \frac{18E_{cs}C}{l_{ave}\left(1 - \frac{c_2}{l_{ave}}\right)^3} \tag{13-4c}$$

in which l_{ave} is the average of the transverse spans on the left and right sides of the centerline of the slab-beam, respectively.

In analyzing edge frames, eq. 13-4c would normally have a value of l_2 in the transverse direction that is continuous, but not for the discontinuous side. Guidance for the determination of the torsional stiffness for an edge frame having a beam cantilevered from the discontinuous edge is not given in ACI 318 or the commentary to ACI 318. If a slab (which may or may not contain a beam) extends outward (cantilevered) from an edge column, torsional flexibility (twist) would be provided by the cantilevered construction. It is appropriate to include this effect of stiffness in the design of construction having this configuration. One can include the effect of the cantilever in the torsional stiffness computation by using twice the length of the cantilever for l_{l2} or l_{r2} in eq. 13-4c.

The constant C in eqs. 13-4a, 13-4b, and 13-4c is equal to:

$$C = \Sigma\left(1 - 0.63\frac{x}{y}\right)\frac{x^3y}{3} \tag{13-5}$$

In using eq. 13-5, the cross section under consideration is divided into rectangular parts in which the dimension of the shorter side is taken to be x, and the dimension of the longer side is taken to be y. The areas of torsional members for different configurations, based upon Fig. 13.7.5.1 in the commentary on ACI 318, are shown in Fig. 13-30.

In the case of a slab-beam containing a beam parallel to its centerline, the value of K_t computed from eq. 13-4a, 13-4b, or 13-4c must be increased to account for the greater stiffness resulting from the parallel beam. The commentary to ACI 318 states that the following relationship must be used for this

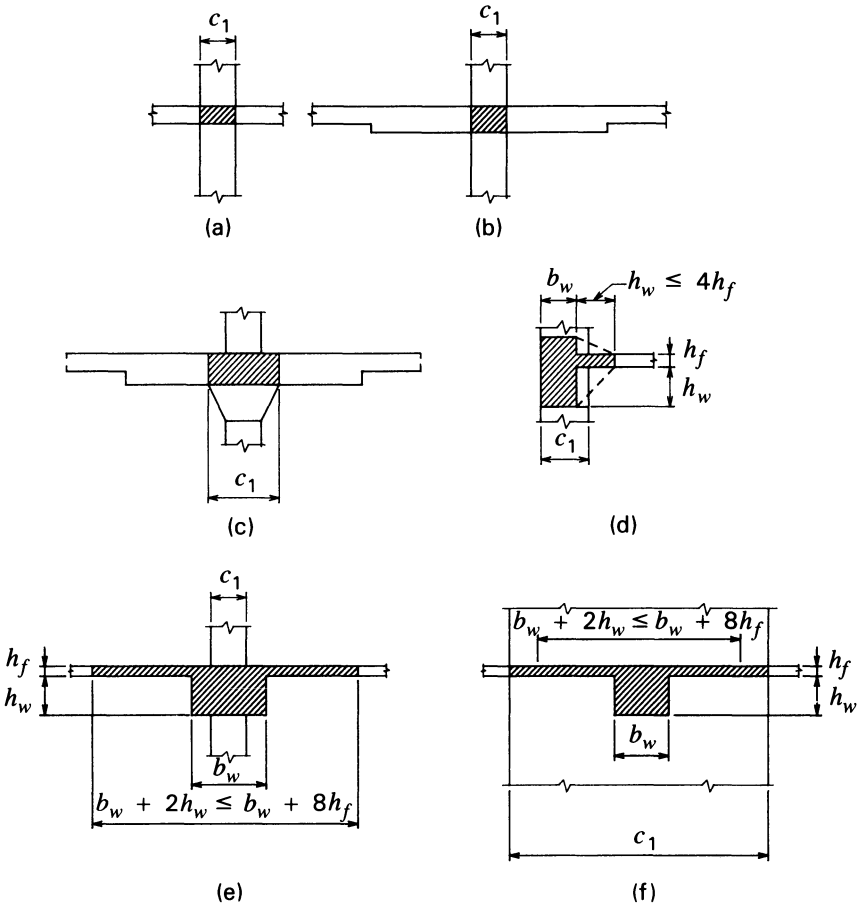

(a) A portion of a flat plate having a width equal to the width of the column (Condition A of Sec. 13.7.5.1 of ACI 318).

(b) A portion of a flat slab without capital having a width equal to the column width (Condition A of Sec. 13.7.5.1 of ACI 318).

(c) A portion of a flat slab with a capital having a width equal to the width of the capital (Condition A of Sec. 13.7.5.1 of ACI 318).

(d) Transverse beam as defined in Sec. 13.2.4 of ACI 318.

(e) Transverse beam as defined in Sec. 13.2.4 of ACI 318.

(f) A portion of a slab having a width equal to the column width plus that part of the transverse beam below (and above if any) the slab (Condition B of Sec. 13.7.5.1 of ACI 318).

Fig. 13-30. Examples of cross sections of torsional members (based upon Sec. 13.2.4, Sec. 13.7.5.1, and Fig. 13.7.5.1 of ACI 318R).

purpose:

$$K_{ta} = K_t \frac{I_{sb}}{I_s} \tag{13-6}$$

in which K_{ta} is the increased torsional stiffness including the effect of the parallel beam, I_{sb} is the moment of inertia of the slab-beam including the stem of the parallel beam shown in Fig. 13-29, and I_s is the moment of inertia of the slab-beam neglecting the stem of the parallel beam.

It is recommended that the reader review the complete contents of ACI 318-83, the Commentary of ACI 318-83 (ACI 318R-83), and all subsequent revisions to these documents before designing cast-in-place prestressed concrete slabs of any type. A paper by Corley and Jirsa, together with a discussion by Eberhardt and Hoffman, provide background information that is an important aid to understanding the action covered in Sec. 13-7 of ACI 318 (Corley and Jirsa 1970; Eberhardt and Hoffman 1971).

ILLUSTRATIVE PROBLEM 13-2 The three-story building shown in plan in Fig. 13-31 has three spans of 36 ft in each of the two orthogonal directions. The exterior columns have their centers located 15 in. from the edge of the slabs and the interior spacing of the columns is 36.0 ft. The story heights, top-of-slab to top-of-slab, are 11.0 ft each from the lowest level through the roof. The roof slab is 9.0 in. thick, and the floor slabs are 11.0 in. thick except in the areas of the drop panels. Drop panels 14.0 in. in thickness, in addition to the slab thicknesses, are provided at the roof and the floors. The plan dimensions of the drop panels are different for the various levels at the corner columns, the edge columns, and the interior columns as will be seen in Fig. 13-32. The nonprestressed reinforced concrete columns, because of architectural considerations, have a diameter of 30.0 in. The concrete in the slabs is sand-lightweight concrete having a specified strength of 4000 psi, an elastic modulus of 2500 ksi, and a unit weight of 115 pcf. The column concrete has a specified strength of 4000 psi, an elastic modulus of 3600 ksi, and a unit weight of 145 pcf. Determine the effective stiffnesses of the equivalent columns for use in a frame analysis as provided in Sec. 13-7 of ACI 318.

SOLUTION: The column heights, as defined in Fig. 13-32, are equal to the floor-to-floor height of 11.0 ft, for all practical purposes, at each level; hence, 11.0 ft is used for the column height at all levels. Using E_{cc} = 3600 ksi, I_c = 39,760 in.^{4}, and L_c = 132 in.

$$K_{c\ \text{above}} = K_{c\ \text{below}} = \frac{4E_{cc}I}{L} = \frac{4 \times 3600 \times 39760}{132} = 4{,}337{,}500\ \text{in.}^4$$

Using x = 23 in. (including the drop panel depth) and y = 30 in., the value of

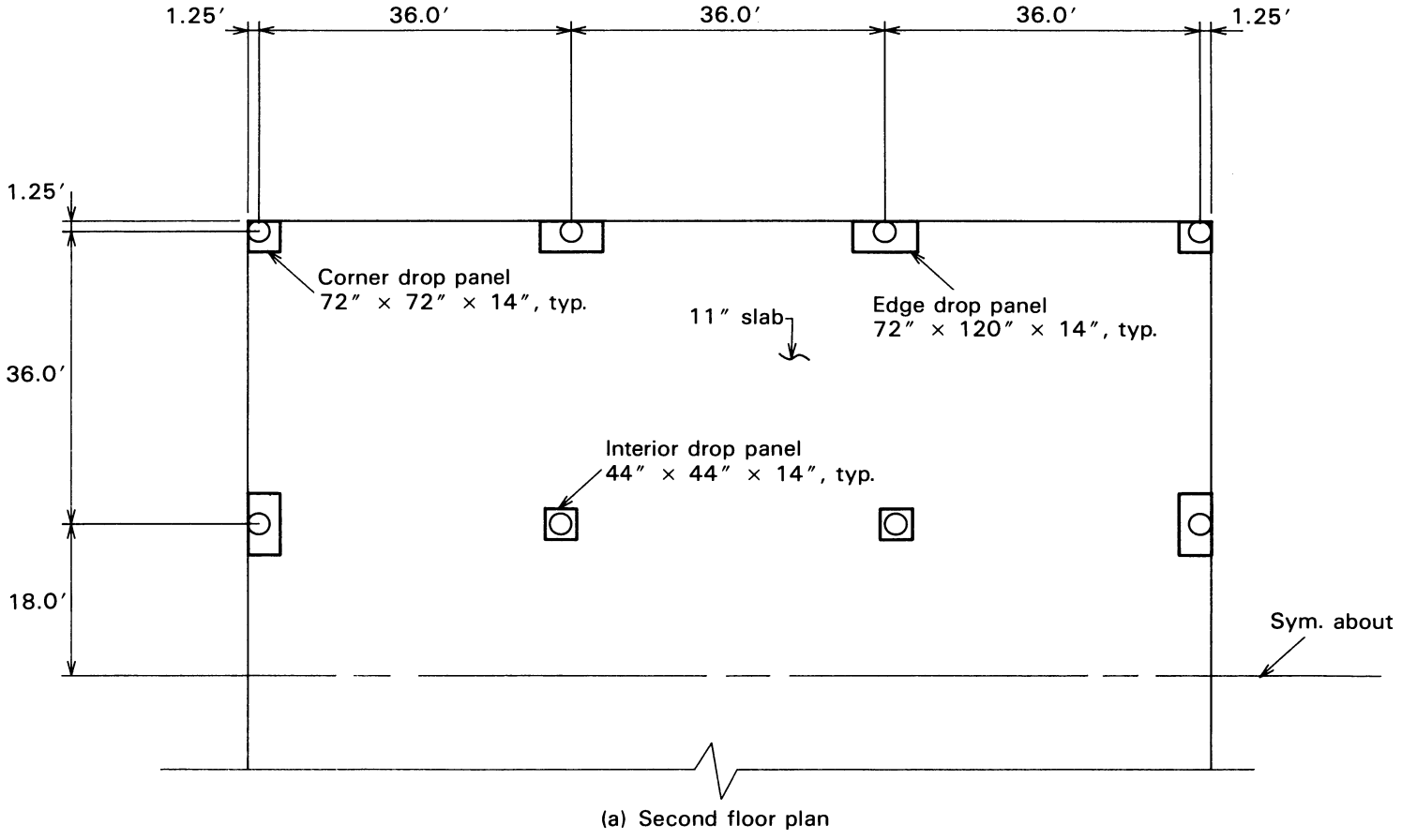

(a) Second floor plan

Fig. 13-31. Plan of three-story building studied in I.P. 13-2. (a) Second floor plan.

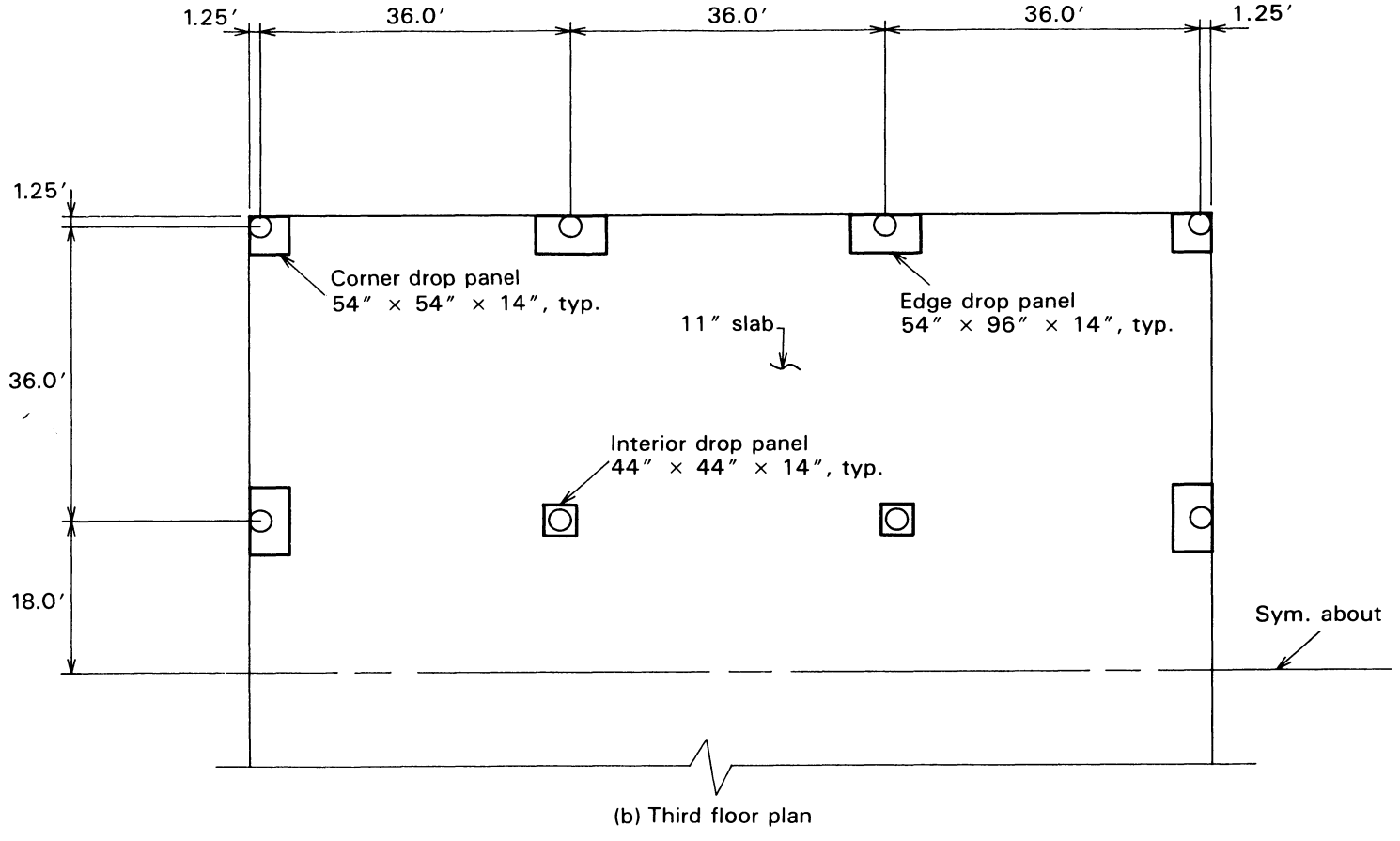

(b) Third floor plan

Fig. 13-31. (*Continued*) (b) Third floor plan.

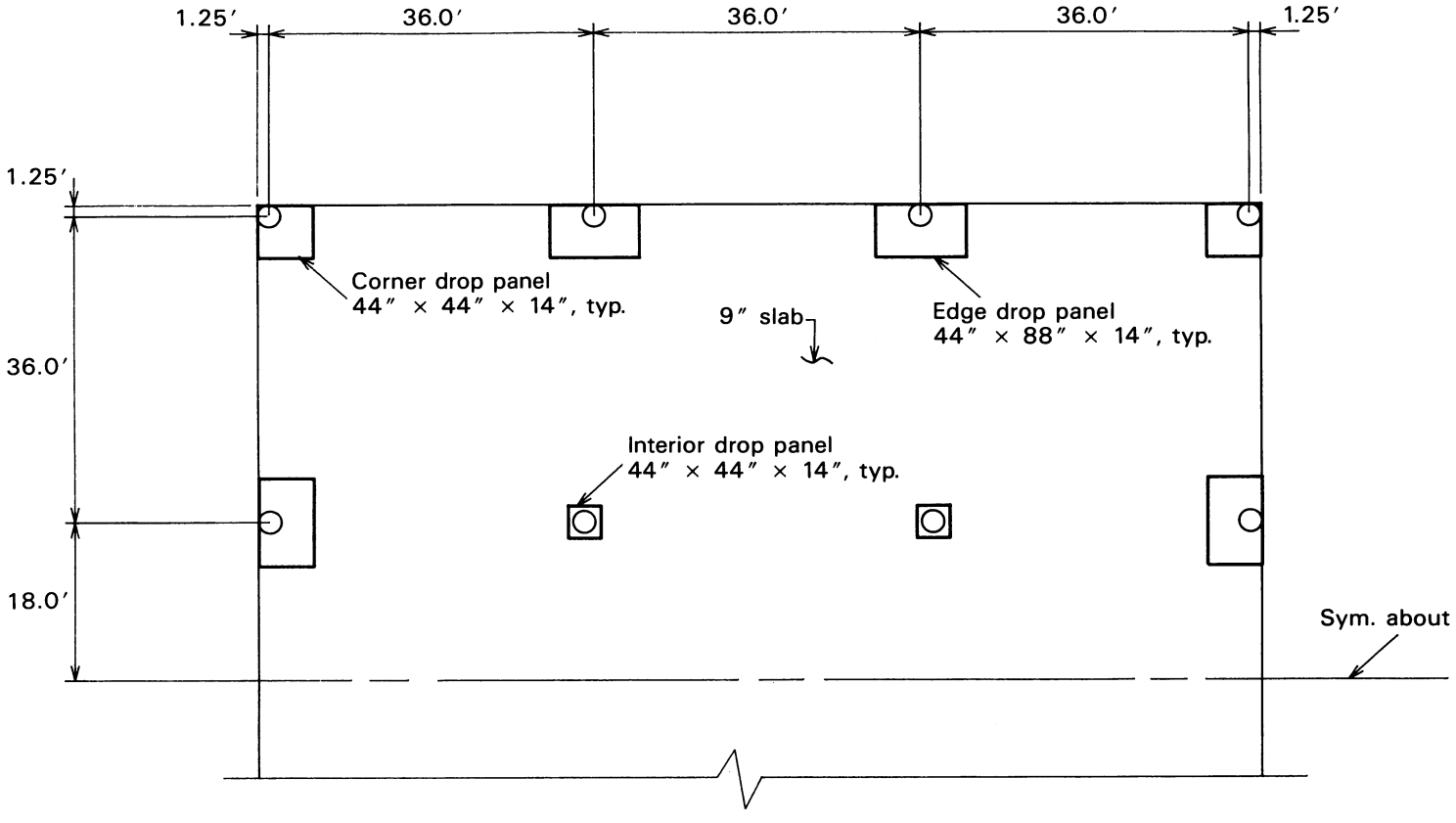

(c) Roof plan

Fig. 13-31. (*Continued*) (c) Roof plan.

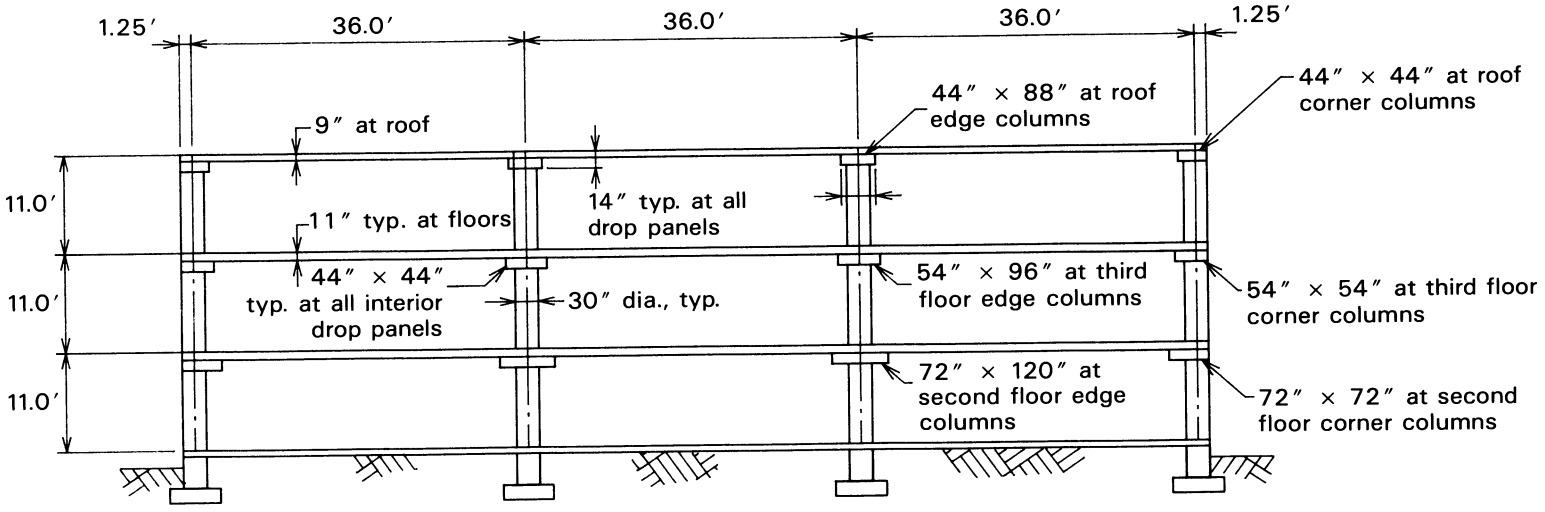

Fig. 13-32. Section through the building analyzed in I.P. 13-2.

TABLE 13-5 Summary of Parameters used in Computation of the Effective Column Lengths and the Effective Column Lengths for I.P. 13-2.

		Exterior Equiv. Frame		Interior Equiv. Frame	
		Roof	Floors	Roof	Floors
K_c	k-in.	4,337,500	8,675,000	4,337,500	8,675,000
C	in.^{4}	62,900	74,200	62,900	74,200
K_t	k-in.	20,523,679	24,215,576	8,131,600	9,594,300
K_{ec}	k-in.	3,580,800	6,387,000	2,828,700	4,555,793
I_{ec}	ft	13	15	17	21

Note: The values for K_c for the roof are for a column below the roof, and those for the floors are for columns above and below.

C becomes:

$$C = \left(1 - 0.063 \times \frac{23}{30}\right)\frac{23^3 \times 30}{3} = 62{,}904 \text{ in.}^4$$

Using $E_{cs} = 2500$ ksi, for an interior column at the roof, the value of K_t is:

$$K_t = \frac{18 \times 2500 \times 62904}{432\left(1 - \dfrac{30}{432}\right)^3} = 8{,}131{,}600 \text{ k-in.}$$

and the stiffness of the equivalent column becomes:

$$K_{ec} = \frac{4{,}337{,}500}{1 + \dfrac{4{,}337{,}500}{8{,}131{,}600}} = 2{,}828{,}700 \text{ k-in.}$$

and the effective column length becomes:

$$L_{ec} = 11 \times \left(1 + \frac{337{,}500}{8{,}131{,}600}\right) = 17 \text{ ft}$$

The values of K_c, C, K_t, K_{ec}, and the effective column lengths are determined to be as summarized in Table 13-5.

13-13 Shear Design for Flat Slabs and Flat Plates

In flat slabs and flat plates, a significant portion of the shear stress at a column is a result of the moment that must be transferred between the slab and the column. The shear stresses resulting from moment transfer at an interior column, together with definitions of the dimensions of the critical sections, are shown

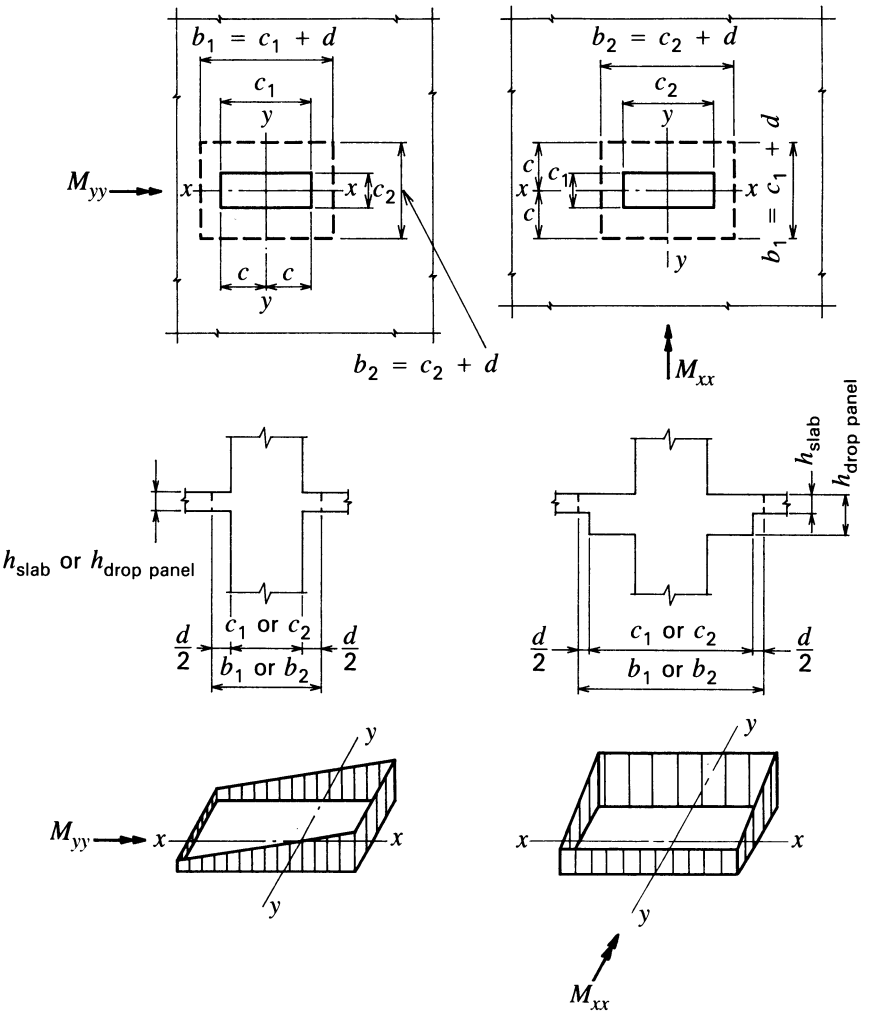

Fig. 13-33. Distribution of shear stresses at an interior column and the dimensions used in their determination.

in Fig. 13-33. The moment may be the result of gravity loads or lateral loads. Only a portion of the moment is assumed to be transferred by flexure. The portions of the moment assumed to be transferred by flexure and shear are:

$$\gamma_f = \frac{1}{1 + \frac{2}{3}\sqrt{\frac{b_1}{b_2}}} \tag{13-7}$$

$$\gamma_v = 1 = \gamma_f$$
$$= 1 - \frac{1}{1 + \frac{2}{3}\sqrt{\frac{b_1}{b_2}}} \qquad (13\text{-}8)$$

in which b_1 is the width of the critical section parallel to the direction of the span, and b_2 is the width of the critical section perpendicular to the direction of the span. The dimensions b_1 and b_2, together with the effective depth, d, are illustrated in Figs. 13-33, 13-34, and 13-35 for interior, edge, and corner columns under moments about the x–x and y–y axes. (*Note*: The values of b_1 and b_2 in these figures are based upon the widths of the column and the thickness of the slab plus the thickness of the drop head or panel at the location of the column, if any. If more critical, the values of b_1 and b_2 should be based upon the widths of the drop head or panel, if any, and d should be taken as the thickness of the slab alone.)

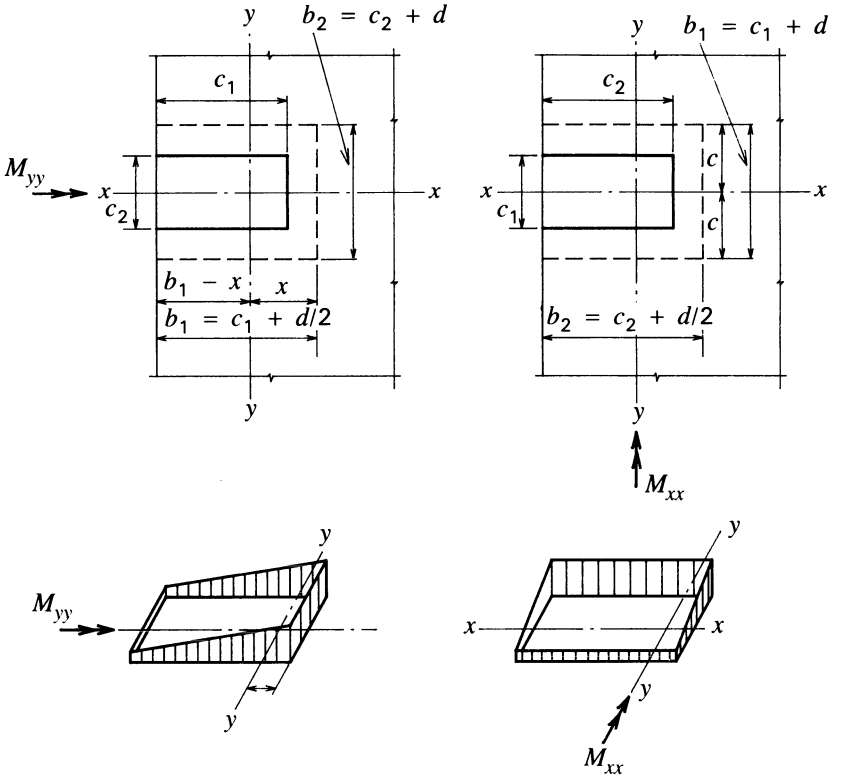

Fig. 13-34. Distribution of shear stresses at an edge (exterior) column and the dimensions used in their determination.

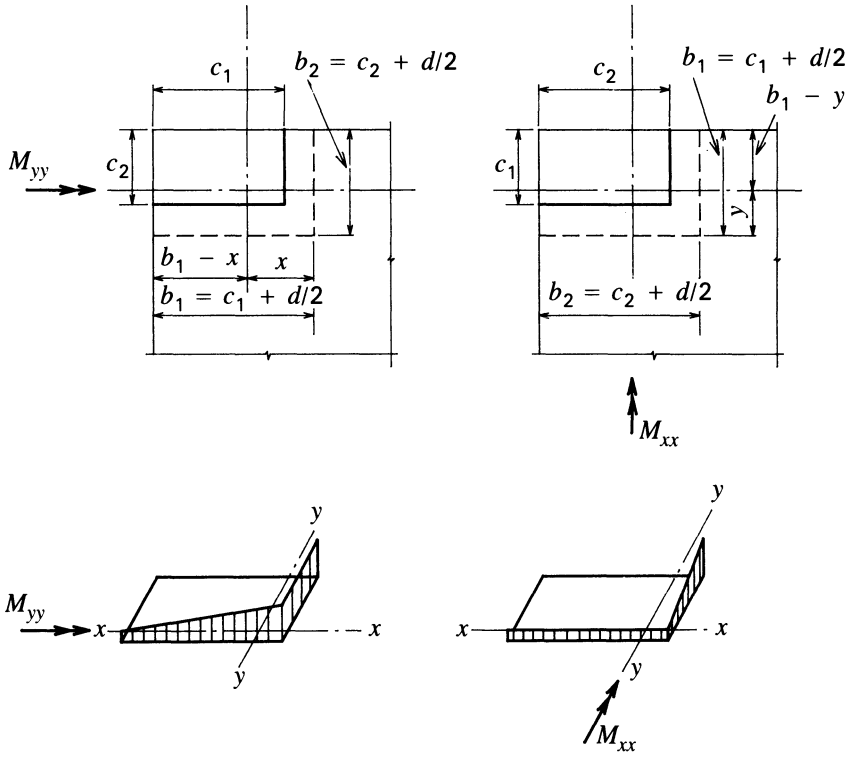

Fig. 13-35. Distribution of shear stresses at a corner column and the dimensions used in their determination.

The maximum shear stress is taken to be the sum of the shear stresses due to the design vertical force, V_u, and to the design moment, M_u. This relationship can be written as:

$$v_u = \frac{V_u}{A_c} + \frac{\gamma_v M_u c}{J_c} \tag{13-9}$$

in which:

A_c = Area of the critical section.

c = Distance from the neutral axis to the fiber under consideration, which, for symmetrical sections, is $\sqrt{\left(\frac{b_1}{2}\right)^2 + \left(\frac{d}{2}\right)^2}$ and, for asymmetrical sections, varies from $\sqrt{x^2 + \left(\frac{d}{2}\right)^2}$ to $-\sqrt{\left(\frac{b_1 - x}{2}\right)^2 + \left(\frac{d}{2}\right)^2}$ or from

$\sqrt{y^2 + \left(\frac{d}{2}\right)^2}$ to $-\sqrt{\left(\frac{b_1 - y}{2}\right)^2 + \left(\frac{d}{2}\right)^2}$. (*Note*: The values of c given above are correct when used with the polar moment of inertia, J_c. However, c frequently is taken to be x, $-(b_1 - x)$, y, or $-(b_1 - y)$ rather than the values given above. The error is so doing is small when b_1 is large in comparison to d.)

J_c = The polar moment of inertia for the critical section.

For an interior column with moments about the x–x or y–y axis, $b_1 = c_1 + d$, $b_2 = c_2 + d$, and:

$$A_c = 2d[(c_1 + d) + (c_2 + d)] = 2d(b_1 + b_2) \tag{13-10}$$

and:

$$J_c = \frac{d(c_1 + d)^3}{6} + \frac{(c_1 + d)d^3}{6} + 2d(c_2 + d)\left(\frac{c_1 + d}{2}\right)^2$$

$$= \frac{db_1^3}{6} + \frac{b_1 d^3}{6} + \frac{db_2 b_1^2}{2} \tag{13-11}$$

For a column along the edge of a slab as shown in Fig. 13-34, the terms b_1 and b_2 are defined in Fig. 13-34, and the area of the critical section with respect to the x–x and y–y axes becomes:

$$A_{cy} = 2db_1 + db_2 \tag{13-12a}$$

$$A_{cx} = db_1 + 2db_2 \tag{13-12b}$$

For moments about the y–y axis, the polar moment of inertia is:

$$J_{cy} = \frac{db_1^3}{6} + \frac{b_1 d^3}{6} + 2db_1(b_1 - x)^2 + b_2 dx^2 \tag{13-13}$$

where:

$$x = \frac{db_1^2}{2db_1 + db_2}$$

For moments about the x–x axis, the polar moment of inertia is:

$$J_{cx} = \frac{db_2^3}{12} + \frac{b_2 d^3}{12} + 2db_1\left(\frac{b_2}{2}\right)^2 \tag{13-14}$$

For a corner column (see Fig. 13-35):

$$A_c = d[b_1 + b_2] \tag{13-15}$$

$$x = \frac{db_1^2}{2A_c} \tag{13-16}$$

$$y = \frac{db_2^2}{2A_c} \tag{13-17}$$

For moments about the y–y and x–x axes, respectively, are:

$$J_c = \frac{db_1^3}{12} + \frac{b_1 d^3}{12} + db_1\left(\frac{b_1}{2} - x\right)^2 + db_2 x^2 \tag{13-18}$$

and

$$J_c = \frac{db_1^3}{12} + \frac{b_1 d^3}{12} + db_1\left(\frac{b_1}{2} - y\right)^2 + db_2 y^2 \tag{13-19}$$

At columns in two-way prestressed concrete slabs meeting the minimum requirements of Sec. 18.9.3 of ACI 318, the nominal shear strength of the concrete at the column, as specified in Sec. 11.12.2.2 of ACI 318, expressed in terms of stress rather than force, is:

$$v_c = \left(\beta_p \sqrt{f'_c} + 0.3 f_{pc} + \frac{V_p}{b_o d}\right) \tag{13-20}$$

where β_p is the lesser of 3.5 and $\alpha_s d/b_o + 1.5$. The values of α_s and b_o, the perimeter of the critical sections, for interior, edge, and corner columns are:

Column type	b_o	α_s
Interior	$2(b_1 + b_2)$	40
Edge	$2b_1 + b_2$ or $b_1 + 2b_2$	30
Corner	$b_1 + b_2$	20

In eq. 13-20, V_p is the vertical component of all effective prestress forces crossing the critical section, and f_{pc} is the average compressive stress in the concrete due to effective prestress forces only (after allowance for all prestress losses). When eq. 13-20 is used, ACI 318 requires that no portion of the column cross section be permitted to be closer to a discontinuous edge than four times the slab thickness, f'_c is not to be taken greater than 5000 psi, and f_{pc} is not to be taken less than 125 psi or more that 500 psi in each of the orthogonal directions. Although not specifically stated in Sec. 11.12.2.3 of ACI 318, the provisions of Sec. 11.2 should be used when lightweight concrete is to be employed. The fact that V_p should be carefully evaluated in thin slabs is emphasized in the ACI–ASCE recommendations. It is pointed out that field placing practices (tolerances, placing errors, etc.) can have a significant effect of the value of V_p, and the term can conservatively be taken to be zero.

For cases when it is not appropriate to use eq. 13-20 for the value of v_c or V_c, the provisions of Sec. 11.12.2.1 of ACI 318, which are for nonprestressed slabs and footings, should be used. The value of V_p can conservatively be taken as zero and should be included in the calculations only if the reverse curvature in the tendons in the vicinity of the supports is included in its determination.

ILLUSTRATIVE PROBLEM 13-3 For the building of I.P. 13-2, compute the shear stresses in the slabs at the corner and edge columns at the second and third floor slabs and the roof if the live loads are 100 psf, nonreducible, 50 psf, reducible to 30 psf, and 12 psf, nonreducible, respectively. The shear forces and moments due to dead loads, live loads, and prestressing are computed to be as summarized in Table 13-6.

SOLUTION: To facilitate the computations, the analysis is based upon a rectangular column having its center 14 in. from the edge of the slab in each of the orthogonal directions as shown in Fig. 13-36b, rather than upon the actual dimensions shown in Fig. 13-36a. The values of the area, polar moment of inertia, and γ_f, together with the numbers of the equations used to compute them, and the maximum slab shear stress for the corner columns and edge columns at the roof and the third and second floors, are summarized in Table

TABLE 13-6 Summary of Shear and Moments for I.P. 13-3.

		Roof	Floor	Floor
Corner columns:				
V_{dl}	k	41	64	64
M_{dlxx}	k-ft	209	340	340
M_{dlyy}	k-ft	209	340	340
V_{ll}	k	7	16	55
M_{llxx}	k-ft	34	90	269
M_{llyy}	k-ft	34	90	269
V_p	k	0	0	0
M_{psxx}	k-ft	−59	−105	−158
M_{psyy}	k-ft	−59	−105	−158
Edge Columns:				
V_{dl}	k	82	128	128
M_{dlxx}	k-ft	418	680	680
M_{dlyy}	k-ft	49	35	35
V_{ll}	k	14	32	110
M_{llxx}	k-ft	66	178	536
M_{llyy}	k-ft	9	17	31
V_p	k	0	0	0
M_{psxx}	k-ft	−119	−209	−317
M_{psyy}	k-ft	0	0	0

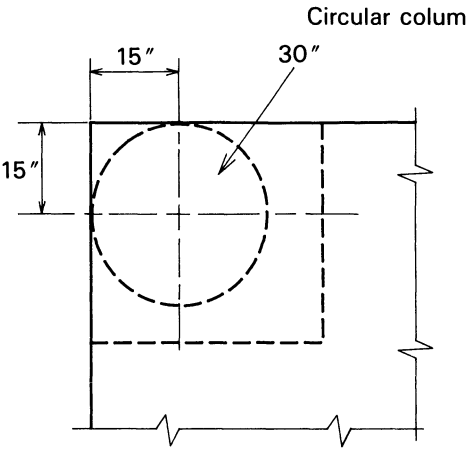

(a) Actual dimensions at corner column for I.P. 13-3

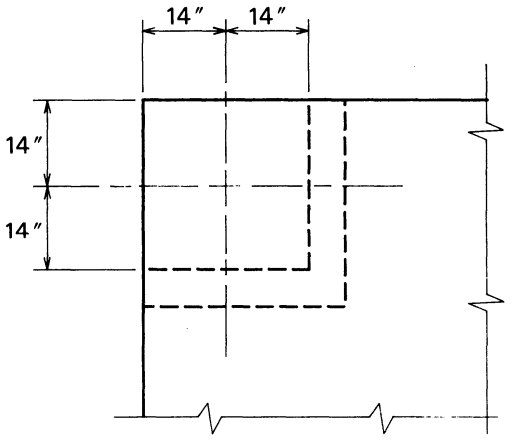

(b) Dimensions used in I.P. 13-3 to facilitate the computations

Fig. 13-36. Plan of corner columns showing (a) actual dimensions and (b) those assumed to facilitate the analysis.

13-7. The value of the first term in eq. 13-20 for the corner and the edge columns is greater than 4; so the maximum value permitted by ACI 318, $4\sqrt{f'_c}$, controls the design. It should be noted that the maximum average shear stress permitted with eq. 13-20 in the sand-lightweight concrete slab is $0.85 \times 4\sqrt{4000} = 215$

TABLE 13-7 Summary of the Values of Area, Polar Moment of Inertia, and γ, Together with the Equations Used to Compute Them, and the Maximum Shear Stress for the Corner Columns and Side Columns at the Roof and Third and Second Floors. The Values of V_c/b_od in the Following Table Were Computed with eq. 11-36 in ACI 318.

			Roof	Floor 3	Floor 2
Corner Columns:					
A_c	in.^{2}	Eq. 13-15	716	1,116	1,458
J_{cx}	in.^{4}	Eq. 13-19	171,793	405,531	900,266
J_{cy}	in.^{4}	Eq. 13-18	171,793	405,531	900,266
γ_{fx}	—	Eq. 13-7	0.40	0.40	0.40
γ_{fy}	—	Eq. 13-7	0.40	0.40	0.40
v_u	psi	Eq. 13-9	189	185	174
$\frac{V_c}{b_od}$	psi	Eq. 13-20	215	215	215
Edge Columns					
A_c	in.^{2}	Eq. 13-12	1,432	2,119	2,688
J_{cx}	in.^{4}	Eq. 13-14	343,585	785,146	1,709,473
J_{cy}	in.^{4}	Eq. 13-13	2,180,817	4,043,180	7,842,356
v_u	psi	Eq. 13-9	134	135	139
$\frac{V_c}{b_od}$	psi	Eq. 13-20	215	215	215

psi; hence, reinforcement is not required at any of the locations studied. It also should be noted that the interior column connections are less critical than those on the periphery of the building because the moments that must be transferred are smaller and the perimeters of the critical section are larger at the interior columns than at the columns on the periphery.

REFERENCES

Aalami, B. O. 1878. Design of Post-Tensioned Floor Slabs. *Concrete International Design and Construction.* Detroit. American Concrete Institute. 11(6):59–67.

Aalami, B. O. and Barth, F. G. 1989. Restraint Cracks and Their Mitigation in Unbonded Post-tensioned Building Structures. *Cracking in Prestressed Concrete Structures.* Detroit. American Concrete Institute.

ACI Committee 318. 1983. *Building Code Requirements for Reinforced Concrete.* Detroit. American Concrete Institute.

ACI Committee 318. 1983. *Commentary on Building Code Requirements for Reinforced Concrete.* Detroit. American Concrete Institute.

ACI Committee 318. 1989. *Building Code Requirements for Reinforced Concrete.* Detroit. American Concrete Institute.

ACI Committee 318. 1989. *Commentary on Building Code Requirements for Reinforced Concrete.* Detroit. American Concrete Institute.

ACI-ASCE Committee 423.1R. 1969. Tentative Recommendations for Concrete Members Prestressed with Unbonded Tendons. *Journal of the American Concrete Institute* 66(2):81-86.

ACI-ASCE Committee 423.3R. 1983. Recommendations for Concrete Members Prestressed with Unbonded Tendons. *Concrete International*. Detroit: American Concrete Institute 5(7):61-76.

ACI-ASCE Committee 423.3R. 1989. Recommendations for Concrete Members Prestressed with Unbonded Tendons. *Structural Journal of the American Concrete Institute*. 86(3):301-18.

Brotchic, J. F. and Wynn, A. J., 1975. *Elastic Deflections and Moments in an Internal Panel of a Flat Plate Structure—Design Information*. Sidney, Australia. Commonwealth Scientific and Industrial Research Organization.

Corley, W. G. and Jirsa, J. O. 1970. Equivalent Frame Analysis for Slab Design. *Journal of the American Concrete Institute* 67(11):875-84.

Csagoly, P. F. and Lybas, J. M. 1989. Advanced Design Method for Concrete Bridge Deck Slabs. *Concrete International Design and Construction* 11(5):53-63.

Eberhardt, A. C. and Hoffman, E. S. 1971. Discussion of the paper "Equivalent Frame Analysis for Slab Design" by W. G. Corley and J. O. Jirsa. *Journal of the American Concrete Institute*. 68(5):397-8.

Kawai, T. 1957. Influence Surfaces for Moments in Slabs Continuous Over Flexible Cross Beams. *International Association for Bridge and Structural Engineering*. 16:117-38.

Kist, H. J. and Bouma, A. L. 1954. An Experimental Investigation of Slabs, Subjected to Concentrated Loads. *International Association for Bridge and Structural Engineering*. 14:85-110.

PCI Design Handbook. 1985. Chicago: Prestressed Concrete Institute.

Precast, Prestressed Concrete Producers and Products. 1969. Chicago. Prestressed Concrete Institute.

Pucher, A. 1964. *Influence Surfaces of Elastic Plates*. New York. Springer-Verlag.

Uniform Building Code. 1976. Whittier, California: International Conference of Building Officials.

Uniform Building Code. 1988. Whittier, California: International Conference of Building Officials.

Westergaard, H. M. 1930. Computation of Stresses in Bridge Slabs Due to Wheel Loads. *Public Roads*. 11:1-23.

14 Bridge Construction

14-1 Introduction

Prestressed concrete has been used extensively in U.S. bridge construction since its first introduction from Europe in the late 1940s. Literally thousands of highway bridges of both precast, prestressed concrete and cast-in-place post-tensioned concrete have been constructed in the United States. Railroad bridges utilizing prestressed concrete have become common as well. The use and evolution of prestressed concrete bridges is expected to continue in the years ahead.

It is not possible to give a comprehensive discussion of all types of prestressed concrete bridges in this book. There are many different types as well as variations within the types. The reader interested in a more comprehensive discussion of the subject is referred to references listed at the end of this chapter.

The following discussion of various factors influencing the design of bridges is presented with respect to fully prestressed simple span bridges unless otherwise stated. The same general principles apply in the design of continuous spans. Partial prestressing is not used in bridge construction to the extent that it is in other types of structures, and hence is not considered in this discussion. In addition, this presentation basically is limited to highway bridges designed for normal truck loadings. The same principles apply to bridges designed for other

purposes and types of loading; however, the span range in which each basic type of framing is most efficient may be altered if the ratio of the dead load to live load is appreciably different with the other types of live loading.

The basic configuration of the most efficient and economical structural elements in prestressed-concrete bridges for any specific structure is a function of the following:

1. Span length
2. Design live and impact loads
3. Configuration of the structure
4. Allowable concrete stresses
5. Size of the structure
6. Site-imposed requirements

The effects of each of these factors are discussed below, as a means of introducing the reader to basic considerations. In subsequent sections various basic types of commonly used highway-bridge construction, as well as some less common yet economical modes of prestressed bridge construction, are discussed, and the limitations of each type are pointed out.

The distance between the supports of a bridge span affects the design in three ways:

1. The dead load of a bridge member, in proportion to the live and total loads, increases as the span is increased. Therefore, for bridges with very short spans, the live load for which the bridge must be designed is very nearly the total load, and, for very long spans, the dead load is of much greater significance than the live load.
2. The moment for which a flexural member must be designed approaches being a function of the square of the span, whereas the shear for which a beam must be designed is basically a direct function of the shear span and the load. Thus, for moving live loads, the shear force in short spans is very large in proportion to the bending moment, and, in long spans, the bending moment is of much greater importance than the shear forces.
3. The impact loads that must be included in the design, which are usually considered as a function of the live load, are smaller for long spans than for short spans.

These three considerations have a significant influence on the optimum cross section for bridge members for different span lengths. Bearing in mind that only relatively nominal tensile stresses are allowed in the precompressed tensile zone under the effect of the total load in most contemporary bridge design, one can see that the principles of elastic design are of greater significance in bridge design than in building design. The strength of a bridge structure, like almost all other structures, is very important and must be great enough to ensure the

safety of persons using the structure even under accidental overloads. Ductility is an important property for assuring safety in bridge construction, as it is in other types of structures.

To facilitate this discussion, it will be assumed that tensile stresses are not to be permitted under full service load. This is done even though, as explained in Sec. 3-19, contemporary design criteria permit tensile stresses in prestressed concrete bridges under some circumstances.

Considering the maximum total moment relationship (see Sec. 4-4):

$$M_t = M_d + M_l = C(e + r^2/y_b) \tag{14-1}$$

it becomes apparent that, because the dead load is very small for short-span bridges, eq. 14-1 approaches:

$$M_t = M_l = C(e + r^2 y_b) \tag{14-2}$$

From eq. 14-2, it follows that when a short simple-span structure is acted upon by dead load alone, the pressure line is located at a distance nearly equal to the eccentricity of the prestressed reinforcement, e_{ps}, below the center of gravity of the section. Therefore, the cross section of the member must have a relatively large bottom flange for resisting the prestressing force during the periods when the live load is not being applied. Solid slabs, hollow slabs, and beams with large top and bottom flanges but with webs of good proportions, all satisfy these conditions. Bridge cross sections of this type utilizing precast sections with prestressed reinforcement are illustrated in Fig. 14-1.

When a bridge span is large, shear is less important than it is in a shorter span, and dead load is a large percentage of the total load. Consideration of the total moment relationship given in eq. 14-1, and of the location of the pressure line under the action of prestressing plus dead load, leads one to recognize that under the condition of no live load, the pressure line in a simple span will be located at a distance equal to M_d/C above the center of gravity of the prestressed reinforcement. Because the dead load is acting at the time of prestressing, a large bottom flange is not needed near midspan to resist the prestressing force during the periods in which the intermittent live load is not applied. In precast construction, unless the prestressing is done in two or more stages, the entire dead load of the structure will not be acting at the time of prestressing, and a bottom flange of moderate size may be needed near midspan to resist the prestressing force temporarily during construction; this is true even for bridges with long spans. In cast-in-place bridges having long spans, on the other hand, T-shaped beams often are very efficient because all of the dead load, with the possible exception of sidewalks and wearing surfaces, is acting at the time of prestressing. Efficient cross sections for simple prestressed bridges with relatively long spans approach those shown in Fig. 14-2 for cast-in-place and precast construction.

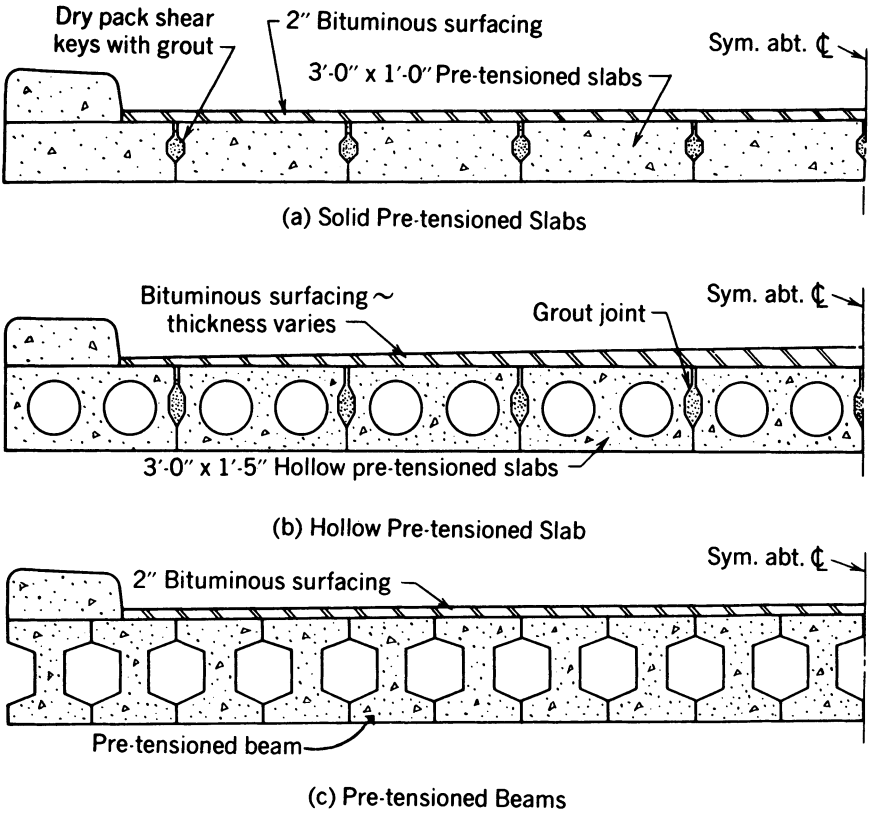

Fig. 14-1. Half-sections of typical prestressed-concrete short-span bridges.

Large compression flanges are required for the development of flexural strength in both long and short spans. Furthermore, in long-span structures where bending moment is of greater importance than shear, a large top flange is necessary for serviceability considerations as well.

The optimum cross sections for spans of moderate length have dimensions falling between those that are desirable for short- and for long-span structures. Hence, I-beams or hollow boxes, as shown in Fig. 14-3, are found to be efficient for bridges of moderate span length.

It should be apparent that exceptionally large live loads, such as those encountered in railroad bridges, would render the use of solid and hollow slabs efficient for spans of moderate length, whereas very light, live loads, such as those found in the design of pedestrian bridges, would permit the use of T-beams, even for relatively short spans.

Structural continuity is an important consideration in bridge design. Short-span continuous bridge structures often experience significant reversals of

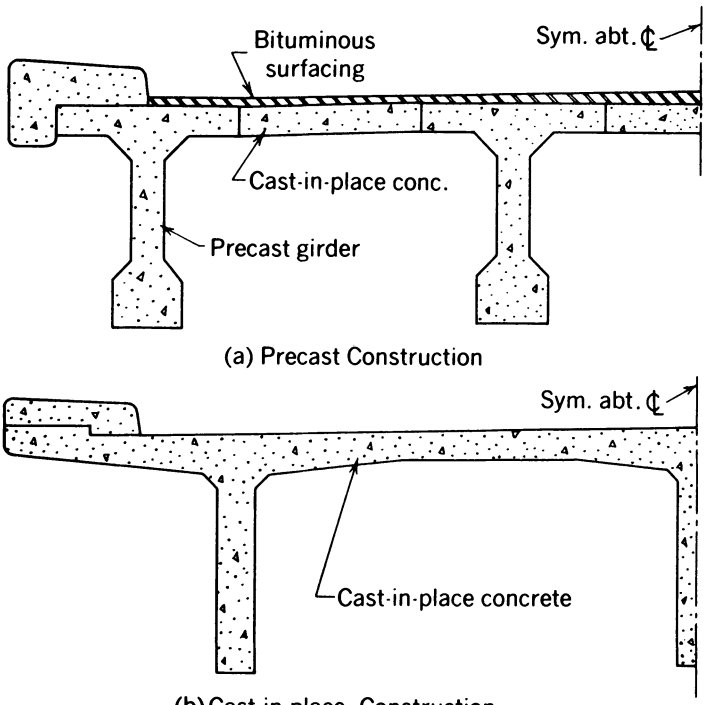

Fig. 14-2. Half-sections of typical long-span bridges.

moment due to live load. In addition, there normally are significant negative live moments at the interior supports and significant positive moments at or near the midspans. Because of this, short-span continuous structures often require cross sections that are approximately symmetrical throughout the full length of the structure. Hollow-box and I-shaped sections are efficient for structures of this type. Frequently, the depth of the superstructure is variable in continuous short-span bridge elements, with the greater depth being near the supports; the basic cross-sectional shape, however, usually is maintained throughout the entire length of the structure. Long-span continuous bridges are not subject to moment reversals to the degree found in short-span structures, and, because of the greater importance of dead load in bridges having long spans, larger top rather than bottom flanges are more efficient in areas of positive moment, with the opposite true at locations of negative moment.

The allowable stresses in the concrete and the prestressing steel have a significant influence on the efficiency of cross-sectional shapes of prestressed concrete elements under specific conditions of span and loading. The allowable concrete stress in the top fibers of precast pretensioned sections has a significant influence on the amount of prestressed reinforcement needed in pretensioned beams. The

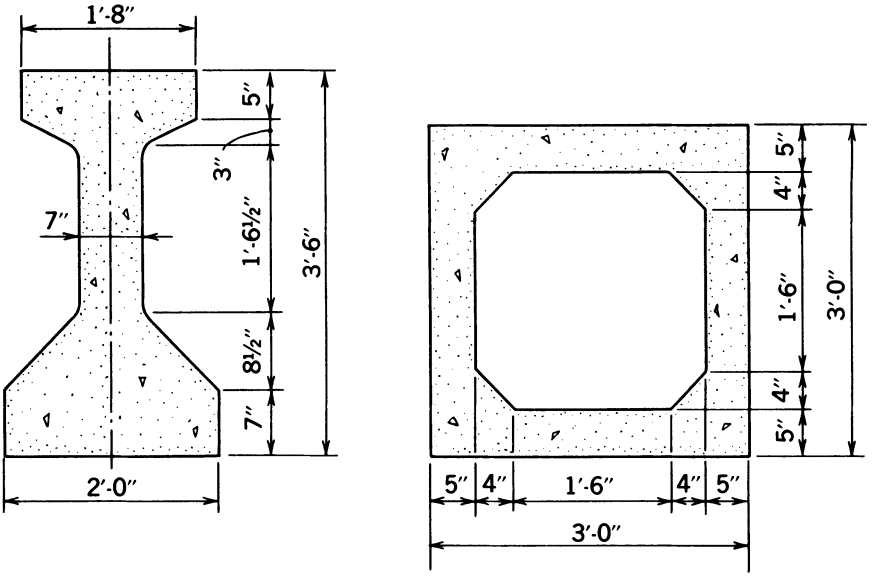

Fig. 14-3. Sections of precast prestressed-concrete beams commonly used in bridges of moderate length.

customary limit of $0.40f'_c$ for compressive stress under service load in bridge design only becomes important for girders having long spans. By using customed-designed members, which could be precast or cast-in-place, and erection techniques designed for a specific long-span bridge, as opposed to the more typical or standard shapes and sizes of members that must be used on smaller projects, a bridge designer often can achieve greater economy in labor and materials than would be possible with the standard or more typical members. It is feasible to use special designs on large projects because the cost of the concrete forms and the plant required to produce special members often does not represent a large portion of the total cost of the work; the opposite is the case on small projects.

In designing small bridges with precast prestressed concrete members, the designer must use elements that require very simple custom-made forms or use standard prestressed concrete products routinely produced by manufacturers or contractors located in the general vicinity of the job site. It normally is not feasible for the relatively large cost of steel forms and plant facilities required for the efficient production of precast prestressed concrete bridge members to be amortized on a single small job.

Each site has certain characteristics that influence or perhaps even dictate which bridge design and construction techniques might be feasible. Among these factors are the purpose of the bridge (i.e., grade separation, river crossing, railroad crossing, etc.), the accessibility of the site from existing precasting

plants, the skew required, the quantity and quality of labor and materials available near the site, and so on. Any of these considerations can have an important bearing on the feasibility of the different types of framing and construction procedures.

The types of framing discussed below in Secs. 14-2 and 14-3 have been used almost without deviation for bridges of short and moderate spans in the United States because the construction procedures that are feasible for small structures of these types are unlikely to be the controlling factors in design. When designing long-span bridges, the designer may be compelled to use cast-in-place or precast construction, either to facilitate construction or to maintain minimum horizontal and vertical clearances during the work. The type of framing that may be economical for a bridge or grade separation structure in a metropolitan area in the United States may be far different from the type of framing that may be economical in some remote location in the world where skilled labor and modern equipment are less available than in more populated areas. Therefore, no further attempts will be made to generalize about the influence of the many factors that affect or control bridge type selection.

14-2 Short-Span Bridges

Short-span bridges, for the purposes of this discussion, will be assumed to have a maximum span of 45 ft. It should be understood that this is an arbitrary figure, and there is no definite line of demarcation between short, moderate, and long spans in highway bridges. As mentioned above, short-span bridges are most efficiently made of precast prestressed-concrete hollow slabs, I-beams, solid slabs or cast-in-place solid slabs, and T-beams of relatively generous proportions.

Precast solid slabs are most economical when used on very short spans. The slabs can be made in any convenient width, but widths of 3 or 4 ft have been common. Keys frequently are cast in the longitudinal sides of the precast units. After the slabs have been erected and the joints between the slabs have been filled with concrete, the keys transfer live load shear forces between the adjacent slabs.

Precast solid slabs may be of the type shown in Fig. 14-1, in which case from 1.5 to 2 in. of asphaltic concrete or other bituminous paving material can be applied to serve as a leveling course and wearing surface. Composite slabs formed of solid precast slabs, as shown in Fig. 14-4, are an efficient design for short-span bridges. In the composite construction, the cast-in-place concrete serves as the leveling course, the wearing surface, and the structural top flange in areas of positive bending moment. The composite topping can be used to develop continuity for live loads, if desired, by placing nonprestressed negative moment reinforcement in the cast-in-place concrete at the locations of the interior supports. Because of the relatively high live load moment, as a fraction of the

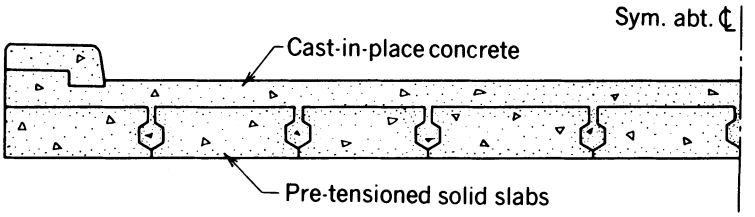

Fig. 14-4. Half-section of a composite precast-slab bridge.

total load moment, and moment reversals, which are characteristic of short-span continuous construction, little is to be gained in first-cost savings through the use of continuity in short-span bridges. Advantages that may lead the designer to specify continuous construction include increased resistance to lateral loads, reduced deflections, better appearance, and the elimination of deck joints.

Precast hollow slabs used in short-span bridges may have round or square voids. They too are generally made in units 3 to 4 ft wide with thicknesses from 18 to 27 in. Precast hollow slabs can be made in any convenient width and depth, and frequently are used in bridges having spans from 20 to 50 ft. Longitudinal shear keys are used in the joints between adjacent hollow slabs in the same way as with solid slabs. Hollow slabs may or may not be used with a composite, cast-in-place concrete topping, but the use of a leveling course of some type normally is required as a means of obtaining an acceptable appearance and levelness.

Transverse reinforcement normally is provided in precast concrete bridge superstructures for the purpose of tying the structure together in the transverse direction. Well-designed ties ensure that the individual longitudinal members forming the superstructure will act as a unit under the effects of the live load. In slab bridge construction, transverse ties most frequently consist of threaded steel bars placed through small holes formed transversely through the member during fabrication. Nuts frequently are used as fasteners at each end of the bars. In some instances, the transverse ties consist of post-tensioned tendons placed, stressed, and grouted after the slabs have been erected. The transverse tie usually extends from one side of the bridge to the other, and is placed along the skew. In a bridge having a large skew, the individual slabs frequently are tied together by connecting adjacent units with short bars that are placed perpendicular to the longitudinal axis of the bridge and only extend between two units. The short bars are offset as required by the skew. This detail is illustrated in Fig. 14-5.

Channel sections of various thicknesses have been used in short-span bridges. The channels are used in the same general way that the solid and hollow slabs are used, with the single exception that a transverse tie of the elements in channel-slab bridges often is developed by bolting the ribs of adjacent channels together, rather than by using tie bars that extend across the entire width of the bridge. This is illustrated in Fig. 14-6.

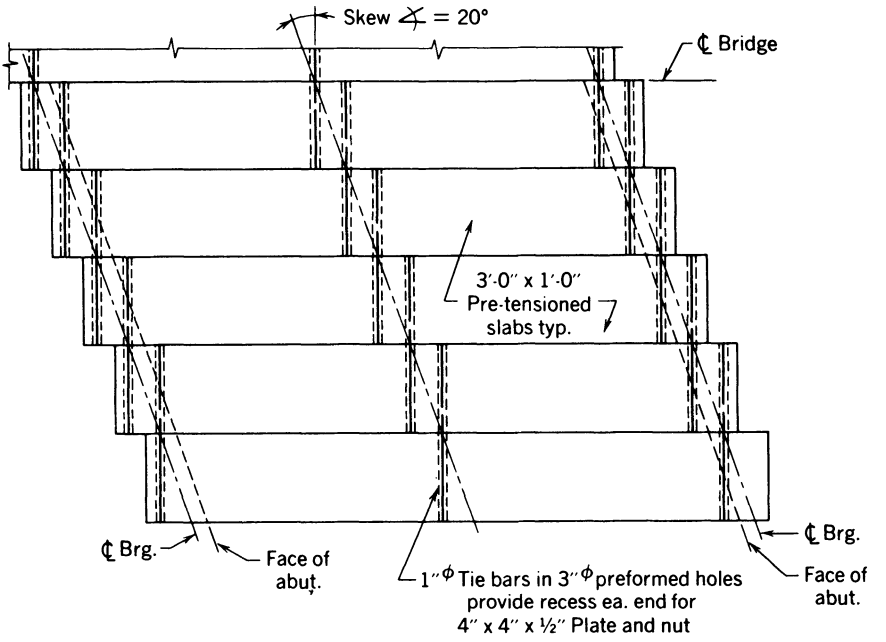

Fig. 14-5. Half-plan of skewed bridge showing staggered transverse tie-bar layout.

The crown or superelevation of the bridge deck, when using any of the short-span bridges of the types discussed above, is developed in one of three ways: (1) by constructing the bearing seats for the precast units on the abutments and piers on straight slopes matching the required crown or superelevation; (2) by constructing the abutment and pier bearing seats level, and achieving the required crown or superelevation with a topping having a variable thickness; or (3) by constructing level bearing seats for each of the precast units in such a way that the top surfaces of the precast units are a series of level steps on which a topping can be placed to obtain the required superelevation or crown. These methods have all been illustrated in Figs. 14-1 through 14-6.

Short-span bridges commonly are made by using composite-stringer construction. This bridge type is illustrated in Fig. 14-7, in which the AASHTO-

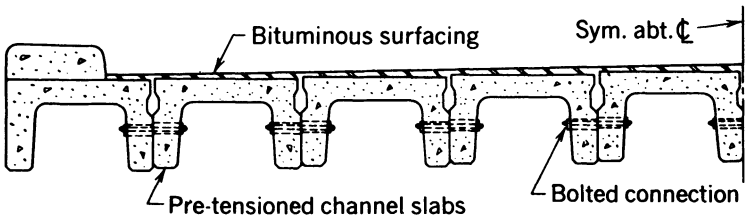

Fig. 14-6. Half-section of a bridge with precast prestressed-concrete channel slabs.

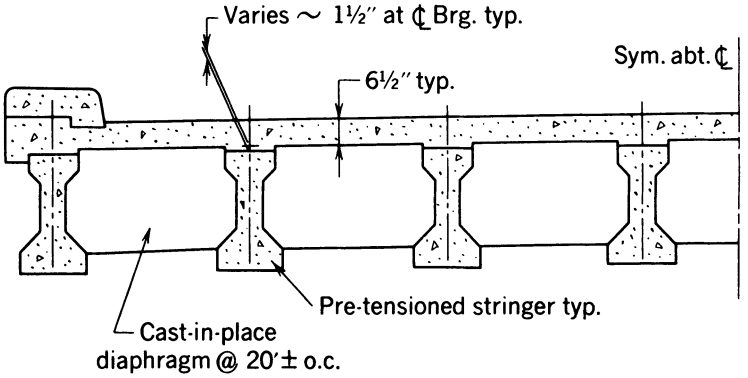

Fig. 14-7. Half-section of a short-span composite-stringer bridge.

PCI Type I bridge stringer is shown. There is little advantage in using composite construction for bridges having short spans from the standpoint of flexural stresses, as the flexural stresses normally are not critical. Furthermore, a precast stringer should have flanges that are wide enough to provide lateral stability during handling, transport, and erection. Top flanges having dimensions that provide stability in handling and transport usually are adequate in the completed structure from the standpoint of lateral buckling even though steps have not been taken to ensure the development of full composite action.

The shear forces imposed on the stringers in short-span bridges frequently are too large to be resisted by the concrete alone. Hence, shear reinforcement normally is required. The amount of shear reinforcement required may be relatively large if the webs of the stringers are relatively thin.

When stringer construction is used for spans between 30 and 45 ft, it generally is considered desirable to use stringers with web thicknesses of 7 to 10 in. as a means of increasing the shear force resisted by the concrete and reducing the amount of web reinforcement required. Stringer spacings used in this type of construction are generally on the order of 4 to 6 ft. When larger spacings are used, the shear stresses in the concrete become difficult to accommodate.

Concrete diaphragms, reinforced with post-tensioned reinforcement or nonprestressed reinforcement, normally are provided transversely at the ends and at intermediate locations along the span in stringer-type bridges. The diaphragms ensure the lateral distribution of the live loads to the various stringers and prevent individual stringers from displacing or rotating significantly with respect to the adjacent stringers. The diaphragms normally are placed along the skew. In bridges in which the skew is large, the intermediate diaphragms may consist of short cast-in-place beams placed perpendicular to the longitudinal axis of the stringers in a staggered configuration across the bridge, in much the same way as is commonly done in steel stringer bridges or in the hollow-slab skew bridge in Fig. 14-5.

No generalities will be made here about the relative cost of each of the above types of construction; construction costs are a function of many variables which prohibit meaningful generalizations. However, it should be noted that the stringer type of construction requires a considerably greater construction depth that is required for solid, hollow, or channel slab bridge superstructures. Stringer construction does not require a separate wearing surface, as do the precast slab types of construction, unless precast slabs are used to span between the stringers in lieu of the more commonly used cast-in-place reinforced concrete deck. Stringer construction frequently requires smaller quantities of superstructure materials than do slab bridges (unless the spans are very short). The construction time needed to complete a bridge after the precast members have been erected is greater with stringer framing than with the slab type of framing.

14-3 Bridges of Moderate Span

Again for the purposes of this discussion only, moderate spans for bridges of prestressed concrete are defined as being from 45 to 80 ft. Prestressed concrete bridges in this span range generally can be divided into two types: stringer-type bridges and slab-type bridges. The majority of the precast prestressed concrete bridges constructed in the United States have been stringer bridges using I-shaped stringers, but a large number of precast prestressed concrete bridges have been constructed with precast hollow-box girders (sometimes also called stringers). Cast-in-place post-tensioned concrete has been used extensively in the construction of hollow-box girder bridges—a form of construction that can be considered to be a slab bridge.

Stringer bridges, which employ a composite, cast-in-place deck slab, have been used in virtually all parts of the United States. For moderate spans, the AASHTO-PCI stringers, Types II and III, frequently are used. These stringers normally are used at spacings of about 5 to 6 ft. The cast-in-place deck is generally from 6.0 to 8.0 in. in thickness. This type of framing is very much the same as that used on composite-stringer construction for short-span bridges (see Fig. 14-7).

The AASHTO-PCI stringer Types I through IV have relatively small flanges, with the top flange smaller than the bottom one. (The dimensions of the AASHTO-PCI stringers are given in Fig. 14-8). Because of the small flanges, relatively large depths of construction are required when these stringers are used. This is a disadvantage in some applications, but not always. A large stringer depth does result in a small prestressing force being required for a specific span and stringer spacing.

In some instances, the bridge construction depth is of great importance, and, in such cases, stringers with larger top and bottom flanges, such as those illustrated in Fig. 14-9, can be used at spacings of from 6 to 8 ft with a significantly

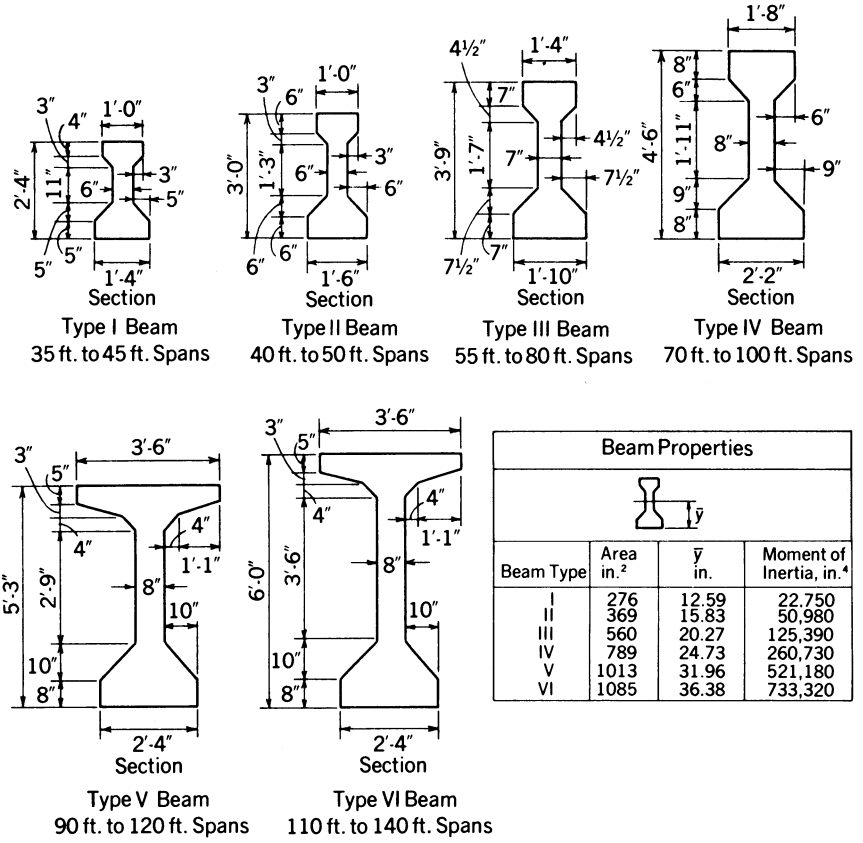

Beam Properties

$\bar{y}$

Beam Type	Area in.^{2}	$\bar{y}$ in.	Moment of Inertia, in.^{4}
I	276	12.59	22,750
II	369	15.83	50,980
III	560	20.27	125,390
IV	789	24.73	260,730
V	1013	31.96	521,180
VI	1085	36.38	733,320

Fig. 14-8. AASHTO-PCI standard bridge stringers.

smaller depth of construction than would be required if stringers with smaller flanges were used.

Another important consideration in the configuration of precast prestressed concrete bridge stringers is the size of the top flange. As has been pointed out, the dead weight of a structure, as well as the stringer alone, becomes greater as the span is increased. The significance of this behavior can best be understood if a stringer with a smaller top flange than bottom flange is analyzed for various stringer spacings on a span of 70 to 80 ft, with composite construction. It frequently will be found that the size of the bottom flange is adequate, and that the capacity and the spacing of the member are limited by the concrete compressive stresses in the smaller top flange. If the span were only 50 ft, and the same procedure were followed, the bottom flange would be found to limit the design. This difference is due to the difference in the ratio of dead to live load that occurs as the span is increased. This restriction can be avoided by

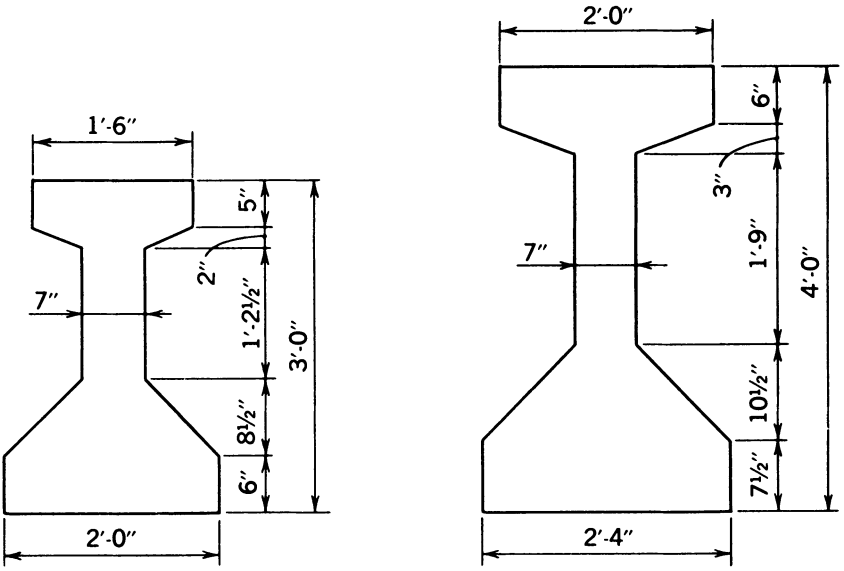

Fig. 14-9. Bridge stringers with large top and bottom flanges.

selecting stringer shapes similar to that shown in Fig. 14-10, when the span is greater than 70 ft.

Composite stringer construction also is used with details similar to those

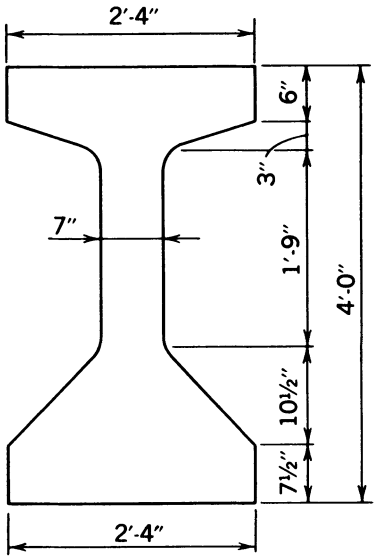

Fig. 14-10. Well-proportioned bridge stringer for span of 60 to 70 ft.

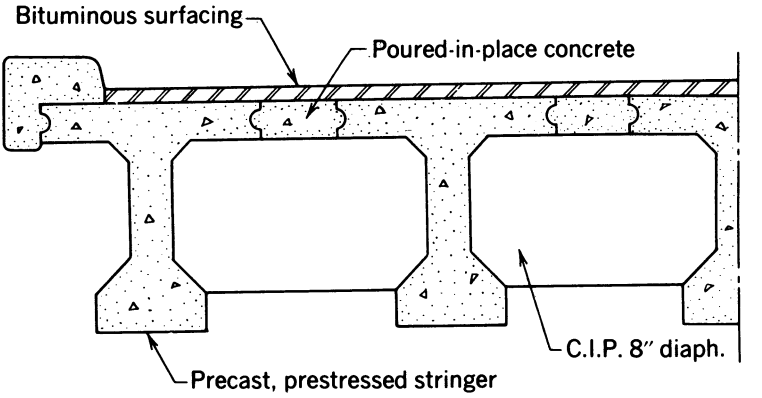

Fig. 14-11. Partial section of a moderate-span bridge.

shown in Fig. 14-11. In this type of framing, the top flange of the girder is reinforced or post-tensioned transversely and forms a portion of the deck of the completed superstructure. The slab between the flanges of the stringers can be either cast-in-place or precast. Another scheme is to cast the stringers with daps near the top for use in supporting precast slabs. This can be done with I-shaped stringers or with hollow stringers, as shown in Fig. 14-12. Still another scheme utilizes precast deck soffit slabs (which serve as forms for the cast-in-place deck topping) adjusted to the corrected elevation during construction through the use of field-cut polystyrene foam supports, as shown in Fig. 14-13.

To eliminate the need for large bottom flanges on stringers in the span range of 50 to 70 ft, two-stage post-tensioning has been employed. This procedure consists of using a T-shaped beam in which 50 to 75 percent of the tendons are stressed before the beam is removed from the casting bed. After the stringer has been erected and the deck has been cast, the remaining tendons are stressed. This construction scheme is restricted to post-tensioned or combined pretensioned and post-tensioned construction. The second-stage post-tensioning,

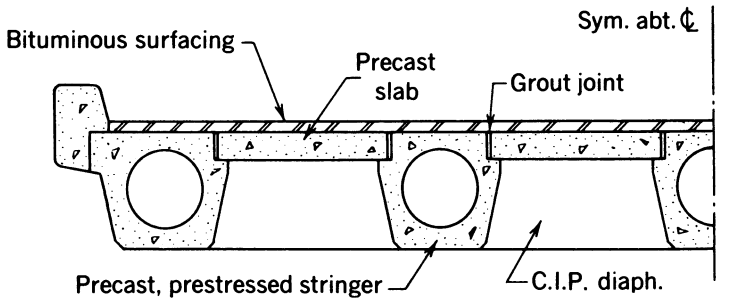

Fig. 14-12. Half-section of a bridge with precast deck slabs.

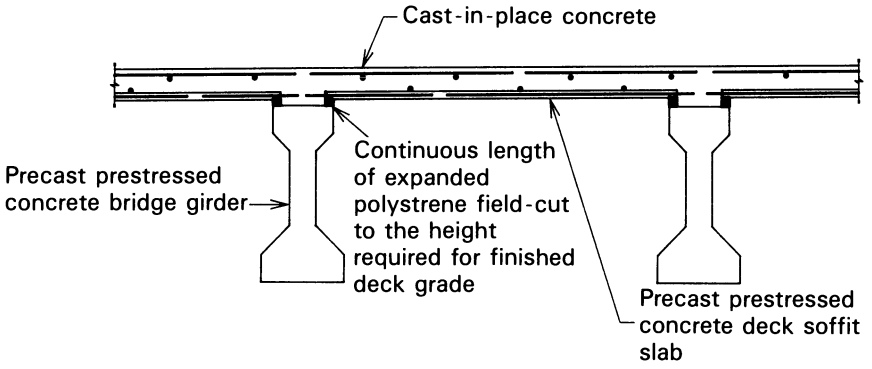

Fig. 14-13. Partial section of a bridge with precast prestressed-concrete slabs used as stay-in-place forms for the deck.

which cannot be done until the deck has attained reasonable strength, may prolong the construction time.

Solid cast-in-place post-tensioned concrete slab bridges have been used in applications where the depth of construction is exceptionally critical. The depth-to-span ratio for simple spans can be from 1 in 26 to 1 in 30. It is more usual in slab-type bridges, however, to use precast, hollow boxes. A typical cross section for an element of this type is illustrated in Fig. 14-3.

Diaphragm details in moderate-span bridges are generally similar to those of the short spans, with the exception that two or three interior diaphragms sometimes are used, rather than just one at midspan as in the short-span bridge.

As in the case of short-span bridges, the minimum depth of construction in bridges of moderate span is obtained by using slab construction, which may be either solid- or hollow-box in cross section. Average construction depths are required when stringers with large flanges are used in composite construction, and large construction depths are required when stringers with small bottom flanges are used. Composite construction may be developed through the use of cast-in-place concrete decks or with precast concrete decks. Lower quantities of materials normally are required with composite construction, and the dead weight of the superstructure normally is less for stringer construction than for slab construction.

14-4 Long-Span Bridges

Prestressed concrete bridges having spans of the order of 100 ft are of the same general types of construction as structures having moderate span lengths, with the single exception that solid slabs are not used for long spans. The stringer spacings are frequently greater (with stringers at 7 to 9 ft) as the span lengths of bridges increase. Because of dead weight considerations, precast hollow-box

construction generally is employed for spans of this length only when the depth of construction must be minimized. Cast-in-place post-tensioned hollow-box bridges with simple and continuous spans frequently are used for spans on the order of 100 ft and longer.

Simple, precast, prestressed stringer construction would be economical in the United States in spans up to 300 ft under some conditions. However, only limited use has been made of this type of construction on spans greater than 100 ft. For very long simple spans, the advantage of precasting frequently is nullified by the difficulties involved in handling, transporting, and erecting the girders, which may have depths as great as 10 ft and weigh over 200 tons. The exceptions to this occur on large projects where all of the spans are over water of sufficient depth and character that precast beams can be handled with floating equipment, when custom girder launchers can be used, and when segmental construction techniques can be used (see Secs. 8-3, 14-5, 18-4, 18-5, and 18-7).

Precast, long-span bridges may approach the general shape illustrated in Fig. 14-14. A very long, narrow, simple-span bridge of cast-in-place construction will approach the cross section shown in Fig. 14-15. These types of bridges may be more accurately described as girder bridges rather than stringer bridges. The general reduction in (or elimination of) the size of the bottom flange, as well as the large top flange supplied in the cross sections of Figs. 14-14 and 14-15, should be noted.

The use of cast-in-place, post-tensioned, box-girder bridges has been extensive. Typical examples of the cross sections are shown in Fig. 14-16. Although structures of these types occasionally are used for spans less than 100 ft, they more often are used for spans in excess of 100 ft and have been used in structures having spans in excess of 300 ft. Structurally efficient in flexure, especially for continuous bridges, the box girder is torsionally stiff and hence an excellent

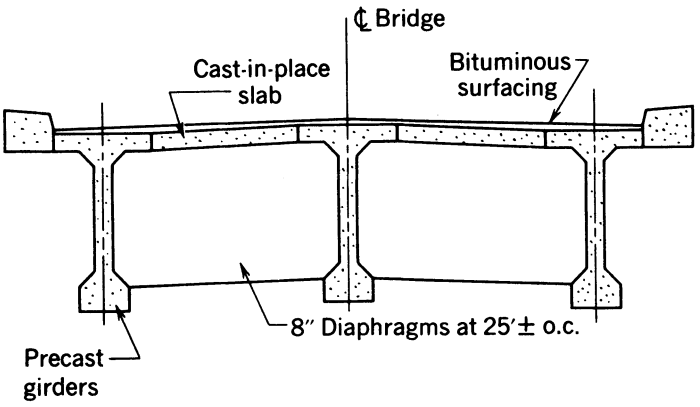

Fig. 14-14. Section of a long-span bridge with precast prestressed-concrete girders.

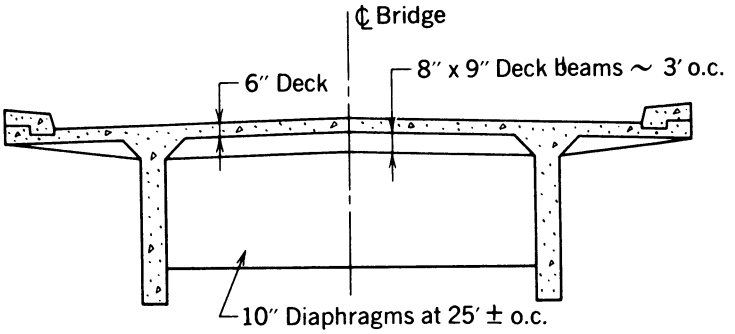

Fig. 14-15. Section of a long-span cast-in-place prestressed-concrete bridge.

type of structure for use on bridges that have horizontal curvature. Some governmental agencies use this form of construction almost exclusively in urban areas where appearance from underneath the superstructure, as well as from the side, is considered important.

14-5 Segmental Bridges

Bridges that are constructed in pieces of various configurations, connected together in some way, frequently are referred to as segmental bridges. The segments may be cast-in-place or precast, elongated units, such as portions of stringers or girders, or relatively short units that are as wide as the completed bridge superstructure.

The Esbly Bridge in France is an example of one of the earliest precast concrete segmental bridges. This bridge is one of five bridges that were made with the same dimensions and utilized the same steel molds for casting the concrete units. All of the bridges span the River Marne, and because of the required navigational clearances and the low grades on the roads approaching the bridge, the depth of construction at the center of each span was restricted. The bridges were formed of precast elements, 6 ft long, and were made in elaborate molds by first casting and steam-curing the top and bottom flanges in which the ends of the web reinforcement were embedded. The flanges were then jacked apart, and held apart by the web forms while the web concrete was cast and cured. Releasing and stripping the web forms resulted in the prestressing of the webs. The 6-ft-long elements were temporarily post-tensioned in the factory into units approximately 40 ft long. The 40 ft units were transported to the bridge site, raised into place, and post-tensioned together longitudinally, after which the temporary post-tensioning was removed. Each span consists of six ribs or beams that were post-tensioned together transversely after they were erected. Hence, the beams are triaxially prestressed. The completed Esbly Bridge consists of a very flat, two-hinged, prestressed concrete arch with a span

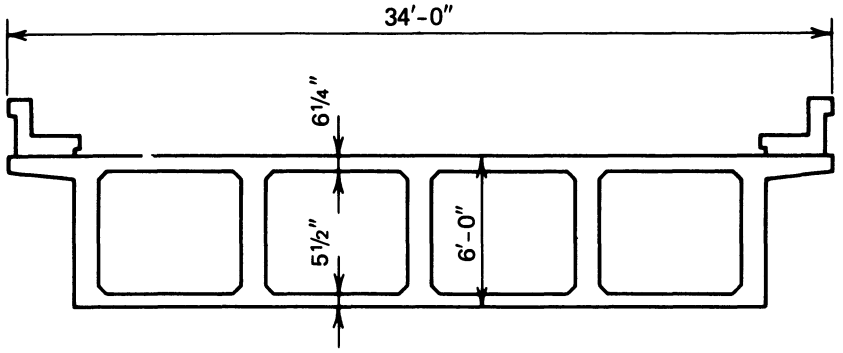

(a) Cross Section of a Box Girder Bridge with Vertical Exterior Webs

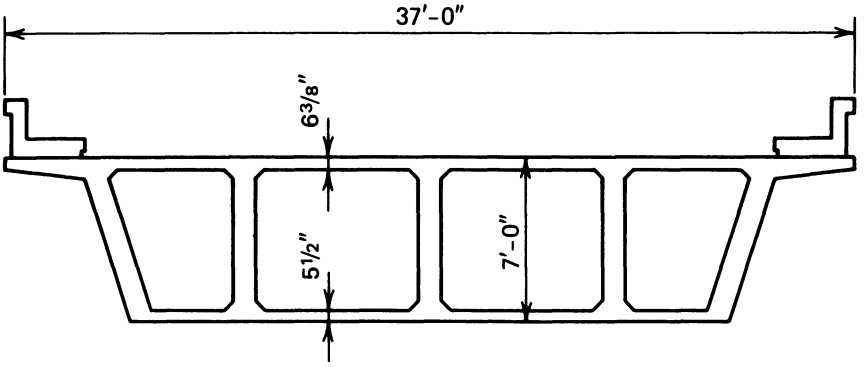

(b) Cross Section of a Box Girder Bridge with Inclined Exterior Webs

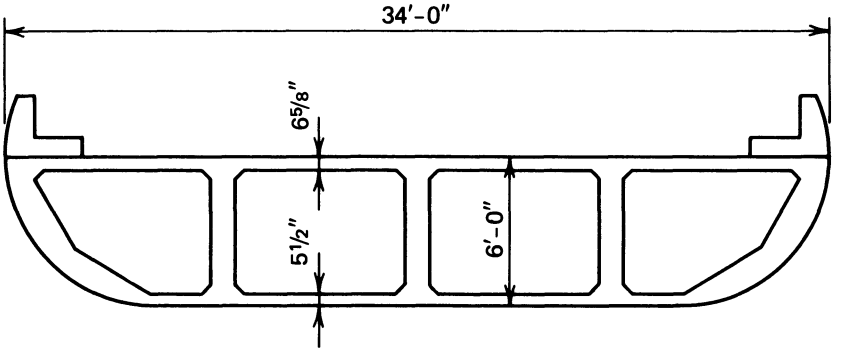

(c) Cross Section of a Box Girder Bridge with Curved Exterior Webs

Fig. 14-16. Typical cross sections of cast-in-place prestressed-concrete box-girder bridges.

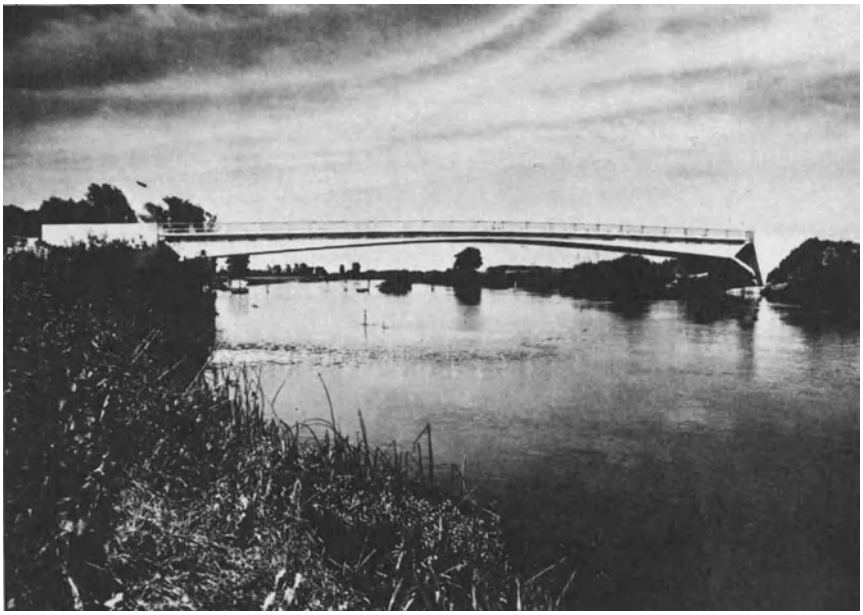

Fig. 14-17. The Esbly bridge across the Marne river in France. (Provided by and reproduced with the permission of the Freyssinet Company, Inc., Charlotte, N.C.)

of 243 ft and a depth at the midspan of about 3 ft. The bridge is shown in Fig. 14-17.

Cast-in-place prestressed concrete segmental construction, in which relatively short, full-width sections of a bridge superstructure are constructed cantilevered from both sides of a pier, originated in Germany shortly after World War II. This procedure sometimes is referred to as balanced cantilever construction. The well-known, late German engineer U. Finsterwalder is credited with being the originator of the technique. The basic construction sequence used in this method is illustrated in Fig. 14-18, which shows that segments, erected one after another on each side of a pier, form cantilevered spans. The construction sequence normally progresses from pier to pier, from one end of the bridge to the other, with the ends of adjacent cantilevers being jointed together to form a continuous deck (see Figs. 10-20, 18-12 and 18-13). The individual segments frequently are made in lengths of 12 to 16 ft in cycles of four to seven days. The method has been used in the United States for bridges having spans as long as 750 ft.

The segmental construction technique also has been used with precast segments. The technique originated in France and has been used in the construction of bridges having spans in excess of 300 ft. The eminent French engineer

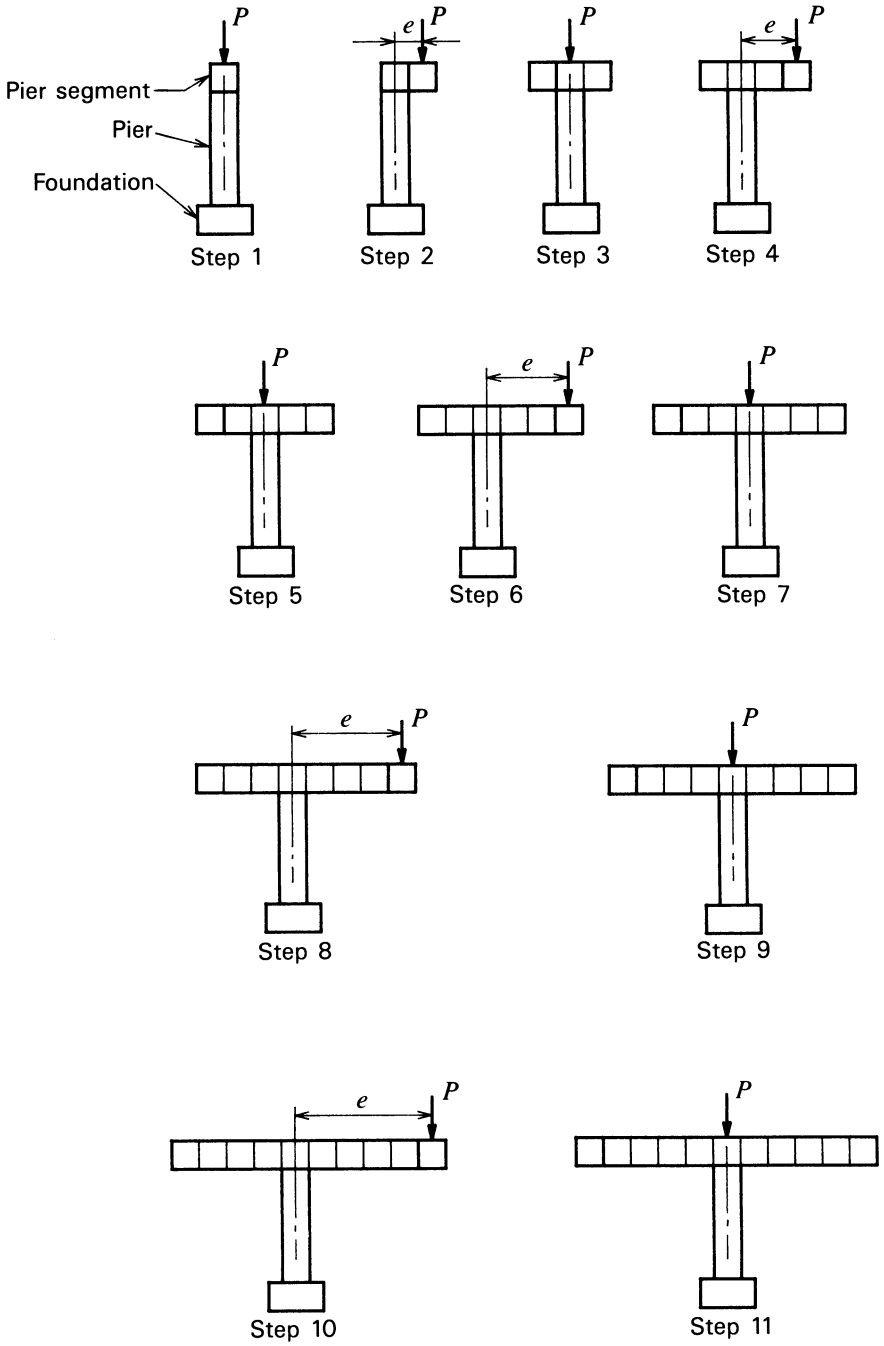

Fig. 14-18. Erection sequence for segmental bridges using the cantilever technique.

Fig. 14-19. The King Fahed Causeway connecting Saudi Arabia and Bahrain constructed of precast segments erected span-by-span. (Provided by and used with the permission of the King Fahed Causeway Authority, El Khobar, Saudi Arabia.)

Jean Muller is credited with originating precast segmental bridge construction using match-cast segments. The precast segments may be erected in balanced cantilever, similar to the method described above for cast-in-place segmental bridges constructed in cantilever, or by using the span-by-span technique described in Sec. 18-6. Precast segments have been made in precasting plants located on the construction site as well as off site. The segments frequently are stored for a period of weeks or months before being moved to the bridge site and erected—a factor having favorable effects on concrete strength, shrinkage, and creep. Construction of precast segmental bridge superstructures normally progresses at a rapid rate once the erection process begins. The erection of precast concrete segments normally does not commence, however, until such time as a large number of segments have been precast and stockpiled because the erection normally can progress at a faster rate than the production of the segments.

The five bridges that form a part of the King Fahed Causeway extending from the eastern shore of Saudi Arabia to the island nation of Bahrain were constructed segmentally using plant-cast precast prestressed concrete span segments. A portion of the causeway, which is 26 kilometers long, is shown in Fig. 14-19.

REFERENCES

Cusens, A. R. and Pama, R. P. 1975. Bridge Deck Analysis. New York. John Wiley & Sons.

French Association for Construction Supervision. Undated.

French Know-How in Bridge Building. Paris. ISTED.

Libby, J. R. and Perkins, N. D. 1976. Modern Prestressed Concrete Highway Bridge Superstructures. San Diego. Grantville Publishing Company.

Mathivat, J. 1979. The Cantilever Construction of Prestressed Concrete Bridges. New York: John Wiley & Sons.

Podolny, W. Jr. and Scalzi, J. B. 1976. Construction and Design of Cable-Stayed Bridges. New York. John Wiley & Sons.

PTI. 1985. Post-Tensioning Manual. Fourth edition. Phoenix. Post-Tensioning Institute. pp 29-40.

15 Pretensioning Equipment and Procedures

15-1 Introduction

Pretensioning, as explained in Sec. 1-4, is the term used for the process of making prestressed concrete in which the prestressed reinforcement is stressed before the concrete is placed. Pretensioned concrete is most commonly made in permanent precasting plants, but, on single construction projects that include a large quantity of pretensioned members, it has been found feasible to construct a pretensioning facility on the job site and amortize it on the one project.

Permanent pretensioning facilities were first constructed in the United States in the early 1950s. Like the early producers of pretensioned concrete, most present-day manufacturers do not limit their products to prestressed concrete but produce other precast concrete products as well. The number of plants and the volume of pretensioned products made in them have steadily increased over the years. The precast prestressed-concrete producers constitute an important part of the U.S. construction industry through their involvement in the production of structural members for buildings, bridges, and piers, as well as structural products such as piling and railroad ties. Many manufacturers of prestressed concrete structural products make architectural concrete products as well. Readers interested in learning more about the products made by precast

prestressed-concrete manufacturers can do so by contacting the Precast/ Prestressed Concrete Institute, the trade organization that represents the precast prestressed-concrete manufacturers.*

The stress in pretensioning tendons must be maintained as nearly constant as possible during placing and curing of the concrete. This can be accomplished in two ways: (1) The tendons are stressed and anchored to individual steel molds designed to withstand the prestressing force as well as the stresses resulting from the plastic concrete. (2) The tendons, after being stressed, are restrained by a special device, called a pretensioning bench or bed. Pretensioning benches also provide a level surface on which the concrete forms are supported.

In addition to these devices, other equipment peculiar to pretensioned construction, including the mechanisms used to stress and release the prestressing tendons, the forms, the vibrators, and the tendon deflectors, are discussed in this chapter.

15-2 Pretensioning with Individual Molds

With the exception of a few firms that have employed stress-resisting molds in the manufacture of double-tee roof slabs and pretensioned spun piles, this technique has not received wide use in the United States. In plants where pretensioned concrete railroad ties and small joists for residential construction are produced, this method has the advantage of allowing individual units to be mass-produced, with products (and molds) moving through the plant in a production cycle, rather than requiring the materials and plant be brought to the molds or forms, as is done when pretensioning benches are used. Another advantage of this method, when employed on small pretensioned products, is that the prestressing plant need not be as large and as elongated as that required in using a conventional pretensioning bench because small pretensioned products in their individual molds can be stacked and need not be arranged in long rows. This advantage applies, but to a lesser degree, with large products that can only be handled with very large cranes and cannot be stacked very high, if at all.

15-3 Pretensioning Benches

Pretensioning benches normally are designed to withstand a specific maximum force applied at a specific maximum eccentricity. Therefore, it is customary, when establishing the capacity of a pretensioning bench, to give the maximum permissible force (shear) and maximum permissible moment that the bench is to safely withstand. The maximum moment normally is expressed in terms of the bench proper (slab portion of the bench, which extends between the uprights at the abutments) and not necessarily in terms of the top surface at the abutments, which may be recessed to accommodate the stressing mechanism.

*Precast/Prestressed Concrete Institute, 175 West Jackson Boulevard, Chicago, Illinois 60604.

Pretensioning benches generally are of the following types:

1. Column type, which may serve as the mold or form, as well as the device that restrains the tendons.
2. Independent-abutment type, in which independent abutments rely upon soil pressure, piling, or rock foundations for stability.
3. Strut-and-tie type.
4. Abutment-and-strut type.
5. Tendon-deflecting type.
6. Portable benches.

As each bench type has its own specific areas of application, the types are discussed separately in the following paragraphs.

One more definition is necessary, before the types of pretensioning benches are discussed, pertaining to the uses to which benches are put. Some benches are designed to produce a specific product and thus may be referred to as fixed benches; other benches are designed to produce any type of product normally encountered in practice and so are termed universal benches.

Column Benches

Column benches rely upon the column action of the bench alone to resist the prestressing force; and the eccentricity of the prestressing force, with respect to the bench, must be confined to relatively low values to achieve efficiency and economy with this type of bench. Therefore, the use of column benches generally is restricted to fixed benches designed to produce a singe-tee, double-tee, or pile. An example of a column-type bench, which is designed to produce double-tee slabs, is shown in Fig. 15-1.

Column-type benches generally are designed according to the usual column design procedures. Adequate safety against crushing of the concrete and buckling must be provided in the design. The dead weight of the bench normally is sufficient to prevent the column from buckling. The buckling could occur (a) with the center of the bench displacing upward, (b) by the two ends displacing upward, or (c) by a combination of center and end displacement, as shown in Fig. 15-2.

Column-type benches normally are not used for universal benches or in benches where a relatively large eccentricity of the prestressing force must be accommodated.

Independent-Abutment Benches

This type of pretensioning bench is composed of two large abutments that are structurally independent of each other as well as of the paving material used as a casting surface between the abutments. When embedded in soil, the abutments may rely exclusively upon the weight of the abutment and passive soil pressure

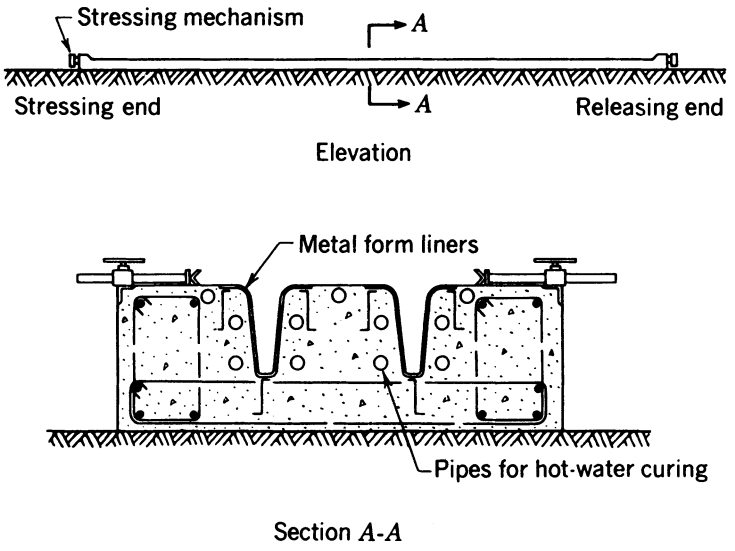

Fig. 15-1. Column-type pretensioning bench for producing double-tee beams.

for stability, but it is more common to incorporate piling in the abutments to increase their stability against sliding and overturning. Abutments of these two types are shown in Fig. 15-3.

When founded on sound rock, independent abutments can be formed by keying into the rock and, if necessary, increasing the resistance of the abutments to overturning by providing ties extending into and anchored in the rock, as shown in Fig. 15-4.

The design of independent abutments requires accurate knowledge of the character of the soil or rock on which the abutments will be located. The effects of long-term loading and variations in loading on the mechanical properties of the foundation material must be known for the abutment design. Because of the difficulty of accurately determining the mechanical properties of the foundation material, few pretensioning facilities employ abutments of this type. When the foundation material is satisfactory for independent abutments, this type of bench is relatively low-cost for long benches. Because the casting surface between the abutments is not a structural component of a bench having independent abutments, it can be considerably lighter than that required for other types of benches.

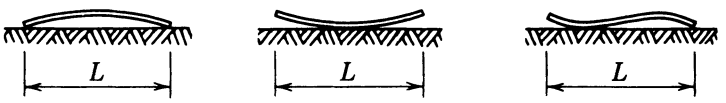

Fig. 15-2. Possible shapes of column buckling.

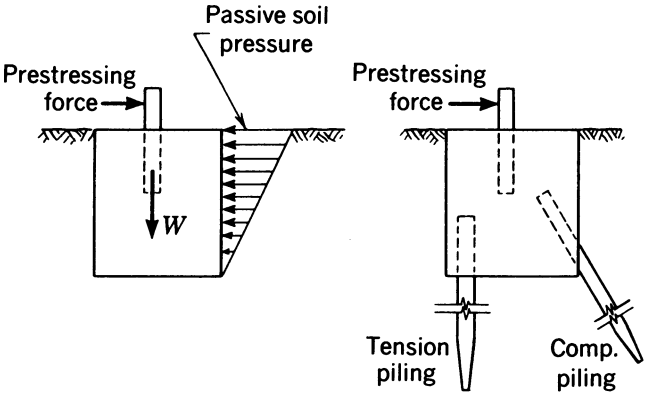

Fig. 15-3. Independent abutments in soil.

Strut-and-Tie Bench

The principle of the strut-and-tie pretensioning bench is shown in Fig. 15-5, where it will be seen that the prestressing force results in a tensile force in the tie and a compressive force in the strut. The uprights are relied upon to distribute the prestressing force to the strut and tie. This type of bench can be used for large eccentricities and is adaptable to universal pretensioning benches. A disadvantage of this type of bench, when large prestressing forces are used, is that the compressive force in the strut is larger than the prestressing force ($C = P + T$), and the dimensions of the strut must be of adequate size to prevent buckling. Another objection to the use of this principle for long benches is

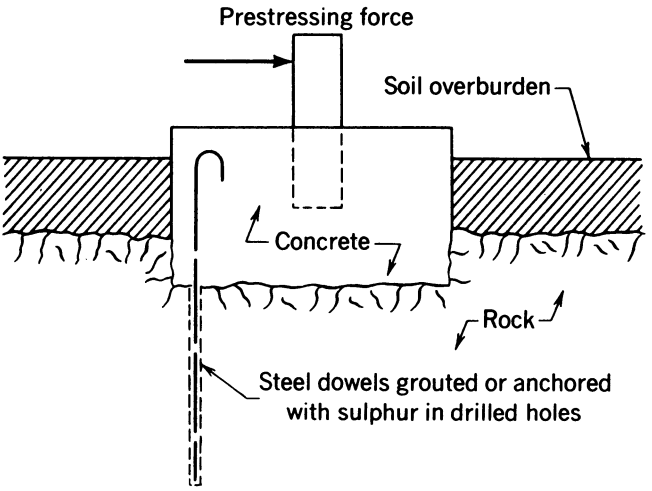

Fig. 15-4. Independent abutment on rock.

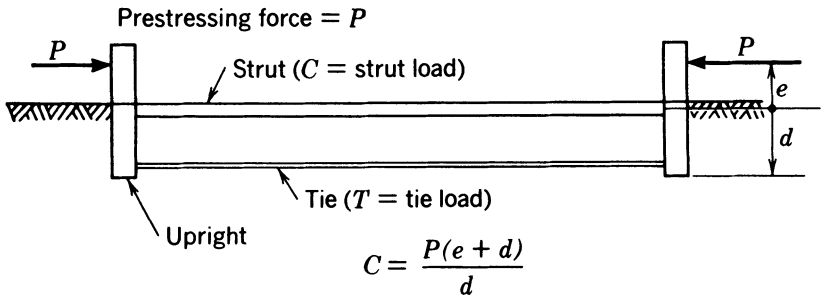

Fig. 15-5. Elevation of strut-and-tie pretensioning bench.

related to the deformations of the bench components due to the prestressing force. The application of the prestressing force causes the tie to lengthen and the strut to shorten. In addition, the effects of the deformations are amplified at the level of the prestressing tendons by the lever action of the uprights. For these reasons, strut-and-tie benches generally are used only on short benches, such as those in laboratories.

Abutment-and-Strut Bench

This is the most common type of pretensioning bench. Its structural principle is illustrated in Fig. 15-6, where it will be seen that the prestressing force has a tendency to overturn the abutments about the concrete hinges, as well as to force the two abutments to slide toward each other. The overturning of the abutment is prevented by the weight of the abutment, and sliding of the abutments is prevented by the slab or strut that separates the two abutments. The provision of the hinge between the abutments and the slab ensures that the slab section is subjected to a direct axial force alone.

The design of this type of bench consists of determining the amount and shape of the concrete abutment that will provide an adequate safety factor against overturning, as well as the reinforcement for the abutment and the proportions of the slab.

The approximate quantity of concrete required for the two abutments for this type of bench can be computed from:

$$Q = 35 + 0.06M \tag{15-1}$$

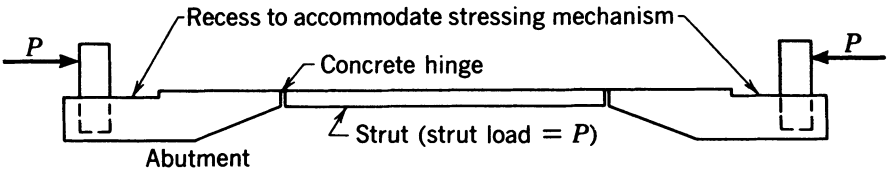

Fig. 15-6. Elevation of abutment-and-strut pretensioning bench.

in which Q is the approximate quantity of concrete in cubic yards, and M is the moment due to prestressing kip-feet for which the bench is designed. For preliminary estimates, the quantity of nonprestressed reinforcement required can be assumed to be 75 pounds per cubic yard. The approximate weight of the structural steel uprights required for the two ends can be computed for:

$$W = 3500 + 6M \tag{15-2}$$

in which W is the approximate weight of the uprights in pounds. The quantity computed from eq. 15-2 does not include the cross beams, templates, pull rods, or other components of the stressing mechanism that may be required.

Tendon-Deflecting Benches

Most of the methods used in deflecting the tendons in pretensioned beams and girders require that the tendons be held down at the lower points by devices attached to the slab portion of the pretensioning bench. The tendons are supported at the high points by devices that bear on the bench. The bench thus is subjected to a series of vertical loads, as well as to the axial load associated with abutment and strut benches. This type of loading and the bench shape usually employed under such conditions are illustrated in Fig. 15-7.

Because of large vertical forces, which may have to be applied at virtually any point along the bench, the use of the concrete hinge characteristic of the abutment and strut bench is not feasible. Furthermore, because the slab portion of the bench is subject to combined bending and direct stress, the slab must be made of reinforced or prestressed concrete rather than concrete that is basically unreinforced, as is used in abutment-and-strut benches. The cost of benches designed for deflected tendons is substantially greater than that of abutment-and-strut benches of equal capacity.

The quantity of materials required for the abutments of a tendon-deflecting bench can be approximated from eqs. 15-1 and 15-2.

Portable Benches

Pretensioning benches that can be moved from job site to job site have been used to a limited degree. The portable benches may be of any of the above types

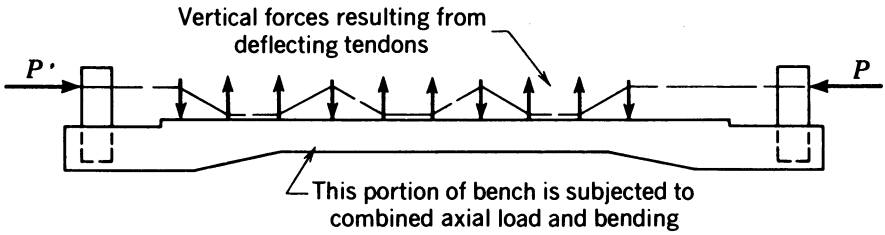

Fig. 15-7. Elevation of a tendon-deflecting pretensioning bench.

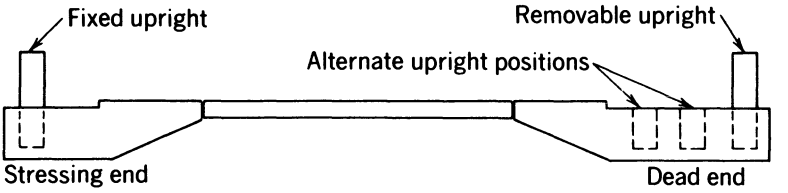

Fig. 15-8. Pretensioning bench with adjustable length.

and may be entirely or only partially portable. An example of a partially portable bench is a bench of the abutment-and-strut type in which the principal components of the abutment are portable, and the strut and counterweight portions of the abutments are not moved.

In the design of universal pretensioning benches, it is often desired to provide a means of adjusting the length of the bench to minimize waste of the pretensioned reinforcement. This has been done by using large pull-rod extensions in the mechanisms used to prestress the tendons (see Sec. 15-4). Another method is to provide a long dead-end abutment with several alternative positions for the dead-end uprights, as illustrated in Fig. 15-8. The provision of an intermediate abutment with removable uprights also has been used successfully. Intermediate abutments designed to withstand the prestressing load from either end of the bench, as shown in Fig. 15-9, have been used to improve the efficiency of pretensioned concrete production.

The maximum force used in the design of a pretensioning bench should be about 15 percent greater than the initial force applied to the bench. Experience has shown that shrinkage of the concrete and temperature variations, which occur during curing and stripping of the concrete, result in the prestressing force's being larger at the time of release than it is immediately after stressing. The increase in stress is a function of (1) the ratio of the length of the prestressed reinforcement embedded in concrete to the total distance between the anchorages at the ends of the bench, (2) the shrinkage characteristics of the cement used in the concrete, (3) the type of curing used, and (4) the air temperature during stripping. The increase in stress in the prestressed reinforcement varies with the ratio of the length of the embedment of the prestressed reinforcement in the concrete to the distance between anchorage points. The increase also is

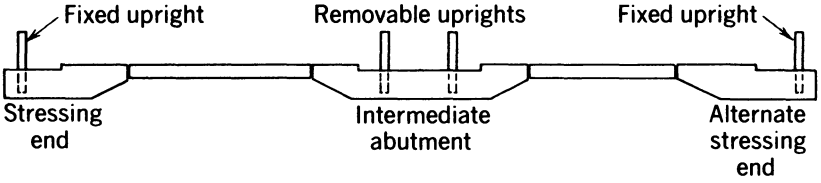

Fig. 15-9. Pretensioning bench with intermediate abutment.

affected by the curing time, being more severe when the air temperature during stripping is low.

15-4 Stressing Mechanisms and Related Devices

The tensioning of pretensioning tendons can be done by stressing each tendon individually or be stressing all the tendons one time. Each method has distinct advantages, and the method that will be used most frequently in a prestressed concrete plant has a significant influence on the design of the stressing mechanism that will be used. It is possible to design the stressing mechanism for the very efficient stressing of tendons individually rather than collectively. It is also possible to design the stressing mechanism in such a way that the tendons can all be released simultaneously with hydraulic jacks rather than by being cut one at a time.

If the stressing is to be done by stressing one stand at a time, the ram used for the stressing normally must have a stroke of 30 to 48 in. and a working capacity of from 10 to 20 tons. The stroke and capacity needed depend upon the length and size of the tendons to be stressed. If the tendons are to be released simultaneously, large rams, whose capacity depends upon the maximum prestressing force for which the bench is designed, must be provided for this purpose. The stroke of the ram used to release the pretensioned tendons is dependent upon the length of the tendons not embedded in the concrete and on whether the release is done in one or several steps.

Releasing the tendons simultaneously with hydraulic rams offers the advantage that the force can be transmitted to the concrete products slowly, so that shock or impact loading is avoided. The result is that the transmission length is minimized. In addition, with this type of equipment the products can be partially released if that becomes necessary or desirable. The principle disadvantage of releasing the tendons with hydraulic jacks is that all of the strain is released at one end of the production line, with the result that the products at the releasing end tend to move away from the releasing end. The amount of movement is a direct function of the elastic deformation of the concrete products and the length of the tendons not embedded in the concrete. When deflected tendons are used, releasing the tendons simultaneously from one or even from both ends may not be possible, as releasing the tendon-deflecting devices before the prestressing force is released may not be feasible. Another advantage of releasing all the tendons at one time is that with this procedure the cutting of the tendons between precast units can be done without adhering to a strict schedule.

Releasing the tendons individually generally is done by cutting them one at a time with an acetylene torch, saw, or hydraulic cutters. The tendons must be cut according to a strict sequence if eccentric loading in the concrete products

is to be minimized, as well as to prevent too many tendons from being cut at one location along the length of the bench. Cutting too many tendons at one location along the bench length will result in the failure of the remaining tendons. In other words, the tendons at each end of each product in the whole line should be cut at approximately the same time.

When all the tendons are to be stressed simultaneously, the rams used to stress the tendons must be of large capacity. Unless the stressing is done in several increments, a procedure that is not recommended for normal operations, the stroke of the rams must be on the order of 30 to 48 in. The same rams used to stress the tendons can be used to release them, but during the releasing operation, the required stroke is smaller.

When the tendons are stressed individually, it is not necessary to apply an initial load to each tendon to equalize their lengths, as is often required (by construction specifications) when all the tendons are stressed simultaneously. Furthermore, if the tendons are being stressed individually and an anchor slips on a tendon during or after the stressing, the tendon that has slipped can easily be prestressed. If, on the other hand, the tendons are all being stressed simultaneously and the tendon slips, it is necessary to release all the tendons and prestress them after the slipped tendon has been reanchored.

It will be found that the cost of the hydraulic jacks is greater in installations designed to stress all the tendons simultaneously than in those designed for the stressing of individual strands. The total labor cost of stressing is about equal with both methods if an initial force must be applied to each tendon before all are stressed simultaneously. More time may be required for stressing the tendons individually when there is a large number of tendons. The time factor can be important in some instances because, in the interest of safety, all work in the vicinity of a pretensioning bench must be stopped during the stressing operation.

The stroke of the rams specified for any particular installation should be based upon the anticipated elongation of the reinforcement during stressing, with an allowance included for slack in the anchorages. The normal theoretical elongation for the pretensioning tendons is between 7 and 8 in. per 100 ft of length. The slack and anchorage take-up is much larger when the tendons are stressed individually than when they are stressed simultaneously. This is so because when the tendons are to be stressed simultaneously, an initial force normally is applied to each tendon individually when their anchorages are installed for the purpose of removing slack and equalizing the initial tendon lengths.

Experience has shown that for prestressing concrete the use of hydraulic rams is preferred over the use of hydraulic jacks. The capacities and strokes needed in pretensioning plants are much more efficiently provided by double-acting hydraulic rams rather than jacks. The latter rely upon internal springs to return the pistons to the closed (or open) position upon the release of the hydraulic

pressure, and this is not efficient when large capacities are needed. The hydraulic rams used in prestressing concrete should be designed to develop the maximum load required in normal operations at a pressure from 5000 to 6000 psi, and to have a maximum rated pressure of not less than 10,000 psi. The pistons of the rams, which are exposed when the ram is extended, should be hard-chrome-plated to protect them against corrosion and other minor damage.

The hydraulic pump used to operate the rams should be designed for a maximum intermittent operating pressure of 10,000 psi and have a minimum continuous operating pressure of 5000 to 6000 psi. The pumping unit assembly, which includes the hydraulic pressure gages, valves, and piping, should be designed as simply as possible to facilitate its use. The unit should be provided with at least one calibrated pressure gage that is not used in routine stressing operations but is reserved for checking the calibration of the gages that are used in normal stressing operations. In addition, the pumping unit should be assembled in such a way that damaged pressure gages can be easily removed and replaced.

The stressing mechanisms used in prestressing benches consist of uprights, pull rods, cross beams, and templates in addition to the hydraulic rams and pumping unit. The uprights, pull rods, cross beams, and templates normally are fabricated of structural steel and, as an assembly, are referred to as the structural frame or simply as the frame. Structural frames are used to transfer the load in the tendons to the abutments and to provide a means of anchoring the tendons, as well as to stress the tendons and, in some cases, release them. Unless screw jacks or hydraulic rams with threaded piston shafts are used to maintain the deformation in the prestressing tendons during the production cycle, the structural frames must be provided with a reliable means of maintaining the deformation. Simple hydraulic jacks or rams cannot maintain a constant strain under load over a period of time.

Several types of structural arrangements can be used for stressing mechanisms. The type best suited for a specific situation depends upon a number of factors, including (1) the capacity of the bench, (2) the type of products to be made on the bench (i.e., fixed or universal bench), (3) the method of stressing to be used, and (4) the method of releasing the prestressing force to be used. Instead of discussing each of these factors individually, three types of structural stressing and releasing systems are described to illustrate differences in the structural arrangements of stressing mechanisms. The designer must determine which arrangement is best suited to the needs of each installation, after carefully weighing the advantages and disadvantages of the different systems.

The first system to be considered is that shown in Fig. 15-10. It consists of cross beams, templates, fixed uprights, and, at the stressing end, vertical beams and pull rods. The vertical beam at the stressing end is held away from the fixed uprights by a strut at the top and the concrete abutment at the bottom. The clear

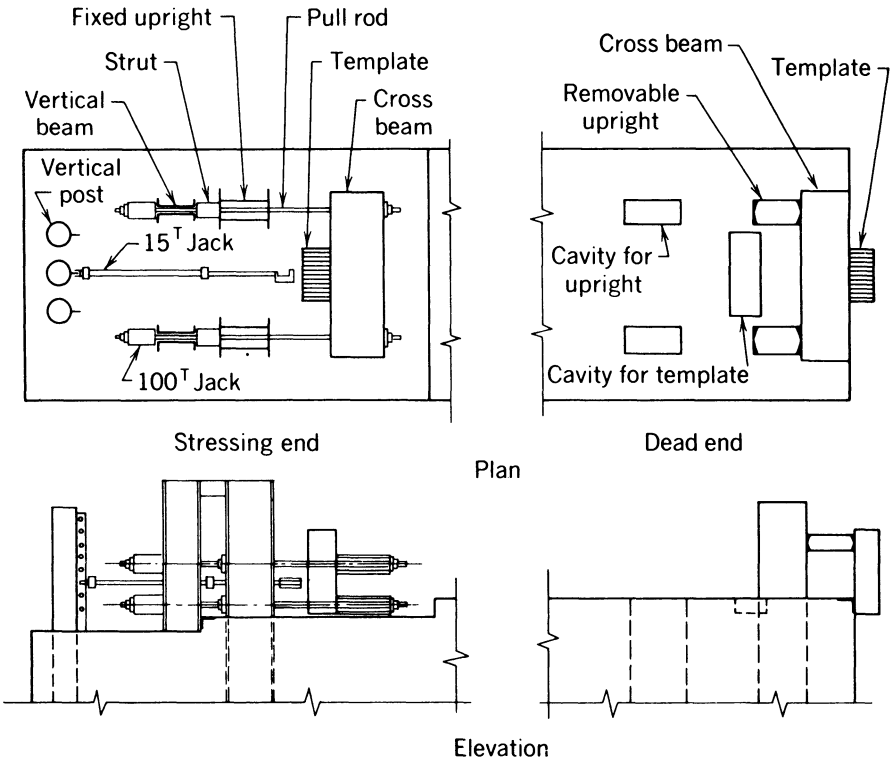

Fig. 15-10. Pretensioning stressing mechanism, type 1.

space between the vertical beams and the fixed uprights is used for nuts and plates that hold the force in the pull rods when the rams are not in use. This system is shown with four, small-stroke, high-capacity center-hole rams (100 ton), with high-strength steel pull rods extending through the rams. The mechanism is intended to be used in stressing tendons individually with the 15-ton long-stroke ram. Alternately, all the tendons can be stressed simultaneously, either by using the four, small-stroke high-capacity rams as shown, and taking several increments of loading to obtain the required elongation of the tendons, or by using four, long-stroke high-capacity rams and obtaining the elongation in one stressing operation. It must be pointed out that unless the center of gravity of the prestressing force is coincident with the center of gravity of the pull rods, the pressures in the four rams will not be equal during stressing (if all tendons are stressed simultaneously) and releasing. This situation can complicate the operation of the hydraulic system and be dangerous if not controlled properly. From the plan view in Fig. 15-10, it will be seen that the area between the uprights is free of obstructions; this is essential when the tendons are to be stressed individually.

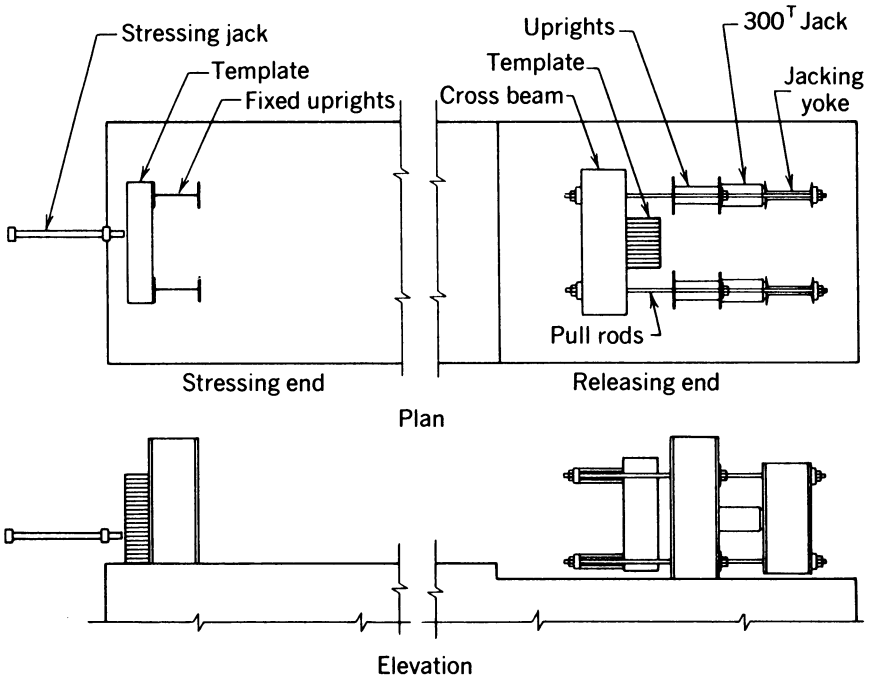

Fig. 15-11. Pretensioning stressing mechanism, type 2.

The system shown in Fig. 15-11 is designed for tensioning the tendons individually at one end and releasing them simultaneously at the other end. The stressing end consists of uprights, which support the template, and has provision for a long-stroke small-capacity stressing jack that may be used with an individual abutment, or that may be of the type that bears directly on the template or anchorage device during stressing. The releasing end in this bench consists of a template, crossbeams, uprights, jacking yokes, and pull rods. The releasing is done with two rams. If so desired, all the tendons could be stressed simultaneously with this bench by stressing from the end normally used for releasing the tendons. This system is less difficult to operate than the system discussed above because the large-capacity rams have been reduced from four to two. By using a releasing mechanism that is a combination of the one shown in Fig. 15-11 and that shown in Fig. 15-12, the number of releasing rams could be reduced to one. It must be emphasized that the center of gravity of the prestressing force and the axis of the releasing ram(s) have to be coincident in this scheme to maintain the stability of the mechanism.

The system shown in Fig. 15-12 is designed for stressing all the tendons simultaneously. Because the ends of the tendons are not accessible to a long-

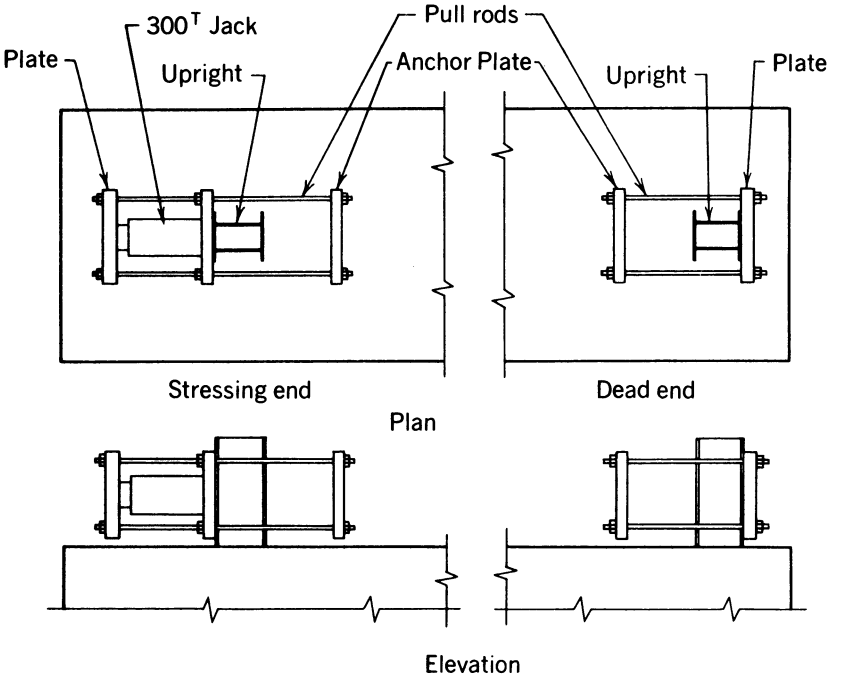

Fig. 15-12. Pretensioning stressing mechanism, type 3.

stroke low-capacity ram in this mechanism, single tendon stressing cannot be used. This mechanism utilizes only one large-capacity ram, which normally would have a long stroke. The ram must be placed at a location that renders its axis coincident with the center of gravity of the prestressing force. If this is not done, the mechanism will not be stable during stressing and releasing.

To simplify the illustrations of the mechanisms in Figs. 15-10 through 15-12, rollers or other devices normally provided to support the movable members are not shown, nor are the devices used to adjust the vertical location of the cross beams and releasing rams. Such accessories should be provided with each type of mechanism to facilitate making adjustments to the mechanism and to aid the operations during stressing and releasing, as well as to reduce the friction in the system during its operations.

The anchorage devices placed on the tendons to connect them to the templates during stressing and curing of the concrete also are a part of the stressing mechanism. Several satisfactory types of devices are available for this purpose, and device selection does not materially affect the operation of the stressing mechanism.

A dynamometer or load cell frequently is used to calibrate the pressure gauge

used with the long-stroke jack in stressing the tendons individually. The dynamometer is not normally used to measure the force in the tendons during routine production because of the risk of breaking the device if an accident occurs.

15-5 Forms for Pretensioning Concrete

Stressing-resisting forms or molds used in the manufacture of pretensioned concrete are special structural elements not normally encountered in practice. For this reason, this discussion will be confined to the forms or molds that are used on pretensioning benches and are not designed to resist a prestressing force.

The desirable features for the forms used in pretensioned concrete are varied, with form requirements differing from product to product. In general, the desirable characteristics of forms can be summarized as follows:

1. High resistance to damage due to rough handling and to the high humidity associated with heat curing. This requirement normally eliminates the use of wood forms, which do not perform well under repeated use, particularly when exposed to hot moist air during curing. Although concrete forms have been used successfully, the lighter steel forms generally are preferred.
2. Precision of form units and dimensions. To facilitate their manufacture and transport, forms generally are made in relatively small panels, connected to form larger sections. It is essential that the panels fit together precisely, and have joints that do not leak.
3. Ease of handling. In erecting or stripping forms, it is essential that individual pieces of the form that must be handled not be awkward to handle, and that they tend to hang plumb when suspended. This characteristic facilitates laying the form on their backs for cleaning, as well as adjusting them to the precise position required during assembly.
4. Design that permits one side of the form to be erected in the final position independently of the opposite side. This facilitates the layout of the member being made, as well as the formation of blockouts and transverse holes through the member, and securing the web reinforcement and post-tensioning units, if any, in the proper locations.
5. Adjustability. The forms or components of the forms should be adjustable, allowing products that have several different shapes to be made from the form or its form components.
6. Resistance to vibration. The forms must be strong enough to withstand the effects of form vibration. Brackets or rails that aid in attaching form vibrators should be supplied with the forms.
7. Rigid structural soffit form. The soffit form must be rigid and must not

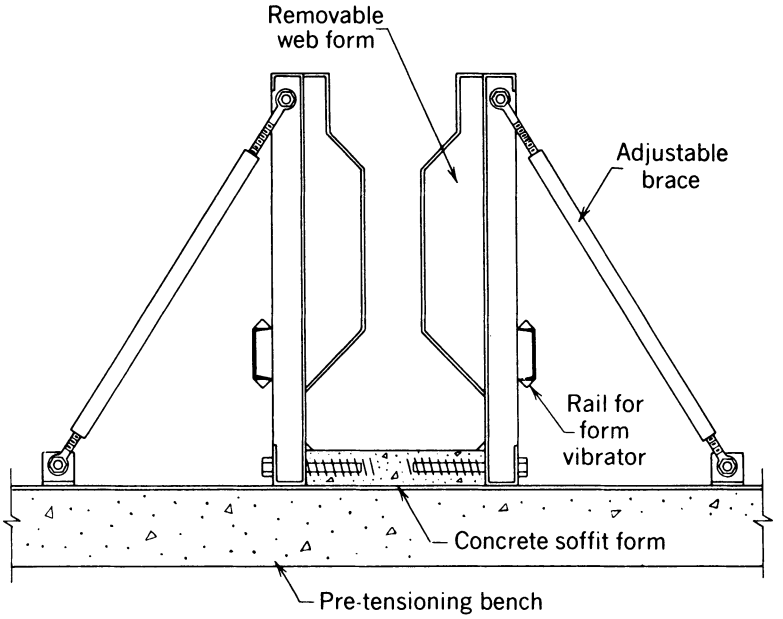

Fig. 15-13. Cross section of an adjustable steel form suitable for the manufacture of pretensioned concrete beams.

deform during use. The soffit form should be a structural element to which side forms can be securely attached (anchored against lateral and uplift loads), and should prevent the side forms from moving during concrete placing. The latter requirement is particularly significant in the manufacture of I-shaped beams having large, bottom flanges on which large uplift forces may occur.

8. Construction that includes a minimum of joints. All joints should be as tight as possible to minimize leakage and bleeding.

An illustration of a type of custom-made form incorporating the above characteristics is presented in Fig. 15-13. It should be noted that the side-form units are narrow, and, when stripped, can easily be turned on their backs to facilitate cleaning. Each side form can be set up independently of the other by attaching it to the concrete soffit and plumbing it with the adjustable brace. The removable web forms can be replaced by web forms of various shapes, and the wastes concrete soffit can be removed and replaced with soffit forms of other widths and heights. In this way, the side forms can be utilized in making a variety of different beam cross sections. The continuous rail on each side form facilitates placing and clamping form vibrators at any location along the form.

15-6 Tendon-Deflecting Mechanisms

As stated previously, it often is desirable in long-span pretensioned-concrete members to have the tendons more eccentric near midspan than at the ends of a beam. In the manufacture of many pretensioned-concrete products, the tendons follow a straight path through the member. If the path of the pretensioned tendons is to be other than straight, vertical forces must be applied to the tendons to change the path. The devices used to apply the vertical forces and deflect the tendons from straight paths are called tendon deflectors or tendon-deflecting mechanisms. These mechanisms frequently consist of devices that support the tendons in the high position and devices that hold the tendons in the lower position. These devices generally are referred to as hold-up devices and hold-down devices, respectively.

In applying the principle of deflected tendons to double-tee roof and floor slabs, it is customary to deflect the tendons at one or two points near midspan, as shown in Fig. 15-14, with the result that the lowest tendon is straight throughout the entire length of the member, and the remaining tendons are spaced apart near the ends of the slab. The steel end forms (or bulkheads) that form the ends of the concrete members also serve as the tendons hold-up and spacing devices. The hold-down devices, which hold the tendons down from the top, are similar to that shown in Fig. 15-15.

Because in double-tee slabs the slope distance from the end bulkhead to the lowest point of the tendon path is rarely of significantly greater length than the horizontal distance between the end bulkhead and the hold-down device, the usual construction procedures is to stress all the tendons to the desired initial stress, install the end bulkheads, place the hold-down devices at the proper locations and push the tendons down one at a time to the lower position using a hydraulic ram temporarily installed in the hold-down devices. The tendons are held in the deflected position with nuts or pins, and the ram is moved to the nest hold-down device. The procedure is repeated until the tendons are deflected at all the hold-down points.

After the concrete has gained sufficient strength to allow the prestress to be released, the hold-down devices are removed, and the pretensioning force is released. If the pretensioning force is released with hydraulic rams from one end of the bench, the slab nearest the releasing end will move a few inches toward the other end of the bench at the time of release; this accounts for the necessity of removing the hold-down devices before releasing the pretensioned tendons.

In the case of deeper members with deflected tendons, the slope length of the deflected tendon path can be significantly greater than the horizontal distance between the deflection points. When this condition exists, it is important that it be considered in calculating the initial stress applied to the tendons.

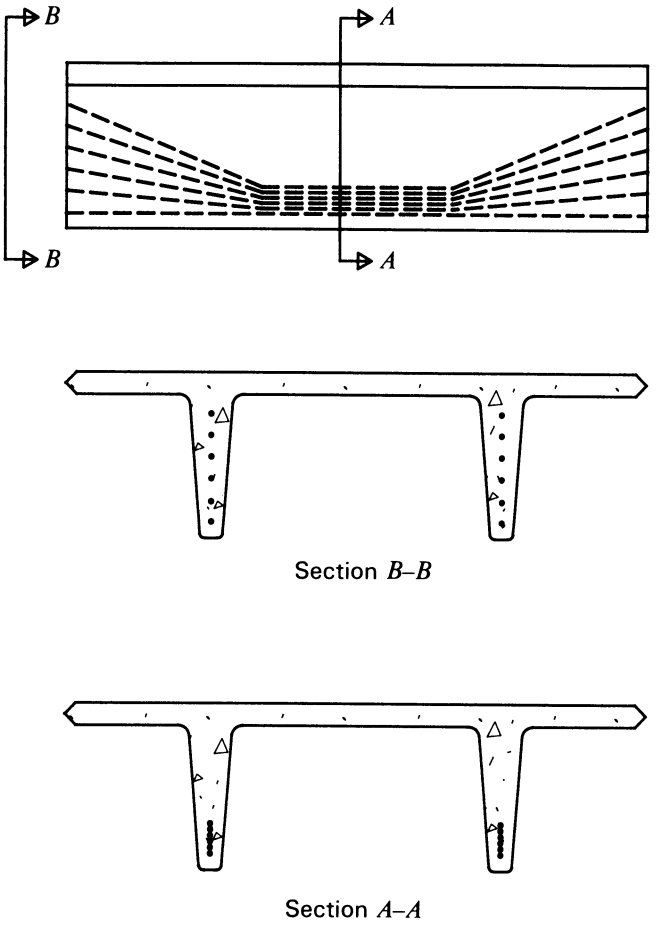

Section *B–B*

Section *A–A*

Fig. 15-14. Double-tee beam with deflected tendons.

At the present time, there is no standard method used to deflect the pretensioning tendons in bridge-girder construction. Several methods have been used or proposed for deflecting the tendons in bridge girders, as described in the following paragraphs.

Jacking Down at the Hold-Down Points

The method is shown schematically in Fig. 15-16. The procedure followed in this system is substantially the same as that used in deflecting the tendons in double-tee slabs, except that the length of the deflected-tendon path may be significantly greater than the length of the straight path, so that the initial

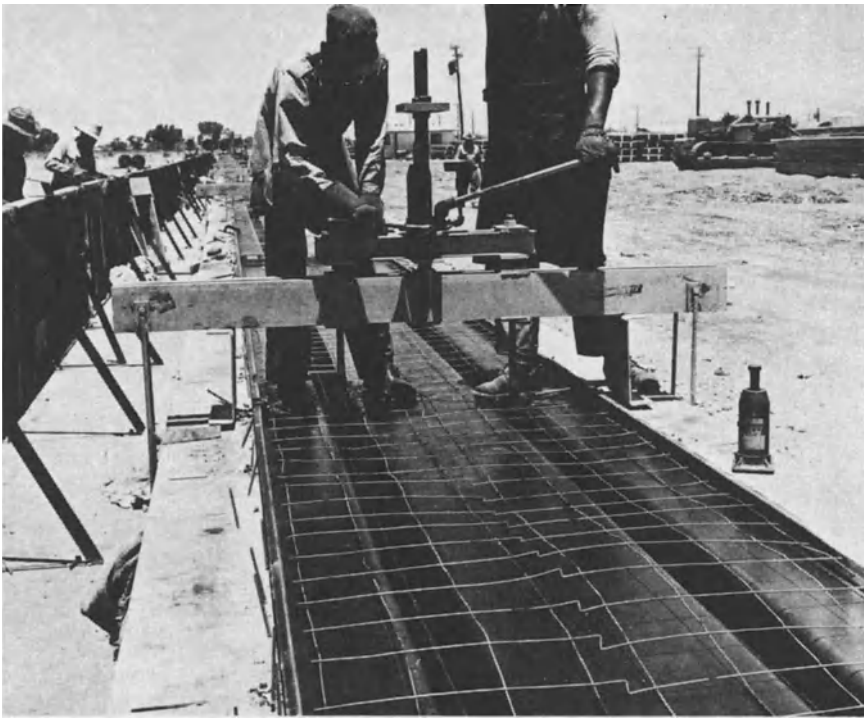

Fig. 15-15. Hold-down device shown spanning a double-tee form with workmen in the process of deflecting the tendons with a hydraulic jack. (Provided by and used with the permission of the FMC Corp., Chicago, Illinois.)

prestress applied to the tendon must be adjusted accordingly. In addition, the end bulkheads normally are not sufficiently strong to act as the hold-up device; so special devices must be supplied for this purpose.

One method of deflecting the tendons in this way is shown in Fig. 15-17. In this method, metal anchors provided in the upper surface of the prestressing

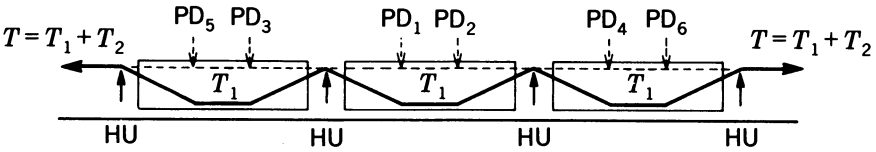

Initial tension T_1, in "up" position. Strand profile and final tension T by push down (PD), which increases strand tension by T_2.

Fig. 15-16. Illustration of jacking down at the hold-down points.

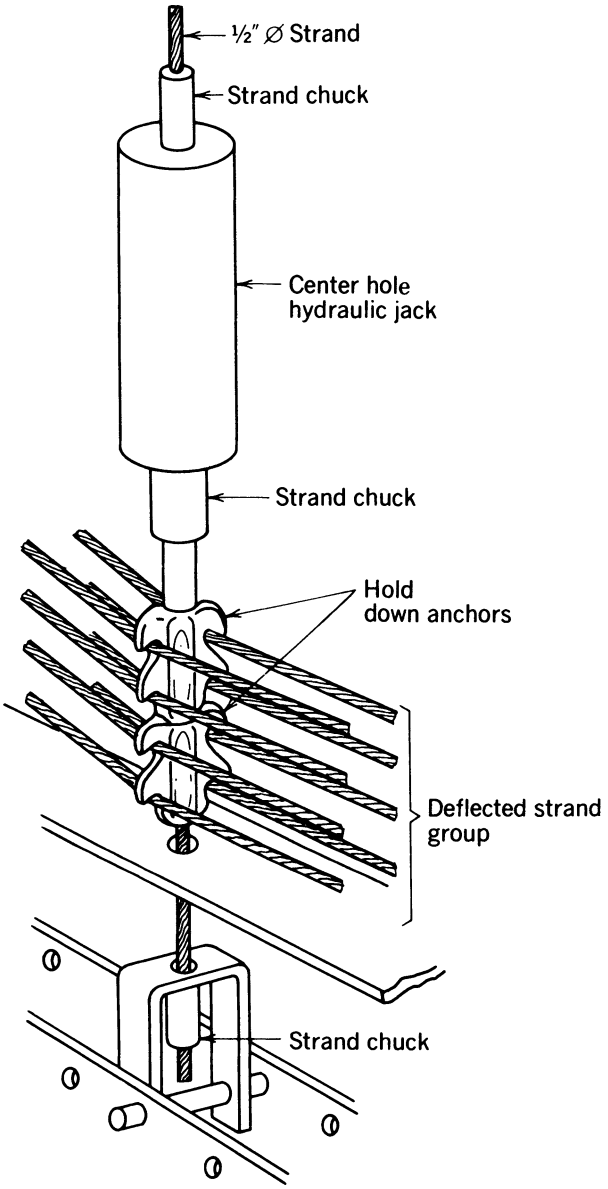

Fig. 15-17. Tendon hold-down device for use with jacking down at the hold-down points.

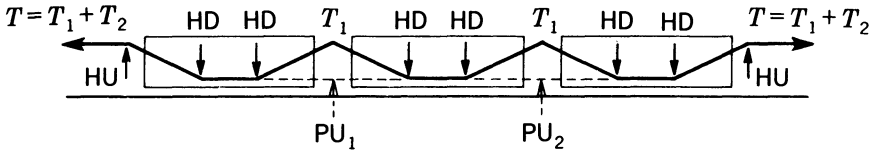

Initial tension T_1, in "down" position. Strand profile and final tension T by push up (PU), which increases strand tension by T_2.

Fig. 15-18. Illustration of jacking up at the hold-up points.

bench are used to anchor the bottom end of the hold-down device, and a center-hole jack is used to jack the tendons down. A strand chuck anchors the tendons in the deflected position. The strand chuck and the hold-down anchors are expended with this procedure. The jacking must be done according to a predetermined sequence in order to equalize the effects of friction along the bench.

Jacking Up at the Hold-Up Points

This procedure, which is shown schematically in Fig. 15-18, is virtually the same as that used in jacking down at the hold-down points. The principal difference is that the tendons are stressed in the lower position, attached securely to the pretensioning bench at the hold-down points by a device that extends through the soffit form, and the tendons are jacked up at the hold-up points (see Fig. 15-19).

After the members are removed from the bench, the cavity at the bottom of the beam at each hold-down point must be patched.

Stressing the Deflected Tendons Individually

Satisfactory results have been obtained in some instances by placing and stressing the tendons in the deflected path. When this procedure is used, some means of reducing the effect of the friction that occurs between the tendons and the hold-down and hold-up devices must be employed. The methods that have been used to reduce the effect of the friction include stressing the tendons from each end, supplying rollers with needle bearings at each hold-down and each hold-up point during the stressing (the low friction rollers are removed after stressing is completed so they can be reused many times), and applying a vibration to the tendons as they are stressed. The vibration reduces the coefficient of friction at the hold-down and hold-up points. Again in this method, the hold-down devices must extend through the soffit form, which results in a cavity that must be patched after the members are removed from the pretensioning bench. The scheme is illustrated in Fig. 15-20.

Each of the methods discussed above has advantages and disadvantages, and

(a)

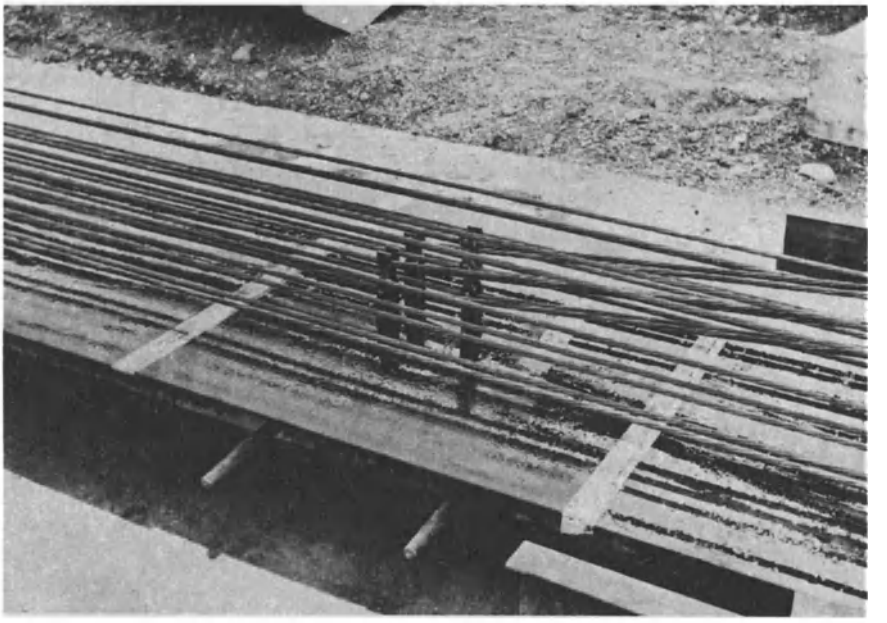

(b)

Fig. 15-19. (a) A general view of the deflecting mechanism, showing the hold-down devices, the deflected tendons, and the tower used to deflect the tendons. (b) The expendable hold-down device attached to a removable portion of the soffit form, which is anchored to the pretensioning bench.

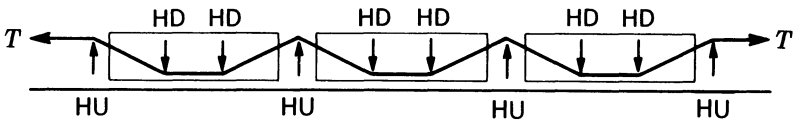

Single or multiple strand tensioning in "draped" pattern. Strand profile established by hold downs (*HD*) and hold ups (*HU*).

Fig. 15-20. Deflected or draped tendons stressed in the deflected position. Single- or multiple-strand tensioning is in the draped position. The strand profile is established by hold-downs (HD) and hold-ups (HU).

the method used on any particular project must be selected on the basis of the available equipment and the desired results. Significant disadvantages of the use of deflected tendons include the large capital investment in the stressing bed, the cost of the deflecting mechanisms, the friction losses that occur along the deflected tendons, the secondary stresses in the tendons where they pass over small-diameter pins and rollers (does not apply to all methods), and the extra labor required to deflect the strands.

16 Post-tensioning Systems and Procedures

16-1 Introduction

Materials and equipment for post-tensioning concrete are available from a number of firms in the United States. These firms market reinforcement for prestressing concrete, ducts, anchorages, accessories, and equipment for stressing and grouting post-tensioned tendons. As a part of their services, the firms normally provide shop drawings for the use of their products and equipment on specific projects. The specialist firms in post-tensioning normally can supply field technicians qualified to supervise and instruct workers in the correct methods and procedures for installing, stressing, and grouting their products. In some regions, the suppliers of post-tensioning materials are subcontractors and contract for the materials installed.

The details of the post-tensioning systems available in the United States are continually changing. For this reason, no attempt will be made to describe the specific details of the various systems. The reader interested in specific details of post-tensioning systems is advised to contact the Post-Tensioning Institute* and request a listing of its members who are suppliers of post-tensioning materials, equipment, and services.

*Post-Tensioning Institute, 301 West Osborn, Phoenix, Arizona 85013.

The primary differences between post-tensioning and pretensioning, from the construction viewpoint, can be summarized as follows:

1. Post-tensioning offers a means of prestressing concrete, either in a precasting plant or at the job site, without requiring a large capital investment in pretensioning facilities.
2. Post-tensioned tendons allow the construction of cast-in-place structures that would not be feasible in pretensioned concrete.
3. Tendons to be post-tensioned can easily be placed on curved paths without special deflecting equipment.
4. Friction losses during stressing normally are significant with post-tensioned tendons, and thus should be considered during design as well as during construction. This is especially true for continuous members, in which friction can have a very significant effect during construction and in service.
5. Each post-tensioned tendon must be stressed individually, and this requirement, in combination with the costs of the end anchorages, ducts or sheaths, special equipment, and grouting of the tendons, normally results in the unit cost (cost per pound of effective prestressing force) of post-tensioned tendons being substantially greater than the cost of pretensioned tendons.
6. Post-tensioning anchorage devices and stressing equipment often are protected by patents, frequently require unique manufacturing techniques and facilities, and require strict quality control during manufacture and use. As a result, each system generally is only available from the patent holder or his or her agent.

In addition to a very brief description of the general types of post-tensioning systems this chapter presents a discussion of construction procedures used in post-tensioned construction, and of the computation of friction losses, gage pressures, and tendon elongations resulting from tendon stressing. Special construction methods and devices unique to post-tensioned construction are discussed as well.

16-2 Description of Post-tensioning Systems

The post-tensioning systems that have been used in this country can be separated into four general categories:

1. Parallel-wire systems
2. Multi-strand systems
3. Single-strand systems
4. High-tensile-strength bar systems

The steels used in the tendons of the various systems have the general characteristics discussed in Chapter 2.

Parallel-wire systems, which were widely used in North America for a number of years, are rarely used now. These systems employ a number of wires bundled or grouped into a unit referred to as a tendon or a cable. The term parallel wire is not a precise means of describing the relative position of the individual wires in the tendons, as, in some instances, the individual wires are bundled or grouped together without spacers and without concern as to whether the individual elements are parallel or not. Hence, the term simply serves as a means of distinguishing systems that employ tendons composed of a number of smooth wires, bundled into groups, from other types of tendons.

The original Freyssinet system was one of the first, if not the first, parallel-wire post-tensioning system in the world. It received its name from the eminent French engineer Eugene Freyssinet, who invented the anchorage device used in the system. The system was introduced in the United States in the early 1950s, when the use of linear prestressed concrete, made with high-strength steel, was beginning to gain momentum. The anchorage device used in this system consists of two parts, normally referred to as the female cone and the male plug. Freyssinet anchorages of two early types are shown in Fig. 16-1. Anchorage cones were used to anchor the wires by the frictional forces resulting from the wedge shape of the male plug and the hole in the female cone.

The original Freyssinet system, which utilized a heavily reinforced concrete female cone and a basically unreinforced male plug, together with tendons composed of smooth, solid wires, has not been marketed in the United States for many years. For a period of time it was replaced with anchorages composed of female cones and male plugs composed of cast steel (rather than reinforced concrete) for use with seven-wire strands. The anchorages marketed as the

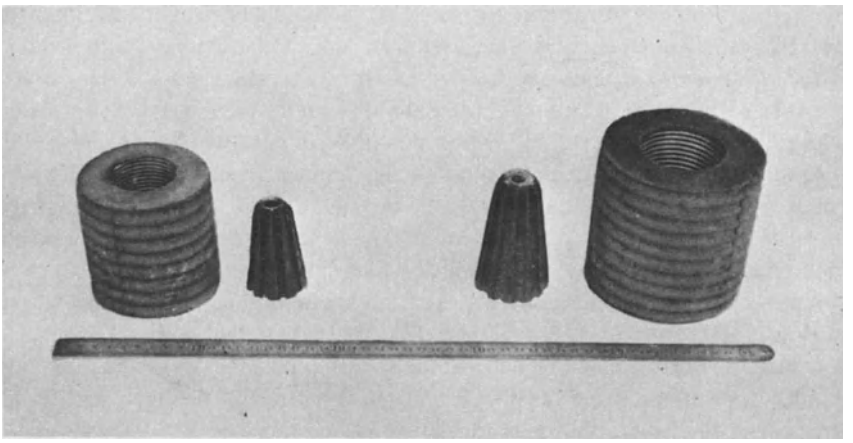

Fig. 16-1. Freyssinet anchorage cones. (Provided by and reproduced with the permission of the Freyssinet Company, Inc., Charlotte, N.C.)

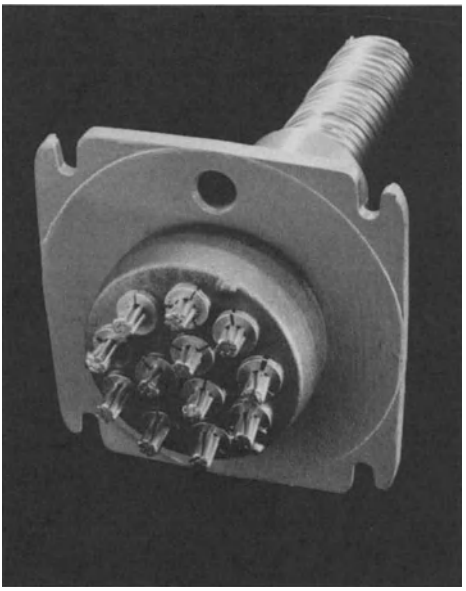

Fig. 16-2. Freyssinet post-tensioning anchorage type K. (Provided by and reproduced with the permission of the Freyssinet Company, Inc., Charlotte, N.C.)

Freyssinet system at the time of publication of this book consist of steel castings designed to anchor a number of seven-wire strands with individual wedge anchors. This anchorage is illustrated in Fig. 16-2.

Special jacks were required to use the early Freyssinet systems. The jacks actually consisted of two rams connected in series; steel wedges on the periphery of the main piston were used to attach the individual wires to the main or stressing ram. Strand anchors were used later in a similar manner, with strands. After the wires or strands had been stressed by the introduction of hydraulic pressure to the main piston, the pressure was maintained in the main piston while hydraulic pressure was applied to the secondary or plugging piston to force the male plug into the cavity of the female cone. The stressing was completed by releasing the pressure in the plugging piston, after which the pressure in the main piston was released. The jack was then disconnected from the tendon by removing the wedges. The post-tensioning operation was completed by cutting and removing the excess wire or strand at the ends of the tendons, and grouting the tendons. Figure 16-3 shows a Freyssinet jack connected to a parallel-wire tendon in the stressing position, as well as a tendon that has been stressed and one that has not been stressed. The mechanics of the stressing sequence are shown in Fig. 16-4.

The Freyssinet anchorage cone was provided with a port through the male plug for the injection of grout after stressing. Before grouting, it was necessary

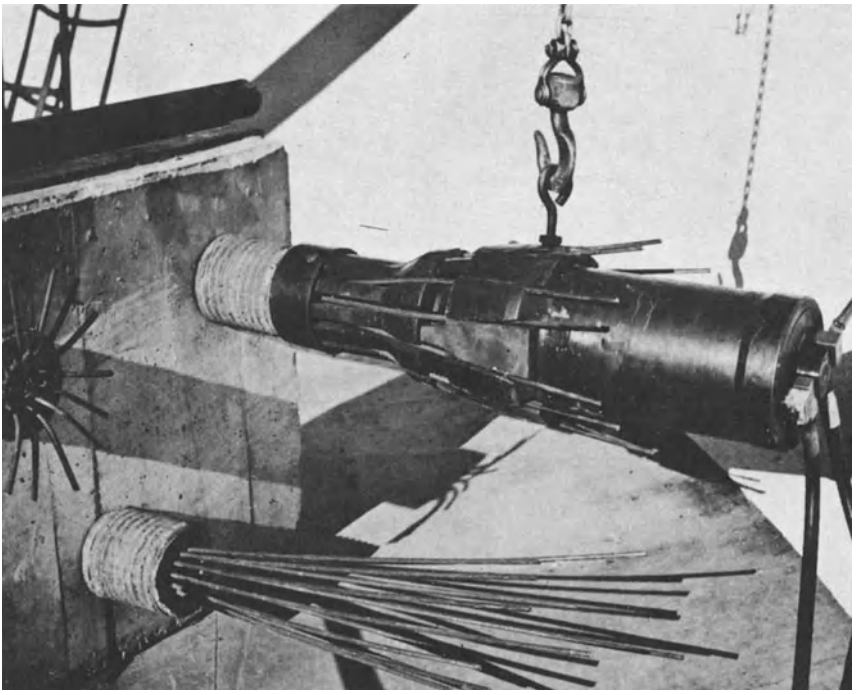

Fig. 16-3. Freyssinet jack in stressing position. (Provided by and reproduced with the permission of the Freyssinet Company, Inc., Charlotte, N.C.).

to plug the openings between the wires, the male plug, and the female cone because large quantities of grout would escape through the openings and reduce the effectiveness of the grouting apparatus if this were not done. The principle of grouting with the Freyssinet system is shown in Fig. 16-4.

Because of the need for a wedge to move longitudinally with the wires, strands, or bars being anchored with a wedge-type anchorage, and thereby develop the lateral forces essential to anchor a tendon by friction, a portion of the elongation of the tendon resulting from prestressing the tendons is lost when the prestressing force is transferred from the jack to the anchorage device. The loss of elongation was enhanced, in the case of the original Freyssinet cones, by the elastic expansion of the female cone that took place upon the anchoring of the tendon. The entire loss of elongation resulting from these actions is referred to as the loss due to the elastic deformation of the anchorage, the loss due to seating the anchorage, or the seating loss.

The loss due to the elastic deformation of the anchorages can be significant under certain conditions (a subject that is discussed further in Sec. 16-6). In some cases the effect of the elastic deformation of the anchorage is beneficial, as will be seen in the discussion of stressing calculations, and some modern

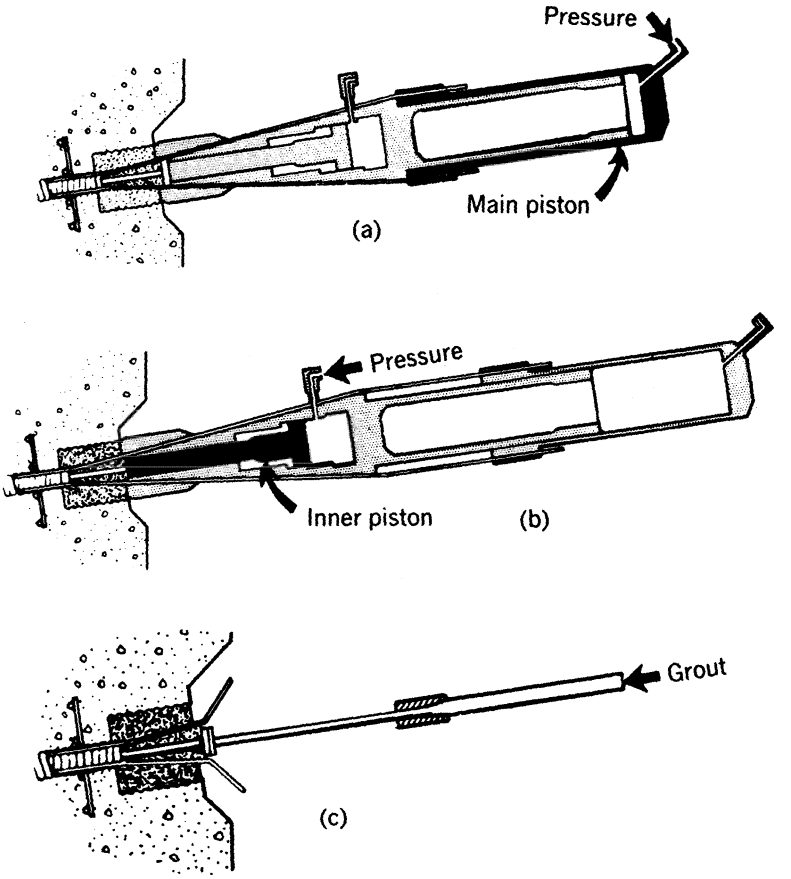

Fig. 16-4. Stressing sequence in the original Freyssinet system. Showing (a) the stressing, (b) the plugging, and (c) the grouting of the tendon. (Provided by and reproduced with the permission of the Freyssinet Company, Inc., Charlotte, N.C.).

post-tensioning systems provide a means of introducing an adjustable reduction in the elongation at the anchorage that simulates the effect of anchorage deformation.

Several multi-strand post-tensioning systems, employing from one to as many as 48 seven-wire strands in each tendon, have been available in the United States. All of the systems rely upon steel wedges or wedge-anchors for the anchorage of the strands. Details of the anchorages, grouting procedures, and stressing equipment should be obtained from the suppliers of the individual systems because the systems are frequently modified and improved.

End anchorage of parallel-wire post-tensioning tendons also has been achieved through the use of enlarged sections, or heads, cold-formed on the ends of wire

having a diameter of 0.25 in. (The cold-formed heads have been referred to as button heads in the technical literature.) Several systems utilizing this principle have been available in the United States, but they no longer are. The basic system has been used with a number of variations, but in all of them, the button heads bear on a stressing ring, block, or disk to which a hydraulic jack is attached for stressing. After stressing, the stressing ring, block, or disk is locked in the stressed position, either with shims or with threaded nuts. Button-headed wires connected to disks that have been stressed and shimmed, are being stressed, and have not been stressed are illustrated in Fig. 16-5.

In the 1950s, tendons composed of a single, large, multi-wire strand, with either swaged or zinc-attached end anchorages, were available in this country. They were very appealing from several viewpoints, but, unfortunately, proved to be uneconomical in competition with other types of tendons. For this reason large-strand tendons have not been available in North America for many years.

Another type of post-tensioning tendon that once was extensively used in the United States utilizes smooth, high-tensile-strength steel bars. Tendons of this type were developed in England, where they are known as Lee-McCall bars. The smooth high-tensile-strength bars have been used with threaded nuts and couplers as well as with wedge-type anchorages, as shown in Fig. 16-6.

High-tensile-strength steel bars are currently available with deformations formed on their exterior surfaces. These deformations are in the form of a helix that permits their use as coarse threads in couplers as well as in anchorages. Deformed bars for prestressing concrete are illustrated in Fig. 16-7 with two

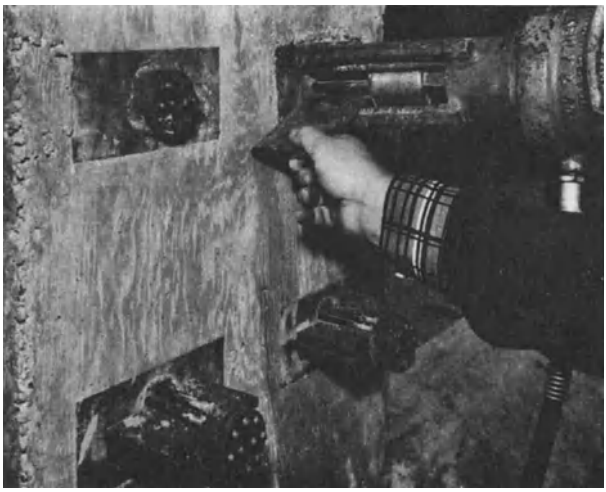

Fig. 16-5. End anchorages of tendons with cold-formed button heads. (Provided by and used with the permission of Prescon, Corp., San Antonio, Texas, a general contractor.)

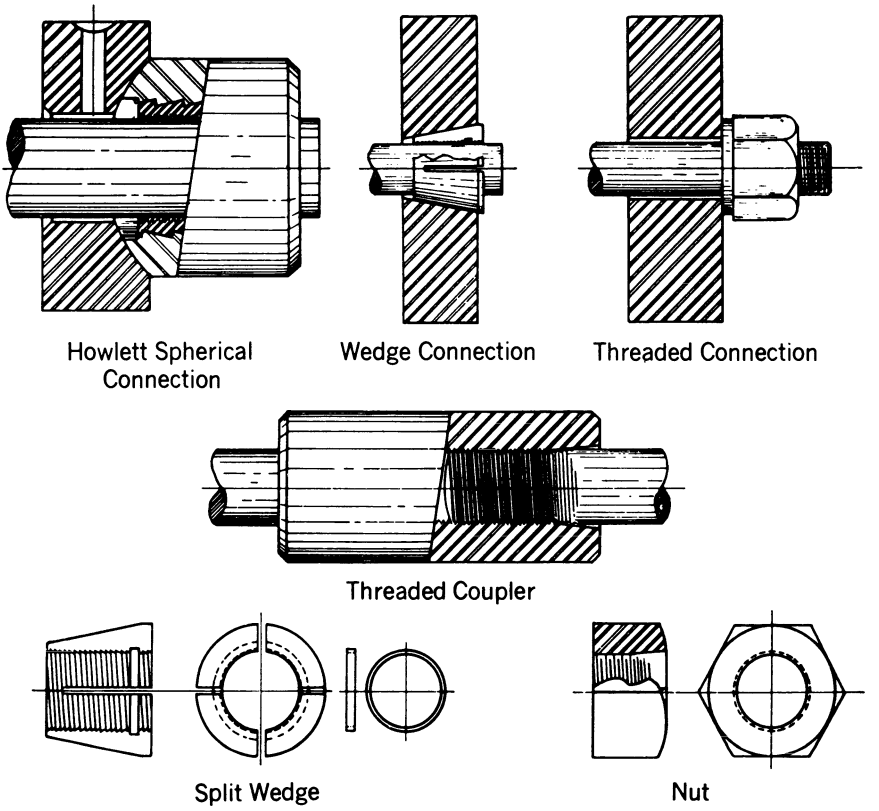

Fig. 16-6. Anchorages and couplers used with bar systems. (Provided by and used with the permission of Howlett Post-tensioning Systems, Berkeley, California.)

types of anchorages. Both of the anchorages incorporate spherical seats that prevent bending moments in the bars because of the axis of the bar not being perpendicular to the anchorage plate. The anchorage shown in Fig. 16-7b, which incorporates tapered surfaces within the anchorages assembly, permits the bearing plate to be several degrees from perpendicular to the anchorage plate without inducing bending moments in the prestressed bar.

Couplers are used to join individual high-strength steel bars together at the job site to form long, continuous bar tendons. The provision of couplers in a prestressed concrete member affects the detailing and construction of the member and must not be overlooked during the preparation of shop drawings and installation of the tendons.

The devices used to stress button-head tendons and high-tensile-strength steel-bar tendons are simple, double-acting center-hole hydraulic rams or jacks. Devices of these types are readily available in many sizes. The center-hole rams

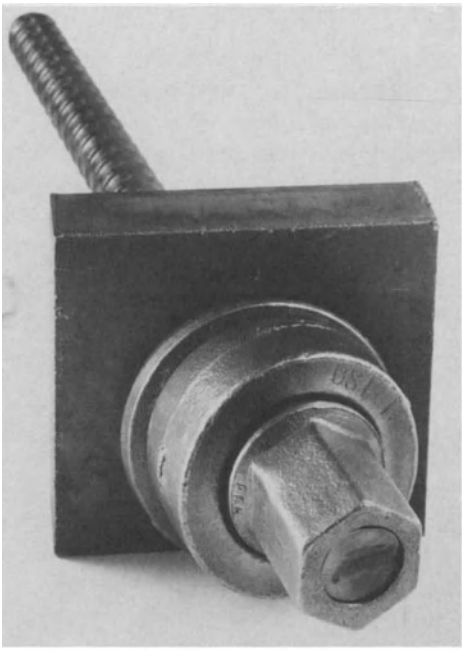

(a)

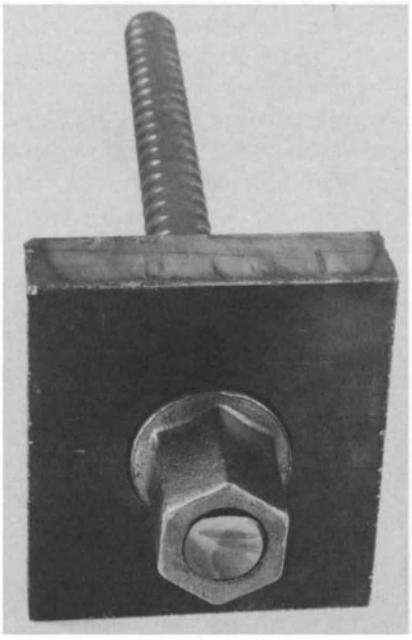

(b)

Fig. 16-7. Anchorages used with thread-bars. (a) Deformed high-strength bar having an anchorage with a spherical seat and tapered shim plate. (b) Deformed high-strength steel bar with a spherical seat. (Based upon data obtained from and used with permission of Dywidag Systems International USA, Inc.)

commonly used at this time are much less expensive and lighter than the stressing devices of equivalent capacity used in most of the early post-tensioning systems.

Each system of post-tensioning offers certain advantages and disadvantages, and no attempt is made here to discuss all the systems or factors that may influence the designer or contractor in selecting a specific system for a particular application. The designer should select and specify the systems that will best meet the requirements of each individual job. In most applications, however, the systems all will work equally well; so the controlling factor is the cost of the materials, equipment, and labor required to install, stress, and grout the tendons.

16-3 Sheaths and Ducts for Post-tensioning Tendons

In prestressed construction, it is essential that the tendons not become bonded to the concrete until after they have been prestressed. In post-tensioned construction, because the tendons cannot be stressed until the concrete has been placed and has attained a significant strength, it is necessary that the concrete be prevented from coming into contact with the tendons before it has hardened. This can be accomplished with any one of three commonly used methods. One method, used for unbonded post-tensioned tendons, is to enclose the tendons in factory-applied materials. This approach permits the tendons to be placed in the forms before the concrete is placed without risk that they will become bonded to the concrete during the placing and curing processes, and thus ensures that they will be free to move at the time of prestressing. Another method involves the use of holes formed in the concrete at the locations where the post-tensioned tendons are to be placed. With this method, after the concrete has been placed and has attained sufficient strength for prestressing, the tendons are inserted in the preformed holes, stressed, and grouted. A third method consists of placing the tendons in metallic tubes that are (a) sufficiently stiff to maintain their shape during the placing and consolidating of the concrete and (b) sufficiently cement-tight to prevent the concrete (and cement) from coming into contact with the reinforcement. External tendons, which usually are placed within the concrete section over relatively short portions of their lengths, generally are placed in metal ducts used to preformed holes where they pass through the concrete sections (i.e., end blocks and deviation blocks), and in plastic pipes where they are not encased in the concrete. External tendons normally are grouted through their lengths after they have been installed and stressed, but they are bonded to the concrete only at the end blocks and deviation blocks.

Unbonded post-tensioned tendons are used in practically all cast-in-place, prestressed concrete used in building construction in the United States. The tendons for this construction usually are fabricated in a factory and shipped to job sites in large rolls. (Coiling them into rolls at the factory facilitates their

transport, handling, and placing.) The tendons prefabricated for unbonded construction normally consist of single seven-wire strands that have been coated with a lubricant containing a rust inhibitor and covered with plastic sheaths extruded over the coated strands. Groups of two or more single-strand tendons frequently are bundled together, after their fabrication as single-strand tendons, to facilitate their handling and placing at the job site. The tendons often must comply with the requirements of the *Specification for Unbonded Single Strand Tendons* published by the Post-Tensioning Institute (PTI 1985). This specification contains requirements for tendons that are intended for use in normal as well as corrosive environments. As described above, tendons of these types are meant to be embedded in the plastic concrete and stressed after the concrete has gained sufficient strength.

Bond post-tensioned tendons also are used in building construction, but the quantity is very small compared to the amount used in unbonded construction. When bonded tendons are to be used in building construction, they frequently are assembled in a factory with the strands placed in flexible metal hoses to facilitate their being coiled for transport to the job site. The tendons are placed in the forms and tied to nonprestressed reinforcement to prevent their displacement during the placing of the concrete. After the concrete has gained sufficient strength and the tendons have been stressed, the metal hoses (ducts) are filled with portland cement grout (see Sec. 16-8).

A high percentage of the post-tensioned tendons used in bridge construction are inserted into holes preformed in the concrete with semirigid, metallic tubing. After the concrete has been placed and has gained sufficient strength for stressing, the tendons are pulled into the preformed holes, stressed, and grouted. Instead of using semirigid or rigid metal tubing, preformed holes can be made with removable rubber tubes. The tubes must be stiffened during concrete placing, either by being inflated with water or air or by the insertion of removable, smooth-steel rods. The rubber tubes are removed from the concrete after it has set.

It is important that ducts and sheathing be protected and not damaged during transport, handling, and placing. The duct should be strong enough to retain its shape during the placing and consolidation of the concrete. If the duct or sheathing is damaged during concrete placing, the tendons may become bonded, or a considerable friction loss may develop during the stressing of the tendons. In some cases, the tendons cannot be stressed to an acceptable level because of the friction or bonding.

16-4 Forms for Post-tensioned Members

Wood forms are commonly used in the construction of cast-in-place prestressed concrete buildings, bridges, and other types of structures. Forms suitable for

the construction of nonprestressed reinforced-concrete structures are suitable for the construction of cast-in-place prestressed-concrete structures. The forms normally require falsework to support them; and because the dead load of the structure supported by the falsework often is redistributed by the application of the prestressing force, special care must be exercised in its design (see Secs. 17-2 and 17-17).

Wood forms have been commonly used in the construction of job-site precast post-tensioned concrete on small projects, where the cost of using steel forms would be prohibitive. Wood forms are not usually made adjustable, but are constructed to produce members of only one size. Well-constructed wood forms properly oiled during use frequently can be used ten or more times before they must be completely reconstructed or discarded. Lining the inside surfaces of wood forms with light-gage metal, or using plastic-impregnated plywood in the forms, reduces the amount of moisture that the wood absorbs from the plastic concrete and increases its life expectancy.

In using wood forms, the method of curing the concrete must be such that expansion of the wood due to absorption of moisture will not crack the concrete. This problem, which is particularly acute with I-shaped beams, necessitates protecting the form surfaces that are not in contact with the concrete as well as the surfaces that are, if water curing is to be used before the form is stripped. Heat- or steam-curing is not recommended for concrete members made in wood forms.

Steel forms frequently are used in the construction of post-tensioned members when the number of reuses of the forms justifies their higher cost.

The same characteristics that are desirable for forms used in the manufacture of pretensioned concrete members are, for the most part, desirable in the manufacture of post-tensioned concrete members (see Sec. 15-5). In the manufacture of pretensioned concrete members, it frequently is necessary to place the soffit form as close to the top surface of the pretensioning bench as possible, to minimize the stress in the uprights and the overturning moment on the abutments. This is not a consideration in post-tensioned construction, and the soffit forms can be built elevated on small columns with elastomeric vibration insulators to maximize the benefits of form vibration. This scheme is illustrated in Fig. 16-8, where it will be seen that the form vibrator can be attached to the soffit form as well as the side forms. The vibrators can be moved along the length of the form as the concrete is placed, or, if desired, vibrators may be positioned at several locations along the length of the form, thus eliminating the need to move them. When form vibration is used, it frequently must be supplemented with internal vibration. The use of elastomeric pads and form vibrators, for all practical purposes, makes the form into a combination form and vibrating table of the type commonly used in the manufacture of small concrete products. The procedure is feasible only in precasting plants.

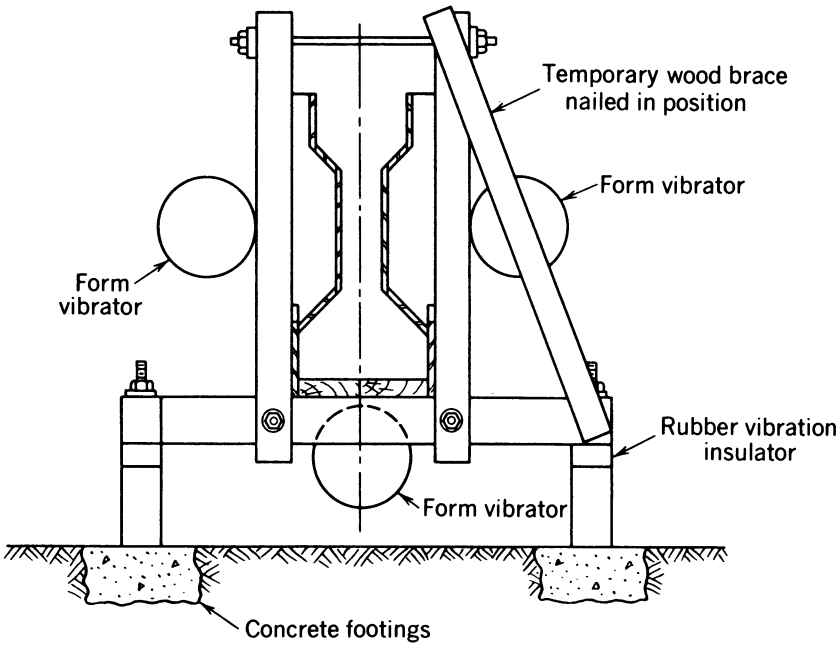

Fig. 16-8. Form designed for use with external (form) vibrators.

16-5 Effect of Friction during Stressing

The forces along the length of a post-tensioned tendon varies because of friction between the tendon and the duct or sheathing. The frictional forces, which are created during stressing, are considered to be a function of two effects: the intentional (primary) curvature or draping of the tendon and the unintentional (secondary) curvature (or wobble) from the intended path. Typical coefficients of friction (μ and K) for each of these effects, which are specified in post-tensioning design criteria in the United States, are listed in Table 16-1. Field tests sometimes are made for the purpose of determining the actual friction coefficients for the materials being used on a specific application.

The stress at any point in a tendon can be determined by substituting the proper coefficients in the relationship:

$$T_0 = T_X e^{(\mu\alpha + KX)} \tag{16-1}$$

in which T_0 is the force at the jacking end; T_X is the force at point X ft from the jacking end; e is the base of the Naperian logarithms; K is the secondary curvature or wobble friction coefficient; μ is the primary curvature friction coefficient; α is the total angle change between the tangents to the tendon at the end and at point X (resultant or sum of the horizontal and vertical angles), in radians;

TABLE 16-1 Typical Coefficients of Friction for each of the Effects Specified in Post-tensioning Design Criteria in the United States

Type of Tendon	Type of Duct	Design Values μ	Design Values K
Uncoated wire or large diameter strands	Bright flexible metal sheath	0.30	0.0020
	Galvanized flexible metal sheath	0.25	0.0015
	Galvanized rigid metal sheath	0.25	0.0002
	Mastic coated, paper or plastic wrapped	0.05	0.0015
Uncoated seven-wire strand	Bright flexible metal sheath	0.30	0.0020
	Galvanized flexible metal sheath	0.25	0.0015
	Galvanized rigid metal sheath	0.25	0.0002
	Mastic coated, paper or plastic wrapped	0.08	0.0014
Bright metal bars	Bright flexible metal sheath	0.20	0.0003
	Galvanized flexible metal sheath	0.15	0.0002
	Galvanized rigid metal sheath	0.15	0.0002
	Mastic coated, paper or plastic wrapped	0.05	0.0002

and X is the distance in feet from the jacking end to the point under consideration.

For values of $(\mu\alpha + KX) \leq 0.30$, Sec. 18.6.2 of ACI 318 permits the use of the following relationship in lieu of eq. 16-1:

$$T_0 = T_X(1 + \mu\alpha + KX) \tag{16-2}$$

The variation in stress in a post-tensioned tendon stressed from one end, according to the above relationship, will be as illustrated in Fig. 16-9. The maximum value of stress in the tendon occurs at the jacking end, and the minimum value at the dead end. If the tendon were stressed from each end simultaneously, the curve would be symmetrical about the midpoint of the tendon and would have the shape of curve *AB* on each side.

For very long tendons and tendons in continuous beams, the effects of friction during post-tensioning should be investigated by the designer at the time when the tendon paths are selected. In this way, the loss of stress due to friction will be determined, and the designer will be alerted to the need, if any, for special friction loss precautions in the project specifications. Special procedures that can be used to reduce the effects of friction include using galvanized duct rather than bright duct, using semirigid duct in lieu of flexible duct, reducing the curvature of the tendons, and lubricating the tendons with water-soluble oil. *Note*: If used, the oil is removed by flushing the ducts with water before the tendons are grouted. The use of water-soluble oil to reduce friction generally is employed only as a last resort when serious friction is encountered on the job site. It is not recommended that this procedure be relied upon during design.

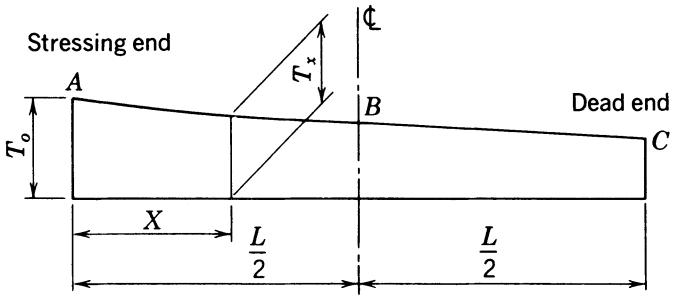

Fig. 16-9. Variation in stress due to friction in a tendon post-tensioned from one end.

ILLUSTRATIVE PROBLEM 16-1 Compute the force that would be expected in a post-tensioned tendon at midspan of a beam that is 100 ft long. The tendon is on a second-degree parabolic path having an ordinate of 3 ft at midspan. Assume that the duct is to be a bright flexible metal hose, and that tendon is to be composed of parallel seven-wire strands. Repeat the computations with galvanized duct.

SOLUTION: Because the tangent of the angle between the tangents to the tendon can be assumed to be numerically equal to the value of the angle expressed in radians, the value of α is found by:

$$\alpha = \tan \alpha = \frac{4e}{L} = \frac{4 \times 3}{100} = 0.12$$

Using the coefficients from Table 16-1:

$$\mu\alpha = 0.30 \times 0.12 = \quad 0.036$$

$$KX = 0.0002 \times 50 = \quad \underline{0.100}$$

$$0.136$$

$$T_0 = T_X e^{0.136} = 1.15 T_X$$

$$T_X = 0.873 T_0$$

With galvanized rather than bright duct, the value of $\mu + KX$ is 0.105 and:

$$T_0 = 1.111 T_X$$

16-6 Elastic Deformation of Post-tensioning Anchorages

As explained in Sec. 16-5, the variation in force and stress along the length of a post-tensioned tendon at the time of stressing is assumed to follow the curve

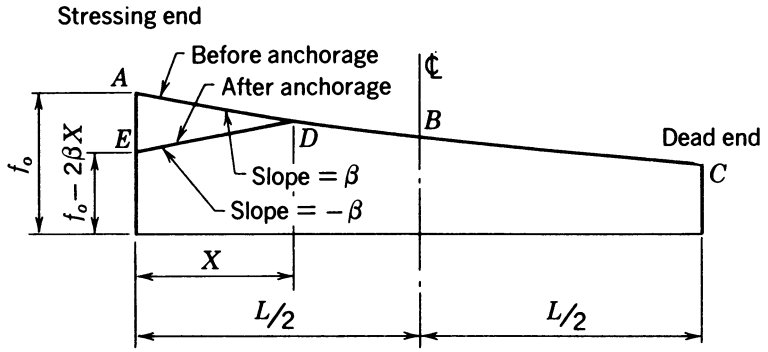

Fig. 16-10. Variation in stress in condition I before and after seating of the anchorage.

ABC in Fig. 16-10. The curve *EDBC* in this figure defines the assumed variation in stress after the tendon has been stressed and anchored. It will be noted that a reduction in the stress at the stressing end of the tendon resulted from the anchoring process (see Sec. 16-2). The reduction in stress occurs when the prestressing force is transferred from the ram or jack to the anchorage device. At this instant, a portion of the elongation of the tendon is lost because of the deformation of the anchorage device. Although some positive-type anchorage devices, such as those used with high-tensile-strength steel threaded bars, when properly applied, have no appreciable deformation of the anchorage, the wedge- or cone-type anchorages often deform significantly as the load is applied to them. (Other types of anchorages, which were used in the past but are no longer used in new construction in the United States, had components stressed in their plastic ranges; several hours were required with these anchorages to reach the limiting value of the anchorage deformation.) The manufacturers anchorages devices accepted for use on a particular project should provide information relative to the anchorage deformation anticipated with the use of their products. Anchorage deformations should be measured in the field, at least periodically, as a means of confirming that the anticipated deformations are being obtained.

To facilitate computation of the effects of anchorage deformation on the stress in a tendon, the curves *AB*, *AD*, *BC*, and *DE* in Fig. 16-10 are assumed to be straight lines. The slopes of lines *AB* and *DE* are assumed to be of equal magnitude, but of opposite sign. Tests have shown these assumptions to be reasonable.

The state of stress indicated in Fig. 16-10 will be referred to as condition I. This condition is characterized by the stress at midspan not being affected by the deformation of the anchorage; that is, the length X is less than one-half the length of the beam. This condition generally occurs in long members or in tendons having relatively high friction. In some instances, it is desirable to stress tendons having stress distributions of this type from one end only, but

because this condition generally exists only in tendons of considerable length, they are more frequently stressed from both ends simultaneously.

The assumed variation in stress referred to as condition II is shown in Fig. 16-11. In this case, the stress at midspan is affected by the deformation of the anchorage: that is, the distance X is greater than one-half the length of the beam. There generally is no advantage to be gained in stressing a tendon simultaneously from both ends if it has this type of stress distribution.

The most severe effects from the deformation of the anchorage are found in short tendons and those with very low friction. In this case, the stress along the entire length of the tendon, including the dead end, is reduced by the deformation of the end anchorage. This condition is characterized by the computed length of distance X being greater than the length of the tendon. The assumed distribution of stress for condition III is illustrated in Fig. 16-12.

A method for determining the effect of anchorage deformation on the stresses after seating of the anchorage consists of the following steps:

1. Determine the relationship between the stress at the stressing end and at midspan (or other critical section) resulting from the friction, as explained in Sec. 16-5. This can be expressed as:

$$f_0 = f_{\ell} e^{\phi}$$

where:

$$\phi = \mu\alpha + \frac{KL}{2}$$

2. Assume that the deformation of the anchorage does not affect the stress at midspan of the beam (condition I), and compute the slope, β, of the curve between midspan and the stressing end as follows:

$$\beta = \frac{2f_{\ell}(e^{\phi} - 1)}{L} \tag{16-3}$$

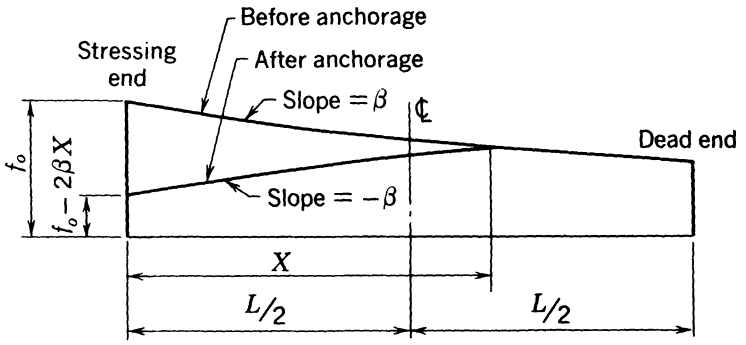

Fig. 16-11. Variation in stress in condition II before and after seating of the anchorage.

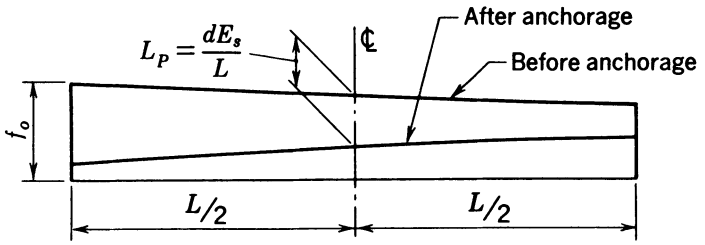

Fig. 16-12. Variation in stress in condition III before and after seating of the anchorage.

3. Compute the length of the tendon on which the stress is reduced by the anchorage deformation as:

$$X = \sqrt{\frac{dE_{ps}}{\beta}} \tag{16-4}$$

where X is the length of tendon that is affected in inches, β is the slope in psi/in., E_{ps} is the modulus of elasticity of the prestressed reinforcement in psi, and d is the deformation of the anchorage in inches.

4. If X is less than $L/2$, condition I exists, the stress at midspan is not affected, and the stress at each end is readily computed if desired.

5. If X is greater than $L/2$, but less than L, condition II exists. The stress loss at midspan resulting from the anchorage deformation is equal to:

$$\Delta f_{\text{℄}} = 2\beta\left(X - \frac{L}{2}\right) \tag{16-5}$$

If this loss is too great to be tolerated, higher initial stresses should be investigated by using a trial procedure until a satisfactory solution is found.

6. If X is found to be greater than L, condition III exists, and the loss at the center of the tendon is equal to:

$$f_{\text{℄}} = \frac{dE_{ps}}{L} \tag{16-6}$$

and the stress after anchorage at the center of the tendon can be computed directly.

It must be emphasized again that the anchorage deformation for some post-tensioning systems is very small and can be reasonably neglected. Anchorage deformations as large as 1 in. have been observed with wedge-type anchors under unusual conditions. It is important to recognize that this phenomenon exists and that it must be taken into consideration during design and construction. This is particularly true when short tendons are to be used.

ILLUSTRATIVE PROBLEM 16-2 Determine the effect of the elastic deformation of the anchorage cone on the stress in the prestressed reinforcement at midspan of a tendon 100 ft long placed on a second-degree parabolic path having a midspan ordinate of 3 ft. The desired stress after anchorage at midspan is 165,000 psi, the deformation of the anchorage is 0.50 in., the modulus of elasticity of the prestressed reinforcement is 28,000,000 psi, and a bright metal duct is to be used. In addition, determine the effect if the duct were to be galvanized rather than bright.

SOLUTION: The effect of friction for these conditions was determined in I.P. 16-1. Using the calculated value for e^{ϕ}, the computation of β and X becomes:

$$\beta = \frac{2 \times 265{,}000 \times 0.15}{100 \times 12} = 41.2 \text{ psi/in.}$$

$$X = \sqrt{\frac{0.50 \times 28 \times 10^6}{41.2}} = 584 \text{ in.} < 600 \text{ in.} = \frac{L}{2}$$

Therefore, condition I exists because the deformation of the anchorage of 0.50 in. does not reduce the stress in the tendon at midspan.

Using galvanized sheath:

$$\beta = 41.2 \times \frac{0.11}{0.15} = 30.2 \text{ psi/in.}$$

$$X = \sqrt{\frac{0.50 \times 28 \times 10^6}{30.2}} = 680 \text{ in.} > 600 \text{ in.} = \frac{L}{2}$$

The reduction in stress at midspan due to the deformation of the anchorage is:

$$f_{\text{℄}} = 2 \times 30.2(680 - 600) = 4830 \text{ psi}$$

Therefore, the stress remaining in the tendon at midspan after the tendon has been anchored is 165,000 − 4800 = 160,200 psi. If the stress at midspan is increased to 169,000 psi at the time of stressing, the values of β, X, and the loss of stress in the prestressed reinforcement at midspan are calculated as follows:

$$\beta = \frac{2 \times 169{,}000 \times 0.11}{1200} = 31.0 \text{ psi}$$

$$X = \sqrt{\frac{0.50 \times 28 \times 10^6}{31.0}} = 672 \text{ in.}$$

and the stress at midspan after the deformation of the anchorage is 169,000 − 2 × 31.0 × 72 = 164,500 psi, which is less than the 165,000 psi required. Hence, the stress at midspan should be increased to 169,500 psi at the time of stressing in order to have 165,000 psi after anchorage.

It should be noted that the stress at the end of the tendon required to obtain 165,000 psi in the tendon at midspan is equal to 165,000 × 1.15 = 190,000 psi when a bright duct is used. When galvanized duct is used, the stress at the end of the tendon required to obtain the desired stress at midspan after anchoring is equal to 169,500 × 1.11 = 188,000 psi. It will be seen that the required tendon stress at the stressing end of the tendon is not materially reduced by the use of galvanized sheath in this case.

ILLUSTRATIVE PROBLEM 16-3 Compute the jacking and initial stresses (stresses before and after anchorage, respectively) for the tendon layout shown in Example V of Appendix B if the tendons are jacked to a force of 6460 kips at each end. The prestressing tendons consist of 208 strands each, having an area of 0.153 sq. in. The friction coefficients are $\mu = 0.25$ and $K = 0.0002$. The elastic modulus of the steel is 27,000 ksi, and the anchorage set is 0.625 in. Determine the location of the maximum and minimum points of stress, assuming the tendons to follow second-degree parabolic paths between the dimensioned points; assume linear variation of stress between these points.

SOLUTION: The friction coefficients, angle changes, and distances between points along the tendon path are summarized in Table 16-2. The computations are summarized in the Table 16-3, as well as in Fig. 16-13.

TABLE 16-2 Friction Coefficients, Angle Changes, and Distances between Points along the Tendon Path for I.P. 16-3.

Point	μ	α	K	ΔX
A				
	0.25	0.0686	0.0002	81.00
B				
	0.25	0.1157	0.0002	64.80
C				
	0.25	0.1157	0.0002	16.20
D				
	0.25	0.1250	0.0002	15.00
E				
	0.25	0.1250	0.0002	60.00
F				
	0.25	0.0740	0.0002	75.00
G				

TABLE 16-3 Summary of Computations for I.P. 16-3.

Point	*H* (ft)	*L* (ft)	Friction factor	Jacking stress (ksi)	Initial stress (ksi)
A	3.610		1.000	202.991	180.890
		81.000			
B	0.833		1.0339	196.334	187.547
		35.343			
		29.456			191.941
C	4.583		1.0781	188.279	188.279
		16.200			
D	5.520		1.1133	182.320	182.320
		0.788			
Pt./min. stress			1.1153	181.992	
		14.211			
E	4.583		1.0797	187.992	187.992
		24.744			
					191.418
		35.255			
F	0.833		1.0340	196.301	186.536
		75.000			
G	3.610		1.000	202.991	179.846

16-7 Computation of Gage Pressures and Elongations

Under optimum condition, the designer of a post-tensioned structure will select a specific system of post-tensioning for use on the project, prepare the computations for gage pressures and elongations needed in the field during construction, and include a summary of the computations on the construction plans. In

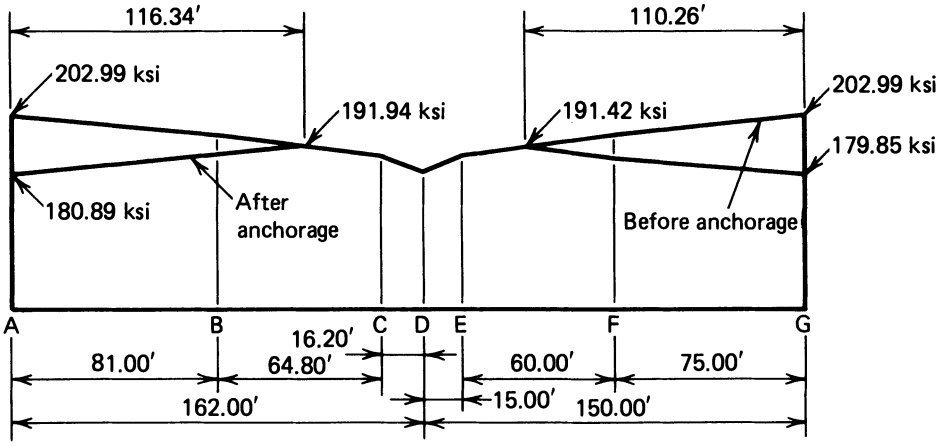

Fig. 16-13. Plot of stresses in the tendon of I.P. 16-3 before and after seating of the anchorage.

following this procedure, the designer is assured that the stressing can be achieved as intended. When the system of post-tensioning is not specified, the computation of gage pressures and elongations must be prepared by the contractor or the contractor's agent and submitted to the engineer for review and acceptance. In the latter case, it is recommended the summary of the stressing data be included on the shop drawings or in a project manual for post-tensioning if one is prepared.

The computations of gage pressures and elongations are conveniently made and summarized by using a form similar to the one in Table 16-4. Some systems of post-tensioning may not require all of the line items included in the list shown in the table, whereas other systems may require more. Hence, the listing should be adjusted for the needs of each specific post-tensioning system.

The length of the prestressing tendon used in the computations normally is taken as the horizontal projection of the tendon. For more precise computations in structures having tendons with large second-degree parabolic curvatures, the

TABLE 16-4 Typical Calculation Sheet for Use in Computing the Gage Pressures and Elongations in Post-tensioning.

Item Number	Tendon Numbers 1	2	3
1. Type of tendon			
2. Area of steel (in.^{2})			
3. Length of tendon (ft)			
4. Length of tendon (in.)			
5. Distance from anchorage to marks (in.) Note: For one-end stressing, use only the length at stressing end. For two-end stressing use the length at both ends			
6. Total length of unit to be stressed (in.)			
7. Desired effective stress (psi)			
8. Losses of prestress.			
a. Elastic shortening*			
b. Relaxation, creep and shrinkage			
9. Desired stress before anchorage deformation (psi)			
10. Effect of anchorage deformation (psi)			
11. Desired jacking stress at center (psi)			
12. Anticipated jacking stress at jack (psi)			
13. Anticipated gauge pressure (psi)			
14. Maximum gauge pressure (psi)			
15. Elongation to be obtained (in.)			
a. Total			
b. Net			
16. Special instructions			

*The losses of prestress should include all the effects listed in Sec. 7-2. The loss due to elastic shortening is often left to be included in the stressing computations. This should be investigated for each job.

tendon length can be computed by using:

$$L' = \left(1 + \frac{8a^2}{3L^2}\right)L \tag{16-7}$$

in which L is the horizontal projection of the tendon, a is the ordinate of the parabolic tendon path, and L' is the true tendon length. Provision is made in the table for the length to be recorded in both feet and inches, as the former is used in the computation of the effect of friction and the latter in the computation of elongations.

The distance from the anchorage to the reference mark or marks on the tendon used in measuring the elongation during stressing is recorded in item 5 in the table. Although this may at first appear to be an unnecessary refinement, it should be noted that with some systems of post-tensioning the distance between the reference mark and the end anchorage may be significant and, if ignored, introduce an unnecessary error in the computation of elongations.

If the designer has specified the final prestressing force required in the structure, rather than the initial force, the computation of the losses of prestress must be made as a part of the computations for the post-tensioning shop drawings (see Sec. 7-3). If the initial tendon stress has been specified, it can be entered directly in item 9. The effect of the deformation of the anchorage, if any, must be computed and entered in item 10. The desired jacking stresses at the midlength and end of the tendon, based upon the computations for the effects of the anchorage deformation, are entered as items 11 and 12, respectively. The value of the jacking stress at the ends is not normally allowed to exceed 70 to 80 percent of the guaranteed minimum ultimate tensile strength of the reinforcement, depending upon the criteria being used.

One normally anticipates that the gage pressure will be greater than the theoretical pressure due to the internal friction of the jack and, in some systems, due to the friction of the tendons where they pass over the anchorage and jack during stressing. The friction can range from 2 to 15 percent, depending upon the post-tensioning system. Calibration of prestressing jacks normally is required as a means of determining a reasonable estimate of the friction. Jack calibration data can be plotted to obtain curves that graphically display the relationship between the gage pressure and the stress in the reinforcement or jacking force. The gage pressure that would be anticipated in obtaining the desired initial stress at the end of the tendon can be taken directly from calibration curves. Gage pressures determined from the calibration curves are referred to as "anticipated" because the actual values are affected by frictional forces and thus are subject to variation. It is customary for the elongations of the tendons measured during stressing to be used as the controlling measurement during prestressing. The usual procedure is to increase the pressure on the jack to the anticipated

pressure and then check the elongation. If the elongation is not within the required tolerances, the pressure is adjusted, without exceeding the maximum permissible pressure, until a satisfactory elongation is obtained. The maximum permissible gage pressure (corresponding to the maximum allowable jacking stress) is determined from the calibration curve in the same way as the anticipated gage pressure.

Before the reference marks used in measuring the elongation of the tendons are placed on the tendons, it is normal procedure to apply a small pressure, about 10 percent of the anticipated gage pressure, to the tendon to firmly tighten the jack to the anchorage and reduce or eliminate any slack that may be in the system. The force or pressure used in removing the slack should not vary during a project, if at all possible, in order to reduce the risk that workers will use an incorrect stressing procedure. This risk is believed to be greater if the initial-force procedure varies on a project.

Because the initial pressure applied to the tendon results in a small stress in the tendon, the amount of elongation that occurs during the application of the remaining force, and is used in controlling the stressing operation, is an increment of the total deformation. Furthermore, because there is a variation in stress along the length of the tendon as a result of friction, an average value for the stress is used in determining the elongation. In the case of stressing from one end only, the average stress is the stress at the midlength of the tendon in most instances, whereas, in the case of stressing from each end simultaneously, the average stress would occur approximately midway between the ends and the midlength of the tendon. After the average stress has been determined, the total and incremental elongations that would result from the average stress can be calculated from the stress–strain characteristic for the specific reinforcement that will be used on the project.

16-8 Construction Procedure in Post-tensioned Concrete

Although the construction details and the system of post-tensioning to be used on a project can have a significant influence on the construction procedure used, experience indicates that several general statements and precautions should be brought to the attention of the reader. Careful planning and attention to details of construction in post-tensioned elements are important and can have a significant influence on the success of projects that include post-tensioned construction.

The procedure normally followed in the construction of post-tensioned beams consists of:

1. Erecting the soffit form and one side form.
2. Placing the ordinary reinforcing steel, reinforcement to be prestressed, and end anchorages.

3. Erecting the second side form.
4. Placing and curing the concrete.
5. Stripping the concrete forms.
6. Stressing the grouting the tendons.

In projects involving the production of many post-tensioned members, the ordinary reinforcing and post-tensioning materials frequently are tied together in a jig and set in the forms as a unit as a means of reducing the time needed to prepare for concrete placement. On smaller jobs, the post-tensioning units normally are tied in place after the reinforcing steel cage is partially or completely assembled in the forms. The latter procedure is much more common, and it must be emphasized that the erection of one side form can facilitate the layout and installation of the nonprestressed reinforcement, inserts, and block-out forms, and can expedite the assembly of post-tensioned members.

When post-tensioning tendons in ducts and sheaths are used, the tendons must be securely tied in place at small intervals in such a way that secondary curvature (wobble) of the tendons is minimized, and the primary curvature of the tendons is reasonably close to the path specified on the drawings.

It is important for the location of the tendons at the midspan of simple flexural members to be close to the locations specified on the drawings. As was shown in Sec. 4-9, the centroidal axis of the tendons does not normally need to be placed within precise limits at points between the midspan of the beam and the ends to achieve satisfactory results. However, it normally is important that a tendon be placed on smooth curves that will minimize friction losses during stressing although it is not of great concern if the tendon is not precisely on the specified path between the locations of maximum moment.

No general statement can be made about the maximum permissible spacing for the ties and supports that secure the post-tensioning tendons in place during placing of the concrete. This is a function of the type and size of tendons, as well as the arrangement of the reinforcing steel and tendon path required.

Care must be exercised in tying tendons in place because it is possible to damage the ducts or sheath during the tying process. This is particularly true with plastic sheaths. A damaged sheath may permit the intrusion of grout and allow the tendons to become bonded to the concrete, thereby making it impossible to stress them.

After the tendons and anchorages have been tied in place, they should be carefully inspected to ensure that they are securely tied at all locations, and there is no possibility of mortar leaking into the sheath or anchorage device during the placing and consolidation of the concrete. Although mortar that leaks into a sheath, duct, or anchorage does not always result in a bonded tendon that is impossible to stress, the labor that is needed to clean the areas affected by the leakage before stressing can be started (or to overcome the high friction in the tendon that may be encountered during stressing) frequently exceeds the

amount of labor required to properly seal the sheath and anchorage before concreting.

When ducts are to be preformed in the concrete, the procedure is very similar to that followed for tendons that are in sheaths or metal hoses. Rubber ducts should not be tied so tightly to the reinforcing that they will be difficult to remove.

The manufacturers of some types of post-tensioning tendons recommend that a tendon be moved back and forth in the sheath during and after the placing of the concrete to ensure that it has not become bonded to the concrete by mortar that may have found its way into the ducts or sheaths. Although there is no technical objection to this procedure, it is not feasible for all systems of post-tensioning, and it is considered unnecessary if sufficient attention is given to the prevention of leaks before the concrete is placed. Rigid sheaths that are placed in the forms without having the tendons in them sometimes become damaged by the internal vibrators used in placing the concrete. This is most likely to occur in areas that are congested with embedded materials, and the damage can be so great as to prevent insertion of the tendons. To guard against this problem, it is recommended that the sheaths be inspected during the concreting operation to confirm that they remain open. This is easily done by pulling (with a small wire or cable) or pushing (with compressed air) a ball through the ducts while the concrete is being placed or immediately thereafter.

The post-tensioning tendons normally are stressed and grouted as soon as possible after the curing of the concrete has been completed. The stressing should be done by following the procedure recommended by the manufacturers of the post-tensioning anchorages and stressing equipment.

Grouting of tendons that are to be bonded normally is done very soon after the completion of the stressing. The grouting procedure used varies with the post-tensioning system. The grouting ports and sheaths of all post-tensioning systems are small and prohibit the use of large-grain sand in the grout. Fine sand is used occasionally for the purpose of reducing the quantity of cement required in the grout. In most cases the grout is neat portland cement grout containing no aggregates, which may or may not contain admixtures.

Recommendations for grouting post-tensioning tendons are included in Sec. 3.3 of the *Post-tensioning Manual* (PTI 1985) as well as in the standard specifications of most of the state departments of transportation. Recent work on improved grouts and grouting techniques for large ground anchors, utilizing grouts having very low water–cement ratios and modern concrete admixtures, and on corrosion protection of prestressing systems in concrete bridges and corrosion protection for prestressed ground anchors, has been published in the technical literature. (Houlsby 1988; Perenchio, Fraczek, and Pfeifer 1989; FIP 1986). Readers interested in corrosion protection of post-tensioned systems should consult these references.

During freezing weather, the grout injected into post-tensioning ducts may freeze and cause cracking of the concrete along the paths of the tendons. This can be avoided by heating the member for 24 to 48 hours after grouting, which allows the grout to harden before it freezes.

If members that are to be post-tensioned will be exposed to freezing weather before the tendons are grouted, the ducts or sheaths should be drained of all water that may collect in the ducts during placing, curing, and storage of the members. If this is not done and water finds its way into the ducts and freezes, the members may crack in the same way as when grout freezes in the ducts. Water should not be allowed to remain in ducts containing post-tensioning tendons for more than just a few days, even if there is no danger of freezing. Corrosion of the reinforcement generally will proceed at a more rapid rate when the tendons are partially submerged in water or stored in a moist environment.

16-9 Post-tensioning with Jacks

It was explained in Sec. 1-3 that concrete sometimes is prestressed with jacks rather than with tendons. A special flat jack made for this purpose is shown in Fig. 16-14. The flat jack is made of metal formed with a bar-bell-shaped cross

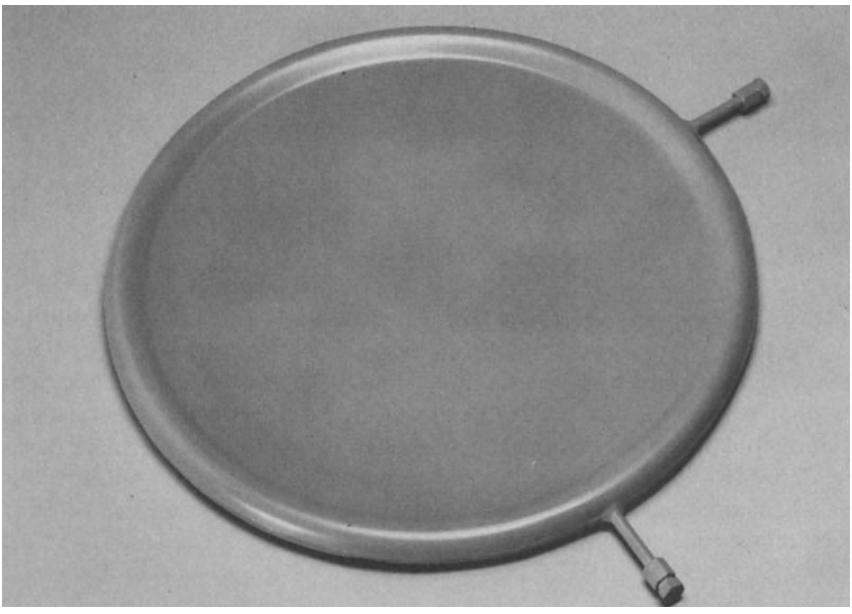

Fig. 16-14. Flat jack used in prestressing concrete. (Provided by and reproduced with the permission of the Freyssinet Company, Inc., Charlotte, N.C.)

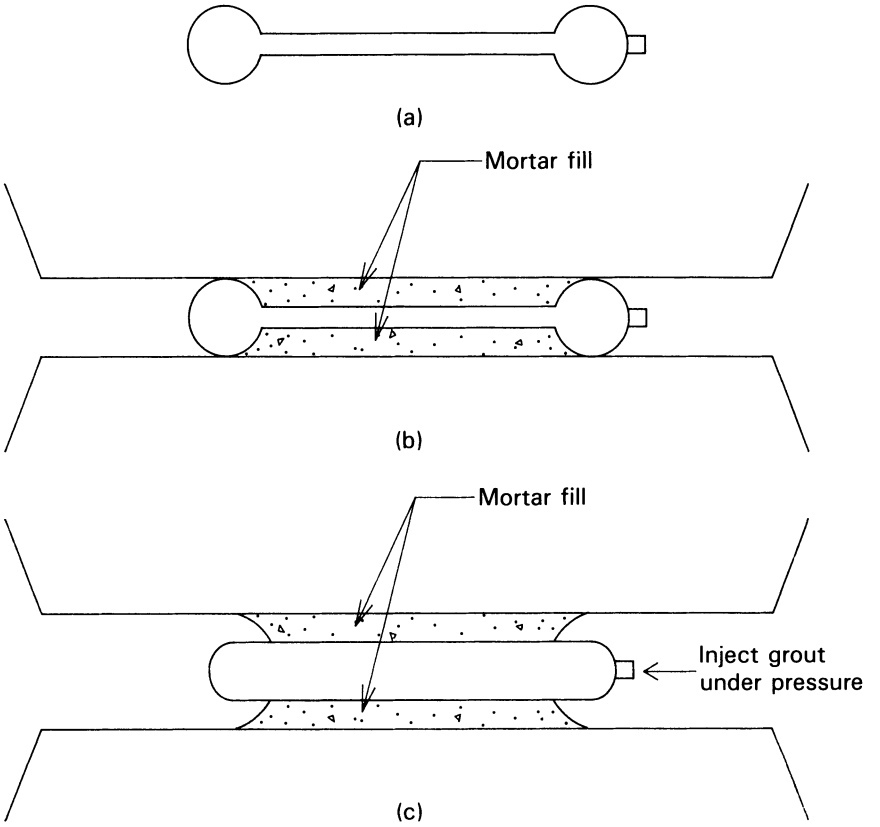

Fig. 16-15. The principle followed in using flat jacks, showing (a) cross section of a jack, (b) jack in position before stressing, and (c) jack in position after stressing.

section, as shown in Fig. 16-15. The jack is used by placing it between two objects to be stressed, filling the space between the jack and the objects, and pressurizing the jack with water, oil, or grout. The pressure causes the jack to expand, as shown in Fig. 16-15. Flat jacks are made in various sizes and can exert very large forces. Their maximum stroke (maximum movement upon being pressurized) is small, normally on the order of an inch or two. Although flat jacks are very special devices that are not commonly used, they can be most helpful in special circumstances.

16-10 Construction of Segmental Beams

Post-tensioned concrete beams may be made of a number of elements or segments post-tensioned together to form a structural unit. This procedure has

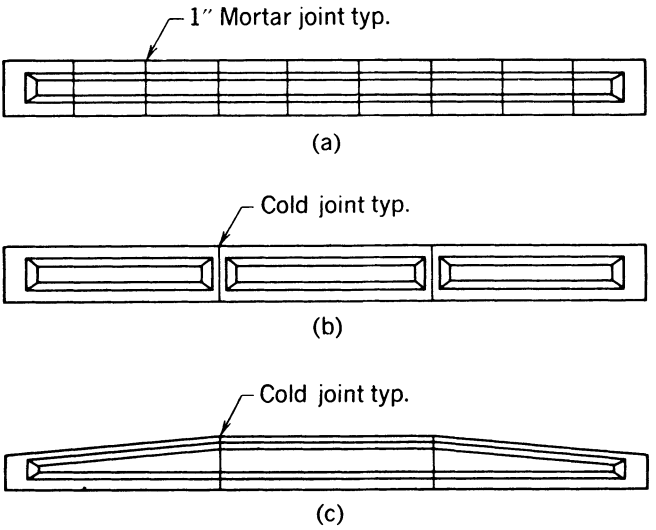

Fig. 16-16. Post-tensioned beams composed of several elements or segments.

been used to facilitate the forming, casting, handling, transporting, and erecting of large beams. Three types of segmental beams are illustrated in Fig. 16-16. It will be seen that a member may be formed of many elements made in small forms on vibrating tables, or of only a few large elements made by the same general procedure used in the construction of monolithic members. Preformed holes, formed with removable rubber tubes or permanent semirigid metallic hoses, are used in segmental members.

Post-tensioned bridge members composed of many small precast segments with mortar joints, as shown in Fig. 16-17, were constructed shortly after World War II. The mortar was necessary in these early structures because the segments were cast individually in molds (not match cast), and the mortar was needed in the joints to assure uniform bearing between the segments. Mortared joints can present some difficulty in the assembly of segmental members because it is difficult to fill the joints and prevent the mortar from entering the post-tensioning ducts and bonding to the tendons. In addition, placing the mortar is labor-intensive: In the case of the Esbly Bridge it was possible to apply the prestress to the segmental beams immediately after the mortar was placed, as the total deformation of the plastic mortar was very small because the widths of the joints were very small. Thin mortar joints cannot fail under the compressive stresses caused by prestressing even if the mortar is partially plastic at the time of stressing. The stresses arch across the joint.

The need for mortar joints in beams made of several elements can be avoided with the match casting technique, which was first used in 1951 in upstate New York. The principle of match casting is simple: The several segments are cast

Fig. 16-17. The Esbly bridge over the Marne River in France. (Provided by and reproduced with the permission of the Freyssinet Company, Inc., Charlotte, N.C.)

against each other at different times and with a light coating in the joint between the members to prevent their becoming bonded to each other. By casting the segments against each other, the unbonded cold joints between the elements have a perfect fit. Because a thin layer of a bond breaker is used between the elements, they can be separated for handling and transportation purposes. Shear keys, which provide vertical and horizontal projections of the end surfaces, are often provided at the ends of each element to facilitate aligning the elements during their assembly in the field. The shear keys normally are not required for structural considerations because of friction and the large compressive force applied to the joint by the prestressing. In contemporary practice, the joints between the individual segments frequently are coated with epoxy resin at the time of reassembly. The epoxy ensures a good fit, provides protection against the intrusion of air and moisture, facilitates the assembly of the segments, and glues the pieces together. A major bridge on which this procedure was used is shown in Fig. 16-18.

When segmented beams composed of only a few pieces are reassembled in the field, it is not necessary to set the elements close together and in precise alignment. It generally is easier and more expeditious to set them on wooden blocks, with a space between the elements. This procedure facilitates placing the post-tensioning tendons in the ducts. The elements can be pulled together

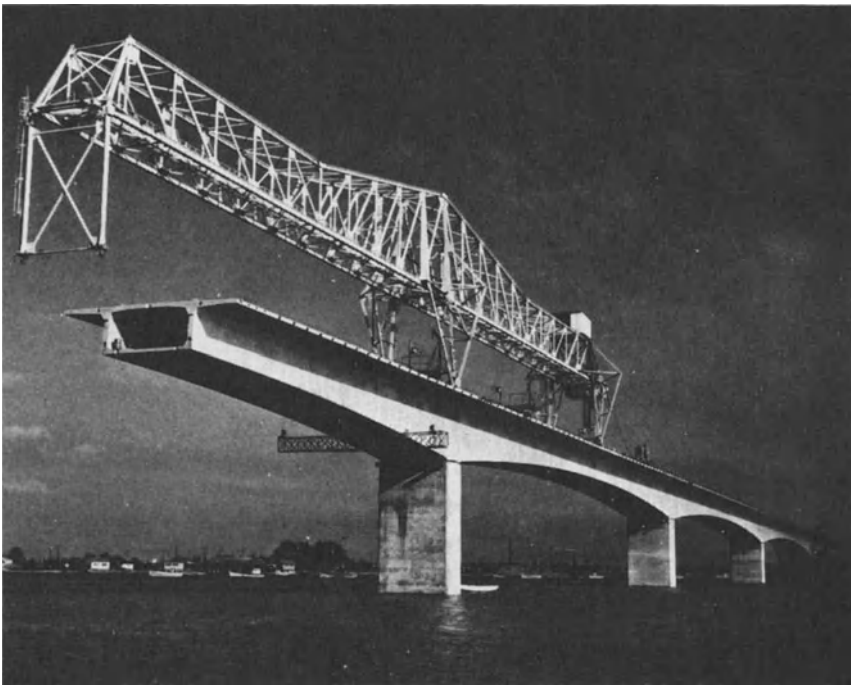

Fig. 16-18. The Oléron Bridge in France. (Provided by and reproduced with the permission of the Freyssinet Company, Inc., Charlotte, N.C.)

and stressed with the aid of post-tensioning jacks after the tendons have been inserted.

REFERENCES

FIP Commission on Prestressing Steels and Systems. 1986. *Corrosion Protection of Unbonded Tendons*. London. Thomas Telford, Ltd.

Houlsby, A. C. 1988. Improvements in Grouting of Large Ground Anchors. *Journal of Geotechnical Engineering*. 114(4):448-67.

Perenchio, W. F., Fraczek, J. and Pfeifer, D. W. 1989. Corrosion Protection of Prestressing Systems in Concrete Bridges. National Cooperative Highway Research Program Report 313.

PTI. 1985. *Post-Tensioning Manual*. Fourth edition. Phoenix. Post-Tensioning Institute.

17 Construction Considerations

17-1 Introduction

The design and fabrication of structural elements must be done with care and understanding to assure the desired quality. This is true of elements made of concrete members having prestressed reinforcement, whether precast or cast-in-place, just as it is for members made with nonprestressed reinforcement or other materials. Most problems that occur during construction are avoidable, and most have been experienced by other individuals. The purpose of this chapter is to describe some of the problems experienced in the fabrication of prestressed-concrete members and, where possible, to provide methods that can be used to avoid them.

17-2 Support-Related Problems

Prestressed concrete beams, both precast and cast-in-place, sometimes are designed to have overhanging ends. A beam of this configuration is shown in Fig. 17-1a. If the beam is constructed on a rigid soffit form, for example, a pretensioning bench as shown in Fig. 17-1b, or stiff falsework, the member will be uniformly supported throughout its length. Upon application of the

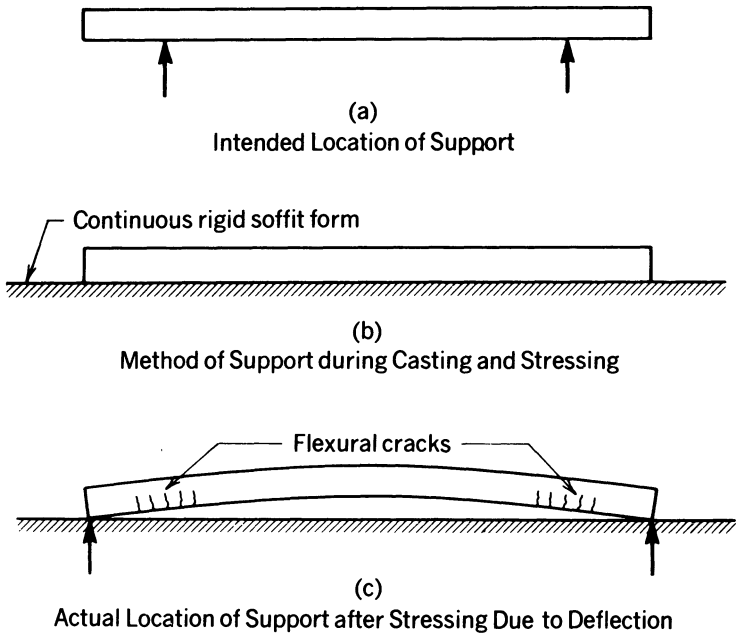

Fig. 17-1. Example of unintended mode of support of a beam cast on a concrete casting bed. (a) Intended locations of supports. (b) Mode of support during casting and prestressing. (c) Deflected shape and locations of supports after prestressing.

prestressing force, the concrete member tends to deflect, and, depending upon the specific conditions, may or may not become supported at the ends of the overhangs, as shown in Fig. 17-1c, rather than at the intended locations of its supports, as shown in Fig. 17-1a. If the bottom fibers of the member are not reinforced for positive moments with bonded reinforcement in the vicinity of the intended supports, wide flexural cracks, as shown in Fig. 17-1c, can occur at those locations. This condition can be mitigated by the provision of bonded reinforcement in the areas that will be subjected to temporary positive bending moments, or avoided by preventing the beam from becoming supported at its ends at the time of prestressing.

Post-tensioned concrete members cast in place on falsework have suffered serious distress, as has the falsework, due to the phenomenon described above, in beams without overhanging ends. Upward deflection of the beam, due to the application of the prestressing force, can transfer the full dead load of the beam, which has been partially carried by each of the falsework bents, so that it is carried by the end bents alone. This is illustrated for a simple beam in Fig. 17-2. After prestressing, the bents at the ends of the member may need to be strong enough to support one-half or more of the total dead load of the

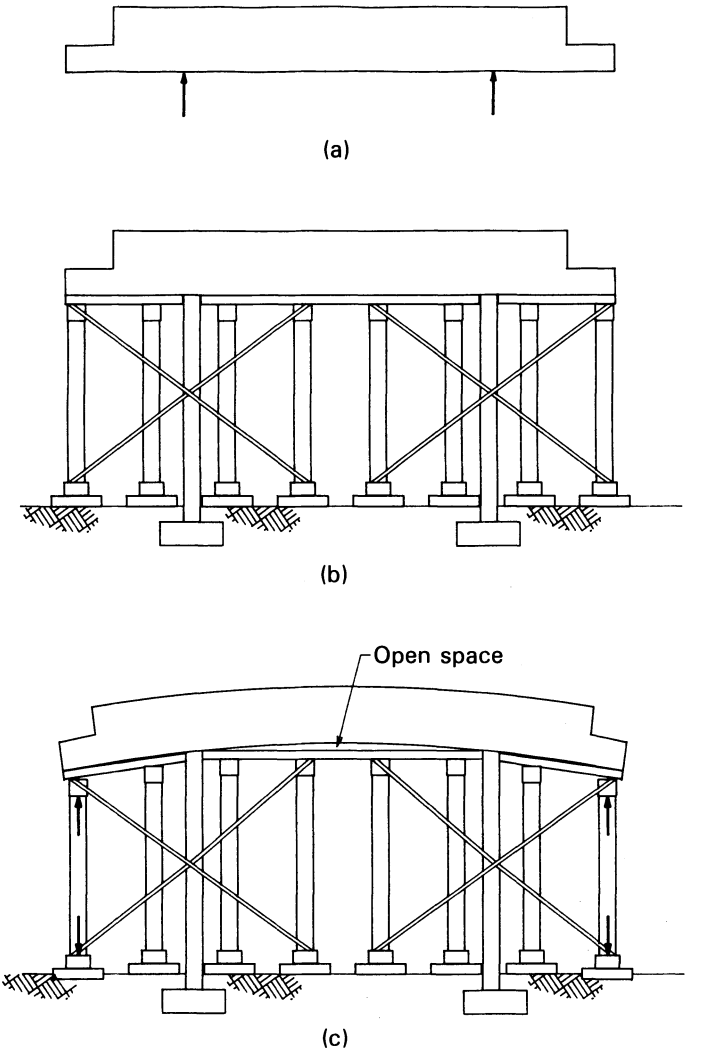

Fig. 17-2. Example of unintended mode of support of a beam cast on falsework. (a) Intended locations of supports. (b) Mode of support during casting and prestressing. (c) Deflected shape and locations of forces at the overhanging ends after prestressing.

prestressed concrete beam (see Sec. 17-17). Special bracing may be required for the end falsework bents as well.

Pretensioned concrete beams can crack at the extreme ends of the beam at the time of transfer of the prestress because of the rotations and horizontal forces resulting from prestressing. This is illustrated in Fig. 17-3. Prestressing causes

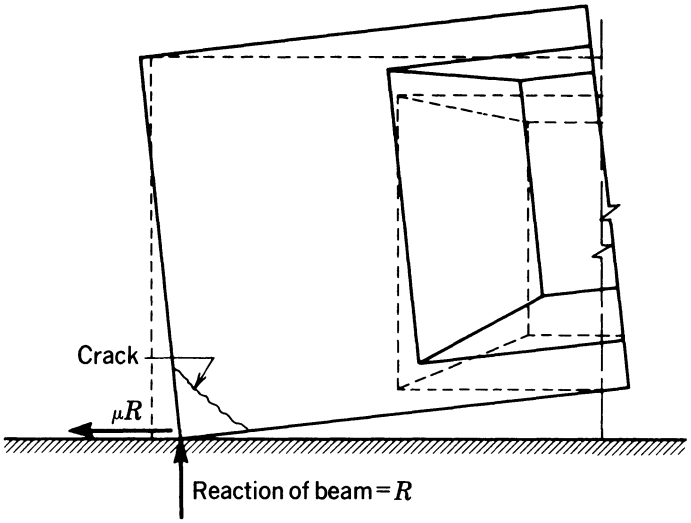

Fig. 17-3. Cracking at the end of a simple beam due to rotation and shortening. The position of the beam before stressing is shown by the broken lines. The coefficient of friction between the beam and the soffit form is denoted by μ.

the beam to be supported by reactions R at each end of the beam. The frictional force, μR, is due to the shortening of the beam and the reaction at the end of the beam. This type of cracking can be avoided either by making it possible for the ends of the beams to rotate without restraint at the time of prestressing or by reinforcing the ends of the beams in such a way that serious cracking will not occur.

The supports at the ends of flexural members sometimes have been detailed to consist of as-cast concrete surfaces bearing on one another, as illustrated in Fig. 17-4. If the two surfaces, the soffit of the supported member and the ledge of the supporting member, are free of foreign materials, smooth, and coplanar (i.e., the two planes are parallel), the bearing stresses may be within acceptable values, and the connection may perform satisfactorily. On the other hand, if the surfaces are not free of foreign materials, smooth, and parallel to each other when joined, or if rotations occur at the end of the supported member due to the effects of applied loads or solar heating of the top surfaces of the supported member, the bearing stresses may not be at acceptable levels, and failure can occur. Elastomeric bearing pads, among other materials, have been used successfully to avoid the problems associated with "dry" concrete-to-concrete joints (see Sec. 12-9).

Another occasionally encountered source of cracking in precast concrete members is a result of insufficient lengths of bearings at supports or connec-

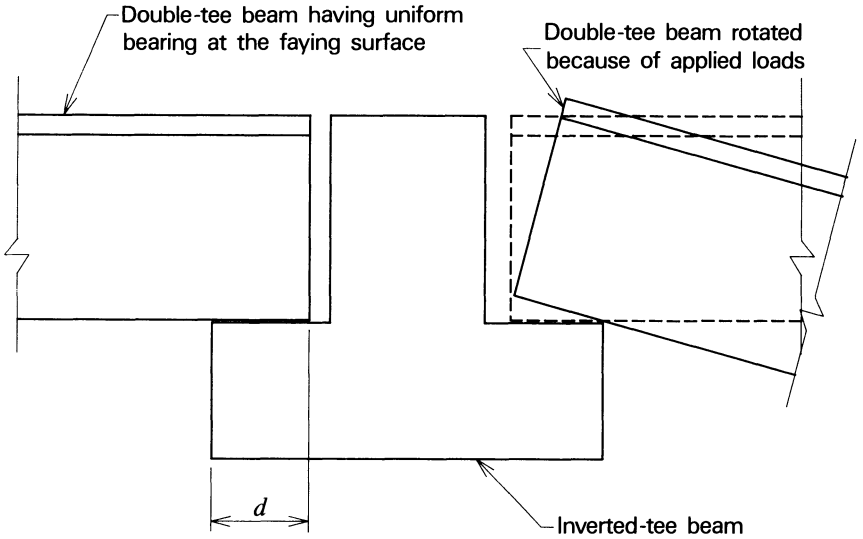

Fig. 17-4. Connection of double-tee beams and inverted-tee beam.

tions. The connection of the stem of a double-tee beam to a cast-in-place ledger is one location where this problem has been experienced. The cracking can be in the form of "heel" cracks in the supported member, in this case the stem of the double-tee beam, or a "toe" crack in the supporting member, in this case the bottom flange of the inverted-tee beam. Several factors can contribute to these types of cracks, including:

1. An insufficient length of bearing. This length is shown as d in Fig. 17-4. The bearing stresses in the concrete of both members are directly dependent upon the length of bearing. This length may be adequate as detailed in the construction documents, but not when the effects of normal precast-concrete manufacturing tolerances are included in the detail. Incorrect location of on-site construction, such as the locations of column and wall foundations, also may cause bearing lengths to be shorter than intended.
2. The horizontal force transferred between the connected members. The transfer may be a result of friction at the faying surfaces, the welding of steel plates embedded in the two members, or another mechanical connection at the location of the supports. The horizontal force can be due to the effects of concrete creep, shrinkage, or temperature change.
3. Rotation of the supported member. The end of the supported member frequently rotates with respect to the supporting member as a result of the application of loads or differential temperature (i.e., a temperature gradient) through the thickness of the supported member.
4. Insufficient anchorage of prestressed reinforcement. The prestressed

reinforcement sometimes does not have an adequate length to develop transfer bond stresses at the end of the supported member.

5. Insufficient anchorage of nonprestressed reinforcement. The anchorage length of nonprestressed reinforcement sometimes is insufficient to develop the required stress in the reinforcement at the ends of the members.
6. Poor quality of construction. Cracking at the connections of precast members sometimes is attributed to the poor quality of the members themselves (i.e., honeycomb, low concrete strength or quality, etc.).

The fact that millions of connections of this type exist and perform in a completely satisfactory way is sufficient proof that many failures that have occurred would have been avoided if the connections had been properly designed, detailed, and constructed (assuming that the failures were not caused by abnormal transient loads such as those from earthquakes and very strong winds).

Settlement of falsework is another type of failure due to unintended performance of supports provided for prestressed-concrete members. The settlement may be due to the normal consolidation of the supporting soils or to other causes. Settlement has been caused by the erosion of soils or by their becoming saturated and losing shear strength when concrete curing water or rainwater was not being diverted away from the soils supporting the construction. Proper attention to all aspects of falsework design and construction can prevent these types of failures.

17-3 Restraint of Volume Changes

The restraint of concrete creep and shrinkage deformations, which was said to be of concern in the design of supports in Sec. 17-2, has been the cause of considerable global cracking in prestressed-concrete structures. These effects must not only be considered locally in a structure having prestressed-concrete components, such as in the design of connections, but also for the structure as a whole (globally).

If the deformations due to elastic shortening, creep, shrinkage, and temperature changes can occur without restraint in a concrete member with prestressed reinforcement, they will not cause stresses in the concrete. If, on the other hand, the deformations due to these effects are restrained, the resulting forces can be large and are limited by the effective force in the prestressed reinforcement and the ability of the restraining member to resist cracking, translation, or rotation.

Prestressed-concrete buildings are more susceptible to the adverse effects of restraint forces than are reinforced-concrete buildings constructed without prestressing. In reinforced-concrete buildings, the creep of concrete tends to reduce the tensile stresses due to concrete shrinkage as well as to increase the transverse deflections of beams and slabs; also in reinforced-concrete buildings, concrete shrinkage has the effect of creating compressive stresses in the

reinforcement and tensile stresses in the concrete, both of which normally are partially relieved by concrete creep and the formation of closely spaced, narrow cracks in the concrete. In buildings in which prestressed concrete is connected to restraining elements, on the other hand, the deformations due to creep and shrinkage of the concrete tend to shorten the prestressed concrete, an effect that in turn transfers a part of the compressive force from the prestressed concrete to the restraining elements; cracking of the prestressed concrete does not reduce the tensile forces in the prestressed reinforcement, but simply transfers the reactions of the prestressing force from the prestressed concrete to the restraining elements (shear walls and frames).

Consider the framing plan of the building shown in Fig. 17-5. The shear walls have been placed at the corners of each of the four sides of the structure to provide stability and resist the effects of lateral loads. This configuration is the least favorable in buildings having prestressed-concrete floors and roofs. Assuming that the building has only one story and the concrete roof is prestressed in each of the orthogonal directions, the tendency for the concrete in the roof to shorten because of the effects of elastic shortening (if the roof is post-tensioned), creep, and shrinkage will be resisted by the shear walls. Considering the deformation in the long direction of the structure, the shortening of the concrete will tend to transfer the prestressing force from the prestressed-concrete roof to the stiff, shear walls at each end of each side of the building. Through arch action, the roof at each end of the building will transfer the forces from the prestressing tendons, from the prestressed-concrete structure between the "arches" at the ends of the building, to the shear walls on each side of the

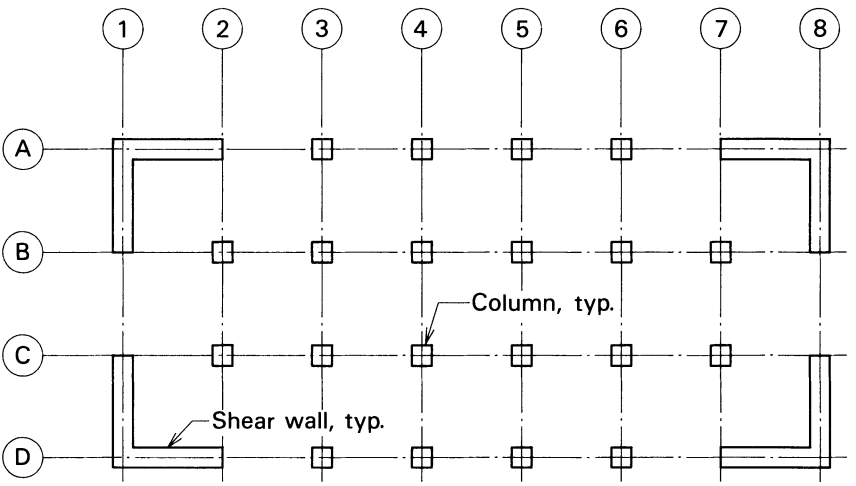

Fig. 17-5. Plan of rectangular building having a prestressed-concrete roof and shear-resisting walls at the corners.

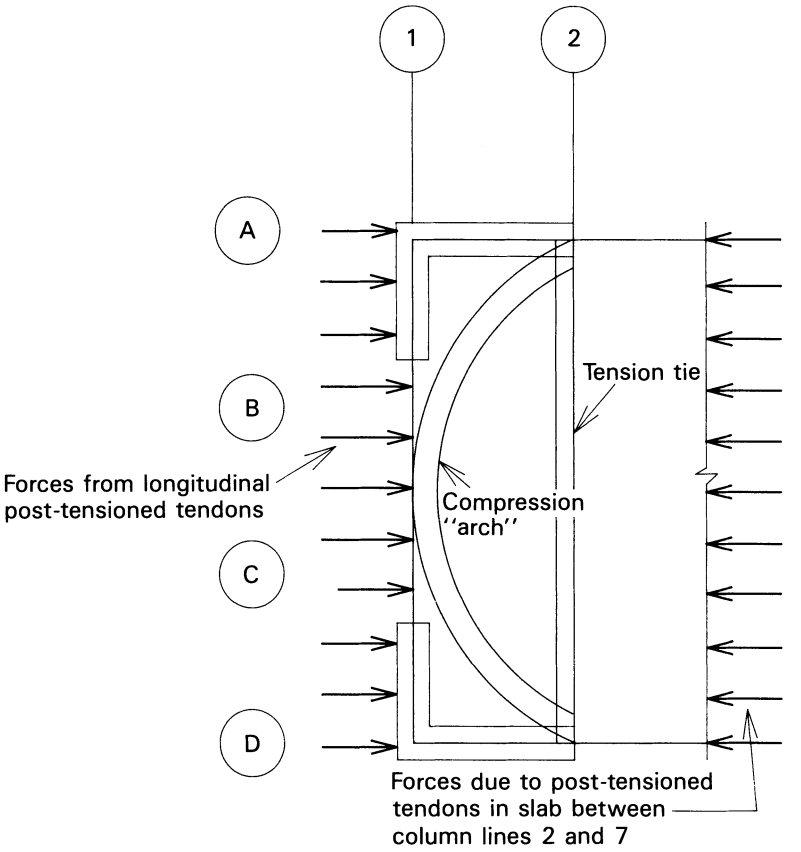

Fig. 17-6. Partial plan of the building shown in Fig. 17-5, showing arch action of the prestressed-concrete roof at one of the narrow ends of the building.

building, as illustrated in Fig. 17-6. If the shear walls are sufficiently strong in shear and flexural strength, as well as able to resist the overturning moment caused by the total effective prestressing force in the longitudinal direction, the entire prestressing force could be transferred to the shear walls. For this to occur, the shrinkage deformation occurring after the roof is connected to the shear walls must be greater than the elastic deformation of the roof due to prestressing. In the narrow direction the roof cannot develop arch action because the depth–span ratio of the diaphragm is not favorable for it. Hence, in the short direction the roof will deform as shown in Fig. 17-7, with a portion of the total prestressing force in the short direction resisted by the shear walls at each end and the remainder resisted by compressive stresses in the concrete in the roof.

The framing plan shown in Fig. 17-8 has the shear walls located near the center of the building length in each of the two orthogonal directions. This is

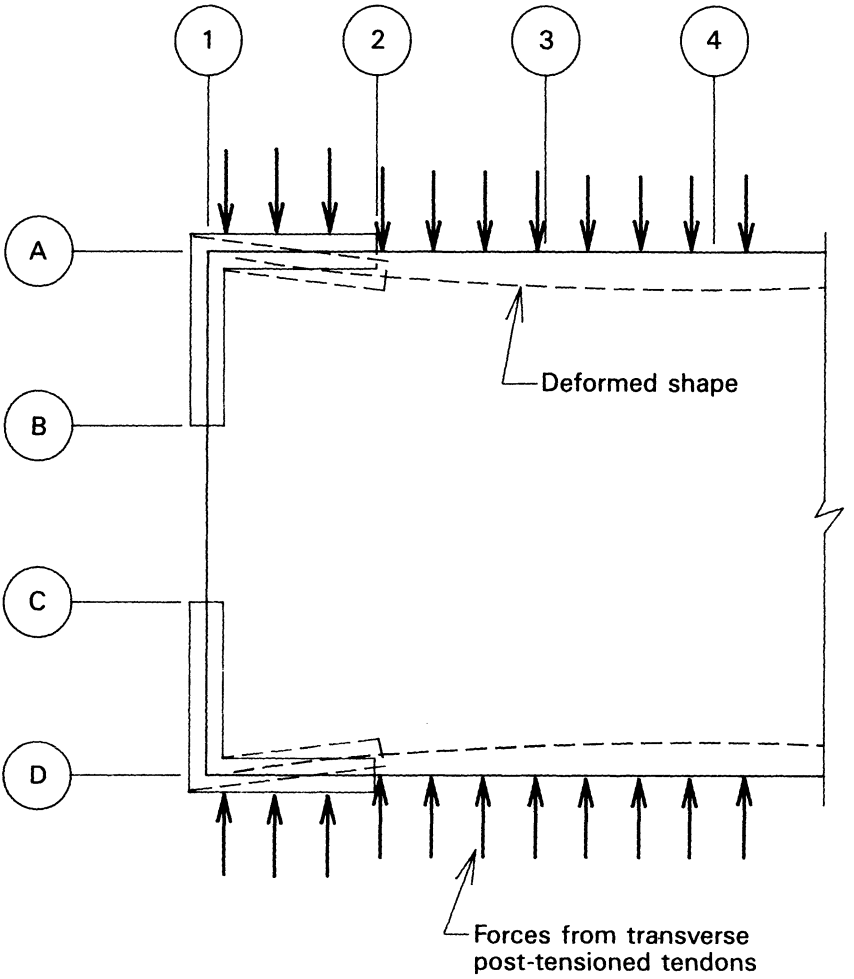

Fig. 17-7. Partial plan of the building shown in Fig. 17-5, showing the transverse deformation of the roof due to the elastic shortening, creep, and shrinkage of the concrete.

the most favorable arrangement of shear walls for buildings with prestressed-concrete roofs and floors because the lateral stability of the structure is provided, with minimum restraint of the creep, shrinkage, and temperature deformations that will occur in the roof and floors. With this configuration, a portion of the prestressing force will be resisted by the shear walls, with an accompanying reduction in the prestressing in the floors or roof in the vicinity of the walls, unless the walls are prestressed by tendons provided in the walls themselves or in the roof areas adjacent to the walls.

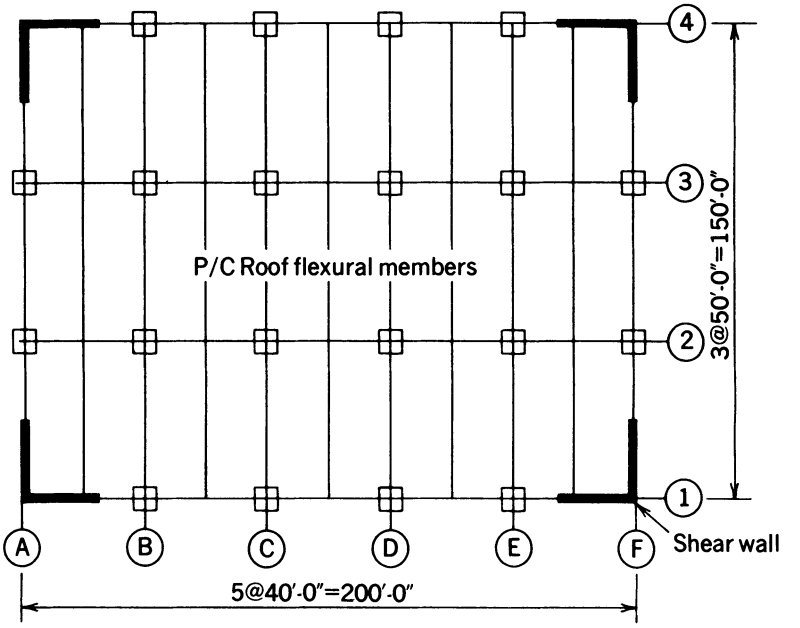

Framing Plan No. 1

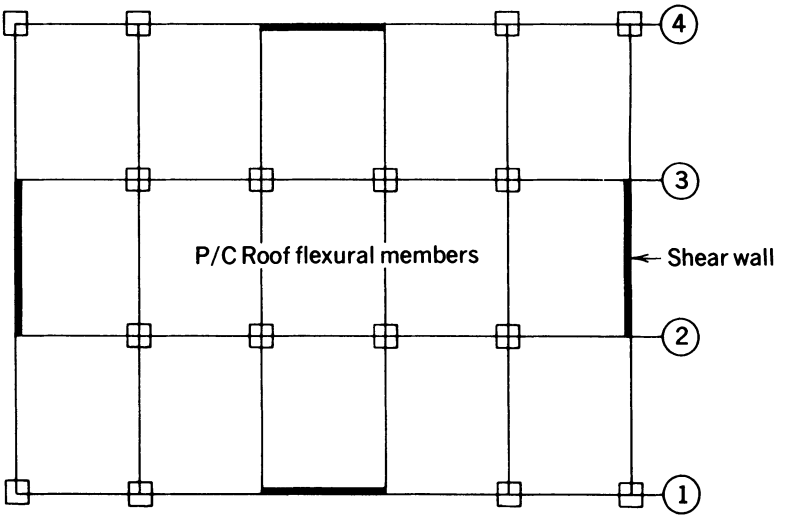

Framing Plan No. 2

Fig. 17-8. Plan of a building with a prestressed-concrete roof and shear-resisting walls near the centers of each exterior wall line.

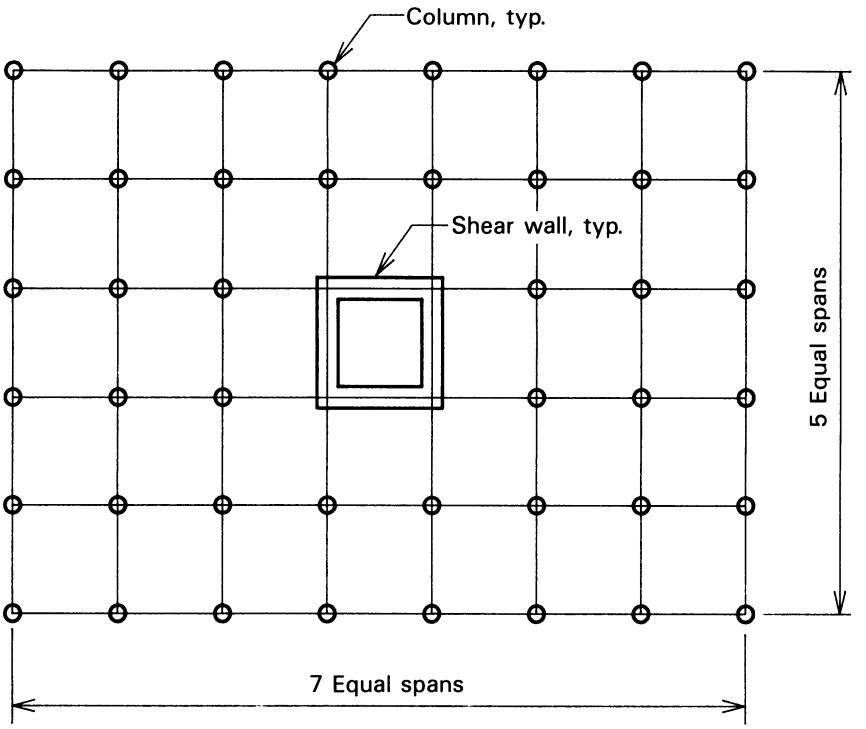

Fig. 17-9. Plan of a building with a prestressed-concrete roof and shear-resisting walls in a core near the center of the structure.

Placing shear walls near the center of square or rectangular buildings, as shown in Fig. 17-9, gives a layout similar to that of the framing plan shown in Fig. 17-8 from the standpoint of roof deformations due to prestressing, creep, and shrinkage. Although this layout should be acceptable in locations with a low risk of seismic activity, its use is not considered appropriate in locations of high seismic risk; high torsional strength is considered necessary for structures that may be exposed to earthquakes.

The effects of restraint of elastic, creep, and shrinkage deformations of concrete are less severe for the upper levels of multistory buildings than for the lowest story. This is so because the deformations, except for the elastic deformation at the time of prestressing, are time-dependent, and if the construction sequence is reasonably rapid, the differential effects of creep and shrinkage deformations are minimized. The lowest story of a multistory building, on the other hand, is similar in behavior to a single-story building with respect to time-dependent deformations. The deflected shapes of two multistory prestressed concrete buildings are shown in Fig. 17-10. One of the buildings has equal story heights throughout the height of the building, and the other has equal story

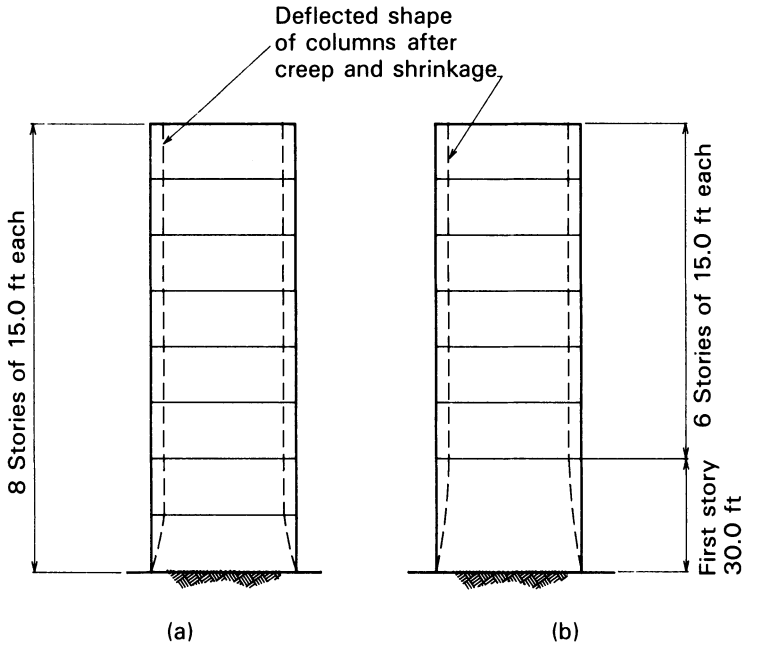

Fig. 17-10. Elevation sections of two multistory buildings having the same heights. (a) Building in which all stories have a height of 15 ft. (b) Building with a first-story height of 30 ft., with the remaining stories having a height of 15 ft.

heights except for the first story, which has a greater height than the others. The longer first-story column lengths in the second building have a favorable effect on the column moments induced by the time-dependent deformations of the prestressed concrete floors and roof.

Cracking in the shear walls and columns of prestressed-concrete buildings, due to the effects of concrete deformation, can be severe. In some cases the cracking has been so serious that new buildings have required repair before being placed in service. Column cracking can be especially serious in split-level parking structures if shear walls are placed at locations that enhance the moments and shear forces in the columns located along the column line between the split levels.

In the manufacture of heat- or steam-cured pretensioned-concrete products, if the curing is stopped before the pretensioned tendons have been released, the concrete members and the tendons exposed between the members cool and contract. The contraction results in an increase in the tension in the exposed tendons between the members because the ends of the tendons are firmly anchored to the abutments of the pretensioning bench. This tensile stress will be aggravated by shrinkage of the concrete if the concrete has not been kept moist during the curing period as well as after the curing has stopped. The

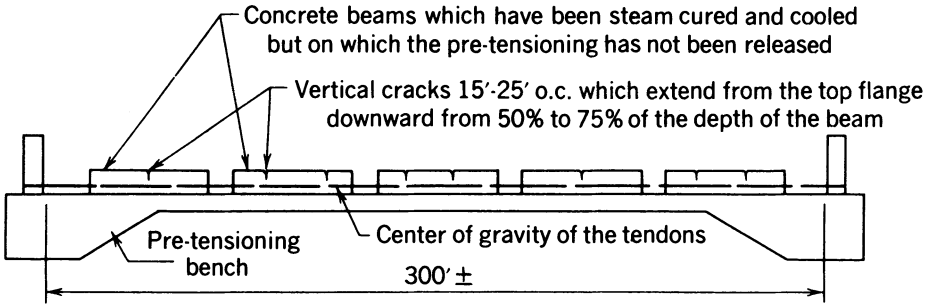

Fig. 17-11. Cracking in pretensioned beams due to shrinkage and temperature deformations aggravated by heat curing.

combined effect can result in the cracking of concrete members at intervals of 15 to 25 ft, as illustrated in Fig. 17-11. In some cases this has resulted in the tendons breaking at the anchorages, which are locations of highly concentrated stresses in the prestressed reinforcement. For this reason, heat or steam curing should never be discontinued for a significant length of time unless the stress in the pretensioning tendons is released (or partially released). If there is a need to discontinue heat or steam curing after a period of time, and the concrete cylinders have not gained sufficient strength to allow the full release of the prestress, the tendons should be partially released to prevent cracking and reduce the risk of tendon breakage. Experience has shown that releasing the tendons about 25 percent of the amount that the tendons would contract if the entire prestress were released is sufficient to avoid cracking. It is best, although not always essential, that the forms be loosened before the partial release is made to avoid the possibility of form damage. Also, a breakdown in the curing facility could result in the cracking of the members; in such an eventuality, under average conditions of design, a partial release of the prestressing force should be made if the concrete strength exceeds 3000 psi.

It is also possible to have relatively wide cracks form in post-tensioned members for similar reasons (temperature drop, concrete shrinkage, or both). This is particularly true in long, large members that have small quantities of nonprestressed reinforcement. The cracks can be avoided by keeping the concrete wet continuously until the main reinforcement is prestressed. In this way, shrinkage deformation will not occur. Another method of avoiding cracking of this kind is to prestress the member, either partially or completely, very soon after curing is completed. In other words, long periods of drying or large temperature variations should be avoided until after the concrete has been prestressed.

The use of unbonded post-tensioned tendons in the construction of buildings in the United States has increased dramatically in the past two decades. They are widely used in the construction of parking, residential, and commercial

buildings, and the increase has been enhanced by changes in allowable stresses at service load in the model building codes. The present codes do not require prestressed concrete to be fully prestressed, and permit the use of partial prestressing with tensile stresses (computed on an uncracked section) exceeding the tensile strength of the concrete. The use of unbonded tendons also has been enhanced by research that has led to the development of alternate tendon-layout configurations for the construction of post-tensioned flat plates. Although this mode of prestressed-concrete construction is used extensively and normally is found to be acceptable from both strength and serviceability standpoints, it frequently results in cracking that is objectionable to some persons. The primary cause of the cracking is the restraint of the concrete deformations associated with prestressed concrete, and not the use of unbonded tendons. The industry appears to recognize this characteristic behavior for this form of prestressed-concrete construction. Some engineers active in the post-tensioning industry suggest that provisions should be included in construction documents for buildings utilizing unbonded post-tensioned tendons to provide for crack repair at a prescribed time after the completion of construction (Aallami and Barth 1989).

When used in the construction of parking structures, unbonded post-tensioned construction often consists of relatively thin, one-way post-tensioned slabs having short spans that extend over beams of considerably greater span and dimension. Cracking frequently is found in the thin slabs (4.5–6.0 in. thick), but not in the thicker and wider beam stems (12–24 in. wide and 36–48. in. thick). It would appear that the cracking in the thinner slabs is enhanced by their drying (and shrinking) more rapidly than the wider beams. In many cases cracking of this type probably could be reduced by water curing the thin slabs over a period of 7 to 14 days, but this step would not be expected to eliminate the cracking.

Some engineers who specialize in the design of buildings prestressed with unbonded tendons advocate providing a caveat on the construction drawings intended to call to the attention of building officials, owners, and contractors the fact that cracking can be expected in cast-in-place post-tensioned buildings, and that in the designer's opinion the presence of cracking is not serious from the standpoints of serviceability and strength.

17-4 Post-tensioning Anchorage Zone Failures

Cracks in end blocks may occur in the loaded face as well as along the paths of the post-tensioned tendons. The cracks are either caused by tensile stresses resulting from the anchorage forces or by an insufficient distance (concrete cover) between the tendon and the edge of the concrete. Control of end-block cracking is best accomplished by providing nonprestressed reinforcing steel in accordance with the methods described in Sec. 8-4, and by providing sufficient

edge distance for the tendons. Concrete quality in the end blocks sometimes is adversely affected by poor concrete consolidation, which is due either to the end block's being congested with reinforcing or to poor workmanship. Congestion—consisting of anchorages, tendons, anchorage zone nonprestressed reinforcement, reinforcement for concrete tensile stresses in the concrete in the vicinity of the supports, and so on—is not uncommon in the ends of beams. However, it is generally preferable to have high-quality, well-compacted concrete at the ends of beams, even if some reinforcement that is considered desirable must be omitted, as opposed to having a beam end that has all the reinforcement considered desirable, but in which the concrete cannot be well compacted.

Occasionally, the concrete in the vicinity of the end anchorages of post-tensioning tendons does not have adequate compressive strength because of poor consolidation or for some other reason. As a result of the low strength, the concrete sometimes fails by crushing at the time of prestressing. This type of failure should not be confused with the splitting type of end-block failures or cracking described in Sec. 8-4. The failures due to splitting tensile stresses are characterized by the concrete in the failed areas being in large pieces, whereas failures due to the crushing of concrete result in severely fractured concrete. The best means of avoiding crushing failures is to take the steps necessary to ensure that the concrete in the vicinity of the anchorages is properly compacted and of good quality.

Concrete crushing failures normally are repaired by removing the fractured concrete and replacing it with good-quality new concrete.

The extreme ends of post-tensioned members have been precast as a means of facilitating the placing and consolidation of the concrete in congested end blocks. When this is done, the end sections normally are cast horizontally rather than in a vertical position. Sometimes they are cast on a vibrating table to further facilitate the placing and consolidating of the concrete.

Large-diameter reinforcing bars placed in the ends of concrete beams in the immediate vicinity of post-tensioning anchorages can result in cracking, spalling, and crushing failures, as the large bars are very rigid and unable to deform in a manner compatible with the deformations of the highly stressed concrete. Hence, the placing of large nonprestressed reinforcing bars in highly compressed anchorage areas should be done with caution, and avoided if possible.

17-5 Shear Cracking

The minimum shear design provisions for prestressed concrete, contained in Chapter 11 of ACI 318-89, are expressed in force relationships but based upon concrete unit-stress considerations. Unfortunately, not all designers understand

this, and this confusion has caused eq. 11-13 of ACI 318 (eq. 6-5 in this book) to be used incorrectly. Shear failures of flexural members have resulted from misinterpretation of the code. The commentary to ACI 318 clearly explains that eq. 11-13 of ACI 318 is intended to predict web-shear cracking when the principal tensile stress is equal to approximately $4\sqrt{f'_c}$ at the centroidal axis of the cross section. Engineers should recognize that when the unit shear stress v_{cw} equals $4\sqrt{f'_c}$ at the centroidal axis (or the intersection of the flange and the web if the centroidal axis is located within the flange), the limiting shear force V_{cw} is equal to the product of the unit stress v_{cw} and $b_w d$, where b_w is the web width. *Note*: The value of b_w should not be taken as the average value of b over the thickness of the beam. This value is illustrated in Fig. 17-12.

Precast prestressed concrete beams sometimes are constructed with overhanging ends and in-span hinges, for use with a suspended or "drop-in" beam. This is done as a means of obtaining distributions of dead- and live-load moments in the completed structure similar to those that would exist in a continuous beam. This configuration is illustrated in Fig. 17-13. Precast beams of this type with post-tensioned tendons have developed cracks following the tendon paths in the overhanging ends. The cracks result from principal tensile stresses, oriented approximately normal to the path of the tendons. This condition of stress occurs at the time when the tendons are stressed only if the large dead-load reaction that is to be supported at the end of the overhang is not in position. This is illustrated in Fig. 17-14a. The vertical component of the prestressing

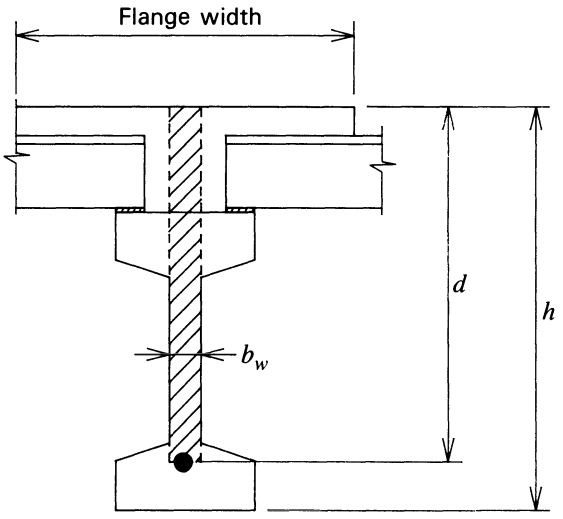

Fig. 17-12. Cross section of a precast prestressed-concrete beam having a composite cast-in-place slab and closure between the ends of double-tee slabs supported by the top flange. The cross-hatched area equals $b_w d$ for eq. 6-5 (ACI 318 eq. 11-13).

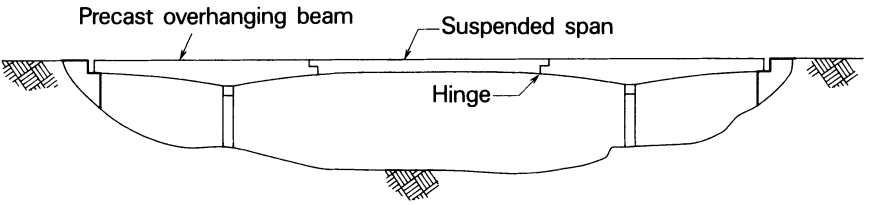

Fig. 17-13. Bridge formed of precast prestressed-concrete girders with overhanging ends supporting precast prestressed-concrete girders suspended from the overhanging ends.

forces in the tendons terminating in the overhanging end of the beam, which act upward in this case, result in large shear forces along the length of the overhanging span (see Secs. 4-6 and 9-9). The dead- and live-load reactions from the suspended span act downward and counteract the upward vertical component of prestressing in the completed structure. This condition is best controlled by stressing some of the tendons before the precast beams are transported to the site, with the remaining tendons being stressed after the suspended span has been erected.

17-6 Tendon Path Cracks

If post-tensioned tendons are grouted during subfreezing temperatures and the concrete member containing the tendons is not protected against freezing, water in the grout that has not hydrated with the cement sometimes freezes. After freezing, the water occupies a greater volume than it occupied before freezing, and the concrete surrounding the frozen water sometimes cracks along the tendon path. Curing the concrete containing the newly grouted tendons with low-pressure steam or moist heat for a short period of time after grouting is an effective way of preventing cracking of this type. In European practice, occasionally some of the mixing water in the grout has been replaced with alcohol during freezing weather for the purpose of lowering the freezing point of the grout and eliminating the cracking. The quality of the grout suffers from this procedure, however, and it can be recommended only under emergency conditions.

Cracks following the paths of post-tensioned tendons have resulted from the settlement of the concrete and the entrapment of water below the ducts in thin-webbed I- or T-shaped members. This is best avoided by using members that do not have unusually thin webs for the size of the ducts being used and by using concrete mixes that have low settlement characteristics.

The use of high pressures in grouting post-tensioned tendons in large ducts also can cause cracks that follow the tendon paths. The risk of this cause of cracking can be evaluated by making simple calculations and comparing the

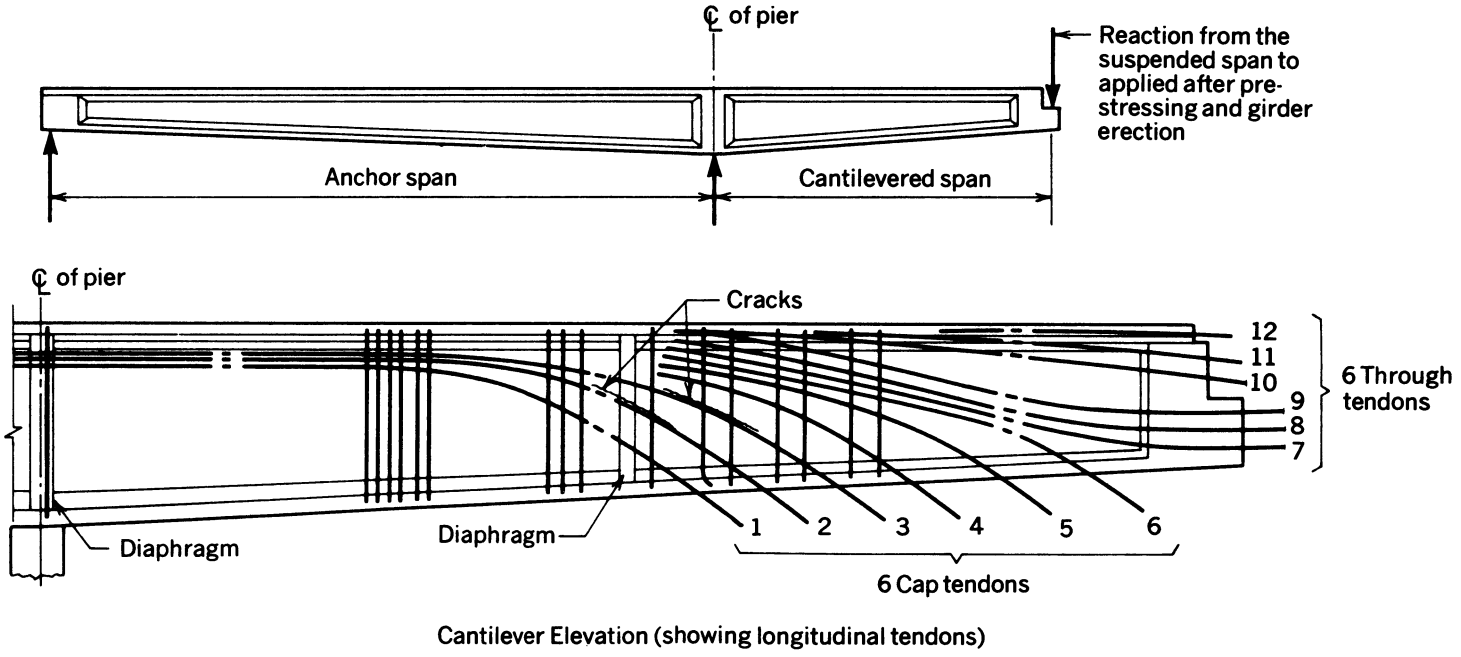

Cantilever Elevation (showing longitudinal tendons)

Fig. 17-14. Bridge beam with an overhanging end span. (a) Elevation of beam. (b) Elevation of overhanging end span showing longitudinal tendons.

tensile stresses in the net concrete section with the anticipated tensile strength of the concrete at the time of grouting. The risk of this type of cracking can be materially reduced and normally eliminated by using grouting pressures appropriate for the size of the tendons being used.

Cracks occurred in the soffits of beams having a combination of post-tensioned and pretensioned tendons, as illustrated in Fig. 17-15. These cracks followed the paths of the post-tensioned tendons in the center portions of the beams where the tendons paths were straight as well as close and parallel to the soffits of the beams. To facilitate the fabrication of the beams, the U-shaped stirrups were oriented with the plane of the stirrup parallel to the centroidal axis of the beams, and thus did not extend transversely across the bottom flange. When first discovered, the cracks were thought to be the result of water freezing in the post-tensioning ducts. Subsequent investigation proved this was not the cause. The cracking was eventually controlled by providing transverse nonprestressed reinforcement in the bottom flanges near the soffit, as shown in Fig. 17-16.

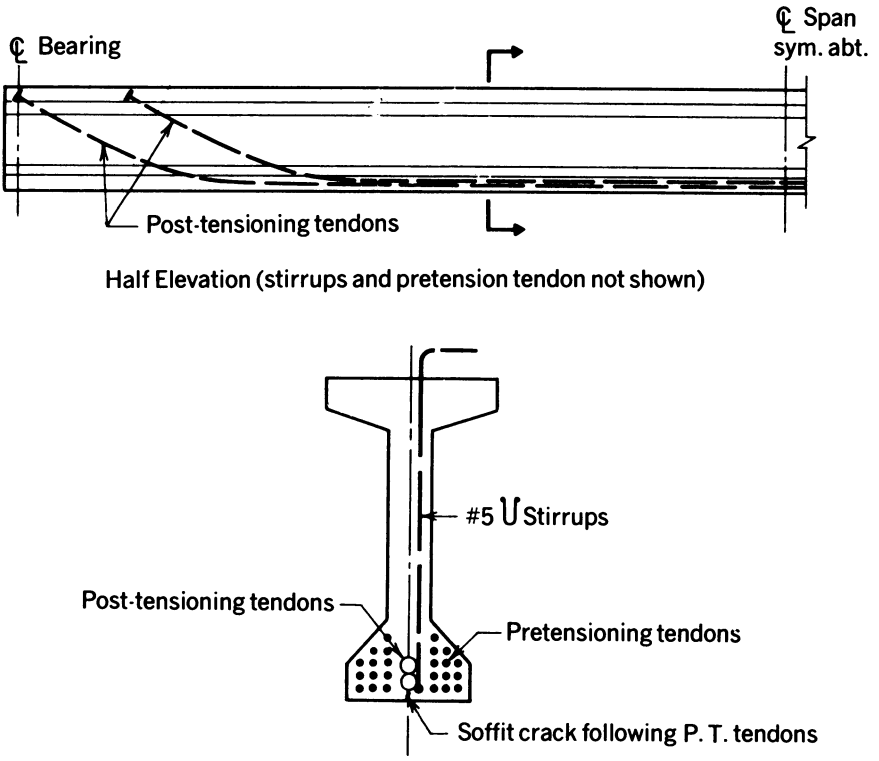

Fig. 17-15. Beam with combined pretensioned and post-tensioned tendons and a crack in the soffit.

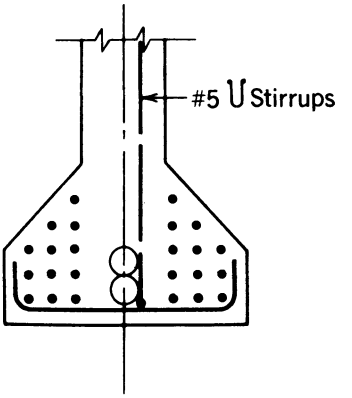

Fig. 17-16. Bottom flange transverse reinforcing.

17-7 Honeycombing

Concrete that has large air voids caused by the failure of the mortar (portland cement, sand, and water) filling the spaces between the coarse aggregate particles is said to be honeycombed. Honeycombing is a result of the concrete's not being completely consolidated. Incomplete consolidation may be due to poor proportioning of the concrete constituents or poor vibration of the concrete during its placing. Poor vibration of concrete frequently is caused by congestion of materials embedded in the concrete (i.e., large quantities of reinforcing steel, other embedded materials, and block-out forms), which inhibits the placing of the concrete in some areas of a member. If the webs of I- and T-shaped members are thin and congested with prestressed and nonprestressed reinforcement, consolidation of the concrete with internal vibrators may be inadequate, with resultant honeycombing.

Honeycombed concrete should be repaired as soon as it is discovered. If concrete curing is continued by keeping the concrete saturated after honeycombing is found, repairs normally can be made that will not adversely affect the strength or durability of the member. The methods of repairing honeycombed concrete contained in ACI 301-84 are recommended (ACI 301 1984).

17-8 Beam Lateral Stability

When long-span precast prestressed-concrete beams are needed, they frequently are designed with narrow flanges as a means of minimizing their weight and cost. If not laterally supported, by a slab or other framing as they normally are in a completed structure, beams with narrow flanges have a tendency to deflect laterally and buckle when lifted, transported, or subjected to transverse load. Precast beams normally have minor imperfections acquired during their fabri-

cation or storage. The imperfections consist of such things as having not been cast perfectly straight, not being perfectly symmetrical about a vertical axis passing through the centroidal axis of the member, having an unintended horizontal eccentricity of the prestressing force, or having a lateral deflection due to solar heating. Although not normally important in the completed structure, the imperfections often create a tendency for the beam to deflect laterally and be unstable under its own dead load alone, during handling and transport. Analytical methods are available for the evaluation of the stability of precast prestressed-concrete beams when suspended from inserts in their tops, as they frequently are during handling in the precasting yard and erection at the job site, as well as when supported at their bottoms on flexible supports, as they normally are when in transport and initially set in place at the job site (Mast 1989).

As a sidelight to this subject, it is interesting to note that the maximum spacing between lateral supports for the compression flange of concrete beams permitted in ACI 318 (Sec. 12.4.1) is 50 times the least width of the compression flange. This code provision, however, is intended to prevent lateral buckling of the compression flange of a beam in a completed structure; it is not meant to apply to the handling and transport of precast concrete members.

17-9 Uniformity of Deflections

The deflection of prestressed-concrete members can present problems during construction when they are significantly different from the deflection anticipated by the structural designer. This difficulty accounts for the use of the detail shown in Fig. 17-17 for precast prestressed-concrete bridge beams used with a cast-in-place concrete deck. The detail anticipates that the deflections of the girders will not be exactly as computed and provides a means of compensating for variations between theoretical and actual deflections. Occasionally, the detail is specified as shown in Fig. 17-18. This detail is not recommended because it cannot be applied to every section of every girder in a bridge; deflection variations between the individual girders prevent this. In addition, when the detail shown in Fig. 17-18 is used, the specified profile and grade of the bridge deck often has to be field-adjusted for the top surface of the finished deck to follow a revised profile that does not compromise the effective depths of the bridge deck reinforcement.

Variations in the deflections of precast concrete beams and slabs used in building construction can present problems during construction if provision has not been made for variations from the theoretical values. Roofing cannot be applied directly to precast concrete surfaces that have abrupt differences in elevation, or over open joints between the individual precast elements, without risk that it will be damaged. For this reason, provisions should be made to

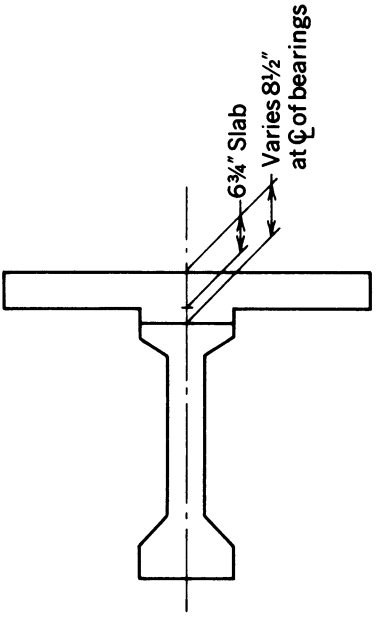

Fig. 17-17. Recommended bridge deck detail.

eliminate the adverse effects of sharp edges and joints where roofing will be applied directly to the surfaces of precast members.

Wind/seismic connections, as discussed in Sec. 12-12 and illustrated in Fig. 12-27, may not align in the erected construction because of differential deflection between adjacent members. If the differential deflection is significant, it may prevent the connection from being completed as shown on the construction

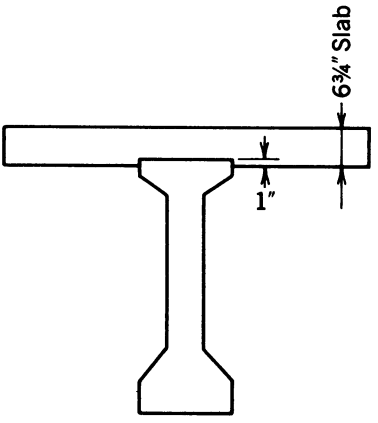

Fig. 17-18. Bridge deck detail that is not recommended.

drawings and intended by the structural designer. This contingency should be addressed in the construction documents. If members having short span lengths, such as those that terminate at a floor penetration, are placed adjacent to members having longer spans, the elevations along the lengths of the members, as well at the intermediate support for the short span, may differ significantly from those of the members having longer spans. This possibility should be addressed in the construction documents and not left for resolution at the construction site.

Floor construction often consists of precast prestressed-concrete elements over which a cast-in-place topping is placed to achieve a smooth, level wearing surface (or a surface having the desired slope). The concrete topping frequently is designed to be bonded to the precast elements and to contribute to the strength of the floor construction through composite action. Conduits for electrical, telephone, and other utilities, which sometimes must cross over each other, frequently are embedded in the cast-in-place topping. The prudent designer will consider these factors in selecting the minimum thickness of the cast-in-place topping as well as in specifying where the minimum thickness is to be provided (i.e., midspan of the precast elements or at their supports).

The variation in deflections between members of identical dimension and composition is undoubtedly the best measure of the quality control achieved in the production of prestressed concrete. It reflects the integration of all the factors that affect the deflections of the members, including the actual physical properties of the concrete, the actual prestressing (i.e., force and eccentricity), the uniformity of concrete dimensions, and so on. The existence of large variations in deflection between members of identical dimensions and materials must be interpreted as an indication of significant variations in the properties of the materials used in the members, the dimensions of the members, and the amount of prestressing force and the eccentricity. A significant difference in age between members that are otherwise identical also can account for a difference in their deflections.

Deflection tolerances and differential deflection tolerances, considered to be normal standards of the industry, have been published by the Prestressed Concrete Institute (PCI 1985). When stricter tolerances are required, the designer is expected to so specify; greater cost must be expected to accompany a reduction in normal tolerances (see Sec. 17-16).

17-10 Composite Concrete Topping

As stated previously, a cast-in-place concrete topping often is placed over the top of precast prestressed-concrete members to provide a flat or level top surface, to increase the flexural strength, to increase the shear strength, to increase the stability of a structure by providing a horizontal diaphragm, or for all of these

purposes. The requirements for horizontal shear strength, as a requisite to reliable composite action in concrete flexural members, are contained in Chapter 17 of ACI 318. The requirements for shear transfer between precast elements and the cast-in-place topping, in construction that does not include nonprestressed reinforcement to tie the two elements together, make it necessary that the contact surfaces be clean, free of laitance, and intentionally roughened. (Intentionally roughened is defined in ACI 318 as the provision of a roughened surface having a full amplitude of approximately 0.25 in.) Although intentional roughening is feasible and straightforward for wet-cast precast elements such as double-tee beams (the most commonly used method of casting concrete), it is not feasible for precast elements, such as hollow-core slabs, that are dry-cast (produced by extruding or slipforming methods). Most manufacturers of wet-cast products, whether they are or are not to be used with composite toppings, do not provide intentional roughening unless it is specified in the contract documents, as it adds to the production cost of precast products. Manufacturers of dry-cast products have proven, through experimental research, that composite action will be provided without intentional roughening, as defined in ACI 318, if these steps are followed correctly:

1. The top surfaces are given a special finish rather than the normally used smooth finish. (The special finish does not, however, provide a roughness equivalent to the 0.25 in. amplitude required by ACI 318.)
2. After transport and erection at the job site, the top surfaces of the products are thoroughly soaked the day before the cast-in-place concrete topping is to be placed.
3. The products are moistened, but not soaked, the day that the concrete topping is placed.

It should be noted that step 1 above normally would be the responsibility of the manufacturer of the precast products, but the other two steps normally would be the responsibility of the purchaser. (Because of this split responsibility, the design professional specifying the use of composite construction that includes dry-cast members should carefully delineate the responsibilities of each of the two parties in the contract documents.)

Experience has shown that composite action is not always achieved as intended by the designer and the contract documents. This may become apparent as a result of failures, or it may be found by accident when, for one reason or another, a "hollow sound" is heard when the surface of the concrete topping is struck with a hammer, or when the structure is surveyed by dragging a heavy chain over the surface of the topping. Coring sometimes is used in investigating the bonding of a cast-in-place topping to precast elements. The cores frequently are studied by using petrographic methods for the purpose of establishing the quality of the concretes used in the construction, as well as the concrete quality

at the very critical interface of the two concretes. The use of a borescope facilitates the examination of the bond of the concrete topping to the precast element at the holes from which cores have been removed. Some engineers question the reliability of using the bond of the topping to the precast concrete in a core removed from the construction; they point out that the coring of the concrete itself may cause the topping and the substrate to become delaminated.

There are literally millions of square feet of precast concrete members that have composite concrete toppings in North America, and the bonding of only a small fraction of a percent of that total area has been questioned. It is believed that composite action can be counted upon with a high degree of confidence if the correct construction methods are used.

17-11 Corrosion of Prestressing Steel

The steel used in prestressing concrete generally is considered to be more sensitive to corrosion than the steel used in nonprestressed reinforced-concrete construction. Furthermore, with the exception of high-strength bars, the steel elements used in prestressing concrete (i.e., wires and strands) are small in comparison to most of the bars used as nonprestressed reinforcement. It is generally agreed, however, that the best protection that the reinforcement can have, whether prestressed or not, is to be surrounded by cement-rich grout or concrete that is well compacted and as impermeable as possible. Grout and concrete are alkaline, and steel has been shown by experiment and experience not to corrode when confined in an alkaline atmosphere.

When the reinforcement is not protected by a sufficient cover of dense concrete and is in a nonalkaline environment that includes oxygen and moisture, corrosion frequently will form on its surface. The products of corrosion, which occupy a volume greater that the uncorroded material, may cause cracking, staining, and eventually spalling of the concrete. Hence, corrosion of the reinforcement must be avoided if reinforced-concrete structures are to have a reasonably long service life.

The use of epoxy-coated reinforcement, for both prestressed and nonprestressed reinforcement, has gained popularity in recent years as a means of protecting ferrous reinforcement against corrosion. Its use, however, generally is limited to bridge decks, marine structures, and large projects where corrosion is a major concern.

The strands shown in Fig. 17-19 were first noticed by a spalled area in the top surface of the prestressed concrete deck of a wharf. The strands were corroded completely through by the action of seawater, which found its way to the upper surface of the deck during heavy storms. The strands were embedded in a mortar-filled joint between precast slabs, and the portland cement mortar, made with a $\frac{3}{8}$-in. maximum-size aggregate, had not been well compacted.

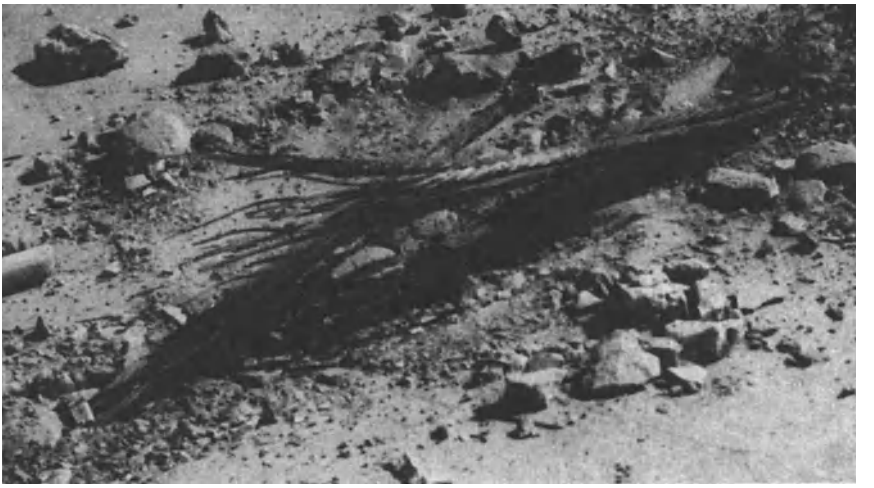

Fig. 17-19. Corroded post-tensioned tendon.

Consequently, the strands were not completely embedded in a cement-rich environment. It is interesting to note that, on the same wharf, a grouted post-tensioned tendon that was exposed to alternating wetting and drying from seawater when a prestressed-concrete pile was damage by the impact of a ship, had bright wires when its sheath was opened and the grout removed. This case clearly demonstrated the ability of portland cement grout to protect tendons in a corrosive environment.

The action of chloride ion, which is present in some premixed compounds formulated for making non-shrink concrete, mortar, and grout, was found to have caused corrosion at the end anchorages of post-tensioning tendons. The non-shrink concrete had been used to replace the concrete under a post-tensioning anchorage that had crushed during stressing. It is believed that the non-shrink concrete was porous and permitted rainwater to penetrate through the patch and reach the anchorage and tendon. This moisture, in combination with the chloride ion and perhaps the metallic aggregate in the premixed material, resulted in the wires being severely corroded in the areas adjacent to the repairs. The use of non-shrink aggregates is not recommended in prestressed concrete construction unless it is first confirmed they do not contain chemicals that are harmful to prestressed reinforcements.

Stress corrosion, which was described in Sec. 2-11, has been blamed for the failure of prestressing wire on at least two projects in North America. One project consisted of prestressed-concrete pipe in which some of the pipe concrete contained calcium chloride and some did not. Stress corrosion was found in varying concentrations in all the pieces of pipe made with concrete containing

calcium chloride, whereas none was found in any pipe that did not contain calcium chloride. Based on this experience, it seems obvious that calcium chloride (and probably any material containing the chloride ion) should not be used in prestressed concrete (Monfore and Verbeck 1962). On the second project, some post-tensioning wires were left ungrouted (after they had been stressed) for a period of several months because of certain difficulties experienced in the construction. When the work was resumed, it was found, upon prestressing of the previously stressed tendons, that some of the wires had corroded and broken. It is believed that this failure would not have happened if the tendons had been grouted reasonably soon after prestressing. New tendons that replaced the corroded ones have given good service for over 35 years.

17-12 Grouting Post-tensioned Tendons

The equipment currently used for mixing and injecting grout into post-tensioned tendons is much more efficient than that used when post-tensioning was introduced in the United States. However, from time to time difficult still will be experienced in grouting, due to such problems as the grout being improperly mixed or proportioned, cement lumps in the grout, improper flushing of the ducts prior to grout injection, unintended obstructions in the post-tensioning ducts, or malfunction of the equipment. A frequent result is that one or more tendons may become partially grouted and plugged before grout has filled the entire duct.

To salvage members with partially grouted tendons, holes must be drilled into the post-tensioning duct with great care to avoid damaging the tendons. The extent of the grouting and the location of obstruction can be determined by a systematic drilling of holes along the length of the tendon. After the extent of the grouting has been determined, the tendons should be flushed with lime water, which is alkaline, and the empty portions of the tendons grouted. The holes drilled to determine the locations of the obstructions in the ducts are used as grouting ports. Grouting procedures are described in Sec. 16-8.

17-13 Coupler Damage

Post-tensioning tendons sometimes are provided with couplers to accommodate a particular construction procedure or to make long tendons out of two or more short ones. The couplers normally are considerably larger in diameter than the tendons and must be provided with a housing larger than the duct in which the tendons are placed, to prevent them from becoming bonded to the concrete. In addition, the housing forms a space for the coupler to move during the stressing operation. If, during stressing, the tendon is released through tendon breakage or some other mishap, or if the distance provided in the coupler housing is not

sufficiently large, the coupler may come to bear on the concrete at the end of the housing. Experience has shown that this can cause spalling of the concrete in the vicinity of the housing.

Care must be taken to ensure that the housings for the couplers are large enough, and that the couplers are properly located in them when the tendon is stressed. If this is not done and the concrete is damaged because of the coupler bearing on the concrete at the end of the housing, the tendon must be unstressed, the fractured concrete removed, and a patch applied to the member. Patches of this type must be applied with care. The use of epoxy mortars may be preferred because this type of damage normally would occur sometime after the curing of the concrete has ceased.

17-14 Dead End Anchorages

Frequently, for one reason or another, it is either necessary or convenient to stress post-tensioned tendons from one end only. When this is done, the end of the tendon where the stressing is done is called the stressing end, and the nonstressing end is frequently referred to as the dead end. In some cases when one-end stressing, is used it is more convenient to use a dead end anchorage that is embedded in the concrete and thus inaccessible during the stressing operation. Care must be taken when inaccessible dead end anchorages are used because it can be very costly to correct dead end anchorages that do not perform as intended.

Wedge-type post-tensioning anchorages at the nonjacking end of tendons must move when the tendons are stressed. The transverse forces that anchor the tendon can be developed only if the wedge moves. Hence, when wedge-type anchorages are used as dead end anchorages, provision must be made to ensure that the tendon and the wedge can move during stressing. If the anchorage is embedded in concrete, provision must be made to prevent the concrete from coming in contact with the wedge and tendon. Details of dead end anchorages vary from one post-tensioning system to another; hence, specific details should be obtained from the suppliers of post-tensioning anchorages.

Dead end anchorages, frequently referred to as pigtail anchorages, have been made by embedding the nonstressing ends of parallel wire and strand tendons in loops or a spiral configuration. An anchorage of this type is shown in Fig. 17-20. Most suppliers of post-tensioning materials supply variations of pigtail anchorages for strand tendons (i.e., post-tensioning anchorages that rely upon bond stresses to anchor the dead end). The method has the advantage of saving the cost of regular anchorage hardware, but it must be executed correctly, or the anchorages will fail from insufficient bond strength, excessive compressive stresses, or spalling of the concrete. When looped or curved wires or strands are used for dead ends, it is recommended that the radii of the bends be computed

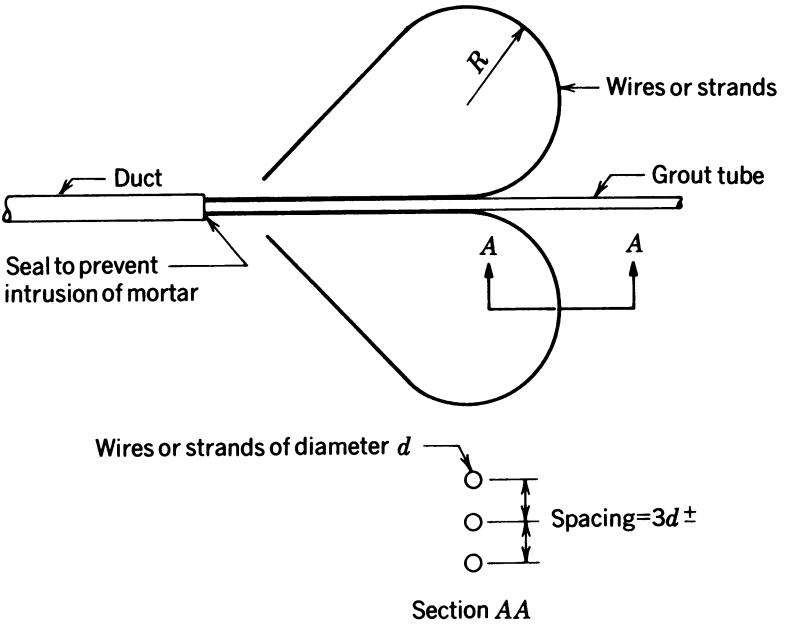

Fig. 17-20. Looped or pigtail anchorage.

by using the relationship for secondary stresses due to tendon curvature given in Sec. 8-11. The bearing stress between the tendons and the concrete should not exceed the compressive strength of the concrete test cylinders. In addition, it is recommended the individual wires or strands in a tendon be carefully held apart with spacers, as shown in Section *AA* of Fig. 17-20, to ensure that each wire or strand will be completely embedded in well-compacted concrete. The wires or strands should not be bundled in the curved portion where bond stresses are developed for anchorage. The concrete in the vicinity of the anchorage should be provided with supplementary nonprestressed reinforcement. If at all possible, tests should be made on the anchorages, with the concrete and details designed for a specific project, to confirm their adequacy before use.

17-15 Congestion of Embedded Materials

The concrete sections of buildings, bridges, and other structures frequently are congested with nonprestressed reinforcement, prestressed reinforcement, end anchorages for post-tensioned tendons, inserts for lifting precast members, expansion joints including their anchorages, anchorages and sole plates for bearings, and other embedded materials and blockout formwork. The most serious congestion normally exists at the ends of flexural members and the intersections of structural members. Frequently, the congested areas are at the locations of the tops of bridge piers where the pier reinforcement, the pier cap

reinforcement, and the superstructure reinforcement come together from all three directions. In buildings the most serious problems with congestion occur where beams, girders, and columns intersect. The problem is the most severe in reinforced concrete frames designed to be ductile.

With designs made and detailed in such a way that it is physically possible to place all of the specified embedded materials as detailed, contractors, often find it is very difficult to place and consolidate the concrete. The problem sometimes is worsened by concrete specifications that require a low slump and relatively large maximum aggregate size. No matter what others may believe, structural designers often are not free to do all they would like to do to mitigate problems of this type. The engineers frequently cannot control the overall dimensions of a structure and must conform to design criteria mandated by law, their contract with their client, or the standard of practice for structural designers. It is important that structural designers be aware of this serious problem and do what they can to facilitate construction.

17-16 Dimensional Tolerances

The owners, designers, and constructors of prestressed concrete structures all should be aware of the dimensional tolerances published by trade and professional organizations that are intended, by the authors, to apply to various aspects of prestressed-concrete members. Relevant documents include publications of the American Association of State Highway and Transportation Officials, the American Concrete Institute, the Precast/Prestressed Concrete Institute, the Concrete Reinforcing Steel Institute, The Post-Tensioning Institute, and numerous government agencies (which are frequently the designers and owners of projects).

The construction documents prepared by structural designers frequently do not address the question of acceptable tolerances to the extent needed to make the intent of the designer and the requirements of the construction contract clear and unambiguous. One reason for this is that there is no single published "super" standard on tolerances that addresses the need for integrating the tolerances published by the different construction trades, owners, government agencies, and professional organizations. If such a document existed, it would be a simple matter for designers to state in the construction documents that the tolerances in the "super" standard should be used unless other values are specified in the specifications (or special provisions) for a specific construction project.

This problem has plagued the construction industry for many years, and many different examples could be given to illustrate the problem; but, for the purpose of this discussion, consider the shear reinforcement and other reinforcement that must be coordinated with the shear reinforcement in the cast-in-place post-tensioned box-girder bridge cross section shown in Fig. 17-21. Assuming that

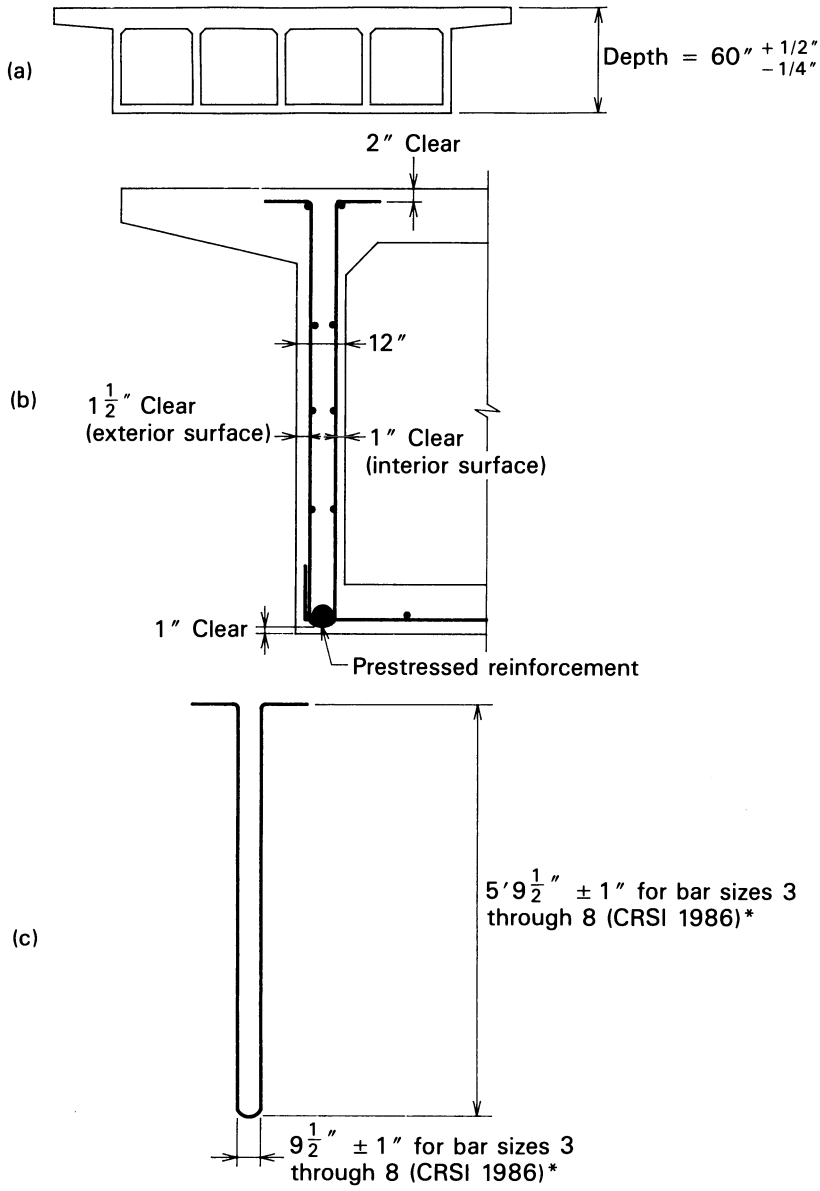

*ACI 315-1980 provides maximum tolerances of ± 1″ for bar sizes 3, 4, and 5 only; provisions for larger bar sizes are not included in ACI 315 1980. It should be noted that the tolerance of ± 1″ is applicable if the total length of the bar exceeds 12.0 ft. If the total length of the bar is less than 12.0 ft, the maximum tolerance would be ± ½″

Fig. 17-21. Cast-in-place prestressed-concrete box-girder bridge details. (a) Cross section. (b) Detail section of the exterior girder. (c) Detail of a typical stirrup.

Standard Specifications for Highway Bridges (AASHTO 1989) was used in the design, the designer would note that Sec. 8.22.1 of Division I of the standard requires a minimum concrete cover of the reinforcement of 2.0 in. and 1.0 in. at the top and bottom surfaces of the section, respectively, and, in addition, would take the following part of Sec. 8.27 of Division II of this standard into account in detailing the bridge:

> 8.27.1 Shear reinforcement shall extend at least to the centroid of the tension reinforcement, and shall be carried as close to the compression and tension surfaces of the member as cover requirements and the proximity of other reinforcement permit. Shear reinforcement shall be anchored at both ends for its design yield strength.
>
> 8.27.2 The ends of single leg, single U, or multiple-U stirrups shall be anchored by one of the following means:
>
> 8.27.21 A standard hook plus an embedment of the sitrrup leg length of at least $0.5l_d$ between the mid-depth of the member $d/2$ and the point of tangency of the hook.
>
> 8.27.2.2 An embedment length of l_d above or below the mid-depth of the member on the compression side but not less than 24 bar or wire diameters or, for deformed bars or deformed wire, 12 inches.
>
> 8.27.2.3 Bending around the longitudinal reinforcement through at least 180 degrees. Hooking or bending stirrups around the longitudinal reinforcement shall be considered effective anchorage only when the stirrups make an angle of at least 45 degrees with the longitudinal reinforcement.
>
> 8.27.2.4 For each leg of welded smooth wire fabric . . .

In addition, Sec. 5.6.1 of Division II of the AASHTO standard states in part:

> Steel reinforcement shall be accurately placed in the positions shown on the plans and firmly held during the placing and setting of concrete. Bars shall be . . .

Based upon the above, one can understand why the designer would detail the stirrups as shown in Fig. 17-21b *and expect them to be placed exactly as shown without tolerance* (because the AASHTO specification does not include placing tolerances for concrete reinforcement). The fabricator of the reinforcing steel, not finding more restrictive requirements in the job specifications, would rely on the tolerances published by either the American Concrete Institute or the Concrete Reinforcing Steel Institute and assume that stirrups would be acceptable if bent as shown in Fig. 17-21c (ACI 315 1980; CRSI 1986). The carpenters, in building the forms for the section, noting that the AASHTO standard

does not specify tolerances for the forms in Sec. 2.4.19, may choose to rely on the formwork tolerances in ACI 117-81 and consider that they have complied with the standard of practice if the forms were constructed within the tolerances shown in Fig. 17-21a. Thus it is apparent that with the tolerances the reinforcing steel fabricator and the carpenters consider appropriate, the clear cover of the reinforcement at the top and bottom of the stirrup could be as little as 1.25 in. or as great as 4.0 in., rather than the 2.5 in. the designer specified on the drawings.

The tolerances considered standard for precast concrete products by the Precast/Prestressed Concrete Institute are published in Chapter 8 of the *PCI Design Handbook* (PCI 1985). It is interesting to note that the PCI recognizes the importance of clearly assigning the responsibility for tolerances in contract documents, and of considering tolerances as part of the conceptual design. Section 8.1.4 of the *PCI Design Handbook* emphasizes the problem of the accumulation of tolerances and the need for contract documents to clearly note special tolerance requirements.

In addition to dimensional tolerances, the principal individuals involved in the design and construction of prestressed concrete should be aware of the tolerances contained in the commonly used standard specifications for the various materials used in prestressed concrete construction.

The designer should give consideration to the dimensional tolerances that might be expected in the construction of prestressed concrete. Special allowances may be required to provide for the fact that concrete members cannot be made to exact dimensions, as is the case with members made of other materials.

Cast-in-place prestressed concrete can be expected to be built within the same dimensional tolerances that one would expect for nonprestressed reinforced-concrete construction. In the case of precast concrete, the designer should specify the maximum dimensional tolerances that he or she is willing to accept. It should be recognized that exceptionally small permissible tolerances would be expected to increase the cost of precast members.

Dimensional tolerances, which may be specified by reference, are contained in *Standard Tolerances for Concrete Construction* (ACI 117 1981) for cast-in-place construction, in *Details and Detailing of Concrete Reinforcement* (ACI 315 1980) for nonprestressed reinforcement, and in the *PCI Design Handbook* for precast prestressed-concrete members (PCI 1985).

17-17 Falsework Design

Cast-in-place prestressed-concrete structures normally are constructed on falsework. The requirements of the falsework are very similar to those for nonprestressed-concrete construction with this very important exception, explained in Sec. 17-2: The act of post-tensioning the reinforcement can result in a redistri-

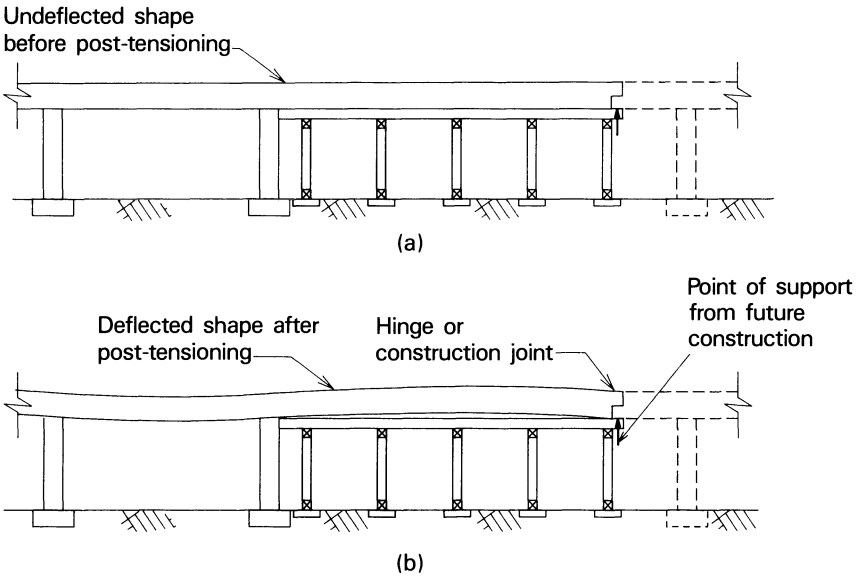

Fig. 17-22. Cast-in-place prestressed-concrete bridge with an in-span hinged or construction joint. (a) Before prestressing with all shores supporting load. (b) After upward deflection due to prestressing and a large reaction being supported by the falsework bent at the joint.

bution of the dead load that can be critical to the strength and stability of the falsework. This must be taken into account in simple beams, as illustrated in Fig. 17-2, and in beams that are continuous on one end and have a construction joint or in-span hinge at the other, as illustrated in Figs. 17-22 and 17-23.

Experience has shown that falsework requires lateral bracing if it is to resist the effects of lateral loads. The lateral loads may be due to wind or impact forces due to vehicular or other types of accidents. (It generally is agreed that it is not economically feasible to design construction falsework for the effects of earth-

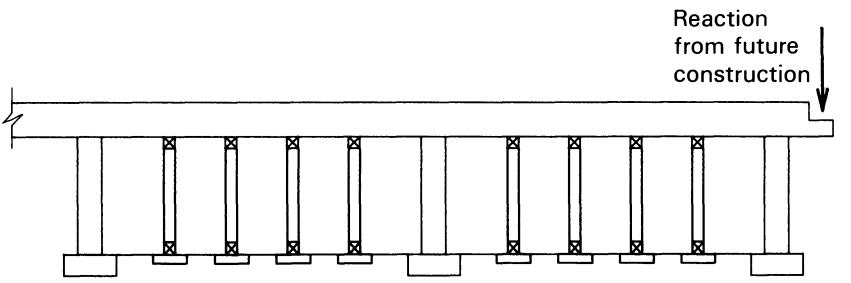

Fig. 17-23. Cast-in-place prestressed-concrete bridge with an in-span hinge or construction joint.

quake.) The bracing provided falsework that is to support prestressed-concrete construction should be designed to be effective for the condition of loading before post-tensioning and after post-tensioning.

Guidance for the design and construction of falsework for cast-in-place concrete construction can be found in *Standard Specifications* (CALTRANS 1988).

17-18 Constructibility

Problems in construction have been associated with prestressed concrete since it was introduced in North America. Although some of the problem related to the construction of post-tensioned structures can exist in members with pretensioned reinforcement, this discussion of constructibility is confined to prestressed, post-tensioned concrete. Post-tensioned prestressed-concrete structures are constructed most often by a general contractor for a specific project on a job site with details and conditions that vary from site to site. Pretensioned prestressed concrete most often consists of plant-produced members having standard details, made on a routine basis by an organization involved in the routine manufacture of precast concrete products. Hence, constructibility issues are routinely resolved in-house by the producer without the constructibility disputes associated with post-tensioned prestressed concrete.

The primary sources of the problems commonly heard from general contractors that relate to the constructibility of post-tensioned concrete structures can be categorized as follows:

1. *Congestion of Embedded Materials.* The materials that are to be embedded in the concrete at some locations, as described in greater detail in Sec. 17-15, sometimes are difficult or even impossible to place as specified on the contract drawings; or if the embedded materials are successfully placed, it is difficult or impossible to place and consolidate the concrete as specified in the contract documents.
2. *Anchorage Zone Reinforcement.* The sizes, shapes, and quantities of nonprestressed reinforcement needed in the anchorage zones of post-tensioned tendons, for the purpose of resisting the effects of tensile splitting and spalling stresses, should be clearly specified in the contract documents. The general contractor should not be made responsible for the design and details of anchorage zone reinforcement.
3. *Interference of Embedded Materials.* The contract drawings should be complete in details and dimensions. It should be possible to place all specified embedded materials, forms for blockouts, concrete, and so on, without interference from the embedded materials and the forms.
4. *Tolerances.* The dimensions of the concrete section, dimensions of embedded materials, and other dimensions that relate to the dimensions of the concrete section and the embedded materials (e.g., concrete clear cover to

reinforcement) should not preclude the use of standard tolerances contained in the publications of trade associations, professional organizations, or the owner.

5. *Erection Methods.* Conceptual structural erection schemes included in contract documents should be workable schemes that provide the clearances necessary for construction operations (i.e., clearance for prestressing jacks, forms, precast elements, etc.) and should identify all materials, both temporary and permanent, needed for the scheme to be workable (Gee 1989).

6. *Geometric Control.* The contract documents should clearly define which of the two parties of the contract (i.e., owner/engineer or general contractor) is responsible for the analytical and field geometric control of segmental structures, cable-stayed structures, etc., during their construction.

7. *Quality Control.* Contract documents should contain specific information on all quality control methods, procedures, or equipment, other than the usual construction equipment and labor responsibilities normally recognized to be the responsibility of the contractor.

The following comments are offered as the author's opinions on how the responsibilities for these problems should be delegated to the parties involved. They are presented in the order in which the problems were listed.

For many years manufacturers of precast concrete products have been aware of the need to identify areas of possible congestion and interference of embedded materials and to resolve the problems, if any, before commencing production. To accomplish this, they have relied upon well-prepared, complete shop drawings. Some of the shop drawings have been drawn to large scales (even full size in some instances) for whole products or portions of products where insufficient clearances or interferences would appear to exist; reinforcing bars must be drawn to their *actual* size, not their nominal size. Skilled and experienced general contractors use these methods as well. This is the obvious solution for avoiding problems of interference between embedded materials and unacceptable congestion in structural concrete members (items 1 and 3 above). It would seem appropriate for the designer to prepare drawings of this type for cast-in-place prestressed-concrete construction, to the extent possible, before the plans and specifications are advertised for bidding. However, the designer can perform these studies only after assuming specific details for the post-tensioning tendons, end anchorages, other embedded materials, and construction methods; if the contractor elects to use post-tensioning details and embedded materials other than those assumed by the designer in the design analysis, the onus should appropriately be on the contractor to identify problems related to constructibility with the materials and construction methods that he or she selects. It also would seem appropriate for the engineer to identify the assumptions that he or she has made in performing a constructibility analysis for congestion and interference. This would assist in identifying responsibility for this aspect of the work in the event of a dispute.

Anchorage zone reinforcement details and quantities present a problem to the

designer of a post-tensioned structure that must be left open to competition during bidding for all available post-tensioning systems—a customary requirement in public works in North America. To design anchorage zone reinforcement correctly, the engineer must know the sizes of the tendons to be used and their exact locations and spacings, as well as the dimensions and details of the end anchorage including any peculiarities of the anchorage that might influence the details of the anchorage zone reinforcement. One obvious solution to the dilemma is for the engineer to assume that a particular post-tensioning system will be used, and to detail the anchorage zone reinforcement for that particular system and make provisions in the contract documents that if other systems are used, the anchorage zone reinforcement must be redesigned at the expense of the contractor. Some owners may not permit this procedure and may not be willing to assume the additional cost of the engineering it would entail. If the successful bidder elects to use a post-tensioning system different from the one used by the engineer, the contractor must provide new details of post-tensioning and anchorage zone reinforcement, satisfactory to the engineer, detailed for use by the system that the contractor chooses. There does not seem to be an easy solution to this problem, but one thing is certain: if the anchorage zone reinforcement is not shown on the contract drawings, the contract documents should make all bidders well aware that this is the case and that the onus is on the successful contractor to provide anchorage zone reinforcement as required for the post-tensioning method that he or she elects to use. Design criteria, acceptable to the owner or engineer, for the anchorage zone reinforcement should be included in the contract documents for the information of the bidders.

Construction tolerances normally do not present serious constructibility problems in the contemporary cast-in-place post-tensioned concrete construction designed by experienced engineers. This has not always been the case, however. There have been disputes over tolerances on this type of project in the past, but, through the cooperation of contractors and engineers, details and methods for avoiding the problems have evolved. Contract documents should be very clear with respect to the tolerance requirements for each specific project. It would seem appropriate for the contract documents to contain graphical and written requirements for the following:

1. Specific tolerances for the actual as-constructed dimensions of the concrete sections, together with a clearly stated method for their measurement.
2. Specific tolerances for the outside dimensions of nonprestressed reinforcement after fabrication, together with a procedure for measurement and confirming its compliance before it is installed.
3. Specific methods for combining the tolerances for embedded items, dimensions of the concrete section, and concrete cover requirements.
4. Specific remedial measures that would be permitted in the event that the specified tolerances are exceeded.

In addition, the contract documents should identify all materials or dimensions that require tolerances that are more restrictive than those specified in trade association documents and consensus standards of organizations related to the construction industry.

The engineer clearly is obligated not to mislead the bidders with respect to erection methods or procedures. All assumptions as to construction loads, sequence of construction, or other limitations used in the design must be clearly stated in the contract documents. If construction engineering analyses, temporary prestressing, materials not shown in the contract documents, and so on, are needed for certain erection procedures, the bidders should be so advised in the contract documents.

The need for clearly defining responsibility for construction surveying, geometric control, testing and inspection, and any uncommon testing requirements such as load tests, strain measurements, stress measurements, and so forth, not normally and routinely performed by a general contractor or subcontractor, should be made very apparent in the contract documents.

REFERENCES

Aalami, B. O. and Barth, F. G. 1989. Restraint Cracks and Their Mitigation in Unbonded Post-Tensioned building Structures. *Cracking in Prestressed Concrete Structures.* Detroit: American Concrete Institute.

ACI Committee 117. 1981. *Standard Tolerances for Concrete Construction.* Detroit. American Concrete Institute.

ACI Committee 301. 1984(88). *Specifications for Structural Concrete for Buildings.* Detroit. American Concrete Institute.

ACI Committee 315. 1980 (revised 1986). *Details and Detailing of Concrete Reinforcement.* Detroit. American Concrete Institute.

American Association of State Highway and Transportation Officials. 1989. *Standard Specifications for Highway Bridges.* Thirteenth Edition, Washington, D.C.

CALTRANS. 1988. *Standard Specifications.* Sacramento. State of California, Department of Transportation.

Concrete Reinforcing Steel Institute. 1986. *Manual of Standard Practice.* Schaumburg, Illinois.

Gee, A. F. 1989. Constructibility of Bridges—A Construction Engineer's View. *Concrete International Design and Construction.* Detroit: American Concrete Institute. 11(5):48-52.

Mast, R. F. 1989. Lateral Stability of Long Prestressed Concrete Beams. *PCI Journal.* 34(1): 34-53.

Monfore, G. E. and Verbeck, G. J. 1962. Corrosion of Prestressed Concrete Wire in Concrete. *ACI Journal.* 32(5): 491-515.

PCI Design Handbook. 1985. Chicago: Prestressed Concrete Institute.

18 Erection of Precast Members

18-1 Introduction

The availability of adequate erection equipment and the feasibility of using the equipment on a specific job site are important considerations in determining whether the use of precast prestressed concrete is appropriate for a specific project. Both factors can have a significant effect on the cost of erecting precast concrete structures. The availability of erection equipment of adequate capacity is of particular importance in the planning and construction of medium- and high-rise buildings where the use of precast concrete is being considered. High reaches require cranes with long booms, and equipping a crane with a long boom can have a significant adverse effect on its lifting capacity. Large mobile cranes of the types required to erect the larger precast members are costly and, most important, are not readily available in all localities. In bridge construction, the use of mobile cranes to erect precast members may not be feasible because of the weights and reaches involved, limited access to the site, the risk of floods, vehicular traffic, or other considerations. The designer must give careful consideration to all the factors affecting the methods that can be used in the construction of a proposed structure, including erection, for each individual structure, and must prepare a design suitable for the job and the conditions of the job site.

18-2 Truck Cranes

Truck cranes commonly are used to erect precast concrete units in the construction of buildings and bridges. In determining the availability of cranes with adequate capacity for a specific project, the designer should be aware of the factors that affect the capacity of a crane and reduce its actual lifting capacity from its maximum rated capacity. The maximum rated capacity of a crane is the maximum load it can lift with a relatively short boom and with the minimum possible load radius. The load radius is the horizontal distance measured from the vertical axis about which the crane cab (or "house") rotates to the vertical axis passing through the center of mass of the load. This is illustrated in Fig. 18-1.

Capacities for specific cranes having rated capacities of 35, 65, and 82 tons are given in Tables 18-1, 18-2, and 18-3. *The data given in the tables are for illustrative purposes only and should not be used for cranes other than those for which the tables were prepared.* It should be understood that for large loads on short radii, the capacity of a crane normally is limited by structural considerations (i.e., strength of the boom, etc.), whereas for loads at larger radii, the capacity normally is limited by the ability of the crane to resist overturning. From Table 18-3 it will be seen that a crane having a rated capacity of 82 tons,

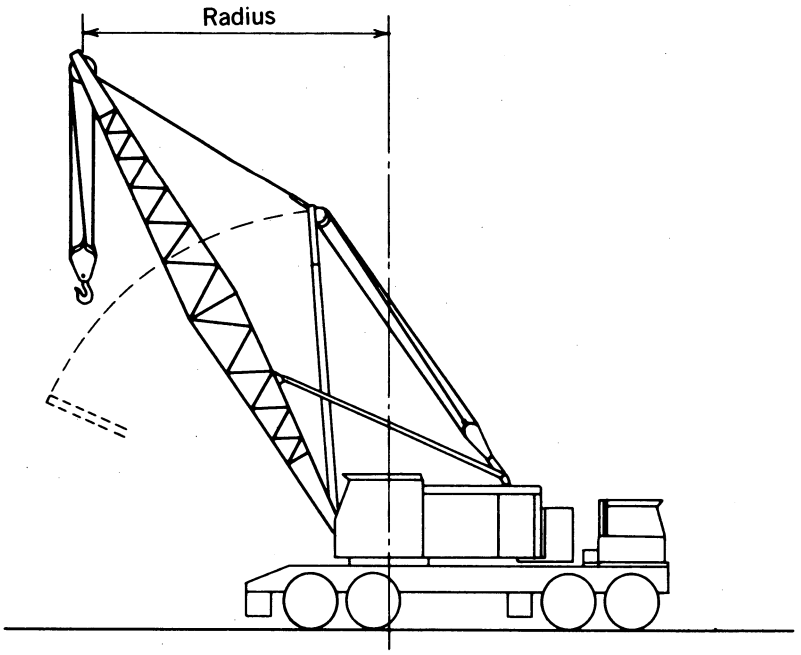

Fig. 18-1. Load radius for a truck crane.

TABLE 18-1 Capacities of a 35-Ton Truck Crane with Angle Boom.

*Capacities are based on machine equipped with Retractable High Gantry, 8 X 4 drive Carrier–9' 0" wide, 12:00 X 20 14-ply rating tires, Power Hydraulic Outriggers, 13,200#ctwt.

BOOM				On Outriggers		On Tires	
Length	Radius	Angle	Point Ht. W	Rear	Side	Rear	Side
35'	10'	79°	40' 9"	70,000*	70,000*	53,100	40,800*
	11'	77°	40' 7"	70,000*	70,000*	46,300	37,800*
	12'	75°	40' 3"	69,300*	69,300*	41,000	35,200*
	13'	74°	39'11"	64,500*	64,500*	36,800	32,300
	14'	72°	39' 9"	60,300*	60,300*	33,300	29,200
	15'	70°	39' 4"	56,600*	56,600*	30,400	26,500
	20'	61°	37' 1"	42,100*	42,100*	21,000	18,100
	25'	51°	33' 9"	32,600*	32,600*	15,900	13,600
	30'	40°	28' 9"	26,500*	26,500*	12,600	10,700
	35'	24°	20' 9"	22,200*	22,200*	10,400	8,800
40'	10'	80°	45'10"	70,000*	70,000*	53,000	40,500*
	11'	79°	45' 8"	70,000*	70,000*	46,200	37,600*
	12'	77°	45' 5"	69,000*	69,000*	40,900	35,000*
	13'	76°	45' 2"	64,200*	64,200*	36,600	32,200
	14'	74°	44'11"	60,100*	60,100*	33,100	29,000
	15'	73°	44' 7"	56,400*	56,400*	30,200	26,400
	20'	65°	42' 8"	41,900*	41,900*	20,800	17,900
	25'	57°	39'10"	32,400*	32,400*	15,700	13,400
	30'	48°	36' 1"	26,300*	26,300*	12,500	10,600
	35'	37°	30' 7"	22,000*	22,000*	10,200	8,600
	40'	23°	21'10"	18,900*	18,900	8,600	7,200
50'	12'	80°	55' 8"	68,600*	68,600*	40,600	34,500*
	13'	79°	55' 5"	63,800*	63,800*	36,300	31,900
	14'	77°	55' 3"	59,600*	59,600*	32,800	28,700
	15'	76°	54'11"	55,900*	55,900*	29,900	26,100
	20'	70°	53' 5"	41,500*	41,500*	20,500	17,600
	25'	64°	51' 4"	32,000*	32,000*	15,400	13,100
	30'	57°	48' 7"	25,900*	25,900*	12,200	10,200
	35'	50°	44'11"	21,600*	21,600*	9,900	8,300
	40'	42°	40' 2"	18,500*	18,500*	8,300	6,900
	50'	20°	23' 9"	13,900	13,500	6,100	4,900
60'	13'	81°	64' 9"	63,300*	63,300*	36,000	31,700
	14'	80°	64' 6"	59,100*	59,100*	32,600	28,500
	15'	79°	65' 3"	55,400*	55,400*	29,600	25,800
	20'	74°	63'11"	41,100*	41,100*	20,200	17,400
	25'	69°	62' 3"	31,600*	31,600*	15,100	12,800
	30'	63°	60' 1"	25,500*	25,500*	11,800	9,900
	35'	58°	57' 3"	21,200*	21,200*	9,600	8,000
	40'	52°	53' 9"	18,100*	18,100*	8,000	6,600
	50'	39°	43'10"	13,600*	13,300	5,800	4,600
	60'	18°	25' 5"	10,500	10,200	4,300	3,400
70'	15'	80°	75' 5"	53,100*	53,100*	29,400	25,500
	20'	76°	74' 4"	40,700*	40,700*	19,900	17,100
	25'	72°	72'11"	31,200*	31,200*	14,800	12,500
	30'	67°	71' 1"	25,100*	25,100*	11,500	9,600
	35'	63°	68' 9"	20,900*	20,900*	9,300	7,700
	40'	58°	65'11"	17,700*	17,700*	7,700	6,300
	50'	48°	58' 4"	13,200*	13,000	5,500	4,300
	60'	36°	47' 2"	10,300	9,900	4,000	3,100
	70'	17°	26'11"	8,100	7,800	3,000	2,200
80'	20'	78°	84' 8"	40,400*	40,400*	19,600	16,800
	25'	74°	83' 4"	30,900*	30,900*	14,500	12,200
	30'	70°	81' 9"	24,700*	24,700*	11,200	9,300
	35'	67°	79' 9"	20,500*	20,500*	9,000	7,400
	40'	63°	77' 5"	17,300*	17,300*	7,400	5,900
	50'	54°	71' 3"	12,900*	12,700	5,100	4,000
	60'	45°	62' 8"	9,900*	9,600	3,700	2,800
	70'	33°	50' 3"	7,900	7,500	2,700	1,900
	80'	16°	28' 5"	6,100*	6,000	1,900	1,200
90'	20'	79°	94'10"	36,300*	36,300*	19,300	16,500
	25'	76°	93' 9"	30,500*	30,500*	14,200	11,900
	30'	73°	92' 4"	24,400*	24,400*	10,900	9,000
	35'	70°	90' 7"	20,100*	20,100*	8,700	7,100
	40'	66°	88' 7"	16,900*	16,900*	7,000	5,600
	50'	59°	83' 3"	12,500*	12,500	4,800	3,700
	60'	51°	76' 2"	9,600*	9,400	3,400	2,400
	70'	42°	66' 8"	7,500*	7,300	2,400	1,600
	80'	31°	53' 2"	5,800*	5,700	1,600	900
	90'	15°	29' 9"	3,900*	3,900*	1,000	400
100'	20'	80°	105' 1"	32,400*	32,400*	19,000	16,200
	25'	77°	103'11"	27,000*	27,000*	13,900	11,600
	30'	74°	102' 9"	22,800*	22,800*	10,600	8,700
	35'	71°	101' 2"	19,300*	19,300*	8,400	6,800
	40'	68°	99' 4"	16,300*	16,300*	6,700	5,300
	50'	62°	94' 9"	12,100*	12,100*	4,500	3,400
	60'	55°	88' 8"	8,800*	8,800*	3,100	2,100
	70'	48°	80' 9"	6,600*	6,600*	2,000	1,200
	80'	40°	70' 4"	5,000*	5,000*	1,300	600
	90'	30°	55'10"	3,600*	3,600*	700	—
	100'	14°	31' 1"	2,300*	2,300*	200	—

(Courtesy of Link-Belt Speeder.)

when used with a 100 ft boom and a load radius of 40 ft, has an approximate capacity of 21 to 23 tons when working on outriggers. The maximum capacity depends upon whether the load is being lifted over the side or over the end of the carrier (truck chassis). This table clearly illustrates the effect of boom length

TABLE 18-2 Capacities of a 65-Ton Truck Crane.

*Capacities are based on machine equipped with Boom Gantry, 8 X 4 drive Carrier—11′ 0″ wide, 14:00 X 20 18-ply rating tires, Power Hydraulic Outriggers, 18,000 lbs. ctwt and 4,000 lbs. Bumper ctwt.

BOOM				ON OUTRIGGERS		ON TIRES	
Length	Radius	Angle	Point Ht. W.	Rear	Side	Rear	Side
40′	12′	78°	45′ 11″	130,000*	130,000*	76,700*	62,310*
	13′	76°	45′ 7″	128,040*	127,140*	73,870*	58,450*
	14′	74°	45′ 4″	119,790*	119,080*	71,250*	55,010*
	15′	73°	45′ 0″	112,500*	111,960*	68,790*	51,930*
	20′	65°	43′ 1″	86,000*	85,930*	47,760	35,510
	25′	57°	40′ 5″	67,530*	66,680	35,540	26,140
	30′	48°	36′ 6″	54,380*	49,320	28,010	20,370
	35′	37°	31′ 1″	44,890*	38,810	22,880	16,460
	40′	23°	22′ 5″	37,240*	31,730	19,150	13,600
50′	13′	79°	55′ 11″	127,360*	127,110*	73,630*	58,370*
	14′	78°	55′ 8″	119,760*	119,050*	71,010*	54,930*
	15′	76°	55′ 5″	112,480*	111,930*	68,560*	51,850*
	20′	70°	53′ 11″	85,980*	85,900*	47,890	35,650
	25′	64°	51′ 10″	67,600*	66,990	35,650	26,250
	30′	58°	48′ 11″	54,490*	49,560	28,100	20,470
	35′	50°	45′ 5″	45,000*	39,030	22,980	16,560
	40′	43°	40′ 7″	38,150*	31,960	19,270	13,730
	50′	21°	24′ 4″	28,390	23,030	14,220	9,870
60′	15′	79°	65′ 10″	112,630*	112,070*	68,410*	51,920*
	20′	74°	64′ 5″	86,080*	85,990*	48,170	35,930
	25′	69°	62′ 8″	67,770*	67,420	35,850	26,450
	30′	63°	60′ 6″	54,670*	49,880	28,250	20,630
	35′	58°	57′ 8″	45,150*	39,270	23,100	16,680
	40′	52°	54′ 2″	38,270*	32,160	19,380	13,830
	50′	39°	44′ 4″	28,580	23,220	14,330	9,980
	60′	19°	26′ 1″	22,060	17,760	11,020	7,440
70′	20′	76°	74′ 10″	85,930*	85,840*	48,150	35,920
	25′	72°	73′ 4″	67,680*	67,530	35,810	26,410
	30′	68°	71′ 6″	54,600*	49,930	28,200	20,580
	35′	63°	69′ 2″	45,080*	39,300	23,050	16,630
	40′	58°	66′ 5″	38,190*	32,170	19,320	13,780
	50′	48°	58′ 11″	28,580	23,220	14,280	9,930
	60′	36°	47′ 10″	22,100	17,800	11,010	7,430
	70′	17°	27′ 7″	17,710	14,130	8,690	5,650
80′	20′	78°	85′ 0″	85,750*	85,660*	48,100	35,870
	25′	74°	83′ 10″	67,560*	67,560*	35,730	26,340
	30′	70°	82′ 2″	54,500*	49,940	28,120	20,490
	35′	67°	80′ 2″	44,980*	39,280	22,960	16,540
	40′	63°	77′-11″	38,090*	32,140	19,220	13,690
	50′	54°	71′ 10″	28,530	23,170	14,180	9,840
	60′	45°	63′ 1″	22,050	17,760	10,930	7,350
	70′	33°	50′ 10″	17,700	14,120	8,640	5,600
	80′	16°	29′ 1″	14,540	11,470	6,920	4,270
90′	20′	79°	95′ 4″	81,510*	81,510*	48,030	35,800
	25′	76°	94′ 2″	67,420*	67,420*	35,640	26,250
	30′	73°	92′ 8″	54,380*	49,920	28,010	20,390
	35′	69°	91′ 0″	44,840*	39,240	22,840	16,430
	40′	66°	89′ 0″	37,950*	32,080	19,110	13,570
	50′	59°	83′ 2″	28,460	23,090	14,060	9,720
	60′	51°	76′ 7″	21,970	17,670	10,810	7,240
	70′	42°	67′ 1″	17,620	14,040	8,530	5,500
	80′	31°	53′ 8″	14,500	11,420	6,840	4,200
	90′	15°	30′ 6″	12,110	9,420	5,510	3,170
100′	25′	77°	104′ 5″	67,260*	67,260*	35,530	26,140
	30′	74°	103′ 2″	54,240*	49,890	27,890	20,270
	40′	68°	99′ 10″	37,790*	32,010	18,980	13,440
	50′	62°	95′ 2″	28,360	23,000	13,930	9,590
	60′	55°	89′ 1″	21,870	17,570	10,680	7,100
	70′	48°	81′ 2″	17,520	13,940	8,400	5,360
	80′	40°	70′ 10″	14,400	11,320	6,720	4,080
	90′	30°	56′ 5″	12,040	9,350	5,410	3,070
	100′	14°	31′ 10″	10,170	7,780	4,350	2,250
110′	25′	79°	114′ 8″	64,820*	64,820*	35,410	26,030
	30′	76°	113′ 6″	54,090*	49,840	27,760	20,150
	40′	70°	110′ 6″	37,630*	31,920	18,840	13,300
	50′	65°	106′ 5″	28,260	22,890	13,790	9,440
	60′	59°	101′ 0″	21,750	17,460	10,530	6,960
	70′	53°	94′ 2″	17,400	13,820	8,260	5,220
	80′	46°	85′ 7″	14,280	11,200	6,580	3,930
	90′	38°	74′ 5″	11,930	9,240	5,280	2,940
	100′	28°	59′ 0″	10,080	7,690	4,240	2,140
	110′	14°	33′ 0″	8,580	6,430	3,370	1,470

BOOM				ON OUTRIGGERS		ON TIRES	
Length	Radius	Angle	Point Ht. W.	Rear	Side	Rear	Side
120′	30′	77°	123′ 10″	53,930*	49,780	27,630	20,010
	40′	72°	121′ 1″	37,460*	31,820	18,690	13,160
	50′	67°	117′ 4″	28,140	22,780	13,630	9,290
	60′	62°	112′ 6″	21,620	17,330	10,380	6,800
	70′	56°	106′ 6″	17,270	13,680	8,100	5,060
	80′	50°	99′ 0″	14,140	11,070	6,420	3,780
	90′	44°	89′ 8″	11,790	9,100	5,130	2,790
	100′	36°	77′ 8″	9,960	7,560	4,090	2,000
	110′	27°	61′ 6″	8,470	6,320	3,250	1,350
	120′	13°	34′ 2″	7,240	5,280	2,520	—
130′	30′	78°	134′ 0″	52,380*	49,720	27,490	19,870
	40′	74°	131′ 6″	37,280*	31,720	18,540	13,010
	50′	69°	128′ 1″	27,960*	22,660	13,470	9,130
	60′	64°	123′ 10″	21,490	17,200	10,210	6,640
	70′	59°	118′ 4″	17,130	13,550	7,940	4,900
	80′	54°	111′ 8″	14,000	10,930	6,260	3,620
	90′	48°	103′ 7″	11,650	8,960	4,960	2,630
	100′	42°	93′ 7″	9,810	7,420	3,940	1,840
	110′	35°	80′ 11″	8,340	6,190	3,090	1,200
	120′	26°	63′ 10″	7,120	5,160	2,390	—
	130′	13°	35′ 4″	6,080	4,290	1,770	—
140′	30′	79°	144′ 2″	47,730*	47,730*	27,340	19,730
	40′	75°	141′ 11″	37,090*	31,610	18,380	12,850
	50′	71°	138′ 10″	27,760*	22,530	13,310	8,970
	60′	66°	134′ 10″	21,360	17,060	10,050	6,480
	70′	62°	129′ 11″	16,980	13,400	7,770	4,740
	80′	57°	123′ 11″	31,850	10,780	6,090	3,450
	90′	52°	116′ 8″	11,500	8,810	4,800	2,460
	100′	46°	107′ 11″	9,660	7,270	3,770	1,680
	110′	40°	97′ 4″	8,190	6,040	2,930	1,040
	120′	33°	84′ 0″	6,980	5,020	2,230	—
	130′	25°	66′ 1″	5,960	4,160	1,640	—
	140′	12°	36′ 5″	5,070	3,420	1,110	—
150′	35′	78°	153′ 5″	39,180*	38,750	21,980	16,580
	40′	76°	152′ 4″	34,890*	31,500	18,220	12,690
	50′	72°	149′ 4″	27,320*	22,400	13,150	8,800
	60′	68°	145′ 8″	21,210*	16,920	9,880	6,310
	70′	64°	141′ 1″	16,840*	13,250	7,600	4,560
	80′	59°	135′ 8″	13,700*	10,630	5,920	3,280
	90′	55°	129′ 2″	11,350*	8,660	4,620	2,290
	100′	50°	121′ 5″	9,510*	7,120	3,600	1,510
	110′	45°	112′ 1″	8,030*	5,880	2,760	—
	120′	39°	100′ 11″	6,820*	4,870	2,070	—
	130′	32°	86′ 11″	5,770*	4,010	1,470	—
	140′	24°	68′ 4″	4,810*	3,290	—	—
	150′	12°	37′ 6″	4,060*	2,640	—	—
160′	35′	79°	163′ 7″	36,070*	36,070*	21,830	15,420
	40′	77°	162′ 6″	31,450*	31,380	18,060	12,530
	50′	73°	159′ 10″	25,070*	22,270	12,980	8,640
	60′	69°	156′ 5″	20,110*	16,770	9,710	6,140
	70′	65°	152′ 2″	16,680*	13,100	7,430	4,390
	80′	61°	147′ 2″	12,760*	10,470	5,740	3,100
	90′	57°	141′ 2″	10,520*	8,500	4,450	2,120
	100′	53°	134′ 5″	8,660*	6,960	3,420	1,330
	110′	48°	125′ 11″	7,110*	5,720	2,590	—
	120′	43°	116′ 2″	5,830*	4,710	1,890	—
	130′	38°	104′ 5″	4,770*	3,860	1,300	—
	150′	23°	70′ 5″	3,130*	2,500	—	—
	160′	11°	38′ 6″	2,540*	1,940	—	—

(Courtesy of Link-Belt Speeder.)

TABLE 18-3 Capacities of an 82-Ton Truck Crane with Tubular "Hi-Lite" Boom.

BOOM			W Boom Point Height	ON OUTRIGGERS		ON TIRES	
Length	R	A		Side	Rear	Side	Rear
40′	12′	78°	45′ 7″	164,000*	164,000*	77,590*	119,850*
	13′	76°	45′ 4″	153,080*	153,380*	72,250*	115,550*
	14′	75°	45′ 2″	143,280*	143,560*	67,540*	104,770
	15′	73°	44′11″	134,610*	134,890*	63,400*	95,160
	20′	66°	43′ 0″	102,000*	103,260*	45,470	64,770
	25′	57°	40′ 4″	80,280*	81,300*	33,570	48,620
	30′	48°	36′ 7″	65,000*	65,850*	26,250	38,580
	35′	38°	31′ 4″	51,800	55,060*	21,290	31,720
	40′	24°	23′ 0″	42,390	45,540*	17,670	26,720
50′	13′	79°	55′ 8″	143,850*	143,850*	72,200*	115,270*
	14′	78°	55′ 6″	140,420*	140,420*	67,510*	105,000
	15′	77°	55′ 4″	134,590*	137,210*	63,360*	95,370
	20′	71°	53′10″	101,890*	103,260*	45,640	64,920
	25′	64°	51′ 8″	80,370*	81,400*	33,700	48,740
	30′	58°	49′ 0″	65,090*	65,940*	26,370	38,690
	35′	51°	45′ 5″	52,060	55,160*	21,410	31,840
	40′	43°	40′10″	42,660	47,210*	17,820	26,860
	45′	34°	34′ 6″	35,930	41,100*	15,090	23,070
	50′	22°	25′ 0″	30,850	34,680*	12,930	20,070
60′	15′	79°	65′ 6″	130,000*	130,000*	63,530*	95,860
	20′	74°	64′ 4″	102,090*	103,380*	45,980	65,230
	25′	69°	62′ 7″	80,580*	81,610*	33,940	48,960
	30′	64°	60′ 5″	65,240*	66,100*	26,560	38,860
	35′	58°	57′ 8″	52,360	55,290*	21,560	31,970
	40′	52°	54′ 2″	42,910	47,330*	17,940	26,980
	50′	39°	44′ 6″	31,060	36,340*	13,050	20,190
	60′	20°	26′10″	23,890	29,090*	9,850	15,750
70′	20′	76°	74′ 7″	100,500*	100,500*	45,960	65,200
	25′	72°	73′ 2″	80,490*	81,520*	33,900	48,910
	30′	68°	71′ 5″	65,150*	65,990*	26,500	38,800
	35′	63°	69′ 1″	52,400	55,180*	21,500	31,910
	40′	59°	66′ 4″	42,930	47,220*	17,890	26,910
	50′	48°	58′11″	31,070	36,270*	13,000	20,130
	60′	36°	47′11″	23,930	29,060*	9,840	15,740
	70′	18°	28′ 6″	19,110	23,920*	7,590	12,610
80′	20′	78°	84′11″	95,000*	95,000*	45,910	65,130
	25′	74°	83′ 8″	80,350*	81,380*	33,820	48,820
	30′	71°	82′ 1″	65,000*	65,860*	26,410	38,700
	35′	67°	80′ 1″	52,380	55,040*	21,400	31,800
	40′	63°	77′10″	42,890	47,080*	17,780	26,800
	50′	55°	71′ 8″	31,020	36,120*	12,900	20,030
	60′	45°	63′ 2″	23,880	28,940*	9,750	14,640
	70′	34°	51′ 1″	19,100	23,850*	7,540	12,550
	80′	17°	30′ 0″	15,630	20,000*	5,860	10,230
90′	20′	79°	95′ 1″	90,000*	90,000*	45,820	65,040
	25′	76°	94′ 0″	77,030*	77,030*	33,720	48,700
	30′	73°	92′ 7″	64,840*	65,690*	26,290	38,570
	35′	70°	90′11″	52,340	54,870*	21,270	31,670
	40′	66°	88′11″	42,830	46,910*	17,650	26,670
	50′	59°	83′ 8″	30,940	35,950*	12,770	19,890
	60′	51°	76′ 8″	23,790	28,760*	9,620	15,510
	70′	42°	67′ 2″	19,010	23,690*	7,420	12,430
	80′	32°	54′ 0″	15,580	19,890*	5,780	10,150
	90′	16°	31′ 6″	12,970	16,920*	4,480	8,350
100′	25′	78°	104′ 4″	72,720*	72,720*	33,590	48,570
	30′	75°	103′ 0″	64,640*	65,490*	26,160	38,430
	35′	72°	101′ 6″	52,270	54,670*	21,130	31,520
	40′	69°	99′ 8″	42,750	46,720*	17,500	26,520
	50′	62°	95′ 1″	30,830	35,760*	12,620	19,730
	60′	56°	89′ 1″	23,680	28,580*	9,470	15,350
	70′	48°	81′ 4″	18,900	23,500*	7,270	12,280
	80′	40°	71′ 0″	15,470	19,710*	5,640	10,010
	90′	30°	56′10″	12,880	16,770*	4,380	8,240
	100′	15°	32′10″	10,840	14,400*	3,340	6,810

BOOM			W Boom Point Height	ON OUTRIGGERS		ON TIRES	
L	R	A		Side	Rear	Side	Rear
110′	25′	79°	114′ 6″	68,000*	68,000*	33,460	48,430
	30′	76°	113′ 5″	62,600*	62,600*	26,010	38,280
	35′	73°	112′ 0″	52,190	54,470*	20,980	31,370
	40′	71°	110′ 5″	42,650	46,510*	17,340	26,350
	50′	65°	106′ 4″	30,710	35,560*	12,450	19,570
	60′	59°	101′ 0″	23,550	28,370*	9,300	15,180
	70′	53°	94′ 2″	18,760	23,300*	7,100	12,120
	80′	46°	85′ 7″	15,340	19,510*	5,480	9,840
	90′	38°	74′ 7″	12,760	16,580*	4,220	8,090
	100′	29°	59′ 5″	10,740	14,250*	3,220	6,690
	110′	14°	34′ 1″	9,090	12,290*	2,370	5,520
120′	30′	77°	123′ 7″	59,140*	59,140*	25,860	38,120
	35′	75°	122′ 5″	52,100	54,270*	20,810	31,200
	40′	72°	120′11″	42,540	46,290*	17,180	26,180
	50′	67°	117′ 2″	30,590	35,320*	12,280	19,390
	60′	62°	112′ 6″	23,410	28,150*	9,130	15,010
	70′	56°	106′ 6″	18,610	23,080*	6,930	11,940
	80′	50°	99′ 1″	15,190	19,300*	5,310	9,670
	90′	44°	89′10″	12,610	16,370*	4,050	7,920
	100′	36°	77′11″	10,590	14,040*	3,050	6,520
	110′	27°	61′11″	8,970	12,130*	2,230	5,380
	120′	14°	35′ 5″	7,610	10,510*	1,530	4,410
130′	30′	78°	133′11″	55,590*	55,590*	25,690	37,950
	35′	76°	132′ 8″	51,160*	51,160*	20,640	31,020
	40′	74°	131′ 5″	42,420	45,400*	17,000	26,000
	50′	69°	128′ 0″	30,450	35,100*	12,100	19,210
	60′	64°	123′ 8″	23,260	27,930*	8,940	14,820
	70′	59°	118′ 4″	18,460	22,850*	6,750	11,750
	80′	54°	111′ 8″	15,030	19,070*	5,120	9,480
	90′	48°	103′ 7″	12,450	16,160*	3,870	7,730
	100′	42°	93′ 8″	10,430	13,830*	2,880	6,340
	110′	35°	81′ 2″	8,820	11,920*	2,060	5,210
	120′	26°	64′ 4″	7,480	10,320*	----	4,260
	130′	13°	36′ 7″	6,350	8,900*	----	3,430
140′	30′	79°	144′ 1″	52,170*	52,170*	25,530	37,780
	35′	77°	143′ 0″	47,450*	47,450*	20,470	30,850
	40′	75°	141′10″	42,300	42,790*	16,820	25,820
	50′	71°	138′ 8″	30,300	34,780*	11,910	19,020
	60′	66°	134′ 8″	23,100	27,680*	8,760	14,630
	70′	62°	129′10″	18,290	22,610*	6,560	11,560
	80′	57°	123′11″	14,860	18,840*	4,930	9,290
	90′	52°	116′ 8″	12,280	15,930*	3,680	7,540
	100′	46°	108′ 0″	10,260	13,600*	2,690	6,150
	110′	41°	97′ 6″	8,650	11,700*	1,880	5,020
	120′	34°	84′ 2″	7,320	10,100*	----	4,080
	130′	25°	66′ 7″	6,200	8,750*	----	3,270
	140′	13°	37′ 8″	5,240	7,480*	----	2,570
150′	35′	78°	153′ 4″	44,330*	44,330*	20,290	30,660
	40′	76°	152′ 1″	39,730*	39,730*	16,640	25,630
	50′	72°	149′ 2″	30,160	31,690*	11,720	18,830
	60′	68°	145′ 7″	22,940	25,900*	8,560	14,430
	70′	64°	141′ 1″	18,130	21,410*	6,360	11,360
	80′	59°	135′ 7″	14,680	16,860*	4,740	9,090
	90′	55°	129′ 2″	12,100	14,410*	3,490	7,340
	100′	50°	121′ 5″	10,090	12,230*	2,490	5,960
	110′	45°	112′ 2″	8,470	10,360*	1,680	4,830
	120′	39°	101′ 1″	7,150	8,880*	----	3,890
	130′	32°	87′ 2″	6,040	7,610*	----	3,090
	140′	24°	68′10″	5,090	6,510*	----	2,400
	150′	12°	38′10″	4,250	5,610*	----	1,780

BOOM			W Boom Point Height	ON OUTRIGGERS		ON TIRES	
L	R	A		Side	Rear	Side	Rear
160′ ②	35′	79°	163′ 6″	41,120*	41,120*	20,110	30,480
	40′	77°	162′ 5″	36,900*	36,900*	16,450	25,440
	50′	73°	159′ 8″	29,270*	29,270*	11,530	18,630
	60′	69°	156′ 4″	22,780	24,000*	8,370	14,240
	70′	65°	152′ 1″	17,960	19,740*	6,160	11,160
	80′	61°	147′ 1″	14,510	15,660*	4,540	8,890
	90′	57°	141′ 2″	11,920	13,140*	3,290	7,140
	100′	53°	134′ 2″	9,900	11,020*	2,290	5,760
	110′	48°	126′ 0″	8,290	9,280*	1,490	4,630
	120′	43°	116′ 4″	6,960	7,770*	----	3,690
	130′	38°	104′ 7″	5,860	6,530*	----	2,890
	140′	31°	90′ 1″	4,910	5,500*	----	2,210
	150′	24°	70′11″	4,100	4,600*	----	1,610
	160′	12°	39′11″	3,370	3,920*	----	----
170′ ②	35′	79°	173′ 8″	38,110*	38,110*	19,930	30,290
	40′	78°	172′ 7″	34,270*	34,270*	16,270	25,250
	50′	74°	170′ 1″	27,170*	27,170*	11,340	18,430
	60′	71°	166′11″	22,100*	22,100*	8,170	14,030
	70′	67°	163′ 1″	17,780	19,920*	5,960	10,960
	80′	63°	158′ 5″	14,330	15,770*	4,330	8,690
	90′	59°	153′ 0″	11,740	13,100*	3,080	6,940
	100′	55°	146′ 7″	9,720	10,840*	2,090	5,550
	110′	51°	139′ 1″	8,100	8,980*	----	4,420
	120′	47°	130′ 5″	6,780	7,460*	----	3,480
	130′	42°	120′ 2″	5,670	6,240*	----	2,690
	140′	37°	107′11″	4,730	5,200*	----	2,010
	150′	30°	92′10″	3,920	4,310*	----	----
	160′	23°	73′ 0″	3,200	3,520*	----	----
	170′	12°	40′11″	2,560	2,820*	----	----
180′ ②	40′	78°	182′11″	31,110*	31,110*	16,070	25,060
	50′	75°	180′ 6″	25,100*	25,100*	11,140	18,230
	60′	72°	177′ 6″	20,350*	20,350*	7,970	13,830
	70′	68°	173′11″	16,600	19,360*	5,760	10,750
	80′	65°	169′ 6″	14,140	15,550*	4,130	8,480
	90′	61°	164′ 6″	11,550	12,710*	2,880	6,730
	100′	58°	158′ 7″	9,530	10,480*	1,890	5,340
	110′	54°	151′ 8″	7,910	8,700*	----	4,210
	120′	50°	143′10″	6,580	7,240*	----	3,280
	130′	45°	134′ 8″	5,480	6,030*	----	2,490
	140′	41°	123′11″	4,540	4,990*	----	1,810
	150′	35°	111′ 2″	3,730	4,100*	----	----
	160′	30°	95′ 6″	3,020	3,320*	----	----
	170′	22°	75′ 0″	2,400	2,640*	----	----
	180′	11°	41′11″	1,830	2,010*	----	----

(Courtesy of Link-Belt Speeder.)

and load radius on the lifting capacity of a truck crane, and structural designers should be aware of these data. It should be noted that the capacity of a truck crane is less when it is used without the benefit of its outriggers and is supported by its tires alone. Outriggers extend transversely from the carrier and increase

the overturning capacity of the crane. It also is important to understand that a crane must be as close as possible to level when lifting large loads. The problems and costs associated with leveling the terrain on which a crane is to operate must be addressed in determining the feasibility of an erection method. If it is necessary to move a large precast member some distance by moving ("walking") with one or more cranes, the ground over which they must move must be made smooth, very nearly level, and firm.

Precast building beams and girders often can be efficiently erected by using truck cranes in combination with small dollies, even when the building dimensions, site conditions, or crane capacity precludes the possibility of the crane setting the members into their final locations. In this case, one or two cranes are used to hoist the precast member to the proper elevation, where it is set on two dollies. The dollies are then used to move the member horizontally to the final location. The dollies can be provided with hydraulic jacks that permit the members to be raised or lowered as needed after they have been positioned horizontally. This method does not work well, however, on sloping floors of the type frequently used in parking garages.

18-3 Crawler Cranes

Crawler cranes with high capacities occasionally are used to erect precast members. Crawler cranes must be moved from site to site on large trailers, so their use is often costly and difficult in developed areas. The load radius for a crawler crane is measured in a manner similar to that of a truck crane (see Fig. 18-2).

The capacities of a 103.5-ton crawler crane are given in Table 18-4. Crawler cranes working under maximum lifts, like truck cranes, must be level and on firm ground.

18-4 Floating Cranes

Floating cranes, some with capacities as great as 1500 metric tons, are available in some parts of the world. The girder shown being erected in Fig. 18-3 weighs 230 tons and is approximately 200 ft long. Cranes of this type are very efficient in erecting precast concrete members in bridges and piers located on or over water. The use of floating cranes is restricted to sites at which the water is relatively calm, without excessive currents or high waves, and of sufficient depth. Truck and crawler cranes sometimes are placed on barges and used as floating cranes.

18-5 Girder Launchers

Large precast bridge girders sometimes are erected with girder launchers of the type shown in Fig. 18-4. Launchers generally incorporate steel trusses, although

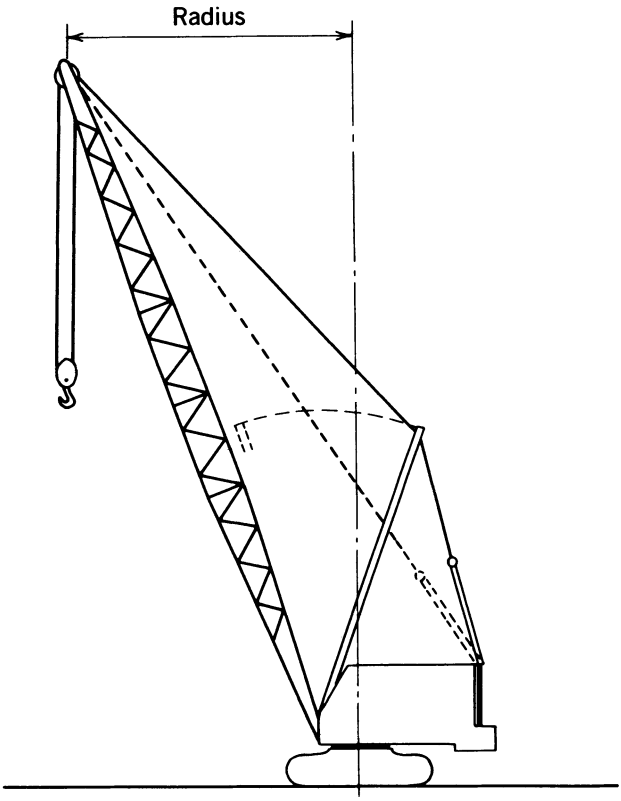

Fig. 18-2. Load radius for a crawler crane.

aluminum has been used. For short spans, steel beams have been used to erect relatively light concrete girders in lie of steel trusses (Stergiou 1967).

There have been many different variations in the construction of girder launchers, but they almost invariably are designed to be advanced from span to span by moving over the previously erected girders and cantilevering out to the next pier. When set in position, the launcher provides an overhead structure strong enough to support the necessary erection loads. Launchers normally are provided with hoists for raising and lowering the precast concrete girders as required in the erection process. Some launchers provide transverse rails and trollies for moving the girders laterally and setting them in their final position. Others are not equipped to move the precast concrete girders transversely, in which case, after being set on the piers, the girders are moved laterally on greased plates until they reach their final position. The sequence in erecting a bridge with a girder launcher is illustrated in Fig. 18-5.

It should be noted that the launcher shown in Fig. 18-5 is approximately 1.7 times the length of the girder that is to be erected. One of the precast concrete

TABLE 18-4 Capacities of a 103.5-Ton Crawler Crane with Tubular "Hi-Lite" Boom.

BOOM			W Boom Point Height	Ctwt. "A"	Ctwt. "AB"
Length	Radius	Angle			
50′	13′	80°	56′ 0″	207,000*	207,000*
	14′	79°	55′10″	185,090*	207,000*
	15′	78°	55′ 8″	160,470*	207,000*
	16′	77°	55′ 6″	144,660	200,000*
	17′	76°	55′ 3″	129,310	187,910
	18′	74°	54′10″	116,830	169,980
	19′	73°	54′ 7″	106,490	155,050
	20′	72°	54′ 4″	97,780	144,720
	25′	66°	52′ 5″	69,010	102,660
	30′	59°	49′10″	52,910	79,140
	35′	53°	46′ 5″	42,600	64,090
	40′	45°	42′ 1″	35,420	53,620
	50′	25°	27′ 8″	26,000	39,940
60′	14′	81°	66′ 0″	185,090*	201,160*
	15′	80°	65′10″	160,470*	197,940*
	16′	79°	65′ 8″	144,660	197,500*
	17′	78°	65′ 5″	129,310	187,910
	18′	77°	65′ 2″	116,830	169,980
	19′	76°	64′11″	106,490	155,050
	20′	75°	64′ 9″	97,780	144,720
	25′	70°	63′ 2″	69,010	102,660
	30′	65°	61′ 1″	52,910	79,140
	35′	60°	58′ 6″	42,600	64,090
	40′	54°	55′ 2″	35,420	53,620
	50′	41°	45′11″	26,000	39,940
	60′	23°	29′ 9″	20,410	31,690
70′	16′	81°	75′11″	144,660	179,500*
	17′	80°	75′ 8″	129,310	179,000*
	18′	79°	75′ 5″	116,830	169,980
	19′	78°	75′ 3″	106,490	155,050
	20′	77°	75′ 0″	97,780	144,720
	25′	73°	73′ 8″	69,010	102,660
	30′	68°	71′11″	52,910	79,140
	35′	64°	69′ 9″	42,600	64,090
	40′	60°	67′ 1″	35,420	53,620
	50′	50°	60′ 0″	26,000	39,940
	60′	38°	49′ 6″	20,410	31,690
	70′	21°	31′ 8″	16,510	26,000
80′	17′	81°	85′ 9″	129,310	164,000*
	18′	80°	85′ 6″	116,830	162,000*
	19′	79.5°	85′ 5″	106,490	155,050
	20′	79°	85′ 3″	97,780	144,720
	25′	75°	84′ 1″	69,010	102,660
	30′	72°	82′ 7″	52,910	79,140
	35′	68°	80′ 9″	42,600	64,090
	40′	64°	78′ 6″	35,420	53,620
	50′	55°	72′ 7″	26,000	39,940
	60′	46°	64′ 5″	20,410	31,690
	70′	35°	52′ 9″	16,510	26,000
	80′	20°	33′ 5″	13,620	21,800
90′	19′	81°	95′ 8″	106,490	147,000*
	20′	80°	95′ 5″	97,780	139,290*
	25′	77°	94′ 5″	69,010	102,660
	30′	74°	93′ 1″	52,910	79,140
	35′	70°	91′ 5″	42,600	64,090
	40′	67°	89′ 6″	35,420	53,620
	50′	60°	84′ 5″	26,000	39,940
	60′	52°	77′ 8″	20,410	31,690
	70′	43°	68′ 7″	16,510	26,000
	80′	33°	55′10″	13,620	21,800
	90′	18°	35′ 1″	11,370	18,560
100′	20′	81°	105′ 7″	97,780	127,550*
	25′	78°	104′ 8″	69,010	102,660
	30′	75°	103′ 6″	52,910	79,140
	35′	72°	102′ 0″	42,600	64,090
	40′	69°	100′ 3″	35,420	53,620
	50′	63°	95′10″	26,000	39,940
	60′	56°	90′ 0″	20,410	31,690
	70′	49°	82′ 4″	16,500	25,980
	80′	41°	72′ 5″	13,580	21,770
	90′	31°	58′ 9″	11,350	18,540
	100′	17°	36′ 8″	9,550	15,970
110′	25′	79°	114′10″	69,010	102,660
	30′	77°	113′ 9″	52,910	79,140
	35′	74°	112′ 5″	42,600	64,090
	40′	71°	110′11″	35,420	53,620
	50′	65°	106′11″	26,000	39,940
	60′	60°	101′ 9″	20,410	31,670
	70′	54°	95′ 2″	16,390	25,870
	80′	47°	86′10″	13,480	21,660
	90′	39°	76′ 1″	11,260	18,460
	100′	30°	61′ 6″	9,500	15,920
	110′	17°	38′ 2″	8,040	13,830
120′	25′	80°	125′ 0″	69,010	101,600*
	30′	78°	124′ 0″	52,910	79,140
	35′	75°	122′10″	42,600	64,090
	40′	73°	121′ 5″	35,420	53,620
	50′	68°	117′10″	26,000	39,940
	60′	63°	113′ 2″	20,250	31,540
	70′	57°	107′ 4″	16,260	25,740
	80′	51°	100′ 1″	13,350	21,540
	90′	45°	91′ 0″	11,140	18,330
	100′	37°	79′ 6″	9,400	15,810
	110′	29°	64′ 1″	7,970	13,760
	120′	16°	39′ 7″	6,760	12,030
130	25′	81°	135′ 2″	69,010	93,280*
	30′	79°	134′ 3″	52,910	79,140
	35′	77°	133′ 2″	42,600	64,090
	40′	74°	131′10″	35,390	53,620
	50′	70°	128′ 7″	25,960	39,900
	60′	65°	124′ 4″	20,110	31,400
	70′	60°	119′ 1″	16,110	25,600
	80′	55°	112′ 8″	13,210	21,390
	90′	49°	104′ 9″	11,000	18,190
	100′	43°	95′ 0″	9,260	15,670
	110′	36°	82′10″	7,840	13,640
	120′	27°	66′ 7″	6,670	11,940
	130′	15°	41′ 0″	5,640	10,490
140′	30′	80°	144′ 7″	52,910	79,140
	35′	77°	143′ 5″	42,540	64,030
	40′	75°	142′ 3″	35,260	53,460
	50′	71°	137′ 4″	25,820	39,750
	60′	67°	135′ 4″	19,950	31,240
	70′	62°	130′ 6″	15,960	25,440
	80′	57°	124′ 8″	13,050	21,230
	90′	52°	117′ 8″	10,840	18,030
	100′	47°	109′ 2″	9,100	15,520
	110′	41°	98′11″	7,700	13,490
	120′	35°	86′ 0″	6,530	11,800
	130′	26°	68′11″	5,540	10,380
	140′	15°	42′ 3″	4,600	9,140
150′	30′	80°	154′ 7″	52,900	75,890*
	35′	78°	153′ 8″	42,400	63,900
	40′	76°	152′ 6″	35,120	53,320
	50′	72°	149′ 9″	25,600	39,600
	60′	68°	146′ 2″	19,790	31,080
	70′	64°	141′ 9″	15,790	25,280
	80′	60°	136′ 5″	12,880	21,060
	90′	55°	130′ 1″	10,670	17,870
	100′	51°	122′ 6″	8,940	15,350
	110′	45°	113′ 6″	7,530	13,320
	120′	40°	102′ 7″	6,370	11,650
	130′	33°	89′ 0″	5,390	10,230
	140′	26°	71′ 3″	4,540	9,020
	150′	14°	43′ 6″	3,780	7,950
160′	30′	81°	164′ 9″	52,810	70,120*
	35′	79°	163′10″	42,290	63,780
	40′	77°	162′ 9″	34,990	53,190
	50′	74°	160′ 2″	25,520	39,460
	60′	70°	156′10″	19,640	30,930
	70′	66°	152′ 9″	15,640	25,120
	80′	62°	147′10″	12,730	20,910
	90′	58°	142′ 0″	10,520	17,710
	100′	53°	135′ 2″	8,780	15,190
	110′	49°	127′ 1″	7,370	13,170
	120′	44°	117′ 7″	6,210	11,490
	130′	38°	106′ 1″	5,240	10,080
	140′	32°	92′ 0″	4,400	8,880
	150′	25°	73′ 6″	3,670	7,830
	160′	14°	44′ 9″	3,000	6,900
170′	35′	80°	174′ 0″	42,170	61,340*
	40′	78°	173′ 0″	34,860	53,060
	50′	75°	170′ 7″	25,380	39,310
	60′	71°	169′ 6″	19,490	30,780
	70′	67°	163′ 8″	15,480	24,970
	80′	64°	159′ 1″	12,570	20,750
	90′	60°	153′ 9″	10,360	17,550
	100′	56°	147′ 5″	8,620	15,040
	110′	51°	140′ 1″	7,220	13,010
	120′	47°	131′ 7″	6,060	11,340
	130′	43°	121′ 6″	5,090	9,930
	140′	37°	109′ 6″	4,250	8,730
	150′	31°	94′10″	3,530	7,700
	160′	24°	75′ 8″	2,890	6,790
	170′	13°	46′ 0″	2,300	5,960
180′	35′	80°	184′ 2″	42,040	55,650*
	40′	79°	183′ 3″	34,720	51,970*
	50′	75°	180′11″	25,230	39,160
	60′	72°	178′ 0″	19,340	30,630
	70′	69°	174′ 5″	15,320	24,810
	80′	65°	170′ 2″	12,410	20,590
	90′	62°	165′ 2″	10,200	17,390
	100′	58°	159′ 5″	8,460	14,880
	110′	54°	152′ 8″	7,060	12,850
	120′	50°	144′10″	5,900	11,180
	130′	46°	135′10″	4,930	9,770
	140′	41°	125′ 4″	4,100	8,580
	150′	36°	112′10″	3,380	7,550
	160′	30°	97′ 7″	2,750	6,640
	170′	23°	77′ 9″	2,180	5,840
	180′	13°	47′ 1″	1,660	5,110
190′	35′	80°	194′ 4″	41,900	49,950*
	40′	79°	193′ 5″	34,580	46,080*
	50′	76°	191′ 3″	25,080	39,010
	60′	73°	188′ 7″	19,180	30,470
	70′	70°	185′ 1″	15,160	24,650
	80′	67°	181′ 2″	12,240	20,430
	90′	63°	176′ 6″	10,030	17,220
	100′	60°	171′ 0″	8,290	14,710
	110′	56°	164′10″	6,890	12,680
	120′	53°	157′ 8″	5,730	11,010
	130′	49°	149′ 5″	4,760	9,610
	140′	45°	140′ 0″	3,940	8,420
	150′	40°	129′ 0″	3,220	7,390
	160′	35°	116′ 0″	2,590	6,490
	170′	30°	100′ 2″	2,040	5,690
	180′	23°	79′ 9″	1,540	4,980
	190′	13°	48′ 3″	1,070	4,320
200′	40′	80°	203′ 7″	34,430	45,200*
	50′	77°	201′ 6″	24,920	35,830*
	60′	74°	198′11″	19,020	30,310
	70′	71°	195′ 9″	14,990	24,480
	80′	68°	192′ 0″	12,080	20,260
	90′	65°	187′ 7″	9,860	17,050
	100′	61°	182′ 6″	8,120	14,540
	110′	58°	176′ 8″	6,720	12,510
	120′	55°	170′ 1″	5,560	10,840
	130′	51°	162′ 6″	4,590	9,440
	140′	47°	153′11″	3,770	8,240
	150′	43°	144′ 1″	3,050	7,220
	160′	39°	132′ 8″	2,430	6,320
	170′	34°	119′ 2″	1,880	5,530
	180′	29°	102′10″	1,380	4,830
	190′	22°	81′ 9″	—	4,190
	200′	12°	49′ 4″	—	3,600

(Courtesy of Link-Belt Speeder.)

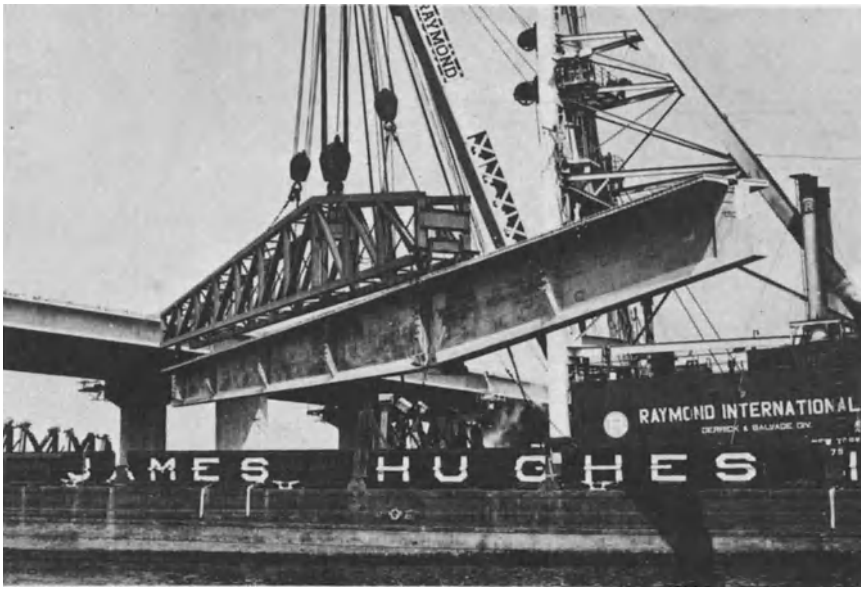

Fig. 18-3. Floating crane erecting a 230-ton girder on Crossbay Parkway Bridge in New York City.

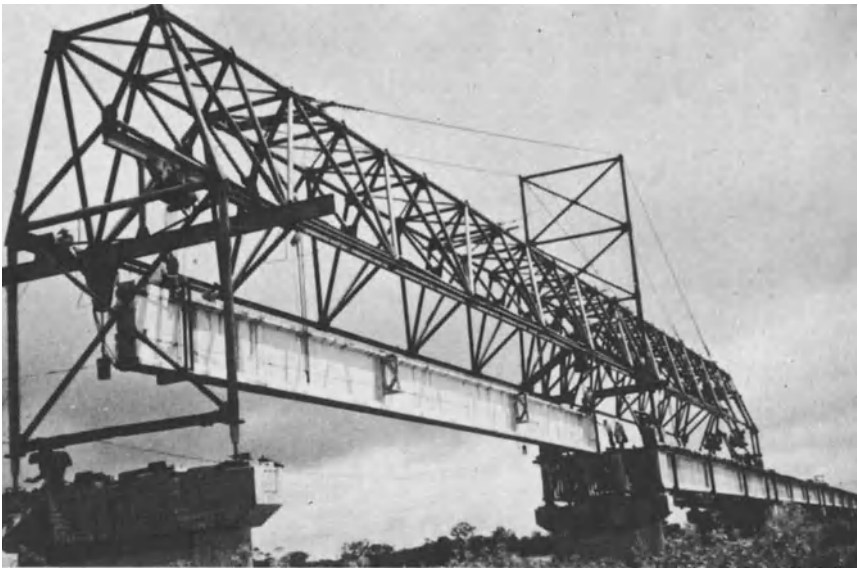

Fig. 18-4. Girder launcher erecting a 70-ton, 130-ft-long girder in Bolivia.

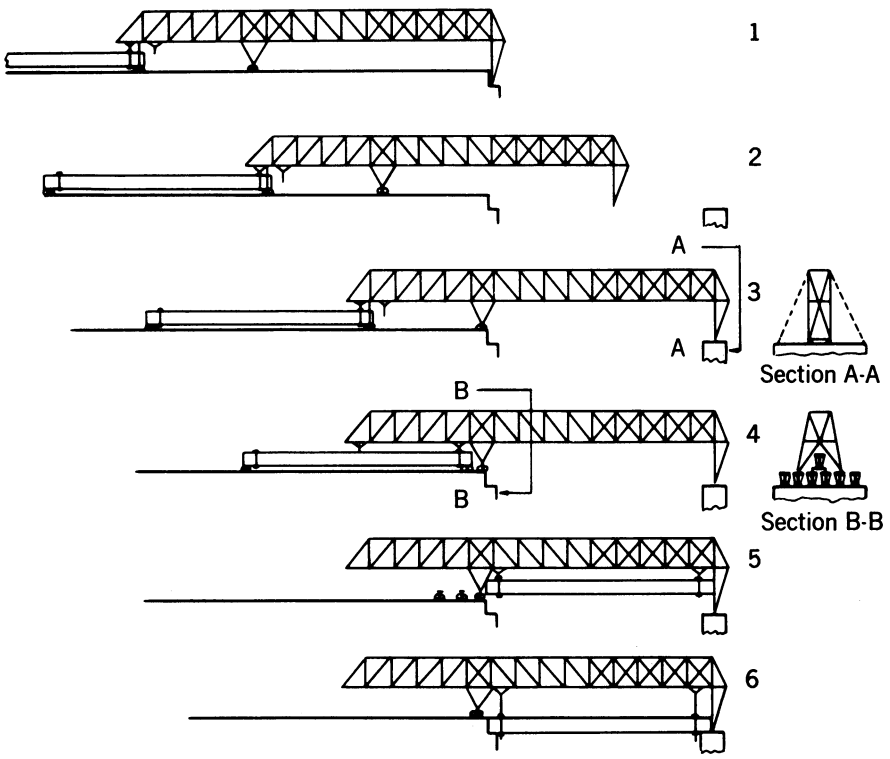

Fig. 18-5. Sequence in using a girder launcher. (1) Launcher assembled with girder connected for a counterweight. (2) Launcher and girder being moved into place for erecting first span. (3) Launcher in place for erecting first span. (4) Girder connected to launcher at outboard end. (5) Girder supported by launcher. (6) Girder erected.

girders is used for a counterweight when the launcher is being advanced into position.

The approximate weights of concrete bridge girders with wide top flanges, and thus suitable for launcher erection without temporary lateral bracing, together with the approximate weights of a launcher truss of sufficient strength for various combinations of weight and span, are shown in Fig. 18-6. The weight of the dollies used to move the precast concrete girders to the launcher, the hoists, and other necessary equipment is approximately equal to that of the launcher itself.

Girder launchers capable of erecting girders 220 ft long and weighing 270 tons have been designed, and their use has proved feasible. For the longer and heavier girders, launchers having guy-cables supported from a central tower, as shown in Fig. 18-4, are considered to be the most economical. For erecting

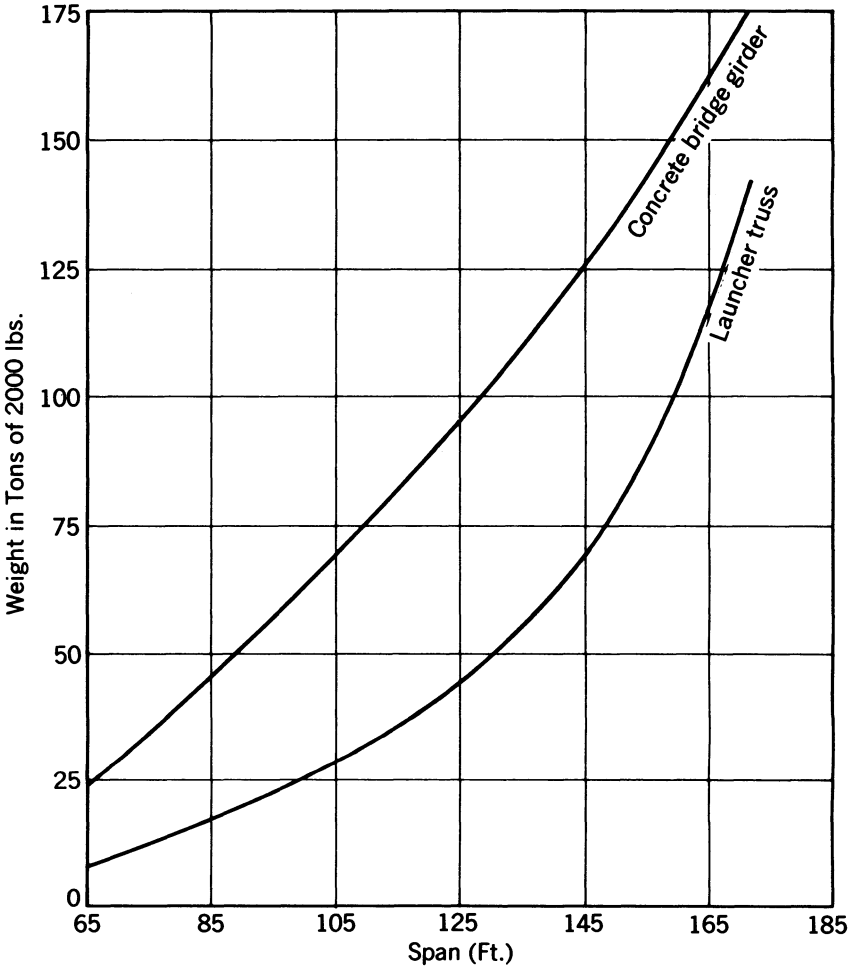

Fig. 18-6. Approximate bridge girder and launcher-truss weights for various spans.

shorter spans, cantilevered trusses, without a central tower, as shown in Fig. 18-7, have proved economical and efficient.

18-6 Falsework

Falsework can be used to erect precast bridge girders economically under conditions where large cranes and girder launchers cannot be used because of inavailability or site conditions. The falsework may consist of wood or steel towers supporting steel or wood beams. The precast girders normally are rolled onto the beams and then slid transversely into place on greased plates. Alternately,

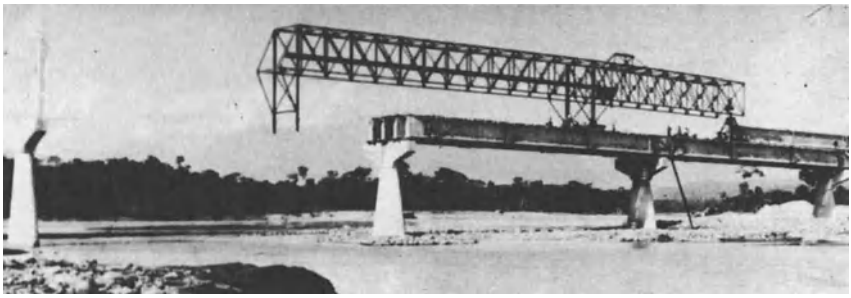

Fig. 18-7. Cantilevered launching truss.

the girders may be precast in segments, assembled, stressed, and grouted on falsework. The latter procedure eliminates the need for moving the assembled girder. Many methods of sliding girders transversely have been used. The details of the scheme used on the Bamako Bridge are shown in Fig. 18-8 (Muller 1960).

Falsework of the types used in cast-in-place construction can be used in the erection of bridges designed to be constructed segmentally with precast concrete segments erected in cantilever. With this technique, the segments can be as large as permitted by the available transport and erection equipment, and the cantilever or negative moment tendons can be placed in the configuration normally used in cantilever construction or extended over the entire length of the cantilevered segments, as shown in Fig. 18-9. The construction is completed

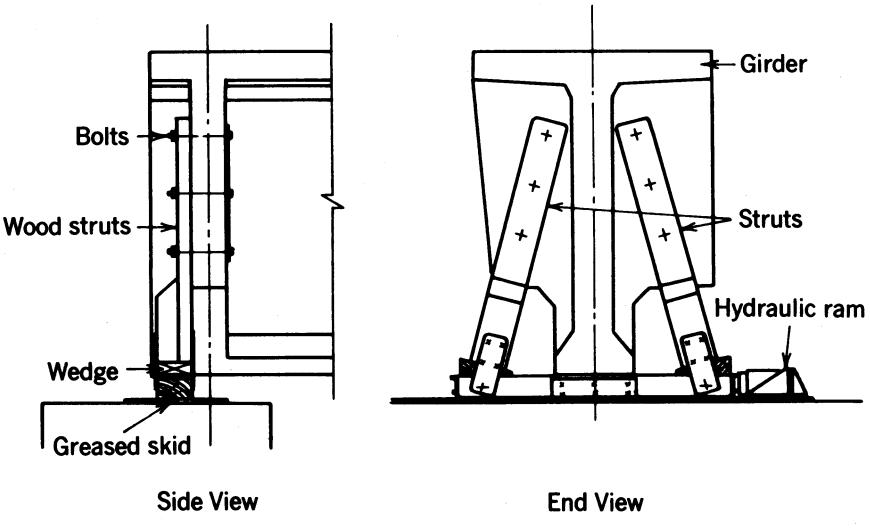

Fig. 18-8. Bamako Bridge apparatus for transverse sliding of girder.

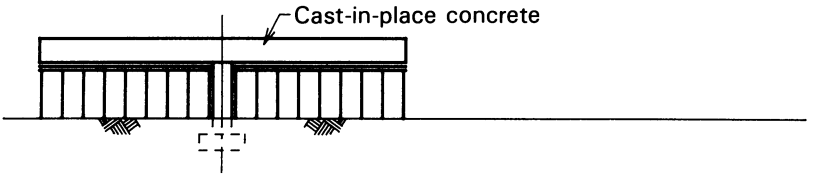

(a) Two cantilevers before post-tensioning

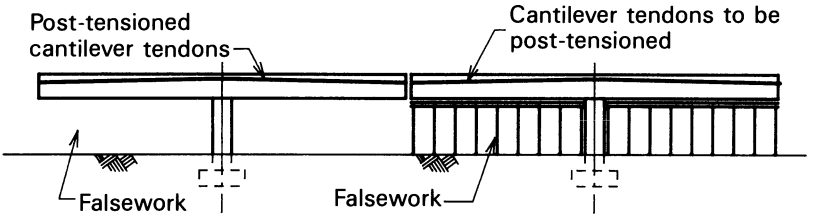

(b) Two sets of two cantilevers

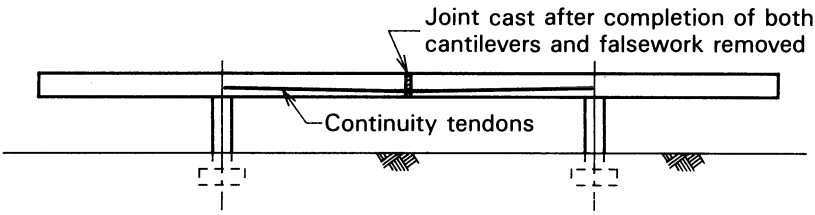

(c) Center span completed by cast-in-place closure and post-tensioning of continuity tendons

Fig. 18-9. Falsework utilized with the cantilever erection technique.

by the placing of the cast-in-place concrete joint between the ends of the cantilevered segments and the installation of the continuity tendons.

Conventional falsework often is used to erect precast segments in the end spans of structures erected in cantilever, and has been used with the span-by-span technique. The latter is illustrated in Fig. 18-10, where it will be seen that the segments are erected on falsework provided with adjustable jacks for "fine grading" the erected segments. The erected segments normally are post-tensioned together first to form simple spans supported at their ends by the piers. After the adjacent span is erected and the cast-in-place closure has been cast and cured, continuity tendons are placed and stressed as shown. In this method, if correctly executed, the falsework bents near the piers do not have to support the entire dead-load reaction of the individual spans segments; this is done by the piers.

Precast concrete segments for a number of bridges have been erected by using falsework trusses rather than the conventional falsework, as illustrated in Fig.

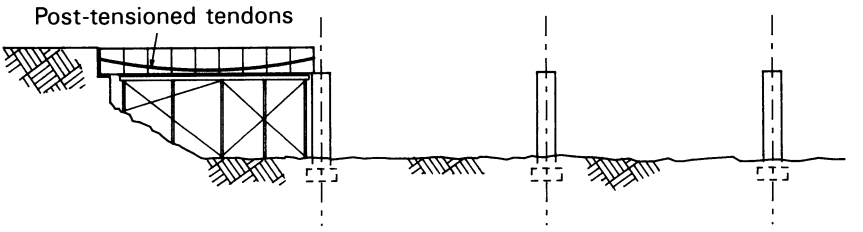

(a) Erection of first span

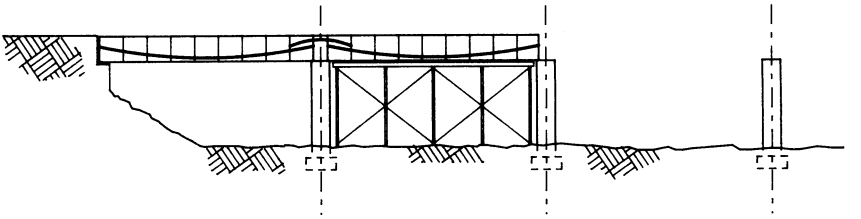

(b) Erection of second span

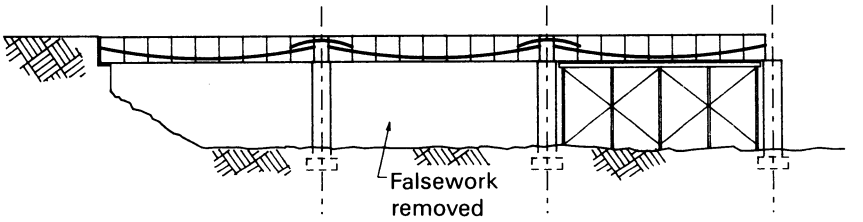

(c) Erection of third span

Fig. 18-10. Falsework utilized with the span-by-span erection technique.

18-11. With this technique the falsework trusses are supported by the piers and moved forward (for multi-span structures) as the erection progresses. The falsework trusses can be designed to support the segments from the soffit of the slab overhangs or from hangers attached to transverse beams that span between the trusses.

18-7 Erection with Gantries

Virtually all large bridges constructed with precast segments have been erected with a gantry or gantries designed expressly for the particular structure. There

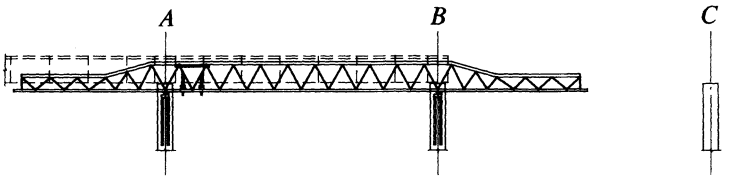

(a) Erection truss in position for erection of span *A–B*

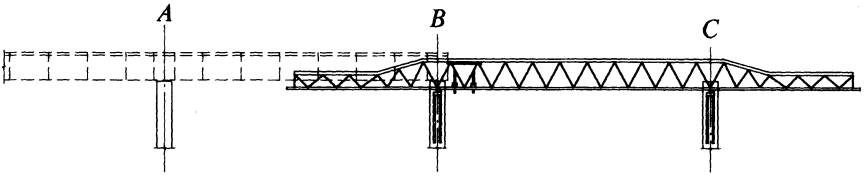

(b) Erection truss in position for erection of span *B–C*

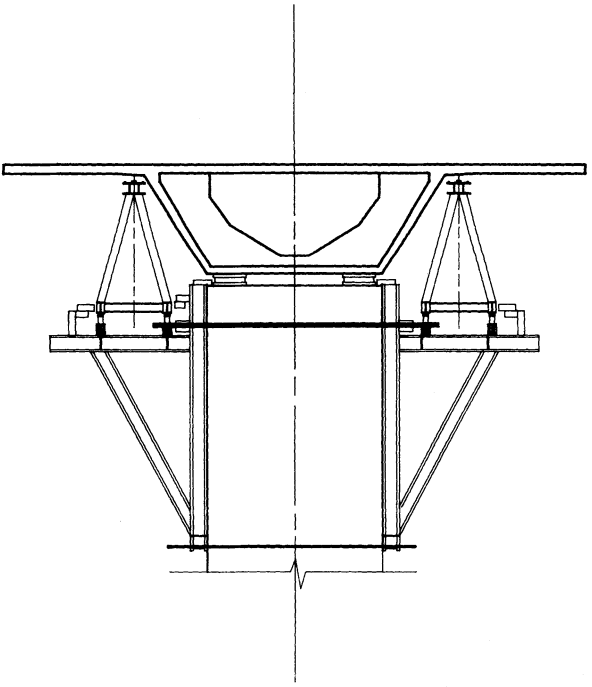

(c) Cross section of erection truss and bridge section.

Fig. 18-11. Trusses utilized with the span-by-span erection technique. (a) Erection truss in position for erecting segments in a span. (b) Erection truss advanced to next span after prestressing of previously erected span. (c) Cross section of erection truss and bridge section.

have been cases, however, in which gantries constructed for one project have been modified and used on a subsequent project or projects. The preferred erection method uses the specially designed gantries because they are capable of erecting the segments at a more rapid rate than other types of equipment and procedures, and, once erected and placed in service, they are completely independent of the terrain (or water) over which they are working. The relatively high first cost of erection gantries cannot be amortized on a bridge of low or moderate cost.

The first erection gantry used to erect precast concrete segments was employed in 1964 on the Oléron bridge in France, shown in Fig. 18-12. The erection was done one segment at a time, with the segments being delivered to the gantry over the top of the previously erected structure. The four gantries used in the erection of the Rio-Niterói bridge in Brazil were able to erect a typical span of 262 ft every seven days. The gantries used on the Rio-Niterói bridge were designed to erect two segments at the same time, with the segments being transported to the gantries on barges, as shown in Figs. 18-13 and 18-14.

The designs of some bridges do not provide sufficient strength at the connection of the superstructure to the substructure to resist the unbalanced moment induced by the cantilever erection technique. In this case, temporary bracing

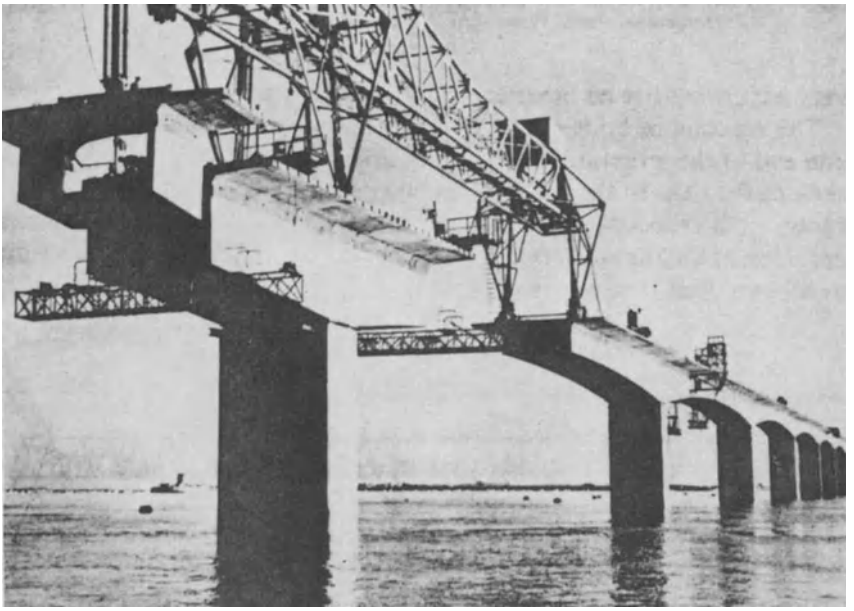

Fig. 18-12. Gantry erecting precast segments on the Oléron Bridge. (Provided by and reproduced with the permission of the Freyssinet Company, Inc., Charlotte, NC)

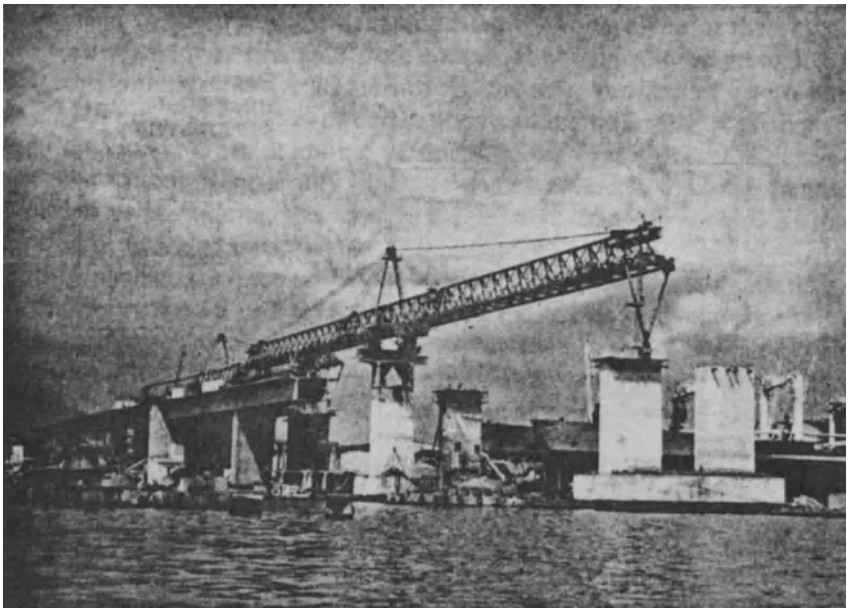

Fig. 18-13. Rio-Niterói Bridge during construction. (Provided by and reproduced with the permission of the Freyssinet Company, Inc., Charlotte, NC)

must be provided to stabilize the structure during the erection process. The bracing has been done by using the erection gantry itself, as shown in Fig. 18-15.

Contemporary erection gantries are much different from the ones used on the Oléron and Rio-Niterói bridges, and their evolution is expected to continue as experience is gained from each new application.

REFERENCES

Muller, J. 1960. Engineering Feats with Post-tensioning. *PCI Journal* 5(4):12–40.

Stergiou, P. 1967. Launcher Erects Post-tensioned Girders. *Civil Engineering*. 37:67-8.

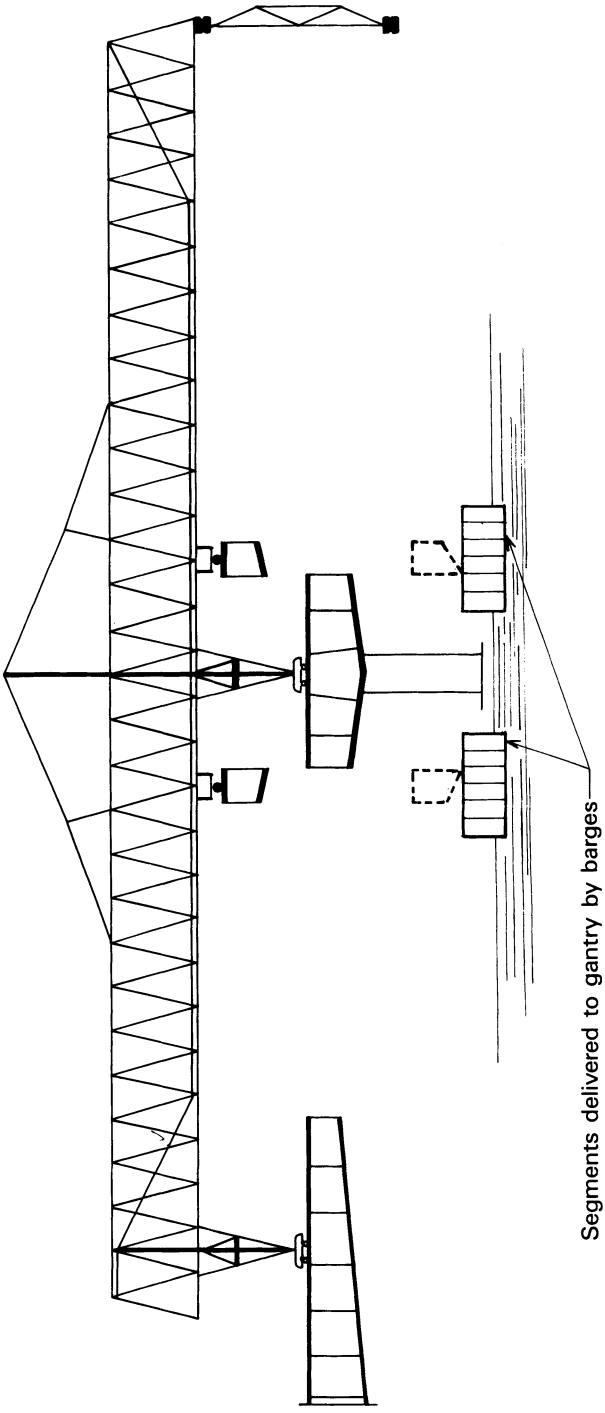

Fig. 18-14. Gantry erecting two segments simultaneously.

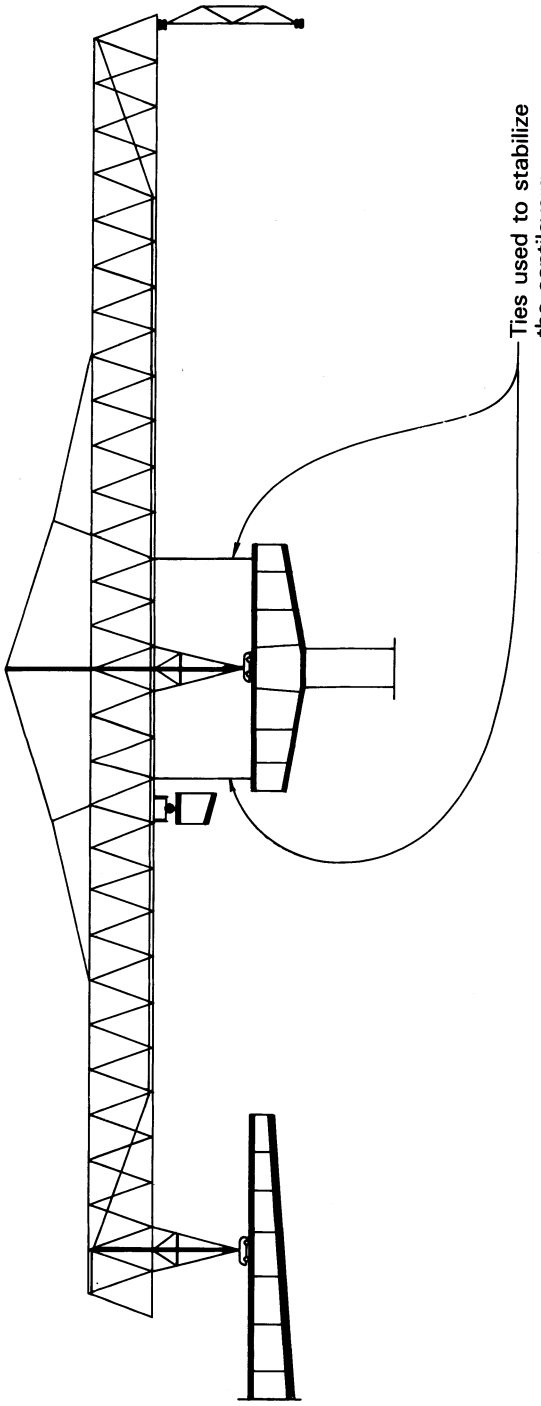

Fig. 18-15. Gantry used to brace the superstructure as well as to erect the segments.

Appendices

A. Recommendations for Estimating Prestress Losses, Prepared by the PCI Committed on Prestress Losses

B. Excerpts from the Eleventh, Thirteenth, and Fourteenth Editions of the AASHTO STANDARD SPECIFICATIONS FOR HIGHWAY BRIDGES

C. Estimating Prestress Losses, by Paul Zia, H. Kent Preston, Norman L. Scott, and Edwin B. Workman

D. Section 11 and Appendix D from *Design of Concrete Structures for Buildings* a National Standard of Canada.

Appendix A

Recommendations for Estimating Prestress Losses

Prepared by

PCI Committee on Prestress Losses

H. KENT PRESTON
Chairman

JAMES M. BARKER
HENRY C. BOECKER, JR.*
R. G. DULL
HARRY H. EDWARDS
TI HUANG
JAIME IRAGORRI
R. O. KASTEN†
HEINZ P. KORETZKY
PAUL E. KRAEMER‡
DONALD D. MAGURA‡
F. R. PREECE
MARIO G. SUAREZ
PAUL ZIA

* Replaced by Mario G. Suarez.
† Replaced by R. G. Dull.
‡ Previous Chairmen.

This PCI Committee report summarizes data on creep and shrinkage of concrete and steel relaxation, and presents both a general and a simplified design procedure for using these data in estimating loss of prestress after any given time period. A Commentary explains the design provisions. Detailed design examples for pretensioned and post-tensioned concrete structures explain the procedures.

This report is reprinted from the copyrighted JOURNAL of the Prestressed Concrete Institute, Vol. 20, No. 4, July–August 1975. Reprinted with permission.

CONTENTS

COMMITTEE STATEMENT

This recommended practice is intended to give the design engineer a comprehensive summary of research data applicable to estimating loss of prestress. It presents a general method whereby losses are calculated as a function of time.

This report contains information and procedures for estimating prestress losses in building applications. The general method is applicable to bridges, although there are some differences between it and the AASHTO *Standard Specifications for Highway Bridges* with respect to individual loss components.

A precise determination of stress losses in prestressed concrete members is a complicated problem because the rate of loss due to one factor, such as relaxation of tendons, is continually being altered by changes in stress due to other factors, such as creep of concrete. Rate of creep in its turn is altered by change in tendon stress. It is extremely difficult to separate the net amount of loss due to each factor under different conditions of stress, environment, loading, and other uncertain factors.

In addition to the foregoing uncertainties due to interaction of shrinkage, creep, and relaxation, physical conditions, such as variations in actual properties of concrete made to the same specified strength, can vary the total loss. As a result, the computed values for prestress loss are not necessarily exact, but the procedures here presented will provide more accurate results than by previous methods which gave no consideration to the actual stress levels in concrete and tendons.

An error in computing losses can affect service conditions such as camber, deflection, and cracking. It has no effect on the ultimate strength of a flexural member unless the tendons are unbonded or the final stress after losses is less than $0.5f_{pu}$.

It is not suggested that the information and procedures in this report provide the only satisfactory solution to this complicated problem. They do represent an up-to-date compromise by the committee of diverse opinions, experience and research results into relatively easy to follow design formulas, parameters, and computations.

CHAPTER 1—GENERAL ASPECTS RELATED TO PRESTRESS LOSSES

1.1—Tensioning of Prestressing Steel

1.1.1—Pretensioned construction

For deflected prestressing steel, loss *DEF*, occurring at the deflecting devices, should be taken into account.

1.1.2—Friction in post-tensioned construction

Loss due to friction in post-tensioned construction should be based upon wobble and curvature coefficients given below, and verified during stressing operations. The losses due to friction between the prestressing steel and the duct enclosure may be estimated by the following equation:

$$FR = T_o[1 - e^{-(Kl_{tx} + \mu\alpha)}] \qquad (1)$$

When $(Kl_{tx} + \mu\alpha)$ is not greater than 0.3, the following equation may be used:

$$FR = T_o(Kl_{tx} + \mu\alpha) \qquad (2)$$

Table 1 gives a summary of friction coefficients for various post-tensioning tendons.

1.2—Anchorage

Loss *ANC*, due to movement of prestressing steel in the end anchorage, should be taken into account. Slip at the anchorage will depend upon the particular prestressing system utilized and will not be a function of time. Realistic allowance should be made for slip or take-up as recommended for a given system of anchorage.

1.3—Transfer of Prestress

Loss due to elastic shortening may be calculated according to the provisions in this recommended practice. The concrete shortening should also include that resulting from subsequent stressing of prestressing steel.

1.4—Effect of Members in Structures

Loss of prestress of a member may be affected by connection to other structural elements or composite action with cast-in-place concrete. Change in prestress force due to these factors should be taken into account based on a rational procedure that considers equilibrium of forces and strain compatibility.

Table 1. Friction coefficients for post-tensioning tendons.

Type of tendon	Wobble coefficient, *K*, per foot	Curvature coefficient, μ
Tendons in flexible metal sheathing		
Wire tendons	0.0010 - 0.0015	0.15 - 0.25
7-wire strand	0.0005 - 0.0020	0.15 - 0.25
High strength bars	0.0001 - 0.0006	0.08 - 0.30
Tendons in rigid metal duct		
7-wire strand	0.0002	0.15 - 0.25
Pre-greased tendons		
Wire tendons and 7-wire strand	0.0003 - 0.0020	0.05 - 0.15
Mastic-coated tendons		
Wire tendons and 7-wire strand	0.0010 - 0.0020	0.05 - 0.15

CHAPTER 2—GENERAL METHOD FOR COMPUTING PRESTRESS LOSSES

2.1—Scope

2.1.1—Materials

2.1.1.1—*Lightweight concrete*—Lightweight aggregate concrete with a unit weight between 90 and 125 lb per cu ft where the unit weight varies because of replacement of lightweight fines with normal weight sand.

2.1.1.2—*Normal weight concrete*—Concrete with an approximate unit weight of 145 lb per cu ft where all aggregates are normal weight concrete aggregates.

2.1.1.3—*Prestressing Steel*—High strength prestressing steel that has been subjected to the stress-relieving process, or to processes resulting in low relaxation characteristics.

2.1.2— Prestressed units

Linearly prestressed members only. Excluded are closed sections prestressed circumferentially.

2.1.3—Curing

2.1.3.1—*Moist cure*—Impermeable membrane curing or other methods to prevent the loss of moisture from the concrete.

2.1.3.2—*Accelerated cure*—Curing in which the temperature of the concrete is elevated to not more than 160F for a period of approximately 18 hours, and steps are taken to retain moisture.

2.1.4—Environment

Prestressed concrete subjected to seasonal fluctuations of temperature and humidity in the open air or to nominal room conditions is covered.

The values for *UCR* and *USH* are based on an average ambient relative humidity of 70 percent.

2.2—Total Loss

2.2.1—Pretensioned construction

$$TL = ANC + DEF + ES + \sum_{t_i}^{t} (CR + SH + RET) \quad (3)$$

2.2.2—Post-tensioned construction

$$TL = \underset{t}{FR} + ANC + ES + \sum_{t_i} (CR + SH + RET) \quad (4)$$

2.3—Loss Due to Elastic Shortening (*ES*)

Loss of prestress due to elastic shortening of the concrete should be calculated based on the modulus of elasticity of the concrete at the time the prestress force is applied.

$$ES = f_{cr}(E_s/E_{ci}) \quad (5)$$

2.3.1—Pretensioned construction

In calculating shortening, the loss of prestress shall be based upon the concrete stress at the centroid of the prestressing force at the section of the member under consideration.

This stress, f_{cr}, is the compressive stress due to the prestressing force that is acting immediately after the prestress force is applied minus the stress due to all dead load acting at that time.

2.3.2—Post-tensioned construction

The average concrete stress between anchorages along each element shall be used in calculating shortening.

2.4—Time-Dependent Losses (General)

Prestress losses due to steel relaxation and creep and shrinkage of concrete are inter-dependent and are time-dependent. To account for changes of these effects with time, a step-by-step procedure can be used with the time interval increasing with age of the concrete. Shrinkage from the time when curing is stopped until the time when the concrete is prestressed should be deducted from the total calculated shrinkage for post-tensioned construction. It is recommended that a minimum of four time intervals be used as shown in Table 2.

When significant changes in loading are expected, time intervals other than those recommended should be used. Also, it is neither necessary, nor always desirable, to assume that the design live load is continually present. The four time intervals above are recommended for minimum non-computerized calculations.

2.5—Loss Due to Creep of Concrete (*CR*)

2.5.1—Loss over each step

Loss over each time interval is given by

$$CR = (UCR)(SCF)(MCF) \times (PCR)(f_o) \quad (6)$$

where f_o is the net concrete compressive stress at the center of gravity of the prestressing force at time t_1, taking into account the loss of prestress force occurring over the preceding time interval.

The concrete stress f_c at the time t_1 shall also include change in applied load during the preceding time interval. Do not include the factor *MCF* for accelerated cured concrete.

Table 2. Minimum time intervals.

Step	Beginning time, t_1	End time, t
1	Pretensioned anchorage of prestressing steel Post-tensioned: end of curing of concrete	Age at prestressing of concrete
2	End of Step 1	Age = 30 days, or time when a member is subjected to load in addition to its own weight
3	End of Step 2	Age = 1 year
4	End of Step 3	End of service life

2.5.2—Ultimate creep loss

2.5.2.1—*Normal weight concrete (UCR)*

Moist cure not exceeding 7 days:

$$UCR = 95 - 20E_c/10^6 \geq 11 \quad (7)$$

Accelerated cure:

$$UCR = 63 - 20E_c/10^6 \geq 11 \quad (8)$$

2.5.2.2—*Lightweight concrete (UCR)*

Moist cure not exceeding 7 days:

$$UCR = 76 - 20E_c/10^6 \geq 11 \quad (9)$$

Accelerated cure:

$$UCR = 63 - 20E_c/10^6 \geq 11 \quad (10)$$

Table 3. Creep factors for various volume to surface ratios.

Volume to surface ratio, in.	Creep factor *SCF*
1	1.05
2	0.96
3	0.87
4	0.77
5	0.68
>5	0.68

Table 4. Creep factors for various ages of prestress and periods of cure.

Age of prestress transfer, days	Period of cure, days	Creep factor, *MCF*
3	3	1.14
5	5	1.07
7	7	1.00
10	7	0.96
20	7	0.84
30	7	0.72
40	7	0.60

Table 5. Variation of creep with time after prestress transfer.

Time after prestress transfer, days	Portion of ultimate creep, *AUC*
1	0.08
2	0.15
5	0.18
7	0.23
10	0.24
20	0.30
30	0.35
60	0.45
90	0.51
180	0.61
365	0.74
End of service life	1.00

Table 6. Shrinkage factors for various volume to surface ratios.

Volume to surface ratio, in.	Shrinkage factor *SSF*
1	1.04
2	0.96
3	0.86
4	0.77
5	0.69
6	0.60

2.5.3—Effect of size and shape of member (SCF)

To account for the effect of size and shape of the prestressed members, the value of *SCF* in Eq. (6) is given in Table 3.

2.5.4—Effect of age at prestress and length of cure (MCF)

To account for effects due to the age at prestress of moist cured concrete and the length of the moist cure, the value of *MCF* in Eq. (6) is given in Table 4. The factors in this table do *not* apply to accelerated cured concretes nor are they applicable as shrinkage factors.

2.5.5—Variation of creep with time (AUC)

The variation of creep with time shall be estimated by the values given in Table 5. Linear interpolation shall be used between the values listed.

2.5.6—Amount of creep over each step (PCR)

The portion of ultimate creep over the time interval t_1 to t, *PCR* in Eq. (6), is given by the following equation:

$$PCR = (AUC)_t - (AUC)_{t_1} \quad (11)$$

2.6—Loss Due to Shrinkage of Concrete *(SH)*

2.6.1—Loss over each step

Loss over each time interval is given by

$$SH = (USH)(SSF)(PSH) \quad (12)$$

2.6.2—Ultimate loss due to shrinkage of concrete

The following equations apply to

both moist cured and accelerated cured concretes.

2.6.2.1—*Normal weight concrete (USH)*

$$USH = 27{,}000 - 3000E_c/10^6 \quad (13)$$

but not less than 12,000 psi.

2.6.2.2—*Lightweight concrete (USH)*

$$USH = 41{,}000 - 10{,}000E_c/10^6 \quad (14)$$

but not less than 12,000 psi.

2.6.3—Effect of size and shape of member (SSF)

To account for effects due to the size and shape of the prestressed member, the value of *SSF* in Eq. (12) is given in Table 6.

2.6.4—Variation of shrinkage with time (AUS)

The variation of shrinkage with time shall be estimated by the values given in Table 7. Linear interpolation shall be used between the values listed.

2.6.5—Amount of shrinkage over each step (PSH)

The portion of ultimate shrinkage over the time interval t_1 to t, *PSH* in Eq. (12), is given by the following equation:

$$PSH = (AUS)_t - (AUS)_{t_1} \quad (15)$$

2.7—Loss Due to Steel Relaxation (*RET*)

Loss of prestress due to steel relaxation over the time interval t_1 to t may be estimated using the following equations. (For mathematical correctness, the value for t_1 at the time of anchorage of the prestressing steel shall be taken as 1/24 of a day so that log t_1 at this time equals zero.)

Table 7. Shrinkage coefficients for various curing times.

Time after end of curing, days	Portion of ultimate shrinkage, *AUS*
1	0.08
3	0.15
5	0.20
7	0.22
10	0.27
20	0.36
30	0.42
60	0.55
90	0.62
180	0.68
365	0.86
End of service life	1.00

2.7.1—Stress-relieved steel

$$RET = f_{st}\{[\log 24t - \log 24t_1]/10\} \times [f_{st}/f_{py} - 0.55] \quad (16)$$

where

$$f_{st}/f_{py} - 0.55 \geq 0.05$$
$$f_{py} = 0.85 f_{pu}$$

2.7.2—Low-relaxation steel

The following equation applies to prestressing steel given its low relaxation properties by simultaneous heating and stretching operations.

$$RET = f_{st}\{[\log 24t - \log 24t_1]/45\} \times [f_{st}/f_{py} - 0.55] \quad (17)$$

where

$$f_{st}/f_{py} - 0.55 \geq 0.05$$
$$f_{py} = 0.90 f_{pu}$$

2.7.3—Other prestressing steel

Relaxation of other types of prestressing steel shall be based upon manufacturer's recommendations supported by test data.

CHAPTER 3—SIMPLIFIED METHOD FOR COMPUTING PRESTRESS LOSSES

3.1—Scope

Computations of stress losses in accordance with the General Method can be laborious for a designer who does not have the procedure set up on a computer program. The Simplified Method is based on a large number of design examples in which the parameters were varied to show the effect of different levels of concrete stress, dead load stress, and other factors. These examples followed the General Method and the procedures given in the Design Examples.

3.2—Principles of the Simplified Method

3.2.1—Concrete stress at the critical location

Compute f_{cr} and f_{cds} at the critical location on the span. The critical location is the point along the span where the concrete stress under full live load is either in maximum tension or in minimum compression. If f_{cds} exceeds f_{cr} the simplified method is not applicable.

f_{cr} and f_{cds} are the stresses in the concrete at the level of the center of gravity of the tendons at the critical location. f_{cr} is the net stress due to the prestressing force plus the weight of the prestressed member and any other permanent loads on the member at the time the prestressing force is applied. The prestressing force used in computing f_{cr} is the force existing immediately after the prestress has been applied to the concrete. f_{cds} is the stress due to all permanent (dead) loads not used in computing f_{cr}.

Table 8. Simplified method equations for computing total prestress loss (*TL*).

Equation number	Concrete weight		Type of tendon			Tensioning		Equations
	NW	LW	SR	LR	BAR	PRE	POST	
N-SR-PRE-70	X		X			X		$TL = 33.0 + 13.8f_{cr} - 4.5f_{cds}$
L-SR-PRE-70		X	X			X		$TL = 31.2 + 16.8f_{cr} - 3.8f_{cds}$
N-LR-PRE-75	X			X		X		$TL = 19.8 + 16.3f_{cr} - 5.4f_{cds}$
L-LR-PRE-75		X		X		X		$TL = 17.5 + 20.4f_{cr} - 4.8f_{cds}$
N-SR-POST-68.5	X		X				X	$TL = 29.3 + 5.1f_{cr} - 3.0f_{cds}$
L-SR-POST-68.5		X	X				X	$TL = 27.1 + 10.1f_{cr} - 4.9f_{cds}$
N-LR-POST-68.5	X			X			X	$TL = 12.5 + 7.0f_{cr} - 4.1f_{cds}$
L-LR-POST-68.5		X		X			X	$TL = 11.9 + 11.1f_{cr} - 6.2f_{cds}$
N-BAR-POST-70	X				X		X	$TL = 12.8 + 6.9f_{cr} - 4.0f_{cds}$
L-BAR-POST-70		X			X		X	$TL = 12.5 + 10.9f_{cr} - 6.0f_{cds}$

Note: Values of TL, f_{cr}, and f_{cds} are expressed in ksi.

3.2.2—Simplified loss equations

Select the applicable equation from Table 8 or 9, substitute the values for f_{cr} and f_{cds} and compute TL or f_{sc}, whichever is desired.

3.2.3—Basic parameters

The equations are based on members having the following properties:

1. Volume-to-surface ratio = 2.0.
2. Tendon tension as indicated in each equation.
3. Concrete strength at time prestressing force is applied:
   3500 psi for pretensioned members
   5000 psi for post-tensioned members
4. 28-day concrete compressive strength = 5000 psi.
5. Age at time of prestressing:
   18 hours for pretensioned members
   30 days for post-tensioned members
6. Additional dead load applied 30 days after prestressing.

Compare the properties of the beam being checked with Items 1 and 2. If there is an appreciable difference, make adjustments as indicated under Section 3.4.

It was found that an increase in concrete strength at the time of prestressing or at 28 days made only a nominal difference in final loss and could be disregarded. For strength at prestressing less than 3500 psi or for 28-day strengths less than 4500 psi, an analysis should be made following Design Example 1.

Wide variations in Items 5 and 6 made only nominal changes in net loss so that further detailed analysis is needed only in extreme cases.

3.2.4—Computing f_{cr}

$$f_{cr} = Af_{st}/A_c + A_s f_{st} e^2/I_c - M'e/I_c \qquad (18)$$

Table 9. Simplified method equations for computing effective prestress (f_{se}).

Equation Number	Concrete weight		Type of tendon			Tensioning		Equations
	NW	LW	SR	LR	BAR	PRE	POST	
N-SR-PRE-70	X		X			X		$f_{se} = f_t - (33.0 + 13.8f_{cr} - 11f_{cds})$
L-SR-PRE-70		X	X			X		$f_{se} = f_t - (31.2 + 16.8f_{cr} - 13.5f_{cds})$
N-LR-PRE-75	X			X		X		$f_{se} = f_t - (19.8 + 16.3f_{cr} - 11.9f_{cds})$
L-LR-PRE-75		X		X		X		$f_{se} = f_t - (17.5 + 20.4f_{cr} - 14.5f_{cds})$
N-SR-POST-68.5	X		X				X	$f_{se} = f_{si} - (29.3 + 5.1f_{cr} - 9.5f_{cds})$
L-SR-POST-68.5		X	X				X	$f_{se} = f_{si} - (27.1 + 10.1f_{cr} - 14.6f_{cds})$
N-LR-POST-68.5	X			X			X	$f_{se} = f_{si} - (12.5 + 7.0f_{cr} - 10.6f_{cds})$
L-LR-POST-68.5		X		X			X	$f_{se} = f_{si} - (11.9 + 11.1f_{cr} - 15.9f_{cds})$
N-BAR-POST-70	X				X		X	$f_{se} = f_{si} - (12.8 + 6.9f_{cr} - 10.5f_{cds})$
L-BAR-POST-70		X			X		X	$f_{se} = f_{si} - (12.5 + 10.9f_{cr} - 15.7f_{cds})$

Note: Values of f_t, f_{si}, f_{cr}, and f_{cds} are expressed in ksi.

3.2.5—Tendon stress for pretensioned members

Except for members that are very heavily or very lightly* prestressed, f_{si} can be taken as follows:

For stress-relieved steel

$$f_{si} = 0.90\, f_t \qquad (19)$$

For low-relaxation steel

$$f_{si} = 0.925\, f_t \qquad (20)$$

3.2.6 Tendon stress for post-tensioned members

Except for members that are very heavily or very lightly* prestressed f_{si} can be taken as

$$f_{si} = 0.95\,(T_o - FR) \qquad (21)$$

3.3—Equations for Simplified Method

3.3.1—Total prestress loss

The equations in Table 8 give total prestress loss TL in ksi. This value corresponds to TL shown in the summaries of Design Examples 1 and 3.

3.3.2—Effective stress

The equations in Table 9 give effective stress in prestressing steel under dead load after losses. This value corresponds to f_{se} shown in the summary of Design Example 1.

As shown in the summary of Design Example 1, the stress existing in the tendons under dead load after all losses have taken place is the initial tension reduced by the amount of the total losses and increased by the stress created in the tendon by the addition of dead load after the member was prestressed. The increase in tendon stress due to the additional dead load is equal to $f_{cds}\,(E_s/E_c)$.

$$f_{se} = f_t - TL + f_{cds}(E_s/E_c) \qquad (22)$$

3.3.3—Explanation of equation number

The equation number in Tables 8 and 9 defines the conditions for which each equation applies:

1. The first term identifies the type of concrete.
   N = normal weight = approximately 145 lb per cu ft
   L = lightweight = approximately 115 lb per cu ft

2. The second term identifies the steel in the tendon:
   SR = stress-relieved
   LR = low-relaxation
   BAR = high strength bar

3. The third term identifies the type of tensioning:
   PRE = pretensioned and is based on accelerated curing
   POST = post-tensioned and is based on moist curing

4. The fourth term indicates the initial tension in percent of f_{pu}:
   For *pretensioned* tendons it is the tension at which the tendons are anchored in the casting bed before concrete is placed.

   For *post-tensioned* tendons it is the initial tension in the tendon at the critical location in the concrete member after losses due to friction and anchor set have been deducted.

*When f_{sr} computed by Eq. (18) using the approximations for f_{s4} is greater than 1600 psi or less than 800 psi the value of f_{s4} should be checked as illustrated in Design Example 2.

3.4—Adjustment for Variations from Basic Parameters

3.4.1—Volume-to-surface ratio

Equations are based on $V/S = 2.0$

V/S ratio	1.0	2.0	3.0	4.0
Adjustment, percent	+3.2	0	−3.8	−7.6

Example: For $V/S = 3.0$, decrease TL by 3.8 percent.

3.4.2—Tendon stress

3.4.2.1—*Pretensioned tendons*

Pretensioned tendons are so seldom used at stresses below those shown for the equations in members where the final stress is important, that examples covering this condition were not worked out. Design Example 1 can be followed if necessary.

3.4.2.2—*Post-tensioned tendons*

Equations are based on $f_{si} = 185{,}000$ psi. If f_{si} is less than 185,000 psi reduce the total stress loss:

For stress-relieved strands

$$\Delta TL = 0.41\,(185{,}000 - f_{si}) \quad (23)$$

For low-relaxation strands

$$\Delta TL = 0.09\,(185{,}000 - f_{si}) \quad (24)$$

For high strength bars which are based on $f_{si} = 0.70\,f_{pu}$

$$\Delta TL = 0.09\,(0.70\,f_{pu} - f_{si}) \quad (25)$$

If f_{si} is greater than the value used in preparing the equations, ΔTL will be a negative number and will therefore increase the value of TL. Note that f_{si} is limited to a maximum of 0.70 f_{pu} by ACI 318-71.

COMMENTARY

In this report a wide range of data has been assimilated to develop a general method for predicting loss of prestress, but including specific numerical values. In addition, creep and shrinkage of concrete and steel relaxation are presented as functions of time. By calculating losses over recommended time intervals, it is possible to take into account the interdependence of concrete and steel deformation.

It must be emphasized that losses, per se, are not the final aim of calculations. What is determined is the stress remaining in the prestressing steel. The stress remaining, however, must be evaluated using rational procedures.

The notation commonly used in the ACI Building Code is adopted wherever possible. For new terms, descriptive letters are used.

References are listed chronologically. Not all the references listed were used in developing the numerical recommendations. They are included because of their value in understanding time-dependent behavior.

Chapter 1—General Aspects Related to Prestress Losses

1.1—Friction losses during post-tensioning are estimated using familiar equations, but with up-dated coefficients (see Reference 30). No known systematic study has been made of

losses that occur at deflecting devices in pretensioned construction. The provision is to warn that friction at these points may produce conditions where the desired steel stresses are not reached.

1.2—Seating losses are particularly important where the length of prestressing steel is short. For this condition, tolerances in seating deformation should not be overlooked.

1.3—The effect of post-tensioning of each individual tendon on previously anchored tendons should be considered. This applies, of course, when pretensioned and post-tensioned systems are combined.

1.4—Many problems have occurred because of unaccounted restraint and the effects of volume changes of concrete cast at different times. There are several references that give techniques for calculating these effects (References 6, 9, 10, 12, 20, 29, 30). This reminder is included here, even though losses are but one factor influenced by structural integration.

Chapter 2—General Method for Computing Prestress Losses

This section presents the range of data studied and, consequently, the range of applicability. Extrapolation has been avoided beyond documented data. In effect, this also shows where additional research is needed. Some practices and conditions common to certain areas of the country cannot be incorporated because no information is available. It is in this situation that experience, engineering judgment, and local sources of information are depended upon.

2.2—Total loss of prestress is the sum of losses due to individual factors. Eqs. (3) and (4) list the factors to be taken into account for each type of construction. The terms *ANC*, *DEF*, and *FR* are defined in Section 1. The remaining terms are defined in Section 2. Losses due to creep, shrinkage, and steel relaxation are the sum of losses during each time interval described in Section 2.4.

2.3—It is not desirable to be "conservative" and assume a low value for the modulus of concrete. The estimated modulus should reflect what is specified for minimum concrete strength and what is specified for permissible variation of concrete strength.

2.4—The step procedure is recommended to realistically approach the actual behavior of prestressed concrete. By this technique, it is possible to evaluate loss of prestress with change in time and change in stress. What is done here is to take into account the interdependence of one deformation on the other. Specific steps are outlined in succeeding sections.

2.5—Ultimate creep is the total amount of shortening measured on standard 6 x 12-in. cylinders. Fig. 1 illustrates that values differ according to the type of cure and the type of concrete (References 2, 14, 15, 21, 24). Ultimate creep is affected by relative humidity as shown in Fig. 2 (References 3, 7, 8, 11, 17). In standard tests, specimens are stored at 50 percent relative humidity. Average relative humidity over the majority of the United States is 70 percent (Reference 18). Eqs. (7), (8), (9), and (10), therefore, are based on data shown in Figs. 1 and 2.

Fig. 3 presents the relationship between creep and the size and shape of the test specimen (see References 7, 11, 17, 19). To apply standard creep data to actual members, a creep factor *SCF* is introduced. Values of *SCF* versus volume to surface ratios are listed in Section 2.5.3.

Similarly, age at loading and extent of moist-cure affect the amount of ultimate creep. Data in Fig. 4 (see Referenecs 3, 4, 11, 14) illustrate the trend. For moist-cured concretes, *UCR* is modified by the factor *MCF* in Section 2.5.4.

A generalization of creep-time data (References 2, 15, 24) was developed to take into account the rate of shortening due to creep. A typical creep curve is shown in Fig. 5. The portion of ultimate creep *AUC* at a given time is listed in Table 5. The amount of creep *PCR* in a given time interval is simply the difference of the amount of creep at the beginning and end of the time interval.

The terms, *SCF*, *MCF*, and *PCR* are non-dimensional. *UCR* was developed from creep data expressed as strain in millionths per psi concrete stress. By multiplying these data by the steel modulus of elasticity, unit steel stress per unit concrete stress was obtained.

Therefore, in Eq. (6), steel stress is obtained by multiplying concrete stress f_c by the product of these four non-dimensional terms. As stated in Section 2.5, f_c is the net concrete stress that results from at least full dead load and possibly some portion of the live load. The amount of live load, if any, present for extended periods is left to the engineer's judgment.

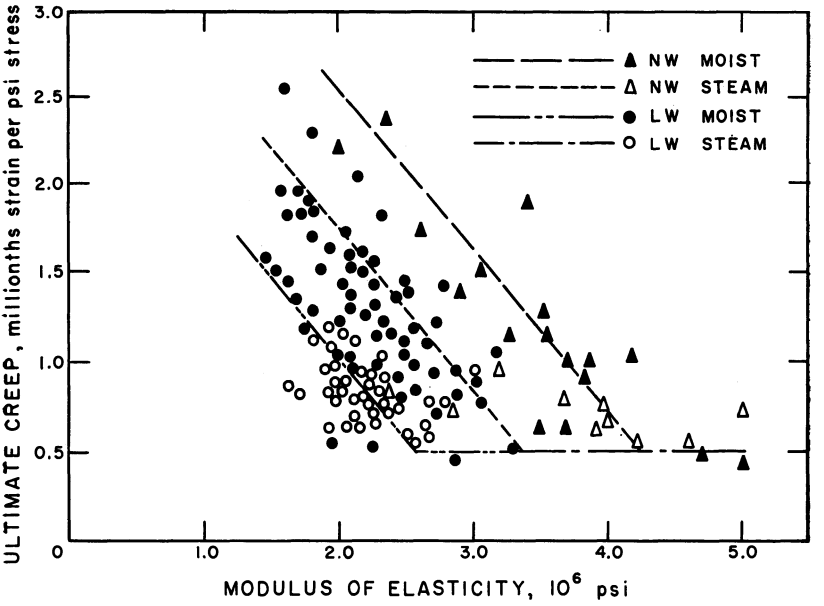

Fig. 1. Ultimate creep versus modulus of elasticity.

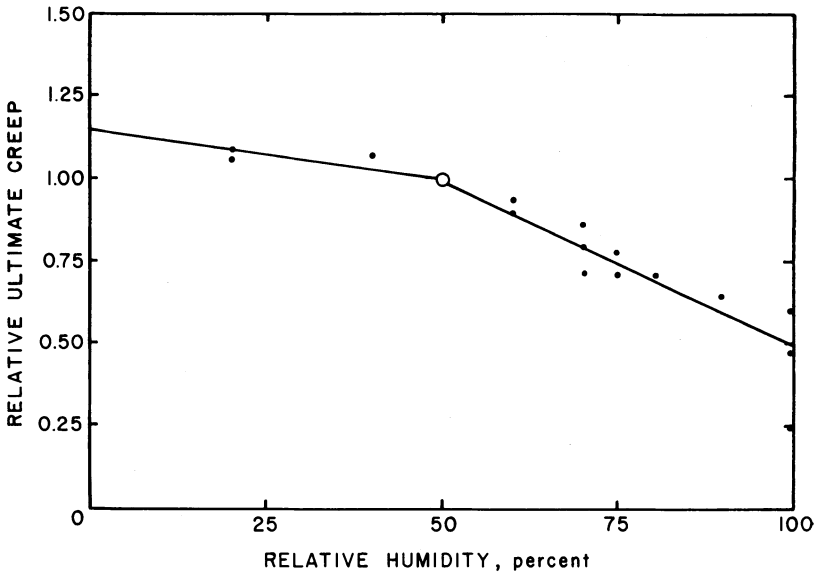

Fig. 2. Relative ultimate creep versus relative humidity.

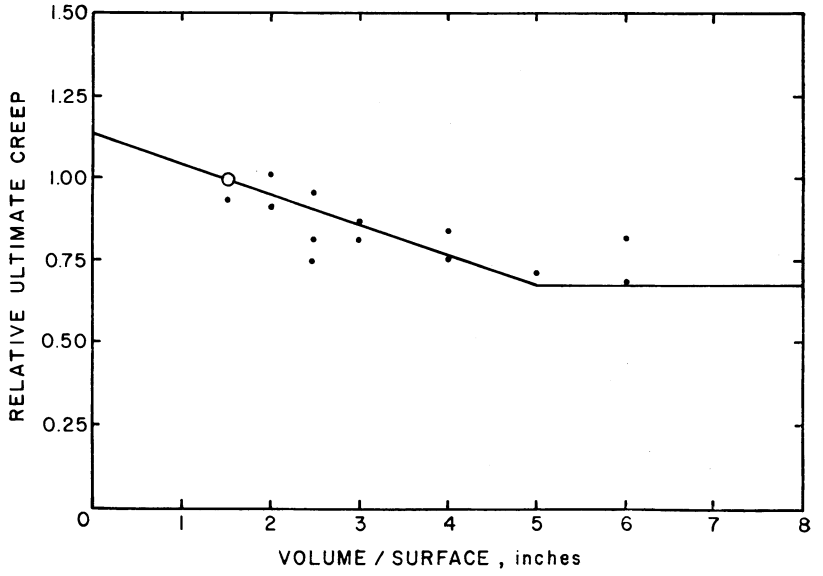

Fig. 3. Relative ultimate creep versus volume to surface ratio.

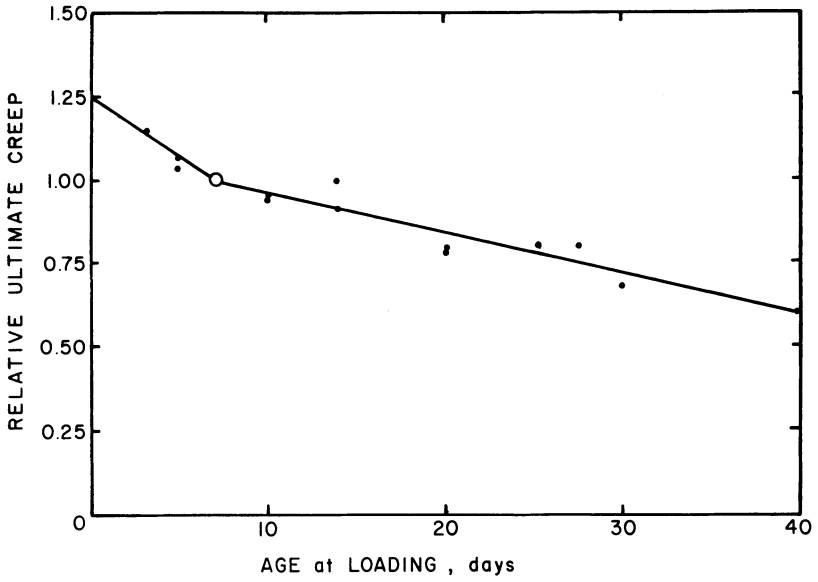

Fig. 4. Relative ultimate creep versus loading age.

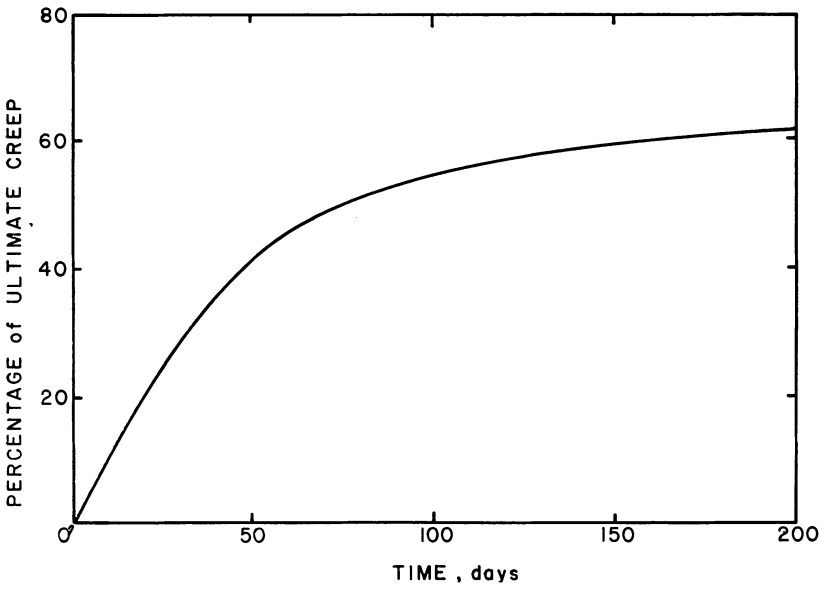

Fig. 5. Percentage of ultimate creep versus time.

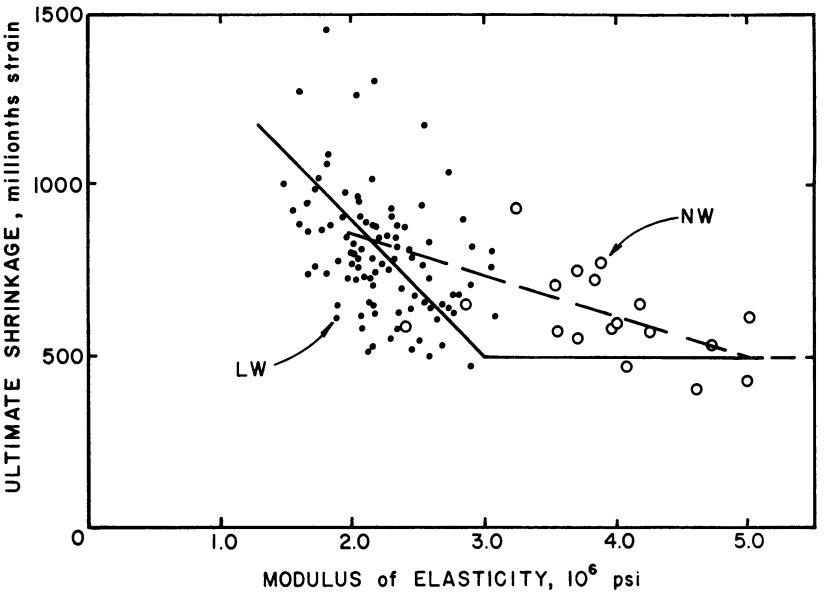

Fig. 6. Ultimate shrinkage versus modulus of elasticity.

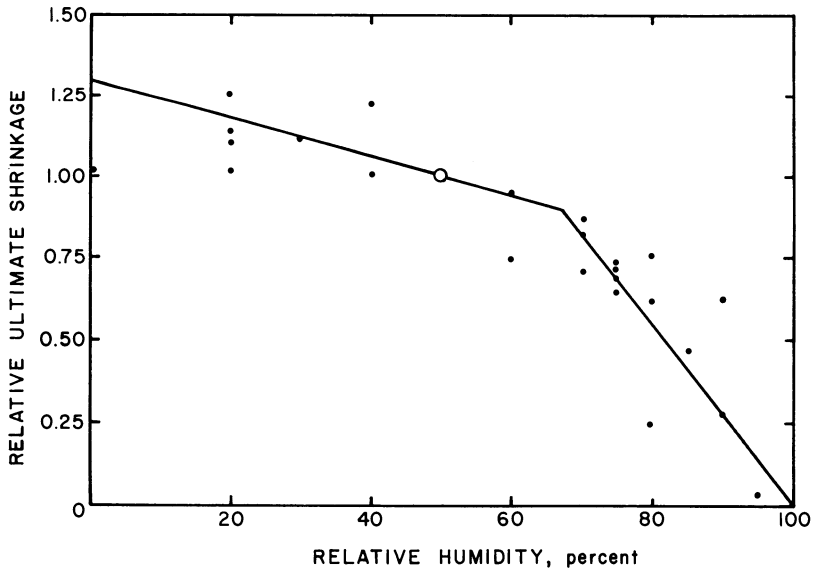

Fig. 7. Relative ultimate shrinkage versus relative humidity.

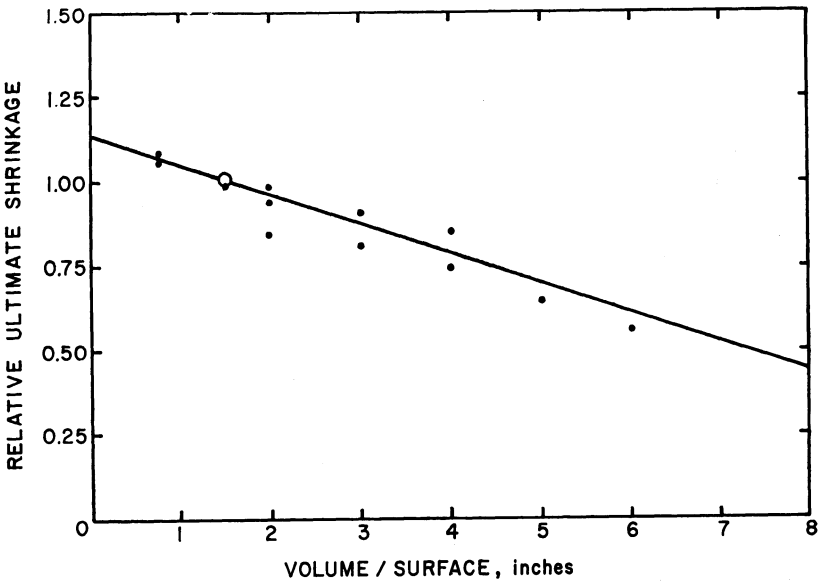

Fig. 8. Relative ultimate shrinkage versus volume to surface ratio.

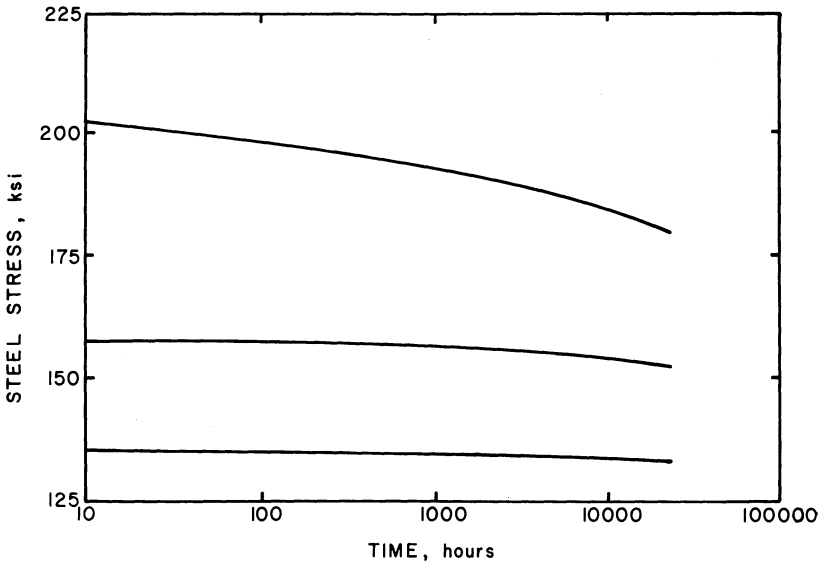

Fig. 9. Prestressing steel stress versus time for stress-relieved steel.

2.6—Comments on loss due to shrinkage are similar to those for creep, except that concrete stress is not a factor. Ultimate shrinkage strain from standard tests is shown in Fig. 6 (References 1, 2, 14, 15, 21, 24). These data were modified to 70 percent relative humidity using information illustrated in Fig. 7 (References 3, 7, 8, 11, 17), and multiplied by the steel modulus of elasticity to obtain Eqs. (13) and (14). *USH* is the loss in steel stress due to shrinkage shortening.

USH is influenced by the size and shape of the prestressed member. Shrinkage volume/surface data are presented in Fig. 8 (References 7, 11 17, 19). The size factor *SSF* is given in Table 6. By multiplying *USH* by *SSF*, standard test data can be applied to actual prestressed members. The variation of shrinkage with time was generalized using data in References 2, 15, and 24. This information is given in Table 7 as the portion of ultimate shrinkage *AUS* for a specific time after the end of curing. The amount of shrinkage *PSH* occurring over a specific time interval is the difference between the amount of shrinkage at the beginning of the time interval and that at the end of the time interval.

The loss of prestress over one time interval due to shrinkage of concrete is stated in Eq. (12).

2.7—Eqs. (16) and (17) (References 13, 32) give the loss of prestress due steel relaxation. The time t_1 in Step 1, listed in Section 2.4, is at anchorage of the prestressing steel. In pretensioned construction, where elevated temperatures are used in curing, losses during curing can be studied more closely using References 5, 22, and 26.

Fig. 9 shows typical steel relaxation with time under constant strain. It is seen that losses are less for lower initial stresses. This illustrates that by taking into account concrete shortening and steel relaxation over a previous time period, subsequent losses are less than that under assumed constant strain.

NOTATION

A_c = gross cross-sectional area of concrete member, sq in.

A_s = cross-sectional area of prestressing tendons, sq in.

ANC = loss of prestress due to anchorage of prestressing steel, psi

AUC = portion of ultimate creep at time after prestress transfer

AUS = portion of ultimate shrinkage at time after end of curing

CR = loss of prestress due to creep of concrete over time interval t_1 to t, psi

DEF = loss of prestress due to deflecting device in pretensioned construction, psi

e = tendon eccentricity measured from center of gravity of concrete section to center of gravity of tendons, in.

E_c = modulus of elasticity of concrete at 28 days taken as $33w^{3/2}\sqrt{f_c'}$, psi

E_{ci} = modulus of elasticity of concrete at time of initial prestress, psi

E_s = modulus of elasticity of steel, psi

ES = loss of prestress due to elastic shortening, psi

f_{cds} = concrete compressive stress at center of gravity of prestressing force due to all permanent (dead) loads not used in computing f_{cr}, psi

f_c = concrete compressive stress at center of gravity of prestressing steel, psi

f_c' = compressive strength of concrete at 28 days, psi

f_{ci}' = initial concrete compressive strength at transfer, psi

f_{cr} = concrete stress at center of gravity of prestressing force immediately after transfer, psi

f_{pu} = guaranteed ultimate tensile strength of prestressing steel, psi

f_{py} = stress at 1 percent elongation of prestressing steel, psi

f_{se} = effective stress in prestressing steel under dead load after losses

f_{si} = stress in tendon at critical location immediately after prestressing force has been applied to concrete

f_{st} = stress in prestressing steel at time t_1, psi

f_t = stress at which tendons are anchored in pretensioning bed, psi

FR = friction loss at section under consideration, psi

I_c = moment of inertia of gross cross section of concrete member, in.^{4}

K = friction wobble coefficient per foot of prestressing steel

l_{tx} = length of prestressing steel from jacking end to point x, ft

MCF = factor that accounts for the effect of age at prestress and length of moist cure on creep of concrete

M_{ds} = moment due to dead weight added after member is prestressed

M' = moment due to loads, including weight of member, at time prestress is applied to concrete

P = final prestress force in member after losses

P_o = initial prestress force in member

PCR = amount of creep over time interval t_1 to t

PSH = amount of shrinkage over time interval t_1 to t

RE = total loss of prestress due to relaxation of prestressing steel in pretensioned construction, psi

REP = total loss of prestress due to relaxation of prestressing steel in post-tensioned construction, psi

RET = loss of prestress due to steel relaxation over time interval t_1 to t, psi

SCF = factor that accounts for the effect of size and shape of a member on creep of concrete

SH = loss of prestress due to shrinkage of concrete over time interval t_1 to t, psi

SSF = factor that accounts for the effect of size and shape of a member on concrete shrinkage

t = time at end of time interval, days

t_1 = time at beginning of time interval, days

T_o = steel stress at jacking end of post-tensioning tendon, psi

T_x = steel stress at any point x, psi

TL = total prestress loss, psi

UCR = ultimate loss of prestress due to creep of concrete, psi per psi of compressive stress in the concrete

USH = ultimate loss of prestress due to shrinkage of concrete, psi

w = weight of concrete, lb per cu ft

α = total angular change of post-tensioning tendon profile from jacking end to point x, radians

μ = friction curvature coefficient

REFERENCES

1. Chubbuck, Edwin R., "Final Report on Research Program for the Expanded Shale Institute," Project No. 238, Engineering Experiment Section, Kansas State College, Manhattan, Kansas, July, 1956.
2. Shideler, J. J., "Lightweight Aggregate Concrete for Structural Use," Development Department Bulletin D-17, Portland Cement Association; see also *ACI Journal*, V. 54, No. 4, October, 1957, pp. 299-328.
3. Troxell, G. E., Raphael, J. M., and Davis, R. E., "Long Time Creep and Shrinkage Tests of Plain and Reinforced Concrete," ASTM Proceedings, Vol. 58, 1958.
4. Ross, A. D., "Creep of Concrete Under Variable Stress," *ACI Journal*, V. 29, No. 9, March, 1958, pp. 739-758.
5. Preston, H. Kent, "Effect of Temperature Drop on Strand Stresses in a Casting Bed," PCI JOURNAL, V. 4, No. 1, June, 1959, pp. 54-57.
6. Freyermuth, C. L., "Design of "Continuous Highway Bridges with Precast, Prestressed Concrete Girders," PCI JOURNAL, V. 14, No. 2, April, 1969, pp. 14-39.
7. Jones, T. R., Hirsch, T. J., and Stephenson, H. K., "The Physical Properties of Structural Quality Lightweight Aggregate Concrete," Texas Transportation Institute, Texas A & M University, College Station, August, 1959.
8. Lyse, I., "Shrinkage and Creep of Concrete," *ACI Journal*, V. 31, No. 8, February, 1960, pp. 775-782.
9. Corley, W. G., Sozen, M. A., and Siess, C. P., "Time-Dependent Deflections of Prestressed Concrete Beams," Highway Research Board Bulletin No. 307, National Academy of Sciences—National Research Council Publication No. 937, 1961.
10. Mattock, A. H., "Precast-Prestressed Concrete Bridges—5. Creep and Shrinkage Studies," Development Department Bulletin D-46, Portland Cement Association; see also Journal of the PCA Research and Development Laboratories, May, 1961.
11. Bugg, S. L., "Long-Time Creep of Prestressed Concrete I-Beams," Technical Report R-212, U.S. Naval Civil Engineering Laboratory, Port Hueneme, California, October 2, 1962.
12. ACI Committee 435, Subcommittee 5, "Deflections of Prestressed Concrete Members," *ACI Journal*, V. 60, No. 12, December, 1963, pp. 1697-1728.
13. Magura, Donald D., Sozen, M. A., and Siess, C. P., "A Study of Stress Relaxation in Prestressing Reinforcement," PCI JOURNAL, V. 9, No. 2, April, 1964, pp. 13-57.
14. Reichard, T. W., "Creep and Drying Shrinkage of Lightweight and Normal-Weight Concretes," National Bureau of Standards Monograph 74, U.S. Department of Commerce, March 4, 1964.
15. Hanson, J. A., "Prestress Loss as Affected by Type of Curing," Development Department Bulletin D-75, Portland Cement Association; see also PCI JOURNAL, V. 9, No. 2, April, 1964, pp. 69-93.
16. Zia, P., and Stevenson, J. F., "Creep of Concrete Under Non-Uniform Stress Distribution and Its Effect on Camber of Prestressed Concrete Beams," Project ERD-100-R, Engineering Research Department, North Carolina State

University, Raleigh, North Carolina, June, 1964.

17. Keeton, J. R., "Study of Creep in Concrete, Phases 1-5," Technical Report Nos. R-333-I, -II, -III, U.S. Naval Civil Engineering Laboratory, Port Hueneme, California, 1965.
18. *Selected Climatic Maps of the United States,* Office of Data Information, Environmental Science Service Administration, U.S. Department of Commerce, 1966.
19. Hansen, T. C., and Mattock, A. H., "Influence of Size and Shape of Member on the Shrinkage and Creep of Concrete," Development Department Bulletin D-103, Portland Cement Association; see also *ACI Journal,* V. 63, No. 2, February, 1966, pp. 267-290.
20. ACI Committee 435, "Deflections of Reinforced Concrete Flexural Members," *ACI Journal,* V. 63, No. 6, June, 1966, pp. 637-674.
21. Furr, H. L., and Sinno, R., "Creep in Prestressed Lightweight Concrete," Texas Transportation Institute, Texas A & M University, College Station, Texas, October, 1967.
22. Navaratnarajah, V., "An Analysis of Stresses During Steam Curing of Pretensioned Concrete," *Constructional Review,* December, 1967.
23. Hickey, K. B., "Creep of Concrete Predicted from the Elastic Modulus Tests," Report No. C-1242, Concrete and Structural Branch, Division of Research, Bureau of Reclamation, Denver, Colorado, January, 1968.
24. Pfeifer, D. W., "Sand Replacement in Structural Lightweight Concrete —Creep and Shrinkage Studies," Development Department Bulletin D-128, Portland Cement Association; see also *ACI Journal,* V. 65, No. 2, February, 1968, p. 131.
25. Rokhsar, A., and Huang, T., "Comparative Study of Several Concretes Regarding Their Potentials for Contributing to Prestress Losses," Fritz Engineering Laboratory Report No. 339.1, Lehigh University, Bethlehem, Pennsylvania, May, 1968.
26. Papsdorf, W., and Schwier, F., "Creep and Relaxation of Steel Wire, Particularly at Highly Elevated Temperatures," *Stahl u. Eisen,* July, 1968; Library Translation No. 84, Cement and Concrete Association, London, July, 1969.
27. Schultchen, E., and Huang, T., "Relaxation Losses in 7/16 in. Diameter Special Grade Prestressing Strands," Fritz Engineering Laboratory Report No. 339.4, Lehigh University, Bethlehem, Pennsylvania, July, 1969.
28. Huang, T., and Frederickson, D. C., "Concrete Strains in Pre-Tensioned Concrete Structural Members—Preliminary Report," Fritz Engineering Laboratory Report No. 339.3, Lehigh University, Bethlehem, Pennsylvania, June, 1969.
29. Branson, D. E., Meyers, B. L., and Kripanarayanan, K. M., "Time-Dependent Deformation of Non-Composite and Composite Sand-Lightweight Prestressed Concrete Structures," Report No. 69-1, Department of Civil Engineering, University of Iowa, Iowa City, February, 1969.
30. ACI Committee 318, "Building Code Requirements for Reinforced Concrete (ACI 318-71)" and "Commentary on Building Code Requirements for Reinforced Concrete (ACI 318-71)," American Concrete Institute, Detroit, Michigan, 1971.
31. Branson, D. E., and Kripanarayanan, K. M., "Loss of Prestress and Camber of Non-Composite and Composite Prestressed Concrete

Structures," Report No. 70-3, Department of Civil Engineering, University of Iowa, Iowa City, Iowa, June, 1970.
32. Glodowski, R. J., and Lorenzetti, J. J., "A Method for Predicting Prestress Losses in a Prestressed Concrete Structure," PCI JOURNAL, V. 17, No. 2, March-April, 1972, pp. 17-31.
33. *Design and Control of Concrete Mixtures,* Portland Cement Association, Old Orchard Road, Skokie, Illinois 60076.
34. *Recommendations for an International Code of Practices for Reinforced Concrete,* published by the American Concrete Institute and the Cement and Concrete Association.
35. *PCI Design Handbook–Precast and Prestressed Concrete,* Prestressed Concrete Institute, Chicago, Illinois, 1971.
36. *Interim Specifications Bridges 1975,* American Association of State Highway and Transportation Officials, Washington, D.C., 1975.

DESIGN EXAMPLES

The following three design examples were prepared solely to illustrate the application of the preceding recommended methods. They do not necessarily represent the real condition of any real structure.

Design aids to assist in calculating prestress losses are included in the *PCI Design Handbook* (see Reference 35). The aids will reduce the calculations required. However, detailed study of losses and time-dependent behavior will follow the steps outlined in the design examples.

The first example applies the general method to a pretensioned double-tee and the second example uses the simplified method for the same member. The third example problem illustrates the general method for a post-tensioned structure.

In these examples it is assumed that the member geometry, load conditions, and other parameters have been defined. Consequently, the detailed moment and stress calculations are omitted.

DESIGN EXAMPLE 1

Pretensioned Double Tee

Reference: *PCI Design Handbook,* p. 3-33.

Data: Double-tee section 10LDT32 + 2.
Strand pattern 128-D1.
Steam cured, lightweight double-tee (115 lb per cu ft) with 2-in. topping of normal weight concrete (150 lb per cu ft).
The beam is designed to carry a live load of 40 psf over a 70-ft span.

Required: Calculate the losses at the critical section, taken as 0.4 span in the *PCI Design Handbook.* $f'_{ci} = 3500$ psi, $f_c' = 5000$ psi

Section properties:

Non-composite

$A = 615$ in.^{2}
$I = 59{,}720$ in.^{4}
$y_b = 21.98$ in.
$y_t = 10.02$ in.
$Z_b = 2717$ in.^{3}
$Z_t = 5960$ in.^{3}
Weight: 491 lb per ft

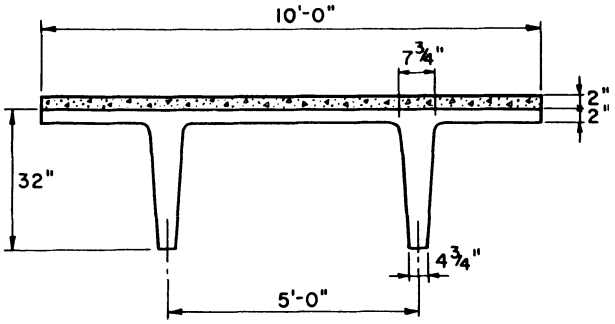

Design Example 1. Cross section of double-tee beam.

Composite

$I = 83{,}001$ in.^{4}
$y_{bc} = 25.40$ in.
$y_{tc} = 8.60$ in.
$Z_b = 3268$ in.^{3}
$Z_t = 9651$ in.^{3}
Weight: 741 lb per ft

The beam is prestressed by twelve ½-in. diameter 270-grade strands, initially tensioned to 0.70 f_{pu}.

Eccentricity of strands:

At ends = 12.98 in.
At center = 18.73 in.
$f_{py} = 230$ ksi

Transfer at 18 hours after tensioning strand, topping cast at age 30 days.

Losses–Basic data

$f'_{ci} = 3500$ psi
$E_{ci} = 115^{1.5}(33\sqrt{3500})$
$= 2.41 \times 10^6$ psi
$f_c' = 5000$ psi
$E_c = 115^{1.5}(33\sqrt{5000})$
$= 2.88 \times 10^6$ psi

Volume to surface ratio $= 615/364$
$= 1.69$

$SSF = 0.985$
$SCF = 0.988$

$UCR = 63 - 20(E_c/10^6)$
(but not less than 11)
$= 63 - 20(2.88) = 11$

$USH = 41{,}000 - 10{,}000(E_c/10^6)$
(but not less than 12,000)
$= 41{,}000 - 10{,}000(2.88)$
$= 12{,}200$ psi

At critical section
$e = 12.98 + 0.8(18.73 - 12.92)$
$= 17.58$ in.

$(UCR)(SCF) = 10.87$

$(USH)(SSF) = 12{,}017$ psi

Stage 1: Tensioning of steel to transfer

$t_1 = 1/24$ day
$t = 18/24$ day
$f_{st} = 189{,}000$ psi

$RET = f_{st}[(\log 24t - \log 24\,t_1)/10] \times [f_{st}/f_{py} - 0.55]$
$= 189{,}000[(\log 18)/10] \times [189/230 - 0.55]$
$= 6450$ psi

Dead load moment at 0.4 span
$M_{DL} = w(x/2)(L - x)$
$= (491/1000)(28/2)(70 - 28)$
$= 289$ ft-kips

Stress at center of gravity of steel due to M_{DL}

$f_c = [289{,}000(12)/59{,}720]\,17.58$
$= 1020$ psi (tension)

Assume $ES \approx 13$ ksi, then
$f_{si} = 189.0 - 6.45 - 13.0$
$= 169.55$ ksi
$P_o = 169.55(12)(0.153)$
$= 311.3$ kips

Stress at center of gravity of steel due to P_o:
$f_c = 311{,}300/615 +$
$311{,}300\,(17.58)^2/59{,}720$
$= 2117$ psi (compression)
$f_{cr} = 2117 - 1020 = 1097$ psi
$ES = f_{cr}(E_s/E_c)$
$= 1097(28.0/2.41)$
$= 12{,}750$ psi ≈ 13 ksi (ok)
$SH = CR = 0$

Total losses in Stage 1 =
$6450 + 12{,}750 = 19{,}200$ psi

Stage 2: Transfer to placement of topping after 30 days

$t_1 = 18/24$ day
$t = 30$ days
$PCR = 0.35$
$PSH = 0.42$
$f_{st} = 189{,}000 - 19{,}200$
$= 169{,}800$ psi
$RET = 169{,}800\,[(\log 720 - \log 18)/10]$
$\times\,[169.8/230 - 0.55]$
$= 5119$ psi

CR $= 10.87(0.35)(1097) = 4173$ psi

SH $= 12{,}017(0.42) = 5047$ psi

Total losses in Stage 2
$5119 + 4173 + 5047 = 14{,}339$ psi

Moment due to weight of topping
$250(28/2)(70 - 28) = 147{,}000$ ft-lb

Stress at center of gravity of steel due to weight of topping
$147{,}000(12)(17.58)/59{,}720 = 519$ psi

Increase in strand stress due to topping
$519(28.0/2.88) = 5048$ psi

Strand stress at end of Stage 2
$169{,}800 - 14{,}339 + 5048 = 160{,}509$ psi

Stage 3: Topping placement to end of one year

$t_1 = 30$ days
$t = 1$ year $= 365$ days
$PCR = 0.74 - 0.35 = 0.39$
$PSH = 0.86 - 0.42 = 0.44$
$f_{st} = 160{,}509$ psi

$RET = 160{,}509\,[(\log 8760 - \log 720)/10] \times [160.5/230 - 0.55]$
$= 2577$ psi

$f_c = 2117(160{,}509/169{,}550) - 1020 - 519$
$= 465$ psi
$CR = 10.87(0.39)(465) = 1971$ psi
$SH = 12{,}017(0.44) = 5287$ psi

Total losses in Stage 3
$2577 + 1971 + 5287 = 9835$ psi

Summary of steel stresses at various stages (Design Example 1)

Stress level at various stages	Steel stress, ksi	Percent
Strand stress after tensioning and deflection ($0.70f_{pu}$)	189.0	100.0
Losses:		
Elastic shortening = 12.75		6.7
Relaxation: 6.45+ 5.12 + 2.58 + 2.54 = 16.69		8.8
Creep: 4.17 + 1.97 + 0.97 = 7.11		3.8
Shrinkage: 5.05 + 5.29 + 1.68 = 12.02		6.4
Total losses, TL	48.57	25.7
Increase of stress due to topping	5.05	2.7
Final strand stress under total dead load (f_{se})	145.48	77.0

Stage 4: One year to end of service life

t_1 = 1 year
t = end of service life (say 40 years)
$PCR = 1 - 0.74 = 0.26$
$PSH = 1 - 0.86 = 0.14$
f_{st} = 160,509 − 9835 = 150,674 psi
$RET = 150{,}674[(\log 350{,}400 - \log 8760)/10] \times [(150.7/230) - 0.55]$
= 2537 psi
$f_c = 2117(150{,}674/169{,}550) - 1020 - 519$
= 343 psi
$CR = 10.87(0.26)(343) = 969$ psi
$SH = 12{,}017(0.14) = 1682$ psi

Total losses in Stage 4 =
2537 + 969 + 1682 = 5188 psi

DESIGN EXAMPLE 2

Application of Simplified Procedure to Design Example 1

Compute f_{cds}

$f_{cds} = eM_{ds}/I$
= 17.58(147)(12)/59,720
= 0.519 ksi

Compute f_{cr}

$f_{cr} = A_s f_{si}/A_c + A_s f_{si} e^2/I_c + M' e/I_c$
$f_{si} = 0.90 f_t = 0.90(189) = 170.1$ ksi
$f_{cr} = 1.84(170.1)/615 + 1.84(170.1)(17.58)^2/59{,}720 - 289(12)(17.58)/59{,}720$
= 0.509 + 1.620 − 1.021
= 1.108 ksi

Equation L-SR-PRE-70 from Table 8 is
$TL = 31.2 + 16.8 f_{cr} - 3.8 f_{cds}$
= 31.2 + 16.8(1.108) − 3.8(0.519)
= 31.2 + 18.61 − 1.97
= 47.84 ksi

Adjustment for volume to surface ratio = 1.69

Use a straight-line interpolation between adjustment values for $V/S = 2.0$ and $V/S = 1.0$

Adjustment = (0.31)(3.2) = + 0.99%

Net TL = 1.0099(47.84) = 48.31 ksi
In Design Example 1, TL = 48.57 ksi
Difference = 0.26 ksi

Compute f_{se}

To find f_{se} in accordance with discussion under Section 3.32, and stress in tendons due to dead load applied after member was prestressed.

This stress is equal to
$f_{cds}(E_s/E_c) = 0.519(28/2.88) = 5.05$ ksi
$f_{se} = 189 - 48.31 + 5.05 = 145.74$ ksi

Note that f_{se} can also be computed from the equations shown in Table 9.

Equation L-SR-PRE-70 from Table 9 is
$f_{se} = f_t - (31.2 + 16.8 f_{cr} - 13.5 f_{cds})$
= 189 − (31.2 + 16.8 × 1.108 − 13.5 × 0.519)
= 189 − (31.2 + 18.61 − 7.01)
= 189 − (42.8)

An adjustment for variations in the basic parameters should be applied to the quantity in parentheses. In this case, adjust for a V/S of 1.69. The adjustment is +0.99 percent. The adjusted quantity becomes
1.0099(42.8) = 43.22
f_{se} = 189 − 43.22 = 145.78 ksi

Checking the assumed value of f_{si}:

In the application of the simplified method to Design Example 1, the value of f_{si} was assumed to be 170.1 ksi.

The following procedure can be used to check the accuracy of this assumed value.

For this example the exact value of f_{si} is the initial stress of 189 ksi reduced by strand relaxation from tensioning to release and by loss due to elastic shortening of the concrete as the prestressing force is applied.

From Section 2.7.1, the relaxation loss in a stress-relieved strand is

$RET = f_{st}[(\log 24t - \log 24t_1)/10] \times [f_{st}/f_{py} - 0.55]$

$f_c = [289{,}000(12)/59{,}720]\,17.58$
$= 1020$ psi (tension)

Assume $ES \approx 13$ ksi, then
$f_{si} = 189.0 - 6.45 - 13.0$
$= 169.55$ ksi
$P_o = 169.55(12)(0.153)$
$= 311.3$ kips

Stress at center of gravity of steel due to P_o:
$f_e = 311{,}300/615 +$
$311{,}300\,(17.58)^2/59{,}720$
$= 2117$ psi (compression)
$f_{cr} = 2117 - 1020 = 1097$ psi
$ES = f_{cr}(E_s/E_c)$
$= 1097(28.0/2.41)$
$= 12{,}750$ psi ≈ 13 ksi (ok)
$SH = CR = 0$

Total losses in Stage 1 =
$6450 + 12{,}750 = 19{,}200$ psi

Stage 2: Transfer to placement of topping after 30 days

$t_1 = 18/24$ day
$t = 30$ days
$PCR = 0.35$
$PSH = 0.42$
$f_{st} = 189{,}000 - 19{,}200$
$= 169{,}800$ psi
$RET = 169{,}800\,[(\log 720 - \log 18)/10]$
$\times\,[169.8/230 - 0.55]$
$= 5119$ psi

$CR = 10.87(0.35)(1097) = 4173$ psi

$SH = 12{,}017(0.42) = 5047$ psi

Total losses in Stage 2
$5119 + 4173 + 5047 = 14{,}339$ psi

Moment due to weight of topping
$250(28/2)(70 - 28) = 147{,}000$ ft-lb

Stress at center of gravity of steel due to weight of topping
$147{,}000(12)(17.58)/59{,}720 = 519$ psi

Increase in strand stress due to topping
$519(28.0/2.88) = 5048$ psi

Strand stress at end of Stage 2
$169{,}800 - 14{,}339 + 5048 = 160{,}509$ psi

Stage 3: Topping placement to end of one year

$t_1 = 30$ days
$t = 1$ year $= 365$ days
$PCR = 0.74 - 0.35 = 0.39$
$PSH = 0.86 - 0.42 = 0.44$
$f_{st} = 160{,}509$ psi

$RET = 160{,}509\,[(\log 8760 - \log 720)/10] \times [160.5/230 - 0.55]$
$= 2577$ psi

$f_c = 2117(160{,}509/169{,}550) - 1020 - 519$
$= 465$ psi
$CR = 10.87(0.39)(465) = 1971$ psi
$SH = 12{,}017(0.44) = 5287$ psi

Total losses in Stage 3
$2577 + 1971 + 5287 = 9835$ psi

Summary of steel stresses at various stages (Design Example 1)

Stress level at various stages	Steel stress, ksi	Percent
Strand stress after tensioning and deflection ($0.70f_{pu}$)	189.0	100.0
Losses:		
Elastic shortening = 12.75		6.7
Relaxation: 6.45+ 5.12 + 2.58 + 2.54 = 16.69		8.8
Creep: 4.17 + 1.97 + 0.97 = 7.11		3.8
Shrinkage: 5.05 + 5.29 + 1.68 = 12.02		6.4
Total losses, TL	48.57	25.7
Increase of stress due to topping	5.05	2.7
Final strand stress under total dead load (f_{se})	145.48	77.0

Stage 4: One year to end of service life

t_1 = 1 year
t = end of service life (say 40 years)
$PCR = 1 - 0.74 = 0.26$
$PSH = 1 - 0.86 = 0.14$
f_{st} = 160,509 − 9835 = 150,674 psi
$RET = 150{,}674[(\log 350{,}400 - \log 8760)/10] \times [(150.7/230) - 0.55]$
= 2537 psi
$f_c = 2117(150{,}674/169{,}550) - 1020 - 519$
= 343 psi
$CR = 10.87(0.26)(343) = 969$ psi
$SH = 12{,}017(0.14) = 1682$ psi

Total losses in Stage 4 =
2537 + 969 + 1682 = 5188 psi

DESIGN EXAMPLE 2

Application of Simplified Procedure to Design Example 1

Compute f_{cds}

$f_{cds} = eM_{ds}/I$
= 17.58(147)(12)/59,720
= 0.519 ksi

Compute f_{cr}

$f_{cr} = A_s f_{si}/A_c + A_s f_{si} e^2/I_c + M' e/I_c$
$f_{si} = 0.90 f_t = 0.90(189) = 170.1$ ksi
$f_{cr} = 1.84(170.1)/615 + 1.84(170.1)(17.58)^2/59{,}720 - 289(12)(17.58)/59{,}720$
= 0.509 + 1.620 − 1.021
= 1.108 ksi

Equation L-SR-PRE-70 from Table 8 is
$TL = 31.2 + 16.8 f_{cr} - 3.8 f_{cds}$
= 31.2 + 16.8(1.108) − 3.8(0.519)
= 31.2 + 18.61 − 1.97
= 47.84 ksi

Adjustment for volume to surface ratio = 1.69

Use a straight-line interpolation between adjustment values for $V/S = 2.0$ and $V/S = 1.0$

Adjustment = (0.31)(3.2) = + 0.99%

Net $TL = 1.0099(47.84) = 48.31$ ksi
In Design Example 1, $TL = 48.57$ ksi
Difference = 0.26 ksi

Compute f_{se}

To find f_{se} in accordance with discussion under Section 3.32, and stress in tendons due to dead load applied after member was prestressed.

This stress is equal to
$f_{cds}(E_s/E_c) = 0.519(28/2.88) = 5.05$ ksi
$f_{se} = 189 - 48.31 + 5.05 = 145.74$ ksi

Note that f_{se} can also be computed from the equations shown in Table 9.

Equation L-SR-PRE-70 from Table 9 is
$f_{se} = f_t - (31.2 + 16.8 f_{cr} - 13.5 f_{cds})$
= 189 − (31.2 + 16.8 × 1.108 − 13.5 × 0.519)
= 189 − (31.2 + 18.61 − 7.01)
= 189 − (42.8)

An adjustment for variations in the basic parameters should be applied to the quantity in parentheses. In this case, adjust for a V/S of 1.69. The adjustment is +0.99 percent. The adjusted quantity becomes
1.0099(42.8) = 43.22
$f_{se} = 189 - 43.22 = 145.78$ ksi

Checking the assumed value of f_{si}:

In the application of the simplified method to Design Example 1, the value of f_{si} was assumed to be 170.1 ksi.

The following procedure can be used to check the accuracy of this assumed value.

For this exam le the exact value of f_{si} is the initial stress of 189 ksi reduced by strand relaxation from tensioning to release and by loss due to elastic shortening of the concrete as the prestressing force is applied.

From Section 2.7.1, the relaxation loss in a stress-relieved strand is

$RET = f_{st}[(\log 24t - \log 24t_1)/10] \times [f_{st}/f_{py} - 0.55]$

For stress-relieved strand
$f_{py} = 0.85(270) = 229.5$ ksi

By definition in Section 2.7.1, when time is measured from zero, $\log 24t_1 = 0$

$$RET = 189[(1.255 - 0)/10] \times [189/229.5 - 0.55] = 6.49 \text{ ksi}$$

Stress loss due to elastic shortening of concrete

$$ES = (E_s/E_c)f_{cr} = (28/0.24)1.108 = 12.93 \text{ ksi}$$

Then, $f_{si} = 189 - 6.49 - 12.93 = 169.58$ ksi
and $0.90\, f_t = 170.10$ ksi

Therefore, there is a $170.10 - 169.58 = 0.52$ ksi stress error in f_{si}.

Consequently, in this particular case there is no need for a second trial.

As an example, assume a large error in the estimated f_{si}, say 10 ksi, and check its effect. The strand relaxation will not change.

Therefore, the change in ES will be

$$\Delta ES = (10/170.1)12.93 = 0.76 \text{ ksi}$$

If desired, the original estimate of f_{si} can be adjusted by 10 ksi and f_{cr} can be recalculated. One such cycle should always give an adequate accuracy.

DESIGN EXAMPLE 3

Post-Tensioned Unbonded Slabs

The following is a procedure for calculating the prestress losses in the longitudinal tendons which extend from end to end of the slab (see sketch showing floor plan and tendon profiles).

Data

$w = 150$ lb per cu ft
f_c' (28 days) = 4000 psi

Prestressed at age 4 days
$f_c' = 3000$ psi

Moist cured 7 days.

Loads

7½-in. slab = 94 psf
Superimposed load = 60 psf
The tendon profile shown is designed to balance 85 psf.

Friction Loss (FR)

The slab is prestressed by 270-grade, ½-in. diameter strand, pregreased and paper wrapped.

Coefficient of friction, $\mu = 0.08$
Wobble coefficient, $K = 0.0015$
$f_{py} = 230$ ksi.

Angular changes along tendon will be:

$$\theta_{AB} = 2(2.5)/[12(12)] = 0.0347 \text{ radians}$$

$$\theta_{BC} = \theta_{EF} = \theta_{FG} = \theta_{KL} = 2(4.0)/[12(9.6)] = 0.0694 \text{ radians}$$

$$\theta_{CD} = \theta_{DE} = \theta_{GH} = \theta_{HK} = 2(1.0)/[12(2.4)] = 0.0694 \text{ radians}$$

Angular change between A and L

$$\alpha = 0.0347 + 4(0.0694) + 4(0.0694) = 0.59 \text{ radians}$$

FR at L (middle of length of slab)

$$= T_o[1 - e^{-(KL + \mu\alpha)}]$$
$$= T_o[1 - e^{-\{(0.0015)(60) + (0.08)(0.59)\}}]$$
$$= T_o[1 - e^{-(0.090 + 0.047)}]$$
$$= 0.128\, T_o$$

The distribution of frictional loss is not uniform, but nearly proportional to $(K + \mu\alpha/L)$. However, the variation of strand stress before anchoring is approximately as shown on p. 72.

Anchorage loss (ANC)

Anchorage set in a single strand anchor
= 1/8 in.
= Shaded area in diagram $\times (1/E_s)$
Area = (1/8)29,000 = 3625 ksi-ft
= 302 ksi-in.

The maximum strand stress after seating of anchorage occurs x ft from end,

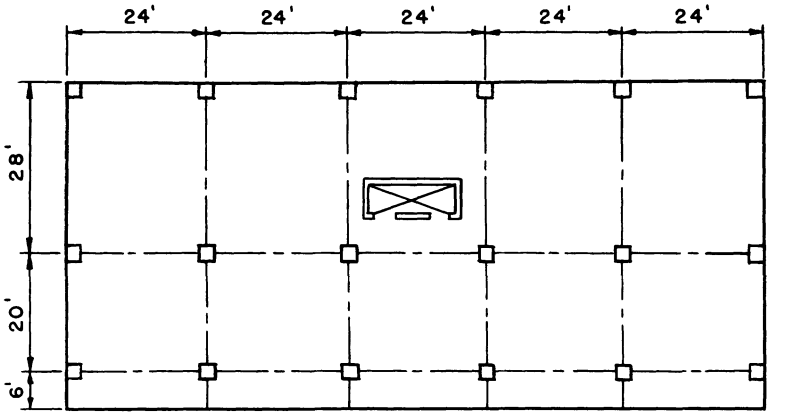

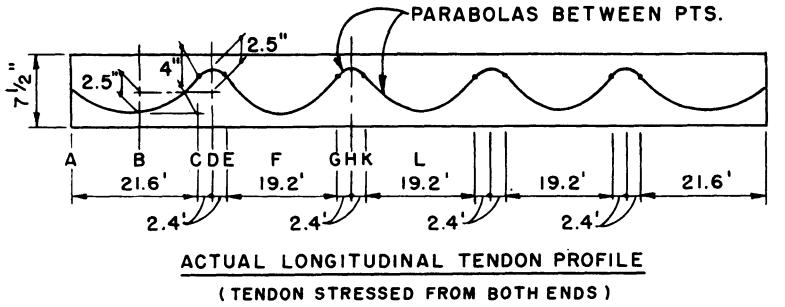

ACTUAL LONGITUDINAL TENDON PROFILE

(TENDON STRESSED FROM BOTH ENDS)

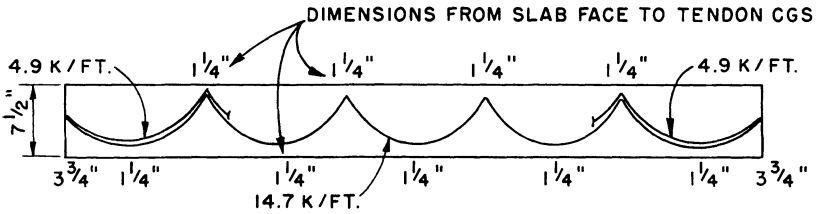

THEORETICAL TENDON PROFILE

(REQUIRED FINAL PRESTRESS FORCE SHOWN)

Design Example 3. Plan and tendon profiles of post-tensioned unbonded slab.

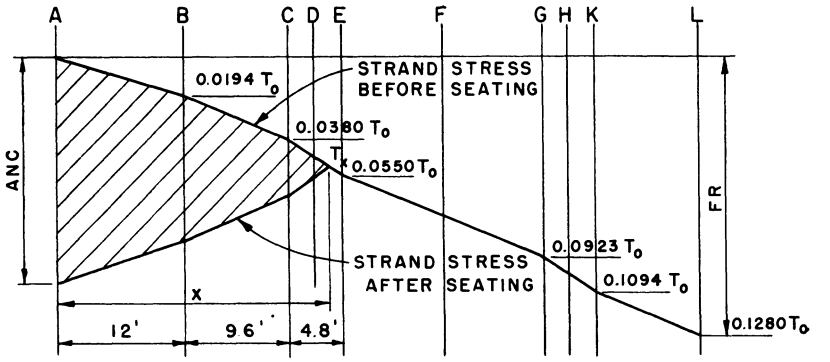

Approximate variation of strand stress.

and this stress T_x must not exceed $0.70f_{pu} = 189$ ksi.

$$T_o - T_x = 0.0380\,T_o + (0.0550 - 0.0380)T_o(x - 21.6)/4.8$$

$$\text{Area} = (T_o - T_x)12 + (0.9806\,T_o - T_x)21.6 + (0.9620\,T_o - T_x)(x - 12)$$

Therefore

$$T_x = 0.9620T_o = 0.0170T_o\,(x - 21.6)/4.8 = 189 \text{ ksi}$$

$$(T_o - T_x)12 + (0.9806T_o - T_x)21.6 + (0.9620T_o - T_x)(x - 12) = 302 \text{ ksi-ft}$$

These equations can be solved by trial and error.

Approximate solution:

$x = 25.5$ ft

$T_o = 200$ ksi

$T_x = 192.4 - 2.8 = 189.6 \approx 189$ ksi

$$\text{Area} = 124.8 + 140.8 + 37.8 = 303.4 \approx 302 \text{ ksi-ft (ok)}$$

For initial end tension before anchorage $T_o = 200$ ksi ($\approx 0.74\,f_{pu}$)

Maximum stress after anchorage

$T_x = 189.6$ ksi

$ANC = 2(T_o - T_x) = 20.8$ ksi

$T_A = 200 - 20.8 = 179.2$ ksi

$FR = 0.128\,T_o = 25.6$ ksi

$T_L = 200 - 25.6 = 174.4$ ksi

Average stress after anchorage:

$T_B = 183.2$ ksi, $T_c = 186.9$ ksi

$$T_{av} = (T_o/60)(0.5)[(0.896)(12) + (0.916)(21.6) + (0.935)(13.5) + (0.948)(4.8) + (0.945)(20.1) + (0.908)(24.0) + (0.891)(14.4) + (0.872)(9.6)] = 182.8 \text{ ksi}$$

Elastic shortening loss (ES)

In post-tensioned structural members, the loss caused by elastic shortening of concrete is only a fraction of the corresponding value in pretensioned members.

The fraction varies from zero if all tendons are tensioned simultaneously to 0.5 if infinitely many sequential steps are used.

In a slab, strands are spaced far apart and it is unlikely that the stretching of one strand will affect stresses in strands other than those immediately neighboring.

A factor of 0.25 will be used.

$$ES = 0.25(E_s - E_{ci})f_{cr}$$

In a design such as this in which the prestress approximately balances the dead load, and the level of prestress is low, a sufficiently close estimate of f_{cr} can be obtained by using the average prestress P/A.

The design final prestress force is 14.7 kips per ft for interior spans and 19.6 kips per ft for end spans. Assuming a long-term prestress loss of 15 percent, the initial prestress force will be 17.3 kips per ft and 23.1 kips per ft, respectively. The average strand stress after anchorage is 182.8 ksi.

Therefore, the required area of steel for the end spans is

$$A_s = 23.1/182.8 = 0.126 \text{ sq in. per ft}$$

This required area is supplied by ½-in. diameter strands spaced at 14 in.

$$A_s = 0.131 \text{ sq in. per ft}$$

Every fourth strand will be terminated in the first interior span, leaving an A_s of 0.098 sq in. per ft.

The actual initial prestressing forces are:

End span
$0.131(182.8) = 23.9$ kips per ft

Interior span
$0.098(182.8) = 17.9$ kips per ft

The average concrete stresses are 266 and 199 psi, respectively.

$$f_{cr} \approx (1/120)[(266)(48) + (199)(72)] = 226 \text{ psi}$$

$$E_{ci} = 33w^{1.5}\sqrt{f_{ci}'} = 33(150)^{1.5}\sqrt{3000} = 3.32 \times 10^6 \text{ psi}$$

$$ES = 0.25(226)(29/3.32) = 494 \text{ psi}$$

After all the strands have been tensioned and anchored:

$$T_{av} = 182.8 - 0.494 = 182.3 \text{ ksi}$$

At midspan of the middle span
Strand stress (at L)

$$174.4 - 0.494 \approx 173.9 \text{ ksi}$$

$$f_{cr} \approx [(173.9)(0.098)]/[(12)(7.5)] \approx 0.189 \text{ ksi}$$

Long-term losses

The calculation for long-term losses will be for the midspan of the middle span (at Section L).

Stage 1: To 30 days after prestressing

Relaxation:

$t_1 = 1/24$ day
$t = 30$ days
$f_{st} = 173.9$ ksi
$f_{st}/f_{py} = 0.756$

$$RET = f_{st}[(\log 24t - \log 24t_1)/10] \times [(f_{st}/f_{py}) - 0.55]$$
$$= 173{,}900(0.2857)(0.206)$$
$$= 10{,}230 \text{ psi}$$

Creep:

$$CR = (UCR)(SCF)(MCF)(PCR)(f_c)$$
$$UCR = 95 - (20E_c/10^6)$$
but not less than 11 psi
$$E_c = 33(150)^{1.5}\sqrt{4000} = 3.83 \times 10^6 \text{ psi}$$
$$UCR = 95 - 76.6 = 18.4 \text{ psi}$$

V/S ratio $= 0.5$(slab thickness)
$= 0.5(7.5)$
$= 3.75$ in.

$SCF = 0.80$
$MCF = 1.07$ (estimated)
$(UCR)(SCF)(MCF) = 15.75$
$f_c = f_{cr} = 189$ psi
$PCR = 0.35$
$CR = 15.75(0.35)(189) = 1042$ psi

Shrinkage:

$$SH = (USH)(SSF)(PSH)$$
$$USH = 27{,}000 - (3000\,E_c/10^6)$$
but not less than 12,000

$USH = 27{,}000 - 11{,}490 = 15{,}510$ psi
$V/S = 3.75$ in.
$SSF = 0.79$
$(USH)(SSF) = 12{,}270$ psi
Time after end of curing = 27 days
$PSH = 0.402$
$SH = 12{,}270(0.402) = 4933$ psi

Total losses in Stage 1:

$RET + CR + SH = 10{,}230 + 1042 + 4933$
$= 16{,}205$ psi

Tendon stress at end of Stage 1
$173{,}900 - 16{,}205 = 157{,}695$ psi

Concrete fiber stress
$189(157{,}695/173{,}900) = 171.4$ psi

Stage 2: To 1 year after prestressing

Relaxation:

$t_1 = 30$ days
$t = 1$ year $= 365$ days
$f_{st} = 157{,}695$ psi
$f_{st}/f_{py} = 157.7/230 = 0.671$
$RET = 157{,}695[(\log 8760 - \log 30)/10] \times [(0.671 - 0.55)]$
$= 2070$ psi

Creep:

$f_c = 171.4$ psi
$PCR = 0.74 - 0.35 = 0.39$
$CR = 15.75(0.39)(171.4) = 1053$ psi

Shrinkage:

$PSH = 0.86 - 0.402 = 0.458$
$SH = 12{,}270(0.458) = 5620$ psi

Total losses in Stage 2:

$2070 + 1053 + 5620 = 8743$ psi

At end of Stage 2, tendon stress at Section L

$157{,}695 - 8743 = 148{,}952$ psi

Concrete fiber stress
$189(148{,}952/173{,}900) = 161.9$ psi

Stage 3: To end of service life (taken as 50 years)

Relaxation:

$t_1 = 1$ year $= 365$ days
$t = 50$ years $= 18{,}250$ days
$\log 24t - \log 24t_1 = 1.699$
$f_{st} = 148{,}952$ psi
$f_{st}/f_{py} = 0.634$
$RET = 148{,}952(0.1699)(0.084)$
$= 2126$ psi

Creep:

$f_c = 161.9$ psi
$PCR = 1 - 0.74 = 0.26$
$CR = 15.75(0.26)(161.9) = 663$ psi

Shrinkage:

$PSH = 1 - 0.86 = 0.14$
$SH = 12{,}270(0.14) = 1718$ psi

Summary of steel stresses at various stages (Design Example 3)

Stress level at various stages	Steel stress, ksi	Percent
Tensioning stress at end	200	
Average stress after seating	182.8	
Middle section stress after seating	174.4	100.0
Losses:		
Elastic shortening	0.5	0.3
Relaxation	14.4	8.2
Creep	2.7	1.6
Shrinkage	12.3	7.0
Total losses after seating	29.9	17.1
Final strand stress at middle section without superimposed load	144.5	82.9

Total long-term losses:

$$RET = 10{,}230 + 2070 + 2126 = 14{,}426 \text{ psi}$$

$$CR = 1042 + 1053 + 663 = 2{,}758 \text{ psi}$$

$$SH = 4933 + 5620 + 1718 = 12{,}271 \text{ psi}$$

$$\text{Total losses} = 29{,}355 \text{ psi}$$

This example shows the detailed steps in arriving at total losses. It is not implied that this effort or precision is required in all design situations.

The *PCI Post-Tensioning Manual* provides a table for approximate prestress loss values which is satisfactory for most design solutions. The value recommended for slabs with stress-relieved 270-kip strand is 30,000 psi which compares with the calculated value of 29,355 psi.

Final tendon stress at Section L

$$175.9 = 29.4 = 144.5 \text{ ksi}$$

Percentage loss after anchorage

$(174.4 - 144.5)/174.4 = 17.1$ percent but greater than 15 percent (assumed initially)

Assuming the same percentage loss prevails over the entire tendon length, the average prestressing forces after losses are 19.8 and 14.8 kips per ft, respectively, which are adequate when compared with the design requirements. Therefore, revision is not needed.

Appendix B

Section 9.16 of the
AASHTO Standard Specifications
for Highway Bridges
Fourteenth Edition
1989

Figure 9.16.2.1.1 of the
AASHTO Standard Specifications for Highway
Bridges 1986 Interim
Thirteenth Edition
1983

Commentary Article 1.6.7(B) and Example
Applications of the AASHTO Standard Specifications
for Highway Bridges 1976 Interim
Eleventh Edition
1973

Appendix B

Section 9.16 of the AASHTO Standard Specifications for Highway Bridges Fourteenth Edition 1989

9.16 LOSS OF PRESTRESS

9.16.1 Friction Losses

Friction losses in post-tensioned steel shall be based on experimentally determined wobble and curvature coefficients, and shall be verified during stressing operations. The values of coefficients assumed for design, and the acceptable ranges of jacking forces and steel elongations shall be shown on the plans. These friction losses shall be calculated as follows:

$$T_0 = T_x e^{(KL + \mu\alpha)} \qquad (9\text{-}1)$$

When $(KL + \mu\alpha)$ is not greater than 0.3., the following equation may be used:

$$T_0 = T_x(1 + KL + \mu\alpha) \qquad (9\text{-}2)$$

The following values for K and μ may be used when experimental data for the materials used are not available:

Type of Steel	Type of Duct	K/ft.	μ
Wire or ungalvanized strand	Bright metal sheathing	0.0020	0.30
	Galvanized metal sheathing	0.0015	0.25
	Greased or asphalt-coated and wrapped	0.0020	0.30
	Galvanized rigid	0.0002	0.25
High-strength bars	Bright metal sheathing	0.0003	0.20
	Galvanized metal sheathing	0.0002	0.15

Friction losses occur prior to anchoring but should be estimated for design and checked during stressing operations. Rigid ducts shall have sufficient strength to maintain their correct alignment without visible wobble during placement of concrete. Rigid ducts may be fabricated with either welded or interlocked seams. Galvanizing of the welded seam will not be required.

9.16.2 Prestress Losses

9.16.2.1 General

Loss of prestress due to all causes, excluding friction, may be determined by the following method.* The method is based on normal weight concrete and one of the following types of prestressing steel: 250- or 270-ksi, seven-wire, stress-relieved strand; 240-ksi stress-relieved wires; or 145- to 160-ksi smooth or deformed bars. Refer to documented tests for data regarding the properties and the effects of lightweight aggregate concrete on prestress losses.

TOTAL LOSS

$$\Delta f_s = SH + ES + CR_c + CR_s \qquad (9\text{-}3)$$

where

Δf_s = total loss excluding friction in pounds per square inch;
SH = loss due to concrete shrinkage in pounds per square inch;
ES = loss due to elastic shortening in pounds per square inch;
CR_c = loss due to creep of concrete in pounds per square inch;
CR_s = loss due to relaxation of prestressing steel in pounds per square inch.

9.16.2.1.1 Shrinkage

Pretensioned Members

$$SH = 17{,}000 - 150\ RH \qquad (9\text{-}4)$$

Post-tensioned Members

$$SH = 0.80(17{,}000 - 150\ RH) \qquad (9\text{-}5)$$

where RH = mean annual ambient relative humidity in percent (see Figure 9.16.2.1.1).

*Should more exact prestress losses be desired, data representing the materials to be used, the methods of curing, the ambient service condition and any pertinent structural details should be determined for use in accordance with a method of calculating prestress losses that is supported by appropriate research data. See also FHWA Report FHWA/RD '85/045, *Criteria for Designing Lightweight Concrete Bridges*.

9.16.2.1.2 Elastic Shortening

Pretensioned Members

$$ES = \frac{E_s}{E_{ci}} f_{cir} \tag{9-6}$$

Post-tensioned Members*

$$ES = 0.5 \frac{E_s}{E_{ci}} f_{cir} \tag{9-7}$$

where

E_s = modulus of elasticity of prestressing steel strand, which can be assumed to be 28×10^6 psi;

E_{ci} = modulus of elasticity of concrete in psi at transfer of stress, which can be calculated from:

$$E_{ci} = 33w^{3/2}\sqrt{f'_{ci}} \tag{9-8}$$

in which w is the concrete unit weight in pounds per cubic foot and f'_{ci} is in pounds per square inch;

f_{cir} = concrete stress at the center of gravity of the prestressing steel due to prestressing force and dead load of beam immediately after transfer; f_{cir} shall be computed at the section or sections of maximum moment. (At this stage, the initial stress in the tendon has been reduced by elastic shortening of the concrete and tendon relaxation during placing and curing the concrete for pretensioned members, or by elastic shortening of the concrete and tendon friction for post-tensioned members. The reductions to initial tendon stress due to these factors can be estimated, or the reduced tendon stress can be taken as $0.63\ f'_s$ for stress relieved strand or $0.69\ f'_s$ for low relaxation strand in typical pretensioned members.)

9.16.2.1.3 Creep of Concrete

Pretensioned and post-tensioned members.

$$CR_c = 12\ f_{cir} - 7\ f_{cds} \tag{9-9}$$

where

f_{cds} = concrete stress at the center of gravity of the prestressing steel due to all dead loads except the dead load present at the time the prestressing force is applied.

*Certain tensioning procedures may alter the elastic shortening losses.

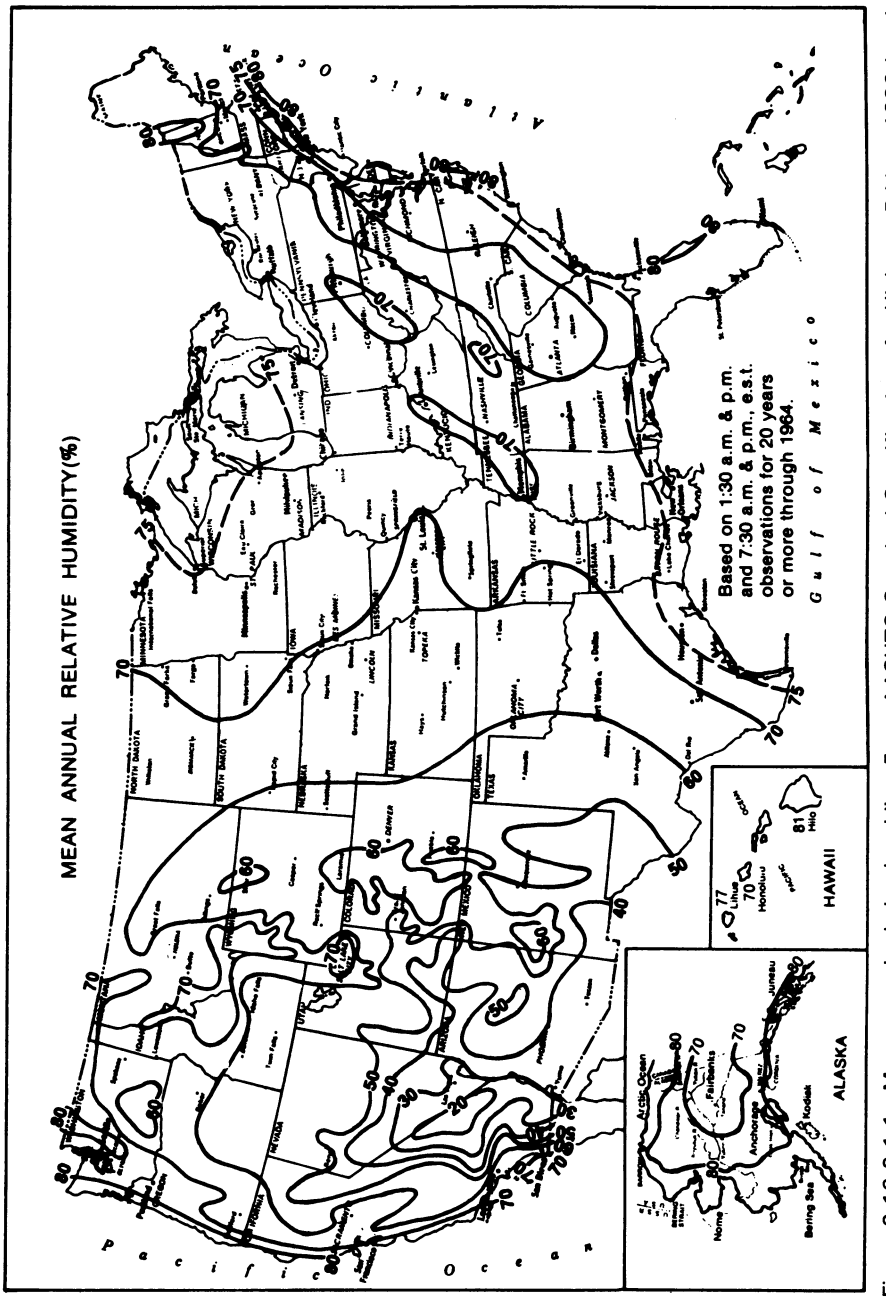

Figure 9.16.2.1.1 Mean annual relative humidity. From AASHTO Standard Specifications for Highway Bridges 1986 Interim; Thirteenth Edition 1983.

*9.16.2.1.4 Relaxation of Prestressing Steel**

Pretensioned Members

250 to 270 ksi Strand

$$CR_s = 20{,}000 - 0.4\,ES - 0.2\,(SH + CR_c)$$

for stress relieved strand (9-10)

$$CR_s = 5{,}000 - 0.10\,ES - 0.05\,(SH + CR_c)$$

for low relaxation strand (9-10A)

Post-tensioned Members

250 to 270 ksi Strand

$$CR_s = 20{,}000 - 0.3\,FR - 0.4\,ES - 0.2(SH + CR_c)$$

for stress relieved strand (9-11)

$$CR_s = 5{,}000 - 0.07\,FR - 0.1\,ES - 0.05(SH + CR_c)$$

for low relaxation strand (9-11A)

240-ksi Wire

$$CR_s = 18{,}000 - 0.3\,FR - 0.4\,ES - 0.2(SH + CR_c) \quad (9\text{-}12)$$

145- to 160-ksi Bars

$$CR_s = 3{,}000$$

where

FR = friction loss stress reduction in psi below the level of $0.70\,f'_s$ at the point under consideration, computed according to Article 9.16.1.

ES, SH, and CR_c = appropriate values as determined for either pre-tensioned or post-tensioned members.

9.16.2.2 Estimated Losses

In lieu of the preceding method, the following estimates of total losses may be used for prestessed members or structures of usual design. These loss values are based on use of normal weight concrete, normal prestress levels, and average exposure conditions. For exceptionally long spans, or for unusual designs, the method in Article 9.16.2.1 or a more exact method shall be used.

*The relaxation losses are based on an initial stress equal to the temporary stress allowed by Article 9.15.1.

Table 16.2.2 Estimate of Prestress Losses

Type of Prestressing Steel	Total Loss	
	f'_c = 4,000 psi	f'_c = 5,000 psi
Pretensioning Strand	—	45,000 psi
Post-Tensioning[a]		
Wire or Strand	32,000 psi	33,000 psi
Bars	22,000 psi	23,000 psi

[a]Losses due to friction are excluded. Friction losses should be computed according to Article 9.16.1.

Commentary Article 1.6.7(B) and Example Applications of the AASHTO Standard Specifications for Highway Bridges 1976 Interim Eleventh Edition 1973

Introduction

The subject revision to Section 1.6.7(B)—Prestress Losses in the 1973 AASHTO Specifications for Highway Bridges is based largely on consideration of research results (1,2)* made available subsequent to the adoption of the current specification, and on a proposed revision of the specifications with respect to losses in post-tensioned bridges presented at the 1972 AASHTO regional Bridge Committee meetings (3).

Precise determination of prestress losses in a given situation is very complex and requires detailed information on the materials to be used, the methods of curing, the ambient exposure conditions, and other detailed construction information that usually is not available to designers. For large and/or special structures such as precast or cast-in-place segmental cantilever bridges it may be appropriate or necessary to obtain this information, in order to maintain control of the geometry of the bridge during construction. For most structures, precise calculation of losses is not necessary, and it is possible to calculate reasonably accurate and satisfactory approximations of prestress losses for general design use.

The necessary level of precision in calculation of losses is subject to both technical and subjective evaluation. It has long been recognized that the value used for loss of prestress does not affect the ultimate strength of a bridge, but is important with respect to serviceability characteristics such as deflection, camber, stresses, and cracking (4). The value used for prestress loss also has an influence on economy in that higher values of losses require somewhat more prestressing steel. However, it has been shown that both the serviceability and economy of prestressed bridges are relatively insensitive to sizeable variations in the value assumed for prestress losses in typical designs (5). None-the-less, there is disagreement between agencies and designers as to what degree of precision is necessary in the calculation of losses, and there is some ambiguity in the research results on this subject, even when attempts are made to relate the research to a common base.

As a result of the above considerations, the subject revision of the AASHTO prestress loss specifications provides for three optional methods of loss calculation as follows:

1) The lump sum loss values in Section 1.6.7(B)(2).
2) The more precise and detailed provisions of Section 1.6.7(B)(1).
3) The use of still more exact procedures for loss calculation under the provisions of the footnote on page one of the proposed revision.

A detailed commentary of considerations related to the first two approaches is presented below. Due to the broad nature of calculations and procedures that might be involved in calculating losses under the provisions of the footnote as noted under the third option above, the discussion of this approach is not included in the commentary.

*Numbers in parenthesis refer to references listed at the end of the commentary.

Section 1.6.7(B)(1)

As compared to the existing specifications, the revision adds consideration of three types of tendons used for post-tensioned structures: 250 or 270 ksi (1724 or 1862 MPa), seven-wire, stress-relieved strand; 240 ksi (1655 MPa), stress-relieved wires; or 145 to 160 ksi (1000 to 1103 MPa) smooth or deformed bars.

The total loss is specified as the direct addition of losses due to shrinkage, elastic shortening, concrete creep, and steel relaxation. Addition of these losses in this manner is an approximation because the losses are to some extent inter-related. As will be discussed below under Section 1.6.7(B)(1)(d), Relaxation of Prestressing Steel, the inter-relationship of losses is considered in the formulas given for relaxation of prestressing steel.

The loss format of addition of four loss components is similar to the procedure outlined in the "Criteria for Prestressed Concrete Bridges" published by the U.S. Department of Commerce, Bureau of Public Roads in 1954 (6). However, the values related to each of the four components in the loss equation have been modified to more accurately reflect the research that has occurred in each area since 1954.

Section 1.6.7 (B)(1)(a)—Shrinkage

The two equations for loss due to concrete shrinkage give similar shrinkage losses to those included in the table in the current specifications. However, the equations have the advantage of eliminating the abrupt jump in shrinkage loss between the three humidity ranges. A map of the United States showing the average annual ambient relative humidity is presented in Fig. 1 (7). This map is to be used as the basis for determining average annual ambient relative humidity for use in calculating shrinkage loss.

The ultimate shrinkage strain of small specimens (8, 9) was assumed to be 550×10^{-6} at 50 percent relative humidity. This is an average value for shrinkage strain, some concretes may inherently shrink somewhat more and others somewhat less. Research indicates that shrinkage strains are reduced 10 to 40 percent by steam curing (10).

Research (11) has shown that shrinkage is related to the size or thickness of the member. This factor is usually expressed as the Volume/Surface ratio of the member. In development of the subject equations an average Volume/Surface ratio of 4 inches (.102 m) was assumed, and the ultimate shrinkage strain was reduced by a factor of 0.77. The volume/surface ratio is effectively one-half the average member thickness and it therefore represents the distance from the drying surface to the center of the member.

Shrinkage loss is also a function of the average ambient relative humidity of the environment. The amount of shrinkage reduces as the humidity increases. In some cases concrete stored under water has been observed to expand slightly. In developing the existing AASHTO specifications, humidity shrinkage factors were assumed as follows (12):

Average Ambient Relative Humidity Percent	Humidity Shrinkage Coefficient
100-75	0.3
75-25	1.0
25-0	1.3

Based on the above assumptions and on assumed modulus of elasticity for steel of 28×10^6 psi ($.193 \times 10^6$ MPa), shrinkage losses were calculated for the table in the existing specifications as the product of the four interior columns in the table below:

Humidity	Shrinkage Strain	Steel Modulus-psi (MPa)	Volume/ Surface Factor	Humidity Factor	Shrinkage Loss-psi (MPa)
100-75	550×10^{-6}	28×10^6 ($.193 \times 10^6$)	0.77	.3	3,540 (24.41)
75-25	550×10^{-6}	28×10^6 ($.193 \times 10^6$)	0.77	1.0	11,800 (81.36)
25-0	550×10^{-6}	28×10^6 ($.193 \times 10^6$)	0.77	1.3	15,250 (105.15)

These shrinkage loss values were rounded to 5,000, 10,000 and 15,000 for use in the existing (1973 edition) AASHTO specifications.

Multiplication of the shrinkage loss equation for post-tensioned design by the factor 0.8 is in consideration of the fact that post-tensioning is not accomplished until the concrete has reached an age of at least seven days at which time 20 percent of the shrinkage is assumed to have occurred. This is a very conservative assumption on time of stressing relative to concrete age for most bridges. A general curve relating shrinkage (or creep) to time is presented in Fig. C1(13). Use of some other reduction factor in the equation for shrinkage loss for post-tensioned applications might be considered if the designer has knowledge that the elapsed time from concrete placement to stressing will be significantly greater than seven days.

In the discussion relative to the subject revision of the loss specification, some expressed the view that the basic ultimate shrinkage strain of 550×10^{-6} was too low, while others suggested that it was too high, and still others felt the value to be satisfactory. This value was retained, and the tabular values in the existing specification were replaced by the two linear equations for reasons described above.

1.6.7(B)(1)(b) ELASTIC SHORTENING.

The table of losses due to elastic shortening in the current AASHTO Specification has been deleted in the revision, and the formula for elastic shortening loss has been generalized by including the ratio of the modulus of elasticity of steel to the modulus of concrete at release. The formula in the current specifications uses a value of 7 for the ratio of the moduli of elasticity.

A significant revision is in the definition of the concrete stress to be used in calculating elastic shortening loss. In the current specifications, this value is given the nomenclature f_{cr} where f_{cr} = average concrete stress at the center of gravity of the prestressing steel at time of release. The reason for using the average value of concrete stress (along the length of the beam) was to avoid the necessity of precise calculation of stresses at each point in a beam *before* a value of the elastic shortening loss could be obtained. It was intended that the average stress value could be estimated or obtained from the table values so that it would not be necessary for designers to use a trial and error process of design iterations in order to obtain a value for the elastic shortening loss. Use of average stress along the center of gravity of the steel is a conservative approximation since the average

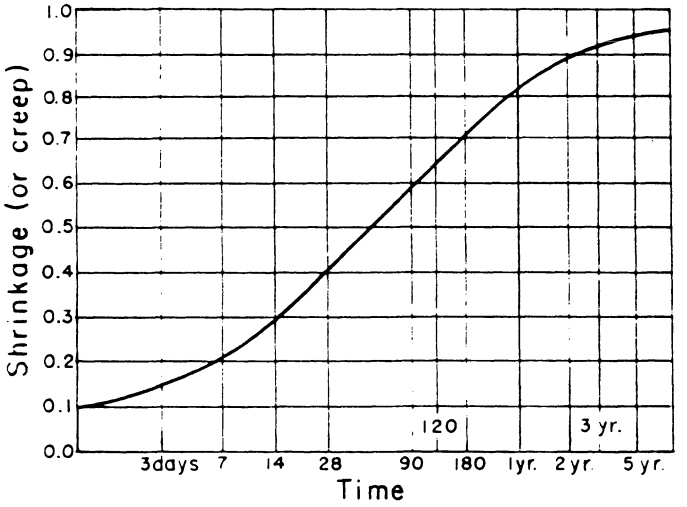

FIG. C1—Shrinkage or creep vs. time

stresses and related elastic shortening is greater than the stress and elastic shortening at the points of maximum moment.

The current specifications were criticized for use of average concrete stresses in calculating both elastic shortening and concrete creep losses. It was pointed out that this process was theoretically incorrect and that the actual elastic shortening loss (and creep loss) is dependent on the concrete stress *at* the section under consideration. In development of the proposed revision, it was agreed that the definition of stress for use in elastic shortening loss calculations would be more precise if related to the section under consideration, and it was acknowledged that this increase in precision might require a trial and error design process. To minimize the amount of additional design calculation, the final specification wording related the concrete stress, f_{cir}, for use in the elastic shortening formula to "...the section or sections of maximum moment," rather than the section under consideration. For a simple span precast design, this change results in a requirement of loss calculation at one point only, whereas relating the definition of f_{cir} to the section under consideration would have required a separate loss calculation at each point where stresses were investigated. For simple span pretensioned designs, it should be understood that the intent of the proposed revision as written is that elastic shortening loss (and concrete creep loss) is to be calculated only at the point of maximum moment, and that this value is to be used as the loss value throughout the length of the beam. For continuous post-tensioned bridges, the intent of this portion of the specification is that the loss value be calculated at each controlling point of maximum positive or negative moment along the length of the structure.

It should be noted that the stress in the tendon for pretensioned products for use in calculating f_{cir} should be reduced from the initial stress value by an amount to allow for elastic shortening of the concrete and for steel relaxation prior to release of the tendon force to the member.* Recognizing that this further complicates the iterative process for the designer, an approximate value of the reduced tendon stress of $0.63\ f_s'$ is provided. This approximation relates to tendons

*See Figures C2 and C3 for steel relaxation losses for constant strain specimens of stress relieved and stabilized 270k(1.2 MN) strand.

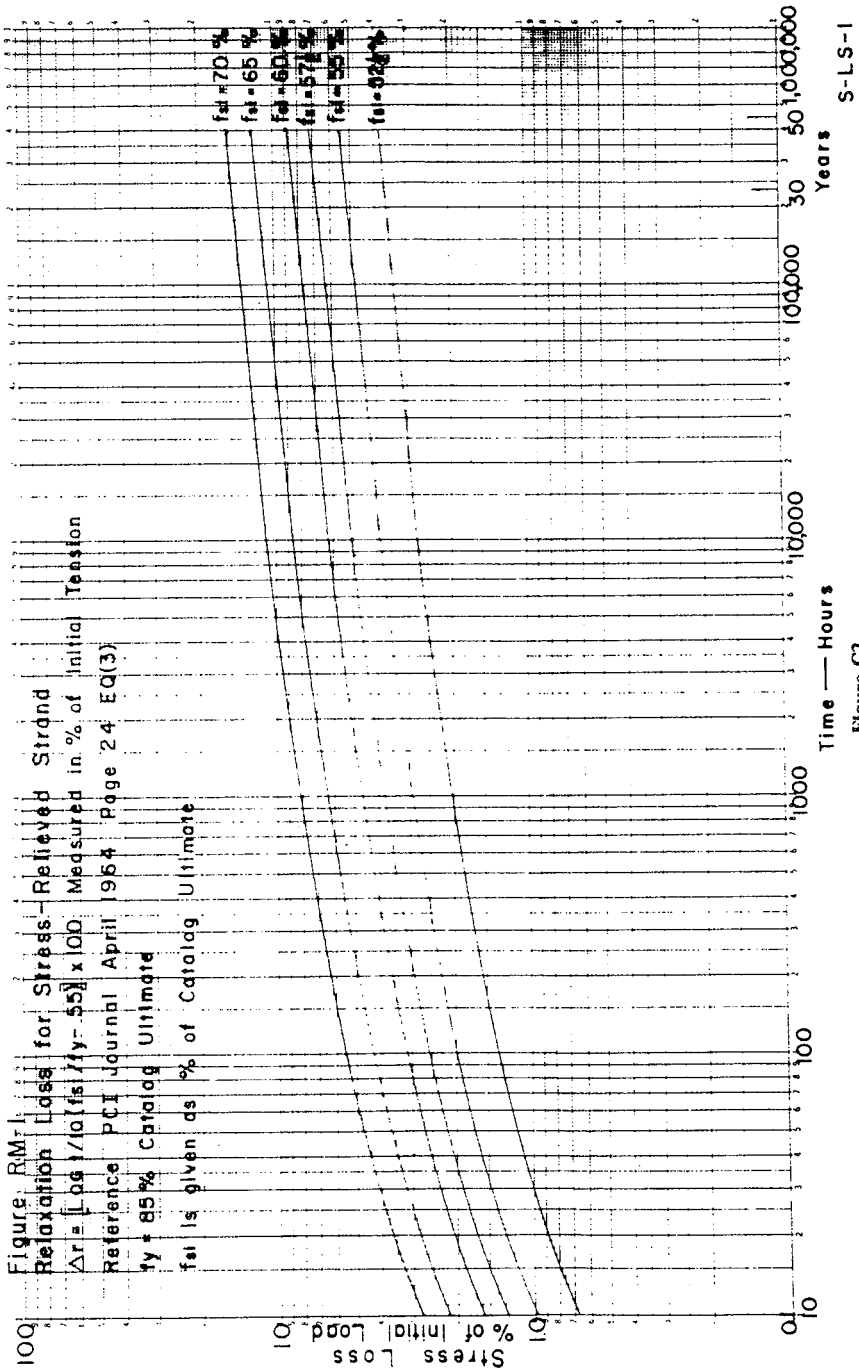
Figure RM-1
Relaxation Loss for Stress-Relieved Strand
Δr = [log t/10(fsi/fy - .55)] x 100 Measured in % of Initial Tension
Reference PCI Journal April 1964 Page 24 EQ(3)
fy = 85% Catalog Ultimate
fsi is given as % of Catalog Ultimate
fsi = 70 %
fsi = 65 %
fsi = 60 %
fsi = 55 %
100
10
1
0
Stress Loss
% of Initial Load
10
100
1000
10,000
100,000
1,000,000
Time — Hours
1
10
30
50
Years
S-LS-1

Figure C2

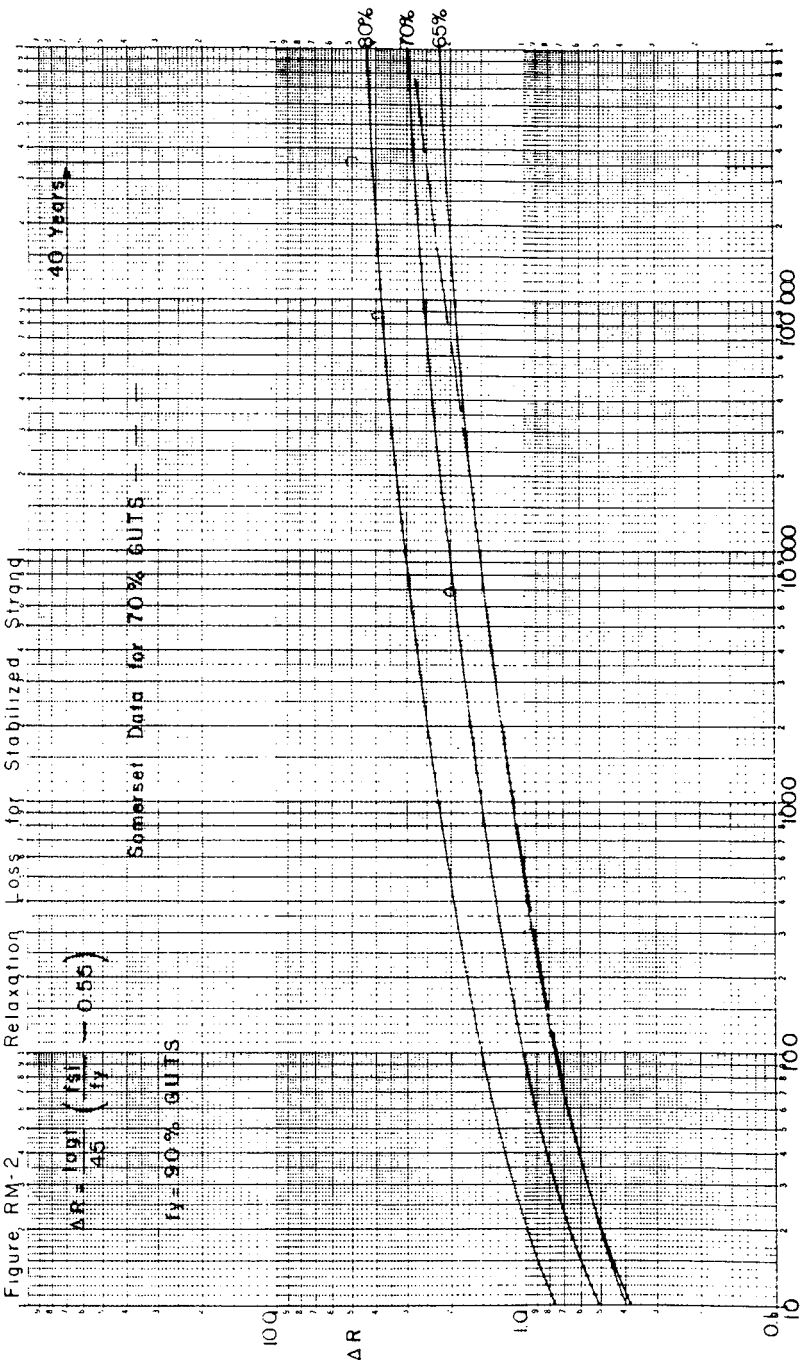
Figure, RM-2, Relaxation Loss, for Stabilized, Strand
ΔR = log t / 45 (fsi / fy − 0.55)
fy = 90% GUTS
Somerset Data for 70% GUTS
40 Years
80%
70%
65%
ΔR
100
10
0.1
10
100
1000
10000
100000
Time — Hours

Figure C3

stressed initially to 0.70 f_s'. Note that initial overstress is permitted so that the initial tendon stress after transfer to concrete is not greater than 0.70 f_s'; this requires more accurate estimates for initial losses to ensure the correct tendon stress at transfer. It is more complicated to obtain the reduced tendon force for calculation of f_{cir} for post-tensioned applications because the reduction depends on both elastic shortening and tendon friction. In addition, the use of initial tendon stresses in excess of 0.70 f_s' is quite common in post-tensioned applications to compensate for anchor seating loss. If the designer is willing to sacrifice some accuracy for convenience in calculation; a value of 0.65 f_s' might be used in calculating f_{cir} for post-tensioned designs. For structures utilizing long tendons where the friction losses become sizeable, this approximation would become quite conservative.

For post-tensioned members with only one tendon, there would be no elastic shortening loss because the member shortening takes place prior to tendon anchorage. However, most post-tensioned applications involve multiple tendons. When multiple tendons are used, the first tendon stressed and anchored sustains elastic shortening loss due to stressing of all subsequent tendons. The last tendon stressed sustains no elastic shortening loss. As a result of this, the formula for elastic shortening loss for post-tensioned structures includes a factor of 0.5 to approximate the total elastic shortening loss as the average loss in all tendons. In some applications, the total elastic shortening loss is eliminated by temporarily overstressing each tendon by the amount of elastic shortening anticipated. While the designer should be aware of this option for special structures, this procedure does complicate the stressing operation and it should only be used where the potential economies in tendon material justify the additional work in the field, and where the stressing crew is sufficiently trained that a different stress level can be specified in each tendon with reasonable assurance that the stressing will be properly carried out.

1.6.7(B)(1)(c) CREEP OF CONCRETE

The formula in the proposed revision for loss due to concrete creep is based on both field measurements and analytical studies conducted at the University of Illinois (1). This formula utilizes the same value of f_{cir} as defined and discussed above in the section on elastic shortening loss. This results in the same complications relative to calculating concrete creep loss as were discussed above with respect to elastic shortening.

The quantity f_{cds} related to the permanent loads applied after prestressing and represents the change of concrete fiber stress at c.g.s. caused by these loads. Usually, the application of load causes the concrete fiber stress at c.g.s. to decrease in magnitude, and thereby reduces the loss due to concrete creep; hence the negative sign in the formula for CR_c.

1.6.7(B)(1)(d) RELAXATION OF PRESTRESSING STEEL

New formulas are added in the section on steel relaxation relative to the various types of steel used for tendons of post-tensioned structures.

The steel relaxation loss formulas for post-tensioned structures utilizing strand and wire tendons include terms reflecting the influence of friction loss. It is intended that steel relaxation losses for post-tensioned structures be computed at the same points of maximum positive and negative moment as were used for

calculation of elastic shortening and concrete creep loss. For post-tensioned structures utilizing bar tendons, a flat value of steel relaxation loss of 3000 psi (20.68 MPa) is specified. Representatives of companies supplying bar tendons have suggested that the steel relaxation loss for bars should also consider the friction loss reduction and other loss modification factors used for strand and wire tendons. While this was acknowledged as theoretically correct, it was considered that such a formula was an unnecessary refinement in view of the very nominal steel relaxation loss specified for bar tendons. This loss value for bar tendons is an arbitrary figure developed on consideration of constant strain steel relaxation loss curves for both smooth and deformed bars (3).

All formulas for steel relaxation loss consider, in an approximate way, the inter-relationship between steel relaxation and other losses. The higher the losses due to elastic shortening, concrete creep, and shrinkage, the lower will be the steel stress and the related steel relaxation loss. This inter-relationship can be evaluated accurately by use of time-related curves for losses due to steel relaxation, shrinkage, and concrete creep, and by use of a step-by-step integration process considering the inter-relationship of the losses. The formulas in the proposed revision were developed to provide approximations of loss values that would be obtained by this more precise integration process.

During final development of the revision, it was suggested that the base loss values of 20,000 psi (137.90 MPa) for strand and 18,000 psi (124.11 MPa) for wire should be modified to reflect the actual constant strain steel relaxation loss for wire and strand which is about 15 percent for tendons stressed to an initial stress of 0.70 f_s'. These values would be about 28,300 psi (195.12 MPa) for strand, and about 25,200 psi (173.75 MPa) for wire. It was felt that this would put the equations in a more direct relationship to research results from constant strain strand tests. While there was agreement that such a procedure would be preferable from a technical standpoint, it was noted that all the modification factors in the formulas would have to be increased so that the net losses would remain the same as those resulting from the proposed equations. Further, it was noted that studies would have to be made to develop appropriate values for the reduction coefficients in the formulas. In view of these considerations, it was decided to retain the equations as previously developed with base loss values of 20,000 psi (137.90 MPa) for strand and 18,000 psi (124.11 MPa) for wire.

In application of the friction loss reduction in the equations for steel relaxation loss for post-tensioned wire and strand tendons, note that the value of FR to be used is limited to the reduction in stress level below stress level of 0.70 f_s'. Post-tensioning tendons are commonly stressed in excess of 0.70 f_s' (usually to about 0.74 f_s') to allow for anchor seating loss. While this process often results in some small portion of the tendon length retaining a stress slightly in excess of 0.70 f_s' immediately after anchoring, the equations for steel relaxation in wire and strand tendons are considered applicable. However, due to this over stressing, it is necessary to limit the value of FR in the equation to the reduction below a stress of 0.70 f_s' (rather than the total friction loss) in order to retain the basic presumption of the equations that the initial stress is 0.70 f_s'.

Steel relaxation increases rapidly with increases in initial stress above 0.70 f_s', and it decreases rapidly as stresses go below 0.70 f_s'. The decreases in stress are considered in the equations. It is emphasized, however, that the equations are not accurate where initial stresses at points of maximum moment exceed 0.70 f_s'. Where such over stressing is specified, an adjustment (increase) should be made in the steel relaxation loss values.

1.6.7(B)(2) LUMP SUM VALUES FOR PRESTRESS LOSS

Nearly all prestressed concrete bridges now in service were designed using the lump sum loss values of 35,000 psi (241.32 MPa) for pretensioned applications and 25,000 psi (172.37 MPa) plus friction for post-tensioned applications. In general the performance and serviceability characteristics of these bridges have been excellent. The revision of prestress losses in the 1971 AASHTO Interim Specifications was motivated by an awareness that research had shown some of the initial assumptions made in developing the initial lump sum loss values might be unconservative. This was particularly true with respect to steel relaxation loss, but applied to some extent to shrinkage and concrete creep losses. However, the basic intent of the provisions of the 1971 AASHTO Interim Specifications on prestress losses was to permit designers to develop lump sum losses that considered the prestress level and exposure conditions of the structure as well as the results of research then available. Some designers inferred an accuracy, or a requirement for precision, in the 1971 Interim Specifications that was not intended. As has been noted above, precise calculation of prestress losses is quite involved and requires detailed information on materials, exposure, and construction procedures not generally available to designers. Further, such precise calculations are usually not warranted from the standpoints of structural economy, serviceability, or strength.

There are numerous factors in the design of prestressed concrete bridges, as with bridges of other materials, that are included in the specifications for the convenience of the designer with the understanding that these factors are only approximations of actual behavior. Some of the provisions of Section 3—Distribution of Loads in the 1973 AASHTO Specifications exemplify such approximations. There are other similar approximations in the specifications, and in regard to prestressed concrete bridge design, a significant conservative approximation exists in the general use of the gross concrete section to compute section properties. Use of transformed section properties for all loads applied after prestressing is perfectly valid technically, and can result in an increase in the bottom section modulus in the order of 10 to 15 percent.

In view of the generally satisfactory performance of bridges designed using lump sum loss values, the conservative approximations in other portions of the specifications, and the convenience to the designer, it was considered desirable that the revision should include lump sum loss values for "prestressed members or structures of usual design." The introductory paragraph to the section indicates that structures of usual design include those of normal weight concrete, normal prestress levels, and average exposure conditions. In addition, it is suggested that the more precise procedures of Section 1.6.7(B)(1) should be used for structures of exceptionally long span or unusual design. The table of lump sum values includes concrete strengths of 4000 and 5000 psi (27.58 and 34.47 MPa). However, the lump sum loss values may be used for bridges with concrete strengths 500 psi (3.45 MPa) above or below the values of 4000 psi and 5000 psi (27.58 and 34.47 MPa) listed in the table headings. Thus, the range of concrete strengths covered by the lump sum loss values may be considered to extend from 3500 psi to 5500 psi (24.13 to 37.92 MPa). These lump sum loss values were developed on the assumption that the full allowable compressive stress of concrete is required by stress conditions during the life of the member. For structures or elements where the concrete strength is determined on the basis of the nominal minimums in the specifications, and where full utilization of the allowable compressive stresses does not occur during the life of the structure, the lump sum loss values will be

somewhat conservative. Such conditions often occur when an over-size section is used for a short span due to the esthetic consideration of matching the depth of section used on a longer adjacent span.

REFERENCES

1. "Proposed Amendment to the AASHO Standard Specifications for Highway Bridges, Article 1.6.7 (B)—Prestress Losses" Submitted by Department of Civil Engineering, University of Illinois, Urbana, in cooperation with Illinois Department of Transportation, Division of Highways under Project IHR-93, "Field Investigation of Prestressed Concrete Highway Bridges."*
2. "Proposed Amendment to the 1971 AASHO Specifications Section 1.6.7 (B) (1)" dated March 20, 1973, submitted by Dr. Ti Huang based on research at Lehigh University for the Pennsylvania Department of Transportation.*
3. "Proposed Revision of AASHO Section 1.6.7 (B) (2)—Prestress Losses for Post-Tensioned Bridges" submitted by C. L. Freyermuth, Director, Post-Tensioning Division, Prestressed Concrete Institute, April 1972.*
4. Committee Closure to Discussion of "Tentative Recommendations for Prestressed Concrete" ACI Journal, Vol. 29, No. 7, January 1958.
5. "A Study of the Practical Significance of Variations in Prestress Losses" by C. L. Freyermuth, Director, Post-Tensioning Division, Prestressed Concrete Institute (Available on request to PCI).
6. "Criteria for Prestressed Concrete Bridges" U.S. Department of Commerce, Bureau of Public Roads, Washington D.C., 1954.
7. "Selected Climatic Maps of the United States" Superintendent of Documents, U.S. Government Printing Office, Washington D.C. 20402.
8. "Design and Control of Concrete Mixtures" Eleventh Edition, Chapter 12, Volume Changes of Concrete, Portland Cement Association, Old Orchard Road, Skokie, Illinois 60076.
9. "Some Aspects of Durability and Volume Change of Concrete for Prestressing" by Paul Klieger, Research Department Bulletin 118, Portland Cement Association, Old Orchard Road, Skokie, Illinois 60076.
10. "Prestress Loss as Affected by Type of Curing" by J. A. Hanson, Development Department Bulletin D-75, Portland Cement Association, Old Orchard Road, Skokie, Illinois 60076.
11. "Influence of Size and Shape of Member on Shrinkage and Creep of Concrete" by Torben C. Hansen and Alan H. Mattock, Development Department Bulletin D-103, Portland Cement Association, Old Orchard Road, Skokie, Illinois 60076.
12. "Tentative Recommendations for Estimating Prestress Losses," PCI Committee on Prestress Losses, Prestressed Concrete Institute, 20 North Wacker Drive, Chicago, Illinois 60606.
13. "International Recommendations for the Design and Construction of Concrete Structures" CEB-FIP Recommendations, Cement and Concrete Association, 52 Grosvenor Gardens, London SW1, England.

*References 1-3 were distributed at AASHTO regional Bridge Committee meetings in 1973 and 1972, but have not been published. Requests for copies of these references should be directed to the agencies concerned.

Appendix C

Estimating Prestress Losses

by Paul Zia, H. Kent Preston, Norman L. Scott, and Edwin B. Workman

Equations for estimating prestress losses due to various causes are presented for pretensioned and post-tensioned members with bonded and unbonded tendons. The equations are intended for practical design applications under normal design conditions as discussed in the commentary. Using the equations, sample computations are carried out for typical prestressed concrete beams selected from the literature. The comparison of the results shows fairly good agreement.

Keywords: beams (supports); creep properties; friction; post-tensioning; **prestressed concrete;** prestressing steels; **prestress loss;** pretensioning; shrinkage; stress relaxation; unbonded prestressing.

Prepared as a part of the work of, and sponsored by, ACI-ASCE Committee 423, Prestressed Concrete.

Introduction

The prestressing force in a prestressed concrete member continuously decreases with time. The factors which contribute to the loss of prestress are well known and they are clearly specified in the current Code.[1] The Code provisions for prestress losses (ACI 318-77, Section 18.6) are written both in performance language and in specific how-to-do-it procedures for losses due to friction. Without detailed analyses, design engineers are permitted to use lump sum loss values as suggested by the Code Commentary.[2] These lump sum loss values were originally proposed by the U.S. Bureau of Public Roads[4] and by the ACI-ASCE Committee 323.[3] Experiences have shown, however, that these lump sum values may not be adequate for some design conditions.

More recently, design recommendations have been developed by others[5,6,7,8,9,10,14] to implement the performance requirements of Section 18.6. Most procedures are relatively complex and convey the impression of an exactness that may not actually exist. The authors, members of ACI-ASCE Committee 423, prepared this report as a means of obtaining reasonably accurate values for the various code-defined sources of loss. A similar procedure was developed and adopted for use in bridge design.[11] It should be noted that the procedures described below are not intended for special structures such as water tanks.

Computation of Losses

Elastic Shortening of Concrete (ES)

For members with bonded tendons,

$$ES = K_{es} E_s \frac{f_{cir}}{E_{ci}} \tag{1}$$

in which

K_{es} = 1.0 for pretensioned members

K_{es} = 0.5 for post-tensioned members when tendons are tensioned in sequential order to the same tension. With other post-tensioning procedures, the value for K_{es} may vary from 0 to 0.5.

$$f_{cir} = K_{cir} f_{cpi} - f_g \tag{2}$$

in which K_{cir} = 1.0 for post-tensioned members

K_{cir} = 0.9 for pretensioned members.

For members with unbonded tendons,

$$ES = K_{es} E_s \frac{f_{cps}}{E_{ci}} \tag{1A}$$

in which f_{cps} = average compressive stress in the concrete along the member length at the center of gravity of the tendons immediately after the prestress has been applied to the concrete.

Creep of Concrete (CR)

For members with bonded tendons,

$$CR = K_{cr} \frac{E_s}{E_c} (f_{cir} - f_{cds}) \tag{3}$$

in which

K_{cr} = 2.0 for pretensioned members
K_{cr} = 1.6 for post-tensioned members

For members made of sand lightweight concrete the foregoing values of K_{cr} should be reduced by 20 percent.

For members with unbonded tendons,

$$CR = K_{cr}\frac{E_s}{E_c} f_{cpa} \qquad (3A)$$

Shrinkage of Concrete (SH)

$$SH = 8.2 \times 10^{-6} K_{sh} E_s (1 - 0.06 \frac{V}{S})(100 - RH) \qquad (4)$$

in which

K_{sh} = 1.0 for pretensioned members

or

K_{sh} is taken from Table 1 for post-tensioned members.

TABLE 1 — Values of K_{sh} for post-tensioned members

Time after end of moist curing to application of prestress, days	1	3	5	7	10	20	30	60
K_{sh}	0.92	0.85	0.80	0.77	0.73	0.64	0.58	0.45

Relaxation of Tendons (RE)

$$RE = [K_{re} - J(SH + CR + ES)]\, C \qquad (5)$$

in which the values of K_{re}, J and C are taken from Tables 2 and 3.

TABLE 2 — Values of K_{re} and J

Type of tendon*	K_{re}	J
270 Grade stress-relieved strand or wire	20,000	0.15
250 Grade stress-relieved strand or wire	18,500	0.14
240 or 235 Grade stress-relieved wire	17,600	0.13
270 Grade low-relaxation strand	5,000	0.040
250 Grade low-relaxation wire	4,630	0.037
240 or 235 Grade low-relaxation wire	4,400	0.035
145 or 160 Grade stress-relieved bar	6,000	0.05

*In accordance with ASTM A416-74, ASTM A421-76, or ASTM A722-75

TABLE 3 — Values of C

f_{pi}/f_{pu}	Stress relieved strand or wire	Stress-relieved bar or low relaxation strand or wire
0.80		1.28
0.79		1.22
0.78		1.16
0.77		1.11
0.76		1.05
0.75	1.45	1.00
0.74	1.36	0.95
0.73	1.27	0.90
0.72	1.18	0.85
0.71	1.09	0.80
0.70	1.00	0.75
0.69	0.94	0.70
0.68	0.89	0.66
0.67	0.83	0.61
0.66	0.78	0.57
0.65	0.73	0.53
0.64	0.68	0.49
0.63	0.63	0.45
0.62	0.58	0.41
0.61	0.53	0.37
0.60	0.49	0.33

Friction

Computation of friction losses is covered in Section 18.6.2 of ACI 318-77[1] and its Commentary.[2] When the tendon is tensioned, the friction losses computed can be checked with reasonable accuracy by comparing the measured elongation and the prestressing force applied by the tensioning jack.

Commentary

Determination of loss of prestress in accordance with Section 18.6.1 of ACI 318-77 usually involves complicated and laborious procedures because the rate of loss due to one factor, such as relaxation of tendons, is continually altered by changes in stress due to other factors such as shrinkage and creep of concrete. Rate of creep is, in turn, altered by the change in tendon stress. Many of these factors are further dependent upon such uncertainties as material properties, time of loading, method of curing of concrete, environmental conditions, and construction details.

The equations presented are intended for a reasonable estimate of loss of prestress from the various sources. They are applicable for prestressed members of normal designs with an extreme fiber compressive stress in the precompressed tensile zone under the full dead load condition ranging from 350 psi (2.41 MPa) to 1750 psi (12.1 MPa) using a minimum concrete cylinder strength f'_c of 4000 psi (27.6 MPa) and a unit weight of concrete of at least 115 pcf (1842.3 kg/m^3). For unusual design conditions, a more detailed procedure should be considered.[8]

Actual losses, greater or smaller than the estimated values, have little effect on the design

strength of a flexural member with bonded tendons unless the final tendon stress after losses is less than 0 .5 f_{pu}. However, they affect service load behavior, such as deflection and camber, connections, or cracking load. Over-estimation of prestress losses can be almost as detrimental as underestimation, since the former can result in excessive camber and horizontal movement.

Careful consideration of losses may be required for simply supported, slender members which may be sensitive to small changes in deflections. For example, shallow beams supporting flat roofs may be subject to ponding if sensitive to deflection.

Elastic Shortening of Concrete

Prestress loss due to elastic shortening of concrete is directly proportional to the concrete strain at the center of gravity of prestressing force immediately after transfer. For example, for members of simple span,

$$f_{cir} = K_{cir} f_{cpi} - f_g$$
$$= K_{cir} \left(\frac{P_{pi}}{A_c} + \frac{P_{pi} e^2}{I_c} \right) - \frac{M_G e}{I_c}$$

The different values for the coefficients K_{es} and K_{cir} account for the difference in the order of transfer. In applying Equation (2), the transformed section of a member may be used in lieu of the gross concrete section.

Creep of Concrete

Part of the initial compressive strain induced in the concrete immediately after transfer is reduced by the tensile strain resulting from the superimposed permanent dead load. Loss of prestress due to creep of concrete is therefore proportional to the net permanent compressive strain in the concrete.

For prestressed members made of sand lightweight concrete, there is a significantly larger amount of loss due to elastic shortening of concrete because of its lower modulus of elasticity, resulting in an overall reduction in loss due to creep. This effect is accounted for by a 20 percent reduction of the creep coefficient. For members made of all lightweight concrete, special consideration should be given to the properties of the particular lightweight aggregate used.

Unbonded Tendons

Since an unbonded tendon can slide within its duct, for most flexural members it does not undergo the same stress induced strain changes as the concrete surrounding it. For this reason, the average compressive stress, f_{cpa}, in the concrete is suggested for use in evaluating prestress losses due to elastic shortening and creep of concrete. This procedure relates the elastic shortening and creep of concrete prestress losses for unbonded tendons to the average member strain, rather than the strain at the point of maximum moment. The somewhat higher residual tensile stress in an unbonded tendon logically results in somewhat higher loss due to steel relaxation.

Shrinkage of Concrete

Shrinkage strain developed in a concrete member is influenced, among other factors, by its volume/surface ratio and the ambient relative humidity. Thus, the effective shrinkage strain ε_{sh} is obtained by multiplying the basic ultimate shrinkage strain ε_{sh} of concrete, taken as 550×10^{-6}, by the factors $(1 - 0.06\ V/S)$ and $(1.5 - 0.015RH)$. Thus

$$\varepsilon_{sh} = 550 \times 10^{-6} \left(1 - 0.06 \frac{V}{S}\right)\left(1.5 - 0.015RH\right)$$

$$= 8.2 \times 10^{-6} \left(1 - 0.06 \frac{V}{S}\right)\left(100 - RH\right)$$

The loss of prestress due to shrinkage is therefore the product of the effective shrinkage ε_{sh} and the modulus of elasticity of prestressing steel. The factor K_{sh} accounts for the reduction in shrinkage due to increased curing period.

It should be noted that for some lightweight concrete, the basic ultimate shrinkage strain ε_{sh} may be greater than the value used here. In addition, the following tabulated correction factors for the effect of the ambient relative humidity may be used in lieu of the expression $(1.5 - 0.015\ RH)$:

Ave. Ambient RH (%)	Correction Factor
40	1.43
50	1.29
60	1.14
70	1.00
80	0.86
90	0.43
100	0.00

Relaxation of Tendons

Relaxation of a prestressing tendon depends upon the stress level in the tendon. Basic relaxation values K_{re} for the different kinds of steel are shown in Table 2. However, because of other prestress losses, there is a continual reduction of the tendon stress, thus causing a reduction in relaxation. The reduction in tendon stress due to elastic shortening of concrete occurs instantaneously. On the other hand, the reduction due to creep and shrinkage takes place in a prolonged period of time. The factor J in Equation (5) is specified to approximate these effects.

Maximum Loss

The total amount of prestress loss due to elastic shortening, creep, shrinkage, and relaxation need

not be more than the values given below if the tendon stress immediately after anchoring does not exceed 0.83 f_{py}:

Type of strand	Maximum Loss psi (MPa) Normal Concrete	Lightweight Concrete
Stress relieved strand	50,000 (345)	55,000 (380)
Low-relaxation strand	40,000 (276)	45,000 (311)

Seating Loss at Anchorage

Many types of anchorage require that the anchoring device "set" from 1/8 in. (3.2 mm) to ¼ in. (6.4 mm) in order to transfer force from the tendon to the concrete. The actual seating loss varies with field technique and anchor type. As the seating loss is small, it is not practicable to measure it with accuracy; therefore it is important to recognize the effects of maximum and minimum values of seating loss. Usually long tendons with curvature will be unaffected by seating loss, since the required tendon elongation generally necessitates stressing to the maximum initial value to overcome friction. For short tendons, however, the elongation corresponding to the range of stress of 70 percent to 80 percent of the ultimate is too small to nullify seating loss, and attempts to obtain the necessary elongation would require exceeding the 80 percent limit with possible rupture of the tendon. Thus, the

TABLE 4 — Beam data from reference 6

Beam No.	Beam section	Deck width x thickness & weight	Transfer at (days)	Cast deck (days)	No. of strands ϕ ½ in.	Initial stress f_{pi} (ksi)	f_{cir} (psi)	f_{cds} (psi)	RH %	V/S (in.)
HG1	AASHTO-III	No Deck	2½	–	20	189	1411	0	80	4.06
HG2	AASHTO-III	96x8-800	1	90	22	189	1622	765	80	4.06
HG3	AASHTO-III	60x5-310	2½	90	22	189	1596	297	50	4.06
HG4	AASHTO-III	96x8-800	7	90	24	189	1721	761	80	4.06
HG5	8 ft Single Tee	96x2-200	2½	90	12	189	1125	695	80	2.07
HG6	8 ft Double Tee	96x2-200	2½	90	24	189	1600	696	80	1.87
HG7	54 in. I-Beam	60x5-310	2½	90	30	189	1554	309	80	3.60
HG8	8 ft Single Tee	96x2-200	2½	90	12	205*	1469	695	80	2.07
HG9	AASHTO-III	96x8-800	2½	90	24	205*	2020	761	80	4.06
HG10	54 in. I-Beam	96x8-800	2½	90	30	205*	1646	796	80	3.60

*Low relaxation strand

$E_s = 28 \times 10^6$ psi, $E_{ci} = 3.5 \times 10^6$ psi and $E_c = 4.2 \times 10^6$ psi

TABLE 5 — Comparison of loss values based on proposed procedure with theoretical results obtained by Hernandez and Gamble (H & G)

Beam No.	Method	ES (psi)	CR (psi)	SH (psi)	RE (psi)	Total (psi)
HG1	Proposed	11288	18813	3473	14964	48538
	H & G	9057	17656	3836	18699	49219
HG2	Proposed	12976	11427	3473	15819	43695
	H & G	10364	15327	3836	18085	47614
HG3	Proposed	12768	17320	8683	14184	52955
	H & G	10202	25840	7195	16743	59981
HG4	Proposed	13768	12800	3473	15494	45535
	H & G	10965	11793	3836	19370	45966
HG5	Proposed	9000	5733	4022	17187	35942
	H & G	8170	9374	5348	18949	41842
HG6	Proposed	12800	12053	4077	15661	44591
	H & G	11264	16069	5348	16840	49522
HG7	Proposed	12432	16600	3600	15105	47737
	H & G	9984	17285	3723	18414	49408
HG8	Proposed	11752	10320	4022	4154	30248
	H & G	10295	16192	5348	4558	36393
HG9	Proposed	16160	16787	3473	3720	40140
	H & G	12816	19780	3835	4564	40996
HG10	Proposed	13168	11333	3600	4070	32171
	H & G	10552	15154	3835	4368	33910

seating loss in short tendons should be deducted from the prestress that is applied to the tendon by the tensioning jack.

Restraining Effect of Adjoining Elements

Loss of prestress to adjoining elements of the structure must be properly evaluated. If a member is in contact with or attached to another member during the post-tensioning operation, there can be a transfer of prestressing force from one member to the other.

After the structure is complete, there will be volume changes due to creep and shrinkage of concrete and to variations of temperature. If the member can not move freely to accommodate these volume changes, there will be a transfer of prestressing force from the prestressed member to the restraining member and a resultant loss of prestress in the prestressed member.

Sample Computations

In order to assess whether the proposed equations are appropriate for estimating prestress losses, the following sample computations have been prepared for typical prestressed beams selected from the test program reported by Hernandez and Gamble.[6] The pertinent data regarding the beams are summarized in Table 4. With the procedures described herein, the computed prestress loss values are compared with the theoretical values obtained by Hernandez and Gamble as shown in Table 5. It should be noted that the theoretical predictions made by Hernandez and Gamble were based on their revised rate of creep method treated as a step-by-step numerical integration procedure with short time intervals. The unit creep and shrinkage strains versus time relationships were based on the 1970 CEB recommendations[13] which were found to be comparable to the field data obtained in their study. It can be seen that the comparisons show fairly good agreement.

Additional sample computations have been carried out on selected double T beams listed in the PCI *Design Handbook*. The double T beam properties are summarized in Table 6. The results are shown in Table 7. It is interesting to note that for those slender beams (i.e., Z2 and S2) with very small superimposed permanent load and under fairly low humidity, the total loss of prestress would be quite significant. With more superimposed permanent load and/or higher humidity, the total prestress loss value is reduced. (Compare S1a and S1b with S1, or S2a and S2b with S2, or S3a with S3.) Comparison of S3a with S4 also shows that the total prestress loss value is somewhat increased for the beam made of lightweight concrete.

TABLE 7 — Results of sample computations for pretensioned beams from PCI *Design Handbook*

Beam No.	*ES* (psi)	*CR* (psi)	*SH* (psi)	*RE* (psi)	Total (psi)
Z1	6896	5693	6268	17171	36028
Z2	16064	19613	10653	13051	59381
Z3	3784	5400	5340	17821	32345
S1	4352	7253	10681	16657	38943
S1a	4352	4880	10681	17013	36926
S1b	4352	4880	5341	17814	32387
S2	16280	27133	10447	11921	65781
S2a	16280	18933	10447	13151	58811
S2b	16280	18933	5224	13934	54371
S3	2816	4693	5224	18090	30823
S3a	2816	3061	5224	18335	29436
S4	5622	5486	5224	17550	33882

$E_c = 28 \times 10^6$ psi
For normal wt. concrete: $E_{ci} = 3.5 \times 10^6$ psi $E_c = 4.2 \times$
For light wt. concrete: $E_{ci} = 2.5 \times 10^6$ psi $E_c = 3.1 \times 1$

TABLE 6 — Beam data from PCI *Design Handbook* for sample computations

Beam No.	Beam Sec.	Span (ft)	Initial prestress P_{pi} (kips)	Initial stress f_{pi} (ksi)	Ecc. e (in.)	D. L. (lbs/ft)	Superimposed assumed permanent load (lbs/ft)	f_{cir} (psi)	f_{cds} (psi)	*RH* (%)	*V/S* (in.)
Z1	8DT24	62	230.6	189	14.15	418	112	862	435	70	1.5
Z2	4DT14	50	173.9	189	7.34	188	56	2008	537	50	1.2
Z3	8DT12	28	115.7	189	4.13	299	40	473	68	75	1.16
S1	8DT12	26	115.7	189	4.13	299	0	544	0	50	1.16
S1a	8DT12	26	115.7	189	4.13	299	120	544	178	50	1.16
S1b	8DT12	26	115.7	189	4.13	299	120	544	178	75	1.16
S2	8DT24	72	404.8	189	13.65	418	0	2035	0	50	1.5
S2a	8DT24	72	404.8	189	13.65	418	120	2035	615	50	1.5
S2b	8DT24	72	404.8	189	13.65	418	120	2035	615	75	1.5
S3	8DT24	42	115.7	189	12.15	418	0	352	0	75	1.5
S3a	8DT24	42	115.7	189	12.15	418	80	352	122.4	75	1.5
S4	8LDT24	42	115.7	189	12.15	320	80	502	122.4	75	1.5

Conclusions

Simple equations for estimating losses of prestress have been proposed which would enable the designer to estimate the various types of prestress loss rather than a lump sum value. It is believed that these equations, intended for practical design applications, would provide fairly realistic values for normal design conditions. For unusual design situations and special structures, more detailed and complex numerical analysis should be used.

Notation

A_c = area of gross concrete section at the cross section considered
A_{ps} = total area of prestressing tendons
CR = stress loss due to creep of concrete
C = a factor used in Eq. (5), see Table 3
e = eccentricity of center of gravity of tendons with respect to center of gravity of concrete at the cross section considered
E_{ci} = modulus of elasticity of concrete at time prestress is applied
E_c = modulus of elasticity of concrete at 28 days
E_s = modulus of elasticity of prestressing tendons. Usually 28,000,000 psi
ES = stress loss due to elastic shortening of concrete
f_{cds} = stress in concrete at center of gravity of tendons due to all superimposed permanent dead loads that are applied to the member after it has been prestressed
f_{cir} = net compressive stress in concrete at center of gravity of tendons immediately after the prestress has been applied to the concrete. See Eq. (2)
f_{cpa} = average compressive stress in the concrete along the member length at the center of gravity of the tendons immediately after the prestress has been applied to the concrete
f_{cpi} = stress in concrete at center of gravity of tendons due to P_{pi}
f_g = stress in concrete at center of gravity of tendons due to weight of structure at time prestress is applied
f_{pi} = stress in tendon due to P_{pi}, $f_{pi} = P_{pi}/A_{ps}$
f_{pu} = ultimate strength of prestressing tendon, psi
I_c = moment of inertia of gross concrete section at the cross section considered
J = a factor used in Eq. (5), See Table 2
K_{cir} = a factor used in Eq. (2)
K_{cr} = a factor used in Eq. (3)
K_{es} = a factor used in Eq. (1)
K_{re} = a factor used in Eq. (5). See Table 2.

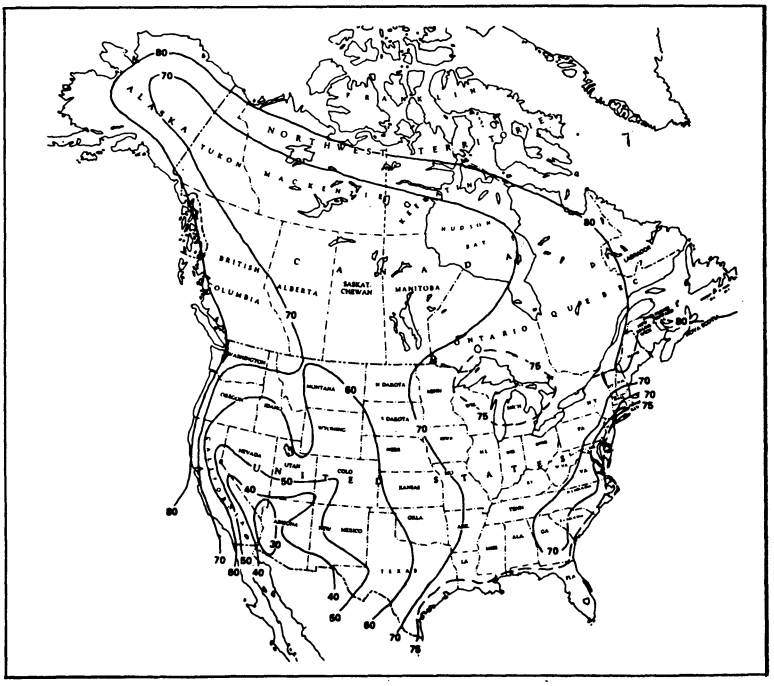

Annual average ambient relative humidity

M_G = bending moment due to dead weight of member being prestressed and to any other permanent loads in place at time of prestressing

P_{pi} = prestressing force in tendons at critical location on span after reduction for losses due to friction and seating loss at anchorages but before reduction for *ES, CR, SH,* and *RE.*

RE = stress loss due to relaxation of tendons

RH = average relative humidity surrounding the concrete member. See annual average ambient relative humidity map appended.

SH = stress loss due to shrinkage of concrete

V/S = volume to surface ratio. Usually taken as gross cross-sectional area of concrete member divided by its perimeter.

1 in. = 25.4 mm
1 ft = .3048 m
1 psi = .0069 MPa
1 ksi = 70.31 kgf/em²

References

1. ACI Committee 318, "Building Code Requirements for Reinforced Concrete (ACI 318-77)," American Concrete Institute, Detroit, 1977, 102 pp.

2. ACI Committee 318, "Commentary on Building Code Requirements for Reinforced Concrete (ACI 318-77)," American Concrete Institute, Detroit, 1977, 132 pp.

3. ACI-ASCE Committee 323, "Tentative Recommendations for Prestressed Concrete," ACI JOURNAL, *Proceedings* V. 54, No. 7, Jan. 1958, pp. 545-578.

4. "Criteria for Prestressed Concrete Bridges," U.S. Department of Commerce, Bureau of Public Roads, Washington, D.C., 1954, 25 pp.

5. Glodowski, R. J., and Lorenzetti, J. J., "A Method for Predicting Prestress Losses in a Prestressed Concrete Structures," *Journal,* Prestressed Concrete Institute, V. 17, No. 2, Mar.-Apr. 1972, pp. 17-31.

6. Hernandez, H. D., and Gamble, W. L., "Time-Dependent Prestress Losses in Pretensioned Concrete Construction," *Structural Research Series* No. 417, Civil Engineering Studies, University of Illinois, Urbana, May 1975, 171 pp.

7. Huang, T., "Prestress Losses in Pretensioned Concrete Structural Members," *Report* No. 339.9, Fritz Engineering Laboratory, Lehigh University, Bethlehem, Pa., Aug. 1973, 100 pp.

8. PCI Committee on Prestress Losses, "Recommendations for Estimating Prestress Losses," *Journal,* Prestressed Concrete Institute, V. 20, No. 4, July-Aug. 1975, pp. 43-75.

9. Sinno, Raouf, and Furr, Howard L., "Hyperbolic Functions of Prestress Loss and Camber," *Proceedings,* ASCE, V. 96, ST4, Apr. 1970, pp. 803-821.

10. Tadros, Maher K.; Ghali, Amin; and Dilger, Walter H., "Time-Dependent Prestress Loss and Deflection in Prestressed Concrete Members," *Journal,* Prestressed Concrete Institute, V. 20, No. 3, May-June 1975, pp. 86-98.

11. *Standard Specifications for Highway Bridges,* 12th Edition, American Association of State Highway and Transportation Officials, Washington, D.C., 1977, 496 pp.

12. Grouni, H. N., "Loss of Prestress Due to Relaxation After Transfer," ACI JOURNAL, *Proceedings* V. 75, No. 2, Feb. 1978, pp. 64-66.

13. "International Recommendations for the Design and Construction of Concrete Structures: Principles and Recommendations," Comite Europeen du Beton/Federation Internationale de la Precontrainte. English Edition, Cement and Concrete Association, London, June 1970, 80 pp.

14. Branson, D. E., and Kripanarayanan, K. M., "Loss of Prestress, Camber and Deflection of Non-Composite and Composite Prestressed Concrete Structures," *Journal,* Prestressed Concrete Institute, V. 16, No. 5, Sept.-Oct. 1971, pp. 22-52.

Received January 25, 1979, and reviewed under Institute publication policies.

Appendix D

Section 11. Shear and Torsion and Appendix D from *Design of Concrete Structures for Buildings* A National Standard of Canada

11. Shear and Torsion

11.0 Notation

a_o = equivalent depth of compression for members in torsion, millimetres (see Equation (11-26))

A_c = area enclosed by outside perimeter of concrete cross section including area of holes, if any, square millimetres

A_{cv} = area of concrete section resisting shear transfer, square millimetres

A_g = gross area of concrete cross section, square millimetres

A_l = total area of longitudinal reinforcement to resist torsion, square millimetres

A_o = area enclosed by shear flow path including area of holes, if any, square millimetres (see Clauses 11.3.7.7 and 11.4.4.8)

A_{oh} = area enclosed by centreline of exterior closed transverse torsion reinforcement including area of holes, if any, square millimetres

A_{ps} = area of prestressed reinforcement in tension zone, square millimetres

A_s = area of nonprestressed tension reinforcement, square millimetres

A_t = area of one leg of closed transverse torsion reinforcement, square millimetres

A_v = area of shear reinforcement perpendicular to the axis of a member within a distance, s, square millimetres

A_{vf} = area of shear-friction reinforcement, square millimetres

A_{vi} = cross sectional area of inclined shear reinforcement within a distance, s, square millimetres

b_o = perimeter of critical section for slabs and footings, millimetres

b_v = minimum effective web width within depth d_v, millimetres (see Clauses 11.4.2.7 and 11.4.2.8)

b_w = web width or diameter of circular section, millimetres (for joist construction defined by Clause 8.11, b_w shall be taken as equal to the average web width)

d = distance from the extreme compression fibre to the centroid of longitudinal tension reinforcement, but need not be less than 0.8h for prestressed members, millimetres (for circular sections d need not be less than the distance from the extreme compression fibre to the centroid of the tension reinforcement in the opposite half of the member)

d_p = distance from the extreme compression fibre to the centroid of prestressed reinforcement, millimetres

d_v = effective shear depth, which can be taken as the distance, measured perpendicular to the neutral axis, between the resultants of the tensile and compressive forces due to flexure but need not be taken less than 0.9d, millimetres

E_s = modulus of elasticity of steel, megapascals

f'_c = specified compressive strength of concrete, megapascals

$\sqrt{f'_c}$ = square root of specified compressive strength of concrete, megapascals

f_{pc} = compressive stress in concrete (after allowance for all prestress losses) at the centroid of the cross section resisting externally applied loads or at the junction of the web and flange when the centroid lies within the flange, megapascals (in a composite member f_{pc} is the resultant compressive stress at the centroid of the composite section or at the junction of the web and flange when the centroid lies within the flange, due to both prestress and moments being resisted by the precast member acting alone)

f_{pu} = specified tensile strength of tendons, megapascals

f_y = specified yield strength of nonprestressed reinforcement, megapascals

f_2 = diagonal compressive stress in concrete, megapascals (see Clause 11.4.2.2)

f_{2max} = diagonal crushing strength of concrete, megapascals (see Clause 11.4.2.3)

h = overall height of member, millimetres

h_b = distance measured from the bottom of a loading interface to the extreme face of a supporting member in the direction of the load but need not be taken less than 75 mm, millimetres

h_1 = overall depth of a supporting member in the direction of the applied shear, millimetres

M_f = factored moment at section, newton millimetres

N_f = factored axial load normal to the cross section occurring simultaneously with V_f; includes effects of tension due to creep and shrinkage, newtons

N_{se} = axial tensile load at specified load, newtons

N_r = factored axial tensile resistance of member, newtons

N_v = equivalent factored axial load caused by shear and torsion, newtons (see Clause 11.4.6)

p_c = outside perimeter of the concrete cross section. millimetres

p_h = perimeter of the centreline of the closed transverse torsion reinforcement, millimetres

p_o = perimeter of the shear flow path (see Clause 11.4.6.1), millimetres

P_{br} = factored axial load resistance at balanced strain conditions, computed using the resistance factors in Clause 9.3, newtons (see Clause 10.3.2)

s = spacing of shear or torsion reinforcement measured parallel to the longitudinal axis of the member, millimetres

T_f = factored torsional moment, newton millimetres

T_{cr} = pure torsional cracking resistance, newton millimetres

T_r = factored torsional resistance provided by circulatory shear flow, newton millimetres

T_{se} = torsion due to specified loads, newton millimetres

v_r = factored shear stress resistance, megapascals

V_c = factored shear resistance provided by tensile stresses in the concrete, newtons

V_{cr} = cracking shear resistance under combined loading, newtons

V_{cw} = factored shear resistance provided by the concrete when diagonal cracking results from excessive principal tensile stress in the web, newtons

V_f = factored shear force at section, newtons

V_p = component in the direction of the applied shear of the effective prestressing force or, in Clause 11.4 for variable depth members, the sum of the component of the effective prestressing force and the components of flexural compression and tension in the direction of the applied shear, positive if resisting applied shear, newtons

V_r = factored shear resistance, newtons

V_s = factored shear resistance provided by shear reinforcement, newtons

V_{se} = shear due to specified loads, newtons

α = angle between inclined stirrups or bent-up bars and the longitudinal axis of the member, degrees

α_f = angle between the shear-friction reinforcement and the shear plane, degrees

β_c = ratio of the long side to short side of the concentrated load or reaction area

γ_f = fraction of unbalanced moment transferred by flexure at slab-column connections (see Clause 13.3.3.3)

γ_v = fraction of unbalanced moment transferred by eccentricity of shear at slab-column connections

$= 1 - \gamma_f$

ϵ_{se} = tensile strain in transverse reinforcement due to specified loads

ϵ_t = tensile strain in transverse reinforcement due to factored loads

ϵ_x = longitudinal strain at mid-depth of the member when the section is subjected to M_f, N_f, and N_v, positive when tensile (see Clause 11.4.2.5)

ϵ_1 = principal tensile strain in cracked concrete due to factored loads

μ = coefficient of friction

θ = angle of inclination of diagonal compressive stresses to the longitudinal axis of the member, degrees

λ = factor to account for low density concrete (see Clause 11.2.3)

ϕ_c = resistance factor for concrete (see Clause 9.3.2)

ϕ_p = resistance factor for prestressing tendons (see Clause 9.3.3)

ϕ_s = resistance factor for reinforcement (see Clause 9.3.3)

11.1 Scope

Provisions of Clause 11 shall apply to the design of structural elements subject to shear or to combined shear and torsion.

Note: *See Appendix D for explanatory comments on Clause 11.*

11.2 General Requirements

11.2.1 Design Methods and Design Considerations

11.2.1.1

One-way flexural members shall be designed for shear and torsion either by the simplified method of Clause 11.3 or the general method of Clause 11.4. In either case the general requirements of Clause 11.2 shall be satisfied.

11.2.1.2

For deep flexural members, walls, shear friction, brackets and corbels, transfer of moments to columns in frames, and slabs and footings, the special provisions of Clauses 11.5 through 11.10 shall apply.

11.2.1.3

In determining shear resistance, the effects of axial tension due to creep, shrinkage, and thermal effects in restrained members shall be considered wherever applicable.

11.2.1.4

For variable depth members, the components of flexural compression and tension in the direction of the applied shear shall be taken into account if their effect is unfavourable and may be taken into account if their effect is favourable.

11.2.1.5
In determining shear resistance, V_r, the effect of any openings in members shall be considered.

11.2.2 Shear and Torsion Reinforcement Details

11.2.2.1 Types of Shear Reinforcement
Transverse reinforcement provided for shear may consist of:
(a) stirrups perpendicular to the axis of the member;
(b) welded wire fabric with transverse wires located perpendicular to the axis of the member, provided that the transverse wires can undergo a minimum elongation of 4% measured over a gauge length of at least 100 mm, which includes at least one cross wire;
(c) stirrups making an angle of 45° or more with the longitudinal tension reinforcement inclined to intercept potential diagonal cracks;
(d) for nonprestressed members, shear reinforcement may consist of No. 35 or smaller longitudinal bars bent to provide an inclined portion having an angle of 30° or more with the longitudinal bars and crossing potential diagonal cracks. However, only the centre three-fourths of the inclined portion of these bars may be considered effective; and
(e) spirals.

11.2.2.2 Anchorage of Shear Reinforcement
Stirrups and other bars or wires used as shear reinforcement shall be anchored at both ends according to Clause 12.13 to develop the design yield strength of the reinforcement.

11.2.2.3 Types of Torsion Reinforcement
Transverse reinforcement provided for torsion may consist of:
(a) closed stirrups perpendicular to the axis of the member;
(b) a closed cage of welded wire fabric with transverse wires meeting the minimum elongation requirements of Clause 11.2.2.1(b) located perpendicular to the axis of the member; and
(c) spirals.

Longitudinal reinforcement is also required.

11.2.2.4 Anchorage of Torsion Reinforcement
Transverse torsion reinforcement shall be anchored:
(a) according to Clause 12.13.2(a) or Clause 12.13.2(b) in regions where the concrete surrounding the anchorage is restrained against spalling (see Clause 11.4.2.7); or

(b) by means of 135° standard hooks where the concrete surrounding the anchorage is unrestrained against spalling.

A longitudinal reinforcing bar or bonded prestressing tendon shall be placed in each corner of the closed transverse reinforcement required for torsion. The nominal diameter of the bar or tendon shall not be less than s/16.

Longitudinal torsion reinforcement shall be anchored in accordance with Clause 12.1.

11.2.2.5 Yield Strength of Shear and Torsion Reinforcement

The yield strength used in design calculations of shear and torsion transverse reinforcement shall not exceed 400 MPa.

11.2.3 Low and Normal Density Concrete

Values of the modification factor, λ, to account for the type of concrete shall be

$\lambda = 1.00$ for normal density concrete;

$\lambda = 0.85$ for structural semi-low density concrete; and

$\lambda = 0.75$ for structural low density concrete.

Linear interpolation may be applied if partial sand replacement is used.

11.2.4 Consideration of Torsion

11.2.4.1

If the magnitude of the torsion, T_f, determined by analysis using stiffnesses based on uncracked sections exceeds $0.25T_{cr}$, then torsional effects shall be considered and torsional reinforcement designed in accordance with Clause 11.3 or 11.4 shall be provided. Otherwise torsional effects may be neglected.

In lieu of more detailed calculations, T_{cr} may be taken as

$$T_{cr} = (A_c^2/p_c)\, 0.4\lambda\phi_c\sqrt{f'_c} \qquad \textbf{(11-1)}$$

for nonprestressed members; and

$$T_{cr} = (A_c^2/p_c)\, 0.4\lambda\phi_c\sqrt{f'_c}\ \sqrt{1 + f_{pc}/(0.4\lambda\phi_c\sqrt{f'_c})} \qquad \textbf{(11-2)}$$

for prestressed members.

11.2.4.2

In a statically indeterminate structure where reduction of torsional moment in a member can occur due to redistribution of internal forces, the maximum factored torsion, T_f, may be reduced to $0.67T_{cr}$ provided that the corresponding adjustments to torsions, moments, and shears are made in the member and in adjoining members to account for the redistribution. For a spandrel beam where the torsion is caused by a slab, the factored torsion in the spandrel can be assumed to vary linearly from zero at midspan to $0.67T_{cr}$ at the face of the support.

11.2.5 Minimum Shear Reinforcement

11.2.5.1

A minimum area of shear reinforcement shall be provided in all regions of flexural members where the factored shear force, V_f, exceeds $0.5V_c$ or the factored torsion, T_f, exceeds $0.25T_{cr}$. This requirement may be waived for:

(a) slabs and footings;
(b) concrete joist construction defined by Clause 8.11;
(c) beams with a total depth of not greater than 250 mm; and
(d) beams cast integrally with slabs with a total depth of not greater than 2.5 times the thickness of the slab nor 600 mm.

11.2.5.2

In lieu of more detailed calculations, V_c in Clause 11.2.5.1 may be taken as $0.2\lambda\phi_c\sqrt{f'_c}\ b_w d$.

11.2.5.3

The minimum shear reinforcement requirements of Clause 11.2.5.1 may be waived if it can be shown by test that the required flexural and shear resistances can be developed when shear reinforcement is omitted. Such tests shall simulate the effects of differential settlement, creep, shrinkage, and temperature change, based on a realistic assessment of such effects occurring in service.

11.2.5.4

Where shear reinforcement is required by Clause 11.2.5.1 or by calculation, the minimum area of shear reinforcement shall be computed by:

$$A_v = 0.35\frac{b_w s}{f_y} \qquad \textbf{(11-3)}$$

11.2.5.5

For prestressed members with an effective prestress force of not less than 40% of the tensile strength of the flexural reinforcement, the minimum area of shear reinforcement may be computed by Equation (11-3) or Equation (11-4).

$$A_v = \frac{A_{ps}}{80} \frac{f_{pu}}{f_y} \frac{s}{d} \sqrt{\frac{d}{b_w}} \qquad \textbf{(11-4)}$$

11.2.5.6

In calculating the term A_v in Equations (11-3) and (11-4), inclined reinforcement and transverse reinforcement used to resist torsion may be included.

11.3 Shear and Torsion Design—Simplified Method

11.3.1 Required Shear Reinforcement

Transverse reinforcement required for shear shall be determined from the requirement that:

$$V_r \geqslant V_f \qquad \textbf{(11-5)}$$

11.3.2 Factored Shear Resistance

The factored shear resistance shall be computed by:

$$V_r = V_c + V_s \qquad \textbf{(11-6)}$$

where

V_c is determined in accordance with Clause 11.3.4 or Clause 11.3.5; and

V_s is determined in accordance with Clause 11.3.6.

11.3.3 Calculation of V_f in Regions Near Supports

11.3.3.1

The shear, V_f, in regions near supports may be reduced in accordance with Clause 11.3.3.2 or 11.3.3.3 when both of the following conditions are satisfied:

(a) the support reaction, in the direction of the applied shear, introduces compression into the end region of the member; and

(b) no concentrated load occurs within a distance, d, from the face of a support for nonprestressed members or within a distance, h/2, for prestressed members.

11.3.3.2

For nonprestressed members, sections located less than a distance, d, from the face of a support may be designed for the same shear, V_f, as that computed at a distance, d.

11.3.3.3

For prestressed members, sections located less than a distance, h/2, from the face of a support may be designed for the same shear, V_f, as that computed at a distance, h/2.

11.3.4 Calculation of V_c—Nonprestressed Members

11.3.4.1

For members subject to shear and flexure only

$$V_c = 0.2\lambda\phi_c\sqrt{f'_c}\, b_w d \qquad \textbf{(11-7)}$$

11.3.4.2

For members subject to axial tension

$$V_c = 0.2\lambda\phi_c\sqrt{f'_c}\left(1 - \frac{N_f}{N_r}\right) b_w d \qquad \textbf{(11-8)}$$

where N_f is positive for tension.

In calculating N_r the influence of the coexisting flexural moment shall be taken into account. Alternatively, N_r may be taken as $0.6\lambda\phi_c\sqrt{f'_c}\, A_g$.

11.3.4.3

For members subject to axial compression

$$V_c = 0.2\lambda\phi_c\sqrt{f'_c}\left(1 - \frac{3N_f}{A_g f'_c}\right) b_w d \qquad \textbf{(11-9)}$$

where N_f is positive for tension.

11.3.5 Calculation of V_c—Prestressed Members

11.3.5.1

For members with an effective prestress force of not less than 40% of the tensile strength of the flexural reinforcement

$$V_c = \left(0.06\lambda\sqrt{f'_c} + 6\frac{V_f d_p}{M_f}\right)\phi_c b_w d \qquad \textbf{(11-10)}$$

but V_c need not be taken as less than $0.2\lambda\phi_c\sqrt{f'_c}\,b_w d$, nor shall it exceed V_{cw} given in Clause 11.3.5.2. The quantity $V_f d_p/M_f$ shall not be taken as greater than 1.0 where M_f is the factored moment occurring simultaneously with V_f at the section considered.

11.3.5.2

V_c shall not exceed V_{cw}

$$V_{cw} = 0.4\lambda\phi_c\sqrt{f'_c}\left(\sqrt{1+\frac{f_{pc}}{0.4\lambda\phi_c\sqrt{f'_c}}}\right)b_w d_p + \phi_p V_p \qquad \textbf{(11-11)}$$

In Equation (11-11) d_p need not be taken less than 0.8h.

11.3.5.3

In pretensioned members the reduced prestress in the transfer length of prestressing tendons shall be considered when computing f_{pc} and V_p. The prestress force may be assumed to vary linearly from zero at the point at which bonding commences, to a maximum at a distance from the end of the tendon equal to the transfer length, assumed to be 50 diameters for strand and 100 diameters for single wire.

11.3.5.4

For prestressed members with an effective prestress force of less than 40% of the tensile strength of the flexural reinforcement, V_c shall be taken as $0.2\lambda\phi_c\sqrt{f'_c}\,b_w d$.

11.3.6 Calculation of V_s

11.3.6.1

When shear reinforcement perpendicular to the axis of a member is used

$$V_s = \frac{\phi_s A_v f_y d}{s} \qquad \textbf{(11-12)}$$

11.3.6.2

When inclined stirrups are used as shear reinforcement

$$V_s = \frac{\phi_s A_{vi} f_y(\sin\alpha + \cos\alpha)d}{s} \qquad \textbf{(11-13)}$$

11.3.6.3

When shear reinforcement consists of a single bar or a single group of parallel bars, all bent up at the same distance from the support:

$$V_s = \phi_s A_{vi} f_y \sin \alpha \qquad \textbf{(11-14)}$$

but not greater than $0.3\lambda\phi_c\sqrt{f'_c}\, b_w d$

11.3.6.4

When shear reinforcement consists of a series of parallel bent-up bars or groups of parallel bent-up bars at different distances from the support, the shear strength, V_s, shall be taken as 0.75 times the value given by Equation (11-13), but not greater than $0.5\lambda\phi_c\sqrt{f'_c}\, b_w d$.

11.3.6.5

Where more than one type of shear reinforcement is used to reinforce the same portion of a member, V_s shall be computed as the sum of the V_s values computed for the various types.

11.3.6.6

For beams designed according to Clause 11.3, V_s shall not be greater than $0.8\lambda\phi_c\sqrt{f'_c}\, b_w d$.

11.3.7 Design of Torsional Reinforcement

11.3.7.1

Where required by Clause 11.2.4, torsion reinforcement shall be provided in addition to the reinforcement required to resist the factored shear, flexure, and axial forces, which act in combination with the torsion.

11.3.7.2

In regions near supports, which satisfy the requirements of Clause 11.3.3, nonprestressed sections located less than a distance, d, from the face of the support may be designed for the same torsion, T_f, as that computed at a distance, d, while prestressed sections located less than a distance h/2 from the face of the support may be designed for the same torsion, T_f, as that computed at a distance, h/2.

11.3.7.3

The transverse reinforcement required for torsion shall be determined from the requirement that $T_r \geqslant T_f$.

11.3.7.4
The factored torsional resistance shall be computed by:

$$T_r = 2A_o\phi_s A_t f_y/s \qquad \textbf{(11-15)}$$

11.3.7.5
The required area, A_l, of longitudinal bars distributed symmetrically around the section shall be computed by:

$$A_l = A_t p_h/s \qquad \textbf{(11-16)}$$

11.3.7.6
In the flexural compression zone of a member the area of longitudinal torsion steel required may be reduced by an amount equal to $M_f/(0.9df_y)$ where M_f is the factored moment at the section acting in combination with T_f.

11.3.7.7
The area enclosed by the torsional shear flow, A_o, may be taken as $0.85A_{oh}$.

11.3.7.8
For hollow sections in torsion, the distance measured from the centreline of the transverse torsion reinforcement to the inside face of the wall shall be not less than $0.5A_{oh}/p_h$.

11.3.7.9
The cross sectional dimensions shall be such that
$(V_f/b_w d) + (T_f p_h/A_{oh}^2)$
does not exceed $0.25\lambda\phi_c f'_c$.

11.3.8 Spacing Limits for Shear and Torsion Reinforcement

11.3.8.1
The spacing of required shear reinforcement placed perpendicular to the axis of a member shall not exceed d/2 in nonprestressed members and 0.75h in prestressed members, nor 600 mm.

11.3.8.2
Inclined stirrups and bent longitudinal reinforcement shall be so spaced that every 45° line, extending toward the reaction from the mid-depth of the member, 0.5d, to the longitudinal tension reinforcement, shall be crossed by at least one line of effective shear reinforcement. (See also Clause 11.2.2.1(d).)

11.3.8.3
When V_s exceeds $0.4\lambda\phi_c\sqrt{f'_c}\,b_w d$, the maximum spacings given in Clauses 11.3.8.1 and 11.3.8.2 shall be reduced by one-half.

11.3.8.4
Spacing of transverse torsion reinforcement shall not exceed $p_h/8$ nor 300 mm.

11.3.8.5
Spacing of longitudinal bars distributed around the perimeter of the transverse torsion reinforcement shall not exceed 300 mm. (See also Clause 11.2.2.4.)

11.3.9 Indirect Loads

11.3.9.1
The provisions of this Clause apply to members loaded by brackets, ledges, or crossbeams.

11.3.9.2
When a load is applied to a side face of a member, additional transverse reinforcement capable of transmitting a tensile force of $(1 - h_b/h_1)$ times the applied factored load shall be provided. In the supporting member, only the additional full depth transverse reinforcement in a region within a distance, h_b, from the shear interface may be assumed effective. In the supported member, only the additional full depth transverse reinforcement within a distance of one-quarter of the effective depth of the supported member on each side of the shear interface may be assumed effective. This requirement may be waived if the interface transmitting the load extends to the top of the supporting member and if the average shear stress on this interface is not greater than $0.25\lambda\phi_c\sqrt{f'_c}$.

11.4 Shear and Torsion Design—General Method

Note: *See Appendix D for explanatory comments on the general method.*

11.4.1 General Principles and Requirements

11.4.1.1

Members shall be designed to have adequate resistance, adequate ductility, and satisfactory performance at service load levels.

11.4.1.2 Resistance

The resistance of members in shear or in shear combined with torsion shall be determined by satisfying applicable conditions of equilibrium and compatibility of strains and by using appropriate stress-strain relationships for reinforcement and for diagonally cracked concrete. Cross sectional dimensions shall be chosen to ensure that the diagonally cracked concrete is capable of resisting the inclined compressive stresses. Longitudinal and transverse reinforcement capable of equilibrating this field of diagonal compression shall be provided.

11.4.1.3 Ductility

The amount of reinforcement in a member shall be such that a reserve of strength exists after initial cracking. In addition, the reinforcement and the cross sectional details and properties shall be such that the transverse reinforcement yields prior to the diagonal crushing of concrete.

11.4.1.4 Serviceability

Cross sectional properties and reinforcement details shall be chosen to ensure adequate control of diagonal cracking at specified loads.

11.4.1.5

The resistance requirements of Clause 11.4.1.2 may be considered satisfied if the concrete crushing limits of Clause 11.4.2 are satisfied, the transverse reinforcement requirements of Clauses 11.4.4 and 11.4.5 are satisfied, the longitudinal reinforcement requirements of Clause 11.4.6 are satisfied, and the requirements of Clause 11.4.7 are satisfied, if applicable.

11.4.1.6

The ductility requirements of Clause 11.4.1.3 may be considered satisfied if the minimum shear reinforcement requirements of Clause 11.2.5 are satisfied and the reinforcement strain limits of Clause 11.4.3 are satisfied.

11.4.1.7

The serviceability requirements of Clause 11.4.1.4 may be considered satisfied if the crack control requirements of Clause 11.4.8 are satisfied.

11.4.2 Diagonal Compressive Stresses in Concrete

11.4.2.1

The cross sectional dimensions may be considered adequate to avoid diagonal crushing of the concrete if:

$$f_2 < f_{2max} \qquad \textbf{(11-17)}$$

11.4.2.2

The diagonal compressive stress in the concrete, f_2, may be computed as:

$$f_2 = \left(\tan\theta + \frac{1}{\tan\theta} \right) \left(\frac{V_f}{b_v d_v} \right) \qquad \textbf{(11-18)}$$

11.4.2.3

The diagonal crushing strength of the concrete, f_{2max}, may be computed as:

$$f_{2max} = \lambda \phi_c f'_c / (0.8 + 170\epsilon_1) \qquad \textbf{(11-19)}$$

however, f_{2max} shall not exceed $\lambda \phi_c f'_c$ unless the concrete is triaxially confined.

11.4.2.4

The principal tensile strain, ϵ_1, may be computed as:

$$\epsilon_1 = \epsilon_x + \frac{\epsilon_x + 0.002}{\tan^2\theta} \qquad \textbf{(11-20)}$$

11.4.2.5

In lieu of determining ϵ_x by performing a plane sections analysis for the section under the loads M_f, N_f and N_v, its value may be taken as 0.002.

11.4.2.6

In evaluating sectional resistance, θ may be chosen to have any value between 15° and 75°; however, the same value of θ must be used in satisfying all of the requirements at a section.

11.4.2.7 Spalling of Concrete Cover

If the shear, V_f, exceeds $\lambda\phi_c\sqrt{f'_c}\,b_w d$ or if torsional reinforcement is required, spalling of the concrete cover shall be accounted for in determining b_v; otherwise spalling may be neglected. If spalling is to be accounted for, the concrete cover down to the centreline of the outermost reinforcement shall be assumed to have spalled off unless the ends of the compression diagonals are restrained against spalling. Transverse reinforcement shall not be anchored in the cover concrete if spalling is to be accounted for.

11.4.2.8

In determining the minimum effective web width, b_v, the diameters of ungrouted ducts or one-half of the diameters of grouted ducts shall be subtracted from the web width at the level of these ducts.

11.4.2.9

For variable depth members or for prestressed members with inclined tendons, the term, V_f, in Equation (11-18) shall be replaced by $(V_f - \phi_p V_p)$.

11.4.2.10

When inclined stirrups are used as shear reinforcement, the term V_f in Equation (11-18) may be replaced by $(V_f - \phi_s A_{vi} f_y d_v \cos\alpha/s)$; however, this term shall not be taken as less than $0.66V_f$.

11.4.2.11

If torsional reinforcement is required by Clause 11.2.4.1, the term $(V_f/b_v d_v)$ in Equation (11-18) shall be replaced by $(V_f/b_v d_v + T_f p_h/A_{oh}^2)$.

11.4.2.12

For hollow sections in torsion the wall thickness may be considered adequate to avoid diagonal crushing of the concrete if the distance from the centreline of the outermost transverse torsional reinforcement to the inside face of the wall exceeds $1.5a_o$. (See Clause 11.4.4.9.)

11.4.3 Yielding of Transverse Reinforcement

11.4.3.1

The cross sectional and reinforcement properties may be considered adequate to ensure the yielding of the transverse reinforcement prior to the diagonal crushing of the concrete if:

$$\epsilon_t > f_y/E_s \qquad \textbf{(11-21)}$$

11.4.3.2

For transverse reinforcement perpendicular to the axis of the member

$$\epsilon_t = \epsilon_1 - \epsilon_x - 0.002 \qquad \textbf{(11-22)}$$

11.4.3.3

For transverse reinforcement inclined to the axis of the member

$$\epsilon_t = 0.5(\epsilon_1 - 0.002) - 0.5(\epsilon_1 + 0.002)\cos 2(\theta + \alpha) \qquad \textbf{(11-23)}$$

11.4.4 Design of Transverse Reinforcement

11.4.4.1

The transverse reinforcement provided shall be at least equal to the sum of that required for shear and that required for the co-existing torsion.

11.4.4.2

The transverse reinforcement required for shear shall be determined from the requirement that $V_r \geqslant V_f$.

11.4.4.3 Factored Shear Resistance

The factored shear resistance shall be computed by:

$$V_r = \frac{\phi_s A_v f_y}{s} \frac{d_v}{\tan\theta} + \phi_p V_p \qquad \textbf{(11-24)}$$

11.4.4.4

If inclined stirrups are used as transverse reinforcement, the term

$$\frac{\phi_s A_{vi} f_y}{s} d_v \left(\frac{\sin\alpha}{\tan\theta} + \cos\alpha \right)$$

shall be added to the expression for V_r.

11.4.4.5

In calculating V_r for nonprestressed members, transverse reinforcement consisting of a series of parallel bent-up bars at different distances from the support may be treated as inclined stirrups, except that d_v shall be replaced by $0.75d_v$ in Clause 11.4.4.4, and the additional shear resistance calculated in Clause 11.4.4.4 shall not exceed $0.3\,\lambda\phi_c\sqrt{f'_c}\,b_v d_v$.

11.4.4.6

The transverse reinforcement required for torsion shall be determined from the requirement that $T_r \geqslant T_f$.

11.4.4.7 Factored Torsional Resistance

The factored torsional resistance shall be computed by

$$T_r = \frac{\phi_s A_t f_y}{s}\,\frac{2A_o}{\tan\theta} \qquad \textbf{(11-25)}$$

11.4.4.8

The area, A_o, enclosed by the torsional shear flow may be computed as $A_{oh} - a_o p_h/2$.

11.4.4.9

The equivalent torsional depth of compression, a_o, may be computed as

$$a_o = \frac{A_{oh}}{p_h}\left[1 - \sqrt{1 - \frac{T_f p_h}{0.7\lambda\phi_c f'_c A_{oh}^2}\left(\tan\theta + \frac{1}{\tan\theta}\right)}\,\right] \qquad \textbf{(11-26)}$$

11.4.4.10 Uniformly Loaded Beams

For a region of a beam supported on its bottom surface and subject to uniform loading on its top surface but not subjected to concentrated applied loads, the transverse reinforcement required within a length $d_v/\tan\theta$ may be determined by using the lowest values of V_f and T_f which occur within this length, provided that the value of θ has been chosen to satisfy the requirements of Clauses 11.4.2 and 11.4.3 using the highest values of V_f and T_f which occur within this length.

11.4.5 Spacing Limits for Transverse Reinforcement

11.4.5.1

Spacing of shear reinforcement placed perpendicular to the axis of member shall not exceed the smallest of $d_v/(3\tan\theta)$, d_v, or 600 mm.

11.4.5.2

Where inclined stirrups or bent longitudinal reinforcement, or both are required to resist shear, they shall be so spaced that every line inclined at an angle θ to the longitudinal axis is crossed by at least three lines of effective shear reinforcement.

11.4.5.3

The spacing of transverse reinforcement provided for torsion shall not exceed $p_h/(8\tan\theta)$.

11.4.6 Design of Longitudinal Reinforcement

11.4.6.1

Longitudinal reinforcement shall be designed by the plane sections theory described in Clause 10 to resist the factored moment, M_f, and the axial load, N_f, together with the additional factored axial tensile load, N_v, acting at mid-depth of the member, except if a design according to Clause 11.4.7 indicates that less reinforcement is required. The equivalent axial tensile load, N_v, shall be computed by:
(a) for members in which torsion can be neglected according to Clause 11.2.4.1

$$N_v = \frac{V_f}{\tan\theta} \qquad \textbf{(11-27)}$$

(b) for other members

$$N_v = \frac{1}{\tan\theta}\sqrt{(V_f)^2 + \left(\frac{T_f p_o}{2A_o}\right)^2} \qquad \textbf{(11-28)}$$

where
p_o may be computed as $(p_h - 4a_o)$

11.4.6.2

For variable depth members or for prestressed members with inclined tendons the term V_f in Equations (11-27) and (11-28) shall be replaced by $(V_f - \phi_p V_p)$.

11.4.6.3
When inclined stirrups are used as shear reinforcement, the term V_f in Equations (11-27) and (11-28) may be replaced by $(V_f - \phi_s A_{vi} f_y d_v \cos \alpha/s)$; however, this term shall not be taken as less than $0.66V_f$.

11.4.6.4
For members subjected to axial compression, N_f, in excess of the balanced load, P_{br}, the cross section shall be capable of resisting the moment, M_f, together with an axial compression load of $N_f + N_v$, where the additional compression, N_v, determined from Equation (11-27) or Equation (11-28) shall be assumed to act at mid-depth.

11.4.6.5
If longitudinal reinforcement is designed to satisfy Clauses 11.4.6 and 12.1, the requirements of Clauses 12.10.3, 12.10.4, 12.10.5, and 12.11.3 may be waived.

11.4.7 Design of Regions Adjacent to Supports, Concentrated Loads, or Abrupt Changes in Cross Section

11.4.7.1
The provisions of this Clause shall apply in determining the resistance of regions near discontinuities, such as abrupt changes in cross sectional dimensions or cross sectional forces, where it is inappropriate to assume that the shear stresses are uniformly distributed over the depth, d_v.

11.4.7.2
These regions shall be idealized as trusses consisting of concrete compressive struts and reinforcing steel tension ties interconnected by nodal zones of multi-directionally compressed concrete. The trusses shall be capable of providing internal load paths for all of the forces acting on the regions.

Note: *See Appendix D for description of nodal zones*

11.4.7.3
The concrete compressive stress in the struts shall not exceed f_{2max} given by Clause 11.4.2.3, where ϵ_1 is determined by considering the strain conditions of the concrete and the reinforcement in the vicinity of the strut.

11.4.7.4
Tension tie reinforcement shall be effectively anchored to transfer the required tension to the nodal zone of the truss in accordance with Clause 12.

11.4.7.5
Unless special confining reinforcement is provided, the concrete compressive stresses in the nodal zones shall not exceed the following limits:

(a) $0.85\phi_c f'_c$ in nodal zones bounded by compressive struts and bearing areas;

(b) $0.75\phi_c f'_c$ in nodal zones anchoring only one tension tie; and

(c) $0.60\phi_c f'_c$ in nodal zones anchoring tension ties in more than one direction.

11.4.7.6
The stress limits in nodal zones may be considered satisfied if the following conditions are met:

(a) the compressive stresses in struts bearing against the nodal zone do not exceed the stress limits given in Clause 11.4.7.5;

(b) the bearing stresses on the nodal zone produced by concentrated loads or reactions do not exceed the stress limits given in Clause 11.4.7.5; and

(c) the tension tie reinforcement is distributed over an effective area of concrete at least equal to the tensile tie force divided by the stress limits given in Clause 11.4.7.5. The effective area of concrete may be assumed to be the area of concrete surrounding the tension tie reinforcement and having the same centroid as that reinforcement.

11.4.7.7
In deep beams and corbels and in regions near direct supports or concentrated loads, where the concrete can be idealized as a series of uninterrupted compressive struts radiating from the nodal zone at the direct support or concentrated load, the concrete compressive stress limits of Clauses 11.4.7.3 and 11.4.7.5 may be considered satisfied by satisfying only the requirements of Clauses 11.4.7.6(b) and 11.4.7.6(c).

11.4.8 Control of Diagonal Cracking

11.4.8.1
The control of diagonal cracking shall be investigated if the shear due to specified loads, V_{se}, is greater than the shear, V_{cr}, causing diagonal cracking.

11.4.8.2

It may be assumed that the control of diagonal cracking at specified loads is adequate if the following three conditions are met:

(a) the spacing of the transverse reinforcement does not exceed 300 mm;

(b) the shear force, V_f, does not exceed $0.6\lambda\phi_c\sqrt{f'_c}\,b_w d$; and

(c) torsion can be neglected according to Clause 11.2.4.1.

11.4.8.3

For members not meeting the requirements of Clause 11.4.8.2 it may be assumed that the control of diagonal cracking at specified loads is adequate if Items (a) and (b) and either Item (c) or Item (d) are met, as follows:

(a) the spacing of the transverse reinforcement does not exceed 300 mm; and

(b) the spacing between longitudinal reinforcing bars along the exposed sides of the member does not exceed 300 mm; and

(c) the calculated strain in the transverse reinforcement at specified loads does not exceed 0.001 for interior exposure and 0.0008 for exterior exposure; or

(d) the value of f_y used in calculating the transverse reinforcement is taken as not greater than 300 MPa.

11.4.8.4

The strain in the transverse reinforcement at specified loads may be calculated as follows:

$$\epsilon_{se} = \left[\frac{V_{se}s}{A_v E_s d_v} + \frac{T_{se}s}{1.6\,A_t E_s A_{oh}} \right] \left[\left(1 - \frac{f_y}{200}\,\frac{f_{pc}}{f'_c} \right) \tan\theta \right]^{0.5} \times \left[1 - \left(\frac{V_{cr}}{V_{se}} \right)^3 \right] \qquad \textbf{(11-29)}$$

where

A_v and A_t are the amounts of transverse reinforcement provided for shear and torsion, respectively.

11.4.8.5

In lieu of more detailed calculations the cracking shear, V_{cr}, may be determined as follows:

(a) for members not subject to torsion

$$V_{cr} = \left[0.2\lambda\sqrt{f'_c}\,\sqrt{1 + f_{pc}/(0.4\lambda\sqrt{f'_c})} \right] b_w d \qquad \textbf{(11-30)}$$

(b) for members subjected to combined shear and torsion, the cracking shear, V_{cr}, may be determined by dividing the value obtained from Equation (11-30) by the factor

$$\sqrt{1 + \left(\frac{p_c b_w d}{2A_c^2} \frac{T_{se}}{V_{se}} \right)^2}$$

(c) the influence of an axial tensile load, N_{se}, can be accounted for by replacing the term, f_{pc}, in Equation (11-30)
by $\left(f_{pc} - \frac{N_{se}}{A_g} \right)$.

11.4.8.6

When inclined stirrups are used as shear reinforcement, the strain in these stirrups may be computed by dividing the value from Equation (11-29) by
$\left[\frac{\sin \alpha}{\tan \theta} + \cos \alpha \right]$
with A_v replaced by A_{vi}.

11.4.8.7

For uniformly loaded beams loaded on the top surface and supported on the bottom, the strain in the transverse reinforcement within a length, $d_v/\tan \theta$, may be determined by using the lowest values of V_{se} and T_{se}, which occur within this length.

11.4.8.8

Concentrated loads that can be transmitted directly to supports by compressive struts satisfying the requirements of Clause 11.4.7 may be neglected when calculating the strain in the transverse reinforcement.

11.5 Special Provisions for Deep Shear Spans

11.5.1

The provisions of Clause 11.5 shall apply for those parts of members in which:
(a) the distance from the point of zero shear to the face of the support is less than 2d; or
(b) a load causing more than 50% of the shear at a support is located less than 2d from the face of the support.

11.5.2
Shear design of deep shear spans shall be in accordance with the requirements of the general method, as specified in Clause 11.4 and modified in accordance with Clause 11.5.3. In particular see Clause 11.4.7.

Note: *Special attention must be given to the anchorage of longitudinal reinforcement in deep beams. See Clauses 11.4.7 and 12.10.6.*

11.5.3 Minimum Shear Reinforcement Requirements for Deep Shear Spans

11.5.3.1
The area of transverse shear reinforcement, A_v, shall not be less than $0.002b_w s$, and s shall not exceed d/5 nor 300 mm.

11.5.3.2
Pairs of longitudinal reinforcing bars shall be distributed over the depth of the beam. The cross sectional area of each pair of bars, with one bar near each face, shall be not less than $0.002b_w$ times the spacing between the pairs of bars. This spacing shall not exceed d/3 nor 300 mm.

11.6 Special Provisions for Walls

11.6.1
The design for shear forces due to concentrated loads acting perpendicular to the face of walls shall be in accordance with the provisions for slabs in Clause 11.10.

11.6.2
The design for shear forces in the plane of walls shall be in accordance with the requirements of Clause 11.3 or 11.4 with minimum reinforcement in accordance with Clause 14.3.

11.6.3
The design for shear strength at construction joints shall be in accordance with the requirements of Clause 11.7.

11.7 Shear Friction

11.7.1
The provisions of Clause 11.7 are to be applied where it is appropriate to consider shear transfer across a given plane, such as an existing or

potential crack, an interface between dissimilar materials, or an interface between two concretes cast at different times.

11.7.2

The resistance of cross sections subject to shear transfer as described in Clause 11.7.1, shall be calculated in accordance with the provisions of Clause 11.7.3 or 11.7.4.

11.7.3

A crack shall be assumed to occur along the shear plane considered. The required area of shear-friction reinforcement, A_{vf}, across the shear plane, may be designed using either Clause 11.7.4 or any other shear transfer design method that results in the prediction of resistance in substantial agreement with results of comprehensive tests.

11.7.3.1

The provisions of Clauses 11.7.5 through 11.7.10 shall apply for all calculations of shear transfer resistance.

11.7.4 Shear Friction Design Method

11.7.4.1

When shear-friction reinforcement is perpendicular to the shear plane, the factored shear resistance, V_r, shall be computed by:

$$V_r = \phi_s A_{vf} f_y \mu \qquad \textbf{(11-31)}$$

where
μ is the coefficient of friction in accordance with Clause 11.7.4.3.

11.7.4.2

When shear-friction reinforcement is inclined to the shear plane at an angle, α_f, such that the shear force produces tension in the shear-friction reinforcement, the factored shear resistance, V_r, shall be computed by:

$$V_r = \phi_s A_{vf} f_y (\mu \sin \alpha_f + \cos \alpha_f) \qquad \textbf{(11-32)}$$

11.7.4.3

The coefficient of friction, μ, in Equation (11-31) and Equation (11-32) shall be:

(a) for concrete placed monolithically 1.25λ;

(b) for concrete placed against hardened concrete with the surface intentionally roughened as specified in Clause 11.7.9 ..... 0.9λ;

(c) for concrete placed against hardened concrete not intentionally roughened ..... 0.5λ; and
(d) for concrete anchored to as-rolled structural steel by headed studs or by reinforcing bars (see Clause 11.7.10) ..... 0.6λ.

11.7.5
The factored shear resistance, V_r, shall not be greater than $0.25\phi_c f'_c A_{cv}$ nor $6.5\phi_c A_{cv}$.

11.7.6
When calculating V_r, the yield strength of the shear-friction reinforcement shall not be taken as greater than 400 MPa.

11.7.7
The net tension across the shear plane shall be resisted by additional reinforcement. The net compression across the shear plane may be taken into account when calculating the required shear-friction reinforcement, provided that only the minimum value of the compression which will occur during the life of the structure is considered

11.7.8
The shear-friction reinforcement shall be appropriately placed along the shear plane and shall be anchored to develop the specified yield strength on both sides by embedment, hooks, or welding to special devices.

11.7.9
For the purpose of Clause 11.7, when concrete is placed against previously hardened concrete, the interface for shear transfer shall be clean and free of laitance. If μ is assumed equal to 0.9λ, the interface shall be roughened to a full amplitude of approximately 5 mm.

11.7.10
When shear is transferred between as-rolled steel and concrete using headed studs or welded reinforcing bars, the steel shall be clean and free of paint.

11.8 Special Provisions for Brackets and Corbels

11.8.1
Brackets and corbels shall be designed in accordance with the requirements of Clause 11.4.7 and the additional requirements of this Clause.

Appendix D
Explanatory Comments to Clause 11, Shear and Torsion

General

Clause 11 of this Standard contains some provisions for shear design that are significantly different from those contained in previous standards. This Appendix is given to assist the design engineer in the application of these new provisions. The clauses are numbered as in Clause 11 with a letter D prefixed.

D11.2.1 Design Methods and Design Considerations

Beams can be designed for shear either by the traditional $V_c + V_s$ approach (see Clause 11.3) or a more general approach based on the Compression Field Theory (see Clause 11.4).

D11.2.2.1 Types of Shear Reinforcement

To effectively increase shear capacity, transverse reinforcement must be capable of undergoing substantial strains prior to failure. Welded wire fabric, particularly if fabricated from small wires and not stress relieved after fabrication, may fail at the cross wire intersections before the required strain is reached.

D11.2.4 Consideration of Torsion

Torques that do not exceed one-quarter of the pure torsional cracking torque will not cause a significant reduction in either flexural or shear strength and hence can be neglected. After cracking, there is a substantial reduction in the torsional stiffness relative to the flexural stiffness. If the torsion in the member is a function of torsional stiffness, the resulting redistribution of internal forces will maintain the maximum torsion in the member at about the cracking torque even as the loads are increased. This cracking torque will be about two-thirds of the pure torsional cracking load.

D11.2.5 Minimum Shear Reinforcement

Minimum shear reinforcement restrains the growth of inclined cracking, and hence increases ductility and provides a warning of failure. Such reinforcement can be omitted if there is no significant

chance of diagonal cracking. It can also be omitted if the member is of minor importance or if the member is part of a redundant structural system which allows substantial redistribution of load and hence will display adequate ductility.

D11.3.4 Calculation of V_c—Nonprestressed Members

Previous standards have given several alternative procedures for calculating V_c. In order to be brief and understandable, this Standard gives only one procedure for calculating V_c. V_c is modified to account for the detrimental effect of axial tension and the beneficial effect of axial compression (see Reference 1). If the axial tension is so high that, acting together with the flexural moment, it will cause yielding of any of the longitudinal reinforcement, then V_c is taken as zero.

D11.3.6.4 Maximum V_s for Parallel Bent-Up Bars

The upper limit has been specified to exclude cases which may exhibit undesirable cracking at service load levels.

D11.3.9 Indirect Loads

The design provisions of Clause 11.3 were developed primarily from tests in which loads pushed down upon the top face of beams while supports pushed up on the bottom face. If loads are applied to the side face of a beam, additional transverse reinforcement is required to support these loads and hang them up to the top face of the member. To be effective, this reinforcement must be placed close to the loaded interface (see Figure D1). Note that in determining the zone of effective reinforcement, h_b need not be taken as being less than 75 mm. If the shear stress is low enough that diagonal cracks are unlikely to form, no additional reinforcement is needed.

D11.4.1 General Principles and Requirements (General Method)

The resistance and behaviour of members in shear or torsion, or both, can be investigated in detail by performing a sectional analysis that considers the equilibrium, compatibility, and stress-strain requirements for different portions of the section. Such an analysis (see Figure D2) would show that the shear stress distribution is not uniform and that the direction of principal compressive stresses changes over the depth of the beam. In lieu of the detailed analysis implied in Clause 11.4.1.1 a more direct procedure, which concentrates on the conditions at mid-depth of the beam, is permitted by Clause 11.4.1.5.

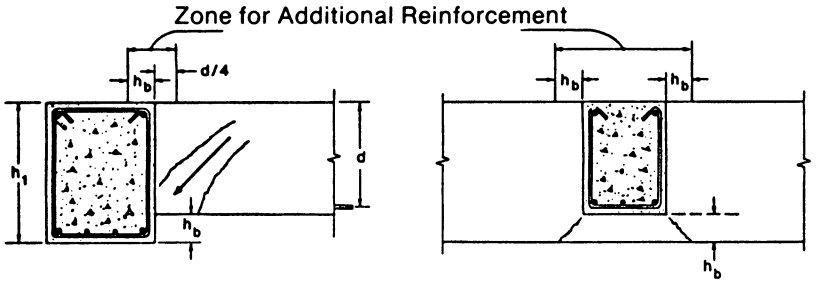

Figure D1
Girder Loaded by Secondary Beam

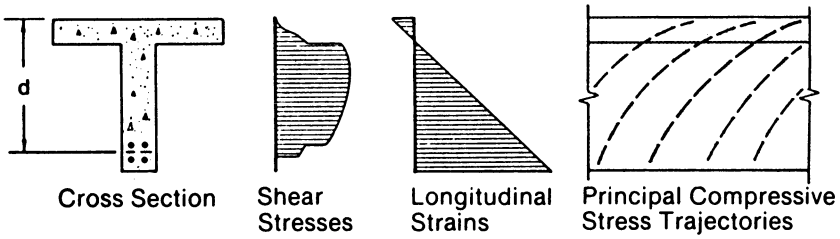

Figure D2
Detailed Study of Beam in Shear

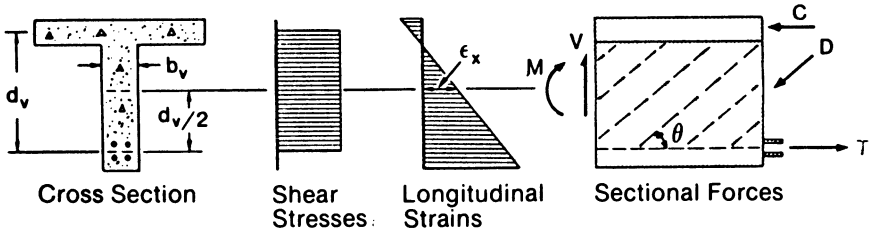

Figure D3
More Direct Procedure for Beam in Shear

In this procedure (see Figure D3) the shear stresses are assumed to be uniformly distributed over an area b_v wide and d_v deep, the direction of the principal compressive stresses (defined by angle θ) is assumed to remain constant over d_v and tensile stresses in cracked concrete are ignored.

D11.4.2 Diagonal Compressive Stresses in Concrete

If the principal tensile stress in the web concrete is zero, then the principal compressive stress in the web concrete will be related to the shear stress on the web concrete by an equilibrium Equation (11-18), which can be derived from the Mohr's circle given in Figure D4. If the web concrete is severely deformed (large ϵ_1), its ability to resist compressive stresses will be substantially reduced. Equation (11-19), which relates the failure value of f_2 to the strain ϵ_1 perpendicular to the direction of f_2 (see Figure D5), was derived from the work reported in Reference 2. The principal tensile strain, ϵ_1, is related to the longitudinal strain at mid-depth, ϵ_x (see Figure D3), the principal compressive strain (assumed to be -0.002), and the principal strain direction (assumed to coincide with the principal stress direction) by compatibility Equation (11-20), which can be derived from the Mohr's circle given in Figure D6. Sections with high axial compression, prestress, or low values of moment will have small web deformations (low ϵ_x and thus low ϵ_1) and hence will be able to tolerate higher shear stresses.

The value of f_{2max} is reduced for lightweight concrete because f_2 must be transmitted across the typically more steeply inclined cracks that formed at lower loads (see Figure D5). Cracks in lightweight concrete usually pass through the aggregate and hence have relatively smooth surfaces that limits their ability to transmit the stresses.

D11.4.2.6

The value of θ can be chosen by the designer. Values of θ smaller than 45° will result in less transverse reinforcement, but more longitudinal reinforcement being required which is usually an economical trade off. As θ is made smaller, f_2, the diagonal compressive stress due to the applied shear, becomes larger and f_{2max}, the limiting value of f_2, becomes smaller. For a given beam the lower limit for θ is set when f_2 reaches f_{2max}. The lower the shear stress on the concrete, the lower the value of θ at which f_2 will equal f_{2max} (see Figure D7).

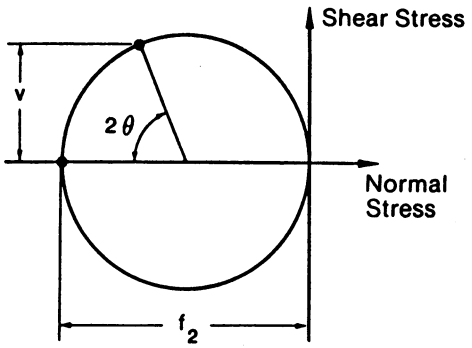

Figure D4
Concrete Stresses in Web of Beam

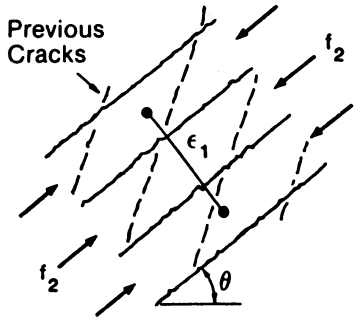

Figure D5
Stress, f_2, and Strain, ϵ_1

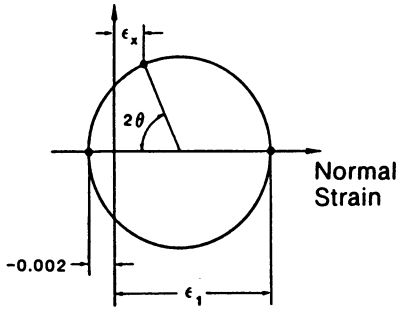

Figure D6
Strains at Mid-depth of Web

D11.4.2.7

Clause 11.4.2.7 discusses spalling of the web at high shears. The outwards thrust of the diagonal compressive stresses in the concrete must be equilibrated by the tensile forces in the transverse reinforcement. Unless the cover concrete is bearing against a flange, the compressive stresses in the cover concrete will need to "curve in" towards the reinforcement (see Figure D8). This changing of direction requires tensile stresses perpendicular to the plane of the stirrups, which may cause the concrete to split along the plane of weakness formed by the stirrups. For members in torsion the highest compressive stresses occur near the outer surface and hence these members are particularly vulnerable to spalling of the concrete cover.

D11.4.2.12

Torsion is assumed to be resisted by a "tube" of uniformly stressed concrete, a_o thick, whose outer surface is the centreline of the outermost transverse torsional reinforcement. The diagonal compressive stresses caused by the torsion will in fact be greater near the outside surface and will reduce to zero at about $1.5a_o$ from this surface.

D11.4.3 Yielding of Transverse Reinforcement

The requirement that the transverse reinforcement must yield prior to crushing of the concrete, limits the maximum shear that a given cross section can resist as shown by the dashed lines in Figure D7.

The geometry of the web deformations is given by Equations (11-22) and (11-23), which can be derived from a Mohr's circle of strain such as that shown in Figure D6.

D11.4.4 Design of Transverse Reinforcement

Transverse reinforcement must be provided to equilibrate the outwards thrust of the diagonal compressive stresses in the concrete. Equations (11-24) and (11-25) express this equilibrium requirement.

As the torsion on a given cross section increases, the thickness, a_o, of the "torsional tube" becomes larger and hence the area enclosed by the centreline of the tube, A_o, becomes smaller. (See Reference 3 for more details.)

The free body diagram in Figure D9 demonstrates why, for uniformly loaded beams, the transverse reinforcement within a length $d_v/\tan\theta$ may be designed to resist the lowest shear within this length as stated in Clause 11.4.4.10.

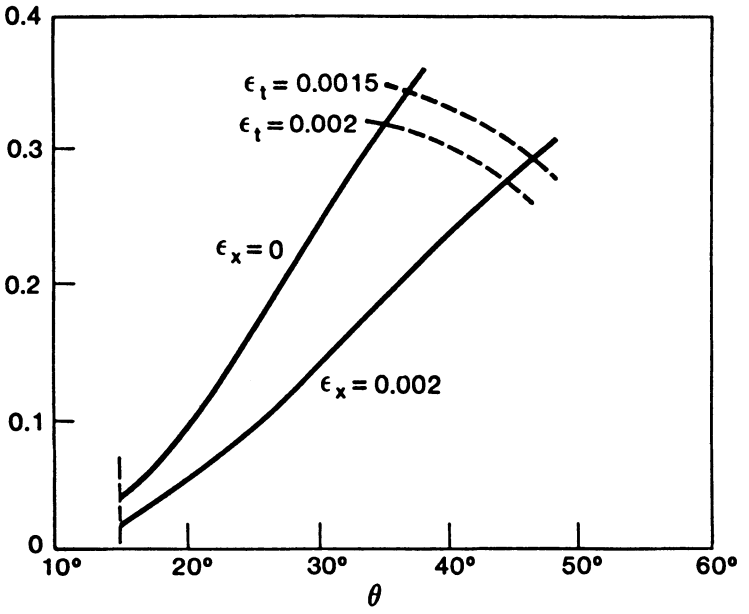

Figure D7
Values for θ at which $f_2 = f_{2max}$

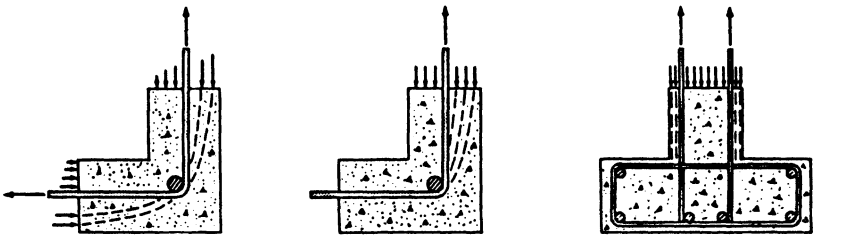

Figure D8
Compressive Stress Trajectories in Concrete Cover

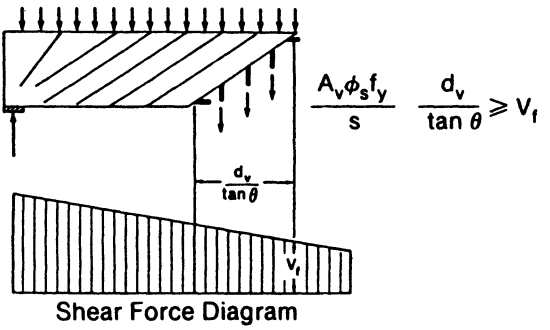

Figure D9
Beam Subjected to Uniform Loading

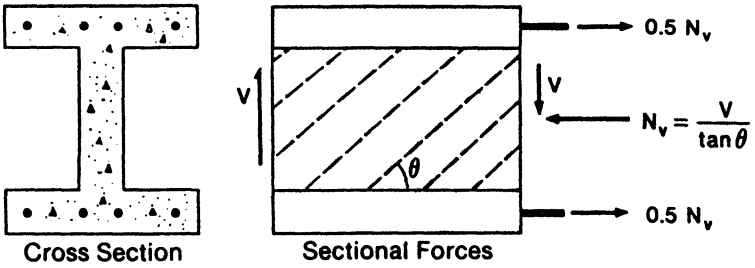

Figure D10
Longitudinal Forces Due to Shear

D11.4.6 Design of Longitudinal Reinforcement

The shear force on the section is resisted by diagonal compressive stresses in the concrete. Thus, in Figure D3, it is the vertical component of the force D that is carrying the shear. The horizontal component of D is equivalent to an axial compression on the concrete of V/tan θ. This unwanted compression needs to be cancelled out by tensile forces in the longitudinal reinforcement (see Figure D10). Thus, shear causes compressive stresses in the concrete and tensile stresses in the longitudinal reinforcement. In terms of the tension in the longitudinal reinforcement, the shear is equivalent to an axial tensile load of V/tan θ.

When both torsion and shear act on a section, the shear stresses due to torsion and shear will add on one side of the section and counteract on the other side. To account for the fact that the torsion and shear effects are not simply additive, the required equivalent tension, N_v, is taken as the square root of the sum of the squares of the individually calculated tensions.

Rather than designing the longitudinal reinforcement at a section to resist moment, M_f, and equivalent axial tension, N_v, it may be more convenient to design only for a larger moment of $M_f + 0.5N_vd_v$. Designing for this increased moment will give essentially the same additional longitudinal reinforcement. Figure D11 illustrates this procedure for a uniformly loaded beam supported by cross girders.

D11.4.6.4

Failure of sections subjected to high axial compressions will be governed by crushing of the concrete in compression rather than yielding of the reinforcement in tension. For such sections, the detrimental effect of the concrete compressive stresses due to shear can be accounted for by adding an equivalent axial compression equal to N_v.

D11.4.6.5

In traditional North American reinforced concrete design procedures, the influence of shear on the longitudinal reinforcement is accounted for by detailing rules about the development of flexural reinforcement. These traditional rules can be waived, if the influence of shear on the longitudinal reinforcement has been accounted for directly.

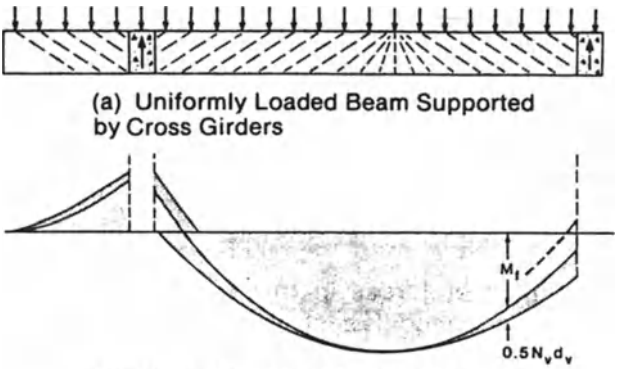

Figure D11
Equivalent Additional Moments Due to Shear

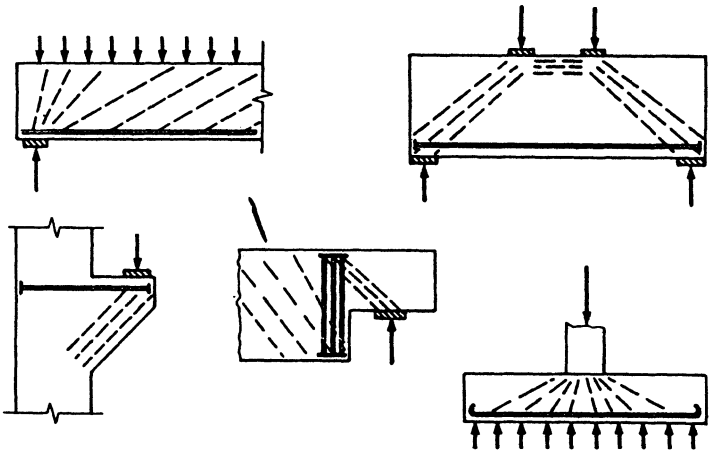

Figure D12
Principal Compressive Stress Trajectories in Regions Near Supports, Concentrated Loads, or Abrupt Changes in Cross Section

D11.4.7 Design of Regions Adjacent to Supports, Concentrated Loads, or Abrupt Changes in Cross Section

The design procedures detailed in Clauses 11.4.2, 11.4.3, 11.4.4, and 11.4.6 are based on the assumptions that the shear stresses are uniformly distributed over the depth, d_v (see Figure D3) and that the principal compressive stress trajectories can be approximated by a series of parallel lines representing the compression field (see Figure D11). In regions near discontinuities, such as those shown in Figure D12, these assumptions do not apply and hence it is appropriate to use procedures that more closely approximate the actual flow of forces.

The internal flow of forces in these disturbed regions can be approximated by truss models such as that shown in Figure D13. The zones of high unidirectional compressive stress in the concrete are modelled as compressive struts, while tension ties are used to model the principal reinforcement. The regions of concrete subjected to multi-directional stresses, where the struts and the ties meet (the nodes of the truss) are represented by "nodal zones".

D11.4.7.3

The reinforcing bars of a tension tie are bonded to the surrounding concrete. Hence, if the reinforcing bars are to yield in tension, there must be an average tensile strain in the concrete. If a tension tie crosses a compressive strut, this tensile straining will reduce the capacity of the concrete to resist compressive stresses. In the direction of the strut the concrete undergoes its highest compressive strain, while in the direction of the bar it must undergo tensile strain (see Figure D14). The largest tensile strain, ϵ_1, will occur in the direction perpendicular to the strut (ie, cracks are assumed to be occurring parallel to the strut). To yield the bar, ϵ_1 must become greater as the angle between the bar and the strut becomes smaller. In this situation Equation (11-20) can be used to determine ϵ_1 if ϵ_x is taken as the average strain in the bar and θ as the angle between the bar and the strut. Equation (11-19) can then be used to determine the maximum possible stress in the strut. (In both applications of Equation (11-20), θ is the angle between the direction in which ϵ_x is measured and the direction of f_{c2}.)

Note that the compressive struts do not have to be of constant cross section along their lengths (the sloping struts in Figure D13 have been taken as being somewhat wider near the bottom). As the force in a strut will be constant, the stress will be inversely proportional to the area.

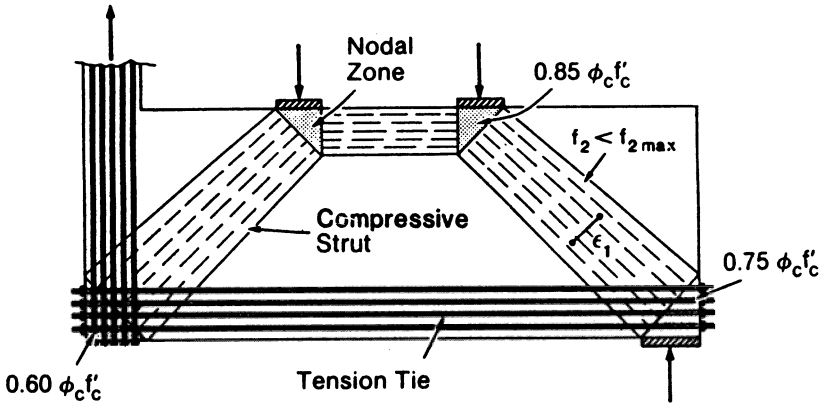

Figure D13
Components of the Truss Model

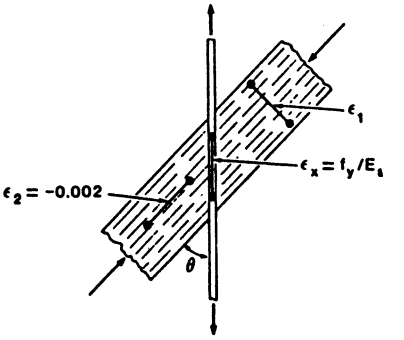

Figure D14
Strain Conditions in Concrete Strut

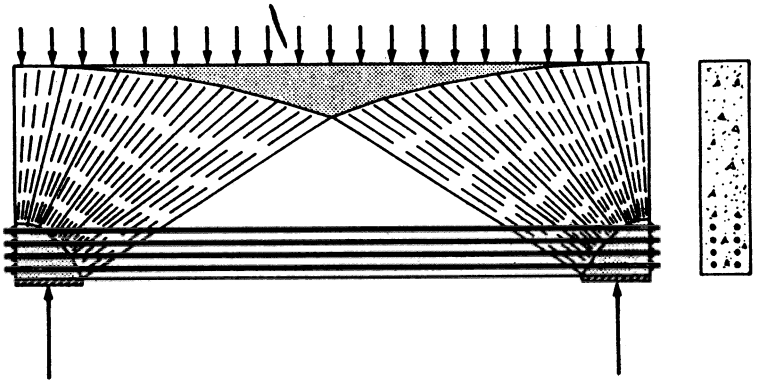

Figure D15
Compressive Struts Radiating from Direct Support

D11.4.7.4

Tension tie reinforcement can be anchored to the nodal zone by appropriate embedment lengths, hooks, or mechanical devices in accordance with the requirements of Clause 12. For the purpose of checking the stresses in the nodal zones, the tie reinforcement can be regarded as being anchored by bearing against the far side of the nodal zone as shown in Figure D13.

D.11.4.7.5

The allowable concrete compressive stresses in nodal zones are related to the degree of confinement of these zones. Thus the zones beneath the loads shown in Figure D13 are allowed to be stressed to $0.85\phi_c f'_c$ (if they were triaxially confined by special reinforcement, higher stresses would be possible) while the zone above the right reaction is restricted to $0.75\phi_c f'_c$ and the zone at the bottom of the left strut is restricted to $0.60\phi_c f'_c$. If the tie reinforcement was really anchored by bearing against metal plates at the back of the nodal zones then these lower limits could be increased to the $0.85\phi_c f'_c$ value.

D11.4.7.7

In situations such as that shown in Figure D15, where the compressive stresses in the concrete can be represented by a series of struts radiating out from a nodal zone, the highest stresses in the concrete will occur at the nodal zone. In such cases the concrete stresses need only be checked at the nodal zones. For the case shown, the truss would be satisfactory if the depth of the top nodal zone at midspan was large enough to ensure that the compressive stress due to the flexural compression was less than $0.85\phi_c f'_c$, if the bearing stress at the supports was less than $0.75\phi_c f'_c$, and if the tension tie reinforcement could resist the flexural tension and was anchored over a sufficient depth of the beam, so that the tension divided by the width of the beam and the depth over which the steel was anchored was less than $0.75\phi_c f'_c$.

The radiating compressive stresses in regions near direct supports will influence the design of the longitudinal reinforcement. In comparison to situations where the support reactions "feed in" over the depth of the beam, less longitudinal reinforcement will be required (compare Figures D11 and D16). In Figure D16 the reinforcement required adjacent to the bottom face near the support remains the same (near the simple support this reinforcement must be anchored over a depth sufficient to satisfy Clause 11.4.7.6(c)), but the reinforcement adjacent to the top face need not exceed the amount required to resist the maximum moment.

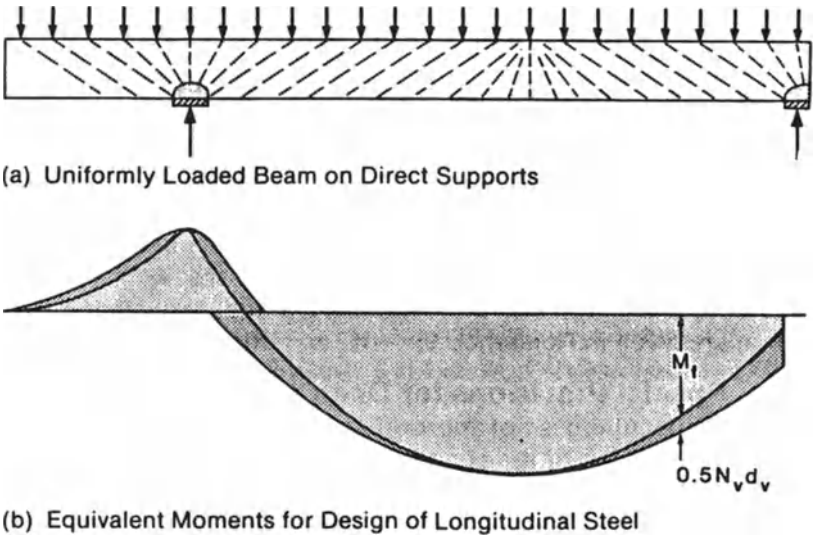

Figure D16
Beam on Direct Supports—Longitudinal Steel Design

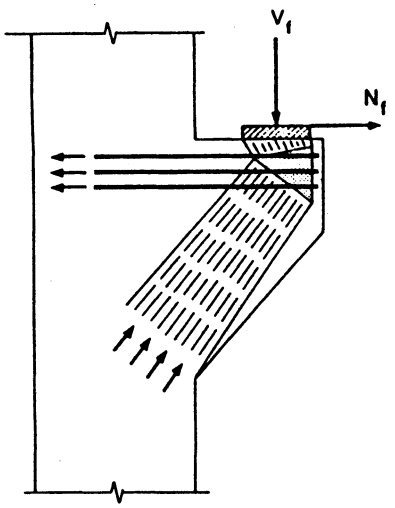

Figure D17
Truss Model of Corbel

D11.4.8 Control of Diagonal Cracking

Excessively wide diagonal cracks are unsightly and increase the risk of corrosion of the reinforcement. Cracking is controlled by limiting the spacing of the reinforcement and by limiting the strain in the transverse reinforcement at service loads. The strain limit of 0.001 was suggested in Reference 4.

Equation (11-29) is based on estimating the principal compressive stress direction at service load (the second factor) and making an allowance for the influence of the tensile stresses in the cracked concrete (the last factor). More details on the derivation of this equation are given in Reference 3.

D11.5 Special Provisions for Deep Shear Spans

The simplified method is not appropriate for the design of deep shear spans. The influence of the shear on the longitudinal reinforcement requirements needs to be calculated directly. Hence the general method is used.

The function of the minimum reinforcement is to control diagonal cracking and to increase the ductility of the member.

D11.8 Special Provisions for Brackets and Corbels

Brackets and corbels are to be designed by the strut and tie models described in Clause 11.4.7 (see Figure D17).

The traditional limits on the corbel dimensions have been retained. Corbels and brackets usually support the ends of beams. With time these beams will shorten due to shrinkage, creep (for prestressed beams), and temperature changes. Unless bearings have been used, which allow these movements to freely occur, the change in length will be resisted by the friction between the beam and the corbel.

D11.10 Special Provisions for Slabs and Footings

These are essentially the ACI provisions for slabs except that the detailed rules for shearhead design have not been reproduced and "nailhead type" shear reinforcement is specifically permitted.

References

1. ACI-ASCE Committee 426. Suggested Revisions to Shear Provisions for Building Codes. *In:* ACI Journal, Vol. 74, No. 9, Detroit, Michigan, Sept. 1977, pp 458—469.
2. F. Vecchio and M.P. Collins. The Response of Reinforced Concrete to In-Plane Shear and Normal Stresses. Publication No. 82-03, University of Toronto, Department of Civil Engineering, March 1982, 242 pp.
3. Michael P. Collins and Denis Mitchell. Shear and Torsion Design of Prestressed and Non-Prestressed Concrete Beams. *In:* Journal of the Prestressed Concrete Institute, Vol. 25, No. 5, Sept./Oct. 1980. Discussion and closure, Vol. 26, No. 6, Nov./Dec. 1981, pp 32—100.
4. ACI-ASCE Committee 426. The Shear Strength of Reinforced Concrete Members. *In:* Journal of the Structural Division, American Society of Civil Engineers, Vol. 99, June 1973, pp 1091—1187.

Index